

IN THE UNITED STATES PATENT AND TRADEMARK OFFICE

In re Patent Application of

Applicants: Bednorz et al.

Serial No.: 08/479,810

Filed: June 7, 1995

For: **NEW SUPERCONDUCTIVE COMPOUNDS HAVING HIGH TRANSITION
TEMPERATURE, METHODS FOR THEIR USE AND PREPARATION**



Date: November 27, 2006

Docket: YO987-074BZ

Group Art Unit: 1751

Examiner: M. Kopec

Commissioner for Patents
United States Patent and Trademark Office
P.O. Box 1450
Alexandria, VA 22313-1450

APPEAL BRIEF

PART IX

CFR 37 § 41.37(c) (1) (ix)

SECTION 1

BRIEF ATTACHMENTS AA TO AZ; BB TO BL

VOLUME 5

Respectfully submitted,

A handwritten signature in black ink, appearing to read "Daniel P. Morris".

Dr. Daniel P. Morris, Esq.
Reg. No. 32,053
(914) 945-3217

IBM CORPORATION
Intellectual Property Law Dept.
P.O. Box 218
Yorktown Heights, New York 10598

BEST AVAILABLE COPY

BRIEF ATTACHMENT AA

IN THE UNITED STATES PATENT AND TRADEMARK OFFICE

In re Patent Application of

Applicants: Bednorz et al.

Serial No.: 08/479,810

Filed: June 7, 1995

For: NEW SUPERCONDUCTIVE COMPOUNDS HAVING HIGH TRANSITION
TEMPERATURE, METHODS FOR THEIR USE AND PREPARATION

Date: March 1, 2005

Docket: YO987-074BZ

Group Art Unit: 1751

Examiner: M. Kopec

Commissioner for Patents
P.O. Box 1450
Alexandria, VA 22313-1450

FIRST SUPPLEMENTAL AMENDMENT

Sir:

In response to the Office Action dated July 28, 2004, please consider the
following:

ATTACHMENT AA

1989

Powder Diffraction File

Inorganic Phases

Alphabetical Index (Chemical and Mineral Name)

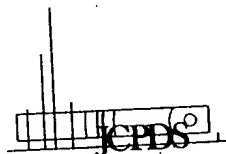


INTERNATIONAL CENTRE FOR DIFFRACTION DATA

Powder Diffraction File

Alphabetical Index Inorganic Phases 1989

Compiled by the JCPDS—International Centre for Diffraction Data in cooperation with the American Ceramic Society, American Crystallographic Association, American Society for Testing and Materials, Australian X-Ray Analytical Association, British Crystallographic Association, The Clay Minerals Society, Deutsche Mineralogische Gesellschaft, The Institute of Physics, The Mineralogical Association of Canada, The Mineralogical Society of America, Mineralogical Society of Great Britain and Ireland, National Association of Corrosion Engineers, and Société Française de Minéralogie et de Cristallographie.



Published by the

INTERNATIONAL CENTRE FOR DIFFRACTION DATA

1601 PARK LANE • SWARTHMORE, PA 19081-2389 • U.S.A.

Copyright © JCPDS International Centre for Diffraction Data 1989
formerly the
Joint Committee on Powder Diffraction Standards

All rights reserved. No part of this publication may be reproduced or transmitted in any form, or by any means, electronic or mechanical, including photocopy, recording, or any information storage and retrieval system, without permission in writing from the publisher.

Printed in U.S.A.
1989

[illegible]

[illegible]

Mercury Bromide Oxide Chloride //Carnanchelite	$\text{Hg}_3\text{O}_2(\text{Cl},\text{Br})_4$	2.67x	2.86x	5.68x	35-510	Mercury Fluoride Hydroxide :	Hg_2FOH	3.78x	2.95x	2.82x	25-558
Mercury Bromide Sulfide :	$\text{Hg}_2\text{Br}_2\text{S}_2$	2.65x	3.06x	3.07x	28-658	Mercury Fluoride Iodide :	Hg_2FI	2.16x	3.57x	4.11x	32-655
Mercury Bromide Sulfide : Copper	$\text{Hg}_2\text{Br}_2\text{S}_2$	2.62x	3.52x	2.52x	38-876	Mercury Fluoride : Potassium	KHgF_3	3.12x	3.12x	3.12x	23-488
Mercury Bromide : Thallium	THgBr_3	3.23x	3.01x	2.45x	18-1349	Mercury Fluoride : Rubidium	RbHgF_3	1.83x	2.25x	3.16x	23-617
Mercury Bromide : Thallium	THgBr_3	2.95x	2.85x	2.81x	16-829	Mercury Fluoride : Silver	Hg_2AgF_3	1.66x	1.94x	3.17x	27-1291
Mercury : Cadmium	CdHg	2.78x	1.50x	1.97x	8-337	Mercury Fluoride Sulfide : Copper	$\text{Hg}_2\text{CuF}_2\text{S}_2$	3.10x	1.90x	1.62x	32-344
Mercury : Cadmium	CdHg_2	2.33x	2.81x	1.51x	18-264	Mercury Fluoride : Silver	Hg_2AgF_3	4.02x	2.70x	2.25x	2-287
Mercury : Cadmium	CdHg_2	2.33x	2.77x	1.50x	32-1361	Mercury Gallium Sulfide :	HgGa_2S_2	3.11x	1.88x	1.65x	39-995
Mercury : Cadmium	CdHg_2	2.33x	2.77x	1.50x	32-1371	Mercury Gallium Sulfide :	HgGa_2S_2	1.85x	3.12x	3.00x	39-996
Mercury : Cadmium	CdHg_2	2.31x	2.78x	1.50x	18-263	Mercury Gallium Telluride :	Ga_2HgTe_2	2.15x	3.45x	1.81x	8-272
Mercury : Calcium	CaHg	2.84x	4.92x	3.48x	33-2951	Mercury : Germanium Lithium	GeHgLi	2.26x	3.68x	1.93x	23-263
Mercury : Calcium	CaHg_2	2.33x	2.26x	2.77x	33-2941	Mercury Germanium Oxide :	Hg_2GeO_2	3.00x	2.41x	2.41x	29-906
Mercury Carbide : Potassium	KHgC_2	2.42x	3.61x	2.31x	38-1235	Mercury Germanium Selenide :	Hg_2GeSe_2	3.28x	2.80x	1.71x	39-1293
Mercury Carbide : Rubidium	RbHgC_2	2.45x	3.09x	3.64x	37-1199	Mercury Germanium Sulfide :	Hg_2GeS_2	3.41x	3.57x	3.04x	21-561
Mercury Carbon Chloride Fluoride Sulfide :	$\text{Hg}_2\text{C}(\text{SCl}_2)_2$	2.76x	4.07x	2.22x	31-852	Mercury Germanium Sulfide : Copper	$\text{Cu}_2\text{HgGeS}_4$	3.13x	1.90x	1.65x	26-543
Mercury Chlorate :	$\text{Hg}(\text{ClO}_3)_2$	4.62x	3.29x	2.19x	1-314	Mercury : Gold	Au_2Hg	2.43x	2.23x	1.23x	26-715
Mercury Chlorate :	$\text{Hg}(\text{ClO}_3)_2$	3.68x	3.36x	2.85x	39-996	Mercury : Gold	Au_2Hg	2.43x	2.23x	1.23x	19-522
Mercury Chlorate Hydroxide :	$\text{Hg}_2(\text{ClO}_3)_2 \cdot 4\text{H}_2\text{O}$	2.68x	5.35x	4.74x	19-803	Mercury : Gold	Au_2Hg	2.39x	2.23x	2.26x	4-780
Mercury Chloride :	HgCl_2	4.37x	2.99x	4.11x	26-3151	Mercury : Gold	$\alpha\text{-Au}_2\text{Hg}$	2.38x	1.24x	2.06x	4-781
Mercury Chloride : Cadamel, syn	HgCl	3.17x	4.15x	2.07x	26-3121	Mercury : Gold	Au_2Hg	2.23x	1.35x	1.25x	4-782
Mercury Chloride :	Hg_2Cl_2	2.73x	1.96x	4.11x	34-1103	Mercury : Iodine	HI_2Hg	2.50x	2.35x	1.39x	20-808
Mercury Chloride : Potassium	K_2HgCl_4	9.16x	3.45x	5.17x	14-817	Mercury : Iodine	HI_2Hg	2.64x	2.39x	1.79x	18-609
Mercury Chloride : Potassium	K_2HgCl_4	9.16x	3.45x	5.17x	14-817	Mercury : Iodine	HI_2Hg	2.42x	1.62x	2.79x	18-609
Mercury Chloride : Potassium	K_2HgCl_4	9.16x	3.45x	5.17x	14-817	Mercury : Iodine	HI_2Hg	2.42x	1.62x	2.79x	18-609
Mercury Chloride : Potassium	K_2HgCl_4	9.16x	3.45x	5.17x	14-817	Mercury : Iodine	HI_2Hg	2.42x	1.62x	2.79x	18-609
Mercury Chloride : Potassium	K_2HgCl_4	9.16x	3.45x	5.17x	14-817	Mercury : Iodine	HI_2Hg	2.42x	1.62x	2.79x	18-609
Mercury Chloride : Potassium	K_2HgCl_4	9.16x	3.45x	5.17x	14-817	Mercury : Iodine	HI_2Hg	2.42x	1.62x	2.79x	18-609
Mercury Chloride : Potassium	K_2HgCl_4										

File No.		
o	Molybdenum Chloride ;	3.07, 3.64, 3.75
o	Molybdenum Chloride ;	6- 482
c	Molybdenum Chloride ;	10- 254
c	Molybdenum Chloride ;	13- 191
c	Molybdenum Chloride ;	23- 352
c	Molybdenum Chloride ;	28- 352
c	Molybdenum Chloride ;	20- 333
c	Molybdenum Chloride ;	31- 556†
c	Molybdenum Chloride ;	36- 732
c	Molybdenum Chloride ;	38- 774
c	Molybdenum Chloride ;	26- 775
c	Molybdenum Chloride ;	19- 609
c	Molybdenum Chloride ;	19- 610
c	Molybdenum Chloride ;	20- 524
c	Molybdenum Chloride ;	20- 525
c	Molybdenum Chloride ;	38- 888
c	Molybdenum Chloride ;	38- 888
c	Molybdenum Chloride ;	27- 307
c	Molybdenum Chloride ;	27- 308
c	Molybdenum Chloride ;	39- 804
c	Molybdenum Chloride ;	9- 292
c	Molybdenum Chloride ;	28- 1366
c	Molybdenum Chloride ;	27- 978
c	Molybdenum Chloride ;	39- 443†
c	Molybdenum Chloride ;	29- 913
c	Molybdenum Chloride ;	27- 710
c	Molybdenum Chloride ;	20- 744
c	Molybdenum Chloride ;	21- 215
c	Molybdenum Chloride ;	21- 216
c	Molybdenum Chloride ;	23- 1194
c	Molybdenum Chloride ;	30- 61
c	Molybdenum Chloride ;	30- 351
c	Molybdenum Chloride ;	20- 1001
c	Molybdenum Chloride ;	21- 1034
c	Molybdenum Chloride ;	20- 748
c	Molybdenum Chloride ;	20- 745
c	Molybdenum Chloride ;	26- 1272
c	Molybdenum Chloride ;	20- 748
c	Molybdenum Chloride ;	6- 546
c	Molybdenum Chloride ;	8- 384
c	Molybdenum Chloride ;	15- 457
c	Molybdenum Chloride ;	35- 787
c	Molybdenum Chloride ;	31- 871
c	Molybdenum Chloride ;	11- 680
c	Molybdenum Chloride ;	36- 863
c	Molybdenum Chloride ;	30- 29
c	Molybdenum Chloride ;	16- 7
c	Molybdenum Chloride ;	37- 1093
c	Molybdenum Chloride ;	19- 12
c	Molybdenum Chloride ;	18- 250
c	Molybdenum Chloride ;	29- 451
c	Molybdenum Chloride ;	37- 1229
c	Molybdenum Chloride ;	22- 211
c	Molybdenum Chloride ;	5- 721
c	Molybdenum Chloride ;	39- 1102
c	Molybdenum Chloride ;	39- 1103
c	Molybdenum Chloride ;	32- 667
c	Molybdenum Chloride ;	30- 572
c	Molybdenum Chloride ;	18- 560
c	Molybdenum Chloride ;	39- 825
c	Molybdenum Chloride ;	17- 911
c	Molybdenum Chloride ;	38- 816
c	Molybdenum Chloride ;	27- 309
c	Molybdenum Chloride ;	31- 403
c	Molybdenum Chloride ;	20- 752
c	Molybdenum Chloride ;	21- 565
c	Molybdenum Chloride ;	12- 691
c	Molybdenum Chloride ;	6- 44
c	Molybdenum Chloride ;	17- 653
c	Molybdenum Chloride ;	20- 752
c	Molybdenum Chloride ;	21- 566
c	Molybdenum Chloride ;	17- 656

BRIEF ATTACHMENT AB

IN THE UNITED STATES PATENT AND TRADEMARK OFFICE

In re Patent Application of

Applicants: Bednorz et al.

Serial No.: 08/479,810

Filed: June 7, 1995

For: NEW SUPERCONDUCTIVE COMPOUNDS HAVING HIGH TRANSITION
TEMPERATURE, METHODS FOR THEIR USE AND PREPARATION

Date: March 14, 2005

Docket: YO987-074BZ

Group Art Unit: 1751

Examiner: M. Kopec

Commissioner for Patents
P.O. Box 1450
Alexandria, VA 22313-1450

THIRD SUPPLEMENTAL AMENDMENT

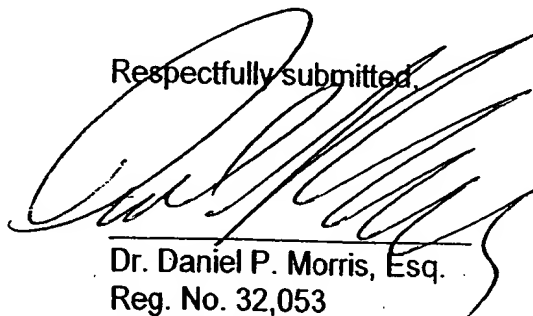
Sir:

In response to the Office Action dated July 28, 2004, please consider the
following:

The attachments referred to herein A to Z and AA are in the FIRST
SUPPLEMENTAL AMENDMENT. The Attachments AB to AG are attached herein.

Please charge any fee necessary to enter this paper and any previous paper to
deposit account 09-0468.

Respectfully submitted,



Dr. Daniel P. Morris, Esq.
Reg. No. 32,053
(914) 945-3217

IBM CORPORATION
Intellectual Property Law Dept.
P.O. Box 218
Yorktown Heights, New York 10598

ATTACHMENT AB

Synthesis of cuprate superconductors*

C N R Rao, R Nagarajan and R Vijayaraghavan

Solid State and Structural Chemistry Unit and CSIR Centre of Excellence in Chemistry, Indian Institute of Science, Bangalore 560012, India

Received 28 August 1992, in final form 19 October 1992

Abstract. There has been unprecedented activity pertaining to the synthesis and characterization of superconducting cuprates in the last few years. A variety of synthetic strategies has been employed to prepare pure monophasic cuprates of different families with good superconducting properties. Besides the traditional ceramic method, other methods such as coprecipitation and precursor methods, the sol-gel method, the alkali flux method and the combustion method have been employed for the synthesis of cuprates. Depending on the requirements, varying conditions such as high oxygen or hydrostatic pressure and low oxygen fugacity are employed in the synthesis. In this review, we discuss the synthesis of the various types of cuprate superconductors and point out the advantages and disadvantages of the different methods. We have provided the necessary preparative details, presenting the crucial information in tabular form wherever necessary.

1. Introduction

Since the discovery of high- T_c superconductivity in the La-Ba-Cu-O system [1], a variety of cuprate superconductors with T_c s going up to 128 K have been synthesized and characterized [2, 3]. No other class of materials has been worked on so widely and intensely in recent years as have the cuprate superconductors. Several methods of synthesis have been employed for preparing the cuprates, with the objective of obtaining pure monophasic products with good superconducting characteristics [3, 4]. The most common method of synthesis of cuprate superconductors is the traditional ceramic method which has been employed for the preparation of a large variety of oxide materials [5]. Although the ceramic method has yielded many of the cuprates with satisfactory characteristics, different synthetic strategies have become necessary in order to control factors such as the cation composition, oxygen stoichiometry, cation oxidation states and carrier concentration. Especially noteworthy amongst these methods are chemical or solution routes which permit better mixing of the constituent cations in order to reduce the diffusion distances in the solid state [3, 6]. Such methods include coprecipitation, use of precursors, the sol-gel method and the use of alkali fluxes. The combustion method or self-propagating high-temperature synthesis (SHS) has also been employed. In this review, we will discuss the preparation of cuprate superconductors by the different methods, mentioning

the special features of each method and the conditions employed for the synthesis. In table 1, we give a list of the cuprate superconductors discussed in this review along with their structural parameters and approximate T_c values. Preparative conditions such as reaction temperature, oxygen pressure, hydrostatic pressure and annealing conditions are specified in the discussion and given in tabular form where necessary. It is hoped that this review will be found useful by practitioners of the subject as well as those freshly embarking on the synthesis of these materials.

2. Ceramic method

The most common method of synthesizing inorganic solids is by the reaction of the component materials at elevated temperatures. If all the components are solids, the method is called the ceramic method [5]. If one of the constituents is volatile or sensitive to the atmosphere, the reaction is carried out in sealed evacuated capsules. Platinum, silica or alumina containers are generally used for the synthesis of metal oxides. The starting materials are metal oxides, carbonates, or other salts, which are mixed, homogenized and heated at a given temperature sufficiently long for the reaction to be completed. A knowledge of the phase diagram is useful in fixing the composition and conditions in such a synthesis.

The ceramic method generally requires relatively high temperatures (up to 2300 K) which are generally attained by resistance heating. Electric arc and skull

* Contribution No 874 from the Solid State and Structural Chemistry Unit.

Table 1. Structural parameters and approximate T_c values of cuprate superconductors.

Cuprate	Structure	T_c (K) (max. value)
1 $\text{La}_2\text{CuO}_{4-x}$	Bmab; $a = 5.355$, $b = 5.401$, $c = 13.15$ Å	39
2 $\text{La}_{2-x}\text{Sr}_x(\text{Ba})\text{CuO}_4$	I4/mmm; $a = 3.779$, $c = 13.23$ Å	35
3 $\text{La}_2\text{Ca}_{1-x}\text{Sr}_x\text{Cu}_2\text{O}_8$	I4/mmm; $a = 3.825$, $c = 19.42$ Å	60
4 $\text{YBa}_2\text{Cu}_3\text{O}_7$	Pmmm; $a = 3.821$, $b = 3.885$, $c = 11.676$ Å	93
5 $\text{YBa}_2\text{Cu}_4\text{O}_8$	Ammm; $a = 3.84$, $b = 3.87$, $c = 27.24$ Å	80
6 $\text{Y}_2\text{Ba}_4\text{Cu}_5\text{O}_{13}$	Ammm; $a = 3.851$, $b = 3.869$, $c = 50.29$ Å	93
7 $\text{Bi}_2\text{Sr}_2\text{CuO}_8$	Amaa; $a = 5.362$, $b = 5.374$, $c = 24.622$ Å	10
8 $\text{Bi}_2\text{CaSr}_2\text{Cu}_2\text{O}_8$	A2aa; $a = 5.409$, $b = 5.420$, $c = 30.93$ Å	92
9 $\text{Bi}_2\text{Ca}_2\text{Sr}_2\text{Cu}_2\text{O}_{10}$	A2aa; $a \sim 5.39$, $b \sim 5.40$, $c \sim 37$ Å	110
10 $\text{Bi}_2\text{Sr}_2(\text{Ln}_{1-x}\text{Ce}_x)_2\text{Cu}_2\text{O}_{10}$	P4/mmm; $a = 3.888$, $c = 17.26$ Å	25
11 $\text{Ti}_2\text{Ba}_2\text{CuO}_6$	A2aa; $a = 5.468$, $b = 5.472$, $c = 23.238$ Å; I4/mmm; $a = 3.868$, $c = 23.239$ Å	92
12 $\text{Ti}_2\text{CaBa}_2\text{Cu}_2\text{O}_8$	I4/mmm; $a = 3.855$, $c = 29.318$ Å	119
13 $\text{Ti}_2\text{Ca}_2\text{Ba}_2\text{Cu}_2\text{O}_{10}$	I4/mmm; $a = 3.85$, $c = 35.9$ Å	128
14 $\text{Ti}(\text{BaLa})\text{CuO}_6$	P4/mmm; $a = 3.83$, $c = 9.55$ Å	40
15 $\text{Ti}(\text{SrLa})\text{CuO}_6$	P4/mmm; $a \sim 3.7$, $c \sim 9$ Å	40
16 $(\text{Ti}_{0.5}\text{Pb}_{0.5})\text{Sr}_2\text{CuO}_8$	P4/mmm; $a = 3.738$, $c = 9.01$ Å	40
17 $\text{TiCaBa}_2\text{Cu}_2\text{O}_7$	P4/mmm; $a = 3.856$, $c = 12.754$ Å	103
18 $(\text{Ti}_{0.5}\text{Pb}_{0.5})\text{CaSr}_2\text{Cu}_2\text{O}_7$	P4/mmm; $a = 3.80$, $c = 12.05$ Å	90
19 $\text{TiSr}_2\text{Y}_{0.5}\text{Ca}_{0.5}\text{Cu}_2\text{O}_7$	P4/mmm; $a = 3.80$, $c = 12.10$ Å	90
20 $\text{TiCa}_2\text{Ba}_2\text{Cu}_2\text{O}_8$	P4/mmm; $a = 3.853$, $c' = 15.913$ Å	110
21 $(\text{Ti}_{0.5}\text{Pb}_{0.5})\text{Sr}_2\text{Ca}_2\text{Cu}_2\text{O}_8$	P4/mmm; $a = 3.81$, $c = 15.23$ Å	120
22 $\text{TiBa}_2(\text{Ln}_{1-x}\text{Ce}_x)_2\text{Cu}_2\text{O}_8$	I4/mmm; $a \sim 3.8$, $c \sim 29.5$ Å	40
23 $\text{Pb}_2\text{Sr}_2\text{Ln}_{0.5}\text{Ca}_{0.5}\text{Cu}_2\text{O}_8$	Cmmm; $a = 5.435$, $b = 5.463$, $c = 15.817$ Å	70
24 $\text{Pb}_2(\text{Sr}, \text{La})_2\text{Cu}_2\text{O}_8$	P2 ₂ ,2; $a = 5.333$, $b = 5.421$, $c = 12.609$ Å	32
25 $(\text{Pb}, \text{Cu})\text{Sr}_2(\text{Ln}, \text{Ca})\text{Cu}_2\text{O}_7$	P4/mmm; $a = 3.820$, $c = 11.826$ Å	50
26 $(\text{Pb}, \text{Cu})(\text{Sr}, \text{Eu})(\text{Eu}, \text{Ce})\text{Cu}_2\text{O}_7$	I4/mmm; $a = 3.837$, $c = 29.01$ Å	25
27 $\text{Nd}_{2-x}\text{Ce}_x\text{CuO}_4$	I4/mmm; $a = 3.95$, $c = 12.07$ Å	30
28 $\text{Ce}_{1-x}\text{Sr}_x\text{CuO}_2$	P4/mmm; $a = 3.902$, $c = 3.35$ Å	110
29 $\text{Sr}_{1-x}\text{Nd}_x\text{CuO}_2$	P4/mmm; $a = 3.942$, $c = 3.393$ Å	40

techniques give temperatures up to 3300 K while high-power CO_2 lasers give temperatures up to 4300 K. The main disadvantages of the ceramic method are the following:

(i) The starting mixtures are inhomogeneous at the atomic level.

(ii) When no melt is formed during the reaction, the entire reaction has to occur in the solid state, first by a phase boundary reaction at the points of contact between the components and later by the diffusion of the constituents through the product phase. With the progress of the reaction, diffusion paths become longer and the reaction rate slower; the reaction can be speeded up to some extent by intermittent grinding between heating cycles.

(iii) There is no simple way of monitoring the progress of the reaction. It is by trial and error that one decides on the appropriate conditions required for the completion of the reaction. Because of this difficulty, with the ceramic method one often ends up with mixtures of reactants and products. Separation of the desired products from such mixtures is difficult, if not impossible.

(iv) Frequently it becomes difficult to obtain a compositionally homogeneous product even where the reaction proceeds nearly to completion.

Despite the above limitations, the ceramic method is widely used for the synthesis of a large variety of inorganic solids. In the case of the cuprate superconductors,

the ceramic method involves mixing and grinding the component oxides, carbonates or other salts, and heating the mixture, generally in pellet form, at the desired temperature. A common variation of the method is to heat a mixture of nitrates obtained by digesting the metal oxides/carbonates in concentrated HNO_3 and evaporating the solution to dryness. Heating is carried out in air or in an appropriate atmosphere, controlling the partial pressure of oxygen when necessary. In the case of thallium cuprates, because of the volatility and poisonous nature of the thallium oxide vapour, reactions are carried out in sealed tubes. In some of the earlier preparations, the thallium cuprates were synthesized in open furnaces. This is however, not recommended. A successful synthesis by the ceramic method depends on several factors which include the nature of the starting materials (the choice of oxides, carbonates), the homogeneity of the mixture of powders, the rate of heating as well as the reaction temperature and duration.

2.1. La_2CuO_4 -related 214 cuprates

Synthesis of alkaline-earth-doped $\text{La}_{1-x}\text{M}_x\text{CuO}_4$ ($\text{M} = \text{Ca}, \text{Sr}$ and Ba) of K_2NiF_4 structure with superconducting transition temperatures up to 35 K is readily achieved by the ceramic method. Typically, the synthesis is carried out by reacting stoichiometric quantities of the oxides and/or carbonates around 1300 K in

oxygen atmosphere at 0.1 K after the sintering step [16]. Metal nitrates have also been used as starting materials for the synthesis [11–13]. By starting with metal nitrates, one obtains a more homogeneous starting mixture, since the hydrated metal nitrates have low melting points leading to a uniform melt in the initial stage of the reaction. Furthermore, nitrates provide an oxidative atmosphere, which is required to obtain the necessary oxygen content.

Stoichiometric La_2CuO_4 is an antiferromagnetic insulator. La_2CuO_4 prepared under high oxygen pressures, however, shows superconductivity ($T_c \sim 35$ K) since the oxygen excess introduces holes just as the alkaline earth dopants [14–16]. $\text{La}_2\text{CuO}_{4+\delta}$ (δ up to 0.05) has been synthesized by annealing La_2CuO_4 under an oxygen pressure of 3 kbar at 870 K [14, 15] or 23 kbar at 1070 K [16]. Oxygen plasma has also been used to increase the oxygen content.

The next homologue of La_2CuO_4 containing two Cu–O layers, $\text{La}_{1-x}\text{Sr}_x\text{CaCu}_2\text{O}_6$ ($T_c \sim 60$ K), has been synthesized by using high oxygen pressures [17]. The synthesis involves heating the sample at an oxygen pressure of around 20 bar at 1240 K. The material prepared at ambient oxygen pressures (in air) is an insulator. Several other high-oxygen-pressure preparations have been reported on the $n=2$ member of the $\text{La}_{2-x}\text{Cu}_2\text{O}_{2+x}$ homologous series by making use of commercially available high-pressure furnaces [18, 19]. In table 2, we have summarized the preparative conditions for 214 and related cuprate superconductors.

2.2. $\text{YBa}_2\text{Cu}_3\text{O}_7$ and other 123 cuprates

Superconducting $\text{YBa}_2\text{Cu}_3\text{O}_{7-\delta}$ with the orthorhombic structure can be easily prepared by the ceramic method. Most of the investigations of the 123 compound, $\text{YBa}_2\text{Cu}_3\text{O}_{7-\delta}$ have been carried out on the materials prepared by reacting Y_2O_3 and CuO with BaCO_3 [20, 21]. It is noteworthy that Rao *et al* [21] obtained monophasic $\text{YBa}_2\text{Cu}_3\text{O}_7$ as the $x=1.0$ member of the $\text{Y}_{3-2x}\text{Ba}_{3+x}\text{Cu}_6\text{O}_{14}$ series. In the method employed for preparing $\text{YBa}_2\text{Cu}_3\text{O}_7$, stoichiometric quantities of high-purity Y_2O_3 , BaCO_3 and CuO are ground thoroughly and heated initially in powder form around 1223 K for a period of 24 h. Following the calcination step, the powder is ground, pelletized and sintered at the same temperature for another 24 h. Finally, annealing is carried out in an atmosphere of oxygen around 773 K for 24 h to obtain the orthorhombic $\text{YBa}_2\text{Cu}_3\text{O}_{7-\delta}$ phase showing 90 K superconductivity. Oxygen annealing has to be carried out below the orthorhombic tetragonal transition temperature (~ 960 K); tetragonal $\text{YBa}_2\text{Cu}_3\text{O}_{7-\delta}$ ($0.6 \leq \delta \leq 1.0$) is not superconducting. Intermittent grinding is necessary to obtain monophasic, homogeneous powders. This kind of complex heating schedule often gives rise to microscopic compositional inhomogeneities. Furthermore, CO_2 released from the decomposition of BaCO_3 can react with $\text{YBa}_2\text{Cu}_3\text{O}_{7-\delta}$ to form non-superconducting

the evolution of CO_2 during the synthesis is to use BaO_2 instead of BaCO_3 . Some of the impurities or side products in the preparation of $\text{YBa}_2\text{Cu}_3\text{O}_7$ are BaCuO_2 , Y_2BaCuO_5 and $\text{Y}_2\text{Cu}_2\text{O}_5$ [24]. The ternary phase diagram given in figure 1 illustrates the complexities of this cuprate system.

Using BaO_2 as the starting material has two advantages. It has a lower decomposition temperature than BaCO_3 and the 123 compound is therefore formed at relatively low temperatures. BaO_2 acts as an internal oxygen source and the duration of annealing in an oxygen atmosphere is reduced to a considerable extent. Sharp superconducting transitions are observed in samples of $\text{YBa}_2\text{Cu}_3\text{O}_{7-\delta}$ made using BaO_2 . Slight excess of copper in the ceramic method is reported to give cuprates with sharper transitions [25]. Preparation of $\text{YBa}_2\text{Cu}_3\text{O}_{7-\delta}$ is accomplished in a shorter period if one employs metal nitrates as the starting materials [13, 23]. In table 2, we present the conditions employed for preparing 123 cuprates by the ceramic method.

Other rare-earth cuprates of the 123 type, $\text{LnBa}_2\text{Cu}_3\text{O}_{7-\delta}$ where $\text{Ln} = \text{La, Nd, Sm, Eu, Gd, Dy, Ho, Er}$ and Tm (all with T_c values around 90 K) have also been prepared by the ceramic method [26, 27]. Oxygen annealing of these cuprates should also be carried out below the orthorhombic–tetragonal transition temperature [3]: La, 754 K; Nd, 837 K; Gd, 915 K; Er, 973 K; Yb, 976 K etc. Nearly 30% of Y can be substituted by Ca in $\text{YBa}_2\text{Cu}_3\text{O}_{7-\delta}$, retaining the basic crystal structure [28]; the T_c decreases with the increase in calcium content. Both La and Sr can be substituted at the Ba site in $\text{YBa}_2\text{Cu}_3\text{O}_{7-\delta}$ [29–31]. With La, monophasic products are obtained for $0 \leq x \leq 1.0$ in $\text{YBa}_{2-x}\text{La}_x\text{Cu}_3\text{O}_{7-\delta}$, the T_c decreasing with increase in x . In the case of Sr substitution, monophasic products are obtained for $0 \leq x \leq 1.25$ in $\text{YBa}_{2-x}\text{Sr}_x\text{Cu}_3\text{O}_{7-\delta}$; high T_c is retained up to $x=1.0$. Ceramic methods have also been used to prepare $\text{YBa}_2\text{Cu}_{3-x}\text{M}_x\text{O}_{7-\delta}$ solid solutions, where M generally stands for a transition element of the first series. In most

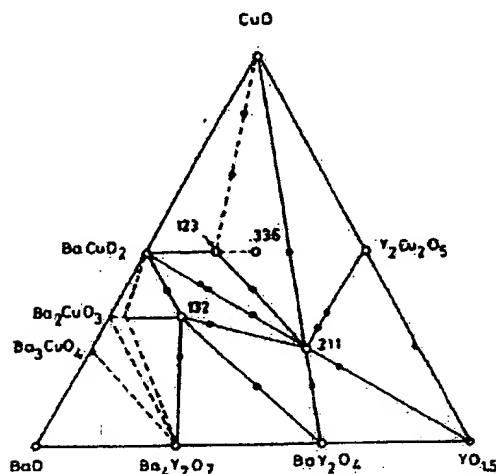


Figure 1. Phase diagram of the Y_2O_3 – BaO – CuO system at 1220 K (from [24]).

Table 2. Preparative conditions for the synthesis of 214, 123, 124 and 247 type cuprates by the ceramic method.

Compound	Starting materials	Preparative conditions			Comments	T_c (K)	Ref.
		Temp. (K)	Time	Gas			
$\text{La}_2\text{CuO}_{4-x}$	$\text{La}_2\text{O}_3, \text{CuO}$	1273 873	24 h 12-48 h	air O_2	3 kbar pressure	35 40	[15] [10]
$\text{La}_{2-x}\text{Sr}_x(\text{Ba}_y)\text{CuO}_4$	$\text{La}_2\text{O}_3, \text{Sr}/\text{BaCO}_3, \text{CuO}$	1393	36 h	O_2		32	[13]
$\text{La}_{1-x}\text{Sr}_x\text{CaCu}_2\text{O}_6$	$\text{La}(\text{NO}_3)_3 \cdot n\text{H}_2\text{O}, \text{Sr}/\text{Ba}(\text{NO}_3)_2, \text{Cu}(\text{NO}_3)_2 \cdot n\text{H}_2\text{O}$	1273	20 h	air			
	$\text{La}_2\text{C}_2\text{O}_7 \cdot 10\text{H}_2\text{O}, \text{Sr}(\text{NO}_3)_2, \text{Ca}(\text{NO}_3)_2 \cdot 4\text{H}_2\text{O}, \text{CuO}$	973	16 h	O_2			
		1173	3 d	O_2			
		1198	3 d	O_2			
$\text{YBa}_2\text{Cu}_3\text{O}_{7-x}$	$\text{Y}_2\text{O}_3, \text{BaCO}_3, \text{CuO}$	1243	2 d	O_2	20 atm	60	[17]
		1223	2 d	air			
	$\text{Y}_2\text{O}_3, \text{BaO}_2, \text{CuO}$	773	1 d	O_2		88	[20]
		1198	2 d	air			
$\text{YBa}_2\text{Cu}_4\text{O}_{10-x}$	$\text{Y}(\text{NO}_3)_3 \cdot n\text{H}_2\text{O}, \text{Ba}(\text{NO}_3)_2, \text{Cu}(\text{NO}_3)_2 \cdot n\text{H}_2\text{O}$	723	1 d	O_2		88	[22]
		1173	18 h	air			
		1223	1 h	O_2		90	[13]
	$\text{Y}_2\text{O}_3, \text{BaCO}_3, \text{CuO}$	1313	—	O_2	400 bar	81	[34]
	$\text{Y}_2\text{O}_3, \text{Ba}(\text{NO}_3)_2, \text{CuO} + \text{equal volumes of } \text{Na}_2\text{CO}_3 \text{ or } \text{K}_2\text{CO}_3$	1023	1 d	O_2	124 major phase + BaCuO_2 impurity	77	[35]
	$\text{Y}_2\text{O}_3, \text{Ba}(\text{NO}_3)_2, \text{CuO} + 0.2\text{M NaNO}_3 \text{ or } \text{KNO}_3 \text{ or } \text{Na}_2\text{O}_2$	1073	3 d	O_2	124 major phase + $\text{BaCuO}_2 + \text{Y}_2\text{BaCuO}_6$	78	[36, 38]
	$\text{Y}_2\text{O}_3, \text{BaCO}_3, \text{CuO}$	1073	3 d	O_2	124 major phase + $\text{BaCuO}_2 + \text{Y}_2\text{BaCuO}_4$	78	[38]
	$\text{Y}_2\text{O}_3, \text{BaCuO}_2, \text{CuO} + 0.2\text{M NaNO}_3 + 10 \text{ drops of dilute HNO}_3$	1088	1 d	air	124 single phase	79	[40]
$\text{Y}_2\text{Ba}_2\text{Cu}_7\text{O}_{19-x}$	$\text{YBa}_2\text{Cu}_3\text{O}_7, \text{CuO}$	1088	2 d	O_2			
		1088	10 d	O_2			
	$\text{Y}_2\text{O}_3, \text{BaCO}_3, \text{CuO}$	1088	3 d	O_2	124 major phase + BaCuO_2	75	[39]
	$\text{Y}_2\text{O}_3, \text{Ba}(\text{NO}_3)_2, \text{CuO}$	1203	8 h	O_2	19 bar	90	[50]
	$\text{Y}_2\text{O}_3, \text{Ba}(\text{NO}_3)_2, \text{CuO} + 0.2\text{M NaNO}_3$	1133	5 d	O_2	Single phase	90	[36]
		1133	4 d	O_2	Single phase	90	[36]

* Other rare-earth derivatives of the type $\text{LnBa}_2\text{Cu}_3\text{O}_7$ are also prepared by this method. Oxygen annealing is carried out below the orthorhombic-tetragonal transition temperature [26, 27].

^b Other rare-earth derivatives of the type $\text{LnBa}_2\text{Cu}_4\text{O}_{10}$ are obtained by a similar procedure [36, 40].

^c Other rare-earth derivatives of the type $\text{Ln}_2\text{Ba}_2\text{Cu}_7\text{O}_{19}$ are prepared by a similar procedure [38, 39].

2.3. $\text{YBa}_2\text{Cu}_4\text{O}_8$ (124), $\text{Y}_2\text{Ba}_4\text{Cu}_7\text{O}_{15}$ (247) and related cuprates

The first bulk synthesis of $\text{YBa}_2\text{Cu}_4\text{O}_8$ was reported by Karpinski *et al* [34] who heated the mixture of oxides at 1313 K, under an oxygen pressure of 400 bar. Synthesis of $\text{YBa}_2\text{Cu}_4\text{O}_8$ by the conventional ceramic method without the use of high oxygen pressure suffered from some limitations due to kinetic factors. Cava *et al* [35] found that additives such as alkali carbonates enhance the reaction rate. The procedure involves two steps. In the first step Y_2O_3 , $\text{Ba}(\text{NO}_3)_2$ and CuO are mixed in the stoichiometric ratio and heated at 1023 K for 16–24 h in an oxygen atmosphere. In the second step, the pre-reacted powder is ground with an approximately equal volume of either Na_2CO_3 or K_2CO_3 powder and pellets of the resulting mixture are heated at 1073 K in flowing oxygen for 3 days. After the reaction, the product is washed with water to remove the excess alkali carbonate and dried by gentle heating in air. The product after this step has $\text{YBa}_2\text{Cu}_4\text{O}_8$ as the majority phase (T_c , 77 K) with little BaCuO_2 impurity. Other reaction rate enhancers such as NaNO_3 , KNO_3 , dilute HNO_3 and Na_2O_2 have also been used successfully (in small quantities) to prepare $\text{YBa}_2\text{Cu}_4\text{O}_8$ [36–38]. The 124 cuprate can also be prepared without the addition of a rate enhancer by the solid state reaction of Y_2O_3 , BaCuO_2 and CuO at 1088 K in flowing oxygen [36]. Synthesis of $\text{YBa}_2\text{Cu}_4\text{O}_8$ from the solid state reaction between $\text{YBa}_2\text{Cu}_3\text{O}_7$ and CuO in flowing oxygen has also been reported [39]. The synthesis of $\text{YBa}_2\text{Cu}_4\text{O}_8$ by the ceramic method generally takes a long time and requires repeated grinding and pelletizing.

Other rare-earth 124 cuprates, $\text{LnBa}_2\text{Cu}_4\text{O}_8$ with $\text{Ln} = \text{Eu, Gd, Dy, Ho}$ and Er have been prepared by the ceramic method under an oxygen pressure of 1 atm [36, 40]. The T_c of these cuprates decreases with the increasing ionic radius of the rare earth. Calcium can be substituted at the Y site up to 10% in $\text{YBa}_2\text{Cu}_4\text{O}_8$, and the T_c increases from 79 K to 87 K in such substituted $\text{YBa}_2\text{Cu}_4\text{O}_8$ [41]. Lanthanum can be substituted for barium in $\text{YBa}_2\text{Cu}_4\text{O}_8$ [42]. Single phases of $\text{YBa}_{2-x}\text{La}_x\text{Cu}_4\text{O}_8$ have been obtained for $0 \leq x \leq 0.4$ with the T_c decreasing with increase in x .

Extensive studies have been carried out on the synthesis of $\text{YBa}_2\text{Cu}_4\text{O}_8$ under high oxygen pressures [43, 44]. The P - T phase diagram of 124, 123 and 247 cuprates is shown in figure 2. High-oxygen pressure synthesis essentially involves the solid state reaction followed by sintering under high oxygen pressures. The typical sintering temperature and the pressure at which synthesis of $\text{YBa}_2\text{Cu}_4\text{O}_8$ has been carried out are 1200 K and 120 atm of oxygen (for 8 h). By the use of high oxygen pressures [45], it is possible to prepare 124 compounds with other rare earths such as Nd and Sm , which is otherwise not possible under ambient pressures.

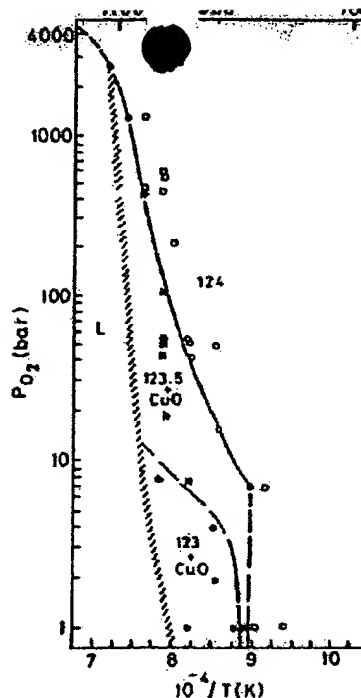


Figure 2. Phase diagram of the 124, 247 and 123 cuprates (from [43]).

A variety of substitutions has been carried out at the Y, Ba and Cu sites in $\text{YBa}_2\text{Cu}_4\text{O}_8$ under high oxygen pressures. Yttrium can be substituted up to 10% by Ca in $\text{YBa}_2\text{Cu}_4\text{O}_8$ giving a T_c of ~ 90 K [46]; 20% Ba has been substituted by Sr without affecting the T_c [47]. Single-phase iron-substituted $\text{YBa}_2\text{Cu}_{4-x}\text{Fe}_x\text{O}_8$ ($0 \leq x \leq 0.05$) has been prepared at an oxygen pressure of 200 bar [48]; the T_c falls monotonically with increasing iron concentration.

Bordet *et al* [49] first reported the preparation of $\text{Y}_2\text{Ba}_4\text{Cu}_7\text{O}_{15}$ under oxygen pressures of 100–200 bar. It was soon realized that $\text{Y}_2\text{Ba}_4\text{Cu}_7\text{O}_{15}$ can be synthesized by the ceramic method under an oxygen pressure of 1 atm by a procedure similar to that employed for $\text{YBa}_2\text{Cu}_4\text{O}_8$, except for the difference in the sintering temperature [36]. There is a narrow stability region between 1123 K and 1143 K for the 247 cuprate to be synthesized under 1 atm oxygen pressure. The best sintering temperature at which the 247 cuprate is formed is 1133 K. Other rare-earth 247 cuprates, $\text{Ln}_2\text{Ba}_4\text{Cu}_7\text{O}_{15}$ ($\text{Ln} = \text{Dy, Er}$), can also be prepared by this method [36, 38]. About 5% of Y can be replaced by Ca in $\text{Y}_2\text{Ba}_4\text{Cu}_7\text{O}_{15}$, and the T_c increases to 94 K [42]. Substitution of La at the Ba site is limited to $\sim 10\%$ in $\text{Y}_2\text{Ba}_4\text{Cu}_7\text{O}_{15}$, where the T_c decreases continuously with increasing lanthanum content [42].

Synthesis of 247 cuprates by the high-pressure oxygen method is generally carried out at 1203 K at an oxygen pressure of around 19 bar (for 8 h). This step is followed by slow cooling (typically 5°C min^{-1}) to room temperature at the same pressure [50]. Other rare-earth 247 compounds, $\text{Ln}_2\text{Ba}_4\text{Cu}_7\text{O}_{15}$ ($\text{Ln} = \text{Eu, Gd, Dy, Ho}$

and Er), have been prepared in the oxygen pressure range of 14–35 bar [50]. Preparative conditions for the 124 and 247 cuprates are given in table 2.

2.4. Bismuth cuprates

Although the ceramic method is widely employed for the synthesis of superconducting bismuth cuprates of the type $\text{Bi}_2(\text{Ca}, \text{Sr})_{n-1}\text{Cu}_n\text{O}_{2n+4+\delta}$, it is generally difficult to obtain monophasic compositions, due to various factors [51, 52]. Both thermodynamic and kinetic factors are clearly involved in determining the ease of formation as well as phasic purity of these cuprates. The $n = 1$ member (2201) of the formula $\text{Bi}_2\text{Sr}_2\text{CuO}_6$ appears to be stable around 1083 K and the $n = 2$ member, $\text{Bi}_2(\text{Ca}, \text{Sr})_2\text{Cu}_2\text{O}_8$ (2122) around 1113 K. The $n = 3$ member, $\text{Bi}_2(\text{Ca}, \text{Sr})_3\text{Cu}_3\text{O}_{10}$ (2223), can be obtained close to the melting point (1123 K) after heating for several days or even weeks. Of all the members of the $\text{Bi}_2(\text{Ca}, \text{Sr})_{n-1}\text{Cu}_n\text{O}_{2n+4+\delta}$ family, the $n = 2$ member (2122) seems to be most stable. Bi_2O_3 , which is often used as one of the starting materials, melts at around 1103 K. Increasing the reaction temperature therefore leads to preferential loss of volatile Bi_2O_3 . This results in micro-inhomogeneities and the presence of the unreacted oxides in the final product. Since these materials contain so many cations, partial reaction between various pairs of oxides leading to the formation of impurity phases in the final product cannot easily be avoided. A noteworthy structural feature of all these bismuth cuprates is the presence of superlattice modulation; the modulation has nothing to do with superconductivity.

Most of the above problems have been overcome by employing the matrix reaction method [53, 54]. This method reduces the number of reacting components and gives better products. In this method, synthesis is carried out by reacting the oxide matrix made from CaCO_3 , SrCO_3 and CuO with Bi_2O_3 in the temperature range of 1083–1123 K in air for a minimum period of 48 h. Quenching the samples in air from the sintering temperature or heating in a nitrogen atmosphere improves the superconducting properties of bismuth cuprates. The matrix reaction method yields monophasic $n = 2$ (2122) and $n = 3$ (2223) compositions showing T_c values of 85 K and 110 K respectively [55, 56]. Partial melting for a short period (~5 min) also favours the rapid formation of the $n = 2$ (2122) and the $n = 3$ (2223) members.

The $n = 1$ member, $\text{Bi}_2\text{Sr}_2\text{CuO}_6$, showing T_c in the range 7–22 K is a rather complicated system and has two structurally different phases near the stoichiometric composition [51, 57–60]. Many workers have varied the Bi/Sr ratio and obtained single-phase materials with a T_c of 10 K at a composition which is strontium deficient, $\text{Bi}_{2.1}\text{Sr}_{1.9}\text{CuO}_6$, [60, 61]. This cuprate is best prepared by reacting the oxides and/or carbonates of the constituent metals at 1123 K in air for extended periods of time. In figure 3 we show the phase diagram of the Bi–Sr–Cu–O system. The phase diagram of the

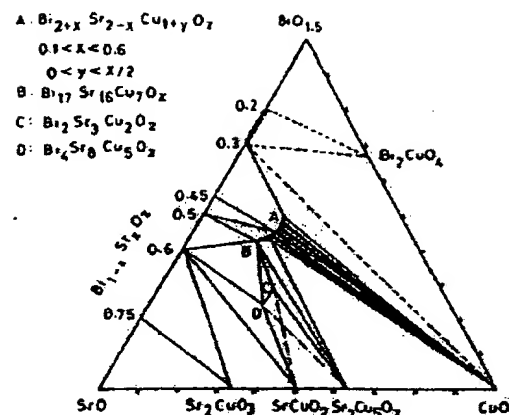


Figure 3. Phase diagram of the Bi–Sr–Cu–O system at 1110 K in air (from [60]).

Bi_2O_3 – SrO – CaO – CuO system at a constant Cu content is shown in figure 4.

Substitution of a small amount of lead for bismuth results in good superconducting samples of $n = 2$ (2122) and $n = 3$ (2223) members. A number of workers have therefore preferred to synthesize both $n = 2$ (2122) and $n = 3$ (2223) members with substitution of lead up to 25% in place of bismuth [58, 63–66]. They are obtained either by direct reaction of oxides and/or carbonates of the cations or by the matrix reaction method.

Other than the matrix reaction method, melt quenching (glass route) [67, 68] and a semi-wet method [6] have been employed for the synthesis of superconducting bismuth cuprates. In the melt quenching method the mixture of starting materials (in the form of oxide and/or carbonates) is melted in a platinum or alumina crucible around 1473 K for a short period in air and then quenched in liquid nitrogen. The quenched specimens are given an annealing treatment around 1103 K in air to obtain the superconducting crystalline cuprates. This method has been shown to produce both $n = 2$ (2122) and lead-doped $n = 3$ (2223) members.

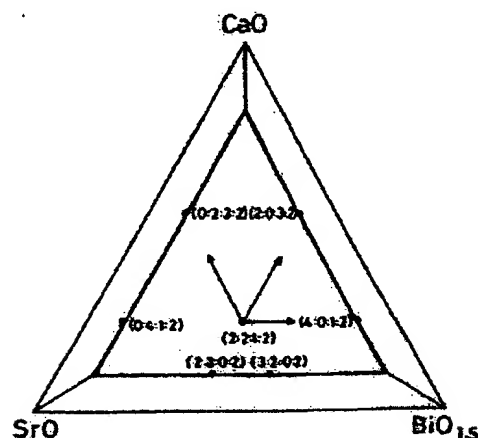


Figure 4. Section through the phase diagram of the Bi_2O_3 – SrO – CaO – CuO system at a constant CuO content of 28.6 mol% (from [62]).

semi-wet method involves the same reaction between two precursors which are precipitated separately. For example, in the preparation of $\text{Bi}_{1.6}\text{Pb}_{0.4}\text{Sr}_2\text{Ca}_2\text{Cu}_3\text{O}_{10}$, a precipitate of Pb, Sr and Ca (as carbonates) and one of Bi and Cu (as oxalates) are reacted at 1138 K in air for a minimum period of 72 h. The duration of the reaction for the formation of 2223 phase is drastically reduced by this method.

The starting composition of the reactant materials plays an important role in the synthesis of these cuprates. For example, strontium deficiency in the $n = 1$ (2201) member favours monophasic compositions [59, 61]. Strontium deficiency also helps in obtaining a phase-pure $n = 2$ (2122) member [70]. Starting with a 4:3:3:4 stoichiometry of Bi:Ca:Sr:Cu, it has been possible to obtain a monophasic 2122 member [54, 71]. The $n = 3$ (2223) phase, on the other hand, is either obtained through the substitution of Bi by Pb (up to 25%) or by taking an excess of Ca and/or Cu [63–66, 72]. The problem of balancing between phase purity and high T_c of the cuprate gives rise to some difficulty in the synthesis of these cuprates. The coexistence of some of the members of the homologous series, especially in the form of polytypic intergrowths of different layered sequences, is also a problem. This problem is also encountered with thallium cuprates [73, 74].

The $n = 4$ phase, $\text{Bi}_{1.3}\text{Pb}_{0.5}\text{Ca}_3\text{Sr}_2\text{Cu}_4\text{O}_{12}$, which was observed in an electron micrograph along with $n = 3$ phase as an intergrowth, was synthesized in bulk by Rao *et al* [75] (with a small proportion of the $n = 3$ phase) by the ceramic method. The $n = 4$ phase has a slightly lower T_c (103 K), than the $n = 3$ phase. This cuprate has also been prepared by Losch *et al* [75].

A variety of substitutions has been carried out in superconducting bismuth cuprates employing the ceramic method [58, 76–79]; some of them are noteworthy. For example, the simultaneous substitution of Bi by Pb and Sr by La in $\text{Bi}_2\text{Sr}_2\text{CuO}_6$ results in a modulation-free superconductor of the formula $\text{BiPbSr}_{1-x}\text{La}_x\text{CuO}_6$ with T_c increased to 24 K [77]. Similarly, co-substitution of Bi by Pb and Ca by Y in the $n = 2$ member (2122) gives a modulation-free superconductor, $\text{BiPbY}_{0.5}\text{Ca}_{0.5}\text{Sr}_2\text{Cu}_2\text{O}_8$ with a T_c of 85 K [77]. Rare-earth substitution for Ca in $\text{Bi}_2\text{CaSr}_2\text{Cu}_2\text{O}_8$ causes the T_c to go up to 100 K without the introduction of the $n = 3$ phase [58, 78]. As mentioned earlier, the $n = 3$ phase is stabilized by the partial substitution of lead in place of bismuth [63–65]. Another significant discovery is the iodine intercalation of the Bi-2122 superconductor [80]. Intercalation does not greatly affect the superconducting properties of the material; clearly, superconductivity is confined to the two-dimensional CuO_2 sheets in these materials.

Synthesis of a new series of superconducting cuprates of the general formula $\text{Bi}_2\text{Sr}_2(\text{Ln}_{1-x}\text{Ce}_x)_2\text{Cu}_2\text{O}_{10}$ (Bi-2222 phase with $\text{Ln} = \text{Sm, Eu, Gd}$) containing a fluorite-like $(\text{Ln}_{1-x}\text{Ce}_x)_2\text{O}_2$ layer between the two CuO_2 sheets has been possible by the ceramic method [81]. Partial substitution of bismuth by lead increases

stability and stabilizes the 2222 structure with other rare earths.

As mentioned earlier, one does not start with an exact stoichiometric composition to obtain the desired final product in the case of superconducting bismuth cuprates. Although structural studies (see for example [84]) indicate the presence of bismuth atoms over strontium and calcium sites as well, it is not possible to prescribe an exact initial composition to obtain the desired final stoichiometry. For example, starting from a nominal composition of $(\text{Bi}_{0.7}\text{Pb}_{0.3})\text{SrCaCu}_2\text{O}_7$, one ends up with the formation of the $n = 3$ (2223) member [65]. Therefore, for the purpose of characterizing the various members of the superconducting bismuth cuprates, one starts with some arbitrary composition and varies the synthetic conditions suitably to obtain the desired final product in pure form. The actual compositions of the final cuprate are quite unexpected (e.g. $\text{Bi}_{1.83}\text{Pb}_{0.30}\text{Sr}_{2.04}\text{Ca}_{1.60}\text{Cu}_3\text{O}_9$) as found from analytical electron microscopy [85]. In table 3 we have summarized the preparative conditions of all the members of $\text{Bi}_2(\text{Ca, Sr})_{n+1}\text{Cu}_n\text{O}_{2n+4}$ family.

2.5. Thallium cuprates

The conventional ceramic method employed for the synthesis of 214, 123 and bismuth cuprates has to be modified in the case of thallium cuprates of the $\text{Tl}_2\text{Ca}_{n-1}\text{Ba}_2\text{Cu}_n\text{O}_{2n+4}$, $\text{TlCa}_{n-1}\text{Ba}_2\text{Cu}_n\text{O}_{2n+3}$ and $\text{TlCa}_{n-1}\text{Sr}_2\text{Cu}_n\text{O}_{2n+3}$ families due to the toxicity and volatility of thallium oxide. In the early days, the reaction was carried out in an open furnace in air or oxygen atmosphere at high temperatures (1150–1180 K) for 5–10 min [86, 87]. In a typical procedure, the mixture of reactants in the form of a pellet was quickly introduced into the furnace maintained at the desired temperature. Since melt–solid reactions take place faster than solid–solid reactions, the product was formed quickly by this method [87]. Although this method requires a very short duration of heating, it results in the loss of thallium, leading to the danger of inhaling thallium oxide vapour. Some workers have taken certain precautions not to release the Tl_2O_3 vapour into the open laboratory, but the method is still not recommended. Furthermore, the formation of the desired phase is not ensured under the open reaction conditions. Synthesis of thallium cuprates has therefore been carried out in closed containers (sealed tubes) by most workers. By this method, both polycrystalline samples and single crystals can be prepared, since the reaction is carried out over longer periods. Better control of stoichiometry, homogeneity of phases and the total avoidance of the inhalation of toxic thallium oxide vapours are some of the advantages of carrying out sealed tube reactions.

Closed reaction conditions have been achieved in different ways. The reactant mixture is sealed in gold [88] or silver tubes [89] or in a platinum [90] or nickel

Table 3. Preparative conditions for the synthesis of bismuth cuprates by the ceramic method.

Starting composition	Conditions*		Product	T_c (K)	Ref.
	Temp. (K)	Time			
$\text{Bi}_2\text{Sr}_2\text{Cu}_2\text{O}_6$	1103	2 d	2201 major phase	20	[51]
$\text{Bi}_2\text{Sr}_2\text{CuO}_6$	1123	1 d	2201 major phase	9	[57]
$\text{Bi}_{2-x}\text{Sr}_{1+x}\text{CuO}_6$	1123	2 d	Single phase	10	[59, 61]
$\text{BiPbSr}_{1-x}\text{La}_x\text{CuO}_6$	1150	1 d	Single phase	24	[77]
$\text{Bi}_{1-x}\text{Ca}_x\text{Sr}_2\text{Cu}_2\text{O}_8$	1103	5 d	Single phase	85	[61]
$\text{Bi}_{1-x}\text{Ca}_x\text{Sr}_{1-x}\text{Cu}_2\text{O}_8^b$	1103	3 d	2122 major phase	80	[63]
$\text{Bi}_{1-x}\text{Ca}_x\text{Sr}_2\text{Cu}_2\text{O}_8$	1108	2 d	2122 single phase	85	[71]
$\text{Bi}_2\text{Sr}_{1-x}\text{Ca}_x\text{Cu}_2\text{O}_8$	1113	3 d	2122 single phase	85	[70]
$\text{BiPbSr}_{2-x}\text{Y}_{0.5}\text{Ca}_{0.5}\text{Cu}_2\text{O}_8$	1200	1 d	2122 single phase	85	[77]
$\text{Bi}_{1-x}\text{Pb}_x\text{Ca}_2\text{Sr}_2\text{Cu}_2\text{O}_8^*$	1140	5 d	2223 major phase	120	[55]
$\text{Bi}_{1-x}\text{Pb}_x\text{Ca}_{2-x}\text{Sr}_{1-x}\text{Cu}_2\text{O}_8^b$	1100	4 d	2223 major phase	105	[64]
$\text{Bi}_{1-x}\text{Pb}_x\text{Sr}_2\text{Ca}_2\text{Cu}_2\text{O}_8$	1153	10 d	2223 single phase	110	[72]
$\text{Bi}_{1-x}\text{Pb}_x\text{Sr}_2\text{CaCu}_{1-x}\text{O}_8$	1153	5 d	2223 major phase	105	[65]
$\text{BiCaSrCu}_2\text{O}_8$	1143	5 d	2223 major phase	120	[65]
$\text{Bi}_{1-x}\text{Pb}_x\text{Ca}_2\text{Sr}_2\text{Cu}_2\text{O}_8$	1133	5 d	2223 major phase	108	[64]
$\text{Bi}_{2-x}\text{Gd}_x\text{Ce}_{0.5}\text{Sr}_2\text{Cu}_2\text{O}_8$	1273	10 h	2222 single phase	30	[81]

* All the preparations carried out in air.

^b Obtained by matrix reaction method.

alloy (Inconel) container [91] closed tightly with a silver lid. Alternatively, the reactant mixture is taken in the form of a pellet, wrapped in a platinum [92] or gold [93] foil and then sealed in a quartz tube. This method has the advantage of carrying out the reaction under a vacuum. Some workers place the reactant pellet in an alumina crucible [94] which is then sealed in a quartz ampoule. Thallium-excess starting compositions have been employed by a few workers to compensate for the thallium loss during the reaction [95].

In the preparation of the thallium cuprates, the matrix reaction method is often employed. Here, a mixed oxide containing all the metal ions other than the volatile thallium oxide is first prepared by reacting the corresponding oxides and/or carbonates around 1200 K for 24 h in air [89, 96]. The freshly prepared mixed oxide is then taken with a calculated quantity of Tl_2O_3 and heated at appropriate temperatures in a sealed tube. This method is desirable when a carbonate is used as the starting material. Some of the thallium cuprates have been prepared by a modified matrix method [97] wherein a thallium-containing precursor such as $\text{Ba}_2\text{Tl}_2\text{O}_3$ is prepared first and then reacted with other components under closed conditions. Thallium-containing precursors are less volatile than Tl_2O_3 , so that the loss of thallium is minimized during the preparation.

Thermodynamic and kinetic factors associated with the synthesis of thallium cuprates are complex due to the existence of various phases which are structurally related and which can therefore intergrow with one another. In fact, one of the common defects that occurs in the thallium cuprates is the presence of random intergrowths between the various layered phases [98]. Furthermore, many of the thallium, lead and bismuth superconductors are metastable phases which are entropy stabilized [99]. The temperature of the reac-

tion, the sintering time and the starting composition are therefore all crucial to obtaining monophasic products (table 4).

The effect of the starting composition is best illustrated by the formation of the $n = 3$ phase of the bilayer thallium cuprates ($\text{Tl}_2\text{Ca}_2\text{Ba}_2\text{Cu}_2\text{O}_{10}$). Synthesis of this compound starting from the stoichiometric mixture of the oxides corresponding to the ideal composition often yields the $n = 2$ member of the family. It was found that starting with compositions rich in Ca and/or Cu (namely $\text{TlCa}_2\text{BaCu}_3\text{O}_9$, $\text{Tl}_2\text{Ca}_2\text{Ba}_2\text{Cu}_3\text{O}_9$) yielded a nearly pure $n = 3$ phase [90, 98, 100]. The actual composition is, however, close to $\text{Tl}_{1.7}\text{Ba}_2\text{Ca}_{2.3}\text{Cu}_3\text{O}_9$. In the case of $\text{TlCaBa}_2\text{Cu}_2\text{O}_8$ (1122) starting from a stoichiometric mixture of oxides corresponding to the ideal stoichiometry always yielded a mixture of 1122 and 2122 phases, the relative proportion of the two being dependent on the conditions. It has been demonstrated recently [101] that thallium-deficient compositions corresponding to $\text{Tl}_{1-x}\text{CaBa}_2\text{Cu}_2\text{O}_8$ ($\delta = 0.0$ to 0.3) yield better monophasic 1122 materials.

The thallium content of the material not only determines the number of Tl-O layers but controls the hole concentration. As mentioned earlier, one of the good starting compositions to obtain $\text{Tl}_2\text{Ca}_2\text{Ba}_2\text{Cu}_3\text{O}_{10}$ (2223) is $\text{TlCa}_2\text{BaCu}_3\text{O}_9$ (1313) which bears little relation to the composition of the final product. Another example is the formation of the $n = 4$ phase, $\text{TlCa}_2\text{Ba}_2\text{Cu}_4\text{O}_{10}$ (1324). Detailed studies [102] have shown that the 2223 phase formed initially transforms to the 1223 phase with an increase in the duration of heating. After prolonged sintering, the 1324 phase is formed at the expense of the 1223 phase. Similar transformations have also been observed in the formation process of $\text{TlCa}_2\text{Ba}_2\text{Cu}_3\text{O}_9$ with five Cu-O layers [103].

The Sr analogue of $\text{TlCa}_{n-1}\text{Ba}_2\text{Cu}_n\text{O}_{2n+3}$ cannot be prepared in pure form. However, they are stabilized by

Starting composition	Conditions			Product	T_c (K)	Ref.
	Temp. (K)	Time	Gas			
$Tl_2Ba_2CuO_8$	1148	3 h	Sealed gold tubes	2201 single phase	84	[88]
$Tl_2CaBa_2Cu_2O_8$	1173	8 h	Sealed gold tubes	2122 single phase	98	[88]
	1150	3 h	Sealed silica ampoule	2122 single phase	95	[98]
$Tl_2Ca_4Ba_2Cu_5O_{10}$	1150	0.5 h	Sealed silica ampoule	2122 single phase	95	[98]
$Tl_4Ca_3Ba_4Cu_5O_{10}$	1150	0.5 h	Sealed silica ampoule	2122 single phase	95	[98]
$Tl_2Ca_2Ba_2Cu_3O_{10}$	1173	6 h	Sealed gold tubes	2223 major phase	105	[88]
	1123	20 min	Sealed silica ampoule	2223 major phase	106	[95]
	1103	12 h				
$TlCa_3BaCu_3O_7$	1153	3 h	Sealed silica ampoules	2223 major phase	125	[100]
$Tl_2CaBa_2Cu_3O_7$	1153	3 h	Sealed silica ampoules	2223 major phase	108	[100]
$TlBa_{1-x}La_{0.5x}CuO_7$	1163	3 h	Sealed silica ampoules	1021 single phase	40	[111]
$TlSrLaCuO_5$	1170	2 h	Sealed silica ampoules	1021 single phase	40	[109]
$TlSr_{2-x}Nd_{0.5x}Cu_2O_7$	1170	2 h	Sealed silica ampoules	1122 major phase	80	[110]
$TlCaBa_2Cu_2O_7$	1170	3 h	Sealed silica ampoules	1122 major phase + 2122 impurity	90	[101]
$Tl_{0.8}CaBa_2Cu_2O_7$	1170	3 h	Sealed silver tubes	1122 major phase	90	[101]
$(Tl_{0.5}Pb_{0.5})CaSr_2Cu_2O_7$	1170	3 h	Sealed silica ampoules	1122 single phase	90	[104]
$Tl(Ca_{0.5}Y_{0.5})Sr_2Cu_2O_7$	1170	3 h	Sealed silver tubes	1122 single phase	90	[92]
$TlCa_2Ba_2Cu_3O_9$	1163	6 h	Sealed silica ampoules	1223 single phase	115	[94]
$(Tl_{0.5}Pb_{0.5})Ca_2Sr_2Cu_3O_9$	1198	3-12 h	Sealed gold tubes	1223 single phase	122	[105]
$Tl_{0.5}Pb_{0.5}Sr_4Cu_3O_9$	1170	2 h	Sealed silica ampoules	1223 major phase	60	[110]

partly substituting Tl by Pb (or Bi) or Ca by yttrium or a trivalent rare earth [92, 104-107]. Thus, $Tl_{0.5}Pb_{0.5}Ca_{n-1}Sr_2Cu_nO_{2n+3}$ shows a T_c of ~ 90 K for $n = 2$ and ~ 120 K for $n = 3$. $TlCa_{0.5}Y_{0.5}Sr_2Cu_2O_7$ also shows a T_c of 90 K. These cuprates in the Tl/Pb-Ca/Ln-Sr-Cu-O systems are prepared in a manner similar to the Tl-Ca-Ba-Cu-O system except that $SrCO_3$ is used in place of $BaCO_3$ or BaO_2 . $Sr_4Ti_2O_7$ has also been used as a starting material in some instances [97]. The $n = 1$ member, TlM_2CuO_5 ($M = Sr$ or Ba) is also stabilized by the substitution of Pb or Bi for Tl or a trivalent rare earth for Sr or Ba [108-111]. All these compounds showing a T_c of 40 K have been prepared by the matrix reaction method.

Single thallium layer cuprates of the general formula $Tl_{1-x}A_{2-x}Ln_2Cu_2O_9$ with $A = Sr, Ba$; $Ln = Pr$ (Nd, Ce) as well as $Tl_{0.5}Pb_{0.5}(Ln_{1-x}Ce_x)_2Sr_2Cu_2O_9$ ($Ln = Pr, Gd$) with a fluorite-type Ln_2O_3 layer have been prepared by the ceramic method [112, 113]. The as-prepared materials are semiconductors. It has been shown by Liu *et al* [114] that annealing $TlBa_2(Eu, Ce)_2Cu_2O_9$ (1222 phase) under an oxygen pressure of 100 bar induces superconductivity with a T_c of ~ 40 K.

As in the case of bismuth cuprates, the final composition of thallium cuprates is unlikely to reflect the composition of the starting mixture. Structural studies [99, 115] have shown that there is cation disorder between Tl and Ca/Sr sites. Therefore, in order to obtain a superconducting composition corresponding to a particular copper content, one has to start with various arbitrary compositions and vary the synthesis conditions. The actual composition of the final product can be quite unexpected (e.g. $Tl_{1.83}Ba_2Ca_{1.44}Cu_3O_9$ or $Tl_{1.86}Ba_{2.01}CuO_9$) as shown by analytical electron microscopy [85]. In table 4 we have listed the pre-

parative conditions employed for the synthesis of thallium cuprates by the ceramic method.

2.6. Lead cuprates

The conditions for the synthesis of superconducting lead cuprates are more stringent than for the other copper oxide superconductors. Direct synthesis of members of the $Pb_2Sr_2(Ln, Ca)Cu_3O_{8+x}$ ($Ln = Y$ or rare earth) family by the reaction of the component metal oxides or carbonates in air or oxygen at temperatures below 1173 K is not possible because of the high stability of $SrPbO_3$ -related perovskite oxides. Preferential loss of the more volatile PbO leads to micro-inhomogeneities. Furthermore, Pb in these compounds is in the 2+ state while part of the Cu is in the 1+ state. Synthesis has therefore to be carried out under mildly reducing conditions, typically in an atmosphere of N_2 containing 1% O_2 . The most common method that has been employed for the synthesis of these lead cuprates is the matrix reaction method [116]. For $Pb_2Sr_2(Ln, Ca)Cu_3O_{8+x}$ ($Ln = Y$ or rare earth), a mixed oxide containing all the metal ions except Pb is made by reacting $SrCO_3$, Ln_2O_3 or Y_2O_3 , $CaCO_3$ and CuO in the appropriate ratios around 1223 K in air for 16 h. The mixed oxide is then taken with an appropriate amount of PbO , ground thoroughly, pelletized and heated in the 1133-1198 K range in a flowing stream of nitrogen containing 1% O_2 for periods between 1 and 16 h. Generally, short reaction times and quenching the product from the sintering temperatures into liquid nitrogen in the same atmosphere gives better-quality samples. Even though this is the common method for preparing $Pb_2Sr_2(Ln, Ca)Cu_3O_{8+x}$, it is not always easy to obtain samples exhibiting good, reproducible

superconducting properties. The lead cuprates from the method described above generally show broad transitions in the $R-T$ curves with negative temperature coefficients of resistance above T_c .

Studies of the dependence of T_c on the calcium concentration in the $\text{Pb}_2\text{Sr}_2\text{Y}_{1-x}\text{Ca}_x\text{Cu}_3\text{O}_{8+x}$ system [117] have shown that heating the samples near the melting point between 1198 and 1228 K for 2 h and post-annealing in flowing nitrogen gas at a temperature between 673 and 773 K improves the superconducting properties of the samples dramatically. Direct one-step synthesis has been achieved [118] by reacting the metal oxides in sealed gold tubes around 1223 K. An alternative route to the direct synthesis from metal oxides and/or carbonates has also been demonstrated [119]. Superconductivity near 70 K has been reported in Ca-free $\text{Pb}_2\text{Sr}_2\text{LnCu}_3\text{O}_{8+x}$ ($\text{Ln} = \text{Y}$ or rare earth) employing the vacuum annealing procedure [120]. Substitution of Pb by Bi in $\text{Pb}_2\text{Sr}_2\text{Y}_{0.5}\text{Ca}_{0.5}\text{Cu}_3\text{O}_{8+x}$ has also been carried out by the ceramic method [121]. About 30% of Pb can be substituted by Bi, and such a substitution increases the T_c up to 100 K. The $n = 0$ member of the $\text{Pb}_2\text{Sr}_2(\text{Ca}_{1-x}\text{Ln}_x)\text{Cu}_{2+2x}\text{O}_{6+2x+x}$ series (namely $\text{Pb}_2(\text{SrLa})\text{Cu}_2\text{O}_{6+x}$) has been prepared successfully by this matrix reaction method [122].

Unlike the 2213-type lead cuprates, superconducting 1212-type lead cuprates of the formula $(\text{Pb}_{0.5}\text{Cu}_{0.5})\text{Sr}_2(\text{Y}_{0.5}\text{Ca}_{0.5})\text{Cu}_2\text{O}_{7-x}$ are synthesized in an oxidizing atmosphere. Several authors have reported direct synthesis as well as reactions under closed conditions [123–127]. In the direct synthesis of these cuprates, care is taken to prevent the loss of Pb by wrapping pellets in gold or platinum foil [127]. Rouillon *et al* [125, 126] have reported the synthesis of 1212 lead cuprates by the direct reaction of the component oxides in evacuated silica ampoules. This method has

the advantage of adjusting the oxygen partial pressure required for the synthesis. Both 2213-type and 1212-type lead cuprates have been prepared using the nitrates of the metal ions as the starting materials [128]. Although this procedure yields 2213 or 1212 phases in a single step, the product obtained always has impurities such as Y_2O_3 , CuO etc.

A superconducting lead cuprate of the formula $(\text{Pb}, \text{Cu})(\text{Eu}, \text{Ce})_2(\text{Sr}, \text{Eu})_2\text{Cu}_2\text{O}_8$ (1222 phase) containing a fluorite layer has been prepared by the direct reaction of the component metal oxides at 1273 K in oxygen atmosphere [129].

High-pressure ceramic synthesis has been employed to prepare lead cuprates of the 1212 type [130, 131]. In order to prepare $\text{Pb}_{0.5}\text{Cu}_{0.5}\text{Sr}_2\text{Y}_{0.5}\text{Ca}_{0.5}\text{Cu}_2\text{O}_{7-x}$, sintering is carried out at 1213 K for 15 h under an oxygen pressure of 100 bar followed by fast cooling to 373 K. The samples obtained from high-pressure oxygen treatment show higher T_c s than those processed at 1 bar pressure of oxygen. Substitution of Y by other rare earths has been possible by this high-oxygen-pressure method [131]. All the rare-earth substituted compounds are superconducting with T_c s in the 50–70 K range. The T_c decreases with increase in the size of the rare earth. In table 5 we summarize the conditions for the synthesis of the various lead cuprates by the ceramic method.

2.7 Electron-doped superconductors

All the cuprates discussed till now are hole superconductors. Synthesis of electron-doped cuprate superconductors of the type $\text{Ln}_{1-x}\text{M}_x\text{CuO}_{4-x}$ ($\text{Ln} = \text{Nd}, \text{Pr}, \text{Sm}, \text{Eu}$; $\text{M} = \text{Ce}, \text{Th}$), possessing the T' structure, is generally achieved by the ceramic method [132–134]. The conditions of synthesis are more stringent since the

Table 5. Conditions for the synthesis of lead cuprates by the ceramic method.

Compound	Starting materials	Conditions			Comments	T_c (K)	Ref.
		Temp. (K)	Time	Gas			
$\text{Pb}_2\text{Sr}_2\text{Ca}_{0.5}\text{Y}_{0.5}\text{Cu}_3\text{O}_{8-x}$	$\text{PbO} + \text{Sr}_2\text{Y}_{0.5}\text{Ca}_{0.5}\text{Cu}_3\text{O}_{8-x}$	1143	1–16 h	$\text{N}_2 + 1\% \text{O}_2$		78	[116]
	Cu_2O_3 matrix						
	$\text{PbO}, \text{PbO}_2, \text{CaO}_2$	1223	12–48 h		Sealed gold tubes	78	[118]
	$\text{SrO}_2, \text{Y}_2\text{O}_3, \text{CuO}$						
$\text{Pb}_2\text{Sr}_2\text{La}_{1.2}\text{Cu}_2\text{O}_{8+x}$	$\text{PbO}, \text{SrCO}_3, \text{Y}_2\text{O}_3$	1073	15 h	air			
	$\text{CaCO}_3, \text{CuO}$	1173	2 h	air			
		1073	1–5 h	N_2		78	[119]
		1063	6 h	N_2	2202 major phase + $\text{Pb}_2\text{LaCu}_{0.5}\text{O}_3$ impurity	28	[122]
$(\text{Pb}_{0.5}\text{Cu}_{0.5})\text{SrLaCuO}_4$	$\text{PbO}, \text{La}_2\text{O}_3$						
	$\text{Sr}_2\text{CuO}_3, \text{CuO}$						
	$\text{PbO}, \text{SrCO}_3, \text{La}_2\text{O}_3$	1073	5 h	air			
$(\text{Pb}_{0.5}\text{Cu}_{0.5})\text{Sr}_2$	CuO	1273	2 h	O_2		25	[123]
	$\text{PbO}, \text{SrCO}_3, \text{Y}_2\text{O}_3$	1123	10 h	air			
	$\text{CaCO}_3, \text{CuO}$	1273	1 h	O_2	1212 major phase + $\text{Sr}_2\text{PbCuO}_{1.5}$ impurity	50	[124]
$(\text{Pb}_{0.5}\text{Cu}_{0.5})\text{Sr}_2(\text{Y}_{0.5}\text{Ca}_{0.5})\text{Cu}_2\text{O}_{7-x}$							
	$\text{PbO} + \text{Sr}_2\text{Y}_{0.5}\text{Ca}_{0.5}\text{Cu}_2\text{O}_{7-x}$	1243	3 h	O_2	1212 major phase + $\text{Sr}_2\text{PbCuO}_{1.5}$ impurity	47	[127]
	$\text{Cu}_{2+2x}\text{O}_3$ matrix						
$(\text{Pb}_{0.5}\text{Sr}_{0.5})\text{Sr}_2$	$\text{PbO}, \text{PbO}_2, \text{Sr}_2\text{CuO}_3$	1108–1223	1–10 h		Evacuated silica tubes	100	[125]
	$\text{Y}_2\text{O}_3, \text{CaO}_2, \text{Cu}_2\text{O}, \text{CuO}$						
$(\text{Pb}_{0.5}\text{Ca}_{0.5})\text{Sr}_2$	$\text{PbO}_2, \text{PbO}, \text{SrO}_2$	1108–1223	1–10 h		Evacuated silica tubes	80	[126]
	$\text{SrCuO}_2, \text{Y}_2\text{O}_3, \text{CaO}, \text{CuO}$						
$(\text{Pb}_{0.5}\text{Cu}_{0.5})\text{Sr}_2(\text{Sr}_{1.75}\text{Eu}_{0.25})$	$\text{PbO}, \text{SrCO}_3, \text{Eu}_2\text{O}_3$	1123	10 h	air	Single phase	25	[129]
	CeO_2, CuO	1323	1 h	O_2	1222		

material, by making sure that extra electron donated by Ce^{4+} or Th^{4+} does not increase the oxygen content of the cuprate. For this reason, samples after calcination and sintering at 1323 K in air (for 24 h) are annealed in a reducing atmosphere (typically Ar, N_2 or dilute H_2) at 1173 K to achieve superconductivity. Samples prepared in this manner show a negative temperature coefficient of resistance above T_c in the R - T curves; the resistivity drop at T_c is also not sharp. An alternative synthetic route involves the reaction of pre-reacted $NdCeO_{3.5}$ material with the required amounts of Nd_2O_3 and CuO at 1253 K for a minimum period of 48 h in flowing oxygen [135]. The samples are then rapidly quenched from 1253 K in an argon atmosphere to achieve superconductivity. This procedure eliminates the slow diffusion of Ce throughout the Nd_2CuO_{4-x} host and gives uniform concentrations of cerium and oxygen. Samples obtained from this route show a sharp transition at 21 K.

Superconductivity with a T_c of 25 K is induced by doping fluorine for oxygen in Nd_2CuO_4 . This has been accomplished by taking NdF_3 as one of the initial reactants [136]. Substitution of either Ga or In for copper in non-superconducting $Nd_{2-x}Ce_xCuO_{4-x}$ also induces superconductivity [137, 138].

2.8. Infinite-layer cuprates

Discovery of superconductivity in cuprates containing infinite CuO_2 layers has been of great importance in understanding the phenomenon. Very high pressures have been employed for obtaining the infinite-layer cuprates. Both hole-doped (e.g. $Ca_{1-x}Sr_xCuO_2$) and electron-doped ($Sr_{1-x}Nd_xCuO_2$) infinite-layer cuprate superconductors with a maximum T_c of 110 K have been reported [139-142]. Infinite-layered cuprates of the type $(Ba, Sr)CuO_2$, $(Ca, Sr)CuO_2$ are synthesized in an oxidizing atmosphere under high hydrostatic pressure [139, 140, 142]. Electron-doped $Sr_{0.88}Nd_{0.14}CuO_2$ is also prepared under high hydrostatic pressures [141]. Metal nitrates are generally used as the starting materials since carbonates of Ba, Sr and Ca have high decomposition temperatures. After decomposing the metal nitrates at around 873-1123 K in air, the product is subjected to high pressure to obtain the superconducting phases $Sr_{0.88}Nd_{0.14}CuO_2$, which superconducts at 40 K, is made under a hydrostatic pressure of 25 kbar at 1273 K. Superconducting $(Ca, Sr)CuO_2$ is prepared at 1273 K under 6 GPa pressure. Deficiency of Sr and Ca as well as the oxidizing atmosphere make this phase superconducting, and the oxidizing atmosphere is provided by heating a capsule containing $KClO_4$ along with the sample. This cuprate has a T_c (onset) of 110 K.

3. Coprecipitation and precursor methods

Coprecipitation involves the separation of a solid containing various ionic species chemically bound to one

another. Coprecipitation can result in the formation of crystalline or amorphous solids. Coprecipitation of well defined stoichiometry with respect to the metal ions is obtained only when the following conditions are satisfied.

(i) The precipitating agent is a multivalent organic compound which can coordinate with more than one metal ion, and the precipitation rate is fast.

(ii) The solid precipitating out of the solution should be really insoluble in the mother liquor.

The anions generally preferred for coprecipitation of oxidic materials are carbonates, oxalates, citrates etc. The same is true of high- T_c cuprates. The precipitates in some instances could be genuine precursors or solid solutions [5, 6]. It is well known that precursor solid solutions drastically bring down diffusion distances for the cations and facilitate reactions in the solid state. We shall not distinguish precursor solid solutions precipitated from solutions from other precursors in this discussion.

The precipitates (carbonate, oxalate etc) are heated at appropriate temperatures in a suitable atmosphere to obtain the desired cuprate. Some of the advantages of the coprecipitation technique over the ceramic method are an homogeneous distribution of components, a decrease in the reaction temperatures and of the duration of annealing, a higher density and a lower particle size of the final product. The major drawback of this route is the control over the stoichiometry of the final product.

3.1. $La_{2-x}Sr_xCuO_4$

La, Sr and Cu in $La_{2-x}Sr_xCuO_4$ are readily coprecipitated as carbonates [11, 12, 143]. For this purpose the required quantities of the various metal nitrates are dissolved together in distilled water. Alternatively, the corresponding oxides are dissolved in nitric acid to give a nitrate solution and the pH of the solution is adjusted to 7-8 by the addition of KOH solution. A solution of K_2CO_3 of appropriate strength is then slowly added under stirring to give a light blue precipitate which is thoroughly washed. The precipitate is dried at 420 K and calcined at 1070 K for 8 h in air. The resulting black powder is ground and pelletized and sintered at 1270 K for 16 h in air to obtain monophasic $La_{1.85}Sr_{0.15}CuO_4$, superconducting at 35 K.

Instead of as carbonate, the metal ions are also readily precipitated as oxalate by the addition of either oxalic acid or potassium oxalate to the solution of metal nitrates [11, 12, 144, 145]. The precipitated oxalate is then decomposed to obtain the cuprate. This method has certain disadvantages:

(i) La^{3+} in the presence of an alkali metal oxalate first yields lanthanum oxalate which further reacts with the precipitating agent to give a double salt. Control of stoichiometry therefore becomes difficult, leading to multiphasic products.

(ii) The relative solubilities of some of the oxalates also pose difficulties. For example, SrC_2O_4 is nearly four times more soluble than SrCO_3 .

3.2. $\text{YBa}_2\text{Cu}_3\text{O}_7$

$\text{YBa}_2\text{Cu}_3\text{O}_7$ and related 123 compounds can be obtained via coprecipitation of the component metals (from a nitrate solution) as a formate [146, 147], acetate [148], oxalate [12, 149–156], hyponitrite [157] or hydroxycarbonate [158, 159]. Some of these precipitates could be genuine precursor compounds as is indeed the case with the hyponitrite.

In oxalate coprecipitation [12, 149–152], oxalic acid solution of appropriate concentration is added to an aqueous solution of mixture of nitrates of Y, Ba and Cu and the pH of the solution is adjusted to 7.5 (by dilute NH_3). The pale green slurry thus formed is digested for 1 h, filtered and dried. The oxalate is converted to orthorhombic $\text{YBa}_2\text{Cu}_3\text{O}_{7-x}$ by heating at 1053 K in air for 5 days followed by oxygenation at 723 K. This procedure, even though successful in making superconducting $\text{YBa}_2\text{Cu}_3\text{O}_{7-x}$ in small particulate form, often results in undesirable stoichiometry because of the moderate solubility of barium oxalate. Furthermore, rare-earth ions in the presence of ammonium oxalate give a double salt with the excess oxalate which competes with the precipitation of copper and barium oxalates. These difficulties can be overcome either by taking a known excess (wt%) of barium and copper or by using triethylammonium oxalate as the precipitant in aqueous ethanol medium [153–155]. The alcoholic medium decreases the solubility of barium oxalate and the pH of the solution is controlled *in situ*.

A better method of homogeneous coprecipitation of oxalates is that of Liu *et al* [156] using urea and oxalic acid. Urea, on heating, is hydrolysed liberating CO_2 and NH_3 , and thus gradually adjusting the pH throughout the solution. The CO_2 liberated controls the bumping of the solution during digestion. The oxalate coprecipitation route is widely described in the literature. The reactive powders obtained by the oxalate coprecipitation method decrease the sintering temperature. The formation of BaCO_3 in the intermediate calcinating step makes it difficult to obtain $\text{YBa}_2\text{Cu}_3\text{O}_{7-x}$ in pure form.

Complete avoidance of the formation of BaCO_3 during the synthesis is possible using the hyponitrite precursor [157]. The hyponitrite precursor is obtained from a nitrate solution of Y, Ba and Cu ions by the addition of an aqueous $\text{Na}_2\text{N}_2\text{O}_2$ solution. The precipitate is converted into superconducting $\text{YBa}_2\text{Cu}_3\text{O}_{7-x}$ by heating at around 973 K in an argon atmosphere, followed by oxygen annealing at 673 K. Although this route provides a convenient means of obtaining the 123 cuprate at much lower temperatures than with other methods, there is a possibility of contamination of alkali metal ions during the course of the precipitation.

$\text{YBa}_2\text{Cu}_3\text{O}_7$ can also be prepared by the hydroxycarbonate method [158, 159]. Here, KOH and K_2CO_3

are employed to precipitate copper as the hydroxide and Y and Ba as the carbonates in the pH range of 7–8. By employing NaOH and Na_2CO_3 , complete precipitation as hydroxycarbonate is attained at a pH of ~ 13 . The product from the above two procedures is homogeneous, showing sharp onset of superconductivity at 92 K. The possibility of contamination by alkali metal ions cannot, however, be avoided.

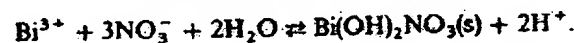
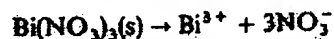
3.3. $\text{YBa}_2\text{Cu}_4\text{O}_8$

$\text{YBa}_2\text{Cu}_4\text{O}_8$ can be prepared by the oxalate route [160] wherein the solution of Y, Ba and Cu nitrates in water is added dropwise into oxalic acid–triethylamine solution under stirring. Complete precipitation of Y, Ba and Cu with the desired stoichiometry of 1:2:4 is achieved in the pH range of 9.3–11.3. The precipitated oxalates are filtered and dried in air at 393 K. The solid obtained is then heated in the form of pellets at 1078 K in flowing oxygen for 2–4 days. The product after quenching in air shows the 124 phase as the major product with a T_c of 79 K.

An alternative coprecipitation route for the synthesis of $\text{YBa}_2\text{Cu}_4\text{O}_8$ is the method of Chen *et al* [161] in which the aqueous nitrate solution of the constituent metal ions is mixed with 8-hydroxyquinoline–triethylamine solution. The precipitated oxine is filtered, washed, dried and sintered at 1088 K in oxygen for 3 days to yield phase-pure $\text{YBa}_2\text{Cu}_4\text{O}_8$ showing a T_c of 80 K. Ethylenediaminetetraacetic acid [161] as well as carbonate routes [162] have also been employed for the preparation of $\text{YBa}_2\text{Cu}_4\text{O}_8$. Coprecipitation using triethylammonium oxalate has been exploited for substituting Sr in place of Ba in $\text{YBa}_2\text{Cu}_4\text{O}_8$ [163].

3.4. Bismuth cuprates

Very few coprecipitation studies have been carried out on the preparation of bismuth cuprates. One reason may be that despite the good sample homogeneity generally obtained through solution methods, the chemistry of bismuth cuprates is rather complex. It is not that easy to find compounds of all the constituent metal ions soluble in a common solvent; controlling the stoichiometry in these cuprates is also difficult in the coprecipitation procedure. Furthermore, bismuth nitrate, which is often used as one of the starting materials, decomposes in cold water to a basic nitrate precipitate as given by



This problem can be overcome to some extent by preparing the nitrate solution of bismuth in nitric acid or by starting with bismuth acetate instead of the nitrate.

Bidentate ligands such as the oxalate are found to react more rapidly than multidentate ligands such as citric acid [164–174] in the coprecipitation process. Complexes of oxalic acid are also more stable than

the stoichiometry because of the relative solubility of BiC_2O_4 or SrC_2O_4 .

A straightforward oxalate coprecipitation is achieved by dissolving the acetates of Bi, Ca, Sr and Cu in glacial acetic acid and then adding excess oxalic acid to the solution [164]. The oxalate precipitate is dried and decomposed at around 1073 K in air and processed in the 1103–1123 K range for periods ranging from 24 h to 4 days, depending on the starting composition. The $n = 2$ (2122) member obtained by this procedure shows zero resistance at 83 K. In another procedure reported by Zhang *et al* [165], first the Sr/Ca/Cu nitrate solutions are mixed in the required molar ratio. Into this solution is poured a solution of bismuth nitrate prepared in nitric acid along with oxalic acid. The complete precipitation occurs at a pH of around 5 (attained by the addition of aqueous NaOH). This process involves the possibility of contamination of sodium ions; this has been circumvented by using $\text{N}(\text{CH}_3)_4\text{OH}$ to adjust the pH of the solution [166] and complete precipitation of the oxalates occurs at a pH of 12. All these procedures, however, produce mixed-phase samples.

For the preparation of the monophasic lead-doped $n = 3$ member (2223), oxalate coprecipitation has been found effective [167–174]. In the procedure reported by Chiang *et al* [171], the molar ratio of the chelating agent (oxalic acid) and the nitrate anions (from the metal nitrate solutions) is fixed at 0.5 and the pH, adjusted by NH_4OH solution, at which complete precipitation occurs is 6.7. The product from this method, $\text{Bi}_{1.4}\text{Pb}_{0.6}\text{Sr}_2\text{Ca}_2\text{Cu}_3\text{O}_y$, after sintering at 1133 K in air for 72 h, shows a T_c of 110 K.

Coprecipitation as oxalates to prepare the lead-doped $n = 3$ member (2223) has been achieved from an ethylene glycol medium using triethylammonium oxalate and oxalic acid [172]. A more easily controlled and reproducible oxalate coprecipitation procedure appears to be that of Shei *et al* [173] where in a mixture of triethylamine and oxalic acid is employed. The advantage of using triethylamine is that it has a higher basicity and a lower complexing ability towards Cu(II) than has ammonia. Control of the stoichiometry of the final product is therefore better obtained with this procedure; precipitation occurs in the pH range 1.5–2.2. The coprecipitated oxalates sintered at 1133 K in air for a minimum period of 72 h give monophasic $\text{Bi}_{1.4}\text{Pb}_{0.6}\text{Sr}_2\text{Ca}_2\text{Cu}_3\text{O}_{10}$ with a T_c of 110 K. It is possible to avoid adjusting the pH in the coprecipitation of oxalates [174]. The procedure involves coprecipitating the oxalates from dilute acetate solutions instead of from nitrate solutions. The oxalates are then converted to nearly phase-pure $\text{Bi}_{1.4}\text{Pb}_{0.6}\text{Sr}_2\text{Ca}_2\text{Cu}_3\text{O}_{10}$ (T_c of 106 K) by sintering at 1123 K in air for 160 h.

Carbonate coprecipitation has also been carried out for the synthesis of superconducting bismuth cuprates [175, 176], but the method does not yield monophasic products.

Coprecipitation of $n = 3$ member cuprates from aqueous solutions as oxalates is hindered by the solubility of thallium oxalate. However, Bernhard and Gritzner [177] have found that complete coprecipitation as oxalates can be achieved by starting with thallium acetate in glacial acetic acid medium. In the procedure reported for the preparation of the $n = 3$ member (2223), stoichiometric amounts of thallium acetate, CaCO_3 , BaCO_3 and copper acetate are dissolved in water containing glacial acetic acid. The solution containing all the cations is then added to a solution of oxalic acid (excess) under stirring. The precipitate, after digestion for 1 h, is filtered, washed and dried. The oxalates are heated in the form of pellets (wrapped in gold foil) at around 1173 K for 6 min in an oxygen atmosphere. The product after annealing in the same atmosphere shows 2223 as the major phase with a T_c of 118 K.

3.6. Lead cuprates

Carbonate coprecipitation is found to be satisfactory for the synthesis of representative members of superconducting lead cuprates [128] of 2213 and 1212 types, namely $\text{Pb}_2\text{Sr}_2\text{Y}_{0.5}\text{Ca}_{0.5}\text{Cu}_3\text{O}_{8.5}$ and $\text{Pb}_{0.5}\text{Sr}_{0.5}\text{Sr}_2\text{Y}_{0.5}\text{Ca}_{0.5}\text{Cu}_2\text{O}_{7.5}$. Coprecipitation as carbonates has been achieved by adding the nitrate solution of the constituent metal ions to an aqueous solution of sodium carbonate (in excess) under constant stirring. The carbonate precipitate thus obtained is washed and dried. The decomposed powder is heated in the form of pellets around 1153 K in a suitable atmosphere. $\text{Pb}_2\text{Sr}_2\text{Ca}_{0.5}\text{Y}_{0.5}\text{Cu}_3\text{O}_{8.5}$ obtained by this method after heating for 4 h in nitrogen containing 1% O_2 showed 2213 as the major phase ($T_c \sim 74$ K) with impurities such as Y_2O_3 , CuO . The 1212 phase obtained after heating in oxygen at 1153 K for 12 h showed a broad transition with a T_c (onset) of 100 K. This method has the advantage of single heating rather than the multistep procedures required in the other methods.

4. Sol-gel process

The sol-gel process is employed in order to get homogeneous mixing of cations on an atomic scale so that the solid state reaction occurs to completion in a short time and at the lowest possible temperature. The term sol often refers to a suspension or dispersion of discrete colloidal particles, while a gel represents a colloidal or polymeric solid containing a fluid component which has the internal network structure wherein both the solid and the fluid components are highly dispersed. In the sol-gel process a concentrated sol of the reactant oxides or hydroxides is converted to a semi-rigid gel by removing the solvent. The dry gel is heated at an appropriate

temperature to obtain the product. Most of the reactions in the sol-gel process occur via hydrolysis and polycondensation.

Two different routes for the sol-gel process are usually described in the literature for the synthesis of high- T_c cuprate superconductors:

- (i) Via molecular precursors (e.g. metal alkoxides) in organic medium;
- (ii) Via ionic precursors in aqueous medium (citrate gel process).

The purity, microstructure and physical properties of the product are controlled by varying the precursor, solvent, pH, firing temperatures and atmosphere of heat treatment.

4.1. 214 Cuprates

Superconducting 214 compounds are prepared both by means of organometallic precursor [178] and by the citrate gel process [11]. Lanthanum 2,4-pentanedionate, barium 2,4-pentanedionate and copper (II) ethyl hexanoate are mixed at room temperature in the appropriate ratios in methoxyethanol medium to obtain the organometallic precursor. After vigorous stirring at room temperature, the precursor gel is converted to monophasic $\text{La}_{1-x}\text{Ba}_x\text{CuO}_4$ (T_c 23 K) by firing at 873 K in oxygen.

In the citrate gel process, a mixture of citric acid and ethylene glycol is added to the solution containing the required quantities of metal nitrates. The resulting solution is vigorously stirred and heated around 393 K. During this process, oxides of nitrogen evolve, resulting in a viscous gel. The gel is decomposed at 673 K in air and the resulting black powder is then given the necessary heat treatment to obtain the superconducting oxide.

4.2. $\text{YBa}_2\text{Cu}_3\text{O}_7$

In the case of $\text{YBa}_2\text{Cu}_3\text{O}_{7-x}$, the alkoxide precursors are both very expensive and difficult to obtain. In addition, the solubility of copper alkoxides is very low in organic solvents and yttrium alkoxides are readily hydrolysed even by a trace of water. Despite these difficulties, superconducting $\text{YBa}_2\text{Cu}_3\text{O}_{7-x}$ has been prepared using alkoxides [157, 179–181]. A simple reaction involving $\text{Y}(\text{OCHMe}_2)_3$, $\text{Ba}(\text{OCHMe}_2)_2$ and $\text{Cu}(\text{NBu}_2)_2$ in THF in an argon atmosphere gives the organometallic precursor [157]. The precursor powder, after removal of the solvent, is sintered at 973 K in flowing argon to obtain tetragonal $\text{YBa}_2\text{Cu}_3\text{O}_{7-x}$. Following oxygenation at 673 K, the product shows a T_c of 85 K. Superconducting properties have been improved by using *n*-butoxides of Y, Ba and Cu in butanol solvent [179].

Alternatively, methoxyethoxides of yttrium, barium and copper have been used as precursors in methoxyethanol-methylethylketone-toluene solvent mixture to prepare $\text{YBa}_2\text{Cu}_3\text{O}_{7-x}$ [180]. In some of the preparations, $\text{Cu}(\text{NO}_3)_2$ (soluble in ethanol) or copper

acetylacetonate (soluble in toluene) is used along with the alkoxides of yttrium and barium to overcome the problem of low solubility of copper alkoxides [182, 183]. Organometallic precursors involving propionates [153] and neodeconates [184] have also been used for preparing $\text{YBa}_2\text{Cu}_3\text{O}_{7-x}$.

Modified sol-gel methods which do not involve the metal alkoxide precursors have been employed by many workers. Thus, Nagano and Greenblatt [185] have employed metal nitrates dissolved in ethylene glycol. After refluxing around 353 K under vigorous stirring, a bluish green colloidal gel is obtained. The gel is converted into orthorhombic $\text{YBa}_2\text{Cu}_3\text{O}_{7-x}$ by heating to 1223 K in flowing oxygen. Precipitating all the three ions as hydroxides also results in fine colloidal particles of the starting materials [186–188]. The precipitation is generally carried out by the addition of NH_4OH [186], $\text{N}(\text{CH}_3)_4\text{OH}$ [187] or $\text{Ba}(\text{OH})_2$ [188] to a solution of metal nitrates (pH range 7–8). These hydroxides are decomposed around 1223 K in oxygen to give $\text{YBa}_2\text{Cu}_3\text{O}_7$ showing a T_c of 93 K.

$\text{YBa}_2\text{Cu}_3\text{O}_{7-x}$ has been prepared by the citrate gel process [189–193]. In this method 1 g equivalent of citric acid is added to each gram equivalent of the metal. The pH of the solution is adjusted to around 6 (either by NH_4OH or by ethylenediamine). Evaporation of the solvent (water) around 353 K, results in a viscous dark blue gel. The gel is decomposed and the powder sintered in the form of pellets at 1173 K in oxygen to obtain orthorhombic $\text{YBa}_2\text{Cu}_3\text{O}_{7-x}$ ($T_c = 93$ K). By this method, ultrafine homogeneous powders (particle size $\sim 0.3 \mu\text{m}$) are obtained. The crucial step in this process is the adjustment of the pH which controls the stoichiometry of the final product. This limitation has been overcome by dispersing the citrate metal ion complexes in a solvent mixture of ethylene glycol and water [194, 195].

Problems such as the formation of BaCO_3 during the calcination step, filtration and contamination of alkali metal ions in the final product are avoided in the sol-gel process. Furthermore, perfect homogeneity is obtained before calcination. The sol-gel process (e.g. citrate process) has the advantage over the other methods in that the gel can be used for making thick and thin superconducting films, fibres etc which have technological importance [179, 185, 186, 196–198].

4.3. $\text{YBa}_2\text{Cu}_4\text{O}_8$

The sol-gel method offers a good alternative to the ceramic method for the synthesis of superconducting $\text{YBa}_2\text{Cu}_4\text{O}_8$. The following procedure has been used to prepare $\text{YBa}_2\text{Cu}_4\text{O}_8$ at 1 atm oxygen pressure [199]. Appropriate quantities of $\text{Y}(\text{n-OC}_4\text{H}_9)_3$, $\text{Ba}(\text{s-OC}_4\text{H}_9)_2$ and $\text{Cu}(\text{s-OBu})_2$ in butanol-xylene mixture are refluxed in an argon atmosphere at 343 K for a period of 30 h. The fine powder after the vigorous reaction is freed from the solvent and dried. The powder is heated in the form of pellets at 1033 K in flowing oxygen to obtain superconducting $\text{YBa}_2\text{Cu}_4\text{O}_8$.

used as the source of copper in this process [200].

In the modified citrate gel process to prepare $\text{YBa}_2\text{Cu}_3\text{O}_x$ [201, 202], 1 g equivalent of citric acid is added for each gram equivalent of the metal and the pH of the solution is adjusted to ~ 5.5 by the addition of ethylenediamine. The resulting clear solution is evaporated to yield a viscous purple gel. The decomposed gel is sintered in flowing oxygen for 3–5 days at 1088 K to obtain nearly monophasic $\text{YBa}_2\text{Cu}_3\text{O}_x$ ($T_c = 66$ K). Kakihana *et al* [203] have reported the preparation of $\text{YBa}_2\text{Cu}_3\text{O}_x$ using a precursor obtained from citrate metal ion complexes uniformly dispersed in a solvent mixture of ethylene glycol and water. This method yields phase-pure $\text{YBa}_2\text{Cu}_3\text{O}_x$ ($T_c \sim 79$ K) and eliminates the need to adjust the pH.

4.4. Bismuth cuprates

There have been very few reports of the preparation of bismuth-based cuprate superconductors by the alkoxy sol-gel method [204]. Some of the difficulties arise because the relevant bismuth/lead alkoxides are not readily available; it is also not easy to get a common organic solvent to dissolve the various metal alkoxides simultaneously. Dhalle *et al* [204] have, however, attempted to synthesize the lead-doped $n = 3$ member (2223) using organometallic precursors involving propionates. The starting materials were taken in the form of nitrates and converted into propionates by the addition of an excess of 100% propyl alcohol. This step was followed by the addition of ammonium hydroxide and ethylene glycol to increase the alkoxy anion concentration, thus in turn increasing the viscosity of the solution. All the solutions were mixed together and dried at 353 K. The resin after calcination at 1123 K in air and sintering at 1118 K gave a mixture of the $n = 3$ and $n = 2$ members.

A simple sol-gel method involving the addition of dilute ammonia to an aqueous solution containing nitrates of Bi, Sr and acetates of Ca, Cu and Pb (until the pH of the solution reached around 5.5) has also been employed to prepare bismuth cuprates [205, 206]. The blue solution after concentrating at around 343 K gives a viscous gel. The gel is decomposed and the powder sintered at around 1128 K in air. The product from this procedure is multiphasic showing a T_c of 104 K. The simplicity of the method and the formation of the $n = 3$ phase in a short time makes it somewhat superior to the conventional ceramic route. The modified citrate gel process has been employed to prepare the $n = 2$ member (2212) in pure form with a T_c of 78 K [193].

4.5. Lead cuprates

The modified citrate gel process has been successfully employed by Mahesh *et al* [207] for the synthesis of lead cuprates of the 2213 or 1212 type. In a typical procedure, a mixture of citric acid and ethylene glycol in

is concentrated at 373 K to get a viscous gel. The gel after decomposition is heated in the form of pellets in the temperature range of 1073–1173 K either in N_2 containing 1% O_2 or in an oxygen atmosphere. $\text{Pb}_2\text{Sr}_2\text{Y}_{0.5}\text{Ca}_{0.5}\text{Cu}_3\text{O}_{8+x}$ obtained from this process shows a sharp superconducting transition at 70 K. The 1212 cuprate also shows a sharp transition at 60 K. This process is superior to the ceramic procedure for synthesizing superconducting lead cuprates.

5. Alkali flux method

Strong alkaline media, either in the form of solid carbonate fluxes, molten hydroxides or highly concentrated alkali solutions can be employed for the synthesis of high- T_c cuprate superconductors. The alkali flux method takes advantage of both the moderate temperatures of the molten media (453–673 K) as well as of the acid-base characteristics of molten hydroxides to simultaneously precipitate oxides or oxide precursors such as hydroxides or peroxides of the constituent metals. The method stabilizes higher oxidation states of the metal by providing an oxidizing atmosphere.

Employing fused alkali hydroxides, Ham *et al* [208] have synthesized superconducting $\text{La}_{2-x}\text{M}_x\text{CuO}_4$ ($\text{M} = \text{K}$ or Na or vacancy) at relatively low temperatures (470–570 K). In this method, stoichiometric quantities of La_2O_3 and CuO are added to a molten mixture containing KOH and NaOH (in an approximately 1:1 ratio) in a Teflon crucible and heated at around 570 K in air for 100 h. The 1:1 mixture of KOH and NaOH melts at 440 K and since the alkali hydroxides generally contain some water, the melt is acidic and can readily dissolve oxides such as La_2O_3 and CuO . The black crystals obtained from the reaction (after washing away the excess hydroxide with water) show a T_c of 35 K. Since the reaction is carried out in alkali hydroxides, incorporation of Na^+ or K^+ ions for La^{3+} in the lattice of La_2CuO_4 cannot be ruled out. It should be noted that superconducting alkali-doped La_2CuO_4 is normally prepared at higher temperatures in sealed gold tubes [209]. Recently, alkaline hypobromite oxidation has been employed to obtain $\text{La}_2\text{CuO}_{4+x}$ with a T_c of 44 K [210].

Superconducting $\text{YBa}_2\text{Cu}_3\text{O}_x$ ($T_c \sim 88$ K) has also been prepared using the fused eutectic of sodium and potassium hydroxides in a similar manner to that described above [211]. The problem of contamination of alkali metals in the preparation of $\text{YBa}_2\text{Cu}_3\text{O}_x$ has been overcome by using the $\text{Ba}(\text{OH})_2$ flux [211]. The procedure involves heating a mixture containing stoichiometric amounts of $\text{Y}(\text{NO}_3)_3 \cdot 6\text{H}_2\text{O}$, $\text{Ba}(\text{OH})_2$ and $\text{Cu}(\text{NO}_3)_2 \cdot 3\text{H}_2\text{O}$ in an open ceramic crucible at around 1023 K in air for a short time (about 10 min) and then slowly cooling the melt to room temperature. Since $\text{Ba}(\text{OH})_2$ has two hydration states, one melting at 351 K and the other at 681 K, the lower-melting hydrate acts as the solvent for the nitrates of copper

and yttrium while the high-melting hydrate serves as the medium for intimate mixing of the reactants. The precipitate obtained from the melt, after washing with water, is sintered in air at around 1173 K followed by oxygenation at 773 K. This method yields an orthorhombic $\text{YBa}_2\text{Cu}_3\text{O}_7$ phase (with little CuO impurity) showing a T_c of 92 K.

The flux method eliminates the need for mechanical grinding and introduction of carbon-containing anions, which is often encountered in the solution routes. Furthermore, the method is efficient and cost-effective.

6. Combustion method

Although many of the solution routes discussed earlier yield homogeneous products, the processes involved are quite complex. Combustion synthesis or self-propagating high-temperature synthesis (SHS), first developed by Merzhanov and Borovinskaya [212], provides a simple and rapid means of preparing inorganic materials, many of which are technologically important. Combustion synthesis is based on the principle that the heat energy liberated by many exothermic non-catalytic solid-solid or solid-gas reactions can self-propagate throughout the sample at a certain rate. This process can therefore occur in a narrow zone which separates the starting substances and reaction products.

Self-propagating combustion has been employed recently in this laboratory to synthesize members of almost all families of cuprate superconductors (except for the thallium cuprates) [213]. The method involves the addition of an appropriate fuel to a solution containing the metal nitrates in the proper stoichiometry. The ratio of the metal nitrates to the fuel is such that when the solution is dried at around 423 K, the solid residue undergoes flash combustion, giving an ash containing the mixture of oxides in the form of very fine particles (particle size 0.3–0.5 μm). The ash is then given proper heat treatment under the desired atmosphere to obtain the cuprate. The small particle size of the ash facilitates the reaction between the metal oxides due to smaller diffusion distances between the cations. Fuels such as urea [213, 214], glycine [213, 215] and tetraformal triazine (TFTA) [216] are generally employed for synthesizing cuprate superconductors. Ultrafine particles of copper metal can also act as an internal fuel wherein the combustion is initiated by flashing a laser beam for a short time [217]. Some of the cuprate superconductors which have been prepared [213] by this route include $\text{La}_{2-x}\text{Sr}_x\text{CuO}_4$ ($T_c = 35$ K), $\text{YBa}_2\text{Cu}_3\text{O}_7$ ($T_c = 90$ K), $\text{YBa}_2\text{Cu}_4\text{O}_8$ ($T_c = 80$ K), $\text{Bi}_2\text{CaSr}_2\text{Cu}_2\text{O}_8$ ($T_c = 85$ K), $\text{Pb}_2\text{Sr}_2\text{Y}_{0.5}\text{Ca}_{0.5}\text{Cu}_3\text{O}_8$ ($T_c = 60$ K) and $\text{Nd}_{2-x}\text{Ce}_x\text{CuO}_4$ ($T_c \sim 30$ K).

7. Other methods

In addition to the various synthetic methods discussed hitherto, a few other methods such as spray drying [218–221], freeze drying [186, 222, 223], use of metallic precursors [224, 225] and electrochemical methods

[226, 227] have also been employed for the preparation of cuprate superconductors in bulk form. In spray drying, a solution containing the metallic constituents, usually in the form of nitrates, is sprayed in the form of fine droplets into a hot chamber. The solvent evaporates instantaneously, leaving behind an intimate mixture of the reactants which on heating at the desired temperature in a suitable atmosphere yields the cuprate. Some of the superconducting cuprates prepared by this method include $\text{YBa}_2\text{Cu}_3\text{O}_7$ ($T_c = 91$ K) [218], $\text{YBa}_2\text{Cu}_4\text{O}_8$ ($T_c = 81$ K) [219] and $\text{Bi}_{1.6}\text{Pb}_{0.4}\text{Sr}_2\text{Ca}_2\text{Cu}_3\text{O}_{10}$ ($T_c = 101$ K) [220, 221]. In freeze drying, the reactants (in a common solvent) are frozen by immersing in liquid nitrogen. The solvent is removed at low pressures to obtain the initial reactants in fine powder form, and these are then processed at an appropriate temperature. For example, $\text{YBa}_2\text{Cu}_3\text{O}_7$ ($T_c = 87$ K) [186], $\text{YBa}_2\text{Cu}_4\text{O}_8$ ($T_c = 79$ K) [222] and $\text{Bi}_{1.6}\text{Pb}_{0.4}\text{Sr}_{1.6}\text{Ca}_2\text{Cu}_3\text{O}_7$ ($T_c = 101$ K) [223] have been prepared by this method.

Metallic precursors have been used in the preparation of 123 and 247 cuprates [224, 225]. For example, oxidizing an Er–Ba–Cu alloy around 1170 K gives superconducting $\text{ErBa}_2\text{Cu}_3\text{O}_7$ with a T_c of 87 K [224]. Similarly $\text{Yb}_2\text{Ba}_4\text{Cu}_8\text{O}_{15}$ has been obtained by heating an alloy composition of YbBa_2Cu_3 (with 33 wt% of silver) under 1 atm oxygen at 1173 K [225].

Making use of electrochemical oxidation, $\text{La}_2\text{CuO}_{4+x}$ with a T_c of 44 K has been prepared at room temperature, which is otherwise possible only by use of high oxygen pressures [226, 227].

8. Oxygen non-stoichiometry

Oxygen stoichiometry plays a crucial role in determining the superconducting properties of many of the cuprates. Thus, stoichiometric La_2CuO_4 is an insulator, while an oxygen-excess material prepared under high oxygen pressures shows superconductivity with a T_c of 35 K [15]. The same holds for the next member of the homologous family, $\text{La}_{2-x}\text{Sr}_x\text{CaCu}_2\text{O}_6$ which is superconducting only when there is an oxygen excess [17]. The excess oxygen donates holes in these two systems. In the case of $\text{YBa}_2\text{Cu}_3\text{O}_{7-x}$, oxygen can be easily removed giving rise to tetragonal non-superconducting $\text{YBa}_2\text{Cu}_3\text{O}_6$. The $\text{YBa}_2\text{Cu}_3\text{O}_6$ material can be prepared by heating $\text{YBa}_2\text{Cu}_3\text{O}_7$ in an argon atmosphere at 973 K for extended periods of time [228]. The variation of T_c with oxygen stoichiometry, δ , is well known [229, 230]. When δ reaches 0.5, there is an intergrowth of $\text{YBa}_2\text{Cu}_3\text{O}_6$ and $\text{YBa}_2\text{Cu}_3\text{O}_7$, and at this composition, the material shows a T_c of 45 K. The $\delta = 0.5$ composition is obtained by quenching $\delta \approx 0$ material, heated in a nitrogen atmosphere at 743 K [231]. Similarly, by quenching $\text{YBa}_2\text{Cu}_3\text{O}_7$ at 783 K in air, $\text{YBa}_2\text{Cu}_3\text{O}_{6.7}$ (showing a T_c of ~ 60 K) is prepared [231]. The T_c of 90 K is found only when $\delta \leq 0.2$. $\text{YBa}_2\text{Cu}_3\text{O}_6$ is readily oxidized back to $\text{YBa}_2\text{Cu}_3\text{O}_7$. It may be noted that this oxidation–reduction process in

Cuprate	T_c (approx.)	Methods of synthesis*
$\text{La}_{2-x}\text{Sr}_x(\text{Ba})\text{CuO}_4$	35	Ceramic*, sol-gel, combustion, coprecipitation
$\text{La}_2\text{Ca}_{1-x}\text{Sr}_x\text{Cu}_2\text{O}_8$	60	Ceramic (high O_2 pressure)*
$\text{La}_2\text{CuO}_{4+\delta}$	40	Ceramic (high O_2 pressure)* alkali-flux, hypobromite*
$\text{YBa}_2\text{Cu}_3\text{O}_{7-\delta}$	90	Ceramic (annealing in O_2)*, sol-gel*, coprecipitation*, combustion
$\text{YBa}_2\text{Cu}_4\text{O}_8$	80	Ceramic (high O_2 pressure), ceramic (with Na_2O_2)* sol-gel*, coprecipitation*
$\text{Bi}_2\text{CaSr}_2\text{Cu}_2\text{O}_8$	90	Ceramic (air-quench)* sol-gel*, combustion, melt (glass) route*
$\text{Bi}_2\text{Ca}_2\text{Sr}_2\text{Cu}_2\text{O}_{10}$	110	Ceramic*, sol-gel, melt route
$\text{TiCaBa}_2\text{Cu}_2\text{O}_{8+\delta}$	90	Ceramic (sealed Ag/Au tube)*
$\text{TiCa}_2\text{Ba}_2\text{Cu}_2\text{O}_{8+\delta}$	115	Ceramic (sealed Ag/Au tube)*
$\text{Ti}_2\text{Ba}_2\text{CuO}_6$	90	Ceramic (sealed Ag/Au tube)*
$\text{Ti}_2\text{CaBa}_2\text{Cu}_2\text{O}_8$	110	Ceramic (sealed Ag/Au tube)*
$\text{Ti}_2\text{Ca}_2\text{Ba}_2\text{Cu}_2\text{O}_{10}$	125	Ceramic (sealed Ag/Au tube)*
$\text{Ti}_{0.5}\text{Pb}_{0.5}\text{CaSr}_2\text{Cu}_2\text{O}_{8+\delta}$	90	Ceramic (sealed Ag/Au tube)*
$\text{Pb}_2\text{Sr}_2\text{Ca}_{1-x}\text{Y}_x\text{Cu}_2\text{O}_8$	70	Ceramic (low O_2 partial pressure)*, sol-gel* (low O_2 partial pressure)
$\text{Pb}_{0.6}\text{Cu}_{0.6}\text{Sr}_2\text{Y}_{0.5}\text{Ca}_{0.6}\text{Cu}_2\text{O}_7$	45	Ceramic (flowing O_2)*
$\text{Nd}_{2-x}\text{Ce}_x\text{CuO}_4$	30	Ceramic (low O_2 partial pressure)*
		Coprecipitation (low O_2 partial pressure)*
$\text{Ca}_{1-x}\text{Sr}_x\text{CuO}_2$	40–110	Ceramic (high pressures)*
$\text{Sr}_{1-x}\text{Nd}_x\text{CuO}_2$	40–110	Ceramic (high pressures)*

* Recommended methods are indicated by asterisks.

* Other rare-earth compounds of this type are also prepared by similar methods. Oxygen annealing is done below the orthorhombic-tetragonal transition.

* Sr analogues of these compounds with different substitutions at Ca and Ti sites are prepared by a similar procedure.

$\text{YBa}_2\text{Cu}_3\text{O}_{7-\delta}$ is of topochemical character. The other analogous rare-earth 123 cuprates also behave in a similar way with respect to the variation of δ with T_c [237].

While $\text{YBa}_2\text{Cu}_4\text{O}_8$ has high oxygen stability, $\text{Y}_2\text{Ba}_4\text{Cu}_7\text{O}_{13-\delta}$ shows a wide range of oxygen stoichiometry ($0 \leq \delta \leq 1$) [233]. The maximum T_c of 90 K is achieved when δ is close to zero, and when δ reaches unity the material shows a T_c of 30 K; there is no structural phase transition accompanying the variation in oxygen stoichiometry. Usually, both yttrium 124 and 247 cuprates and their rare-earth analogues, prepared by the ceramic method under 1 atm oxygen pressure, show δ close to zero.

Bismuth cuprates of the type $\text{Bi}_2(\text{Ca}, \text{Sr})_{1-x}\text{Cu}_x\text{O}_{8+\delta}$ are best prepared by quenching the samples in air or by annealing in a nitrogen atmosphere at appropriate temperatures [53, 234]. Heating the samples in an oxygen atmosphere is no good, possibly because the extra oxygen may add on to the Bi-O layers. In the case of the lead-doped $n = 3$ member (2223), preparing the samples under low partial pressures of oxygen is found to increase the volume fraction of the superconducting phase [235, 236]. The $n = 1$ member, $\text{Bi}_2\text{Sr}_2\text{CuO}_{6+\delta}$ shows metallic behaviour when there is excess oxygen [237]. By annealing in a reducing atmosphere (Ar or N_2), the excess oxygen can be removed to induce superconductivity.

Oxygen stoichiometry has a dramatic influence on the superconducting properties of thallium cuprates [94, 108, 109, 238–246]. For example, thallium cuprates of the $\text{TiCa}_{1-x}\text{Ba}_x\text{Cu}_2\text{O}_{8+\delta}$ family, derivatives of the

$\text{TiCa}_{1-x}\text{Sr}_x\text{Cu}_2\text{O}_{8+\delta}$ family and $\text{Ti}_2\text{Ba}_2\text{CuO}_6$ often have excess oxygen when prepared in sealed tubes. By annealing these samples in a reducing atmosphere (Ar, dilute H_2 , N_2 or vacuum) at appropriate temperatures, the excess oxygen is removed to induce superconductivity in some cases [108, 109, 238]. Annealing at low oxygen partial pressures or in a reducing atmosphere also increases the T_c of some of the superconducting thallium cuprates to higher values by decreasing the oxygen content [94, 239–246]. These variations are clearly related to the hole concentration where the number of holes decreases by removing excess oxygen, thereby giving the optimal concentration required for maximal T_c [247].

In lead cuprates of the $\text{Pb}_2\text{Sr}_2(\text{La}, \text{Ca})\text{Cu}_2\text{O}_{8+\delta}$ (2213) type, increasing the oxygen content of the material by annealing in an oxygen atmosphere oxidizes the Pb^{2+} and Cu^{1+} without affecting the CuO_2 sheets, which governs the superconductivity in this material [248]. Though this system shows a wide range of oxygen stoichiometry (associated with a structural phase transition from orthorhombic to tetragonal symmetry), maximum T_c is observed for any given composition where δ is close to zero [249]. Samples with $\delta \approx 0$ are therefore prepared by annealing in a nitrogen atmosphere containing little oxygen. The lead 1212 cuprates, on the other hand, are best prepared in a flowing oxygen atmosphere. The samples obtained after the oxygen treatment are often not superconducting since there is an oxygen excess. The samples are quenched in air at around 1073 K in order to achieve superconductivity [250].

Superconducting properties of the electron-doped superconductors, $\text{Nd}_{1-x}\text{Ce}_x\text{CuO}_{4-x}$, are sensitive to the oxygen content. The as-prepared samples which are semiconducting have oxygen content greater than four. Samples with oxygen content less than four are obtained by annealing in a reducing atmosphere (N_2 , Ar or dilute H_2) at around 1173 K. Maintaining the oxygen stoichiometry at less than four is essential for having an oxidation state of Cu less than 2+ in this material [25].

9. Concluding remarks

In the earlier sections we presented details of the preparative methods for the synthesis of various families of cuprate superconductors. In addition, we also examined the advantages and disadvantages of the different methods. Since more than one method of synthesis has been employed for preparing any given cuprate, it becomes necessary to make the right choice of method in any given situation. In order to assist in making such a choice, we have tabulated in table 6 the important preparative methods employed to synthesize some of the representative cuprates, where the recommended methods are also indicated.

Acknowledgment

The authors thank the various agencies, especially the National Superconductivity Research Board, University Grants Commission and the US National Science Foundation for support of the research related to cuprate superconductors.

References

- [1] Bednorz J G and Müller K A 1986 *Z. Phys.* B 64 189
- [2] Sleight A W 1988 *Science* 242 1519
- [3] Rao C N R (ed) 1991 *Chemistry of High Temperature Superconductors* (Singapore: World Scientific)
- [4] Rao C N R 1991 *Phil. Trans. R. Soc. A* 336 595
- [5] Rao C N R and Gopalakrishnan J 1989 *New Directions in Solid State Chemistry* (Cambridge: Cambridge University Press)
- [6] Rao C N R 1992 *Mater. Sci. Eng.* at press
- [7] Uchida S, Takagi H, Kitazawa K and Tanaka S 1987 *Japan. J. Appl. Phys.* 26 L1
- [8] Cava R J, Vandover R B, Batlogg B and Rietman E A 1987 *Phys. Rev. Lett.* 58 408
- [9] Ganguly P, Mohan Ram R A, Sreedhar K and Rao C N R 1987 *Solid State Commun.* 62 807
- [10] Tarascon J M, Greene L H, McKinnon W R, Hull G W and Geballe T H 1987 *Science* 235 1373
- [11] Wang H *et al* 1987 *Inorg. Chem.* 26 1474
- [12] Bhat V, Ganguli A K, Nanjundaswamy K S, Mohan Ram R A, Gopalakrishnan J and Rao C N R 1987 *Phase Transitions* 10 87
- [13] Kaplan M L and Hauser J J 1988 *Mater. Res. Bull.* 23 287
- [14] Demazeau G, Trése F, Planche Th F, Chevalier B, Broréau J, Michel C, Hervieu M, Raveau B, Lejay P, Sulpice A and Tournier T 1988 *Physica C* 153-155 824
- [15] Schriber E, Morosin B, Merriell R M, Heava P F, Venturini E L, Kurak J F, Nigney P J, Baughman R J and Ginley D S 1988 *Physica C* 152 121
- [16] Zhou J, Sinha S and Goodenough J B 1989 *Phys. Rev. B* 39 12331
- [17] Cava R J, Batlogg B, Vandover R B, Krajewski J J, Waszczak J V, Flemming R M, Peck W Jr, Rupp L W Jr, Marsh P, James A C W P and Schneemeyer L F 1990 *Nature* 345 6026
- [18] Kinoshita K, Shibata H and Yamada T 1991 *Physica C* 176 433
- [19] Okai B 1991 *Japan. J. Appl. Phys.* 30 L179
- [20] Cava R J, Batlogg B, Vandover R B, Murphy D W, Sunshine S, Siegrist T, Rameika J P, Rietman E A, Zahurak S and Espinosa G P 1987 *Phys. Rev. Lett.* 58 1676
- [21] Rao C N R, Ganguly P, Raychaudhuri A K, Mohan Ram R A and Sreedhar K 1987 *Nature* 326 856
- [22] Leskela M, Mueller C H, Truman J K and Holloway P H 1988 *Mater. Res. Bull.* 23 1469; Hepp A F and Gajer J R 1988 *Mater. Res. Bull.* 23 693
- [23] Rao C N R 1988 *J. Solid State Chem.* 74 147
- [24] Clarke D R 1987 *Int. J. Mod. Phys.* B1 170
- [25] Umarji A M and Nanjundaswamy K S 1987 *Pramana-J. Phys.* 29 L611
- [26] Tarascon J M, McKinnon W R, Greene L H, Hull L W and Vogel E M 1987 *Phys. Rev. B* 36 226
- [27] Alario-Franco M A, Moran-Miguel E, Saez-Puche R, Garcia-Alvarado F, Amador U, Barabona M, Fernandez F, Perez-Frias M T and Vincent J L 1988 *Mater. Res. Bull.* 23 313
- [28] Manthiram A, Lee S J and Goodenough J B 1988 *J. Solid State Chem.* 73 278
- [29] Cava R J, Batlogg B, Flemming R M, Sunshine S A, Ramirez A, Rietman E A, Zahurak S M and Vandover R B 1988 *Phys. Rev. B* 37 5912
- [30] Somasundaram P, Nanjundaswamy K S, Umarji A M and Rao C N R 1988 *Mater. Res. Bull.* 23 1139
- [31] Veal B M, Kwok W K, Umezawa A, Crabtree G W, Jorgensen J D, Downey J W, Nowicki L J, Mitchell A W, Paulikas A P and Sowers C H 1987 *Appl. Phys. Lett.* 51 279
- [32] Tarascon J M, Barbour P, Miceli P F, Greene L H, Hull G W, Eibschutz M and Sunshine S A 1988 *Phys. Rev. B* 37 7458
- [33] Xu Y, Sabatini R L, Moodenbaugh A R, Zhu Y, Shyu S G, Suenaga M, Dennis K W and McCallum R W 1990 *Physica C* 169 205
- [34] Karpinski J, Kaldos E, Jilek E, Rusicek S and Bucher B 1988 *Nature* 336 660
- [35] Cava R J, Krajewski J J, Peck W F Jr, Batlogg B, Rupp L W Jr, Fleming R M, James A C W P and Marsh P 1989 *Nature* 338 328
- [36] Pooke D M, Buckley R G, Presland M R and Tallon J L 1990 *Phys. Rev. B* 41 6616
- [37] Hurng W M, Wu S F and Lee W H 1990 *Solid State Commun.* 76 647
- [38] Rao C N R, Subbanna G N, Nagarajan R, Ganguli A K, Ganapathi L, Vijayaraghavan R, Bhat S V and Raju A R 1990 *J. Solid State Chem.* 85 163
- [39] Jin S, O'Bryan, Gallagher P K, Tietel T H, Cava R J, Fastnacht R A and Kammlott G W 1990 *Physica C* 165 415
- [40] Adachi S, Adachi H, Setsune K and Wada K 1991 *Physica C* 175 523
- [41] Buckley R G, Tallon J L, Pooke D M and Presland M R 1990 *Physica C* 165 391
- [42] Buckley R G, Pooke D M, Tallon J L, Presland M R, Flower N E, Staines M P, Johnson H L, Meylan M, Williams G V M and Bowden M 1991 *Physica C* 174 383

- 1707 *Physica C* 100 727
- [44] Tallon J L and Lusk J 1990 *Phys. Rev. B* 41 7236
- [45] Morris D E, Nickel J H, Wei J Y T, Asmar N G, Scott J S, Scheven U M, Hultgren C T, Markelz A G, Post J E, Heaney P J, Veblen D R and Hazen R M 1989 *Phys. Rev. B* 39 7347
- [46] Miyatake T, Gotoh S, Koshizuka N and Tanaka S 1989 *Nature* 341 41
- [47] Wada T, Sakurai T, Suzuki N, Koriyama S, Yamauchi H and Tanaka S 1990 *Phys. Rev. B* 41 11209
- [48] Morris D E, Marathe A P and Sinha A P B 1990 *Physica C* 169 386
- [49] Bordet P, Chailout C, Chevanas J, Hoveau J L, Marezio M, Karpinski J and Kaldis E 1988 *Nature* 334 596
- [50] Morris D E, Asmar N G, Wei J Y T, Sid R L, Nickel J H, Scott J S and Post J E 1989 *Physica C* 162-164 955
- [51] Michel C, Hervieu M, Borel M M, Grandin A, Deslandes F, Provost J and Raveau B 1987 *Z. Phys.* B 68 421
- [52] Maeda H, Tanaka Y, Fukutomi M and Asano T 1988 *Japan. J. Appl. Phys.* 27 L209
- [53] Rao C N R, Ganapathi L, Vijayaraghavan R, Ranga Rao G, Kumari Murthy and Mohan Ram R A 1988 *Physica C* 156 827
- [54] Sastry P V P S S, Gopalakrishnan I K, Sequeira A, Rajagopal H, Gangadharan K, Phatak G M and Iyer R M 1988 *Physica C* 156 230
- [55] Sastry P V P S S, Yakhmi J V and Iyer R M 1989 *Physica C* 161 656
- [56] Wang Z, Statt B W, Lee M J G, Bagheri S and Rutter J 1991 *J. Mater. Res.* 6 1160
- [57] Torrance J B, Tokura Y, LaPlaca S J, Huang T C, Savoy R J and Nazzari A I 1988 *Solid State Commun.* 66 703
- [58] Tallon J L, Buckley R G, Presland M R, Gilbert P W, Brown I W M, Bowden M and Goguel R 1989 *Phase Transitions* 19 171
- [59] Garcia-Alvarado F, Moran E, Alario-Franco M A, Gonzalez M A, Vincent J L, Cheetham A K and Chippindale A M 1990 *J. Less Common Metals* 164-165 643
- [60] Ikeda Y, Ito H, Shimomura S, Oue Y, Inaba K, Hiroi Z and Takano M 1989 *Physica C* 159 93
- [61] Maeda A, Hase M, Tsukada I, Noda K, Takebayashi S and Uchinokura K 1990 *Phys. Rev. B* 41 6418
- [62] Sinclair D C, Irvine J T S and West A R 1992 *J. Mater. Chem.* 2 579
- [63] Agostinelli E, Bohandy J, Green W J, Phillips T E, Kim B F, Adrian F J and Moorjani K 1989 *J. Mater. Res.* 4 1103
- [64] Ganapathi L, Sujata Krishna, Kumari Murthy, Vijayaraghavan R and Rao C N R 1988 *Solid State Commun.* 67 967; Statt B W, Wang Z, Lee M J G, Yakhmi J V, Decamargo P C, Major J F and Rutter J W 1988 *Physica C* 156 251
- [65] Balachandran U, Shi D, Dos Santos D I, Graham S W, Patel M A, Tani B, Vandervoort K, Claus H and Poeppel R B 1988 *Physica C* 156 649
- [66] Green S M, Jiang C, Mei Y, Luo H L and Politis C 1988 *Phys. Rev. B* 38 5016
- [67] Varma K B R, Rao C N R and Rao C N R 1989 *Appl. Phys. Lett.* 54 69
- [68] Komatsu T, Sato R, Hirose C, Matusita K and Yamashita T 1988 *Japan. J. Appl. Phys.* 27 L2293
- [69] Pandey D, Mahesh R, Singh A K, Tiwari V S and Kak S K 1991 *Physica C* 184 135
- [70] Bloom I, Frommelt J M, Hash M C, Lanagan M T, Gruber C S, Gyo G, Gallagher P K, O'Bryan H M, Johnson S, Anichini S, Zaburak S M, Jin S and Sherwood R C 1988 *Phys. Rev. B* 38 757
- [72] Shi F, Rong T S, Zhou S Z, Wu X F, Du J, Shi Z H, Cui C G, Jin R Y, Zhang J L, Ran Q Z and Shi N C 1990 *Phys. Rev. B* 41 6541
- [73] Rao C N R, Mohan Ram R A, Ganapathi L and Vijayaraghavan R 1988 *Pramana-J. Phys.* 30 L495
- [74] Zandbergen H W, Huang Y K, Menken M J V, Li J N, Kadowaki K, Menovsky A A, Van Tendeloo G and Amelinckx S 1988 *Nature* 332 620
- [75] Rao C N R, Vijayaraghavan R, Ganapathi L and Bhat S V 1989 *J. Solid State Chem.* 79 177; Losch S, Budin H, Eibl O, Hartmann M, Rentschler T, Rygula M, Kemmler-Sack S and Heubener R P 1991 *Physica C* 177 271
- [76] Darriet J, Soethout C J P, Chevalier B and Etourneau J E 1989 *Solid State Commun.* 69 1093
- [77] Manivannan V, Gopalakrishnan J and Rao C N R 1991 *Phys. Rev. B* 43 8686
- [78] Rao C N R, Nagarajan R, Vijayaraghavan R, Vasanthacharya N Y, Kulkarni G U, Ranga Rao G, Umarji A M, Somasundaram P, Subbanna G N, Raju A R, Sood A K and Chandrabhas N 1990 *Supercond. Sci. Technol.* 3 242
- [79] Manthiram A and Goodenough J B 1988 *Appl. Phys. Lett.* 53 420
- [80] Xiang X D, McKernan S, Vareka W A, Zeitl A, Corkill J L, Barbee T W III and Cohen M L 1990 *Nature* 348 145
- [81] Tokura Y, Arima T, Takagi H, Uchida S, Ishigaki T, Asano H, Beyers R, Nazzari A I, Laccorre P and Torrance J B 1989 *Nature* 342 890
- [82] Remschnig K, Tarascon J M, Ramesh R, Hull G W and Rogi P 1990 *Physica C* 170 284
- [83] Arima T, Tokura Y, Takagi H, Uchida S, Beyers R and Torrance J B 1990 *Physica C* 168 79
- [84] Sequeira A, Rajagopal H, Ganapathi L, Vijayaraghavan R and Rao C N R 1989 *Int. J. Mod. Phys.* 3 445; Lee P, Gao Y, Sheu H S, Petricek V, Restori R, Coppens P, Darovskikh A, Phillips J C, Sleight A W and Subramanian M A 1989 *Science* 244 62
- [85] Cheetham A K, Chippindale A M, Hibbs S J and Woodley C J 1989 *Phase Transitions* 19 223
- [86] Sheng Z Z and Hermann A M 1988 *Nature* 332 55, 138
- [87] Shimakawa Y, Kubo Y, Manoko T, Nakabayashi Y and Igarashi H 1988 *Physica C* 156 97
- [88] Torardi C C, Subramanian M A, Gopalakrishnan J, McCarron E M, Calabrese J C, Morrissey K J, Askew T R, Flippens R B, Chowdhry U, Sleight A W and Cox D E 1988 *High Temperature Superconductivity* (ed R M Metzger) (New York: Gordon and Breach) p 117
- [89] Vijayaraghavan R, Rangavittal N, Kulkarni G U, Grantscharova E, Guru Row T N and Rao C N R 1991 *Physica C* 179 183
- [90] Goretta K C, Chen J G, Chen N, Hash M O and Shi D 1990 *Mater. Res. Bull.* 25 791
- [91] Schilling A, Ott H R and Hulliger F 1989 *Physica C* 157 144
- [92] Rao C N R, Ganguli A K and Vijayaraghavan R 1989 *Phys. Rev. B* 40 2505; Ganguli A K, Vijayaraghavan R and Rao C N R 1989 *Phase Transitions* 19 213
- [93] Parkin S S P, Lee V Y, Nazzari A I, Savoy R, Huang T C, Gorman G and Beyers R 1988 *Phys. Rev. B* 38 6531
- [94] Martin C, Maignan A, Provost J, Michel C, Hervieu M, Tournier R and Raveau B 1990 *Physica C* 168 8

- [95] Barry J C, Iqbal Z, Ramakrishna B L, Sharma R, Eckhardt H and Reidinger F 1989 *J. Appl. Phys.* 65 5207
- [96] Gopalakrishnan I K, Sastry P V P S S, Gangadharan K, Phatak G M, Yakhmi J V and Iyer R M 1988 *Appl. Phys. Lett.* 53 414
- [97] Li S and Greenblatt M 1989 *Physica C* 157 365
- [98] Ganguli A K, Nanjundaswamy K S, Subbanna G N, Rajumon M K, Sarma D D and Rao C N R 1988 *Mod. Phys. Lett. B* 2 1169
- [99] Sleight A W 1991 *Phys. Today* 44 24
- [100] Parkin S S P, Lee V Y, Engler E M, Nazzari A I, Huang T C, Gorman G, Savoy R and Beyers R 1988 *Phys. Rev. Lett.* 60 2539
- [101] Vijayaraghavan R, Gopalakrishnan J and Rao C N R 1992 *J. Mater. Chem.* 2 237
- [102] Suigze R, Herbayashi M, Terasada N, Jo M, Shimomura T and Ihara H 1988 *Japan. J. Appl. Phys.* 27 1709
- [103] Suigze R, Herbayashi M, Terasada N, Jo M, Shimomura T and Ihara H 1989 *Physica C* 157 131
- [104] Ganguli A K, Nanjundaswamy K S and Rao C N R 1988 *Physica C* 156 788
- [105] Subramanian M A, Torardi C C, Gopalakrishnan J, Gai P L, Calabrese J C, Askew T R, Flippin R B and Sleight A W 1988 *Science* 242 249
- [106] Subramanian M A, Gai P L and Sleight A W 1990 *Mater. Res. Bull.* 25 101
- [107] Pan M H and Greenblatt M 1991 *Physica C* 176 80
- [108] Pan M H and Greenblatt M 1991 *Physica C* 184 235
- [109] Ganguli A K, Manivannan V, Sood A K and Rao C N R 1989 *Appl. Phys. Lett.* 55 2664
- [110] Manivannan V, Ganguli A K, Subbanna G N and Rao C N R 1990 *Solid State Commun.* 74 87
- [111] Manako T, Shimakawa Y, Kubo Y, Satoh T and Igarashi H 1989 *Physica C* 158 143
- [112] Martin C, Bourgault D, Hervieu M, Michel C, Provost J and Raveau B 1989 *Mod. Phys. Lett.* B3 993
- [113] Vijayaraghavan R 1992 *PhD Thesis Indian Institute of Science*
- [114] Liu R S, Hervieu M, Michel C, Maignan A, Martin C, Raveau B and Edwards P P 1992 *Physica C* 197 131
- [115] Torardi C C, Subramanian M A, Calabrese J C, Gopalakrishnan J, Morrissey K J, Askew T R, Flippin R B, Chowdhry U and Sleight A W 1988 *Science* 240 631
- [116] Cava R J *et al* 1988 *Nature* 336 211
- [117] Koike Y, Masuzawa M, Noji T, Sunagawa H, Kawabe H, Kobayashi N and Saito Y 1990 *Physica C* 170 130
- [118] Subramanian M A, Gopalakrishnan J, Torardi C C, Gai P L, Boyes E D, Askew T R, Flippin R B, Farneth W E and Sleight A W 1989 *Physica C* 157 124
- [119] Kadowaki K, Menken M J V and Moleman A C 1989 *Physica C* 159 165
- [120] Ramprasad, Soti N C, Adhikary K, Malik S K and Tomy C V 1990 *Solid State Commun.* 76 667
- [121] Retoux R, Michel C, Hervieu M and Raveau B 1989 *Mod. Phys. Lett.* B3 591
- [122] Zandbergen H W, Fu W T, Van Ruitenbeck J M and Amelinckx S 1989 *Physica C* 159 81
- [123] Adachi S, Seisune K and Wasa K 1990 *Japan. J. Appl. Phys.* 29 L890
- [124] Maeda T, Sakuyama K, Koriyama S, Yamauchi H and Tanaka S 1991 *Phys. Rev. B* 43 7866
- [125] Rouillon T, Provost J, Hervieu M, Groult D, Michel C and Raveau B 1989 *Physica C* 159 201
- [126] Rouillon T, Maignan A, Hervieu M, Michel C, Groult D and Raveau B 1990 *Physica C* 171 7
- [127] Liu R S, Wu S F, Gamson I, Edwards P P, Maignan A, Rouillon T, Groult D and Raveau B 1991 *J. Solid State Chem.* 93 276
- [128] Mohan Ram R A and Clearfield A 1991 *Chem. Mater.* 3 313
- [129] Maeda T, Sakuyama K, Koriyama S, Ichinose A, Yamauchi H and Tanaka S 1990 *Physica C* 169 133
- [130] Tang X X, Morris D E and Sinha A P B 1991 *Phys. Rev. B* 43 7936
- [131] Liu H B and Morris D E 1991 *Phys. Rev. B* 44 5369
- [132] Tokura Y, Takagi H and Uchida S 1989 *Nature* 337 345
- [133] Markert J T and Maple M B 1989 *Solid State Commun.* 70 145
- [134] Markert J T, Early E A, Bjornholm T, Ghanaty S, Lee B W, Neumier J J, Price R D, Seaman C L and Maple M B 1989 *Physica C* 159 178
- [135] Lopez-Morales M E, Savoy R J and Grant P M 1990 *J. Mater. Res.* 5 2041
- [136] James A C W P, Zahurak S M and Murphy D W 1989 *Nature* 338 240
- [137] Felner I, Yaron U, Yeshurun Y, Yacoby E R and Wolfus Y 1989 *Phys. Rev. B* 40 11366
- [138] Ayoub N Y, Almasan C C, Early E A, Markert J T, Seaman C L and Maple M B 1990 *Physica C* 170 211
- [139] Takano M, Azuma M, Hiroi Z, Bando Y and Takeda Y 1991 *Physica C* 176 441
- [140] Takano M, Hiroi Z, Azuma M and Takeda Y 1992 *Chemistry of High Temperature Superconductors* (ed C N R Rao) (Singapore: World Scientific) p 243
- [141] Smith M G, Manthiram A, Zhou J, Goodenough J B and Markert J T 1991 *Nature* 351 549
- [142] Azuma M, Hiroi Z, Takano M, Bando Y and Takeda Y 1992 *Nature* 356 775
- [143] Capone D W, Hinks D G, Jorgensen J D and Zhang Z K 1987 *Appl. Phys. Lett.* 50 543
- [144] Bednorz J G, Takashige M and Müller K A 1987 *Mater. Res. Bull.* 22 819
- [145] Jorgensen J D, Schuttler H B, Hinks D G, Capone D W, Zhang K, Brodsky M B and Scalapino D 1987 *Phys. Rev. Lett.* 58 1024
- [146] Otamiri J C and Anderson A 1990 *J. Mater. Res.* 5 1388
- [147] Panayappan R M, Guy J T, Binstead R, Toynsneau V L and Cooper J C 1988 *Phys. Rev. B* 37 3727
- [148] McIntyre P C, Cima M J, Man Fai Ng, Chiu R C and Rhine W E 1990 *J. Mater. Res.* 5 2771
- [149] Manthiram A and Goodenough J B 1987 *Nature* 329 701
- [150] Wang X Z, Henry M, Livage J and Rosenmann I 1987 *Solid State Commun.* 64 881
- [151] Clark R J, Harrison L L, Skirius S A and Wallace W J 1990 *Mod. Cryst. Liq. Cryst.* 184 377
- [152] Vos A, Carleer R, Mullens J, Yperman J, Vanhees I and Van Poucke L C 1991 *Eur. J. Solid State Inorg. Chem.* 28 657
- [153] Vilminot S, Hadigui S El and Desory A 1988 *Mater. Res. Bull.* 23 521
- [154] Pramanik P, Biswas S, Singh C, Bhattacharya D, Dey T K, Sen D, Ghatak S K and Chopra K L 1988 *Mater. Res. Bull.* 23 1693
- [155] Kellner K, Wang X Z, Gritzer G and Bauvale D 1991 *Physica C* 173 208
- [156] Liu R S, Chang C T and Wu P T 1989 *Inorg. Chem.* 28 154
- [157] Horowitz H S, McInnis S J, Sleight A W, Druliner J D, Gai P L, Van Kavelaar M J, Wagner J L, Biggs B D and Poon S J 1989 *Science* 243 66
- [158] Kini A M, Geiser U, Kao H C I, Carlson D K, Wang H H, Monaghan M R and Williams J M 1987 *Inorg. Chem.* 26 1834

- [160] Ho J S, Lin R S, Chang C T and Edwards P P 1991 *J. Chem. Soc. Chem. Commun.* 609
- [161] Chen W L, Huang Y, Wu M K, Wang M J, Chen D H, Sheen S R and Chang C T 1991 *Physica C* 185-189 483
- [162] Guptasarma P, Palkar V R and Multani M R 1991 *Solid State Commun.* 77 769
- [163] Liu R S, Ho J S, Chang C T and Edwards P P 1991 *J. Solid State Chem.* 92 247
- [164] Das Santos D I, Balachandran U, Gutschow R A and Poeppel R B 1990 *J. Non-Cryst. Solids* 121 441
- [165] Zhang Y, Fang Z, Muhammed M, Rao K V, Skumryev V, Medelii H and Costa J L 1989 *Physica C* 157 108
- [166] Marbach G, Stotz S, Klee M and Devries J W C 1989 *Physica C* 161 111
- [167] Takano M, Takada J, Oda K, Kitaguchi H, Miura Y, Ikeda Y, Tomi Y and Mazaki H 1988 *Japan. J. Appl. Phys.* 27 L1041
- [168] Chen F H, Hoo K S and Tseng T Y 1990 *J. Mater. Sci.* 25 3338
- [169] Hagberg J, Vusimaki A, Levoska J and Leppavuori S 1989 *Physica C* 160 369
- [170] Gritzner G and Bernhard K 1991 *Physica C* 181 201
- [171] Chiang C, Shie C Y, Huang Y T, Lee W H and Wu P T 1990 *Physica C* 170 383
- [172] Chen D Y, Shie C Y, Sheen S R and Chang C T 1991 *Japan. J. Appl. Phys.* 30 1198
- [173] Shie C Y, Liu R S, Chang C T and Wu P T 1990 *Inorg. Chem.* 29 3117
- [174] Bernhard K, Gritzner G, Wang X Z and Bauerle D 1990 *J. Solid State Chem.* 86 293
- [175] Schrodt D J et al 1988 *Solid State Commun.* 67 871
- [176] Borik M, Chernikov M, Dubov I, Osiko V, Veselago V, Yakowets Y and Stepankin V 1992 *Supercond. Sci. Technol.* 5 151
- [177] Bernhard K and Gritzner G 1992 *Physica C* 196 259
- [178] Kordas G, Wu K, Brahme U S, Friedmann T A and Ginsberg D M 1987 *Mater. Lett.* 5 417
- [179] Shibata S, Kitagawa T, Okazaki H, Kimura T and Murakami T 1988 *Japan. J. Appl. Phys.* 27 L53
- [180] Kordas G, Moore G A, Jorgensen J D, Rotella F, Hitterman R L, Volin K J and Faber J 1991 *J. Mater. Chem.* 1 175
- [181] Katayama S and Sekine M 1990 *J. Mater. Res.* 5 683
- [182] Murakami H, Yaegashi S, Nishino J, Shiohara Y and Tanaka S 1990 *Japan. J. Appl. Phys.* 29 2715
- [183] Catania P, Hovnanian N, Cot L, Pham Thi M, Kormann R and Ganne J P 1990 *Mater. Res. Bull.* 25 631
- [184] Bowmer T N and Shokoohi F K 1991 *J. Mater. Res.* 6 670
- [185] Nagano M and Greenblatt M 1988 *Solid State Commun.* 67 595
- [186] Barboux P, Tarascon J M, Greene L H, Hull G W and Bagley B G 1988 *J. Appl. Phys.* 63 2725
- [187] Fujiki M, Hikita M and Sukegawa K 1987 *Japan. J. Appl. Phys.* 26 L1159
- [188] Karis T E and Economy J 1991 *J. Mater. Res.* 6 1623
- [189] Cho C T and Dunn B 1987 *J. Am. Ceram. Soc.* 70 C375
- [190] Blank D H A, Kruidhof H K and Flokstra J 1988 *J. Phys. D: Appl. Phys.* 21 226
- [191] Sanjines R, Ravindranathan Thampi K and Kiwi J 1988 *J. Am. Ceram. Soc.* 71 512
- [192] Yang Y M, Out P, Zhao B R, Zhao Y Y, Li L, Ran Q Z and Jin R Y 1989 *J. Appl. Phys.* 66 312
- [193] Liu R S, Wang W N, Chang C T and Wu P T 1989 *Japan. J. Appl. Phys.* 28 L2155
- [194] Lee H K, Kim D and Sucks S I 1989 *J. Appl. Phys.* 65 2563
- [196] Katayama S and Sekine M 1991 *J. Mater. Res.* 6 1629; 1991 *J. Mater. Chem.* 1 1031
- [197] Zhang S C, Messing G L, Huebner W and Coleman M M 1990 *J. Mater. Res.* 5 1806
- [198] Sakka S, Kozuka H and Zhuang H 1990 *Mol. Cryst. Liq. Cryst.* 184 359
- [199] Koriyama S, Ikemachi T, Kawano T, Yamauchi H and Tanaka S 1991 *Physica C* 185-189 519
- [200] Murakami H, Yaegashi Y, Nishino J, Shiohara Y and Tanaka S 1990 *Japan. J. Appl. Phys.* 29 L445
- [201] Liu R S, Jones R, Bennett M J and Edwards P P 1990 *Appl. Phys. Lett.* 57 920
- [202] Koyama K, Junod A, Graf T, Triscone G and Muller J 1991 *Physica C* 185-189 461
- [203] Kakihana M, Kall M, Borjesson L, Mazaki H, Yasuoka H, Berastegui P, Eriksson S and Johansson L G 1991 *Physica C* 173 377
- [204] Dhalie M, Van Haesendonck C, Bruynseraede Y, Kwarcia J and Van der Biest O 1990 *J. Less Common Metals* 164-165 663
- [205] Tanaka K, Nozue A and Kamiya K 1990 *J. Mater. Sci.* 25 3551
- [206] Masuda Y, Ogawa R, Kawate Y, Tateishi T and Hara N 1992 *J. Mater. Res.* 7 292
- [207] Mahesh R, Nagarajan R and Rao C N R 1992 *J. Solid State Chem.* 96 2
- [208] Ham W K, Holland G F and Stacy A M 1988 *J. Am. Chem. Soc.* 110 5214
- [209] Subramanian M A, Gopalakrishnan J, Torardi C C, Askew T R, Flippen R B, Sleight A W, Liu J J and Poon J J 1988 *Science* 240 495
- [210] Rudolf P and Schöhlhorn R 1992 *JCS Chem. Commun.* 1158
- [211] Coppa N, Nichols D H, Schwegler J W, Crow J E, Myer G H and Salomon R E 1989 *J. Mater. Res.* 4 1307; Coppa N, Kebede A, Schwegler J W, Perez I, Salomon R E, Myer G H and Crow J E 1990 *J. Mater. Res.* 5 2755
- [212] Merzhanov A G and Borovinskaya I P 1972 *Dokl. Acad. Nauk.* 204 366
- [213] Mahesh R, Vikram A Pavate, Om Prakash and Rao C N R 1992 *Supercond. Sci. Technol.* 5 174
- [214] Varma H, Warrier K G and Damodaran A D 1990 *J. Am. Ceram. Soc.* 73 3103
- [215] Pederson L R, Maupin G D, Weber W J, McReady D J and Stephens R W 1991 *Mater. Lett.* 10 437
- [216] Sundar Manoharan S, Prasad V, Subramanyam S V and Patil K C 1992 *Physica C* 190 225
- [217] Lepart J P and Varma A 1991 *Physica C* 184 220
- [218] Kourtakis K, Robbins M and Gallagher P K 1989 *J. Solid State Chem.* 82 290
- [219] Kourtakis K, Robbins M, Gallagher P K and Tiefel T 1989 *J. Mater. Res.* 4 1289
- [220] Tomizawa T, Matsunaga H, Fujishiro M and Kakegawa H 1990 *J. Solid State Chem.* 89 212
- [221] Tripathi R B and Johnson D W Jr 1991 *J. Am. Ceram. Soc.* 74 247
- [222] Horn J, Borner H, Semmelhack H C, Lippold B, Hermann J, Wurlitz M, Krotzsch M, Boehnke U, Schlenkerich F and Frenzel Ch 1991 *Solid State Commun.* 79 483
- [223] Song K H, Liu H K, Dou S and Sorrell C C 1990 *J. Am. Ceram. Soc.* 73 1771
- [224] Matsuzaki K, Inoue A, Kimura H, Aoki K and Masumoto T 1987 *Japan. J. Appl. Phys.* 26 L1310
- [225] Kogure T, Kontra R, Yurek G J and Vander Sande J B 1988 *Physica C* 156 45
- [226] Grenier J C, Wattiaux A, Lagueyette N, Park J C, Marquestaut E, Etourneau J and Pouchard M 1991 *Physica C* 173 139

BRIEF ATTACHMENT AC

IN THE UNITED STATES PATENT AND TRADEMARK OFFICE

In re Patent Application of

Applicants: Bednorz et al.

Serial No.: 08/479,810

Filed: June 7, 1995

For: NEW SUPERCONDUCTIVE COMPOUNDS HAVING HIGH TRANSITION
TEMPERATURE, METHODS FOR THEIR USE AND PREPARATION

Date: March 14, 2005

Docket: YO987-074BZ

Group Art Unit: 1751

Examiner: M. Kopec

Commissioner for Patents
P.O. Box 1450
Alexandria, VA 22313-1450

THIRD SUPPLEMENTAL AMENDMENT

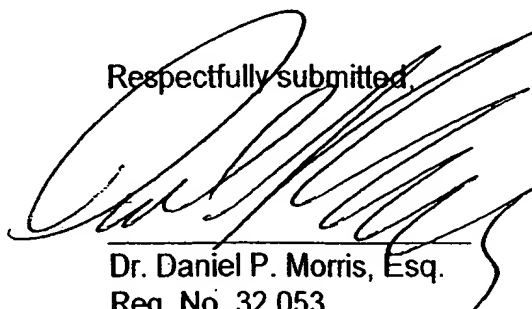
Sir:

In response to the Office Action dated July 28, 2004, please consider the
following:

The attachments referred to herein A to Z and AA are in the FIRST
SUPPLEMENTAL AMENDMENT. The Attachments AB to AG are attached herein.

Please charge any fee necessary to enter this paper and any previous paper to
deposit account 09-0468.

Respectfully submitted,



Dr. Daniel P. Morris, Esq.
Reg. No. 32,053
(914) 945-3217

IBM CORPORATION
Intellectual Property Law Dept.
P.O. Box 218
Yorktown Heights, New York 10598

ATTACHMENT AC



HIGH TEMPERATURE

C. N. R. Rao and A. K. Raychaudhuri

The following tables give properties of a number of high temperature [redacted] Table 1 lists the crystal structure (space group and lattice constants) and the critical transition temperature T_c for the more important high temperature [redacted] so far studied. Table 2 gives energy gap, critical current density, and penetration depth in the superconducting state. Table 3 gives electrical and thermal properties of some of these materials in the normal state. The tables were prepared in November 1992 and updated in November 1994.

REFERENCES

1. Ginsburg, D.M., Ed., *Physical Properties of High-Temperature* [redacted] Vols. I—III, World Scientific, Singapore, 1989—1992.
2. Rao, C.N.R., Ed., *Chemistry of High-Temperature* [redacted] World Scientific, Singapore, 1991.
3. Shackelford, J.F., *The CRC Materials Science and Engineering Handbook*, CRC Press, Boca Raton, 1992, 98—99 and 122—123.
4. Kaldis, E., Ed., *Materials and Crystallographic Aspects of HT_c Superconductivity*, Kluwer Academic Publ., Dordrecht, The Netherlands, 1992.
5. Malik, S.K. and Shah, S.S., Ed., *Physical and Material Properties of High Temperature* [redacted] Nova Science Publ., Commack, N.Y., 1994.
6. Chmaissem, O. et al., *Physica*, C230, 231—238, 1994.
7. Antipov, E.V. et al., *Physica*, C215, 1—10, 1993.

HIGH TEMPERATURE SUPERCONDUCTORS

C. N. R. Rao and A. K. Raychaudhuri

The following tables give properties of a number of high temperature superconductors. Table 1 lists the crystal structure (space group and lattice constants) and the critical transition temperature T_c for the more important high temperature superconductors so far studied. Table 2 gives energy gap, critical current density, and penetration depth in the superconducting state. Table 3 gives electrical and thermal properties of some of these materials in the normal state. The tables were prepared in November 1992 and updated in November 1994.

REFERENCES

1. Ginsburg, D.M., Ed., *Physical Properties of High-Temperature Superconductors*, Vols. I—III, World Scientific, Singapore, 1989—1992.
2. Rao, C.N.R., Ed., *Chemistry of High-Temperature Superconductors*, World Scientific, Singapore, 1991.
3. Shackelford, J.F., *The CRC Materials Science and Engineering Handbook*, CRC Press, Boca Raton, 1992, 98—99 and 122—123.
4. Kaldis, E., Ed., *Materials and Crystallographic Aspects of HT_c-Superconductivity*, Kluwer Academic Publ., Dordrecht, The Netherlands, 1992.
5. Malik, S.K. and Shah, S.S., Ed., *Physical and Material Properties of High Temperature Superconductors*, Nova Science Publ., Commack, N.Y., 1994.
6. Chmaissem, O. et al., *Physica*, C230, 231—238, 1994.
7. Antipov, E.V. et al., *Physica*, C215, 1—10, 1993.

Table 1
Structural Parameters and Approximate T_c Values of High-Temperature Superconductors

Material	Structure	T_c /K (maximum value)
$\text{La}_2\text{CuO}_{4+\delta}$	Bmab; $a = 5.355$, $b = 5.401$, $c = 13.15$ Å	39
$\text{La}_{2-x}\text{Sr}_x(\text{Ba}_y\text{CuO}_4)$	I4/mmm; $a = 3.779$, $c = 13.23$ Å	35
$\text{La}_2\text{Ca}_{1-x}\text{Sr}_x\text{Cu}_2\text{O}_6$	I4/mmm; $a = 3.825$, $c = 19.42$ Å	60
$\text{YBa}_2\text{Cu}_3\text{O}_7$	Pmmm; $a = 3.821$, $b = 3.885$, $c = 11.676$ Å	93
$\text{YBa}_2\text{Cu}_4\text{O}_8$	Ammm; $a = 3.84$, $b = 3.87$, $c = 27.24$ Å	80
$\text{Y}_2\text{Ba}_4\text{Cu}_7\text{O}_{15}$	Ammm; $a = 3.851$, $b = 3.869$, $c = 50.29$ Å	93
$\text{Bi}_2\text{Sr}_2\text{CuO}_6$	Amaa; $a = 5.362$, $b = 5.374$, $c = 24.622$ Å	10
$\text{Bi}_2\text{CaSr}_2\text{Cu}_2\text{O}_8$	A_2aa ; $a = 5.409$, $b = 5.420$, $c = 30.93$ Å	92
$\text{Bi}_2\text{Ca}_2\text{Sr}_2\text{Cu}_3\text{O}_{10}$	A_2aa ; $a = 5.39$, $b = 5.40$, $c = 37$ Å	110
$\text{Bi}_2\text{Sr}_2(\text{Ln}_{1-x}\text{Ce}_x)_2\text{Cu}_2\text{O}_{10}$	P4/mmm; $a = 3.888$, $c = 17.28$ Å	25
$\text{Ti}_2\text{Ba}_2\text{CuO}_6$	A_2aa ; $a = 5.468$, $b = 5.472$, $c = 23.238$ Å; I4/mmm; $a = 3.866$, $c = 23.239$ Å	92
$\text{Ti}_2\text{CaBa}_2\text{Cu}_2\text{O}_8$	I4/mmm; $a = 3.855$, $c = 29.318$ Å	119
$\text{Ti}_2\text{Ca}_3\text{Ba}_2\text{Cu}_3\text{O}_{10}$	I4/mmm; $a = 3.85$, $c = 35.9$ Å	128
$\text{Ti}(\text{BaLa})\text{CuO}_5$	P4/mmm; $a = 3.83$, $c = 9.55$ Å	40
$\text{Ti}(\text{SrLa})\text{CuO}_5$	P4/mmm; $a = 3.7$, $c = 9$ Å	40
$(\text{Ti}_{0.5}\text{Pb}_{0.5})\text{Sr}_2\text{CuO}_5$	P4/mmm; $a = 3.738$, $c = 9.01$ Å	40
$\text{TiCaBa}_2\text{Cu}_2\text{O}_7$	P4/mmm; $a = 3.856$, $c = 12.754$ Å	103
$(\text{Ti}_{0.5}\text{Pb}_{0.5})\text{CaSr}_2\text{Cu}_2\text{O}_7$	P4/mmm; $a = 3.80$, $c = 12.05$ Å	90
$\text{TiSr}_2\text{Y}_{0.5}\text{Ca}_{0.5}\text{Cu}_2\text{O}_7$	P4/mmm; $a = 3.80$, $c = 12.10$ Å	90
$\text{TiCa}_2\text{Ba}_2\text{Cu}_3\text{O}_8$	P4/mmm; $a = 3.853$, $c = 15.913$ Å	110
$(\text{Ti}_{0.5}\text{Pb}_{0.5})\text{Sr}_2\text{Ca}_2\text{Cu}_3\text{O}_9$	P4/mmm; $a = 3.81$, $c = 15.23$ Å	120
$\text{TiBa}_2(\text{La}_{1-x}\text{Ce}_x)_2\text{Cu}_2\text{O}_9$	I4/mmm; $a = 3.8$, $c = 29.5$ Å	40
$\text{Pb}_2\text{Sr}_2\text{La}_{0.5}\text{Ca}_{0.5}\text{Cu}_3\text{O}_8$	Cmmm; $a = 5.435$, $b = 5.463$, $c = 15.817$ Å	70
$\text{Pb}_2(\text{SrLa})_2\text{Cu}_2\text{O}_6$	P22 ₁ 2; $a = 5.333$, $b = 5.421$, $c = 12.609$ Å	32
$(\text{Pb,Cu})\text{Sr}_2(\text{La,Ca})\text{Cu}_2\text{O}_7$	P4/mmm; $a = 3.820$, $c = 11.826$ Å	50
$(\text{Pb,Cu})(\text{Sr,Eu})(\text{Eu,Ce})\text{Cu}_2\text{O}_x$	I4/mmm; $a = 3.837$, $c = 29.01$ Å	25
$\text{Nd}_{2-x}\text{Ce}_x\text{CuO}_4$	I4/mmm; $a = 3.95$, $c = 12.07$ Å	30
$\text{Ca}_{1-x}\text{Sr}_x\text{CuO}_2$	P4/mmm; $a = 3.902$, $c = 3.35$ Å	110
$\text{Sr}_{1-x}\text{Nd}_x\text{CuO}_2$	P4/mmm; $a = 3.942$, $c = 3.393$ Å	40
$\text{Ba}_{0.6}\text{K}_{0.4}\text{BiO}_3$	Pm3m; $a = 4.287$ Å	31
$\text{Rb}_2\text{CsC}_{60}$	$a = 14.493$ Å	31
$\text{NdBa}_2\text{Cu}_3\text{O}_7$	Pmmm; $a = 3.878$, $b = 3.913$, $c = 11.753$	58

BRIEF ATTACHMENT AD

IN THE UNITED STATES PATENT AND TRADEMARK OFFICE

In re Patent Application of

Applicants: Bednorz et al.

Serial No.: 08/479,810

Filed: June 7, 1995

For: NEW SUPERCONDUCTIVE COMPOUNDS HAVING HIGH TRANSITION
TEMPERATURE, METHODS FOR THEIR USE AND PREPARATION

Date: March 14, 2005

Docket: YO987-074BZ

Group Art Unit: 1751

Examiner: M. Kopec

Commissioner for Patents
P.O. Box 1450
Alexandria, VA 22313-1450

THIRD SUPPLEMENTAL AMENDMENT

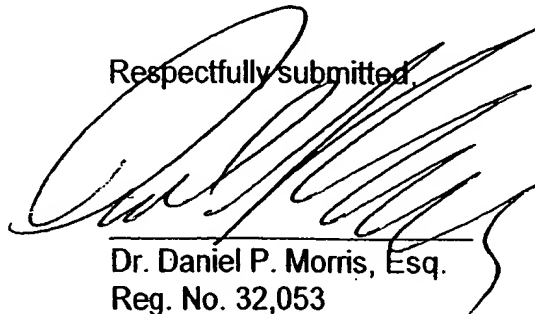
Sir:

In response to the Office Action dated July 28, 2004, please consider the
following:

The attachments referred to herein A to Z and AA are in the FIRST
SUPPLEMENTAL AMENDMENT. The Attachments AB to AG are attached herein.

Please charge any fee necessary to enter this paper and any previous paper to
deposit account 09-0468.

Respectfully submitted,



Dr. Daniel P. Morris, Esq.
Reg. No. 32,053
(914) 945-3217

IBM CORPORATION
Intellectual Property Law Dept.
P.O. Box 218
Yorktown Heights, New York 10598

ATTACHMENT AD

THEORY OF SUPERCONDUCTIVITY

By

M. von LAUE

Kaiser-Wilhelm-Institut für physikalische und Elektro-Chemie
Berlin—Dahlem

Translated by

LOTHAR MEYER

University of Chicago, Chicago, Illinois

and

WILLIAM BAND

The State College of Washington, Pullman, Washington



ACADEMIC PRESS INC., PUBLISHERS

New York, 1952

Fundamental Facts

(a) Superconductivity was discovered in 1911 by Kamerlingh-Onnes.¹ He was the first to liquefy helium and so to produce temperatures below 10°K . With this new technique he was able to observe the continued decrease of the electrical resistance of metals with decreasing temperature. With mercury, in contrast to other metals, he was astonished to find that the resistance completely vanished, almost discontinuously, at about 4.2°K (Fig. 1-1). Today superconductivity is known in 18 other metals (see Table 1-1) whereas in others, e. g., gold and bismuth, the conductivity remains normal far below even 1°K . Many alloys and compounds can also become superconducting, in particular the frequently used niobium nitride which has a transition temperature as high as 20°K . However, among these latter substances hysteresis phenomena mentioned in the "Introduction" are so much more strongly evident that in testing the present theory we prefer to employ only the "good" superconductors, i. e., the pure elements.

In the ideal case the resistance vanishes completely and discontinuously at a transition temperature T_c . Actually the resistance-temperature curve does fall more sharply the more the specimen is like a single crystal and the smaller the measuring current used. Because the drop always occurs in a measurable temperature range, the experimental definition of the transition temperature is to some extent arbitrary. The temperature at which the direct-current resistance reaches one half of the value it had just before the drop is generally given as the transition temperature, because this can be measured accurately. However, a high-frequency investigation to be described in Chap. 16 (f) indicates that the foot of the curve where

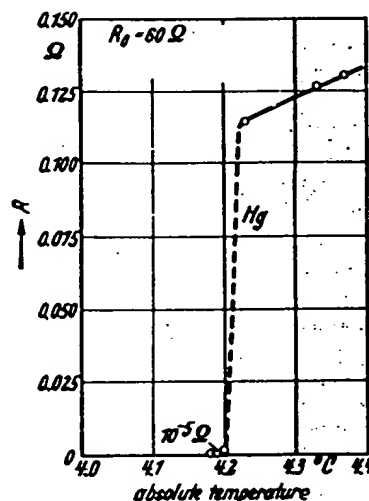


Fig. 1-1. Appearance of superconductivity in mercury according to H. Kamerlingh-Onnes (1911). The ordinate is the resistance R ; R_0 , the resistance of solid mercury extrapolated to 0°C , is 60 ohms.

¹H. Kamerlingh-Onnes, *Commun. Leiden*, 120b, 122b, 124c, (1911).

BRIEF ATTACHMENT AE

IN THE UNITED STATES PATENT AND TRADEMARK OFFICE

In re Patent Application of

Applicants: Bednorz et al.

Serial No.: 08/479,810

Filed: June 7, 1995

For: **NEW SUPERCONDUCTIVE COMPOUNDS HAVING HIGH TRANSITION
TEMPERATURE, METHODS FOR THEIR USE AND PREPARATION**

Date: March 14, 2005

Docket: YO987-074BZ

Group Art Unit: 1751

Examiner: M. Kopec

Commissioner for Patents
P.O. Box 1450
Alexandria, VA 22313-1450

THIRD SUPPLEMENTAL AMENDMENT

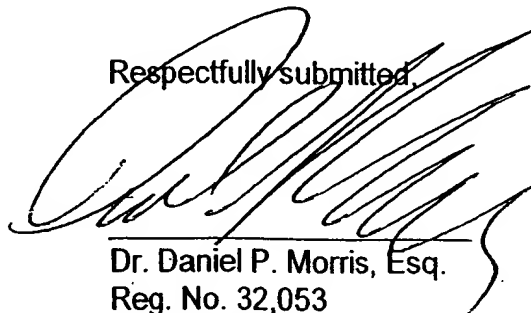
Sir:

In response to the Office Action dated July 28, 2004, please consider the following:

The attachments referred to herein A to Z and AA are in the **FIRST SUPPLEMENTAL AMENDMENT**. The Attachments AB to AG are attached herein.

Please charge any fee necessary to enter this paper and any previous paper to deposit account 09-0468.

Respectfully submitted,



Dr. Daniel P. Morris, Esq.
Reg. No. 32,053
(914) 945-3217

IBM CORPORATION
Intellectual Property Law Dept.
P.O. Box 218
Yorktown Heights, New York 10598

ATTACHMENT AE

(12)

EUROPEAN PATENT APPLICATION

(21) Application number: **87100961.9**

(51) Int. Cl.⁴ **H01L 39/12**

(22) Date of filing: **23.01.87**

(43) Date of publication of application:
27.07.88 Bulletin 88/30

(84) Designated Contracting States:
AT BE CH DE ES FR GB GR IT LJ LU NL SE

(71) Applicant: **International Business Machines Corporation**
Old Orchard Road
Armonk, N.Y. 10504(US)

(72) Inventor: **Bednorz, Johannes Georg, Dr.**
Sonnenbergstrasse 47
CH-8134 Adliswil(CH)
Inventor: **Müller, Carl Alexander, Prof.Dr.**
Haldenstrasse 54
CH-8908 Hedingen(CH)
Inventor: **Takashige, Masaaki, Dr.**
Rottfarbweg 1
CH-8803 Rüschlikon(CH)

(74) Representative: **Rudack, Günter O., Dipl.-Ing.**
IBM Corporation Säumerstrasse 4
CH-8803 Rüschlikon(CH)

(54) **New superconductive compounds of the K₂NiF₄ structural type having a high transition temperature, and method for fabricating same.**

(57) The superconductive compounds are oxides of the general formula $RE_{2-x}AE_xTM.O_{4-y}$, wherein RE is a rare earth, AE is a member of the group of alkaline earths or a combination of at least two member of that group, and TM is a transition metal, and wherein $x < 0.3$ and $0.1 \leq y \leq 0.5$. The method for making these compounds involves the steps of coprecipitating aqueous solutions of the respective nitrates of the constituents and adding the coprecipitate to oxalic acid, decomposing the precipitate and causing a solid-state reaction at a temperature between 500 and 1200°C for between one and eight hours, forming pellets of the powdered product at high pressure, sintering the pellets at a temperature between 500 and 1000°C for between one half and three hours, and subjecting the pellets to an additional annealing treatment at a temperature between 500 and 1200°C for between one half and five hours in a protected atmosphere permitting the adjustment of the oxygen content of the final product.

EP 0 275 343 A1

NEW SUPERCONDUCTIVE COMPOUNDS OF THE KNIF₂ STRUCTURAL TYPE HAVING A HIGH TRANSITION TEMPERATURE, AND METHOD FOR FABRICATING SAME

Field of the Invention

The invention relates to a new class of superconductors, in particular to components of the K_2NiF_4 type of structure having superconductor properties below a relatively high transition temperature, and to a method for manufacturing those compounds.

Background of the Invention

Superconductivity is usually defined as the complete loss of electrical resistance of a material at a well-defined temperature. It is known to occur in many materials: About a quarter of the elements and over 1000 alloys and components have been found to be superconductors. Superconductivity is considered a property of the metallic state of the material, in that all known superconductors are metallic under the conditions that cause them to superconduct. A few normally non-metallic materials, for example, become superconductive under very high pressure, the pressure converting them to metals before they become superconductors.

Superconductors are very attractive for the generation and energy-saving transport of electrical power over long distances, as materials for forming the coils of strong magnets for use in plasma and nuclear physics, in nuclear resonance medical diagnosis, and in connection with the magnetic levitation of fast trains. Power generation by thermonuclear fusion, for example, will require very large magnetic fields which can only be provided by superconducting magnets. Certainly, superconductors will also find application in computers and high-speed signal processing and data communication.

While the advantages of superconductors are quite obvious, the common disadvantage of all superconductive materials so far known lies in their very low transition temperature (usually called the critical temperature T_c) which is typically on the order of a few degrees Kelvin. The element with the highest T_c is niobium (9.2 K), and the highest known T_c is about 23 K for Nb_3Ge at ambient pressure.

Accordingly, most known superconductors require liquid helium for cooling and this, in turn, requires an elaborate technology and as a matter of principle involves a considerable investment in cost and energy.

It is, therefore, an object of the present inven-

tion to propose compositions for high- T_c superconductors and a manufacturing method for producing compounds which exhibit such a high critical temperature that cooling with liquid helium is obviated so as to considerably reduce the cost involved and to save energy.

The present invention proposes to use compounds having a layer-type structure of the kind known from potassium nickel fluoride K_2NiF_4 . This structure is in particular present in oxides of the general composition $RE_2TM.O_4$, wherein RE stands for the rare earths (lanthanides) and TM stands for the so-called transition metals. It is a characteristic of the present invention that in the compounds in question the RE portion is partially substituted by one member of the alkaline earth group of metals, or by a combination of the members of this alkaline earth group, and that the oxygen content is at a deficit.

For example, one such compound that meets the description given above is lanthanum copper oxide La_2CuO_4 in which the lanthanum -which belongs to the IIIB group of elements-is in part substituted by one member of the neighboring IIA group of elements, viz. by one of the alkaline earth metals (or by a combination of the members of the IIA group), e.g., by barium. Also, the oxygen content of the compound is incomplete such that the compound will have the general composition $La_{2-x}Ba_xCuO_{4-y}$, wherein $x \leq 0.3$ and $y < 0.5$.

Another example for a compound meeting the general formula given above is lanthanum nickel oxide wherein the lanthanum is partially substituted by strontium, yielding the general formula $La_{2-x}Sr_xNiO_{4-y}$. Still another example is cerium nickel oxide wherein the cerium is partially substituted by calcium, resulting in $Ce_{2-x}Ca_xNiO_{4-y}$.

The following description will mainly refer to barium as a partial replacement for the lanthanum in a La_2CuO_4 compound because it is the Ba-La-Cu-O system which is, at least at present, the best understood system of all possible. Some compounds of the Ba-La-Cu-O system have been described by C. Michel and B. Raveau in Rev. Chim. Min. 21 (1984) 407, and by C. Michel, L. Er-Rakho and B. Raveau in Mat. Res. Bull., Vol. 20, (1985) 667-671. They did, however, not find nor try to find, superconductivity.

Experiments conducted in connection with the present invention have revealed that high- T_c superconductivity is present in compounds where the rare earth is partially replaced by any one or more of the other members of the same IIA group of elements, i.e. the other alkaline earth metals. Ac-

tually, the T_c of $\text{La}_2\text{CuO}_{4-y}$ with Sr^{2+} is higher and is superconductivity-induced diamagnetism larger than that found with Ba^{2+} and Ca^{2+} .

As a matter of fact, only a small number of oxides is known to exhibit superconductivity, among them the Li-Ti-O system with onsets of superconductivity as high as 13.7 K, as reported by D.C. Johnston, H. Prakash, W.H. Zachariasen and R. Visvanathan in *Mat. Res. Bull.* 8 (1973) 777. Other known superconductive oxides include Nb-doped SrTiO_3 and $\text{BaPb}_{1-x}\text{Bi}_x\text{O}_3$, reported respectively by A. Baratoff and G. Binnig in *Physics* 108B (1981) 1335, and by A.W. Sleight, J.L. Gillson and F.E. Bierstedt in *Solid State Commun.* 17 (1975) 27.

The X-ray analysis conducted by Johnston et al. revealed the presence in their Li-Ti-O system of three different crystallographic phases, one of them, with a spinel structure, showing the high critical temperature. The Ba-La-Cu-O system, too, exhibits a number of crystallographic phases, namely with mixed-valent copper constituents which have itinerant electronic states between non-Jahn-Teller Cu^{3+} and Jahn-Teller Cu^{2+} ions.

This applies likewise to systems where nickel is used in place of copper, with Ni^{3+} being the Jahn-Teller constituent, and Ni^{2+} being the non-Jahn-Teller constituent.

The existence of Jahn-Teller polarons is conducting crystals was postulated theoretically by K.H. Hoeck, H. Nickisch and H. Thomas in *Helv. Phys. Acta* 56 (1983) 237. Polarons have large electron-phonon interactions and, therefore, are favorable to the occurrence of superconductivity at high critical temperatures.

Generally, the Ba-La-Cu-O system, when subjected to X-ray analysis reveals three individual crystallographic phases, viz.

- a first layer-type perovskite-like phase, related to the K_2NiF_4 structure, with the general composition $\text{La}_{2-x}\text{Ba}_x\text{CuO}_{4-y}$, with $x \ll 1$ and $y \geq 0$;
- a second, non-conducting CuO phase; and
- a third, nearly cubic perovskite phase of the general composition $\text{La}_{1-x}\text{Ba}_x\text{CuO}_{3-y}$, which appears to be independent of the exact starting composition,

as has been reported in the paper by J.G. Bednorz and K.A. Müller in *Z. Phys. B - Condensed Matter* 64 (1988) 189-193. Of these three phases the first one appears to be responsible for the high- T_c superconductivity, the critical temperature showing a dependence on the barium concentration in that phase. Obviously, the Ba^{2+} substitution causes a mixed-valent state of Cu^{2+} and Cu^{3+} to preserve charge neutrality. It is assumed that the oxygen deficiency, y , is the same in the doped and undoped crystallites.

Both La_2CuO_4 and LaCuO_3 are metallic conduc-

tors at high temperatures in the absence of barium. Actually, both are metals like LaNiO_3 . Despite their metallic character, the Ba-La-Cu-O type materials are ceramics, as are the other compounds of the $\text{RE}_2\text{TM}_2\text{O}_4$ type, and their manufacture more or less follows the known principles of ceramic fabrication. The preparation of a Ba-La-Cu-O compound, for example, in accordance with the present invention typically involves the following manufacturing steps:

- Preparing aqueous solutions of the respective nitrates of barium, lanthanum and copper and coprecipitation thereof in their appropriate ratios.
- Adding the coprecipitate to oxalic acid and forming an intimate mixture of the respective oxalates.
- Decomposing the precipitate and causing a solid-state reaction by heating the precipitate to a temperature between 500 and 1200°C for one to eight hours.

- Pressing the resulting product at a pressure of about 4 kbar to form pellets.

- Re-heating the pellets to a temperature between 500 and 900°C for one half to three hours for sintering.

It will be evident to those skilled in the art that if the partial substitution of the lanthanum by strontium or calcium is desired, the particular nitrate thereof will have to be used in place of the barium nitrate of the example described above. Also, if the copper of this example is to be replaced by another transition metal, the nitrate thereof will obviously have to be employed.

Experiments have shown that the partial contents of the individual compounds in the starting composition play an important role in the formation of the phases present in the final product. While, as mentioned above, the final Ba-La-Cu-O system obtained generally contains the said three phases, with the second phase being present only to a very small amount, the partial substitution of lanthanum by strontium or calcium (and perhaps beryllium) will result in only one phase existing in the final $\text{La}_{2-x}\text{Sr}_x\text{CuO}_{4-y}$ or $\text{La}_{2-x}\text{Ca}_x\text{CuO}_{4-y}$, respectively, provided $x < 0.3$.

With a ratio of 1:1 for the respective (Ba, La) and Cu contents, one may expect the said three phases to occur in the final product. Setting aside the said second phase, i.e. the CuO phase, whose amount is negligible, the relative volume amounts of the other two phases are dependent on the barium contents in the $\text{La}_{2-x}\text{Ba}_x\text{CuO}_{4-y}$ complex. At the 1:1 ratio and with an $x \approx 0.02$, the onset of a localization transition is observed, i.e., the resistivity increases with decreasing temperature, and there is no superconductivity.

With $x = 0.1$ at the same 1:1 ratio, there is a resistivity drop at the very high critical temperature of 35 K.

With a (Ba,La) versus Cu ratio of 2:1 in the starting composition, the composition of the $\text{La}_2\text{CuO}_4\text{:Ba}$ phase, which was assumed to be responsible for the superconductivity, is imitated, with the result that now only two phases are present, the CuO phase not existing. With a barium content of $x = 0.15$, the resistivity drop occurs at $T_c = 26$ K.

The method for preparing the Ba-La-Cu-O complex involves two heat treatments for the precipitate at an elevated temperature for several hours. In the experiments carried out in connection with the present invention it was found that best results were obtained at 900°C for a decomposition and reaction period of 5 hours, and again at 900°C for a sintering period of one hour. These values apply to a ratio 1:1 composition as well as to a 2:1 composition.

For the ratio 2:1 composition, a somewhat higher temperature is permissible owing to the melting point of the composition being higher in the absence of excess copper oxide. Yet it is not possible by high-temperature treatment to obtain a one-phase compound.

Measurements of the dc conductivity were conducted between 300 and 4.2 K. For barium-doped samples, for example, with $x < 0.3$, at current densities of 0.5 A/cm^2 , a high-temperature metallic behavior with an increase in resistivity at low temperatures was found. At still lower temperatures, a sharp drop in resistivity ($>90\%$) occurred which for higher current densities became partially suppressed. This characteristic drop was studied as a function of the annealing conditions, i.e. temperature and oxygen partial pressure. For samples annealed in air, the transition from itinerant to localized behavior was not found to be very pronounced, annealing in a slightly reducing atmosphere, however, led to an increase in resistivity and a more pronounced localization effect. At the same time, the onset of the resistivity drop was shifted towards higher values of the critical temperature. Longer annealing times, however, completely destroy the superconductivity.

Cooling the samples from room temperature, the resistivity data first show a metal-like decrease. At low temperatures, a change to an increase occurs in the case of Ca compounds and for the Ba-substituted samples. This increase is followed by a resistivity drop, showing the onset of superconductivity at 22 ± 2 K and 33 ± 2 K for the Ca and Ba compounds, respectively. In the Sr compound, the resistivity remains metallic down to the resistivity drop at 40 ± 1 K. The presence of localization effects, however, depends strongly on alkaline-earth ion concentration and sample preparation, that is to say, annealing conditions and also on the density which have to be optimized. All samples with low

concentrations of Ca, Sr, and Ba show a strong tendency to localization before the resistivity drop occur.

Apparently, the onset of the superconductivity, i.e. the value of the critical temperature T_c , is dependent, among other parameters, on the oxygen content of the final compound. It seems that a certain oxygen deficiency is necessary for the material to have a high- T_c behavior. In accordance with the present invention, the method described above for making the $\text{La}_2\text{CuO}_4\text{:Ba}$ complex is complemented by an annealing step during which the oxygen content of the final product can be adjusted. Of course, what was said in connection with the formation of the $\text{La}_2\text{CuO}_4\text{:Ba}$ compound, likewise applies to other compounds of the general formula $\text{RE}_2\text{TM}_x\text{O}_{4-y}\text{AE}$, such as, e.g. $\text{Nd}_2\text{NiO}_4\text{:Sr}$.

In the cases where a heat treatment for decomposition and reaction and/or for sintering was performed at a relatively low temperature, i.e. at no more than 950°C , the final product is subjected to an annealing step at about 900°C for about one hour in a reducing atmosphere. It is assumed that the net effect of this annealing step is a removal of oxygen atoms from certain locations in the matrix of the $\text{RE}_2\text{TM}_x\text{O}_4$ complex, thus creating a distortion in its crystalline structure. The O_2 partial pressure for annealing in this case may be between 10^{-1} and 10^{-5} bar.

In those cases where a relatively high temperature (i.e. above 950°C) was employed for the heat treatment, it might be advantageous to perform the annealing step in a slightly oxidizing atmosphere. This would make up for an assumed exaggerated removal of oxygen atoms from the system owing to the high temperature and resulting in a too severe distortion of the system's crystalline structure.

Resistivity and susceptibility measurements, as a function of temperature, of Sr^{2+} and Ca^{2+} -doped $\text{La}_2\text{CuO}_{4-y}$ ceramics show the same general tendency as the Ba^{2+} -doped samples: A drop in resistivity $\rho(T)$, and a crossover to diamagnetism at a slightly lower temperature. The samples containing Sr^{2+} actually yielded a higher onset than those containing Ba^{2+} and Ca^{2+} . Furthermore, the diamagnetic susceptibility is about three times as large as for the Ba samples. As the ionic radius of Sr^{2+} nearly matches the one of La^{3+} , it seems that the size effect does not cause the occurrence of superconductivity. On the contrary, it is rather adverse, as the data on Ba^{2+} and Ca^{2+} indicate.

The highest T_c 's for each of the dopant ions investigated occur for those concentrations where, at room temperature, the $\text{Re}_{2-x}\text{TM}_x\text{O}_{4-y}$ structure is close to the orthorhombic-tetragonal structural phase transition which may be related to the substantial electron-phonon interaction enhanced by the substitution. The alkaline-earth substitution of

the rare earth metal is clearly important, and quite likely creates TM ions with no e_g Jahn-Teller orbitals. Therefore, the absence of these J.-T. orbitals, that is, J.-T. holes near the Fermi energy probably plays an important role for the T_c enhancement.

Claims

1) Superconductive compound of the $RE_2TM.O_4$ type having a transition temperature above 28 K, wherein the rare earth (RE) is partially substituted by one or more members of the alkaline earth groups of elements (AE), and wherein the oxygen content is adjusted such that the resulting crystal structure is distorted and comprises a phase of the general composition $RE_{2-x}AE_xTM.O_{4-y}$, wherein TM represents a transition metal, and $x < 0.3$ and $y < 0.5$.

2) Compound in accordance with claim 1, wherein the rare earth (RE) is lanthanum and the transition metal (TM) is copper.

3) Compound in accordance with claim 1, wherein the rare earth is cerium and the transition metal is nickel.

4) Compound in accordance with claim 1, wherein the rare earth is lanthanum and the transition metal is nickel.

5) Compound in accordance with claim 1, wherein barium is used as a partial substitute for the rare earth, with $x < 0.3$ and $0.1 \leq y \leq 0.5$.

6) Compound in accordance with claim 1, wherein calcium is used as a partial substitute for the rare earth, with $x < 0.3$ and $0.1 \leq y \leq 0.5$.

7) Compound in accordance with claim 1, wherein strontium is used as a partial substitute for the rare earth, with $x < 0.3$ and $0.1 \leq y \leq 0.5$.

8) Compound in accordance with claim 1, wherein the rare earth is lanthanum and the transition metal is chromium.

9) Compound in accordance with claim 1, wherein the rare earth is neodymium and the transition metal is copper.

10) Method for making superconductive compounds of the $RE_2TM.O_4$ type, with RE being a rare earth, TM being a transition metal, the compounds having a transition temperature above 28 K, comprising the steps of:

- preparing aqueous solutions of the nitrates of the rare earth and transition metal constituents and of one or more of the alkaline earth metals and coprecipitation thereof in their appropriate ratios;
- adding the coprecipitate to oxalic acid and forming an intimate mixture of the respective oxalates;
- decomposing the precipitate and causing a solid-state reaction by heating the precipitate to a temperature between 500 and 1200°C for a period of

time between one and eight hours;

- allowing the resultant powder product to cool;
- pressing the powder at a pressure of between 2 and 10 kbar to form pellets;

5 - re-adjusting the temperature of the pellets to a value between 500 and 1000°C for a period of time between one half and three hours for sintering;

- subjecting the pellets to an additional annealing treatment at a temperature between 500 and 1200°C for a period of time between one half and 5 hours in a protected atmosphere permitting the adjustment of the oxygen content of the final product which has a final composition of the form $RE_2 \cdot xTM.O_{4-y}$, wherein $x < 0.3$ and $0.1 < y < 0.5$.

11) Method in accordance with claim 10, wherein the protected atmosphere is pure oxygen.

12) Method in accordance with claim 10, wherein the protected atmosphere is a reducing atmosphere with an oxygen partial pressure between 10^{-1} and 10^{-5} bar.

13) Method in accordance with claim 10, wherein the decomposition step is performed at a temperature of 900°C for 5 hours, and wherein the annealing step is performed at a temperature of 900°C for one hour in a reducing atmosphere with an oxygen partial pressure between 10^{-1} and 10^{-5} bar.

14) Method in accordance with claim 10, wherein lanthanum is used as the rare earth and copper is used as the transition metal, and wherein barium is used to partially substitute for the lanthanum, with $x < 0.2$, wherein the decomposition step is performed at a temperature of 900°C for 5 hours, and wherein the annealing step is performed in a reducing atmosphere with an oxygen partial pressure on the order of 10^{-3} bar and at a temperature of 900°C for one hour.

15) Method in accordance with claim 10, wherein lanthanum is used as the rare earth and nickel is used as the transition metal, and wherein barium is used to partially substitute for the lanthanum, with $x < 0.2$, wherein the decomposition step is performed at a temperature of 900°C for 5 hours, and wherein the annealing step is performed in a reducing atmosphere with an oxygen partial pressure on the order of 10^{-3} bar and at a temperature of 900°C for one hour.

16) Method in accordance with claim 10, wherein lanthanum is used as the rare earth and copper is used as the transition metal, and wherein calcium is used to partially substitute for the lanthanum, with $x < 0.2$, wherein the decomposition step is performed at a temperature of 900°C for 5 hours, and wherein the annealing step is performed in a reducing atmosphere with an oxygen partial pressure on the order of 10^{-3} bar and at a temperature of 900°C for one hour.

17) Method in accordance with claim 10, wherein lanthanum is used as the rare earth and copper is used as the transition metal, and wherein strontium is used to partially substitute for the lanthanum, with $x < 0.2$, wherein the decomposition step is performed at a temperature of 900°C for 5 hours, and wherein the annealing step is performed in a reducing atmosphere with an oxygen partial pressure on the order of 10^{-3} bar and at a temperature of 900°C for one hour.

18) Method in accordance with claim 10, wherein cerium is used as the rare earth and nickel is used as the transition metal, and wherein barium is used to partially substitute for the cerium, with $x < 0.2$, wherein the decomposition step is performed at a temperature of 900°C for 5 hours, and wherein the annealing step is performed in a reducing atmosphere with an oxygen partial pressure on the order of 10^{-3} bar and at a temperature of 900°C for one hour.

5

10

15

20

25

30

35

40

45

50

55

6

BRIEF ATTACHMENT AF

IN THE UNITED STATES PATENT AND TRADEMARK OFFICE

In re Patent Application of

Applicants: Bednorz et al.

Serial No.: 08/479,810

Filed: June 7, 1995

For: **NEW SUPERCONDUCTIVE COMPOUNDS HAVING HIGH TRANSITION
TEMPERATURE, METHODS FOR THEIR USE AND PREPARATION**

Date: March 14, 2005

Docket: YO987-074BZ

Group Art Unit: 1751

Examiner: M. Kopec

Commissioner for Patents
P.O. Box 1450
Alexandria, VA 22313-1450

THIRD SUPPLEMENTAL AMENDMENT

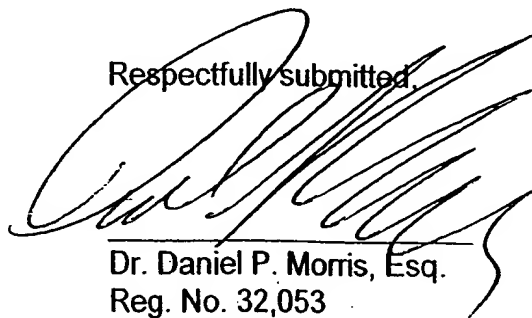
Sir:

In response to the Office Action dated July 28, 2004, please consider the following:

The attachments referred to herein A to Z and AA are in the **FIRST SUPPLEMENTAL AMENDMENT**. The Attachments AB to AG are attached herein.

Please charge any fee necessary to enter this paper and any previous paper to deposit account 09-0468.

Respectfully submitted,



Dr. Daniel P. Morris, Esq.
Reg. No. 32,053
(914) 945-3217

IBM CORPORATION
Intellectual Property Law Dept.
P.O. Box 218
Yorktown Heights, New York 10598

ATTACHMENT AF

COPPER OXIDE SUPERCONDUCTORS

Charles P. Poole, Jr.
Timir Datta
Horacio A. Farach

with help from

M. M. Rigney
C. R. Sanders

*Department of Physics and Astronomy
University of South Carolina
Columbia, South Carolina*



WILEY

A Wiley-Interscience Publication

JOHN WILEY & SONS

New York • Chichester • Brisbane • Toronto • Singapore

61

Copyright © 1988 by John Wiley & Sons, Inc.

All rights reserved. Published simultaneously in Canada.

Reproduction or translation of any part of this work beyond that permitted by Section 107 or 108 of the 1976 United States Copyright Act without the permission of the copyright owner is unlawful. Requests for permission or further information should be addressed to the Permissions Department, John Wiley & Sons, Inc.

Library of Congress Cataloging in Publication Data:

Poole, Charles P.

Copper oxide superconductors / Charles P. Poole, Jr., Timir Datta, and Horacio A. Farach; with help from M. M. Rigney and C. R. Sanders.
p. cm.

"A Wiley-Interscience publication."

Bibliography: p.

Includes index.

I. Copper oxide superconductors. I. Datta, Timir. II. Farach, Horacio A. III. Title.

QC611.98.C64P66 1988

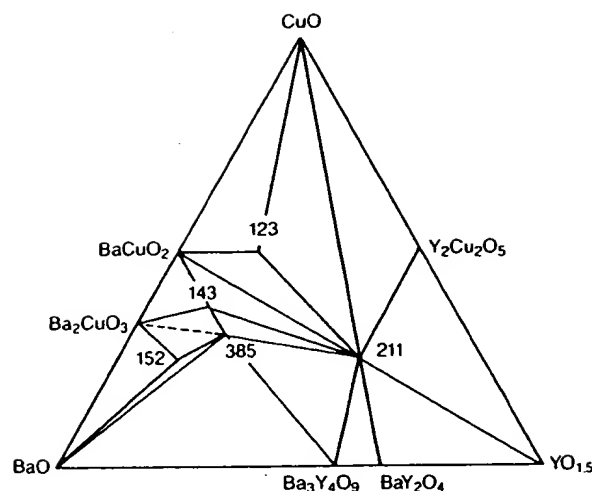
539.6'23-dc 19 88-18569 CIP

ISBN 0-471-62342-3

Printed in the United States of America

10 9 8 7 6 5 4 3 2 1

62



Compound	Slowly cooled to room temperature
123 - $\text{YBa}_2\text{Cu}_3\text{O}_{6.5+\delta}$	O_7
143 - $\text{YBa}_4\text{Cu}_3\text{O}_{8.5+\delta}$	O_9
385 - $\text{Y}_3\text{Ba}_8\text{Cu}_5\text{O}_{17.5+\delta}$	O_{18}
152 - $\text{YBa}_5\text{Cu}_2\text{O}_{8.5+\delta}$	O_9
211 - Y_2BaCuO_5	
$\text{Ba}_2\text{CuO}_{3+\delta}$	O_{33}

Fig. V-2. Ternary phase diagram of the Y_2O_3 -BaO-CuO system at 950°C . The green phase [Y_2BaCuO_5 , (211)] the superconducting phase [$\text{YBa}_2\text{Cu}_3\text{O}_{7-\delta}$, (123)], and three other compounds are shown in the interior of the diagram (DeLee).

B. METHODS OF PREPARATION

In this section three methods of preparation will be described, namely, the solid state, the coprecipitation, and the sol-gel techniques (Hatfi). The widely used solid-state technique permits off-the-shelf chemicals to be directly calcined into superconductors, and it requires little familiarity with the subtle physicochemical processes involved in the transformation of a mixture of compounds into a superconductor. The coprecipitation technique mixes the constituents on an atomic scale and forms fine powders, but it requires careful control of the pH and some familiarity with analytical chemistry. The sol-gel procedure requires more competence in analytical procedures.

In the solid-state reaction technique one starts with oxygen-rich compounds of the desired components such as oxides, nitrates, or carbonates of Ba, Bi, La, Sr, Tl, Y, or other elements. Sometimes nitrates are formed first by dissolving oxides in nitric acid and decomposing the solution at 500°C before calcination

$\text{SrCaCuO}_{7-\delta}$ (a) aluminum-doped sample calcined at and (g) calcined

the same tem-

the early work l out with thin paration tech- ch samples. n, and others entative tech-

bulk supercon- h as thin films ys of checking or subsolidus Fig. V-2 con- l-point oxides $^\circ$, (Ba_3CuO_4), 7), along the ig green phase n the interior urther, Kuzzz,). Compounds workers. The so), and then

(e.g., Davis, Holla, Kelle). These compounds are mixed in the desired atomic ratios and ground to a fine powder to facilitate the calcination process. Then these room-temperature-stable salts are reacted by calcining for an extended period (≈ 20 hr) at elevated temperatures ($\approx 900^\circ\text{C}$). This process may be repeated several times, with pulverizing and mixing of the partially calcined material at each step. As the reaction proceeds, the color of the charge changes. The process usually ends with a final oxygen anneal followed by a slow cool down to room temperature of the powder, or pellets made from the powder, by sintering in a cold or hot press. Sintering is not essential for the chemical process, but for transport and other measurements it is convenient to have the material pelletized. A number of researchers have provided information on this solid-state reaction approach (e.g., Allge, Finez, Galla, Garla, Gopal, Gubse, Hajk1, Hatan, Herrm, Hikal, Hirab, Jayar, Maen1, Mood1, Mood2, Neume, Poepp, Polle, Qadri, Rhyne, Ruzic, Saito, Sait1, Sawa1, Shamo, Takit, Tothz, Wuzz3).

Some of the earlier works on foils, thick films, wires, or coatings employed a suspension of the calcined powder in a suitable organic binder, and the desired product was obtained by conventional industrial processes such as extruding, spraying, or coating.

In the second or coprecipitation process the starting materials for calcination are produced by precipitating them together from solution (e.g., Asela, Bedno, Leez7, Wang2). This has the advantage of mixing the constituents on an atomic scale. In addition the precipitates may form fine powders whose uniformity can be controlled, which can eliminate some of the labor. Once the precipitate has been dried, calcining can begin as in the solid-state reaction procedure. A disadvantage of this method, at least as far as the average physicist or materials scientist is concerned, is that it requires considerable skill in chemical procedures.

Another procedure for obtaining the start-up powder is the sol-gel technique in which an aqueous solution containing the proper ratios of Ba, Cu, and Y nitrates is emulsified in an organic phase and the resulting droplets are gelled by the addition of a high-molecular-weight primary amine which extracts the nitric acid. This process was initially applied to the La materials, but has been perfected for YBaCuO as well (Cimaz, Hatfi).

When using commercial chemical supplies to facilitate the calcination process a dry or wet (acetone) pregrinding with an agate mortar and pestle or a ball mill is recommended. Gravimetric amounts of the powdered precursor materials are thoroughly mixed and placed in a platinum or ceramic crucible. Care must be taken to ensure the compatibility of the ceramic crucible with the chemicals to obviate reaction and corrosion problems.

Complete recipes for the YBa* material have been described (e.g., Gran2). Typically, the mixture of unreacted oxides is calcined in air or oxygen around 900°C for 15 hr. During this time the YBaCuO mixture changes color from the green Y_2BaCuO_5 phase to the dark gray $\text{YBa}_2\text{Cu}_3\text{O}_{7-\delta}$ compound. Then the charge is taken out, crushed, and scanned with X rays to determine its purity. If warranted by the powder pattern X-ray scan, the calcination process is repeated. Often, at this stage the material is very oxygen poor, and electrically it is semi-

conducting
sintered for
at $\approx 3^\circ\text{C}/\text{min}$
perature is
conductor
quenching
sand blasting
another oxide
serve the same

An examination
metric amount
ing them in
dures several
same temperature
shows the
curve.

WARNING
precautions:
the high-
oxides in air
powdered,
oxides in flow
temperature (S

Allen H.
information on
Pharmacology
antidote for
cussess case

C. ADDITIONAL

This section
the preparation

In one case
were calcined
compressive
(Graham). The
 1100°C . Still
for YBa* a
distinct from

Another
or Yb, Ba
tained sub

ired atomic
cess. Then
xtended pe-
be repeated
material at
The process
wn to room
ntering in a
ess, but for
erial pellet-
lid-state re-
jkl, Hatan,
epp, Polle,
Vuzz3).

employed a
the desired
extruding,

calcination
ela, Bedno,
n an atomic
formity can
cipitate has
re. A disad-
erials scien-
rocedures.
el technique
Cu, and Y
are gelled by
ts the nitric
is been per-

ination pro-
stle or a ball
or materials
. Care must
chemicals to

.g., Gran2).
ngen around
lor from the
d. Then the
its purity. If
is repeated.
ly it is semi-

conducting or even nonconducting. After pelletizing at $>10^5$ psi the pellet is sintered for several hours at $\approx 900^\circ\text{C}$ in flowing oxygen and then slowly cooled at $\approx 3^\circ\text{C}/\text{min}$ down to room temperature. Slow cooling from the elevated temperature is important for producing the low-temperature orthorhombic superconductor phase. The tetragonal nonsuperconducting phase may be obtained by quenching. The pellet may be used as is or it may be cut into suitable sizes by sand blasting, with a diamond saw, or with an arc. After vigorous machining another oxygen anneal (450°C , 1 hr, slow cool down) is often required to preserve the superconducting properties.

An example of preparing a Bi-based superconductor involves mixing gravimetric amounts of high-purity Bi_2O_3 , SrCO_3 , CaCO_3 , and CuO powders, calcining them in air at 750 – 890°C , regrinding them, and then repeating these procedures several times. Then pellets of the calcined product were sintered at the same temperature and quenched to room temperature (Chuz5). Figure V-1 shows the effect of sample treatment on the resistance versus temperature curve.

WARNING: As was mentioned above, thallium is a toxic material and proper precautions must be taken when working with it. It is useful to start by preparing the high-quality precursor compound BaCu_3O_4 or $\text{Ba}_2\text{Cu}_3\text{O}_5$ by reacting the oxides in air at 925°C for 24 hr. Then appropriate amounts of Tl_2O_3 are added, powdered, and pelletized. The pellet is then heated to 880 – 910°C for a few minutes in flowing oxygen, and at the onset of melting it is quenched to room temperature (Shen1).

Allen Hermann has suggested consulting the following references for information on thallium poisoning and antidotes thereto: H. Heydlauf, *Euro. J. Pharmacol.* 6, 340 (1969), which discusses thallium poisoning and describes the antidote ferric cyanoferrate, and *Int. J. Pharmacol.* 10, 1 (1974), which discusses cases of thallium intoxication treated with Prussian Blue.

C. ADDITIONAL COMMENTS ON PREPARATION

This section will treat some additional methods which have been employed for the preparation of samples.

In one experiment coprecipitated nitrates of La, Sr, Cu, and Na carbonate were calcined for 2 hr at 825°C , pressed into pellets, and then subjected to shock compression of ≈ 20 GPa at an estimated peak temperature of $\approx 1000^\circ\text{C}$ (Graha). The best superconductivity was observed after 1 hr of air exposure at 1100°C . Shock compression fabrication has also been reported (Murrz, Murr1) for YBa_* and other rare-earth derivatives. This process produced "monoliths," distinct from the usual composites.

Another technique involved the formation of a precursor alloy of Eu, Ba, Cu or Yb, Ba, Cu by rapid solidification, with the superconducting materials obtained subsequently by oxidation (Halda). A novel method involved preparing

the superconductors from molten Ba-Cu oxides and solid rare-earth-containing materials. In principle this process may be better controlled and complicated shapes can be molded or cast (Herma).

Pulsed current densities of $300\text{--}400\text{ Å/cm}^2$ with rise times of $0.6\text{ }\mu\text{sec}$ at room temperature were used to convert the weakly semiconducting phase of YBaCuO to the stable metallic phase (Djure, Djur1).

A claim was made that thermal cycling from cryogenic temperatures to 240 K raised the T_c of YBa* and YBaCuO-F (with some F substituting for O) to 159 K. Cycling above 140 K lowered T_c . This cycling process could possibly change the density of twins and thereby enhance T_c .

A freeze-drying technique was reported as producing sintered materials homogeneous in composition and small in porosity (Stras). The low-temperature firing of oxalates ($T < 780^\circ\text{C}$) has also been reported as producing a homogeneous material of small grain size (Manth).

Both Bi and Pb act as fluxes during the sintering process (Kilco). Bismuth substitution appears to reduce the normal state resistivity by about an order of magnitude without affecting the superconducting properties.

A convenient method of separating the superconducting particles from a powdered mixture using magnetic levitation has been reported (Barso). This may be used to select the superconducting fraction after each calcination process.

D. FILMS

The new ceramic oxide superconductors presently lack mechanical properties such as ductility which are needed for high-current applications like magnet wire fabrication (Jinzz-Jinz3) and power transmission. To circumvent some of these deficiencies for microelectronic applications one can prepare thin films on suitable substrates. Some devices such as Josephson junctions require thin superconducting films. Many workers have discussed the preparation and properties of LaSrCuO- (e.g., Adach, Delim, Kawas, Koinu, Matsu, Nagat, Naito, Tera1) and YBaCuO- (e.g., Burbi, Charz, Evett, Gurvi, Hause, Hongz, Inamz, Kwozz, Kwoz1, Manki, Scheu, Somek, Wuzz4) type films.

Almost every conceivable thin-film deposition technique such as electron beam evaporation, molecular beam epitaxy, sputtering, magnetron, laser ablation, screening, and spraying has been tried with the copper oxide system. Some of these techniques require expensive, elaborate apparatus, although descriptions of simple thin-film deposition systems are also available (e.g., see Koin1). Some representative examples of deposition procedures will be discussed.

Epitaxial films of $\text{YBa}_2\text{Cu}_3\text{O}_{7-\delta}$ on (100) SrTiO_3 were produced using three separate electron beam sources (e.g., Chaud, Chau1, Laibo). The deposition was done in $10^{-4}\text{--}10^{-3}$ torr O_2 with a substrate temperature of 400°C . The deposited films were atomically amorphous with a broad X-ray peak. The epitaxial ordering was achieved upon annealing in O_2 at 900°C with the orthorhombic c axis essentially perpendicular to the plane.

High-quality beam to evaporate torr (Hammo, Cited film in oxygen 750°C for 1 hr, furnace.

Superconducting (Ma was Ar or an Ar 10^{-7} torr and, v $\text{ZrO}_2\text{--}9\%\text{ Y}_2\text{O}_3$ films. The films gen annealing. Properties depended conditions, con

Films of dysprosium beam epitaxy (process was monitored copper was incorporated amorphous Ba high-temperatu

Films of $\text{Y}_{1-x}\text{Ba}_x\text{Cu}_3\text{O}_{7-\delta}$ with thickness of 500 Å deposited on SrTiO_3 pellet of YBaCuO. The evaporation rate was 6 Hz , $\approx 30\text{ nsec}$ heated to 450°C they appeared oxygen annealed hours. Standard superconductivity achieved LaSr* (Moorj)

Films were deposited and Cu in layers at 200°C and 10^{-4} torr layers to diffuse superconducting composite conductivity with Y_2O_3 , and Ba

Some $5000\text{--}10000\text{ Å}$ vacuum dc-magnetron was 0.2 Å/sec substrate distance

orth-containing
and complicated

0.6 μ sec at room
temperature of YBaCuO

temperatures to 240 K
(or O) to 159 K.
It changes the

of materials how
low-temperature
is a homogeneous

(silico). Bismuth
out an order of

isles from a pow-
er). This may be
in process.

nical properties
like magnet wire
at some of these
in films on suit-
able thin super-
conducting and properties
(t, Naito, Tera1)
Inamz, Kwozz,

such as electron
beam, laser abla-
tion system. Some
though descrip-
tion, see Koin1).
discussed.

used using three
The deposition
400°C. The de-
position. The epitaxial
orthorhombic c

High-quality superconducting films were obtained using a multiple electron beam to evaporate metallic sources in a flow of molecular oxygen at $4-5 \times 10^{-6}$ torr (Hammo, Ohzzz). The deposition rate was 10 Å/sec. To anneal the deposited film in oxygen it was heated for 3-6 hr in a flow of oxygen at 650°C, raised to 750°C for 1 hr, then to 850°C for 1 hr, and finally slowly cooled down in the furnace.

Superconducting films were prepared using a double ion beam sputtering arrangement (Madak). The target beam was Ar at 40 mA, and the substrate beam was Ar or an Ar-O₂ mixture at 10-500 eV and 2 mA. The base pressure was 5×10^{-7} torr and, with the gas, 4×10^{-4} torr. The best substrate materials such as ZrO₂-9% Y₂O₃ did not appreciably interact, diffuse, or change the deposited films. The films were $\approx 1 \mu$ m thick and were rendered superconducting by oxygen annealing. Zero resistance was attained at 88 K. The superconducting properties depended upon the ion beam energy, substrate temperature, annealing conditions, composition, and the extent of poisoning from the substrate.

Films of dysprosium barium copper oxide were grown (Webbz) by molecular beam epitaxy (MBE) using a Varian 360 MBE system, and the nucleation process was monitored by reflection high-energy electron diffraction (RHEED). The copper was incompletely oxidized in metallic microcrystals growing in a sea of amorphous Ba and Dy. After deposition superconducting films were obtained by high-temperature oxygen annealing.

Films of Y_{1.1}Ba_{1.5}Cu₃O_{6.4} approximately 3300 Å thick with a surface roughness of 500 Å were prepared (Dijkk, Inamz, Wuzz4). These films were deposited on SrTiO₃, sapphire, and vitron carbon by evaporation from a single bulk pellet of YBaCuO 1 cm diameter and 0.2 cm thick at a pressure of 5×10^{-7} torr. The evaporation was produced by several thousand pulses of laser irradiation (3-6 Hz, ≈ 30 nsec width, 1 J/pulse, 2 J/cm²). For best results the substrate was heated to 450°C. As deposited thin films were well bonded to the substrate and they appeared shiny dark brown and were electrically insulating. The films were oxygen annealed at 900°C for 1 hr and then slowly cooled over a period of several hours. Standard four-probe resistivity measurements indicated the onset of superconductivity around 95 K and, for a (100) SrTiO₃ substrate, with zero resistivity achieved near 85 K. The laser ablation technique was also employed for LaSr* (Moorj) and YBa* (Nara1).

Films were obtained from sandwiched multilayers by depositing Y₂O₃, BaO, and Cu in layers (Nasta, Tsaur) on ZrO₂, MgO, and sapphire substrates at 200°C and 10^{-5} torr. Oxygen treatment for 1-2 hr at $\approx 850^\circ\text{C}$ permitted the layers to diffuse, homogenize, and oxygenate, and thereby form the superconducting compound (Baozz). Films on Ni have also been reported in which superconductivity was obtained by a diffusion process involving the Cu substrate, Y₂O₃, and BaCO₃ composite (Tachi).

Some 5000-Å thick films of YBaCuO have been deposited using an ultrahigh vacuum dc-magnetron getter-sputter deposition system. The deposition rate was 0.2 Å/sec, the substrate temperature was 1050°C, and the target-to-substrate distance was 12 cm. The scattering was done in an Ar-O₂ atmosphere.

The X-ray and electron microscope examinations indicated some variation among the substrates arranged on the heater. Inhomogeneities were observed even within the film made on a single substrate. As deposited the films were oxygen deficient, and annealing produced suitable compositions. The reversible oxygen incorporation was monitored by the systematic splitting of the strongest X-ray peaks. The oxygen diffusion coefficient at 600°C was 10^{-15} m²/sec and the activation energies for desorption and absorption were 1.1 and 1.7 eV, respectively. The highest onset temperature was 99 K with complete superconduction at 40 K. Exposure to water inhibited the superconductor (Barns, Kishi, Yanzz). A device structure with a Y₂O₃ barrier has also been studied (Blami).

Another work showed that films produced by dc magnetron sputtering are copper deficient if the substrate-to-target distance is large or if the substrate is at an elevated temperature (Leez5).

Superconducting YBaCuO thin films with a large surface area (≈ 5 cm \times 5 cm) were grown on Al₂O₃, sapphire, and MgO up to a 500°C substrate temperature by magnetron and diode techniques. Rutherford back scattering (RBS) indicated a uniform composition across magnetron-deposited film areas with diameters up to 5 cm, and the diode film composition homogeneity was even better, but over a smaller area (≈ 2.5 cm diameter). The as-deposited films were annealed in oxygen at different temperatures and exposure times. Prolonged high-temperature annealing ($> 850^\circ\text{C}$) increased the impurity phase. The highest T_c films had a wide range of composition, with the maximum T_c film copper rich. On the basis of an in-situ resistivity study of YBa* thin films a rapid heating to about 900°C in flowing helium followed by slow cool down in flowing oxygen was recommended (David).

The post-deposition anneal cycle was avoided by producing the films in a high-pressure reactive evaporation process involving rapid thermal annealing (Lathr). Smooth films were obtained on zirconia and SrTiO₃ substrates. Screen printing of oxide superconducting films is also possible (Budha, Fuzz1), and simple spray deposition has been reported (Gupta). Films have also been made by coating and spinning off the solutions. Aqueous and aqueous-alcoholic mixed solutions of the metal nitrates (Coop2), metal acetates in dilute acetic acid (Rice1), and sol-gels (Kram1) have all been reported. These processes are potentially important for commercial superconducting coatings on silicon (Kram1), on yttrium-stabilized zirconia (YSZ), on SrTiO₃ (Coop2, Gupta), and on MgO (Gupta, Rice1).

E. SINGLE CRYSTALS

The bulk properties of oxide superconductors are averages over components parallel and perpendicular to the Cu-O planes. In addition, for orthorhombic samples there is an averaging over properties that differ for the a and b directions in this plane. This in-plane anisotropy is especially pronounced for the YBa* 123 structure in which the Cu-O-Cu-O chains lie along the b axis. The

best way to u
crystals. Und
anisotropy ca
twinning pro
gle crystals.

A numbe
X-ray diffrac
(e.g., Crabt,
and micro-R
scribe how s
Crystal Grov

Millimete
oxide flux (
Taka4, Zhoi
contaminati
a hot press (
(Satoz).

Small sing
der which w
sphere and t
ture also pro
melting a st
followed by

A gold cr
(1 \times 2 \times 0.
was heated i
400°C at 25'
on the surfa
the crucible

A detaile
crystal by th
1:3 and 2:5
multistep te
found at the
crucibles. P
crucibles we
ported. A s
DyBa* as la

F. ALIGNI

Clearly high
of supercon

some variation were observed in the films were. The reversible of the strongest m^2/sec and the 1.7 eV, respectively (Kishi, Yanzz). sputtering are a substrate is at

area ($\approx 5 \text{ cm} \times$ substrate temperature. Sputtering (RBS) in areas with density was even better. sited films were mes. Prolonged base. The high- T_c film copper ns a rapid heat- in flowing oxy-

g the films in a normal annealing substrates. Screen (a, Fuzz1), and also been made reous-alcoholic dilute acetic acid esses are potential silicon (Kram1),), and on MgO

ver components or orthorhombic a and b directions for the b axis. The

best way to understand these materials is through experiments on perfect single crystals. Unfortunately, untwinned YBa* crystals are not available so the a, b anisotropy cannot be resolved. Tetragonal superconductors should not have this twinning problem. In this work twinned monocrystals will be referred to as single crystals.

A number of experiments have been carried out on monocrystals such as X-ray diffraction (e.g., Borde, Hazen, Lepad, Siegr, Onoda), magnetic studies (e.g., Crabt, Schn1, Worth), mechanical measurements (e.g., Cookz, Dinger), and micro-Raman spectroscopy (e.g., Hemle). In this section we will briefly describe how such crystals are made. The December 1987 issue of the *Journal of Crystal Growth* was devoted to superconductors.

Millimeter-size $(\text{La}_{1-x}\text{Sr}_x)_2\text{CuO}_4$ single crystals were grown in a molten copper oxide flux (Kawa1). Another basic technique employs other fluxes (Haned, Taka4, Zhou1), namely, PbF_2 , B_2O_3 , PbO , PbO_2 , with the risk of possible Pb contamination. LaSr* crystals were also grown by the solid phase reaction using a hot press of pellets (Iwazu) and rapid quenching of a nonstoichiometric melt (Satoz).

Small single crystals of $\text{YBa}_2\text{Cu}_3\text{O}_{7-\delta}$ have been prepared from a sintered powder which was formed into a pellet and then heated, first in a reducing atmosphere and then in an oxidizing one at 925°C . Annealing a stoichiometric mixture also produced monocrystals (Liuzz). Millimeter-size crystals were grown by melting a stoichiometric mixture of $\text{YBa}_2\text{Cu}_3\text{O}_{7-\delta}$ plus excess CuO at 1150°C followed by holding at 900°C for 4 days (Damen, see also Fine1).

A gold crucible on a gold or alumina sheet was used to obtain free-standing ($1 \times 2 \times 0.1 \text{ mm}$) single crystals of YBa* (Kaise, Kais1, Holtz). A charge of 2 g was heated in air at $200^\circ\text{C}/\text{hr}$ and held at 975°C for 1.5 hr, then it was cooled to 400°C at $25^\circ\text{C}/\text{hr}$. The molten charge creeps and forms single crystals and twins on the surfaces. The larger crystals formed in the space between the bottom of the crucible and the gold support sheet.

A detailed account has appeared of the preparation of a 123 compound single crystal by the flux method (Zhou1). The flux mole ratio $\text{BaO}_2:\text{CuO}$ was between 1:3 and 2:5, and the nutrient $\text{Y}_2\text{O}_3:\text{BaO}_2:\text{CuO}$ mole ratios were 0.5:2:3. A multistep temperature process was employed. Black single crystals of YBa* were found at the bottom and at the edge between the wall and the bottom of the crucibles. Platinum crucibles seemed to contaminate the samples so alumina crucibles were recommended. Crystals as large as $2 \times 2 \times 0.3 \text{ mm}^3$ were reported. A similar technique was used to produce single crystals of YBa* and DyBa* as large as 4 mm (Schn1).

F. ALIGNED GRAINS

Clearly high-quality single crystals are important for understanding the physics of superconductors. However, much useful information about anisotropies can

be obtained by studying the properties of aligned grains, which are much easier to fabricate.

A superconducting sample can be initially a collection of randomly oriented grains, but various techniques can be used to partially orient these grains so that the *c* axis lies preferentially in a particular direction. For example uniaxial compression tends to orient compacted grains, with compressed 90- μm particles exhibiting more alignment than compressed 10- μm particles (Glowa). Epoxy-embedded grains have been aligned under the influence of an applied magnetic field and pressure (Arend).

X-ray and magnetic measurements have been reported on aligned crystalline grains of YBa* (Farr1). Optical studies have also been made on aligned grains. The critical current density for samples cut parallel to the compression axis of such grains was nearly isotropic with respect to the direction of an applied magnetic field, and it was a factor of 6 smaller than that for the samples cut perpendicular to this axis (Glowa).

G. REACTIVITY

The oxide superconductors are not inert materials, but rather they are sensitive to exposure to certain gases and to surface contact with particular materials. Great care must be exercised to avoid contamination from water vapor and carbon dioxide in the atmosphere. In addition these materials are catalytic to oxygenation reactions, and these factors result in the occurrence of various chemical and other interactions, especially at elevated temperatures. The granular and porous nature of the materials has an accelerating effect on such reactions.

Samples of YBaCuO may degrade in a matter of days when exposed to an ordinary ambient atmosphere; they react readily with liquid water, acids, and electrolytes, and moderately with basic solutions. The reaction with water (Barns, Kishi, Yanzz) produces nonsuperconducting cuprates. The effects of acetone and other organics (McAnd) have been determined, and stable carboxyl groups have been found in the YBaCuO lattice (Parmi).

Hydrogen enters the YBaCuO lattice at elevated temperatures and forms a solid solution. Low concentrations have very little effect and high concentrations degrade the superconducting properties (Berni, Reill, Yang3). The effects of exposure to oxygen at elevated temperature and oxidation have been discussed several places in this review (e.g., Blend, Engle, Tara3).

The foregoing evidence for the reactivity of the oxide superconductors makes it necessary to consider methods of passivation or protecting them from long-term degradation. An epoxy coating was found to provide some protection (Barns). Coating the surface with metals can be deleterious since metals such as Fe (Gaoz1, Hillz, Weave) and Ti (Meyel) react with the surface of LaSrCuO or YBaCuO. There is evidence for the passivation of the surface of LaSr* with gold (Meyer).

H. THERM

Thermogra
ple during
oxygen con
an oxidizin
procedures
the method
John4, Lee
ferential th
procedures

I. CHECK

After a san
conductor.
mine whetl
supercondu
ity sample.
the magne
sharp, high
-1/4 π . Tl
of the susc
the fraction

In addit
chemical co
tion is dedu
material. (C
XPS, elect
probe that
investigato
tent is muc
back-scatter
tents, and

The stru
ily checked
constants a
or orthorho
indicate a g
for LaSr* (C
used to cor

H. THERMOGRAVIMETRIC ANALYSIS

Thermogravimetric analysis (TGA) consists of monitoring the weight of a sample during a heating or cooling cycle. For example, one might determine the oxygen content of a superconducting material by measuring its weight change in an oxidizing (O_2 or air) or reducing (e.g., 4% H_2 in Ar) atmosphere. Typical procedures consist of heating or cooling at $20^\circ C/min$. The relative accuracy of the method is about 0.005 (Ongz1). Many workers (e.g., Beye3, Hauck, Huan1, John4, Leez7, Maruc, Ohish, Ongz1, Tara7, Zhuzz) are now using TGA or differential thermal analysis (DTA) routinely during their sample preparation procedures.

I. CHECKS ON QUALITY

After a sample has been prepared it is necessary to check its quality as a superconductor. Most investigators employ the four-probe resistivity check to determine whether it superconducts, and at what temperature it transforms to the superconducting state. A sharp, high T_c transition is an indicator of a high-quality sample. Another widely used quality control method is the determination of the magnetic susceptibility of the specimen. Good quality is indicated by a sharp, high T_c transition with both the flux exclusion and flux expulsion close to $-1/4\pi$. This is, in a sense, a more fundamental check on quality since the value of the susceptibility far below the transition temperature is a good indicator of the fraction of the sample that is superconducting (see Section III-D).

In addition to its superconducting properties, it is also of interest to know the chemical composition and the structure of the specimen. The nominal composition is deduced from the relative proportions of the various cations in the starting material. Chemical analysis and some more sophisticated techniques such as XPS, electrospectroscopic chemical analysis (ESCA), and an electron microprobe that is favorable for low-atomic-weight elements are applicable here. Most investigators only report the cation concentrations in the specimen. Oxygen content is much more difficult to determine, but is important to know. Rutherford back-scattering experiments (John1, Wuzz1, Wuzz4) can provide oxygen contents, and metallography characterizes grain sizes.

The structures of the oxide superconductors described in Chapter VI are easily checked by the X-ray powder pattern method. Many articles list the lattice constants a , b , c of samples and mention whether they are tetragonal ($a = b \neq c$) or orthorhombic ($a \approx b \neq c$). Narrow lines and the absence of spurious signals indicate a good, single-phase sample. Typical X-ray diffraction powder patterns for $LaSr^*$ (Skelt) and YBa^* presented in Figs. V-3 and V-4, respectively, may be used to compare with patterns obtained from freshly prepared samples.

h easier

oriented
s so that
ial com-
icles ex-
Epoxy-
magnetic

ystalline
l grains.
1 axis of
ed mag-
perpen-

sensitive
aterials.
and car-
c to oxy-
chemical
ular and
tions.
ed to an
ids, and
th water
cts of ac-
carboxyl

l forms a
ntrations
cts of ex-
ssed sev-

rs makes
om long-
rotection
ls such as
SrCuO or
with gold

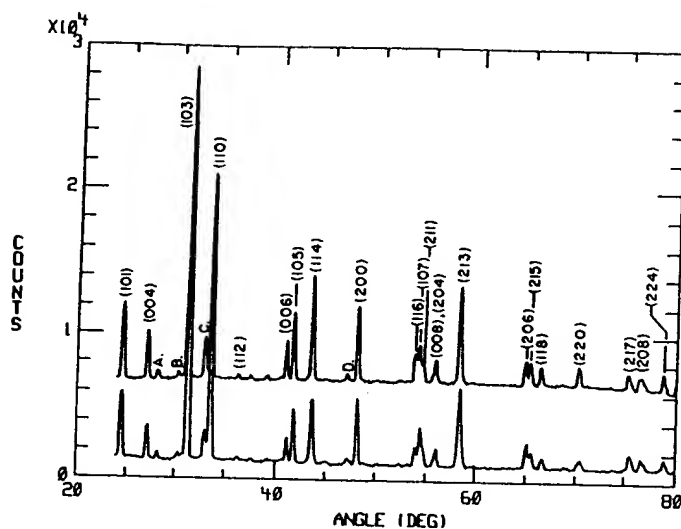


Fig. V-3. Room-temperature (upper curve) and 24-K (lower curve) X-ray diffraction powder patterns of $(\text{La}_{0.925}\text{Ba}_{0.075})_2\text{CuO}_4$ (Skelt).

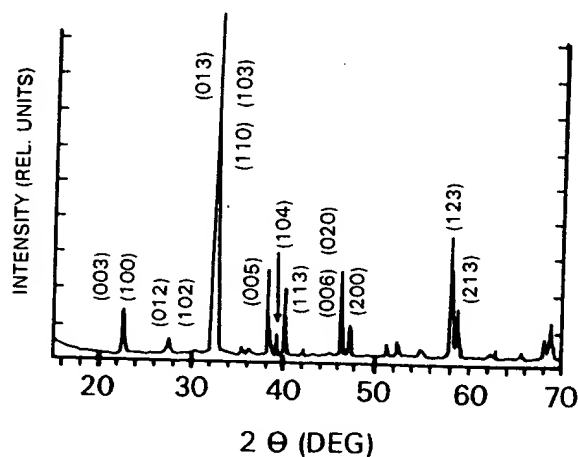


Fig. V-4. Room-temperature X-ray diffraction powder pattern of $\text{YBa}_2\text{Cu}_3\text{O}_7$. (Provided by C. Almasan, J. Estrada, and W. E. Sharp.)

J. RESIS

A measur
temperati
becomes
sharp dro
to apply a
such a tw
Most resi
described
method (I
silver glaz
portance
port J_c m

The sp
in a suita
probe con
and out o
between t
conductin
with the c
ment volt

J. RESISTIVITY MEASUREMENT

A measurement of the resistance $R(T)$ or resistivity $\rho(T)$ of a material versus the temperature is the principal technique employed to determine when a material becomes superconducting. The transition temperature manifests itself by a sharp drop in resistivity to zero. The simplest way to make this measurement is to apply a voltage across the sample and measure the current flow through it, but such a two-probe method (Baszy) is not very satisfactory, and is seldom used. Most resistivity determinations are made with the four-probe technique to be described below, although more sophisticated arrangements such as a six-probe method (Kirsch) can also be used. The fabrication of low-resistance contacts by silver glazing has been reported (Vand2). These researchers pointed out the importance of a low-contact resistance ($\rho < 10 \mu\Omega/\text{mm}^2$ at 77 K) for making transport J_C measurements.

The specimen resistance as a function of temperature is generally determined in a suitable cryostat by attaching leads or electrodes to it in the standard four-probe configuration. Two leads or probes carry a known constant current I into and out of the specimen, and the other two leads measure the potential drop between two equipotential surfaces resulting from the current flow. For superconducting specimens the leads are often arranged in a linear configuration, with the contacts for the input current on the ends, and those for the measurement voltage near the center.

ray diffraction

U_3O_7 . (Provided

T. J. WATSON RESEARCH CENTER LIBRARY

BRIEF ATTACHMENT AG

IN THE UNITED STATES PATENT AND TRADEMARK OFFICE

In re Patent Application of

Applicants: Bednorz et al.

Serial No.: 08/479,810

Filed: June 7, 1995

For: NEW SUPERCONDUCTIVE COMPOUNDS HAVING HIGH TRANSITION
TEMPERATURE, METHODS FOR THEIR USE AND PREPARATION

Date: March 14, 2005

Docket: YO987-074BZ

Group Art Unit: 1751

Examiner: M. Kopec

Commissioner for Patents
P.O. Box 1450
Alexandria, VA 22313-1450

THIRD SUPPLEMENTAL AMENDMENT

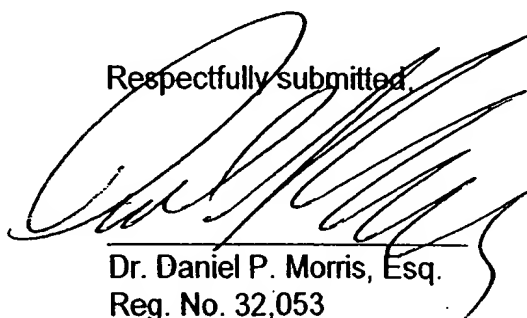
Sir:

In response to the Office Action dated July 28, 2004, please consider the
following:

The attachments referred to herein A to Z and AA are in the FIRST
SUPPLEMENTAL AMENDMENT. The Attachments AB to AG are attached herein.

Please charge any fee necessary to enter this paper and any previous paper to
deposit account 09-0468.

Respectfully submitted,



Dr. Daniel P. Morris, Esq.
Reg. No. 32,053
(914) 945-3217

IBM CORPORATION
Intellectual Property Law Dept.
P.O. Box 218
Yorktown Heights, New York 10598

ATTACHMENT AG

CONDUCTIVITY

TS

ERCONDUCTIVITY

DUCTIVITY

The New Superconductors

Frank J. Owens

*Army Armament Research Engineering and Development Center
Picatinny, New Jersey
and Hunter College of the City University of New York
New York, New York*

and

Charles P. Poole, Jr.

*Institute of Superconductivity
University of South Carolina
Columbia, South Carolina*

on order will bring delivery of
d only upon actual shipment.

Plenum Press • New York and London

Library of Congress Cataloging-in-Publication Data

On file

ISBN 0-306-45453-X

© 1996 Plenum Press, New York
A Division of Plenum Publishing Corporation
233 Spring Street, New York, N. Y. 10013

10 9 8 7 6 5 4 3 2 1

All rights reserved

No part of this book may be reproduced, stored in a retrieval system, or transmitted in any form or by any means, electronic, mechanical, photocopying, microfilming, recording, or otherwise, without written permission from the Publisher

Printed in the United States of America

Table 8.1. Progress in Raising the Superconducting Transition Temperature T_c Since the Discovery of Cuprates in 1986

Material	T_c (K)	Year
$\text{Ba}_x\text{La}_{5-x}\text{Cu}_5\text{O}_9$	30–35	1986
$(\text{La}_{0.9}\text{Ba}_{0.1})_2\text{Cu}_4\text{O}_{4-x}$ (at 1-GPa pressure) ^a	52	1986
$\text{YBa}_2\text{Cu}_3\text{O}_{7-x}$	95	1987
$\text{Bi}_2\text{Sr}_2\text{Ca}_2\text{Cu}_3\text{O}_{10}$	110	1988
$\text{Tl}_2\text{Ba}_2\text{Ca}_2\text{Cu}_3\text{O}_{10}$	125	1988
$\text{Tl}_2\text{Ba}_2\text{Ca}_2\text{Cu}_3\text{O}_{10}$ (at 7-GPa pressure)	131	1993
$\text{HgBa}_2\text{Ca}_2\text{Cu}_3\text{O}_{8+x}$	133	1993
$\text{HgBa}_2\text{Ca}_2\text{Cu}_3\text{O}_{10}$ (at 30-GPa pressure)	147	1994

^aA pressure of 1 GPa is about 10,000 atm.

While this increase in T_c itself is an amazing result, a high-transition temperature is not the only property required to make new compounds useful for applications. For example if materials are to be used as wires in magnets, they must be malleable and ductile rather than brittle; in addition they must have high critical currents in large magnetic fields. Critical currents as high as those in niobium-tin have not yet been achieved in forms of the new materials that can easily be made into wires, although there are reports of comparable values in thin films on various substrates.

The Holy Grail that is being sought is a transition temperature much above room temperature. We say much above because devices must operate significantly below the transition T_c so that the critical current J_c and critical magnetic field B_c are sufficiently high. Very close to the transition temperature, the critical magnetic field is usually quite small, but we see from Figs. 3.4 and 3.5 that B_c and J_c continuously increase as the temperature is lowered below T_c . We need an operating temperature far below the critical surface in Fig. 3.15 so that both B_c and J_c are sufficiently large for the desired application.

8.3. LAYERED STRUCTURE OF THE CUPRATES

All cuprate superconductors have the layered structure shown in Fig. 8.1: The flow of supercurrent takes place in conduction layers, and binding layers support and hold together the conduction layers. Conduction layers contain copper-oxide (CuO_2) planes of the type shown in Fig. 8.2; each copper ion (Cu^{2+}) is surrounded by four oxygen ions (O^{2-}). These planes are held together in the structure by calcium (Ca^{2+}) ions located between them, as indicated in Fig. 8.3. An exception to this is the yttrium compound in which the intervening ions are the element yttrium (Y^{3+}) instead of calcium. These CuO_2 planes are very close to being flat. In the normal state above T_c , conduction electrons released by copper atoms move about on these

Figure 8.1. Layering scheme for different sequences for several cuprates.

Figure 8.2. Arrangement in a CuO_2 plane of the con

Transition Temperature T_c
in 1986

Year
1986
1986
1987
1988
1988
1993
1993
1994

t, a high-transition temperature superconductor useful for applications in magnets, they must be able to have high critical temperature as those in niobium-tin superconductors that can easily be made in thin films on various substrates.

At a temperature much above the transition temperature, the superconductor must operate significantly below the critical magnetic field B_c . At low temperature, the critical magnetic field is about 0.4 and 3.5 that B_c and J_c are low. We need an operating temperature so that both B_c and J_c are high.

ES

As shown in Fig. 8.1: The conduction and binding layers support the structure. The conduction layers contain copper-oxide planes. The copper ion (Cu^{2+}) is surrounded in the structure by calcium ions. An exception to this is the element yttrium (Y^{3+}) which is being flat. In the normal state, the atoms move about on these planes.

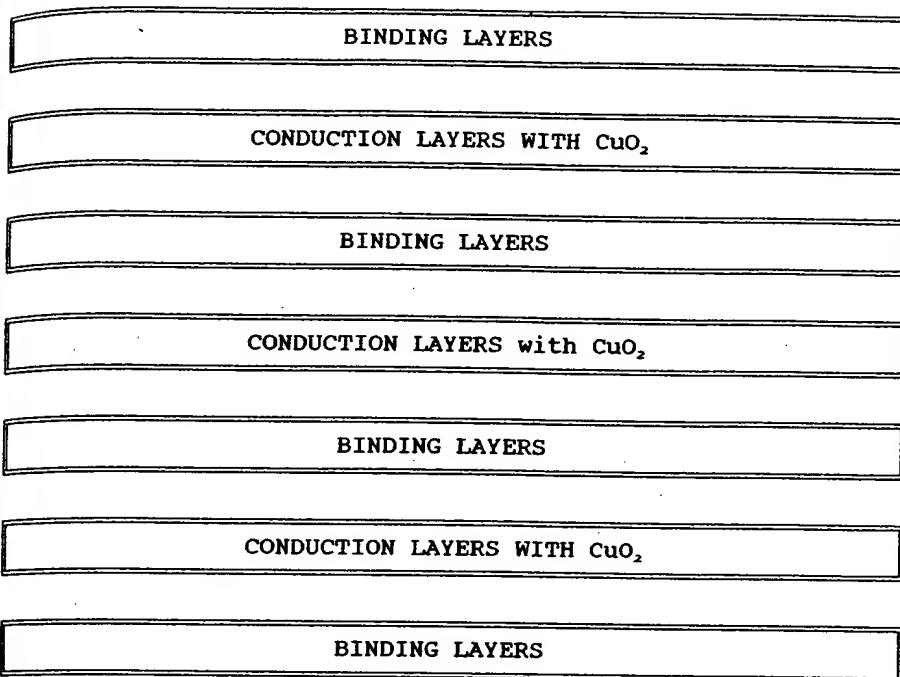


Figure 8.1. Layering scheme of the cuprate superconductors. Figure 8.3 shows details of the conduction layers for different sequences of copper oxide planes, and Fig. 8.4 presents details of the binding layers for several cuprates.

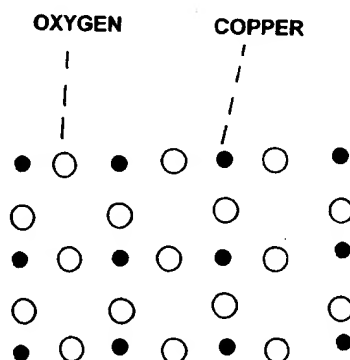
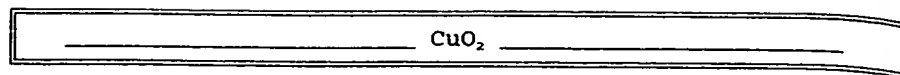
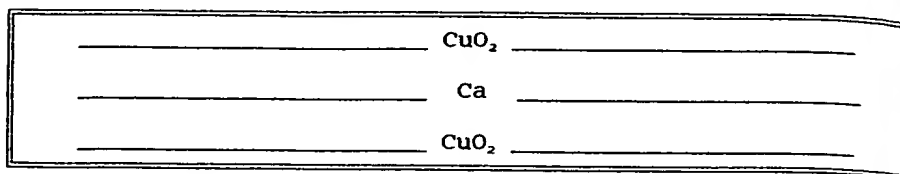


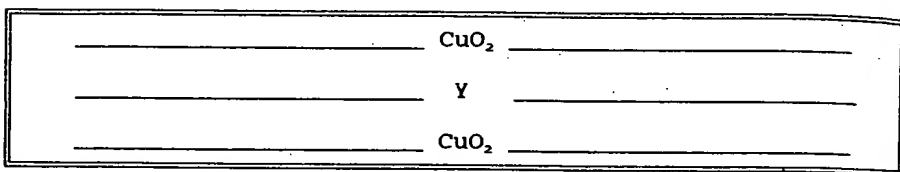
Figure 8.2. Arrangement of copper and oxygen atoms in a CuO_2 plane of the conduction layer.



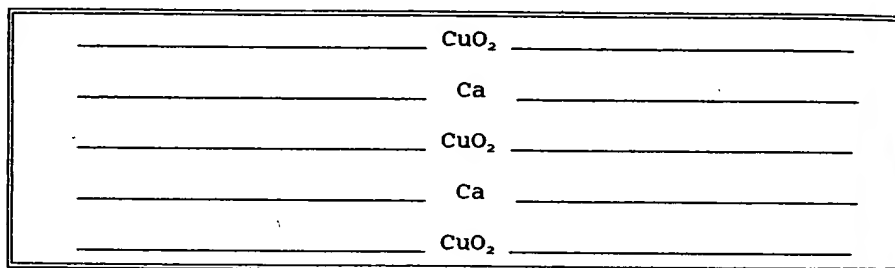
Conduction layer with one copper oxide plane



Conduction layer with two copper oxide planes



Conduction layer of yttrium compound with two copper oxide planes

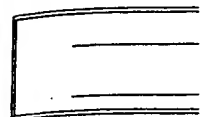


Conduction layer with three copper oxide planes

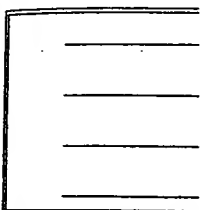
Figure 8.3. Conduction layers of the various cuprate superconductors showing sequences of CuO_2 and Ca (or Y) planes in the conduction layers of Fig. 8.1.

CuO_2 planes carrying electric current. In the superconducting state below T_c , these same electrons form the Cooper pairs that carry the supercurrent in the planes.

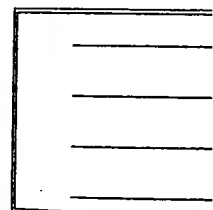
Each particular cuprate compound has its own specific binding layer consisting mainly of sublayers of metal oxides MO, where M is a metal atom; Fig. 8.4 gives the sequences of these sublayers for the principal cuprate compounds. These binding layers are sometimes called *charge reservoir layers* because they contain



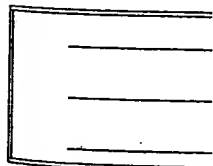
Neodyn



Bismu



Thalli



Mercur

Figure 8.4. Sequences of metal ions. The parent

CHAPTER 8

oxide plane

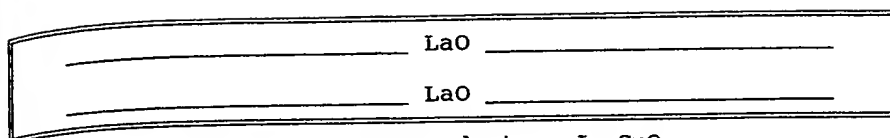
oxide planes

two copper oxide planes

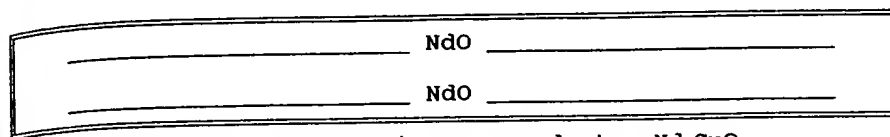
oxide planes

ctors showing sequences of CuO_2 and

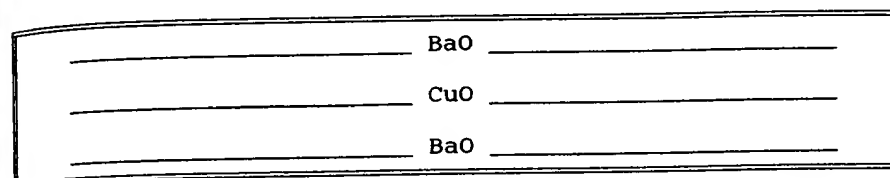
conducting state below T_c , these supercurrent in the planes. specific binding layer consisting is a metal atom; Fig. 8.4 gives 1 cuprate compounds. These *ir layers* because they contain



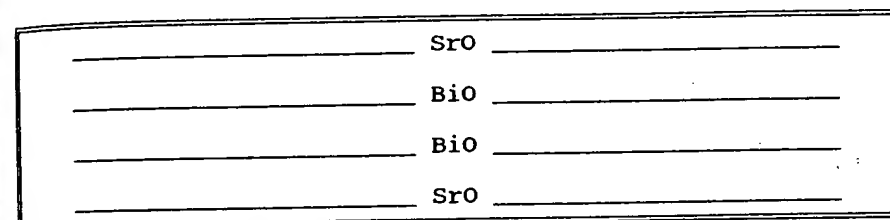
Lanthanum Superconductor La_2CuO_4



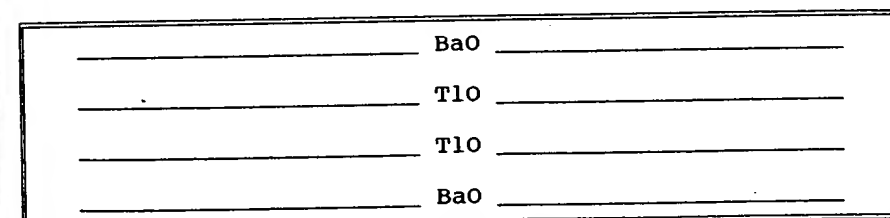
Neodymium (electron) Superconductor Nd_2CuO_4



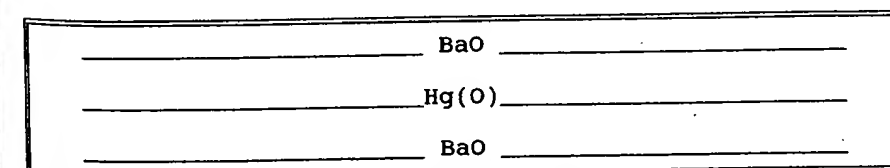
Yttrium Superconductor $\text{YBa}_2\text{Cu}_3\text{O}_7$



Bismuth Superconductor $\text{Bi}_2\text{Sr}_2\text{Ca}_{n-1}\text{Cu}_n\text{O}_{2n+4}$



Thallium Superconductor $\text{Tl}_2\text{Ba}_2\text{Ca}_{n-1}\text{Cu}_n\text{O}_{2n+4}$



Mercury Superconductor $\text{HgBa}_2\text{Ca}_{n-1}\text{Cu}_n\text{O}_{2n+2}$

Figure 8.4. Sequences of MO sublayers in the binding layers of Fig. 8.1, where M stands for various metal ions. The parentheses around the oxygen atom O in the lowest panel indicates partial occupancy.

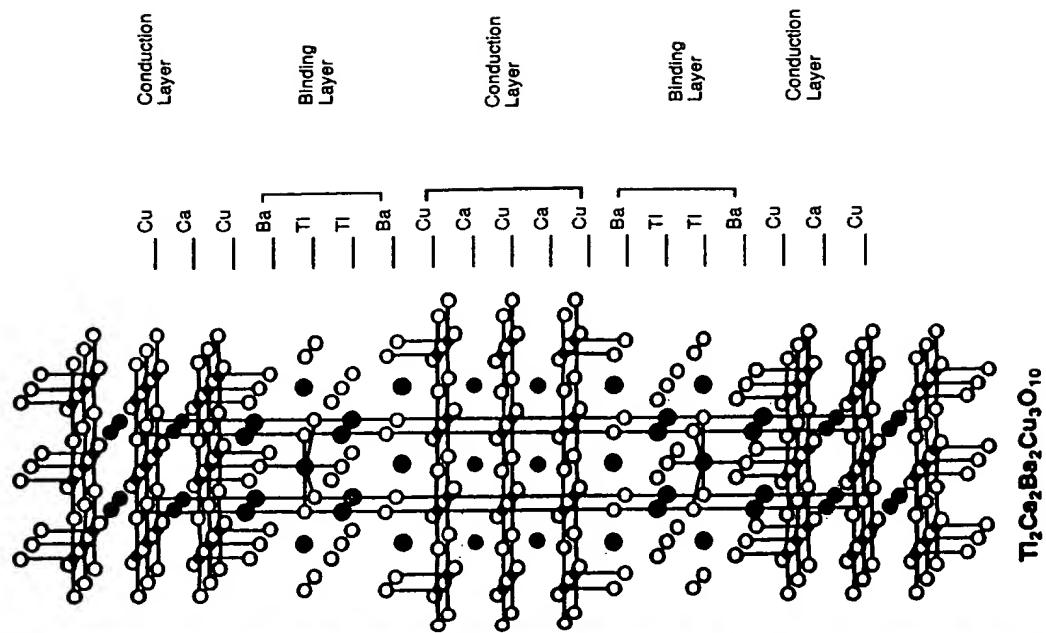
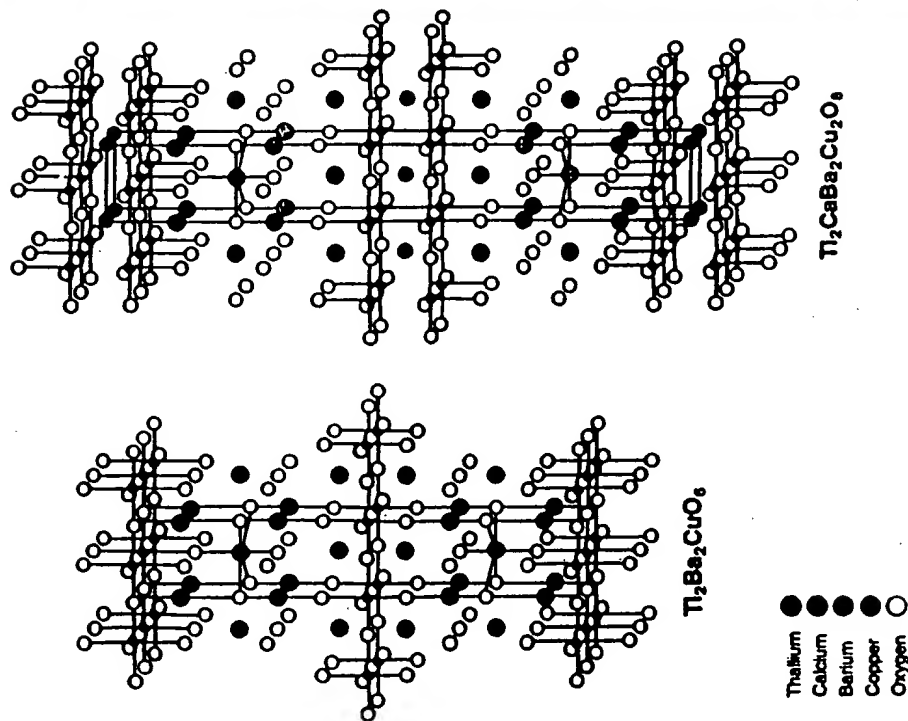


Figure 8.5. (Continued)

Figure 8.5. Layering schemes of three thallium compound superconductors $\text{Tl}_2\text{Ba}_2\text{Ca}_{n-1}\text{Cu}_n\text{O}_{2n+4}$ where there are $n = 1, 2, 3$ CuO_2 planes in the conduction layers, from left to right. (Adapted from Toraldi et al., *Science* 240, 631 (1988).)

of randomly oriented grains. In the current flow capability of

$\text{La}_{1-x}\text{Sr}_x\text{CuO}_4$ are hole-type perovskite, (Nd_{1-x} ions rather than holes. The have trivalent positive ions:

(8.6)

(8.7)

tium (Sr^{2+}) and cerium (Ce^{4+}),

CuO_4) (8.8)

La_2CuO_4) (8.9)

one extra electron to form an antiferromagnetic state. The perovskite is hole-like. Any part both of these examples of perovskite, but not identical structures; because most experiments are not

STRUCTURES

referred to as ceramics, they are perovskite refers to the particular mineral perovskite, calcium titanate. The parts of the lanthanum compound perovskite, with Cu present in the positions not shown in Fig. 8.9) positions. Similarities between these two compounds and La_2CuO_4 a perovskite-type

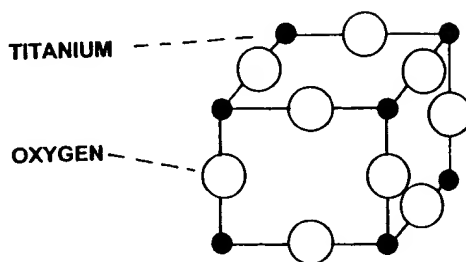


Figure 8.9. Sketch of the cubic unit cell of the mineral Perovskite, CaTiO_3 , showing titanium at the vertices and oxygen in the middle of the edges. Calcium, not shown, is in the center of the cube.

In contrast the ceramic designation is not based on structural grounds but on the similarity of the cuprate-superconducting compound and ceramic manufacturing process. For example La-Sr-Cu-O is made by heating mixtures of lanthanum oxide, strontium carbonate, and copper oxide in air at $900\text{--}1000^\circ\text{C}$ for 20 hours. Proportions of atoms in the initial mixture should be the same as in the end product, and for the compound $(\text{La}_{0.9}\text{Sr}_{0.1})_2\text{CuO}_4$ the ratio $\text{La}:\text{Sr}:\text{Cu}$ is 1.8:0.2:1. Materials are usually ground to a fine mixture before heating; after heating in air, they are cooled, pressed into pellets, and reheated from $900\text{--}1000^\circ\text{C}$ for several more hours.

We see in Fig. 8.10 that the superconductor $(\text{La}_{1-x}\text{Sr}_x)_2\text{CuO}_4$ has only one copper oxide plane in its conduction layer and each copper ion is surrounded by

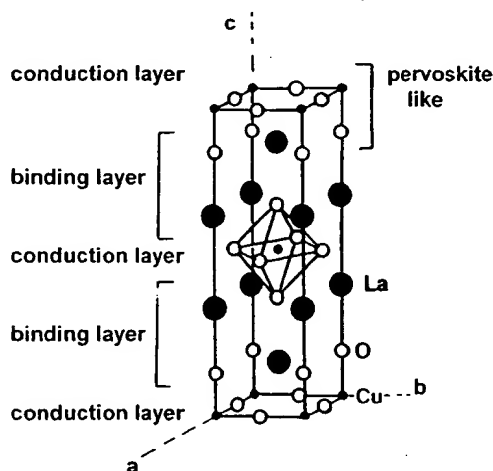


Figure 8.10. Atom positions in the tetragonal unit cell of the La_2CuO_4 compound. When strontium is substituted for lanthanum in the superconducting compound $(\text{La}_{1-x}\text{Sr}_x)_2\text{CuO}_4$ it replaces lanthanum in some of the La sites.

BRIEF ATTACHMENT AH

IN THE UNITED STATES PATENT AND TRADEMARK OFFICE

In re Patent Application of

Applicants: Bednorz et al.

Serial No.: 08/479,810

Filed: June 7, 1995

For: NEW SUPERCONDUCTIVE COMPOUNDS HAVING HIGH TRANSITION
TEMPERATURE, METHODS FOR THEIR USE AND PREPARATION

Date: March 1, 2004

Docket: YO987-074BZ

Group Art Unit: 1751

Examiner: M. Kopec

Commissioner for Patents
P.O. Box 1450
Alexandria, VA 22313-1450

FIFTH SUPPLEMENTAL AMENDMENT

Sir:

In response to the Office Action dated February 4, 2000:

ATTACHMENT 16

IN THE UNITED STATES PATENT AND TRADEMARK OFFICE

In re Patent Application of
J. Bednorz et al.

Date: December 15, 1998

Serial No. 08/303,561

Group Art Unit: 1105

Filed: September 9, 1994

Examiner: M. Kopec

For: NEW SUPERCONDUCTIVE COMPOUNDS HAVING HIGH TRANSITION
TEMPERATURE, AND METHODS FOR THEIR USE AND PREPARATION

AFFIDAVIT UNDER 37 C.F.R. 1.132

Commissioner of Patents and Trademarks
Washington, D. C. 20231

Sir:

I, David B. Mitzi, being duly sworn, do hereby depose and state:

That I received a B. S. E. degree in Electrical Engineering/Engineering Physics (1985) from Princeton University and a PhD. degree, in Applied Physics (1990) from Stanford University, California.

That I have worked as a research staff member in Solid State Chemistry at the Thomas Watson Research Center of the International Business Machines Corporation in Yorktown Heights, NY from 1990 to the present.

That I have worked in the fabrication of and characterization of high temperature superconductor and related materials from 1990 to the present.

That I have reviewed the above-identified patent application and that I have reviewed the above-identified patent application and acknowledge that it represents the work of Bednorz and

YO987-074BY

Muller, which is generally recognized as the first discovery of superconductivity above 26°K and that subsequent developments in this field have been based on this work.

That all the high temperature superconductors which have been developed based on the work of Bednorz and Muller behave in a similar manner, conduct current in a similar manner and have similar magnetic properties.

That once a person of skill in the art knows of a specific transition metal oxide composition which is superconducting above 26°K, such a person of skill in the art, using the techniques described in the above-identified patent application, which includes all known principles of ceramic fabrication known at the time the application was filed, can make the transition metal oxide compositions encompassed by the claims in the above identified application, without undue experimentation or without requiring ingenuity beyond that expected of a person of skill in the art. This is why the work of Bednorz and Muller was reproduced so quickly after their discovery and why so much additional work was done in this field within a short period of their discovery.

The general principles of ceramic science referred to by Bednorz and Mueller in their patent application can be found in many books and articles published before their discovery. An exemplary list of books describing the general principles of ceramic fabrication are:

- 1) Introduction to Ceramics, Kingery et al., Second Edition, John Wiley & Sons, 1976, in particular pages 5-20, 269-319, 381-447 and 448-513, a copy of which is with the Affidavit of Thomas Shaw submitted December 15, 1998.
- 2) Polar Dielectrics and Their Applications, Burfoot et al., University of California Press, 1979, in particular pages 13-33, a copy of which is with the Affidavit of Thomas Shaw submitted December 15, 1998.
- 3) Ceramic Processing Before Firing, Onoda et al., John Wiley & Sons, 1978, the entire book, a copy of which is with the Affidavit of Thomas Shaw submitted December 15, 1998.

4) Structure, Properties and Preparation of Perovskite-Type Compounds, F.S. Glasco, Pergamon Press, 1969, in particular pages 159-186, a copy of which is with the Affidavit of Thomas Shaw submitted December 15, 1998.

An exemplary list of articles applying their general principles of ceramic fabrication to the types of materials described in applicants' specification are (these references are cited on applicant's 1449 form submitted August 5, 1987 and in PTO Form 892 in Paper # 20, Examiner's action dated August 8, 1990):

1) Oxygen Defect K_2NiF_4 - Type Oxides: The Compounds $La_{2-x}Sr_xCuO_{4-x/2+}$, Nguyen et al., Journal of Solid State Chemistry 39, 120-127 (1981).

2) The Oxygen Defect Perovskite $BaLa_4Cu_5O_{13.4}$, A Metallic Conductor, C. Michel et al., Mat. Res. Bull., Vol. 20, pp. 667-671, 1985.

3) Oxygen intercalation in mixed valence copper oxides related to the perovskite, C. Michel et al., Revue de Chemie minerale, p. 407, 1984.

4) Thermal Behaviour of Compositions in the Systems $x BaTiO_3 + (1-x) Ba(Ln_{0.5}B_{0.5})O_3$, V.S. Chincholkar et al. Therm. Anal. 6th, Vol. 2., p. 251-6, 1980.

By: 

David B. Mitzi

Sworn to before me this 15th day of December, 1998


Notary Public

DANIEL P. MORRIS
NOTARY PUBLIC, State of New York
No. 4888876
Qualified in Westchester County
Commission Expires March 16, 1999

YO987-074BY

BRIEF ATTACHMENT AI

IN THE UNITED STATES PATENT AND TRADEMARK OFFICE

In re Patent Application of

Applicants: Bednorz et al.

Serial No.: 08/479,810

Filed: June 7, 1995

For: NEW SUPERCONDUCTIVE COMPOUNDS HAVING HIGH TRANSITION
TEMPERATURE, METHODS FOR THEIR USE AND PREPARATION

Date: March 1, 2004

Docket: YO987-074BZ

Group Art Unit: 1751

Examiner: M. Kopec

Commissioner for Patents
P.O. Box 1450
Alexandria, VA 22313-1450

FIFTH SUPPLEMENTAL AMENDMENT

Sir:

In response to the Office Action dated February 4, 2000:

ATTACHMENT 17

IN THE UNITED STATES PATENT AND TRADEMARK OFFICE

In re Patent Application of
J. Bednorz et al.

Date: December 15, 1998

Serial No. 08/303,561

Group Art Unit: 1105

Filed: September 9, 1994

Examiner: M. Kopec

For: NEW SUPERCONDUCTIVE COMPOUNDS HAVING HIGH TRANSITION
TEMPERATURE, AND METHODS FOR THEIR USE AND PREPARATION

AFFIDAVIT UNDER 37 C.F.R. 1.132

Commissioner of Patents and Trademarks
Washington, D. C. 20231

Sir:

I, Timothy Dinger, being duly sworn, do hereby depose and state:

That I received a B. S. degree in Ceramic Engineering (1981) from New York State College of Ceramics, Alfred University, an M. S. degree (1983) and a PhD. degree (1986), both in Material Science from the University of California at Berkley.

That I have worked as a research staff member in Material Science at the Thomas Watson Research Center of the International Business Machines Corporation in Yorktown Heights, NY from 1986 to the present.

That I have worked in the fabrication of and characterization of high temperature superconductor materials from 1987 to 1991.

That I have reviewed the above-identified patent application and acknowledge that it represents the work of Bednorz and Muller, which is generally recognized as the first discovery of

YO987-074BY

superconductivity above 26°K and that subsequent developments in this field have been based on this work.

That all the high temperature superconductors which have been developed based on the work of Bednorz and Muller behave in a similar way, conduct current in a similar manner and have similar magnetic properties.

That once a person of skill in the art knows of a specific transition metal oxide composition which is superconducting above 26°K, such a person of skill in the art, using the techniques described in the above-identified patent application, which includes all known principles of ceramic fabrication known at the time the application was filed, can make the transition metal oxide compositions encompassed by the claims in the above identified application, without undue experimentation or without requiring ingenuity beyond that expected of a person of skill in the art. This is why the work of Bednorz and Muller was reproduced so quickly after their discovery and why so much additional work was done in this field within a short period of their discovery.

The general principles of ceramic science referred to by Bednorz and Mueller in their patent application can be found in many books and articles published before their discovery. An exemplary list of books describing the general principles of ceramic fabrication are:

- 1) Introduction to Ceramics, Kingery et al., Second Edition, John Wiley & Sons, 1976, in particular pages 5-20, 269-319, 381-447 and 448-513, a copy of which is with the Affidavit of Thomas Shaw submitted December 15, 1998
- 2) Polar Dielectrics and Their Applications, Burfoot et al., University of California Press, 1979, in particular pages 13-33, a copy of which is with the Affidavit of Thomas Shaw submitted December 15, 1998.
- 3) Ceramic Processing Before Firing, Onoda et al., John Wiley & Sons, 1978, the entire book, a copy of which is with the Affidavit of Thomas Shaw submitted December 15, 1998.

4) Structure, Properties and Preparation of Perovskite-Type Compounds, F.S. Glasco, Pergamon Press, 1969, in particular pages 159-186, a copy of which is with the Affidavit of Thomas Shaw submitted December 15, 1998.

An exemplary list of articles applying their general principles of ceramic fabrication to the types of materials described in applicants' specification are (these references are cited on applicant's 1449 form submitted August 5, 1987 and in PTO Form 892 in Paper # 20, Examiner's action dated August 8, 1990):

- 1) Oxygen Defect K_2NiF_4 - Type Oxides: The Compounds $La_{2-x}Sr_xCuO_{4-x/2+}$, Nguyen et al., Journal of Solid State Chemistry 39, 120-127 (1981).
- 2) The Oxygen Defect Perovskite $BaLa_4Cu_5O_{13.4}$, A Metallic Conductor, C. Michel et al., Mat. Res. Bull., Vol. 20, pp. 667-671, 1985.
- 3) Oxygen intercalation in mixed valence copper oxides related to the perovskite, C. Michel et al., Revue de Chemie minerale, p. 407, 1984.
- 4) Thermal Behaviour of Compositions in the Systems $x BaTiO_3 + (1-x) Ba(Ln_{0.5}B_{0.5})O_3$, V.S. Chincholkar et al. Therm. Anal. 6th, Vol. 2., p. 251-6, 1980.

By: Timothy A. Dinger
Timothy Dinger

Sworn to before me this 16th day of December, 1998

Sandra M. Emma

Notary Public

SANDRA M. EMMA
Notary Public, State of New York
No. 01PO4935290
Qualified in Westchester County
Commission Expires July 5, 2000

BRIEF ATTACHMENT AK

IN THE UNITED STATES PATENT AND TRADEMARK OFFICE

In re Patent Application of

Applicants: Bednorz et al.

Serial No.: 08/479,810

Filed: June 7, 1995

Date: March 1, 2004

Docket: YO987-074BZ

Group Art Unit: 1751

Examiner: M. Kopec

For: NEW SUPERCONDUCTIVE COMPOUNDS HAVING HIGH TRANSITION
TEMPERATURE, METHODS FOR THEIR USE AND PREPARATION

Commissioner for Patents
P.O. Box 1450
Alexandria, VA 22313-1450

FIFTH SUPPLEMENTAL AMENDMENT

Sir:

In response to the Office Action dated February 4, 2000:

ATTACHMENT 19

AK

IN THE UNITED STATES PATENT AND TRADEMARK OFFICE

Applicants: J. Bednorz et al.

Date: December 15, 1998

Serial No. 08/303,561

Group Art Unit: 1105

Filed: September 9, 1994

Examiner: M. Kopec

For: NEW SUPERCONDUCTIVE COMPOUNDS HAVING HIGH
TRANSITION TEMPERATURE, AND METHODS FOR THEIR
USE AND PREPARATION

The Commissioner of Patents and Trademarks
Washington, D.C. 20231

AFFIDAVIT UNDER 37 CFR 1.132

Sir:

I, Thomas M. Shaw, being duly sworn, do hereby depose and state:

I received a B.S. degree in Metallurgy from the University of Liverpool, Liverpool, England and a M.S. and PhD. degree in Materials Science (1981) from the University of California, Berkeley.

I have worked as a postdoctoral researcher in the Material Science Department of Cornell University from 1981-1982. I worked at Rockwell International Science Center in Thousand Oaks, California from 1982-1984 as a ceramic scientist. I have worked as a research staff member in Ceramics Science at the Thomas J. Watson Research

Center of the International Business Machines Corporation in Yorktown Heights, N.Y.
from 1984 to the present.

I have worked in the fabrication of and characterization of ceramic materials of various types, including superconductors and related materials from 1984 to the present.

Attached is a resume of my publications. I have reviewed the above-identified patent application and acknowledge that it represents the work of Bednorz and Mueller, which is generally recognized as the first discovery of superconductivity above 26°K and that subsequent developments in this field have been based on this work.

That all the high temperature superconductors which have been developed based on the work of Bednorz and Mueller behave in a similar manner, conduct current in a similar manner and have similar magnetic properties.

That once a person of skill in the art knows of a specific transition metal oxide composition which is superconducting above 26°K, such a person of skill in the art, using the techniques described in the above-identified patent application, which includes all known principles of ceramic fabrication known at the time the application was filed, can make the transition metal oxide compositions encompassed by the claims in the above-identified application, without undue experimentation or without requiring ingenuity beyond that expected of a person of skill in the art. This is why the

work of Bednorz and Mueller was reproduced so quickly after their discovery and why so much additional work was done in this field within a short period of their discovery.

The general principles of ceramic science referred to by Bednorz and Mueller in their patent application can be found in many books and articles published before their discovery. An exemplary list of books describing the general principles of ceramic fabrication are:

- 1) Introduction to Ceramics, Kingery et al., Second Edition, John Wiley & Sons, 1976, in particular pages 5-20, 269-319, 381-447 and 448-513, a copy of which is attached herewith.
- 2) Polar Dielectrics and Their Applications, Burfoot et al., University of California Press, 1979, in particular pages 13-33, a copy of which is attached herewith.
- 3) Ceramic Processing Before Firing, Onoda et al., John Wiley & Sons, 1978, the entire book, a copy of which is attached herewith.
- 4) Structure, Properties and Preparation of Perovskite-Type Compounds, F.S. Glasco, Pergamon Press, 1969, in particular pages 159-186, a copy of which is attached herewith.

An exemplary list of articles applying their general principles of ceramic fabrication to the types of materials described in applicants' specification are (these references are cited on applicant's 1449 form submitted August 5, 1987 and in PTO Form 892 in Paper # 20, Examiner's action dated August 8, 1990):

- 1) Oxygen Defect K_2NiF_4 - Type Oxides: The Compounds $La_{2-x}Sr_xCuO_{4-x/2+\delta}$, Nguyen et al., Journal of Solid State Chemistry 39, 120-127 (1981).
- 2) The Oxygen Defect Perovskite $BaLa_4Cu_5O_{13.4}$, A Metallic Conductor, C. Michel et al., Mat. Res. Bull., Vol. 20, pp. 667-671, 1985.

- 3) Oxygen intercalation in mixed valence copper oxides related to the perovskite, C. Michel et al., Revue de Chemie minerale, p. 407, 1984.
- 4) Thermal Behaviour of Compositions in the Systems $x \text{BaTiO}_3 + (1-x) \text{Ba}(\text{Ln}_{0.5} \text{B}_{0.5}) \text{O}_3$, V.S. Chincholkar et al. Therm. Anal. 6th, Vol. 2., p. 251-6, 1980.

By: Thomas M. Shaw
Thomas M. Shaw

Sworn to before me this 14th day of December, 1998.

Sandra M. Emma
Notary Public

SANDRA M. EMMA
Notary Public, State of New York
No. 01PO4935290
Qualified in Westchester County
Commission Expires July 5, 2000

BRIEF ATTACHMENT AJ

IN THE UNITED STATES PATENT AND TRADEMARK OFFICE

In re Patent Application of

Applicants: Bednorz et al.

Serial No.: 08/479,810

Filed: June 7, 1995

Date: March 1, 2004

Docket: YO987-074BZ

Group Art Unit: 1751

Examiner: M. Kopec

For: NEW SUPERCONDUCTIVE COMPOUNDS HAVING HIGH TRANSITION
TEMPERATURE, METHODS FOR THEIR USE AND PREPARATION

Commissioner for Patents
P.O. Box 1450
Alexandria, VA 22313-1450

FIFTH SUPPLEMENTAL AMENDMENT

Sir:

In response to the Office Action dated February 4, 2000:

ATTACHMENT 18

AJ

IN THE UNITED STATES PATENT AND TRADEMARK OFFICE

In re Patent Application of
J. Bednorz et al.

: Date: December 15, 1998

Serial No. 08/303,561

: Group Art Unit: 1105

Filed: September 9, 1994

: Examiner: M. Kopec

For: NEW SUPERCONDUCTIVE COMPOUNDS HAVING HIGH TRANSITION
TEMPERATURE, AND METHODS FOR THEIR USE AND PREPARATION

AFFIDAVIT UNDER 37 C.F.R. 1.132

Commissioner of Patents and Trademarks
Washington, D. C. 20231

Sir:

I, Chang C. Tsuei, being duly sworn, do hereby depose and state:

That I received a B. S. degree in Mechanical Engineering from National Taiwan University (1960) and M. S. and PhD. degrees, in Material Science (1963, 1966) respectively from California Institute of Technology.

That I have worked as a research staff member and manager in the physics of superconducting, amorphous and structured materials at the Thomas Watson Research Center of the International Business Machines Corporation in Yorktown Heights, New York from 1973 to the present. (See attached Exhibit A for other professional employment history.)

That I have worked in the fabrication of and characterization of high temperature superconductor and related materials from 1973 to the present.

That I have reviewed the above-identified patent application and acknowledge that it represents the work of Bednorz and Muller, which is generally recognized as the first discovery of
YO987-074BY

superconductivity above 26°K and that subsequent developments in this field have been based on this work.

That all the high temperature superconductors which have been developed based on the work of Bednorz and Muller behave in a similar manner, conduct current in a similar manner and have similar magnetic properties.

That once a person of skill in the art knows of a specific transition metal oxide composition which is superconducting above 26°K, such a person of skill in the art, using the techniques described in the above-identified patent application, which includes all known principles of ceramic fabrication known at the time the application was filed, can make the transition metal oxide compositions encompassed by the claims in the above identified application, without undue experimentation or without requiring ingenuity beyond that expected of a person of skill in the art. This is why the work of Bednorz and Muller was reproduced so quickly after their discovery and why so much additional work was done in this field within a short period of their discovery.

The general principles of ceramic science referred to by Bednorz and Mueller in their patent application can be found in many books and articles published before their discovery. An exemplary list of books describing the general principles of ceramic fabrication are:

- 1) Introduction to Ceramics, Kingery et al., Second Edition, John Wiley & Sons, 1976, in particular pages 5-20, 269-319, 381-447 and 448-513, a copy of which is with the Affidavit of Thomas Shaw submitted December 15, 1998.
- 2) Polar Dielectrics and Their Applications, Burfoot et al., University of California Press, 1979, in particular pages 13-33, a copy of which is with the Affidavit of Thomas Shaw submitted December 15, 1998.
- 3) Ceramic Processing Before Firing, Onoda et al., John Wiley & Sons, 1978, the entire book, a copy of which is with the Affidavit of Thomas Shaw submitted December 15, 1998.

4) Structure, Properties and Preparation of Perovskite-Type Compounds, F.S. Glasco, Pergamon Press, 1969, in particular pages 159-186, a copy of which is with the Affidavit of Thomas Shaw submitted December 15, 1998.

An exemplary list of articles applying their general principles of ceramic fabrication to the types of materials described in applicants' specification are (these references are cited on applicant's 1449 form submitted August 5, 1987 and in PTO Form 892 in Paper # 20, Examiner's action dated August 8, 1990):

- 1) Oxygen Defect K_2NiF_4 - Type Oxides: The Compounds $La_{2-x}Sr_xCuO_{4-x/2+}$, Nguyen et al., Journal of Solid State Chemistry 39, 120-127 (1981).
- 2) The Oxygen Defect Perovskite $BaLa_4Cu_5O_{13.4}$, A Metallic Conductor, C. Michel et al., Mat. Res. Bull., Vol. 20, pp. 667-671, 1985.
- 3) Oxygen intercalation in mixed valence copper oxides related to the perovskite, C. Michel et al., Revue de Chemie minerale, p. 407, 1984.
- 4) Thermal Behaviour of Compositions in the Systems $x BaTiO_3 + (1-x) Ba(Ln_{0.5}B_{0.5})O_3$, V.S. Chincholkar et al. Therm. Anal. 6th, Vol. 2., p. 251-6, 1980.

By: Chang C. Tsuei
Chang C. Tsuei

Sworn to before me this 16th day of December, 1998

Sandra M. Emma

Notary Public

SANDRA M. EMMA
Notary Public, State of New York
No. 01PO4935290
Qualified in Westchester County
Commission Expires July 5, 2000

YO987-074BY

CHANG C. TSUEI

Education

California Institute of Technology, M.S. (1963), Ph.D. (1966)

National Taiwan University, B.S. (1960)

Professional Employment

1993 - present - Research Staff Member

1983 - 1993 - Manager, Physics of Structured Materials

1979 - 1983 - Manager, Physics of Amorphous Materials

1974 - 1975 - Acting Manager, Superconductivity

1973 - 1979 - Research Staff Member

Harvard University: 1980 (Summer)

Visiting Scholar in Applied Physics

Stanford University: 1982 (Sept.) - 1983 (April)

Visiting Scholar in Applied Physics

California Institute of Technology

1972 - 1973 - Senior Research Associate in Applied Physics

1969 - 1972 - Senior Research Fellow in Materials Science

1966 - 1969 - Research Fellow in Materials Science

Exhibit A

YO987-074BY

BRIEF ATTACHMENT AK

IN THE UNITED STATES PATENT AND TRADEMARK OFFICE

In re Patent Application of

Applicants: Bednorz et al.

Serial No.: 08/479,810

Filed: June 7, 1995

Date: March 1, 2004

Docket: YO987-074BZ

Group Art Unit: 1751

Examiner: M. Kopec

For: NEW SUPERCONDUCTIVE COMPOUNDS HAVING HIGH TRANSITION
TEMPERATURE, METHODS FOR THEIR USE AND PREPARATION

Commissioner for Patents
P.O. Box 1450
Alexandria, VA 22313-1450

FIFTH SUPPLEMENTAL AMENDMENT

Sir:

In response to the Office Action dated February 4, 2000:

ATTACHMENT 19

AK

IN THE UNITED STATES PATENT AND TRADEMARK OFFICE

Applicants: J. Bednorz et al.

Date: December 15, 1998

Serial No. 08/303,561

Group Art Unit: 1105

Filed: September 9, 1994

Examiner: M. Kopec

For: NEW SUPERCONDUCTIVE COMPOUNDS HAVING HIGH
TRANSITION TEMPERATURE, AND METHODS FOR THEIR
USE AND PREPARATION

The Commissioner of Patents and Trademarks
Washington, D.C. 20231

AFFIDAVIT UNDER 37 CFR 1.132

Sir:

I, Thomas M. Shaw, being duly sworn, do hereby depose and state:

I received a B.S. degree in Metallurgy from the University of Liverpool, Liverpool, England and a M.S. and PhD. degree in Materials Science (1981) from the University of California, Berkeley.

I have worked as a postdoctoral researcher in the Material Science Department of Cornell University from 1981-1982. I worked at Rockwell International Science Center in Thousand Oaks, California from 1982-1984 as a ceramic scientist. I have worked as a research staff member in Ceramics Science at the Thomas J. Watson Research

Center of the International Business Machines Corporation in Yorktown Heights, N.Y.
from 1984 to the present.

I have worked in the fabrication of and characterization of ceramic materials of various types, including superconductors and related materials from 1984 to the present.

Attached is a resume of my publications. I have reviewed the above-identified patent application and acknowledge that it represents the work of Bednorz and Mueller, which is generally recognized as the first discovery of superconductivity above 26°K and that subsequent developments in this field have been based on this work.

That all the high temperature superconductors which have been developed based on the work of Bednorz and Mueller behave in a similar manner, conduct current in a similar manner and have similar magnetic properties.

That once a person of skill in the art knows of a specific transition metal oxide composition which is superconducting above 26°K, such a person of skill in the art, using the techniques described in the above-identified patent application, which includes all known principles of ceramic fabrication known at the time the application was filed, can make the transition metal oxide compositions encompassed by the claims in the above-identified application, without undue experimentation or without requiring ingenuity beyond that expected of a person of skill in the art. This is why the

work of Bednorz and Mueller was reproduced so quickly after their discovery and why so much additional work was done in this field within a short period of their discovery.

The general principles of ceramic science referred to by Bednorz and Mueller in their patent application can be found in many books and articles published before their discovery. An exemplary list of books describing the general principles of ceramic fabrication are:

- 1) Introduction to Ceramics, Kingery et al., Second Edition, John Wiley & Sons, 1976, in particular pages 5-20, 269-319, 381-447 and 448-513, a copy of which is attached herewith.
- 2) Polar Dielectrics and Their Applications, Burfoot et al., University of California Press, 1979, in particular pages 13-33, a copy of which is attached herewith.
- 3) Ceramic Processing Before Firing, Onoda et al., John Wiley & Sons, 1978, the entire book, a copy of which is attached herewith.
- 4) Structure, Properties and Preparation of Perovskite-Type Compounds, F.S. Glasco, Pergamon Press, 1969, in particular pages 159-186, a copy of which is attached herewith.

An exemplary list of articles applying their general principles of ceramic fabrication to the types of materials described in applicants' specification are (these references are cited on applicant's 1449 form submitted August 5, 1987 and in PTO Form 892 in Paper # 20, Examiner's action dated August 8, 1990):

- 1) Oxygen Defect K_2NiF_4 - Type Oxides: The Compounds $La_{2-x}Sr_xCuO_{4-x/2+\delta}$, Nguyen et al., Journal of Solid State Chemistry 39, 120-127 (1981).
- 2) The Oxygen Defect Perovskite $BaLa_4Cu_5O_{13.4}$, A Metallic Conductor, C. Michel et al., Mat. Res. Bull., Vol. 20, pp. 667-671, 1985.

- 3) Oxygen intercalation in mixed valence copper oxides related to the perovskite, C. Michel et al., Revue de Chemie minerale, p. 407, 1984.
- 4) Thermal Behaviour of Compositions in the Systems $x \text{BaTiO}_3 + (1-x) \text{Ba}(\text{Ln}_{0.5} \text{B}_{0.5}) \text{O}_3$, V.S. Chincholkar et al. Therm. Anal. 6th, Vol. 2., p. 251-6, 1980.

By: Thomas M. Shaw
Thomas M. Shaw

Sworn to before me this 14th day of December, 1998.

Sandra M. Emma
Notary Public

SANDRA M. EMMA
Notary Public, State of New York
No. 01PO4935290
Qualified in Westchester County
Commission Expires July 5, 2000

BRIEF ATTACHMENT AL

IN THE UNITED STATES PATENT AND TRADEMARK OFFICE

In re Patent Application of

Applicants: Bednorz et al.

Serial No.: 08/479,810

Filed: June 7, 1995

For: NEW SUPERCONDUCTIVE COMPOUNDS HAVING HIGH TRANSITION
TEMPERATURE, METHODS FOR THEIR USE AND PREPARATION

Date: March 1, 2004

Docket: YO987-074BZ

Group Art Unit: 1751

Examiner: M. Kopec

Commissioner for Patents
P.O. Box 1450
Alexandria, VA 22313-1450

FIFTH SUPPLEMENTAL AMENDMENT

Sir:

In response to the Office Action dated February 4, 2000:

ATTACHMENT 20

AL

IN THE UNITED STATES PATENT AND TRADEMARK OFFICE

Applicants: J. Bednorz et al.

Date: December 18, 1998

Serial No. 08/303,561

Group Art Unit: 1105

Filed: September 9, 1994

Examiner: M. Kopec

For: NEW SUPERCONDUCTIVE COMPOUNDS HAVING HIGH
TRANSITION TEMPERATURE, AND METHODS FOR THEIR
USE AND PREPARATION

The Commissioner of Patents and Trademarks
Washington, D.C. 20231

AFFIDAVIT UNDER 37 CFR 1.132

Sir:

I, Peter R. Duncombe, being duly sworn, do hereby depose and state:

I received a B.A. degree in Chemistry from the State University of New York at New Paltz, New Paltz, N.Y. and a M.S. degree in Chemical Engineering (1983) from the State University of New York at Buffalo, Buffalo, N.Y.

I have worked as a graduate research assistant in the Chemical Engineering Department of SUNY at Buffalo from 1980-1983. I have worked as a chemical engineer in Ceramics Science at the Thomas J. Watson Research Center of the International Business Machines Corporation in Yorktown Heights, N.Y. from 1984 to the present.

I have worked in the fabrication of and characterization of ceramic materials of various types, including superconductors and related materials from 1984 to the present.

Attached is a resume of my publications (Attachment A).

I have reviewed the above-identified patent application and acknowledge that it represents the work of Bednorz and Mueller, which is generally recognized as the first discovery of superconductivity above 26°K and that subsequent developments in this field have been based on this work.

That all the high temperature superconductors which have been developed based on the work of Bednorz and Mueller behave in a similar manner, conduct current in a similar manner and have similar magnetic properties.

That once a person of skill in the art knows of a specific transition metal oxide composition which is superconducting above 26°K, such a person of skill in the art, using the techniques described in the above-identified patent application, which includes all known principles of ceramic fabrication known at the time the application was filed, can make the transition metal oxide compositions encompassed by the claims in the above-identified application, without undue experimentation or without requiring ingenuity beyond that expected of a person of skill in the art. This is why the

work of Bednorz and Mueller was reproduced so quickly after their discovery and why so much additional work was done in this field within a short period of their discovery.

The general principles of ceramic science referred to by Bednorz and Mueller in their patent application can be found in many books and articles published before their discovery. An exemplary list of books describing the general principles of ceramic fabrication are:

- 1) Introduction to Ceramics, Kingery et al., Second Edition, John Wiley & Sons, 1976, in particular pages 5-20, 269-319, 381-447 and 448-513, a copy of which is attached herewith.
- 2) Polar Dielectrics and Their Applications, Burfoot et al., University of California Press, 1979, in particular pages 13-33, a copy of which is attached herewith.
- 3) Ceramic Processing Before Firing, Onoda et al., John Wiley & Sons, 1978, the entire book, a copy of which is attached herewith.
- 4) Structure, Properties and Preparation of Perovskite-Type Compounds, F.S. Glasco, Pergamon Press, 1969, in particular pages 159-181, a copy of which is attached herewith.

An exemplary list of articles applying their general principles of ceramic fabrication to the types of materials described in applicants' specification are (these references are cited on applicant's 1449 form submitted August 5, 1987 and in PTO Form 892 in Paper # 20, Examiner's action dated August 8, 1990):

- 1) Oxygen Defect K_2NiF_4 - Type Oxides: The Compounds $La_{2-x}Sr_xCuO_{4-x/2+\delta}$, Nguyen et al., Journal of Solid State Chemistry 39, 120-127 (1981).
- 2) The Oxygen Defect Perovskite $BaLa_4Cu_5O_{13.4}$, A Metallic Conductor, C. Michel et al., Mat. Res. Bull., Vol. 20, pp. 667-671, 1985.

3) Oxygen intercalation in mixed valence copper oxides related to the perovskite, C. Michel et al., *Revue de Chemie minerale*, p. 407, 1984.

4) Thermal Behaviour of Compositions in the Systems $x \text{BaTiO}_3 + (1-x) \text{Ba}(\text{Ln}_{0.5} \text{B}_{0.5}) \text{O}_3$, V.S. Chincholkar et al. *Therm. Anal.* 6th, Vol. 2., p. 251-6, 1980.

I have recorded research notes relating to superconductor oxide (perovskite) compounds in technical notebook IV with entries from November 12, 1987 to June 14, 1988 and in technical notebook V with entries continuing from June 7, 1988 to May 2, 1989. Complete copies of each of these notebooks are attached - Attachment B - Book IV and Attachment C - Book V. Below is a listing of some of the compounds I prepared and recorded in these notebooks according to the teaching as described in the Bednorz and Mueller patent application using the general principles of ceramic science as described in the books and articles listed above.

In Book IV, $\text{Y}_1\text{Ba}_2\text{Cu}_3\text{O}_x$ batch C1 pellet pressing, sintering notes and powder processing specifications start on page 2 and continue intermittently to pg. 40 (pg. 13 has superconductive susceptibility curves for pellet 9). Batch C2 $\text{Y}_1\text{Ba}_2\text{Cu}_3\text{O}_3$ detailed from pages 14 to 47.

In Book V green phase (Y_2BaCuO_x) microstructural photomicrographs are logged on pages 15-17 with notes continuing to pg. 19. The perovskite superconductor BiSrCaCu oxide ($\text{Bi}_{2.15}\text{Sr}_{1.68}\text{Ca}_{1.7}\text{Cu}_2\text{O}_{8+\delta}$) and related perovskites $\text{Ca}_{(2-x)}\text{Sr}_x\text{CuO}_x$ and $\text{Bi}_2\text{Sr}_2\text{CuO}_x$ synthesis notations start and continue through pg. 61 with microstructural photomicrographs.

A series of $Y_1Ba_2Cu_3O_x$ stoichiometric perturbations to study compositional effects on 2nd phase or grain boundary phases and their effect on conductivity (resistivity), sintering behavior etc., continue until the end of the book notes on the page dated May 2, 1989 (page not numbered). These are typical perovskite synthetic procedures, microstructural photomicrographs, powder processing methods, characteristic susceptibility curve(s), sintering behavior and the like. Additional notes may be available in later notebooks.

The undersigned affiant swears further that all statements made herein of his own knowledge are true and that all statements made on information and belief are believed to be true; and further that these statements were made with the knowledge that willful false statements and the like so made are punishable by fine or imprisonment, or both, under Section 1001 of Title 18 of the United States Code and that such willful false statements may jeopardize the validity of the application or patent issuing thereon.

By: Peter R. Duncombe
Peter R. Duncombe

Sworn to before me this 18th day of December, 19 98.

Sandra M. Emma
Notary Public

SANDRA M. EMMA
Notary Public, State of New York
No. 01PO4935290
Qualified in Westchester County
Commission Expires July 5, 2000

ATTACHMENT A

1. Compensation doping of Ba_{0.7}Sr_{0.3}TiO₃ thin films
Copel, M Baniecki, JD Duncombe, PR Kotecki, D
Laibowitz, R Neumayer, DA Shaw, TM
APPLIED PHYSICS LETTERS V73 N13 SEP 28 1998 P1832-1834
2. Method for Forming Noble Metal Oxides and Structures Formed Thereof. June 1998.
Duncombe, P. R. Hummel, J. P. Laibowitz, R. B.
Neumayer, D. A. Saenger, K. L. Schrott, A. G.
RC 98A 41575
3. Growth of Bismuth Titanate Films By Chemical Vapor Deposition and Chemical Solution Deposition. March 1998. RC-21124
Neumayer, D. A. Duncombe, P. R. Laibowitz, R. B.
Shaw, T. Purtell, R. Grill, A.
4. Dielectric relaxation of Ba_{0.7}Sr_{0.3}TiO₃ thin films from 1 mHz to 20 GHz Baniecki, JD
Laibowitz, RB Shaw, TM Duncombe, PR
Neumayer, DA Kotecki, DE Shen, H Ma, QY
APPLIED PHYSICS LETTERS V72 N4 JAN 26 1998 P498-500
5. Contrasting magnetic and structural properties of two La manganites with the same doping levels
McGuire, T.R. Duncombe, P.R. Gong, G.Q. Gupta, A. Li, X.W. Pickart, S.J. Crow, M.L.
J. Appl. Phys. (USA) Vol.83, No.11 1 June 1998 P7076-8
6. Effects of Annealing Conditions on Charge Loss Mechanisms in MOCVD (Ba_{0.7},Sr_{0.3})TiO₃ Thin Film Capacitors.
Baniecki, J.D., Laibowitz, RB Shaw, TM Duncombe, PR Saenger, KL Cabral C
Kotecki, DE , Shen, H , Lian, J., Ma, QY
7. Low Operating Voltage and High Mobility Field Effect Transistors Comproising Pentacene and Relatively High Dielectric Constant Insulators RC21233(94806) 7/17/98
Dimitrakopoulos, CD Purushothaman S , Kymissis J. Callegari A. , Neumayer DA,
Duncombe PR, Laibowitz RB, Shaw JM
8. Maximum Magnetoresistance in Granular Manganite/Insulator System close to Percolation Threshold PACS 10/06/98
DK Petrov, L Krusin-Elbaum, JZ Sun, C Feild, & PR Duncombe
9. Magnetoresistance and Hall Effect of Chromium Dioxide Epitaxial Thin Films
X.W. Li, A. Gupta, T.R. McGuire, P.R. Duncombe, Gang Xiao
10. Progress Report on High-k dielectric material: amorphous BST from solgel (09/98)
P. Andry, D. Neumayer, P. Duncombe, C. Dimitrakopoulos, F. Libsch, A. Grill, R. Wisnieff

RC21352 (96175) 2 Dec 1998

SEND

MAIN
MENU

OTHER
OPTIONS

INCOMPLETE

Personal Inventor History

Name: Duncombe, P.R. Serial: 155139 Loc: RES YORKTOWN
Patent Pts: 36 TDB Pts: 1 Total Pts: 37 Plateau Lvl: 3
Plateau Date: 10/24/98 File Update: 11/02/98
Awards Due: None

Title: NOVEL METAL ALKOXYALKOXIDECARBOXYLATES AND USE TO FORM FILMS

06/17/98 Opened as Discl YO8980231

Status: Filed

06/22/98 Discl Review

Action: File

① 09/04/98 Filed as Docket YO998254 in US

Rating: 2

Pts: 3

Co-inventors: Neumayer, D.A.

Title: SELECTIVE GROWTH OF FERROMAGNETIC FILMS FOR MAGNETIC MEMORY, STORAGE-BASED DEVICES, AND OTHER DEVICES

06/17/98 Opened as Discl YO8980225

Status: Filed

06/29/98 Discl Review

Action: File

④ 10/15/98 Filed as Docket YO998268 in US

Rating: 2

Pts: 3

Co-inventors: Guha, S. Gupta, A. Bojarczuk, N.A. Karasinski, J.M.

Title: BEOL DECOUPLING CAPACITOR MATERIALS

01/28/98 Opened as Discl YO8980024 in US

Status: Opened

06/24/98 Discl Review

Action: File

Co-inventors: Rosenberg, R. Ning, T.H. Shaw, T.M. Edelstein, D.C. Neumayer, D.A. Laibowitz, R.B.

③ "FABRICATION OF Strontium Bismuth Titanate/Bismuth Titanate Multilayer Ferroelectric"
Title: FERROELECTRIC THIN FILM STRUCTURES

10/01/97 Opened as Discl YO8970512 in US

Status: Opened

09/16/98 Discl Review

Action: File

② 10/30/98 SENT TO COUNSEL (L. Schick)
Co-inventors: Shaw, T.M. Neumayer, D.A. Laibowitz, R.B.

Title: CAPACITORS WITH AMORPHOUS DIELECTRICS AND IMPROVED DIELECTRIC PROPERTIES MADE USING SILICON SURFACES AS ELECTRODES

06/06/97 Opened as Discl YO8970261 in US

Status: Opened

Co-inventors: Shaw, T.M. Neumayer, D.A. Laibowitz, R.B.

Title: FABRICATION OF THIN FILM FIELD EFFECT TRANSISTOR COMPRISING AN ORGANIC SEMICONDUCTOR AND CHEMICAL SOLUTION DEPOSITED METAL OXIDE

03/25/97 Opened as Discl YO8970113

Status: Filed

03/25/97 Discl Review

Action: File

03/25/97 Filed as Docket YO997083 in US

Rating: 2

Pts: 3

⑥ 03/24/98 Filed as Docket YO997083 in JA

Rating: 2

03/16/98 Filed as Docket YO997083 in TA

Rating: 2

03/12/98 Filed as Docket YO997083 in KO

Rating: 2

04/24/98 Last Office Action

Co-inventors: Purushothaman, S. Dimitrakopoulos, C.D. Furman, B.K. Neumayer, D.A. Laibowitz, R.B.

Title: NOVEL ALKOXYALKOXIDES AND USE TO FORM FILMS

10/30/96 Opened as Discl YO8960411

Status: Filed

03/10/97 Discl Review

Action: File

⑤ 01/30/98 Filed as Docket YO997069 in US

Rating: 2

Pts: 3

Co-inventors: Neumayer, D.A.

Title: THIN-FILM FIELD-EFFECT TRANSISTOR WITH ORGANIC SEMICONDUCTOR REQUIRING LOW OPERATING VOLTAGES

09/11/96 Opened as Discl YO8960358

Status:Filed

03/04/97 Discl Review

Action:File

03/25/97 Filed as Docket YO997057 in US

Rating: 2

Pts:3

03/12/98 Filed as Docket YO997057 in KO.

Rating: 2

04/10/98 Last Office Action

Co-inventors: Purushothaman, S. Dimitrakopoulos, C.D. Furman, B.K. Neumayer, D.A. Laibowitz, R.B.

X Title: HIGH DIELECTRIC CONSTANT, BARIUM LANTHANUM TITANATE THIN FILM CAPACITORS FOR RANDOM ACCESS

06/20/96 Opened as Discl YO8960255 in US

Status:Opened

Co-inventors: Gupta, A. Shaw, T.M. Laibowitz, R.B.

Title: METHOD FOR FORMING NOBLE METAL OXIDES AND STRUCTURES FORMED THEREOF

10/30/95 Opened as Discl YO8950450

Status:Filed

11/12/96 Discl Review

Action:File

11/05/97 Filed as Docket YO996239 in US

Rating: 2

Pts:3

10/20/98 Filed as Docket YO996239 in JA

Rating: 2

07/30/98 Filed as Docket YO996239 in TA

Rating: 2

Co-inventors: Schrott, A.G. Saenger, K.L. Hummel, J.P. Neumayer, D.A. Laibowitz, R.B.

Title: PEROXIDE ETCHANT PROCESS FOR PEROVSKITE-TYPE OXIDES

10/23/95 Opened as Discl YO8950434

Status:Filed

08/08/97 Discl Review

Action:File

04/08/98 Filed as Docket YO997256 in US

Rating: 2

Pts:3

Co-inventors: Rosenberg, R. Cooper, E.I. Laibowitz, R.B.

Title: RF TRANSPONDER FOR METALLIC SURFACES

08/02/95 Opened as Discl YO8950329 in US

Status:Opened

Co-inventors: Afzali-ardakani, A. Feild, C.A. Duan, D.W. Brady, M.J. Moskowitz, P.A.

Title: METHOD FOR CLEANING THE SURFACE OF A DIELECTRIC

09/06/95 Opened as Discl FI8950292

Status:Filed

09/06/95 Sent to Evaluator

02/05/96 Evaluated

Action:Search

04/19/96 Discl Review

Action:File

12/06/96 Filed as Docket FI996047 in US

Rating: 2

Pts:3

11/29/97 Filed as Docket FI996047 in KO

Rating: 2

05/26/97 Filed as Docket FI996047 in TA

Rating: 2

06/11/98 Last Office Action

Co-inventors: Kotecki, D.E. Wildman, H.S. Yu, C. Natzle, W. Laibowitz, R.B.

Title: NANO PHASE FABRICATION OF COPPER-GLASS CERAMIC COMPOSITE VIAS IN CORDIERITE SUBSTRATES

10/05/92 Opened as Discl YO8920907 in US

Status:Published

10/08/92 Sent to Evaluator

12/17/92 Discl Review

Action:Publish

01/06/93 Mailed to Tech Discl Bulletin

09/02/93 Published

Pts:1

Co-inventors: Kang, S.K. Shaw, T.M. Brady, M.J.

Title: METHOD OF SINTERING ALUMINUM NITRIDE

11/06/92 Opened as Discl FI8920668 in US

Status:Closed

11/06/92 Sent to Evaluator

12/18/92 Closed

Co-inventors: Takamori, T. Shinde, S.L.

Title: METHOD OF SINTERING ALUMINUM NITRIDE

11/06/92 Opened as Discl 18920667 in US Status:Closed
11/06/92 Sent to Evaluator
12/18/92 Closed
Co-inventors: Takamori, T. Shinde, S.L.

Title: ALUMINUM NITRIDE BODY AND METHOD FOR FORMING SAID BODY UTILIZING A VITREOUS SINTERING ADDITIVE
08/13/92 Opened as Discl FI8920525 Status:Filed
08/17/92 Sent to Evaluator
09/29/92 Evaluated Action:Search
12/23/92 Discl Review Action:File
05/10/95 Filed as Docket FI992168B in US Rating: 2 Pts:3
05/28/96 Issued as Patent 5520878 in US
Co-inventors: Takamori, T. Shinde, S.L.

Title: ALUMINUM NITRIDE BODY AND METHOD FOR FORMING SAID BODY UTILIZING A VITREOUS SINTERING ADDITIVE
08/13/92 Opened as Discl FI8920525 Status:Filed
08/17/92 Sent to Evaluator
09/29/92 Evaluated Action:Search
12/23/92 Discl Review Action:File
12/22/93 Filed as Docket FI992168A in US Rating: 2 Pts:3
01/09/96 Issued as Patent 5482903 in US
Co-inventors: Takamori, T. Shinde, S.L.

Title: GOLD DOPING OF YBA2CU307-8 AS A MEANS OF INCREASING TRANSPORT CRITICAL CURRENT DENSITY
02/12/92 Opened as Discl YO8920161 in US Status:Closed
02/14/92 Sent to Evaluator
05/15/92 Closed
Co-inventors: Daeumling, M. Shaw, T.M.

Title: PROCESS FOR PRODUCING CERAMIC CIRCUIT STRUCTURES HAVING CONDUCTIVE VIAS
07/19/89 Opened as Discl YO8890552 Status:Filed
07/25/89 Sent to Evaluator
08/10/89 Evaluated Action:Search
07/30/90 Discl Review Action:File
12/17/92 Filed as Docket YO990091B in US Rating: 2 Pts:3
08/16/94 Issued as Patent 5337475 in US
Co-inventors: Vallabhaneni, R.V. Giess, E.A. Farooq, S. Cooper, E.I. Kim, Y.H. Vanhise, J.A. Aoude, F.Y. Muller-landau, F. Shaw, R.R. Walker, G.F. Rita, R.A. Neisser, M.O. Park, J.M. Shaw, T.M. Brownlow, J.M. Kim, J. Knickerbocker, S.H.

Title: VIA PASTE COMPOSITIONS AND USE THEREOF TO FORM CONDUCTIVE VIAS IN CIRCUITIZED CERAMIC SUBSTRATES
07/19/89 Opened as Discl YO8890552 Status:Filed
07/25/89 Sent to Evaluator
08/10/89 Evaluated Action:Search
07/30/90 Discl Review Action:File
03/20/91 Filed as Docket YO990091A in US Rating: 2 Pts:3
02/01/94 Issued as Patent 5283104 in US
Co-inventors: Vallabhaneni, R.V. Giess, E.A. Farooq, S. Cooper, E.I. Kim, Y.H. Vanhise, J.A. Aoude, F.Y. Muller-landau, F. Shaw, R.R. Walker, G.F. Rita, R.A. Neisser, M.O. Park, J.M. Shaw, T.M. Brownlow, J.M. Kim, J. Knickerbocker, S.H.

Call your award coordinator, IPL department, or T/L 826-2680 for help.

SEND

MAIN
MENU

OTHER
OPTIONS

- T.R. McGuire, A. Gupta, P.R. Duncombe, M. Rupp, J.Z. Sun, R.B. Laibowitz, W.J. Gallagher & G. Xiao "Magnetoresistance and Magnetic Properties of $(\text{La}_{1-x})\text{MnO}_3$ Thin Films" 3M Conf. Proc: 4/96
- T.R. McGuire, P.R. Duncombe, G.Q. Gong, A. Gupta, X.W. Li & G. Xiao "Magnetoresistance & Magnetic Properties of $(\text{La}_{1-x})\text{MnO}_3$ (Vacancy) Bulk Materials" 11/96 3M conf CMR Open Forum entry
- J.Z. Sun, L. Krusin-Elbaum, A. Gupta, G. Xiao, P.R. Duncombe, W.J. Gallagher & S. P. Parkin "Magneto-Transport in Doped Manganate Perovskites" 3M conference 11/12-15/96 Atlanta, Georgia
- P. Lecoeur, A. Gupta, P.R. Duncombe, G. Gong & G. Xiao "Emission Studies of the Gas-Phase Oxidation of Mn during Pulsed Laser Deposition Manganates in O_2 & N_2O Atmospheres" JAP 80(1), 7/1/96
- J.Z. Sun, L. Krusin-Elbaum, A. Gupta, G. Xiao, P.R. Duncombe, W.J. Gallagher & S.S.P. Parkin "Colossal Magnetoresistance in Doped Manganate Perovskites" IBM J&D to appear 1996/97
- A. Gupta, G.Q. Gong, G. Xiao, P.R. Duncombe, P. Trouilloud, P. Lecoeur, Y.Y. Wang, V.P. Dravid, & J.Z. Sun "Grain Boundary Effects on the Magnetoresistance Properties of Perovskite Manganite Films"
- J.Z. Sun, W.J. Gallagher, P.R. Duncombe, L. Krusin-Elbaum, R.A. Altman, A. Gupta, Y. Lu, G.Q. Gong & G. Xiao "Observation of Large Low-field Magnetoresistance in Tri-layer Perpendicular Transport Devices Made Using Doped Manganate Perovskites" to appear Appl. Phys. Lett.
- J.Z. Sun, L. Krusin-Elbaum, P.R. Duncombe, A. Gupta & R. B. Laibowitz "Spin-Polarized Tunneling in Doped Perovskite Manganate Trilayer Junctions" APL submission 11/96
- T.R. McGuire, P.R. Duncombe, C.Q. Gong, A. Gupta, X.W. Li & G. Xiao "Interlayer Exchange Coupling & Magnetoresistance Of LCMO/LSMO 67/33 Multilayers" APL submission
- R.B. Laibowitz, T.M. Shaw, D.E. Kotecki, S. Tiwari, A. Gupta, A. Grill, & P.R. Duncombe "Properties and Applications of Thin Films of Lead Lanthanum Titanate (PLT) and Barium Strontium Titanate (BST) APS mtg 3/18-22/96
- P.R. Duncombe, S.L. Shinde, & T. Takamori "Aluminum Nitride Body Utilizing A Vitreous Sintering Additive" US05482903 1/9/96 (EF Plaque)
- P.R. Duncombe, S.L. Shinde, & T. Takamori "Aluminum Nitride Body & Method for Forming Said Body Utilizing a Vitreous Sintering Additive" US05520878 issued 5/28/96; I.A. Patent issue Award: 8/96
- Ali Afzali-Ardakani, Mike Brady, Dah-Wei Duan, Peter Duncombe, Chris Feild, and Paul Moskowitz "RF Transponder for Metallic Surfaces" Docket#:YO895-0329 submitted: 8/2/95
- D.E. Kotecki, R.B. Laibowitz, W. Natze, C. Yu, H. Wildman, P.R. Duncombe "Method for Cleaning the Surface of BST Prior to Electrode Deposition" Application #:FI996047 draft #1 under review
- E.I. Cooper, P.R. Duncombe, R.B. Laibowitz, "Peroxide Etchant Process for Titanate Dielectrics" Docket: YO895-0434 rated file; in prep.
- D.A. Neumayer, P.R. Duncombe, R.B. Laibowitz, & A. Grill "Sol-Gel Processing of BaSrTiO_3 Films" submitted to International Symposium on Integrated Ferroelectrics (ISIF: 3/2-5/97) Santa Fe, N.M.
- A. Grill, R. Laibowitz, D. Beach, D. Neumayer & P.R. Duncombe "Effect of Base Electrode on the Crystallization & Electrical Properties of PLT" IBM RC 20402 (90185) 3/5/96
- D.A. Neumayer, P.R. Duncombe, R.B. Laibowitz & A. Grill "Effect of TiO_x Nucleation Layer on Crystallization of Sol-Gel Derived $\text{Bi}_4\text{Ti}_3\text{O}_{12}$ Films" ISIF submission 3/97
- C.D. Dimitrakopoulos, P.R. Duncombe, B.K. Furman, R.B. Laibowitz, D. Neumayer, S. Purushothaman, J. Shaw "Field Effect Transistor for Low Voltage Operation" Disclosure YO896-0358 rated file: 9/11/96
- R.B. Laibowitz, P.R. Duncombe, D. Neumayer, K.L. Saenger, A.G. Schrott "Noble Metal Surfaces" YO896-04xx rated "file" 10/96
- T. Shaw, R.B. Laibowitz, P.R. Duncombe & A. Gupta "High Dielectric Constant Barium Lanthanum Titanate-Based DRAM Structures" Disclosure #: YO898-0681 rated File 5/96 in preparation
- D. Neumayer, P.R. Duncombe "Fabrication of Barium Strontium Titanate Films" YO896-04xx rated File 10/96 in preparation

IBM Commitments:

To Win

To Execute

To Teamwork

ATTACHMENT B

T01001

Technical Notebook
Book IV

User's Initials and Last Name:

P DUNCOMBE

Employee Serial:

15513P

Date of First Entry:

Date of Last Entry:

Security Classification:

11/12/87 6/88

MOTAR

11/12

IBM Technical Notebook

1

70/30 - 25-25 } C1 GEP 2 - ~ 12:30 start

3.094 0.574 0.179 4.07
1.458 0.455 0.760

"63.9" 123 basis
84.6!?

~ 4 hrs

3.047
≤ ~ 1.5% loss

0.515 0.158
1.308 0.401 0.539

5.65

88.7 better
P1 → 83.4

11/12

11/13 SrTiO₃ - ST3 → 32 hrs ST2 pes. → 48

SrTiO₃ ⇒ ST3 ⇒ coded in morning see book III, pg (A7)

4.024 0.510 ✓ 0.240 ✓ ~ 5.01 "1.04(2)% dense"
no airt loss 1.295 0.610 0.803 same Sally

~ 48 hrs (+ cooling 3 mornings, stepwise) sintering pellet

Cutting record

start 0.425 (0)
+ 0.060 Δ - saw (0.015) = 0.045 ~ 1.14 mm w/ flattening ~ 1 mm ✓
0.485 (Δ 0) ↳ 0.042 (1.08 mm) OK
0.060
0.545 (0.045 Δ resid; actual ⇒ 0.052 → 1.32 mm
(55) 0.0465 1.18 mm

0.0523

bottom (0.6-0.69) not flat 1.52 mm

The above understood

Date

and
hv

Date

10/13

2

PRE

IBM Technical Notebook

STA - some security on 1 side (a slice worth)

4.178 0.584 10.287 3.316
 1.483 0.729 1.26

way final piece of
 ST2 @ 4.55
68.9
 average

will remove Monday morning ~ 6:16 AM, SAT-6 SW, ~ 63+ hours projected

10/16

4.169 0.510 ~ 0.250 4.98 1.035 <CONSISTENT>
 (0.2%) 1.295 0.635 0.837

G1

ISO-26,000 - URL-3300

4.01 0.578 0.248 0.542 3.46
 1.468 0.630 ~~0.498~~

density est. (figure 65%) => 5.785 RANGE (5.37-6.27)

C1Z41

10/17 3300 / 26,000 EXTREMELY SHINY, flat surface, with sharp convex pellet
 3.105 0.566 0.193(4) 3.90 61.2%
 1.438 0.490 0.796

G1 16 hrs

3.985 0.578 0.250 (no change) 3.738 (lost 0.5% density)

10:18

in hot furnace, packed T_c - 520C

	T_c	T_s	T_{SET}	
20	977	745	971	to 'push' ΔT
21	↓	838	✓	
22		898		
23		935		
24		949	956	23 1/2 → 951
2:23				~ SET-PT.
2:54	435			"OFF" for slow-cool (first stepped to 840)

The above understood

Date

and

Date

IBM Technical Notebook

3

10/17

C12F1 \rightarrow pellet multiply cracked as if organic residue vaporized, evidence of vapor transport to support plate, etc. ~~ex Na~~

2.925 80.18

5.5%

9.79 - 3.105 \Rightarrow 6.685

10/18

G1 - post 4.044 split in 4 pieces (seem wet on cooling)

G2 4.1	0.579	0.253	3.75	✓ pellet slightly disfigured, but ok.
	1.471	0.643	1.093	

33

4.155				
0.510	0.220		5.64	about expected density
1.295	0.559	0.736		

D.D.1 Pre

3.10	0.5765	0.191
------	--------	-------

3.11

0.513	0.165			
1.303	0.419	0.559	5.61	88.2

5.75

4
11/24

IBM Technical Notebook

Thermodyne Tube furnace set-up specs.

thermocouple: dia. ~0.255 length 20" + USED 23"

Set-up complete w/ plug in jacks, ext. wire, 5 couples.

11/30 Analytical Submissions

C1 - 0.75 g	$Y_{0.02} Ba_{0.98} Cu_{0.6}$	Y, Ba, Cu
C2 - 1.1	Y_2O_3	Y , trace 99%
C3 - 2.0	BaO	Ba ,
C4 - 1.0	TiO_2	Ti , trace
C5 - 2.0	$SrTiO_3$ pre	Sr, Ti , trace
C6 - 1.0	↓ post mill	↓
C7 2.0	DRC 123.	Y, Ba, Cu
C8	DD 123	Y, Ba, Cu
C9	off comp 2.11	

IBM Technical Notebook

5

'New' $30 \xrightarrow{20.25} g$ GRINDING CHARGE of $SrTiO_3$ in mill (3:10)
O₂, compressed AIR, CO₂ cylinders obtained w/ regulations off (4:17)
Ar

YIELD $\rightarrow 20.4 g$ \therefore MUST BE SOME FROM old batch or ZrO_2
COMBINED w/ OLD POWDER $\rightarrow 23 g$ of milled powder

12/2 C1. batch 45.6 grams left
39.56 g (16 g kept for files)
 $\frac{10.5}{29.5}$ left for pellets
 ~ 10 for grinding charge TFE/Toluene

NEW BOTTLES ORDERED, NO TEFLON AVAILABLE, - approx - 60 hrs total

$SrTiO_3$ pellets $\rightarrow 10-10$ (29 hrs) down 1 \therefore 2-24 (12?) $\sim 12-12$ (24) Thus

ST5, ST6 - start 10 A.M. 12/8, numerous interruptions due to furnace malfunctions, out 12:00 P.M. 12/10
ST5 edge chips 1 side OK otherwise 21 ISO.

*1 4.08 0.285 0.584
0.52

(#01) 0.237 0.520 4.94 1.027
0.602 1.321 0.825

ST6 large chip during iso pressing in $\frac{3}{4}$ side, must do

#1 4.128 0.586 0.886
~~0.520~~ ~~0.825~~

4.15 0.513 0.249 4.92 1.023
1.303 0.632(5) 0.843

*1 bracketing crack

The above understood
and witnessed by:

Date

and

Date

6

IBM Technical Notebook

950C Run

POST GREEN	C1P9	3.108	0.577	0.185	3.92	61.5
			1.466	0.470	0.793	
POST	3.1	0.514	0.161	5.66	88.9%	
	no loss	1.306	0.409	0.548		
POST GREEN	DRC 2	0.579	0.177	4.19	65.8	
	3.204	1.471	0.450	0.765		
POST	3.2	0.551	0.165	4.96	77.9	
	no loss	1.400	0.419	0.645		

17/

pellets not in best shape after 150 at 26000

975C Run

POST	C1P10	0.574	0.185	3.99	61.8	
	3.090	1.458	0.470	0.785		
POST	3.056	0.508	0.157	5.88	92.3	PROBABLY 93
	1% loss	1.288	0.399	0.510	+3.4%	

* DRC 3	0.579	0.181	4.24	66.6% ~	
	3.318	1.471	0.460	0.782	

POST	crack still apparent, but holding	3.293	0.547	0.168	0.647	5.08	79.9 + 2%
	0.75% loss	0.389	0.427				

C1P10 Pyrometer 91.8 → 92 ∴ mostly closed porosity (95% of on peak density basis)

* cracked in 1/2, but holding. Will go w/ see if it heats.

To Temp @ 4:05 → 2 HRS 6:05 RAMP DOWN

4:00 P.M. 12/8 start cooling, OK NOT FLOWING WHEN ARRIVED, THOUGH COULD HAVE HAD BACK PRESSURE

IBM Technical Notebook

12-8

7/3 7

100% E/G mix \Rightarrow new wght calc.

(4.0 g) E basis (transferred to jar for physical mixing)

$$92.0913 \text{ g / mM section} \therefore \frac{4.0}{92.0913} = 0.0434 \text{ mM}$$

0.0434 mM is BASIS for mix of 0.7 mM Ectectic

$$0.0434 / 0.7 = 0.0620 \text{ mM total} \therefore 0.3 \text{ mM } 211$$

$$0.3 (0.0620) = 0.0186 \text{ mM } (94.6725 \text{ g / mM } 211) = 1.761 \text{ g } 211$$

$$\begin{array}{r} 1.761 \text{ g } 211 \\ 4.0 \text{ g } E \\ \hline 5.761 \text{ g mix} \end{array}$$

$$\text{tare } 0.83 \quad \begin{array}{r} 5.76 \\ 5.68 \text{ recovered} \\ \hline 0.08 \text{ g loss on mixing} \end{array}$$

5.53 after gundng (light loss on transfer)

1 pellet pressed \Rightarrow EG1 \Rightarrow to temp 12/10 @ 3:40-45 NOT OUT TO BE 5:45

$$\begin{array}{cccccc} 2.57 & 0.580 & 0.153 & & 3.88 & "60.9" \rightarrow 74\%? \\ & 1.473 & 0.389 & 0.663 & & \end{array}$$

Rel. density calc $0.3 (6.00) + 0.7 (4.9) \Rightarrow 5.23$ approx theoretical
 \uparrow EMPIRICAL D's

$$\begin{array}{cccccc} 2.543 & \sim 0.611 & 0.161 & & 2.825 \\ (1\% \text{ wght loss}) & 1.55 & 0.480 & 0.90 & \end{array}$$

Restarted for overwrite RUN

8

IBM Technical Notebook

III. DENSITY WORKSHEET

STEREOPHOTOGRAPHIC
TRUE POWDER DENSITY

SAMPLE I.D. 660 DATE 12-9-87
SOURCE PPD OPERATOR PRD
TOTAL WEIGHT 18.855 g. OUTCASSING CONDITIONS
TARE WEIGHT 4.061 g.
SAMPLE WEIGHT 14.794 g.
ADDED VOLUME, V_A cc
CELL HOLDER VOLUME, V_C cc

$$\text{OPERATIONAL EQUATION } V_p = V_c \cdot \left[\frac{V_A}{1 - \rho_p/\rho_s} \right]$$

V_p = Volume of Powder (cc)
 V_c = Volume of Sample Cell Holder (cc)
 V_A = Added Volume
 P_2 = Pressure Reading after Pressurizing Cell
 P_3 = Pressure Reading after Added V_A

DATA	RUN 1	RUN 2
P_2	18.367	18.488
P_3	18.362	5.013
V_p	7.023 cc	3.034 cc
DENSITY	4.89 g/cc	4.88 g/cc

± 0.24 (6%)
 4.85 ± 0.13
{pressure}

III. DENSITY WORKSHEET

STEREOPHOTOGRAPHIC
TRUE POWDER DENSITY

SAMPLE I.D. 660 DATE 12-9-87
SOURCE PPD OPERATOR PRD
TOTAL WEIGHT 12.606 g. OUTCASSING CONDITIONS
TARE WEIGHT 4.061 g.
SAMPLE WEIGHT 8.545 g.
ADDED VOLUME, V_A cc
CELL HOLDER VOLUME, V_C cc

$$\text{OPERATIONAL EQUATION } V_p = V_c \cdot \left[\frac{V_A}{1 - \rho_p/\rho_s} \right]$$

V_p = Volume of Powder (cc)
 V_c = Volume of Sample Cell Holder (cc)
 V_A = Added Volume
 P_2 = Pressure Reading after Pressurizing Cell
 P_3 = Pressure Reading after Added V_A

DATA	RUN 1	RUN 2
P_2	18.367	18.488
P_3	18.362	5.013
V_p	7.023 cc	3.034 cc
DENSITY	4.89 g/cc	4.88 g/cc

± 0.24 (6%)
 4.85 ± 0.13
{pressure}

III. DENSITY WORKSHEET

STEREOPHOTOGRAPHIC
TRUE POWDER DENSITY

SAMPLE I.D. 211 DATE 12-9-87
SOURCE PPD OPERATOR PRD
TOTAL WEIGHT 19.662 g. OUTCASSING CONDITIONS
TARE WEIGHT 4.061 g.
SAMPLE WEIGHT 15.601 g.
ADDED VOLUME, V_A cc
CELL HOLDER VOLUME, V_C cc

$$\text{OPERATIONAL EQUATION } V_p = V_c \cdot \left[\frac{V_A}{1 - \rho_p/\rho_s} \right]$$

V_p = Volume of Powder (cc)
 V_c = Volume of Sample Cell Holder (cc)
 V_A = Added Volume
 P_2 = Pressure Reading after Pressurizing Cell
 P_3 = Pressure Reading after Added V_A

DATA	RUN 1	RUN 2
P_2	18.557	18.828
P_3	5.084	5.057
V_p	2.578 cc	2.736 cc
DENSITY	6.05 g/cc	6.088 g/cc

± 0.3
 $(5.05 - 6.35)$
 ± 0.24 (6%)
{pressure}

STEREOPHOTOGRAPHIC
TRUE POWDER DENSITY

SAMPLE I.D. 123 DATE 12-9-87
SOURCE PPD OPERATOR PRD
TOTAL WEIGHT 21.026 g. OUTCASSING CONDITIONS
TARE WEIGHT 4.061 g.
SAMPLE WEIGHT 16.965 g.
ADDED VOLUME, V_A cc
CELL HOLDER VOLUME, V_C cc

$$\text{OPERATIONAL EQUATION } V_p = V_c \cdot \left[\frac{V_A}{1 - \rho_p/\rho_s} \right]$$

V_p = Volume of Powder (cc)
 V_c = Volume of Sample Cell Holder (cc)
 V_A = Added Volume
 P_2 = Pressure Reading after Pressurizing Cell
 P_3 = Pressure Reading after Added V_A

DATA	RUN 1	RUN 2
P_2	18.598	18.596
P_3	5.078	5.078
V_p	2.73 cc	2.73 cc
DENSITY	6.21 g/cc	6.21 g/cc

The above understood
and understood by

Date

and

Date

IBM Technical Notebook

9

III. DENSITY WORKSHEET

STEREOPHONIC TRUE POWDER DENSITY

SAMPLE I.D. 123-344 DATE 12-9
SOURCE DNAIDS OPERATOR PRD
TOTAL WEIGHT 19.700 g. OUTCASSING CONDITIONS
TARE WEIGHT 4.061 g.
SAMPLE WEIGHT 15.639 g. ADDED VOLUME, V_A 18.57 cc
CELL HOLDER VOLUME, V_C 34.8 cc

$$\text{OPERATIONAL EQUATION } V_p = V_c \cdot \left[\frac{V_A}{1 - P_2/P_1} \right]$$

V_p = Volume of Powder (cc)
 V_c = Volume of Sample Cell Holder (cc)
 V_A = Added Volume
 P_1 = Pressure Reading after Pressurizing Cell
 P_2 = Pressure Reading after Added V_A

R=3.646

DATA
R=3.646

ROW 1	ROW 2	ROW 3
P_1 <u>18.603</u>	<u>18.561</u>	<u>18.561</u>
P_2 <u>5.103</u>	<u>5.091</u>	<u>5.091</u>
V_p <u>2.523</u> cc	cc	cc
DENSITY <u>6.199</u> g/cc	g/cc	g/cc

no page

16

III. DENSITY WORKSHEET

STEREOPHONIC ROW 2 TRUE POWDER DENSITY

SAMPLE I.D. 123 DATE 12-9
SOURCE C1 OPERATOR PRD
TOTAL WEIGHT 21.949 g. OUTCASSING CONDITIONS
TARE WEIGHT 4.061 g.
SAMPLE WEIGHT 17.888 g. ADDED VOLUME, V_A 34.85 cc
CELL HOLDER VOLUME, V_C 34.85 cc

$$\text{OPERATIONAL EQUATION } V_p = V_c \cdot \left[\frac{V_A}{1 - P_2/P_1} \right]$$

V_p = Volume of Powder (cc)
 V_c = Volume of Sample Cell Holder (cc)
 V_A = Added Volume
 P_1 = Pressure Reading after Pressurizing Cell
 P_2 = Pressure Reading after Added V_A

R=3.648

DATA

ROW 1	ROW 2	ROW 3
P_1 <u>18.508</u>		
P_2 <u>5.014</u>		
V_p <u>3.087</u> cc	cc	cc
DENSITY <u>6.13</u> g/cc	g/cc	g/cc

16

III. DENSITY WORKSHEET

STEREOPHONIC TRUE POWDER DENSITY

SAMPLE I.D. 123 DATE 12-9-87
SOURCE C1-344 OPERATOR PRD
TOTAL WEIGHT 19.959 g. OUTCASSING CONDITIONS
TARE WEIGHT 4.063 g.
SAMPLE WEIGHT 15.896 g. ADDED VOLUME, V_A 18.57 cc
CELL HOLDER VOLUME, V_C 34.8 cc

$$\text{OPERATIONAL EQUATION } V_p = V_c \cdot \left[\frac{V_A}{1 - P_2/P_1} \right]$$

V_p = Volume of Powder (cc)
 V_c = Volume of Sample Cell Holder (cc)
 V_A = Added Volume
 P_1 = Pressure Reading after Pressurizing Cell
 P_2 = Pressure Reading after Added V_A

R=3.58

DATA
R=3.58

ROW 1	ROW 2	ROW 3
P_1 <u>18.677</u>	<u>18.643</u>	
P_2 <u>5.218</u>	<u>5.208</u>	
V_p <u>1.703</u> cc	cc	cc
DENSITY <u>6.10</u> g/cc	<u>6.105</u> g/cc	g/cc

NOT BACK TO ZERO

16

STEREOPHONIC TRUE POWDER DENSITY

SAMPLE I.D. C1P10 DATE 12-10-87
SOURCE C1-975782 OPERATOR PRD
TOTAL WEIGHT 6.613 g. OUTCASSING CONDITIONS
TARE WEIGHT 4.061 g.
SAMPLE WEIGHT 2.552 g. ADDED VOLUME, V_A 18.57 cc
CELL HOLDER VOLUME, V_C 34.8 cc

$$\text{OPERATIONAL EQUATION } V_p = V_c \cdot \left[\frac{V_A}{1 - P_2/P_1} \right]$$

V_p = Volume of Powder (cc)
 V_c = Volume of Sample Cell Holder (cc)
 V_A = Added Volume
 P_1 = Pressure Reading after Pressurizing Cell
 P_2 = Pressure Reading after Added V_A

R=3.485

DATA
R=3.485

ROW 1	ROW 2	ROW 3
P_1 <u>18.198</u>	<u>18.182</u>	
P_2 <u>5.208</u>	<u>5.217</u>	
V_p <u>0.9355</u> cc	cc	cc
DENSITY <u>5.809</u> g/cc	g/cc	g/cc

6.13 → 95.6
6.37 → 91.8 (92)

16

→ 16.48 + 58.75

The above understood
and witnessed by

Date

and
by

Date

IBM Technical Notebook

10
12/10

Powders for Analysis \Rightarrow Now entered @ conf. time
12/11, SENSITIVITIES NOT ENOUGH
Need to increase by 10X at least.

~~#1~~ - Species Description
 Y_2O_3 left exposed to air

TiO_2

C1 $YBaCu$
1 2 3

DD1

DRC

P11

EI $Y_{0.02}Ba_{0.38}Cu_{0.6}$

off comp

off comp

Table I - Precision¹ of Metals determined by ICP in $La_{1-x}Sr_xCuO_4$ and $YBa_2Cu_3O_7$ Thin Films.

Element	x^2	S.D.	R.S.D. (%)
La	1.80	0.08	4.64
Sr	0.20	0.01	5.52
Cu	1.00	0.14	3.52
Y	1.00	0.05	5.60
Ba	2.04	0.07	3.43
Cu	3.00	0.11	3.67

¹Based on 7 determinations

²Calculated atomic ratios

For 123

$Y (0.533) \Rightarrow \pm 0.019 \quad 0.314 - 0.352$

$Ba (0.667) \Rightarrow \pm 0.023 \quad 0.544 - 0.690$

$Cu (1.00) \Rightarrow \pm 0.036 \quad 0.963 - 1.0367$

Theoretical wgt % calcs.

IBM Technical Notebook

$TiO_2 \Rightarrow 47.90/79.8988 \rightarrow 59.95$

Anal 1
57.3

CRRR reported.

$SrCO_3 \Rightarrow 87.62/147.62935 \rightarrow 59.35$

ACT ANALYZED

$BaCO_3 \Rightarrow 137.34/197.34435 \rightarrow 69.59(2)$

$BaO \Rightarrow 89.566 \quad 88.9 \quad 99.26 !$

$SrTiO_3 \Rightarrow Sr \Rightarrow 47.74(5) \quad M.W. 183.5182$
 $Ti \Rightarrow 26.10(1)$

(

C5- 22.2
19.4

Ti
 Sr

85.05% (15% poor)
"3.48% rich"

C6 24.2
50.6

Ti
 Sr

92.72 (7.3% poor)
"5.98% rich"

86.5
92.5

The above understood
and witnessed by

Date

and
by


Date

IBM Technical Notebook

12/14 both well shaped pellets

C1P11 - 15026

3.673 0.574 0.215 4.03 63.3
1.458 0.546 0.9116

92+  from T. SHAW

C1fp(#)? 15026

3.058 0.560 0.200 3.606 56.6 as usual
1.437 0.523 0.848

- final microstructure full of liquid, br metal g.s. } cracking
- no final density recorded

12/16 pellets in furnace from 12/14 in a purge.

To temp (10°C/min ramp from RT) @ 10:50 A.M.

Low (leading) side undershoot 974, high (downside) overshoot 978.

Stable variation 974-976 ✓

start ramp down ^{1:00} (12:50 p.m. (to 600C where soak for 48 hours)

$$\left\{ \text{Diff coef: } 2 \times 10^{-5} \frac{\text{m}^2}{\text{s}} \times 2 \times 10^{-15} \frac{\text{m}^2}{\text{s}} \times \frac{t^2}{(0.348 \text{ m})^2} = 2.153 \times 10^{-14} \frac{\text{ft}^2}{\text{s}} \right\}$$

The above understood
and witnessed by _____

Date _____

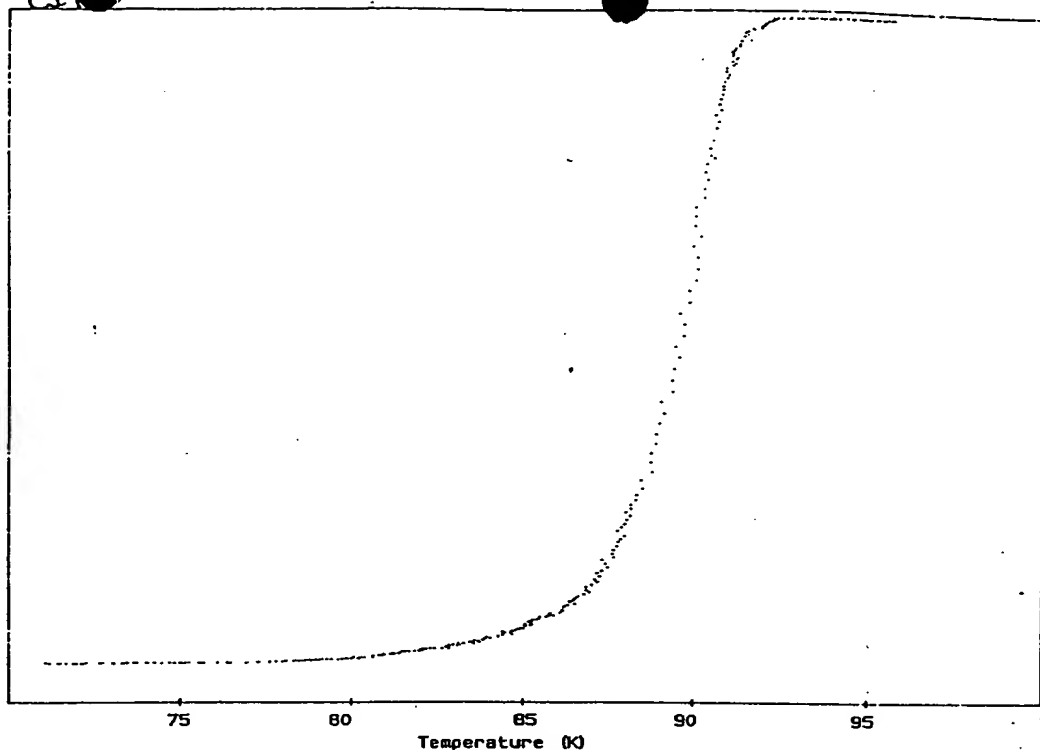
and
by _____

Date _____

0.00

ΔI

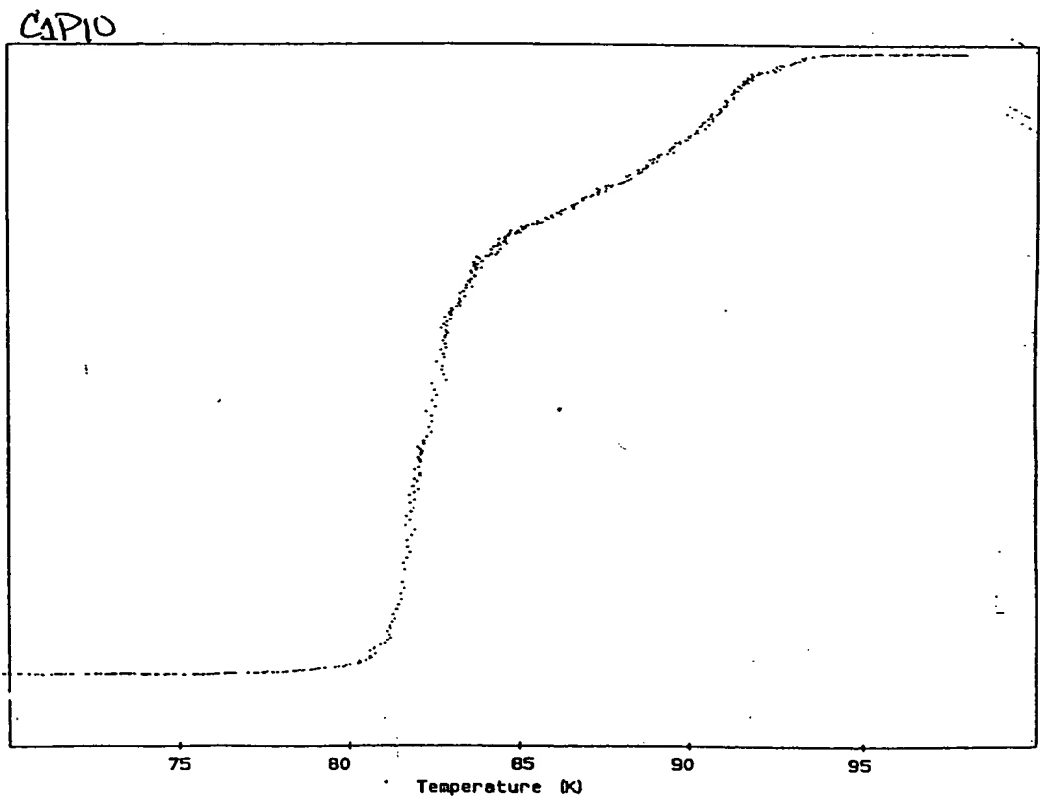
0.17



0.00

ΔI

-0.17



The above understood
and witnessed by

Date

and
by

Date

IBM Technical Notebook

14 C2 Batch $\rightarrow \frac{1}{2} \text{Ba}_2\text{Cu}_3\text{O}_7$ 200g

from C1 batch calc. (pg. 54 Book III) \rightarrow 72 Book II

$\frac{1}{2} \text{O}_3 \Rightarrow$ 17.1535 \Rightarrow 17.1707 \Rightarrow x2 34.34

$\text{BaCO}_3 \Rightarrow$ 48.5934 100 \Rightarrow x2 93.1868

BaCO_3 conversion: 93.1868 $\frac{197.35}{153.34} = 119.932(3) \div 0.99 \Rightarrow$ 121.14(4)

$\text{CuO} \Rightarrow$ 36.25(81) \Rightarrow 36.2893(4) \Rightarrow x2 72.57(9)

O.K. everything is Ba rich by analysis, so why not not correct \rightarrow 119.93

Apply $\frac{1}{2}$.

BaCO_3

tare: $\frac{279.67}{+ \frac{120.54}{400.21}}$ won't read, but will tare

reads: 120.57(4-6) was $\frac{4}{5}$

CuO

tare: 0.87/7
reads: 72.58 transfered quant. tare to zero w/ paper

$\frac{34.34}{5}$ $\frac{1}{2} \frac{1}{3}$ transfered quant
paper weighs 0.1 after checked due to static glove charge
but after glove/charge removal 0.00. Think OK since
cal. w/ paper glove while (not more than 0.3% error)

Expected }
tot right } 227.46 g dry

BaO - 5.72 g/c BaCO_3 - 4.43 $\frac{1}{2} \text{O}_3$ - 3.01 CuO - 6.3 - 6.49

\therefore if bumping occurs w/ selective loss, BaCO_3 should preferentially be lost ~~if~~ not ~~well~~ uniformly suspended.

Except for 1 bump (0.06 g recovered) \Rightarrow very smooth, overestful preparations. Placed in drying oven for weekend drying. (oven cleaned before use also)

12/21 after breaking up cubes and re-baking under vac @ 70C for 3^{1/2} hrs.

~~Prick~~ #1 transferal

ideally want 75 per cent

$$\begin{array}{r} 166.6790.97 \\ \text{tax } - 86.21 \\ \hline 80.46 \\ -.01 \end{array}$$
 g. recovery

Totals
80.46
77.74
68.29

$\frac{226.49}{226.49}$ expected 227.46 (99.57%)

0.3 g recovered on ~~leaf~~ brushy lke.

CRUX 2 172.72
94.98

77.74
+ 0.03 "recovery"

$\frac{226.79}{227.16}$
 $\frac{110}{\text{total}}$
 $\underline{\underline{99.7\%}}$

CRX 3 $\begin{array}{r} 173.46 \\ 105.17 \\ \hline 68.29 \end{array}$ "white"

Rxn. Run 1 \Rightarrow W { on 12/10/11 320 ramp to 940C, 450 cool ramp
14 hrs + 3 up + 2 down = 20 hrs total

12/22 11:00 AM - 1:00 PM

{12/21}

IBM Technical Notebook

12/17-18 CENTUR ST₁₀ RUN

2:00-1700 psi Air usage 16 hr soak @ 1800 w/ 500 psi up/400 down rate
Running Si-Christy RUN Prog. 05

So for 12/21 → (*) ST₁₀ RUN 24 hrs → 1000 psi
16
40 hrs → 1500 psi max permissible

Set for 36 → Ramp started @ 4:25 p.m. 12/21
3 hrs to temp
4:25
36 hours soak
40:25

1600 psi @ 300C ramp up. 4.25
44.5 hours total should be O.K

(3 hrs → 1000) → 15,000 projected usage.

12/22 9:00 AM

19.3 soak hours left ∴ Δt → 16.7 + 3 → 19.7 (16-11250) psi → 4750

∴ 241.1 psi/hr. 19.3 + 4.25 = 23.55 (241.1 psi/hr) = 5,680

11250 - 5680 = remainder of 5,572 psi } could run longer if rate remains constant

6:00 PM

11,250 - 9,000 → 2,250 / (16.7 - 10.2) = 2250 / 6.5 = 346.2 !

346.2 (10.2 + 4.25) = 65,000 psi + (9000) = 4,000 to spare ✓

12-22

IBM Technical Notebook

17

C2 RXN seems good, NO APPARENT LIQUID, LARGE SHRINKAGE
NO VISIBLE GREEN, GOOD BLACK COLOR, BEFORE UNLOADING.

~~Post weight.~~

CRUX #1
initial

166.97
86.21
80.76

100%
EXPECTED RXN weight.

loss calc.

227.46 theoretical powder

$$80.76 + (80.76 \times (-0.1182)) = 71.214$$

$$\frac{120.54}{227.46} = 0.52994 \text{ wt \% } \text{FeCO}_3$$

CRUX #2
initial

172.72
94.98
77.74

$$\frac{153.34}{197.35} (0.52994) = 0.41176$$

as above

$$= 68.551$$

$$\Delta = 0.52994 - 0.41176 = 0.1182\% \text{ total}$$

↑
wrong?

CRUX #3

173.46
105.17
68.29

as above

$$= \frac{60.218}{199.983} \text{ total}$$

$$\frac{0.997}{0.997} = 200.58 \checkmark \checkmark \text{ OK.}$$

Actual yields - 1A HR RXN @ 940C

CRUX #2
2.27g weight loss

170.45
~~94.98~~
75.47

total weight
initial time
75.47

above expected
weight
6.919
(9.489)

% RXN
24.7

CRUX #4
2.09g weight loss

169.92
86.21
78.71

78.71

7.496
(9.546)

21.5

CRUX #3
1.55g weight loss

171.91
105.17
66.74

66.74

6.522
(8.072)

19.2

21.8% } O.K.
aver?

consistent

The above understood

Date

and
by

Date

Date

18 Recheck of wght bxs calc.

IBM Technical Notebook

$ \begin{array}{r} \text{Ba} \quad 137.34 \\ 0 \quad 15.9994 \\ \hline 153.3394 \approx 153.34 \\ \sim 153.34 \end{array} $	$ \begin{array}{r} \text{Ba} \quad 137.34 \\ 30s \quad 47.9982 \\ \hline 12.01885 \\ 197.34935 \\ \sim 197.35 \end{array} $
-------------------------------------------------------------------------------------------------------------------------------------	--------------------------------------------------------------------------------------------------------------------------------------

$$\frac{153.34}{197.35} = 0.776975 \quad (120.54) = 93.6589999 \quad 126.881 \text{ g}$$

$$26.881 \text{ g} / 3 \text{ cruc.} = \sim 8.96 \text{ g/crucible} \sim \text{correct}$$

Individual wght measures during grinding

12/29

aux 3 66.72 unloaded

$$\begin{array}{r}
 105.17 \text{ tare} \\
 171.82 \text{ loaded} \\
 171.91 \text{ previously} \\
 \hline
 0.09 \text{ g loss} = 0.135\% \\
 66.74
 \end{array}$$

$$\begin{array}{r}
 169.38 \\
 171.82 \\
 \hline
 -2.44 \text{ loss} \\
 + 1.55 \\
 \hline
 3.99
 \end{array}$$

crux ②

$$\begin{array}{r}
 86.20 \text{ tare (0.19/20)} \\
 78.75 \text{ load (-0.02) } 78.73 \\
 78.69 \text{ gain after grinding} \\
 \hline
 0.06 \text{ g loss } 0 > 0.076\% \text{ loss} \\
 164.85 \\
 78.65 \text{ 0.09 g loss} = 0.115\% \text{ loss}
 \end{array}$$

$$\begin{array}{r}
 161.68 \\
 164.85 \\
 \hline
 -3.17 \text{ loss} \\
 + 2.27 \\
 \hline
 5.44 \text{ total to date}
 \end{array}$$

crux ①

$$\begin{array}{r}
 75.49/8 \text{ unloaded} \\
 94.99/8 \text{ tare} \\
 75.46 \text{ load (precru)} \\
 \hline
 170.44 \text{ loaded} \\
 75.46 \text{ 0.03 loss}
 \end{array}$$

$$\begin{array}{r}
 167.18 \\
 170.44 \\
 \hline
 -3.26 \text{ loss} \\
 + 2.05 \\
 \hline
 5.31
 \end{array}$$

The above understood
and witnessed by

Date

and
by

Date

IBM Technical Notebook

19

Samples were incompletely converted, as right loss indicated. Top was black, but went through a transition of greens progressively over crucible. Ground powder was a dull forest green. Cux 1 slightly darker than 2 & 3. All had white hard agglomerates (presumably B_2O_3). Tops inhibited oxygen flow throughout crucible. No tops used for second run. Heat treatment.

2/29 New losses consistent w/ cux loading. Conversion now up to 70.8 ~ 71%. Well reground and reweighed initial weighing loss

cux 2
unloaded 95.02
ground 72.10

cux 1
grd. 86.21 ✓
75.40

cux 3
grd pot 105.19
64.15

cux 1 } 192.24 } 188.21 -4.03 22.82 expected 26.807 (85.1%)
(3 crucibles) 86.24/1

cux 2 } 199.53 } 195.48 -4.05
95.01

Reground, to 1 crucible

286.00
86.27
199.73 & 202.47 to start
(before grd)

$\% (202.47 - 199.73) = 2.74 \text{ g loss } (1.35 \%)$

IBM Technical Notebook

Night Loss Summary (by rxn) { crucible

Crucible #	Initial	Post ①	Post ②	Post ③	Crucible
1	80.76	78.71	75.48	102.0	1 & 3
2	77.74	75.47	72.20	100.47	2
3	68.29	66.74	64.21	202.47	
Thermet	226.79	220.92	211.89		
	227.46				

Final gnd into 1 crucible: pre 202.47
 gnd post 199.73
 loss 2.74g (1.35% \Rightarrow 1g spill of saved powder)

Was 85% reacted before this run.
 Total loss so far slightly less than 2432g / 27.46 (88.5-85%)

Expect less than, but approx. 3.0 g loss for complete rxn.

0.52994% B_2O_3 { (0.77895% of B_2O_3 is B_2O)

Look for 283g total upon cooling!

1/5 initial wght. 288.00
 post 284.17
 001.83g

199.73 initial
 197.59 unloaded
 2.14

1/4 SrTiO_3 synthesis ^{IBM Technical Notebook} references book III pgs. 77, A3

21

TiO_2 - 79.8988 g/m

SrCO_3 - 147.6235

SrTiO_3 - 183.5182

SrO - 103.6194

Ti - 47.90

in SrTiO_3 26.1009

Sr - 87.62

in 47.7446

Take transferred amount to SHAKER JAR (SrCO_3) as basis for TiO_2 addition

$$\cancel{201.66 \text{ g base}} \frac{48.50}{147.6235} \times 1.328(54) \text{ moles} \times 79.8988 \text{ g/TiO}_2 = 26.2499$$

$$= 26.2541$$

~~110.85~~

$$\begin{array}{r} 251.07 \\ 202.56 \\ \hline 48.50 \end{array}$$

$$\begin{array}{r} 251.07 \\ 26.25 / 999 = 26.2763 \\ \hline 277.32 \text{ target } 277.3(5) \end{array}$$

actual 277.35/6

The above understood
and witnessed by

Date

and
by

Date

22

IBM Technical Notebook

COMPS SCRIPT A1 dated 87/12/02 14:32:25 Page 1

Date: 2 December 1987, 13:24:31 EST
 From: PLECHAT at YKIVMZ
 To: PRD

The laboratory results on your samples are:

# C1	Y	Ba	Cu O	Cu=1, ICP
	0.03	0.68	X	
# C2	Y	...	78.1 % (V/V)	
# C3	Ba	...	88.9 %	
# C4	Ti	...	57.3 %	/ error due to static electr. during weighing of sample/
# C5	Ti	...	22.2 %	
	Sr	...	49.4 %	
# C6	Ti	...	24.2 %	
	Sr	...	50.6 %	
# C7	Y	Ba	Cu O	Cu=1
	0.34	0.71	X	
# C8	Y	Ba	Cu O	
	0.34	0.71	X	
# C9	Y	Ba	Cu O	
	2.37	1.10	X	

MHP

Date: 21 October 1987, 10:45:18 EDT
 From: PLECHAT at YKIVMZ
 To: PRD

The laboratory results on your samples are:

# C1	Y	Ba	Cu O	Cu=1, ICP
	0.35	0.72	X	
# C1f	Y	Ba	Cu O	
	0.33	0.70	X	
# C5	Y	Ba	Cu O	
	2.21	1.06	X	

Other results to follow from Olson,

MHP

Note: I have produced a light green compound from 123 with
 the formula: Y Ba Cu O. If interested get in touch
 12 3 X
 with me.

threshold
T_i consistently low 26e1
Sr consistently high 47.7

The above understood
 and witnessed by

Date

and
by

Date

IBM Technical Notebook

2:

41
21
28.17
tare 86.61
196.56

initial 197.59
196.56
1.03 g lost during grinding

Post
196.56
194.16
-2.40

Lost another 2.4 g.. Must be totally converted @ Ruopant.

UNIaxial - 7,000 / 0.371 = 18,870 PSI
0.126 0.161 2.53 4.19 65.8
0.320 1.55 0.604

C2P1 green
no final dms. 2d

C2P2 → Will leave notes on pusher later, too busy. Still see 110. on crucible however, disheartening.

→ 1 mill 4.2 um PSD 10-1 ~ flat dist.

green 27 isopressed

3.59 0.580 0.194 4.274 67.1% (high vs C1)
1.473 0.493 0.84

C2P3- mill 2 2.53 um ave., much better behaved pellet

(Green)

3.55 0.576 0.210 3.96 62.2% (good agreement w/ C1)
1.463 0.533 0.896

C2P2- removed @ 600°C ⇒ 20° up to 800, 10° to 975, 20° down

3.59 0.554 0.186 4.89 76.8% ! terrible
1.407 0.472 0.734 slightly higher dms
pellet attrition

1/13

C2P3 3.57 0.517 0.185 5.57
1.313 0.47 0.636

87.4%

~ 88

IBM Technical Notebook

24 1/13

C2P4 3,775 uni/26,000 1sc

988 1 transient 796 peak
 2HRS/600 over

3.50/1

0.576 0.206
 1.463 0.523

3.987 0.819

62.6% consistent

1/14

3.49

0.515 0.180
 1.308 0.457

5.68 0.614

89.2

C2P5

3775/24

990

3.18

0.577 0.199
 1.466 0.505

3.74 0.85

58.7%

3.15

0.496 0.168
 1.26 0.427

5.92 0.532

92.9

pellet has stress cracking and photo microstructure with
 large grain interior and peripheral eggshell of small grains.

The above understood
 and witnessed by

Date

and
 by

Date

Dates:

Date and sign every entry. Have entry witnessed. Submit anything possibly new or important.

THIS FORM IS:
☐ Unclassified
☐ IBM Confidential
☐ IBM Confidential

☐ IBM Confidential-Restricted
☐ Registered IBM Confidential
 *Register with local Recorder

IBM Technical Notebook

21

TEST III
 DATE 1/1/80
 SAMPLE 12-1000
 SOLVENT ISO

• CONDITIONS
 BALLS: 2.000"
 BALLS: 6.700"
 BALLS: 6.700"
 BALLS: 6.700"
 BALLS: 6.700"
 BALLS: 6.700"
 BALLS: 6.700"
 BALLS: 6.700"
 BALLS: 6.700"
 BALLS: 6.700"

• TIME 0.0 - 10.0 SEC

• DATA



• DISTRIBUTION TABLE BY VOL.

DATE	TIME	RESPONSE
1.00-1.00	0.0	0.0
1.00-1.00	0.0	0.0
1.00-1.00	0.0	0.0
1.00-1.00	0.0	0.0
1.00-1.00	0.0	0.0
1.00-1.00	0.0	0.0
1.00-1.00	0.0	0.0
1.00-1.00	0.0	0.0
1.00-1.00	0.0	0.0
1.00-1.00	0.0	0.0

• DISTRIBUTION GRAPH BY VOL.



TEST III
 DATE 1/1/80
 SAMPLE 12-1000
 SOLVENT ISO

• CONDITIONS
 BALLS: 2.000"
 BALLS: 6.700"
 BALLS: 6.700"
 BALLS: 6.700"
 BALLS: 6.700"
 BALLS: 6.700"
 BALLS: 6.700"
 BALLS: 6.700"
 BALLS: 6.700"
 BALLS: 6.700"

• TIME 0.0 - 10.0 SEC

• DATA



• DISTRIBUTION TABLE BY VOL.

DATE	TIME	RESPONSE
1.00-1.00	0.0	0.0
1.00-1.00	0.0	0.0
1.00-1.00	0.0	0.0
1.00-1.00	0.0	0.0
1.00-1.00	0.0	0.0
1.00-1.00	0.0	0.0
1.00-1.00	0.0	0.0
1.00-1.00	0.0	0.0
1.00-1.00	0.0	0.0
1.00-1.00	0.0	0.0

• DISTRIBUTION GRAPH BY VOL.



TEST III
 DATE 1/1/80
 SAMPLE 12-1000
 SOLVENT ISO

• CONDITIONS
 BALLS: 2.000"
 BALLS: 6.700"
 BALLS: 6.700"
 BALLS: 6.700"
 BALLS: 6.700"
 BALLS: 6.700"
 BALLS: 6.700"
 BALLS: 6.700"
 BALLS: 6.700"
 BALLS: 6.700"

• TIME 0.0 - 10.0 SEC

• DATA



• DISTRIBUTION TABLE BY VOL.

DATE	TIME	RESPONSE
1.00-1.00	0.0	0.0
1.00-1.00	0.0	0.0
1.00-1.00	0.0	0.0
1.00-1.00	0.0	0.0
1.00-1.00	0.0	0.0
1.00-1.00	0.0	0.0
1.00-1.00	0.0	0.0
1.00-1.00	0.0	0.0
1.00-1.00	0.0	0.0
1.00-1.00	0.0	0.0

• DISTRIBUTION GRAPH BY VOL.

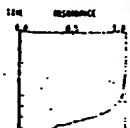


TEST III
 DATE 1/1/80
 SAMPLE 12-1000
 SOLVENT ISO

• CONDITIONS
 BALLS: 2.000"
 BALLS: 6.700"
 BALLS: 6.700"
 BALLS: 6.700"
 BALLS: 6.700"
 BALLS: 6.700"
 BALLS: 6.700"
 BALLS: 6.700"
 BALLS: 6.700"
 BALLS: 6.700"

• TIME 0.0 - 10.0 SEC

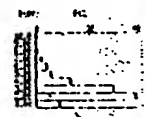
• DATA



• DISTRIBUTION TABLE BY VOL.

DATE	TIME	RESPONSE
1.00-1.00	0.0	0.0
1.00-1.00	0.0	0.0
1.00-1.00	0.0	0.0
1.00-1.00	0.0	0.0
1.00-1.00	0.0	0.0
1.00-1.00	0.0	0.0
1.00-1.00	0.0	0.0
1.00-1.00	0.0	0.0
1.00-1.00	0.0	0.0
1.00-1.00	0.0	0.0

• DISTRIBUTION GRAPH BY VOL.

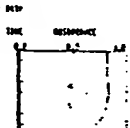


TEST III
 DATE 1/1/80
 SAMPLE 12-1000
 SOLVENT ISO

• CONDITIONS
 BALLS: 2.000"
 BALLS: 6.700"
 BALLS: 6.700"
 BALLS: 6.700"
 BALLS: 6.700"
 BALLS: 6.700"
 BALLS: 6.700"
 BALLS: 6.700"
 BALLS: 6.700"
 BALLS: 6.700"

• TIME 0.0 - 10.0 SEC

• DATA



• DISTRIBUTION TABLE BY VOL.

DATE	TIME	RESPONSE
1.00-1.00	0.0	0.0
1.00-1.00	0.0	0.0
1.00-1.00	0.0	0.0
1.00-1.00	0.0	0.0
1.00-1.00	0.0	0.0
1.00-1.00	0.0	0.0
1.00-1.00	0.0	0.0
1.00-1.00	0.0	0.0
1.00-1.00	0.0	0.0
1.00-1.00	0.0	0.0

• DISTRIBUTION GRAPH BY VOL.



The above understood

Date

and
 by

Date

IBM Technical Notebook

28 1/19 (18, 17, 16, 15 26th Aug)

NOTE → C1 powder

C1 P12, 13, 14, 15 3775/26, 5

C1 P12

3.04	0.574	0.178	3.92	61.5%
	1.478	0.452	0.7755	
3.01	0.506	0.153	5.966	93.66%
	1.285	0.389	0.509(5)	

C1 P13

3.00	0.574	0.175	3.93(4)	61.8%
	1.478	0.444(6)	0.7626	
2.97	0.506	0.150	6.01	94.35
	1.285	0.381	0.494	

C1 P14 (*)

2.89	0.574	0.169	3.92(7)	61.6%
	1.478	0.429	0.736	

C1 P15 (*)

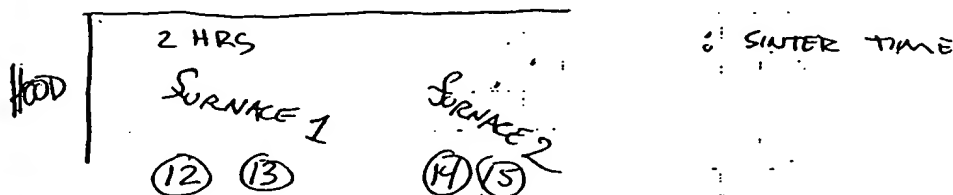
3.05	0.575	0.179	4.00	62.8%
	1.460(6)	0.455	0.762(6)	

(*) NO DATA ON final pellets - Tom took

IBM Technical Notebook

29

1/19 Runs in furnace as: all ramps 10°C/min



1/19 A.M. ↓
4:10 P.M. 4:25 P.M.
to temp (97.5°C)
6:10 P.M.
Ramp down to 600°C soak
1/20 1:19 P.M.
Ramp down to RT
check 2:22 (270°C)

Pellet thickness experiment DD mill powder 3775/26,000

DT2.0

2.04	0.575	0.119		4.03	63.3 %
2.01	1.460(5)	0.302	0.506		
	0.507	0.100		6.09	
	1.288	0.234	0.33		95.6

DT1.5

1.54	0.575	0.090		4.01	62.95 %
1.51	1.460(5)	0.229	0.384		
	0.509	0.075		6.04	94.8
	1.293	0.190(5)	0.250		

DT1.0K

1.09	0.575	0.065		3.95	62.0 %
	1.460(5)	0.165	0.276		

The above understood and witnessed by

Date

and by

Date

30

IBM Technical Notebook

Cutting Calculations for C1P12, B

$$\begin{array}{r} 0.108 \\ 0.06 \\ \hline 0.048/3 = 0.016 \end{array} \quad 3 \text{ blade thickness} + 0.05$$

C1P12 (0.025) 5 = 0.125
 (0.025) 6 = 0.150 \neq O.K. from micrometer

use 2 cuts { no 'parallelism'

$$\begin{array}{r} 0.050 \\ 0.040 \\ \hline 0.11/3 = 0.037 + 0.015 = 0.052 \end{array} \quad \text{no from edge}$$

1 cut MADE, BUT PELLET HAS CRACK

$$\begin{array}{r} (0.025) 6 = 0.150 \\ 0.040 \\ \hline 0.11/3 = 0.037 + 0.015 = 0.052 \end{array}$$

1/21

DT 1.751 in furnace/no green data (5°C ramp to try to eliminate sinter-cracking)

DT 1.75(2)

1.88	0.575	0.111	3.98	62.5	never run
	1.465	0.282	0.472		

The above understood
 and witnessed by _____

Date: _____

and
 by _____

Date _____

IBM Technical Notebook

31

Stereopycnometer

1/27/88 {25/26 supply, miller repair}
28
29, 2/01

See sheets

Data Points (Multiples)

"	D _A		D _P
"83"	82.95	DRC, DDP12	95.8
"86"	86.4	JP262, C1P3, C1P2	92.2
"89"	89.3	C1P1, C1P4, C1P7	89.56
"91"	91.3	C1P1, C1P5, C1P8	91.9

NOTE pack: 99.3-95.8

← $\Delta 86.4 - 89.3 = \Delta 3\%$

Single Point trends ⊗

87.5	87.5	JP1	83	seems to NOT clear, could be closed
77		C2P2	95.4	DEFINITELY wide open
"93"	93	DDP13	86.6	indicates closure

⊗ small volumes yield low D values for closed porosity.

32

3500/26,000

IBM Technical Notebook

2/02 Saturday: Porosity Inquiry C1 & C2 @ 975
{ 10°/min ramp from RT, 2 HOUR SOAK, 10°/min to RT no
O₂ equilibration. In order from left to right in rows,

C1P16

3.03	0.575	0.178		4.00	62.8	} GOOD NEW	polished
	1.460(5)	0.452	0.757				
3.00	0.500	0.152		5.92	92.9		
	1.293	0.386	0.507				

C1P17

3.26	0.575	0.191		4.01	62.9(5)	} GOOD NEW	
	1.460(5)	0.485	0.812(5)				
3.22	0.508	0.164		5.94	92.8		
	1.290	0.4166	0.544(5)				

C2P6

3.16	0.575	0.191		3.82(6)	60.0	} GOOD NEW	
	1.460(5)	0.493	0.826				
3.11	0.497	0.160		6.12	96.1		
	1.262	0.406	0.507(8)				

C2P7 ^{chip}

3.21	0.575	0.199		3.79	59.5	} GOOD NEW	polished
	1.460(5)	0.505(5)	0.847				
3.16	0.497	0.164		6.065	95.2		
	1.262	0.4166	0.521				

C2P7 good & dense, but exterior cracking due to oxygen penetration.
Will guide cool by opening furnace. Quench.

The above understood
and witnessed by _____

Date _____

and
by _____

Date _____

IBM Technical Notebook

33

ITEM

C2-8 3.08 0.573 0.191 3.82
1.155 0.485 0.806
3.06(5) 0.529 0.158 5.53
1.328 0.399 0.553

59.97 \Rightarrow ~60%
comparable to previous
see
86.8

C1-18 3.07 0.578 0.178 4.01
1.468 0.452 0.765
3.03 0.497 0.158 6.04
1.267 0.401 0.5016

62.95 ~ 63%
comparable to previous
94.8

2/12

HP-4 green 5,000/27,000

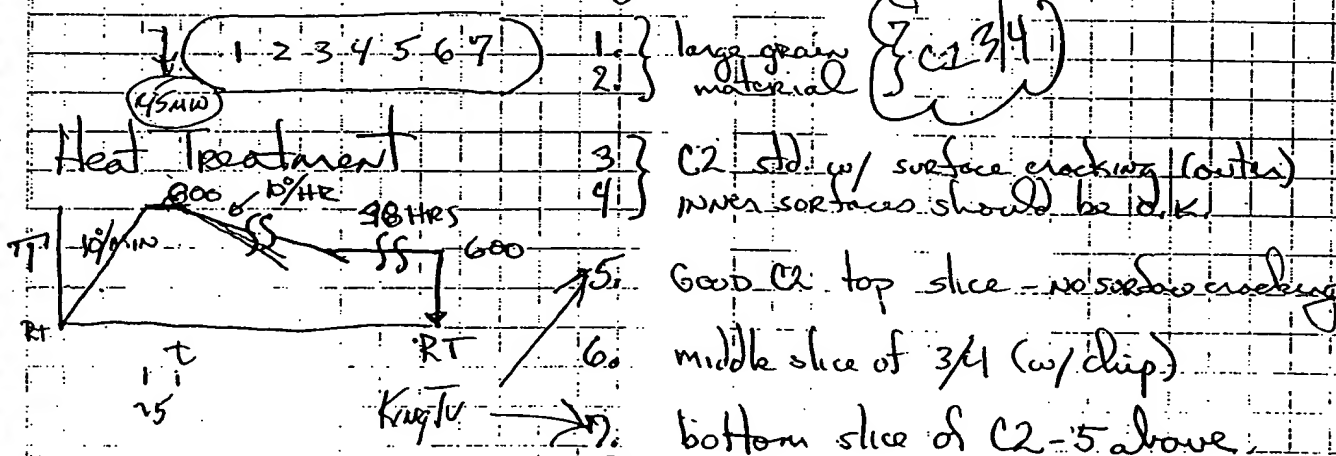
13.98 0.947 ~0.301
2.405 0.764(5) 3.473

4.02(5) 63.2

Cling C2-8 dry
ST 0.50

Boat Spots \rightarrow positioning I.D.

2/15



START: 4:50 PM 2/12 \rightarrow 6:15 start ramp down 20 HRS to soak point
QUENCH 2:50 2/15 \rightarrow 3:00 ~ 30 HRS

34 2/17 3500/26750

IBM Technical Notebook

C2-9	3.09	0.575	0.193		3.76	59.0%
		1.460(5)	0.490	0.821		
	3.06	0.510	0.168			
		1.295	0.427	0.562		85.5 !

C2-10	3.06	0.575	0.191		3.77	59.2%
		1.460(5)	0.485	0.812(5)		
	3.02(5)	0.501	0.164		5.77	90.6
	3	1.272(5)	0.417	0.530		89.6

Furnace Oz purge > 1 HR @ 29⁽³²⁾ 12:10 P.M. ∴ 945/10 =
 94.5 mins / 60 min / HR = 1.575 HRS OR 1 hr 34.5 mins (1:45 START
 1:45-2:15 (1/2 hr sinter) w/ guard. SINTER)

C2-11	3.02	0.575	0.188		3.775	59.3% O.K.
		1.460(5)	0.477(5)	0.80		
	2.98	0.505	0.159		5.71	89.64 ~90
		1.283	0.404	0.522		

The above understood
 and witnessed by

Date

and
 by

Date

D₅₀ 4 μ m

D₅₀ 6 μ m

D₅₀ 6-7

D₅₀ 9

35

IBM Technical Notebook

NOTES CRP-500
PARTICLE ANALYZER

DATE 2/18
SAMPLE C2-III OF
SOLVENT 150

D₅₀ 0.83

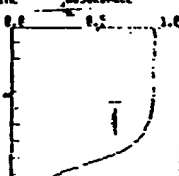
• CONDITIONS

SOLV. FISC 2.16 (CP)
SOLV. PENS 0.79 (CC)
SAMP. PENS 6.37 (G/CC)
D (MAX) 16.6 (PC)
D (MIN) 1.00 (PC)
D (D₅₀) 1.00 (PC)
SPEED 500 (RPM)

• TIME 0.4 4 RIN 15 SEC

• DATE

TIME DISPERGANCE

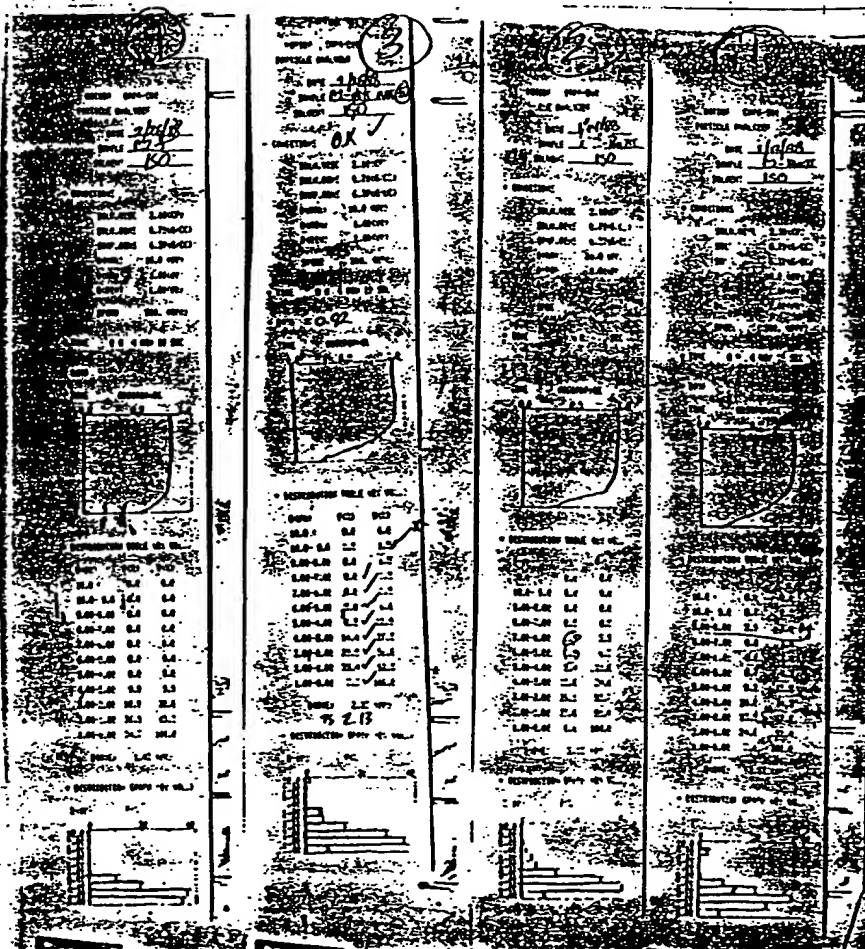
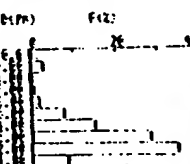


• DISTRIBUTION TABLE (BY VOL.)

D (PC)	F (C)	D (C)
10.0 - 5.0	0.0	0.0
5.00 - 4.00	2.0	2.0
4.00 - 3.00	0.5	3.2
3.00 - 2.00	0.7	3.9
2.00 - 1.00	1.0	5.7
1.00 - 0.00	7.0	13.5
	15.1	26.6
	26.2	56.6
	34.7	91.5
	6.2	100.0

D (MAX) 2.24 (PC)

• DISTRIBUTION GRAPH (BY VOL.)



C2 PSDS

- 1) C2 MILL PASS II
- 2) C2 + PASS III of 1/2 of ①
- 3) C2 MILL PASS IV of other 1/2 of ①
- ④ fines from ①, ②, ③ III

⑤ 3rd MILLING WAS ineffective due to clogged bag
& powder charged channels.

The above understood
and witnessed by

Date

and
by

Date

36 SrTiO_3 3/4 Synthesis (see Book III page 77 for work-up) IBM Technical Notebook

Prep:

SrCO_3	tare	206.15	
		50.00 g	desired
		256.15	
		256.15/6	actual wght
		0.0	Δ
TiO_2		27.062	desired
		283.212	desired
		283.22	actual wght
		+0.01	Δ
		+0.01	scale replace
		~ 0.0	Δ net

1 hr + mixing

Transfer

	tare	89.20	
		166.23	final wght
		77.03 ⁺	
		77.062	expected
		-0.03 g	Δ 0.04

185.56	total prelim wght w/ top
19.33 g	top

theoretical expected	151.36	w/ out top	150.97
	19.33		
	170.69	w/ top	

$14.87 + 62.16 = 77.03 \sim \text{correct}$

Ramp @ 700C/hr to 1450C \Rightarrow to temp $\sim 3:25$

$0.39/150.97$ (0.258% loss)

GROUND yield $\Rightarrow 61.39/62.16 \Rightarrow 98.8\%$
 $\sim 1\%$ grinding loss

Clean X-RAY. MOL. 1 HOUR.

Syn PROJECT COMPLETE
 3/5

3/4/88

C2 pellets

C2P12-15
C2P16-17

IBM Technical Notebook
1 III
2 IV

3700/27000

37

C2P12
3/21 →
page 44

3.075
(3.08)

0.572
1.453

0.191
0.485

0.804

3.825

60.0

C2P13
3/21 →
page 44

3.02
(3.02)

0.573
1.455

0.188
0.477(5)

0.794

3.803(5)

59.7

C2P14
page 47

3.11

0.574
1.458

0.192(3)
0.488

0.815

3.82

59.9

C2P15
page 47

3.11

0.574(5)
1.459

0.192(3)
0.488

0.816

59.8

C2P²16

3.25

0.573
1.455

0.202
0.513

0.853

59.8

C2P²17
SR clipped

3.22 → add 0.02
(3.24) calc

0.573
1.455

0.202
0.513

0.853

59.6⁺

38 SrTiO_3 GB Doping IBM Technical Notebook

10g SrTiO_3 w/ 2 wt % B_2O_3 added

Sp. g - 8.8 m.p. 820°C

10g + 0.2g $\text{B}_2\text{O}_3 \Rightarrow 10.2$

0.2g Ag_2O 7.14g/cc Decomposes above 300°C

$\text{AgNO}_3 \gg$ mp 212°C bp > decomp 169.8749 mol

4.388g/cc

0.2g $\text{Ag}_2\text{O} \times \Rightarrow 231.7394$

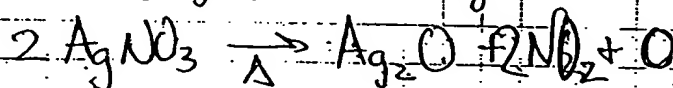
169.8749g AgNO_3
 g/mol

$\Rightarrow 0.733, 1.364$

0.2g $\text{Ag}_2\text{O} \times \frac{169.8749 \text{ g/mol}}{231.7394 \text{ g/mol}} = 0.1466 \approx 0.15\text{g}$ OK

$\times 2 = 0.29$

0.2g $\text{AgNO}_3 \times 169.8749$



~~0.2g $\text{Ag}_2\text{O} \times \frac{231.7394 \text{ g/mol}}{169.8749 \text{ g/mol}} = 0.278\text{g} \text{AgNO}_3$~~

IBM Technical Notebook

129500 Doped SiO_2 pellets

STA-1 3.10 0.581 0.196
1.476 0.498
3.0 0.525 0.178
1.334 0.452

STA-3 deformed, SiO_2 basis 3/5
3.64 75.7
0.852 4.75 98.8
0.632

STA-2 3.25 0.581 0.208
1.476 0.521
3.14 0.525 0.185
1.334 0.470

3.65 75.9
0.891 4.78 99.1 ← polish
0.657

129 STB-1 3.03 0.587 0.191
1.491 0.485
2.88 ← 2.72 0.599 0.174
(chip) 1.370 0.470 0.644

3.58 74.4
0.847 4.47 92.9

STB-2 3.17 0.586 0.197
1.488 0.500
3.03 ← 3.21 0.179
1.370 0.455

3.646 75.9
0.869(5) 4.52 94

129500 STB-3 3.77 0.583 0.237
1.481 0.60
3.61 ← 3.74 0.534 0.216
deformed 1.356 0.549 0.793

3.66 76.1
1.03 4.55 94.6 ← polish

ST-D1 3.62 0.585 0.235 ^{varies}
1.486 0.597
3.60 ← 3.67 0.527 0.210
1.339 0.533 0.7505

1.03(5) 3.55 72.8
4.77 99.2 ← polish

Comments - green D^* fairly consistent, even w/ pressure variation

40

IBM Technical Notebook

DD-X

37/22000

2.88

0.573

0.169

1.455

0.429

C.713

4.04

63.4%

2.83

0.508

0.144

1.290

0.366

C.478

93

DD-Y

2.99

0.575

0.174

1.46(5)

0.442

0.740(5)

4.04

63.4%

2.93

0.509

0.149

1.293

0.379

C.498

92.4

10°C/min RAMP IN NEW Al_2O_3 CRUCIBLE ON FRESH DD POWDR.
 975°C FOR 2 HOURS { QUENCH. 20min O_2 PURGE.

The above understood
 and witnessed by

Date

and
 by

Date

Date and sign every entry. Have entry witnessed. Submit only anything possibly new and alive.

ve. sibly important
L. osure of

THIS PAGE IS:
☐ Unclassified
☐ IBM Confidential
☐ IBM Confidential

Only

☐ IBM Confidential-Restricted
☐ Registered IBM Confidential
Register with local Recorder

IBM Technical Notebook

41

MOPIEF CARP-500
PARTICLE ANALYZER

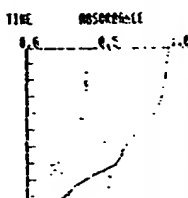
DATE 2/24/88
SAMPLE 2/24
SOLVENT ISO

• CONDITIONS

SOLV. VISC 2.75(CP)
SOLV. DENS 0.7916(G/CC)
SAMP. DENS 0.8416(G/CC)
D(RX) 10.0 (PP)
D(RIN) 1.00 (PP)
D(DIN) 1.00 (PP)
SPEED 500. (RPM)

• TIME 0.0 4.0 20.0 SEC

• DATA

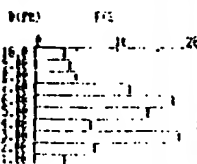


• DISTRIBUTION TABLE (BY VOL.)

D(RX)	F(C)	P(C)
10.0-0.0	0.0	0.0
10.0-5.0	3.5	12.5
9.00-0.00	4.2	17.7
8.00-7.00	4.0	22.5
7.00-6.00	11.0	34.2
6.00-5.00	16.0	50.0
5.00-4.00	12.0	64.7
4.00-3.00	6.0	71.0
3.00-2.00	17.0	85.2
2.00-1.00	7.2	94.2
1.00-0.00	3.7	100.0

D(RX) 5.00 (PP)

• DISTRIBUTION GRAPH (BY VOL.)



MOPIEF CARP-500
PARTICLE ANALYZER

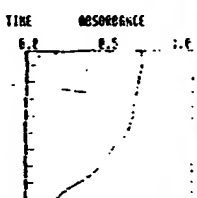
DATE 2/24/88
SAMPLE 2/24
SOLVENT ISO

• CONDITIONS

SOLV. VISC 2.75(CP)
SOLV. DENS 0.7916(G/CC)
SAMP. DENS 0.8416(G/CC)
D(RX) 10.0 (PP)
D(RIN) 1.00 (PP)
D(DIN) 1.00 (PP)
SPEED 500. (RPM)

• TIME 0.0 4.0 20.0 SEC

• DATA

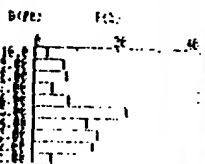


• DISTRIBUTION TABLE (BY VOL.)

D(RX)	F(C)	P(C)
10.0-0.0	0.0	0.0
10.0-5.0	2.5	2.5
9.00-0.00	7.2	10.0
8.00-7.00	7.0	17.7
7.00-6.00	4.4	22.1
6.00-5.00	0.2	30.0
5.00-4.00	22.0	52.0
4.00-3.00	12.0	65.0
3.00-2.00	15.0	81.0
2.00-1.00	14.0	95.0
1.00-0.00	4.5	100.0

D(RX) 4.12 (PP)

• DISTRIBUTION GRAPH (BY VOL.)



MOPIEF CARP-500
PARTICLE ANALYZER

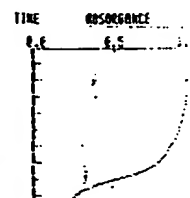
DATE 2/24/88
SAMPLE 2-24/88
SOLVENT ISO

• CONDITIONS

SOLV. VISC 2.10(CP)
SOLV. DENS 0.7916(G/CC)
SAMP. DENS 0.8416(G/CC)
D(RX) 10.0 (PP)
D(RIN) 1.00 (PP)
D(DIN) 1.00 (PP)
SPEED 500. (RPM)

• TIME 0.0 4.0 20.0 SEC

• DATA

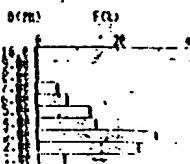


• DISTRIBUTION TABLE (BY VOL.)

D(RX)	F(C)	P(C)
10.0-0.0	0.0	0.0
10.0-5.0	0.0	0.0
9.00-0.00	0.0	0.0
8.00-7.00	0.0	0.0
7.00-6.00	5.1	5.1
6.00-5.00	12.7	12.7
5.00-4.00	12.7	25.5
4.00-3.00	14.0	39.5
3.00-2.00	25.2	64.6
2.00-1.00	24.7	89.3
1.00-0.00	6.3	100.0

D(RX) 2.45 (PP)

• DISTRIBUTION GRAPH (BY VOL.)



The above understood
and witnessed by

Date

and
by

Date

42

IBM Technical Notebook

3/15 DC batch II SP_4O_3

per ton 206.11 (206, unstable
 $\frac{256.06(7)}{49.95} g$ loss 0.05 (0.1%) desired 50g

$\frac{27.06^2}{283.122}$ target
 $\frac{283.13}{27.07}$ actual ✓
 $\frac{17.02}{+0.008}$ total

$\frac{88.34(15)}{17.02}$ Pt. cur. tone
 $\frac{165.36(7)}{165.34}$ total above
 expected comb. weight
 0.03 g error max. ✓ OK. (0.04% error)

~184.54 (19.20 tone) ✓ expect ~154.0 w/out top

150.15 after cooling!

3/16 41.20 < 100 mesh = 59.85 g

ST-D2 3750/25,000
 (2.9μm) 3.04 0.583 0.206 3.38 70.3 %
 m. II 1.481 0.523 0.900
 3.017 0.514 0.181 4.90 1.02 %
 1.306 0.460 0.616

The above understood
and witnessed by

Date

and
by

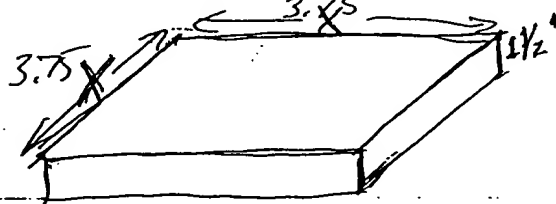
Date

7070 GLASS count

1 1/2"

70% density - $2.13 \text{ g/cc} \Rightarrow \frac{\text{kg}}{1000 \text{ g}} \times \frac{0.00571 \text{ lb}}{3.73 \times 10^{-4} \text{ kg}} \frac{\text{cc}}{\text{cc}}$

$0.00571 \frac{\text{lb}}{\text{cc}} \times \frac{16.387 \text{ cc}}{3.75 \text{ in}^3} = 0.0936 \frac{\text{lb}}{\text{in}^3}$ try conv.



$4.08 \times 4.08 \times 1.5 = 21.32 \text{ in}^3$

$\frac{21.32 \text{ in}^3}{24.9696} \times \frac{0.0936 \text{ lb}}{\text{in}^3} = 1.99 \text{ lb}$

$1.5 \times^2 (0.0936 \frac{\text{lb}}{\text{in}^3}) = 2$

$1.5 (0.0936 \frac{\text{lb}}{\text{in}^3}) \times^2 = 2 \text{ lb}$

4.78^2

$0.209 \times^2 = 2 \text{ lb}$

$\times^2 = 16.86$

$\times = 3.77 \text{ in}$

check density conversion: $2.13 \frac{\text{g}}{\text{cc}} \times \frac{1 \text{ lb}}{453.59 \text{ g}} \times \frac{3.73 \times 10^{-4} \text{ kg}}{1 \text{ cc}} =$

OK

$\frac{0.00213 \text{ kg}}{\text{cc}} \times \frac{1 \text{ lb}}{453.59 \text{ kg}} = 0.0048965 \frac{\text{lb}}{\text{cc}}$

$1 \text{ lb} = 4.535 \times 10^{-4} \text{ kg}$
 $1 \text{ lb} = 0.435 \text{ kg}$

$0.0048965 \frac{\text{lb}}{\text{cc}} \times \frac{16.387 \text{ cc}}{\text{in}^3} = 0.08 \frac{\text{lb}}{\text{in}^3}$

4x4x1.5 OR 5x5x1

@ 1" thick $0.08 \times^2 = 2$
 $\times^2 = 25$
 $\times = 5$

44

IBM Technical Notebook

3/21 1st pellet 700C for 12 hrs. \Rightarrow START @ 3 to RAMP @
 10°/MIN to 800C for 16-17 hrs.

C2P12 for green data on all pellets see pg 37

C2PB 2nd pellet 750C to run concurrently

Peter,

Since we didn't get to discuss this experiment in more detail, here is what needs to happen.

5 pellets - C2
 1st) - 700° C ~12 hr O₂ 308
 2nd) - 750° C ~12 hr O₂ 302
 3rd) - 800° C " "
 4th) - 850° C " "

After three intermediate temperature anneal,
 weigh and measure each pellet. If no sintering,
 or at least a negligible amount, has occurred, then
 re-fire each sample for 12 hrs again at the same
 intermediate temperature and then sinter each pellet
 for 2 hrs at 950° C. Ramp from the intermediate
 T to 950° C fast (~20° C/min).

Also sinter the 5th pellet at 950° C
 for 2 hrs, this is the control pellet. Thanks
 and have a good week.

Puane

3/23 Temp raised to 950° C @ 9:00
 to temp @ 9:15 am

C2P12 3.06 (Δ -0.02)
 3.01

0.572 0.191 no sintering, but 0.65% wght loss:
 0.50 0.163 5.65 88.7
 1.27 0.414 0.533 CRACKING = closing

C2P13 3.01 (Δ -0.05)
 2.97

0.572 0.187 no sintering, but 0.60% wght loss:
 0.504 0.163 5.57 87.4
 1.280 0.414 0.533 NO CRACKING = open

The above understood
 and witnessed by

Date

and
by

Date

IBM Technical Notebook

45

3/21 SiTiO_3 DRC-batch 2 \rightarrow fine coll after 3rd milling \rightarrow 11g yield
 after cleaning ~ 2g loss to machine
 3g loss to blow-out
 fines \rightarrow 1.34 μm ave
 medium \rightarrow \geq 2.2 μm RANGE (2.2-2.8)
 approx. expectations { 18% fines
 82% medium
 61g / 72 orig.
 ~ 85% yield

STD 1f-1 0.570 0.212 3.09 64.2% versus 72.1
 2.74 1.448 0.538(5) 0.887 3um probe

In furnace ~ 3:00 p.m., tripped off @ 975 2X, cooled to 1400C, then to 1600C.

Temp recovered/reset to 1650 @ 4:30 p.m..

3/22 RAN all NITE! 24 HRS @ 3:00 p.m. Tuesday, 42 HRS @ 9:00 a.m. Weds.
 2.70 0.487 0.178 4.97 1.033% same as old!
 1.237 0.452 0.543

Peter:

✓ started
 - Cut, section and polish Cu-Bi shot (Start Plan)

start/finish 21/22

- Try firing one pellet of SiTiO_3 to 1350C overnight

- Try slip casting a pellet of SiTiO_3

\rightarrow Finest Jet mill SiTiO_3 grade down to ~ 1 μm . This will require "fining" the jet mill. Run for 1650C overnight

USED fines, fine 21/2

✓ - Make water bath of SiTiO_3 ?

tare 202.33 * approx. due to instability - spans down: sometimes stable
 60.00 TRANSFER. 165.22 act weight

act weight 252.33 target
 252.33 * 100
 100.00 Δ 0.0

tare 88.17
 77.05 wght max
 77.07 expected
 ~ 0.03% loss

27.062
 279.392
 out weight 279.4 ~ 0.01

POST/16HR 150.02
 + 14.87 g expected loss
 164.89
 15.2g actual loss

write-up 3/23, pwr 3/24

IBM Technical Notebook

46/3/23

C3-Synthesis
(Reference)

Synthesis
BaCO₃

target → 277.72 to zero
weight: ?

3/23 398.24-6 total
120.52-54 (-0.02%)

CaO

target → 0.89 → zeroed
weight: 72.58 (7/9) 3/23

transferral quant

4/20/3

target · 0.85 → zeroed 3/23
weight 34.35

total expected ⇒ 227.46
transferral quant, +0.03%

Overwrite @ 70C in 30" vacuum after "bump free" isopropanol mixing

3/24
#1 cur 230.56 230.41
116.57 #2 117.17
113.99 + 113.24 ⇒ 227.23

0.1% loss or

Prior to removing from bkr after overwrite, cake broken up and "pudged", then let cool under vacuum to remove any sol. resid.

In Surface @ 12:30

POST 219.22
3/25 102.65
101.79

218.36

500C/Hr Ramps, 955 RWT in flowing oxygen

218.34
101.17 ⇒ 203.82
100.94

202.13 0.83% loss

318.71

The above understood
and witnessed by

Date

and
by

Date

3/23 from pg 44 TREATMENT INQUIRY

C2P14 & C2P15 ⇒ original green of info on pg 37; both 3.11 then

C2P14: (800°C pretreat), purge - 2120 p.m. 59.9 ad. : 18 HRS
3.09 0.573 0.191 3.83 60.1 no appreciable sintering
1.455 0.485 0.806
3.07 0.522 0.171 5.125 80.5 apparently sintering
1.326 0.434 0.599 appreciable

C2P15: (850°C pretreat), purge as above - 59.8 ad. : 18 HRS
3.09 0.565 0.187 4.02 63.1 slight amount of sintering
1.435 0.475 0.768
3.08 0.531 0.174 4.87 76.5% initial sintering "appreciable"
1.319 0.442 0.632

C2P18 (CONTROL) 37/27500
2.92 0.574 0.180 3.83 60.1% O.K.
1.458 0.457 0.763
2.86 0.501 0.152 5.82 91.4
3/28 1.273 0.386 0.491
Post 48 hr (2nd 2A) - C3 batch

pre → 318.71
post → 316.88
(-) 1.83
702.13
200.30
199.23 initial yield

48/23 from page 45 IBM Technical Notebook

STD-1f grain size slightly larger - interior fairly uniform
 ~25 μ m away occasional
 50 μ m grain

Re-sintered overite to check for additional growth.
 Further polishing of 40 hr sample slice yields numerous 40-50 μ m
 GRAINS! Growth seems probable!

3/24

Summary from 45

Grain 2.74 1.448 0.538(5) 0.887

3.09 64.2

40 HR @ 2.70 1.237 0.452 0.543

4.97 100.33

1645C

slice back up to 1650 @ 5:00 PM (4 hr earlier due to control couple failure)
 63 HRS SHUT OFF @ 1:45 PM 3/24 (42 hr)

The above understood
 and witnessed by _____

Date

and

Date

3/24 from pg 45

after additional 12 hr rxn time $\frac{150.02}{149.81}$: Assume constant rxn
~ 0.21 g

total loss: 165.22 initial 1
150.02 16 HR - 15.20 98.6% reacted
149.81 28 HR - .21 1.4%
15.41 CASE FOR MINOR porosity?

- > 61 gs recovered after mortar grinding.
- > 2 HRS on shaker mill w/ 5mm balls.
- > 60.4 g shaker yield
- > 48.8 g MI JET YIELD

PSD
2.91 μ m ave. Flatter than jet, but not much better ϕ size.

Slip-cast calculations: die 0.9" id. \Rightarrow 2.286 cm $\frac{0.762 \text{ cm}}{0.3 \text{ "desired green thickness}}$
 $\frac{\pi \cdot (2.286)^2}{4} (0.762) = 3.1275 \text{ cc } (\uparrow 8.81 \text{ g/cc}) = 15 \text{ g } \text{SrTiO}_3 (\uparrow 0.6 \text{ g}) = 9.0 \text{ g}$
approx density

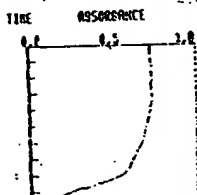
50

IBM Technical Notebook

MODEL CAP-500
 PARTICLE ANALYZER
 DATE 3/1/80
 SAMPLE ST-103-DRC2
 SOLVENT ISO
 NAME MT
 • CONDITIONS
 SOLV. VISC 2.10 (CP)
 SOLV. DENS 0.79 (G/CC)
 SAMP. DENS 4.81 (G/CC)
 D(CHE) 16.0 (PH)
 D(CHE) 1.00 (PH)
 D(CHE) 1.00 (PH)
 SPEED 500 (RPM)

• TIME 0.0 6.0 12.0 SEC

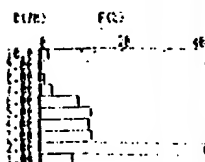
• DATA



• DISTRIBUTION TABLE (BY VOL.)

D(CHE)	F(CHE)	F(CHE)
10.0 - 0.0	0.0	0.0
10.0 - 5.0	1.0	1.0
5.00 - 0.00	0.0	1.0
0.00 - 7.00	1.0	2.0
7.00 - 6.00	2.0	5.0
6.00 - 5.00	9.5	15.0
5.00 - 4.00	12.5	27.0
4.00 - 3.00	12.1	35.0
3.00 - 2.00	12.6	50.0
2.00 - 1.00	35.6	5.0
1.00 - 0.00	7.9	100.0
D(CHE)	2.20 (PH)	

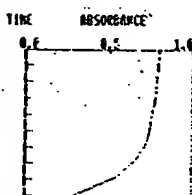
• DISTRIBUTION GRAPH (BY VOL.)



MODEL CAP-500
 PARTICLE ANALYZER
 DATE 3/1/80
 SAMPLE ST-103
 SOLVENT MT
 • CONDITIONS
 SOLV. VISC 2.10 (CP)
 SOLV. DENS 0.79 (G/CC)
 SAMP. DENS 4.81 (G/CC)
 D(CHE) 16.0 (PH)
 D(CHE) 1.00 (PH)
 D(CHE) 1.00 (PH)
 SPEED 500 (RPM)

• TIME 0.0 6.0 12.0 SEC

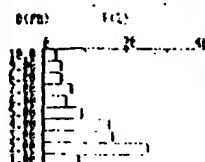
• DATA



• DISTRIBUTION TABLE (BY VOL.)

D(CHE)	F(CHE)	F(CHE)
10.0 - 0.0	0.0	0.0
10.0 - 5.0	1.0	1.0
5.00 - 0.00	0.0	1.0
0.00 - 7.00	1.0	2.0
7.00 - 6.00	2.0	10.0
6.00 - 5.00	5.4	24.0
5.00 - 4.00	9.2	32.0
4.00 - 3.00	16.0	45.0
3.00 - 2.00	17.0	61.0
2.00 - 1.00	25.0	91.0
1.00 - 0.00	0.4	100.0
D(CHE)	2.55 (PH)	

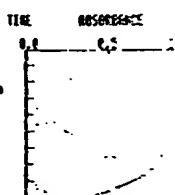
• DISTRIBUTION GRAPH (BY VOL.)



MODEL CAP-500
 PARTICLE ANALYZER
 DATE 3/1/80
 SAMPLE ST-103
 SOLVENT MT
 • CONDITIONS
 SOLV. VISC 2.10 (CP)
 SOLV. DENS 0.79 (G/CC)
 SAMP. DENS 4.81 (G/CC)
 D(CHE) 16.0 (PH)
 D(CHE) 1.00 (PH)
 D(CHE) 1.00 (PH)
 SPEED 500 (RPM)

• TIME 0.0 6.0 12.0 SEC

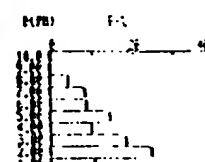
• DATA



• DISTRIBUTION TABLE (BY VOL.)

D(CHE)	F(CHE)	F(CHE)
10.0 - 0.0	0.0	0.0
10.0 - 5.0	0.0	0.0
5.00 - 0.00	0.0	0.0
0.00 - 7.00	0.0	0.0
7.00 - 6.00	0.4	12.0
6.00 - 5.00	0.7	21.0
5.00 - 4.00	10.4	36.0
4.00 - 3.00	5.5	45.0
3.00 - 2.00	16.0	64.0
2.00 - 1.00	24.0	89.0
1.00 - 0.00	16.7	100.0
D(CHE)	2.70 (PH)	

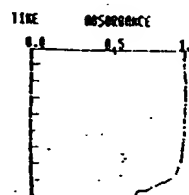
• DISTRIBUTION GRAPH (BY VOL.)



MODEL CAP-500
 PARTICLE ANALYZER
 DATE 3/1/80
 SAMPLE ST-103-DRC2
 SOLVENT ISO
 NAME MT
 • CONDITIONS
 SOLV. VISC 2.10 (CP)
 SOLV. DENS 0.79 (G/CC)
 SAMP. DENS 4.81 (G/CC)
 D(CHE) 16.0 (PH)
 D(CHE) 1.00 (PH)
 D(CHE) 1.00 (PH)
 SPEED 500 (RPM)

• TIME 0.0 6.0 12.0 SEC

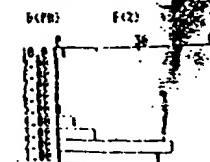
• DATA



• DISTRIBUTION TABLE (BY VOL.)

D(CHE)	F(CHE)	F(CHE)
10.0 - 0.0	0.0	0.0
10.0 - 5.0	0.0	2.0
5.00 - 0.00	0.0	2.0
0.00 - 7.00	0.0	2.0
7.00 - 6.00	0.0	2.0
6.00 - 5.00	0.0	2.0
5.00 - 4.00	0.0	3.0
4.00 - 3.00	5.0	9.0
3.00 - 2.00	13.4	23.0
2.00 - 1.00	43.0	64.0
1.00 - 0.00	35.0	100.0
D(CHE)	1.34 (PH)	

• DISTRIBUTION GRAPH (BY VOL.)



The above understood

Date

and

Date

IBM Technical Notebook

51

3/20

10g $\text{SrCO}_3 \Rightarrow 0.06774$ moles
 $\underline{5.412 \text{ g } \text{Tl}_2\text{O}_2}$

15.412g total

$\underline{15.48}$ after mixing RECOVERY
 $\underline{.27}$

2/25/93 Note
 Density calculations here were done using paper lit. which is now known to be in error. It is 5.116 not 4.82

Dave's unreacted $\text{SrCO}_3/\text{Tl}_2\text{O}_2$ { new batch SrTiO_3 -

8.975 0.584 0.242

2.42 0.458 0.190
 1.16 0.483 0.510

(4.745)

(98.6)

NOT TOO GOOD

⊗ 2.91 0.585 0.194

2.90 0.488 0.173
 1.326 0.439 0.606

(4.785)

(99.5)

NOT TOO GOOD

52 A/ SrTiO_3 grow growth IBM Technical Notebook

pellet 2 of fines

2.22	0.572	0.169	3.12	64.9%	~ same as before
	1.453	0.429	0.711		
2.19	0.487	0.144	4.98	<u>103.5%</u>	= 103.5
	1.237	0.366	0.440		

2.71	0.580	0.176	3.56	74.0%	
Daves xcess	1.473	0.447	0.762		
TiO_2					
estimate on 1/2	0.518	0.262	0.160	4.86	<u>\$1.01</u>
etc 35	1.32	0.406	0.556		101.-
(2.70)	1.32	0.406			

~ O.K. by wght.

The above understood

Date

and

Date

IBM Technical Notebook



0.0676 $\times 2$ 0.13525 g batches
0.125 0.25
0.125
STOIC as nitrate
0.036 \rightarrow SAME
0.154 0.308

M.W. 53
79.90 0.0676
147.63
101.96
181.88 3.337 690C
183.5182

13.531 TiO_2 moles 0.16935 0.00084675 = $\frac{1}{2}$ mole %
 \downarrow
 $\frac{25.00}{38.531} \text{ SrCO}_3$

0.00084675 moles (79.90) \rightarrow 0.06766 + 13.531 = 13.46

0.00084675 (147.63) \rightarrow 0.125 + 25. = 24.875

Summary of additions, quantities

	excess	SUB 1	SUB 2	excess 2
TiO_2 re	13.5986 13.6662	13.443	13.531	13.531
SrCO_3	25.00	25.00	24.875	25.125
Al_2O_3	—	0.086*	—	—
V_2O_5	—	—	0.154* 0.16	—

* these quants are $\times 2$ since there are 2 moles of Al { $\text{V}_{1/2}$ Al_2O_3 } V_2O_5

Correction: $\frac{.16}{147.63} = 0.00108$ moles SrCO_3

$\frac{0.00108 \text{ moles}}{0.00169}$ { 64% with loss due to decanting approx
70% stoic or 30% off addition excess
 V_2O_5 }

The above understood and witnessed by

Date

and by

Date

54 4/5

IBM Technical Notebook

Sub2 $\frac{1}{2}O_5$ 1 mol % stoichiometric / not excess (see pg 53)

25.0 g $SrCO_3$ weighed & transferred to beaker

0.16 g removed

0.16 g $\frac{1}{2}O_5$ added (~20% saturated in hot water, decont'd)

MISTAKE, now uncorrectable. Should have been:

$0.00084675 \cdot (2) = 0.0016935$ g $SrCO_3$ removed

$0.0016935 \cdot (147.63) = 0.25$ g however, decont'g over residual pack reduced actual $\frac{1}{2}O_5$ addition, and though NONSTOICHIOMETRIC (slightly) will use to see what happens,

$\frac{38.62}{38.53}$ g red after overnight vac. @ ~90°C
 initial
 0.51 loss in mixing 1.3 %

$\frac{88.88}{38.08}$ tare (zeroed)
 406 extra due to final beaker scrape ✓

In furnace to temp by 12:00, 4/6/88 16 HRS 8 A.M 4/7

'Severe' sintering, dark black appearance of pack body

$\frac{126.96}{117.68}$
 ~ 0.05 g spillage
 $\frac{117.73}{117.73}$

$25g SrCO_3 \times \frac{103.62}{147.63} \approx 17.55$

$\frac{126.96}{117.68}$
 $\frac{126.96}{117.68}$
 $\frac{9.28}{9.28}$

~ 7.40 g expected loss

26.18 g ground yield

! some bound water?

See 57 & 58
 FOR ENTERED

The above understood and witnessed by _____

Date

and
for

Date

Sub 1 ~~Al₂O₃~~ → 1 mol % added as nitrate

$$0.00084695(2) = 0.0016935 \text{ moles} // \text{Al(NO}_3)_3 \cdot 9\text{H}_2\text{O} \quad 375.14$$

$\frac{1}{2}$ mol % 1 mol % Al 1:1 so use 0.0016935 moles

$$0.0016935 \text{ moles Al nitrate} \left(\frac{375.14 \text{ g}}{\text{mole}} \right) = 0.6353 \text{ g}$$

(303192)

So remove 0.0016935 moles TiO₂ ∴ 0.0016935(79.9) = 0.135 g TiO₂

$$\begin{array}{r} 13.531 \\ - 0.135 \\ \hline 13.396 \text{ g TiO}_2, \end{array} \quad 0.6353 \text{ g Al nitrate in soln}$$

$$\begin{array}{r} 38.29 \text{ mix yield} \\ 39.03 \text{ theoretical} \\ \hline 0.74 \text{ mix loss} \end{array} \quad 1.9\%$$

$$0.6353 \text{ g} \left(\frac{101.9612}{375.14} \right) = 0.173 - \Delta 0.46$$

$$\begin{array}{r} 87.55 \text{ tare (removed)} \\ 38.27 \text{ note: nitrate decomposes in hot water. Must explain some of loss} \\ \hline 49.28 \end{array} \quad \begin{array}{r} 39.03 \\ - 0.46 \\ \hline 38.57 \\ 38.27 \Rightarrow 0.3^+ \text{ mix loss} \end{array}$$

In furnace to temp by 12:00 p.m., 4/6/88 ⇒ 16 hrs 8 am 4/7
little sintering of powder, light SrTiO₃ color, mottled,

$$\begin{array}{r} 118.54 \\ 127.82 \\ \hline - 9.28 \text{ g} \end{array} \quad \text{same as SUB 2! looking the same, even though exact loss is coincidence}$$

yield → 27 g

see 57 / 58
SINTERED
DATA

56

IBM Technical Notebook

Two Oxides

119

Figs. 296-301

SrO-SiO₂

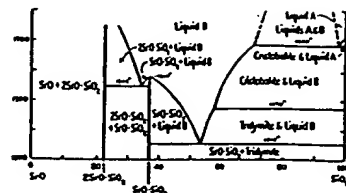


FIG. 296.—System SrO-SiO₂.

P. Eskola, *Am. J. Sci.*, 5th Ser., 4, 336 (1922); modified by J. W. Geck, *ibid.*, 5th Ser., 13, 19 (1927); see also P. C. Knoch, *J. Am. Chem. Soc.*, 52 [4] 1640 (1930).

ZnO-Al₂O₃

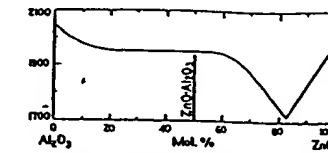


FIG. 299.—Liquidus curve of system ZnO-Al₂O₃.

E. M. Bunting, *Bur. Standards J. Research*, 8 [2] 220 (1932); R. F. 412.

SrO-TiO₂

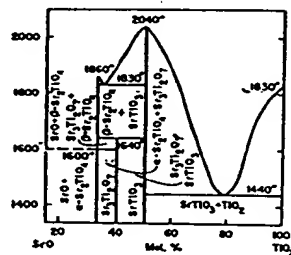


FIG. 297.—System SrO-TiO₂.

Miroslawa Dryl and Wladyslaw Trachetowski, *Rach. Chem.*, 31, 492 (1957).

ZnO-B₂O₃

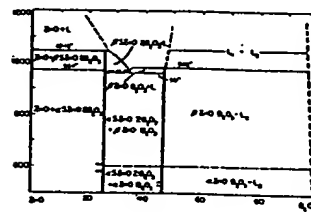


FIG. 300.—System ZnO-B₂O₃.

D. E. Harrison and F. A. Hammett, *J. Electrochem. Soc.*, 103 [9] 406 (1956); see also, "Structure of Zinc Bismuthate, ZnO(BiO₃)", F. Smith, S. Garcia-Blanco, and L. Berthel, *Anales Real Soc. Espan. Fis. Quim. (Madrid) Ser. A (Nouv. Dec.)*, 263-268 (1961).

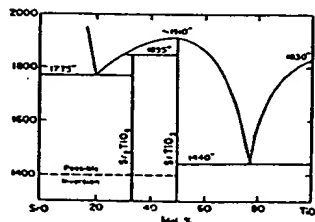


FIG. 298.—System SrO-TiO₂; tentative.

Rustum Roy; private communication, 1957.

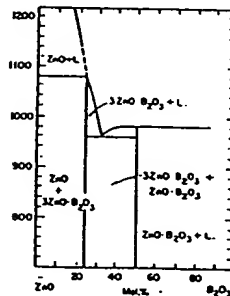


FIG. 301.—System ZnO-B₂O₃.

Yu. S. Leonov, *Zhur. Neorg. Khim.*, 3, 1246 (1958).

Two Oxides

93

Figs. 2334-2336

SrO-TiO₂

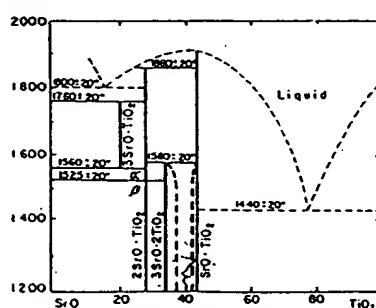


FIG. 2334.—System SrO-TiO₂. SrO-TiO₂ is extended to approximately the 65O:35TiO₂ composition.

Alejo Corco and Franco Mazzanti, *Ann. Chim. (Rome)*, 53, 802 (1953).

SrO-ZrO₂

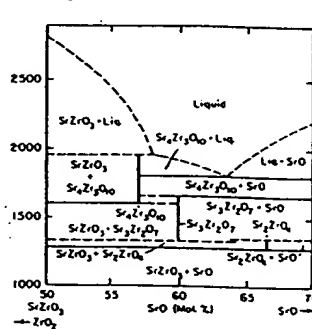


FIG. 2335.—System SrO-ZrO₂.

Gilbert Tilley and Monique Percey y Jorba, *Rev. Rouss. Temp. Refractories*, 1 [4] 237 (1964).

The above understood

Date

and

Date

These Diagrams
 (arrows)
 for SrO-TiO₂
 system and
 asserted others

Excess SrTiO_3

(Excess 2) IBM Technical Notebook

(Excess 1) ➡

57

13.531 TiO_2
➡ 13.53-

25.25 SrTiO_3
25.28

13.6 TiO_2
13.61

25.00 Sr
25.02
.03 to

zero off after addition
probably static

In drying oven @ ~100C under house vacuum @ 1:30 p.m. 4/6/61

38.72 after drying
87.87 weighed crucible
126.59 w/ addition
118.85
7.74

38.43 after drying
87.07
125.50
117.59
7.71

25 g x $\frac{101.86}{375.14} = 6.795$ 17.5

$\frac{6.795}{7.74} = 88.25\%$ + 12% excess loss
 $7.5 / 7.7 = 97.5\%$

#1 TiO_2

#2 SrCO_3

NO GREEN DATA TAKEN

➡ NO GREEN DATA

N_2 2.75 0.520 0.159 4.96 1.03
1.321 0.404 0.554
2.71 0.529 0.160 4.71 97.9
1.344 0.406 0.576

3.01 0.517 0.175 5.0 1.04
EXCHANGE 1.313 0.444(5) 0.60
3.00 0.520 0.176 4.89 1.02
1.321 0.447 0.613

SiB_2 2.38 0.540 0.135 4.69 97.5
1.372 0.343 0.507
 N_2 2.41 0.554 0.141 4.31 89.6
1.410 0.358 0.559

SiB_2 2.56 0.529 0.150 4.74 98.2
1.314 0.381 0.5405
2.60 0.526 0.151 4.83 1.00
1.336 0.384 0.538

58

IBM Technical Notebook

SUBSTITUTION 1: Al_2O_3 1 mol % 16 HRS. RUN
 " 2: Y_2O_3 ↓
 " N_2 O_2
 1: 100.4 98.5
 2: 89.6 97.5

EXCESS DOPING 1: $1/2$ mol % Ti_2O_3
 " 2: $1/2$ $SrCO_3$
 " N_2 O_2
 1: 97.4 103
 2: 102 104

MECHANICAL MANIPULATION
 fines: 103.4
 fines $1/3$ med $2/3$ mix: 102.3
 MED: 100.4

4/11 Phase Co/Bi studies IBM Technical Notebook

59

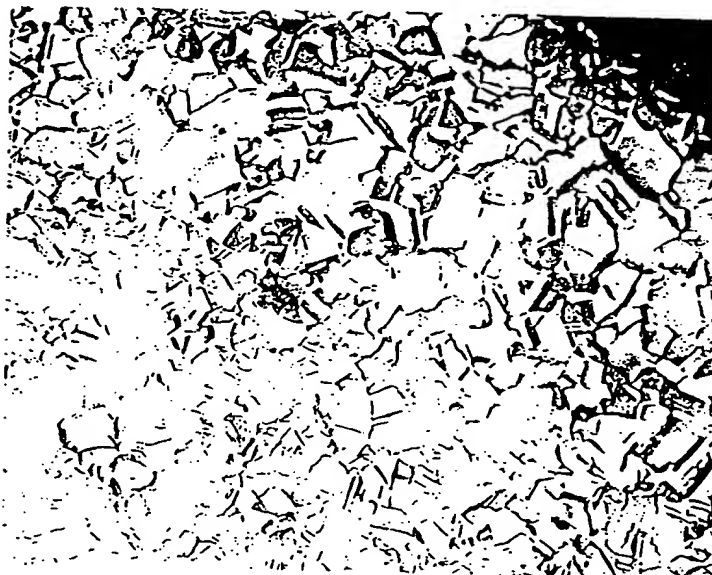
600C overnite N_2 treatment on as rec'd material (Cu)



INTERIOR
INHOMOGENEOUS
(ABNORMAL)
GRAIN GROWTH

100X

100 μ m



EXTERIOR
INHOMOGENEOUS

100 μ m

The above understood
and witnessed by _____

Date _____

and
by _____

Date _____

60

IBM Technical Notebook

1, 3, 10% Bi in copper

5 g total per batch

4.95 post 750C

$g Bi: 5(0.01) = 0.05 \quad 5(0.03) = 0.15 \quad 5(0.10) = 0.5 g$

Cu $\underline{4.95} \quad \underline{4.85} \quad \underline{4.50}$

actual $0.05-6 \quad 0.15-0.16 \quad 0.50-1$

$4.95-6 \quad 5.00 \quad 4.99-5.0$

recovery $4.87 \text{ added to } 5.00 \quad 4.99 - \quad 4.95$

5.00
 $4.98 \text{ after } 400C \text{ over (not disturbed)} \quad 4.90 \text{ after } 400C \text{ overwrite}$

Reloaded 1% & will continue w/ 3%. Will make a new 10%
 And a 50% and fire @ 750C. Crucible shortage → will likely
 modify above.

50/50

2.5g Bi, 2.5g Cu

10% Bi

3% as above

g Bi: 2.51 actual

post Cu $\underline{5.01}$

Cu 2.40

crucible
total

1.34
 $\underline{6.34}$
 5.00
 (1.34)

Post 750C

6.3
 (4.91)

0.51
 $\underline{5.02(3)}$ total
 $4.51(2)$

Post 750C

$1.32(3)$
 $\underline{6.24}$
 5.07
 4.92

6.21
 (4.89)

100% RESULT

NOTE: INITIAL 400C (420C) follow (1-10%) percentages of Bi
 did not produce expected densification/solidification of pucks.

IBM Technical Notebook

61

25% { 35% Bi/Cu melts \leq 1 Bi crucible filling

25%
 $0.028(5) = 1.25 \text{ g Bi}, 3.75 \text{ Cu}$

6.33 PRE
 $\frac{1.33}{5.00}$

36
1.75 Bi ; 3.25 Cu

6.25(4) loaded
 $\frac{1.30(1)}{4.95}$ starting total

6.30 post $\Delta = 0.03$
Possible post density: 0.315, 0.385
4.97 0.800, 0.978 0.6 8.28

6.23 $\Delta = -0.02$

90.
definitely smaller volume, higher density

Argon/H₂ Bi filling

13.32 post

2.2 PRE

13.18

11.86

0.148

13.30 after slag removal

25%

1.26 Bi

5.03 w/Cu

filled 12.82
cruc: $\frac{11.39(46)}{11.43}$

CRUX \Rightarrow

post 12.81

ARGON/H₂ 25% Bi Run \leftarrow Pellet Run \rightarrow

pellet: 4.87 0.485 0.222 7.25 79%
1.232 0.564 0.672

$8.96 \times 0.75 + 0.25(9.8) =$
 $6.72 + 2.45 = 9.17$

French started 2 HR purge 3:35 " pellet bloating due to Bi vaporization?"
4.84 0.483 0.234

B₁₂O₃: sp. g. 8.8 m.p. 820°C

62

IBM Technical Notebook

SnTiO_3 Grain Growth Experiment - MECHANICAL MEASURES

- 1) PSD weighting
- 2) fines full density & free sintering of polished surface
- 3) reacted to constant weight (1st batch) sintering as in #2

Fines = F

2.04	0.570	0.155		3.14	65.3
	1.498	0.394	0.649		
2.01	0.488	0.132		4.975	10.84
	1.239(5)	0.335	0.409		

Fine/medium = FM

2.19	0.577	0.154		3.32	69.0
	1.465	0.391	0.659		
2.17	0.504	0.135		4.92	102.3
	1.28	0.343	0.441		

changed μ

2.46(7)	0.582	0.165		3.43(5)	71.4
	1.478	0.419	0.719		
2.46*	0.589	0.147		4.85	100.4
	1.318	0.373	0.509		

REMARKS \rightarrow * some powder adhered

IBM Technical Notebook

4-12-88⁶³

Sintering Regime

Rapid Temp w/ 10 cc/min O₂

1550C initial set, after REACHING temp for 1 HR, 1640C overnight
5:20 p.m. ~ 1100C, T_{control} blown. @ ~ 30-45 minutes @ 1540.
Restarted @ ~ 5:55 & brought directly to 1640C.

The above understood
and witnessed by _____

Date _____

and
by _____

Date _____

644-26-88

IBM Technical Notebook

LEAK TESTING - S.O. TORR HIGH VAC

25 millitor after continued pumping through system
STARTING WITH roughing in

Will check pumpdown through HVAC valve alone
tomorrow.

4/27 → Vacation

4/28 Pump down through high vac initially unsuccessful, must
have been stuck valve, but after freeing can get down
to ~50 millitor in 15 minutes. Will continue pumping.

1/2 40

Down to 10 thru rough, 30 w/ HVAC only,
Rather quick leak-back when both closed off indicating
leaks in system:

- 1) FURNACE
- 2) Elbow connection
- 3) Pump

See page 78

5/13 Promised CSS test Monday (Chad!)

5/13

First Milling - AutoSeed - Teflon liner (13

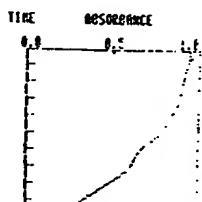
48.17 g known, but "few" acia before total processed right. checks

49.69 g yield

NORIDE CAPR-SEE
PARTICLE ANALYZER
DATE 5/13
SAMPLE C3-Proc I
SOLVENT ISO
Teflon liner
• CONDITIONS
SOLV. VISC 2.10 CCP
SOLV. DENS 0.7516/CC
SAMP. DENS 6.3416/CC
D(CRUS) 10.0 (PH)
D(CRIM) 1.00 (PH)
D(CRIS) 1.00 (PH)
SPEED 500. (PPH)

• TIME 0 H 4 MIN 20 SEC

• GATE

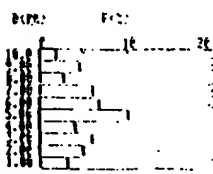


• DISTRIBUTION TABLE (BY VOL.)

D(PH)	F(%)	R(%)
10.0 - 9.0	49.7	49.7
9.00-8.00	1.0	51.6
8.00-7.00	4.5	54.1
7.00-6.00	2.7	56.6
6.00-5.00	6.1	64.5
5.00-4.00	6.9	71.7
4.00-3.00	10.2	81.5
3.00-2.00	4.0	85.5
2.00-1.00	6.0	91.5
1.00-0.00	5.0	96.6
0.00-0.00	3.2	100.0

(AVERAGE) 5.85 (PH)

• DISTRIBUTION GRAPH (BY VOL.)



The above
and witnessed by

PASS II 5/10

47.6 g yield: much fluffier, looks
~ like 5um powder.

IMMEDIATELY REMILLING

pg. 66 for PSD sheets ~2g loss

PASS III 45.8
45.8

PASS IV 44.5
~ 18.0 5 pellets
26.9

4 High large particle % 41.7 vs 18 for C2

4 overall ave. ~10 vs 5-6 for C2

however distribution seems similar { some
bypassing must have occurred.

Will work on Tuesday.

Date

and
by

Date

This Page Is:
☐ Unclassified
☐ IBM Internal Use Only
☐ IBM Confidential

IBM Confidential-Restricted
Registered IBM Confidential
**Register with local Recorder*

anything a w gn y entry. Have every possibly important
ed. Submit an Invention Disclosure of
ssibly new and inventive.

66

IBM Technical Notebook

Date

IBM Technical Notebook

67

B₁/C₀ 25/75 ~~erocible packed~~, sinter overnite in Ar/H₂(5)
@ 750C.

#₁ → < ~~100~~ mesh Cu, spherical ("new")

#₂ → ^{10μm} ~~100 mesh spherical Cu~~ (old)

#₃ → penetration
10μm spherical

#2: 1.25/5.01
6.31
ceux 1.34
5.00

#1: 1.25/5.00
6.35
1.35
5.00

POST 6.31

6.32

8.0-8.5 mm L

8.37

9.65-9.75 mm dia

9.65-10.0

After interruptions: 5/24/ start cut { polishing
6/8/88 Finish: 6/8/88 after

{ Porosity is reduced, and 3rd ^(grey) 'oxide' has been eliminated }
in forming gas.

The above understood
and witnessed by _____

Date _____

and
by _____

Date _____

68 C3- P1-5 Green Data { IBM Technical Notebook } Picked up mill test on
 150275 G mm mm { Sinter } Material ruined
 C3P1 3.59 1.470 0.779 0.80 70.5
3.33
 C3P2 3.33 1.477 0.442 4.40 69%
 2.93 0.757
 C3P3 3.58 1.472 0.478 4.40 69%
 0.813
 C3P4 3.37 1.476 0.440
 C3P5 3.53 1.474 0.471 5.52 87 even w/ cracks
 3.19! 1.331 0.415 0.577 pick OK. I think
 Mill no good.

NOTES: PELLETS SEEM TO HAVE SHED ORGANIC/GAS?!
 looks like the pellet melted in plastic container.
 15026 UNIC 6200 20% → 550, 10% → 975, 2 HRS,
 C3P6 2.52 1.50 0.32 4.46 70.1%
 coarse 2.50 1.482 0.316 0.565 4.55 71%
 0.55

The above understood
 and witnessed by

Date

and
by

Date

Calcinations - 750C IN @ 8:00 P.M. 5/17/88 out 9:00 AM 5/18 69

TiO₂ - Green 3-9's

$$\begin{array}{r} 16.3620 \\ - 0.8610 \\ \hline 15.501 \text{ g TiO}_2 \text{ weighed} \end{array}$$

$$\begin{array}{r} 89.4610 \text{ crux} \\ 105.0174 \text{ crux + TiO}_2 \end{array}$$

15.5564 g TiO₂ by difference

$$\begin{array}{r} \text{s/r Post} \\ 105.0174 \\ \hline 104.9395 \\ 0.0779 \end{array} \text{ gaining } \Delta T > \Delta T_{\text{CO}_2}$$

$$15.501 = 0.5\% +$$

$$\begin{array}{r} \text{EQ} \rightarrow 105.0084 \\ \hline 105.0174 \\ 0.0090 / 0.0779 = 88.5\% \text{ bal} \end{array}$$

$$99.64\% \rightarrow 0.3\% \Delta + 0.0554$$

SnCO₃

$$\begin{array}{r} 18.4193 \\ 0.8710 \\ \hline 17.5473 \end{array} \rightarrow \begin{array}{r} 0.8732 \\ \hline 17.5441 \end{array}$$

$$\Delta 0.0032 \approx \Delta \Delta D.S. !!$$

$$\begin{array}{r} 109.9615 \\ 92.3660 \\ \hline 17.5955 \end{array} \Delta + 0.0514$$

$$\Delta \Delta D.S. \Rightarrow 0.004 \text{ g} \sim 4 \text{ mg calibrate}$$

$$\begin{array}{r} \text{Post } 109.9615 \\ 109.8870 \\ \hline 0.0745 \end{array} \text{ gaining } 17.5441 = 0.4\%$$

$$\begin{array}{r} \text{EQ } 109.9510 \\ \hline 109.9615 \\ 0.0105 \end{array} 85.6\% \text{ back}$$

5/19 TiO₂ { ~~SnCO₃~~ 2nd Cal POST

$$\begin{array}{r} 105.0174 \\ 104.8670 \\ \hline 0.15 \end{array} (-0.0003 \text{ cal})$$

$$\sim 1\%$$

$$\begin{array}{r} 109.9615 \\ 109.8580 \\ \hline 0.1035 \end{array} (-0.0003 \text{ cal})$$

$$\sim 0.6\%$$

☐ Unclassified
☐ IBM Internal Use Only
☐ IBM Confidential

☐ Confidential-Restricted
Registered IBM Confidential
*Register with local Recorder

Date and . every entry. Have every possibly important
essed. Submit an Invention Disclosure of
possibly new and inventive.

70

IBM Technical Notebook

The above understood
and witnessed by _____

Date _____

and
by _____

Date _____

IBM Technical Notebook

71

HF Silicon Etch/Wash/Buffer Solns.

~~80g~~ 80g NH_4F in 120g H_2O (distilled) \Rightarrow 120cc 40 wt. % NH_4F REAGENT

actual soln is 40:1 ~~10:1~~ $\sim 170^\circ\text{C}$

BHF \rightarrow 40 parts NH_4F reagent : 1 part HF (49 wt%) soln.

QUENCH \rightarrow 10:1 DI : NH_4OH reagent 50ml:500ml

BHF clean \rightarrow 10:1:2.2 (NH_4F :HF:Glycerin)
reagent 49

16(10)=160 16(1)=16 16(2.2)=35.2 = 211 ml
320
350
(190) (35) (77)

MSG:FROM: SARDESAI--FSHVMCC TO: MDT --YKIVMT
To: MDT --YKIVMT

05/18/88 12:39:40

From: Viraj Sardesai
8-533-8545, SCL Pers Metals, GTD E. Fishkill
IBM INTERNAL USE ONLY (Unless otherwise specified)
SUBJECT: BHF concentrations used in SCL

Michael,

We use 40:1 BHF for pre platinum, emitter screen ox removal and for s metal pre clean.

The chemical is commercially available premixed solution and has 40 parts (by volume) of 40 wt pct NH_4F solution mixed with 1 part of 49 wt pct HF solution. Both NH_4F and HF are in aqueous solutions. Manufacturer specs the HF concentration to 0.61 to 0.77 moles per liter and specific gravity of 1.106.

For S postL/O BHF clean 10:1:2.2 (NH_4F :HF:Glycerin) is used prepared similarly and quenched in 10:1 NH_4OH solution (28 Wt pct NH_4OH solution diluted to 10 times its volume in DI water).

cc: SZECSY --FSHVMCC

HOUGHTON--FSHVMCC

Regards,
VIRAJ

FSHVMCC(SARDESAI), D/11G B/322 Z/ST1

***** OUR TEAMWORK MAKES THE DIFFERENCE ! *****

BHF concentrations used in SCL

BHF

BHF CLEAN

The above understood and witnessed by

Date

and by

Date

☐ IBM Internal Use Only
☐ IBM Confidential

ered IBM Confidential
Register with local Recorder

entry w
thin

ry entry. Have every possibly important
Submit an invention Disclosure of
ssibly new and inventive.

72

IBM Technical Notebook

The above understood
and witnessed by _____

Date

and
by _____

Date

5/18 Polymilling

IBM Technical Notebook - mill #2

73

40g batch yield

I 36.8

II 33.4

III 31.3

IV 28.4

V 25.75

DO

PSD 1 2 Δ

6.94 4.84 3

3.65 3.21 3

3.53

2.98!

3.1!

(2) bag charger required

3 actually higher error 7% @ 7.

2.5 New bag

The above understood and witnessed by _____

Date _____

and by _____

Date _____

ISO 28,

74

IBM Technical Notebook

MARGAL GREEN
 DENSITIES

C3P6	3.29	1.474	0.971		4.11	64.6
				0.80		
	3.23	1.343	0.416	0.59	5.48	<u>86.2</u> !
C3P7	3.19	1.476	0.955		4.00	64.5
				0.779		
	3.13	1.343	0.404	0.57	5.49	86.3
C3P8	3.21	1.473	0.962	0.787		64.1
	3.16	1.341	0.409	0.577	5.48	86.2
C3P9	3.08	1.474	0.441		4.09	64.3
				0.7525		
	3.02	1.336	0.391	0.548	5.51	<u>86.6</u>

} TO
 KING-TU

NOTES: PELLETS W @ 4:55 with flowing O₂ (bottled, dessicated)
 Heating started @ 5:15 @ 20°/min (97C @ start)
 @ 265C cut back to 10°/min; to reach sinter T' @ 6:35 p.m.
 Sintering @ 975C for 2HRS. till 8:35 p.m.
 Quench { remove.

The above understood
 and witnessed by _____

Date _____

and
 by _____

Date _____

IBM Technical Notebook

75

995C sister
CSP10 3.18 1.474 0.453 4.114 64.7
3.11 1.338 0.399 0.773cc 5.54 87.2
0.561

no (appreciable) liq. ϕ !

T3 "leg"

yield
10.35

PASS
II

$\Delta \rightarrow$ MILL #1

Ave. part dia.
<100 mesh

29.~

I

10 !

12g leaks

3.29

21.5

II

8 !

~1g leak

3.11

18.5

III

3 !

4.0⁺ g of ~20 μ m powder in mill neck

22.4 total max yield

☐ IBM Internal Use Only
☐ IBM Confidential

☐ "Stered IBM Confidential"
ster with local Recorder

entry witne.
anyth

very entry. have every possibly impo
Submit an Invention Disclosure of
possibly new and inventive.

76

IBM Technical Notebook

The above understood
and witnessed by _____

Date _____

and
by _____

Date _____

"T3" pellets IBM Technical Notebook

C3P10-18

9750

C3P10 ①	3.14	1.461	0.473		3.975	62.50
	✓3.08	1.308	0.400	0.79	5.75	<u>90.4</u>
				0.536		

C3P12 ②	3.28	1.462	0.495			
C	✓3.21	1.308	0.417	0.56	5.73	<u>90.0</u>

C3P12 ③	3.04	1.463	0.450			
	2.97	1.308	0.388	0.54	5.68	89.31
		1.310	0.385	0.523	5.756	90.5
		1.306		0.516		

RECHECK TOMORROW

C3P14	3.21	1.464	0.473			
	✓3.14	1.308	0.405	0.548	5.77-8	<u>90.7-9</u>
		1.306				

10000

C3P15	3.04	1.461	0.458			
	2.97	1.298	0.386	0.511	5.81	91.35

C3P16 (pellets)	3.08	1.466	0.457			
	3.02	1.301	0.390	0.519	5.82	91.5

C3P17	3.28	1.464	0.492		5.75	<u>90.4</u>
	3.22	1.298	0.422	0.568	5.82	91.5
	(3.28)					

chip offset

The above understood and witnessed by

Date

and by

Date

78 6/8/88

IBM Technical Notebook

Centorr HVAC system close to finished with leak testing,
preliminary operation checks.

System mechanical pump down < 20-30 minutes

Torbo molecular ↓ down → to 5×10^{-5} within 1 hr
with attachments to mid 6's by 1:00 p.m.
Start was 9:15 originally.

Block-off flange, new Centorr purge / plug fittings still
needed. Failure seal test req'd.

The above understood
and witnessed by _____

Date _____

and
by _____

Date _____

IBM Technical Notebook

7

Bi/Cu Free-Crucible Sinter Vacuum Run

To glass shop 6/17/88. Batch size to be 4.0 g to allow for ease of manipulation during sealing of quartz tube.

$$4.0 (0.25) = 1.00 \text{ g Bi}$$

$$\downarrow (0.75) = 3.00 \text{ g Cu (will use 10 \mu m Cu powder)}$$

$$\begin{array}{r} \text{Bi} \rightarrow 1.00 (0.99) \\ \text{Cu to } 4.03 \\ \text{Cu } 3.03 \end{array}$$

$$\text{from JAR } 4.02 (1)$$

$$\begin{array}{r} \text{cruc } 1.33 \\ \text{w/ mix } 5.33 (4) \\ 4.00 (1) \\ \hline 4.04 \end{array}$$

$$\begin{array}{r} \sim 24.8\% \\ 75.2\% \end{array} \quad \begin{array}{r} \sim 25 \\ 75 \end{array}$$

Re-do - spilled in glass shop

6/9 New crucible shape/size for stability

lets take 5.0 g batch

$$1.25/5.0 (\pm 0.01)$$

$$\begin{array}{r} \text{crucible } 3.35 \\ \text{w/ mix } 8.35 \\ \hline 5.00 \end{array}$$

6/14 After overnite sinter & removal from quartz tube

cruc. & sinter 8.30g (some spillage w/ tube before heat treatment)

no appreciable vapor product seen

CONCLUSIONS: Vacuum doesn't appear to work as well as Ar/H₂. Sample full of holes, but no evidence of oxidation, so holes are real. Again, no evidence of vapor phase deposition in tube.

The above understood
and witnessed by _____

Date _____

and
by _____

Date _____

IBM Technical Notebook

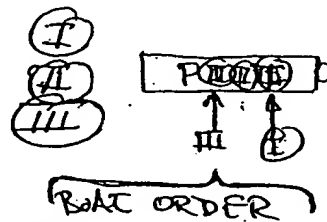
80 6/14/88

To do: 10, 20, 25 % in Ar/H₂(s)

(VACATION)
 MONDAY
 RUN!

WENDS 6/22/88

5 gram batches: 0.25 (5) = 1.25 B. / 3.75 C
 0.20 (5) = 1.00 B. / 4.00 C
 0.10 (5) = .5 B. / 4.5 C



(I) 5 gram w/ new conical crucible
 mix 9.03
 time 1.03
 5.00
 PRE

voids, but some areas seem OK.
 less small voids, some good regions versus (II),
 however larger voids & mystery. Need
 repeating, maybe larger times.

(II)
 9.00
 time 4.00
 5.00

seems very good, no large voids, mic exam not
 microscopic exam shows many small 'pockets'
 or voids. Usually circular

(III) 6.31
 time 1.31
 5.00 'nominal loss possible'

did not densify fully

Sitting Milling Results

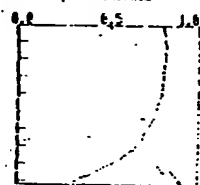
 MODER CAPA-SEE
 PARTICLE ANALYZER

 DATE 3/24/88
 SAMPLE S-103-3
 SOLVENT ISO
 MT-MED
• CONDITIONS
SIGHT IMPROVEMENT
 SOLV. VISC 2.10 (CP)
 SOLV. DENS 0.7916 (CC)
 SAMP. DENS 4.816 (CC)
 D(CRUX) 16.8 (PP)
 D(CHIF) 1.00 (PP)
 D(CDIF) 1.00 (PP)
 SPEED 500. (PP)

• TIME 0 H 6 MIN 0 SEC

• DATE D=0.8

TIME ABSORBANCE

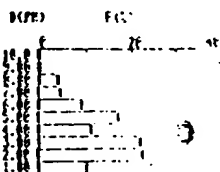


• DISTRIBUTION TABLE (BY VOL.)

D(PH)	F(2)	F(3)
10.0 - 9.0	0.0	0.0
9.0 - 8.0	0.0	0.0
8.0 - 7.0	0.0	0.0
7.0 - 6.0	0.0	0.0
6.0 - 5.0	0.0	0.0
5.0 - 4.0	0.0	0.0
4.0 - 3.0	0.0	0.0
3.0 - 2.0	0.0	0.0
2.0 - 1.0	0.0	0.0
1.0 - 0.0	0.0	0.0

D(CRUX) 2.75 (PP)

• DISTRIBUTION GRAPH (BY VOL.)


 MODER CAPA-SEE
 PARTICLE ANALYZER

 DATE 3/24/88
 SAMPLE S-103-102
 SOLVENT ISO
 MT-S

• CONDITIONS

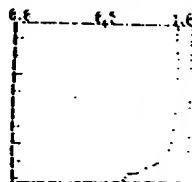
 SOLV. VISC 2.10 (CP)
 SOLV. DENS 0.7916 (CC)
 SAMP. DENS 4.816 (CC)
 D(CRUX) 16.8 (PP)
 D(CHIF) 1.00 (PP)
 D(CDIF) 1.00 (PP)

SPEED 500. (PP)

• TIME 0 H 6 MIN 0 SEC

• DATE

TIME ABSORBANCE

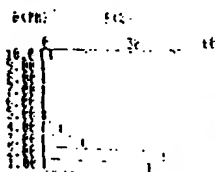


• DISTRIBUTION TABLE (BY VOL.)

D(PH)	F(2)	F(3)
10.0 - 9.0	0.0	0.0
9.0 - 8.0	0.0	0.0
8.0 - 7.0	0.0	0.0
7.0 - 6.0	0.0	0.0
6.0 - 5.0	0.0	0.0
5.0 - 4.0	0.0	0.0
4.0 - 3.0	0.0	0.0
3.0 - 2.0	0.0	0.0
2.0 - 1.0	0.0	0.0
1.0 - 0.0	0.0	0.0

D(CRUX) 1.34 (PP)

• DISTRIBUTION GRAPH (BY VOL.)


 MODER CAPA-SEE
 PARTICLE ANALYZER

 DATE 3/24/88
 SAMPLE S-103-102
 SOLVENT ISO
 MT-S

• CONDITIONS

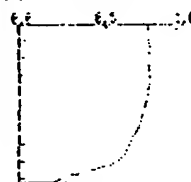
 SOLV. VISC 2.10 (CP)
 SOLV. DENS 0.7916 (CC)
 SAMP. DENS 4.816 (CC)
 D(CRUX) 16.8 (PP)
 D(CHIF) 1.00 (PP)
 D(CDIF) 1.00 (PP)

SPEED 500. (PP)

• TIME 0 H 6 MIN 0 SEC

• DATE

TIME ABSORBANCE

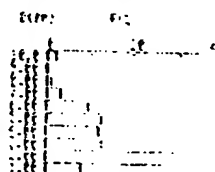


• DISTRIBUTION TABLE (BY VOL.)

D(PH)	F(2)	F(3)
10.0 - 9.0	0.0	0.0
9.0 - 8.0	0.0	0.0
8.0 - 7.0	0.0	0.0
7.0 - 6.0	0.0	0.0
6.0 - 5.0	0.0	0.0
5.0 - 4.0	0.0	0.0
4.0 - 3.0	0.0	0.0
3.0 - 2.0	0.0	0.0
2.0 - 1.0	0.0	0.0
1.0 - 0.0	0.0	0.0

D(CRUX) 2.20 (PP)

• DISTRIBUTION GRAPH (BY VOL.)



Administrative Notes

C3 Milling RESULTS - T1: TeFlow T2: Polyu T3: PolyN

T1

NOTES: CAPP-SET
PARTICLE ANALYZER

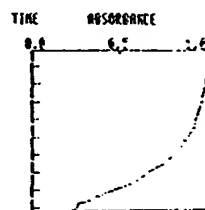
DATE 5/17
SAMPLE C3-PV
SOLVENT ISO

• CONDITIONS

T1 →
SOLV. VISC 2.18 (CP)
SOLV. DENS 6.79 (G/CC)
SAMP. DENS 6.36 (G/CC)
D(CMAX) 10.0 (PM)
D(CMIN) 1.00 (PM)
D(CIV) 1.00 (PM)
SPEED 500. (RPM)

• TIME 0 H 4 MIN 20 SEC

• DATA

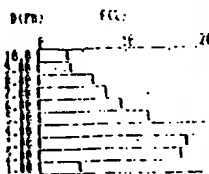


• DISTRIBUTION TABLE (BY VOL.)

D(PH)	F(%)	R(%)
10.0 <	0.0	0.0
10.0-9.0	3.3	3.7
9.00-8.00	3.6	6.9
8.00-7.00	6.1	13.8
7.00-6.00	7.7	20.7
6.00-5.00	9.5	30.2
5.00-4.00	12.6	42.8
4.00-3.00	15.6	58.4
3.00-2.00	16.8	75.2
2.00-1.00	16.2	91.4
1.00-0.00	4.6	100.0

D(AVE): 3.43 (PM)

• DISTRIBUTION GRAPH (BY VOL.)



NOTES: CAPP-SET
PARTICLE ANALYZER

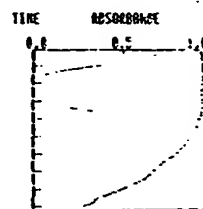
DATE 5/17
SAMPLE C3-PV
SOLVENT ISO

• CONDITIONS 0.097

SOLV. VISC 2.18 (CP)
SOLV. DENS 6.79 (G/CC)
SAMP. DENS 6.36 (G/CC)
D(CMAX) 10.0 (PM)
D(CMIN) 1.00 (PM)
D(CIV) 1.00 (PM)
SPEED 500. (RPM)

• TIME 0 H 4 MIN 20 SEC

• DATA

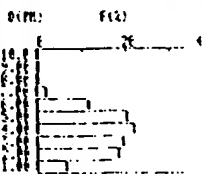


• DISTRIBUTION TABLE (BY VOL.)

D(PH)	F(%)	R(%)
10.0 <	0.0	0.0
10.0-9.0	0.0	0.0
9.00-8.00	0.0	0.0
8.00-7.00	0.0	0.0
7.00-6.00	2.1	2.1
6.00-5.00	11.5	13.6
5.00-4.00	26.2	33.8
4.00-3.00	21.5	55.7
3.00-2.00	15.4	75.1
2.00-1.00	10.3	93.4
1.00-0.00	6.6	100.0

D(AVE): 3.26 (PM)

• DISTRIBUTION GRAPH (BY VOL.)



NOTES: CAPP-SET
PARTICLE ANALYZER

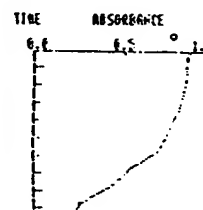
DATE 5/17
SAMPLE C3-PV
SOLVENT ISO

• CONDITIONS 0.097

SOLV. VISC 2.18 (CP)
SOLV. DENS 6.79 (G/CC)
SAMP. DENS 6.36 (G/CC)
D(CMAX) 10.0 (PM)
D(CMIN) 1.00 (PM)
D(CIV) 1.00 (PM)
SPEED 500. (RPM)

• TIME 0 H 4 MIN 20 SEC

• DATA



• DISTRIBUTION TABLE (BY VOL.)

D(PH)	F(%)	R(%)
10.0 <	0.0	0.0
10.0-9.0	0.0	0.0
9.00-8.00	2.0	21.6
8.00-7.00	6.6	27.7
7.00-6.00	9.2	36.8
6.00-5.00	9.8	46.6
5.00-4.00	12.6	59.2
4.00-3.00	17.6	76.9
3.00-2.00	9.0	86.7
2.00-1.00	9.0	95.8
1.00-0.00	4.2	100.0

D(AVE): 4.73 (PM)

• DISTRIBUTION GRAPH (BY VOL.)



T2 Part I

MOTIP CAPA-500
PARTICLE ANALYZERDATE 5/19
SAMPLE C3-PI-T2
SOLVENT 150

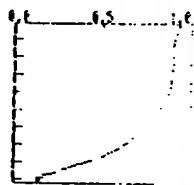
• CONDITIONS

SOLV. VISC 2.10 cP
SOLV. DENS 0.7916 g/cc
SAMP. DENS 0.3616 g/cc
D(CHX) 10.0 cP
D(CHN) 1.00 cP
D(CHV) 1.00 cP
SPEED 500 cP

• TIME 0 H 4 MIN 26 SEC

• DATE ~0.9

TIME RESONANCE

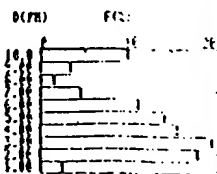


• DISTRIBUTION TABLE (BY VOL.)

D(PH)	F(2)	F(2)
10.0-9.0	0.0	0.0
9.0-8.0	5.6	5.6
8.0-7.0	3.4	12.0
7.0-6.0	1.2	14.6
6.0-5.0	4.5	19.2
5.0-4.0	11.2	30.4
4.0-3.0	14.1	44.5
3.0-2.0	15.6	60.1
2.0-1.0	19.4	79.5
1.0-0.0	10.0	89.5
0.0-0.0	2.5	100.0

D(AVE) 3.65 cP

• DISTRIBUTION GRAPH (BY VOL.)

MOTIP CAPA-500
PARTICLE ANALYZERDATE 5/19
SAMPLE C3-PI-T2
SOLVENT 150

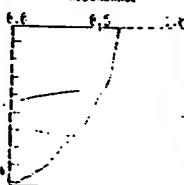
• CONDITIONS

SOLV. VISC 2.10 cP
SOLV. DENS 0.7916 g/cc
SAMP. DENS 0.3616 g/cc
D(CHX) 10.0 cP
D(CHN) 1.00 cP
D(CHV) 1.00 cP
SPEED 500 cP

• TIME 0 H 4 MIN 26 SEC

• DATE ~0.57

TIME RESONANCE

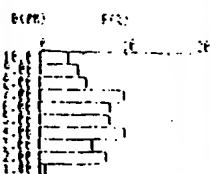


• DISTRIBUTION TABLE (BY VOL.)

D(PH)	F(2)	F(2)
10.0-9.0	36.4	36.4
9.0-8.0	3.2	39.6
8.0-7.0	4.2	43.8
7.0-6.0	5.5	49.3
6.0-5.0	5.6	54.9
5.0-4.0	6.2	61.1
4.0-3.0	6.1	67.2
3.0-2.0	9.5	76.7
2.0-1.0	6.2	82.9
1.0-0.0	7.6	90.5
0.0-0.0	0.7	100.0

D(AVE) 6.94 cP

• DISTRIBUTION GRAPH (BY VOL.)

MOTIP CAPA-500
PARTICLE ANALYZERDATE 5/19
SAMPLE C3-PI-T2
SOLVENT 150

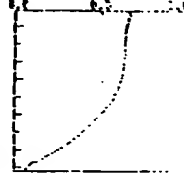
• CONDITIONS

SOLV. VISC 2.10 cP
SOLV. DENS 0.7916 g/cc
SAMP. DENS 0.3616 g/cc
D(CHX) 10.0 cP
D(CHN) 1.00 cP
D(CHV) 1.00 cP
SPEED 500 cP

• TIME 0 H 4 MIN 26 SEC

• DATE ~0.67

TIME RESONANCE

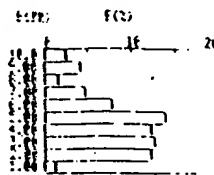


• DISTRIBUTION TABLE (BY VOL.)

D(PH)	F(2)	F(2)
10.0-9.0	27.1	27.1
9.0-8.0	2.5	29.6
8.0-7.0	4.1	33.7
7.0-6.0	1.5	35.2
6.0-5.0	4.6	39.8
5.0-4.0	7.5	47.3
4.0-3.0	13.0	60.3
3.0-2.0	12.3	72.6
2.0-1.0	12.7	85.3
1.0-0.0	12.2	97.5
0.0-0.0	1.2	100.0

D(AVE) 4.04 cP

• DISTRIBUTION GRAPH (BY VOL.)



Administrative Notes

TR PART 2

MOBILE CAPA-504
PARTICLE ANALYZER

DATE 5/9
SAMPLE CS-73-D
SOLVENT 150

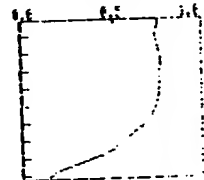
• CONDITIONS

SOLV. VISC 2.10 (CP)
SOLV. DENS 0.79 (G/CC)
SAMP. DENS 6.36 (G/CC)
D(CMAX) 10.0 (PM)
D(CMIN) 1.00 (PM)
D(C10) 1.00 (PM)
SPEED 500. (RPM)

• TIME 0 R 4 MIN 20 SEC

• DATE ~0.7

TIME ABSORBANCE

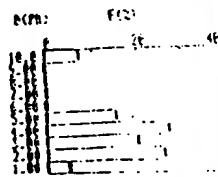


• DISTRIBUTION TABLE (BY VOL.)

D(PM)	F(2)	F(3)
10.0 - 9.0	0.0	0.0
9.0 - 8.00	7.2	7.2
8.00 - 7.00	0.0	7.2
7.00 - 6.00	0.0	7.2
6.00 - 5.00	0.3	7.6
5.00 - 4.00	15.1	22.7
4.00 - 3.00	27.0	49.7
3.00 - 2.00	20.0	69.7
2.00 - 1.00	25.6	95.3
1.00 - 0.00	4.7	100.0

D(CAVE) 2.50 (PM)

• DISTRIBUTION GRAPH (BY VOL.)



MOBILE CAPA-504
PARTICLE ANALYZER

DATE 5/9
SAMPLE CS-73-D
SOLVENT 150

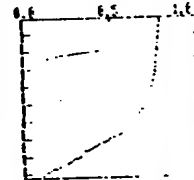
• CONDITIONS

SOLV. VISC 2.10 (CP)
SOLV. DENS 0.79 (G/CC)
SAMP. DENS 6.36 (G/CC)
D(CMAX) 10.0 (PM)
D(CMIN) 1.00 (PM)
D(C10) 1.00 (PM)
SPEED 500. (RPM)

• TIME 0 R 4 MIN 20 SEC

• DATE ~0.7

TIME ABSORBANCE



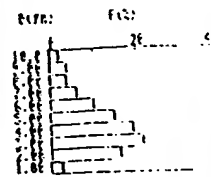
• DISTRIBUTION TABLE (BY VOL.)

D(PM)	F(2)	F(3)
10.0 - 9.0	0.0	0.0
9.0 - 8.00	2.2	2.2
8.00 - 7.00	3.5	6.0
7.00 - 6.00	3.7	9.8
6.00 - 5.00	6.2	16.0
5.00 - 4.00	10.1	26.6
4.00 - 3.00	15.0	41.6
3.00 - 2.00	19.0	60.6
2.00 - 1.00	21.4	81.5
1.00 - 0.00	16.0	97.5
1.00 - 0.00	2.5	100.0

D(CAVE) 2.50 (PM)

NO MIXING / RAG CHANGE

• DISTRIBUTION GRAPH (BY VOL.)



MOBILE CAPA-504
PARTICLE ANALYZER

DATE 5/9/83
SAMPLE CS-73-D
SOLVENT 150

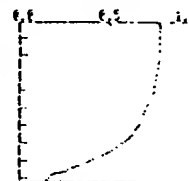
• CONDITIONS

SOLV. VISC 2.10 (CP)
SOLV. DENS 0.79 (G/CC)
SAMP. DENS 6.36 (G/CC)
D(CMAX) 10.0 (PM)
D(CMIN) 1.00 (PM)
D(C10) 1.00 (PM)
SPEED 500. (RPM)

• TIME 0 R 4 MIN 20 SEC

• DATE

TIME ABSORBANCE

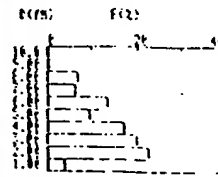


• DISTRIBUTION TABLE (BY VOL.)

D(PM)	F(2)	F(3)
10.0 - 9.0	0.0	0.0
9.0 - 8.00	0.0	0.0
8.00 - 7.00	0.0	0.0
7.00 - 6.00	0.0	0.0
6.00 - 5.00	0.0	0.0
5.00 - 4.00	0.0	0.0
4.00 - 3.00	0.0	0.0
3.00 - 2.00	0.0	0.0
2.00 - 1.00	0.0	0.0
1.00 - 0.00	0.0	0.0

D(CAVE) 3.21 (PM)

• DISTRIBUTION GRAPH (BY VOL.)



T2 (cont.)

HORIZA EMP-500
PARTICLE ANALYZER

DATE
SAMPLE C3-P5-T2
SOLVENT:

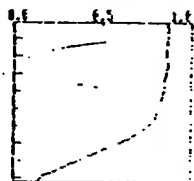
• CONDITIONS

SOLV. VISC 2.10 (CP)
SOLV. DENS 0.79 (G/CC)
SAMP. DENS 6.36 (G/CC)
D(CRX) 10.0 (PH)
D(CIK) 1.00 (PH)
D(CIV) 1.00 (PH)
SPEED 500 (RPM)

• TIME 0 H 4 MIN 20 SEC

• DATE 0.87

TIME ABSORBANCE

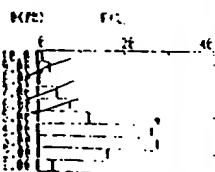


• DISTRIBUTION TABLE (BY VOL.)

D(PH)	F(%)	G(%)
10.0-9.0	0.0	0.0
9.0-8.0	1.2	1.2
8.0-7.0	2.0	3.2
7.0-6.0	0.1	4.6
6.0-5.0	4.4	6.4
5.0-4.0	7.3	15.8
4.0-3.0	11.8	27.5
3.0-2.0	26.2	53.7
2.0-1.0	27.3	81.0
1.0-0.0	15.1	96.1
0.0-0.0	3.4	100.0

D(CRV) 3.14 (PH)

• DISTRIBUTION GRAPH (BY VOL.)


HORIZA EMP-500
PARTICLE ANALYZER

DATE 9/19
SAMPLE C3-P5-T2
SOLVENT: H2O

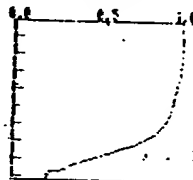
• CONDITIONS

SOLV. VISC 2.10 (CP)
SOLV. DENS 0.79 (G/CC)
SAMP. DENS 6.36 (G/CC)
D(CRX) 10.0 (PH)
D(CIK) 1.00 (PH)
D(CIV) 1.00 (PH)
SPEED 500 (RPM)

• TIME 0 H 4 MIN 20 SEC

• DATE 0.9

TIME ABSORBANCE

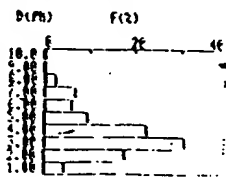


• DISTRIBUTION TABLE (BY VOL.)

D(PH)	F(%)	G(%)
10.0-9.0	0.0	0.0
9.0-8.0	0.0	0.0
8.0-7.0	0.0	0.0
7.0-6.0	2.2	2.2
6.0-5.0	6.0	9.1
5.0-4.0	6.6	15.8
4.0-3.0	9.6	24.6
3.0-2.0	22.5	47.1
2.0-1.0	36.4	77.0
1.0-0.0	10.6	95.7
0.0-0.0	4.3	100.0

D(CRV) 2.91 (PH)

• DISTRIBUTION GRAPH (BY VOL.)



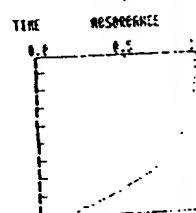
Administrative Notes

T1 versus T2 versus T3 for various passes

NOIRIF CAPP-SEC
PARTICLE ANALYZER
DATE 5/12
SAMPLE C3-P1-B
SOLVENT ISO

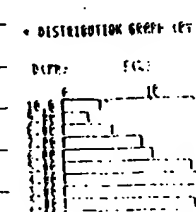
• CONDITION (T3)
SOLV. VISC 2.10(CP)
SOLV. DENS 0.7916(CC)
SAMP. DENS 6.3616(CC)
D(CHEX) 10.0 (PP)
D(CHEX) 1.00(CP)
D(CHEX) 1.00(CP)
SPEED 500. (CPH)

• TIME 0 h 4 min 20 sec
• DATA 0.9



• DISTRIBUTION TABLE (BY VOL.)

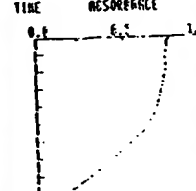
D(CP)	F(C)	F(C)
10.0	0.0	0.0
10.0-9.0	4.2	4.2
9.0-8.0	2.5	7.0
8.0-7.0	5.0	12.0
7.0-6.0	9.0	21.0
6.0-5.0	11.0	31.0
5.0-4.0	14.0	45.0
4.0-3.0	16.0	61.0
3.0-2.0	17.0	78.0
2.0-1.0	15.0	93.0
1.0-0.0	4.0	100.0
D(AVE)	3.79 (PP)	



NOIRIF CAPP-SEC
PARTICLE ANALYZER
DATE 5/12
SAMPLE C3-P1-B
SOLVENT

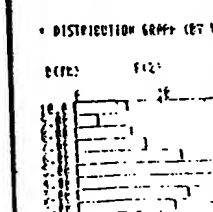
• CONDITION 0.75
SOLV. VISC 2.10(CP)
SOLV. DENS 0.7916(CC)
SAMP. DENS 6.3616(CC)
D(CHEX) 10.0 (PP)
D(CHEX) 1.00(CP)
D(CHEX) 1.00(CP)
SPEED 500. (CPH)

• TIME 0 h 4 min 20 sec
• DATA (T1)



• DISTRIBUTION TABLE (BY VOL.)

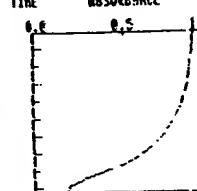
D(CP)	F(C)	F(C)
10.0	0.0	0.0
10.0-9.0	4.2	4.2
9.0-8.0	2.5	6.7
8.0-7.0	6.0	12.7
7.0-6.0	6.0	18.7
6.0-5.0	12.0	30.7
5.0-4.0	16.0	46.7
4.0-3.0	19.0	65.7
3.0-2.0	12.0	77.7
2.0-1.0	11.0	88.7
1.0-0.0	3.7	100.0
D(AVE)	4.14 (PP)	



NOIRIF CAPP-SEC
PARTICLE ANALYZER
DATE 5/12
SAMPLE C3-P1-B
SOLVENT

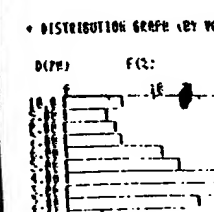
• CONDITION NO CHANGE
SOLV. VISC 2.10(CP)
SOLV. DENS 0.7916(CC)
SAMP. DENS 6.3616(CC)
D(CHEX) 10.0 (PP)
D(CHEX) 1.00(CP)
D(CHEX) 1.00(CP)
SPEED 500. (CPH)

• TIME 0 h 4 min 20 sec
• DATA (T2)



• DISTRIBUTION TABLE (BY VOL.)

D(CP)	F(C)	F(C)
10.0	0.0	0.0
10.0-9.0	6.5	6.5
9.0-8.0	4.7	11.2
8.0-7.0	5.6	16.8
7.0-6.0	6.3	23.1
6.0-5.0	10.7	33.7
5.0-4.0	12.7	46.4
4.0-3.0	16.5	62.9
3.0-2.0	10.0	72.9
2.0-1.0	14.7	87.6
1.0-0.0	3.0	100.0
D(AVE)	3.79 (PP)	



FINAL **C3-T3** - RESULTS: NECIC, MIX { premix medium

NO. 100
PARTICLE

SAMPLE
SOLVENT

• CONDITIONS

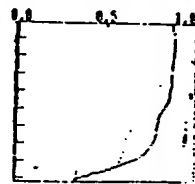
SOLV. VISC 2.10 (CP)
SOLV. DENS 0.79 (G/CC)
SAMP. DENS 6.36 (G/CC)
D(CMAX) 10.0 (PP)
D(CMIN) 1.00 (PP)
D(CDIV) 1.00 (PP)
SPEED 500. (RPM)

NECK

• TIME 0 H 4 MIN 20 SEC

• DATA

TIME ABSORBANCE



• DISTRIBUTION TABLE (BY VOL.)

D (PP)	F (%)	R (%)
10.0	0.0	0.0
9.0-9.9	0.0	0.0
8.0-8.9	0.0	0.0
7.0-7.9	2.4	2.4
6.0-6.9	13.3	4.4
5.0-5.9	10.5	14.5
4.0-4.9	13.3	20.6
3.0-3.9	6.5	34.5
2.0-2.9	17.6	51.5
1.0-1.9	9.0	87.4
1.0-0.0	0.0	100.0

D(CAVE) 2.00 (PP)

• DISTRIBUTION GRAPH (BY VOL.)

D (PP) F (%)



NO. 100
PARTICLE ANALYZER

DATE 5/22
SAMPLE C3-T3-MIX
SOLVENT P32

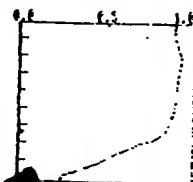
• CONDITIONS

SOLV. VISC 2.10 (CP)
SOLV. DENS 0.79 (G/CC)
SAMP. DENS 6.36 (G/CC)
D(CMAX) 10.0 (PP)
D(CMIN) 1.00 (PP)
D(CDIV) 1.00 (PP)
SPEED 500. (RPM)

• TIME 0 H 4 MIN 20 SEC

• DATA *DN 0.9*

TIME ABSORBANCE



• DISTRIBUTION TABLE (BY VOL.)

D (PP)	F (%)	R (%)
10.0	0.0	0.0
9.0-9.9	0.0	0.0
8.0-8.9	0.0	0.0
7.0-7.9	2.4	2.4
6.0-6.9	13.3	4.4
5.0-5.9	10.5	14.5
4.0-4.9	13.3	20.6
3.0-3.9	6.5	34.5
2.0-2.9	17.6	51.5
1.0-1.9	9.0	87.4
1.0-0.0	0.0	100.0

D(CAVE) 2.00 (PP)

• DISTRIBUTION GRAPH (BY VOL.)

D (PP) F (%)



NO. 100
PARTICLE ANALYZER

DATE 5/22
SAMPLE C3-T3-MIX
SOLVENT P32

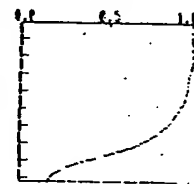
• CONDITIONS

SOLV. VISC 2.10 (CP)
SOLV. DENS 0.79 (G/CC)
SAMP. DENS 6.36 (G/CC)
D(CMAX) 10.0 (PP)
D(CMIN) 1.00 (PP)
D(CDIV) 1.00 (PP)
SPEED 500. (RPM)

• TIME 0 H 4 MIN 20 SEC

• DATA

TIME ABSORBANCE



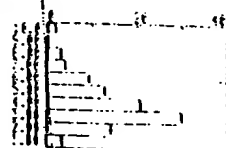
• DISTRIBUTION TABLE (BY VOL.)

D (PP)	F (%)	R (%)
10.0	0.0	0.0
9.0-9.9	0.0	0.0
8.0-8.9	0.0	0.0
7.0-7.9	2.4	2.4
6.0-6.9	13.3	4.4
5.0-5.9	10.5	14.5
4.0-4.9	13.3	20.6
3.0-3.9	6.5	34.5
2.0-2.9	17.6	51.5
1.0-1.9	9.0	87.4
1.0-0.0	0.0	100.0

D(CAVE) 2.00 (PP)

• DISTRIBUTION GRAPH (BY VOL.)

D (PP) F (%)



100179

Technical Notebook

Book V

Initials and Last Name:

NCOMBE, P.

Serial:

139

Date of First Entry:

6/7/88

Date of Last Entry:

5/89

Security Classification:

42 11-17-88

IBM Technical Notebook

Survey 2212 sintering time versus rel density

<u>h</u>	<u>rel D(%)</u>	<u>wt</u>
0	68.4	
✓ (0.08)	65.9	6.97
✓ 0.25	61.1	
✓ 0.5	59.7	
(16) (70)	54	✓
✓ 120	51	✓

small pellet, density determination probably not as accurate

16h (not listed in book)

POST

0.88 1.15 0.216 0.22 4.0 / 6.45 62

REDO

11-2-88 0011 Analytical IBM Technical Notebook

El.	wt %	theo. M%	ANA M%
Ca	22.4	0.86	0.875
Sr	8.24	0.14	0.147
Cu	40.6	1	1

Example calc. ✓
 $\frac{Ca\ wt\ \%}{Ca\ wt\ \%} = 0.639 / 0.639 = 1$
 $\frac{Sr\ wt\ \%}{Sr\ wt\ \%} = 0.094 / 0.639 = 0.147$
 $\frac{Cu\ wt\ \%}{Cu\ wt\ \%} = 0.539 = 0.825$

11/3 0011 pellet 2 for 16h diffusion sinter
 Pre 4000/30,000 slightly irregular

2.85	1.531	0.496	0.913	~3.12	/4.95 = 63 — perfect
2.81	~1.36	0.44	0.639	4.4	↓ = <u>89</u>
			0.64		

0201 4,000/30,000 PRE

3.78	1.365	0.494	0.723	5.23	= 72.4% (too high?)
------	-------	-------	-------	------	---------------------

11/4 0011-2 cut into 2 slices. Didn't add block thickness so irregular.
 1 ~ 2.30 cm thick 1 ~ 0.179 cm

↓ Post will use for first press
 875C for 30 hrs → pellet has warped, grown large voids like xstals and sagged. Obviously metastable.

previous 3h sinter showed no evidence of instability.

11-2-88


IBM Technical Notebook

44 11-9 2201 pellets
 3200/28
 2013 2.99 1.351 0.415 0.595 5.02 69.7
 2.96 ~1.306 0.372 0.498 ~5.98 ~83.3+
 2013 min 872C SINTER (SLD ATTAINMENT 12 MIN TERSUS 1. T_{int} = T_{AT} + 3 min)
 open possibly
 pycnometer
 86
 air = 85

3300/30
 2014 1.16 1.082 0.245 0.225 5.16 71.7
 1.15 1.050* 0.210* 0.182 6.32
 (87.5) 5 min.
 double

2015 1.17 1.086 0.248 0.230 5.09 70.7
 { broken before
 sintering
 reground
 repressed } pellet 201-11

2016 0.99 1.094 0.205 0.193 5.13 71.25
 *† 0.98 1.06 0.185^{lip} 0.163 6.01
 * (0.178) 0.158 6.2
 to temp 1845
 out 2.15
 36 min

*(†): 201-4,5 some evidence of drooping

 edge droop
 in pellet. reduce temp 5C

2700/29
 2017 1.2 1.086 0.258 0.238(5) 5.03 69.9
 1.01 ~1.05 0.185 0.165
 1.06 1.19 1.05 ~0.225 0.195 6.1 84.7
 to temp 2727-8
 15
 2.145
 15

11-10 Sintering Summary <2201 data>

45

	temp	SINTER	green	POST.	201-2
201-8	872C	2min	71.25	85.6	C11-2201 P3 pressed pellet (large die) 86.1 ave
201-3	872	12-3	69.7	86	
201-4	875C	5	71.7	87.5	
201-9	872C	5	71-	84.7	
201-7	872C	15	69.9	84.7	
201-6	875C	30	71.25	83.5	
201-10	872C	1h	70.4	86.7 → 85	
201-1	875C	2h		84-	
201-2	875	30h		76.1 → 79	

not sintered
201-11

Record keeping: 201-2 30h 875C ~ 75% (pyc): irregular pellet growth
resulting in varying local densities
201-3 0.608 dia. pellet for pressure diffusion sinter
201-5 regd → 201-11

11-11 Gas pycnometry gives an averaged rel density for pellets 1, 7, 8, 9
(wght 4.6g) of 86.75g vs 84.75 (reasonable agreement), mostly
closed porosity.

The above understood
and witnessed by

Date

and
by

Date

46
11-14 SINTER 870-875°C IBM Technical Notebook

NOTE: [ALL SINTER TIMES ARE 1 MW attainment + 1 MW EQ SOAK + Δ SINTER time]

201-8 perfect pellet ~3000/29000


POST	1.19	1.081	0.253	0.232	5.13	71.25	green
2 MW	1.17	1.038	0.225	0.190	6.16	85.6	

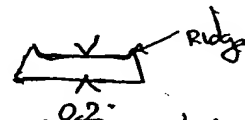
POST	201-9 12	1.075	0.259	0.235	5.11	71.00	green
5 MW	1.19	1.036	0.231	0.195	6.10	84.7	

POST	201-10 1.10	1.083	0.236	0.217	5.07	70.4	
1h	1.09	1.057*	0.2†	0.175(5)	6.21	86.25 (accurate?)	see below

201-11 Pellet was reg'd & repressed from broken pellet. Also, die ran from results, w much high uniaxial pressure (of true edge) 12,000

1.169	0.252	0.24	5.04	70.00
-------	-------	------	------	-------

* linear average dia due to slumping. (- 
 † w pellet interior after edge ridge worn away



? probably slightly less due to exclusion of ridge volume and linear average approx. after flattening; 15 μm

201-10	0.90†	1.057	0.168	0.147	6.12	85	better (more accurate)
--------	-------	-------	-------	-------	------	----	------------------------

11 2.96 (298)
 201-11 1.357 0.412 0.596 4. 496 5.0 (69.4)

2.935 ~1.315 0.365 0.496 5.94 82.5
 2.945

11-12

201-11 cut "whats" larger flattened and polished.

0011-2201 sandwich $\sim 0.353 - 0.363$ thick.

> From Furnace top to bottom of "weight plate" $1\frac{3}{32}" @ 462C$
assuming ~ 6 lbs. for RAM & plate & x-sectional pellet area
of $0.212 in^2$ load $\Rightarrow 28$ psi

Diffusion sintering set @ $860C$ for ~ 12 hrs.

Rel density from measurement of 201-11 $\sim 83\%$. On inspection of internal polished surface numerous burnout-like occlusions present. Some degree of open porosity, also.

Pyc. rel. den = 88% thus Δ attributable to open porosity.

0011 rel density from measure $\sim 89\%$. No pyc reading done 16h sinter @ $975C$.

4:30 pm T @ $859C$ assume start of diffusion sintering
Plate height $1\frac{3}{8}"$ ($\frac{3}{32}"$ expansion due to TCE from $462C$)
(No RT measure made, but not significant)

48

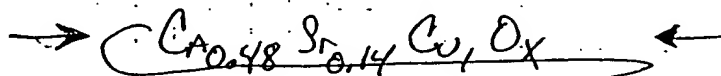
IBM Technical Notebook

11-28-88 <INSERT>

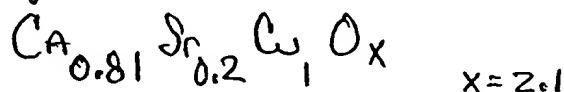
Results (by microprobe) of $\text{Ca}_{0.8}\text{Sr}_{0.2}\text{CuO}_x$ melt xstals

Melt composition was from pgs. 27-29

Composition was not $\text{Ca}_{0.86}\text{Sr}_{0.14}\text{Cu}_1\text{O}_x$ in melt, but rather



from which xstals grew of CaSrCuO_x with stoic.



Atomic wght fractions were:

Ca	0.195
Sr	0.05
Cu	0.242
O	0.513 (by difference)

Melt temp. was 1000C for 16h with cooling virtually, but
 NOT TOTALLY A QUENCH. UNCONTROLLED RATE REGULATED BY PLENOR
 thermal mass

11-22

Balance Bi Powders for Run

2212 - ^{~g}30.5

2201 - 12.5

0011 - 33.5

2nd Diffusion Run 2hr RAMP to 866C @ 100C plate space = 1 7/32

0011 slice studied @ 0.18 cm (not measured when finished, either was 2201 or sandwich, will try to approx)

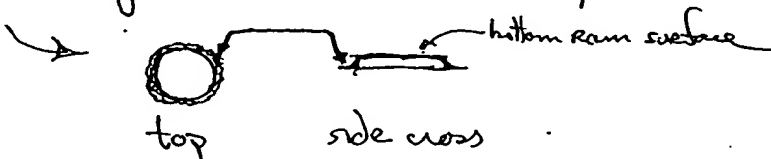
2201 ~ same 0.18

loose ~ 0.23 - 0.2 x 0.03/slice ∴ 0.18 → 0.15 0.17 → 0.14
 so sandwich might be ~ 0.29 cm (80% of run #1)

Approx thickness by height of plate differences @ 866C 1 12/32 - 1 9/32

12/32 - 9/32 = 0.23 cm ∴ 0.29 - 0.23 = 0.06 too small → 871C peak

RESULTS: "Bi" pellet has spread, apparently melting. Total thickness 0.18 cm.
 has generated crystalline (?) skirt around pellet periphery.



0.18 cm = 0.07" slice ~ square 0.07 + 0.015 = 0.085

50

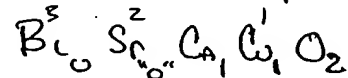
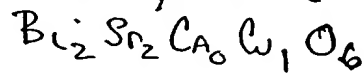
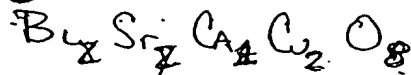
IBM Technical Notebook

0011-2201 Mix Calculations

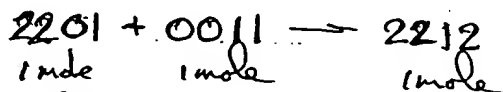
wt% wt%
 0011 2201

*✓ +2

*✓ +5



From "ideal" state.



	A.W.	0011	2201	2212
B _{1.2}	208.98	-	417.96	417.96
Sr	87.62	-	175.24	175.24
Ca	40.08	40.08	-	40.08
C	63.54	63.54	63.54	127.08
O	15.9994		95.9964	127.9952

$$135.6188 + 752.7341 = 888.3552$$

B _{1.2}	0(0.14)(0.86)1	(2.15)(1.6)(0)(1)	(2.15)(1.6)(1.17)(2)
	449.307	449.307	449.307
Sr	12.2168	140.192	147.2016
Ca	34.488	-	40.32816
C	63.54	63.54	127.08
O	31.9988	~95.9964*	*127.9952

142.2744

749.0354

891.912296 / (891.3098)

% dev

+8.6%

*(5.825)15.9994
 93.19651

99.6% (2.15 etc)

The above understood and witnessed by

Date

and

Date

IBM Technical Notebook

51

CONTINUATION...

1 mole "0011" + 1 mole 2201 \rightarrow 011 + 529 wt% 2201

142.2744g

752.7364g

$$142.2744g + (0.02)(142.2744) = 145.12g$$

2.84549

2 wt%

Batch
15

9.49
9.485

0.19

9.675

batch size

$$142.2744g + (0.05)(142.2744) = 149.38812g$$

7.11372

5 wt%

9.485

~0.475
0.48

9.96

batch size

For Stoic (molar) mix = $1.423g + 7.53g = 8.95g$ batch size

Total Usage 0011 2201

20.393 8.192

% 61 66

	cc	cc	vol%	wt%
roll	2.37	0.0264	1.0%	2
table	2.37	0.0736	3	5
	0.356	1.045	25%	storic

STOIC: 2201 2.15 1.6 0 1

"0011" 0 0.14 0.86 1

2.15 1.74 0.86 2 versus poly 2.15 1.68 1.17 2

The above understood and witnessed by

Date

and hv

Date

52 Stoic Mixing

IBM Technical Notebook

0011 2201

~1.43 g ~7.53

MIX STARTING @ 3:00 P.M., 50mls isopropyl
5cc ZrO_2 balls
2/3 full

NOTE: From bottom pg 51 can be seen this Additive approach will
yield a theoretical molar comp { 0.1 M larger in Sr
0.31 M less in Ca

i.e. Strontia rich, Calcium poor

8.96 g added initially, 8.85 g recovered: 1.2% loss (98.8 yield)

Stoic 1 Pre 2700/27,500

3.11 1.36 0.486 0.706 4.41 ~68.9

$0.25(4) + 0.75(7.2) = 6.4$ vol% basis, ~ density calc

Rxn. (SINTER) temp to be 850°C

Pellet melted indicating lower mp, $1/2 \phi$ exists in system, later
x-rayed. Predominantly 1 lath-like ϕ w/ exaggerated growth
as in 2201 120h sample.

12-5

4:20 P.M. // 4:25 @ temp.

0011-3 placed in preheated rapid temp set @ 951C ($T_{\text{imp}} = 975\text{C}$)
for overnite sintering.
No per data on density due to irregular shape caused by
pellet crumbling during isopressing.
unipress $\rightarrow 6000, 150 - 29,000$ PSI. wght $\sim 3.1\text{g}$ ^{3.0-2.9}

12/6

9:30 Slow cooling begun $\therefore \Delta T_{\text{inter}} = 17\text{h}$ @ 875C

Post 2.86g ~ 0.460 mm thick radius might have been ~ 1.58

estimated density 0.666cc @ 3.1g $\sim 4.68/4.00 \approx 93$ (may be high)
 3.0 4.5 \downarrow 90 better

0011-3

0.181" thick

Slice 1 $\rightarrow 0.09$ " after cleaning // post polish \rightarrow N/R

Slice 2 $\rightarrow 0.074$
0.179 ✓

2201-8

1.028 dia \therefore area = $\pi D^2/4 = 0.85\text{in}^2$
 0.409 $= 0.525\text{in}^2$

$5.75\text{lbs}/.525\text{in}^2 \sim 11\text{psi}$

2201-8 (top)



Pellet configuration @ START $\sim 3:55\text{p.m.}$ thickness - 0.34mm

0011-3

Ramp $\rightarrow 434$ Set point - 800C Dwell - 12h $1\frac{1}{2}$ @ 380C

12/7 Result: no melting, pellets bonded by little deformation.

12/8 After 24h 825C Anneal no evidence of lica., but bond breaks
after handling at pellet interface with some "rxn etching" of
0011 pellet surface having thin, ^{upper} layer of 2201 (or rxn prod)
behind.

54
12-6

IBM Technical Notebook

~~4/18/80~~
 SECOND 2201 Synthesis Ref pg 25 $\text{Bi}_{2.15}\text{Sr}_{1.6}\text{Ca}\text{Cu}_1\text{O}_8$

$\text{Bi} \approx \text{Bi}_2\text{O}_3 : 30.0543 \times 2 = 60.1086 \quad 60.11$

$\text{Sr} @ \text{SrCO}_3 : 14.1724 \quad 28.3448 \quad 28.35$

$\text{Cu} @ \text{CuO} : \frac{4.7724}{48.9991 \text{ g}} \quad \frac{9.5448}{97.9982 \text{ g}} \quad 9.54$

$\sim 0.7019 \text{ conversion factor for } \text{CO}_2 \rightarrow 0 \quad 28.3448 (0.702) = 19.898$

Estimate $\sim 89 \text{ g}$ "batch recovery"
 $\frac{97.9982}{89.55} \text{ CO}_2 \text{ loss}$

12-7

$\text{Bi}_2\text{O}_3 \quad \begin{array}{r} \text{tare} \quad 202.54 \\ \text{tare} \quad 262.68 \\ \hline 60.13 \end{array} \quad 60.13 - 60.11 = +0.02 \checkmark$

$\text{SrCO}_3 \quad \begin{array}{r} \text{tare} \quad 262. \\ \text{tare} \quad 291.03 \\ \hline 28.35 \end{array} \quad \begin{array}{l} < 28.3835 \text{ wgt} \\ 28.36 \text{ tared} \end{array} \quad 28.36$

$\text{CuO} \quad \begin{array}{r} 300.57 \\ 291.03 \\ \hline 9.54 \end{array} \quad (300.57/9.54) \text{ wgt } 9.55$

12-8 $97.92 / \text{recovery after drying overnite}$
 $98.02 \text{ theoretical} = 99.9\% \text{ yield} \quad 0.1\% \text{ mixing loss}$

to pg 56

The above understood and witnessed by

Date

and

Date

IBM Technical Notebook

55

12-7-88

0.11
9.49
9.48
0.02
9.46

0.48

22.01
0.48
0.50
> .01
0.49

theor.

wtd

Reed

actual = 9.95

std. 1.5h 5min ZnO₂/Iso
grind mix, screening & drying.

12-8-88

Recovery : 9.84 g / 9.86g theoretical = 99.8% > 0.2% loss

60.87
cont take 51.04/5
9.83 transferred

0011-2201-5W(3V)-1

Post 8500/29,000

2.31 1.17 0.704 0.690 3.35 ~67%

Pellet bigger than usual, 1.75g max in future might be considered.

1.183 0.715 CRACKED, measurements ~~1.183~~

12-9

5W-2 900C 8500/39000

1.27 1.174 0.382 0.414 3.07 61.4!

3:55 in preheated furnace → 4:00 to temp @ 900C
POST 5 MIN

1.24 1.11 0.36 0.349 3.55 71—

15 MIN NO SIGNIFICANT CHANGE

12-12 to temp ~ 10:20 A.M. (check: 10:45 → no slumping) → SNTER till 12:30

12:15 A.M. do-cool initiated

11:45

~2h

1.24 1.053 0.33 0.29 4.28 ~86%

The above understood
and witnessed by

Date

and

Date

56

IBM Technical Notebook

12-8-88 2201 SYNII cont. (from 1454)

crucible temp $\begin{array}{r} 186.68 \\ - 88.79 \\ \hline 97.89 \end{array}$ $\xrightarrow{\text{spill}}$ 186.68 \rightarrow 192.29 w/ top

10:00 A.M. \rightarrow 575C hold 1h
 11:00 \rightarrow 800C
 12-9 11:00 AM cool, required to < 100 mesh

$\begin{array}{r} 182.23 \\ - 88.95 \\ \hline 93.28 \end{array}$ (weight after sintered powder removed)

$\begin{array}{r} 93.44 \\ - 88.79 \\ \hline 4.65 \end{array}$ if 88.79 used
 184.02 after grinding
 $\begin{array}{r} 88.95 \\ - 93.28 \\ \hline -4.33 \end{array}$ to temp. (866C) @ 1:00 p.m.
 $\Delta 1.21$ w grinding 1.3%
 $97.88 - 93.28 = 4.6$
 $97.89 - 89.55 = 8.34$ } 55% REACTED

1:00 - 5:00 pm 866C, shut down for weekend (very resistant saw eye)

12-12-88

to temp 866C @ 10:00 A.M.
 off @ 7:00 A.M. 12/13/88

PARTIAL MELTING, "CLASSIC" EUTECTIC lamellar and large 2201 lathes.

Date and sign every entry. Have
entry witnessed. Submit an Inver
anything possibly relevant.

possibly important
disclosure of

☐ Unclassified
☐ IBM Internal Use
☐ Confidential

☐ IBM Confidential-Restricted
☐ Registered IBM Confidential
"Register with local Recorder"

~~12-14-88 2201 Sys III~~

IBM Technical Notebook

57

~~memory for bus: 202.75~~

The above understood
and witnessed by _____

Date _____

and
by _____

Date _____

58 12-14-88 **SYNTH 2201** IBM Technical Notebook

mixing jar tare 202.75

Be as Be_2O_3 30.0543

Sr as $SrCO_3$ 14.1724

C. as CO 4.7724

x 2 = 60.11

28.35

9.55

98.01

- 8.5 CO_2 loss

89.51

$Sr/Be = 0.744$

$Sr 0.8 Sr = 1.72$

Be_2O_3 262.86

tare 202.75

60.11

291.20 (19)

262.86

28.34 (5)

300.75

291.20

9.55

PRE CAL I

crucible + 185.84

tare 87.99

97.85

$97.85/98.01 = 0.2\%$ max loss

12-20 Post 750C 16h calcination

crucible + 181.15

↓

87.98

93.17

post gen 92.70

no rxn w/ Pt. ; lime green color/bottom, uniform throat

except for top 1/2 edges (grey)

$93.17 - 97.85 = -4.68 / 8.5 = 55\%$ CO_2 lost

post gr

crucible + 180.70

↓

87.98

(92.72)

12-21-88 Post 790C 20h calcination

178.10

87.98

90.12

Material looks very good, smooth indicating lamellar structure
 Uniformly black, sparkling, smooth body. An outer shell
 89% \approx rxn close to completion $\approx 98\%$
 and inner core structure. (see below)



inner sub-core
 outer shell
 air space

to page 60

The above understood
 and witnessed by _____

Date

and
 hv

Date

12-14-8

IBM Technical Notebook

5

$Y_1Ba_2Cu_3O_x$ Implantation Experiment

PRE - film on $SrTiO_3$ 3500/30000

3.07 $\phi.448$ 0.485 0.799 3.84 ~60.4 %

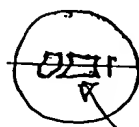


line 'MARKER' || to long axis of triangular $SrTiO_3$ implant
implant orientation - NOTE: MARK ON UNDERSIDE of pellet

film side opposite

3.02 1.271 0.34 0.508 6.02 94-95

3.05 1.448 0.476 0.784 3.89 ~61



line 'MARKER' || to long cutting axis of two pellets (cut on line)
implant orientation - see NOTE above for polished side over

2.99 1.272 0.391 0.497 6.02 94-95

5

5:12 p.m. 475C @ 10C/min to 975 $\Delta 500C/10C/min = 50min$ ~ 6:00 pm

Cutting $SrTiO_3$ implant: measures 0.5" on SAW (0.025-0.505 tangents)

$$\frac{1.272}{2.54} = 0.485 \checkmark$$

The above understood
and witnessed by _____

Date _____

and
by _____

Date _____

60

IBM Technical Notebook

12-21-88 Calkination III 2201-B3

X-RAY SHOWS DISTINCTLY NOT SINGLE ϕ , even though material looks "OK"

total 177.04
 curx 87.98
 89.06 88.2

12-22-88

175.7 - (-1.34) slight sticking (RXN) w/ cur. bottom
 87.98
 87.72 - 89.51 (theo.) = 1.79 g greater than theoretical loss
 could be grinding loss 2%

PRE
 850 cal

174.93 total
 87.93 tare (after air cleaning)
 87. - g 0.72 g grinding loss (consistent w/ previous losses)
 + X-ray slide

POST
 12-22-88

174.83
 87.93
 86.90 - $\Delta 0.10$ 100% RXN! non-staining weight
 not overconcluding but not surprising
 batch #1 wasn't either

IBM Technical Notebook

61

12-27-88

Summary various RXN pellets:

5 wt% 2201 in 0011 for 16h @ 850C SEM

5 wt% 2201 in 0011 for 2h @ 975C SEM

{ 0011-2201 ~~submicron mixture~~ ~~pressure-banded~~ pellet: 13h 850C } when
1/2 Ø formation, exaggerated grain growth/warpage

0011 @ 975C 17h SEM STD.

2201 @ 875C 1h SEM STD.

2212 @ 853C 5min SEM STD.

The above understood
and witnessed by _____

Date

and

Date

62

IBM Technical Notebook

12-29-88 Dave's Compositions

#	Y	Ba	Cu	Y	Ba	Cu
	(0.157)	(0.33)	(0.50)	0.17	0.33	0.50
	0.15	0.33	0.52	0.8639	1.9038	3—
	0.17	0.35	0.48	1.0625	2.1875	3—
	0.19	0.33	0.48	1.1875	2.0625	3—
	0.19	0.31	0.50	1.14	1.86	3—

Calculated Compositions (calculations next page)

	Y	Ba*	Cu	total	
1)	1.91937 (1.92)	6.51253 (6.51)	3.97697 (3.98)	12.48	←
2)	1.69356 (1.69)	6.51253 (6.51)	4.13605 (4.14)	12.34	←
3)	1.92	6.90723 (6.91)	3.81789 (3.82)	12.65	
4)	2.14518 (2.15)	6.51 0.33	3.82 0.48	12.48	←
5)	2.15	6.1783 (6.18) .31	3.98	12.31	←

* Ba as BaCO₃
Y as Y₂O₃
Cu as CuO } NOTE → no purity corrections applied yet

The above understood
and witnessed by ...

Date

and
by

Date

IBM Technical Notebook

63

1/3/89

Calculations for weights summarized on page 62

2) $y_{0.15} Ba_{0.33} Co_{0.52}$

$y = 0.15 (225.8082) / 2 = 16.9356 g$

$Ba = 0.33 (197.3494) = 65.1253 g BaCO_3$

$Co = 0.52 (79.5394) = 41.3605 g Co$

3) $y_{0.17} Ba_{0.35} Co_{0.48}$

$y = 0.17 (225.8082) / 2 = 19.1937 g$

$Ba = 0.35 () = 69.0723 g BaCO_3$

$Co = 0.48 () = 38.1789 g Co$

4) $y_{0.19} Ba_{0.33} Co_{0.48}$

$y = 21.4518 Ba = 65.1253 Co = 38.1789$

5) $y_{0.19} Ba_{0.31} Co_{0.50}$

$y = 21.4518 Ba = 61.1783 Co = 39.7697$

1) $y_{0.17} Ba_{0.33} Co_{0.50}$

$19.1937 65.1253 39.7697$

The above understood
and witnessed by

Date

and

Date

1/8/89

64

1) ~~88.5~~ (TRIAL #1)
 O_2 FIRED

IBM Technical Notebook

$2 \rightarrow 88.5409$ $\frac{1}{0.17} Ba_{0.33} Cu_{0.5}$

$\frac{1}{2} O_3 - 1.92$

$CO - 3.98(1)$

$BaCO_3 = 6.51$
 6.58867

$\frac{88.53}{76.06}$
 $\frac{12.47}{12.43}$

$\frac{2.3125}{0.3900}$
 1.922

$\frac{4.3712}{0.3900}$
 $3.98(12)$

$\frac{6.9665}{6.7785}$
 0.3888
 6.9685

post dry $\frac{12.43}{12.43}$

$6.5777 = 1248$

$\rightarrow 91.6\% \text{ recovery total } - \Delta = 0.05$

1-9-89

10.95 g after 2nd 16h 950C O_2 calcination

$6.5777 \cdot \left(\frac{153.8394}{197.3510} \right) = 5.11$
 0.777
 $-\Delta 1.47$

$\frac{12.43}{1.47}$
 10.96

1/17 Dave) post 1h grind = 1.86 μm 3000/30,000

P1 1.68 1.136 0.408 0.4135 4.06 63.8%

In O_2 @ ~3:00 p.m. 1/10/89, to temp @ 950C projected 4:30 5:00 \rightarrow 9:00

16h 1.64 1.011 0.354 0.284 5.775 90.8 (91)

1/4/88

4) ~~Pre~~ fired
O₂

Y_{0.19} Ba_{0.33} Co_{0.48}

~~1.89~~ 6.51 ~~3.82~~
~ 2.15

3.8217

.3865

4.2082

Y₂O₃ =

2.5342 6.9623 4.2093
0.3865 0.384 0.3865
2.1477 6.5783 3.8218

→ 12.55 g

1/10/88

Second generation started after grinding. No evidence of liq formation. Powder looks good already.

10.99 g after 2nd calcination;

10.76 post grind

~~6.58~~ (.777) = 5.11 - Δ 1.47

12.55
1.47
11.08 g expected:

Recovered

1/17

P1 Pre 2500/30,000 to temp @ ~ 5:00 p.m.

1.60 1.14 0.399 0.4073 3.93 62% ✓

1/18

1.58 1.055 v 0.365 0.319 4.95 77.8%

Green φ peaks coming up in x-ray.

66

IBM Technical Notebook

5) 4.19 Ba 0.31 Co 0.50
 (.99) $\frac{1}{2}O_3 - 2.14(13)$ $\frac{1}{2}O_3 - 2.14(13)$ $\frac{1}{2}O_3 - 2.14(13)$
 2.3760 $\frac{1}{2}O_3 - 2.14(13)$ $\frac{1}{2}O_3 - 2.14(13)$
 2.3761 $\frac{1}{2}O_3 - 2.14(13)$ $\frac{1}{2}O_3 - 2.14(13)$
 0.2287 $\frac{1}{2}O_3 - 2.14(13)$ $\frac{1}{2}O_3 - 2.14(13)$
 2.1474 $\frac{1}{2}O_3 - 2.14(13)$ $\frac{1}{2}O_3 - 2.14(13)$
 6.4690 $\frac{1}{2}O_3 - 2.14(13)$ $\frac{1}{2}O_3 - 2.14(13)$
 0.2229 $\frac{1}{2}O_3 - 2.14(13)$ $\frac{1}{2}O_3 - 2.14(13)$
 6.2411 $\frac{1}{2}O_3 - 2.14(13)$ $\frac{1}{2}O_3 - 2.14(13)$
 4.2092 $\frac{1}{2}O_3 - 2.14(13)$ $\frac{1}{2}O_3 - 2.14(13)$
 0.2282 $\frac{1}{2}O_3 - 2.14(13)$ $\frac{1}{2}O_3 - 2.14(13)$
 $3.9810 \Rightarrow 12.3695$ $\frac{1}{2}O_3 - 2.14(13)$ $\frac{1}{2}O_3 - 2.14(13)$

12.34(3) collected after mix // 12.34/12.37 $\sim \Delta 0.24\%$ ✓

$6.2411 - 4.8493 = 1.392$

$\frac{63.50}{51.17} = 12.33$ $\frac{62.20}{51.17} = 11.03$ $\Delta 1.3/1.39 = 93.5\%$

11.00 post GRND

$\frac{62.17}{51.18} = 10.99$

post CA II 62.11

$\frac{11.63}{10.75}$

Post GRND 10.46
 PRE 1.60 1.440 0.244 0.40 4.00 62.9
 Post 1.56 1.266 0.210 0.267 6.00 (94-91)

Good densification, no apparent liq, CO islands present,

The above understood and witnessed by

Date

and by

Date

IBM Technical Notebook

67

2201

P1B3 2500/30000
PRE 1.94 1.09 0.391 0.365 5.315 73.8%
Post 15 min @ 860
1.94 1.06 0.359 0.313 6.2 86%

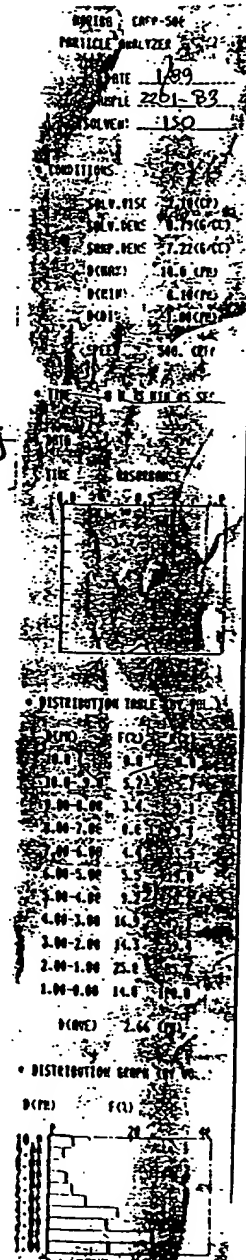
2 wt % 2201 in 0011 1/18/88

9.49
0.19
9.58
some leaking during 0.5h mix : 9.05 g
9.05 g
8.68 g Small
0.37 g loss
8.68 g
0.37 g

2 wt % P1 4200/30,000 to temp @ ~5:00 p.m.
Pre 1.70 1.163 0.499 0.53 3.21 ~64.2
1.69 1.21 0.525 0.60 2.82 56.4
1.194 - 1.227
same slumping
- Δ 12%

Cuts yield : 1.57 mm inside 0.30
1.12 mm center 0.25
polished → 1.79 mm outside 0.380 (two)

+ 26.52 26.03 25.94
post 25.52 25.52 25.45
1000 → 1000 μm 490



The above understood
and witnessed by _____

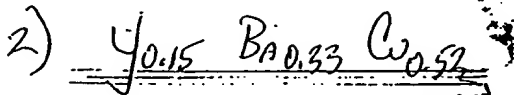
Date

and

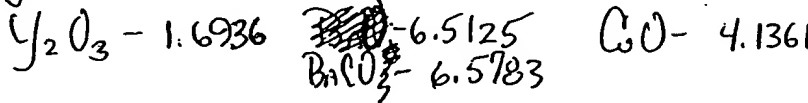
Date

68

IBM Technical Notebook



little loss: 74.55



$(.22705) \frac{1.9206}{\underline{0.2288}}$
 ~ 1.6936

$\frac{6.8066}{\underline{0.2284(8)}}$
 6.5782

$\frac{4.3651}{\underline{0.2288}}$
 $4.1363 - (0.2284) \sim 12.41$ total

1/17 1st CALCINATION

$\frac{66.53}{\underline{54.16}}$ (12.37 measured from weighing)
 12.37 $\sim 12.41 = -\Delta 0.3\%$

$6.5783(.277) = 5.111 (-1.47)$ 12.37
 ~ 10.90 expected yield (less transfer losses)

1/18 POST $\frac{66.53}{\underline{65.15(05)}}$ $- \Delta 1.38(48)$ $\frac{54.20}{\underline{54.2}}$ $\frac{65.05}{\underline{54.2}}$ $\frac{10.85}{\underline{10.85}}$ \sim total rxn.

2nd CAL (16h as above)

1/19 POST $\frac{65.02}{\underline{54.2}}$ $\frac{10.82}{\underline{10.82}}$ \sim constant 10.79 recovery

Notes: large liq stains (formation) during 1st/2nd cal unlike

PRE P1 1 & A where liq was suppressed in 1st cal { minor in 2nd }
 $3380/30,000$ 75C @ 5:16 p.m. temp @ 7:45, 16h \rightarrow 11:45 A.M.

1.60 1.414 0.258 0.405 3.95 62.1%

1.57 1.227 0.216 0.255 6.16 96.9

IBM Technical Notebook

69

1) O_2

4) O_2

2) O_2

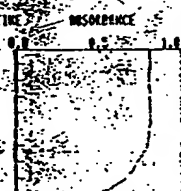
3) O_2 1h iso

PSD's
5) O_2

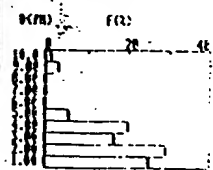
DATE 1-10-89
SAMPLE Y. B. 33605
SOLVENT ISO-1

• CONDITIONS
SOLV. VISC 2.10 (CP)
SOLV. DENS 0.7916 (CC)
SAMP. DENS 0.3416 (CC)
D(COX) 10.0 (CP)
D(CIN) 0.10 (CP)
D(CIV) 1.00 (CP)
SPEED 500 (RPM)

• TIME 0.0 4 MIN 20 SEC

• DATA
TIME ABSORBANCE


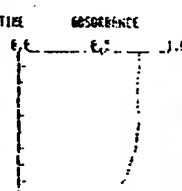
• DISTRIBUTION TABLE (BY VOL.)
D(CPX) F(C) R(C)
10.0-9.0 1.2 1.2
9.0-8.0 2.3 4.1
8.0-7.0 0.0 4.1
7.0-6.0 0.0 4.1
6.0-5.0 0.0 4.1
5.0-4.0 5.5 5.6
4.0-3.0 13.0 25.5
3.0-2.0 16.5 46.6
2.0-1.0 26.0 74.5
1.0-0.0 25.1 100.0
D(CVE) 1.00 (CP)

• DISTRIBUTION GRAPH (BY VOL.)
D(CPX) F(C)


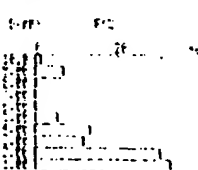
DATE 1-13-88
SAMPLE Y. B. 33605
SOLVENT ISO

• CONDITIONS
SOLV. VISC 2.10 (CP)
SOLV. DENS 0.7916 (CC)
SAMP. DENS 0.3416 (CC)
D(COX) 10.0 (CP)
D(CIN) 0.10 (CP)
D(CIV) 1.00 (CP)
SPEED 500 (RPM)

• TIME 0.0 4 MIN 20 SEC

• DATA 0.7
TIME ABSORBANCE


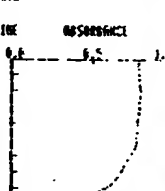
• DISTRIBUTION TABLE (BY VOL.)
D(CPX) F(C) R(C)
10.0-9.0 1.2 1.2
9.0-8.0 0.0 0.0
8.0-7.0 0.0 0.0
7.0-6.0 0.0 0.0
6.0-5.0 0.0 0.0
5.0-4.0 11.2 11.2
4.0-3.0 13.2 26.5
3.0-2.0 11.4 36.6
2.0-1.0 29.6 67.6
1.0-0.0 32.2 100.0
D(CVE) 1.00 (CP)

• DISTRIBUTION GRAPH (BY VOL.)
D(CPX) F(C)


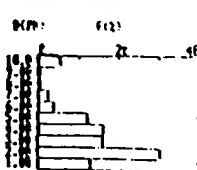
DATE 1-20-89
SAMPLE Y. B. 33605
SOLVENT ISO

• CONDITIONS D-0.8
SOLV. VISC 2.10 (CP)
SOLV. DENS 0.7916 (CC)
SAMP. DENS 0.3416 (CC)
D(COX) 10.0 (CP)
D(CIN) 0.10 (CP)
D(CIV) 1.00 (CP)
SPEED 500 (RPM)

• TIME 0.0 4 MIN 20 SEC

• DATA
TIME ABSORBANCE



• DISTRIBUTION TABLE (BY VOL.)
D(CPX) F(C) R(C)
10.0-9.0 1.2 1.2
9.0-8.0 5.4 5.4
8.0-7.0 0.0 5.4
7.0-6.0 0.0 5.4
6.0-5.0 3.0 11.4
5.0-4.0 12.2 23.6
4.0-3.0 16.2 40.0
3.0-2.0 16.2 56.2
2.0-1.0 30.0 86.2
1.0-0.0 13.8 100.0
D(CVE) 2.20 (CP)

• DISTRIBUTION GRAPH (BY VOL.)
D(CPX) F(C)



DATE 1-27-89
SAMPLE Y. B. 33605
SOLVENT ISO

• CONDITIONS D-9.6
SOLV. VISC 2.10 (CP)
SOLV. DENS 0.7916 (CC)
SAMP. DENS 0.3416 (CC)
D(COX) 10.0 (CP)
D(CIN) 0.10 (CP)
D(CIV) 1.00 (CP)
SPEED 500 (RPM)

• TIME 0.0 4 MIN 20 SEC

• DATA
TIME ABSORBANCE



• DISTRIBUTION TABLE (BY VOL.)
D(CPX) F(C) R(C)
10.0-9.0 1.2 1.2
9.0-8.0 5.4 5.4
8.0-7.0 0.0 5.4
7.0-6.0 0.0 5.4
6.0-5.0 3.0 11.4
5.0-4.0 12.2 23.6
4.0-3.0 16.2 40.0
3.0-2.0 16.2 56.2
2.0-1.0 30.0 86.2
1.0-0.0 13.8 100.0
D(CVE) 1.00 (CP)

• DISTRIBUTION GRAPH (BY VOL.)
D(CPX) F(C)



DATE 1-24-89
SAMPLE Y. B. 33605
SOLVENT ISO

• CONDITIONS
SOLV. VISC 2.10 (CP)
SOLV. DENS 0.7916 (CC)
SAMP. DENS 0.3416 (CC)
D(COX) 10.0 (CP)
D(CIN) 0.10 (CP)
D(CIV) 1.00 (CP)
SPEED 500 (RPM)

• TIME 0.0 4 MIN 20 SEC

• DATA
TIME ABSORBANCE


• DISTRIBUTION TABLE (BY VOL.)
D(CPX) F(C) R(C)
10.0-9.0 1.2 1.2
9.0-8.0 5.4 5.4
8.0-7.0 0.0 5.4
7.0-6.0 0.0 5.4
6.0-5.0 3.0 11.4
5.0-4.0 12.2 23.6
4.0-3.0 16.2 40.0
3.0-2.0 16.2 56.2
2.0-1.0 30.0 86.2
1.0-0.0 13.8 100.0
D(CVE) 1.00 (CP)

• DISTRIBUTION GRAPH (BY VOL.)
D(CPX) F(C)


The above understood
and witnessed by

Date

and

Date

70

IBM Technical Notebook

$$\begin{array}{lcl}
 S_{r7} C_{12} D \rightarrow S_{0.37} C_{0.63} O_{19} & S_{rD} & C_{10} \\
 38.34 & 50.1078 & \\
 S_{rC} D \rightarrow S_{0.5} C_{0.5} D_7 & 51.8077 & 39.7677 \\
 S_{rC} D \rightarrow S_{0.67} C_{0.33} D_3 & 69.4250 & 26.248 \\
 S_{rD} = 103.6194 \rightarrow S_{rD}_3 & 142.63 & 142.47 \\
 C_{10} = 79.5334 & & \\
 3.83 & 5.02 & \\
 3.834 & 5.0178 & \rightarrow 8.8538 \\
 (5.11) 5.18077 & 3.97677 & (5.78) \rightarrow 9.1579 \\
 (6.29) 6.9425 & 26.248 & (6.63) \rightarrow 9.5673 \\
 \downarrow & \downarrow & \\
 5.46 & 5.02 & 10.48 \\
 7.38 & 3.98 & 11.36 \\
 9.89 & 26.34 & 12.52 \\
 S_{rD} & C_{10} &
 \end{array}$$

The above understood

Date

and

Date

1/17/89

CO11-5 at 201 @ 8500 for attempted TCM prep.

slice 2 - 1.28 mm - 1280 μ m

slice 3 - 0.68 680 μ m

slice 2 prep: mounted side 1 measures ~ 27.64
12.80
 $\frac{26.30 - (3.5)}{1.34 - 1.29}$

am: 300 μ 1340
 $\frac{980}{2} = 490 - 490$

20 8's on "soft" 15 μ m grids ~ 900 } 150 8's on 6 give 770
850 target
720 μ m before starting second side

26.40 after mount 20 \rightarrow 26.21
25.69
0.71 ✓
25.69
520

150 \rightarrow 26.16
1430

150 \rightarrow 26.06
330 ✓

72

IBM Technical Notebook

3) O_2 fixed

$Y_{O_2} = 0.17$ $Bu = 0.35$ $Co = 0.48$

$Y_{O_2} = 1.9213$

$BuCO_2 = 6.9770$

$CO = 3.8217$

2.1495
 0.2288
 1.9212

7.2050
 0.2277
 6.9773
 5.4214

4.0499
 0.2281
 3.8218

4.0498

Some bumping, but very good mix as should be true. 12.35 post mix

12.72 of expected REDO (Bumping too critical)

$Y_{O_2} = 1.9213$

$BuCO_2 = 6.9770$

$CO = 3.8217$

2.1425
 0.2240
 1.9215

7.1973
 0.2200
 6.9773

4.0425
 0.2210
 3.8218

4.0427
total
12.72

Mix recovery after accurate drying: $12.63/12.72 = \Delta 0.7\%$ (acceptable)

63.82
low 51.19

Post 62.35
 51.20
 11.19

Cal #I: 3:57 1900 w 5:15 est temp attainment
4:25 486C ~ seems correct

(11.17 expected)
Post cal II

Post grind I: 11.21 \rightarrow 11.14 62.35

62.24
 51.20
 11.05

Very little liq formation compared to #2. Apparently need excess Bu and Co for larger liq.

0.2 g loss due to Si carbon from tube (pre-grow) 10.8

The above understood

Date

and

Date

1/27

IBM Technical Notebook

73

10.97 collected: white top layer on powder. Dry. Flake-cake
very agglomerated/brittle and does not easily pick out when
brushed. Had to dry grind in order to produce decent prod.

10.25 recovered for dry grind

P1 3500/29000

1.62 1.425 0.266 0.424 3.82 60—%

1.52 1.321 0.245 0.336 4.52 71 %

Pre grind & Post grind x-rays show change of some peaks
in two x-rays, however sintering calculation of pellet may
refer to products to original ϕ 's. Will do x-ray of pellet

also.
Post: some slumping.

The above understood
and witnessed by _____

Date _____

and
by _____

Date _____

74. 4/10/87 125 Variation Study IBM Technical Notebook Property Pellets
ave = 62.5

#1 P2 3.000/50,000
1.04 1.138 0.256 0.260 4 62.3
1.01 1.046 .22 0.187 5.34 84

#2 P2 1
1.02 1.123 0.264 0.261(5) 9.90 67.3
1.00 9.87 .22 0.168(6) 5.75 93.6

#3 P2 ✓
1.04 1.154 0.248 0.258 4.03 63.4
1.024 1.024 .224 0.184 5.54 87

Pellets 15 Pellets @ ~10:30 A.M. 2/17/87 10°/min (pre-warmed)
Tc Ts
10:30 259 239 (?)
→ 10:45 442 518 +Δ75 Ts
11:50 900 sp 944

non early exits P@ 300 west down
by 25.50 estimated time to reach
st point would be 45 mins. or
11:30 @ +Δ50 pre-warmed
or 95°C then relaxation over
ensuing 20 mins of 60°C. Delay
in pull run requires time
w.c. BC. is probably close.
project over 2 hrs 1:45 Mon.

1:45 PM 2/17/87 in furnace @ 600C project over 2 hrs 1:45 Mon.

see page 145

2/6/89

IBM Technical Notebook

75

Experiments to look at
Carbonate in 123

clean gas with ascorbic

Sample 1: dense closed

porosity, 0.791%

cut sections from center

Sample 2: open porosity

0.87%

center section

thin slices on aggregate

(2) 3 pellets of each (Peter)

center sections of each

(1) T am / EELSS (P. Batson)

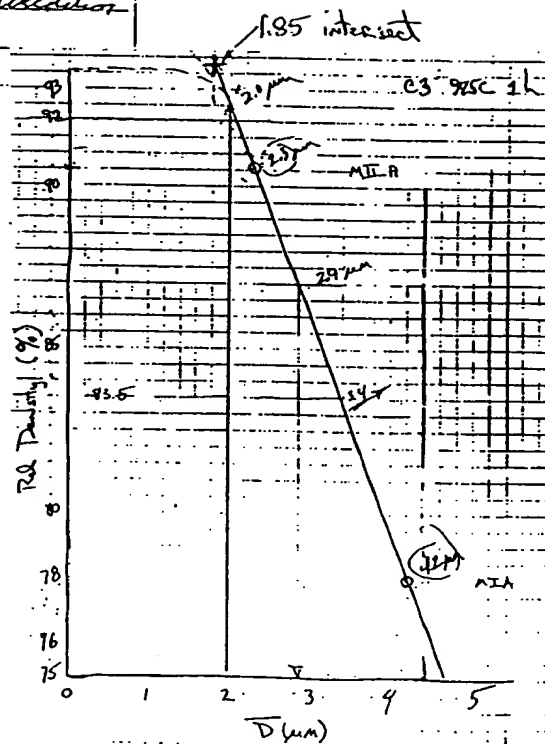
(2) Magnetometer (T. Magnus)

(3) Induction (Diane Davis)

(4) CO₂ evolution on dissolution

(5) X-ray lattice

(6) XPS



The above understood

Date

and
by

Date

NOPIER CAP-104
 PARTICLE ANALYZER
 DATE 2/18/89
 SAMPLE C3-PA 11
 SOLVENT ISO

• CONDITIONS: MICA

SOLV. VISC 1.00 CP
 SOLV. DENS 0.79 G/CC
 SHAP. DENS 0.34 G/CC
 D(0.0) 10.0 MP
 D(0.1) 0.10 MP
 D(0.2) 1.00 MP
 SPEED 500.0 RPM

• TIME 0.0 MIN 20 SEC
 DATE 0.8

TIME RESONANCE

• DISTRIBUTION TABLE (BY VOL.)

D(μm)	F(%)	D(μm)	F(%)
0.0	0.0	10.0	0.0
0.1	0.0	10.1	0.0
0.2	0.0	10.2	0.0
0.3	0.0	10.3	0.0
0.4	0.0	10.4	0.0
0.5	0.0	10.5	0.0
0.6	0.0	10.6	0.0
0.7	0.0	10.7	0.0
0.8	0.0	10.8	0.0
0.9	0.0	10.9	0.0
1.0	0.0	11.0	0.0
1.1	0.0	11.1	0.0
1.2	0.0	11.2	0.0
1.3	0.0	11.3	0.0
1.4	0.0	11.4	0.0
1.5	0.0	11.5	0.0
1.6	0.0	11.6	0.0
1.7	0.0	11.7	0.0
1.8	0.0	11.8	0.0
1.9	0.0	11.9	0.0
2.0	0.0	12.0	0.0
2.1	0.0	12.1	0.0
2.2	0.0	12.2	0.0
2.3	0.0	12.3	0.0
2.4	0.0	12.4	0.0
2.5	0.0	12.5	0.0
2.6	0.0	12.6	0.0
2.7	0.0	12.7	0.0
2.8	0.0	12.8	0.0
2.9	0.0	12.9	0.0
3.0	0.0	13.0	0.0
3.1	0.0	13.1	0.0
3.2	0.0	13.2	0.0
3.3	0.0	13.3	0.0
3.4	0.0	13.4	0.0
3.5	0.0	13.5	0.0
3.6	0.0	13.6	0.0
3.7	0.0	13.7	0.0
3.8	0.0	13.8	0.0
3.9	0.0	13.9	0.0
4.0	0.0	14.0	0.0
4.1	0.0	14.1	0.0
4.2	0.0	14.2	0.0
4.3	0.0	14.3	0.0
4.4	0.0	14.4	0.0
4.5	0.0	14.5	0.0
4.6	0.0	14.6	0.0
4.7	0.0	14.7	0.0
4.8	0.0	14.8	0.0
4.9	0.0	14.9	0.0
5.0	0.0	15.0	0.0
5.1	0.0	15.1	0.0
5.2	0.0	15.2	0.0
5.3	0.0	15.3	0.0
5.4	0.0	15.4	0.0
5.5	0.0	15.5	0.0
5.6	0.0	15.6	0.0
5.7	0.0	15.7	0.0
5.8	0.0	15.8	0.0
5.9	0.0	15.9	0.0
6.0	0.0	16.0	0.0
6.1	0.0	16.1	0.0
6.2	0.0	16.2	0.0
6.3	0.0	16.3	0.0
6.4	0.0	16.4	0.0
6.5	0.0	16.5	0.0
6.6	0.0	16.6	0.0
6.7	0.0	16.7	0.0
6.8	0.0	16.8	0.0
6.9	0.0	16.9	0.0
7.0	0.0	17.0	0.0
7.1	0.0	17.1	0.0
7.2	0.0	17.2	0.0
7.3	0.0	17.3	0.0
7.4	0.0	17.4	0.0
7.5	0.0	17.5	0.0
7.6	0.0	17.6	0.0
7.7	0.0	17.7	0.0
7.8	0.0	17.8	0.0
7.9	0.0	17.9	0.0
8.0	0.0	18.0	0.0
8.1	0.0	18.1	0.0
8.2	0.0	18.2	0.0
8.3	0.0	18.3	0.0
8.4	0.0	18.4	0.0
8.5	0.0	18.5	0.0
8.6	0.0	18.6	0.0
8.7	0.0	18.7	0.0
8.8	0.0	18.8	0.0
8.9	0.0	18.9	0.0
9.0	0.0	19.0	0.0
9.1	0.0	19.1	0.0
9.2	0.0	19.2	0.0
9.3	0.0	19.3	0.0
9.4	0.0	19.4	0.0
9.5	0.0	19.5	0.0
9.6	0.0	19.6	0.0
9.7	0.0	19.7	0.0
9.8	0.0	19.8	0.0
9.9	0.0	19.9	0.0
10.0	0.0	20.0	0.0

• DISTRIBUTION GRAPH (BY VOL.)

NOPIER CAP-104
 PARTICLE ANALYZER
 DATE 2/18/89
 SAMPLE C3-PA 11
 SOLVENT ISO

• CONDITIONS: MICA

SOLV. VISC 1.00 CP
 SOLV. DENS 0.79 G/CC
 SHAP. DENS 0.34 G/CC
 D(0.0) 10.0 MP
 D(0.1) 0.10 MP
 D(0.2) 1.00 MP
 SPEED 500.0 RPM

• TIME 0.0 MIN 20 SEC
 DATE 0.8

TIME RESONANCE

• DISTRIBUTION TABLE (BY VOL.)

D(μm)	F(%)	D(μm)	F(%)
0.0	0.0	10.0	0.0
0.1	0.0	10.1	0.0
0.2	0.0	10.2	0.0
0.3	0.0	10.3	0.0
0.4	0.0	10.4	0.0
0.5	0.0	10.5	0.0
0.6	0.0	10.6	0.0
0.7	0.0	10.7	0.0
0.8	0.0	10.8	0.0
0.9	0.0	10.9	0.0
1.0	0.0	11.0	0.0
1.1	0.0	11.1	0.0
1.2	0.0	11.2	0.0
1.3	0.0	11.3	0.0
1.4	0.0	11.4	0.0
1.5	0.0	11.5	0.0
1.6	0.0	11.6	0.0
1.7	0.0	11.7	0.0
1.8	0.0	11.8	0.0
1.9	0.0	11.9	0.0
2.0	0.0	12.0	0.0
2.1	0.0	12.1	0.0
2.2	0.0	12.2	0.0
2.3	0.0	12.3	0.0
2.4	0.0	12.4	0.0
2.5	0.0	12.5	0.0
2.6	0.0	12.6	0.0
2.7	0.0	12.7	0.0
2.8	0.0	12.8	0.0
2.9	0.0	12.9	0.0
3.0	0.0	13.0	0.0
3.1	0.0	13.1	0.0
3.2	0.0	13.2	0.0
3.3	0.0	13.3	0.0
3.4	0.0	13.4	0.0
3.5	0.0	13.5	0.0
3.6	0.0	13.6	0.0
3.7	0.0	13.7	0.0
3.8	0.0	13.8	0.0
3.9	0.0	13.9	0.0
4.0	0.0	14.0	0.0
4.1	0.0	14.1	0.0
4.2	0.0	14.2	0.0
4.3	0.0	14.3	0.0
4.4	0.0	14.4	0.0
4.5	0.0	14.5	0.0
4.6	0.0	14.6	0.0
4.7	0.0	14.7	0.0
4.8	0.0	14.8	0.0
4.9	0.0	14.9	0.0
5.0	0.0	15.0	0.0
5.1	0.0	15.1	0.0
5.2	0.0	15.2	0.0
5.3	0.0	15.3	0.0
5.4	0.0	15.4	0.0
5.5	0.0	15.5	0.0
5.6	0.0	15.6	0.0
5.7	0.0	15.7	0.0
5.8	0.0	15.8	0.0
5.9	0.0	15.9	0.0
6.0	0.0	16.0	0.0
6.1	0.0	16.1	0.0
6.2	0.0	16.2	0.0
6.3	0.0	16.3	0.0
6.4	0.0	16.4	0.0
6.5	0.0	16.5	0.0
6.6	0.0	16.6	0.0
6.7	0.0	16.7	0.0
6.8	0.0	16.8	0.0
6.9	0.0	16.9	0.0
7.0	0.0	17.0	0.0
7.1	0.0	17.1	0.0
7.2	0.0	17.2	0.0
7.3	0.0	17.3	0.0
7.4	0.0	17.4	0.0
7.5	0.0	17.5	0.0
7.6	0.0	17.6	0.0
7.7	0.0	17.7	0.0
7.8	0.0	17.8	0.0
7.9	0.0	17.9	0.0
8.0	0.0	18.0	0.0
8.1	0.0	18.1	0.0
8.2	0.0	18.2	0.0
8.3	0.0	18.3	0.0
8.4	0.0	18.4	0.0
8.5	0.0	18.5	0.0
8.6	0.0	18.6	0.0
8.7	0.0	18.7	0.0
8.8	0.0	18.8	0.0
8.9	0.0	18.9	0.0
9.0	0.0	19.0	0.0
9.1	0.0	19.1	0.0
9.2	0.0	19.2	0.0
9.3	0.0	19.3	0.0
9.4	0.0	19.4	0.0
9.5	0.0	19.5	0.0
9.6	0.0	19.6	0.0
9.7	0.0	19.7	0.0
9.8	0.0	19.8	0.0
9.9	0.0	19.9	0.0
10.0	0.0	20.0	0.0

• DISTRIBUTION GRAPH (BY VOL.)

NOPIER CAP-104
 PARTICLE ANALYZER
 DATE 2/18/89
 SAMPLE C3-PA 11
 SOLVENT ISO

• CONDITIONS: MICA

SOLV. VISC 1.00 CP
 SOLV. DENS 0.79 G/CC
 SHAP. DENS 0.34 G/CC
 D(0.0) 10.0 MP
 D(0.1) 0.10 MP
 D(0.2) 1.00 MP
 SPEED 500.0 RPM

• TIME 0.0 MIN 20 SEC
 DATE 0.8

TIME RESONANCE

• DISTRIBUTION TABLE (BY VOL.)

D(μm)	F(%)	D(μm)	F(%)
0.0	0.0	10.0	0.0
0.1	0.0	10.1	0.0
0.2	0.0	10.2	0.0
0.3	0.0	10.3	0.0
0.4	0.0	10.4	0.0
0.5	0.0	10.5	0.0
0.6	0.0	10.6	0.0
0.7	0.0	10.7	0.0
0.8	0.0	10.8	0.0
0.9	0.0	10.9	0.0
1.0	0.0	11.0	0.0
1.1	0.0	11.1	0.0
1.2	0.0	11.2	0.0
1.3	0.0	11.3	0.0
1.4	0.0	11.4	0.0
1.5	0.0	11.5	0.0
1.6	0.0	11.6	0.0
1.7	0.0	11.7	0.0
1.8	0.0	11.8	0.0
1.9	0.0	11.9	0.0
2.0	0.0	12.0	0.0
2.1	0.0	12.1	0.0
2.2	0.0	12.2	0.0
2.3	0.0	12.3	0.0
2.4	0.0	12.4	0.0
2.5	0.0	12.5	0.0
2.6	0.0	12.6	0.0
2.7	0.0	12.7	0.0
2.8	0.0	12.8	0.0
2.9	0.0	12.9	0.0
3.0	0.0	13.0	0.0
3.1	0.0	13.1	0.0
3.2	0.0	13.2	0.0
3.3	0.0	13.3	0.0
3.4	0.0	13.4	0.0
3.5	0.0	13.5	0.0
3.6	0.0	13.6	0.0
3.7	0.0	13.7	0.0
3.8	0.0	13.8	0.0
3.9	0.0	13.9	0.0
4.0	0.0	14.0	0.0
4.1	0.0	14.1	0.0
4.2	0.0	14.2	0.0
4.3	0.0	14.3	0.0
4.4	0.0	14.4	0.0
4.5	0.0	14.5	0.0
4.6	0.0	14.6	0.0
4.7	0.0	14.7	0.0
4.8	0.0	14.8	0.0
4.9	0.0	14.9	0.0
5.0	0.0	15.0	0.0
5.1	0.0	15.1	0.0
5.2	0.0	15.2	0.0
5.3	0.0	15.3	0.0
5.4	0.0	15.4	0.0
5.5	0.0	15.5	0.0
5.6	0.0	15.6	0.0
5.7	0.0	15.7	0.0
5.8	0.0	15.8	0.0
5.9	0.0	15.9	0.0
6.0	0.0	16.0	0.0
6.1	0.0	16.1	0.0
6.2	0.0	16.2	0.0
6.3	0.0	16.3	0.0
6.4	0.0	16.4	0.0
6.5	0.0	16.5	0.0
6.6	0.0	16.6	0.0
6.7	0.0	16.7	0.0
6.8	0.0	16.8	0.0
6.9	0.0	16.9	0.0
7.0	0.0	17.0	0.0
7.1	0.0	17.1	0.0
7.2	0.0	17.2	0.0
7.3	0.0	17.3	0.0
7.4	0.0	17.4	0.0
7.5	0.0	17.5	0.0
7.6	0.0	17.6	0.0
7.7	0.0	17.7	0.0
7.8	0.0	17.8	0.0
7.9	0.0	17.9	0.0
8.0	0.0	18.0	0.0
8.1	0.0	18.1	0.0
8.2	0.0	18.2	0.0
8.3	0.0	18.3	0.0
8.4	0.0	18.4	0.0
8.5	0.0	18.5	0.0
8.6	0.0	18.6	0.0
8.7	0.0	18.7	0.0
8.8	0.0	18.8	0.0
8.9	0.0	18.9	0.0
9.0	0.0	19.0	0.0
9.1	0.0		

2/7/89

IBM Technical Notebook

77

PI mill $D = 4.21 \mu m$ (guide)

3333/28500

Pre wght: 3.46 (of 3.5) some deformation during iso pressing, but slight
minimal so hardness can be deduced.

Post 975C 1h

3.41 1.402 0.448 0.69 4.94 77.7 \rightarrow 78% 4.2 too low

PII mill $D = 2.34 \mu m$ (slow)

PRE 3900/29,000

3.46 1.453 0.543 0.9 3.84 60.5 reasonable

3.40 1.285 0.456 0.59 5.76 90.6 \langle NEED SLIGHTLY HIGHER \rangle

Tomorrow \rightarrow will mill in

the

Yields: PRE MI: 48g

gap B

gap A { 24 MIIA: 20g
16 MIIA: #

20.5

error in pre-weights

78

M4A $\bar{D} = 1.85$

IBM Technical Notebook

PRE - 4000/30,000

$20/\mu\text{m}$ to 675 $10/\mu\text{m}$ to 975
 1h 975C } given

P3 (3.40) 1.452 0.543 0.9 3.78
~~3.38~~
 3.48 1.265 0.460 0.518 1.602 94.6

stent

P4 (3.41) 1.462 0.540 0.91 3.75
 3.60 1.274 0.468 0.506 1.604 95

honey

P5 (3.93)⁺ 1.457 0.561 0.935 3.67
 3.60 1.280 0.482 0.62 5.81
 3.65 5.89

57.7⁺ $\rightarrow \geq 58$

91.4⁺
~~92.6~~ } Probably even higher

MIFB - 4000/30,000 80 μm

P6 (3.53) 1.463 0.508 0.85 4.17 65.6
 3.53 1.38 0.464 0.674 5.24 (82.4)

stent

P7 (3.54) 1.462 0.504 0.85 4.165 65.5
 3.59 1.358 0.462 0.668 5.36 (84.5)

honey

P8 (3.56) 1.463 0.507 0.85 4.19 65.9
 3.73 1.352 0.453 0.65 5.73 90.2

* laminated on 1 side, not severe (must be 'repelletized' pellet)

P9 4000/30000

3.57 1.462 0.517 0.87 4.1 64.5

3.56 1.354 0.463 0.666 5.35 84.2

P10 fines 4/3 as above

1.53 1.436 0.254 0.411 3.72 58.5 was expected

1.54 1.254 0.207 0.256 6.02 94.7 { doesn't look good

Pellet cutting NEXT (see pg 80 for plan overview)

Pellet 3 & 4 dedicated to vertical & horiz. slicing

Pellets 6 & 7

from tangent saw cut edge: 1 mm slices are 0.055" w/ blade

Low Density Vertical slices: 1 1.2 slices } 7 altogether + one piece
6 1.0 slices } and polished end (unusable)

Horizontal: 2 1.0 slices mid section
1 0.5 top
1 1.0 bottom

High Density

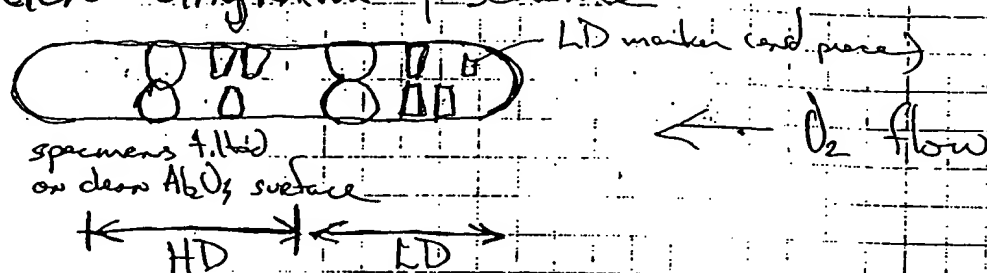
vertical: 5 slices (and lost to chipping) 1 end polished
~2mm 1 polished thick chunk
~1.2mm 3 oxygenated
horiz: 1 SAs
2 mid section
1 ea top & bottom (top chipped)

2/15/89

IBM Technical Notebook

Oxygenation Diagram { scheme

Top View



2/14 in and to 600C @ 20C/min; 10C/min to 800C

15 min SOAK AND start ramp to 600C @ 0.17C/min (10/h)

To 600C @ 1:30 p.m. 2/15/89 in deg, CO₂-free O₂.

Pellet (1) 0.5C

1 mm vertical slices 19mm to 800C, 10/h to 600 deg (48h), quench.

- 1) 1 slice for Jaccard Press (Raman)
- 2) 1 slice for Alex for XPS of fracture surface
- 3) save remainder for future use (desiccated)
- 2) 1 extra slice oxygenated

Pellet (2) 0.5C

1 mm horizontal slices 4 up outer slices discarded

- 1) 1 slice (10mm) ground to ~0.5mm { cut 3 3mm discs w/ ultrasonic in isopropanol etc (if possible).
1 disc to Tom
2 discs for TEM
1 spare
- 2) 1 slice dedicated to T vs T to Dave's spec

Pellet (3) 0.5C

spare for ① x-ray lattice
② CO₂ evolution

The above understood

Date

and
by

Date

2/16/89

C4 Synthesis Preparation/Notes (ref book IV, pg 46, pg 14)

	oxide wt. frac.	atomic % $\frac{1}{4} \text{ Ba, C}$	oxide M.W.
$\frac{1}{2} \text{ O}_3$	0.1751	.17	225.81
BaO	0.4651	.33	153.34

CO : 0.3625 ~ .5 79.54

Example Calc: wt frac deriv

$\frac{1}{2} \text{ O}_3$	225.81 g	$\times \frac{.17 \text{ mole}}{1 \text{ mole}} = \frac{38.39}{2} = 19.19$	$19.19 / 109.56 = 0.1751$
BaO	153.34	$\times .33 = 50.60$	$50.6 / 109.56 = 0.4618(5)$
CO	79.54	$\times .5 = 39.77$	$39.77 / 109.56 = 0.363$
			0.9999

17.51 g $\frac{1}{2} \text{ O}_3$

46.18 g BaO

 $\left\{ \begin{array}{l} 197.35 \times 46.18 \\ 153.34 \end{array} \right\} 59.43 \text{ g BaCO}_3$

$\frac{1}{2} \text{ O}_3$	19.19 / .99 = 19.209 \rightarrow 19.21	$\approx \times 1.5$	28.81(5)	28.82
BaCO ₃	50.60(2) \times (197.35 / 153.34) = 65.12(5)		97.69	97.69
CO	39.77 / .99 = 39.87		59.71(5)	59.72

$$97.69 (0.1777) = 75.91 - 97.69 =$$

$$\begin{array}{r} 186.23 \\ - 21.78 \\ \hline 164.45 \end{array}$$

A2

Administrative Notes

FINAL Batch Size for REASONABLE BULK HANDLING

$$\frac{1}{2}O_2 \quad 17.51 / .999 = 17.52(7) \approx 17.53$$

$$BaCO_3 \quad 65.12(5) / .9999 = 65.12(5) \approx 65.13 \quad \rightarrow 343.78$$

$$CO \quad 39.77 / .999 = 39.80(9) \approx 39.81$$

$$122.47$$

$$\begin{array}{r} 343.78(7) \\ \times 278.65 \\ \hline 65.13 \quad \checkmark \quad (\Delta 0.01?) \end{array} \quad BaCO_3 \quad \frac{1}{2}O_2 \quad 17.53 \quad \text{weighed/transformed}$$

$$\begin{array}{r} 382.46 \\ + 343.78(7) \\ \hline 39.78 \quad (\Delta 0.03) \end{array} \quad CO \quad \text{Mixing yield} \quad \begin{array}{r} 122.29 \\ \hline 122.47 \end{array} \quad \begin{array}{r} 99.85\% \\ - \Delta 0.15 \end{array}$$

$$\begin{array}{r} 151.42 \quad \text{OK} \\ \times 37.89 \\ \hline 57.93 \end{array} \quad \text{tare 1} \quad \begin{array}{r} 140.48 \\ \times 82.12 \\ \hline 58.36 \end{array} \quad \text{tare 2} \quad \begin{array}{r} 140.48 \\ \times 82.12 \\ \hline 58.36 \end{array} \quad \rightarrow X \text{ bad hunt dimensions}$$

$$58.36 = 122.29 \quad \checkmark$$

$$\begin{array}{r} 146.97(6) \\ 88.61 \\ \hline 58.36 \end{array} \quad \text{sintered much more / some lca form}$$

$$\begin{array}{r} 151.42 \\ \times 144.37 \\ \hline 7.05 \\ 87.55 \end{array} \quad \text{tare 1} \quad \begin{array}{r} 146.97 \\ \times 141.74 \\ \hline 5.23 \\ 88.64 \end{array} \quad \text{tare 2} \quad \begin{array}{r} 146.97 \\ \times 141.74 \\ \hline 5.23 \\ 88.64 \end{array} \quad \begin{array}{l} \text{less sintered, less lca} \\ - 12.28 \text{ (O}_2 \text{ loss vs} \\ 14.53 \text{ expected} \\ 105\% \text{ reached)} \\ 2.25 \text{ to go} \end{array}$$

$$\text{after gross} \quad 108.71 / 110. = 98.8\% \quad - \Delta 1.2\%$$

$$\begin{array}{r} 197.383 \quad (2) \\ 88.64 \\ \hline 108.69 \end{array}$$

	$\gamma\text{Al}_2\text{O}_3$	BaCO_3	Cu_2O	SIS / Result
C4-1	0.17	0.33	0.5	assumed, store pack
	0.16	0.36	0.5	analytical determination

C4-2	0.17	0.33	0.5	analytical <u>lig</u>
------	------	------	-----	-----------------------

Δ	+0.01	-0.03	-
----------	-------	-------	---

C4-3	0.16	0.35	0.5	analytical
------	------	------	-----	------------

Δ	-0.01	+0.02	-
----------	-------	-------	---

Δ_{net}	-	-0.01	-
-----------------------	---	-------	---

-3E	0.165	0.35	0.5
-----	-------	------	-----

Δ	-0.005	+0.02	-
----------	--------	-------	---

Δ_{net}	+0.005	-0.01	-
-----------------------	--------	-------	---

C4-4	0.16	0.34	0.5	analytical
------	------	------	-----	------------

Δ	-	-0.01	-
----------	---	-------	---

Δ_{net}	-	-0.02	-
-----------------------	---	-------	---

C4-5	0.16	0.34	0.49	analytical
------	------	------	------	------------

Δ	-	-	-0.01
----------	---	---	-------

Δ_{net}	-	-0.02	-0.01
-----------------------	---	-------	-------

Species Imputation \rightarrow trace content,

C4-6	0.16	0.34	0.478	$\text{Cu}_2\text{O} \rightarrow \text{Cu}_2\text{O}$
------	------	------	-------	-------------------------------------------------------

Δ	-	-	-0.022
----------	---	---	--------

$\text{BaCO}_3 \rightarrow \text{Ba(OH)}_2$

Δ_{net}	-	-0.02	-0.03
-----------------------	---	-------	-------

$\gamma\text{-}\text{Fe}_2\text{O}_3 \rightarrow \gamma\text{-}\text{Fe}_2\text{O}_3$ X

C4-7	0.16	0.34	0.478
------	------	------	-------

Δ	-	-	+0.008
----------	---	---	--------

Δ_{net}	-	-0.02	-0.022 \uparrow
-----------------------	---	-------	-------------------

C4-7 TRANSFORM TO STOIC basis

$\frac{1}{2}O_2$	$Ba(O_2)$	$Cu(O)$	
0.17	0.31	0.498	0.48

Correct for fuel batched

$\frac{1}{2}O_2$ is good as received

$BaCO_3$ is Barium rich by 0.02 at %

CuO is Copper rich by 0.02 at %

A3

Administrative Notes

Post: Cal II in 60 hrs @ 950C in O_2

3/27

195.52 \rightarrow post 88.84 (O₂g. rxn.)

88.64

106.88 - 108.69 = 1.81 / 2.25 = 80.5% of remainder

 $\frac{12.28}{14.09 / 14.53 \text{ theo.}} = 97\% \uparrow$ less

Minimal liq. formation.

99.57g yield (due to contamination)

{ further contamination upon re-submission to the for cal II reduces yield further

Peaks @ ~30.2, 29.4, 28.5 2θ Dunsberg. May be $BiCl_3$, but could also be 2θ

$$n\lambda = 2d \sin \theta \Rightarrow d = \frac{\lambda}{2 \sin \theta} \quad 100 = 3.72$$

something wrong here

$$3.72 = \frac{\lambda}{2 \sin \theta}$$

$$4.803 = \sin^2 \theta$$

4/19

From Hechtly: $1/96 Ba_{2.16} Cu_3$ ($1/92 Ba_{2.72} Cu_1$) $O_{2.2}$ In reference to VARIATIONAL study: $\frac{0.116 \pm 0.005}{0.36 \pm 0.01} \cdot 0.5 = 1.02$

2/17/89 pag 4

975C

Property Pellet for information study - On

2 g pellets should give enof material for 4.4 mm thick sintered body allowing a slice to be cut up an interior & exterior surface.

7.5 g #1 stock 1.92 used for pellet (.17 .33 .5)

7.6 g #2 stock 1.90 ↓ (.15 .33 .52)

8.5 g #3 stock . . . (17 .35 .48)

9 #4

2.7 #5 to 600C @ 20/min; 10/min to 975C 4131-625C
3600/29,000 Quench 1h 510

#1 P3

1.92	1.144	0.479	0.489	3.93	61.8
1.90	1.0	0.4	0.314	6.05	95-

#2 P3

1.91	1.126	0.490	0.488	3.91	61.5
1.88(?)	0.98	0.412	0.311	6.045	95-

#3 P3

1.95	1.133	0.503	0.507	3.85	60.5
1.85	0.998	0.43	0.336	5.51	86.6

#4 P2

1.90	1.139	0.481	0.490	3.88	61-
1.86	1.05	0.43	0.37	5.03	79-

#5 P3

1.88	1.145	0.46	0.474	3.99	62.7
1.86	0.993	0.388	0.300	6.2	97.5
	1.05	0.41			

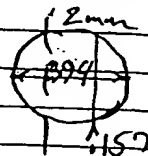
#1-5

Pellets showing oxygenation @ 600C for 66 hrs in O_2

0.394 inches

0.157 in for center cut

eOB ~ 2 mm



#1 P41 Pre 63.5%

Post 1.85 1.025 0.406 0.335 5.52 87

2/28 Property Pellet Summary (to date)

	cbic	11g	X	X	CO	REA#	
	#1	#2	#3	#4	#5		
oxygenated	975	(95)	95	(87)	(79)	97.5	R3
no furnace 2/28	'950 II'	(84)	(94)	—	—	(87)	R2
	950	87	Roane				R4
MICRO STRUCTURES	ORIG 950	91	'97'	71	78	92	Davis

950 II #1 & #5 pellets to temp @ 600C then 10C/min Ramp @ 6:15 pm
 > oxygenation RUN
 Out 10:00 A.M. 3/2 40 h O_2

$$5 \text{ cc} \times \frac{6.36 \text{ g}}{\text{cc}} = 31.8 \text{ g}$$

$$\frac{\pi (2.54)^2}{4} X = 5 \text{ cc}$$

$$5.07 \text{ cm}^2 X = 5 \text{ cc}$$

$$X = 5 \text{ cc} / 5.07 \text{ cm}^2$$

$$X \approx 1 \text{ cm} \text{ or } 1/2 \text{ inch} - 1 \text{ inch with sheepage}$$

4/24/89

#1 - Cu wt% Cu 28.7

wt% holes 36.0

Hole Concentration Conversion Formula:

Data: wt% Cu (total): 28.7

wt% holes: 36.0

$$\frac{\text{wt\% holes} - \text{wt\% Cu}_{\text{tot}}}{\text{Cu}_{\text{tot}}} = \frac{36 - 28.7}{28.7} = 0.254$$

average over
valence

∴ add Cu valence (2) = 2.25 = average valence Cu

$$2.25 (\text{Cu}_{\text{tot}}) = 2.25 (3) = 6.75 \text{ total Cu val}$$

↑
from sample
y. Ba₂Cu₃^{2.25}

$$+ 7.00 \text{ total Ba+Y val}$$

13.75

⑦

total charges

Take total charges & divide by two for O²⁻

$$13.75/2 = 6.88 \text{ O atoms} \Rightarrow \text{YBa}_2\text{Cu}_3\text{O}_{6.88}$$

2.25

see
page after
next

Notes to Kristy concerning Pellet Forming precalculations

To estimate pellet ^{weight} _{pack} for pellet pressing:

A. take dia & approx. height desired

1. calculate volume in cc. $(1.2 \frac{1.22^2}{4} \times 0.35 \times \pi) = 0.41 \text{ cc}$

B. Assume some reasonable 'green' density (unfired pressed pellet)

0.6-0.8 (60-80%) usual. for metals > 0.70 w/ small

ave. part. dias. (ie. 3mm).

$\frac{0.41 \text{ cc}}{0.8} \times 9.0 \frac{\text{g}}{\text{cc}} \approx 3 \text{ g of pack.}$ ← density theoretical

I pressed @ between 16,000 & 20,000 psi.

low side for pure metal ∴

$\frac{X}{(\text{dia})^2} = \text{desired pressure}$ where X = 1" scale pressure

$X \approx 4,000 \text{ for } 0.48" \text{ dia. die.}$

K-26

K-11

MODEL: RPP-500
PARTICLE ANALYZER
DATE: 3/1/89
SAMPLE: 150
SOLVENT: 150

• CONDITIONS
SOLV. VISC: 2.10 (CP)
SOLV. DENS: 0.7916 (G/CC)
SAMP. DENS: 2.61 (G/CC)
D(CHE): 10.0 (PH)
D(CHE): 0.10 (PH)
D(CHE): 1.00 (PH)
SPEED: 500 (RPM)

TIME: 13 MIN 27 SEC

DATA: 0.95

TIME: 0.5

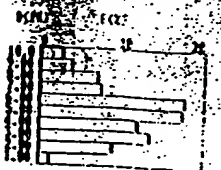


• DISTRIBUTION TABLE (BY VOL.)

D(CHE)	F(1)	F(2)
10.0-9.0	0.5	0.5
9.0-8.0	2.0	11.5
8.0-7.0	3.0	15.1
7.0-6.0	7.0	22.1
6.0-5.0	7.4	29.6
5.0-4.0	17.6	47.2
4.0-3.0	7.2	64.2
3.0-2.0	11.5	76.1
2.0-1.0	23.4	87.6
1.0-0.0	9.6	98.7
0.0-0.0	1.2	100.0

D(CHE): 4.84 (PH)

• DISTRIBUTION GRAPH (BY VOL.)



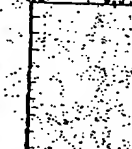
MODEL: RPP-500
PARTICLE ANALYZER
DATE: 3/14/89
SAMPLE: 150
SOLVENT: 150

• CONDITIONS
SOLV. VISC: 2.10 (CP)
SOLV. DENS: 0.7916 (G/CC)
SAMP. DENS: 3.97 (G/CC)
D(CHE): 10.0 (PH)
D(CHE): 0.10 (PH)
D(CHE): 1.00 (PH)
SPEED: 500 (RPM)

TIME: 8 MIN 7 MIN 36 SEC

DATA: 0.9

TIME: 0.5

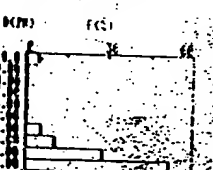


• DISTRIBUTION TABLE (BY VOL.)

D(CHE)	F(1)	F(2)
10.0-9.0	0.0	0.0
9.0-8.0	4.5	4.5
8.0-7.0	0.0	4.5
7.0-6.0	0.0	4.5
6.0-5.0	0.0	4.5
5.0-4.0	0.0	4.5
4.0-3.0	5.5	10.6
3.0-2.0	10.6	20.6
2.0-1.0	20.6	40.6
1.0-0.0	51.5	100.0

D(CHE): 0.97 (PH)

• DISTRIBUTION GRAPH (BY VOL.)



Analytical Results for C3 H_x/LD STUDY - H66



IBM
RESEARCH CENTER

ANALYTICAL
LABORATORY

Request for Analysis

Use Ball Point Pen

REQUESTOR <u>T. S. Piken</u>	PROJECT NO. _____	REQUEST NO. _____
DEPARTMENT _____	LOCATION _____	ROOM <u>25-225</u> PHONE _____
REQUESTOR'S SAMPLE IDENTIFICATION <u>H66x, LDox</u>		
APPROXIMATE COMPOSITION AND HISTORY OF SAMPLE <u>Yt₂O₃ Cu Oxide</u>		
ANALYSES REQUESTED _____		
ANALYSIS METHOD _____		
<u>Cu</u> ANALYTICAL RESULTS		
	<u>H66</u>	<u>LD</u>
<u>Wt% H66x</u>	<u>33.5</u>	<u>34.2</u>
<u>Wt% Cu</u>	<u>(23.5)</u>	<u>27.6</u>
<u>2.21</u>		<u>2.26</u>
<u>6.81</u>		<u>4.689</u>
<u>tot Cu = 3%</u>		
<u>4 Cu</u>		
<u>After Reox: H66x</u>	<u>28.7</u>	<u>Wt% Cu ← 2.86</u>
<u>pure @ 500C</u>	<u>36</u>	<u>h66x</u>
DATE SUBMITTED <u>5/1/07</u>	DATE REPORTED <u>5/24/07</u>	NOTES/REFERENCE <u>4/11/07 p. 121</u>
ANALYST <u>T. S. Piken</u>	APPROVED _____	

Nº

Notes to Kristy concerning ~~the~~ FORMING precalculations

To estimate pellet weight for pellet pressing:

A. take dia & approx. height desired

1. calculate volume in cc. (i.e. $\frac{(1.22 \text{ cm})^2 \times 0.35 \text{ cm} \times \pi}{4}$) = 0.41 cc

B. Assume some reasonable 'green' density (within pressed pellet)

0.6-0.8 (60-80%) usual for metals > 0.70 w/ small

ave. part. diam. (i.e. 3 μm).

$$\frac{0.41 \text{ cc}}{0.8} \times 9.0 \frac{\text{g}}{\text{cc}} \approx 3 \text{ g of powder}$$

(density theoretical)

I pressed @ between 16,000 & 20,000 psi.

low side for pure metal \therefore

$$\frac{X}{(dia)^2} = \text{desired pressure} \quad \text{where } X = 1'' \text{ scale pressure}$$

$$X \approx 4,000 \text{ for } 0.48'' \text{ dia. die.}$$

4/24/89

#1 - Cu wt% Cu 28.7

wt% holes 36.0

Hole Concentration Conversion Formula:

Data: wt% Cu (total): 28.7

wt% holes: 36.0

see
page after
next

$$\frac{\text{wt\% holes} - \text{wt\% Cu}_{\text{tot}}}{\text{Cu}_{\text{tot}}} = \frac{36 - 28.7}{28.7} = 0.254$$

average over
valence

 \therefore add Cu valence (2) = 2.25 = average valence Cu

$$2.25 (\text{Cu}_{\text{tot}}) = 2.25 (3) = 6.75 \text{ total Cu val}$$

↑
from sample
2.25

$$y. \text{Ba}_2 \text{Cu}_3$$

$$+ 7.00 \text{ total Ba+Y val}$$

$$\frac{13.75}{4} = 3.44$$

⑦

total charges

Take total charges / divide by two for O^{2-}

$$13.75 / 2 = 6.88 \text{ O atoms} \Rightarrow y \text{Ba}_2 \text{Cu}_3 \text{O}_{6.88}$$

2.25

Notes to Kristy concerning PELLE FORMING precalculations

To estimate pellet weight for pellet pressing:

A. take dia & apprx. height desired

$$1. \text{ calculate volume in cc. } \left(\frac{1.22 \text{ cm}^2 \times 0.35 \text{ cm} \times \pi}{4} \right) = 0.41 \text{ cc}$$

B. Assume some reasonable 'green' density (unfired pressed pellet)

0.6-0.8 (60-80%) usual. for metals > 0.70 or small

ave. part. diam. (ie. 3mm).

$$\left(0.41 \text{ cc} / 0.8 \right) \times 9.0 \frac{\text{g}}{\text{cc}} \approx 3 \text{ g of powder}$$

(density theoretical)

I pressed @ between 16,000 & 20,000 psi.

low side for pure metal \therefore

$$\frac{X}{(\text{dia})^2} = \text{desired pressure where } X = 1^{\text{st}} \text{ side pressure}$$

$$X \approx 4,000 \text{ for } 0.48'' \text{ dia. dia.}$$

DATE: 3/1/89
 PARTICLE ANALYZE:

 SOLV: 150
 SAMPLE: 150

• CONDITIONS

 SOLV. VISC: 2.10 (CP)
 SOLV. DENS: 0.79 (G/CC)
 SAMP. DENS: 2.61 (G/CC)
 D(CR): 10.0 (PH)
 D(CR): 0.10 (PH)
 D(CR): 1.00 (PH)
 SPEED: 500 (RPM)

TIME: 0 h 13 min 27 sec

DATE: 0.95

TIME: ABSORBANCE



• DISTRIBUTION TABLE (BY VOL.)

D(CR)	F(C)	D(C)
10.0-9.0	8.5	8.5
9.0-8.0	2.8	11.3
8.0-7.0	3.2	15.1
7.0-6.0	7.0	22.1
6.0-5.0	7.4	29.6
5.0-4.0	17.6	47.2
4.0-3.0	27.3	64.5
3.0-2.0	31.5	76.4
2.0-1.0	33.4	89.8
1.0-0.0	5.0	96.8
0.0-0.0	1.2	100.0

D(CR): 4.84 (PH)

• DISTRIBUTION GRAPH (BY VOL.)


 DATE: 3/1/89
 PARTICLE ANALYZE:

 SOLV: 150
 SAMPLE: 150

• CONDITIONS

 SOLV. VISC: 2.10 (CP)
 SOLV. DENS: 0.79 (G/CC)
 SAMP. DENS: 3.97 (G/CC)
 D(CR): 10.0 (PH)
 D(CR): 0.10 (PH)
 D(CR): 1.00 (PH)
 SPEED: 500 (RPM)

TIME: 0 h 7 min 36 sec

DATE: 0.9

TIME: ABSORBANCE

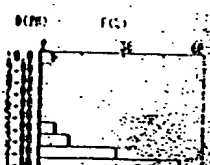


• DISTRIBUTION TABLE (BY VOL.)

D(CR)	F(C)	D(C)
10.0-9.0	0.0	0.0
9.0-8.0	4.5	4.5
8.0-7.0	0.0	4.5
7.0-6.0	0.0	4.5
6.0-5.0	0.0	4.5
5.0-4.0	0.0	4.5
4.0-3.0	5.5	10.0
3.0-2.0	10.5	20.5
2.0-1.0	20.0	40.5
1.0-0.0	51.5	100.0

D(CR): 0.52 (PH)

• DISTRIBUTION GRAPH (BY VOL.)



Analytical Results for C3 AL/LD STUDY - H6es

IBM

IBM
RESEARCH CENTER

ANALYTICAL
LABORATORY

Request for Analysis

Use Ball Point Pen

REQUESTOR <u>T. S. Hines</u>	PROJECT NO.	REQUEST NO.
DEPARTMENT	LOCATION	ROOM <u>25-220</u>
REQUESTOR'S SAMPLE IDENTIFICATION <u>H6es, LDex</u>		
APPROXIMATE COMPOSITION AND HISTORY OF SAMPLE <u>Y17.5% Cu Oxide</u>		
ANALYSES REQUESTED		
ANALYSIS METHOD		
ANALYTICAL RESULTS		
	H.D.	L.D.
<u>Wt% H6es</u>	<u>33.5</u>	<u>34.2</u>
<u>Wt% Cu</u>	<u>(27.5)</u>	<u>27.6</u>
<u>2.31</u>		<u>2.21</u>
<u>6.81</u>		<u>7.689</u>
$\frac{6.81}{2.31} = 2.95\%$		
<u>Aster. Perm: LDex 28.7</u> <u>Wt% Cu ← 2.56</u> <u>pure @ spec 36</u> <u>h6es</u>		
DATE LABORED <u>5/20/87</u>	DATE REPORTED <u>5/24/87</u>	NOTES/REFERENCE <u>1/11/84 p. 12</u>
ANALYST <u>T. S. Hines</u>	APPROVAL	

No

Recalculating Pre HD, LD values w/ 28.7% C_w

$$\text{HD holes } 33.5 \therefore \frac{33.5 - 28.7}{28.7} = 0.167$$

$$2 + 0.167 = 2.167 (3) = +6.50$$

$$\begin{array}{r} + 7 \\ \hline 13.50 / 2 = 6.75 \Rightarrow \text{y Ba}_2\text{Cu}_3 \text{ } ^{2.167} 0.675 \end{array}$$

$$\text{LD } \frac{34.2 - 28.7}{28.7} = 0.192 \quad 2.192 (3) = 6.58$$

$$\begin{array}{r} + 7 \\ \hline 13.58 / 2 = 6.79 \end{array}$$

$$\therefore \text{y Ba}_2\text{Cu}_3 \text{ } ^{2.192} 0.679$$

with original anal. C_w values

$$\text{HD } \frac{33.5 - 27.5}{27.5} = 0.22 \quad 2.22 (3) = 6.66 + 7 = 13.66 / 2 = 6.83$$

$$\text{LD } \frac{34.2 - 27.0}{27} = 0.27 \quad 2.27 (3) = 6.81 + 7 = 13.81 / 2 = 6.90(5)$$

$$\text{w/ ave. } 27.5 + 27 = 27.25$$

$$\text{LD } \frac{34.2 - 27.25}{27.25} = 0.25(5) \quad 2.255 (3) = 6.765 = 13.765 / 2 = 6.88$$

$$\text{HD } \frac{33.5 - 27.25}{27.25} = 0.23 \quad 2.23 (3) = 6.69 \text{ } \left(\text{ } \right) \text{ } ^{0.23} 6.845 \text{ } ^{0.23} \text{ } ^{0.23}$$

Composition #	Rel Pellet density (%) [*]	Actual Density ²	Green Rel S	Green act S
1	84 (90.8)	5.34	62.8 4.0	
2	98.8	5.95	61.5	3.90
3	71	4.52	60-	3.82
4	77.8	4.95	62	3.93
5	87 (91)	5.54	63.9 4.03	

* after 1h sinter @ 950C

BRIEF ATTACHMENT AM

IN THE UNITED STATES PATENT AND TRADEMARK OFFICE

In re Patent Application of

Applicants: Bednorz et al.

Serial No.: 08/479,810

Filed: June 7, 1995

For: NEW SUPERCONDUCTIVE COMPOUNDS HAVING HIGH TRANSITION
TEMPERATURE, METHODS FOR THEIR USE AND PREPARATION

Date: April 14, 2005

Docket: YO987-074BZ

Group Art Unit: 1751

Examiner: M. Kopec

Commissioner for Patents
P.O. Box 1450
Alexandria, VA 22313-1450

SIXTH SUPPLEMENTAL AMENDMENT

Sir:

In response to the Office Action dated July 28, 2004, please consider the
following:

RECEIPT

IN THE UNITED STATES PATENT AND TRADEMARK OFFICE

In re Patent Application of

Applicants: Bednorz et al.

Serial No.: 08/479,810

Filed: June 7, 1995

For: NEW SUPERCONDUCTIVE COMPOUNDS HAVING HIGH TRANSITION
TEMPERATURE, METHODS FOR THEIR USE AND PREPARATION



Date: April 14, 2005

Docket: YO987-074BZ

Group Art Unit: 1751

Examiner: M. Kopec

Commissioner for Patents
P.O. Box 1450
Alexandria, VA 22313-1450

AFFIDAVIT UNDER 37 C.F.R. 1.132

Sir:

I, Thomas M. Shaw, being duly sworn, do hereby depose and state:

1. I received a B. S. degree in Metallurgy from the University of Liverpool, Liverpool, England and a M. S. and a Ph.D. degree in Material Science (1981) from the University of California, Berkeley.

2. I refer to Attachments A to Z and AA herein which were submitted in a separate paper designated as "FIRST SUPPLEMENTAL AMENDMENT" in response to the Office Action dated July 28, 2004. I also refer to Attachments AB to AG which were submitted in a separate paper designated as "THIRD SUPPLEMENTAL AMENDMENT" in response to the Office Action dated July 28, 2004.

3. I have worked as a postdoctoral researcher in the Material Science Department of Cornell University from 1981-1982. I have worked at Rockwell International Science Center in Thousand Oaks, California from 1982-1984 as a ceramic scientist. I have worked as a research staff member in Ceramics Science at the Thomas J. Watson Research Center of the International Business Machines Corporation in Yorktown Heights, New York from 1984 to the present.

IBM
YORKTOWN
2005 APR 20 PM 2:29
INTELLECTUAL PROPERTY
LAW DEPT.

IN THE UNITED STATES PATENT AND TRADEMARK OFFICE

In re Patent Application of

Applicants: Bednorz et al.

Serial No.: 08/479,810

Filed: June 7, 1995

Date: April 14, 2005

Docket: YO987-074BZ

Group Art Unit: 1751

Examiner: M. Kopec

For: **NEW SUPERCONDUCTIVE COMPOUNDS HAVING HIGH TRANSITION
TEMPERATURE, METHODS FOR THEIR USE AND PREPARATION**

Commissioner for Patents
P.O. Box 1450
Alexandria, VA 22313-1450

AFFIDAVIT UNDER 37 C.F.R. 1.132

Sir:

I, Thomas M. Shaw, being duly sworn, do hereby depose and state:

1. I received a B. S. degree in Metallurgy from the University of Liverpool, Liverpool, England and a M. S. and a Ph.D. degree in Material Science (1981) from the University of California, Berkeley.
2. I refer to Attachments A to Z and AA herein which were submitted in a separate paper designated as "FIRST SUPPLEMENTAL AMENDMENT" in response to the Office Action dated July 28, 2004. I also refer to Attachments AB to AG which were submitted in a separate paper designated as "THIRD SUPPLEMENTAL AMENDMENT" in response to the Office Action dated July 28, 2004.
3. I have worked as a postdoctoral researcher in the Material Science Department of Cornell University from 1981-1982. I have worked at Rockwell International Science Center in Thousand Oaks, California from 1982-1984 as a ceramic scientist. I have worked as a research staff member in Ceramics Science at the Thomas J. Watson Research Center of the International Business Machines Corporation in Yorktown Heights, New York from 1984 to the present.

4. I have worked in the fabrication of and characterization of ceramic materials of various types, including superconductors and related materials from 1984 to the present.

5. My resume and list of publications is in Attachment 1 included with this affidavit.

6. This affidavit is in addition to my affidavit dated December 15, 1998. I have reviewed the above-identified patent application (Bednorz-Mueller application) and acknowledge that it represents the work of Bednorz and Mueller, which is generally recognized as the first discovery of superconductivity in a material having a $T_c \geq 26^\circ\text{K}$ and that subsequent developments in this field have been based on this work.

7. All the high temperature superconductors which have been developed based on the work of Bednorz and Mueller behave in a similar manner, conduct current in a similar manner, have similar magnetic properties, and have similar structural properties.

8. Once a person of skill in the art knows of a specific type of composition described in the Bednorz-Mueller application which is superconducting at greater than or equal to 26°K , such a person of skill in the art, using the techniques described in the Bednorz-Mueller application, which includes all principles of ceramic fabrication known at the time the application was initially filed, can make the compositions encompassed by the claims of the Bednorz-Mueller application, without undue experimentation or without requiring ingenuity beyond that expected of a person of skill in the art of the fabrication of ceramic materials. This is why the work of Bednorz and Mueller was reproduced so quickly after their discovery and why so much additional work was done in this field within a short period after their discovery. Bednorz and Mueller's discovery was first reported in Z. Phys. B 64 page 189-193 (1996).

9. The techniques for placing a superconductive composition into a superconducting state have been known since the discovery of superconductivity in 1911 by Kamerlingh-Onnes.

10. Prior to 1986 a person having a bachelor's degree in an engineering discipline, applied science, chemistry, physics or a related discipline could have been trained within one year to reliably test a material for the presence of superconductivity and to flow a superconductive current in a superconductive composition.

11. Prior to 1986 a person of ordinary skill in the art of fabricating a composition according to the teaching of the Bednorz-Mueller application would have: a) a Ph.D. degree in solid state chemistry, applied physics, material science, metallurgy, physics or a related discipline and have done thesis research including work in the fabrication of ceramic materials; or b) have a Ph.D. degree in these same fields having done experimental thesis research plus one to two years post Ph.D. work in the fabrication of ceramic materials; or c) have a master's degree in these same fields and have had five years of materials experience at least some of which is in the fabrication of ceramic materials. Such a person is referred to herein as a person of ordinary skill in the ceramic fabrication art.

12. The general principles of ceramic science referred to by Bednorz and Mueller in their patent application and known to a person of ordinary skill in the ceramic fabrication art can be found in many books and articles published before their discovery, priority date (date of filing of their European Patent Office patent application EPO 0275343A1, January 23, 1987) and initial US Application filing date (May 22, 1987). An exemplary list of books describing the general principles of ceramic fabrication are:

a) Introduction to Ceramics, Kingery et al., Second Edition, John Wiley & Sons, 1976, in particular pages 5-20, 269-319, 381-447 and 448-513, a copy of which is in Attachment B.

b) Polar Dielectrics and Their Applications, Burfoot et al., University of California Press, 1979, in particular pages 13-33, a copy of which is in Attachment C.

- c) Ceramic Processing Before Firing, Onoda et al., John Wiley & Sons, 1978, the entire book, a copy of which is in Attachment D.
- d) Structure, Properties and Preparation of Perovskite-Type Compounds, F. S. Galasso, Pergamon Press, 1969, in particular pages 159-186, a copy of which is in Attachment E.

These references were previously submitted with the Affidavit of Thomas Shaw submitted December 15, 1998.

13. An exemplary list of articles applying the general principles of ceramic fabrication to the types of materials described in Applicants' specification are:

- a) Oxygen Defect K_2NiF_4 - Type Oxides: The Compounds $La_{2-x}Sr_xCuO_{4-x/2+}$, Nguyen et al., Journal of Solid State Chemistry 39, 120-127 (1981). See Attachment F.
- b) The Oxygen Defect Perovskite $BaLa_4Cu_5O_{13.4}$, A Metallic (This is referred to in the Bednorz-Mueller application at page 21, lines 1-2) Conductor, C. Michel et al., Mat. Res. Bull., Vol. 20, pp. 667-671, 1985. See Attachment G.
- c) Oxygen Intercalation in Mixed Valence Copper Oxides Related to the Perovskite, C. Michel et al., Revue de Chemie Minerale, 21, p. 407, 1984. (This is referred to in the Bednorz-Mueller application at page 27, lines 1-2). See Attachment H.
- d) Thermal Behaviour of Compositions in the Systems $x BaTiO_3 + (1-x) Ba(Ln_{0.5}B_{0.5})O_3$, V.S. Chincholkar et al., Therm. Anal. 6th, Vol. 2., p. 251-6, 1980. See Attachment I.

14. The Bednorz-Mueller application in the paragraph bridging pages 6 and 7 states in regard to the high T_c materials:

These compositions can carry supercurrents (i.e., electrical currents in a substantially zero resistance state of the composition) at temperatures greater than 26°K. In general, the compositions are characterized as mixed transition metal oxide systems where the transition metal oxide can exhibit multivalent behavior. These compositions have a layer-type crystalline structure, often perovskite-like, and can contain a rare earth or rare earth-like element. A rare earth-like element (sometimes termed a near rare earth element is one whose properties make it essentially a rare earth element. An example is a group IIIB element of the periodic table, such as La. Substitutions can be found in the rare earth (or rare earth-like) site or in the transition metal sites of the compositions. For example, the rare earth site can also include alkaline earth elements selected from group IIA of the periodic table, or a combination of rare earth or rare earth-like elements and alkaline earth elements. Examples of suitable alkaline earths include Ca, Sr, and Ba. The transition metal site can include a transition metal exhibiting mixed valent behavior, and can include more than one transition metal. A particularly good example of a suitable transition metal is copper. As will be apparent later, Cu-oxide based systems provide unique and excellent properties as high T_c superconductors. An example of a superconductive composition having high T_c is the composition represented by the formula RE-TM-O, where RE is a rare earth or rare earth-like element, TM is a nonmagnetic transition metal, and O is oxygen. Examples of transition metal elements include Cu, Ni, Cr etc. In particular, transition metals that can exhibit multi-valent states are very suitable. The rare earth elements are typically elements 58-71 of the periodic table, including Ce, Nd, etc.

15. In the passage quoted in paragraph 14 the general formula is RE-TM-O "where RE is a rare earth or rare earth-like element, TM is a nonmagnetic transition metal, and O is oxygen." This paragraph states "Substitutions can be found in the rare earth (or rare earth-like) site or in the transition metal sites of the compositions. For example, the rare earth site can also include alkaline earth elements selected from group IIA of the periodic table, or a combination of rare earth or rare earth-like elements and alkaline earth elements." Thus applicants teach that RE can be something other than an rare earth. For example, it can be an alkaline earth, but is not limited to a alkaline earth element. It can be an element that has the same effect as an alkaline earth or rare-earth element, that is a rare earth like element. Also, this passage teaches that TM can be substituted with another element, for example, but not limited to, a rare earth, alkaline earth or some other element that acts in place of the transition metal.

16. The following table is compiled from the Table 1 of the Article by Rao (See Attachment AB) and the Table of high T_c materials from the "CRC Handbook of Chemistry and Physics" 2000-2001 Edition (See Attachment AC). An asterisk in column 5 indicated that the composition of column 2 does not come within the scope of the claims allowed in the Office Action of July 28, 2004.

17. I have reviewed the Office Action dated July 28, 2004, which states at page 6 "The present specification is deemed to be enabled only for compositions comprising a transition metal oxide containing at least a) an alkaline earth element and b) a rare-earth element of Group IIIB element." I disagree for the reasons given herein.

18. Composite Table

1	2	3	4	5	6	7
#	MATERIAL	RAO ARTICLE	HANDBOOK OF CHEM & PHYSICS		ALKALINE EARTH ELEMENT	RARE EARTH ELEMENT
1	$\text{La}_2\text{CuO}_{4+\delta}$	√	√	*	N	Y
2	$\text{La}_{2-x}\text{Sr}_x(\text{Ba}_x)\text{CuO}_4$	√	√		Y	Y
3	$\text{La}_2\text{Ca}_{1-x}\text{Sr}_x\text{Cu}_2\text{O}_6$	√	√		Y	Y

4	YBa ₂ Cu ₃ O ₇	√	√		Y	Y
5	YBa ₂ Cu ₄ O ₈	√	√		Y	Y
6	Y ₂ Ba ₄ Cu ₇ O ₁₅	√	√		Y	Y
7	Bi ₂ Sr ₂ CuO ₆	√	√	*	Y	N
8	Bi ₂ CaSr ₂ Cu ₂ O ₈	√	√	*	Y	N
9	Bi ₂ Ca ₂ Sr ₂ Cu ₃ O ₁₀	√	√	*	Y	N
10	Bi ₂ Sr ₂ (Ln _{1-x} Ce _x) ₂ Cu ₂ O ₁₀	√	√		Y	Y
11	Tl ₂ Ba ₂ CuO ₆	√	√	*	Y	N
12	Tl ₂ CaBa ₂ Cu ₂ O ₈	√	√	*	Y	N
13	Tl ₂ Ca ₂ Ba ₂ Cu ₃ O ₁₀	√	√	*	Y	N
14	Tl(BaLa)CuO ₅	√	√		Y	Y
15	Tl(SrLa)CuO ₅	√	√		Y	Y
16	(Tl _{0.5} Pb _{0.5})Sr ₂ CuO ₅	√	√	*	Y	N
17	TlCaBa ₂ Cu ₂ O ₇	√	√	*	Y	N
18	(Tl _{0.5} Pb _{0.5})CaSr ₂ Cu ₂ O ₇	√	√	*	Y	N
19	TlSr ₂ Y _{0.5} Ca _{0.5} Cu ₂ O ₇	√	√		Y	Y
20	TlCa ₂ Ba ₂ Cu ₃ O ₈	√	√	*	Y	N
21	(Tl _{0.5} Pb _{0.5})Sr ₂ Ca ₂ Cu ₃ O ₉	√	√	*	Y	N
22	TlBa ₂ (Ln _{1-x} Ce _x) ₂ Cu ₂ O ₉	√	√		Y	Y
23	Pb ₂ Sr ₂ Ln _{0.5} Ca _{0.5} Cu ₃ O ₈	√	√		Y	Y
24	Pb ₂ (Sr,La) ₂ Cu ₂ O ₆	√	√		Y	Y
25	(Pb,Cu)Sr ₂ (Ln,Ca)Cu ₂ O ₇	√	√		Y	Y
26	(Pb,Cu)(Sr,Eu)(Eu,Ce)Cu ₂ O _x	√	√		Y	Y
27	Nd _{2-x} Ce _x CuO ₄	√	√	*	N	Y
28	Ca _{1-x} Nd _x CuO ₂	√			Y	Y
29	Sr _{1-x} Nd _x CuO ₂	√	√		Y	Y
30	Ca _{1-x} Sr _x CuO ₂		√	*	Y	N
31	Ba _{0.6} K _{0.4} BiO ₃		√	*	Y	N
32	Rb ₂ C ₅ C ₆₀		√	*	N	Y
33	NdBa ₂ Cu ₃ O ₇		√		Y	Y
34	SmBaSrCuO ₇		√		Y	Y
35	EuBaSrCu ₃ O ₇		√		Y	Y
36	BaSrCu ₃ O ₇		√	*	Y	N
37	DyBaSrCu ₃ O ₇		√		Y	Y
38	HuBaSrCu ₃ O ₇		√		Y	Y
39	ErBaSrCu ₃ O ₇ (Multiphase)		√		Y	Y
40	TmBaSrCu ₃ O ₇ (Multiphase)		√		Y	Y

41	YBaSrCu ₃ O ₇		√	*	Y	Y
42	HgBa ₂ CuO ₂		√	*	Y	N
43	HgBa ₂ CaCu ₂ O ₆ (annealed in O ₂)		√	*	Y	N
44	HgBa ₂ Ca ₂ Cu ₃ O ₈		√	*	Y	N
45	HgBa ₂ Ca ₃ Cu ₄ O ₁₀		√	*	Y	N

19. The first composition, La₂ Cu O_{4+δ}, has the form RE₂CuO₄ which is explicitly taught by Bednorz and Mueller. The δ indicates that there is a nonstoichiometric amount of oxygen.

20. The Bednorz-Mueller application teaches at page 11, line 19 to page 12, line 7:

An example of a superconductive compound having a layer-type structure in accordance with the present invention is an oxide of the general composition RE₂TMO₄ where RE stands for the rare earths (lanthanides) or rare earth-like elements and TM stands for a transition metal. In these compounds the RE portion can be partially substituted by one or more members of the alkaline earth group of elements. In these particular compounds, the oxygen content is at a deficit. For example, one such compound that meets this general description is lanthanum copper oxide La₂CuO₄...

21. The Bednorz-Mueller application at page 15, last paragraph states "Despite their metallic character, the Ba-La-Cu-O type materials are essentially ceramics, as are other compounds of the RE₂ TMO₄ type, and their manufacture generally follows known principles of ceramic fabrication."

22. Compound number 27 of the composite table contains Nd and Ce, both rare earth elements. All of the other compounds of the composite table, except for number 32, have O and one of the alkaline earth elements which as stated above is explicitly taught by applicants. Compound 31 is a BiO_3 compound in which TM is substituted by another element, here Bi, as explicitly taught by Applicants in the paragraph quoted above.

23. The rare earth elements are Sc, Y, La, Ce, Pr, Nd, Pm, Sm, Eu, Gd, Tb, Dy, Ho, Er, Tm, Yb, and Lu. See the Handbook of Chemistry and Physics 59th edition 1978-1979 page B262 in Appendix A. The transition elements are identified in the periodic table from the inside front cover of the Handbook of Chemistry and Physics in Appendix A.

24. The basic theory of superconductivity has been known many years before Applicants' discovery. For example, see the book "Theory of Superconductivity", M. von Laue, Academic Press, Inc., 1952 (See Attachment AD).

25. In the composite table, compound numbers 7 to 10 and 31 are Bismuth (Bi) compounds. Compound number 12 to 22 are Thallium (Tl) compounds. Compound numbers 23 to 26 are lead (Pb) compounds. Compounds 42 to 45 are Mercury (Hg) compounds. Those compounds that do not come within the scope of an allowed claims (the compounds which are not marked with an asterisk in column 3 of the composite table) are primarily the Bi, Tl, Pb and Hg compounds. These compounds are made according to the principles of ceramic science known prior to applicant's filing date. For example, Attachments J, K, L, and M contain the following articles:

Attachment J - Phys. Rev. B. Vol. 38, No. 16, p. 6531 (1988) is directed to Thallium compounds.

Attachment K - Jap. Joun. of Appl. Phys., Vol. 27, No. 2, p. L209-L210 (1988) is directed to Bismuth (Bi) compounds.

Attachment L - Letter to Nature, Vol. 38, No. 2, p. 226 (18 March 1993) is directed to Mercury (Hg) compounds.

Attachment M - Nature, Vol. 336, p. 211 (17 November 1988) is directed to Lead (Pb) based compounds.

26. The article of Attachment J (directed to Tl compounds) states at page 6531, left column:

The samples were prepared by thoroughly mixing suitable amounts of Tl_2O_3 , CaO, BaO_2 , and CuO, and forming a pellet of this mixture under pressure. The pellet was then wrapped in gold foil, sealed in quartz tube containing slightly less than 1 atm of oxygen, and baked for approximately 3 h at $\approx 880^\circ C$.

This is according to the general principles of ceramic science known prior to applicant's priority date.

27. The article of Attachment K (directed to Bi compounds) states at page L209:

The Bi-Sr-Ca-Cu-O oxide samples were prepared from powder reagents of Bi_2O_3 , $SrCO_3$, $CaCO_3$ and CuO. The appropriate amounts of powders were mixed, calcined at $800-870^\circ C$ for 5 h, thoroughly reground and then cold-pressed into disk-shape pellets (20 mm in diameter and 2 mm in thickness) at a pressure of 2 ton.cm^2 . Most of the pellets were sintered at about $870^\circ C$ in air or in an oxygen atmosphere and then furnace-cooled to room temperature.

This is according to the general principles of ceramic science known prior to applicant's priority date.

28. The article of Attachment L (directed to Hg compounds) states at page 226:

The samples were prepared by solid state reaction between stoichiometric mixtures of $\text{Ba}_2\text{CuO}_{3+\delta}$ and yellow HgO (98% purity, Aldrich). The precursor $\text{Ba}_2\text{CuO}_{3+\delta}$ was obtained by the same type of reaction between BaO_2 (95% purity, Aldrich) and CuO (NormalPur, Prolabo) at 930°C in oxygen, according to the procedure described by De Leeuw et al.⁶. The powders were ground in an agate mortar and placed in silica tubes. All these operations were carried out in a dry box. After evacuation, the tubes were sealed, placed in steel containers, as described in ref. 3, and heated for 5 h to reach ~800°C. The samples were then cooled in the furnace, reaching room temperature after ~10 h.

This is according to the general principles of ceramic science known prior to applicant's priority date.

29. The article of Attachment M (directed to Pb compounds) states at page 211, left column:

The preparative conditions for the new materials are considerably more stringent than for the previously known copper-based superconductors. Direct synthesis of members of this family by reaction of the component metal oxides or carbonates in air or oxygen at temperatures below 900°C is not possible because of the stability of the oxidized SrPbO_3 -based perovskite. Successful synthesis is accomplished by the reaction of PbO with pre-reacted (Sr, Ca, Ln) oxide precursors. The precursors are prepared from oxides and carbonates in the appropriate metal ratios, calcined for 16 hours (in dense Al_2O_3 crucibles) at 920-980°C in air with one intermediate grinding.

This is according to the principles of ceramic science known prior to applicant's priority date.

30. A person of ordinary skill in the art of the fabrication of ceramic materials would be motivated by the teaching of the Bednorz-Mueller application to investigate compositions for high superconductivity other than the compositions specifically fabricated by Bednorz and Mueller.

31. In Attachment U, there is a list of perovskite materials from pages 191 to 207 in the book "Structure, Properties and Preparation of Perovskite-Type Compounds" by F. S. Galasso, published in 1969, which is Attachment E hereto. This list contains about 300 compounds. Thus, what the term "Perovskite-type" means and how to make these compounds was well known to a person of ordinary skill in the art in 1969, more than 17 years before the Applicants' priority date (January 23, 1987).

This is clear evidence that a person of skill in the art of fabrication of ceramic materials knows (prior to Applicants' priority date) how to make the types of materials in Table 1 of the Rao Article and the Table from the Handbook of Chemistry and Physics as listed in the composite table above in paragraph 17.

32. The standard reference "Landholt-Börnstein", Volumn 4, "Magnetic and Other Properties of Oxides and Related Compounds Part A" (1970) lists at page 148 to 206 Perovskite and Perovskite-related structures. (See Attachment N). Section 3.2 starting at page 190 is entitled "Descriptions of perovskite-related structures". The German title is "Perowskit-ähnliche Strukturen". The German word "ähnliche" can be translated in English as "like". The Langenscheidt's German-English, English-German Dictionary 1970, at page 446 translates the English "like" as the German "ähnliche". (See Attachment O). Pages 126 to 147 of Attachment N describes "crystallographic and magnetic properties of perovskite and perovskite-related compounds", see title of Section 3 at page 126. Section 3.2.3.1 starting at page 192 of "Landholt-Börnstein" Vol. 4 (See Attachment N) is entitled "Bismuth Compounds". Thus Bismuth

perovskite-like compounds and how to make them were well known more than 16 years prior to Applicants' priority date. Thus the "Landholt Börnstein" book published in 1970, more than 16 years before Applicants' priority date (January 23, 1987), shows that the term "perovskite-like" or "perovskite related" is understood by persons of skill in the art prior to Applicants' priority date. Moreover, the "Landholt-Börnstein" book cites references for each compound listed. Thus a person of ordinary skill in the art of ceramic fabrication knows how to make each of these compounds. Pages 376-380 of Attachment N has figures showing the crystal structure of compounds containing Bi and Pb.

33. The standard reference "Landholt-Börnstein, Volume 3, Ferro- and Antiferroelectric Substances" (1969) provides at pages 571-584 an index to substances. (See Attachment P). This list contains numerous Bi and Pb containing compounds. See, for example pages 578 and 582-584. Thus a person of ordinary skill in the art of ceramic fabrication would be motivated by Applicants' application to fabricate Bi and/or Pb containing compounds that come within the scope of the Applicants' claims.

34. The standard reference "Landholt-Börnstein Volume 3 Ferro- and Antiferroelectric Substances" (1969) (See Attachment P) at page 37, section 1 is entitled "Perovskite-type oxides." This standard reference was published more than 17 years before Applicants' priority date (January 23, 1987). The properties of perovskite-type oxides are listed from pages 37 to 88. Thus the term perovskite-type was well known and understood by persons of skill in the art of ceramic fabrication prior to Applicants' priority date and more than 17 years before Applicants' priority date persons of ordinary skill in the art knew how to make Bi, Pb and many other perovskite, perovskite-like, perovskite-related and perovskite-type compounds.

35. At page 14, line 10-15 of the Bednorz-Mueller application, Applicants' state "samples in the Ba-La-Cu-O system, when subjected to x-ray analysis, revealed three individual crystallographic phases V.12. a first layer-type perovskite-like phase, related to the K_2NiF_4 structure ..." Applicants' priority document EP0275343A1 filed July 27, 1988, is entitled "New Superconductive Compounds of the K_2NiF_4 Structural Type Having a High Transition Temperature, and Method for Fabricating Same." See (See Attachment AE). The book "Structure and Properties of Inorganic Solids" by Francis S. Galasso, Pergamon Press (1969) at page 190 lists examples of Thallium (Tl) compounds in the K_2NiF_4 structure. (See Attachment Q). Thus based on Applicants' teachings prior to Applicants' priority date, a person of ordinary skill in the art of ceramic fabrication would be motivated to fabricate Thallium based compounds to test for high T_c superconductivity.

36. The book "Crystal Structures" Volume 4, by Ralph W. G. Wyckoff, Interscience Publishers, 1960 states at page 96 "This structure, like these of $Bi_4Ti_2O_{12}$ (IX, F_{12}) and Ba $Bi_4Ti_4O_4$ (XI, 13) is built up of alternating Bi_2O_2 and perovskite-like layers." Thus layer of perovskite-like Bismuth compounds was well known in the art in 1960 more than 26 years before Applicants' priority date. (See Attachment R).

37. The book "Modern Oxide Materials Preparation, Properties and Device Applications" edited by Cockayne and Jones, Academic Press (1972) states (See Attachment S) at page 155 under the heading "Layer Structure Oxides and Complex Compounds":

"A large number of layer structure compounds of general formula $(Bi_2O_2)^{2+}(A_{x-1}B_xO_{3x+1})^{2-}$ have been reported (Smolenskii et al. 1961; Subbarao, 1962), where A = Ca, Sr, Ba, Pb, etc., B = Ti, Nb, Ta and x = 2, 3, 4, or 5. The structure had been previously investigated by Aurivillius (1949) who described them in terms of Alternate $(Bi_2O_2)^{2+}$ layers and perovskite layers of oxygen octahedra. Few have been found to be ferroelectric and include $SrBi_2Ta_2O_9$ ($T_c = 583^\circ K$), $PbBi_2Ta_2O_9$ ($T_c = 703^\circ K$), $BiBi_3Ti_2TiO_{12}$ or

$\text{Bi}_4\text{Ti}_3\text{O}_{12}$ ($T_c = 948^\circ\text{K}$), $\text{Ba}_2\text{Bi}_4\text{Ti}_5\text{O}_{18}$ ($T_c = 598^\circ\text{K}$) and $\text{Pb}_2\text{Bi}_4\text{Ti}_5\text{O}_{18}$ ($T_c = 583^\circ\text{K}$). Only bismuth titanate $\text{Bi}_4\text{Ti}_3\text{O}_{12}$ has been investigated in detail in the single crystal form and is finding applications in optical stores (Cummins, 1967) because of its unique ferroelectric-optical switching properties. The ceramics of other members have some interest because of their dielectric properties. More complex compounds and solid solutions are realizable in these layer structure oxides but none have significant practical application."

Thus the term layered oxides was well known and understood prior to Applicants' priority date. Moreover, layered Bi and Pb compounds were well known in 1972 more than 15 years before Applicants' priority date.

38. The standard reference "Landolt-Börnstein, Volume 3, Ferro and Antiferroelectric Substances" (1969) at pages 107 to 114 (See Attachment T) list "layer-structure oxides" and their properties. Thus the term "layered compounds" was well known in the art of ceramic fabrication in 1969 more than 16 years prior to Applicants' priority date and how to make layered compounds was well known prior to applicants priority date.

39. Layer perovskite type Bi and Pb compounds closely related to the Bi and Pb high T_c compounds in the composite table above in paragraph 17 have been known for some time. For example, the following is a list of four articles which were published about 35 years prior to Applicants' first publication date:

(1) Attachment V - "Mixed bismuth oxides with layer lattices", B. Aurivillius, Arkiv Kemi 1, 463, (1950).

(2) Attachment W - "Mixed bismuth oxides with layered lattices ", B. Aurivillius, Arkiv Kemi 1, 499, (1950).

(3) Attachment X - "Mixed bismuth oxides with layered lattices ", B. Aurivillius, Arkiv Kemi 2, 519, (1951).

(4) Attachment Y - "The structure of $\text{Bi}_2\text{NbO}_5\text{F}$ and isomorphous compounds", B. Aurivillius, Arkiv Kemi 5, 39, (1952).

These articles will be referred to as Aurivillius 1, 2, 3 and 4, respectively.

40. Attachment V (Aurivillius 1), at page 463, the first page, has the subtitle "I. The structure type of $\text{CaNb}_2\text{Bi}_2\text{O}_9$. Attachment V states at page 463:

X-ray analysis ... seemed to show that the structure was built up of $\text{Bi}_2\text{O}_2^{2+}$ layers parallel to the basal plane and sheets of composition $\text{Bi}_2\text{Ti}_3\text{O}_{10}^-$. The atomic arrangement within the $\text{Bi}_2\text{Ti}_3\text{O}_{10}^-$ sheets seemed to be the same as in structure of the perovskite type and the structure could then be described as consisting of $\text{Bi}_2\text{O}_2^{2+}$ layers between which double perovskite layers are inserted.

41. Attachment V (Aurivillius 1) at page 464 has a section entitled " $\text{PbBi}_2\text{Nb}_2\text{O}_9$ Phase". And at page 471 has a section entitled " $\text{Bi}_3\text{NbTiO}_9$ ". And at page 475 has a table of compounds having the " $\text{CaBi}_2\text{Nb}_2\text{O}_9$ structure" listing the following compounds $\text{Bi}_3\text{NbTiO}_9$, $\text{Bi}_3\text{TaTiO}_9$, $\text{CaBi}_2\text{Nb}_2\text{O}_9$, $\text{SrBi}_2\text{Nb}_2\text{O}_9$, $\text{SrBi}_2\text{Ta}_2\text{O}_9$, $\text{BaBi}_2\text{Nb}_2\text{O}_9$, $\text{PbBi}_2\text{Nb}_2\text{O}_9$, $\text{NaBi}_5\text{Nb}_4\text{O}_{18}$, $\text{KBi}_5\text{Nb}_4\text{O}_{18}$. Thus Bi and Pb layered perovskite compounds were well known in the art about 35 years prior to Applicants' priority date.

42. Attachment W (Aurivillius 2) at page 499, the first page, has the subtitle "II Structure of $\text{Bi}_4\text{Ti}_3\text{O}_{12}$ ". And at page 510, Fig. 4 shows a crystal structure in which "A denotes a perovskite layer $\text{Bi}_2\text{Ti}_3\text{O}_{10}^-$, C $\text{Bi}_2\text{O}_2^{2+}$ layers and B unit cells of the hypothetical perovskite structure BiTiO_3 .

43. Attachment X (Aurivillius 3) has at page 519, the first page, the subtitle "III Structure of $\text{BaBi}_4\text{Ti}_4\text{O}_{15}$ ". And in the first paragraph on page 519 states referring to the articles of Attachments V (Aurivillius 1), and W (Aurivillius 2) "X ray studies on the compounds $\text{CaBi}_2\text{Nb}_2\text{O}_9$ [the article of Attachment V] and $\text{Bi}_4\text{Ti}_3\text{O}_{12}$ [the article of Attachment W] have shown that the comparatively complicated chemical formulae of these compounds can be explained by simple layer structures being built up from $\text{Bi}_2\text{O}_2^{2+}$ layers and perovskite layers. The unit cells are pictured schematically in Figs. 1a and 1c." And Fig. 4 at page 526 shows "One half of a unit cell of $\text{BaBi}_4\text{Ti}_4\text{O}_{15}$. A denotes the perovskite region and B the Me_2O_4 layer" where Me represents a metal atom.

44. Attachment Y (Aurivillius 4) is direct to structures having the $\text{Bi}_3\text{N}_{10}\text{O}_3\text{F}$ structure.

45. Attachment AA is a list of Hg containing solid state compounds from the 1989 Powder Diffraction File Index. Applicants do not have available to them an index from prior to Applicants' priority date. The Powder Diffraction File list is a compilation of all known solid state compounds with reference to articles directed to the properties of these compositions and the methods of fabrication. From Attachment AA it can be seen, for example, that there are numerous examples of Hg based compounds. Similarly, there are examples of other compounds in the Powder Diffraction File. A person of ordinary skill in the art is aware of the Powder Diffraction File and can from this file find a reference providing details on how to fabricate these compounds. Thus persons of ordinary skill in the art would be motivated by Applicants' teaching to look to the Powder Diffraction File for examples of previously fabricated composition expected to have properties similar to those described in Applicants' teaching.

46. It is generally recognized that it is not difficult to fabricate transition metal oxides and in particular copper metal oxides that are superconductive after the discovery by Applicants of composition, such as transition metal oxides, that are high T_c superconductors. This is noted in the book "Copper Oxide Superconductors" by Charles P. Poole, Jr., Timir Datta and Horacio A. Farach, John Wiley & Sons (1998),

referred to herein as Poole 1988: Chapter 5 of Poole 1988 (See Attachment AF) in the book entitled "Preparation and Characterization of Samples" states at page 59 "[c]opper oxide superconductors with a purity sufficient to exhibit zero resistivity or to demonstrate levitation (Early) are not difficult to synthesize. We believe that this is at least partially responsible for the explosive worldwide growth in these materials". Poole 1988 further states at page 61 "[i]n this section three methods of preparation will be described, namely, the solid state, the coprecipitation, and the sol-gel techniques (Hatfi). The widely used solid-state technique permits off-the-shelf chemicals to be directly calcined into superconductors, and it requires little familiarity with the subtle physicochemical process involved in the transformation of a mixture of compounds into a superconductor." Poole 1988 further states at pages 61-62 "[i]n the solid state reaction technique one starts with oxygen-rich compounds of the desired components such as oxides, nitrates or carbonates of Ba, Bi, La, Sr, Ti, Y or other elements. ... These compounds are mixed in the desired atomic ratios and ground to a fine powder to facilitate the calcination process. Then these room-temperature-stable salts are reacted by calcination for an extended period (~20hr) at elevated temperatures (~900°C). This process may be repeated several times, with pulverizing and mixing of the partially calcined material at each step." This is generally the same as the specific examples provided by Applicants and as generally described at pages 8, line 19, to page 9, line 5, of the Bednorz-Mueller application which states "[t]he methods by which these superconductive compositions can be made can use known principals of ceramic fabrication, including the mixing of powders containing the rare earth or rare earth-like, alkaline earth, and transition metal elements, coprecipitation of these materials, and heating steps in oxygen or air. A particularly suitable superconducting material in accordance with this invention is one containing copper as the transition metal." Consequently, it is my opinion that Applicants have fully enabled high T_c materials oxides and their claims.

47. Charles Poole et al. published another book in 1995 entitled "Superconductivity" Academic Press which has a Chapter 7 on "Perovskite and Cuprate Crystallographic Structures". (See Attachment Z). This book will be referred to as Poole 1995.

At page 179 of Poole 1995 states:

V. PEROVSKITE-TYPE SUPERCONDUCTING STRUCTURES

In their first report on high-temperature superconductors Bednorz and Müller (1986) referred to their samples as "metallic, oxygen-deficient ... perovskite-like mixed-valence copper compounds." Subsequent work has confirmed that the new superconductors do indeed possess these characteristics.

I agree with this statement.

48. The book "The New Superconductors", by Frank J. Owens and Charles P. Poole, Plenum Press, 1996, referred to herein as Poole 1996 in Chapter 8 entitled "New High Temperature Superconductors" starting a page 97 (See Attachment AG) shows in Section 8.3 starting at page 98 entitled "Layered Structure of the Cuprates" schematic diagrams of the layered structure of the cuprate superconductors. Poole 1996 states in the first sentence of Section 8.3 at page 98 "All cuprate superconductors have the layered structure shown in Fig. 8.1." This is consistent with the teaching of Bednorz and Mueller that "These compositions have a layer-type Crystalline Structure often Perovskite-like" as noted in paragraph 14 above. Poole 1996 further states in the first sentence of Section 8.3 at page 98 "The flow of supercurrent takes place in conduction layers and bonding layers support and hold together the conduction layers". The caption of Fig. 8.1 states "Layering scheme of the cuprate superconductors". Fig. 8.3 shows details of the conduction layers for difference sequence of copper oxide planes and Fig. 8.4 presents details of the bonding layers for several of the cuprates which include binding layers for lanthanum superconductor La_2CuO_4 , neodymium superconductor Nd_2CuO_4 , yttrium superconductor $\text{YBa}_2\text{Cu}_3\text{O}_{2n+4}$, bismuth

superconductor $\text{Bi}_2\text{Sr}_2\text{Ca}_{n-1}\text{Cu}_n\text{O}_{2n+4}$, thallium superconductor $\text{Tl}_2\text{Ba}_2\text{Ca}_{n-1}\text{Cu}_n\text{O}_{2n+4}$, and mercury superconductor $\text{HgBa}_2\text{Ca}_{n-1}\text{Cu}_n\text{O}_{2n+2}$. Fig. 8.5 at pages 102 and 103 show a schematic atomic structure showing the layering scheme for thallium superconductors. Fig. 8.10 at page 109 shows a schematic crystal structure showing the layering scheme for La_2CuO_4 . Fig. 8.11 at page 110 shows a schematic crystal structure showing the layering scheme for $\text{HgBa}_2\text{Ca}_2\text{Cu}_3\text{O}_{8+x}$. The layering shown in Poole 1996 for high T_c superconductors is consistent with the layering as taught by Bednorz and Mueller in their patent application.

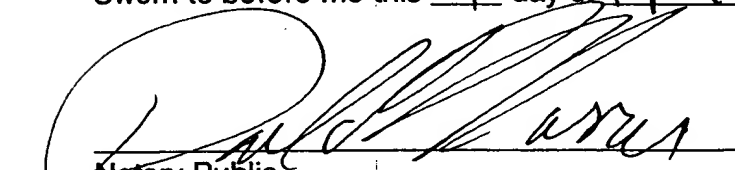
49. Thus Poole 1988 states that the high T_c superconducting materials "are not difficult to synthesize" and Poole 1995 states that "the new superconductors do indeed possess [the] characteristics" that Applicants' specification describes these new superconductors to have. Poole 1996 provide details showing that high T_c superconductors are layered or layer-like as taught by Bednorz and Mueller. Therefore, as of Applicants' priority date persons of ordinary skill in the art of ceramic fabrication were enabled to practice Applicants' invention to the full scope that it is presently claimed, including in the claims that are not allowed from the teaching in the Bednorz-Mueller application without undue experimentation that is by following the teaching of Bednorz and Mueller in combination with what was known to persons of ordinary skill in the art of ceramic fabrication. The experiments to make high T_c superconductors not specifically identified in the Bednorz-Mueller application were made by principles of ceramic fabrication prior to the date of their first publication. It is within the skill of a person of ordinary skill in the art of ceramic fabrication to make compositions according to the teaching of the Bednorz-Mueller application to determine whether or not they are high T_c superconductors without undue experimentation.

50. I have personally made many samples of high T_c superconductors following the teaching of Bednorz and Mueller as found in their patent applications. In making these materials it was not necessary to use starting materials in stoichiometric proportions to produce a high T_c superconductor with insignificant secondary phases or multi-phase compositions, having a superconducting portion and a non-superconducting portion, where the composite was a high T_c superconductor. Consequently, following the teaching of Bednorz and Mueller and principles of ceramic science known prior to their discovery, I made, and persons of skill in the ceramic arts were able to make, high T_c superconductors without exerting extreme care in preparing the composition. Thus I made and persons of skill in the ceramic arts were able to make high T_c superconductors following the teaching of Bednorz and Mueller, without experimentation beyond what was well known to a person of ordinary skill in the ceramic arts prior to the discovery by Bednorz and Mueller.

51. I hereby swear that all statements made herein of my knowledge are true and that all statements made on information and belief are believed to be true; and further, that these statements were made with the knowledge that willful false statements and the like so made are punishable by fine or imprisonment, or both, under Section 1001 of Title 18 of the United States Code and that such willful false statements made jeopardize the validity of the application or patent issued thereon.

Date: 14th April 2005 By: Thomas M. Shaw
Thomas M. Shaw

Sworn to before me this 14 day of April, 2005.


Notary Public

DANIEL P. MORRIS
NOTARY PUBLIC, State of New York
No. 4888676
Qualified in Westchester County
Commission Expires March 16, ~~19~~ 2007

ATTACHMENT 1

Thomas M. Shaw

IBM Thomas J. Watson Research Center
P.O. Box 218
Yorktown Heights, NY 10598
Phone: (914) 945-3196

Education:

1981 Ph.D.	Materials Science - University of California at Berkeley
1978 Masters of Science	Materials Science - University of California at Berkeley
1975 Bachelors of Science	Engineering in Metallurgy and Materials Science - University of Liverpool

Work Experience:

1994-Present Research Staff Member at IBM Thomas J. Watson Research Center working in Materials Science
1984-1994 Research Staff Member at IBM Thomas J. Watson Research Center working in Ceramics Science
1982-1984 Member of the technical staff at Rockwell International Science Center working in Ceramics Science
1981-1982 Postdoctoral Associate at Cornell University working in Ceramics Science

Professional Positions:

A fellow of the American Ceramics Society

Honors:

1981 John E. Dorn Award for thesis.

Publications:

Has authored or co-authored more that 150 publications and 21 patents.

His research interests include, ferroelectric thin films, processing and microstructure control of ceramic materials, microscopy of materials, interfacial energy driven processes, liquid phase sintering, porous materials, diffusion in thin films, electrical and mechanical properties materials and the reliability of interconnect structures.

** TX STATUS REPORT **

AS OF APR 14 '05 15:06 PAGE.01

IBM

	DATE	TIME	TO/FROM	MODE	MIN/SEC	PGS	CMD#	STATUS
09	04/14	14:59	917032991475	UF--S	07'24"	029		OK

BRIEF ATTACHMENT AN

IN THE UNITED STATES PATENT AND TRADEMARK OFFICE

In re Patent Application of

Applicants: Bednorz et al.

Serial No.: 08/479,810

Filed: June 7, 1995

For: NEW SUPERCONDUCTIVE COMPOUNDS HAVING HIGH TRANSITION
TEMPERATURE, METHODS FOR THEIR USE AND PREPARATION

Date: April 5, 2005

Docket: YO987-074BZ

Group Art Unit: 1751

Examiner: M. Kopec

Commissioner for Patents
P.O. Box 1450
Alexandria, VA 22313-1450

FIFTH SUPPLEMENTAL AMENDMENT

Sir:

In response to the Office Action dated July 28, 2004, please consider the
following:

IN THE UNITED STATES PATENT AND TRADEMARK OFFICE

In re Patent Application of

Date: April 4, 2005

Applicants: Bednorz et al.

Docket: YO987-074BZ

Serial No.: 08/479,810

Group Art Unit: 1751

Filed: June 7, 1995

Examiner: M. Kopec

For: NEW SUPERCONDUCTIVE COMPOUNDS HAVING HIGH TRANSITION
TEMPERATURE, METHODS FOR THEIR USE AND PREPARATION

Commissioner for Patents
P.O. Box 1450
Alexandria, VA 22313-1450



AFFIDAVIT UNDER 37 C.F.R. 1.132

Sir:

I, Chang C. Tsuei, being duly sworn, do hereby depose and state:

1. I received a B. S. degree in Mechanical Engineering from National Taiwan University (1960), and M. S. and Ph.D. degrees in Material Science (1963, 1966) respectively from California Institute of Technology.
2. I refer to Attachments A to Z and AA herein which were submitted in a separate paper designated as "FIRST SUPPLEMENTAL AMENDMENT" in response to the Office Action dated July 28, 2004. I also refer to Attachments AB to AG which were submitted in a separate paper designated as "THIRD SUPPLEMENTAL AMENDMENT" in response to the Office Action dated July 28, 2004.
3. I have worked as a research staff member and manger in the physics of superconducting, amorphous and structured materials at the Thomas J. Watson Research Center of the International Business Machines Corporation in Yorktown Heights, New York from 1973 to the present.
4. I have worked in the fabrication of and characterization of high temperature superconductor and related materials from 1973 to the present.

IBM
YORKTOWN
2005 APR -6 PM 1:10
INTELLECTUAL PROPERTY
DEPT.

IN THE UNITED STATES PATENT AND TRADEMARK OFFICE

In re Patent Application of

Date: April 4, 2005

Applicants: Bednorz et al.

Docket: YO987-074BZ

Serial No.: 08/479,810

Group Art Unit: 1751

Filed: June 7, 1995

Examiner: M. Kopec

For: NEW SUPERCONDUCTIVE COMPOUNDS HAVING HIGH TRANSITION
TEMPERATURE, METHODS FOR THEIR USE AND PREPARATIONCommissioner for Patents
P.O. Box 1450
Alexandria, VA 22313-1450**AFFIDAVIT UNDER 37 C.F.R. 1.132**

Sir:

I, Chang C. Tsuei, being duly sworn, do hereby depose and state:

1. I received a B. S. degree in Mechanical Engineering from National Taiwan University (1960), and M. S. and Ph.D. degrees in Material Science (1963, 1966) respectively from California Institute of Technology.
2. I refer to Attachments A to Z and AA herein which were submitted in a separate paper designated as "FIRST SUPPLEMENTAL AMENDMENT" in response to the Office Action dated July 28, 2004. I also refer to Attachments AB to AG which were submitted in a separate paper designated as "THIRD SUPPLEMENTAL AMENDMENT" in response to the Office Action dated July 28, 2004.
3. I have worked as a research staff member and manger in the physics of superconducting, amorphous and structured materials at the Thomas J. Watson Research Center of the International Business Machines Corporation in Yorktown Heights, New York from 1973 to the present.
4. I have worked in the fabrication of and characterization of high temperature superconductor and related materials from 1973 to the present.

IN THE UNITED STATES PATENT AND TRADEMARK OFFICE

In re Patent Application of

Applicants: Bednorz et al.

Serial No.: 08/479,810

Filed: June 7, 1995

For: **NEW SUPERCONDUCTIVE COMPOUNDS HAVING HIGH TRANSITION
TEMPERATURE, METHODS FOR THEIR USE AND PREPARATION**

Date: April 4, 2005

Docket: YO987-074BZ

Group Art Unit: 1751

Examiner: M. Kopec

Commissioner for Patents
P.O. Box 1450
Alexandria, VA 22313-1450

AFFIDAVIT UNDER 37 C.F.R. 1.132

Sir:

I, Chang C. Tsuei, being duly sworn, do hereby depose and state:

1. I received a B. S. degree in Mechanical Engineering from National Taiwan University (1960), and M. S. and Ph.D. degrees in Material Science (1963, 1966) respectively from California Institute of Technology.

2. I refer to Attachments A to Z and AA herein which were submitted in a separate paper designated as "FIRST SUPPLEMENTAL AMENDMENT" in response to the Office Action dated July 28, 2004. I also refer to Attachments AB to AG which were submitted in a separate paper designated as "THIRD SUPPLEMENTAL AMENDMENT" in response to the Office Action dated July 28, 2004.

3. I have worked as a research staff member and manger in the physics of superconducting, amorphous and structured materials at the Thomas J. Watson Research Center of the International Business Machines Corporation in Yorktown Heights, New York from 1973 to the present.

4. I have worked in the fabrication of and characterization of high temperature superconductor and related materials from 1973 to the present.

5. My resume and list of publications is in Attachment 1 included with this affidavit.

6. This affidavit is in addition to my affidavit dated December 15, 1998. I have reviewed the above-identified patent application (Bednorz-Mueller application) and acknowledge that it represents the work of Bednorz and Mueller, which is generally recognized as the first discovery of superconductivity in a material having a $T_c \geq 26^\circ\text{K}$ and that subsequent developments in this field have been based on this work.

7. All the high temperature superconductors which have been developed based on the work of Bednorz and Mueller behave in a similar manner, conduct current in a similar manner, have similar magnetic properties, and have similar structural properties.

8. Once a person of skill in the art knows of a specific type of composition described in the Bednorz-Mueller application which is superconducting at greater than or equal to 26°K , such a person of skill in the art, using the techniques described in the Bednorz-Mueller application, which includes all principles of ceramic fabrication known at the time the application was initially filed, can make the compositions encompassed by the claims of the Bednorz-Mueller application, without undue experimentation or without requiring ingenuity beyond that expected of a person of skill in the art of the fabrication of ceramic materials. This is why the work of Bednorz and Mueller was reproduced so quickly after their discovery and why so much additional work was done in this field within a short period after their discovery. Bednorz and Mueller's discovery was first reported in Z. Phys. B **64** page 189-193 (1996).

9. The techniques for placing a superconductive composition into a superconducting state have been known since the discovery of superconductivity in 1911 by Kamerlingh-Onnes.

10. Prior to 1986 a person having a bachelor's degree in an engineering discipline, applied science, chemistry, physics or a related discipline could have been trained within one year to reliably test a material for the presence of superconductivity and to flow a superconductive current in a superconductive composition.

11. Prior to 1986 a person of ordinary skill in the art of fabricating a composition according to the teaching of the Bednorz-Mueller application would have: a) a Ph.D. degree in solid state chemistry, applied physics, material science, metallurgy, physics or a related discipline and have done thesis research including work in the fabrication of ceramic materials; or b) have a Ph.D. degree in these same fields having done experimental thesis research plus one to two years post Ph.D. work in the fabrication of ceramic materials; or c) have a master's degree in these same fields and have had five years of materials experience at least some of which is in the fabrication of ceramic materials. Such a person is referred to herein as a person of ordinary skill in the ceramic fabrication art.

12. The general principles of ceramic science referred to by Bednorz and Mueller in their patent application and known to a person of ordinary skill in the ceramic fabrication art can be found in many books and articles published before their discovery, priority date (date of filing of their European Patent Office patent application EPO 0275343A1, January 23, 1987) and initial US Application filing date (May 22, 1987). An exemplary list of books describing the general principles of ceramic fabrication are:

a) Introduction to Ceramics, Kingery et al., Second Edition, John Wiley & Sons, 1976, in particular pages 5-20, 269-319, 381-447 and 448-513, a copy of which is in Attachment B.

b) Polar Dielectrics and Their Applications, Burfoot et al., University of California Press, 1979, in particular pages 13-33, a copy of which is in Attachment C.

- c) Ceramic Processing Before Firing, Onoda et al., John Wiley & Sons, 1978, the entire book, a copy of which is in Attachment D.
- d) Structure, Properties and Preparation of Perovskite-Type Compounds, F. S. Galasso, Pergamon Press, 1969, in particular pages 159-186, a copy of which is in Attachment E.

These references were previously submitted with the Affidavit of Thomas Shaw submitted December 15, 1998.

13. An exemplary list of articles applying the general principles of ceramic fabrication to the types of materials described in Applicants' specification are:

- a) Oxygen Defect K_2NiF_4 - Type Oxides: The Compounds $La_{2-x}Sr_xCuO_{4-x/2+}$, Nguyen et al., Journal of Solid State Chemistry 39, 120-127 (1981). See Attachment F.
- b) The Oxygen Defect Perovskite $BaLa_4Cu_5O_{13.4}$, A Metallic (This is referred to in the Bednorz-Mueller application at page 21, lines 1-2) Conductor, C. Michel et al., Mat. Res. Bull., Vol. 20, pp. 667-671, 1985. See Attachment G.
- c) Oxygen Intercalation in Mixed Valence Copper Oxides Related to the Perovskite, C. Michel et al., Revue de Chemie Minerale, 21, p. 407, 1984. (This is referred to in the Bednorz-Mueller application at page 27, lines 1-2). See Attachment H.
- d) Thermal Behaviour of Compositions in the Systems $x BaTiO_3 + (1-x) Ba(Ln_{0.5} B_{0.5}) O_3$, V.S. Chincholkar et al., Therm. Anal. 6th, Vol. 2., p. 251-6, 1980. See Attachment I.

14. The Bednorz-Mueller application in the paragraph bridging pages 6 and 7 states in regard to the high T_c materials:

These compositions can carry supercurrents (i.e., electrical currents in a substantially zero resistance state of the composition) at temperatures greater than 26°K. In general, the compositions are characterized as mixed transition metal oxide systems where the transition metal oxide can exhibit multivalent behavior. These compositions have a layer-type crystalline structure, often perovskite-like, and can contain a rare earth or rare earth-like element. A rare earth-like element (sometimes termed a near rare earth element is one whose properties make it essentially a rare earth element. An example is a group IIIB element of the periodic table, such as La. Substitutions can be found in the rare earth (or rare earth-like) site or in the transition metal sites of the compositions. For example, the rare earth site can also include alkaline earth elements selected from group IIA of the periodic table, or a combination of rare earth or rare earth-like elements and alkaline earth elements. Examples of suitable alkaline earths include Ca, Sr, and Ba. The transition metal site can include a transition metal exhibiting mixed valent behavior, and can include more than one transition metal. A particularly good example of a suitable transition metal is copper. As will be apparent later, Cu-oxide based systems provide unique and excellent properties as high T_c superconductors. An example of a superconductive composition having high T_c is the composition represented by the formula RE-TM-O, where RE is a rare earth or rare earth-like element, TM is a nonmagnetic transition metal, and O is oxygen. Examples of transition metal elements include Cu, Ni, Cr etc. In particular, transition metals that can exhibit multi-valent states are very suitable. The rare earth elements are typically elements 58-71 of the periodic table, including Ce, Nd, etc.

15. In the passage quoted in paragraph 14 the general formula is RE-TM-O "where RE is a rare earth or rare earth-like element, TM is a nonmagnetic transition metal, and O is oxygen." This paragraph states "Substitutions can be found in the rare earth (or rare earth-like) site or in the transition metal sites of the compositions. For example, the rare earth site can also include alkaline earth elements selected from group IIA of the periodic table, or a combination of rare earth or rare earth-like elements and alkaline earth elements." Thus applicants teach that RE can be something other than an rare earth. For example, it can be an alkaline earth, but is not limited to a alkaline earth element. It can be an element that has the same effect as an alkaline earth or rare-earth element, that is a rare earth like element. Also, this passage teaches that TM can be substituted with another element, for example, but not limited to, a rare earth, alkaline earth or some other element that acts in place of the transition metal.

16. The following table is compiled from the Table 1 of the Article by Rao (See Attachment AB) and the Table of high T_c materials from the "CRC Handbook of Chemistry and Physics" 2000-2001 Edition (See Attachment AC). An asterisk in column 5 indicated that the composition of column 2 does not come within the scope of the claims allowed in the Office Action of July 28, 2004.

17. I have reviewed the Office Action dated July 28, 2004, which states at page 6 "The present specification is deemed to be enabled only for compositions comprising a transition metal oxide containing at least a) an alkaline earth element and b) a rare-earth element of Group IIIB element." I disagree for the reasons given herein.

18. Composite Table

1	2	3	4	5	6	7
#	MATERIAL	RAO ARTICLE	HANDBOOK OF CHEM & PHYSICS		ALKALINE EARTH ELEMENT	RARE EARTH ELEMENT
1	$\text{La}_2\text{CuO}_{4+\delta}$	√	√	*	N	Y
2	$\text{La}_{2-x}\text{Sr}_x(\text{Ba}_x)\text{CuO}_4$	√	√		Y	Y
3	$\text{La}_2\text{Ca}_{1-x}\text{Sr}_x\text{Cu}_2\text{O}_6$	√	√		Y	Y

4	YBa ₂ Cu ₃ O ₇	√	√		Y	Y
5	YBa ₂ Cu ₄ O ₈	√	√		Y	Y
6	Y ₂ Ba ₄ Cu ₇ O ₁₅	√	√		Y	Y
7	Bi ₂ Sr ₂ CuO ₆	√	√	*	Y	N
8	Bi ₂ CaSr ₂ Cu ₂ O ₈	√	√	*	Y	N
9	Bi ₂ Ca ₂ Sr ₂ Cu ₃ O ₁₀	√	√	*	Y	N
10	Bi ₂ Sr ₂ (Ln _{1-x} Ce _x) ₂ Cu ₂ O ₁₀	√	√		Y	Y
11	Tl ₂ Ba ₂ CuO ₆	√	√	*	Y	N
12	Tl ₂ CaBa ₂ Cu ₂ O ₈	√	√	*	Y	N
13	Tl ₂ Ca ₂ Ba ₂ Cu ₃ O ₁₀	√	√	*	Y	N
14	Tl(BaLa)CuO ₅	√	√		Y	Y
15	Tl(SrLa)CuO ₅	√	√		Y	Y
16	(Tl _{0.5} Pb _{0.5})Sr ₂ CuO ₅	√	√	*	Y	N
17	TlCaBa ₂ Cu ₂ O ₇	√	√	*	Y	N
18	(Tl _{0.5} Pb _{0.5})CaSr ₂ Cu ₂ O ₇	√	√	*	Y	N
19	TlSr ₂ Y _{0.5} Ca _{0.5} Cu ₂ O ₇	√	√		Y	Y
20	TlCa ₂ Ba ₂ Cu ₃ O ₈	√	√	*	Y	N
21	(Tl _{0.5} Pb _{0.5})Sr ₂ Ca ₂ Cu ₃ O ₉	√	√	*	Y	N
22	TlBa ₂ (Ln _{1-x} Ce _x) ₂ Cu ₂ O ₉	√	√		Y	Y
23	Pb ₂ Sr ₂ Ln _{0.5} Ca _{0.5} Cu ₃ O ₈	√	√		Y	Y
24	Pb ₂ (Sr,La) ₂ Cu ₂ O ₆	√	√		Y	Y
25	(Pb,Cu)Sr ₂ (Ln,Ca)Cu ₂ O ₇	√	√		Y	Y
26	(Pb,Cu)(Sr,Eu)(Eu,Ce)Cu ₂ O _x	√	√		Y	Y
27	Nd _{2-x} Ce _x CuO ₄	√	√	*	N	Y
28	Ca _{1-x} Nd _x CuO ₂	√			Y	Y
29	Sr _{1-x} Nd _x CuO ₂	√	√		Y	Y
30	Ca _{1-x} Sr _x CuO ₂		√	*	Y	N
31	Ba _{0.6} K _{0.4} BiO ₃		√	*	Y	N
32	Rb ₂ C ₅ C ₆₀		√	*	N	Y
33	NdBa ₂ Cu ₃ O ₇		√		Y	Y
34	SmBaSrCuO ₇		√		Y	Y
35	EuBaSrCu ₃ O ₇		√		Y	Y
36	BaSrCu ₃ O ₇		√	*	Y	N
37	DyBaSrCu ₃ O ₇		√		Y	Y
38	HuBaSrCu ₃ O ₇		√		Y	Y
39	ErBaSrCu ₃ O ₇ (Multiphase)		√		Y	Y
40	TmBaSrCu ₃ O ₇ (Multiphase)		√		Y	Y

41	YBaSrCu ₃ O ₇		√	*	Y	Y
42	HgBa ₂ CuO ₂		√	*	Y	N
43	HgBa ₂ CaCu ₂ O ₆ (annealed in O ₂)		√	*	Y	N
44	HgBa ₂ Ca ₂ Cu ₃ O ₈		√	*	Y	N
45	HgBa ₂ Ca ₃ Cu ₄ O ₁₀		√	*	Y	N

19. The first composition, La₂ Cu O_{4+δ}, has the form RE₂CuO₄ which is explicitly taught by Bednorz and Mueller. The δ indicates that there is a nonstoichiometric amount of oxygen.

20. The Bednorz-Mueller application teaches at page 11, line 19 to page 12, line 7:

An example of a superconductive compound having a layer-type structure in accordance with the present invention is an oxide of the general composition RE₂TMO₄ where RE stands for the rare earths (lanthanides) or rare earth-like elements and TM stands for a transition metal. In these compounds the RE portion can be partially substituted by one or more members of the alkaline earth group of elements. In these particular compounds, the oxygen content is at a deficit. For example, one such compound that meets this general description is lanthanum copper oxide La₂CuO₄...

21. The Bednorz-Mueller application at page 15, last paragraph states "Despite their metallic character, the Ba-La-Cu-O type materials are essentially ceramics, as are other compounds of the RE₂ TMO₄ type, and their manufacture generally follows known principles of ceramic fabrication."

22. Compound number 27 of the composite table contains Nd and Ce, both rare earth elements. All of the other compounds of the composite table, except for number 32, have O and one of the alkaline earth elements which as stated above is explicitly taught by applicants. Compound 31 is a BiO_3 compound in which TM is substituted by another element, here Bi, as explicitly taught by Applicants in the paragraph quoted above.

23. The rare earth elements are Sc, Y, La, Ce, Pr, Nd, Pm, Sm, Eu, Gd, Tb, Dy, Ho, Er, Tm, Yb, and Lu. See the Handbook of Chemistry and Physics 59th edition 1978-1979 page B262 in Appendix A. The transition elements are identified in the periodic table from the inside front cover of the Handbook of Chemistry and Physics in Appendix A.

24. The basic theory of superconductivity has been known many years before Applicants' discovery. For example, see the book "Theory of Superconductivity", M. von Laue, Academic Press, Inc., 1952 (See Attachment AD).

25. In the composite table, compound numbers 7 to 10 and 31 are Bismuth (Bi) compounds. Compound number 12 to 22 are Thallium (Tl) compounds. Compound numbers 23 to 26 are lead (Pb) compounds. Compounds 42 to 45 are Mercury (Hg) compounds. Those compounds that do not come within the scope of an allowed claims (the compounds which are not marked with an asterisk in column 3 of the composite table) are primarily the Bi, Tl, Pb and Hg compounds. These compounds are made according to the principles of ceramic science known prior to applicant's filing date. For example, Attachments J, K, L, and M contain the following articles:

Attachment J - Phys. Rev. B. Vol. 38, No. 16, p. 6531 (1988) is directed to Thallium compounds.

Attachment K - Jap. Journ. of Appl. Phys., Vol. 27, No. 2, p. L209-L210 (1988) is directed to Bismuth (Bi) compounds.

Attachment L - Letter to Nature, Vol. 38, No. 2, p. 226 (18 March 1993) is directed to Mercury (Hg) compounds.

Attachment M - Nature, Vol. 336, p. 211 (17 November 1988) is directed to Lead (Pb) based compounds.

26. The article of Attachment J (directed to Tl compounds) states at page 6531, left column:

The samples were prepared by thoroughly mixing suitable amounts of Tl_2O_3 , CaO, BaO_2 , and CuO, and forming a pellet of this mixture under pressure. The pellet was then wrapped in gold foil, sealed in quartz tube containing slightly less than 1 atm of oxygen, and baked for approximately 3 h at $\approx 880^\circ C$.

This is according to the general principles of ceramic science known prior to applicant's priority date.

27. The article of Attachment K (directed to Bi compounds) states at page L209:

The Bi-Sr-Ca-Cu-O oxide samples were prepared from powder reagents of Bi_2O_3 , $SrCO_3$, $CaCO_3$ and CuO. The appropriate amounts of powders were mixed, calcined at $800-870^\circ C$ for 5 h, thoroughly reground and then cold-pressed into disk-shape pellets (20 mm in diameter and 2 mm in thickness) at a pressure of 2 ton. cm^2 . Most of the pellets were sintered at about $870^\circ C$ in air or in an oxygen atmosphere and then furnace-cooled to room temperature.

This is according to the general principles of ceramic science known prior to applicant's priority date.

28. The article of Attachment L (directed to Hg compounds) states at page 226:

The samples were prepared by solid state reaction between stoichiometric mixtures of $\text{Ba}_2\text{CuO}_{3+\delta}$ and yellow HgO (98% purity, Aldrich). The precursor $\text{Ba}_2\text{CuO}_{3+\delta}$ was obtained by the same type of reaction between BaO_2 (95% purity, Aldrich) and CuO (NormalPur, Prolabo) at 930°C in oxygen, according to the procedure described by De Leeuw et al.⁶. The powders were ground in an agate mortar and placed in silica tubes. All these operations were carried out in a dry box. After evacuation, the tubes were sealed, placed in steel containers, as described in ref. 3, and heated for 5 h to reach $\sim 800^\circ\text{C}$. The samples were then cooled in the furnace, reaching room temperature after ~ 10 h.

This is according to the general principles of ceramic science known prior to applicant's priority date.

29. The article of Attachment M (directed to Pb compounds) states at page 211, left column:

The preparative conditions for the new materials are considerably more stringent than for the previously known copper-based superconductors. Direct synthesis of members of this family by reaction of the component metal oxides or carbonates in air or oxygen at temperatures below 900°C is not possible because of the stability of the oxidized SrPbO_3 -based perovskite. Successful synthesis is accomplished by the reaction of PbO with pre-reacted (Sr, Ca, Ln) oxide precursors. The precursors are prepared from oxides and carbonates in the appropriate metal ratios, calcined for 16 hours (in dense Al_2O_3 crucibles) at 920 - 980°C in air with one intermediate grinding.

This is according to the principles of ceramic science known prior to applicant's priority date.

30. A person of ordinary skill in the art of the fabrication of ceramic materials would be motivated by the teaching of the Bednorz-Mueller application to investigate compositions for high superconductivity other than the compositions specifically fabricated by Bednorz and Mueller.

31. In Attachment U, there is a list of perovskite materials from pages 191 to 207 in the book "Structure, Properties and Preparation of Perovskite-Type Compounds" by F. S. Galasso, published in 1969, which is Attachment E hereto. This list contains about 300 compounds. Thus, what the term "Perovskite-type" means and how to make these compounds was well known to a person of ordinary skill in the art in 1969, more than 17 years before the Applicants' priority date (January 23, 1987).

This is clear evidence that a person of skill in the art of fabrication of ceramic materials knows (prior to Applicants' priority date) how to make the types of materials in Table 1 of the Rao Article and the Table from the Handbook of Chemistry and Physics as listed in the composite table above in paragraph 17.

32. The standard reference "Landolt-Börnstein", Volume 4, "Magnetic and Other Properties of Oxides and Related Compounds Part A" (1970) lists at page 148 to 206 Perovskite and Perovskite-related structures. (See Attachment N). Section 3.2 starting at page 190 is entitled "Descriptions of perovskite-related structures". The German title is "Perowskit-ähnliche Strukturen". The German word "ähnliche" can be translated in English as "like". The Langenscheidt's German-English, English-German Dictionary 1970, at page 446 translates the English "like" as the German "ähnliche". (See Attachment O). Pages 126 to 147 of Attachment N describes "crystallographic and magnetic properties of perovskite and perovskite-related compounds", see title of Section 3 at page 126. Section 3.2.3.1 starting at page 192 of "Landolt-Börnstein" Vol. 4 (See Attachment N) is entitled "Bismuth Compounds". Thus Bismuth

perovskite-like compounds and how to make them were well known more than 16 years prior to Applicants' priority date. Thus the "Landholt Börnstein" book published in 1970, more than 16 years before Applicants' priority date (January 23, 1987), shows that the term "perovskite-like" or "perovskite related" is understood by persons of skill in the art prior to Applicants' priority date. Moreover, the "Landholt-Börnstein" book cites references for each compound listed. Thus a person of ordinary skill in the art of ceramic fabrication knows how to make each of these compounds. Pages 376-380 of Attachment N has figures showing the crystal structure of compounds containing Bi and Pb.

33. The standard reference "Landholt-Börnstein, Volume 3, Ferro- and Antiferroelectric Substances" (1969) provides at pages 571-584 an index to substances. (See Attachment P). This list contains numerous Bi and Pb containing compounds. See, for example pages 578 and 582-584. Thus a person of ordinary skill in the art of ceramic fabrication would be motivated by Applicants' application to fabricate Bi and/or Pb containing compounds that come within the scope of the Applicants' claims.

34. The standard reference "Landholt-Börnstein Volume 3 Ferro- and Antiferroelectric Substances" (1969) (See Attachment P) at page 37, section 1 is entitled "Perovskite-type oxides." This standard reference was published more than 17 years before Applicants' priority date (January 23, 1987). The properties of perovskite-type oxides are listed from pages 37 to 88. Thus the term perovskite-type was well known and understood by persons of skill in the art of ceramic fabrication prior to Applicants' priority date and more than 17 years before Applicants' priority date persons of ordinary skill in the art knew how to make Bi, Pb and many other perovskite, perovskite-like, perovskite-related and perovskite-type compounds.

35. At page 14, line 10-15 of the Bednorz-Mueller application, Applicants' state "samples in the Ba-La-Cu-O system, when subjected to x-ray analysis, revealed three individual crystallographic phases V.12. a first layer-type perovskite-like phase, related to the K_2NiF_4 structure ..." Applicants' priority document EP0275343A1 filed July 27, 1988, is entitled "New Superconductive Compounds of the K_2NiF_4 Structural Type Having a High Transition Temperature, and Method for Fabricating Same." See (See Attachment AE). The book "Structure and Properties of Inorganic Solids" by Francis S. Galasso, Pergamon Press (1969) at page 190 lists examples of Thallium (Tl) compounds in the K_2NiF_4 structure. (See Attachment Q). Thus based on Applicants' teachings prior to Applicants' priority date, a person of ordinary skill in the art of ceramic fabrication would be motivated to fabricate Thallium based compounds to test for high T_c superconductivity.

36. The book "Crystal Structures" Volume 4, by Ralph W. G. Wyckoff, Interscience Publishers, 1960 states at page 96 "This structure, like these of $Bi_4Ti_2O_{12}$ (IX, F_{12}) and $BaBi_4Ti_4O_4$ (XI, 13) is built up of alternating Bi_2O_2 and perovskite-like layers." Thus layer of perovskite-like Bismuth compounds was well known in the art in 1960 more than 26 years before Applicants' priority date. (See Attachment R).

37. The book "Modern Oxide Materials Preparation, Properties and Device Applications" edited by Cockayne and Jones, Academic Press (1972) states (See Attachment S) at page 155 under the heading "Layer Structure Oxides and Complex Compounds":

"A large number of layer structure compounds of general formula $(Bi_2O_2)^{2+}$ $(A_{x-1}B_xO_{3x+1})^{2-}$ have been reported (Smolenskii et al. 1961; Subbarao, 1962), where A = Ca, Sr, Ba, Pb, etc., B = Ti, Nb, Ta and x = 2, 3, 4, or 5. The structure had been previously investigated by Aurivillius (1949) who described them in terms of Alternate $(Bi_2O_2)^{2+}$ layers and perovskite layers of oxygen octahedra. Few have been found to be ferroelectric and include $SrBi_2Ta_2O_9$ ($T_c = 583^\circ K$), $PbBi_2Ta_2O_9$ ($T_c = 703^\circ K$), $BiBi_3Ti_2TiO_{12}$ or

$\text{Bi}_4\text{Ti}_3\text{O}_{12}$ ($T_c = 948^\circ\text{K}$), $\text{Ba}_2\text{Bi}_4\text{Ti}_5\text{O}_{18}$ ($T_c = 598^\circ\text{K}$) and $\text{Pb}_2\text{Bi}_4\text{Ti}_5\text{O}_{18}$ ($T_c = 583^\circ\text{K}$). Only bismuth titanate $\text{Bi}_4\text{Ti}_3\text{O}_{12}$ has been investigated in detail in the single crystal form and is finding applications in optical stores (Cummins, 1967) because of its unique ferroelectric-optical switching properties. The ceramics of other members have some interest because of their dielectric properties. More complex compounds and solid solutions are realizable in these layer structure oxides but none have significant practical application."

Thus the term layered oxides was well known and understood prior to Applicants' priority date. Moreover, layered Bi and Pb compounds were well known in 1972 more than 15 years before Applicants' priority date.

38. The standard reference "Landolt-Börnstein, Volume 3, Ferro and Antiferroelectric Substances" (1969) at pages 107 to 114 (See Attachment T) list "layer-structure oxides" and their properties. Thus the term "layered compounds" was well known in the art of ceramic fabrication in 1969 more than 16 years prior to Applicants' priority date and how to make layered compounds was well known prior to applicants priority date.

39. Layer perovskite type Bi and Pb compounds closely related to the Bi and Pb high T_c compounds in the composite table above in paragraph 17 have been known for some time. For example, the following is a list of four articles which were published about 35 years prior to Applicants' first publication date:

(1) Attachment V - "Mixed bismuth oxides with layer lattices", B. Aurivillius, Arkiv Kemi 1, 463, (1950).

(2) Attachment W - "Mixed bismuth oxides with layered lattices ", B. Aurivillius, Arkiv Kemi 1, 499, (1950).

(3) Attachment X - "Mixed bismuth oxides with layered lattices ", B. Aurivillius, Arkiv Kemi 2, 519, (1951).

(4) Attachment Y - "The structure of $\text{Bi}_2\text{NbO}_5\text{F}$ and isomorphous compounds", B. Aurivillius, Arkiv Kemi 5, 39, (1952).

These articles will be referred to as Aurivillius 1, 2, 3 and 4, respectively.

40. Attachment V (Aurivillius 1), at page 463, the first page, has the subtitle "I. The structure type of $\text{CaNb}_2\text{Bi}_2\text{O}_9$. Attachment V states at page 463:

X-ray analysis ... seemed to show that the structure was built up of $\text{Bi}_2\text{O}_2^{2+}$ layers parallel to the basal plane and sheets of composition $\text{Bi}_2\text{Ti}_3\text{O}^{2-}_{10}$. The atomic arrangement within the $\text{Bi}_2\text{Ti}_3\text{O}^{2-}_{10}$ sheets seemed to be the same as in structure of the perovskite type and the structure could then be described as consisting of $\text{Bi}_2\text{O}_2^{2+}$ layers between which double perovskite layers are inserted.

41. Attachment V (Aurivillius 1) at page 464 has a section entitled " $\text{PbBi}_2\text{Nb}_2\text{O}_9$ Phase". And at page 471 has a section entitled " $\text{Bi}_3\text{NbTiO}_9$ ". And at page 475 has a table of compounds having the " $\text{CaBi}_2\text{Nb}_2\text{O}_9$ structure" listing the following compounds $\text{Bi}_3\text{NbTiO}_9$, $\text{Bi}_3\text{TaTiO}_9$, $\text{CaBi}_2\text{Nb}_2\text{O}_9$, $\text{SrBi}_2\text{Nb}_2\text{O}_9$, $\text{SrBi}_2\text{Ta}_2\text{O}_9$, $\text{BaBi}_2\text{Nb}_2\text{O}_9$, $\text{PbBi}_2\text{Nb}_2\text{O}_9$, $\text{NaBi}_5\text{Nb}_4\text{O}_{18}$, $\text{KBi}_5\text{Nb}_4\text{O}_{18}$. Thus Bi and Pb layered perovskite compounds were well known in the art about 35 years prior to Applicants' priority date.

42. Attachment W (Aurivillius 2) at page 499, the first page, has the subtitle "II Structure of $\text{Bi}_4\text{Ti}_3\text{O}_{12}$ ". And at page 510, Fig. 4 shows a crystal structure in which "A denotes a perovskite layer $\text{Bi}_2\text{Ti}_3\text{O}^{2-}_{10}$, C $\text{Bi}_2\text{O}_2^{2+}$ layers and B unit cells of the hypothetical perovskite structure BiTiO_3 .

43. Attachment X (Aurivillius 3) has at page 519, the first page, the subtitle "III Structure of $\text{BaBi}_4\text{Ti}_4\text{O}_{15}$ ". And in the first paragraph on page 519 states referring to the articles of Attachments V (Aurivillius 1), and W (Aurivillius 2) "X ray studies on the compounds $\text{CaBi}_2\text{Nb}_2\text{O}_9$ [the article of Attachment V] and $\text{Bi}_4\text{Ti}_3\text{O}_{12}$ [the article of Attachment W] have shown that the comparatively complicated chemical formulae of these compounds can be explained by simple layer structures being built up from Bi_2O_2^+ layers and perovskite layers. The unit cells are pictured schematically in Figs. 1a and 1c." And Fig. 4 at page 526 shows "One half of a unit cell of $\text{BaBi}_4\text{Ti}_4\text{O}_{15}$. A denotes the perovskite region and B the Me_2O_4 layer" where Me represents a metal atom.

44. Attachment Y (Aurivillius 4) is direct to structures having the $\text{Bi}_3\text{N}_{10}\text{O}_3\text{F}$ structure.

45. Attachment AA is a list of Hg containing solid state compounds from the 1989 Powder Diffraction File Index. Applicants do not have available to them an index from prior to Applicants' priority date. The Powder Diffraction File list is a compilation of all known solid state compounds with reference to articles directed to the properties of these compositions and the methods of fabrication. From Attachment AA it can be seen, for example, that there are numerous examples of Hg based compounds. Similarly, there are examples of other compounds in the Powder Diffraction File. A person of ordinary skill in the art is aware of the Powder Diffraction File and can from this file find a reference providing details on how to fabricate these compounds. Thus persons of ordinary skill in the art would be motivated by Applicants' teaching to look to the Powder Diffraction File for examples of previously fabricated composition expected to have properties similar to those described in Applicants' teaching.

46. It is generally recognized that it is not difficult to fabricate transition metal oxides and in particular copper metal oxides that are superconductive after the discovery by Applicants of composition, such as transition metal oxides, that are high T_c superconductors. This is noted in the book "Copper Oxide Superconductors" by Charles P. Poole, Jr., Timir Datta and Horacio A. Farach, John Wiley & Sons (1998), referred to herein as Poole 1988: Chapter 5 of Poole 1988 (See Attachment AF) in the book entitled "Preparation and Characterization of Samples" states at page 59 "[c]opper oxide superconductors with a purity sufficient to exhibit zero resistivity or to demonstrate levitation (Early) are not difficult to synthesize. We believe that this is at least partially responsible for the explosive worldwide growth in these materials". Poole 1988 further states at page 61 "[i]n this section three methods of preparation will be described, namely, the solid state, the coprecipitation, and the sol-gel techniques (Hatfi). The widely used solid-state technique permits off-the-shelf chemicals to be directly calcined into superconductors, and it requires little familiarity with the subtle physicochemical process involved in the transformation of a mixture of compounds into a superconductor." Poole 1988 further states at pages 61-62 "[i]n the solid state reaction technique one starts with oxygen-rich compounds of the desired components such as oxides, nitrates or carbonates of Ba, Bi, La, Sr, Ti, Y or other elements. ... These compounds are mixed in the desired atomic ratios and ground to a fine powder to facilitate the calcination process. Then these room-temperature-stable salts are reacted by calcination for an extended period (~20hr) at elevated temperatures (~900°C). This process may be repeated several times, with pulverizing and mixing of the partially calcined material at each step." This is generally the same as the specific examples provided by Applicants and as generally described at pages 8, line 19, to page 9, line 5, of the Bednorz-Mueller application which states "[t]he methods by which these superconductive compositions can be made can use known principals of ceramic fabrication, including the mixing of powders containing the rare earth or rare earth-like, alkaline earth, and transition metal elements, coprecipitation of these materials, and heating steps in oxygen or air. A particularly suitable superconducting material in accordance with this invention is one containing copper as the transition metal."

Consequently, it is my opinion that Applicants have fully enabled high T_c materials oxides and their claims.

47. Charles Poole et al. published another book in 1995 entitled "Superconductivity" Academic Press which has a Chapter 7 on "Perovskite and Cuprate Crystallographic Structures". (See Attachment Z). This book will be referred to as Poole 1995.

At page 179 of Poole 1995 states:

V. PEROVSKITE-TYPE SUPERCONDUCTING STRUCTURES

In their first report on high-temperature superconductors Bednorz and Müller (1986) referred to their samples as "metallic, oxygen-deficient ... perovskite-like mixed-valence copper compounds." Subsequent work has confirmed that the new superconductors do indeed possess these characteristics.

I agree with this statement.

48. The book "The New Superconductors", by Frank J. Owens and Charles P. Poole, Plenum Press, 1996, referred to herein as Poole 1996 in Chapter 8 entitled "New High Temperature Superconductors" starting a page 97 (See Attachment AG) shows in Section 8.3 starting at page 98 entitled "Layered Structure of the Cuprates" schematic diagrams of the layered structure of the cuprate superconductors. Poole 1996 states in the first sentence of Section 8.3 at page 98 "All cuprate superconductors have the layered structure shown in Fig. 8.1." This is consistent with the teaching of Bednorz and Mueller that "These compositions have a layer-type Crystalline Structure often Perovskite-like" as noted in paragraph 14 above. Poole 1996 further states in the first sentence of Section 8.3 at page 98 "The flow of supercurrent takes place in conduction layers and bonding layers support and hold together the conduction layers". The caption of Fig. 8.1 states "Layering scheme of the cuprate superconductors". Fig. 8.3 shows details of the conduction layers for difference sequence of copper oxide

planes and Fig. 8.4 presents details of the bonding layers for several of the cuprates which include binding layers for lanthanum superconductor La_2CuO_4 , neodymium superconductor Nd_2CuO_4 , yttrium superconductor $\text{YBa}_2\text{Cu}_3\text{O}_{2n+4}$, bismuth superconductor $\text{Bi}_2\text{Sr}_2\text{Ca}_{n-1}\text{Cu}_n\text{O}_{2n+4}$, thallium superconductor $\text{Tl}_2\text{Ba}_2\text{Ca}_{n-1}\text{Cu}_n\text{O}_{2n+4}$, and mercury superconductor $\text{HgBa}_2\text{Ca}_{n-1}\text{Cu}_n\text{O}_{2n+2}$. Fig. 8.5 at pages 102 and 103 show a schematic atomic structure showing the layering scheme for thallium superconductors. Fig. 8.10 at page 109 shows a schematic crystal structure showing the layering scheme for La_2CuO_4 . Fig. 8.11 at page 110 shows a schematic crystal structure showing the layering scheme for $\text{HgBa}_2\text{Ca}_2\text{Cu}_3\text{O}_{8+x}$. The layering shown in Poole 1996 for high T_c superconductors is consistent with the layering as taught by Bednorz and Mueller in their patent application.

49. Thus Poole 1988 states that the high T_c superconducting materials "are not difficult to synthesize" and Poole 1995 states that "the new superconductors do indeed possess [the] characteristics" that Applicants' specification describes these new superconductors to have. Poole 1996 provide details showing that high T_c superconductors are layered or layer-like as taught by Bednorz and Mueller. Therefore, as of Applicants' priority date persons of ordinary skill in the art of ceramic fabrication were enabled to practice Applicants' invention to the full scope that it is presently claimed, including in the claims that are not allowed from the teaching in the Bednorz-Mueller application without undue experimentation that is by following the teaching of Bednorz and Mueller in combination with what was known to persons of ordinary skill in the art of ceramic fabrication. The experiments to make high T_c superconductors not specifically identified in the Bednorz-Mueller application were made by principles of ceramic fabrication prior to the date of their first publication. It is within the skill of a person of ordinary skill in the art of ceramic fabrication to make compositions according to the teaching of the Bednorz-Mueller application to determine whether or not they are high T_c superconductors without undue experimentation.

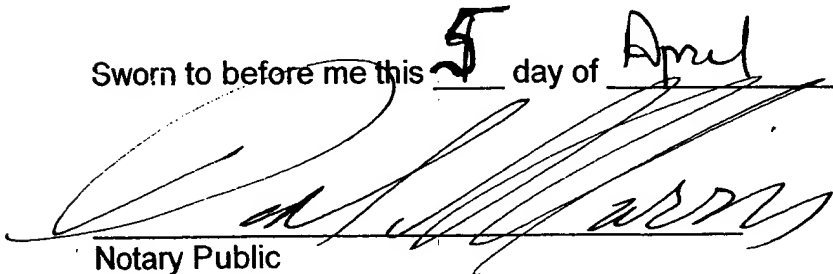
50. I have personally made many samples of high T_c superconductors following the teaching of Bednorz and Mueller as found in their patent applications. In making these materials it was not necessary to use starting materials in stoichiometric proportions to produce a high T_c superconductor with insignificant secondary phases or multi-phase compositions, having a superconducting portion and a non-superconducting portion, where the composite was a high T_c superconductor. Consequently, following the teaching of Bednorz and Mueller and principles of ceramic science known prior to their discovery, I made, and persons of skill in the ceramic arts were able to make, high T_c superconductors without exerting extreme care in preparing the composition. Thus I made and persons of skill in the ceramic arts were able to make high T_c superconductors following the teaching of Bednorz and Mueller, without experimentation beyond what was well known to a person of ordinary skill in the ceramic arts prior to the discovery by Bednorz and Mueller.

51. I hereby swear that all statements made herein of my knowledge are true and that all statements made on information and belief are believed to be true; and further, that these statements were made with the knowledge that willful false statements and the like so made are punishable by fine or imprisonment, or both, under Section 1001 of Title 18 of the United States Code and that such willful false statements made jeopardize the validity of the application or patent issued thereon.

Date: April 5, 2005

By: Chang C. Tsuei
Chang C. Tsuei

Sworn to before me this 5 day of April, 2005.


Notary Public

DANIEL P. MORRIS
NOTARY PUBLIC, State of New York
No. 4888676
Qualified in Westchester County
Commission Expires March 16, 19

2007

Attachment 1

Chang C. Tsuei

IBM Thomas J. Watson Research Center
P.O. Box 218
Yorktown Heights, NY 10598
Phone: (914) 945-2799
Fax: (914) 945-2141

Education:

Ph.D. 1966 Materials Science - California Institute of Technology
M.S. 1963 Materials Science - California Institute of Technology
B.S. 1960 Mechanical Engineering - National Taiwan University

Professional Positions:

IBM Thomas J. Watson Research Center

1993 – Present	Research Staff Member, Superconductivity
1983 – 1993	Manager, Physics of Structured Materials
1979 – 1983	Manager, Physics of Amorphous Materials
1974 – 1975	Acting Manager, Superconductivity
1973 – 1979	Research Staff Member

Universite Paris-Sud

1996 – 1997	Invited Professor in Solid State Physics
-------------	------------------------------------------

Harvard University

1980 (summer)	Visiting Scholar in Applied Physics
---------------	-------------------------------------

Stanford University

09/1982 – 04/1983	Visiting Scholar in Applied Physics
-------------------	-------------------------------------

California Institute of Technology

1972 – 1973	Senior Research Associate in Applied Physics
1969 – 1972	Senior Research Fellow in Materials Science
1966 – 1969	Research Fellow in Materials Science

Honors:

2000 Dynamic Achiever Award from the Organization of Chinese Americans
2000 IBM Corporate Award
1998 Bodo von Borries Lectureship sponsored by the Bodo von Borries Stiftung of Germany.
1998 Co-recipient of the Oliver E. Buckley Condensed Matter Physics Prize of the American Physical Society
1996-1997 Appointment as Invited Professor at the Universite Paris-Sud
1996 Elected to Academia Sinica
1996 Academic Achievement Award from the Chinese American Academic and Professional Society
1995 IBM Outstanding Innovation Award for contributions to the work on half integer flux quantization observed with a scanning SQUID microscope
1992 Max Planck Research Prize from the Max Planck Society and the Alexander von Humbolt Foundation of Germany
1990 IBM Outstanding Technical Achievement Award for contributions to the understanding of electrical properties of grain boundaries in high- T_c superconductors
1984 IBM Invention Achievement Award

1980 Invention Achievement Award

Professional Societies Honors:

2001 Fellow of the American Association for the Advancement of Science

1996 Academician of Academia Sinica

1974 Fellow of American Physical Society

Publications: available upon request

BRIEF ATTACHMENT AO

IN THE UNITED STATES PATENT AND TRADEMARK OFFICE

In re Patent Application of

Applicants: Bednorz et al.

Serial No.: 08/479,810

Filed: June 7, 1995

For: NEW SUPERCONDUCTIVE COMPOUNDS HAVING HIGH TRANSITION
TEMPERATURE, METHODS FOR THEIR USE AND PREPARATION

Date: April 5, 2005

Docket: YO987-074BZ

Group Art Unit: 1751

Examiner: M. Kopec

Commissioner for Patents
P.O. Box 1450
Alexandria, VA 22313-1450

FIFTH SUPPLEMENTAL AMENDMENT

Sir:

In response to the Office Action dated July 28, 2004, please consider the
following:

IN THE UNITED STATES PATENT AND TRADEMARK OFFICE

In re Patent Application of

Applicants: Bednorz et al.

Serial No.: 08/479,810

Filed: June 7, 1995

For: NEW SUPERCONDUCTIVE COMPOUNDS HAVING HIGH TRANSITION
TEMPERATURE, METHODS FOR THEIR USE AND PREPARATION

Date: April 4, 2005

Docket: YO987-074BZ

Group Art Unit: 1751

Examiner: M. Kopec

Commissioner for Patents
P.O. Box 1450
Alexandria, VA 22313-14502005 APR -6 PM 1:10
INTELLECTUAL PROPERTY
LAW DEPT.
IBM
YORKTOWNAFFIDAVIT UNDER 37 C.F.R. 1.132

Sir:

I, Timothy Dinger, being duly sworn, do hereby depose and state:

1. I received a B. S. degree in Ceramic Engineering (1981) from New York State College of Ceramics, Alfred University, an M. S. degree (1983) and a Ph.D. degree (1986), both in Material Science from the University of California at Berkeley.
2. I refer to Attachments A to Z and AA herein which were submitted in a separate paper designated as "FIRST SUPPLEMENTAL AMENDMENT" in response to the Office Action dated July 28, 2004. I also refer to Attachments AB to AG which were submitted in a separate paper designated as "THIRD SUPPLEMENTAL AMENDMENT" in response to the Office Action dated July 28, 2004.
3. I have worked as a research staff member in Material Science at the Thomas J. Watson Research Center of the International Business Machines Corporation in Yorktown Heights, New York from 1986 to 2001. From 2001 to the present, I have worked as an I/T Manager in the IBM Chief Information Officer organization.
4. I have worked in the fabrication of and characterization of high temperature superconductor materials from 1987 to 1991.

IN THE UNITED STATES PATENT AND TRADEMARK OFFICE

In re Patent Application of

Applicants: Bednorz et al.

Serial No.: 08/479,810

Filed: June 7, 1995

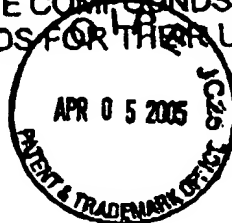
For: NEW SUPERCONDUCTIVE COMPOUNDS HAVING HIGH TRANSITION
TEMPERATURE, METHODS FOR THEIR USE AND PREPARATION

Date: April 4, 2005

Docket: YO987-074BZ

Group Art Unit: 1751

Examiner: M. Kopec

Commissioner for Patents
P.O. Box 1450
Alexandria, VA 22313-1450**AFFIDAVIT UNDER 37 C.F.R. 1.132**

Sir:

I, Timothy Dinger, being duly sworn, do hereby depose and state:

1. I received a B. S. degree in Ceramic Engineering (1981) from New York State College of Ceramics, Alfred University, an M. S. degree (1983) and a Ph.D. degree (1986), both in Material Science from the University of California at Berkeley.
2. I refer to Attachments A to Z and AA herein which were submitted in a separate paper designated as "FIRST SUPPLEMENTAL AMENDMENT" in response to the Office Action dated July 28, 2004. I also refer to Attachments AB to AG which were submitted in a separate paper designated as "THIRD SUPPLEMENTAL AMENDMENT" in response to the Office Action dated July 28, 2004.
3. I have worked as a research staff member in Material Science at the Thomas J. Watson Research Center of the International Business Machines Corporation in Yorktown Heights, New York from 1986 to 2001. From 2001 to the present, I have worked as an I/T Manager in the IBM Chief Information Officer organization.
4. I have worked in the fabrication of and characterization of high temperature superconductor materials from 1987 to 1991.

IN THE UNITED STATES PATENT AND TRADEMARK OFFICE

In re Patent Application of

Applicants: Bednorz et al.

Serial No.: 08/479,810

Filed: June 7, 1995

For: NEW SUPERCONDUCTIVE COMPOUNDS HAVING HIGH TRANSITION
TEMPERATURE, METHODS FOR THEIR USE AND PREPARATION

Date: April 4, 2005

Docket: YO987-074BZ

Group Art Unit: 1751

Examiner: M. Kopec

Commissioner for Patents
P.O. Box 1450
Alexandria, VA 22313-1450

AFFIDAVIT UNDER 37 C.F.R. 1.132

Sir:

I, Timothy Dinger, being duly sworn, do hereby depose and state:

1. I received a B. S. degree in Ceramic Engineering (1981) from New York State College of Ceramics, Alfred University, an M. S. degree (1983) and a Ph.D. degree (1986), both in Material Science from the University of California at Berkeley.
2. I refer to Attachments A to Z and AA herein which were submitted in a separate paper designated as "FIRST SUPPLEMENTAL AMENDMENT" in response to the Office Action dated July 28, 2004. I also refer to Attachments AB to AG which were submitted in a separate paper designated as "THIRD SUPPLEMENTAL AMENDMENT" in response to the Office Action dated July 28, 2004.
3. I have worked as a research staff member in Material Science at the Thomas J. Watson Research Center of the International Business Machines Corporation in Yorktown Heights, New York from 1986 to 2001. From 2001 to the present, I have worked as an I/T Manager in the IBM Chief Information Officer organization.
4. I have worked in the fabrication of and characterization of high temperature superconductor materials from 1987 to 1991.

5. My resume and list of publications is in Attachment 1 included with this affidavit.

6. This affidavit is in addition to my affidavit dated December 15, 1998. I have reviewed the above-identified patent application (Bednorz-Mueller application) and acknowledge that it represents the work of Bednorz and Mueller, which is generally recognized as the first discovery of superconductivity in a material having a $T_c \geq 26^\circ\text{K}$ and that subsequent developments in this field have been based on this work.

7. All the high temperature superconductors which have been developed based on the work of Bednorz and Mueller behave in a similar manner, conduct current in a similar manner, have similar magnetic properties, and have similar structural properties.

8. Once a person of skill in the art knows of a specific type of composition described in the Bednorz-Mueller application which is superconducting at greater than or equal to 26°K , such a person of skill in the art, using the techniques described in the Bednorz-Mueller application, which includes all principles of ceramic fabrication known at the time the application was initially filed, can make the compositions encompassed by the claims of the Bednorz-Mueller application, without undue experimentation or without requiring ingenuity beyond that expected of a person of skill in the art of the fabrication of ceramic materials. This is why the work of Bednorz and Mueller was reproduced so quickly after their discovery and why so much additional work was done in this field within a short period after their discovery. Bednorz and Mueller's discovery was first reported in Z. Phys. B **64** page 189-193 (1996).

9. The techniques for placing a superconductive composition into a superconducting state have been known since the discovery of superconductivity in 1911 by Kamerlingh-Onnes.

10. Prior to 1986 a person having a bachelor's degree in an engineering discipline, applied science, chemistry, physics or a related discipline could have been trained within one year to reliably test a material for the presence of superconductivity and to flow a superconductive current in a superconductive composition.

11. Prior to 1986 a person of ordinary skill in the art of fabricating a composition according to the teaching of the Bednorz-Mueller application would have: a) a Ph.D. degree in solid state chemistry, applied physics, material science, metallurgy, physics or a related discipline and have done thesis research including work in the fabrication of ceramic materials; or b) have a Ph.D. degree in these same fields having done experimental thesis research plus one to two years post Ph.D. work in the fabrication of ceramic materials; or c) have a master's degree in these same fields and have had five years of materials experience at least some of which is in the fabrication of ceramic materials. Such a person is referred to herein as a person of ordinary skill in the ceramic fabrication art.

12. The general principles of ceramic science referred to by Bednorz and Mueller in their patent application and known to a person of ordinary skill in the ceramic fabrication art can be found in many books and articles published before their discovery, priority date (date of filing of their European Patent Office patent application EPO 0275343A1, January 23, 1987) and initial US Application filing date (May 22, 1987). An exemplary list of books describing the general principles of ceramic fabrication are:

a) Introduction to Ceramics, Kingery et al., Second Edition, John Wiley & Sons, 1976, in particular pages 5-20, 269-319, 381-447 and 448-513, a copy of which is in Attachment B.

b) Polar Dielectrics and Their Applications, Burfoot et al., University of California Press, 1979, in particular pages 13-33, a copy of which is in Attachment C.

- c) Ceramic Processing Before Firing, Onoda et al., John Wiley & Sons, 1978, the entire book, a copy of which is in Attachment D.
- d) Structure, Properties and Preparation of Perovskite-Type Compounds, F. S. Galasso, Pergamon Press, 1969, in particular pages 159-186, a copy of which is in Attachment E.

These references were previously submitted with the Affidavit of Thomas Shaw submitted December 15, 1998.

13. An exemplary list of articles applying the general principles of ceramic fabrication to the types of materials described in Applicants' specification are:

- a) Oxygen Defect K_2NiF_4 - Type Oxides: The Compounds $La_{2-x}Sr_xCuO_{4-x/2+*}$, Nguyen et al., Journal of Solid State Chemistry 39, 120-127 (1981). See Attachment F.
- b) The Oxygen Defect Perovskite $BaLa_4Cu_5O_{13.4}$, A Metallic (This is referred to in the Bednorz-Mueller application at page 21, lines 1-2) Conductor, C. Michel et al., Mat. Res. Bull., Vol. 20, pp. 667-671, 1985. See Attachment G.
- c) Oxygen Intercalation in Mixed Valence Copper Oxides Related to the Perovskite, C. Michel et al., Revue de Chemie Minerale, 21, p. 407, 1984. (This is referred to in the Bednorz-Mueller application at page 27, lines 1-2). See Attachment H.
- d) Thermal Behaviour of Compositions in the Systems $x BaTiO_3 + (1-x) Ba(Ln_{0.5} B_{0.5}) O_3$, V.S. Chincholkar et al., Therm. Anal. 6th, Vol. 2., p. 251-6, 1980. See Attachment I.

14. The Bednorz-Mueller application in the paragraph bridging pages 6 and 7 states in regard to the high T_c materials:

These compositions can carry supercurrents (i.e., electrical currents in a substantially zero resistance state of the composition) at temperatures greater than 26°K. In general, the compositions are characterized as mixed transition metal oxide systems where the transition metal oxide can exhibit multivalent behavior. These compositions have a layer-type crystalline structure, often perovskite-like, and can contain a rare earth or rare earth-like element. A rare earth-like element (sometimes termed a near rare earth element) is one whose properties make it essentially a rare earth element. An example is a group IIIB element of the periodic table, such as La. Substitutions can be found in the rare earth (or rare earth-like) site or in the transition metal sites of the compositions. For example, the rare earth site can also include alkaline earth elements selected from group IIA of the periodic table, or a combination of rare earth or rare earth-like elements and alkaline earth elements. Examples of suitable alkaline earths include Ca, Sr, and Ba. The transition metal site can include a transition metal exhibiting mixed valent behavior, and can include more than one transition metal. A particularly good example of a suitable transition metal is copper. As will be apparent later, Cu-oxide based systems provide unique and excellent properties as high T_c superconductors. An example of a superconductive composition having high T_c is the composition represented by the formula RE-TM-O, where RE is a rare earth or rare earth-like element, TM is a nonmagnetic transition metal, and O is oxygen. Examples of transition metal elements include Cu, Ni, Cr etc. In particular, transition metals that can exhibit multi-valent states are very suitable. The rare earth elements are typically elements 58-71 of the periodic table, including Ce, Nd, etc.

15. In the passage quoted in paragraph 14 the general formula is RE-TM-O "where RE is a rare earth or rare earth-like element, TM is a nonmagnetic transition metal, and O is oxygen." This paragraph states "Substitutions can be found in the rare earth (or rare earth-like) site or in the transition metal sites of the compositions. For example, the rare earth site can also include alkaline earth elements selected from group IIA of the periodic table, or a combination of rare earth or rare earth-like elements and alkaline earth elements." Thus applicants teach that RE can be something other than an rare earth. For example, it can be an alkaline earth, but is not limited to a alkaline earth element. It can be an element that has the same effect as an alkaline earth or rare-earth element, that is a rare earth like element. Also, this passage teaches that TM can be substituted with another element, for example, but not limited to, a rare earth, alkaline earth or some other element that acts in place of the transition metal.

16. The following table (in paragraph 18) is compiled from the Table 1 of the Article by Rao (See Attachment AB) and the Table of high T_c materials from the "CRC Handbook of Chemistry and Physics" 2000-2001 Edition (See Attachment AC). An asterisk in column 5 indicated that the composition of column 2 does not come within the scope of the claims allowed in the Office Action of July 28, 2004.

17. I have reviewed the Office Action dated July 28, 2004, which states at page 6 "The present specification is deemed to be enabled only for compositions comprising a transition metal oxide containing at least a) an alkaline earth element and b) a rare-earth element of Group IIIB element." I disagree for the reasons given herein.

18. Composite Table

1	2	3	4	5	6	7
#	MATERIAL	RAO ARTICLE	HANDBOOK OF CHEM & PHYSICS		ALKALINE EARTH ELEMENT	RARE EARTH ELEMENT
1	$\text{La}_2\text{CuO}_{4+\delta}$	√	√	*	N	Y
2	$\text{La}_{2-x}\text{Sr}_x(\text{Ba}_x)\text{CuO}_4$	√	√		Y	Y
3	$\text{La}_2\text{Ca}_{1-x}\text{Sr}_x\text{Cu}_2\text{O}_6$	√	√		Y	Y

4	YBa ₂ Cu ₃ O ₇	√	√		Y	Y
5	YBa ₂ Cu ₄ O ₈	√	√		Y	Y
6	Y ₂ Ba ₄ Cu ₇ O ₁₅	√	√		Y	Y
7	Bi ₂ Sr ₂ CuO ₆	√	√	*	Y	N
8	Bi ₂ CaSr ₂ Cu ₂ O ₈	√	√	*	Y	N
9	Bi ₂ Ca ₂ Sr ₂ Cu ₃ O ₁₀	√	√	*	Y	N
10	Bi ₂ Sr ₂ (Ln _{1-x} Ce _x) ₂ Cu ₂ O ₁₀	√	√		Y	Y
11	Tl ₂ Ba ₂ CuO ₆	√	√	*	Y	N
12	Tl ₂ CaBa ₂ Cu ₂ O ₈	√	√	*	Y	N
13	Tl ₂ Ca ₂ Ba ₂ Cu ₃ O ₁₀	√	√	*	Y	N
14	Tl(BaLa)CuO ₅	√	√		Y	Y
15	Tl(SrLa)CuO ₅	√	√		Y	Y
16	(Tl _{0.5} Pb _{0.5})Sr ₂ CuO ₅	√	√	*	Y	N
17	TlCaBa ₂ Cu ₂ O ₇	√	√	*	Y	N
18	(Tl _{0.5} Pb _{0.5})CaSr ₂ Cu ₂ O ₇	√	√	*	Y	N
19	TlSr ₂ Y _{0.5} Ca _{0.5} Cu ₂ O ₇	√	√		Y	Y
20	TlCa ₂ Ba ₂ Cu ₃ O ₈	√	√	*	Y	N
21	(Tl _{0.5} Pb _{0.5})Sr ₂ Ca ₂ Cu ₃ O ₉	√	√	*	Y	N
22	TlBa ₂ (Ln _{1-x} Ce _x) ₂ Cu ₂ O ₉	√	√		Y	Y
23	Pb ₂ Sr ₂ Ln _{0.5} Ca _{0.5} Cu ₃ O ₈	√	√		Y	Y
24	Pb ₂ (Sr,La) ₂ Cu ₂ O ₆	√	√		Y	Y
25	(Pb,Cu)Sr ₂ (Ln,Ca)Cu ₂ O ₇	√	√		Y	Y
26	(Pb,Cu)(Sr,Eu)(Eu,Ce)Cu ₂ O _x	√	√		Y	Y
27	Nd _{2-x} Ce _x CuO ₄	√	√	*	N	Y
28	Ca _{1-x} Nd _x CuO ₂	√			Y	Y
29	Sr _{1-x} Nd _x CuO ₂	√	√		Y	Y
30	Ca _{1-x} Sr _x CuO ₂		√	*	Y	N
31	Ba _{0.6} K _{0.4} BiO ₃		√	*	Y	N
32	Rb ₂ C ₅ C ₆₀		√	*	N	Y
33	NdBa ₂ Cu ₃ O ₇		√		Y	Y
34	SmBaSrCuO ₇		√		Y	Y
35	EuBaSrCu ₃ O ₇		√		Y	Y
36	BaSrCu ₃ O ₇		√	*	Y	N
37	DyBaSrCu ₃ O ₇		√		Y	Y
38	HuBaSrCu ₃ O ₇		√		Y	Y
39	ErBaSrCu ₃ O ₇ (Multiphase)		√		Y	Y
40	TmBaSrCu ₃ O ₇ (Multiphase)		√		Y	Y

41	YBaSrCu ₃ O ₇		√	*	Y	Y
42	HgBa ₂ CuO ₂		√	*	Y	N
43	HgBa ₂ CaCu ₂ O ₆ (annealed in O ₂)		√	*	Y	N
44	HgBa ₂ Ca ₂ Cu ₃ O ₈		√	*	Y	N
45	HgBa ₂ Ca ₃ Cu ₄ O ₁₀		√	*	Y	N

19. The first composition, La₂ Cu O_{4+δ}, has the form RE₂CuO₄ which is explicitly taught by Bednorz and Mueller. The δ indicates that there is a nonstoichiometric amount of oxygen.

20. The Bednorz-Mueller application teaches at page 11, line 19 to page 12, line 7:

An example of a superconductive compound having a layer-type structure in accordance with the present invention is an oxide of the general composition RE₂TMO₄ where RE stands for the rare earths (lanthanides) or rare earth-like elements and TM stands for a transition metal. In these compounds the RE portion can be partially substituted by one or more members of the alkaline earth group of elements. In these particular compounds, the oxygen content is at a deficit. For example, one such compound that meets this general description is lanthanum copper oxide La₂CuO₄...

21. The Bednorz-Mueller application at page 15, last paragraph states "Despite their metallic character, the Ba-La-Cu-O type materials are essentially ceramics, as are other compounds of the RE₂ TMO₄ type, and their manufacture generally follows known principles of ceramic fabrication."

22. Compound number 27 of the composite table contains Nd and Ce, both rare earth elements. All of the other compounds of the composite table, except for number 32, have O and one of the alkaline earth elements which as stated above is explicitly taught by applicants. Compound 31 is a BiO_3 compound in which TM is substituted by another element, here Bi, as explicitly taught by Applicants in the paragraph quoted above.

23. The rare earth elements are Sc, Y, La, Ce, Pr, Nd, Pm, Sm, Eu, Gd, Tb, Dy, Ho, Er, Tm, Yb, and Lu. See the Handbook of Chemistry and Physics 59th edition 1978-1979 page B262 in Appendix A. The transition elements are identified in the periodic table from the inside front cover of the Handbook of Chemistry and Physics in Appendix A.

24. The basic theory of superconductivity has been known many years before Applicants' discovery. For example, see the book "Theory of Superconductivity", M. von Laue, Academic Press, Inc., 1952 (See Attachment AD).

25. In the composite table, compound numbers 7 to 10 and 31 are Bismuth (Bi) compounds. Compound number 12 to 22 are Thallium (Tl) compounds. Compound numbers 23 to 26 are lead (Pb) compounds. Compounds 42 to 45 are Mercury (Hg) compounds. Those compounds that do not come within the scope of an allowed claims (the compounds which are not marked with an asterisk in column 3 of the composite table) are primarily the Bi, Tl, Pb and Hg compounds. These compounds are made according to the principles of ceramic science known prior to applicant's filing date. For example, Attachments J, K, L, and M contain the following articles:

Attachment J - Phys. Rev. B. Vol. 38, No. 16, p. 6531 (1988) is directed to Thallium compounds.

Attachment K - Jap. Joun. of Appl. Phys., Vol. 27, No. 2, p. L209-L210 (1988) is directed to Bismuth (Bi) compounds.

Attachment L - Letter to Nature, Vol. 38, No. 2, p. 226 (18 March 1993) is directed to Mercury (Hg) compounds.

Attachment M - Nature, Vol. 336, p. 211 (17 November 1988) is directed to Lead (Pb) based compounds.

26. The article of Attachment J (directed to Tl compounds) states at page 6531, left column:

The samples were prepared by thoroughly mixing suitable amounts of Tl_2O_3 , CaO, BaO_2 , and CuO, and forming a pellet of this mixture under pressure. The pellet was then wrapped in gold foil, sealed in quartz tube containing slightly less than 1 atm of oxygen, and baked for approximately 3 h at $\approx 880^\circ C$.

This is according to the general principles of ceramic science known prior to applicant's priority date.

27. The article of Attachment K (directed to Bi compounds) states at page L209:

The Bi-Sr-Ca-Cu-O oxide samples were prepared from powder reagents of Bi_2O_3 , $SrCO_3$, $CaCO_3$ and CuO. The appropriate amounts of powders were mixed, calcined at $800-870^\circ C$ for 5 h, thoroughly reground and then cold-pressed into disk-shape pellets (20 mm in diameter and 2 mm in thickness) at a pressure of 2 ton.cm². Most of the pellets were sintered at about $870^\circ C$ in air or in an oxygen atmosphere and then furnace-cooled to room temperature.

This is according to the general principles of ceramic science known prior to applicant's priority date.

28. The article of Attachment L (directed to Hg compounds) states at page 226:

The samples were prepared by solid state reaction between stoichiometric mixtures of $\text{Ba}_2\text{CuO}_{3+\delta}$ and yellow HgO (98% purity, Aldrich). The precursor $\text{Ba}_2\text{CuO}_{3+\delta}$ was obtained by the same type of reaction between BaO_2 (95% purity, Aldrich) and CuO (NormalPur, Prolabo) at 930°C in oxygen, according to the procedure described by De Leeuw et al.⁶. The powders were ground in an agate mortar and placed in silica tubes. All these operations were carried out in a dry box. After evacuation, the tubes were sealed, placed in steel containers, as described in ref. 3, and heated for 5 h to reach $\sim 800^\circ\text{C}$. The samples were then cooled in the furnace, reaching room temperature after ~ 10 h.

This is according to the general principles of ceramic science known prior to applicant's priority date.

29. The article of Attachment M (directed to Pb compounds) states at page 211, left column:

The preparative conditions for the new materials are considerably more stringent than for the previously known copper-based superconductors. Direct synthesis of members of this family by reaction of the component metal oxides or carbonates in air or oxygen at temperatures below 900°C is not possible because of the stability of the oxidized SrPbO_3 -based perovskite. Successful synthesis is accomplished by the reaction of PbO with pre-reacted (Sr, Ca, Ln) oxide precursors. The precursors are prepared from oxides and carbonates in the appropriate metal ratios, calcined for 16 hours (in dense Al_2O_3 crucibles) at 920 - 980°C in air with one intermediate grinding.

This is according to the principles of ceramic science known prior to applicant's priority date.

30. A person of ordinary skill in the art of the fabrication of ceramic materials would be motivated by the teaching of the Bednorz-Mueller application to investigate compositions for high superconductivity other than the compositions specifically fabricated by Bednorz and Mueller.

31. In Attachment U, there is a list of perovskite materials from pages 191 to 207 in the book "Structure, Properties and Preparation of Perovskite-Type Compounds" by F. S. Galasso, published in 1969, which is Attachment E hereto. This list contains about 300 compounds. Thus, what the term "Perovskite-type" means and how to make these compounds was well known to a person of ordinary skill in the art in 1969, more than 17 years before the Applicants' priority date (January 23, 1987).

This is clear evidence that a person of skill in the art of fabrication of ceramic materials knows (prior to Applicants' priority date) how to make the types of materials in Table 1 of the Rao Article and the Table from the Handbook of Chemistry and Physics as listed in the composite table above in paragraph 17.

32. The standard reference "Landolt-Börnstein", Volumn 4, "Magnetic and Other Properties of Oxides and Related Compounds Part A" (1970) lists at page 148 to 206 Perovskite and Perovskite-related structures. (See Attachment N). Section 3.2 starting at page 190 is entitled "Descriptions of perovskite-related structures". The German title is "Perowskit-ähnliche Strukturen." The German word "ähnliche" can be translated in English as "like". The Langenscheidt's German-English, English-German Dictionary 1970, at page 446 translates the English "like" as the German "ähnliche". (See Attachment O). Pages 126 to 147 of Attachment N describes "crystallographic and magnetic properties of perovskite and perovskite-related compounds", see title of Section 3 at page 126. Section 3.2.3.1 starting at page 192 of "Landolt-Börnstein" Vol. 4 (See Attachment N) is entitled "Bismuth Compounds". Thus Bismuth

perovskite-like compounds and how to make them were well known more than 16 years prior to Applicants' priority date. Thus the "Landholt Börnstein" book published in 1970, more than 16 years before Applicants' priority date (January 23, 1987), shows that the term "perovskite-like" or "perovskite related" is understood by persons of skill in the art prior to Applicants' priority date. Moreover, the "Landholt-Börnstein" book cites references for each compound listed. Thus a person of ordinary skill in the art of ceramic fabrication knows how to make each of these compounds. Pages 376-380 of Attachment N has figures showing the crystal structure of compounds containing Bi and Pb.

33. The standard reference "Landholt-Börnstein, Volume 3, Ferro- and Antiferroelectric Substances" (1969) provides at pages 571-584 an index to substances. (See Attachment P). This list contains numerous Bi and Pb containing compounds. See, for example pages 578 and 582-584. Thus a person of ordinary skill in the art of ceramic fabrication would be motivated by Applicants' application to fabricate Bi and/or Pb containing compounds that come within the scope of the Applicants' claims.

34. The standard reference "Landholt-Börnstein Volume 3 Ferro- and Antiferroelectric Substances" (1969) (See Attachment P) at page 37, section 1 is entitled "Perovskite-type oxides." This standard reference was published more than 17 years before Applicants' priority date (January 23, 1987). The properties of perovskite-type oxides are listed from pages 37 to 88. Thus the term perovskite-type was well known and understood by persons of skill in the art of ceramic fabrication prior to Applicants' priority date and more than 17 years before Applicants' priority date persons of ordinary skill in the art knew how to make Bi, Pb and many other perovskite, perovskite-like, perovskite-related and perovskite-type compounds.

35. At page 14, line 10-15 of the Bednorz-Mueller application, Applicants' state "samples in the Ba-La-Cu-O system, when subjected to x-ray analysis, revealed three individual crystallographic phases V.12. a first layer-type perovskite-like phase, related to the K_2NiF_4 structure ..." Applicants' priority document EP0275343A1 filed July 27, 1988, is entitled "New Superconductive Compounds of the K_2NiF_4 Structural Type Having a High Transition Temperature, and Method for Fabricating Same." See (See Attachment AE). The book "Structure and Properties of Inorganic Solids" by Francis S. Galasso, Pergamon Press (1969) at page 190 lists examples of Thallium (Tl) compounds in the K_2NiF_4 structure. (See Attachment Q). Thus based on Applicants' teachings prior to Applicants' priority date, a person of ordinary skill in the art of ceramic fabrication would be motivated to fabricate Thallium based compounds to test for high T_c superconductivity.

36. The book "Crystal Structures" Volume 4, by Ralph W. G. Wyckoff, Interscience Publishers, 1960 states at page 96 "This structure, like these of $Bi_4Ti_2O_{12}$ (IX, F_{12}) and $BaBi_4Ti_4O_4$ (XI, 13) is built up of alternating Bi_2O_2 and perovskite-like layers." Thus layer of perovskite-like Bismuth compounds was well known in the art in 1960 more than 26 years before Applicants' priority date. (See Attachment R).

37. The book "Modern Oxide Materials Preparation, Properties and Device Applications" edited by Cockayne and Jones, Academic Press (1972) states (See Attachment S) at page 155 under the heading "Layer Structure Oxides and Complex Compounds":

"A large number of layer structure compounds of general formula $(Bi_2O_2)^{2+}(A_{x-1}B_xO_{3x+1})^{2-}$ have been reported (Smolenskii et al. 1961; Subbarao, 1962), where A = Ca, Sr, Ba, Pb, etc., B = Ti, Nb, Ta and x = 2, 3, 4, or 5. The structure had been previously investigated by Aurivillius (1949) who described them in terms of Alternate $(Bi_2O_2)^{2+}$ layers and perovskite layers of oxygen octahedra. Few have been found to be ferroelectric and include $SrBi_2Ta_2O_9$ ($T_c = 583^\circ K$), $PbBi_2Ta_2O_9$ ($T_c = 703^\circ K$), $BiBi_3Ti_2TiO_{12}$ or

$\text{Bi}_4\text{Ti}_3\text{O}_{12}$ ($T_c = 948^\circ\text{K}$), $\text{Ba}_2\text{Bi}_4\text{Ti}_5\text{O}_{18}$ ($T_c = 598^\circ\text{K}$) and $\text{Pb}_2\text{Bi}_4\text{Ti}_5\text{O}_{18}$ ($T_c = 583^\circ\text{K}$). Only bismuth titanate $\text{Bi}_4\text{Ti}_3\text{O}_{12}$ has been investigated in detail in the single crystal form and is finding applications in optical stores (Cummins, 1967) because of its unique ferroelectric-optical switching properties. The ceramics of other members have some interest because of their dielectric properties. More complex compounds and solid solutions are realizable in these layer structure oxides but none have significant practical application."

Thus the term layered oxides was well known and understood prior to Applicants' priority date. Moreover, layered Bi and Pb compounds were well known in 1972 more than 15 years before Applicants' priority date.

38. The standard reference "Landolt-Börnstein, Volume 3, Ferro and Antiferroelectric Substances" (1969) at pages 107 to 114 (See Attachment T) list "layer-structure oxides" and their properties. Thus the term "layered compounds" was well known in the art of ceramic fabrication in 1969 more than 16 years prior to Applicants' priority date and how to make layered compounds was well known prior to applicants priority date.

39. Layer perovskite type Bi and Pb compounds closely related to the Bi and Pb high T_c compounds in the composite table above in paragraph 17 have been known for some time. For example, the following is a list of four articles which were published about 35 years prior to Applicants' first publication date:

(1) Attachment V - "Mixed bismuth oxides with layer lattices", B. Aurivillius, Arkiv Kemi 1, 463, (1950).

(2) Attachment W - "Mixed bismuth oxides with layered lattices ", B. Aurivillius, Arkiv Kemi 1, 499, (1950).

(3) Attachment X - "Mixed bismuth oxides with layered lattices ", B. Aurivillius, Arkiv Kemi 2, 519, (1951).

(4) Attachment Y - "The structure of $\text{Bi}_2\text{NbO}_5\text{F}$ and isomorphous compounds", B. Aurivillius, Arkiv Kemi 5, 39, (1952).

These articles will be referred to as Aurivillius 1, 2, 3 and 4, respectively.

40. Attachment V (Aurivillius 1), at page 463, the first page, has the subtitle "I. The structure type of $\text{CaNb}_2\text{Bi}_2\text{O}_9$. Attachment V states at page 463:

X-ray analysis ... seemed to show that the structure was built up of $\text{Bi}_2\text{O}_2^{2+}$ layers parallel to the basal plane and sheets of composition $\text{Bi}_2\text{Ti}_3\text{O}_{10}^-$. The atomic arrangement within the $\text{Bi}_2\text{Ti}_3\text{O}_{10}^-$ sheets seemed to be the same as in structure of the perovskite type and the structure could then be described as consisting of $\text{Bi}_2\text{O}_2^{2+}$ layers between which double perovskite layers are inserted.

41. Attachment V (Aurivillius 1) at page 464 has a section entitled " $\text{PbBi}_2\text{Nb}_2\text{O}_9$ Phase". And at page 471 has a section entitled " $\text{Bi}_3\text{NbTiO}_9$ ". And at page 475 has a table of compounds having the " $\text{CaBi}_2\text{Nb}_2\text{O}_9$ structure" listing the following compounds $\text{Bi}_3\text{NbTiO}_9$, $\text{Bi}_3\text{TaTiO}_9$, $\text{CaBi}_2\text{Nb}_2\text{O}_9$, $\text{SrBi}_2\text{Nb}_2\text{O}_9$, $\text{SrBi}_2\text{Ta}_2\text{O}_9$, $\text{BaBi}_2\text{Nb}_2\text{O}_9$, $\text{PbBi}_2\text{Nb}_2\text{O}_9$, $\text{NaBi}_5\text{Nb}_4\text{O}_{18}$, $\text{KBi}_5\text{Nb}_4\text{O}_{18}$. Thus Bi and Pb layered perovskite compounds were well known in the art about 35 years prior to Applicants' priority date.

42. Attachment W (Aurivillius 2) at page 499, the first page, has the subtitle "II Structure of $\text{Bi}_4\text{Ti}_3\text{O}_{12}$ ". And at page 510, Fig. 4 shows a crystal structure in which "A denotes a perovskite layer $\text{Bi}_2\text{Ti}_3\text{O}_{10}^-$, C $\text{Bi}_2\text{O}_2^{2+}$ layers and B unit cells of the hypothetical perovskite structure BiTiO_3 .

43. Attachment X (Aurivillius 3) has at page 519, the first page, the subtitle "III Structure of $\text{BaBi}_4\text{Ti}_4\text{O}_{15}$ ". And in the first paragraph on page 519 states referring to the articles of Attachments V (Aurivillius 1), and W (Aurivillius 2) "X ray studies on the compounds $\text{CaBi}_2\text{Nb}_2\text{O}_9$ [the article of Attachment V] and $\text{Bi}_4\text{Ti}_3\text{O}_{12}$ [the article of Attachment W] have shown that the comparatively complicated chemical formulae of these compounds can be explained by simple layer structures being built up from $\text{Bi}_2\text{O}_2^{2+}$ layers and perovskite layers. The unit cells are pictured schematically in Figs. 1a and 1c." And Fig. 4 at page 526 shows "One half of a unit cell of $\text{BaBi}_4\text{Ti}_4\text{O}_{15}$. A denotes the perovskite region and B the Me_2O_4 layer" where Me represents a metal atom.

44. Attachment Y (Aurivillius 4) is direct to structures having the $\text{Bi}_3\text{N}_{10}\text{O}_3\text{F}$ structure.

45. Attachment AA is a list of Hg containing solid state compounds from the 1989 Powder Diffraction File Index. Applicants do not have available to them an index from prior to Applicants' priority date. The Powder Diffraction File list is a compilation of all known solid state compounds with reference to articles directed to the properties of these compositions and the methods of fabrication. From Attachment AA it can be seen, for example, that there are numerous examples of Hg based compounds. Similarly, there are examples of other compounds in the Powder Diffraction File. A person of ordinary skill in the art is aware of the Powder Diffraction File and can from this file find a reference providing details on how to fabricate these compounds. Thus persons of ordinary skill in the art would be motivated by Applicants' teaching to look to the Powder Diffraction File for examples of previously fabricated composition expected to have properties similar to those described in Applicants' teaching.

46. It is generally recognized that it is not difficult to fabricate transition metal oxides and in particular copper metal oxides that are superconductive after the discovery by Applicants of composition, such as transition metal oxides, that are high T_c superconductors. This is noted in the book "Copper Oxide Superconductors" by Charles P. Poole, Jr., Timir Datta and Horacio A. Farach, John Wiley & Sons (1998), referred to herein as Poole 1988: Chapter 5 of Poole 1988 (See Attachment AF) in the book entitled "Preparation and Characterization of Samples" states at page 59 "[c]opper oxide superconductors with a purity sufficient to exhibit zero resistivity or to demonstrate levitation (Early) are not difficult to synthesize. We believe that this is at least partially responsible for the explosive worldwide growth in these materials". Poole 1988 further states at page 61 "[i]n this section three methods of preparation will be described, namely, the solid state, the coprecipitation, and the sol-gel techniques (Hatfi). The widely used solid-state technique permits off-the-shelf chemicals to be directly calcined into superconductors, and it requires little familiarity with the subtle physicochemical process involved in the transformation of a mixture of compounds into a superconductor." Poole 1988 further states at pages 61-62 "[i]n the solid state reaction technique one starts with oxygen-rich compounds of the desired components such as oxides, nitrates or carbonates of Ba, Bi, La, Sr, Ti, Y or other elements. ... These compounds are mixed in the desired atomic ratios and ground to a fine powder to facilitate the calcination process. Then these room-temperature-stable salts are reacted by calcination for an extended period (~20hr) at elevated temperatures (~900°C). This process may be repeated several times, with pulverizing and mixing of the partially calcined material at each step." This is generally the same as the specific examples provided by Applicants and as generally described at pages 8, line 19, to page 9, line 5, of the Bednorz-Mueller application which states "[t]he methods by which these superconductive compositions can be made can use known principals of ceramic fabrication, including the mixing of powders containing the rare earth or rare earth-like, alkaline earth, and transition metal elements, coprecipitation of these materials, and heating steps in oxygen or air. A particularly suitable superconducting material in accordance with this invention is one containing copper as the transition metal."

Consequently, it is my opinion that Applicants have fully enabled high T_c materials oxides and their claims.

47. Charles Poole et al. published another book in 1995 entitled "Superconductivity" Academic Press which has a Chapter 7 on "Perovskite and Cuprate Crystallographic Structures". (See Attachment Z). This book will be referred to as Poole 1995.

At page 179 of Poole 1995 states:

V. PEROVSKITE-TYPE SUPERCONDUCTING STRUCTURES

In their first report on high-temperature superconductors Bednorz and Müller (1986) referred to their samples as "metallic, oxygen-deficient ... perovskite-like mixed-valence copper compounds." Subsequent work has confirmed that the new superconductors do indeed possess these characteristics.

I agree with this statement.

48. The book "The New Superconductors", by Frank J. Owens and Charles P. Poole, Plenum Press, 1996, referred to herein as Poole 1996 in Chapter 8 entitled "New High Temperature Superconductors" starting a page 97 (See Attachment AG) shows in Section 8.3 starting at page 98 entitled "Layered Structure of the Cuprates" schematic diagrams of the layered structure of the cuprate superconductors. Poole 1996 states in the first sentence of Section 8.3 at page 98 "All cuprate superconductors have the layered structure shown in Fig. 8.1." This is consistent with the teaching of Bednorz and Mueller that "These compositions have a layer-type Crystalline Structure often Perovskite-like" as noted in paragraph 14 above. Poole 1996 further states in the first sentence of Section 8.3 at page 98 "The flow of supercurrent takes place in conduction layers and bonding layers support and hold together the conduction layers". The caption of Fig. 8.1 states "Layering scheme of the cuprate superconductors". Fig. 8.3 shows details of the conduction layers for difference sequence of copper oxide

planes and Fig. 8.4 presents details of the bonding layers for several of the cuprates which include binding layers for lanthanum superconductor La_2CuO_4 , neodymium superconductor Nd_2CuO_4 , yttrium superconductor $\text{YBa}_2\text{Cu}_3\text{O}_{2n+4}$, bismuth superconductor $\text{Bi}_2\text{Sr}_2\text{Ca}_{n-1}\text{Cu}_n\text{O}_{2n+4}$, thallium superconductor $\text{Tl}_2\text{Ba}_2\text{Ca}_{n-1}\text{Cu}_n\text{O}_{2n+4}$, and mercury superconductor $\text{HgBa}_2\text{Ca}_{n-1}\text{Cu}_n\text{O}_{2n+2}$. Fig. 8.5 at pages 102 and 103 show a schematic atomic structure showing the layering scheme for thallium superconductors. Fig. 8.10 at page 109 shows a schematic crystal structure showing the layering scheme for La_2CuO_4 . Fig. 8.11 at page 110 shows a schematic crystal structure showing the layering scheme for $\text{HgBa}_2\text{Ca}_2\text{Cu}_3\text{O}_{8+x}$. The layering shown in Poole 1996 for high T_c superconductors is consistent with the layering as taught by Bednorz and Mueller in their patent application.

49. Thus Poole 1988 states that the high T_c superconducting materials "are not difficult to synthesize" and Poole 1995 states that "the new superconductors do indeed possess [the] characteristics" that Applicants' specification describes these new superconductors to have. Poole 1996 provide details showing that high T_c superconductors are layered or layer-like as taught by Bednorz and Mueller. Therefore, as of Applicants' priority date persons of ordinary skill in the art of ceramic fabrication were enabled to practice Applicants' invention to the full scope that it is presently claimed, including in the claims that are not allowed from the teaching in the Bednorz-Mueller application without undue experimentation that is by following the teaching of Bednorz and Mueller in combination with what was known to persons of ordinary skill in the art of ceramic fabrication. The experiments to make high T_c superconductors not specifically identified in the Bednorz-Mueller application were made by principles of ceramic fabrication prior to the date of their first publication. It is within the skill of a person of ordinary skill in the art of ceramic fabrication to make compositions according to the teaching of the Bednorz-Mueller application to determine whether or not they are high T_c superconductors without undue experimentation.

50. I have personally made many samples of high T_c superconductors following the teaching of Bednorz and Mueller as found in their patent applications. In making these materials it was not necessary to use starting materials in stoichiometric proportions to produce a high T_c superconductor with insignificant secondary phases or multi-phase compositions, having a superconducting portion and a non-superconducting portion, where the composite was a high T_c superconductor. Consequently, following the teaching of Bednorz and Mueller and principles of ceramic science known prior to their discovery, I made, and persons of skill in the ceramic arts were able to make, high T_c superconductors without exerting extreme care in preparing the composition. Thus I made and persons of skill in the ceramic arts were able to make high T_c superconductors following the teaching of Bednorz and Mueller, without experimentation beyond what was well known to a person of ordinary skill in the ceramic arts prior to the discovery by Bednorz and Mueller.

51. I hereby swear that all statements made herein of my knowledge are true and that all statements made on information and belief are believed to be true; and further, that these statements were made with the knowledge that willful false statements and the like so made are punishable by fine or imprisonment, or both, under Section 1001 of Title 18 of the United States Code and that such willful false statements made jeopardize the validity of the application or patent issued thereon.

Date: April 4, 2005

By: Timothy R. Dinger
Timothy Dinger

Sworn to before me this 4th day of April, 2005.

Eileen C. Daly
Notary Public

Eileen C. Daly
Notary Public, State of New York
No. 01DA5037543
Qualified in Dutchess County
Commission Expires February 26, 2007

50. I have personally made many samples of high T_c superconductors following the teaching of Bednorz and Mueller as found in their patent applications. In making these materials it was not necessary to use starting materials in stoichiometric proportions to produce a high T_c superconductor with insignificant secondary phases or multi-phase compositions, having a superconducting portion and a non-superconducting portion, where the composite was a high T_c superconductor. Consequently, following the teaching of Bednorz and Mueller and principles of ceramic science known prior to their discovery, I made, and persons of skill in the ceramic arts were able to make, high T_c superconductors without exerting extreme care in preparing the composition. Thus I made and persons of skill in the ceramic arts were able to make high T_c superconductors following the teaching of Bednorz and Mueller, without experimentation beyond what was well known to a person of ordinary skill in the ceramic arts prior to the discovery by Bednorz and Mueller.

51. I hereby swear that all statements made herein of my knowledge are true and that all statements made on information and belief are believed to be true; and further, that these statements were made with the knowledge that willful false statements and the like so made are punishable by fine or imprisonment, or both, under Section 1001 of Title 18 of the United States Code and that such willful false statements made jeopardize the validity of the application or patent issued thereon.

Date: April 4, 2005

By: Timothy R. Dinger
Timothy Dinger

Sworn to before me this 4th day of April, 2005.

Eileen C. Daly
Notary Public

Eileen C. Daly
Notary Public, State of New York
No. 01D43037545
Qualified in Dutchess County
Commission Expires February 20 2007

Attachment 1

Timothy R. Dinger
IBM Corporate Headquarters
Enterprise On Demand Transformation and CIO Organization
294 Route 100
Somers, NY 10589

Telephone: (914) 766-3507
FAX: (914) 766-7145
e-mail address: dinger@us.ibm.com

Title

IBM Corporate Headquarters, Enterprise On Demand Transformation and CIO Organization - Manager, B2B Technology Strategy and Architecture, (2001 - present). Responsibility to define B2B technology strategy and architecture for IBM's On Demand Infrastructure and reduce that strategy to practice by developing and maintaining IBM's edge-of-enterprise B2B Gateway in support of the IBM Business Unit B2B strategies.

Education

Ph.D. (1986) - Materials Science and Engineering, University of California at Berkeley
M.S. (1983) - Materials Science and Engineering, University of California at Berkeley
B.S. (1981) - Ceramic Engineering, Alfred University

Professional Experience

Information Systems Department, IBM Research Division, Yorktown Heights, NY, Senior Manager/Research Staff Member - Watson Information Systems, (1998-2001). Responsibilities included financial planning and decision-making for IBM's worldwide Research Division (8 laboratories worldwide) and formation of and coordination of the Research Division's program to influence and support the goals of the IBM CIO.

Information Systems Department, IBM Research Division, Yorktown Heights, NY, Manager/Research Staff Member - Server Systems Engineering, (1997 - 1998).

Physical Sciences Department, IBM Research Division, Yorktown Heights, NY, Manager/Research Staff Member - Center for Scalable Computing Solutions, (1994-1996).

Semiconductor Research and Development Center, IBM Microelectronics Division, East Fishkill, NY, Manager/Research Staff Member - Advanced Logic Interconnection Technology, (1993-1994).

Semiconductor Research and Development Center, IBM Microelectronics Division, East Fishkill, NY, Technical Assistant to John E. Kelly III, the Director of the SRDC (1993).

IBM Thomas J. Watson Research Center, Yorktown Heights, NY, Manager/Research Staff Member, Interconnection Performance and Reliability Group, Semiconductor Research and Development Center (1991 - 1993).

IBM T.J. Watson Research Center, Research Staff Member, Ceramic Materials Group, System Technology and Science Department (1987 - 1991).

IBM T.J. Watson Research Center, Postdoctoral Fellow, Exploratory Packaging Materials and Processes Group, Semiconductor Science and Technology Department (1986-1987).

University of California, Berkeley, CA, Graduate Student Research Assistant (1981-1985).

Lawrence Livermore National Laboratory, Livermore, CA, Research Assistant, Ceramic Science Group (1981).

Selected Publications (currently author/coauthor of 47 publications, 5 U.S. Patents)

T.P. Smith III, T.R. Dinger, D.C. Edelstein, J.R. Paraszczak, and T.H. Ning, "The Wiring Challenge: Complexity and Crowding," Future Trends in Microelectronics: Reflections on the Road to Nanotechnology, S. Luryi, J. Xu, and A. Zaslavsky, eds. NATO ASI Series, Vol. 323, Kluwer Academic Publishers, Boston, pp. 45-56, 1996.

T.R. Dinger, T.K. Worthington, W.J. Gallagher and R.L. Sandstrom, "Direct Observation of Electronic Anisotropy in Single-Crystal $Y_1Ba_2Cu_3O_x$," *Phys. Rev. Lett.*, 58, [25], 2687-2690(1987).

T.K. Worthington, W.J. Gallagher, and T.R. Dinger, "Anisotropic Nature of High-Temperature Superconductivity in Single-Crystal $Y_1Ba_2Cu_3O_{7-x}$," *Phys. Rev. Lett.*, 59, [10], 1160-1163(1987).

T.R. Dinger and S.W. Tozer, "Old Behaviour in New Materials," *Nature*, 332, 204, 17 March 1988.

T.R. Dinger, R.S. Rai and G. Thomas, "Crystallization Behavior of a Glass in the Y_2O_3 - SiO_2 -AlN System," *J. Am. Cer. Soc.*, 71, [4], 236-44(1988).

G.J. Dolan, G.V. Chandrashekhar, T.R. Dinger, C. Feild and F. Holtzberg, "Vortex Structure in $YBa_2Cu_3O_7$ and Evidence for Intrinsic Pinning," *Phys. Rev. Lett.*, 62, [7], 827-830(1989).

G.J. Dolan, F. Holtzberg, C. Feild, and T.R. Dinger, "Anisotropic Vortex Structure in $Y_1Ba_2Cu_3O_7$," *Phys. Rev. Lett.*, 62, [18], 2184-2187(1989).

T.R. Dinger, G.J. Dolan, D. Keane, T.R. McGuire, T.K. Worthington, R.M. Yandrofski and Y. Yeshurun, "Flux Pinning in Single-Crystal $\text{YBa}_2\text{Cu}_3\text{O}_{7-x}$," High Temperature Superconducting Compounds: Processing and Related Properties, Proceedings of the 1989 Symposium on High Temperature Superconducting Oxides: Processing and Related Properties, 118th Annual Meeting of TMS-AIME, Las Vegas, Nevada, February 27 - March 3, 1989, Edited by S.H. Whang and A. DasGupta, The Minerals, Metals & Materials Society, Warrendale, PA, 1989, pp. 23-40.

Awards

IBM Major Outstanding Technical Achievement Award - 2005

IBM Outstanding Technical Achievement Award - 2004

IBM Second Plateau Invention Achievement Award - 1994

IBM First Plateau Invention Achievement Award - 1991

IBM Outstanding Technical Achievement Award - 1989

IBM First Patent Application Award - 1989

Atlantic Richfield Foundation Fellowship (U.C. Berkeley) - 1985

Regent's Fellowship (U.C. Berkeley) - 1984

A.L. Ehrman Memorial Scholarship and S.M. Tasheira Scholarship (U.C. Berkeley) - 1982

Summa Cum Laude (Alfred University, College of Engineering, 1st in class) - 1981

Alcoa Scholarship (Alfred University) - 1981

Refractories Foundation Scholarship (Alfred University) - 1980

Kodak Scholarship (Alfred University) - 1979

Tredennick Scholarship - 1988 through 1981

Pennsylvania State University Scholar (declined) - 1997

National Merit Scholarship Competition finalist - 1977

Professional Organizations and Affiliations

Chairman, Technical Advisory Board, E2open Corporation

Association of Computing Machinery (ACM)

Institute of Electronics and Electrical Engineers (IEEE)

BRIEF ATTACHMENT AP

RECEIPT

IN THE UNITED STATES PATENT AND TRADEMARK OFFICE

In re Patent Application of

Applicants: Bednorz et al.

Serial No.: 08/479,810

Filed: June 7, 1995

For: NEW SUPERCONDUCTIVE COMPOUNDS HAVING HIGH TRANSITION
TEMPERATURE, METHODS FOR THEIR USE AND PREPARATION

Date: April 12, 2006

Docket: YO987-074BZ

Group Art Unit: 1751

Examiner: M. Kopec

Mail Stop: AF

Commissioner for Patents

P.O. Box 1450

Alexandria, VA 22313-1450



SECOND AMENDMENT AFTER FINAL REJECTION

Sir:

In response to the Final Office Action dated October 20, 2005 and the Advisory
Action dated December 28, 2005, please consider the following:

IN THE UNITED STATES PATENT AND TRADEMARK OFFICE

In re Patent Application of

Date: April 10, 2006

Applicants: Bednorz et al.

Docket: YO987-074BZ

Serial No.: 08/479,810

Group Art Unit: 1751

Filed: June 7, 1995

Examiner: M. Kopec

For: NEW SUPERCONDUCTIVE COMPOUNDS HAVING HIGH TRANSITION
TEMPERATURE, METHODS FOR THEIR USE AND PREPARATION

Commissioner for Patents

P.O. Box 1450

Alexandria, VA 22313-1450

AFFIDAVIT OF DENNIS NEWNS

UNDER 37 C.F.R. 1.132

Sir:

I, Dennis Newns, declare that:

1. I received a B. A. degree in Chemistry from Oxford University United Kingdom in 1964 and a Ph.D. degree in Theoretical Physical Chemistry from the University of London in 1967.

2. I am a theoretical solid state scientist. My resume and curriculum vitae are attached.
3. The USPTO response dated October 20, 2005 at page 4 regarding the subject application cites Schuller et al "A Snapshot View of High Temperature Superconductivity 2002" (report from workshop on High Temperature Superconductivity held April 5-8, 2002 in San Diego) which the examiner states "discusses both the practical applications and theoretical mechanisms relating to superconductivity."
4. The Examiner at page 4 of the Office Action cites page 4 of Schuller et al which states:

"Basic research in high temperature superconductivity, because the complexity of the materials, brings together expertise from materials scientists, physicists and chemists, experimentalists and theorists... It is important to realize that this field is based on complex materials and because of this materials science issues are crucial. Microstructures, crystallinity, phase variations, nonequilibrium phases, and overall structural issues play a crucial role and can strongly affect the physical properties of the materials. Moreover, it seems that to date there are no clear-cut directions for searches for new superconducting phases, as shown by the serendipitous discovery of superconductivity in MgB_2 . Thus studies in which the nature of chemical bonding and how this arises in existing superconductors may prove to be fruitful. Of course, "enlightened" empirical searches either guided by chemical and

materials intuition or systematic searches using well-defined strategies may prove to be fruitful. It is interesting to note that while empirical searches in the oxides gave rise to many superconducting systems, similar (probable?) searches after the discovery of superconductivity in MgB_2 have not uncovered any new superconductors. "

5. The Examiner at pages 4 -5 of the Office Action cites pages 5- 6 of Schuller et al which state:

"The theory of high temperature superconductivity has proven to be elusive to date. This is probably as much caused by the fact that in these complex materials it is very hard to establish uniquely even the experimental phenomenology, as well as by the evolution of many competing models, which seem to address only particular aspects of the problem. The Indian story of the blind men trying to characterize the main properties of an elephant by touching various parts of its body seems to be particularly relevant. It is not even clear whether there is a single theory of superconductivity or whether various mechanisms are possible. Thus it is impossible to summarize, or even give a complete general overview of all theories of superconductivity and because of this, this report will be very limited in its theoretical scope."

6. The Examiner at page 5 of the Office Action cites page 7 of Schuller et al which states:

"Thus far, the existence of, a totally new superconductor has proven impossible to predict from first principles. Therefore their discovery has been based largely on empirical approaches, intuition, and, even serendipity. This unpredictability is at the root of the excitement that the condensed matter community displays at the discovery of a new material that is superconducting at high temperature."

7. I am submitting this declaration to clarify what is meant by predictability in theoretical solid state science. All solid state materials, even elemental solids, present theoretical problems. That difficulty begins with the basic mathematical formulation of quantum mechanics and how to take into account all interactions that are involved in atoms having more than one electron and where the interactions between the atoms may be covalent, ionic or Van der Waals interactions. A theory of a solid is based on approximate mathematical formalisms to represent these interactions. A theoretical solid state scientist makes an assessment using physical intuition, mathematical estimation and experimental results as a guide to focus on features of the complex set of interactions that this assessment suggests are dominate in their effect on the physical phenomena for which the theorist is attempting to develop a theory. This process results in what is often referred to as mathematical formalism. This formalism is then applied to specific examples to determine whether the formalism produces computed results that agree with measured experimental results. This process can be considered a "theoretical experiment." For example, applying the theoretical formalism to a particular crystal

structure comprised of a particular set of atoms to compute a value of a desired property is in this context a “theoretical experiment.”

8. Even when a successful theoretical formalism is developed, that formalism does not produce a list of materials that have a particular property that is desired. Rather for each material of interest the same “theoretical experiment” must be conducted. Moreover, even if such a “theoretical experiment” indicates that the particular material investigated has the property, there is no assurance that it does without experimentally fabricating the material and experimentally testing whether it has that property.
9. For example, semiconductors have been studied both experimentally and theoretically for more than 50 years. The theory of semiconductors is well understood. A material is a semiconductor when there is a filled valence band that is separated from the next empty or almost empty valence band by an energy that is of the order of the thermal energy of an electron at ambient temperature. The electrical conductivity of the semiconductor is controlled by adding dopants to the semiconductor crystal that either add electrons to the empty valence band or remove electrons from the filled valence band. Notwithstanding this theoretical understanding of the physical phenomena of semiconductivity, that understanding does not permit either a theoretical or experimental solid state scientist to know *a priori* what materials will in fact be a semiconductor. Even with the well developed semiconductor theoretical formalisms, that theory cannot be asked the question “can you list for me all materials that will be a semiconductor?” Just as an experimentalist must do, the theoretical scientist must select a particular material for

examination. If the particular material already exists an experimentalist can test that material for the semiconducting property. If the particular material does not exist, the theoretical solid state scientist must first determine what the crystal structure will be of that material. This in of itself may be a formidable theoretical problem to determine accurately. Once a crystal structure is decided on, the theoretical formalism is applied in a "theoretical experiment" to determine if the material has the arraignment of a fully filled valence and an empty valence band with the correct energy spacing. Such a theoretical experiment generally requires the use of a computer to compute the energy band structure to determine if for the selected composition the correct band configuration is present for the material to be a semiconductor. This must be verified by experiment. Even with the extensive knowledge of semiconducting properties such computations are not 100% accurate and thus theory cannot predict with 100% accuracy what material will be a semiconductor. Experimental confirmation is needed. Moreover, that a theoretical computation is a "theoretical experiment" in the conceptual sense not different than a physical experiment. The theorist starting out on a computation, just as an experimentalist staring out on an experiment, has an intuitive feeling that, but does not know whether, the material studied will in fact be a semiconductor. As stated above solid state scientists, both theoretical and experimental, are initially guided by physical intuition based on prior experimental and theoretical work. Experiment and theory complement each other, at times one is ahead of the other in an understanding of a problem, but which one is ahead changes over time as an understanding of the physical phenomena develops.

10. This description of the semiconductor situation is for illustration of the capability of theory in solid state science where there is a long history of both experimental and theoretical developments.
11. Superconductivity was first discovered by H. Kammerlingh Onnes in 1911 and the basic theory of superconductivity has been known many years before Applicants' discovery. For example, see the book "Theory of Superconductivity", M. von Laue, Academic Press, Inc., 1952 (See Attachment AD of the Third Supplementary Amendment dated March 1, 2005). Prior to applicants' discovery superconductors were grouped into two types: Type I and Type II.
12. The properties of Type I superconductors were modeled successfully by the efforts of John Bardeen, Leon Cooper, and Robert Schrieffer in what is commonly called the BCS theory. A key conceptual element in this theory is the pairing of electrons close to the Fermi level into Cooper pairs through interaction with the crystal lattice. This pairing results from a slight attraction between the electrons related to lattice vibrations; the coupling to the lattice is called a phonon interaction. Pairs of electrons can behave very differently from single electrons which are fermions and must obey the Pauli exclusion principle. The pairs of electrons act more like bosons which can condense into the same energy level. The electron pairs have a slightly lower energy and leave an energy gap above them on the order of .001 eV which inhibits the kind of collision interactions which lead to ordinary resistivity. For temperatures such that the thermal energy is less than the band gap, the material exhibits zero resistivity.

13. There are about thirty pure metals which exhibit zero resistivity at low temperatures and have the property of excluding magnetic fields from the interior of the superconductor (Meissner effect). They are called Type I superconductors. The superconductivity exists only below their critical temperatures and below a critical magnetic field strength. Type I and Type II superconductors (defined below) are well described by the BCS theory.
14. Starting in 1930 with lead-bismuth alloys, a number of alloys were found which exhibited superconductivity; they are called Type II superconductors. They were found to have much higher critical fields and therefore could carry much higher current densities while remaining in the superconducting state.
15. Ceramic materials are expected to be insulators -- certainly not superconductors, but that is just what Georg Bednorz and Alex Muller, the inventors of the patent application under examination, found when they studied the conductivity of a lanthanum-barium-copper oxide ceramic in 1986. Its critical temperature of 30 K was the highest which had been measured to date, but their discovery started a surge of activity which discovered materials exhibiting superconducting behavior in excess of 125 K. The variations on the ceramic materials first reported by Bednorz and Muller which have achieved the superconducting state at much higher temperatures are often just referred to as high temperature superconductors and form a class of their own.
16. It is generally believed by theorists that Cooper pairs result in High T_c superconductivity. What is not understood is why the Cooper pairs remain together at the higher temperatures. A phonon is a vibration of the atoms about their

equilibrium positions in a crystal. As temperature increases these vibrations are more complex and the amplitude of these vibrations is larger. How the Cooper pairs interact with the phonons at the lower temperature, when these oscillations are less complex and of lower amplitude, is understood, this is the BCS theory. Present theory is not able to take into account the more complex and larger amplitude vibrations that occur at the higher temperatures.

17. The article of Schuller referred to by the Examiner in paragraphs 4, 5 and 6 present essentially the same picture.
18. In paragraph 4 above Schuller states "Of course, 'enlightened' empirical searches either guided by chemical and materials intuition or systematic searches using well-defined strategies may prove to be fruitful. It is interesting to note that while empirical searches in the oxides gave rise to many superconducting systems, similar (probable?) searches after the discovery of superconductivity in MgB_2 have not uncovered any new superconductors." Schuller is acknowledging that experimental researchers using intuition and systematic searches found the other known high T_c superconductors. Systematic searching is applying what is known to the experimental solid state scientist, that is, knowledge of how to fabricate compounds of the same class as the compounds in which Bednorz and Muller first discovered High T_c superconductivity. That a similar use of intuition and systematic searching "after the discovery of superconductivity in MgB_2 have not uncovered any new superconductors" is similar to a "theoretical experiment" that after the computation is done does not show that the material studied has the property being investigated, such as semiconductivity. The Schuller article was published in April 2002

approximately one year after the experimental discovery of superconductivity in MgB_2 was reported on in March 2001 (Reference 8 of the Schuller article. See paragraph 19 of this affidavit.) This limited time of only one year is not sufficient to conclude that systematic searching "after the discovery of superconductivity in MgB_2 " cannot uncover any new superconductors. Experimental investigations of this type are not more unpredictable than theoretical investigations since the experimental investigation has a known blue print or course of actions, just as does a "theoretical experiment." Just as an physical experimental investigation may lead to a null result a "theoretical experiment" may lead to a null result. In the field of High T_c superconductivity physical experiment is as predictable as a well developed theory since the experimental procedures are well known even though very complex. Experimental complexity does not mean the field of High T_c superconductivity is unpredictable since the methods of making these material are so well known.

19. In paragraph 4 above Schuler refers the discovery of MgB_2 citing the paper of Nagamatsu et al. Nature Vol. 410, March 2001 in which the MgB_2 is reported to have a T_c of 39 K, a layered graphite crystal structure and made from powders using know ceramic processing methods. MgB_2 has a substantially simpler structure than the first samples reported on by Bednorz and Muller and therefore can be more readily investigated theoretically. There have been recent reports by Warren Pickett of the University of California at Davis and by Marvin L. Cohen and Steven Louie at the University of California at Berkeley describing progress in a theoretical understanding of the T_c of MgB_2 . It is not surprising that progress in the theory of

superconductivity at 39 K has been made based on this relatively simple material.

In fact a few months after the Schuller article was published in April 20002 Marvin

.L. Cohen and Steven Louie were authors on an article Choi, HJ; Roundy, D; Sun,

H; Cohen, ML; Louie, SG "First-principles calculation of the superconducting

transition in MgB_2 within the anisotropic Eliashberg formalism " PHYSICAL REVIEW

B; JUL 1, 2002; Vol. 66; p 20513. The following is from the Abstract of this article:

" We present a study of the superconducting transition in MgB_2 using the ab initio pseudopotential density-functional method, a fully anisotropic Eliashberg equation, and a conventional estimate for μ^* . Our study shows that the anisotropic Eliashberg equation, constructed with ab initio calculated momentum-dependent electron-phonon interaction and anharmonic phonon frequencies, yields an average electron-phonon coupling constant $\lambda=0.61$, a transition temperature $T_c=39$ K, and a boron isotope-effect exponent $\alpha(B)=0.32$. The calculated values for T_c , λ , and $\alpha(B)$ are in excellent agreement with transport, specific-heat, and isotope-effect measurements, respectively. The individual values of the electron-phonon coupling $\lambda(k,k')$ on the various pieces of the Fermi surface, however, vary from 0.1 to 2.5. The observed T_c is a result of both the raising effect of anisotropy in the electron-phonon couplings and the lowering effect of anharmonicity in the relevant phonon modes." (Emphasis added)

Thus the statement of the Schuller article in paragraph 5 above "The theory of high temperature superconductivity has proven to be elusive to date" is not totally accurate since shortly after the publication of the Schuller article a theory of the T_c of MgB_2 was published by Marvin .L. Cohen and Steven Louie.

A month later they expanded on this in the article Choi, HJ; Roundy, D; Sun, H; Cohen, ML; Louie, SG "The origin of the anomalous superconducting properties of MgB_2 " NATURE, AUG 15, 2002;Vol 418; pp 758-760. The following is from the Abstract of this article:

" Magnesium diboride ... differs from ordinary metallic superconductors in several important ways, including the failure of conventional models ... to predict accurately its unusually high transition temperature, the effects of isotope substitution on the critical transition temperature, and its

anomalous specific heat A detailed examination of the energy associated with the formation of charge-carrying pairs, referred to as the 'superconducting energy gap', should clarify why MgB_2 is different. Some early experimental studies have indicated that MgB_2 has multiple gaps.... Here we report an ab initio calculation of the superconducting gaps in MgB_2 and their effects on measurable quantities. An important feature is that the electronic states dominated by orbitals in the boron plane couple strongly to specific phonon modes, making pair formation favourable. This explains the high transition temperature, the anomalous structure in the specific heat, and the existence of multiple gaps in this material. Our analysis suggests comparable or higher transition temperatures may result in layered materials based on B, C and N with partially filled planar orbitals. (Emphasis added)

Thus the statement in the Schuller article in paragraph 5 above "Thus far, the existence of, a totally new superconductor has proven impossible to predict from first principles" was shown by the work of Marvin .L. Cohen and Steven Louie published shortly after the article of Schuller also to be not totally accurate.

20. In paragraph 5 above Schuller states "The theory of high temperature superconductivity has proven to be elusive to date." As stated above although solid state theorist believe that Cooper Pairs are the mechanism of the High T_c superconductors, we do not as of yet completely understand how to create a mathematical formalism that takes into account the atomic vibrations at these higher temperatures to theoretically permit that electrons to remain paired.

21. In paragraph 5 above Schuller further states "This is probably as much caused by the fact that in these complex materials it is very hard to establish uniquely even the experimental phenomenology." Even though these materials are complex that complexity does not have to be understood to make these material since experimental solid state scientists well understand the method of making these materials. The book "Copper Oxide Superconductors" by Charles P. Poole, Jr.,

Timir Datta and Horacio A. Farach, John Wiley & Sons (1998), [(See Attachment 23 of The Fifth Supplemental Amendment dated March 1, 2004)] referred to herein as Poole 1988 states in Chapter 5 entitled "Preparation and Characterization of Samples" states at page 59:

"Copper oxide superconductors with a purity sufficient to exhibit zero resistivity or to demonstrate levitation (Early) are not difficult to synthesize. We believe that this is at least partially responsible for the explosive worldwide growth in these materials".

Poole et al. further states at page 61:

"In this section three methods of preparation will be described, namely, the solid state, the coprecipitation, and the sol-gel techniques (Hatfi). The widely used solid-state technique permits off-the-shelf chemicals to be directly calcined into superconductors, and it requires little familiarity with the subtle physicochemical process involved in the transformation of a mixture of compounds into a superconductor."

22. It is thus clear that experimentalists knew, at the time of Benor and Muller's discovery, how to make the High T_c class of material and that to do so it was not necessary to precisely understand the experimental phenomenology.

23. Charles Poole et al. published another book in 1995 entitled "Superconductivity" Academic Press which has a Chapter 7 on "Perovskite and Cuprate Crystallographic Structures". (See Attachment Z of the First Supplementary Amendment dated

March 1, 2005). This book will be referred to as Poole 1995. At page 179 of Poole 1995 states:

"V. PEROVSKITE-TYPE SUPERCONDUCTING STRUCTURES

In their first report on high-temperature superconductors Bednorz and Müller (1986) referred to their samples as "metallic, oxygen-deficient ... perovskite-like mixed-valence copper compounds." Subsequent work has confirmed that the new superconductors do indeed possess these characteristics."

24. Thus Poole 1988 states that the high T_c superconducting materials "are not difficult to synthesize" and Poole 1995 states that "the new superconductors do indeed possess [the] characteristics" that Applicants' specification (the patent application currently under examination) describes these new superconductors to have.

25. In paragraph 5 above Schuller states:

"The theory of high temperature superconductivity has proven to be elusive to date. This iscaused by the fact ... the evolution of many competing models, which seem to address only particular aspects of the problem. The Indian story of the blind men trying to characterize the main properties of an elephant by touching various parts of its body seems to be particularly relevant. It is not even clear whether there is a single theory of superconductivity or whether various mechanisms are possible. Thus it is impossible to summarize, or even give a complete general overview of all theories of superconductivity and because of this, this report will be very limited in its theoretical scope."

The initial development of a theory always considers the problem from many different aspects until the best and most fruitful approach is realized. That at this time "It is not even clear whether there is a single theory of superconductivity or whether various mechanisms are possible" does not mean that experimental solid state scientists do not know how to make this class of High T_c materials. As stated by Poole 1988 and Poole 1995 the experimental solid state scientist does know how to make this class of High T_c materials.

26. The Examiner at page 5 of the Office Action cites page 7 of Schuller et al which states:

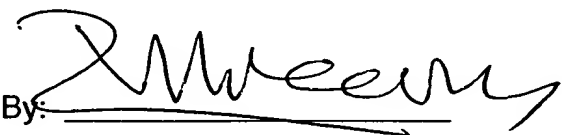
"Thus far, the existence of, a totally new superconductor has proven impossible to predict from first principles. Therefore their discovery has been based largely on empirical approaches, intuition, and, even serendipity. This unpredictability is at the root of the excitement that the condensed matter community displays at the discovery of a new material that is superconducting at high temperature."

A first principles theory that accurately predicts all physical properties of a material does not exist for as simple a material as water in its solid form as ice which may very well be the most extensively studied solid material. Most theories of solid state materials have phenomenological components that are approximations based on empirical evidence. As stated above solid state theoretical scientists have not as of yet formulated a theoretical formalism that accounts for electrons remaining paired as Cooper pairs at higher temperatures. But this does not prevent experimental scientists from fabricating materials that have structurally similar properties to the

materials first discovered by Bednorz and Muller. This is particularly true since the basic theory of superconductivity were also well known at the time of their discovery and the methods of making these materials was well known at the time of their discovery. It was not necessary at the time of their discovery to have the specific theoretical mechanism worked out in detail in order to make samples to test for High Tc superconductivity. Even Schuller acknowledges "empirical searches in the oxides gave rise to many superconducting systems."

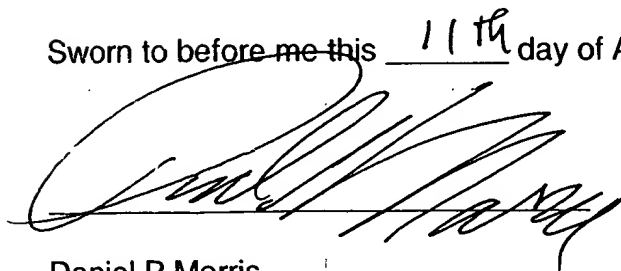
27. I hereby declare that all statements made herein of my knowledge are true and that all statements made on information and belief are believed to be true; and further, that these statements were made with the knowledge that willful false statements and the like so made are punishable by fine or imprisonment, or both, under Section 1001 of Title 18 of the United States Code and that such willful false statements made jeopardize the validity of the application or patent issued thereon.

Date: 04/11/06

By: 

Dennis Newns

Sworn to before me this 11th day of April _____, 2006.



Daniel P Morris

DANIEL P. MORRIS
NOTARY PUBLIC, State of New York
No. 4888676
Qualified in Westchester County
Commission Expires March 16, 192007

Dr. Dennis M. Newns

Address: Physical Science Division, IBM T.J. Watson Laboratory, Yorktown Hgts, NY.

Phone: (914) 945-3014

E-mail: dennisn@us.ibm.com

Professional Preparation and Appointments

1986-Present Physical Science Division, IBM T.J. Watson Laboratory.

1981 Reader, Imperial College London.

1971 Lecturer, Imperial College London.

1969 Postdoctoral Fellow, Department of Physics, Cambridge University.

1967 Postdoctoral Fellow, James Franck Institute, University of Chicago.

1967 Ph.D, Imperial College London.

Relevant Publications

1. "Polaronic Effects in Mixed and Intermediate Valence Compounds",
D.M. Newns and A. C. Hewson,
J. Phys. C, 12 1665 (1979).
2. "Mott transition field effect transistor",
D.M. Newns, J.A. Misewich, and C.C. Tsuei,
Appl. Phys. Lett. 73 780 (1998).
3. "Room-temperature ferromagnetic nanotubes controlled by electron or hole doping",
L. Krusin-Elbaum, D.M. Newns and H. Zeng,
Nature 431 672 (2004).
4. "Charge-exchange in atom-surface scattering - thermal versus quantum-mechanical non-adiabaticity",
R. Brako and D.M. Newns,
Surf. Sci. 108 253 (1981).
5. "Desorption induced by multiple electronic-transitions",
JA Misewich, TF Heinz and D.M. Newns,
Phys. Rev. Lett. 68 3737 (1992).

Significant Publications

1. "On the solution of the Coqblin-Schrieffer Hamiltonian by the large-N expansion technique", N. Read and D.M. Newns, *J. Phys. C* **16** 3273 (1983).
2. "Anomalous isotope effect and vanhove singularity in superconducting Cu oxides", C.C. Tsuei, D.M. Newns and C.C. Chi, *Phys. Rev. Lett.* **65** 2724-2727 (1990).
3. "Effect of parallel velocity on charge fraction in ion-surface scattering", J. Vanwunnik, R. Brako, K. Makoshi and D.M. Newns, *Surf. Sci.* **12** 618-623 (1983).
4. "Quasi-classical transport at a van hove singularity in cuprate superconductors", D.M. Newns, C.C. Tsuei and R.P. Huebener, *Phys. Rev. Lett.* **73** 1695-1698 (1994).
5. "Self-Consistent Model of Hydrogen Chemisorption" D. Newns, *Phys. Rev.* **178** 1123-1135 (1969).

Synergistic Activities

1. Work with undergraduate and high school interns as part of the IBM summer research program.
2. Interact with students at APS March meeting lunches.

Recent Collaborators

W. Donath, M. Shabes, B. Lengfield, M. Eleftheriou, P. Pattnaik, C. Zhou, I. Morgenstern, T. Husslein, P.B. Moore, Q.F. Zhong, L. Krusin-Elbaum, H. Zeng, H.J. Wen, R. Ludeke, T. Doderer, M.L. Klein, J.A. Misewich, C.C. Tsuei, and G.J. Martyna.

Graduate and Postdoctoral Advisors

Thesis Advisor : E.P. Wohlfarth, Imperial College, London.

Postdoctoral Advisor : P.W. Anderson, University of Chicago.

Postdoctoral Advisor : P.W. Anderson, Princeton University.

BRIEF ATTACHMENT AQ

RECEIPT

IN THE UNITED STATES PATENT AND TRADEMARK OFFICE

In re Patent Application of

Applicants: Bednorz et al.

Serial No.: 08/479,810

Filed: June 7, 1995

For: NEW SUPERCONDUCTIVE COMPOUNDS HAVING HIGH TRANSITION
TEMPERATURE, METHODS FOR THEIR USE AND PREPARATION

Date: April 12, 2006

Docket: YO987-074BZ

Group Art Unit: 1751

Examiner: M. Kopec

Mail Stop: AF

Commissioner for Patents

P.O. Box 1450

Alexandria, VA 22313-1450



SECOND AMENDMENT AFTER FINAL REJECTION

Sir:

In response to the Final Office Action dated October 20, 2005 and the Advisory
Action dated December 28, 2005, please consider the following:

IN THE UNITED STATES PATENT AND TRADEMARK OFFICE

In re Patent Application of

Applicants: Bednorz et al.

Serial No.: 08/479,810

Filed: June 7, 1995

Date: February 2, 2006

Docket: YO987-074BZ

Group Art Unit: 1751

Examiner: M. Kopec

For: NEW SUPERCONDUCTIVE COMPOUNDS HAVING HIGH TRANSITION
TEMPERATURE, METHODS FOR THEIR USE AND PREPARATION

Commissioner for Patents
P.O. Box 1450
Alexandria, VA 22313-1450

DECLARATION OF GEORG BEDNORZ
UNDER 37 C.F.R. 1.132

Sir:

I, J.Georg Bednorz , declare that:

1. I am a coinventor of the referenced application.
2. I received a M. S. Degree in Mineralogy/Crystallography (1976) from the University of Muenster in Germany and a Ph.D. degree in Natural Science (1982) from the Swiss Federal Institute of Technology (ETH) in Zuerich - Switzerland.

3. The USPTO response dated October 20, 2005 at page 7 cites the following web page <http://www.nobelchannel.com/learningstudio/introduction.sps?id=295&eid=0>

Which states

It is worth noting that there is no accepted theory to explain the high-temperature behavior of this type of compound. The BCS theory, which has proven to be a useful tool in understanding lower-temperature materials, does not adequately explain how the Cooper pairs in the new compounds hold together at such high temperatures. When Bednorz was asked how high-temperature superconductivity works, he replied, "If I could tell you, many of the theorists working on the problem would be very surprised."

4. This declaration is to explain the meaning of the statement attributed to me "If I could tell you, many of the theorists working on the problem would be very surprised" in response to a question from the interviewer about the mechanism of High Tc superconductivity.

5. Following the discovery of the High Tc superconductivity in oxides by my coinventor Alex Mueller and me, the enormous research effort conducted by experimentalist specialized in different disciplines of solid state science created a very complex scenario. After our discovery new layered perovskite-like CuO-compounds with comparable and higher Tc were discovered of the type that are reported on in our original publication and that are described in our patent application. These new materials were made according to known principles of ceramic science that we described in our patent application. The rapid experimental developments were guided by previous work on materials having related the composition and structure. This enormous amount of new information collected over a short period of time made it hard to get a clear picture at that time of the experimental situation for both experimental specialists and theorists. In addition to showing superconductivity at temperatures higher than previously observed, this new information included novel and unusual properties, so far unexplained in the superconducting and normal state. I am an experimental scientist and in the field of solid state science, because of the complexities of theory and experiment, workers in the field are either experimentalist or theorist and typically not both. In this field, including the field of high Tc superconductivity, theory utilizes complex mathematical procedures about which theorists are experts. Thus theorists working in the field would have been surprised if, I, as an experimentalist, had been the sole person in the field to gain a sufficient overview and experimental and theoretical insight, to propose a final theory of high temperature superconductivity at this early stage of research.

6. I hereby declare that all statements made herein of my knowledge are true and that all statements made on information and belief are believed to be true; and further, that these statements were made with the knowledge that willful false statements and the like so made are punishable by fine or imprisonment, or both, under Section 1001 of Title 18 of the United States Code and that such willful false statements made jeopardize the validity of the application or patent issued thereon.

Date:

Feb. 24 / 2006

By:

J. Georg Bednorz
J. Georg Bednorz

BRIEF ATTACHMENT AR

IN THE UNITED STATES PATENT AND TRADEMARK OFFICE

In re Patent Application of

Applicants: Bednorz et al.

Serial No.: 08/479,810

Filed: June 7, 1995

Date: March 1, 2004

Docket: YO987-074BZ

Group Art Unit: 1751

Examiner: M. Kopec

For: NEW SUPERCONDUCTIVE COMPOUNDS HAVING HIGH TRANSITION
TEMPERATURE, METHODS FOR THEIR USE AND PREPARATION

Commissioner for Patents
P.O. Box 1450
Alexandria, VA 22313-1450

FIFTH SUPPLEMENTAL AMENDMENT

Sir:

In response to the Office Action dated February 4, 2000:

ATTACHMENT 57

AR



UNITED STATES DEPARTMENT OF COMMERCE
Patent and Trademark Office

Address: COMMISSIONER OF PATENTS AND TRADEMARKS
Washington, D.C. 20231

SERIAL NUMBER	FILING DATE	FIRST NAMED INVENTOR	ATTORNEY-DOCKET NO.
07/053,307	05/22/87	HELNOK7	Y0987-074

EXAMINER
6078, J

J. DAVID ELLETT
JRM INTELLECTUAL PROPERTY LAW DEPT.
P.O. BOX 218
YORKTOWN HEIGHTS, NY 10568

ART UNIT	PAPER NUMBER
	115

DATE RATED: 04/25/91

DUE 7/25/91

☒ This application has been examined ☒ Responsive to communication filed on 2/13/91 ☒ This action is made final.

A shortened statutory period for response to this action is set to expire 3 month(s), days from the date of this letter. Failure to respond within the period for response will cause the application to become abandoned. 35 U.S.C. 133

Part I THE FOLLOWING ATTACHMENT(S) ARE PART OF THIS ACTION:

- | | |
|-------------------------------------------------------------------------------------|---------------------------------------------------------------------------------|
| 1. <input type="checkbox"/> Notice of References Cited by Examiner, PTO-892. | 2. <input type="checkbox"/> Notice re Patent Drawing, PTO-848. |
| 3. <input type="checkbox"/> Notice of Art Cited by Applicant, PTO-1449. | 4. <input type="checkbox"/> Notice of Informal Patent Application, Form PTO-152 |
| 5. <input type="checkbox"/> Information on How to Effect Drawing Changes, PTO-1474. | 6. <input type="checkbox"/> |

Part II SUMMARY OF ACTION

1. ☒ Claims 1-95 are pending in the application.
Of the above, claims 12-26, 36-39, 55-59, + 64 are withdrawn from consideration.
2. ☐ Claims have been cancelled.
3. ☐ Claims are allowed.
4. ☒ Claims 1-11, 27-35, 40-54, 60-63 + 65-68 are rejected.
5. ☐ Claims are objected to.
6. ☐ Claims are subject to restriction or election requirement.
7. ☐ This application has been filed with informal drawings under 37 C.F.R. 1.85 which are acceptable for examination purposes.
8. ☐ Formal drawings are required in response to this Office action.
9. ☐ The corrected or substitute drawings have been received on Under 37 C.F.R. 1.84 these drawings are ☐ acceptable; ☐ not acceptable (see explanation or Notice re Patent Drawing, PTO-848).
10. ☐ The proposed additional or substitute sheet(s) of drawings, filed on has (have) been ☐ approved by the examiner; ☐ disapproved by the examiner (see explanation).
11. ☐ The proposed drawing correction, filed has been ☐ approved; ☐ disapproved (see explanation).
12. ☐ Acknowledgement is made of the claim for priority under U.S.C. 119. The certified copy has ☐ been received ☐ not been received ☐ been filed in parent application, serial no. filed on
13. ☐ Since this application appears to be in condition for allowance except for formal matters, prosecution as to the merits is closed in accordance with the practice under Ex parte Quayle, 1935 C.D. 11; 453 O.G. 213.
14. ☐ Other

1. Applicant's election with traverse of Group I in Paper No. 22 is acknowledged. The traversal is on the ground(s) that the claims of Groups I, II and III are not distinct. This is not found persuasive because the Examiner maintains that the superconductive product, process of making and method of use are directed to patentally distinct inventions. Although there are broad "process" and "method" claims that appear to encompass a great deal of subject matter, the limitations in the dependent claims distinguish the claims of the Groups I, II and III.

The requirement is still deemed proper and is therefore made FINAL.

2. The objection to the specification and objection of claims 1-11, 27-35, 40-54, 60-63 and 65-68 under 35 USC 112, first paragraph, is maintained.

3. The following is a quotation of the first paragraph of 35 U.S.C. § 112:

The specification shall contain a written description of the invention, and of the manner and process of making and using it, in such full, clear, concise, and exact terms as to enable any person skilled in the art to which it pertains, or with which it is most nearly connected, to make and use the same and shall set forth the best mode contemplated by the inventor of carrying out his invention.

The specification is objected to under 35 U.S.C. § 112, first paragraph, as failing to provide an enabling disclosure commensurate with the scope of the claims.

4. The Applicants assert that "the scope of the claims as presently worded is reasonable and fully merited" (page 17 of

Serial No. 07/53,307

-3-

Art Unit 115

response). The Examiner disagrees. The present claims are broad enough to include a substantial number of inoperable compositions.

5. The rejection of claims 1-11, 27-35, 40-54, 60-63 and 65-68 under 35 USC 112, second paragraph is maintained.

6. Claims 1-11, 27-35, 40-54, 60-63 and 65-68 are rejected under 35 U.S.C. § 112, second paragraph, as being indefinite for failing to particularly point out and distinctly claim the subject matter which applicant regards as the invention.

7. The amended term "rare earth-like" is vague. With respect to the lack of stoichiometry, Applicants argue the superconductive properties can be measured as the composition is varied. This is unpersuasive because the present claims broad enough to require an undue amount of experimentation.

8. The Examiner maintains that the term "doping" is vague. Neither the claim or the specification discuss the limits of the effective amounts of doping.

9. The Applicants assert that a discussion of "electron-phonon interactions to produce superconductivity" is found in the specification. The Examiner maintains that the term is not adequately explained. The specification fails to teach how one determines how to enhance the "electron-phonon" interactions?

10. The term "at least four elements" is indefinite considering the number of elements in the periodic table.

Serial No. 07/53,307

-4-

Art Unit 115

11. The rejection of claims 1-11, 27-35, 40-54, 60-63 and 65-68 under 35 USC 102/103 is maintained.

12. Claims 1-11, 27-35, 40-54, 60-63 and 65-68 are rejected under 35 U.S.C. § 102(b) as anticipated by or, in the alternative, under 35 U.S.C. § 103 as obvious over each of Shaplygin et.al., Nguyen et.al., Michel et.al. (Mat. Res. Bull. and Revue de Chimie).

13. The Applicants argue that "no prima facie case has been made that the composition anticipates or renders obvious the subject matter" (page 28 of response). The Examiner maintains that these materials appear to be identical to those presently claimed except that the superconductive properties are not disclosed. Applicants have not provided any evidence that the compositions of the cited references are in any way excluded by the language of the present claims, i.e. Applicants have failed to show that these materials are not superconductive. Applicant's composition claims do not appear to exclude these materials.

14. Applicants further argue that under United States patent law they are entitled to claim compositions which might happen to overlap a portion of the concentration ranges broadly recited in the cited references. "The broad statement of a concentration range in the prior art does not necessarily preclude later invention within the concentration range" (page 29 of response). The Examiner fails to understand how Applicant's incredibly broad claims, some of

Serial No. 07/53,307

-5-

Art. Unit 115

which require only the presence of a "doped transition metal oxide" (see claim 42), in anyway fall "within" the scope of the compositions disclosed in the prior art. The cited references disclose very specific compositions that not only fall within the scope of the claims, but appear to be identical to those compositions disclosed in the specification as being superconducting. The Examiner maintains that these materials are inherently superconductive and therefore render the claim unpatentable.

15. With respect to Applicants arguments under 35 USC 103 regarding the "question of non-analogous art" and the assertion the cited prior art is irrevelant to the present claim, the Examiner maintains that for the present "composition" claims the references directed to what appear to be identical materials (both in composition and inherent properties) are clearly relevant. The cited individual disclosures appear to be sufficient to maintain the rejection, the Examiner is not relying on any secondary references to modify the teachings in the references.

16. The rejection of claims 1-2, 5-11, 40-44, 46, 48, 51-54, 60, 62 and 66 under 35 USC 102/103 is maintained.

17. Claims 1-2, 5-11, 40-44, 46, 48, 51-54, 60, 62 and 66 are rejected under 35 U.S.C. § 102(b) as anticipated by or, in the alternative, under 35 U.S.C. § 103 as obvious over each of Perron-

Serial No. 07/53,307

-6-

Art Unit 115

Simon et.al., Mossner et.al., Chincholkar et.al., Amad et.al.,
Blasse et.al., Kurihara et.al. and Anderton et.al.

18. This rejection is maintained for the reasons set forth in the previous paragraphs. The Examiner maintains that the cited references appear to disclose materials which inherently provide superconductive properties and therefore render the present claims unpatentable.

19. THIS ACTION IS MADE FINAL. Applicant is reminded of the extension of time policy as set forth in 37 C.F.R. § 1.136(a).

A SHORTENED STATUTORY PERIOD FOR RESPONSE TO THIS FINAL ACTION IS SET TO EXPIRE THREE MONTHS FROM THE DATE OF THIS ACTION. IN THE EVENT A FIRST RESPONSE IS FILED WITHIN TWO MONTHS OF THE MAILING DATE OF THIS FINAL ACTION AND THE ADVISORY ACTION IS NOT MAILED UNTIL AFTER THE END OF THE THREE-MONTH SHORTENED STATUTORY PERIOD, THEN THE SHORTENED STATUTORY PERIOD WILL EXPIRE ON THE DATE THE ADVISORY ACTION IS MAILED, AND ANY EXTENSION FEE PURSUANT TO 37 C.F.R. § 1.136(a) WILL BE CALCULATED FROM THE MAILING DATE OF THE ADVISORY ACTION. IN NO EVENT WILL THE STATUTORY PERIOD FOR RESPONSE EXPIRE LATER THAN SIX MONTHS FROM THE DATE OF THIS FINAL ACTION.

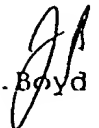
Any inquiry concerning this communication or earlier communications from the examiner should be directed to John Boyd whose telephone number is (703) 308-3314.

Any inquiry of a general nature or relating to the status of this application should be directed to the Group receptionist whose telephone number is (703) 308-0661.

Serial No. 07/53,307

-7-

Art Unit 115


J. Boyd

April 24, 1991

PAUL LIEBERMAN
SUPERVISORY PRIMARY EXAMINER
ART UNIT 115

BRIEF ATTACHMENT AS

IN THE UNITED STATES PATENT AND TRADEMARK OFFICE

In re Patent Application of

Applicants: Bednorz et al.

Serial No.: 08/479,810

Filed: June 7, 1995

Date: March 1, 2004

Docket: YO987-074BZ

Group Art Unit: 1751

Examiner: M. Kopec

For: NEW SUPERCONDUCTIVE COMPOUNDS HAVING HIGH TRANSITION
TEMPERATURE, METHODS FOR THEIR USE AND PREPARATION

Commissioner for Patents
P.O. Box 1450
Alexandria, VA 22313-1450

FIFTH SUPPLEMENTAL AMENDMENT

Sir:

In response to the Office Action dated February 4, 2000:

ATTACHMENT 39

Inorganic Chemistry

AN ADVANCED TEXTBOOK

THERALD MOELLER

*Associate Professor of Chemistry
University of Illinois*

New York · JOHN WILEY & SONS, Inc.

London · CHAPMAN & HALL, Limited

Attachment A pages

COPYRIGHT, 1952

BY

JOHN WILEY & SONS, INC.

All Rights Reserved

This book or any part thereof must not be reproduced in any form without the written permission of the publisher.

Library of Congress Catalog Card Number: 52-7487

PRINTED IN THE UNITED STATES OF AMERICA

Attachment A page 2

Emphasis up
quite generally
istry, inorganic
followed by the
istry, and, sub:
strongly empha
More recently,
inorganic chem
rather than up
remarkable the
and continue to
position that it

Unfortunately
expanded in a
university stud
their freshman
courses. Thes
dents with the
them of its sco
that is to be d
they have conc
technology. &
Sober reflectio
modern and ac

For a numb
semester lectur
the field from
existing probl
advanced und
At the gradua
upon which th
chemistry are
enrollments ar

Those who l
suitable textbo
sequence, they

clathrate compounds. In crystallized compounds, especially those of the type of ordinary compounds, the components are not free to escape. Each the compounds, CO_2 , CO , HCN , $(\text{p-H}_2\text{NC}_6\text{H}_4)_2$, $(\text{C}_6\text{H}_5\text{O})_2\text{SO}_2$, gas elements

ate compounds of importance

ponent. This crystal together, of suitable size,

may result from the crystal or

the time when

interest but are possible arrangements lead to them is

S

as of chemistry. on bond formation and its applicational combination. departure from not possess the considerations on-stoichiometric (1950); *Research*, 1,

ric compounds as opposed to the normal Daltonide or stoichiometric compounds. As examples, one may cite certain metallic hydrides such as $\text{VH}_{2.14}$, $\text{CeH}_{1.11}$ (p. 411); certain oxides such as $\text{TiO}_{1.7-1.8}$, $\text{FeO}_{1.044}$, $\text{WO}_{2.88-2.92}$; such sulfides, selenides, and tellurides as $\text{Cu}_{1.7}\text{S}$, $\text{Cu}_{1.6}\text{Se}$, $\text{Cu}_{1.6}\text{Te}$, $\text{CuFeS}_{1.94}$; the tungsten bronzes, Na_xWO_3 ; etc. Combinations of these types are particularly common among minerals.

Lack of true stoichiometry of this type is associated with so-called *defect crystal lattices*. Defects in a crystal lattice amount to variations from the regularity which characterizes the material as a whole. They are of two types:

1. *Frenkel defects*, in which certain atoms or ions have migrated to interstitial positions some distance removed from the "holes" which they vacated.
2. *Schottky defects*, in which "holes" are left in random fashion throughout the crystal because of migration of atoms or ions to the surface of the material.

Although both types of defect probably characterize crystals of non-stoichiometric compounds, the Schottky defects are the more important. Obviously detectable departure from true stoichiometric composition can result only if serious defects are present. It would follow, therefore, that many apparently stoichiometric compounds are not truly so. If excess metal is present in a crystal, it may also result from partial reduction of high-valent cations; whereas if excess non-metal is present, higher valent cations or lower valent anions than those normally present may be responsible. Many instances are known of multiple oxidation number in a single crystal. Non-stoichiometric compounds often show semi-conductivity, fluorescence, and centers of color. For a comprehensive discussion of this rather complex subject, a detailed review²² should be consulted.

SUMMARY OF BOND TYPES

The important linkages which hold together the components of crystalline solids and their general characteristics may be summarized as follows:

1. *Ionic linkages*, in which the crystals are made up of regular geometrical arrangements of positive and negative ions. Such solids tend to possess high melting and boiling points, are hard and difficult to deform, and tend to be soluble in polar solvents. When dissolved in such solvents or fused, they are excellent conductors. Crystals

²² J. S. Anderson: *Ann. Reports*, 43, 104 (1946).

Attachment A page 3

overcome. Such cage compounds have been called *clathrate* compounds²⁰ (Latin *clathratus*, enclosed by cross bars of a grating). In general, they occur when mixtures of the components are crystallized under optimum conditions. Their properties are roughly those of the enclosing material. Such compounds are stable at ordinary temperatures with respect to decomposition into their components, but melting or dissolution permits the enclosed component to escape. Examples are hydroquinone compounds which approach the composition $(C_6H_6O)_x \cdot X$ ($X = HCl, HBr, H_2S, CH_3OH, SO_2, CO_2, HCN$, etc.); amine compounds containing sulfurous acid, e.g. $(p-H_2NC_6H_4-NH_2)_x \cdot H_2SO_3$; phenol compounds, e.g. $(C_6H_5O)_x \cdot SO_2$, $(C_6H_5O)_x \cdot SO_3$, $(C_6H_5O)_x \cdot CO_2$; and certain compounds of the inert gas elements (pp. 382-383).

It is obvious that the conditions under which clathrate compounds can form are limited and highly specific. Among those of importance are:

1. An open crystal structure in the enclosing component. This necessitates directed linkages holding the molecule and crystal together, sufficient extension of the groups to form a cavity of suitable size, and a rigid structure.
2. Small access holes to the enclosed cavity. This may result from either proper disposition of groups in the formation of the crystal or sufficient surface area in the enclosing groups.
3. Ready availability of the trapped component at the time when the cavity is closed.

Such compounds are of considerable theoretical interest but are lacking in practical importance. Information on possible arrangements in clathrate compounds and the structures which lead to them is to be found in Powell's discussions.²⁰

NON-STOICHIOMETRIC COMPOUNDS

The law of definite proportions is one of the basic tenets of chemistry. Its validity is indicated by the restrictions imposed upon bond formation where electrons are involved as already outlined, and its application is generally the assumed basis for any type of chemical combination. There are, however, many instances of apparent departure from this rule among *solid* compounds. Such compounds do not possess the exact compositions which are predicted from electronic considerations alone and are commonly referred to as Berthollide or non-stoichiometric.

²⁰ H. M. Powell: *J. Chem. Soc.*, 1948, 61; *Endeavour*, 9, 154 (1950); *Research*, 1, 353 (1947-1948).

Attachment page 4

*Fundamentals
of
chemistry
a
modern
introduction*

FRANK BRESCIA

JOHN ARENTS

HERBERT MEISLICH

AMOS TURK

*Department of Chemistry
The City College of the
City University of New York*



ACADEMIC PRESS

New York and London

Attachment A page 5

*The text of this book was set in Monotype
MODERN 8A printed and bound by The Maple Press Company.
The book is printed on Thor Cote Plate by Bergstrom Paper
Company. The binding is Tonero offset cloth,
Arkwright-Intertaken Inc.
The design of the text and cover was created by Betty Binns.
The drawings are by F. W. Taylor.*

COPYRIGHT © 1966, BY ACADEMIC PRESS INC.
All rights reserved.

No part of this book may be reproduced in any form,
by photostat, microfilm, or any other means, without
written permission from the publishers.

ACADEMIC PRESS INC.
111 Fifth Avenue, New York, New York 10003

United Kingdom Edition published by
ACADEMIC PRESS INC. (LONDON) LTD.
Berkeley Square House, London W.1

Library of Congress catalog card number: 65-26049
First Printing, January, 1966
Second Printing, April, 1966

PRINTED IN THE UNITED STATES OF AMERICA

Attachment A page 6

matter: the mass of a chemically reacting system remains constant. This law is consistent with the data obtained with the most precise balances available. If matter is created or destroyed, the quantity is less than can be detected with the best available balance.

4.2 THE LAW OF DEFINITE PROPORTIONS

Analyses of compounds show that when elements form a given compound, they always combine in the same ratio by weight. For example, independently of the source or method of formation, silicon dioxide, SiO_2 , contains 46.7% by weight of silicon and 53.3% of oxygen. This knowledge is summarized in the *law of definite proportions: the weight composition of a given compound is constant.*

EXAMPLE 1 10.0 g of silicon dust, Si, is exploded with 100.0 g of oxygen, O_2 , forming silicon dioxide, SiO_2 . How many grams of SiO_2 are formed and how many grams of O_2 remain uncombined?

ANSWER Since 46.7 g of Si combines with 53.3 g of O_2 , the quantity of O_2 required per gram of Si is

$$\frac{53.3 \text{ g } \text{O}_2}{46.7 \text{ g Si}}$$

and, therefore, for 10.0 g of Si, the quantity of O_2 required is

$$10.0 \text{ g Si} \times \frac{53.3 \text{ g } \text{O}_2}{46.7 \text{ g Si}} = 11.4 \text{ g } \text{O}_2$$

Hence, the weight of SiO_2 formed is $10.0 \text{ g} + 11.4 \text{ g} = 21.4 \text{ g}$ and the weight of uncombined O_2 is $100.0 \text{ g} - 11.4 \text{ g} = 88.6 \text{ g}$.

4.3 THE ATOMIC THEORY

The weight relationships of substances participating in chemical reactions are clearly explained in terms of the atomic theory. Although John Dalton (1803) is generally recognized as the inventor of the theory, he was anticipated by other scientists, particularly William Higgins (1789). Thus, it appears that the law of multiple proportions (Section 4.4) was foreshadowed by Higgins and Dalton from their respective atomic theories. A verified prediction made by a theory constitutes the strongest argument in its favor. However, the novel and central point of Dalton's activities was the attempt to determine the relative weights of atoms. This goal focused attention upon the theory, and revealed a new field of human endeavor that ultimately made chemistry a systematized body of knowledge.

The assumptions of the atomic theory were

- (i) *The elements are composed of indivisible particles called atoms.*
- (ii) *All the atoms of a given element possess identical properties, for example, mass.*



BRIEF ATTACHMENT AT

IN THE UNITED STATES PATENT AND TRADEMARK OFFICE

In re Patent Application of

Applicants: Bednorz et al.

Serial No.: 08/479,810

Filed: June 7, 1995

For: NEW SUPERCONDUCTIVE COMPOUNDS HAVING HIGH TRANSITION
TEMPERATURE, METHODS FOR THEIR USE AND PREPARATION

Date: March 1, 2004

Docket: YO987-074BZ

Group Art Unit: 1751

Examiner: M. Kopec

Commissioner for Patents
P.O. Box 1450
Alexandria, VA 22313-1450

FIFTH SUPPLEMENTAL AMENDMENT

Sir:

In response to the Office Action dated February 4, 2000:

ATTACHMENT 42

AT

THEORY OF SUPERCONDUCTIVITY

By

M. von LAUE

Kaiser-Wilhelm-Institut für physikalische und Elektro-Chemie
Berlin—Dahlem

Translated by

LOTHAR MEYER

University of Chicago, Chicago, Illinois

and

WILLIAM BAND

The State College of Washington, Pullman, Washington



ACADEMIC PRESS INC., PUBLISHERS

New York, 1962

SYMBOLS

A	vector potential	H^0	external homogeneous magnetic field
a_p	undetermined constants, $p = 1, 2, \dots$	H_c	critical magnetic field
a	a numerical ratio	H_e	internal and external values of H
a_p	undetermined constants, $p = 1, 2, \dots$	$H_0(x)$	Hankel's function of x , first kind-zero order
B	magnetic induction	$H_1(x)$	Hankel's function of x , first kind first order
β	reciprocal penetration depth	I	electric current in a line or current in a surface
c	velocity of light	i	electric current density vector
C_m	closed curves $m = 1, 2, \dots$	i_α	components of i , $\alpha = 1, 2, 3$
c_N, c_S	specific heats per mol of normal and superconducting phases	i_1, i_2, i_3	i_1, i_2, i_3 , components of i , cartesian or polar
x	an undetermined multiplier	i_0	ohmic current density vector
D	electric displacement	i^*	supercurrent density vector
d	distance	i_m	maximum current density vector
δA	work done in virtual displacement	i_n	current density normal to a given surface element
δA	work done in material displacement	i_s	surface density of current
δF	change in free energy in virtual displacement	$(i \cdot G)$	scalar product of i and G
δn	virtual displacement of a surface element	i	square root of minus one
$d\sigma$	surface element	$I_n(x)$	Bessel functions, $n = 0, 1, 2$
ds	line element	k	complex wave number
$d\tau$	volume element	k_n	complex wave number for normal conductor
∂u	material displacement	K_n or K_y	total force on a surface element due to electromagnetic stress
∂V	potential energy change due to material displacement	K	force per unit volume in matter due to Maxwell-London stresses
E	electric field intensity	L	a length
E_0	electric field components, $a = 1, 2, 3$	λ	superconductivity constant
E	total energy	λ_{ab}	superconductivity tensor $a, \beta = 1, 2, 3$
E_0	amplitude of E waves	M	intensity of permanent magnetisation
$[E \times H]$	vector product of E and H	μ	magnetic permeability
ϵ	dielectric constant	N	number of superconducting electrons per cubic centimeter
F	free energy	n	unit normal vector
f_N, f_S	free energy per mol of normal and superconducting phases	n_i, n_s	unit normal vector directed inwards or outwards
F	force per unit area due to Maxwell stresses	ν	frequency (numerical)
G	free energy of supercurrent	P_n	force on surface due to London stresses
G_n	electromagnetic momentum associated with the supercurrent	p_{ap}	coefficients of induction $a, \beta = 1, 2, \dots$
γ	a numerical factor	p''	self-induction for superconductors
H	magnetic field intensity vector	p''	mutual induction between super- and normal conductor
H_1	components of H , $a = 1, 2, 3$	φ	azimuthal angle
		Φ	imaginary part of a complex function
		Φ	electrostatic or magnetostatic potential
		ψ	real part of a complex function
		Ψ	superconduction scalar potential
		Q	quantity of heat
		Q	cross cut in n -ply connected region
		Q	rate of flow of energy in radiation field

x

R_c real part of complex function
a radius

R, R_c

r, θ, φ internal and external radii
polar coordinates

ρ

charge density

ρ^0

charge density for ohmic current carriers
charge density for supercurrent carriers

s_N, s_s

entropy per mol in normal and superconducting phases
linear dimensions of a surface

S

S_C "period" of a multiple valued function on a curve C
equal to the flux of induction thru the loop C

σ

electric conductivity

σ_{ω}

electric conductivity tensor $\alpha, \beta = 1, 2, 3$

T

temperature in $^{\circ}K$

T_c

transition temperature for superconductivity

$T(E)$

Maxwell stress tensor

$T(H)$

Maxwell stress tensor

t

time

τ_a

numerical constants $a = 1, 2, \dots$

θ

latitude angle

θ_N, θ_s

Debye temperatures for normal and superconducting phases
The London stress tensor in superconductor $\alpha, \beta = 1, 2, 3$

U

total energy of the field

U

real part of complex function W

u

a general function of position and time

V

volume or potential

V

imaginary part of complex function W

v

electromotive force

w

resistance

ω

a complex function

ω

angular frequency

$W(\)$

differential operator for the telegrapher's equation

x, y, z

x_1, x_2, x_3

x

cartesian coordinates

χ

cartesian coordinates

χ

permeability

χ

a function in the complex plane

z

z

ζ

ζ

complex impedance

ζ

a function in the complex plane

ζ

a variable of integration

CHAPTER 1

Fundamental Facts

(a) Superconductivity was discovered in 1911 by Kamerlingh-Onnes.¹ He was the first to liquefy helium and so to produce temperatures below 10° K. With this new technique he was able to observe the continued decrease of the electrical resistance of metals with decreasing temperature. With mercury, in contrast to other metals, he was astonished to find that the resistance completely vanished, almost discontinuously, at about 4.2° K (Fig. 1-1). Today superconductivity is known in 18 other metals (see Table 1-1) whereas in others, e. g., gold and bismuth, the conductivity remains normal far below even 1° K. Many alloys and compounds can also become superconducting, in particular the frequently used niobium nitride which has a transition temperature as high as 20° K. However, among these latter substances hysteresis phenomena mentioned in the "Introduction" are so much more strongly evident that in testing the present theory we prefer to employ only the "good" superconductors, i. e., the pure elements.

In the ideal case the resistance vanishes completely and discontinuously at a transition temperature T_c . Actually the resistance-temperature curve does fall more sharply the more the specimen is like a single crystal and the smaller the measuring current used. Because the drop always occurs in a measurable temperature range, the experimental definition of the transition temperature is to some extent arbitrary. The temperature at which the direct-current resistance reaches one half of the value it had just before the drop is generally given as the transition temperature, because this can be measured accurately. However, a high-frequency investigation to be described in Chap. 16 (f) indicates that the foot of the curve where

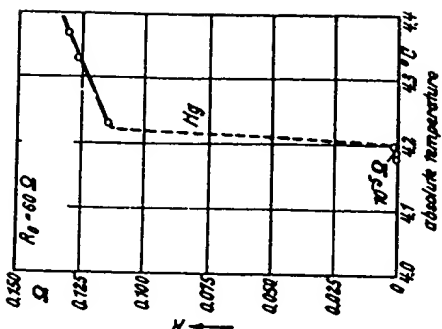


Fig. 1-1. Appearance of superconductivity in mercury according to H. Kamerlingh-Onnes (1911). The ordinate is the resistance R ; R_0 , the resistance of solid mercury extrapolated to 0° C, is 60 ohms.

¹H. Kamerlingh-Onnes, *Commun. Leiden*, 120b, 122b, 124c, (1911).

the d-c resistance becomes unmeasurably small represents the true transition point. Because of this uncertainty Table 1-1 quotes the transition points only to one-tenth of a degree.

Table 1-1

Superconducting Elements			
Name	Atomic Number	Transition Temperature	Crystallographic System
Aluminum	13	1.2 °K	Cubic
Titanium	22	0.5 °K	Cubic and hexagonal
Vanadium	23	4.3 °K	Cubic
Zinc	30	0.9 °K	Hexagonal
Gallium	31	1.1 °K	Rhombohedral
Zirconium	40	0.7 °K	Cubic and hexagonal
Niobium	41	9.2 °K	Cubic
Cadmium	48	0.6 °K	Hexagonal
Indium	49	3.4 °K	Tetragonal
Tin	50	3.7 °K	Tetragonal†
Lanthanum	57	4.7 °K	Cubic and hexagonal
Hafnium	72	0.3 °K	Hexagonal
Tantalum	73	4.4 °K	Cubic
Rhenium	75	0.9 °K	Hexagonal
Mercury	80	4.2 °K	Rhombohedral
Thallium	81	2.4 °K	Cubic and hexagonal
Lead	82	1.2 °K	Cubic
Thorium	90	1.4 °K	Cubic
Uranium	92	0.8 °K	Rhombohedral

* The atomic structure does not change during the transition from normal conductor to superconductor therefore the crystal class does not change either. The classes are defined according to Schoenflies.

† Besides the tetragonal white tin there exists a gray modification with a crystal structure of the diamond type which, however, does not become superconducting.

In order to obtain curves such as in Fig. 1-1, the resistance is calculated from the potential drop along a wire carrying a current. For this purpose the leads for the current, and are connected to a highly sensitive potentiometer. But if one merely wishes to verify the complete disappearance of the resistance below the transition temperature T_c , experiments with persistent currents, also due to Kamerlingh-Onnes,² are far more convincing and exact.

(b) One possible procedure is to place a ring or short-circuited coil in a magnetic field while its temperature is still above T_c , cool it down until superconductivity appears, and then remove it from the field. The induced

² H. Kamerlingh-Onnes, *Commun. Leiden*, 140b, 141b, (1914).

1. FUNDAMENTAL FACTS

3

electromotive force produces a current in the superconductor which will persist indefinitely unchanged in magnitude as long as superconductivity remains. The ring forms an ideal permanent magnet, and, when placed in an external homogeneous magnetic field, it experiences a torque corresponding to its magnetic moment. Two rings with persistent currents attract or repel each other, depending on their relative orientations, just as for ordinary currents, except that no emf's are needed to maintain them. It does not matter whether the rings are homogeneous or consist of several different superconductors, or whether their temperature is constant in space or time; it is only necessary that no part of the ring shall leave the superconducting state.³ Should this occur, the current is quenched almost instantaneously. For example, a ring carrying a persistent current may be cut at some point across which a galvanometer has been connected through normally conducting leads. Before the cut is made, the galvanometer will register zero current; but at the instant that the ring is broken, it will show a short current impulse. The energy of the persistent current, for the most part magnetic energy, is then transformed into Joule heat in the normally conducting wires.

A necessary condition for the existence of any persistent current is that the superconductor form a doubly connected body or, briefly, a ring, or more generally a multiply connected body. No persistent currents can exist in a simply connected body such as a sphere. Results that apparently contradict this arise because only parts of the specimen, among them doubly or multiply connected parts, may become superconducting, while the rest of the specimen remains either normal or in the intermediate state (see Chap. 12 (g) and 19). An electromagnet using the persistent current has been described by E. Justi.⁴

(c) In contrast to the normal current, which we shall call the ohmic current, the superconducting current (or supercurrent) does not penetrate very far into the specimen. It has been known for a long time that the superconductivity of thin tin films on copper or some other normally conducting metal, even down to a thickness of only 10^{-6} cm, does not differ from the superconductivity of thick tin wires. The contradictory evidence found by Burton⁵ using somewhat thinner films is outweighed by the observations of Shalnikov⁶ and by those of Appleyard and Misener⁷ using lead, tin, and mercury films as thin as 5×10^{-7} cm. These workers found practically the same transition temperatures as in the bulk metals, the small differences observed being within the experimental error.

The first quantitative estimates of the penetration depth of the supercurrent and its associated magnetic field derived from observational evidence,

³ It is fairly certain that temperature fluctuations have no effect because no investigator has ever mentioned any such effect.

⁴ E. Justi, *Elektronen*, Z., 68, 577 (1942).

⁵ E. F. Burton, *Nature*, 138, 459 (1934).

⁶ A. Shalnikov, *Nature*, 142, 74 (1938).

⁷ T. S. Appleyard and A. D. Misener, *Nature*, 142, 474 (1938).

were made by the author⁹ from the experimental results of Pontius using lead wires⁸ (Fig. 18-1). Appleyard, Bristow, and H. London¹⁰ and a year later Shoenberg¹¹ found the same order of magnitude, namely 10^{-6} cm, using films and spherical drops of mercury. This holds for temperatures within a few tenths of a degree below the transition temperature T_c . However, if we are within one-tenth of a degree of T_c , according to the above work of Shoenberg, the penetration depth increases suddenly and appears to become infinitely great at the transition point (see Fig. 11-3). This means that in a certain sense the electrical properties of the superconductor change continuously into those of the normal conductor. The measurements by McLennan, Burton, Pitt and Wilhelm¹² and H. London¹³ on the high-frequency resistance of superconductors also fit in with this concept: the resistance to rapid oscillations showed no discontinuity at the transition point, but joined smoothly at T_c with that of the high-frequency resistance of the normal conductor (Fig. 16-2).

(d) The transition from normal to superconductor does not change the form or the volume of the specimen; its lattice remains the same not only in its symmetry but also in its three lattice constants. This was proved for lead by Kamerlingh-Onnes and Keesom using x-ray analysis.¹⁴ The coefficient of thermal expansion (which incidentally is very small) does not change at the transition. Of special significance is the optical identity of the two phases, because in normal conductors the optical constants are intimately related to the electrical conductivity. The observations of Daunt, Keely, and Mendelssohn,¹⁵ of Hirschlaff,¹⁶ and of Hilsch¹⁷ revealed no difference in the appearance of the metal. One cannot tell by visual observation whether the metal is normal or superconducting.

(e) The relation between superconductivity and magnetic field is of the highest significance. The first steps toward disclosing this relation were made in 1913 by Kamerlingh-Onnes¹⁸ who noticed that at each temperature there existed a critical value H_c of the magnetic field that would destroy the superconductivity. We can obtain the simplest and clearest results by putting a wire in a longitudinal magnetic field, i. e.,

⁹M. V. Laue, *Ann. Physik*, **82**, 71, 253 (1938).

¹⁰R. B. Pontius, *Nature*, **189**, 1065 (1937).

¹¹T. S. Appleyard, T. R. Bristow, and H. London, *Nature*, **148**, 453 (1939).

¹²D. Shoenberg, *Nature*, **148**, 434 (1939).

¹³E. Laurmann and D. Shoenberg, *Nature*, **160**, 747 (1948).

¹⁴C. McLennan, A. C. Burton, A. Pitt, and J. O. Wilhelm, *Proc. Roy. Soc. (London)*, **186**, 52 (1932); **188**, 245 (1934).

¹⁵H. London, *Proc. Roy. Soc. (London)*, **176**, 522 (1940).

¹⁶W. H. Keesom and H. Kamerlingh-Onnes, *Commun. Leiden*, **174b** (1924).

¹⁷J. G. Daunt, T. C. Keely, and K. Mendelssohn, *Phil. Mag.*, **28**, 264 (1937).

¹⁸E. Hirschlaff, *Proc. Cambridge Phil. Soc.*, **88**, 140 (1937).

¹⁹R. Hilsch, *Physik. Z.*, **40**, 592 (1939).

²⁰H. Kamerlingh-Onnes, *Commun. Leiden Supplement* **85** (1913).

1. FUNDAMENTAL FACTS

parallel to the axis of the wire. The dependence of the a-c resistance on the magnetic field H for this case is shown in Fig. 1-2, while Fig. 1-3 shows the critical value of the magnetic field as a function of temperature for several metals.

Figure 1-4 shows an extrapolation of these curves down to the absolute zero of temperature according to a relation that is empirically confirmed in some cases:

$$H_c = a(T_c^2 - T^2)$$

At $T = 0$ the tangent of this curve is horizontal, as thermodynamics demands (Chap. 17). The maximum values of H_c at $T = 0$ lie between 100 and 1000 oersteds for pure metals and may be much higher for alloys and compounds.

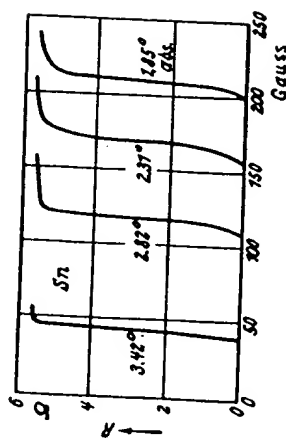


Fig. 1-2. Transition to superconductivity in a longitudinal magnetic field for tin at different temperatures. (After Steiner and Grassmann, *Supraleitung*, Braunschweig, 1937.)

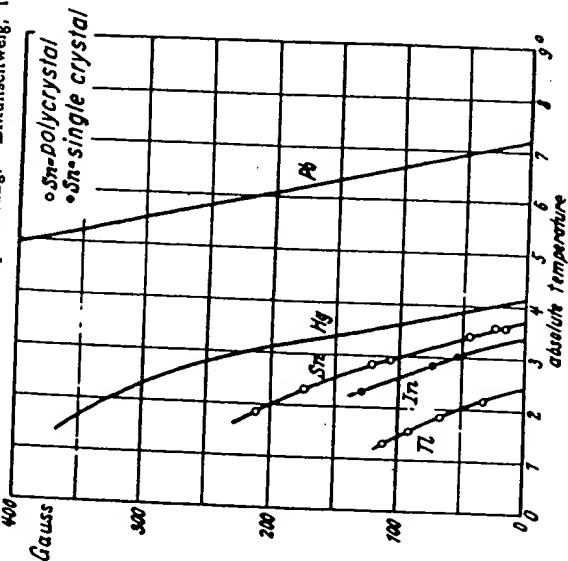


Fig. 1-3. Critical value of the magnetic field H_c as a function of temperature for different metals. (After Steiner and Grassmann, *Supraleitung*, Braunschweig, 1937.)

THE THEORY OF SUPERCONDUCTIVITY

A current I produces at the surface of a straight wire of radius R a magnetic field H :

$$H = \frac{I}{2\pi c R} \quad (1-1)$$

in Lorentz units, which we shall generally employ.¹⁹ We should therefore expect to find a critical value I_c of the current which would destroy superconductivity, and this has been confirmed by observation. According to eq. (1-1) the relation between I_c and H_c ought to be

$$I_c = 2\pi c R H_c \quad (1-2)$$

This was first pointed out by Silsbee,²⁰ and it is therefore called the Silsbee hypothesis. Most measurements do not agree with eq. (1-2), although in one case it has been confirmed by a very careful series of measurements by Shubnikov and Alexejevski.²¹ This is one of the weakest points in our understanding of superconductivity; a failure of eq. (1-2) means nothing less than a failure of the fundamental Maxwell relation connecting curl H and current density i . No one at present credits such a failure, and the theory developed here is based essentially on this equation. It is to be hoped that experimental work will soon be able to remove this uncertainty.

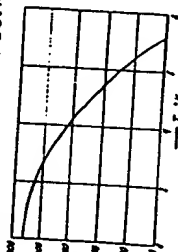


Fig. 1-4. Critical value of the magnetic field H_c as a function of temperature for lead (approximate curve).

essentially on this equation. It is to be hoped that experimental work will soon be able to remove this uncertainty.

(1) The earliest theory of superconductivity visualized the superconductor as simply a conductor with zero resistance. But on the Maxwell theory this assumption would have an important consequence; the interior of a perfect conductor would be completely shut off electromagnetically from any outside influence. If such a conductor were placed in a static magnetic induction, would diverge in front and converge behind as if going round a body of zero permeability (Fig. 1-5). But the result would be different were one to put the specimen in an external field while it was still above the transition temperature T_c , and then cool it in the field until the resistance disappeared. Above T_c , the lines of force would go through the metal without difficulty because the permeability of the metals under consideration is practically unity so long as they are in the normal state. This theory however asserts that the appearance of superconductivity cannot by itself alter the field. The lines of force would still go through the specimen undeviated. On the contrary, Meissner and Ochsenfeld²² showed in 1933 that the final

¹⁹ If I is measured in amperes and H in oersteds $H \approx 0.2 I/R$.

²⁰ F. B. Silsbee, *J. Washington Acad. Sci.*, 6, 597 (1916); Pap. Bureau of Standards 14, 307 (1917).

²¹ L. W. Shubnikov and N. E. Alexejevski, *Nature*, 188, 804 (1936).

²² W. Meissner and R. Ochsenfeld, *Naturwissenschaften*, 21, 787 (1933).

W. Meissner, *Physik. Z.*, 86, 931 (1934).

1. FUNDAMENTAL FACTS

state is in fact identical in the two cases — it does not depend on the previous history. In a singly connected superconductor everything is uniquely determined by its temperature and the apparatus producing the external field: in an n -ply connected body there is a possibility of $n - 1$ persistent currents and their magnetic fields whose strengths are optional within certain limits. But in any case the interior of a sufficiently thick superconductor is field free. The field-free state is the only state in such a superconductor.

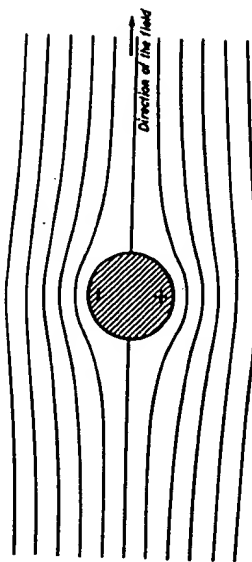


Fig. 1-5. The transverse field near a superconducting circular cylinder. The lines of force are plotted from the equation, in polar coordinates:

$$(r - R^2/\rho) \sin \theta = C \quad \text{for } C = 0, \pm 1/2 R, \pm R, \pm 3R/2, \pm 2R, \pm 5R/2, \dots$$

+ or — means the supercurrent flows toward or away from the reader respectively.

This fact permits us to interpret the super- and normal conductors as two phases of the same substance, whereas according to the older theory the state inside the superconductor was not determined intrinsically. Under this condition we can now apply thermodynamics to the equilibrium between the normal and the superconducting state (see Chap. 17). The London extension of the Maxwell theory is also based essentially on the expulsion of the field, called the Meissner effect.

(2) The older conception permitted us to calculate the field deformation near a thick superconductor accurately enough when the cooling precedes the application of the field. It showed that the distortion of the lines of force at certain points of the surface increases the field strength (see Fig. 1-5); for a superconducting sphere in a homogeneous field by a maximum factor $3/2$, for a circular cylinder in a transverse field by a factor 2, and for an elliptical cylinder with cross-sectional axes a and b by the factor $(1 + b/a)$ when the field is parallel to the a axis.

It was thus possible in 1932 — even before the Meissner discovery — for the author²³ to explain the fact that a transverse external field $1/2 H_c$ was sufficient to quench the superconductivity in a wire. It was also predicted that an elliptical cylinder would show a greater decrease of the apparent

²³ M. v. Laue, *Physik. Z.*, 88, 793 (1932).

critical value than a circular cylinder if the field were perpendicular to the greater axis; also for a sphere the apparent critical value would amount to $(2/3)H_c$ (see Chap. 10 (c) and (d), and Chap. 11). All these predictions were confirmed by an extensive series of measurements by de Haas and co-workers^{24, 25}. In this work it was also found that the most certain indication of the breakdown of superconductivity was not the reappearance of an ohmic resistance, but the appearance of a magnetic field in the interior of the specimen as detected by means of small bismuth wires placed in cavities in the specimen. The whole specimen does not immediately become normally conducting with the disappearance of superconductivity; instead the "intermediate state" almost always appears, a mechanical mixture of normal and superconducting parts (Chap. 19). As long as the latter form a connected path they take over the conduction of the current exclusively. (h) Finally our book will discuss thermal measurements, e. g., the heat required in the transition to normal from superconducting states, whenever this takes place in a magnetic field; or the specific heats of the normal and superconductors. But we shall postpone any more detailed discussion of this until Chap. 17 where the thermodynamics will reveal relations between these caloric phenomena and the critical magnetic field.

CHAPTER 2

Current Distribution Between Superconductors in Parallel

(a) If between two points of a normally conducting system there are n branches with resistances r_1, r_2, \dots, r_n , then the ratios of the direct currents

$$I_1 : I_2 : \dots : I_n = \frac{1}{r_1} : \frac{1}{r_2} : \dots : \frac{1}{r_n}$$

This rule of Kirchhoff's remains valid when one branch becomes superconducting, e. g., $r_n = 0$. This states that $I_1 = I_2 = \dots = I_{n-1} = 0$; i. e., the superconductor short-circuits all the other branches. If we apply an emf to such a system consisting of one and the same metal above the transition temperature, then the rule still holds even if we cool the metal until superconductivity appears. The appearance of superconductivity... does not change the individual currents if the total current $\sum_{k=1}^n I_k$ is kept constant. As a matter of fact any (possible) cause for such a change disappears as the mutual inductions between all the currents I_k vanish.

²⁴W. J. de Haas and J. M. Casimir-Jonker, *Physica*, **1**, 291 (1934).
²⁵W. J. de Haas and O. A. Guineau, *Physica*, **1**, 291 (1934).
²⁶W. J. de Haas, A. D. Engelkes, and O. A. Guineau, *Physica*, **4**, 595 (1937).

2. CURRENT DISTRIBUTION — PARALLEL SUPERCONDUCTORS 9

If initially all values of $r_k = 0$, the Kirchhoff rule cannot be applied at all. The calculation of the current distribution must be based upon the fact that the current is initiated by means of a voltage V , formed between the junctions, which changes with time and dies out as soon as the currents become stationary, the whole process being described in terms of the laws of induction. In using these laws we have to assume that the inductive coupling between the n branches is much stronger than their coupling with the leads to the junctions. This condition is fulfilled by inserting coils with considerable mutual inductance in the branches and by having the leads in the form of straight wires which do not come too close to the coils. The magnetic field of the system is then mainly confined to the vicinity of the coils.

Under these conditions the magnetic field strength H is a linear function of the currents I_k at every point; the energy density $\frac{1}{2} H^2$ and also the total magnetic energy

$$\frac{1}{2} \int H^2 dx dy dz = \frac{1}{2} \sum_{k,l} \dot{p}_{kl} I_k I_l$$

is therefore a quadratic form in I_k . This form is necessarily positive and definite, i. e., all \dot{p}_{kl} , the determinant of the \dot{p}_{kl} , as well as all subdeterminants symmetrical with respect to the diagonal, are positive. For $n = 2$,

$$\dot{p}_{11} > 0, \quad \dot{p}_{22} > 0, \quad \dot{p}_{11}\dot{p}_{22} - \dot{p}_{12}^2 > 0 \quad (2-1)$$

The \dot{p}_{kl} are the coefficients of self induction, the "mixed" terms \dot{p}_{kl} are the coefficients of mutual induction. $\dot{p}_{kl} = \dot{p}_{lk}$ identically.

It is possible to derive Maxwell's equations from the principle of least action by considering the electric energy as the potential energy and the magnetic energy as the kinetic energy. If electric currents are flowing, the work $V \cdot \delta e$ performed by the emf's has to be taken into consideration, where δe is the amount of electricity transported in a given direction by the current I . Here we have to do with quasi-stationary processes for which the electric energy vanishes compared with the magnetic energy. Under the assumption that the magnetic energy is the only energy depending on the currents, this principle now reads:

$$\delta \int \left(\frac{1}{2} \sum_{k,l} \dot{p}_{kl} I_k I_l - V \sum_k e_k \right) dt = 0 \quad (2-2)$$

As $-I_k = de_k/dt$ is the velocity corresponding to the coordinate e_k , the corresponding Euler equations are

$$\frac{d}{dt} \left(\sum_l \dot{p}_{kl} I_l \right) - V = 0 \quad (k = 1, 2, \dots, n) \quad (2-3)$$

and we recognize these as the usual induction equations. They are immediately integrable with respect to time t , and if all I_k are zero at $t = 0$ we obtain

$$\sum_i \dot{p}_{ni} I_i = \int V dt \quad (2-4)$$

This holds for all times, including the final state in which all I_k have become stationary and $V = 0$ by eq. (2-3). Unfortunately the quantity $\int V dt$ is not determined by the experiment, but only the current $I = \sum_k I_k$ in the steady state, namely by a galvanometer in the leads. However, together with the equation $I = \sum_k I_k$, eq. 2-4 forms $n + 1$ linear relations between the $n + 1$ unknowns I_1, I_2, \dots, I_n and $\int V dt$. For the special case $n = 2$, eq. 2-4 gives

$$\dot{p}_{11} I_1 + \dot{p}_{12} I_2 = \dot{p}_{21} I_1 + \dot{p}_{22} I_2 = \int V dt \quad (2-5)$$

Therefore because $I_1 + I_2 = I$ we have

$$I_1 = \frac{\dot{p}_{22} - \dot{p}_{12}}{\dot{p}_{11} + \dot{p}_{22} - 2\dot{p}_{12}} I, \quad I_2 = \frac{\dot{p}_{11} - \dot{p}_{12}}{\dot{p}_{11} + \dot{p}_{22} - 2\dot{p}_{12}} I \quad (2-6)$$

We regard I as positive; a positive I_k means that this current flows in the same direction as I ; a negative I_k means that it has the opposite direction.

According to eq. 2-1 and because the geometric mean of two positive quantities lies below the arithmetic mean:

$$|\dot{p}_{12}| < \sqrt{\dot{p}_{11}\dot{p}_{22}} < \frac{1}{2}(\dot{p}_{11} + \dot{p}_{22})$$

The denominator in eq. 2-6 is therefore always positive. However, it may very well be that $\dot{p}_{12} > \dot{p}_{22}$; but then because of eq. 2-1 $\dot{p}_{11} > \dot{p}_{12}$. In this case $I_2 > I$, $I_1 < 0$. The current in the first branch flows opposite to the input current, an impossible occurrence in normal conduction.¹ After they were derived theoretically by the author,² eq. 2-6 including the last inference, was confirmed quantitatively by Justi and Zickner.³

If a current I^0 was already flowing at time $t = 0$, with branch currents I_1^0 and I_2^0 , then these currents are superimposed on the system under consideration: in the first branch the current $I_1 + I_1^0$ will now flow, in the second $I_2 + I_2^0$. If in particular $I^0 = -I$, then, as can easily be computed, $I_1 + I_1^0 = -(I_2 + I_2^0)$, and the leads carry no current. Therefore if we have introduced a current before cooling down to the superconducting state, and after the cooling we cut off the supply leads, then a persistent current remains in the ring consisting of the two branches. We recognize here a second method of producing persistent currents. This

¹ Under certain circumstances it may happen that the absolute value of I_i can be greater than I .

² See Chap. 1, footnote 23.

³ E. Justi and G. Zickner, *Phys. Z.*, 42, 258 (1941).

2. CURRENT DISTRIBUTION — PARALLEL SUPERCONDUCTORS 11

has also been proved experimentally by Justi and Zickner. If we now feed in still another current I' , then this is independent of the persistent current, and its branch currents I'_1 and I'_2 calculated from eq. 2-6 are superimposed on the persistent current.

(b) Equation 2-4 allows yet another interpretation. If we ask which distribution of the current I minimizes the magnetic energy $1/2 \sum_k \dot{p}_{kk} I_k$, using the Lagrange undetermined multiplier α we find the conditions

$$\left(\frac{\partial}{\partial I_i} \right) \left(\frac{1}{2} \sum_k \dot{p}_{kk} I_k - \alpha \sum_k I_k \right) = 0$$

$$\sum_k \dot{p}_{ik} I_k = \alpha \quad (i = 1, 2, \dots, n)$$

However, from this and from

$$\sum_i I_i = I$$

we get the same relations between the I_i and I as from eq. 2-4. The current distribution in the branched superconducting circuit adjusts itself so as to minimize the magnetic energy. This minimum is, according to eq. 2-6,

$$\frac{1}{2} \frac{\dot{p}_{11}\dot{p}_{22} - \dot{p}_{12}^2}{\dot{p}_{11} + \dot{p}_{22} - 2\dot{p}_{12}} I^2$$

This is important for the understanding of Sizoo's experiments.⁴ In fact, in his experiment, $\dot{p}_{11}\dot{p}_{22} - \dot{p}_{12}^2$ is very nearly zero. On supplying a current, no magnetic field at all is produced — to this approximation; the field strength remains zero at every point in space. If before feeding in I there are already two currents I_1^0 and I_2^0 flowing in the branches which produce a magnetic field because they are not in the ratio $I_1 : I_2$, then this addition of I does not change anything in the magnetic field; a new field is merely superimposed on the old one, which in our case is zero. This conclusion also remains valid if we choose $I = -(I_1^0 + I_2^0)$, i. e., if we simply cut off the leads. All this had been found experimentally by Sizoo in 1926 and it was his work that instigated the discussion presented here.

According to eq. 2-5

$$(\dot{p}_{11} - \dot{p}_{21}) I_1 - (\dot{p}_{22} - \dot{p}_{12}) I_2 = 0$$

In the approximation used here, which allows us to ascribe its own induction coefficient to each of the two unclosed branches (strictly speaking only for closed circuits), the left-hand side of this equation is the flux of induction through the superconducting ring formed by the two branches. The fact that the flux of induction retains its initial value, i. e., zero, even if currents are switched on, corresponds to a theorem which will be discussed in general in Chap. 12.

⁴ G. J. Sizoo, Thesis, Leiden, 1926.

(c) The experiments under discussion not only confirm the complete disappearance of the resistances r_A but also show that there is no noticeable amount of any other energy depending on the current to be added to the magnetic energy. Such an energy would have to be added to the magnetic energy in the principle of least action, equation 2-2, and would disturb the linearity of the relations between the I_A and I , if it were a quadratic function of the I_A . Otherwise it would at least cause the induction coefficients applicable to these experiments to deviate from the ρ_A values as measured with ohmic currents. Neither possibility occurs in practice. We shall find in Chaps. 5 and 12 that a specific superconduction energy actually does appear, but that in the experiments under discussion and in many other similar experiments, it is far too small an amount to show up against the magnetic energy.

As we indicated in Chap. 1 (c), superconductors have an ohmic resistance for varying currents, in spite of the fact that their d. c. resistance is zero. In the measurements mentioned in this paragraph however the variations were much too slow for this effect to be appreciable.

CHAPTER 3

Fundamental Equations of the Maxwell-London Theory^{1,2}

(a) In most experimental work we observe effects on the field surrounding the superconductor caused by the phenomena occurring inside the superconductor. To be of any value, therefore, the theory must retain Maxwell's equations for empty space. We shall simplify the Maxwell equations by limiting the discussion to isotropic substances or cubic crystals. This restriction can easily be lifted if necessary, but so far no such necessity has arisen. We therefore introduce the three vectors \mathbf{E} , \mathbf{D} , and \mathbf{i} , the first of which is the field intensity, the second the displacement, and the third the current density. There exist between them the relations

$$\mathbf{D} = \epsilon \mathbf{E} \quad \mathbf{i} = \sigma \mathbf{E} \quad (3-1)$$

The dielectric constant ϵ and the conductivity σ are positive constants of the material depending only on temperature. For the magnetic field we need three more vectors \mathbf{H} , \mathbf{B} , and \mathbf{M} , i. e., the field intensity, the magnetic induction, and the induction due to permanent magnetization present only in permanent magnets that may be in the field. For these we have the relation

¹F. London, Une conception nouvelle de la supraconductivité, Paris, 1937.

²M. v. Laue, (a) *Ann. Physik*, 42, 65 (1942); (b) 48, 223 (1943); (c) 2, 183 (1948); (d) 8, 31 (1948); (e) 8, 40 (1948); (f) *Z. Physik*, 125, 517 (1949).

3. FUNDAMENTAL EQUATIONS

13

$$\mathbf{B} = \mu \mathbf{H} + \mathbf{M} \quad (3-2)$$

Here μ is a constant depending only on temperature, taken to be unity for ferromagnetics where \mathbf{M} is not zero. Hysteresis effects are not included in eq. 3-2, it is true, except implicitly in the behavior of \mathbf{M} . In Lorentz units, which we shall use throughout unless specifically stated otherwise, the Maxwell equations themselves now have the form

$$\begin{aligned} \text{I} \quad \text{curl } \mathbf{E} &= -\frac{1}{c} \frac{\partial \mathbf{B}}{\partial t} & \text{II} \quad \text{curl } \mathbf{H} &= \frac{1}{c} \left(\frac{\partial \mathbf{i}}{\partial t} + \mathbf{i} \right) \\ \text{III} \quad \text{div } \mathbf{B} &= 0 & \text{IV} \quad \text{div } \mathbf{D} &= \rho \end{aligned}$$

ρ is the space charge density.

(b) For the superconductor we put $\epsilon = 1$ from the outset, as Maxwell's theory does for all metallic conductors. An important feature of London's generalization is that the permeability $\mu = 1$. Moreover, $\mathbf{M} = 0$, because no ferromagnetic material shows superconductivity. So \mathbf{D} coincides with \mathbf{E} and \mathbf{B} with \mathbf{H} . Equations I — IV are simplified to

$$\begin{aligned} \text{I,} \quad \text{curl } \mathbf{E} &= -\frac{1}{c} \frac{\partial \mathbf{H}}{\partial t} & \text{II,} \quad \text{curl } \mathbf{H} &= \frac{1}{c} \left(\frac{\partial \mathbf{i}}{\partial t} + \mathbf{i} \right) \\ \text{III,} \quad \text{div } \mathbf{H} &= 0 & \text{IV,} \quad \text{div } \mathbf{E} &= \rho \end{aligned}$$

Now — and this introduces something essentially new — the current \mathbf{i} and the density ρ are each split into two parts by this theory, namely the ohmic current \mathbf{i}^0 together with the appropriate density ρ^0 , and the supercurrent \mathbf{i}^s with the corresponding density ρ^s .

$$\text{V} \quad \mathbf{i} = \mathbf{i}^0 + \mathbf{i}^s \quad \rho = \rho^0 + \rho^s$$

Between each sort of current and the corresponding density we assume a continuity equation:

$$\text{VI} \quad \text{div } \mathbf{i}^0 + \frac{\partial \rho^0}{\partial t} = 0, \quad \text{div } \mathbf{i}^s + \frac{\partial \rho^s}{\partial t} = 0$$

Equation VI gives a definite meaning to the coupling of ρ^0 with \mathbf{i}^0 and of ρ^s with \mathbf{i}^s . Only the continuity equation for the total current \mathbf{i} and the total density ρ follows in the known way from II, and IV. The subdivision carried out here therefore represents an essentially new assumption. Incidentally, ρ^0 shall include not only the contribution from the mobile carriers of the ohmic current \mathbf{i}^0 , but also that from the fixed atoms which is constant in time, and for a homogeneous superconductor uniform in space. This is completely consistent with eq. VI. ρ^s shall be due only to the carriers of the supercurrent. We are forced to this assertion because in eq. 13-10 ρ^s appears as a factor in a product which can be related only to the supercurrent.

For the ohmic current, Ohm's law, i. e., a linear relationship between \mathbf{j}^0 and \mathbf{E} , shall still be valid in superconductors. For a crystal it always has the form

$$\mathbf{j}^0 = \sum_{\rho} \sigma_{\alpha\rho} \mathbf{E}_{\rho} \quad \text{VII}$$

and for mathematical reasons $\sigma_{\alpha\rho}$ is a tensor of the second rank which we call the conductivity tensor. For cubic crystals it simplifies to a scalar conductivity σ , and eq. VII is replaced by the equation

$$\mathbf{j}^0 = \sigma \mathbf{E} \quad \text{VIIa}$$

The $\sigma_{\alpha\rho}$ are of the dimensions t^{-1} . The order of magnitude of σ and likewise the principal values $\sigma_{\alpha\alpha}$ of the tensor for normally conducting pure metals at the low temperatures under discussion is of the order 10^{19} sec^{-1} . According to experiments to be described in Chap. 16, we may also ascribe the same order of magnitude to the superconductor in spite of the fact that actual measurements are not available.

Finally, London's fundamental equations for the supercurrent appear as essentially new equations in the theory. We formulate them for an arbitrary crystal by associating with the vector \mathbf{l} a vector \mathbf{G} for the super-momentum per unit charge and by postulating a linear relation between them in terms of the tensor³ $\lambda_{\alpha\beta}$ the sums being over $\alpha, \beta = 1, 2, 3$:

$$\mathbf{G}_{\alpha} = \sum_{\beta} \lambda_{\alpha\beta} \mathbf{l}_{\beta} \quad \text{VIII}$$

which simplifies for cubic crystals to read

$$\mathbf{G} = \lambda \mathbf{l} \quad \text{VIIIa}$$

And for \mathbf{G} we introduce the following two differential equations due to London⁴

$$\text{IX} \quad \frac{\partial \mathbf{G}}{\partial t} = \mathbf{E} \quad \text{X} \quad \text{curl } \mathbf{G} = -\mathbf{H}$$

According to Chap. 1 (c), London's constant λ is a function of temperature that increases beyond all limit as we approach the transition temperature

³This tensor was introduced by M. von Laue (see footnote 2d).

⁴These equations can be combined relativistically in the form

$$c \left(\frac{\partial P_m}{\partial x_n} - \frac{\partial P_n}{\partial x_m} \right) = M_{nm} \quad m, n = 1, 2, 3, 4$$

if one puts $M_{14} = -i\mathbf{E}$, etc., $M_{23} = H$, etc., and $x_4 = ict$; the four vector \mathbf{P} is reduced to the supermomentum by identifying $P_{\alpha} = U_{\alpha}$, $\alpha = 1, 2, 3$, and $P_4 = 0$ for the system at rest.

Here we have written x_1, x_2 , and x_3 for x, y, z , but this can scarcely lead to any misunderstanding.

3. FUNDAMENTAL EQUATIONS

15

from below. The tensor $\lambda_{\alpha\beta}$ must have the same property. The dimensions of its components are $[\text{time}]^2$.

The most general tensor of second rank is asymmetrical, but from Table 1-1 all the crystal classes in which superconductivity has been observed have such high crystallographic symmetry that all tensor constants must be symmetrical, i. e., interchanging their suffixes does not change their value.⁵ We therefore put

$$\begin{aligned} \sigma_{\alpha\beta} &= \sigma_{\beta\alpha} \\ \lambda_{\alpha\beta} &= \lambda_{\beta\alpha} \end{aligned} \quad (3-3)$$

In Chap. 13 (b) this will turn out to be a necessary condition for the possibility of superconductivity. It can also be understood in this way why deformations which distort the natural symmetry of the crystals easily destroy the superconductivity — as has often been observed.

We shall find in Chap. 5 that

$$\frac{1}{2} (\mathbf{l} \cdot \mathbf{G}) = \frac{1}{2} \sum_{\alpha\beta} \lambda_{\alpha\beta} \mathbf{l}_{\alpha} \mathbf{l}_{\beta} \quad (3-4)$$

is the density of the free energy that is connected with the supercurrent. By requiring that it be positive, not only in the cubic system where it equals $\frac{1}{2} \lambda (\mathbf{l})^2$, but also under all circumstances, we conclude that the components $\lambda_{\alpha\alpha}$ with two identical suffixes, the determinant of all the $\lambda_{\alpha\beta}$, and the three symmetrical subdeterminants

$$\begin{vmatrix} \lambda_{\alpha\alpha} & \lambda_{\alpha\beta} \\ \lambda_{\beta\alpha} & \lambda_{\beta\beta} \end{vmatrix}$$

are all positive. These are the necessary and sufficient conditions that the quadratic form $\sum_{\alpha\beta} \lambda_{\alpha\beta} \mathbf{l}_{\alpha} \mathbf{l}_{\beta}$ shall be positive and definite. But as $\sum_{\alpha\beta} \sigma_{\alpha\beta} \mathbf{E}_{\alpha} \mathbf{E}_{\beta}$ is also positive and definite (it is the expression for the Joule heat, see Chap. 5), the conductivity tensor obeys the same conditions. The quadratic surfaces corresponding to these tensors:

$$\sum_{\alpha\beta} \lambda_{\alpha\beta} x_{\alpha} x_{\beta} = \text{constant} \quad \text{and} \quad \sum_{\alpha\beta} \sigma_{\alpha\beta} x_{\alpha} x_{\beta} = \text{constant}$$

are therefore ellipsoids. If their axes are chosen as coordinates, then all the tensor components with unlike suffixes vanish, and those with two like suffixes give the principal values $\lambda_1, \lambda_2, \lambda_3$ of the tensor.

In the crystal classes in which superconductivity has been detected to date (Table 1-1) the axes of these ellipsoids are completely fixed and

⁵This is also true for all superconducting compounds and alloys. Compare Max von Laue, footnote 2c; in this reference, a table appears giving all crystal classes together with the properties of all second-rank tensors that can belong to them, like the tensors $\lambda_{\alpha\beta}$ and $\sigma_{\alpha\beta}$, that can form a linear relation between two polar vectors. In these particular cases the polar vectors are \mathbf{l} and \mathbf{G} , \mathbf{P} , and \mathbf{E} .

coincide with the principal crystallographic axes. In the rhombic system, i. e., for gallium and uranium, they are mutually perpendicular but not of equal length. In the tetragonal and hexagonal systems the surfaces are ellipsoids of revolution whose unequal axes coincide with the principal crystallographic axes. Therefore two of the principal values of the tensor are equal. We need scarcely mention the cubic system for which the ellipsoid degenerates into a sphere.

As the determinant of $\lambda_{\alpha\beta}$ differs from zero the three equations VIII can be solved for the components i_{α} . Thus not only does it follow from $i = 0$ that $G = 0$, but also conversely from $G = 0$ that $i = 0$.

It is a significant feature of this theory that the ohmic current and the supercurrent are essentially independent of each other and are only coupled in a secondary way through the magnetic field with which they are both related.

The fundamental equations of this chapter are not all independent. Equation III, is given by forming the divergence of λ ; eq. I, by forming the curl of eq. IX and using eq. X. Nevertheless by retaining eqs. I, and III, we show more clearly that the London theory does not do away with the Maxwell theory, but only supplements it. There is no contradiction in the system of equations.

(c) In addition to the differential equations, the theory still needs to be completed by boundary conditions at all surfaces where the constants of the theory undergo sudden changes, as at the surface of the specimen. Such boundary conditions do not represent new additions; they are limiting forms of the differential equations themselves. For instance B, D, and i have finite time derivatives everywhere, and hence eqs. I and II lead through Stokes' theorem regarded as applying to a "surface curl" to the result that the tangential components of both fields are continuous across any surface. Also, according to eq. III we may say that the "surface divergence" of B is zero; therefore if we indicate two opposite normals of the surface of discontinuity by n_1 and n_2 we obtain

$$B_{n_1} + B_{n_2} = 0 \quad (3-5)$$

Similarly, according to eq. IV, when a surface charge density exists we have

$$D_{n_1} + D_{n_2} = \rho \quad (3-6)$$

These two equations hold for the superconductor if we replace B by H and D by E. The following new boundary conditions then have to be added: of the current densities i^0 and i' are related to the surface charge densities ρ^0 and ρ' by the equations:

$$i^0_{n_1} + i^0_{n_2} = \frac{\partial \rho^0}{\partial t}, \quad i'_{n_1} + i'_{n_2} = \frac{\partial \rho'}{\partial t} \quad (3-7)$$

Finally because H is finite everywhere, eq. X requires that the tangential components of i be everywhere continuous across every surface:

3. FUNDAMENTAL EQUATIONS

17

$$G_{\alpha} = G_i, \quad (3-8)$$

$$\lambda_1 i_{\alpha} = \lambda_2 i'_{\alpha}, \quad (3-9)$$

This means that at the boundary between two cubic crystal superconductors the superconductor with the smaller λ carries the higher tangential current; it behaves as if it were the better superconductor. Increasing temperature increases the constant, as already stated, thus impairing the superconductor.

(d) Although, as already mentioned, we shall generally use Lorentz units, we have also enumerated the changes involved in the transition to electrostatic units. In these units the fundamental eqs. II and IV become

$$\text{curl } H = \frac{1}{c} \left(\frac{\partial D}{\partial t} + 4\pi i \right) \quad \text{and} \quad \text{div } D = 4\pi \rho$$

Equations I, III, and VII remain unchanged. In general, the transformation is effected by the equations:

$$\begin{aligned} \rho_L &= \sqrt{4\pi} \rho_{EL}, & i_L &= \sqrt{4\pi} i_{EL}, & E_L &= \frac{E_{EL}}{\sqrt{4\pi}}, \\ H_L &= \frac{H_{EL}}{\sqrt{4\pi}}, & B_L &= \frac{B_{EL}}{\sqrt{4\pi}}, & (\sigma_{\alpha\beta})_L &= 4\pi (\sigma_{\alpha\beta})_{EL} \end{aligned} \quad (3-10)$$

The question arises: shall the tensor components $\lambda_{\alpha\beta}$ have the same values in both systems so that $G_L = \sqrt{4\pi} G_{EL}$ and the eqs. IX and X have to be replaced by

$$4\pi \frac{\partial G_{EL}}{\partial t} = E \quad \text{and} \quad 4\pi c \text{curl } G_{EL} = -H?$$

We decide instead in favor of taking over eqs. IX and X unchanged in the electrostatic system and derive the transformations:

$$G_L = \frac{G_{EL}}{\sqrt{4\pi}}, \quad (\lambda_{\alpha\beta})_L = \frac{(\lambda_{\alpha\beta})_{EL}}{4\pi} \quad (3-11)$$

We shall find out the advantages of this convention in Chaps. 15 and 16. There the pure number $\nu \sigma \lambda$, where ν is a frequency, has the same value in both systems of units, and plays an important part in the theory of oscillations similar to the part played by the scalar product $(i \cdot G)$ in what follows.

(e) Even though we intend to present London's theory in a phenomenological manner, we wish nevertheless to point out the atomic theory basis from which it developed historically. Fritz and Heinz London⁶ attempted in 1935 to make the fundamental eqs. IX and X, which they wrote in the form

$$IX'' \quad \frac{\partial \lambda i'}{\partial t} = E \quad X'' \quad c \text{curl } (\lambda i) = -H$$

⁶F. and H. London, *Physicon*, 2, 241 (1935).

seem plausible from quantum theoretical considerations. In this way they found a relation between the constant λ and the charge e , the mass m of the electron, and the number N of the superconducting electrons per unit volume, namely,

$$\lambda = \frac{m}{e^2 N} \quad (3-12)$$

However, eq. IXa had already been derived in 1933 by Becker, Heller, and Sauter⁷ on a purely mechanical basis. They took the electric field as the only force acting on the electron, so that

$$m \frac{dv}{dt} = eE;$$

where v is the velocity of the electron. Furthermore, as the current density is $i = eNv$ one arrives at eqs. IXa and 3-12 if one neglects the difference between the partial time derivative $\partial/\partial t$ (at constant coordinates) and d/dt (referring to a moving particle): this is permissible for sufficiently small velocities. Equation IXa can be derived from eq. IXa by means of Maxwell's equation 1 under the physically self-evident assumption that no field existed prior to a certain time 0. Thus if one takes the curl of eq. IXa and integrates from $t = 0$ to t , one gets:

$$\text{curl}(\lambda i) = \int_0^t \text{curl} E dt = -\frac{1}{c} \mathbf{H}$$

To this extent this entire theory was contained in the "acceleration theory" of Becker and co-workers.

We shall not go further into this atomic picture here although in Chap. 13 we shall make use of the picture to explain the Maxwell-London stresses, assuming that neither the lattice formed by the ions nor the ohmic conduction electrons exert any force on the mechanism of the supercurrent.

To make a rough estimate of λ from 3-12 we take aluminum as an example. The lattice cell contains four atoms and has an edge of 4×10^{-8} cm. In one cubic centimeter therefore there are 1.6×10^{23} cells and 6.4×10^{22} atoms. If we assume the number N of superconducting electrons to be the same, with $m = 9 \times 10^{-28}$ gm and $e_L = \sqrt{4\pi} e_{EL} = \sqrt{4\pi} \times 4.8 \times 10^{-10} = 1.7 \times 10^{-9}$ Lorentz unit, it follows that

$$\lambda_{Li} = 2 \times 10^{-32} \text{ sec}^2 \quad (3-13)$$

or according to 3-11.

$$\lambda_{EL} = 2.5 \times 10^{-31} \text{ sec}^2$$

But probably the number N is much smaller, and λ accordingly greater.

⁷R. Becker, G. Heller, and F. Sauter, *Z. Physik*, 86, 772 (1933).

CHAPTER 4

Space Charges in Superconductors

Space charges may be formed in a superconductor by irradiating it with fast cathode rays which are sooner or later trapped inside the superconductor. The theory must lead to plausible conclusions about the super- of such charges, and this requirement has played a role in its development. We assume the crystal to be cubic, λ and σ constants in space and time. From eqs. VI, IXa, and IVa respectively there follow the equations

$$\frac{\partial \rho^i}{\partial t^i} = -\text{div} \frac{\partial i^i}{\partial t^i} = -\frac{1}{\lambda} \text{div} E = -\frac{\rho}{\lambda} = -\frac{(\rho^0 + \rho^i)}{\lambda}$$

while from eqs. IV, VIIa, and VI correspondingly

$$\rho = \text{div} E = \frac{1}{\sigma} \text{div} i^0 = -\frac{1}{\sigma} \frac{\partial \rho^0}{\partial t}$$

Therefore the differential equations

$$\frac{\partial \rho^i}{\partial t^i} + \frac{(\rho^0 + \rho^i)}{\lambda} = 0 \quad \frac{\partial \rho^0}{\partial t} + \sigma(\rho^0 + \rho^i) = 0 \quad (4-1)$$

hold for the two unknowns ρ^i and ρ^0 . They are solved under the assumption that

$$\rho^0 = \rho^0 e^{-\alpha t^i} \quad \rho^i = \rho^i e^{-\alpha t^i} \quad (4-2)$$

which transform the differential equations into the algebraic relations

$$(\alpha^2 + \lambda^{-1}) \rho^i + \lambda^{-1} \rho^0 = 0 \quad (4-3)$$

$$\sigma \rho^i + (\sigma - \alpha) \rho^0 = 0$$

Putting the determinant of the coefficients equal to zero yields for α the equation

$$\alpha^3 - \sigma \alpha^2 + \lambda^{-1} \alpha = 0 \quad (4-4)$$

To each root of this equation there corresponds a certain ratio ρ^i/ρ^0 . Carrying through the calculation gives

$$\begin{aligned} \alpha_1 &= \frac{1}{2} (\sigma + \sqrt{\sigma^2 - 4\lambda^{-1}}), & \left(\frac{\rho^i}{\rho^0} \right)_1 &= -\frac{1}{2} \left(1 - \sqrt{1 - \frac{4}{\sigma^2 \lambda}} \right) \\ \alpha_2 &= \frac{1}{2} (\sigma - \sqrt{\sigma^2 - 4\lambda^{-1}}), & \left(\frac{\rho^i}{\rho^0} \right)_2 &= -\frac{1}{2} \left(1 + \sqrt{1 - \frac{4}{\sigma^2 \lambda}} \right) \\ \alpha_3 &= 0, & \left(\frac{\rho^i}{\rho^0} \right)_3 &= -1 \end{aligned} \quad (4-5)$$

The general solution of eq. 4-1 therefore reads

$$\begin{aligned} \rho^0 &= A_1 e^{-\alpha_1 t^i} + A_2 e^{-\alpha_2 t^i} + A_3 \\ \rho^i &= -\frac{1}{2} \left(1 - \sqrt{1 - \frac{4}{\sigma^2 \lambda}} \right) A_1 e^{-\alpha_1 t^i} - \frac{1}{2} \left(1 + \sqrt{1 - \frac{4}{\sigma^2 \lambda}} \right) A_2 e^{-\alpha_2 t^i} - A_3 \end{aligned}$$

A_1, A_2, A_3 are constants of integration, i. e., invariable with time, but otherwise arbitrary functions of position. a_1 and a_2 can be complex, but both roots always have real parts. When a_1 and a_2 are complex, there are superposed vibrations of ρ^0 and ρ^1 which decay with time until $\rho = \rho^0 + \rho^1$ becomes zero. The equations do not require that the individual densities of conduction are independent. This is related to the fact that the two mechanisms already disappeared in the final state when the total density $\rho = 0$.

On the whole the phenomenological theory does not say anything about the individual densities in the final state, except that where a current i is flowing, ρ^1 cannot be zero. Otherwise the momentum $\rho^1 \lambda i$ of the supercurrent, which we shall meet with in eq. 13-10, should equally well be zero. Because the field equations are linear, the decay of ρ takes place independently of, and is superimposed upon, all other processes that occur in the superconductor. When we investigate these other processes, therefore, we neglect the space charge completely and always put $\text{div } \mathbf{E} = 0$ in place of IV.

In order to do this it is necessary that σ and λ do not change in time or space. If these constants were to vary because of temperature inequalities for example, or varying composition of an alloy, then the space charges would change according to other laws. Nevertheless in a stationary state the superconductor is charge free under all circumstances. From eq. VIII it follows, namely, that if $\partial/\partial t = 0$, then $\mathbf{E} = 0$, and therefore according to eq. IV, where σ is a symmetrical tensor. The above calculation cannot be applied to a noncubic crystal show how we can also draw conclusions about the decay in this case. In a normal conductor with a cubic lattice the charge decays according to eq. III, as can be seen by forming the divergence of eq. III. This result is well known, but having regard to the magnitude of σ it is doubtful whether the Maxwell theory will still be valid for such a rapid decay. It is also doubtful in our theory of superconductivity. However, it is significant that the theory does lead to plausible results, and its conclusions about the decay should be at least qualitatively correct.

CHAPTER 5

The Conservation of Energy

(a) We obtain the energy principle for the space outside the superconductor in the known manner by forming the scalar product of eq. I with $(-\mathbf{H})$ and of II with \mathbf{E} , adding the results and applying the rule

$$(\mathbf{P} \cdot \text{curl } \mathbf{Q}) - (\mathbf{Q} \cdot \text{curl } \mathbf{P}) = \text{div } [\mathbf{Q} \times \mathbf{P}] \quad (5-1)$$

5. THE CONSERVATION OF ENERGY

21

The result is immediately

$$-c \text{div } [\mathbf{E} \times \mathbf{H}] = \left(\mathbf{E} \cdot \frac{\partial \mathbf{D}}{\partial t} \right) + \left(\mathbf{H} \cdot \frac{\partial \mathbf{B}}{\partial t} \right) + (\mathbf{E} \cdot \mathbf{i}) \quad (5-2)$$

According to eqs. 3-1 and 3-2 and because $\partial \mathbf{M} / \partial t = 0$, this takes the form

$$\frac{\partial}{\partial t} \left(\frac{1}{2} \epsilon F^2 + \frac{1}{2} \mu H^2 \right) + \sigma E^2 + c \text{div } [\mathbf{E} \times \mathbf{H}] = 0 \quad (5-3)$$

Within the differential sign are the density of electrical energy $\frac{1}{2} \epsilon E^2$ and of magnetic energy $\frac{1}{2} \mu H^2$; σF^2 gives the Joule heat per unit time, and $c [\mathbf{E} \times \mathbf{H}]$ is the flux density of electromagnetic energy, the so-called Poynting vector.

Proceeding in the same manner with eqs. I, and II, we find for the interior of the superconductor, instead of eq. 5-2

$$-c \text{div } [\mathbf{E} \times \mathbf{H}] = \left(\mathbf{E} \cdot \frac{\partial \mathbf{E}}{\partial t} \right) + \left(\mathbf{H} \cdot \frac{\partial \mathbf{H}}{\partial t} \right) + (\mathbf{E} \cdot \mathbf{i}) \quad (5-4)$$

or, also according to eqs. VII, VIII, and IX

$$\frac{\partial}{\partial t} \left(\frac{1}{2} E^2 + \frac{1}{2} H^2 + \frac{1}{2} \sum_{\alpha\beta} \lambda_{\alpha\beta} i_\alpha i_\beta \right) + \sum_{\alpha\beta} \sigma_{\alpha\beta} E_\alpha E_\beta + c \text{div } [\mathbf{E} \times \mathbf{H}] = 0 \quad (5-5)$$

In a superconductor there is, in addition to the electric and magnetic energy, a specific energy of the supercurrent having a density

$$\frac{1}{2} \sum_{\alpha\beta} \lambda_{\alpha\beta} i_\alpha i_\beta = \frac{1}{2} (\mathbf{i} \cdot \mathbf{G}) \quad (5-6)$$

or, for the cubic case

$$\frac{1}{2} \lambda i^2 \quad (5-7)$$

This is the only difference from the older theory. If we wish to combine the laws of conservation, eqs. 5-3 and 5-5, which will be useful later, we put

$$\frac{1}{2} \epsilon E^2 + \frac{1}{2} \mu H^2 + \frac{1}{2} (\mathbf{i} \cdot \mathbf{G}) \quad (5-8)$$

for the total energy density. Our assumptions in Chap. 3 (b) about the tensors λ and σ ensure that the two sums in eq. 5-5 are always positive. Therefore it follows from eq. 5-5 that the energy of any electric field will be entirely dissipated by Joule heat if energy is not supplied from outside. Therefore if the superconductor does contain space charges, they must vanish. For if they were assumed to remain, there would exist an electric field without a magnetic field strength; the Poynting vector would be zero, and according to eq. 5-5 the field energy would decrease until the field and therefore also its charges become zero, contradicting the hypothesis. The conclusion drawn in Chap. 4 about the decay of the total space charge density ρ in superconductors with a cubic lattice structure is in this way applicable to all superconductors.

Stationary magnetic fields are, however, possible in which a supercurrent appears but no electric field strength. In deriving the energy law,

eq. 5-5, it is assumed that the $\lambda_{\alpha\beta}$ do not change with time, just as in eq. 5-2 ϵ and μ have to be constant. All these constants of the material depend on temperature. Therefore eqs. 5-2 and 5-5 can be used for isothermal processes only. The kinds of energy appearing here are therefore free energies in the sense of thermodynamics. The actual energy E is connected with the free energy F ¹ by the relation $E = F - T \partial F / \partial T$. Consequently the energy of the supercurrent per unit volume is

$$\frac{1}{2} \sum_{\alpha\beta} \left(\lambda_{\alpha\beta} - T \frac{\partial \lambda_{\alpha\beta}}{\partial T} \right) \mathbf{L}_{\alpha} \cdot \mathbf{L}_{\beta}$$

or for the cubic case

$$\frac{1}{2} \left(\lambda - T \frac{\partial \lambda}{\partial T} \right) \mathbf{L}^2$$

Reversing signs, the second terms, i. e., the expressions

$$\frac{1}{2} T \sum_{\alpha\beta} \frac{\partial \lambda_{\alpha\beta}}{\partial T} \mathbf{L}_{\alpha} \cdot \mathbf{L}_{\beta} \quad \text{or} \quad \frac{1}{2} T \frac{\partial \lambda}{\partial T} \mathbf{L}^2$$

represent the heat which has to be removed from the superconductor during isothermal production of the supercurrent \mathbf{L} . As λ increases with T they are positive, and immediately below the transition temperature they are quite considerable.

CHAPTER 6

The Telegrapher's Equation for Superconductors with Cubic Crystal Structure

It is known that by eliminating all field vectors but one from among Maxwell's field equations one obtains a partial differential equation for the remaining vector, the so-called telegrapher's equation which occupies a position intermediate between the wave equation $\Delta u - (1/c^2) \partial^2 u / \partial t^2 = 0$ and the equation for heat conduction $\Delta u - k \partial u / \partial t = 0$. We now wish to perform this elimination for the superconductivity theory. We assume all constants of the material to be unvarying in time and space. The lattice shall be cubic. We form the curl of \mathbf{H} . Then from the rule

$$\text{curl curl } \mathbf{P} = \text{grad div } \mathbf{P} - \Delta \mathbf{P} \quad (6-1)$$

¹This is the Helmholtz free energy $F = E - TS$, not the Gibbs free energy $G = E - TS + PV + HM$.

6. THE TELEGRAPHER'S EQUATION

23

and according to III, we obtain $-\Delta \mathbf{H}$ on the left-hand side. The result is therefore:

$$-\Delta \mathbf{H} = \frac{1}{c} \left\{ \text{curl } \frac{\partial \mathbf{E}}{\partial t} + \text{curl } \mathbf{i}^0 + \text{curl } \mathbf{i}^1 \right\}$$

We transform the right-hand side of this by means of eqs. I, VII, and IX; the first term yields $-(1/c^2) \partial^2 \mathbf{H} / \partial t^2$, the second $-(\sigma/c^2) \partial \mathbf{H} / \partial t$, and the third $-\mathbf{H}/c^2 \lambda$. Consequently

$$W(\mathbf{H}) \equiv \Delta \mathbf{H} - \frac{1}{c^2} \frac{\partial^2 \mathbf{H}}{\partial t^2} - \frac{\sigma}{c^2} \frac{\partial \mathbf{H}}{\partial t} - \frac{\mathbf{H}}{c^2 \lambda} = 0 \quad (6-2)$$

Now we form the curl of eq. I₁. Because of IV, with $\rho = 0$ the only term we get on the left-hand side is $-\Delta \mathbf{E}$. By using eqs. II, and VII, then eqs. VIII and IX we reduce the right-hand side to

$$\begin{aligned} -\frac{1}{c} \text{curl } \frac{\partial \mathbf{H}}{\partial t} &= -\frac{1}{c^2} \left(\frac{\partial^2 \mathbf{E}}{\partial t^2} + \frac{\partial \mathbf{i}^0}{\partial t} + \frac{\partial \mathbf{i}^1}{\partial t} \right) \\ &= -\frac{1}{c^2} \left(\frac{\partial^2 \mathbf{E}}{\partial t^2} + \sigma \frac{\partial \mathbf{E}}{\partial t} + \frac{\mathbf{E}}{\lambda} \right) \end{aligned}$$

Consequently

$$W(\mathbf{E}) \equiv \Delta \mathbf{E} - \frac{1}{c^2} \left(\frac{\partial^2 \mathbf{E}}{\partial t^2} + \sigma \frac{\partial \mathbf{E}}{\partial t} + \frac{\mathbf{E}}{\lambda} \right) = 0 \quad (6-3)$$

If we again form the curl of eq. 6-2 it follows because of eq. II, and because the operator W can be interchanged with the operation of forming the curl:

$$W \left(\frac{\partial \mathbf{E}}{\partial t} + \mathbf{i} \right) = 0$$

By combining this with eq. 6-3 differentiated with respect to t , one gets

$$W(\mathbf{i}) = 0$$

On the other hand, multiplying eq. 6-3 by σ and using eq. VII give

$$W(\mathbf{i}^0) = 0 \quad (6-4)$$

Consequently by subtracting the last two equations, one finds from eq. V

$$W(\mathbf{i}^1) = 0 \quad (6-5)$$

The generalized telegrapher's equation $W(u) = 0$ therefore holds for each component of any of the field vectors with respect to cartesian coordinates. If the vectors were resolved in terms of curvilinear coordinates special treatment would be necessary.

Most experiments with superconductivity deal with stationary fields, so that their study constitutes the most important part of the theory. For

this case the equation for $\nabla^2(u)$ is reduced to its first and its last terms: we are left with the differential equation

$$\Delta u - \beta^2 u = 0 \quad (6-6)$$

where u , as stated, represents a component of any field vector and where

$$\beta^2 = \frac{1}{c^2 \lambda} \quad (6-7)$$

Chaps. 7 and 11 will deal with this differential equation.

All the above is expressed in Lorentz units. In electrostatic units the last two terms in eq. 6-1 gain a factor 4π . So in place of eq. 6-7

$$\beta^2 = \frac{4\pi}{c^2 \lambda} \quad (\text{in esu}) \quad (6-8)$$

According to eq. 5-11 β has the same value in both systems of units.

CHAPTER 7

Stationary Fields

(a) As mentioned in Chap. 4 it follows from eq. IX that $E = 0$ in the stationary case. Furthermore by eq. I, E is the gradient of a scalar potential and so the superconductor is a region of constant potential even when the tensor components $\lambda_{\alpha\beta}$ vary with position in space. By eq. VII there is no ohmic current; it is deprived of its potential gradient by the presence of the supercurrent, i. e., it is short circuited. Therefore no experiment using direct current can enable us to detect the finite conductivity of the superconductor. The only significant field vectors are the current i and the magnetic field H . These vectors are more strongly coupled than in the normal conductor, because there exists between them not only the generally valid relation II, which here simplifies to

$$\text{curl } H = \frac{i}{c} \quad (7-1)$$

but also eq. IX applying specifically to superconductors:

$$\text{curl } G = -\frac{H}{c}, \quad \left(G_\alpha = \sum_\beta \lambda_{\alpha\beta} i_\beta \right) \quad (7-2)$$

Everything we can say about the stationary case is based on the combined application of these two laws. This excludes the possibility of a current-free magnetic-potential field in a normal conductor. From $\text{curl } H = 0$ it follows that $i = 0$, $G = 0$, and $H = 0$. Strictly speaking there is no

7. STATIONARY FIELDS

outside field into which one could place a superconductor carrying a current. The current distribution changes with any attempt to do so in such a way as to annul the outside field. It is possible to keep the current strength constant, and if one considers only the total current strength, one may use the term "external field". In the following sections we shall follow this through for the superconductor with cubic crystal structure.

In many of the examples to be considered the field inside the superconductor is desired when the field in the surrounding space is known. It follows from a general theorem that the solution is unique. In fact, if we form the scalar product of eq. 7-1 with G and of eq. 7-2 with $(-H)$, add the two, and apply the rule 5-1, we obtain

$$\text{div } [H \times G] = \frac{1}{c} \{ (i \cdot G) + H^2 \} \quad (7-3)$$

Integrating eq. 7-3 over the volume of the superconductor and using Gauss' theorem¹

$$\int_S \text{div } [H \times G] d\tau = - \int_S [H \times G]_n d\sigma$$

we get

$$\frac{1}{c} \int_S \{ (i \cdot G) + H^2 \} d\tau = \int_S [G \times H]_n d\sigma \quad (7-4)$$

The suffix S below the integral signs indicates that the volume integral extends over the volume of the superconductor and the surface integral over its entire surface.²

Now the normal component of the vector product $[G \times H]$ contains only the tangential components of G and H . If either $G_t = 0$ or $H_t = 0$ over the whole surface, then the right side of eq. 7-4 is zero. The left side, however, vanishes only if $H = 0$ and $G = 0$ or $i = 0$ at every point of the superconductor.

Consider two fields $H^{(1)}$, $i^{(1)}$ and $H^{(2)}$, $i^{(2)}$ which coincide everywhere over the boundary either with respect to H_{tang} or to G_{tang} . Equation 7-4

¹ n_i indicates the inner normal on the surface $d\sigma$.

² If one uses the Gauss theorem for multiply connected regions, as we do later in Chap. 12, it is first necessary to produce singly connected regions by making a sufficient number of cuts and adding the new cross sections to the surface. Sometimes the cross sections make appreciable contributions. Here this is not the case because G and H are singlevalued functions of position, so that the contributions from both sides of any cross section cancel each other. Equation 7-4 therefore holds also for multiply connected superconductors.

³ According to eq. 3-4, $(i \cdot G)$ is necessarily positive with the exception of the case where $i = 0$, $G = 0$.

holds equally well for the difference field $\mathbf{H}' = \mathbf{H}^{(1)} - \mathbf{H}^{(2)}$; $\mathbf{H}' = \mathbf{H}^{(1)} - \mathbf{H}^{(2)}$ because all our differential equations are linear; it follows then that the difference field vanishes throughout the volume: $\mathbf{H}' = 0$, $\mathbf{H}' = 0$. The stationary field in a superconductor is therefore uniquely determined by the tangential components at its surface of either the magnetic field or of the electromagnetic momentum of the supercurrents. This corresponds with the theorem of potential theory according to which the potential gradient in a region is uniquely fixed by its tangential components over the surface; these fix the surface potential to within an additive constant, and this in turn fixes the potential in the interior. The vectors \mathbf{G} and \mathbf{H} on the right-hand side of eq. 7-4 here refer to the inner side of the surface. It is also possible here to insert for \mathbf{H} its value on the outside of the surface because by Chap. 3 (c) the tangential component of \mathbf{H} is continuous across the surface. In this way the field in the interior is uniquely determined by the external magnetic field.

(b) For the homogeneous superconductor with a cubic lattice, eq. 7-2 can be simplified to read

$$\lambda \operatorname{curl} \mathbf{H} = -\frac{1}{c} \mathbf{H} \quad (7-5)$$

If we form the curl of eq. 7-1, then the fundamental eq. III, and eq. 7-5 together with the theorem 6-1 give us

$$\Delta \mathbf{H} - \beta^2 \mathbf{H} = 0, \quad \beta^2 = \frac{1}{c^2 \lambda} \quad (7-6)$$

Conversely, if we form the curl of eq. 7-5, then use eqs. VI and 7-1, we get

$$\Delta \mathbf{H} - \beta^2 \mathbf{H} = 0 \quad (7-7)$$

Thus we come back at once to eqs. 6-6 and 6-7.

(c) The simplest conceivable example is that of a superconductor filling one half of space $z > 0$, so having the plane $z = 0$ as its boundary. If in outside space $z < 0$, there is a homogeneous magnetic field \mathbf{H}^0 , then eq. 6-6 can be solved by putting

$$\mathbf{H} = \mathbf{H}^0 e^{-\beta z} \quad (7-8)$$

Because $\operatorname{div} \mathbf{H} = 0$, \mathbf{H}^0 must be zero. We can turn the x and the (perpendicular) y directions in such a manner that \mathbf{H}^0 also vanishes. Then it follows that for the field strength in the superconductor

$$\mathbf{H}_x = \mathbf{H}_y = 0, \quad \mathbf{H}_z = \mathbf{H}^0 e^{-\beta z} \quad (7-9)$$

Therefore according to eq. 7-1 the equations⁴

$$i_x = -c \frac{\partial \mathbf{H}_y}{\partial z} = \beta c \mathbf{H}^0 e^{-\beta z} = \lambda^{-1/2} \mathbf{H}^0 e^{-\beta z} \quad (7-10)$$

$$i_y = i_z = 0$$

⁴In electrostatic units $i_x = H^0 e^{-\beta z} / \sqrt{4\pi\lambda}$, compare eqs. 3-10 and 3-12.

represent the supercurrent vector field. We gather from this that the current density at the surface depends only on the field strength \mathbf{H}^0 there. \mathbf{i} , \mathbf{H} , and the inner normal of the superconductor are perpendicular to each other and form a right-handed system like the coordinate system x, y, z adopted here. The field penetrates the superconductor only to a depth of the order of magnitude β^{-1} . It forms a protecting layer of that thickness under which lies a region protected from the influence of the field. This result is fundamental because it can be taken over for the case of curved surfaces provided only that the superconductor is thick compared with the penetration depth β^{-1} . In this lies the explanation of the Meissner effect.

The surface density of the current is

$$i_s = \int_0^\infty i_x dz = c \mathbf{H}^0 \quad (7-11)$$

In electrostatic units eq. 7-11 reads, by eq. 3-10

$$i_s = \frac{c \mathbf{H}^0}{4\pi} \quad (7-12)$$

and if the current is measured in amperes, $i_s = 10 \mathbf{H}^0 / 4\pi$: nearly 80 amp are flowing per centimeter across each magnetic line of force at $\mathbf{H}^0 = 100$ oersteds. The penetration depth is

$$\beta^{-1} = c / \sqrt{\lambda}$$

or $\beta^{-1} = c / \sqrt{\lambda / 4\pi}$ in electrostatic units, by eq. 7-6. It is of the order of magnitude 10^{-6} cm if we assume for λ the order of magnitude 10^{-31} sec^2 , which is correct, according to present knowledge, for temperatures $\frac{1}{2} T_0$ or more below the transition temperature. Approaching the transition temperature T_0 , it appears to increase like λ without limit.

(d) We now consider the field and current distribution in thin superconductors, i. e., those with thickness no longer great compared with the penetration depth. We first treat the example of a plane parallel slab extending from $z = -d$ to $z = +d$. In the outside space let there be homogeneous magnetic fields \mathbf{H}^\pm where $z < -d$ and \mathbf{H}^+ where $z > d$, both in the y direction. The differential equation $\Delta \mathbf{H} - \beta^2 \mathbf{H} = 0$ and the condition $\operatorname{div} \mathbf{H} = 0$ are satisfied by

$$\mathbf{H}_x = \mathbf{H}_z = 0, \quad \mathbf{H}_y = a \cosh(\beta z) + b \sinh(\beta z) \quad (7-13)$$

It follows from eq. 7-1 that the current density is

$$i_y = i_x = 0, \quad i_z = -c \frac{\partial \mathbf{H}_y}{\partial z} = -\lambda^{-1/2} \{a \sinh(\beta z) + b \cosh(\beta z)\} \quad (7-14)$$

The boundary condition that H_z be continuous at $z = \pm d$ yields two equations for the constants a and b :

$$a \cosh(\beta d) + b \sinh(\beta d) = H^+, \quad a \cosh(\beta d) - b \sinh(\beta d) = H^- \quad (7-15)$$

The solution of these is

$$a = \frac{(H^+ + H^-)}{2 \cosh(\beta d)}, \quad b = \frac{(H^+ - H^-)}{2 \sinh(\beta d)} \quad (7-16)$$

If $\beta d \gg 1$ there exists a protected region free from field and current between two protecting layers of thickness $1/\beta$. If $\beta d \ll 1$, by expanding eqs. 7-13, 7-14, and 7-16 in series we find to a first approximation

$$H_z = \frac{1}{2}(H^+ + H^-) + \frac{1}{2} \frac{(H^+ - H^-)z}{d}, \quad I_x = c \frac{(H^- - H^+)}{2d} \quad (7-17)$$

surface current density

$$i_z = 2d I_x = c(H^- - H^+)$$

is therefore evenly distributed over the slab, the magnetic field increases linearly with z if the field strengths differ on the two sides of the slab. If, however, $H^+ = H^-$, no current flows, and the field is constant. If in a homogeneous magnetic field we place a sufficiently thin superconducting sheet parallel to the field strength, the field penetrates the sheet without being disturbed. For arbitrary thickness, but with $H^+ = H^-$, eqs. 7-13 and 7-14 simplify to

$$H_y = H + \frac{\cosh(\beta z)}{\cosh(\beta d)}, \quad I_x = -H + \frac{\sinh(\beta z)}{\sqrt{\lambda} \cosh(\beta d)} \quad (7-18)^s$$

(c) Consider now the same slab with a surface current density⁴ i_z with no magnetic field other than that produced by i_z . The current density is certainly an even function of z as the positive and negative z directions are equivalent, and we therefore need those solutions of the fundamental eqs. 7-14 for which $a = -b$. Also by eq. 7-13 H_z is an odd function of z , and consequently $H^- = -H^+$. Thus by eq. 7-15

$$b = \frac{H^+}{\sinh(\beta d)}$$

and

$$I_x = -H + \frac{\cosh(\beta z)}{\sqrt{\lambda} \sinh(\beta d)}, \quad H_y = H + \frac{\sinh(\beta z)}{\sinh(\beta d)} \quad (7-19)$$

^sWith regard to the sign of I_x it must be noticed that for the boundary surface $z = +d$, the z direction is the outer normal, and not, as in eq. 7-10 the inner normal. ⁴We cannot speak of the total current in this case because the slab is unlimited in extent in the y direction.

Now we still have to calculate H^+ from i_z . The equation

$$i_z = \int_{-d}^d I_x dz = -2cH^+ \quad (7-20)$$

will serve for this. So the final result reads

$$I_x = \frac{1}{2} \beta i_z \frac{\cosh(\beta z)}{\sinh(\beta d)}, \quad H_y = -i_z \frac{\sinh(\beta z)}{2c \sinh(\beta d)} \quad (7-21)$$

For a thick slab ($\beta d \gg 1$) one finds again that the field and current are concentrated in two protecting layers adjacent to the boundary surface. For thin sheets ($\beta d \ll 1$), eq. 7-21 simplifies to

$$I_x = \frac{i_z}{2d}, \quad H_y = \frac{i_z z}{2cd} \quad (7-22)$$

The current is therefore evenly distributed through the thickness of the sheet.

(f) To generalize the results obtained from these examples a mean value theorem for scalar space functions u that obey the differential equation

$$\Delta u - \beta^2 u = 0 \quad (7-23)$$

proves to be useful. We describe a sphere of radius r around an arbitrary point P in the three-dimensional domain of the function and form the mean value over its surface satisfying the equation

$$\Delta \bar{u} - \beta^2 \bar{u} = 0 \quad (7-24)$$

Since however \bar{u} depends only on r

$$\Delta \bar{u} = \frac{1}{r^2} \frac{\partial}{\partial r} \left(r^2 \frac{d\bar{u}}{dr} \right)$$

and the differential eq. 7-24 has the solutions

$$\bar{u} = \text{const.} \frac{\sinh(\beta r)}{\beta r} \quad \text{and} \quad \bar{u} = \text{const.} \frac{\cosh(\beta r)}{\beta r}$$

The second of these must be rejected because it increases without limit at $r = 0$. If we go to $r = 0$ in the first one, we see that the constant must be u_P , therefore we find

$$u_P = \frac{\bar{u} \beta r}{\sinh(\beta r)} \quad (7-25)$$

The factor multiplying \bar{u} decreases from 1 to arbitrary small values with increasing r . For $\beta = 0$ it would always be 1, and eq. 7-25 would go over into the well-known mean value theorem of potential theory, according to which the function \bar{u} cannot have either a maximum or a minimum at any point P . However here, with $\beta > 0$, the equation says only that the absolute value $|u_P|$ is smaller than the absolute value $|\bar{u}|$, excluding a maximum of $|\bar{u}|$ at P , but certainly permitting a minimum. The highest values of $|u|$ never lie in the interior, but always on the boundary of the region in which the differential eq. 7-23 holds; for points on the surface it is not possible to construct such spheres so that eq. 7-25 does not apply.

The components H_x , H_y , and H_z of the magnetic field strength satisfy the differential eq. 7-23; therefore we find according to this theorem that

$$(H_x^2)^p < (\bar{H}_x)^2$$

However, the mean square fluctuation over the surface of the sphere,

$$\frac{1}{4\pi r^2} \int (\bar{H}_x - \bar{H}_x)^2 |d\sigma| = \frac{1}{4\pi r^2} \int H_x^2 |d\sigma| - (\bar{H}_x)^2 = \bar{H}_x^2 - (\bar{H}_x)^2$$

is necessarily positive; therefore *a fortiori*

$$(H_x^2)^p < \bar{H}_x^2$$

Since corresponding relations hold for H_y and H_z , we find by summation

$$(H^2)^p < \bar{H}^2$$

One can prove in the same manner that

$$(H^2)^p < (\bar{H})^2$$

There exists no maximum of the magnetic field strength or the current density in the interior of a superconductor. The highest values of H^2 and i^2 are always located at the surface. The possibility of minima is demonstrated by the examples in sections (d) and (e) and also by those in the following paragraphs. This is the general theory of the Meissner effect.

If u depends only on two coordinates, the mean value is formed over a circle with radius r around the point P . Then

$$\Delta u = \frac{1}{r} \frac{d}{dr} \left(r \frac{du}{dr} \right)$$

and eq. 7-25 is replaced by

$$u^p = \frac{1}{I_0(\beta r)} \bar{u} \quad (7-26)^7$$

where $I_0(x)$ is the Bessel function of zero order to be discussed in more detail in Chap. 8. Since with increasing r , $I_0(\beta r)$ increases continuously from 1 and finally exceeds all limits,⁸ all conclusions drawn from eq. 7-25 can be taken over in the two-dimensional case.

(g) However, there are limits to be set to the Meissner effect which can be derived from eq. 7-25 or 7-26. If the region where the differential eq. 7-23 holds is small compared with the penetration depth β^{-1} then $\beta r \ll 1$ and $u^p = u$, i. e., in such a region any solution of eq. 7-23 coincides with a solution of the potential equation $\Delta u = 0$. Then the Meissner effect becomes undetectable. Examples are contained in the approximations 7-17 and 7-22 for the thin sheet; as a matter of fact in this case i^p and H_p do satisfy the potential equation.

In an infinitely long straight cylinder of arbitrary but small cross section with its axis along the z direction, we can consider

$$i_z^p = \text{constant}$$

⁷ $i_z = \sqrt{-1}$.

⁸ Compare the series expansion of eq. 8-6.

as the first approximation, because in this way $\Delta i_z^p = 0$. The supercurrent is then distributed in exactly the same way as an ohmic current. If, keeping the current density i_z constant, we decrease all the dimensions of the cross section by a factor a , then the magnetic field strength decreases at corresponding points like a because of Stokes' theorem it follows from eq. II, for any surface lying entirely inside the conductor that

$$\int \mathbf{H} \cdot d\mathbf{s} = \frac{1}{c} \int i \cdot d\sigma$$

and the surface of integration decreases like a^2 while the circumference decreases like a . Equation IX shows that the ratio of curl i to i decreases like a . This justifies neglecting curl i in eq. 7-23. We can take this result over without hesitation for a curved wire provided that the radius of curvature is great compared with the dimensions of the cross section.

On the other hand if we place a sufficiently small superconductor of arbitrary shape in a static magnetic field of strength H^0 , then the field continues unchanged through the superconductor because it obeys the differential equation $\Delta H = 0$. As here H is curl free, no current is produced on this approximation. This is not a contradiction of eq. 7-5 because if we integrate that equation over a surface lying entirely inside the superconductor and transform the integral on the left side to a line integral over the circumference by means of Stokes' theorem we get

$$c \int \lambda i \cdot d\mathbf{s} = - \int \mathbf{H} \cdot d\sigma \quad (7-28)$$

We apply this to two geometrically similar superconductors which may differ in their superconductivity constants λ_1 and λ_2 . Let L_1 and L_2 be corresponding linear intervals. We choose two corresponding surfaces in the superconductors; the integrals on the right-hand side of eq. 7-28 are then in the ratio $(L_1/L_2)^2$. Corresponding parts of the circumferences however are in the ratio L_1/L_2 . Consequently the ratio of the current density components i_a at corresponding points of the two bodies is,

$$\frac{i_{a1}}{i_{a2}} = \frac{\lambda_2 L_1}{\lambda_1 L_2} = \sqrt{\frac{\lambda_2}{\lambda_1} \frac{\beta_1 L_1}{\beta_2 L_2}}$$

Therefore for every sufficiently small superconductor every component i_a of i , $a = 1, 2, 3$, can be developed in a series the first term of which has the form

$$i_a = H^0 \tau_a \frac{\beta L}{\sqrt{\lambda}} \quad (7-29)$$

The quantities τ_a here are pure numbers, depending only on the relative positions and the shapes, but no longer on λ or the size of the specimen. Examples will be found in eqs. 10-2 and 11-12 as well as in the discussion following eq. 10-16.

These results do not hold without restriction for multiply connected superconductors because in this case there exist surfaces (see Chap. 12)

that extend partly outside the superconductor, in spite of the fact that their perimeters lie completely inside it. It is not then permissible to apply eq. 7-2 which is valid only for surfaces entirely within the superconductor. We shall see that in this case a persistent current, independent of H^0 , can be superposed on the currents obeying eq. 7-29.

(h) According to Chap. 3 the constant λ is a function of temperature. Immediately below the transition temperature it is very great, and so is the penetration depth $\beta^{-1} = c/\lambda$. (See eq. 7-6.) Every specimen is then "small" in the sense of the present considerations, the magnetic field penetrates it undisturbed. With decreasing temperature λ decreases, at first very rapidly indeed. This initiates the expulsion of the field — the Meissner effect. If the specimen is wrapped with a normally conducting induction coil, one can follow this process by means of the induced current; it decreases the flux of induction through the coil. Such experimental tests have often been carried out. In one instance Stark, Steiner, and Schoeneck⁹ observed a "paramagnetic" effect in the induced current, i. e., an effect that corresponds to an increase in flux of induction, which preceded the expulsion of the field. There is as yet no explanation for this. It would not help to ascribe to the superconductor a permeability μ deviating from 1. According to eq. 6-7 the former value $1/c^2 \lambda$ of β^2 merely acquires a factor μ . As the observations concern β , this would change the conversion from β to λ , but would offer no explanation of the induction experiments.¹⁰

(i) We shall try to apply some of the above results to superconductors with noncubic crystal structure and consider again the simplest case: the superconductor fills half of space, $x_3 > 0$, and at its surface there is a static homogeneous magnetic field H^0 the direction of which we again take as the x_3 axis. The boundary conditions for $x_3 = 0$ are therefore

$$H_1 = 0, \quad H_3 = H^0 \quad (7-30)$$

The other boundary condition is again the gradual vanishing of all field vectors as x_3 increases toward infinity. The Maxwell eq. II, ($\text{curl } H = 1/c$)

⁹J. Stark, K. Steiner, and H. Schoeneck, *Phys. Z.*, **88**, 887 (1937).

¹⁰Another discrepancy with the theory appeared sometimes in such experiments in that the total induced current impulse seemed to be less, occasionally even much less, than would be consistent with the complete expulsion of the field. The objection to these measurements is that the whole specimen had actually not become superconducting, but only a ring-shaped outer part of it. The cooling is effected from outside, so once such a ring is formed, it holds the enclosed flux of induction constant, as described in detail in Chap. 12, no matter how the external field is changed. The other parts remain in the intermediate state due to the influence of the field. In the superconducting ring a persistent current is produced by switching off the field, (Chap. 12). A test for this would consist in looking for the magnetic field of such a persistent current after the external field has been switched off, but it seems that this test has never been made in such experiments.

7. STATIONARY FIELDS

33

and the London eq. X ($c \text{ curl } G = -H$) reduce according to eq. VIII to the following:

$$i_1' = -c \frac{\partial H_2}{\partial x_3}, \quad i_2' = c \frac{\partial H_1}{\partial x_3} \quad (7-31)$$

$$H_1 = c \frac{\partial G_2}{\partial x_3} = c \left(\lambda_{21} \frac{\partial i_1'}{\partial x_3} + \lambda_{22} \frac{\partial i_2'}{\partial x_3} \right) \quad (7-32)$$

$$H_2 = -c \frac{\partial G_1}{\partial x_3} = -c \left(\lambda_{11} \frac{\partial i_1'}{\partial x_3} + \lambda_{12} \frac{\partial i_2'}{\partial x_3} \right)$$

Because of the divergence conditions i_3' and H_3 vanish. Elimination of i_1' leads to the differential equations

$$\begin{aligned} \lambda_{22} \frac{\partial^2 H_1}{\partial x_3^2} - \lambda_{21} \frac{\partial^2 H_2}{\partial x_3^2} - \frac{H_1}{c^2} &= 0 \\ -\lambda_{12} \frac{\partial^2 H_1}{\partial x_3^2} + \lambda_{11} \frac{\partial^2 H_2}{\partial x_3^2} - \frac{H_2}{c^2} &= 0 \end{aligned} \quad (7-33)$$

which here replaces eq. 7-6. The most obvious way to solve these is by introducing a new coordinate system x_1' and x_2' rotated about the x_3 axis, in which the tensor component λ_{12} vanishes. These are the "relative" principal axes of the tensor (i. e., relative to the plane $x_3 = 0$), the principal axes of the ellipse formed by the intersection of this plane and the ellipsoid of the tensor: $\sum \lambda_{\alpha\beta} x_\alpha x_\beta = \text{constant}$. This ellipse gives the

"relative principal values" λ_1' and λ_2' of the tensor. Introducing these changes in eq. 7-33 yields at once the two solutions:

$$(1) \quad H_1' = H_1^{0'} e^{-\beta_1' x_3}, \quad H_2' = 0 \quad (\beta_2' = 1/c \sqrt{\lambda_2'})$$

$$\begin{aligned} i_1' &= 0, & i_2' &= -H_1^{0'} e^{-\beta_1' x_3} / \lambda_2' \\ G_1' &= 0, & G_2' &= -\sqrt{\lambda_2'} H_1^{0'} e^{-\beta_1' x_3} \end{aligned} \quad (7-34)$$

$$(2) \quad \begin{aligned} H_1' &= 0, & H_2' &= H_2^{0'} e^{-\beta_2' x_3} \\ i_1' &= H_2^{0'} e^{-\beta_2' x_3} / \lambda_1', & i_2' &= 0 \\ G_1' &= \sqrt{\lambda_1'} H_2^{0'} e^{-\beta_2' x_3}, & G_2' &= 0 \end{aligned} \quad (\beta_1' = 1/c \sqrt{\lambda_1'}) \quad (7-35)$$

The integration constants $H_1^{0'}$ and $H_2^{0'}$ are the external magnetic field strength components in the directions x_1' and x_2' respectively. However, the boundary condition 7-30 must hold with respect to the coordinates x_1 and x_2 . Denoting the angle between x_1 and x_1' by φ , as in Fig. 7-1, we have to put $H_2^{0'} = H^{0'} \cos \varphi$; $H_1^{0'} = -H^{0'} \sin \varphi$. Finally transforming the vector components of eqs. 7-34 and 7-35 back into the components with respect to x_1 and x_2 .

$$H_1 = H_1' \cos \varphi + H_2' \sin \varphi, \quad H_2 = -H_1' \sin \varphi + H_2' \cos \varphi, \text{ etc.}$$

and we find

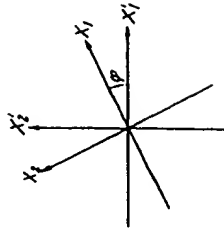


Fig. 7-1. Illustrating transformation of coordinates to principal axes.

$$\begin{aligned}
H_1 &= H^0 \{ e^{-\beta_1' x_1} - e^{-\beta_1' x_2} \} \cos \varphi \sin \varphi \\
H_2 &= H^0 \{ e^{-\beta_1' x_1} \cos^2 \varphi + e^{-\beta_1' x_2} \sin^2 \varphi \} \\
I_1' &= H^0 \{ (1/\Lambda_1') e^{-\beta_1' x_1} \cos^2 \varphi + (1/\Lambda_2') e^{-\beta_1' x_2} \sin^2 \varphi \} \\
I_2' &= -H^0 \{ (1/\Lambda_1') e^{-\beta_1' x_1} - (1/\Lambda_2') e^{-\beta_1' x_2} \} \cos \varphi \sin \varphi \\
G_1 &= H^0 \{ \sqrt{\Lambda_1'} e^{-\beta_1' x_1} \cos^2 \varphi + \sqrt{\Lambda_2'} e^{-\beta_1' x_2} \sin^2 \varphi \} \\
G_2 &= -H^0 \{ \sqrt{\Lambda_1'} e^{-\beta_1' x_1} - \sqrt{\Lambda_2'} e^{-\beta_1' x_2} \} \cos \varphi \sin \varphi
\end{aligned} \quad (7-36)$$

According to Chap. 3 (b), the relative principal values Λ_1' , Λ_2' are positive, therefore the decay constants β_1' and β_2' are certainly real. Because of the boundary condition at infinity, we must take them to be positive.

According to this, a noncubic crystal superconductor in a magnetic field also has a protecting layer under which exists a field-free region. In contrast to the case with a scalar λ , the decay does not follow one exponential function but two. Furthermore, the magnetic field strength in the protecting layer does not have the same direction x_3 everywhere, as in the outside space, nor does the current density have the same direction x_1 everywhere perpendicular to this. Neither does the scalar product $(\mathbf{i} \cdot \mathbf{H})$ vanish. However, the two parts of the energy density, that due to the supercurrent and that due to the magnetic field, remain equal to each other, because from eq. 7-36

$$\frac{1}{2} (\mathbf{i} \cdot \mathbf{G}) = \frac{1}{2} H^0 \quad (7-37)$$

Also the total surface current $\oint \mathbf{i} \cdot d\mathbf{x}_3$ flows perpendicular to H^0 and its value is defined exclusively by H^0 through eq. 7-36:

$$\oint_0^\infty I_1' dx_3 = c H^0, \quad \oint_0^\infty I_2' dx_3 = 0 \quad (7-38)$$

This can of course be deduced directly from the Maxwell equations. All these differences vanish either if the relative principal values Λ_1' and Λ_2' are equal, or if the external field coincides in direction with one of the relative principal axes, i. e., if $\varphi = 0$ or $\pi/2$. Then we return to one of the solutions 7-34 or 7-35.

One might also apply this solution to slightly curved conductors in so far as they are thick compared with the penetration depths $(\beta_1')^{-1}$ and $(\beta_2')^{-1}$, by considering the respective tangent planes as the x_3 plane. For thin superconductors, however, the conditions are different. We see easily from eq. 7-33 that for a sufficiently thin plate the external magnetic field penetrates without hindrance and that a supercurrent is evenly distributed over it. From this we infer that the conclusions drawn in (I) for thin cubic crystal superconductors may also be applied to other lattices. As a confirmation of this we find in Chap. 8 (c) and Chap. 11 (I), that the solutions of London's equations, which lead to the above conclusions for cubic crystal cylinders and spheres, can under suitable conditions be applied to other crystal lattice forms.

¹¹ ϵ_3 is generally not zero but $\epsilon_3 \approx \lambda_{31} I_1' + \lambda_{32} I_2'$.

CHAPTER 8

The Current Flowing in a Wire

(a) In sections (a) to (d) we shall discuss a circular cylinder of radius R carrying a current I in the direction of its axis, the z axis. We assume the current to be confined to a coaxial cylindrical shell so that we shall have a well-defined axially symmetrical external field. We assume the material of the superconductor to have a homogeneous cubic crystalline structure. We use cylindrical coordinates, the distance r from the axis, the azimuth angle θ measured from an arbitrary direction, forming a right-handed system with z in the order r, θ, z (compare Fig. 8-1). In these coordinates the components of the vector curl are

$$\text{curl}_r \mathbf{A} = \frac{1}{r} \frac{\partial A_z}{\partial \theta} - \frac{\partial A_\theta}{\partial z}$$

$$\text{curl}_\theta \mathbf{A} = \frac{\partial A_r}{\partial z} - \frac{\partial A_z}{\partial r}$$

$$\text{curl}_z \mathbf{A} = \frac{1}{r} \frac{\partial(r A_\theta)}{\partial r} - \frac{1}{r} \frac{\partial A_r}{\partial \theta}$$

and for a scalar u :

$$\Delta u = \frac{1}{r} \frac{\partial}{\partial r} \left(r \frac{\partial u}{\partial r} \right) + \frac{1}{r^2} \frac{\partial^2 u}{\partial \theta^2} + \frac{\partial^2 u}{\partial z^2} \quad (8-2)$$

In what follows we shall use solutions of the differential equation $\Delta u - \beta^2 u = 0$ of the form

$$u = f(r) e^{n\theta} e^{\pm k z} \quad (n \text{ an integer}) \quad (8-3)$$

Then $f(r)$ must satisfy the equation

$$\frac{1}{r} \frac{d}{dr} \left(r \frac{df}{dr} \right) + \left(k^2 - \beta^2 - \frac{n^2}{r^2} \right) f = 0 \quad (8-4)$$

By the substitution $x = \sqrt{k^2 - \beta^2} r$ this is transformed into the Bessel equation

$$\frac{1}{x} \frac{d}{dx} \left(x \frac{df}{dx} \right) + \left(1 - \frac{n^2}{x^2} \right) f = 0 \quad (8-5)$$

The solutions of eq. 8-5 which remain finite for $x = 0$ are the Bessel functions $J_n(x)$, namely,



Fig. 8-1. Cylindrical coordinates r, θ for a wire. The z axis is directed toward the reader; Λ is the intersection of the z axis with the plane of the diagram.

$$\begin{aligned}
 I_0(x) &= 1 - \frac{(\frac{1}{2}x)^2}{(1!)^2} + \frac{(\frac{1}{2}x)^4}{(2!)^2} - \dots + \frac{(-1)^m (\frac{1}{2}x)^{2m}}{(m!)^2} \dots \\
 I_1(x) &= \frac{\frac{1}{2}x}{0!1!} - \frac{(\frac{1}{2}x)^3}{1!2!} + \frac{(\frac{1}{2}x)^5}{2!3!} - \dots + \frac{(-1)^m (\frac{1}{2}x)^{2m+1}}{m!(m+1)!} \dots \\
 I_2(x) &= \frac{(\frac{1}{2}x)^2}{0!2!} - \frac{(\frac{1}{2}x)^4}{1!3!} + \frac{(\frac{1}{2}x)^6}{2!4!} - \dots + \frac{(-1)^m (\frac{1}{2}x)^{2m}}{(m-1)!(m+1)!} \dots
 \end{aligned} \quad (8-6)$$

One may verify that these series satisfy the following equations:

$$\begin{aligned}
 \frac{dI_0(x)}{dx} &= -I_1(x) \\
 \frac{dI_1(x)}{dx} &= I_0(x) - \frac{1}{x} I_1(x) \\
 \frac{1}{x} \frac{d[x I_1(x)]}{dx} &= I_0(x) \\
 \int_0^x I_0(\xi) d\xi &= x I_1(x) \\
 \int_0^x I_1(\xi) d\xi &= x^2 I_2(x) \\
 I_0(x) + I_2(x) &= \frac{2}{x} I_1(x)
 \end{aligned} \quad (8-7)$$

For real arguments, x , the functions $I_n(x)$ oscillate about zero and have an infinity of roots. For pure imaginary arguments, the functions increase monotonically without limit with increasing argument.

(b) Let us consider an infinitely long homogeneous superconducting circular cylinder. By symmetry the current density is parallel to the axis and depends only on r . Therefore I must obey the differential eq. 8-4 with $n=0$ and $k=0$. The substitution used in the transition to eq. 8-5 is now $x = i\beta r$ and so

$$I_1 = C I_0(i\beta r), \quad I_2 = I_0 = 0 \quad (8-8)$$

The integration constant is determined by the condition that a total current I flows through the cross section. Consequently,

$$I = 2\pi \int_0^R r I_1 dr = 2\pi C \int_0^R r I_0(i\beta r) dr = 2\pi \frac{CR}{\beta} [-I_1(i\beta R)]$$

(see eq. 8-7). From this it follows that

$$C = \frac{I i\beta / 2\pi R}{I_1(i\beta R)}, \quad I_1 = \frac{i\beta I}{2\pi R} \frac{I_0(i\beta r)}{I_1(i\beta R)} \quad (8-9)$$

ince according to eq. 8-6 $I_0(i\beta r)$ is real and positive, while $I_1(i\beta r)$ is positive imaginary, the right sides of these equations are positive real.

The magnetic field strength is determined by the fundamental eq. X:

$$\mathbf{H} = -c \lambda \text{curl} \mathbf{I}$$

Therefore according to eq. 8-1

$$\mathbf{H}_r = \mathbf{H}_\theta = 0, \quad \mathbf{H}_z = c \lambda \frac{\partial I_z}{\partial r} = i c \lambda \beta C \left(\frac{dI_0(x)}{dx} \right)_{x=i\beta r} \quad (8-10)$$

that is by eqs. 8-7 and 6-7:

$$\mathbf{H}_\theta = \sqrt{\lambda C} [-I_1(i\beta r)] = \frac{I}{2\pi c R} \frac{I_1(i\beta r)}{I_1(i\beta R)} \quad (8-11)$$

We can check this equation by setting $r = R$. At the surface of the cylinder carrying a total current I we must have

$$\mathbf{H}_\theta = \frac{I}{2\pi c R} \quad (8-12)$$

and this actually is the result.

The Bessel functions $I_0(i\beta r)$ and $I_1(i\beta r)$ increase toward infinity as $e^{r/\lambda}$. If βR is a high number, the wire therefore thick compared with the penetration depth, then according to eq. 8-9 with $\beta r \gg 1$, I_1 contains the factor $e^{-r/\lambda}$. The current, and likewise the magnetic field, lie almost entirely in a protecting layer of thickness β^{-1} . On the other hand $I_0(i\beta r)$ has a minimum at $x=0$ (equal to 1), and if $\beta R \ll 1$, then the current density I increases only slightly from the axis to the perimeter — it is more or less evenly distributed over the section. Both results were to have been expected according to Chap. 7.

(c) Now let the cylinder consist of a normally conducting part where $x < 0$ and a superconducting part where $x > 0$. According to Chap. 7 the electrostatic potential is constant inside the superconductor. The boundary plane at $x=0$ is thus an equipotential surface for the normal conductor; therefore the current flows exactly as in a wire of unlimited length, namely, it is evenly distributed over the cross section. The current density is

$$I_1 = \frac{I}{\pi R^2} \quad (z < 0)$$

The magnetic lines of force here are circles around the axis of the wire. Since $\int \mathbf{H}_\theta \cdot d\mathbf{s}$ integrated round a circle of radius $r < R$ must equal the total current through the circle, $I \cdot r^2/R^2$, divided by c , we have

$$\mathbf{H}_\theta = \frac{r \cdot I}{2\pi c R^2} \quad (z < 0) \quad (8-13)$$

On entering the superconductor the current must restrict itself to the boundary layers. We have therefore to take into account a radial component I_r in the neighborhood of the boundary plane. Because of this it is more expedient to start with the magnetic field strength which even at this point has by symmetry only a component H_θ independent of θ . For large positive values of x we can use the solution 8-11 directly; in the neighborhood of $x=0$, however, other terms have to be added that decrease with increasing x .

As already mentioned, the differential equation $\Delta u - \beta^2 u = 0$ holds for \mathbf{H}_z and \mathbf{H}_r , but not for \mathbf{H}_θ , which is associated with a curvilinear coordinate. Since, however,

$$\mathbf{H}_z = -\mathbf{H}_\theta \sin \theta, \quad \mathbf{H}_r = \mathbf{H}_\theta \cos \theta$$

we may write, using an a priori undetermined constant u_p ,

$$\mathbf{H}_\theta = f(r) e^{-\sqrt{c^2 \beta^2 + \beta^2} x}$$

so that we get

$$\mathbf{H}_r = i \mathbf{H}_z = f(r) e^{i\theta} e^{-\sqrt{c^2 \beta^2 + \beta^2} x}$$

Comparison with eq. 8-3 proves that $f(r)$ must be a solution of eq. 8-4 with $n = 1$ and $k = \sqrt{\alpha_p^2 + \beta^2}$, i. e.,

$$f(r) = I_1(\alpha_p r)$$

inconsistent with eq. 8-12, an equation which must still hold; we therefore determine α_p by the requirement that

$$I_1(\alpha_p R) = 0 \quad (8-14)$$

As there are infinitely many zeros of $I_1(x)$, a discrete but infinite set of real α_p values satisfy this condition.

In this way we arrive at the following series for H_θ :

$$H_\theta = \frac{I}{2\pi c R} \left[\frac{I_1(\alpha \beta r)}{I_1(\alpha \beta R)} + \sum_{p=1}^{\infty} \alpha_p I_1(\alpha_p r) e^{-\sqrt{\alpha_p^2 + \beta^2} r} \right] \quad (z > 0) \quad (8-15)$$

and now have only the coefficients α_p to calculate. For this purpose the continuity condition for H_θ at $z = 0$ is available. Because of eq. 8-13

$$\sum_{p=1}^{\infty} \alpha_p I_1(\alpha_p r) = \frac{r}{R} - \frac{I_1(\alpha \beta r)}{I_1(\alpha \beta R)} \quad (8-16)$$

must hold identically in r . To carry out the calculations two relations are available which we accept without proof:

$$\int_0^R r I_1(\gamma r) I_1(\delta r) dr = \frac{[\delta R I_1(\gamma R) I_0(\delta R) - \gamma R I_1(\delta R) I_0(\gamma R)]}{(\gamma^2 - \delta^2)} \quad (8-17)$$

From the first of these follows the important fact that the functions $I_1(\alpha_p r)$ selected by eq. 8-14 form an orthogonal system, i. e.,

$$\int_0^R r I_1(\alpha_p r) I_1(\alpha_q r) dr = 0 \quad \text{for } \alpha_p \neq \alpha_q$$

Multiplying eq. 8-16 by $r I_1(\alpha_q r)$ and integrating from 0 to R therefore eliminates all the coefficients except α_q and yields for it the value

$$\alpha_q = \frac{\int_0^R r \left[\frac{r}{R} - \frac{I_1(\alpha \beta r)}{I_1(\alpha \beta R)} \right] I_1(\alpha_q r) dr}{\int_0^R r I_1^2(\alpha_q r) dr}$$

The integration can be carried out easily by means of eqs. 8-7 and 8-17. The result is

8. CURRENT FLOWING IN A WIRE

$$\alpha_q = -\frac{1}{2\alpha_q R} \left\{ \frac{1}{I_0(\alpha_q R)} + \frac{\alpha_q^2(\alpha_q^2 + \beta^2)}{I_2(\alpha_q R)} \right\}$$

Because of the last of the equations 8-7, eq. 8-14 is $I_2(\alpha_q R) = -I_0(\alpha_q R)$ so

$$\alpha_q = -\frac{1}{2\alpha_q R} \cdot \frac{\beta^2(\alpha_q^2 + \beta^2)}{I_0(\alpha_q R)} \quad (8-18)$$

We get the current density now from the fundamental eq. 11:
 $I = c \text{ curl } H$

According to eqs. 8-1, 8-7, and 8-15 this yields

$$I_r = -c \frac{\partial H_\theta}{\partial z} = \frac{I}{2\pi R} \sum_{p=1}^{\infty} \alpha_p \left[\frac{1}{\alpha_p^2 + \beta^2} I_1(\alpha_p r) e^{-\sqrt{\alpha_p^2 + \beta^2} r} \right]$$

$$\begin{aligned} I_z &= \frac{c}{r} d(r H_\theta)/dr \\ &= \frac{I}{2\pi R} \left[\frac{\alpha \beta I_0(\alpha \beta r)}{I_1(\alpha \beta R)} + \sum_{p=1}^{\infty} \alpha_p \alpha_p I_0(\alpha_p r) e^{-\sqrt{\alpha_p^2 + \beta^2} r} \right] \end{aligned} \quad (8-19)$$

Because of eq. 8-14 I_r vanishes at the surface of the cylinder $r = R$ as required. The same is true at $r = 0$ because $I_1(0) = 0$.

Furthermore, as soon as $\beta z \gg 1$, both I_r and that part of I_z represented by the sum over p vanish. Then I_z assumes the same value as for the infinitely long superconducting cylinder given in eq. 8-9. The transition from the even current distribution that still exists at the boundary $z = 0$ to the distribution that characterizes the superconductor is effected in a distance β^{-1} .

The first roots of eq. 8-14 are

$$\alpha_1 R = 3.83, \quad \alpha_2 R = 7.02, \quad \alpha_3 R = 10.2, \quad \alpha_4 R = 16.6 \dots$$

If therefore $\beta R \geq 100$ (with $\beta = 10^5 \text{ cm}^{-1}$, $R = 10^{-3} \text{ cm}$ is sufficient for this), these first α_p are all small compared with β . Then I_r is great compared with the contribution to I_z from the sum over p . But according to what has been said in section (b) about the exponential decay of the first terms, this contribution to I_z is practically the only one in the region where r is considerably smaller than R . So in this region the lines of flow, which leave the boundary of the normal conductor evenly distributed and perpendicular to the boundary, bend sharply into the radial direction. They have to do this because the major portion of the current must be deflected from the interior of the wire into the protecting layer of thickness β^{-1} adjoining the cylinder's surface, and do this within a distance of β^{-1} in the z direction.

The thinner the wire the greater become the α_p , and if $\beta R \ll 1$ they are considerably greater than β . According to eq. 8-18 the coefficients α_p then all decrease, and with them the sum in eq. 8-19, and so also the radial

current I_r . The latter is no longer needed because, according to (b) the current is uniformly distributed over the cross section even in the superconductor.

(d) Let the cylinder now consist of two superconductors touching in the plane $z = 0$. Let the poorer superconductor lie below this plane; $z < 0$, reciprocal penetration depth β' , and therefore to the greater depends on β so transition phenomena must now appear on both sides of the boundary.

For $z > 0$ we can retain the expression 8-15 with the values of a_p given by eq. 8-14, and also the consequent eq. 8-19. For $z < 0$ we write down the analogous expression:

$$H_\theta' = \frac{I}{2\pi c R} \left\{ \frac{I_1(\epsilon\beta r)}{I_1(\epsilon\beta R)} + \sum_{p=1}^{\infty} a_p' I_1(a_p r) e^{+\sqrt{a_p'^2 + \beta'^2} z} \right\} \quad (z < 0) \quad (8-20)$$

he resulting calculation of the current distribution differs from eq. 8-19 not only in the sign of the exponents but also in the sign of the right-hand side of the equations for I_r . We have two boundary conditions to evaluate the coefficients a_p and a_p' , first the continuity of H_θ and second (see Chap. 3, eq. 3-9)

$$\lambda I_r = \lambda' I_r'$$

according to eq. 6-7 we can also write for this

$$\frac{I_r}{I_r'} = \frac{\beta^2}{\beta'^2} \quad (8-21)$$

This second condition is fulfilled identically in r only if the corresponding coefficients in the two series for I_r and I_r' are in the ratio β^2/β'^2 :

$$\frac{a_p'}{a_p} \sqrt{\frac{(a_p^2 + \beta^2)}{(a_p'^2 + \beta'^2)}} = -\frac{\beta^2}{\beta'^2}$$

or

$$a_p' = -a_p \left(\frac{\beta'}{\beta} \right)^2 \sqrt{\frac{(a_p^2 + \beta^2)}{(a_p'^2 + \beta'^2)}} \quad (8-22)$$

The continuity of H_θ , however, requires that

$$\sum_{p=1}^{\infty} (a_p - a_p') I_1(a_p r) = \frac{I_1(\epsilon\beta' r)}{I_1(\epsilon\beta' R)} - \frac{I_1(\epsilon\beta r)}{I_1(\epsilon\beta R)} \quad (8-23)$$

identically in r . Applying the method used in (b) we conclude:

$$a_p - a_p' = -\frac{2a_p}{R I_0(a_p R)} \frac{\beta'^2}{(a_p^2 + \beta^2)} \quad (8-24)$$

This equation and 8-22 determine both a_p and a_p' . We see that if we assume $\beta' = \beta$ all the a_p and the a_p' vanish, as indeed must be so.

The transformation from one current distribution to the other takes place in two layers adjoining the boundary plane $z = 0$ of thickness β^{-1}

8. CURRENT FLOWING IN A WIRE

41

and β'^{-1} respectively. It is effected by radial currents in both superconductors. To find the contributions of each of the two conductors, we compare the integrals $\int_0^\infty I_r dz$ and $\int_{-\infty}^0 I_r dz$. As

$$I_r = -c \frac{\partial H_\theta}{\partial z}$$

both yield the same value for $(H_\theta)_{z=0}$. The greater absolute value of I_r , which according to eq. 8-21 occurs in the better superconductor, is compensated by the smaller depth of the boundary layer. In the three cases treated here the magnetic field outside the superconductor is known *a priori*. The solutions therefore come under the uniqueness theorem of Chap. 7 (a).

(c) The solutions of section (b), i. e., of the problem of the infinitely long cylinder carrying a current, can be applied to noncubic crystal superconductors only if one of the axes of the ellipsoid representing the tensor $\lambda_{\alpha\beta}$ coincides with the axis of the cylinder. We call this axis the x_3 axis. If I_r has this direction everywhere then by eq. VIII the supermomentum has only one component G_3 . The only tensor component that enters the calculation is the principal value λ_3 . It is only necessary to replace β in eqs. 8-9 and 8-10 by

$$\beta_3 = \frac{1}{c \sqrt{\lambda_3}} \quad (8-25)$$

to take over the former solution. Its uniqueness is again guaranteed by the theorem of Chap. 7 (a).

(f) It has not yet been possible to give a rigorous solution of our problem for a cylinder with an elliptical cross section, except in the approximation corresponding to the "thick" cylinder. In this case the circumference of the surface is a line of force of the external magnetic field. This field is irrotational and its potential obeys the equation $\Delta \phi = 0$, but it increases with each turn around the cylinder by the "period"

$$-\oint \mathbf{H} \cdot d\mathbf{s} = -\frac{I}{c}$$

where, as before, I means the total current in the cylinder. Let the axes of the elliptical cross section be a and b ($a > b$). The "thick" cylinder is characterized by the fact that the smallest radius of curvature b^2/a at the ends of the greater axis is great compared with the penetration depth β^{-1} . The same holds *a priori* for b .

It is well known that if a functional relation $\zeta = \zeta(x)$ exists between two complex variables $\zeta = x + iy$ and $x = \psi + i\varphi$, then ψ and φ are solutions of the potential equation. In the present problem

$$\zeta = C \cosh(a\chi) = C [\cosh(a\psi) \cos(a\varphi) + i \sinh(a\psi) \sin(a\varphi)] \quad (8-26)$$

can be adjusted to the given boundary conditions. The constants C and a are available for this purpose.

Thus it follows from eq. 8-26 that

$$x = C \cosh(\alpha\psi) \cos(\alpha\varphi), \quad y = C \sinh(\alpha\psi) \sin(\alpha\varphi) \quad (8-27)$$

Elimination of φ yields

$$\left[\frac{x}{\cosh(\alpha\psi)} \right]^2 + \left[\frac{y}{\sinh(\alpha\psi)} \right]^2 = C^2 \quad (8-28)$$

The curves $\psi = \text{constant}$ are everywhere orthogonal to the curves $\varphi = \text{constant}$ and so represent the lines of force. If we fix a value ψ_0 in such a way that

$$a = C \cosh(\alpha\psi_0) \quad \text{and} \quad b = C \sinh(\alpha\psi_0)$$

or

$$C^2 = a^2 - b^2, \quad \tanh(\alpha\psi_0) = \frac{b}{a} \quad (8-29)$$

then the surface of the cylinder contains the corresponding line of force, required by the one boundary condition. All the other lines of force are ellipses confocal with the cross section of the cylinder. The period of the potential has the prescribed value if we put

$$a = -\frac{2\pi c}{I} \quad (8-30)$$

The magnitude H of the field strength follows from the general equation according to eq. 8-26:

$$H = \frac{1}{C|a|\sinh(\alpha\chi)} = \frac{1}{\{C|a|[\sinh^2(\alpha\psi)\cos^2(\alpha\varphi) + \cosh^2(\alpha\psi)\sin^2(\alpha\varphi)]\}^{1/2}} \quad (8-31)$$

In particular the field strength at the surface $\psi = \psi_0$ is (see eq. 8-29)

$$H^0 = \frac{I}{2\pi c} [a^2 \sin^2(\alpha\varphi) + b^2 \cos^2(\alpha\varphi)]^{-1/2} \quad (8-32)^1$$

Consequently at the end point of the greater axis ($y = 0$, $\sin(\alpha\varphi) = 0$, eq. 8-27), H^0 is a maximum exceeding the minimum at the end of

¹The transformation from φ to the polar angle $\theta = \arctan y/x$ can be effected by an equation following from eq. 8-27:

$$\tan \theta = \tanh(\alpha\psi) \tan(\alpha\varphi)$$

Applying this to eq. 8-32 we have to put $\tan \theta = (b/a) \tan(\alpha\varphi)$ according to eq. 8-29. The result is

$$H^0 = \frac{I}{2\pi c} \sqrt{\frac{(a^2 \sin^2 \theta + b^2 \cos^2 \theta)}{(a^4 \sin^2 \theta + b^4 \cos^2 \theta)}}$$

the smaller axis [$x = 0$ and $\cos(\alpha\varphi) = 0$] by the factor a/b . According to eq. 7-38 this statement is equally true of the surface density of the supercurrent, whatever the crystal structure of the conductor. If d is the perpendicular distance of an interior point from the surface, then according to eq. 7-10 for a cubic lattice, the current density within the protecting layer is

$$i_s = H^0 \chi^{-1/2} e^{-\beta d} \quad (8-33)$$

and practically no current is flowing in the protected region beneath.

(g) The fact that the supercurrent prefers protruding edges is no peculiarity of the elliptical cylinder, but a general characteristic of this current. It is caused by the well-known fact that when the lines of force envelope the surface of a body, the field intensity is considerably increased at such edges. The potential theory proves this as follows.

If as in section (f) we start from the conformal mapping $\chi = -iC\zeta^n$ then ψ , the real part of χ , equals $C|\zeta|^n \sin(n\theta)$; we take n to be a fraction between $1/2$ and 1. The line of force $\psi = 0$ consists of the radial lines $\theta = 0$ and $\theta = \pi/n$. In our mapping we see the representation of a field whose lines of force run along the surface of the superconductor filling the space $\pi/n < \theta < 2\pi$. At the protruding edge $\zeta = 0$

$$H = \left| \frac{d\chi}{d\zeta} \right| = nC|\zeta|^{n-1}$$

becomes infinite. If the edge is not mathematically sharp, but rounded, H remains finite, but in any case becomes especially large compared with the surrounding field. If we choose $n > 1$ we get a re-entrant edge and see that H decreases to zero therein.

In a column with rectangular cross section the strongest current runs along the four edges.

However this holds only under the conditions for a "thick" superconductor, and this excludes mean radii of curvature comparable with or smaller than the penetration depth β^{-1} . In extremely thin superconductors the supercurrent is distributed evenly over the cross section in accordance with Chap. 7 (g).

$$\frac{dH_0(x)}{dx} = -H_1(x) \quad (9-4)$$

and is a solution of the differential eq. 8-5 with $n = 1$. $H_1(x)$ is negative real everywhere, becoming infinite like $-2/(\pi y)$; it increases monotonically reaching the value zero only for infinitely large positive values of y . It now follows from eq. 8-3 as in eq. 8-10 that

$$H_0 = c \lambda \frac{\partial I_1}{\partial r} = \sqrt{\frac{2}{\pi}} [C - i I_1(\beta r) + D H_1(\beta r)] \quad (9-5)$$

According to eqs. 9-1 and 9-2, the equations determining the constants C and D are

$$\begin{aligned} -i C I_1(\beta R_i) + D H_1(\beta R_i) &= \frac{\beta I'}{2\pi R_i} \\ -i C I_1(\beta R_o) + D H_1(\beta R_o) &= \frac{\beta(I + I')}{2\pi R_o} \end{aligned} \quad (9-6)$$

We need not write out the solution explicitly. For a thick hollow cylinder, i. e., when $R_o - R_i \gg \beta^{-1}$, the first terms in eqs. 9-3 and 9-5 decrease toward the interior and can be neglected completely in the neighborhood of R_i , and similarly the second terms decrease toward the outside and are negligible near R_o . Then we have simply

$$C = \frac{(I + I')(\beta/2\pi R_i)}{I_1(\beta R_i)}, \quad D = \frac{I'(\beta/2\pi R_o)}{H_1(\beta R_o)} \quad (9-7)$$

Comparing this value of C with that in eq. 8-9 we see that the outer protecting layer of the cylindrical shell now carries the current $I + I'$. The equation for D shows that the protecting layer adjoining the inner surface carries the current $-I'$ because $H_1(\beta R_i)$ is negative and $i H_0(\beta r)$ in eq. 9-3 is positive. (See Fig. 9-1.) And this must be so; because a circle $r = \text{constant}$ within the protected interior of the cylindrical shell must enclose zero net current because $H = 0$ on the circle. This current $-I'$ on the inner wall of the shell must be compensated by an additional current $+I'$ in the outer surface in order to have the total current I for the whole cylinder. Also it is only in this way that we can satisfy at the inner wall the rule that the current, the magnetic field strength, and the inner normal to the superconductor form a right-handed system.

For thin hollow cylinders, $R_o - R_i \ll \beta^{-1}$, one develops the two cylinder functions of eq. 9-5 in powers of $r - R_m$ starting from $R_m = \frac{1}{2}(R_o + R_i)$. One sees without calculation that, to a first approximation there is a linear transition from one to the other of the two values of H_0 prescribed by eqs. 9-1 and 9-2. This corresponds to the linear transition in the thin plane parallel plate of Chap. 7, eq. 7-17.

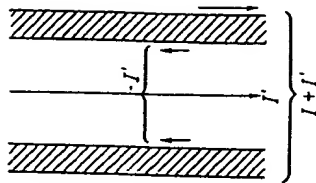


Fig. 9-1. Current distribution in a hollow superconducting cylinder with a coaxial wire. I is the net current in the superconducting cylinder; I' is the current in the coaxial wire.

The Current Flowing in a Hollow Cylinder

(a) For our present discussion let us consider a hollow cylinder with an inner radius R_i and outer radius R_o . Let the cylinder be homogeneous, superconducting, and have cubic crystal structure; let a total current I flow along it. But also let a wire, either normal or superconducting, be placed along the axis of the cylinder and carry another current I' . We consider I or I' to be positive if they flow in the positive z direction. We imagine the circuit to be closed by means of a coaxial cylindrical shell at infinity, as in Chap. 8.

Under these circumstances the magnetic field strength at the inner cylindrical surface $r = R_i$ is

$$H_0 = \frac{I'}{2\pi c R_i} \quad (r = R_i) \quad (9-1)$$

because a circle of radius R_i encloses the current I' . A circle lying in the outer cylindrical surface ($r = R_o$), however, encloses the total current $I + I'$. Consequently the field strength there is

$$H_0 = \frac{I + I'}{2\pi c R_o} \quad (r = R_o) \quad (9-2)$$

From these conditions we can obtain the fields within the cylinder uniquely according to the theorem of Chap. 7 (a).

The current is parallel to z and depends only on r just as for the solid cylinder [Chap. 8 (b)]. Furthermore I_1 is again a solution of the differential equation $\Delta u - \beta^2 u = 0$. But eq. 8-8 is insufficient because we cannot satisfy both conditions 9-1 and 9-2 with only one integration constant. However, we are relieved of the requirement that I_1 must remain finite for $r = 0$ because the domain of the desired solution does not extend so far. Therefore we can generalize the expression 8-8 as follows:

$$I_1 = C I_0(\beta r) + i D H_0(\beta r) \quad (9-3)$$

where $H_0(x)$ is the Hankel function of the first kind¹ and zero order, namely, that solution of the differential eq. 8-5 with $n = 0$ which becomes logarithmically infinite at the origin; $I_0(x)$ also satisfies eq. 8-5. $H_0(x)$ is so defined that $i H_0(\beta y)$ is positive real for positive real y and behaves at $y = 0$ like $-(2/\pi) \ln y$; it decreases monotonically with increasing y , and finally vanishes asymptotically. The Hankel function of the first kind and first order $H_1(x)$ is connected with $H_0(x)$ by the relation

¹We can omit the usual suffix 1 because we shall not have to deal with the Hankel function of the second kind.

The solution given in eqs. 9-6 and 9-7 can be generalized to non-cubic crystals as in Chap. 8 (e) if one principal axis of the tensor falls in the direction of the cylinder. One only has to replace β by the β_s of eq. 8-25. Everything that follows in this chapter holds independently of all crystallographic properties.

As explained in Chap. 1 every "thick" superconductor (there have been scarcely any experiments done on thin hollow cylinders) can stand only a certain critical value H_c at its surface. According to eqs. 9-1 and 9-2 this sets a limit for the superconducting state of the hollow cylinder:

$$|I'| < 2\pi c R_i H_c, \quad |I + I'| < 2\pi c R_o H_c \quad (9-8)$$

If we plot I and I' as coordinates in a plane (Fig. 9-2) the interior of the shaded parallelogram represents the region of superconductivity. This simple consequence of the Slisbee hypothesis has never been checked experimentally in a rigorous manner.

(b) Figure 9-3 represents the cross section of an arrangement of normal and superconducting parts symmetrical with respect to the z axis. Leads in the z axis may supply the current I . We ask what part of I flows through the inner solid cylinder, and what part flows through the outer hollow cylinder. This is decided not in the superconductor, but in the normal conductor. The circular sections K and the annular ring R in the figure have the same potential because the electrostatic potential in a superconductor is constant. Potential theory applied to the interior of the normal conductor then tells us what part of I takes the path through the inner cylinder.

This current enters the superconductor at K and must finally reach the lower lead. As it cannot penetrate deeply into the superconductor, it can only go along the boundary of the superconductor, as sketched in the figure. It flows, in fact, across the plane R and there joins the current $I - I'$ that enters the outer surface of the superconductor from above. The full current then flows down the outer surface to the lower leads.

The uniqueness of the solution sketched here is again guaranteed by the theorem of Chap. 7 (a). To begin with, owing to the symmetry of the arrangement, the magnetic field is known for all boundaries.

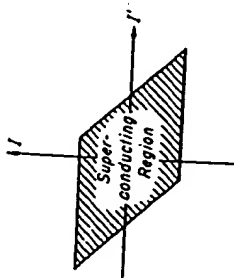


Fig. 9-2. Diagrammatic representation of Slisbee's hypothesis for a hollow superconducting cylinder. I is the net current in the superconducting cylinder; I' is the current in the coaxial wire.

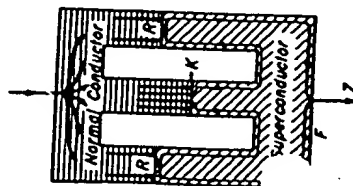


Fig. 9-3. Current distribution at the boundaries between normal and superconducting parts of a cylinder.

ries, e. g., the lower surface F of the superconductor. After solving the potential problem for the normal conductor (which is possible only in one way) our knowledge of I , allows us to find the field distribution first in the hollow space between the inner cylinder and the outer shell, secondly at the boundaries K and R of the superconductor, and therefore at all surfaces of the latter.

(c) Figure 9-4 represents a similar arrangement only in this case the whole shaded area is to be superconducting. Again we imagine the current I to be fed in at Z' and carried back by a third cylinder C_3 coaxial with C_1 and C_2 . This shields the field from outside because a curve enclosing it encloses a net current zero. The circuit for the current I_1 flowing in C_1 is completed by the inner walls of C_2 and the two superconducting caps. It does not affect the outside at all, so long as the superconducting parts are thick compared with the penetration depth, but neither can it be influenced from the outside. It is a persistent current in what is here actually a doubly connected body. Its energy is substantially of magnetic nature and is located in the hollow space between C_1 and C_2 and has the form $a I_1^2$; the value of the constant a is of no importance.

Fig. 9-4. Doubly connected superconductor in the same arrangement as in Fig. 9-3.

One can also consider this apparatus from another point of view. The parts formed by sections at A and B can be regarded as superconductors in parallel in the sense of Chap. 2. In order to permit the current strength I_2 in the cylinder C_2 a current $I_1 + I_2$ must flow along its outer walls because the inner wall carries the current $-I_1$. Consequently the energy located between C_2 and C_3 (and to an unimportant degree also in the protecting layer of C_2) is of the form $\gamma (I_1 + I_2)^2$. Writing the total energy $a I_1^2 + \gamma (I_1 + I_2)^2$ in the form $\frac{1}{2} (\rho_{11} I_1^2 + \rho_{22} I_2^2 + 2 \rho_{12} I_1 I_2)$ we have $\rho_{12} = \gamma$. According to eq. 2-6 it follows that if there were no current in the system initially, I_1 would remain zero after switching on the current I , while any initial current I_1 would remain unchanged by switching on I .

These considerations, although leading to no new results, nevertheless show the intimate relations between the discussion of Chap. 2 and the theory explained in Chap. 3 and later chapters.

The requirements that H_z goes over continuously into H_r at $r = R_i$ and to H_i at $r = R_o$ serve to determine the constants C and D .

If the walls of the cylinder are thick compared with β^{-1} we can in eq. 10-4 neglect the first term when $r = R_i$ and the second term when $r = R_o$, as we did in Chap. 9 (a). We then have to put

$$C = \frac{H_i}{J_0(\beta R_i)}, \quad D = \frac{H_i}{i H_0(\beta R_i)} \quad (10-6)$$

This leads back to eq. 10-1 for the layer at the outer boundary, while for the neighborhood of the inner boundary it follows that

$$H_i = H_i \frac{H_0(\beta r)}{H_0(\beta R_i)}, \quad i_\theta = -H_i \frac{H_1(\beta r)}{i \sqrt{2} H_0(\beta R_i)} \quad (10-7)$$

Since $H_1(\beta r)$ is negative while $H_0(\beta R_i)$ is positive, the current for positive H_i has again the direction of increasing θ . A field-free region is located between the two protective layers where these equations hold.

Let us choose $H_i = 0$. If we ascribe to the cylinder a finite length which, however, is great compared with its diameter, eqs. 10-7 are still valid except in the neighborhood of the ends. Here we have an example of a persistent current, because indeed a hollow cylinder is a doubly connected body.

Let us assume the cylinder to be thin ($R_o - R_i \ll \beta^{-1}$) and choose $H_i = H_o$. Writing R_m for the arithmetic mean between R_i and R_o , the first terms of the expansion will now suffice:

$$H_z = (H_i)_{R_m} + \left(\frac{\partial H_z}{\partial r} \right)_{R_m} (r - R_m)$$

If the right-hand side has to assume the same value; H_z at $r = R_i$, i. e., at $r - R_m = -\frac{1}{2}(R_o - R_i)$, as it does at $r = R_o$, i. e., at $r - R_m = \frac{1}{2}(R_o - R_i)$, then $(\partial H/\partial r)_{R_m}$ must be zero; consequently according to eq. 10-5 $(i_\theta)_{R_m}$ is also zero. This again confirms the general argument of Chap. 7 (b) for thin specimens.

The solutions given in eqs. 10-1 and 10-2, 10-4 and 10-5 remain valid for noncubic crystals provided the ellipsoid of the tensor $\lambda_{\theta\rho}$ has an axis of symmetry (say x_3) in the direction of the axis of the cylinder, and the two principal values λ_1 and λ_2 coincide. Then for this problem the supermomentum is in fact always in the same direction as the supercurrent, just as in the cubic case, while

$$\beta_1 = \frac{1}{c \sqrt{\lambda_1}} \quad (10-8)$$

replaces β in the calculation.

(c) Now let us imagine a solid cylinder of radius R with no longitudinal current, placed in a field perpendicular to its axis — a transverse field. The field does not remain homogeneous as the lines of force must go around the cylinder if the latter is not too thin, i. e., they are deflected by it as shown in Fig. 1-5. If we are not satisfied with the approximation used in the figure, which regards the superconductor as completely impenetrable to the field (a case for which the distortion of the field can easily be

CHAPTER 10

The Cylinder in a Homogeneous Magnetic Field

(a) We now place a homogeneous superconducting cylinder in a longitudinal magnetic field; no current flows in the direction of its axis; the external field has everywhere the same strength $H_z = H^0$ outside the surface of the cylinder.

In the interior of the cylinder H_z has to satisfy the equation $\Delta u - \beta^2 u = 0$ and must moreover depend only on the distance r from the axis. Like the current density i_r in Chap. 8 (b) which satisfied the same conditions, H_z must therefore be proportional to $J_0(\beta r)$. The boundary condition that H_z be continuous is then obviously satisfied by

$$H_z = H^0 \frac{J_0(\beta r)}{J_0(\beta R)} \quad (10-1)$$

We find the current density from $i = c \operatorname{curl} H$. According to eq. 8-1 this reads:

$$i_r = i_\theta = 0, \quad i_z = -c \frac{\partial H_z}{\partial r} = -c H^0 \frac{J_1(\beta r)}{\sqrt{2} J_0(\beta R)} \quad (10-2)$$

From eq. 8-7 $dJ_0(x)/dx = -J_1(x)$. From the form of these two Bessel functions, discussed in Chap. 8 (b) it also follows here that the influence of the field on a thick wire is confined to a protecting layer of thickness β^{-1} . The currents that provide this protection flow in the direction of increasing θ when H^0 is positive because $-J_1(\beta r)$ is positive. This corresponds to the rule that current, field strength, and inner normal to the superconductor — here the negative r direction — form a right handed system. For a thin wire ($\beta R \ll 1$) the flat minimum of $J_0(\beta r)$ at $r = 0$ shows that the field penetrates almost without loss. In this case

$$i_\theta = -\frac{1}{2} \frac{H^0 \beta r}{\sqrt{2}} \quad (10-3)$$

This becomes identical with eq. 7-29 if one puts $L = R$ and $\tau_m = -r/2 R$.

(b) Now let us consider a hollow cylinder with radii R_i and R_o having field strength $H_z = H_i$ in the bore, whereas outside there is a homogeneous field $H_z = H_o$. Within the superconductor H_z has to satisfy the same differential equation as in case (a); but for the reasons we have discussed in Chap. 9 (a) in connection with the hollow cylinder carrying a current, we now write down the analogous expression to eq. 9-3:

$$H_z = C J_0(\beta r) + i D H_0(\beta r) \quad (10-4)$$

From this it follows, as in (a) (compare also eq. 9-5) that

$$i_z = -c \frac{\partial H_z}{\partial r} = -c \beta C J_1(\beta r) - c \beta D H_1(\beta r) \quad (10-5)$$

calculated by potential theory) we have to try to determine the internal and external field simultaneously. We come here for the first time to an example in which the external field cannot be specified in advance. The uniqueness theorem of Chap. 7 (a) is no longer applicable; instead we shall need a more general uniqueness theorem worked out in Chap. 12 (d). Introduce rectangular coordinates in a plane perpendicular to the wire to supplement the polar coordinates r and θ used hitherto:

$$x = r \cos \theta, \quad y = r \sin \theta$$

Suppose the intensity of the homogeneous field has the positive direction and magnitude H^0 . Its potential would then be

$$\phi = -H^0 x = -H^0 r \cos \theta$$

According to potential theory a completely impenetrable cylinder would act at points outside it as a dipole sheet, and its potential would be of the form $1/(a/r) \cos \theta$, with $a = R^2$. We therefore seek a rigorous solution of the problem in the following form with a at first undetermined:

$$\phi = -H^0 \left(r + \frac{a}{r} \right) \cos \theta \quad (10-9)$$

Because $H = -\text{grad } \phi$ it follows that

$$H_r = -\frac{\partial \phi}{\partial r} = H^0 \left(1 - \frac{a}{r^2} \right) \cos \theta$$

$$H_\theta = -\frac{1}{r} \frac{\partial \phi}{\partial \theta} = -H^0 \left(1 + \frac{a}{r^2} \right) \sin \theta \quad (10-10)$$

(We see that eq. 10-10 yields $H_\theta = 0$ for $a = R^2$ and $r = R$, corresponding to the case of impenetrability.)

H_θ is therefore proportional to $\sin \theta$ on the boundary as well as in the external space. Remembering the intimate connection between the current density and the tangential component of magnetic field, which we first noted when discussing thick specimens, it is natural to put inside the cylinder

$$I_r = I_\theta = 0, \quad I_z = f(r) \sin \theta \quad (10-11)$$

Since I_z must be a solution of $\Delta u - \beta^2 u = 0$, the differential eq. 8-4 with $k = 0$ and $u = 1$ must be satisfied by $f(r)$. Furthermore $f(r)$ must remain finite and continuous at $r = 0$ so that

$$f(r) = C I_1(\epsilon \beta r), \quad I_z = \epsilon C I_1(\epsilon \beta r) \sin \theta \quad (10-12)$$

where C is an integration constant. From $H = -c \lambda \text{curl } I$ and eq. 8-1 it follows therefore that

$$\begin{aligned} H_r &= -\frac{c \lambda}{r} \frac{\partial I_z}{\partial \theta} = -\frac{c \lambda C}{r} \epsilon I_1(\epsilon \beta r) \cos \theta \\ &= -\frac{\sqrt{\lambda C}}{\beta r} \epsilon I_1(\epsilon \beta r) \cos \theta \end{aligned} \quad (10-13)$$

$I_1 \cos \theta$ is the real part of the function ζ^{-1} of the complex variable $\zeta = x + iy$ and in this way a solution of the potential equation.

and, noting one of the eqs. 8-7,

$$H_\theta = c \lambda \frac{\partial I_z}{\partial r} = -\sqrt{\lambda C} \left[I_0(\epsilon \beta r) - \frac{1}{\epsilon \beta r} I_1(\epsilon \beta r) \right] \sin \theta \quad (10-14)$$

For boundary conditions we have the continuity of the two components of H at $r = R$. These can be satisfied by the above expressions, and this justifies our chosen procedure. As a comparison of eqs. 10-13 and 10-14 with 10-10 shows, we have only to adjust the constants a and C so that

$$H^0 \left(1 - \frac{a}{R^2} \right) = \frac{\sqrt{\lambda C}}{\epsilon \beta R} I_1(\epsilon \beta R) \quad (10-15)$$

$$H^0 \left(1 + \frac{a}{R^2} \right) = \sqrt{\lambda C} \left[I_0(\epsilon \beta R) - \frac{1}{\epsilon \beta R} I_1(\epsilon \beta R) \right]$$

These requirements yield:

$$C = \frac{2 H^0}{\sqrt{\lambda} I_0(\epsilon \beta R)}, \quad 1 - \frac{a}{R^2} = \frac{2 I_1(\epsilon \beta R)}{\epsilon \beta R I_0(\epsilon \beta R)} \quad (10-16)$$

$$I_z = \frac{2 H^0 \sin \theta \epsilon I_1(\epsilon \beta r)}{\sqrt{\lambda} I_0(\epsilon \beta R)}$$

According to eqs. 10-13 and 10-14 the magnetic lines of force in the interior of the cylinder must be such that $I_z = \text{constant}$. For thick cylinders this means

$$\frac{\epsilon I_1(\epsilon \beta r)}{I_0(\epsilon \beta R)} = -e^{-\beta(R-r)} \quad (10-17)$$

The right-hand side of the equation for a becomes zero, and a assumes the potential theory value R^2 , and at the surface, according to eq. 10-10 we shall have

$$(H_\theta)_R = -2 H^0 \sin \theta$$

The maximum $2 H^0$ of $|H_\theta|$ illustrates the doubling of the field strength due to field deformation discussed in Chap. 1 (g). From eqs. 10-16 and 10-17, however, it follows that

$$I_z = -2 H^0 \lambda^{-1/2} e^{-\beta(R-r)} \sin \theta = \lambda^{-1/2} (H_\theta)_R e^{-\beta(R-r)}$$

The same result would be obtained from eq. 7-10 by adapting to a cylindrical surface the equation given there for a plane boundary. Such a step would be justified for a thick cylinder. The protecting layer obeys the same laws here as at a plane surface. I_z is negative for positive θ , i. e., in the upper part of Fig. 1-5, so the current is flowing away from the reader; this fact corresponds to the general rule that current, magnetic field, and internal normal form a right-handed system.

According to eq. 10-17 and the equation for a in 10-16 we have, for a thick cylinder

$$a = R^2 \left(1 - \frac{2}{\epsilon \beta R} \right)$$

The magnetic moment is decreased by the factor $(1 - 2/\beta R)$ compared with the case of a completely vanishing penetration depth ($\beta \rightarrow \infty$). For thin cylinders ($\beta R \ll 1$), $I_0(\beta R) = 1$ and $I_1(\beta R) = \frac{1}{2}\beta R$. (Compare the series 8-6). The right-hand side of equation 10-16 for a now becomes equal to unity and $a = 0$. According to eq. 10-9 the field now penetrates the cylinder without being deflected and no longer induces any current in it, because, according to eq. 10-16 I , vanishes like βR in agreement with eq. 7-29.

According to eq. 8-6 we have the following series expansions:

$$\begin{aligned} \frac{I_1(x)}{I_0(x)} &= 1 + \frac{(\frac{1}{2}x)^2}{1 \cdot 1 \cdot 2!} + \frac{(\frac{1}{2}x)^4}{2! \cdot 3!} + \dots + \frac{(\frac{1}{2}x)^{2m}}{m! (m+1)!} + \dots \\ I_0(x) &= 1 + \frac{(\frac{1}{2}x)^2}{(1!)^2} + \frac{(\frac{1}{2}x)^4}{(2!)^2} + \dots + \frac{(\frac{1}{2}x)^{2m}}{(m!)^2} + \dots \end{aligned}$$

In the second series the coefficients of all powers of x are greater than the corresponding coefficients in the first series, therefore $I_0(x) > 2I_1(x)/x$, and it increases with increasing x more rapidly than $2I_1(x)/x$. The right-hand side of eq. 10-16 for a is therefore smaller than unity for all values of βR and continually decreases with increasing R but without becoming negative. Therefore a increases with increasing R monotonically from 0 to R^2 , the limit already mentioned.

Figure 10-1 shows the form of the lines of force for three different values of βR . In the external space the lines follow the same course as with a diamagnetic specimen. However, whereas inside a diamagnetic body they would be straight, here they are more or less curved.

If the temperature is lowered, starting from the transition temperature, the penetration depth $\beta^{-1} = c/\lambda$ is at first great, and so βR is a small number for any given value of R . Later β^{-1} decreases and βR increases. The figures represent in this way the gradual expulsion of the field from the interior of the specimen. The final phase, $\beta R \gg 1$ is shown in Fig. 1-5.

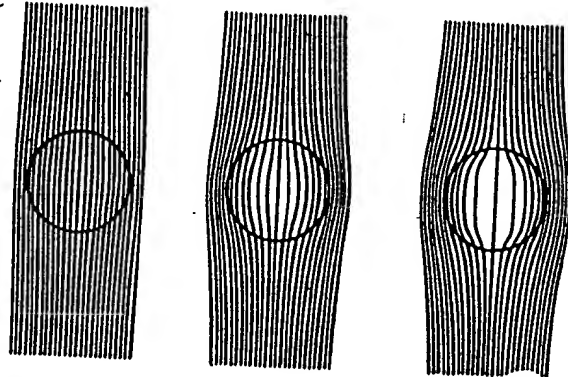


Fig. 10-1. Lines of force for a thin superconducting cylinder in a transverse homogeneous magnetic field for different ratios of diameter to penetration depth. a) $\beta R = 1$; b) $\beta R = 2$; c) $\beta R = 3$

this way the gradual expulsion of the field from the interior of the specimen. The final phase, $\beta R \gg 1$ is shown in Fig. 1-5.

10. THE CYLINDER IN A HOMOGENEOUS MAGNETIC FIELD 53

As the current here has only one component i_z , the solution implied by eqs. 10-12, 10-13, and 10-14 can be taken over for noncubic crystals under the same conditions as set up in Chap. 8 (e).

(d) No rigorous solution can yet be given for an elliptical cylinder in an external field; just as was the case for the cylinder carrying a current treated in Chap. 8 (d), we must confine ourselves again to the approximation that holds only for "thick" cylinders. The boundary curve must then be a field line. The solution is trivial for the longitudinal field: everywhere in the external space the field strength H_z is constant and equal to H_0 , and the current density can be calculated by eq. 7-10.

For the transverse field, however, we assume that the field strength forms an angle $\theta_0 < \frac{1}{2}\pi$ with the a axis at a great distance from the cylinder. For the description of the field we use, as in Chap. 8 (e) a function of the complex variable $\zeta = x + iy$, which we shall call $W = U + iV$, and take U as the potential. We define W in terms of the complex parameter $\chi = \psi + i\varphi$, namely,

$$W = -\frac{1}{2} H_0 \sqrt{a^2 - b^2} \left(e^{-i\chi} + \frac{a+b}{a-b} e^{-x+i\varphi} \right) \quad (10-18)$$

$$\zeta = \sqrt{a^2 - b^2} \cosh \chi$$

The second of these equations follows from eq. 8-26 by putting $\alpha = 1$ there. In analogy to eq. 8-27 we have here

$$x = \sqrt{a^2 - b^2} \cosh \psi \cos \varphi, \quad y = \sqrt{a^2 - b^2} \sinh \psi \sin \varphi \quad (10-19)$$

and the curves $\psi = \text{constant}$ are the confocal ellipses

$$\frac{x^2}{\cosh^2 \psi} + \frac{y^2}{\sinh^2 \psi} = a^2 - b^2 \quad (10-20)$$

Let the contour of the cylinder correspond to the value ψ_0 , so that

$$\sqrt{a^2 - b^2} \cosh \psi_0 = a, \quad \sqrt{a^2 - b^2} \sinh \psi_0 = b$$

$$e^{+\psi_0} = \sqrt{\frac{a+b}{a-b}} \quad (10-21)$$

The curves $\varphi = \text{constant}$, however, are the hyperbolas confocal to these ellipses:

$$\frac{x^2}{\cosh^2 \varphi} - \frac{y^2}{\sinh^2 \varphi} = a^2 - b^2 \quad (10-22)$$

ψ and φ are called elliptical coordinates. To make them single valued we restrict them to the ranges of values 0 to $+\infty$ for ψ and 0 to 2π for φ . Each of the above hyperbolas then corresponds to four φ values: if $\varphi = \varphi_0$ is the semi-axis in the first quadrant ($x > 0, y > 0$), then $\varphi = \pi - \varphi_0$ is the semi-axis in the second quadrant ($x < 0, y > 0$), $\varphi = \pi + \varphi_0$ that in the third quadrant ($x < 0, y < 0$) and $\varphi = 2\pi - \varphi_0$ in the fourth ($x > 0, y < 0$).

*The assumption that $\theta_0 > \frac{1}{2}\pi$ leads to nothing new.

From eq. 10-18 it follows that

$$\begin{aligned} U &= -\frac{1}{2} H^0 \sqrt{\frac{a^2 - b^2}{a^2}} \left\{ e^{\psi} + \frac{a+b}{a-b} e^{-\psi} \right\} \cos(\varphi - \theta_0) \\ V &= -\frac{1}{2} H^0 \sqrt{\frac{a^2 - b^2}{a^2}} \left\{ e^{\psi} - \frac{a+b}{a-b} e^{-\psi} \right\} \sin(\varphi - \theta_0) \end{aligned} \quad (10-23)$$

Because of the way they were derived from eq. 10-18, U and V are solutions of the potential equation. ψ is infinite at infinity, according to eq. 10-19. Therefore at infinity

$$\begin{aligned} U &= -\frac{1}{2} H^0 \sqrt{\frac{a^2 - b^2}{a^2}} e^{\psi} (\cos \varphi \cos \theta_0 + \sin \varphi \sin \theta_0) = \\ &= -H^0 (x \cos \theta_0 + y \sin \theta_0) \end{aligned}$$

The field is therefore homogeneous at infinity, and inclined at an angle θ_0 to the x axis. The field line $V = 0$ consists first of those parts of the hyperbolas $\varphi = \theta_0$ and $\varphi = \pi + \theta_0$ which lie outside the ellipse ψ_0 (since these formulas are valid outside), and secondly of the ellipse ψ_0 , because according to eq. 10-21 on this ellipse

$$e^{\psi_0} = \frac{a+b}{a-b} e^{-\psi_0}$$

The expression 10-18 thus satisfies all the imposed conditions.

We proceed to the calculation of $|H| = |dW/d\zeta|$. From eq. 10-18

$$\begin{aligned} \frac{dW}{d\zeta} &= \frac{(dW/d\chi)}{(d\zeta/d\chi)} = -\frac{H^0}{2 \sinh \chi} \left(e^{\chi - i\theta_0} - \frac{a+b}{a-b} e^{-\chi + i\theta_0} \right) \\ &= \frac{H^0 \left[\frac{a+b}{a-b} e^{-\chi - i(\varphi - \theta_0)} - e^{\chi + i(\varphi - \theta_0)} \right]}{2 (\sinh \psi \cos \varphi + i \cosh \psi \sin \varphi)} \end{aligned}$$

Along the ellipse ψ_0 we have from eq. 10-21

$$|H| = \left| \frac{dW}{d\zeta} \right| = \frac{H^0 (a+b) \sin(\varphi - \theta_0)}{\sqrt{a^2 \sin^2 \varphi + b^2 \cos^2 \varphi}}$$

The maximum of this expression is at the point where

$$\tan \varphi = -\frac{b^2}{a^2} \cot \theta_0, \quad \text{i. e., } \frac{y}{x} = -\frac{b^2}{a^2} \cot \theta_0$$

a diameter of the ellipse is drawn in the direction θ_0 , the conjugate diameter (parallel to the tangents at the ends of the first one) is given by

$$\frac{y}{x} = -\frac{b^2}{a^2} \cot \theta_0$$

If $b \ll a$ the maximum field therefore lies considerably nearer to the major axis of the ellipse than this diameter, except when $\theta_0 = 0$ or $\frac{1}{2}\pi$. The maximum value itself amounts to

$$|H|_{\max} = H^0 \left(\frac{1}{a} + \frac{1}{b} \right) \sqrt{\frac{1}{a^2 \sin^2 \theta_0} + \frac{b^2 \cos^2 \theta_0}{a^2}} \quad (10-24)$$

11. THE SPHERE IN A HOMOGENEOUS MAGNETIC FIELD 55

For $\theta_0 = 0$ the factor multiplying H^0 becomes $(1 + b/a)$ and is thus smaller than the factor 2 appearing in the circular cylinder. For $\theta = \frac{1}{2}\pi$ however, the factor becomes $1 + a/b > 2$. This confirms the statement made in Chap. 1 (g) about the intensifying of the field. It is at once evident that this intensification is greater when the cylinder forces the field to diverge around its major axis than if it exposed only its minor axis to the field.

The expression 10-24 is needed to calculate the limiting value of H^0 that destroys the superconductivity in the cylinder [Chap. 17 (f)].

CHAPTER 11

The Sphere in a Homogeneous Magnetic Field

(a) We introduce polar coordinates in space, r, θ, φ , forming a right-handed system in that order (Fig. 11-1). The following equations hold for the curl of a vector A

$$\begin{aligned} \text{curl}_r A &= \frac{1}{r \sin \theta} \left[\frac{\partial}{\partial \theta} (\sin \theta A_\varphi) - \frac{\partial A_\theta}{\partial \varphi} \right] \\ \text{curl}_\theta A &= \frac{1}{r \sin \theta} \frac{\partial A_r}{\partial \varphi} - \frac{1}{r} \frac{\partial(r A_\varphi)}{\partial r} \\ \text{curl}_\varphi A &= \frac{1}{r} \frac{\partial(r A_\theta)}{\partial r} - \frac{1}{r} \frac{\partial A_r}{\partial \theta} \end{aligned} \quad (11-1)$$

The differential equation $\Delta u - \beta^2 u = 0$ in these coordinates reads:

$$\frac{1}{r^2} \frac{\partial}{\partial r} \left(r^2 \frac{\partial u}{\partial r} \right) + \frac{1}{r^2 \sin \theta} \frac{\partial}{\partial \theta} \left(\sin \theta \frac{\partial u}{\partial \theta} \right) + \frac{1}{r^2 \sin^2 \theta} \frac{\partial^2 u}{\partial \varphi^2} - \beta^2 u = 0 \quad (11-2)$$

We can solve this equation for the present problem by separation of the variables:

$$u = f(r) \sin \theta e^{i\varphi} \quad (11-3)$$

Direct calculation shows that

$$\frac{1}{r^2} \frac{\partial}{\partial r} \left(r^2 \frac{\partial u}{\partial r} \right) + \frac{1}{r^2 \sin^2 \theta} \frac{\partial^2 u}{\partial \varphi^2} = -\frac{2}{r^2} f(r) \sin \theta e^{i\varphi}$$

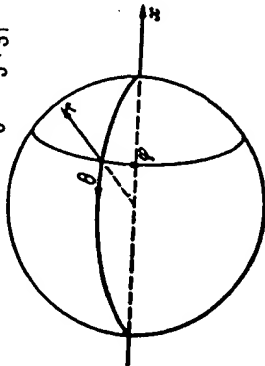
so we can divide eq. 11-2 by the factor $\sin \theta e^{i\varphi}$ common to all terms and we are left with the ordinary differential equation for $f(r)$:

$$\frac{1}{r^2} \frac{d}{dr} \left(r^2 \frac{df}{dr} \right) - \left(\beta^2 + \frac{2}{r^2} \right) f = 0 \quad (11-4)$$

The solution of this that remains finite at $r = 0$ is

$$\begin{aligned} I(r) &= \frac{1}{\beta r} \cosh(\beta r) - \left(\frac{1}{\beta r}\right)^2 \sinh(\beta r) \\ &= \frac{(\beta r)}{3} + \frac{(\beta r)^3}{5 \cdot 3!} + \dots + \frac{(\beta r)^m}{(m+2)m!} + \dots \end{aligned} \quad (11-5)$$

I is positive because $\tanh \beta r < \beta r$ for all positive values of r . For large values of βr



$$I = \frac{1}{2} (\beta r)^{-1} e^{\beta r} \quad (11-6)$$

(b) Let the polar axis $\theta = 0$ and likewise the positive x axis be in the direction of the homogeneous magnetic field. If the field were undisturbed its potential would be

$$\Phi = -H^0 r \cos \theta$$

Fig. 11-1. The polar coordinates r, θ, ϕ .

The r arrow is pointed upwards.

If the sphere were completely impenetrable to the lines of force it would act as a dipole, as shown by potential theory and as will be confirmed later. This would contribute to the potential a term of the form $r^{-2} \cos \theta$. Therefore in analogy to the procedure of Chap. 10 (c) we now seek a solution for the space outside the sphere in the form

$$\Phi = -H^0 \left(r + \frac{a}{r^2} \right) \cos \theta \quad (11-7)$$

Here $4\pi a H^0$ represents the magnetic moment of the sphere². With positive a it is in the negative x direction and thus opposite to the field. The magnetic field strength $H = -\text{grad } \Phi$ follows immediately from eq. 11-7:

$$\begin{aligned} H_r &= -\frac{\partial \Phi}{\partial r} = H^0 \left(1 - \frac{2a}{r^3} \right) \cos \theta \\ H_\theta &= -\frac{1}{r} \frac{\partial \Phi}{\partial \theta} = -H^0 \left(1 + \frac{a}{r^3} \right) \sin \theta \\ H_\phi &= 0 \end{aligned} \quad (11-8)$$

As can be expected from symmetry the lines of force lie in meridian planes $\phi = \text{constant}$. According to Chap. 7 (c) the current must be perpendicular to the lines of force, at least for thick superconductors, and

² Together with r^{-1} itself, all its derivatives with respect to the rectangular coordinates x, y, z are also solutions of $\Delta u = 0$. But $\partial(r^{-1})/\partial x = -x/r^3 = -\cos \theta/r^2$ since we have chosen $x = r \cos \theta$.

³ This is in Lorentz units. In electrostatic units the moment is $a H^0$.

near the surface, so we must expect it to flow along the latitude — circles $r = \text{const}$, $\theta = \text{constant}$. Therefore for the interior of the sphere we try

$$I_r = I_\theta = 0, \quad I_\phi = C/(r) \sin \theta \quad (11-9)$$

If for $I(r)$ we assume the same function as in eq. 11-5, then according to (a) the components of the current

$$I_r = -I_\phi \sin \theta, \quad I_\theta = I_\phi \cos \theta$$

satisfy the differential equation $\Delta u - \beta^2 u = 0$. From the relation $H = -c \lambda \text{curl } I$ we have from eq. 11-1:

$$H_r = -\frac{c \lambda}{r} \sin \theta \frac{\partial (\sin \theta I_\phi)}{\partial \theta} = -\frac{2\sqrt{\lambda}}{\beta r} C/(r) \cos \theta \quad (11-10)$$

$$H_\theta = -\frac{c \lambda}{r} \frac{\partial (r I_\phi)}{\partial r} = \frac{\sqrt{\lambda} C}{\beta r} [\sinh(\beta r) - I(r)] \sin \theta$$

To check whether these equations are correct we show, as in Chap. 10 (c) that they fulfil the boundary conditions at the surface of the sphere $r = R$. These require the continuity of the two nonvanishing components of H . According to eqs. 11-8 and 11-10 we should have

$$H^0 \left(1 - \frac{2a}{R^3} \right) = -\frac{2\sqrt{\lambda}}{\beta R} C/(R)$$

$$H^0 \left(1 + \frac{a}{R^3} \right) = \frac{\sqrt{\lambda} C}{\beta R} [I(R) - \sinh(\beta R)]$$

As a matter of fact we can satisfy these conditions by means of the adjustable constants a and C . For this purpose we have to put

$$C = -\frac{3H^0 \beta R}{2\sqrt{\lambda} \sinh(\beta R)}, \quad a = \frac{1}{2} \left[1 - \frac{3/(R)}{\sinh \beta R} \right] R^3 \quad (11-11)$$

Evidently I_ϕ is negative; the current flows against the arrow in Fig. 11-1. From eq. 11-10 we now have the equations

$$\frac{\partial}{\partial r} (r \sin \theta I_\phi) dr + \frac{\partial}{\partial \theta} (r \sin \theta I_\phi) d\theta = 0, \quad \text{i. e., } r \sin \theta I_\phi = \text{constant}$$

or $r/(r) \sin^2 \theta = \text{constant}$. These, with $\phi = \text{constant}$, determine the magnetic lines of force in the interior.

(c) The discussion proceeds in the same way as in Chap. 10 (c). From eqs. 11-9, 11-10, and 11-11 it follows that for a large sphere ($\beta R \gg 1$) and high values of βr that

$$\begin{aligned} I_\phi &= -\frac{3H^0 R}{2\sqrt{\lambda} r} e^{-\beta(R-r)} \sin \theta \\ H_r &= 0, \quad H_\theta = -\frac{3H^0 R}{2r} e^{-\beta(R-r)} \sin \theta \end{aligned} \quad (11-12)$$

Again this means the formation of a protective layer around a field-free interior. Furthermore, we conclude from eqs. 11-11 and 11-6 that

$$-a = \frac{1}{2} \left(1 - \frac{3}{\beta R} \right) R^3 \quad (11-13)$$

Using this value it follows from eq. 11-8 in agreement with eq. 11-12 that at $r = R$:

$$H_r = 0, \quad H_\theta = -\frac{3}{2} H^0 \sin \theta \quad (11-14)$$

The first equation proves that in this approximation the sphere appears from the outside as if it were totally impenetrable to the lines of force; the second equation proves that the intensification of the field due to its distortion leads to a maximum one and a half times the original field strength H^0 , as already mentioned in Chap. 1 (g). Figure 1-5 is valid qualitatively for the field distribution in a meridian plane of the sphere in spite of the fact that it is drawn for the cylindrical problem. For small βR values, however, according to eq. 11-5 $J(R)$ becomes $(1/3)\beta R$, so from eq. 11-11 we have

$$C = -\frac{3H^0}{2\sqrt{\lambda}}, \quad a = 0 \quad (11-15)$$

As at the same time it follows from eq. 11-9 that

$$I_r = -\frac{1}{2} H^0 \left(\frac{\beta r}{\sqrt{\lambda}} \right) \sin \theta \quad (11-16)$$

and from eq. 11-10 that

$$H_r = H^0 \cos \theta, \quad H_\theta = -H^0 \sin \theta \quad (11-17)$$

According to the last equation H is in the x direction and has the magnitude H^0 . The magnetic field penetrates the sphere without hindrance as was to be expected from Chap. 7 (f), whereas eq. 11-16 for I_r has the same general form as eq. 7-29. Choosing the length of the superconductor L equal to R in order to duplicate eq. 11-16 one has to put $-\frac{1}{2}(r/R) \sin \theta$ for the pure number τ_a which depends only on the position of the origin in the superconductor.

We conclude from the expansion 11-5 and the known series

$$\sinh(\beta R) = \beta R + \frac{(\beta R)^3}{3!} + \frac{(\beta R)^5}{5!} + \dots + \frac{(\beta R)^{2m+1}}{(2m+1)!} \dots$$

that $\sinh(\beta R)$ increases faster with increasing βR than $J(R)$. Therefore by eq. 11-11 a grows monotonically with βR from 0 to $\frac{1}{2}\beta R^3$, the magnetic

¹ It follows from eq. 11-10 for the center of the sphere $r = 0$ exactly

$$(H_r)_{r=0} = \frac{H^0 \beta R \cos \theta}{\sinh(\beta R)}, \quad (H_\theta)_{r=0} = -\frac{H^0 \beta R \sin \theta}{\sinh(\beta R)}$$

This gives H the direction of the x axis, as was to be expected from symmetry, and the magnitude $H^0 \beta R / \sinh(\beta R)$. This can be used to confirm the mean value theorem of eq. 7-25.

moment $4\pi a H^0$ goes from 0 to $2\pi R^3 H^0$, and the moment per unit volume and unit field strength increases from 0 to $\frac{1}{2}$.

A nonmagnetic layer, e. g., of colloidal spheres of mercury dispersed in gelatine, must become increasingly diamagnetic below the transition temperature, 4.17° K, the greater the moment per unit volume due to the spheres. If there are N such spheres per unit volume, the latter has a moment $4\pi a N H^0$; the permeability is therefore $\chi = 4\pi a N$. If each sphere has a radius R and they occupy a fraction V per unit volume, then $N = 3V/4\pi R^3$ so that

$$\chi = \frac{3V a}{\pi R^3}$$

For large values of βR :

$$a = \frac{1}{2} R^3$$

according to Fig. 11-2. Relative susceptibility of a slab containing superconducting colloidal mercury spheres as a function of temperature. (After Shoenberg.)

$$\chi_\infty = \frac{3V}{2\pi}$$

and in this way we get for $\beta R \ll 1$ a somewhat better approximation than used above:

$$\frac{\chi}{\chi_\infty} = \frac{a}{\frac{1}{2} R^3} = 1 - \frac{3}{\sinh(\beta R)} = \frac{1}{15} (\beta R)^2 \quad (11-18)$$

(d) Shoenberg⁴ [Chap. 1 (c)] used the above method to determine the superconductivity constant λ as a function of temperature. He knew from the amount of mercury in emulsion what the permeability χ_0 would be if the βR of the small spheres were great compared with unity. Actually the permeability was only some thousandths of this (see Fig. 11-2) and dropped much lower still as the transition temperature was approached. Shoenberg knew only that the average radius of the spheres was about 0.5×10^{-5} cm. To obtain information about β he started from eq. 11-18. If we indicate values of χ , β , and λ at $T = 2.5^\circ$ K by an inferior 2.5, we have, from eqs. 11-18 and 6-7

$$\frac{\chi}{\chi_{2.5}} = \left(\frac{\beta}{\beta_{2.5}} \right)^2 = \frac{\lambda_{2.5}}{\lambda}$$

⁴ D. Shoenberg, *Nature*, 148, 454 (1939).

E. Laurmann and D. Shoenberg, *Nature*, 160, 747 (1948).

By means of this equation Shoenberg was able to plot his experimental data as in Fig. 11-3, which shows λ/λ_0 as a function of T . They agree excellently with the values found by Appleyard and co-workers⁴ [Chap. I (c)] using another method [see Chap. 18 (c)]. λ becomes infinite at T , like $(T_c - T)^{-1}$ because χ goes to zero like $(T_c - T)$ in Fig. 11-2.

(e) If we specify a line of force by its distance in the undistorted part of the field from the central line of force that is directed toward the center of the sphere, its equation can easily be derived from eq. 11-7 and reads

$$\left(r^2 - \frac{2a}{r}\right) \sin^2 \theta = C^2, \quad \varphi = \text{constant}$$

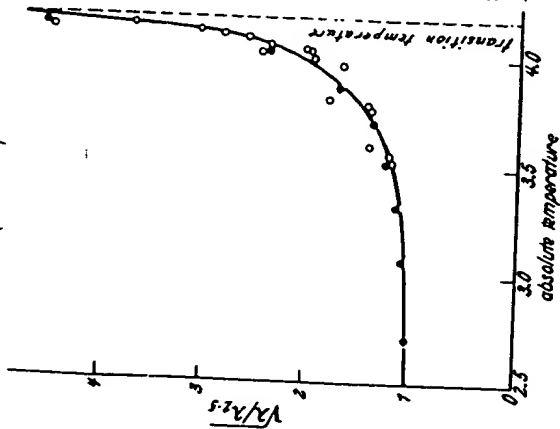


Fig. 11-3. The superconductivity constant λ for mercury as a function of temperature. ● measurements of Appleyard, Bristow, and London; ○ measurements of Shoenberg.

(f) The eqs. 11-9, 11-10, and 11-11 remain true for noncubic crystals if the ellipsoid of the tensor λ_{cd} has rotational symmetry and the axis of symmetry lies in the x direction. Only then β can be replaced by $\beta_1 = 1/c\sqrt{A_1}$ where A_1 is the principal value of the tensor for a direction perpendicular to the axis of symmetry.

⁴T. S. Appleyard, T. R. Bristow, and H. London, *Nature*, 148, 433 (1939).

CHAPTER 12

Persistent Currents

(a) A classical method for the treatment of electromagnetic problems uses the vector potential A in conjunction with the scalar potential ϕ . In the static case ϕ becomes the electrostatic potential and it is therefore a generalization of the latter. A and ϕ are defined by requiring

$$B = \text{curl } A \quad (12-1)$$

$$E = -\frac{1}{c} \frac{\partial A}{\partial t} - \text{grad } \phi \quad (12-2)$$

From these it follows at once that

$$\text{div } B = 0, \quad \frac{1}{c} \frac{\partial B}{\partial t} = \frac{1}{c} \text{curl } \frac{\partial A}{\partial t} = -\text{curl } E$$

which agrees with the fundamental eqs. I and III (Chap. 3). To obtain the fundamental eqs. II and IV also, we must now add a condition on $\text{div } A$, which we may do because no vector is completely defined by giving only its curl. We require that

$$\text{div } A + \frac{\epsilon \mu}{c^2} \frac{\partial \phi}{\partial t} = 0 \quad (12-3)$$

According to eqs. 12-2 and 3-1 we now have

$$\text{div } D = \text{div}(\epsilon E) = \epsilon \text{div } E + (E \cdot \text{grad } \epsilon)$$

$$= -\frac{\epsilon}{c} \frac{\partial}{\partial t} \text{div } A - \epsilon \Delta \phi + (E \cdot \text{grad } \epsilon)$$

$$= \frac{\epsilon^2 \mu}{c^2} \frac{\partial^2 \phi}{\partial t^2} - \epsilon \Delta \phi + (E \cdot \text{grad } \epsilon)$$

and if we subject ϕ to the condition

$$\Delta \phi - \frac{\epsilon \mu}{c^2} \frac{\partial^2 \phi}{\partial t^2} = -\rho + \frac{1}{\epsilon} (E \cdot \text{grad } \epsilon) \quad (12-4)$$

we recover eq. IV ($\text{div } D = \rho$). In order to obtain eq. II we use eqs. 12-1, and 12-3 and the vector rule 6-1 to obtain

$$\text{curl } B = \text{curl curl } A = \text{grad div } A - \Delta A = -\text{grad} \left(\frac{\epsilon \mu}{c^2} \frac{\partial \phi}{\partial t} \right) - \Delta A$$

$$= -\frac{\epsilon \mu}{c} \left[\frac{\partial E}{\partial t} + \frac{1}{c} \frac{\partial^2 A}{\partial t^2} \right] - \frac{1}{c} \frac{\partial \phi}{\partial t} \text{grad}(\epsilon \mu) - \Delta A \quad (12-5a)$$

Also according to eqs. 3-2 and I f:

$$\begin{aligned} \text{curl } B &= \text{curl}(\mu H) + \text{curl } M = \mu \text{curl } H - [\mu \times \text{grad } \mu] + \text{curl } M \\ &= \frac{\mu}{c} \left(\frac{\partial E}{\partial t} + I \right) - [\mu \times \text{grad } \mu] + \text{curl } M \end{aligned} \quad (12-5b)$$

The necessary and sufficient condition for the validity of eq. 11 follows by subtracting the right-hand sides of 12-5a and 12-5b:

$$\Delta A - \frac{\varepsilon \mu}{c^2} \frac{\partial^2 A}{\partial t^2} = -\frac{\mu}{c} |\mathbf{I} - \text{curl } \mathbf{M} + \frac{1}{c} \frac{\partial \Phi}{\partial t} \text{grad}(\varepsilon \mu) + [\mathbf{H} \times \text{grad} \mu] \quad (12-6)$$

We accept eqs. 12-4 and 12-6 as valid throughout all space. The \mathbf{I} here always means the sum of ohmic and supercurrents.

The most frequent application of eq. 12-1 consists in the transformation of the integral $\int_C \mathbf{B} \cdot d\sigma$ over a surface C into the line integral around the boundary by Stokes' theorem:

$$\int_C (\mathbf{B} \cdot d\sigma) = \int_C (\mathbf{A} \cdot d\mathbf{s}) \quad (12-7)$$



Fig. 12-1. Illustration for Stokes' theorem, eq. 12-7. The normal vector $d\sigma$ points toward the reader.

Figure 12-1 shows the relation between the direction of the normal vector $d\sigma$ and the sense $d\mathbf{s}$ in which the line integral traverses the boundary. The justification for using the same symbol C to specify both surface and loop is that all surfaces with the same loop as boundary have the same integral $\int_C (\mathbf{B} \cdot d\sigma)$ because of $\text{div } \mathbf{B} = 0$.

(b) We now have to explain the concept of the multiply connected region. In a simply connected or singly connected region of space two closed curves C and C' which lie completely within the region, but are otherwise quite arbitrary, can be transformed into each other by continuous deformation without either of them leaving the region. In particular C can be contracted to a point, because C' can be chosen to be an infinitesimal loop around this point. Such curves also exist in a doubly connected region; we call them curves of the first kind. Besides these there are curves of the second kind which can be transformed in the described manner into each other but not into curves of the first kind. It is impossible to reduce them to a point (Fig. 12-2a). We have to distinguish "sets of curves for an n -ply connected region".

All curves of the same kind can be transformed into each other in the described manner but not curves of one set into curves of another set. The possibility of reduction to a point is reserved for curves of the first kind. We assign once and for all the same arbitrary sense of traversal to all curves of the same kind. The line integrals over such curves are defined to follow this sense of traversal, which we shall call the sense of the curve or circuit.

¹Curves that can be reduced by continuous deformation to a curve C_1 together with a curve C_2 within a triply connected region do not constitute a new kind of curve. A similar statement holds for n -ply connected regions.

In a singly connected region of space every finite and continuous scalar function Ψ is unique if its gradient is uniquely defined, e. g., by physical quantities, because for any closed curve C in the region

$$\oint_C (d\mathbf{s} \cdot \text{grad } \Psi) = \int_C (d\sigma \cdot \text{curl grad } \Psi)$$

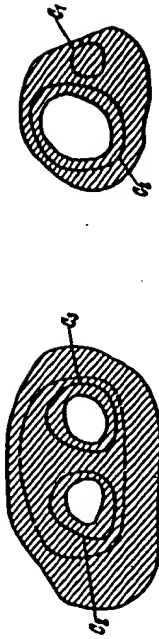


Fig. 12-2. (a) Curves C_1 and C_2 in a doubly connected region. (b) Curves C_1 and C_2 in a triply connected region. The dotted line is not a new kind of curve because it can be reduced to a curve C_3 together with a curve C_1 .

and the right side vanishes because $\text{curl grad } \Psi \equiv 0$. This conclusion holds only for curves of the first kind in a doubly connected region if Ψ is defined only within the region. Since these curves can be contracted to a point, we can draw surfaces of which they are the boundaries completely within the region of interest. For a curve of the second kind, such a surface necessarily extends outside the region. Otherwise it would also be possible to reduce these curves to a point. Consequently, for a curve of the second kind C_2 ,

$$\int_{C_2} (d\mathbf{s} \cdot \text{grad } \Psi) = S_{C_2}$$

can differ from zero and be either positive or negative. However, the integral has the same value for all curves C_2 . For two such curves C_2 and C_2' ,

$$\int_{C_1} (d\mathbf{s} \cdot \text{grad } \Psi) - \int_{C_2'} (d\mathbf{s} \cdot \text{grad } \Psi) = \iint_{C_1} (d\sigma \cdot \text{curl grad } \Psi)$$

The surface integral extends over a surface bounded by the curves C_2 and C_2' lying completely within the region and is therefore zero because of the present theorem. In an n -ply connected region the integral $\int (d\mathbf{s} \cdot \text{grad } \Psi)$ has the same value for all curves C_m (any given $m \leq n$) but has different values for curves of different kind. It is zero for curves of the first kind, as before.

A doubly connected region is made simply connected by a cut Q , i. e., a surface intersecting every curve C_2 once and only once, destroying all C_2 as closed curves. All curves still remaining closed are now of the first kind. The boundaries of the cut necessarily lie in the surface of the region.

Otherwise Q would not cut all the curves C_m . Except for this requirement there is complete freedom of choice of position and form of Q . ($n-1$) cross-sectional cuts Q_m , ($m=2, 3, \dots, n$) are needed to produce a simply connected region from an n -ply connected one. Q_m cuts all closed curves C_m . In the single region formed in this way only closed curves of the first kind C_1 exist and the scalar Ψ is unique in such a region. Consider two points 1 and 2 lying on opposite sides of, and immediately adjacent to, the cut Q_m . Ψ differs at 1 and 2 by

$$\Psi_2 - \Psi_1 = \int_1^2 (ds \cdot \text{grad } \Psi) = \int_{C_m} (ds \cdot \text{grad } \Psi) = S_{C_m}$$

The points 1 and 2 must be chosen in such a way that the path from 1 to 2 that does not pass through the cut at Q_m has the same sense as the curve C_m . As S_{C_m} has the same value for all curves C_m the jump in Ψ at the cut is the same for all points on it.

These cuts are necessary if one wishes to apply Stokes' theorem in a multiply connected region to a vector ΨS , the product of a unique vector S with Ψ . Applied to the cut region

$$\int \text{div}(\Psi S) d\tau = - \int \Psi S \cdot d\sigma$$

and every cut Q_m makes two contributions to the surface integral which differ formally only in the directions of the inner normals $d\sigma_1$ and $d\sigma_2$. The sum of these two contributions is

$$-(\Psi_1 - \Psi_2) \int_{C_m} (S \cdot d\sigma_1) = S_{C_m} \int (S \cdot d\sigma_1) \quad (12-8)$$

The fact that the two contributions do not in general cancel each other proves that the Gauss theorem can be applied directly only to singly connected regions. According to what has been agreed to about the points 1 and 2, the normal $d\sigma_1$ has the same direction as the sense of the curves C_m . (c) From eq. 12-1 and the fundamental equation X: $H = -c \text{curl } G$ it follows that

$$\text{curl}(cG + A) = 0 \quad (12-9)$$

Therefore a superconduction scalar potential Ψ exists for which

$$\text{grad } \Psi = cG + A \quad (12-10)$$

As there is no supercurrent outside the superconductor this potential is defined only in the interior. The integral

$$S_C = \int_C (ds \cdot \text{grad } \Psi) = \int_C ds (cG + A) \\ = c \int_C (G \cdot ds) + \int_C A \cdot ds \quad (12-11)$$

therefore has the value zero for any closed curve C in a singly connected superconductor; in a doubly connected superconductor (in the form of a ring) it is likewise zero for curves of the first kind, but has in general a unique value S_{C_2} different from zero. In an n -ply connected superconductor the integral has the same value S_{C_m} for all curves of the m^{th} kind. The superconduction potential Ψ is multiple valued ("periodic") with the "periods" S_{C_m} .

We differentiate eq. 12-10 with respect to time and use the fundamental equation IX ($E = \partial G / \partial t$) and also eq. 12-2 to obtain

$$-c \text{grad } \Phi = \text{grad } \frac{\partial \Psi}{\partial t} \quad (12-12)$$

The potential Φ is defined in all space, and is therefore unique. Integrating eq. 12-12 over a closed curve C_m within the superconductor:

$$\frac{d}{dt} \int_{C_m} (ds \cdot \text{grad } \Psi) = \frac{dS_{C_m}}{dt} = 0 \quad (12-13)$$

The integrals S_C do not change with time so long as the specimen remains superconducting. This is still true if during a phase transition the superconducting material grows at the expense of the normal material so causing the ring to become thicker, or, if it shrinks, by the reverse process.

The explanation of the persistent current contained in these theorems is due to F. London.

All experiments on the persistent current have been done with doubly connected superconductors, e. g., in the form of a ring or a closed coil. Moreover, the superconductor has always been thick compared with the penetration depth. If the curve C_2 be placed in the field-free interior, $G = 0$ on the curve and it follows from eq. 12-11 that

$$S_C = \int_C B \cdot d\sigma \quad (12-14)$$

From this eq. 12-13 shows that the flux of induction through any surface that encloses the bore of the ring and protrudes through the protective layer into the field free interior (which adds but little) is constant, see Fig. 12-3.

Therefore if a ring has been placed in a magnetic field while still above its transition temperature, and if on cooling below the transition a certain flux of induction is trapped in the bore of the ring, this will remain there until superconductivity is destroyed: it is "frozen in." If the external field

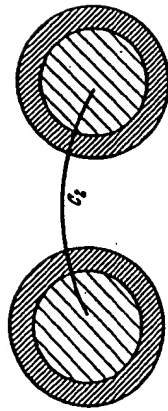


Fig. 12-3. Illustrating a curve C_2 lying entirely within the field-free bore of a ring. Darkly shaded area represents the protective layer; lightly shaded area represents the protected interior.

is switched off, the ring acts as a permanent magnet due to this flux of induction. The great achievement of the London theory is that it logically combines this freezing-in process with the Meissner effect, i. e., the fact that the field inside a superconductor does not get frozen in but is expelled.

If a superconducting ring initially free of current is placed in a magnetic field, the lines of force will go around it according to eq. 12-14; its bore remains permanently field free.

It should be emphasized once more that eq. 12-14 holds only for "thick" rings; for "thin" ones the line integral in S_C (eq. 12-11) cannot be neglected. In such rings the flux of induction does not freeze in. Immediately below the transition temperature every specimen is effectively thin, as has been repeatedly pointed out. The flux which according to eq. 12-14 remains constant, is not necessarily identical with the flux that passed through the bore before the ring became superconducting.

The ohmic current has not been mentioned in the above discussion. This does not mean that it is zero under the circumstances of the problem, that we have neglected it. On the contrary our conclusions are completely rigorous and independent of what happens to the ohmic current during the changes under consideration. Strictly speaking, the ohmic current has always to play its role as consumer of energy during the processes, the more strongly the more rapid the process. The fact that nothing of this kind can be detected in actual experiments, is due to the relatively slow rate of change at practicable frequencies.¹

¹In multiply connected specimens carrying a persistent current the superconduction potential is certainly not zero everywhere, according to the argument in the text. However, we may ask whether perhaps it does not vanish identically for a singly connected superconductor in a static magnetic field? This question has to be answered in the negative, in so far as we understand by Λ the potential introduced in (a) and describing the total magnetic field. This can already be seen for the cubic crystal where especially simple conditions prevail because \mathbf{j} and \mathbf{G} have the same directions. Owing to eq. 12-10 and the boundary condition $\Lambda_n' = 0$ (and therefore also $\mathbf{G}_n = 0$) we must have

$$\frac{\partial \Psi}{\partial n} = \Lambda_n$$

and it is certainly not generally true that $\Lambda_n = 0$. However, by relinquishing the representation of the whole field, we could introduce a potential for the interior of the superconductor alone:

$$\Lambda' = \Lambda - \text{grad } \Psi$$

For this potential we should have

$$\epsilon(\mathbf{i} + \Lambda') = 0$$

Equation 12-1 would be retained in the form $\mathbf{H} = \text{curl } \Lambda'$. Whereas according to eq. 12-3 $\text{div } \Lambda = 0$ for stationary fields generally, the relation $\text{div } \Lambda' = 0$ would follow from eq. 12-10 only for cubic crystals. It is only for these crystals that the equation $\text{div } \mathbf{G} = 0$ follows from $\text{div } \mathbf{j} = 0$. Because of this restriction, no special significance can be attached to the potential Λ' .

(d) Let us calculate the "period" of the superconduction potential

$$S_C = \int \mathbf{H} \cdot d\sigma = 2\pi \int_0^\infty r H_r dr$$

in the example of a hollow cylinder of cubic crystal material, with an inner radius R and field H_i in the interior hollow space [Chap. 9 (a)]. The integral with respect to r should extend as far as a circle situated in the protected field-free space inside the superconductor. This is expressed in the formula by writing the upper limit as infinite.

Now for $r < R$, $H_r = H_i$, whereas for $r > R$, according to eq. 10-7

$$H_r = H_i \frac{H_0(\iota\beta r)}{H_0(\iota\beta R)}$$

so according to the theorem

$$\int_0^\infty \iota H_0(\zeta) d\zeta = -x H_1(x)$$

we obtain

$$S_C = 2\pi R^2 H_i \left[\frac{1}{2} - \frac{1}{\iota\beta R} \frac{H_1(\iota\beta R)}{H_0(\iota\beta R)} \right]$$

The second term in the bracket is positive real, as it should be, because both $\iota H_0(\iota\beta R)$ and $-H_1(\iota\beta R)$ are also positive real. For large βR this term is vanishingly small compared with the first term because the ratio of the two Hankel functions becomes unity. For small βR , however, it becomes the dominant term, even increasing without limit as βR decreases, because $-H_1(\iota\beta R)$ becomes $2/\pi\beta R$, and $\iota H_0(\iota\beta R) \rightarrow -(2/\pi) \ln(\beta R)$ in this limit. Thus we get

$$S_C = -\frac{2\pi H_i}{\beta^2 \ln(\beta R)} \quad (12-15)$$

S_C therefore vanishes when $R = 0$ as in this case, of course, the hollow cylinder becomes a simply connected solid cylinder.

If we imagine the temperature of a given hollow cylinder to be increased, then its λ increases, and consequently β and βR decrease, approaching zero when the transition temperature T is reached. The factor multiplying H_i increases without limit, and since S_C remains constant, according to what has been said above, H_i must accordingly decrease. The physical reason for this is the increase in the penetration depth β^{-1} . The field penetrates the superconductor and spreads over a continuously increasing area, so its intensity has to decrease because of the constancy of the total flux S_C . The superconduction potential Ψ is proportional to the angle θ because of axial symmetry: thus

$$\Psi = \frac{\theta}{2\pi} S_C$$

and Ψ satisfies the potential equation³ $\Delta \Psi = 0$. This must be so for all stationary currents in cubic-crystal superconductors according to eqs. 12-10 and 12-3 because from $\text{div } \mathbf{I} = 0$ it follows for such crystals that $\text{div } \mathbf{Q} = 0$.

(c) When there is a persistent current in a ring, it has a magnetic moment. Does the direction of the moment depend on the way in which it has been produced? This and similar questions are answered by the uniqueness theorem for a superconductor in a stationary field. We derive it now under the assumption that no ohmic current is supplied from outside.

We form the scalar product of 12-10 with $\mathbf{I}/2c$, and integrate over the volume of an arbitrary (homogeneous or inhomogeneous) superconductor as indicated by the suffix s under the integral sign. This yields

$$\frac{1}{2} \int_V (\mathbf{I} \cdot \mathbf{G}) d\tau + \frac{1}{2c} \int_V (\mathbf{A} \cdot \mathbf{I}) d\tau = \frac{1}{2c} \int_V (\mathbf{I} \cdot \text{grad } \Psi) d\tau \quad (12-16)$$

Using the formula

$$(\mathbf{I} \cdot \text{grad } \Psi) + \Psi \text{div } \mathbf{I} = \text{div } (\Psi \mathbf{I})$$

the right-hand integral in eq. 12-16 can be transformed into

$$-\frac{1}{2c} \int_V (\Psi \text{div } \mathbf{I}) d\tau - \frac{1}{2c} \int_V \Psi (\mathbf{I} \cdot d\sigma)$$

Now because of the assumed stationary conditions in the interior, the fundamental eq. VI becomes $\text{div } \mathbf{I} = 0$, and at the surface eq. 3-7 gives $\mathbf{I} \cdot \mathbf{n} = 0$. Therefore nothing remains of the above expressions except the contribution of the cross-sectional cuts which eventually have to be introduced. For the time being we assume the superconductor to be doubly connected so we need only one cut. By eq. 12-8 its contribution is

$$-\frac{1}{2c} (\Psi_1 - \Psi_2) \int_C \mathbf{I} \cdot d\sigma_1 = \frac{1}{2c} S_C \int_C \mathbf{I} \cdot d\sigma_1 \quad (12-17)$$

We write

$$\int_C \mathbf{I} \cdot d\sigma_1 = I_s \quad (12-18)$$

the current in the ring. As $d\sigma_1$ is in the same direction as the curves C_2 , I_s is positive if the current flows in the same sense as C_2 , otherwise it is negative. Equation 12-16 is transformed in this way into

$$\frac{1}{2} \int_V (\mathbf{I} \cdot \mathbf{G}) d\tau = \frac{S_C I_s}{2c} - \frac{1}{2c} \int_V (\mathbf{A} \cdot \mathbf{I}) d\tau \quad (12-19)$$

On the other hand, the magnetic energy of the field is, by eqs. 5-8 and 3-2

$$\frac{1}{2} \int_V \mu H^2 d\tau = \frac{1}{2} \int_V (\mathbf{H} \cdot \mathbf{B}) d\tau = \frac{1}{2} \int_V (\mathbf{H} \cdot \mathbf{M}) d\tau$$

³ Δ is the imaginary part of the complex function $\ln(x + iy)$.

where the suffix V indicates that the integral extends over the whole of space, whereas the suffix P indicates that it extends over only the permanent magnets in the field. By eq. 12-1 and the rule 5-1 we have

$$\frac{1}{2} \int_V (\mathbf{H} \cdot \mathbf{B}) d\tau = \frac{1}{2} \int_V (\mathbf{H} \cdot \text{curl } \mathbf{A}) d\tau = \frac{1}{2} \int_V (\mathbf{A} \cdot \text{curl } \mathbf{H}) d\tau - \frac{1}{2} \int_V ((\mathbf{A} \times \mathbf{H}) \cdot d\sigma)$$

The surface integral vanishes over the sphere at infinity because there \mathbf{H} behaves like R^{-3} . The tangential components of \mathbf{H} and \mathbf{A} are continuous at surfaces of discontinuity, therefore the normal component of $[\mathbf{A} \times \mathbf{H}]$ which depends only on these tangential components is also continuous and does not contribute anything. Therefore

$$\frac{1}{2} \int_V \mu H^2 d\tau = \left(\frac{1}{2c} \right) \int_V (\mathbf{A} \cdot \mathbf{I}) d\tau - \frac{1}{2} \int_P (\mathbf{H} \cdot \mathbf{M}) d\tau \quad (12-20)$$

The field is produced by the ohmic current in the normally conducting coils together with the corresponding supercurrent in the superconductor, and also by any persistent current that may be present. We designate the coils by the suffix c under the integral sign. Splitting up the right-hand side of eq. 12-20 in this way yields:

$$\frac{1}{2} \int_V \mu H^2 d\tau = \frac{1}{2c} \int_V (\mathbf{A} \cdot \mathbf{I}) d\tau + \frac{1}{2c} \int_c (\mathbf{A} \cdot \mathbf{I}) d\tau - \frac{1}{2} \int_P (\mathbf{H} \cdot \mathbf{M}) d\tau$$

Adding this equation to 12-19 we get

$$\frac{1}{2} \int_V (\mathbf{I} \cdot \mathbf{G}) d\tau + \frac{1}{2} \int_V \mu H^2 d\tau = \frac{1}{2c} \left\{ S_C I_s + \int_c (\mathbf{A} \cdot \mathbf{I}) d\tau \right\} - \frac{1}{2} \int_P (\mathbf{H} \cdot \mathbf{M}) d\tau \quad (12-21)$$

According to eq. 5-8 the left-hand side of this is the total energy of the field U , which is necessarily positive or zero, the latter only if $\mathbf{I} = 0$ and $\mathbf{H} = 0$ everywhere. This equation implies the following theorem.

The "period" S_C of the superconduction potential in the ring, together with the ohmic currents and the permanent magnets determine uniquely the magnetic field of the supercurrent. This is because if we assume two different fields with the same ohmic currents and permanent magnets, the difference between the two fields also satisfies the differential equations of the London theory. Therefore eq. 12-21 may be expressed in terms of this difference, but the right-hand side vanishes by hypothesis.

For a singly connected superconductor the first term of the right-hand side is missing; it is therefore current free in the absence of external excitation; otherwise the apparatus producing the field determines the situation uniquely. This theorem also guarantees the uniqueness of the solution of those examples in Chaps. 10 and 11 which are not covered already by the uniqueness theorem of eq. 7-4. Equation 12-21 admits the possibility of an independent persistent current in a ring, but otherwise the ring is determined in all details by specifying its S_C . For instance its

magnetic moment is equal to ScP where P is a vectorial factor depending only on the geometry of the ring and the intensive functions of position λ, ρ . The magnetic moment can only assume two opposite directions; the sign of Sc decides which one. In so far as the persistent current alone is exciting the field, the direction of the current is such as to make ScI' positive. If as in Fig. 12-1 the current flows in the positive sense, assigned to all curves C_2 in the ring, then the magnetic lines of force that pass through the ring have the direction of $d\sigma$, i. e., they come toward the reader. If we place a ring carrying a persistent current in an additional external magnetic field, then an induced current is superposed on the original current. In spite of the constancy of Sc the resulting current strength I' can become zero or even reverse in sign.

Let a normally conducting specimen be placed in a magnetic field and then cooled down until it becomes superconducting; then there is a considerable flux of induction through the ring but no current, or only a very weak current. Which of these possibilities is realized depends upon the detailed course of events during the cooling process and is difficult to determine. Switching off the magnetic field does not change the flux, but the current increases to the strength determined by the total flux and the form of the specimen. This is a common method of producing persistent currents.

To generalize eq. 12-21 for an n -ply connected superconductor we replace the one term ScI' by $(n-1)$ terms of the same kind. The corresponding statement applies if several separate superconductors are present in the field.

Because of its magnetic moment every superconductor that has a persistent current must experience a torque in a homogeneous magnetic field in addition to that due to field deformation caused by the shape of the specimen.⁴

(f) Let us assume two superconductors, both with persistent currents I and I' , to be moving relative to each other. The forces between them perform work, and for lack of any other source of energy, at the expense of the energy $ScI' + Sc'I'$. Because Sc and Sc' are constants according to eq. 12-14 a change of energy is only possible by a change of the strengths of the currents.

Suppose the superconductors to be rings formed by circles rotated around axes of symmetry that do not intersect the circles (Fig. 12-4). Let them be in such a relative position that at first they are at a great distance from each other and their axes of symmetry coincide. In this situation let the

⁴Why is it that there is in the theory of ohmic currents and their magnetic fields, no uniqueness theorem corresponding to eq. 12-21? This is because in this case the question of current distribution is answered uniquely by electrostatics and because after solving this problem the magnetic field can be deduced unambiguously from the current density. It is impossible to separate the problem of the superconductor into two parts in this way.

current I flow in the first ring, but zero current in the second one. Let the rings now be brought together. The resulting lines of force are then as sketched diagrammatically in the figure. If the current I flows away from the reader on the right-hand side (at the minus sign), then the current in the second ring flows toward the reader on the right-hand side. This follows from the rule [Chap. 7 (c)] that inner normal of the conductor, current, and magnetic field form a right-handed system. The antiparallel currents I_1 and I_2 repel each other; bringing the rings together requires the performance of work and produces an increase of the field energy ScI_1I_2 , and thus an increase of I_2 . However I_2' is also increased because the lines of force crowd together near the second ring and create a greater field strength the smaller the distance.

If a current I_2^0 is initially flowing in the second ring when at infinite separation, then the current $I_2^0 - I_2$ flows at the smaller distance, and there is attraction or repulsion depending on whether this expression is positive or negative. We have a stable equilibrium, at least with respect to motion along the axis, because a further approach leads to repulsion, and increase of distance to attraction. For example, in Justi's persistent current electro-magnet the current strength decreases when it is attracting iron and the flux of induction remains constant [Chap. 1 (b)].

(g) A famous experiment performed in 1924 is in apparent contradiction to this argument. Kamerlingh-Onnes⁵ excited a persistent current in a hollow sphere of lead and so apparently in a singly connected region. He produced the current by the usual method of bringing the specimen, while at a higher temperature, into a magnetic field and then cooling it to become superconducting. The sphere showed a magnetic moment after removing the field and experienced the corresponding torque in any external field. This great investigator concluded that the paths of the current could not be displaced in the superconducting body. If they could be, the forces exerted by the external field would be unable to move the sphere because it has no preferential direction.

From later experience the following explanation can be given for the above observation. The cooling of the hollow sphere immersed in liquid helium did not proceed everywhere with the same speed. At first one or may be several annular zones became superconducting while the rest of

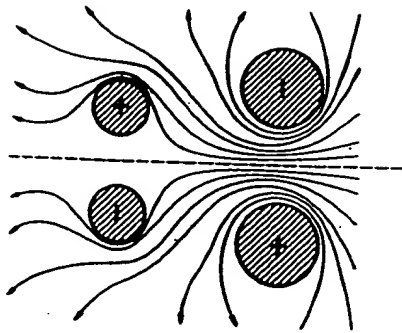


Fig. 12-4. Two superconducting rings with magnetic field lines.

⁵H. Kamerlingh-Onnes, *Commun. Leiden Supplement*, 50a, (1924).

the sphere remained normal. With the approach of temperature equilibrium the whole sphere had not become superconducting; instead, after the first zone had once trapped a certain amount of flux, the latter remained unchanged in the nonsuperconducting remainder of the sphere which stayed in the intermediate state (Chap. 19). With increasing concentration of the lines of force as the annular ring of superconducting material grew and the cross section of the normal material decreased, the field strength increased finally beyond the critical value H_c in the rest of the sphere and so prevented the complete establishment of the superconducting state.

Actually therefore the supercurrent was flowing in one or in several rings. Its magnetic moment was attached rigidly to this ring, and therefore also to the sphere, so the latter was forced to orient itself in an external field. This follows inevitably from the uniqueness theorem. However, even though Kamerlingh-Onnes failed to interpret his experiments, his question whether the current lines are displaced in a superconductor under the influence of an external magnetic field is still perfectly legitimate. This is discussed in Chap. 13.

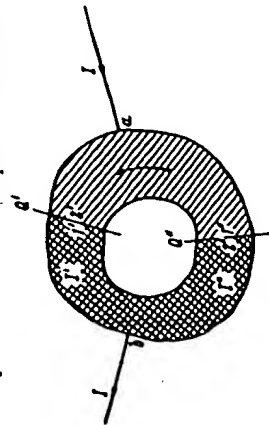


Fig. 12-5. Superconducting ring with normally conducting leads. The arrow shows the "sense" of the ring and also the positive I' current direction. A positive current I'' flows in the opposite direction. The sense of the ring is from $2'$ to $1'$ and from $2''$ to $1''$.

(h) In the examples discussed in the last paragraph and in section (d) it was assumed that no ohmic current was supplied to the doubly connected superconductor from outside. But now let us imagine that at two points a and b on the surface of the superconductor, normally conducting wires are soldered through which a current I is supplied, entering at a and leaving at b , see Fig. 12-5. The ohmic current is distributed through the superconductor with a current I' flowing in the path that goes from a to b in the same direction as the "sense" of the ring (which we arbitrarily choose for all from $2'$ to $1'$), and a current I'' in the other path. We regard the currents as positive if they are flowing from a to b . However, we know from Chap. 2 that one of them can be negative. This is true particularly if a persistent current is superimposed on the supplied current. In general

$$I' + I'' = I \quad (12-22)$$

This modified assumption does not alter eq. 12-10. Therefore eqs. 12-11 and 12-13 together with the theorems derived from them remain valid. But the integral on the right-hand side of eq. 12-16

$$\int (\mathbf{i} \cdot \text{grad } \Psi') d\tau = - \int \Psi' (\mathbf{i} \cdot d\mathbf{a})$$

acquires another value because it is no longer true that $\mathbf{i} \cdot \mathbf{a} = 0$ everywhere over the surface. Suppose the cut that contributes to the integral is made first in the branch carrying the current I' ; this cut may be called Q' and the function Ψ' for this case will be written Ψ'' . The integral then becomes

$$-(\Psi_a' - \Psi_b'') I + S_c I'$$

If we displace the cut to the other branch and call it Q'' , and the corresponding function Ψ'' , the surface integral becomes in the same way

$$-(\Psi_a'' - \Psi_b'') I - S_c I''$$

Here I'' has a minus sign because a positive I'' has, by hypothesis, a direction opposite to the sense of the ring. The two values are equal because their difference

$$[(\Psi_a' - \Psi_b'') - (\Psi_b' - \Psi_a'')] I - (I' + I'') S_c = 0$$

This can be seen in the simplest way from eq. 12-22 by making use of the undetermined additive constant in the definition of Ψ' to make $\Psi_a' = \Psi_b''$. In this case Ψ' and Ψ'' are equal throughout the whole singly shaded region in Fig. 12-5 between the two cuts that enclose the point a whereas in the other cross-hatched area between the two cuts enclosing the point b we have $\Psi'' - \Psi' = S_c$. Equation 12-21 is now replaced either by

$$\frac{1}{2} \int (\mathbf{i} \cdot \mathbf{G}) d\tau + \frac{1}{2} \int \mu H^2 d\tau = \frac{1}{2c} [(\Psi_b'' - \Psi_a'') I + S_c I' + \int (\mathbf{A} \cdot \mathbf{i}) d\tau] - \frac{1}{2} \int (\mathbf{H} \cdot \mathbf{M}) d\tau \quad (12-23)$$

or by

$$\frac{1}{2} \int (\mathbf{i} \cdot \mathbf{G}) d\tau + \frac{1}{2} \int \mu H^2 d\tau = \frac{1}{2c} [(\Psi_b'' - \Psi_a'') I - S_c I'' + \int (\mathbf{A} \cdot \mathbf{i}) d\tau] - \frac{1}{2} \int (\mathbf{H} \cdot \mathbf{M}) d\tau$$

the term containing S_c has the positive or negative sign if the current is in the positive sense I' or the negative sense I'' respectively. This agrees with the sign of the corresponding term in eq. 12-21.

This alteration does not affect the uniqueness theorem which we linked with eq. 12-21 because the current I supplied to the superconductor belongs to the ohmic currents of the external field. Also I becomes zero for the difference field between two fields corresponding to the same "period" S_c , the same ohmic currents, and the same permanent magnets.

(i) Considered as the source of its field, a persistent current has, according to eq. 12-21, only the energy $U = S_c I^2$. However, S_c is proportional to I , and we may write

$$\frac{S_c}{c} = p'' I \quad (12-24)$$

and we see from the equation

$$U = \frac{1}{2} p^{ss} I_s^2 \quad (12-25)$$

that p^{ss} is the coefficient of self-induction of the superconducting ring. It differs from the self-induction for an ohmic current in that in U there is also in p^{ss} there is a positive term due to the energy of the supercurrent. However, this term is usually quite insignificant compared with the magnetic energy, because the superconductivity occurs for the most part only in thin layers where, due to the continuity of the components of H , most of the energy density is of the same order of magnitude as in adjoining parts of the outside space (see eq. 7-37). This positive contribution is annulled in thick specimens by the far greater negative contribution from the expulsion of the field.⁶ This idea can be carried through quantitatively only for special cases because the external magnetic field outside a superconductor is generally different from that for an ohmic conductor.

From eqs. 12-14 and 12-24 it follows that for a thick superconductor the coefficient of self-induction is equal to the flux through its own current circuit divided by the velocity of light c and the current strength. For thin superconductors there is a correction according to eq. 12-11. It is well known that this theorem does not hold for normal conductors, because it is then impossible to define the flux through its own current circuit in so far as the latter is considered to have extension in space, whereas if it is considered infinitely thin, the flux is no longer finite.

If there are ohmic currents of strength I^e present in addition to the persistent current, we get

$$Sc = p^{ss} I_s + \sum_e p^{ee} I_e$$

a linear function of all the current strengths. Furthermore, because the vector potential A is a linear sum of all the contributions from the separate currents, eq. 12-21 gives for the field energy, omitting the magnetic contribution,

$$U = \frac{1}{2} \sum_{ss} p^{ss} I_s I_s$$

This summation is extended over all the ohmic currents as well as the persistent current. The coefficients of induction between the persistent current and the ohmic currents are also affected by the energy of the supercurrent in the same way as the self-induction p^{ss} . Beyond this we can say nothing without further information about the effect of the expulsion of the field.

⁶However, in a cable with the return path formed by its shell at a small distance from the inner conductor, supposing the shell to be superconducting, the superconductivity energy could be responsible for almost one-half of the coefficient of self-induction.

With regard to the other coefficients, the self-induction and the mutual inductions between the ohmic currents are also affected by the presence of the superconductor, just as they depend on the magnetic permeability in their neighborhood. One method for measuring the penetration depth β^{-1} and the constant λ is based on this fact. It was devised by Casimir⁷ and used with success by Laurmann and Shoenberg⁸; although not absolute, it gives the dependence on temperature. A long solenoid is wound around a superconducting cylinder and a shorter induction coil is wound tightly around its center; their mutual induction is measured. The greater the penetration depth, the greater the flux of induction through the measuring coil due to the long solenoid, and so the greater their mutual induction. Two different specimens of mercury gave slightly different results in this experiment, and this is a reminder of the fact that the constant λ is really a tensor.

CHAPTER 13

The Maxwell and London Stresses

(a) Kamerlingh-Onnes in 1924 raised the question whether the track of the supercurrent could be displaced in the superconductor under the influence of an external magnetic field [see Chap. 12 (g)]. He started from the assumption that in any case in the steady state the carriers of the supercurrent do not experience any forces due to the material itself, i. e., to the atoms and the carriers of the ohmic current, for otherwise persistent currents would be impossible. His question was, however, inconsequential in so far as the supercurrent already has its own magnetic field, so that the problem exists even before any external field enters the picture. Our present ideas about the current distribution had not been developed in 1924. We now have a clear picture of the current concentration in the protecting layer and we know that the current, magnetic field, and the inner normal to the surface form a right-handed system (Chap. 7), and therefore that the force per unit volume $\frac{1}{2} [j \times H]$ due to its own magnetic field is directed toward the interior of the superconductor (current, field, and force also form a right-handed system). We may therefore raise the question: Why does the magnetic field not push the current into the interior? How can the current in the thin protecting layer have any stability at all?

Another question is intimately connected with this. A rod carrying a supercurrent I and located in a magnetic field H perpendicular to the axis of the cylinder, experiences a force $\frac{1}{2} I H$ per unit length. Upon what does this force act? If the supercurrent mechanism experiences no force

⁷H. G. B. Casimir, *Physica*, 7, 887 (1940).

⁸E. Laurmann and D. Shoenberg, *Nature*, 160, 747 (1948).

due to the material, neither can it exert force on the material: action and reaction must be equal. And yet the force due to the magnetic field certainly has to act first on the supercurrent mechanism, and through this somehow on the rod.

The answer can only be that the forces act on the material discontinuity at the surface. It is there that the interaction between matter and the supercurrent carriers must be located, and not in the interior. If such forces were not present even at the surface, the carriers would be able to escape from the metal, which certainly does not happen. The theory answers all these questions in terms of the London stresses. The force ordinarily exerted by the field can be calculated from the divergence of the Maxwell stresses, which are defined in terms of the electric and magnetic fields; similarly the London stresses, which depend only on the supercurrent, take care of the force exerted by the magnetic field on the supercurrent mechanism, and in fact locate it at the surface instead of throughout the body of the material. The supercurrent hangs as it were from the surface like a curtain, the magnetic field of the current corresponds to the weight of the curtain, the London stresses correspond to the elastic forces holding the curtain to its curtain rod and prevent it from falling into the interior. This is how we can answer Kamerlingh-Onnes' question.

The point therefore is to find a stress tensor that depends only on the current density \mathbf{i} and that has a divergence that everywhere just compensates the force resulting from the Maxwell stresses in the magnetic field.¹ London's fundamental equations IX and X are needed to carry this through mathematically. They enter as the necessary and sufficient conditions for the system of London stresses to just compensate the Maxwell forces. The whole current distribution is fixed by this equilibrium condition. We regard the fact that it makes such a compensation possible as inherently the strongest point in favor of the theory.

This compensation is not entirely necessary for inhomogeneous superconductors or non stationary currents. The discussion of the general equation 13-10 actually leads to completely new points of view.

(b) To begin with we define nine quantities in terms of two arbitrary vector functions of position \mathbf{P} and \mathbf{Q} :

$$\Theta_{\alpha\beta}(\mathbf{P}, \mathbf{Q}) = P_\beta Q_\alpha - \frac{1}{2} \delta_{\alpha\beta} \sum_\gamma P_\gamma Q_\gamma \quad (\alpha, \beta = 1, 2, 3) \quad (13-1)$$

They form the components of a tensor of the second rank because the two parts $P_\beta Q_\alpha$ and $\frac{1}{2} \delta_{\alpha\beta} \sum_\gamma P_\gamma Q_\gamma$ are each tensors themselves.² Written in greater detail the definition 13-1 reads:

$$\Theta_{11}(\mathbf{P}, \mathbf{Q}) = \frac{1}{2} (P_1 Q_1 - P_2 Q_2 - P_3 Q_3) \\ \Theta_{23} = P_3 Q_2, \quad \Theta_{32} = P_2 Q_3, \quad \text{etc.} \quad (13-2)$$

¹As we later put $-\text{div } \Theta$ equal to the force acting on the material we have to regard a positive $\Theta_{\alpha\alpha}$ as a pressure, a negative one as a tension.

² $\delta_{\alpha\beta} = 1$ for $\alpha = \beta$, otherwise zero.

We now form the divergence of this tensor, i. e., the vector of which the x_1 component is³

$$\text{div}_1 \Theta(\mathbf{P}, \mathbf{Q}) = \frac{\partial \Theta_{11}}{\partial x_1} + \frac{\partial \Theta_{12}}{\partial x_2} + \frac{\partial \Theta_{13}}{\partial x_3} \quad (13-3)$$

Carrying through the calculation yields

$$\text{div}_1 \Theta(\mathbf{P}, \mathbf{Q}) = Q_1 \text{div } \mathbf{P} - [\mathbf{P} \times \text{curl } \mathbf{Q}]_1 + \frac{1}{2} \left(\sum_\gamma P_\gamma \frac{\partial Q_\gamma}{\partial x_1} - \sum_\gamma Q_\gamma \frac{\partial P_\gamma}{\partial x_1} \right) \quad (13-4)$$

Now we set $\mathbf{P} = \mathbf{i}$, $\mathbf{Q} = \mathbf{Q}$, i. e., $Q_\alpha = \sum_\beta \lambda_{\alpha\beta} i_\beta$ (see eq. VIII Chap. 3); then because of the symmetry relation 3-3 ($\lambda_{\alpha\beta} = \lambda_{\beta\alpha}$), the two sums cancel each other, at least if the $\lambda_{\alpha\beta}$ are independent of x_α . Otherwise there remains a term:

$$\frac{1}{2} \sum_{\alpha\beta} i_\alpha i_\beta \frac{\partial \lambda_{\alpha\beta}}{\partial x_1}$$

By writing the tensor of third rank with components $\partial \lambda_{\alpha\beta} / \partial x_\gamma$ as $\nabla(\lambda_{\alpha\beta})$, the following vector equation results:

$$\text{div } \Theta(\mathbf{i}, \mathbf{Q}) = Q \text{div } \mathbf{i} - [\mathbf{i} \times \text{curl } \mathbf{Q}] + \frac{1}{2} \sum_{\alpha\beta} i_\alpha i_\beta \nabla(\lambda_{\alpha\beta}) \quad (13-5)$$

Now we use the continuity equation VI and the fundamental equation X to obtain

$$\text{div } \Theta(\mathbf{i}, \mathbf{Q}) = -Q \frac{\partial \rho}{\partial t} + \frac{1}{c} [\mathbf{i} \times \mathbf{H}] + \frac{1}{2} \sum_{\alpha\beta} i_\alpha i_\beta \nabla(\lambda_{\alpha\beta}) \quad (13-6)$$

Finally remembering IX we write

$$-Q \frac{\partial \rho}{\partial t} = -\frac{\partial}{\partial t} (\rho' G) + \rho' \frac{\partial G}{\partial t} = -\frac{\partial}{\partial t} (\rho' G) + \rho' E,$$

and find in this way that

$$\text{div } \Theta(\mathbf{i}, \mathbf{Q}) = \rho' E + \frac{1}{c} [\mathbf{i} \times \mathbf{H}] + \frac{1}{2} \sum_{\alpha\beta} i_\alpha i_\beta \nabla(\lambda_{\alpha\beta}) - \frac{\partial}{\partial t} (\rho' G) \quad (13-7)$$

On the other hand, if we form the Maxwell stress tensors $T(\mathbf{E})$ and $T(\mathbf{H})$ for the interior of the superconductor where we do not need to distinguish between \mathbf{D} and \mathbf{E} or between \mathbf{B} and \mathbf{H} , we have

$$T(\mathbf{E}) = -\Theta(\mathbf{E}, \mathbf{E}), \quad T(\mathbf{H}) = -\Theta(\mathbf{H}, \mathbf{H}) \quad (13-8)$$

Remembering the Maxwell equations I, and IV, it follows from 13-4 that

$$-\text{div } \{T(\mathbf{E}) + T(\mathbf{H})\} = \mathbf{E} \text{div } \mathbf{E} - [\mathbf{E} \times \text{curl } \mathbf{E}] + \mathbf{H} \text{div } \mathbf{H} - [\mathbf{H} \times \text{curl } \mathbf{H}] \\ = \rho E + \frac{1}{c} [\mathbf{i} \times \mathbf{H}] + \frac{1}{c} \frac{\partial}{\partial t} [\mathbf{E} \times \mathbf{H}] \quad (13-9)$$

³ See previous footnote.

Here ρ is the total density $\rho^0 + \rho'$, I the total current $I^0 + I'$. Subtracting from eq. 13-7 yields

$$-\operatorname{div} [T(E) + T(H) + \Theta(I, G)] = \rho^0 E + \frac{1}{c} [I^0 \times H] - \frac{1}{2} \sum_{\alpha\beta} I_{\alpha}' I_{\beta}' \nabla (\lambda_{\alpha\beta}) + \frac{\partial}{\partial t} \left\{ \frac{1}{c} [E \times H] + \rho' G \right\} \quad (13-10)$$

This equation constitutes the momentum law.

In the stationary state E and I^0 vanish (Chap. 7), and for the homogeneous body the double sum vanishes. In the stationary state, the Maxwell stresses of the magnetic field and the London stresses of the supercurrent result in no net force on the interior of a homogeneous superconductor, as was required. The symmetry of the tensor $\lambda_{\alpha\beta}$ is found to be a necessary and sufficient condition for this. In a time-dependent field the ohmic current mechanism exerts the force $\rho^0 E + (1/c) [I^0 \times H]$ per unit volume; it serves to change the mechanical momentum density. Moreover, the forces due to the three stress tensors produce an increase in the well-known electromagnetic momentum $(1/c) [E \times H]$ and of the momentum density of the supercurrent $\rho' G$. (This is why we have called G the supermomentum.) Discussion of the double sum in eq. 13-10 is deferred until later. This also shows why we were not permitted to put the superconduction charge density ρ' equal to zero even in the stationary state where ρ is zero (see Chaps. 4 and 5): the momentum $\rho' G$ is without doubt always present in the stationary current.

(c) The Maxwell stresses do not act on the surface of a superconductor except in the case (not to be discussed here) that the material immediately across the surface has a dielectric constant or a permeability differing from unity. As all the components of E and H are continuous across the boundary, according to the boundary conditions of Chap. 3 (c), the tensors $T(E)$ and $T(H)$ have equal components on either side of the surface, and so have no "surface divergence." However, the London tensor $\Theta(I, G)$ does have a surface divergence because the supercurrent ceases at the surface. Let $P_{(n)}$ be this negative surface divergence, the n referring to the inner normal of the surface; its components are

$$P_{(n)\alpha} = - \sum_{\beta} \Theta_{\alpha\beta} \cos(n, x_{\beta}) \quad (13-11)$$

Using the definition 13-1 and introducing the unit vector n in the direction n , we can write vectorially

$$P_{(n)} = -i_{\alpha}' G + \frac{1}{2} (I' \cdot G) n \quad (13-12)$$

$P_{(n)}$ is the force exerted by the supercurrent on the surface per unit area. This is the only ponderomotive force exerted by the current.

Wherever there is no current entering (or leaving) across the surface, $i_{\alpha}' = 0$, a tension $\frac{1}{2} (I' \cdot G)$ acts toward the interior. At points where

current enters there is a tangential component of the force due to the first term in 13-12.

In cubic crystals, $G = \lambda I'$ has the same direction as I' everywhere. Then the current streamline is the only intrinsic direction and must be a principal axis of the tensor $\Theta(I, G)$. As can be seen from the equations

$$\Theta_{11} = \frac{1}{2} \lambda \{ I_1'^2 - I_2'^2 - I_3'^2 \}; \quad \Theta_{23} = \Theta_{32} = \lambda I_2' I_3' \quad (13-13)$$

this tensor becomes symmetrical. Putting the x_1 axis parallel to the current, the components $\Theta_{\alpha\beta}$ with mixed suffixes vanish and we get

$$\Theta_{11} = \frac{1}{2} \lambda I'^2, \quad \Theta_{22} = \Theta_{33} = -\frac{1}{2} \lambda I'^2 \quad (13-14)$$

In this case therefore a pressure $\frac{1}{2} \lambda I'^2$ acts along the current line, and an equal tension perpendicular to it. It manifests itself at the surface where $i_{\alpha}' = 0$ as a tension $\frac{1}{2} \lambda I'^2$ directed toward the interior.

We can illustrate the meaning of the double sum in eq. 13-10 for the cubic crystal case where it reduces to

$$-\frac{1}{2} I'^2 \operatorname{grad} \lambda \quad (13-15)$$

Where two superconductors with different λ 's make contact, the stresses give rise to a force on the boundary. In case the current crosses the boundary perpendicularly, $(I_{\alpha}')_1 = (I_{\alpha}')_2$ and eq. 13-15 gives the difference between the two pressures along the current lines: $\frac{1}{2} \lambda_1 I'^2 (\lambda_1 - \lambda_2)$. Where, however, the two currents flow parallel to the boundary, $\lambda_1 (I_1') = \lambda_2 (I_2') = C$ according to eq. 3-9, and the integral of eq. 13-15 over the thickness of the boundary layer yields the difference between the two tensions: $\frac{1}{2} C^2 (1/\lambda_2 - 1/\lambda_1)$.

In all these cases the force given by eq. 13-15 is directed toward the better superconductor, with the smaller λ .

(d) The stress system assumes a particularly simple form in the fully developed protective layer of a thick cubic crystal conductor. With the z axis of coordinates along the inner normal, eqs. 7-9 and 7-10 give

$$H_x = H_z = 0, \quad I_y' = I_z' = 0, \quad H_y = \sqrt{\lambda} I_x'$$

Therefore in the z direction the pressure $\frac{1}{2} H^2$ of the magnetic field and the tension $\frac{1}{2} \lambda I_x'^2$ of the current cancel each other at every point. In the direction of the current, however, the pressure $\frac{1}{2} H^2$ and $\frac{1}{2} \lambda I_x'^2$ are equal and have to be added together, but because they do not depend on z they give rise to no resultant force, in agreement with eq. 13-10.

(e) To answer a question remaining from section (a) we now calculate from the London stresses the force exerted on a superconducting cylinder of cubic crystalline material carrying a current I in a transverse magnetic field H^0 . Figure 13-1 represents a cross section of the cylinder, and if H^0 is in the x direction, the current produced by this field flows toward the reader at a and away from the reader at b . If the current I flows toward the reader, the current at a is greater than that at b . The stronger inward

tension at a and its neighborhood results in a force from a toward b , in the y direction in the figure. This force, the current I , and the field H^0 form a right-handed system as they should.

The numerical calculation can be carried out by the methods of Chap. 8 (a) and Chap. 10 (c). From eq. 8-9 the density of the current I at $r = R$ is

$$I_z^{(1)} = \frac{\epsilon \beta I I_0 (\epsilon \beta R)}{2 \pi R I_1 (\epsilon \beta R)}$$

The current density due to the field H^0 according to eq. 10-16 is

$$I_z^{(2)} = \frac{2 \epsilon H^0 \sin \theta I_1 (\epsilon \beta R)}{\sqrt{\lambda} I_0 (\epsilon \beta R)}$$

The inward tension therefore has the strength

$$\frac{1}{2} \lambda (I_z^{(1)} + I_z^{(2)})^2$$

If this is multiplied by $-\sin \theta$, we obtain its contribution to the total force on the surface K , the value of which is

$$K_y = -\frac{1}{2} R \lambda \int_0^{2\pi} [(I_z^{(1)})^2 + I_z^{(2)2} + 2 I_z^{(1)} I_z^{(2)}] \sin \theta d\theta$$

Because $\int_0^{2\pi} \sin \theta d\theta = \int_0^{2\pi} \sin^2 \theta d\theta = 0$ and $\int_0^{2\pi} \sin^2 \theta d\theta = \pi$, this reduces

$$K_y = -R \lambda \int_0^{2\pi} I_z^{(1)} I_z^{(2)} \sin \theta d\theta = \frac{I H^0}{c}$$

(f) An example of the tangential component of the force K would be given by a Barlow's wheel made of superconducting cubic crystal material. This consists of a circular disk in a magnetic field parallel to its axis that would be homogeneous in the absence of the disk; current is supplied through the axis of the disk and is drawn off through a normal conductor at its perimeter. If the disk is thick compared with the penetration depth, the field is distorted by the Meissner effect and considerably increased at the periphery, while according to Chap. 7 (g) the field would penetrate a thin disk relatively undisturbed, assuming it still to be of cubic crystalline structure.

The above stresses act on the two circular faces of the disk. Because they are parallel to the axis they produce no angular momentum. However, near the point where the current leaves the disk there is a tangential current

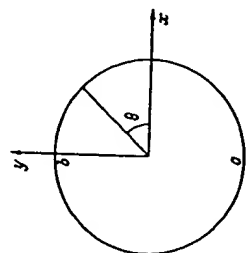


Fig. 13-1. Cylindrical coordinates for a superconducting cylinder. The x axis and the current I point toward the reader, and H^0 is in the x direction.

I_θ flowing along the periphery which is proportional to H^0 and protects the interior of the (thick) superconductor from the field. At the point where the current leaves, there is a tangential force $\mathcal{O}_{r,\theta} = \lambda I_z^{(1)} I_\theta$ that does produce angular momentum. The calculation shows that with a thin disk the force has the same value as for a normal conductor, while with a thick disk it has the same direction but is much weaker.*

The reality of the Maxwell stresses in empty space is vouchsafed by the principle of relativity. In so far as the energy density has reality in all inertial systems connected by a Lorentz transformation, the same reality must be ascribed to the stress components that are transformed along with this energy density and form with it a "world tensor." It is difficult to believe that this does not also hold for the Maxwell stresses. However, it is not inconceivable that the London stresses are purely a convenient mathematical fiction. In what follows we assume the contrary.

(g) Because in the above examples the net force and the torque are acting on an essentially rigid body, we could have started from the external magnetic stresses $\mathcal{T}(\mathbf{H})$ instead of from the London stresses in the interior; which stresses exist in the interior is of no importance for such a calculation so long as all the stress tensors are symmetrical.

In order to carry through this alternative, we recall the two well-known integral theorems of the tensor theory; it is possible by partial integration to transform certain volume integrals of an arbitrary asymmetrical tensor $t_{\alpha\beta}$ into surface integrals. Let n again mean the inner normal, then we have first

$$\iint \left[\frac{\partial t_{11}}{\partial x_1} + \frac{\partial t_{12}}{\partial x_2} + \frac{\partial t_{13}}{\partial x_3} \right] d\tau = - \int [t_{11} \cos(n x_1) + t_{12} \cos(n x_2) + t_{13} \cos(n x_3)] d\sigma \quad (13-16)^*$$

and secondly,

$$\begin{aligned} \iint \left\{ x_2 \left(\frac{\partial t_{31}}{\partial x_1} + \frac{\partial t_{32}}{\partial x_2} + \frac{\partial t_{33}}{\partial x_3} \right) - x_3 \left(\frac{\partial t_{21}}{\partial x_1} + \frac{\partial t_{22}}{\partial x_2} + \frac{\partial t_{23}}{\partial x_3} \right) \right\} d\tau = \\ = - \iint \left\{ x_2 [t_{31} \cos(n x_1) + t_{32} \cos(n x_2) + t_{33} \cos(n x_3)] - x_3 [t_{21} \cos(n x_1) + \right. \\ \left. + t_{22} \cos(n x_2) + t_{23} \cos(n x_3)] \right\} d\sigma + \int (t_{32} - t_{23}) d\tau \quad (13-17) \end{aligned}$$

*W. Heisenberg and M. v. Laue, *Z. Physik*, 124, 514 (1948). With regard to the present state of our knowledge about supercurrents and surface phenomena, one might perhaps doubt whether the torque is acting on the disk itself or on the normally conducting wire that leads the current out of the disk. The phenomenological theory described here cannot answer this question, but we could imagine the leads replaced by a cold emission from the periphery through the surrounding space when it could conceivably be decided experimentally whether or not the torque acts on the wheel.

* In this and subsequent formulas $d\sigma$ is not a vector.

The force per unit area on any surface due to the tensor $T(H)$ now has the components

$$F_{n\alpha} = \sum_{\beta} T_{\alpha\beta} \cos(n, x_{\beta}) \quad (13-18)$$

which can be written together in vector form:⁵

$$\mathbf{F}_n = -H_n \mathbf{H} + H^2 \mathbf{n} \quad (13-19)$$

(\mathbf{n} is again the unit vector normal).

The difference in sign between the right-hand sides of eqs. 13-18 and 13-11 is due to the fact that the Maxwell stresses we are discussing here lie outside the space element, whereas the London stresses are inside it. The resultant force on this element is, according to eq. 13-16,

$$-\int \operatorname{div} T(H) d\tau = \int \mathbf{F}_n d\sigma \quad (13-20)$$

and the torque due to the Maxwell stresses is:

$$-\int [\mathbf{r} \times \operatorname{div} T(H)] d\tau = \int [\mathbf{r} \times \mathbf{F}_n] d\sigma \quad (13-21)^6$$

By using eq. 13-20 one can easily calculate from \mathbf{F}_n , e. g., the force $(1/c) I H^0$ acting on the cylinder carrying a current in a magnetic field treated in (c).

We now want to find the conditions under which the net force and the torque due to the Maxwell stresses in the outside space coincide with the net force and the torque due to the London stresses in the interior.

The volume integral for the Maxwell stresses on the right-hand side of eq. 13-17 vanishes because the tensor $T(H) = -\Theta(H, H)$ is symmetrical, according to eq. 13-2. It also vanishes for the tensor $\Theta(i, G)$ in a cubic crystalline superconductor because in this case $G = \lambda i$. Therefore integrating eq. 13-11 over the volume of the superconductor, using eqs. 13-16 and 13-17, we conclude that

$$-\int \operatorname{div} \Theta(i, G) d\tau = -\int K_n d\sigma \quad (13-22)$$

and

$$-\int [\mathbf{r} \times \operatorname{div} \Theta(i, G)] d\tau = -\int [\mathbf{r} \times K_n] d\sigma \quad (13-23)$$

For the homogeneous superconductor in a stationary state we have, according to eq. 13-10, $\operatorname{div} T(H) = -\operatorname{div} \Theta(i, G)$. Therefore

$$\int \mathbf{F}_n d\sigma = \int K_n d\sigma, \quad \int [\mathbf{r} \times \mathbf{F}_n] d\sigma = \int [\mathbf{r} \times K_n] d\sigma \quad (13-24)$$

The net resultant force acting on an arbitrary superconductor can be calculated equally well either from the Maxwell stresses in the outside space or from the London stresses in the interior. The two methods give

⁵Because according to eqs. 13-8 and 13-1, $T_{\alpha\beta}(H) = -H_{\alpha} H_{\beta} + \frac{1}{2} \delta_{\alpha\beta} H^2$.

⁶ \mathbf{r} is the vector whose components are the x_{α} .

the same results for the torque of the force only if the superconductor is of cubic crystal material. This always is true, although the separate forces \mathbf{F}_n and K_n may have the same value, namely, $\mathbf{F}_n = K_n = \frac{1}{2} H^2 \mathbf{n}$, only for thick superconductors (compare eqs. 13-12, 13-19, and 7-37) and where no current is entering or leaving the superconductor.

However, when in Chap. 17 we calculate the work performed by the magnetic field during an arbitrary displacement of the phase boundary between normal and superconducting material, we have to start from the forces K_n due to the London stresses, because they alone yield the actual force on every element of the surface.

(b) We still have to consider the term $\int (i_{32} - i_{23}) d\tau$ in eq. 13-17 as applied to the tensor $\Theta(i, G)$. In the first place this equation, the other terms of which represent torques, shows that $i_{32} - i_{23}$ is the x component of a polar vector. We therefore introduce the vector θ with the components

$$\theta_1 = \Theta_{23} - \Theta_{32}, \quad \theta_2 = \Theta_{31} - \Theta_{13}, \quad \theta_3 = \Theta_{12} - \Theta_{21} \quad (13-25)$$

which according to eq. 13-2 we can also write vectorially as

$$\theta = [G \times i] \quad (13-26)$$

Equation 13-23 obviously has to be supplemented to read

$$-\int [\mathbf{r} \times \operatorname{div} \Theta(i, G)] d\tau = -\int [\mathbf{r} \times K_n] d\sigma + \int \theta d\tau \quad (13-27)$$

We can apply this equation not only to the whole volume of the superconductor but also to any part of it, provided only we keep in mind that in this case the forces K_n are not effective, but are completely compensated by the London stresses from outside the region of integration. Equation 13-27 therefore states: The London stresses in a noncubic crystal superconductor produce a torque θ per unit volume. Because of the equality between action and reaction the material, in the stationary state, has to exert a torque $\theta' = -\theta$ on the superconduction mechanism. This result at first seems most surprising.

In classical mechanics there are already cases where a torque is necessary to maintain uniform motion. For example, a rigid body moving through liquid thrusts the latter to one side, in the absence of special symmetry conditions, and an impulse component perpendicular to the velocity \mathbf{v} is associated with the motion of the body. As this impulse is displaced along with the body, the angular momentum is changing by $[\mathbf{v} \times \mathbf{G}]$ per unit time, where \mathbf{G} represents the momentum of the body. If a torque of this direction and magnitude did not act on the body it would not be able to persist in its uniform motion. See Fig. 13-2.

Section (b) showed us that a momentum $\rho' G$ per unit volume is associated with the supercurrent. The concept of a velocity \mathbf{v} of the super-

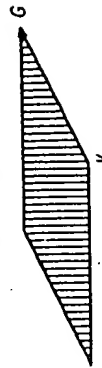


Fig. 13-2. The shaded area represents the vector product $[\mathbf{v} \times \mathbf{G}]$ i. e., the increase in angular momentum per unit time.

current is alien to the phenomenological theory. However, in so far as it has any meaning at all, it certainly has the value given by $\rho^s v = i^s$. Then the required torque per unit volume becomes

$$\theta' = [v \times \rho^s Q] = [i^s \times Q]$$

and this actually is equal to $-\theta$.

The combination of eqs. 13-27 and 13-10 gives for the whole superconductor

$$\int [r \times F_s] d\sigma = \int [r \times K_s] d\sigma + \int \theta' d\tau \quad (13-28)$$

instead of the second equation of 13-24.

The torque due to the Maxwell stresses in outside space, $\int [r \times F_s] \cdot d\sigma$ i. e., the moment of all the forces acting on the superconductor from outside, serves to increase the mechanical angular momentum of the superconductor and any other bodies rigidly connected with it by the amount $\int [r \times K_s] \cdot d\sigma$; according to this equation angular momentum is also imparted to the superconducting mechanism.

(b) The results of this chapter concerning ponderomotive forces and the torque due to the field are so important for the further development of the theory that we wish to confirm them in the next chapter by expressing them in terms of an electrodynamic potential, at least for the stationary case. We derive this potential itself by a plausible generalization of the usual potential of the Maxwell theory.

CHAPTER 14

The Electrodynamic Potential

(a) We shall prove the following theorem with the unimportant restriction that only one superconductor is situated in the field, and the more important restriction that no ohmic current is supplied: In any quasi-stationary change of the field, occurring as a consequence of displacements¹ of the conductors, the work ∂A performed by the field is equal to the decrease of electrodynamic potential $-\partial V$ defined by

$$V = \frac{SJ}{c} - \int_V \left\{ \frac{1}{2} \mu H^2 + (M \cdot H) + \frac{1}{2} (i^s \cdot Q) \right\} d\tau \quad (14-1)$$

As in Chap. 12, I is the current flowing in the superconductor when the latter is in the form of a ring, S is the time invariant period of the superconduction potential ψ ; if the superconductor is singly connected the

¹Compare Von Laue reference ϵ and f in footnote 2, Chapter 3.

14. THE ELECTRODYNAMIC POTENTIAL

first term is absent. The integration has to be extended over the whole of space (as indicated by the suffix V). In the term $(M \cdot H)$ the integration is taken only over the volume of the permanent magnets, in the term $\frac{1}{2} (i^s \cdot Q)$ only over the volume of the superconductor: these two volumes are mutually exclusive, and the observation that no ferromagnetics ever become superconducting is therefore significant for the following proof. Electric field vectors do not appear because of our assumption that at every instant the state is infinitesimally near to a stationary state.

Let the material displacement be ∂u , a continuous vector function of position. The proof of the above theorem is effected as soon as we can express the decrease in potential in the form

$$-\partial V = \int_V \left\{ (K \cdot \partial u) + \frac{1}{4} (\theta \cdot \text{curl } \partial u) \right\} d\tau \quad (14-2)$$

where K means the force per unit volume determined by the well-known electrodynamic laws, and θ is the torque given by eq. 13-26. In other words we must show that the right-hand side of this expression is the work ∂A done by the field. The boundary conditions are that all material constants, including λ_{θ} and μ do not change their values at any material point, furthermore that the ohmic current flows through any material surface with the same strength $\int i_{\perp}^0 d\sigma'$ before and after the displacement, and also that the permanent magnetism $\int M_s d\sigma'$ remains unchanged.² We shall therefore have

$$\partial \int i_{\perp}^0 d\sigma' = 0, \quad \partial \int M_s d\sigma' = 0 \quad (14-3)$$

We assume the condition of the constant ohmic current strength to be realized by arranging for suitable changes of the electromotive forces to compensate all changes of induction due to the displacements. We cannot introduce such a condition for the annular current in a superconductor. For this current it is the potential period S (Chap. 12) and not the current strength that remains unchanged, and for the current density here we have eq. 12-10,

$$cQ + A = \text{grad } \psi \quad (14-4)$$

(b) To formulate the assumptions under discussion mathematically we use at first some well-known equations. If $\delta\mu$ means the change of the parameter μ at a material point, $\partial\mu$, the change at a point fixed in space, the following relation holds:

$$\delta\mu = \partial\mu + (\partial u \cdot \text{grad } \mu)$$

As $\delta\mu$ shall be zero, we have to put

$$\partial\mu = -(\partial u \cdot \text{grad } \mu) \quad (14-5)$$

Furthermore, the change of flux of an arbitrary vector through a material surface integrates to

$$\delta \int K_s d\sigma' = \int \{ \partial K + \partial u \text{ div } K - \text{curl } [\partial u \times K] \} d\sigma'$$

² $d\sigma'$, in contrast to $d\sigma$, is a surface element participating in the displacement.

Therefore if we remember that here the stationary state means $\text{div } i^0 = 0$, the conditions 14-3 yield

$$\partial i^0 = \text{curl} [\partial u \times i^0] \quad (14-6)$$

$$\partial M = -(\text{div } M) \partial u + \text{curl} [\partial u \times M] \quad (14-7)$$

Although the above considerations are based on well-known theorems³ we shall have to leave the proof of the next equation to the Appendix, namely that under the condition that the $\lambda_{\alpha\beta}$ do not change at any material point, the changes $\partial \lambda_{\alpha\beta}$ at a fixed point in space satisfy the equation

$$\frac{1}{2} \sum_{\alpha\beta} i_{\alpha'} i_{\beta'} \partial \lambda_{\alpha\beta} = -\frac{1}{2} \sum_{\alpha\beta} i_{\alpha'} i_{\beta'} (\partial u \nabla \lambda_{\alpha\beta}) + \frac{1}{2} (\text{curl } \partial u \cdot [G \times i^0]) \quad (14-8)$$

It is obvious that throughout the superconductor

$$\text{and at its boundary} \quad \text{div } i^0 = 0 \quad (14-9)$$

We take into account only one surface of discontinuity, namely the surface of the superconductor, and assume all other transitions to be continuous. In particular the permanent magnetization M must go continuously to zero as we move from the interior of a permanent magnet; the actual conditions there can be taken care of afterwards by going to the limit.

(c) We proceed to the proof of eq. 14-2. According to eq. 14-1 we have

$$-\partial V = -\frac{S}{c} \partial I + \partial \int_V \left\{ \frac{1}{2} \mu H^2 + (M \cdot H) + \frac{1}{2} (i^0 \cdot G) \right\} d\tau$$

The right-hand side can be split into six terms of the following type:

$$-\partial V = \sum_{n=1}^6 \partial I_n - \frac{S}{c} \partial I$$

$$\partial I_1 = \int_V (B \cdot \partial H) d\tau$$

$$\partial I_2 = \int_P (H \cdot \partial M) d\tau$$

$$\partial I_3 = \frac{1}{2} \int_V H^2 \partial \mu d\tau$$

$$\partial I_4 = \int_S (G \cdot \partial i^0) d\tau \quad (14-11)^4$$

³See for example, Margenau and Murphy, *Mathematics of Physics and Chemistry*, D. Van Nostrand, New York Chapter IV.

⁴As before the suffixes s and P mean that the integration has to extend over the superconductor or the permanent magnets respectively.

$$\partial I_5 = \frac{1}{2} \int_S \sum_{\alpha\beta} i_{\alpha'} i_{\beta'} \partial \lambda_{\alpha\beta} d\tau$$

This is because

$$\frac{1}{2} \partial (i^0 \cdot G) = \frac{1}{2} \partial \left(\sum_{\alpha\beta} i_{\alpha'} i_{\beta'} \lambda_{\alpha\beta} \right) = \sum_{\alpha\beta} \lambda_{\alpha\beta} i_{\alpha'} i_{\beta'} \partial i_{\alpha'} + \frac{1}{2} \sum_{\alpha\beta} i_{\alpha'} i_{\beta'} \partial \lambda_{\alpha\beta}$$

and

$$\frac{1}{2} \int_V \partial (i^0 \cdot G) d\tau = \partial I_4 + \partial I_5$$

We now use eq. 12-1, the theorem 5-1, and the fundamental equation II to rewrite ∂I_1 in the form

$$\partial I_1 = \int_V (\text{curl } A \cdot \partial H) d\tau = \int_V (\text{curl } \partial H \cdot A) d\tau = \frac{1}{c} \int_V [(A \cdot \partial i^0) + (A \cdot \partial i^0)] d\tau$$

Consequently by eq. 14-4,

$$\partial I_1 + \partial I_4 = \frac{1}{c} \left[\int_V (A \cdot \partial i^0) d\tau + \int_S (\text{grad } \Psi \cdot \partial i^0) d\tau \right]$$

However, partial integration over the superconductor yields

$$\frac{1}{c} \int_S (\text{grad } \Psi \cdot \partial i^0) d\tau = -\frac{1}{c} \int_S \Psi \text{div } \partial i^0 d\tau - \frac{1}{c} \int_S \Psi \partial i_{n'} \cdot d\sigma$$

The first term vanishes because of eq. 14-9, and the surface makes no contribution because of eq. 14-10. But with a doubly connected body, a cut Q makes a contribution to the surface integral (compare eq. 12-17):

$$-\frac{1}{c} \int_Q \Psi \partial i_{n'} \cdot d\sigma = \frac{1}{c} (\Psi_2 - \Psi_1) \partial I = \frac{S}{c} \partial I$$

The sign is determined by the convention of Chap. 12 that a positive current flows through the cut in the direction $2 \rightarrow 1$. On the other hand, according to eqs. 14-6 and 12-1:

$$\frac{1}{c} \int_V (A \cdot \partial i^0) d\tau = \frac{1}{c} \int_V (A \cdot \text{curl} [\partial u \times i^0]) d\tau$$

$$= \frac{1}{c} \int_V (B \cdot [\partial u \times i^0]) d\tau = \frac{1}{c} \int_V (\partial u \cdot [i^0 \times B]) d\tau$$

Consequently we have

$$\partial I_1 + \partial I_4 = \frac{S}{c} \partial I + \int_V (\partial u \cdot [i^0 \times B]) d\tau \quad (14-12)$$

Again, using eqs. 13-26 and 14-8 we can rewrite

$$\partial I_3 = \frac{1}{2} \iint_V \left[- \sum_{\alpha\beta} \mathbf{t}_\alpha \cdot \mathbf{l}_\beta \nabla \lambda_{\alpha\beta} + (\theta \cdot \text{curl } \partial \mathbf{u}) \right] d\tau \quad (14-13)$$

Furthermore, by eq. 14-7, the theorem 5-1, and the fundamental equation III (remembering that the supercurrent \mathbf{v} is absent from the interior of the permanent magnets) we get

$$\begin{aligned} \partial I_3 &= \int_V \left\{ \mathbf{H} \cdot (\text{curl } [\partial \mathbf{u} \times \mathbf{M}] - \partial \mathbf{u} \text{ div } \mathbf{M}) \right\} d\tau \\ &= \int_V \left\{ \frac{1}{c} ((\partial \mathbf{u} \times \mathbf{M}) \cdot \mathbf{v}) - (\partial \mathbf{u} \cdot \mathbf{H} \text{ div } \mathbf{M}) \right\} d\tau \\ &= \int_V \left\{ -\frac{1}{c} (\partial \mathbf{u} \cdot [\mathbf{v} \times \mathbf{M}]) - (\partial \mathbf{u} \cdot \mathbf{H} \text{ div } \mathbf{M}) \right\} d\tau \end{aligned} \quad (14-14)$$

finally it follows from eq. 14-5 that

$$\partial I_3 = -\frac{1}{2} \int_V \mathbf{H}^2 (\partial \mathbf{u} \cdot \text{grad } \mu) d\tau \quad (14-15)$$

By adding together eqs. 14-12 to 14-15 and using eq. 14-11 we obtain

$$-\partial V = \int_V \left\{ (\mathbf{K} \cdot \partial \mathbf{u}) + \frac{1}{2} (\theta \cdot \text{curl } \partial \mathbf{u}) \right\} d\tau \quad (14-16)$$

with the value of the vector \mathbf{K} given by

$$\mathbf{K} = \frac{1}{c} [\mathbf{v} \times \mu \mathbf{H}] - \mathbf{H} \text{ div } \mathbf{M} - \frac{1}{2} \mathbf{H}^2 \text{ grad } \mu - \frac{1}{2} \sum_{\alpha\beta} \mathbf{t}_\alpha \cdot \mathbf{l}_\beta \nabla \lambda_{\alpha\beta} \quad (14-17)$$

This is the most general expression for the force exerted by a stationary magnetic field on a unit volume of matter. The first term represents the effect of the field on ohmic current, the second term is the effect on the density of permanent magnetic charges as measured by $-\text{div } \mathbf{M}$, the third is the equally familiar force on regions of magnetic inhomogeneity, the fourth is the force on an inhomogeneous superconductor appearing in 13-10. Equations 14-16 and 14-17 contain therefore the proof of the earlier statement that $\mathbf{K} = 0$ for the homogeneous superconductor, for then, by eq. 13-10 $\mathbf{K} = 0$.

(d) The theorem $\partial A = -\partial V$ comes from the Maxwell theory, and our definition 14-1 is simply a plausible extension of the definition of that theory. That we have arrived at exactly the same conclusions about the force \mathbf{K} and the torque θ by a line of reasoning that avoids the stress concept used in Chap. 13 on the argument about the London stresses seems to us to be a valuable confirmation of the essential truth of that theory. In addition, the observation that ferromagnetics are unable to show super-

conductivity appears in a new light. Otherwise we would have found in eq. 14-14 another term

$$-\frac{1}{c} (\partial \mathbf{u} \cdot [\mathbf{v} \times \mathbf{M}])$$

also entering the expression for the force \mathbf{K} , and this would have been in conflict with the fact that the existence of persistent currents demands that \mathbf{K} be zero in a homogeneous superconductor. It seems as though permanent magnetism and superconductivity are mutually exclusive not only in the temperature ranges that happen to have been observed to date, but also fundamentally so.

(e) According to eq. 12-21 the total (available) energy of the field is

$$U = \frac{1}{2} \int_V \{ \mu \mathbf{H}^2 + (\mathbf{v} \cdot \mathbf{G}) \} d\tau = \frac{1}{2c} \left\{ S I + \int_V (\mathbf{A} \cdot \mathbf{v}) d\tau \right\} - \frac{1}{2} \int_V (\mathbf{H} \cdot \mathbf{M}) d\tau \quad (14-18)$$

and so according to eq. 14-1,

$$V = \frac{1}{2c} \left[S I - \int_V (\mathbf{A} \cdot \mathbf{v}) d\tau \right] - \frac{1}{2} \int_V (\mathbf{H} \cdot \mathbf{M}) d\tau \quad (14-19)$$

If the field is produced only by an annular current I and permanent magnets, then $V = U$ and the work $\partial A = -\partial U$. Conversely if the field is produced by ohmic currents, $V = -U$ and $\partial A = \partial U$. The amount of work $2 \partial A$ has then to be performed by the electromotive forces keeping the currents constant. This second point differs from the corresponding theorem of the Maxwell theory in that here superconductors (but with no annular currents) are permitted to be in the field.

Eliminating the term $S I/c$ from eq. 14-1 by means of eq. 12-19 we get a new expression for V of which we shall make immediate use, namely,

$$V = \frac{1}{c} \int_V (\mathbf{A} \cdot \mathbf{v}) d\tau + \frac{1}{2} \int_V (\mathbf{v} \cdot \mathbf{G}) d\tau - \int_V \left[\frac{1}{2} \mu \mathbf{H}^2 + (\mathbf{M} \cdot \mathbf{H}) \right] d\tau \quad (14-20)$$

(f) With the help of the potential V we shall now confirm the theorem of Chap. 13 (c) that the surface of the superconductor experiences an inward pull $\frac{1}{2} (\mathbf{v} \cdot \mathbf{G})$ at all points where there is no current entering or leaving. For this purpose we ignore all displacements of matter, but displace the boundary between a superconducting and a chemically identical normal conducting phase in such a way that every surface element $d\sigma$ suffers a displacement $\partial \mathbf{u}$ normal to $d\sigma$. We take $\partial \mathbf{u}$ to be positive if $d\sigma$ moves toward the interior of the superconductor. If before the displacement the superconducting phase occupied the region s , afterwards it occupies the smaller region s' . A finite change therefore takes place in the layer $s \rightarrow s'$; supercurrent and supermomentum suddenly drop to zero. But as this layer is infinitely thin, the effects of this change at all other points in space is infinitesimal. In general μ and $\lambda_{\alpha\beta}$ do not change at all, and the same is true of the current density \mathbf{v} , as we shall again keep the ohmic currents constant.

Starting from eq. 14-20 we split the change $-\partial V$ into five parts:

$$\begin{aligned}
 -\partial V &= \sum_{k=1}^5 \partial I_k \\
 \partial I_1 &= -\frac{1}{c} \int_V \partial(A \cdot v) d\tau \\
 \partial I_2 &= -\int_V (G \cdot \partial v) d\tau \\
 \partial I_3 &= \int_V (B \cdot \partial H) d\tau \\
 \partial I_4 &= \int_{s-s'} (A \cdot v) d\tau \\
 \partial I_5 &= \frac{1}{2} \int_{s-s'} (v \cdot G) d\tau
 \end{aligned} \quad (14-21)$$

The transformation proceeds as follows.

First, by eq. 14-4 we have

$$\partial I_1 + \partial I_3 = -\frac{1}{c} \int_V [(\text{grad } \Psi \cdot \partial v + (v \cdot \partial A))] d\tau$$

Then in spite of the infinitesimal ∂H in the layer $s-s'$ by which the superconductor is reduced, $\text{curl } \partial H = -v/c$ is finite, but $\partial v = 0$ everywhere; remembering this and using eq. 12-1 and the theorem 5-1 it follows that

$$\partial I_3 = \frac{1}{c} \int_V \left[\int_{s-s'} (A \cdot \partial v) d\tau - \int_{s-s'} (A \cdot v) d\tau \right]$$

Adding up ∂I_1 to ∂I_3 the contributions of the layer $s-s'$ cancel. Again recalling eq. 14-4 there remains

$$\begin{aligned}
 \sum_{k=1}^5 \partial I_k &= \frac{1}{c} \int_V [(\{A - \text{grad } \Psi\} \cdot \partial v) - (v \cdot \partial A)] d\tau \\
 &= -\int_V \left\{ (G \cdot \partial v) + \frac{1}{c} (v \cdot \partial A) \right\} d\tau
 \end{aligned}$$

Now because of the symmetry of the tensor $\lambda_{\alpha\beta}$, which enters once more as an important condition, we have

$$(G \cdot \partial v) = \sum_{\alpha\beta} \lambda_{\alpha\beta} G_\alpha \partial v_\beta = \sum_{\alpha\beta} \lambda_{\alpha\beta} \partial v_\alpha v_\beta = (v \cdot \partial G)$$

and so from eqs. 14-4 and 14-9 and the constancy of $S = \Psi_2 - \Psi_1$ we have

$$\begin{aligned}
 \sum_{k=1}^5 \partial I_k &= -\int_V \left\{ v \cdot \partial \left[G + \frac{A}{c} \right] \right\} d\tau = -\frac{1}{c} \int_V (v \cdot \text{grad } \partial \Psi) d\tau \\
 &= \frac{1}{c} \int_V \Psi' \text{div } v d\tau - \int_V \partial(\Psi_2 - \Psi_1) = 0
 \end{aligned} \quad (14-22)$$

There remains only the term ∂I_5 in eq. 14-21 to be considered. In the layer $s-s'$ however, putting the volume element $d\tau = d\sigma' \cdot du$ we get by surface integration

$$\partial A = -\partial V = \frac{1}{2} \int_V (v \cdot G) \partial u \cdot d\sigma' \quad (14-23)$$

From this we deduce that $\frac{1}{2} (v \cdot G)$ is in fact the pull acting over the element $d\sigma'$ toward the interior of the superconductor.

(g) From the section (f) we can also make the following deduction. Given the relative positions of all bodies, the ohmic currents in them, the permanent magnetism, and the potential "period" S of all possible annular currents which may eventually appear, the stationary field adjusts itself to minimize the electrodynamic potential.

If we disregard the displacements ∂u , the integrals ∂I_4 and ∂I_5 in eq. 14-21 vanish for every virtual displacement of the field. Then eq. 14-22 gives

$$-\partial V = \sum_{k=1}^3 I_k = 0$$

If there is no ohmic current contributing to the field, then $V = U$ according to section (e). The field adjusts itself to minimize the free energy. Also a persistent current by itself corresponds to a minimum of the free energy, of course with the boundary condition that the potential "period" S be given. Without such a condition the law of the minimum free energy cannot be proved.

CHAPTER 15

Electric Waves in Superconductors with Cubic Crystal Structure

(a) According to the fundamental equation IX changes in time always produce an electric intensity E in a superconductor; this in turn produces an ohmic current density j^0 in addition to the supercurrent, and also Joule heat according to the energy equation 5-5. This is the fundamental difference from static fields. To describe periodic waves, in what follows we always use complex expressions for the field strengths and all quantities linearly related to them. The waves will be designated by their angular frequency ω , the numerical frequency ν being $\omega/2\pi$. All the complex expressions are taken proportional to $e^{i\omega t}$.

It follows from VII a and IX for cubic crystal superconductors that

$$j^0 = \sigma E = \omega \sigma \lambda v e^{i\omega t/2} \quad (15-1)$$

The supercurrent i_s is therefore lagging in phase by a quarter period behind the ohmic current and the field strength E . For the ratio of the amplitudes of the two waves we have

$$\frac{|i_0|}{|i_s|} = \omega \sigma \lambda \quad (15-2)$$

The greater ω the greater the influence of i_0 compared with i_s . The pure number $\omega \sigma \lambda$ which we encounter here for the first time, will play a fundamental role in the ensuing calculations. The total current density is connected with the field strength by the relation

$$i = i_0 + i_s = E \frac{\omega \sigma \lambda - i}{\omega \lambda} \\ = E \frac{1 + i \omega \sigma \lambda}{i \omega \lambda} \quad (15-3)$$

(b) Because of the inevitable production of Joule heat a progressive wave in a superconductor is damped just as in a normal conductor. For a plane polarized wave progressing in the z direction we write

$$E_x = E_0 \exp i \omega \left\{ t - \frac{(n - i\kappa)z}{c} \right\}, \quad E_y = E_z = 0 \quad (15-4)$$

This satisfies the condition $\text{div } E = 0$. According to the fundamental relation I it follows from this that

$$H_x = 0, \quad H_y = (n - i\kappa) E \exp i \omega \left\{ t - \frac{(n - i\kappa)z}{c} \right\}, \quad H_z = 0 \quad (15-5)$$

Consequently for waves in a superconductor the electric field strength, magnetic field strength, and direction of propagation are perpendicular to each other and form in this order a right-handed system, as is otherwise known to be the case. However, unlike the behavior of waves in a non-conductor, E and H do not oscillate in phase, E in general lagging in phase behind H . The amplitude decreases with increasing z by the factor $e^{-\omega \kappa z/c}$, the energy density by $e^{-2\omega \kappa z/c}$. κ is called the extinction coefficient, the refractive index. Both are pure numbers and functions of ω .

Inserting the value of E from eq. 15-4 in the telegrapher's equation $W(E) = 0$ (compare Chap. 6: it is equally possible to insert the value of H from eq. 15-5 in $W(H) = 0$), because

$$W(E) = \Delta E - \frac{1}{c^2} \frac{\partial^2 E}{\partial t^2} - \frac{\sigma}{c^2} \frac{\partial E}{\partial t} - \frac{E}{\lambda^2 c^2} \\ (n - i\kappa)^2 = (\omega^2 \lambda^2 - 1 - i \omega \sigma \lambda) \omega^2 \lambda \quad (15-6)$$

one obtains the relation

The two real numbers n and κ are determined by

$$n^2 = \frac{1}{2} \left[(\omega^2 \lambda^2 - 1) + \sqrt{(\omega^2 \lambda^2 - 1)^2 + (\omega \sigma \lambda)^2} \right] \\ \kappa^2 = \frac{1}{2} \left[-(\omega^2 \lambda^2 - 1) + \sqrt{(\omega^2 \lambda^2 - 1)^2 + (\omega \sigma \lambda)^2} \right] \quad (15-7)$$

If $\omega^2 \lambda^2 < 1$, then $n < \kappa$ and the wavelength $2\pi c/\omega n$ is greater than the logarithmic damping factor, i. e., the distance in which the amplitude decreases by a factor $e^{-2\kappa}$ or 0.2%. No wave can actually develop at all under such circumstances. The field is quasistatic and its distribution in space is similar to a static one. If indeed $\omega^2 \lambda^2$ and $\omega \sigma \lambda$ are small numbers, the following approximations hold:

$$n = \frac{1}{2} \omega \sigma \lambda^2, \quad \kappa = \frac{1}{\omega \lambda^2} \gg n \quad (15-8)$$

This can be seen in the simplest way by forming $n^2 - \kappa^2$ and $2n\kappa$ from eq. 15-8, and comparing with eq. 15-6. Since in this case $\omega \kappa/c = \beta$, the amplitude decreases by the factor $e^{-\beta z}$ just as in the static case.

On the other hand if $\omega^2 \lambda^2 > 1$, then $n > \kappa$ according to eq. 15-7, and the wavelength is therefore smaller than the logarithmic damping factor, so a whole series of waves is produced with only gradually decreasing amplitude. If indeed $\omega^2 \lambda^2 \gg 1$, then the unity in the numerator of eq. 15-6 is negligible and we obtain the approximate values

$$n = 1 + \frac{(\sigma/\omega)^2}{8}, \quad \kappa = \frac{\sigma}{2\omega} \quad (15-9)$$

which no longer depend on the superconductivity constant λ .

But such a condition can only be realized immediately below the transition temperature where λ is comparatively large. As soon as λ attains values of the order 10^{-81} sec² at somewhat lower temperatures, this condition is hardly possible any longer because, just as with the Maxwell theory, our theory cannot be regarded as valid for arbitrarily high frequencies. Let us consider the situation with mercury for which direct determinations of β , and therefore also of λ , are available (see Chap. 1 and 12). Its conductivity σ at room temperatures is about 10^{17} sec⁻¹ in Lorentz units (4π times its value in esu); it is about 500 times greater just above the transition temperature: 10^{19} sec⁻¹. Therefore for $\omega = 10^{10}$ per sec, $\omega^2 \lambda^2 = 10^{-11}$, and $\omega \sigma \lambda^2 = 10^{-2}$ (short Hertzian waves, high radio frequency), and for $\omega = 10^{14}$ per sec, $\omega^2 \lambda^2 = 10^{-3}$ and $\omega \sigma \lambda^2 = 10^2$ (infrared waves).

In the first case the ohmic current is about one hundred times smaller than the supercurrent; in the second case about one hundred times greater, according to eq. 15-2. In the first case the unity is the dominating term in the numerator of eq. 15-6; in the second case the number $i \omega \sigma \lambda$, so that, just as for a normal conductor,

$$n - i\kappa = (1 - i) \sqrt{\frac{\sigma}{2\omega}} \quad (15-10)$$

This indicates a complete identity between normal and superconductors for all optical processes. If only the supercurrent were to exist in the superconductor, then the superconductor would be transparent. The fact that there is no visible difference between the normal and the superconductor [Chap. 1 (d)] is a decisive proof of the existence of the ohmic current.

For $\omega = 10^{14}$ per sec and $\sigma = 10^{19}$ per sec, eq. 15-10 gives n and κ the order of magnitude between 10^8 and 10^9 .

(c) If $\omega = 10^{10}$ per sec then according to the above figures the conditions for the validity of eq. 15-8 are satisfied. The refractive index n then has the order of magnitude 10^8 and the extinction coefficient 10^8 for radio frequency waves. The reflectivity of a specimen for a wave incident perpendicularly from empty space can be calculated from the well-known optical expression

$$\frac{(n-1)^2 + \kappa^2}{(n+1)^2 + \kappa^2} = 1 - \frac{4n}{n+1} = 1 - 2\omega^2 \sigma \lambda'^4 \quad (15-11)$$

Under the present conditions this expression can be simplified to read

$$\frac{1 + \left(\frac{n-1}{\kappa}\right)^2}{1 + \left(\frac{n+1}{\kappa}\right)^2} = 1 - 2\omega^2 \sigma \lambda'^4 \quad (15-11)$$

Consequently that fraction of the energy given by the second term is absorbed in the superconductor and amounts, according to the figures used above, to about 10^{-6} .

CHAPTER 16

The High-Frequency Resistance of Superconductors

(a) A direct current is distributed uniformly over the cross section of a normally conducting cylinder. Alternating current, however, is confined to a thin layer at the surface which becomes thinner with increasing frequency. The induction from the magnetic field of the alternating current itself protects the interior from the current. This is the "skin effect" that exists in conductors of any form. In the superconductor a tendency to the same effect already exists even with the direct current because of the coupling between the supercurrent and the magnetic field expressed by eq. X. For high frequency alternating current this Meissner effect and the skin effect reinforce each other. The penetration depth of the field of such an alternating current is then smaller than for direct current in the super-

¹ See the discussion of eq. 16-18 for the meaning of the number $\omega^2 \sigma \lambda'^4$.

16. HIGH-FREQUENCY RESISTANCE

conductor and smaller than for alternating current of the same frequency in a normal conductor. The skin effect eventually causes a very substantial decrease in the cross section that actually carries the current in a normal conductor and thus may cause a considerable increase of the resistance. A changing field, according to Chaps. 7 and 15, produces an average resistance in a superconductor. This resistance increases with increasing frequency not only because of the decrease of the conducting cross section, but also because of the increasing transfer of current from the supercurrent to the ohmic current in accordance with eq. 15-2. We shall describe this increase quantitatively for the cubic crystal material.

(b) First we have to determine the current density as a function of position. The telegrapher's equation of Chap. 6 for the total current density reads:

$$W(i) \equiv \Delta i - \frac{1}{c^2} \frac{\partial^2 i}{\partial t^2} - \frac{\sigma}{c^2} \frac{\partial i}{\partial t} - \frac{1}{\lambda^2} i = 0$$

For periodic processes this becomes

$$\Delta i - i(\omega^2 + i\omega\sigma + \lambda^{-2}) = 0$$

As we are confining ourselves to frequencies less than 10^{10} per sec, the first term in the brackets is small compared with the second term when $\sigma = 10^{19}$ per sec (see Chap. 15). We therefore neglect this term and write

$$\Delta i - k^2 i = 0$$

for superconductors where

$$k = \frac{(1 + i\omega\sigma\lambda)^{1/2}}{c/\lambda} \quad (16-1)$$

As the neglected term arises from the term $\partial E/\partial t$ in the fundamental equation II, it means we are neglecting the displacement current as compared with the conduction current. We complete the definition of k by choosing both its roots to be positive, i. e., both the real and the imaginary part of k shall be positive.

Going to the limit $\lambda \rightarrow \infty$ leads to the normal conductor, because in this limit the last term of $W(i)$ vanishes and instead of eq. 16-1 we have the differential equation

$$\Delta i - k_n^2 i = 0, \quad k_n = \frac{\sqrt{i\omega\sigma}}{c} \quad (\text{normal conductor}) \quad (16-2)$$

In both cases the boundary conditions are: $\text{div } i = 0$, i is finite and continuous throughout the interior; and, because we are discussing quasi-stationary currents, $i_n = 0$ at all surfaces; and finally integration of i

¹ The following relation exists between k and the refractive index and extinction coefficient:

$$k = i\omega \frac{(n - i\kappa)}{c}$$

over any cross section yields the total current strength $I e^{i\omega t}$. We treat I as a real quantity.

We obtain the magnetic field from the current density by the fundamental equation II, which, neglecting the displacement current, reads:

$$\text{curl } \mathbf{H} = \frac{1}{c} \quad (16-3)$$

In the external space we have the additional requirement that \mathbf{H} is the negative gradient of a potential obeying the equation $\Delta \varphi = 0$. Besides requiring that \mathbf{H} be divergence free, the boundary conditions require also that \mathbf{H} be finite and continuous at the surface of the conductor, and vanish sufficiently rapidly at infinity. The calculations are carried out in the same way for both the superconductor and the normal conductor except that in the first case one has to use the \mathbf{k} of eq. 16-1 and in the other the \mathbf{k}_n of eq. 16-2.

We can also derive the electric field from the current density. For the normal conductor we use the fundamental equation VII a,

$$\mathbf{E} = \frac{1}{\sigma} \quad (\text{normal conductor})$$

while for the superconductor we use eq. 15-3,

$$\mathbf{E} = \frac{i\omega\lambda}{(1 + i\omega\sigma\lambda)} \quad (\text{superconductor})$$

We can therefore derive the field strength for the superconductor from that of the normal conductor by multiplying the latter by the factor

$$\frac{i\omega\sigma\lambda}{(1 + i\omega\sigma\lambda)} \quad (16-4)$$

The last step consists of determining the Poynting energy current vector $c[\mathbf{E} \times \mathbf{H}]$. The divergence of the time average of this vector gives the Joule heat per unit volume and unit time, and the integral $c \int [\mathbf{E} \times \mathbf{H}] \cdot d\sigma$ is therefore the Joule heat developed in the enclosed volume per unit time. From the complex solutions for \mathbf{E} and \mathbf{H} obtained in the manner just described, we calculate the time average of the Joule heat as the real part of $\frac{1}{2} c [\mathbf{E} \times \mathbf{H}^*]$,³ where \mathbf{H}^* is the complex conjugate to \mathbf{H} .

³If one has the complex representations for two field quantities A and B :

$$A = A_0 e^{i\omega t} = |A_0| e^{i(\omega t - \varphi)}, \quad B = B_0 e^{i\omega t} = |B_0| e^{i(\omega t - \psi)}$$

they each represent two real quantities, one pair of which is

$$A = |A_0| \cos(\omega t - \varphi), \quad B = |B_0| \cos(\omega t - \psi)$$

The time average of the product of the two quantities is then

$$\frac{1}{2} |A_0| |B_0| \cos(\varphi - \psi)$$

This result can be obtained most simply from the complex representation as

$$\frac{1}{2} \text{Real Part of } (A B^*)$$

16. HIGH-FREQUENCY RESISTANCE

97

Having calculated $\frac{1}{2} c [\mathbf{E} \times \mathbf{H}^*]$ for the normal conductor, we obtain its value for the superconductor by substituting \mathbf{k} for \mathbf{k}_n and multiplying by the factor 16-4. From the real part of this we derive the Joule heat Q and the resistance

$$R = \frac{Q}{I^2} \quad (16-5)$$

As the factor 16-4 becomes unity, and $\mathbf{k} \rightarrow \mathbf{k}_n$ when λ approaches infinity, the resistance of the superconductor goes over continuously into that of the normal conductor at the transition temperature provided that the conductivity σ is not discontinuous there.

The simplest solutions of the differential equations 16-1 and 16-2, corresponding to the plane waves already discussed in Chap. 15, are

$$\mathbf{H} = \mathbf{H}_0 e^{-kz} \quad \text{or} \quad \mathbf{H} = \mathbf{H}_0 e^{-k_n z}$$

Evidently the real part of \mathbf{k} , or of \mathbf{k}_n , respectively, determines the decrease of amplitude with increasing z . Separating the real and imaginary parts of \mathbf{k} and \mathbf{k}_n ,

$$k = \frac{1}{c\sqrt{2\lambda}} \{ [1 + \sqrt{1 + (\omega\sigma\lambda)^2}]^{1/2} + i [-1 + \sqrt{1 + (\omega\sigma\lambda)^2}]^{1/2} \} \quad (16-6)$$

$$k_n = \sqrt{\frac{1}{2} \omega \sigma \frac{(1+i)}{c}} \quad (16-7)$$

The real part of \mathbf{k} is thus greater than that of \mathbf{k}_n , or waves in the superconductor decay more rapidly toward the interior than they do in the normal conductor, other things being equal, as already observed in section (a).

(c) Using the method described above we calculate the a-c resistance of a circular cylinder of radius R carrying a current $I e^{i\omega t}$, first for a normal conductor. We use the same cylindrical coordinates as in Chap. 8. As the differential equation 16-2 differs from $\Delta u - \beta^2 u = 0$ only in the notation used for the constants, we can take over eq. 8-9 for the current by replacing β by k_n and I by $I e^{i\omega t}$

$$I_r = 0, \quad I_\theta = 0, \quad I_z = \frac{i k_n I e^{i\omega t}}{2\pi R} \frac{I_0(i k_n r)}{I_1(i k_n R)} \quad (16-8)$$

Taking over eq. 8-11 in the same way satisfies eq. 16-3:

$$H_r = 0, \quad H_\theta = \frac{I}{2\pi c R} \frac{I_1(i k_n r)}{I_1(i k_n R)}, \quad H_z = 0 \quad (16-9)$$

For thin cylinders ($k_n R \ll 1$) to a first approximation $I_0(x) = 1$ and $I_1(x) = \frac{1}{2} x$; compare the series 8-6. We therefore conclude, as in Chap. 8, that the current is uniformly distributed over the cross section in this case. For thick cylinders ($k_n R \gg 1$) we have approximately:

$$I_0(i k_n r) = (2\pi i k_n r)^{-1/2} \left(1 + \frac{1}{8 k_n r} \right) \exp \left(k_n r + \frac{1}{4} \pi i \right) \\ I_1(i k_n r) = (2\pi i k_n r)^{-1/2} \left(1 - \frac{3}{8 k_n r} \right) \exp \left(k_n r + \frac{3}{4} \pi i \right) \quad (16-10)^3$$

³It is essential here that the real part of k_n be positive.

It follows that I and H decay exponentially with decreasing r . There is a protective layer of thickness $(\text{Re } k_n)^{-1}$ in this case and the skin effect is pronounced.

The Poynting energy flow vector has only one component, an r component with magnitude $c E_r H_\theta = - (c/\sigma) I_r H_\theta$. The mean rate at which energy enters unit length of the cylinder is therefore

$$Q = 2\pi R \frac{c}{2\sigma} \text{Re}(I_r H_\theta^*)_{r=R} \quad (16-11)$$

Let Z be defined in such a way that

$$Q = I^2 \text{Re}(Z) \quad (16-12)$$

so that by eq. 16-5 the resistance per unit length is

$$W = \text{Re}(Z) \quad (16-13)$$

However, from eqs. 16-8 and 16-9

$$Z = \frac{1}{\sigma \pi R^2} \left(\frac{1}{2} k_n R \right) \frac{J_0(k_n R)}{J_1(k_n R)} \quad (\text{normal conductor}) \quad (16-14)$$

The first fraction is the d-c resistance of the normal conductor. For thin cylinders the other fractions reduce to unity according to eq. 8-6.

This well-known result for the a-c resistance of the normal conductor holds for the superconductor if we write k instead of k_n and multiply with the factor 16-4. The resistance then becomes the real part of

$$Z = \frac{1}{\sigma \pi R^2} \left[\frac{i\omega\sigma\lambda}{(1+i\omega\sigma\lambda)} \right] \left(\frac{1}{2} k R \right) \frac{J_0(k R)}{J_1(k R)} \quad (\text{superconductor}) \quad (16-15)$$

(d) We limit the discussion of this equation to the case of a thick cylinder, $(|k| R \gg 1)$. From eq. 16-10 it follows for this case that

$$\frac{J_0(k R)}{J_1(k R)} = -i \left(1 + \frac{1}{2kR} \right) \quad (16-16)$$

Noticing eq. 16-1 we see that this reduces eq. 16-14 to

$$Z = \frac{1}{2\pi c R} \left(\frac{i\omega}{\sqrt{1+i\omega\sigma\lambda}} \right) \left[1 + \frac{1}{2} c \sqrt{\lambda} \frac{(1+i\omega\sigma\lambda)^{-1/2}}{R} \right] \quad (16-17)$$

Assume at first that $\omega\sigma\lambda \ll 1$, which is surely justified when $\omega \lesssim 10^{10}$ per sec and $\lambda = 10^{-31}$ sec² (see Chap. 15). Developing the denominator of eq. 16-16 in series we then find

$$Z = \frac{\omega^2\sigma\lambda^{1/2}}{4\pi c R} + \frac{\omega^3\sigma\lambda^2}{4\pi R^2} + i \left(\frac{\omega\lambda^{1/2}}{2\pi c R} + \frac{\omega\lambda}{4\pi R^2} \right) \quad (16-18)$$

Consider the real part of eq. 16-17, the resistance W . Its value is

$$W = \frac{\omega^2\sigma\lambda^{1/2}}{4\pi c R} = \frac{(\omega\sigma\lambda)^{1/2}}{4\pi\sigma c R \sqrt{\lambda}} \quad (16-19)$$

except for an additional term only $c/\sqrt{\lambda} \div R$ compared with the first term $(c/\sqrt{\lambda})$ is the penetration depth).

The resistance turns out to be proportional to $(\omega\sigma\lambda)^{1/2}$ because the number $\omega\sigma\lambda$ is a measure of the extent to which the ohmic current participates in the transport of electricity, whereas the Joule heat is proportional to the square of I . In the denominator of eq. 16-18 there is the product of the cylinder's circumference, $2\pi R$, and the penetration depth $c/\sqrt{\lambda}$, and this is an approximate measure of the area that carries the current. Multiplying this is the conductivity σ , because it is this product of cross-sectional area and conductivity that matters. We may take $c/\sqrt{\lambda}$ rather than the reciprocal of the real part of k to be the penetration depth because the supercurrent far outweighs the ohmic current in the present approximation.

Equation 16-18 can be used for all temperatures that are at least some tenths of a degree below the transition temperature, for λ then has the assumed order of magnitude, 10^{-31} sec². With increasing temperature λ increases and so does the resistance. However, some tenths of a degree below the transition temperature, λ becomes so great that the equation fails.

To discuss the temperature dependency of the resistance in general we introduce the auxiliary quantity θ defined by

$$\omega\sigma\lambda = \tan \theta \quad 0 < \theta \leq \frac{1}{2}\pi \quad (16-19)$$

Neglecting the small second term inside the bracket in eq. 16-16 we get the transformation

$$2\pi c R Z = i\omega \sqrt{\lambda} \cos \theta e^{-1/2} i\theta$$

The real part of this is therefore

$$2\pi c R W = \sqrt{\frac{\omega}{\sigma}} \sqrt{\omega\sigma\lambda} \cos \theta \sin \frac{1}{2}\theta = \sqrt{\frac{\omega}{\sigma}} \sqrt{\sin \theta} \sin \frac{1}{2}\theta$$

At the transition temperature $\lambda = \infty$ and therefore $\theta = \frac{1}{2}\pi$. As the conductivity has perhaps a different value σ_c at the transition temperature than at lower temperatures, we have to put

$$2\pi c R W_c = \sqrt{\frac{\omega}{2\sigma_c}} \quad (16-20)$$

Dividing eq. 16-20 into the previous equation yields

$$\sqrt{\frac{\sigma}{\sigma_c}} \frac{W}{W_c} = \sqrt{2} \sin \theta \sin \frac{1}{2}\theta \quad (16-21)$$

From the way it was derived, eq. 16-20 evidently gives the resistance of a normal conductor having conductivity σ_c , assuming a pronounced skin effect; $\text{Re}(k_n R) \gg 1$. This is easily confirmed from eqs. 16-3 and 16-15. Therefore eq. 16-21 again shows that there is a continuous transition from the high-frequency resistance of the normal conductor to that of the superconductor.

(e) All quantities depending on the geometry of the superconductor have disappeared from eq. 16-21, and in fact this equation holds for other forms than the straight circular cylinder.

To see this let us consider a normal conductor having some elongated form to the ends of which the current leads are attached, at a distance L apart. It could, for example, be a wire wound in the form of a coil. Its d-c resistance would be $L/\sigma A$, where A is the mean cross section. However for alternating current with pronounced skin effect, the current does not fill the whole cross section, but only a thin superficial layer the thickness of which is given by $(\text{Re } k_n)^{-1}$. Let the cross section of this surface layer have a mean linear dimension S normal to its thickness. Then the resistance becomes $W = L(\text{Re } k_n)/\sigma S$.

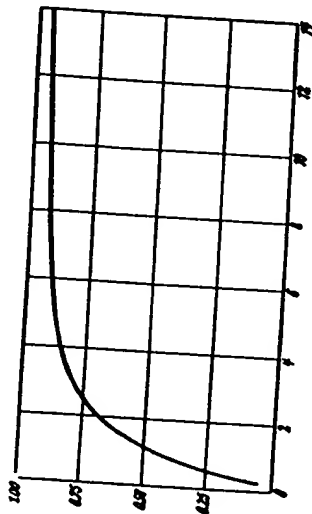


Fig. 16-1. Curve of $1/2 \sin \theta \sin \frac{1}{2} \theta$ against $\tan \theta$.

As the example of the cylinder shows, the calculation leads initially to a complex quantity Z the real part of which is the resistance W . The equation for Z can be nothing else than $Z = L k_n / \sigma S$ because the real and imaginary parts of k_n do not appear explicitly. In fact the eq. 16-13 does have this form if we remember that it refers to $L = 1$, and if, in accordance with eq. 16-15 we put the ratio of the Bessel functions equal to $-i$. Going over to the superconductor, which requires the replacement of k_n by k and the multiplication by the factor 16-4 we obtain

$$Z = \frac{L k}{S \sigma (1 + i \omega \sigma \lambda)}$$

By again applying eq. 16-15 we confirm that the factor (L/S) equals the factor $(1/2 \pi R)$ in eq. 16-14. This means, however, that the transformation that followed eq. 16-19 can be applied exactly to the expressions $c S Z/L$ and $c S W/L$, thus again leading to eq. 16-21.⁴ We repeat: In all these examples it is important that the skin effect should already be pronounced

⁴A. Sommerfeld (*Ann. Physik* (4) 24, 609 (1907)) has calculated the correction pronounced skin effect, it consists of a real factor depending only on the spacing between successive windings of the coil and the radius of the wire. The same factor has to multiply $W = \text{Re } (Z)$, it can be taken over unchanged for the superconducting wire and so cancels in eq. 16-21 when forming the ratio W/W' .

in the normal conductor. It is only if the smallest possible value of $|k|$, namely $|k_n|$, satisfies the condition $|k| R \gg 1$ that eq. 16-21 can be used for the cylinder.

(f) Let us reduce the temperature T starting from the transition temperature T_c . According to eq. 16-19 θ then decreases monotonically with λ , and the same is true of the function $1/2 \sin \theta \sin \frac{1}{2} \theta$ (Fig. 16-1). If finally the number $\omega \sigma \lambda$ becomes small compared with unity, owing to the decrease of λ , then also $\theta \ll 1$ and $1/2 \sin \theta \sin \frac{1}{2} \theta$ has the value $(\omega \sigma \lambda)^{1/2}$. Therefore, according to eq. 16-21, we have

$$W = W_c \sqrt{\frac{\sigma_c}{2\omega} \omega^2 \sigma \lambda^{1/2}}$$

in agreement with eq. 16-17. W should decrease monotonically between this value and W_c , provided the conductivity σ remains constant. However, the curves published by McLennan and co-workers [Chap. 1 (c)] for the resistance of tantalum as a function of temperature for frequency $\omega = 2\pi \cdot 1.14 \times 10^7$ per sec, i. e., the upper curve of Fig. 16-2 shows an initial maximum at which W is 4% higher than W_c , and only after this does the expected decrease appear. If this maximum is real,⁵ it can only be interpreted as due to the conductivity σ starting to decrease at the transition temperature; according to eq. 16-21 the product $\sqrt{\sigma} W$ must decrease immediately below the transition temperature.

It is evidently impossible to determine both σ and λ as functions of T from a single empirical curve. But by using the empirical curve for W we can try to find a plausible form for σ as a function of T such that one derives a curve for λ that has a steep decline just below T_c , similar to that found in the experiments of Appleyard and Shoenberg with mercury (Chap. 1 (c)). If W and σ are given for a certain T , then eq. 16-21 ascribes to this T a certain θ value, and eq. 16-19 a certain λ to this θ . We try the form

$$\frac{\sigma}{\sigma_c} = 0.6 + 0.4 \times e^{-5(T_c - T)} \quad (16-22)$$

⁵Recent work on resonant cavities instead of wires failed to show this maximum. J. C. Slater, E. Maxwell, P. Marcus, *Phys. Rev.* 76, 1332, (1949).

B. Pippard, *Proc. Roy. Soc. (London)*, 191, 370, 385, 399 (1947). 208, 195, 210, (1950).

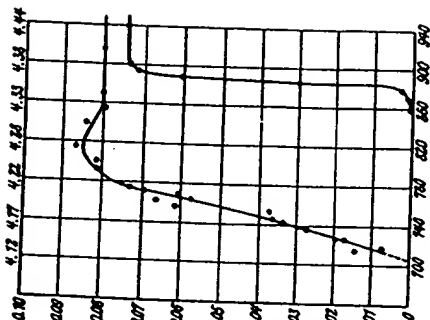


Fig. 16-2. Resistance of tantalum near the transition temperature.

according to which σ decreases to $0.6 \sigma_1$ within one degree and then remains constant. The empirical values of σ_1 differ. The finding of McLennan and his co-workers that the d-c resistance of tantalum at T_1 is 0.07 of the resistance at 0°C leads to $\sigma_1 = 1.30 \times 10^{19}$ per sec in Lorentz units, and we shall use this value. If it is wrong by a factor α , then all σ values have to be multiplied by α and all λ values by $1/\alpha$, which does not change the form of the λ curve. The result of this calculation is shown in Fig. 16-3. The curve has indeed the expected form. Figure 11-3 gives the measurements of λ for mercury for comparison.

If this is considered a sufficient confirmation of the theory, we can proceed to ask how the W curve would be affected by going to higher frequencies. We see that the curve must be considerably raised by this at the lowest temperatures where W is still just noticeable, because of the factor ω^2 in eq. 16-18. It must also be raised at higher temperatures because according to eq. 16-19 θ increases with ω , and so therefore does the right-hand side of eq. 16-21 at a given temperature (σ and λ fixed). However, this increase is less serious the greater $\omega \sigma \lambda$ already is, namely, the nearer T approaches T_1 . As we already saw, θ has its greatest possible value $\pi/2$ for all frequencies at T_1 itself, so that W remains equal to W_1 there. The rise of the W curve up to W_1 becomes less steep with higher frequencies, and the curve should rise appreciably above the zero level at lower temperatures as shown in Fig. 16-2.

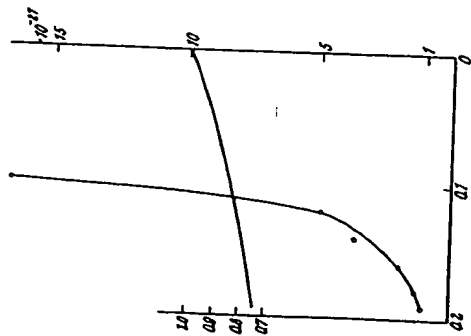


Fig. 16-3. Superconductivity constant and relative conductivity of tantalum as a function of temperature. Abscissa: temperature difference $T_1 - T$, increasing toward the left. Ordinate: the steeper curve is the superconductivity constant in sec given by the scale on the right-hand side; the flat curve is (σ/α_1) given by the left-hand scale according to the assumption 16-22.

(e) H. London measured the resistance of superconducting tin at frequencies of about 10^{10} cycles per second by producing eddy currents in an ellipsoidal specimen and calculating the heat produced by measuring the rate of evaporation of the helium bath. He also found that the high frequency resistance of the normal conductor passes continuously into that of the superconductor at the transition temperature, and that there is then a steep drop when we further decrease the temperature.

The considerations of this chapter become meaningless — as does the Maxwell theory itself — if the mean free path of the electrons becomes

comparable with or greater than the penetration depth. Deviations of this kind were first observed by Pippard⁶ and by Slater and co-workers.⁷ A theoretical treatment of this problem has been given by Reuter and Sondheimer⁸ and Slater *et al.*⁷

CHAPTER 17

Thermodynamics of the Transition between Normal and Superconducting Phases

(a) It was the Meissner effect that led to the idea that the superconducting and the normally conducting states are different phases of the same material in the sense that diamond and graphite are different phases of carbon. Earlier, when it was supposed that any arbitrary magnetic field could be "frozen in" within the interior of a superconductor (see Chap. 1) one had to presume an infinity of different superconducting states, and this excluded the phase idea. We know now, however, that the interior of a sufficiently thick superconductor in a stationary state is field free, protected by the thin surface layer, regardless of its history. Even if the metal is too thin to form this protective layer, the field in its interior is uniquely determined by the conditions imposed by the magnetic field in its neighborhood at the moment of interest, and independent of its previous history, always supposing this field to be stationary and changes of state as quasi-stationary just as we do in all thermodynamic arguments.

However, the superconducting and normally conducting phases are much more alike than are diamond and graphite. At all temperatures they have the same lattice structure, not only with regard to symmetry characteristics, but also the same lattice constants. Shape and volume are completely preserved during the transition. This point is essential to the following application of thermodynamics. It would not be if the transition between the two phases were effected by means of an intermediate vapor phase, a certain amount of one phase evaporating, the same amount condensing into the other solid phase. But in the present case one solid phase changes directly into the other, which is in contact with it; only the identity of the two lattices prevents the system from splitting into more or less minute fractions (being of the form single crystal \rightarrow polycrystal which would naturally exclude any reversibility).

⁶B. Pippard, *Proc. Roy. Soc. (London)*, 191, 370, 385, 399 (1947).

⁷J. C. Slater, E. Maxwell, P. Marcus, *Phys. Rev.* 76, 1332, (1949).

⁸G. E. H. Reuter and E. H. Sondheimer, *Proc. Roy. Soc. (London)*, 195 A, 336 (1948).

Incidentally Keesom and Kok¹ (for tellurium) and van Laer and Keesom² (for tin) have experimentally compared the heats of reaction during the transition both from the superconducting to the normal state and during the reverse transition and have found them equal, as required for reversibility.

A further assumption, supported indeed by the arguments of Chap. 5, is that the free energy of the magnetic field, including the superconduction energy is added to the free energy of the specimen, and so there is no free energy of interaction. This permits the following concept. The field is a "machine" exerting the forces on the surface of the superconductor that are given by the London stress system as discussed in Chap. 13. These forces perform work in so far as the surface is displaced, and this work serves to change the free energy of the material during isothermal displacements. The free energy of the field does not enter such a calculation, the internal changes of the "machine" being irrelevant for the energy balance in the specimen.

As shown in Chaps. 13 and 14 the force due to the field at a point where no current crosses the surface — the current lines being parallel to the surface — is a stress of amount $\frac{1}{2}(\mathbf{i} \cdot \mathbf{G})$ directed toward the interior of the superconductor. We shall calculate this example first.

(b) To do this we write f_s and f_N for the free energies ($f = e - Ts$) per mol of the superconductor and normal conductor respectively and V for the mol volume common to both phases, with $d\sigma$ a surface element of the superconductor and δn a virtual displacement of this element in the direction of its normal. δn is taken positive for displacements toward the interior of the superconductor as in Chap. 14 (f). It is necessarily positive wherever the superconductor borders upon empty space or a chemically different specimen, but δn can be negative if the superconductor joins on to a chemically identical normal conductor. For positive δn , $d\sigma \cdot \delta n/V$ mols of the superconductor change into normal conductor; the tension of the London stresses performs work $\frac{1}{2}(\mathbf{i} \cdot \mathbf{G}) \delta n \cdot d\sigma$ (Chaps. 13 and 14) while the free energy of the material increases by $(f_N - f_s) d\sigma \cdot \delta n/V$. For negative δn the corresponding number of mols of normal conductor change into superconductor; the work done by the forces becomes negative. Naturally it is impossible for a single element alone to be displaced as the continuity of the boundary must be preserved, but an arbitrary infinitesimal displacement δn can be ascribed to any element $d\sigma$ of the surface. The total number of mols going over from one phase into the other is $\int \delta n \cdot d\sigma/V$ and the work done by the forces is

$$\delta A = \int \frac{1}{2}(\mathbf{i} \cdot \mathbf{G}) \delta n \cdot d\sigma \quad (17-1)$$

The corresponding change in free energy is

¹W. H. Keesom and J. A. Kok, *Physica*, 1, 503 (1934).

²P. H. van Laer and W. H. Keesom, *Physica*, 5, 993 (1938).

$$\delta F = \left[\frac{(f_N - f_s)}{V} \right] \int \delta n \cdot d\sigma \quad (17-2)$$

From the two principal laws of thermodynamics one concludes that for a spontaneous isothermal transition $\delta A > \delta F$. The necessary condition that a transition shall not occur is therefore

$$\delta A \leq \delta F$$

Applied to the displacement of the boundary this gives

$$\frac{1}{2} \int (\mathbf{i} \cdot \mathbf{G}) \delta n \cdot d\sigma \leq \left[\frac{(f_N - f_s)}{V} \right] \int \delta n \cdot d\sigma$$

Since δn can be either positive or negative, the inequality must reduce to equality: because if for some choice of δn the right-hand side were greater than the left side, it would be smaller for the opposite choice of δn . Furthermore, as δn is an arbitrary function of position on the surface, equilibrium must exist at every point:

$$\frac{1}{2}(\mathbf{i} \cdot \mathbf{G}) = \frac{(f_N - f_s)}{V} \quad (17-3)$$

This is the equilibrium condition for the boundary between super- and normal conductor. If δn is necessarily positive at the surface of a superconductor bordering empty space or a chemically different specimen the condition for conservation of superconductivity is

$$\frac{1}{2}(\mathbf{i} \cdot \mathbf{G}) \leq \frac{(f_N - f_s)}{V} \quad (17-4)$$

In this form both conditions are valid for "thick" superconductors with fully developed protective layers, as well as for the "thin" superconductors in which the magnetic field penetrates more or less completely. Since experiments almost always deal with "thick" superconductors these conditions are usually expressed instead in terms of the magnetic field at the surface, derived from the supercurrent there by the eq. 7-37 valid for "thick" superconductors. We define a field strength H_c by

$$\frac{1}{2} H_c^2 = \frac{(f_N - f_s)}{V} \quad (17-5)$$

The condition 17-3 for the boundary between super- and normal conductor reads

$$H = H_c \quad (17-6)$$

and the condition 17-4 for a boundary surface adjacent to empty space or a chemically different material:

$$H \leq H_c \quad (17-7)$$

This justifies our considering H_c defined by eq. 17-5 as a critical field. It is a necessary consequence of this theory that if H exceeds this value at any point of the free surface of a "thick" superconductor its superconductivity is destroyed.

If the magnetic field gives rise only to permanent magnetism and annular currents in superconductors, then according to Chap. 14 (e) the work δA performed by the field is equal to the decrease $(-\delta U)$ of the free energy of the field. Equation 17-3 states that in this case the sum of the free energy of the field and the specimen is conserved during the reversible phase transition. This statement however does not hold if ohmic currents are also produced, or if only ohmic currents are produced by the field. In this case the system (field plus specimen) is not a closed system. Additional electrostatic forces are required to fulfill the condition that the ohmic currents remain constant. If we wish to use the theorem of constant free energy we have to be quite clear about how the field is produced.

(c) These conclusions can also be derived for a "thick" superconductor from the volume forces exerted according to Chap. 13 by the Maxwell stresses, $[1 \times H]/c$, on the supercurrent mechanism of the London theory. These forces are distributed over the thickness of the protecting layer. However, in the "thick" superconductor this protecting layer undergoes the virtual displacement δn as a whole without alteration of field or current distribution, so that we can calculate the work done by these forces per unit surface as the product of the resultant force per unit area times δn . As there is no field inside the layer, the resultant force is the pressure $\frac{1}{2} H^2$ of the lines of force on the outside, by Chap. 13. In this way we get the equilibrium condition

$$\delta A = \frac{1}{2} \int H^2 \delta n \cdot d\sigma \leq \left[\frac{(N - I_s)}{V} \right] \int \delta n \cdot d\sigma$$

and from this, the eqs. 17-6 and 17-7. This conclusion cannot be assumed so easily for thin superconductors where the field and current distribution change in a complicated fashion with a displacement δn of the surface.

This derivation has the advantage of being based more directly on the Meissner effect, i. e., the existence of the protective layer, than was the first derivation; but the latter is more general and can be used also for thin specimens.

(d) The free energies f_N and f_S are functions of the temperature T . We neglect their dependence on pressure or elastic stress because most experiments have been performed on strain-free specimens at one atmosphere which is effectively zero pressure. According to eq. 17-5 the critical value H_c is also a function of T . From thermodynamics we have⁵

$$s = - \frac{df}{dT} \quad (17-8)$$

for the entropy per mol, s , and we obtain eq. 17-5 by neglecting the extremely small changes in volume V at these temperatures in accordance with Nernst's theorem, thus:

$$s_N - s_S = - \frac{1}{2} V \frac{d(H_c^2)}{dT} = - V H_c \frac{dH_c}{dT} \quad (17-9)$$

⁵ The specific heat does not depend on magnetic field (see discussion of Fig. 17-2) so we may write d/dT instead of $(\partial/\partial T)_H$.

This is the increase in entropy associated with the transfer of one mol from the superconducting to the normal state. Multiplying by T we get the amount of heat that has to be supplied with this transition:

$$Q = - \frac{1}{2} V T \frac{d(H_c^2)}{dT} = - V T H_c \frac{dH_c}{dT} \quad (17-10)$$

Further we have the following expression for the specific heat per mol at constant pressure:

$$c = T \frac{ds}{dT} = - T \frac{d^2 f}{dT^2} \quad (17-11)$$

So from eq. 17-9 we have

$$c_N - c_S = - \frac{1}{2} V T \frac{d^2(H_c^2)}{dT^2} = - V T \left[\frac{dH_c}{dT} \right]^2 + H_c \frac{d^2 H_c}{dT^2} \quad (17-12)$$

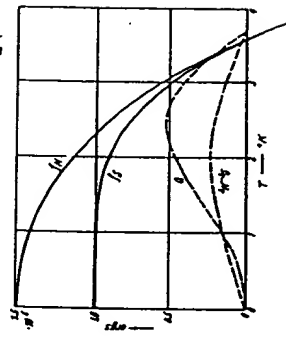


Fig. 17-1. Thermodynamic functions for tin below the transition temperature f_N and f_S are the free energies per mol in the normal and superconducting states. The curves split at the transition temperature 3.7°K . Only the difference $f_N - f_S$ has physical meaning. The upper dotted curve gives the heat Q in ergs per mol to be supplied during the transition of the superconductor into the normally conducting state. The lower dotted curve is the entropy difference $s_N - s_S$ in ergs per mol degree. The figures used come from eqs. 17-16 and 17-17:

$$f_N = -2.54 \times 10^3 \text{ T}^4 - 8.40 \times 10^3 \text{ T}^2 + 1.50 \times 10^4 \text{ erg/mol}$$

$$f_S = -5.92 \times 10^3 \text{ T}^4 + 1.00 \times 10^4 \text{ erg/mol}$$

$$s_N - s_S = -1.35 \times 10^3 \text{ T}^3 + 1.68 \times 10^4 \text{ T erg/mol deg}$$

$$Q = -1.35 \times 10^3 \text{ T}^4 + 1.68 \times 10^4 \text{ T}^2 \text{ erg/mol}$$

(e) These relations were first derived by Rutgers⁴ and by Casimir and Gorter.^{5,6} We shall discuss them now in the light of the free energy curves, f_N and f_S as functions of T , represented in Fig. 17-1. The slopes or tangents

⁴ A. J. Rutgers, *Physica*, 1, 1055 (1934); 8, 999 (1936). See also P. Ehrenfest, *Proc. Roy. Acad. (Amsterdam)*, 86, 153 (1933).

⁵ H. B. G. Casimir and C. J. Gorter, *Physica*, 1, 300 (1934).

⁶ A formulation also valid for thin superconductors was given by Max von Laue, see Chap. 1, footnote 7, and Chap. 3, footnote 2 (f).

give the corresponding entropy, by eq. 17-8. H_c is zero at the transition temperature T_c , by definition, therefore $/N = /s$ there according to eq. 17-5, and the two curves coincide. Experiment shows that dH_c/dT is finite at T_c , so that by eq. 17-9 the two curves have a common tangent there. But by eq. 17-12 the curves differ in their second derivatives, i. e., curvature. For $T < T_c$, we always have $/N > /s$ according to eq. 17-5.

We cannot produce the curve of $/s$ above T_c , because the superconductor does not exist there, not even as a phase that is unstable with respect to the normal conductor. We arrive at this conclusion first from the fact that the supercurrent constant becomes infinite at T_c , so that no value can be ascribed to λ above T_c . Secondly, from the fact that when $/N = /s$ so that the common point of the two curves would be a stationary point; $/N$ would then be greater than $/s$ above T_c , also, which is inconsistent with the whole concept of phase transitions. Approaching the transition from above, the free energy curve divides at T_c in such a way that the two branches originating at T_c have the same initial tangent.

Experience shows that H_c increases monotonically with decreasing temperature. According to eq. 17-5 the same must be true of $(/N - /s)$. At $T = 0$, $s_N - s_N$ must vanish by the Nernst theorem. Therefore by eq. 17-9 it follows that $(dH_c/dT)_{T=0} = 0$. The parabola drawn in Fig. 1-4 for H_c satisfies this condition and also the condition that dH_c/dT remains finite at T_c , without however being fixed by these conditions. On the other hand $dH_c/dT < 0$ and therefore by eq. 17-10 $Q > 0$: *The transition from the superconducting to the normally conducting state requires heat: the converse process liberates heat.* $Q = 0$ only at the absolute zero where also the factor dH_c/dT in eq. 17-10 vanishes as well as T , and at the transition temperature T_c where the factor H_c vanishes. Between these temperatures Q has at least one maximum. If the H_c -temperature curve is exactly parabolic as in Fig. 1-4 the only maximum is at $T = T_c/\sqrt{2} = 0.707 T_c$. From the finite value of dH_c/dT at T_c we conclude by eq. 17-12 that $dH_c/dT = 0$ and d^2H_c/dT^2 is still small, $c_N - c_S$ must be positive if d^2H_c/dT^2 is everywhere negative as in Fig. 1-4. In between there must be an intersection of the curves of c_N and c_S as functions of T . The entropy difference $s_N - s_S$ has a maximum at this point, by eq. 17-11. If the $H_c - T$ curve were exactly parabolic, this intersection would occur at $T = T_c/\sqrt{3} = 0.577 T_c$. At $T = 0$ both c_N and c_S are zero by the Nernst theorem.

In these calculations current density i and field strength H were expressed in Lorentz units. Transforming to electrostatic units H_c has to be multiplied by the factor $1/4\pi$, according to eq. 3-10. Equations 17-5, 17-10, and 17-12 expressed in electrostatic units read:

$$\frac{V H_c^2}{8\pi} = /N - /s \quad (17-13)$$

$$Q = \left(\frac{V T}{8\pi} \right) \frac{dH_c^2}{dT} \quad (17-14)$$

$$c_N - c_S = - \frac{V T d^2(H_c^2)}{8\pi dT^2} \quad (17-15)$$

According to eqs. 3-10 and 3-11 the general conditions 17-3 and 17-4 retain their form in the electrostatic system.

We are now in a position to derive from eq. 17-12 an equation that has often been used to check the theory against experimental evidence. By partial integration we have

$$- \int_{T_c}^{T_s} (c_N - c_S) dT = \frac{1}{2} V \int_{T_c}^{T_s} T \frac{d^2(H_c^2)}{dT^2} dT = \frac{1}{2} V \left\{ T \frac{d(H_c^2)}{dT} \Big|_{T_c}^{T_s} - \int_{T_c}^{T_s} d(H_c^2) dT \right\}$$

At T_c , $H_c = 0$ and $d(H_c^2)/dT = 0$. Using these expressions and eq. 17-10 to transform the right-hand side we obtain

$$-Q = \frac{1}{2} V H_c^2 + \int_{T_c}^{T_s} (c_N - c_S) dT \quad (17-16)$$

This equation expresses the energy principle for the following cycle: Consider one mol of substance:

1. Cool the superconducting phase from the transition temperature T_c to T . To effect this we have to supply the (negative) amount of heat $-\int_{T_c}^T c_S dT$.

2. Transform the superconducting phase into the normally conducting phase isothermally by application of the magnetic field H_c ; this requires the supply of heat Q and the performance of work $\frac{1}{2} V H_c^2$ (see Chaps. 13 and 14).

3. Heat the normally conducting phase in the magnetic field H_c from T to T_c for which we have to supply heat amounting to $\int_T^{T_c} c_N dT$.

4. Remove the magnetic field and transform the material at T_c into the superconducting state. This step requires no heat and no work. By equating the sum of all these amounts of heat and work to zero we obtain eq. 17-13.

If Fig. 1-4 is correct, H_c for lead increases to almost 1000 oersteds. V , the quotient of the mass of one mol, 207 g., and the density, 11.3 g./cm³, is about 18.5 cm³. Therefore $/N - /s = 7.5 \times 10^6$ erg = 1.8×10^{-2} cal.

For comparison we may mention that the difference of free energies of water and ice per mol is about 1.6×10^6 erg at 0° C and approximately

10^6 dynes/cm² pressure; and 4.6×10^8 erg at -20°C and about 1.9×10^9 dynes/cm².

In the neighborhood of the transition temperature, where H_c is smaller by one or two powers of 10, $f_N - f_S$ is smaller by two to four powers of 10 and therefore quite small compared with the above values for water and ice. Using the equation for the transition curve from which Fig. 1-4 was drawn,

$$H_c = a(T_i^2 - T^2), \quad a = 17.3 \text{ oersted/deg}^2, \quad T_i = 7.3^\circ$$

Calculating the maximum of the heat of transition at 5.2° and the difference between the specific heats at the transition temperature, we find:

$$Q_{\text{max}} = 6.2 \times 10^8 \text{ erg} = 1.5 \times 10^{-2} \text{ cal} \quad (\text{lead})$$

and

$$(c_N - c_S)T_i = 6.9 \times 10^5 \text{ erg/deg} = 1.6 \times 10^{-2} \text{ cal/deg} \quad (\text{lead})$$

These figures at least give some idea of the magnitude of the values under discussion.

(f) The Rutgers-Gorter-Casimir equations 17-5, 17-9, 17-10, and 17-12 have been confirmed for several metals. We may mention here the measurements on Zn by Keesom and van Laar.⁸ In Fig. 17-2 the points C show the experimental results for the molar heat found in the absence of a magnetic field. Starting above the transition temperature T_i , these points at first lie on the curve of c_N against T . At the transition temperature, 3.7°K , the points suddenly jump to higher values and trace the curve for c_S . The points Δ were measured in the presence of a field of 299 oersteds, and the points \bullet in a field of 139 oersteds. As these fields prevented the appearance of superconductivity, all these points lie on the curve for c_N which apparently does not depend on the field strength. This is an important confirmation of our assumption that the thermodynamic functions of the normal conductor are uninfluenced by a magnetic field. Although c_S lies much higher than c_N at the transition temperature, the two curves intersect each other at 1.9° as required in section (c).

The authors were able to represent the c_S curve by Debye's law for molar heat:

$$c_S = 464.5 \left(\frac{T}{\theta_S} \right)^3 \text{ cal deg}^{-1}, \quad \theta_S = 140^\circ \quad (17-17)$$

However, in order to obtain a good representation of c_N they had to add to the T^3 term a linear term in T :

$$c_N = 464.5 \left(\frac{T}{\theta_N} \right)^3 + 4 \times 10^{-1} T \text{ cal deg}^{-1}, \quad \theta_N = 185^\circ \quad (17-18)$$

In fact, even with this additional term there are still discrepancies above 3.5°K . The second term may be interpreted as the specific heat of the conduction electrons on the Sommerfeld theory of metallic conductivity.

⁷ Calculated as the product of pressure and change of volume.

⁸ W. H. Keesom and P. H. van Laar, *Physica*, 6, 193 (1938). The value $\theta_c = 140^\circ$ was taken from their Fig. 2.

The difference $c_N - c_S$ is thus of the form $aT^3 + \beta T$. This leads to the parabola for H_c as a function of T , by eq. 17-12 and the conditions $dH_c/dT = 0$ at $T = 0$ and $H_c = 0$ at $T = T_i$. The authors also emphasize that eq. 17-12 is well satisfied if their measurements are combined with those of de Haas and Engelke⁹ on H_c .

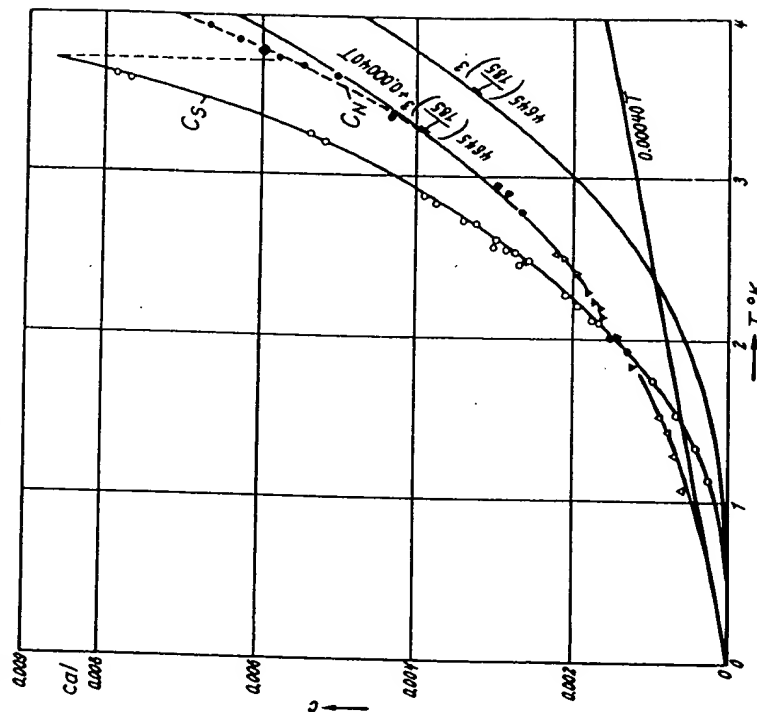


Fig. 17-2. Atomic heat of normal and superconducting tin as a function of temperature.

The jump in the atomic heat of tin at T_i is 1.26×10^5 erg/deg $= 3.0 \times 10^{-3}$ cal/deg, according to Fig. 17-2, and so considerably smaller than that found in lead [section (e)]. In addition to the f_N and f_S curves in Fig. 17-1 we have also plotted the entropy difference, using the values from eqs. 17-17 and 17-18:

⁹ W. J. de Haas and Miss A. D. Engelke, *Physica*, 4, 325 (1937).

$$-(s_N - s_S) = \int_{\tau_e}^{\tau_e} \frac{1}{T} (c_N - c_S) dT \quad (17-19)$$

and also the heat of the transformation $Q = T(s_N - s_S)$.

Keesom and van Laer¹⁰ examined the validity of eq. 17-3 by measuring the heat of transformation Q and the specific heats of tin. They find agreement between calculated and measured values of Q to within 5% in the least favorable case. The confirmation of eq. 17-19 in the same paper shows that the assumption of a reversible phase transition is justified.

(g) A homogeneous magnetic field does not generally need to have the full strength H_c in order to quench the superconductivity of any body placed in it. As shown in Chaps. 9 to 11 for many examples, and depicted in Fig. 1-5, the distortion of the field by the superconductor produces an intensification of the field at the surface of that body. This suffices for the quenching of the superconductivity if the intensification raises the field at some point to beyond H_c . If we write α for the ratio of the maximum field strength at the surface to the field strength at a great distance from the specimen, the critical value of this latter field is H_c/α . In the sequel we must distinguish carefully between this value, depending on the form of the specimen, and the critical H_c that depends only on the material of the specimen and the temperature.

For a "thick" elliptical cylinder with axes a and b , the a axis forming the angle θ with the direction of the field we have, by eq. 10-24:

$$\alpha = \left(\frac{1}{a} + \frac{1}{b} \right) \sqrt{\frac{a^2 \sin^2 \theta + b^2 \cos^2 \theta}{ab}} \quad (17-20)$$

The intensification factor α therefore varies with θ between $1 + b/a$ and $1 + a/b$. This has been confirmed at least qualitatively by de Haas and Casimir-Jonker [Chap. 1 (f)]. For the thick circular cylinder $\alpha = 2$, for the "thick" sphere $\alpha = 3/2$, see Chap. 11.

CHAPTER 18

The Critical Magnetic Field for Thin Superconductors

(a) It is only for "thick" superconductors that the field strength H_c defined in eq. 17-5 is a critical value exceeding which at any point of the free surface would destroy the superconductivity. Equation 7-37 between current density and magnetic field strength at the surface holds only for a fully developed protective layer. For "thin" superconductors in which the protective layer is not fully developed, we have to go back to the more

¹⁰ W. H. Keesom and P. H. van Laer, *Physica*, 3, 371 (1936).

general equations 17-3 and 17-4. These equations, remembering eq. 17-5, can be written:

$$\begin{aligned} (\mathbf{i} \cdot \mathbf{G}) &= H_c^2, & \text{equilibrium condition for the boundary between} \\ & & \text{superconductor and normal conductor} \\ (\mathbf{i} \cdot \mathbf{G}) &\leq H_c^2, & \text{condition for preserving superconductivity} \\ & & \text{at a free surface} \end{aligned} \quad (18-1)$$

In what follows we discuss cubic crystal superconductors with $(\mathbf{i} \cdot \mathbf{G}) = \lambda \mathbf{i}^2$. However, the results are qualitatively valid for other forms.

Consider two geometrically similar thin superconductors of the same material and at the same temperature such that the linear dimensions of the smaller specimen can be obtained from those of the larger one by multiplication by the factor $\alpha < 1$. Let the two specimens be placed in the same homogeneous magnetic field H^0 ; then the ratio of the current density \mathbf{i} in the smaller specimen to that at the corresponding point in the larger specimen is, according to Chap. 7 (f) equal to α .

Since \mathbf{i} is proportional to H^0 we have to increase H^0 by the factor α^{-1} to get the same stress $\frac{1}{2} \lambda \mathbf{i}^2 = \frac{1}{2} H_c^2$ at corresponding points on the surface of the smaller specimen. The critical value of H^0 needed to quench superconductivity increases by the factor α^{-1} when the dimensions of the specimen are decreased by the factor α . The smaller the disturbance of the field caused by a small superconductor, the less it is influenced by the field.

(b) We shall prove this for a few examples. For a plane parallel plate of thickness $2d$ with field strength H^0 at both sides we have by eq. 7-18

$$\lambda \mathbf{i}^2 = (H^0)^2 \tanh^2 \beta d$$

According to eq. 18-1 the superconductivity is quenched at the critical value

$$H^0 = H_c \coth \beta d > H_c \quad (18-2)$$

For a "thick" plate this is approximately

$$H^0 = H_c (1 + 2e^{-2\beta d}) \quad (18-3)$$

and for a "thin" one

$$H^0 = H_c \frac{[1 + (\beta d)^2/3]}{\beta d} \quad (18-4)$$

The denominator βd corresponds to the factor α in the theorem of (a).

The current density at the surface of a cylinder of radius R in a longitudinal field H^0 is, according to eq. 10-2, given by:

$$\lambda (\mathbf{i} \cdot \mathbf{r})^2 = (H^0)^2 \left[-\frac{I_1(\epsilon \beta R)}{I_0(\epsilon \beta R)} \right]^2$$

The critical value is therefore

$$H^0 = H_c \left[\frac{I_0(\epsilon \beta R)}{I_1(\epsilon \beta R)} \right] > H_c \quad (18-5)$$

By using eq. 16-15 for the ratio of the Bessel functions for large values of βR we find

$$H^0 = H_c \left(1 + \frac{1}{2\beta R} \right) \quad (18-6)$$

For small values of βR , however, the series 8-6 gives

$$H^0 = 2H_c \frac{1 + \frac{1}{8}(\beta R)^2}{\beta R} \quad (18-7)$$

For a cylinder in a transverse field the current density at the surface is, by eq. 10-16, a maximum at $\theta = \frac{1}{2}\pi$. At this angle

$$(i_r)^2 r_{\frac{1}{2}\pi} = 4(H^0)^2 \left[-\frac{i I_1(i\beta R)}{I_0(i\beta R)} \right]^2$$

This value is four times the value for longitudinal fields. Therefore we have simply to divide the right-hand sides of eqs. 18-5, 18-6, and 18-7 by 2 to get the corresponding results for the transverse field.

The current density at the surface of a sphere of radius R has a maximum on the equatorial plane $\theta = \frac{1}{2}\pi$. According to eqs. 11-1, 11-9, and 11-5 we have

$$\lambda (i_r)^2 r_{\frac{1}{2}\pi} = (H^0)^2 \left\{ \frac{3}{2} [\coth \beta R - (\beta R)^{-1}]^2 \right\}$$

A homogeneous field can therefore be increased without destroying the superconductivity only as far as the critical value:

$$H^0 = \frac{3}{2} H_c [\coth \beta R - (\beta R)^{-1}]^{-1} > \frac{2H_c}{3} \quad (18-8)$$

This means for $\beta R \gg 1$, up to

$$H^0 = \frac{2}{3} H_c \left(1 + \frac{1}{\beta R} \right) \quad (18-9)$$

while with $\beta R \ll 1$, up to

$$H^0 = 2H_c \frac{1 + \frac{1}{15}(\beta R)^2}{\beta R} \quad (18-10)$$

The denominator βR in eqs. 18-7 and 18-10 again corresponds to the a factor in the theorem of section (a).

(c) We follow these examples by three paradoxes. At the two boundaries $\pm d$ of a plane parallel plate of thickness $2d$ carrying current i per centimeter, the current density and magnetic field are given by eq. 7-21:

$$|i_r| = \frac{1}{2} \beta I \coth \beta d, \quad |H_r| = \frac{I}{2c}$$

The critical value of i that quenches superconductivity is such that $\lambda i_c^2 = H_c^2$. Therefore the critical current and the corresponding field intensity are respectively

$$i_c = 2c H_c \tanh \beta d, \quad |H_c| = H_c \tanh \beta d \quad (18-11)$$

The critical current therefore decreases with decreasing βd finally going to zero; the same is true of the corresponding magnetic field. The mean critical current density, however, namely,

$$\frac{i_c}{2d} = \frac{H_c}{\sqrt{\lambda}} \frac{\tanh \beta d}{\beta d} \quad (18-12)$$

increases to a maximum value $H_c/\sqrt{\lambda}$.

The current density at the surface of a wire of radius R carrying current i is, by eq. 8-9

$$(i_r)_R = \frac{\beta I}{2\pi R} \frac{I_0(i\beta R)}{I_1(i\beta R)}$$

To find the maximum possible supercurrent we must put $\lambda i_c^2 = H_c^2$. This gives the maximum possible mean current density

$$\frac{i_c}{\pi R^2} = -i \frac{H_c}{\beta \sqrt{\lambda} R} \frac{I_1(i\beta R)}{I_0(i\beta R)} \quad (18-13)$$

The ratio of the Bessel functions decreases more slowly than βR , the mean current density therefore increases, but more slowly than $(\beta R)^{-1}$. In particular for large βR we have

$$\frac{i_c}{\pi R^2} = \frac{2H_c}{\beta \sqrt{\lambda} R} \left(1 - \frac{1}{2\beta R} \right) \quad (18-14)$$

and for small βR

$$\frac{i_c}{\pi R^2} = \frac{H_c}{\sqrt{\lambda}} \left[1 - \frac{1}{8}(\beta R)^2 \right] \quad (18-15)$$

$H_c/\sqrt{\lambda}$ is again the maximum possible current density. The magnetic field produced by this maximum current at the surface of the wire is

$$\frac{i_c}{2\pi c R} = -\frac{H_c i I_1(i\beta R)}{I_0(i\beta R)} \quad (18-16)$$

and is thus smaller than H_c , and the more so the smaller βR , vanishing with βR . These examples do not actually contradict the theorem of section (a), because in both these cases the superconductor was not put into an already existing field. The field outside would not exist without the current i .

The above results can easily be demonstrated and generalized. The maximum possible current load is characterized by the fact that the current density attains the value $H_c/\sqrt{\lambda}$ for which the stress is $\frac{1}{2} \lambda i_c^2 = \frac{1}{2} H_c^2$ at one or more points on the surface (in both the above examples actually over the whole surface). The mean current density required for this in a "thick" superconductor is actually very small compared with $H_c/\sqrt{\lambda}$ because of the extended protected region beneath the protecting layer. However, the mean density for a very "thin" superconductor is equal to $H_c/\sqrt{\lambda}$ because the current is uniformly distributed over the whole cross section. It can never increase beyond this value under any circumstances.

because according to Chap. 7 the maximum current density is always at the surface. As the cross section decreases toward zero, the maximum possible current and the magnetic field at the surface produced by this current also decrease toward zero. This is shown by eqs. 18-11 and 18-12 for a wire and eqs. 18-14, and 18-16 for a plate.

(d) The third of the mentioned paradoxes is of a different kind. If the bore of a hollow thick cylindrical superconductor contains a magnetic field H^0 , then according to eqs. 10-7 and 10-6 the current on the walls is given by

$$\lambda I_0 = (H^0)^2 \left[\frac{H_1(\epsilon \beta R)}{H_0(\epsilon \beta R)} \right]^2$$

To make this equal to H_c^2 we must have¹

$$H^0 = -H_c \frac{H_0(\epsilon \beta R)}{H_1(\epsilon \beta R)} \quad (18-17)$$

The factor multiplying H_c is less than unity and is smaller the smaller βR . Whereas for large βR we have

$$H^0 = H_c \left(1 - \frac{1}{2\beta R} \right) \quad (18-18)$$

for indefinitely decreasing values of βR the maximum possible value of H^0 goes to zero according to the equation

$$H^0 = -H_c \beta R \log \beta R$$

This decrease with decreasing βR is again no contradiction to section (a), as we are not considering a "thin" superconductor.²

As already mentioned in Chap. 12 (g), it can happen that, upon cooling down a normally conducting metal in a magnetic field, at first only an annular part of the specimen becomes superconducting. Normal conductivity remains within the bore of this ring, and a number of lines of force, or rather a certain flux of induction $\int \mathbf{B} \cdot d\mathbf{o}$ is present there. This flux must remain constant (Chap. 12) with further progress of the cooling. If the bore becomes smaller, the field intensity must increase. We see therefore that the bore cannot become arbitrarily small. The critical value of the field strength decreases with the decreasing dimensions of the bore, so that in any case a state will be reached where any further shrinking of the bore will cause the magnetic field to exceed this critical value.

(e) We now come to the measurements of the critical value for "thin" superconductors. Pontius [Chap. 1 (c)] measured the critical values of a longitudinal field for lead wires at 4.2°, i. e., 3.1° below the transition temperature. The radii of the wires were of the order of magnitude 10⁻⁴ cm

¹ $H_0(\epsilon \beta R)$ and $-H_1(\epsilon \beta R)$ are positive as mentioned in Chap. 10.

² The equations of section (b), (c), and (d) were first given by M. v. Laue in the paper already quoted: *Ann. Physik*, 82, 71, 253 (1938). An error in sign in that paper led to a wrong result for the cylinder in a transverse field. The numerical values used in section (e) are also taken from that paper.

to 10⁻³ cm. Figure 18-1 shows his observations compared with a theoretical curve calculated, not from eq. 18-6, but by the somewhat more exact equation³

$$\left(\frac{H_c}{H^0} \right)^2 = 1 - \frac{1}{\beta R} + \text{terms in } \frac{1}{(\beta R)^2} \quad (18-19)$$

It has been assumed that $H_c = 537$ oersteds, and then that $\beta = 4.78 \times 10^4$ cm⁻¹ to yield by eq. 6-7 the value for λ :

$$\lambda = 4.8 \times 10^{-3} \text{ sec}^2 \text{ in Lorentz units}$$

or by eq. 6-8 the 4π times greater value

$$\lambda = 6.0 \times 10^{-30} \text{ sec}^2 \text{ in esu.}$$

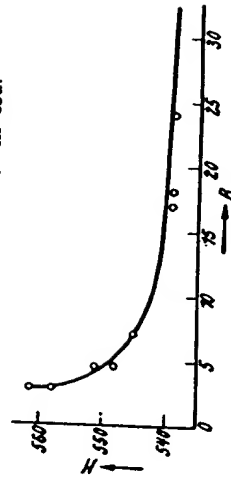


Fig. 18-1. The limiting field strength H^0 in Oersteds as function of the radius R of the wire (in 10⁻⁴ cm units) for lead at 4.2° K. The theoretical curve according to eq. 18-19 and the points observed by Pontius.

This good agreement between the calculated and observed values not only supports the theory in general, but also supports the orders of magnitude for β and λ proposed by F. London from quantum mechanical considerations. This calculation was made in 1938 and was the first one to be based on observational data.

There are also data for thin films. Shalnikov [Chap. 1 (c)] used a lead film 1.4×10^{-6} cm thick and a tin film 1.1×10^{-6} cm thick and found

$$\frac{I_1(\epsilon X)}{I_0(\epsilon X)} = \frac{d [\log I_0(\epsilon X)]}{d X}$$

and by eq. 16-10

$$I_0(\epsilon X) = \frac{e^X (1 + 1/8 X)}{\sqrt{2\pi X}}$$

therefore

$$-\frac{I_1(\epsilon X)}{I_0(\epsilon X)} = 1 - \frac{1}{X} + \text{terms in } \frac{1}{X^2}$$

Equation 18-6 should be more exactly

$$H^0 = H_c \left[1 + \frac{1}{2\beta R} + \frac{3}{8(\beta R)^2} \right]$$

that the critical magnetic field strength required to quench superconductivity was far higher than the critical value H_c found for "thick" films. However, the critical current load was much smaller than that calculated from H_c on the Silsbee hypothesis. He found these results for temperatures ranging over several degrees. They correspond qualitatively with the results of sections (b) and (c). They agree also qualitatively with those of Appleyard and Misener [Chap. 1 (c)] on the critical magnetic field values in mercury films from 4×10^{-6} to 1×10^{-4} cm thick. Shalnikov's results do not seem suitable for a quantitative check of eq. 18-2 or the determination of β because they do not agree quantitatively with the measurements of Appleyard, Bristow, and H. London [Chap. 1 (c)] for mercury films of a similar thickness. The last mentioned authors, however, arrived at an estimate of the relative value of β at any T to its value at 2.5°K in the following manner. As the critical value depends only on the product βd , they selected from among their data at different temperatures and thicknesses those which yielded the same critical value. Then βd must have the same value for all these cases; thus

$$\frac{\beta_T}{\beta_{2.5}} = \frac{d_{2.5}}{d_T}$$

But by eq. 6-7 β is inversely proportional to the square root of λ . In this way the authors found the relation between $\sqrt{\lambda}$ and T shown in Fig. 11-3, which also shows in a striking manner the results of a completely different determination made by Shoenberg [Chap. 11 (d)].

Incidentally all these measurements of the critical magnetic field when used in eq. 18-2 to calculate β lead to the expected result that, sufficiently far below the transition temperature, β has the order of magnitude of 10^5 cm^{-1} .

(1) The whole argument of Chaps. 17 and 18 depends on the condition emphasized in Chap. 17 (a) that no current shall be entering or leaving the superconductor at the points of interest on its surface. It is only under this condition that the London stresses give rise to the tensile stress $\frac{1}{2} \lambda j^2$ toward the interior of the superconductor. Where there is a current being supplied from outside and where j has no tangential component, the tension is replaced by a pressure of the same amount directed outwards. In general if both normal and tangential components of j exist, the force is inclined to the surface. The tangential component is exactly zero only at a few points on the surface of a "thick" superconductor. For example we saw in Chap. 8 (c) that in a superconducting cylinder of radius R to which a current is supplied through a normally conducting cylinder of the same thickness, the tangential component j_t almost everywhere over the interface greatly exceeds the normal component j_n as long as $\beta R \gg 1$. Only on the axis $r = 0$ and at the circumference $r = R$ is $j_t = 0$. Only in areas around these radii of extension β^{-1} is $j_t \gg j_n$.

For a "thin" cylinder or more generally a "thin" superconductor of arbitrary cross section in which the supercurrent, like the ohmic current

in the normal conductor, spreads uniformly over the cross section [Chap. 7 (a)], the tangential component at the interface vanishes. At such points, provided the normally conducting leads consist of the same material as the superconductor, thermodynamic equilibrium between the two phases would depend on the condition (compare eq. 17-3)

$$-\frac{1}{2} (j \cdot G) = \frac{(j_n - j_s)}{V}$$

This condition cannot be satisfied, because at any temperature at which the superconductor can exist at all, i.e., any temperature below T_c , $j_n - j_s > 0$ according to Chap. 17 (c) and Fig. 17-1 whereas $(j \cdot G)$ is positive according to Chap. 3. The current at the interface can therefore only strengthen the tendency of the superconductor to grow at the expense of the normal conductor. Certain as yet unexplained relaxation phenomena which often blur the sharpness of the phase transition may be related to this point.

CHAPTER 19

The Intermediate State

(a) If the superconductivity of a specimen is quenched isothermally by an increasing external magnetic field, it does not transform immediately and completely into the normally conducting state. The nearest approach to a sudden complete transition is found with straight wires in longitudinal fields. However, even in this case the resistance does not change from zero to its final value in one single jump. The transition is by no means continuous, but takes place in several separate jumps. Thus if, following Justi¹ one wraps around the specimen an induction coil connected with an oscillograph or a telephone, and subjects the specimen to a continuously increasing magnetic field, one observes current impulses caused by sudden large changes in the flux of induction.

In other cases where the transition is much slower it can be followed through all its intermediate stages by placing minute bismuth wires inside cavities in the specimen and measuring their resistance as a function of the external field, as was done by de Haas and his collaborators. The resistance of bismuth changes in a known manner with the local magnetic field strength. This arrangement, which naturally is limited to thick superconductors, demonstrates the gradual penetration of the external field. It is impossible for a normally conducting shell to form either completely or partly round a superconducting core. The thermodynamics of Chap. 17 requires the existence of the critical magnetic field H_c corresponding to the prevailing

¹E. Justi, *Physik Z.*, 48, 130 (1942); *Ann. Physik*, 48, 84 (1942).

temperature at every point on the boundary between any such normal envelope and the core. On the other hand, the lines of force, according to electrodynamics, must be parallel to the boundary surface. These two requirements are mathematically inconsistent.

(b) In the first place it is out of the question for the normally conducting shell to enclose the superconducting core completely. There must exist places (either curves or at least points) on the boundary surface where the incident lines of force divide sharply into two lines parallel to the surface. (For a spherical core this would occur at the poles, see Fig. 1-5.) The field strength at these points is zero according to potential theory because the field direction is indefinite, and so cannot equal H_c .

Let us confine ourselves for the moment to two-dimensional problems. Let the boundary of the core S consist of two parts S_1 and S_2 ; at S_1 the core borders either on empty space or on a normal conductor of chemically different material, and at S_2 on the normally conducting shell. Both S_1 and S_2 may consist of several separate sections. We assume each section to be an analytic curve i. e., they can be represented by equations of the form $x = f(s)$, $y = g(s)$ where f and g are analytic functions.

At each point where a section of S_1 meets the adjacent section of S_2 it is not permissible for them to form an angle with each other. Such an angle would make a kink in S_1 ; if the kink were re-entrant the field strength, according to potential theory, would be zero; if the kink were raised (convex), the field would be extremely large (mathematically infinite); in any case it could not be equal to H_c at such kinks. The above parametric representation therefore holds uniformly over the whole boundary curve S , and therefore H on the boundary must also be an analytic function of the parameter s . As it is constant and equal to H_c over all parts of S_2 , it must also be equal to H_c over S_1 in spite of the fact that it must also be zero at some points.

The same inconsistency is found in the three-dimensional case. We can ascribe to any part of the boundary, whether it belongs to S_1 or to S_2 an analytical representation in terms of two parameters: $x = f(s, t)$, $y = g(s, t)$, $z = h(s, t)$. No singularities are permitted at any point where sections of S_1 and S_2 touch, because they would cause zeros or infinities in H . Therefore the analytical representation holds uniformly over the whole boundary S . Then H is also an analytical function of s and t . Because it is constant and equal to H_c over S_2 , it must also be constant over S_1 in spite of the fact that places must exist where $H = 0$.³ So if a piece of material cannot be either normally conducting as a whole nor superconducting, it must be in an "intermediate state" representing a mixture of alternating superconducting and normally conducting regions.

The difficulty discussed above for thick superconductors does not exist for small superconducting regions dispersed through a normal conductor, because such small regions do not disturb the magnetic field, according to

³M. v. Laue, *Physik. Z.*, 48, 274 (1942).

Chap. 7, and are themselves barely affected by the field, according to Chap. 18.

These conclusions are confirmed by an experiment by Shubnikov and Nachutin.³ They quenched the superconductivity of a sphere in a magnetic field and measured the electric resistance parallel and perpendicular to the external field before the sphere had become completely normally conducting. Long after resistance had appeared in the direction perpendicular to the field, they could find no resistance in the direction parallel to the field. This is difficult to explain except in terms of coexisting normal and superconducting regions. It suggests, moreover, that the superconducting regions are much more extended in the direction of the field than in the transverse direction. This fits in with the argument of Chap. 18 (b) according to which a cylinder or any other elongated specimen loses its superconductivity much more easily in a transverse field than in a longitudinal one.

(c) The earliest method of recognizing superconductivity was to observe the disappearance of the d—c resistance. However this method is hardly suitable for distinguishing between the superconducting and the intermediate states because the normally conducting regions will not participate in carrying the current so long as the current can find a closed path through the superconducting regions. A far better criterion for the break down of the superconducting state is the disappearance of the Meissner effect, i. e., the appearance of a magnetic field within the interior of the specimen. In this way it is possible to understand why the first measurable resistance

of a wire in a transverse field has been observed at $H^0 = 0.58 H_c$,⁴ whereas according to theory [Chap. 18 (b)] and the experiments to be mentioned immediately, superconductivity is already destroyed when $H^0 = 0.50 H_c$.

In order to observe the field penetration, de Haas and Casimir-Jonker⁴ inserted minute bismuth wires, as described above, in holes in a tin wire 0.7 cm in diameter, see Fig. 19-1. They measured the increase of resistance of the bismuth wires while gradually increasing the external magnetic field H^0 . Figure 19-2 shows the results when the plane of the wires is perpendicular to the field H^0 ; Fig. 19-3 when it is parallel. The critical value H_c can be recognized in both diagrams at the point where the resistance curves meet the resistance curve of a bismuth wire exposed to the external field H^0 , and indicated in Fig. 19-2 by the dotted line. This point is where the specimen allows the external field to penetrate it completely. In Fig. 19-2

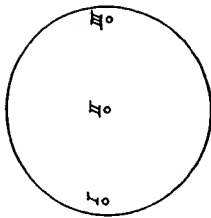


Fig. 19-1. Cross section through tin cylinder with bismuth probe wires inserted at I, II, and III. (After W. J. de Haas and J. M. Casimir-Jonker.)

³L. Shubnikov and J. Nachutin, *J. Exp. Theoret. Phys. (U.S.S.R.)*, 7, 566 (1937).

⁴W. J. de Haas, J. Voogd, and J. M. Casimir-Jonker, *Physica*, 1, 281 (1934).

⁵W. J. de Haas, and J. M. Casimir-Jonker, *Physica*, 1, 291 (1934).

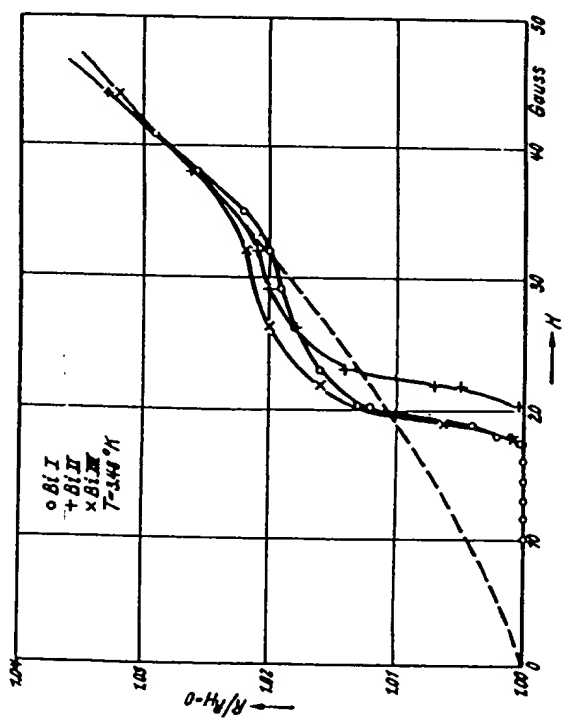


Fig. 19-2. Increase of resistance in the bismuth probe wires due to penetration of a magnetic field normal to the plane of the wires.

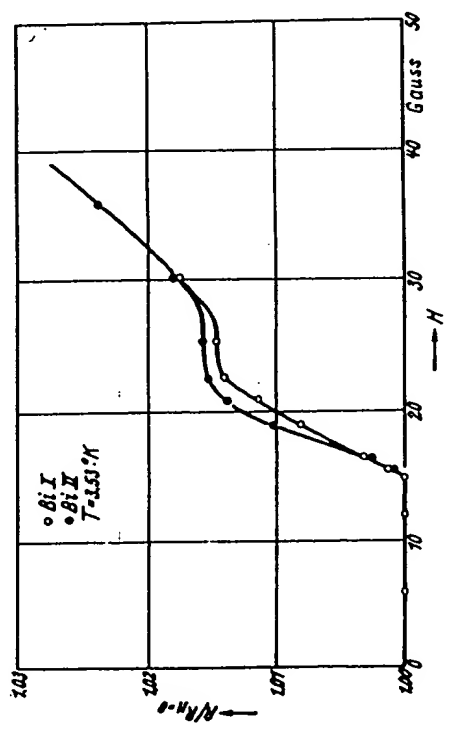


Fig. 19-3. Increase of resistance in the bismuth probes due to penetration of a magnetic field parallel to the plane of the wires.

H_c falls at about 36 oersteds; in Fig. 19-3 at about 30 oersteds because of the slightly higher temperature. One sees that the first sign of the field penetration occurs in both diagrams at the field $H^0 = \frac{1}{2} H_c$, i. e., at 18 and 15 oersteds respectively, as required by theory. The wire II was placed in the axis of the wire, so the fact that its curve reacted only at 20 oersteds does not alter the fact that both the wires I and III, placed nearer the outside of the wire, show the breakdown of superconductivity already at 18 oersteds.

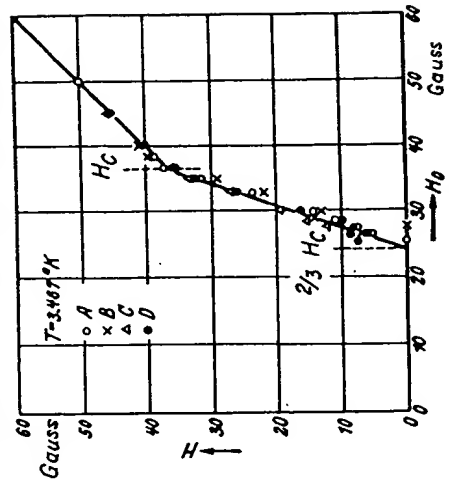
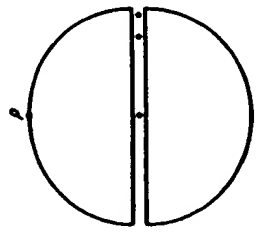


Fig. 19-4. Cross section of a tin sphere cut across an equatorial plane with bismuth wires inserted at the points shown. (After W. J. de Haas and O. A. Guineau.)

Fig. 19-5. Magnetically induced isothermal transition from super- to normal conduction in a single crystal tin sphere. Points marked A, B, C represent magnetic field strengths shown by the bismuth probes of Fig. 19-4, D the field strength at the pole P of the sphere.

The theory has been confirmed more exactly for the case of a sphere where, according to Chap. 18 (b) the critical value should be $H^0 = 2 H_c/3$. de Haas and Guineau⁶ cut a tin sphere (1.65 cm in diameter) into two hemispheres and placed them 0.03 mm apart (Fig. 19-4). In the space between the two halves they placed three bismuth wires, one in the center, the second 0.55 cm and the third 0.75 cm from the center. The field strengths calculated from the resistance decrease in the bismuth wires are shown in Fig. 19-5 as a function of H^0 which in this experiment was perpendicular to the plane of the cut. The magnetic field strength at the pole P of the sphere is also plotted. All four curves coincide exactly. They start at 24 oersteds, and at 36 oersteds they join the straight line $H = H^0$, indicating that the protective influence of the tin sphere has completely disappeared. Thus the critical value H_c is 36 oersteds, and the limiting value H^0 for superconductivity is $2/3 H_c$.

⁶W. J. de Haas and O. A. Guineau, *Physica*, 8, 182 (1936).

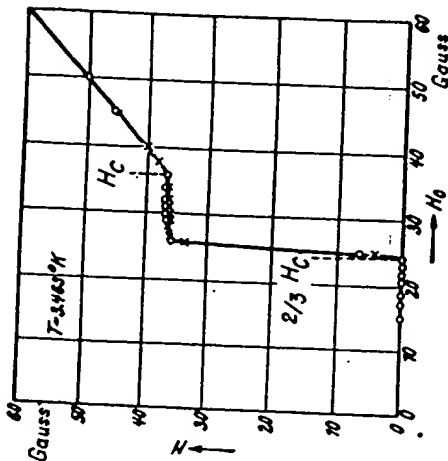


Fig. 19-6. Magnetically induced isothermal transition from super- to normal conduction of a single crystal tin sphere. The field strengths are measured in a hole bored through the center of the sphere parallel to the field.

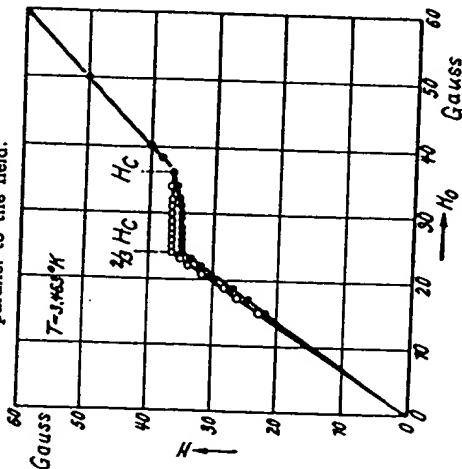


Fig. 19-7. Magnetically induced isothermal transition from super- to normal conduction in a single crystal tin sphere. \circ -field strength exactly on the equator of the sphere; \bullet -field strength at a point on the plane of the equator slightly outside the sphere.

This is further confirmed by experiments presented in Fig. 19-6, in which the bismuth wires were placed inside a channel parallel to the field through the center of the sphere to measure the field penetration. The field jumps almost discontinuously to the value 36 oersteds when the external field reaches the value 24 oersteds, and remains practically constant until H^0 also reaches the value 36 oersteds. From then on the sphere no longer disturbs the field, and it follows the line $H = H^0$.

Figure 19-7 explains why the field jumps immediately to 36 oersteds in spite of the fact that H^0 is still smaller than this value. In this experiment two bismuth wires were placed in the equatorial plane, one exactly on the equator of the sphere (which was not cut like the one in Fig. 19-6), the other a little above the surface of the sphere. In this case the measured field H follows a straight line $H = 3H^0/2$ and shows the intensification of the field at the equator of a superconducting sphere [Chap. 11 (b)]. At $H^0 = 24$, and $H = 36$ oersteds, however, the superconductivity breaks down, and H at first remains constant at this value as shown in Fig.

19-6. As soon as H^0 also reaches 36 oersteds the undisturbed field H^0 exists throughout the sphere, as shown again in this diagram.

The experiments represented in Figs. 19-4 and 19-5 have been repeated by Meshkowsky and Shalnikov⁷ with a considerably narrower slit. Also instead of three fixed bismuth wires they used a movable bismuth probe which they displaced continuously along the diameter, registering field strengths at each position. For wider slits and relatively thick bismuth probes they confirmed the results of Fig. 19-5. But with an especially thin slit, namely, 1.2×10^{-2}

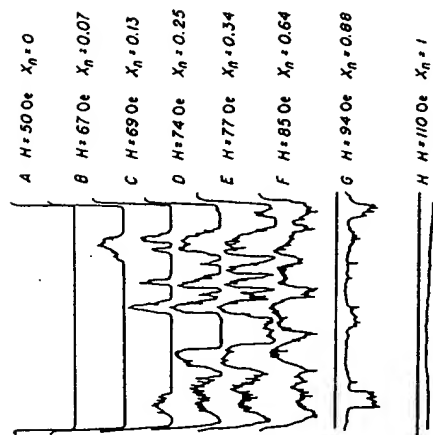


Fig. 19-8. Magnetic field strength as function of position within a narrow equatorial slit in a single crystal tin sphere measured by movable bismuth probes, according to Meshkowsky and Shalnikov.

The authors emphasize the fact that it is impossible to reproduce the curves exactly, although their general character remains the same with repeated experiments. The irregularity of the intermediate state is demonstrated by the accidental form of the field distribution.

⁷A. Meshkowsky and A. Shalnikov, *J. Physics (U.S.S.R.)* 11 (1947).

CHAPTER 20

A Nonlinear Extension of the Theory¹

(a) According to Chap. 17 the breakdown of superconductivity becomes inevitable for thermodynamic reasons as soon as the energy density $\frac{1}{2}(\mathbf{i} \cdot \mathbf{G})$ reaches the critical value $[(N - f_s)/V]$ at any point of the surface, the transformation into the normally conducting phase starting at that point (eq. 17-4). For a "thick" superconductor, we can, according to eq. 7-37 put $\frac{1}{2}(\mathbf{i} \cdot \mathbf{G}) = \frac{1}{2}H_0^2$ and this leads to the critical value of the magnetic field strength given by eq. 17-5. However, the atomic theory of superconductivity recently developed by Heisenberg² leads to the idea of a maximum density of the supercurrent that cannot be exceeded because of quantum theoretical restrictions. The question arises: Is this a new stability condition for the superconducting phase? Is the breakdown of superconductivity possible from within, and how is this related with thermodynamics?

The maximum current density I_m like the critical magnetic field strength H_c must be a function of temperature. They are both zero at the transition temperature T_c . Also I_m is zero at absolute zero temperature and has a maximum, according to current estimates, in the neighborhood of $\frac{1}{2}T_c$. According to Chap. 1, Fig. 1-4, the critical field H_c increases continuously with decreasing temperature. This different behavior emphasizes the importance of the following question: If the maximum current density, and therefore for a wire of given thickness the maximum total current, decreases toward zero with decreasing temperature, how can the supercurrent produce the field strength at the surface required by thermodynamics for the breakdown of superconductivity?

There is no upper limit to the current density in the theory so far presented in this book. We shall make it possible to include such a maximum current by means of a nonlinear extension of the theory without sacrificing very many of its results. This step was also suggested by the fact that experimentalists have for some time doubted whether the penetration depth of a transverse field in a wire is actually independent of the field strength in the manner required for the theory of Chap. 9.*

¹Compare the following references:

M. v. Laue, *Ann. Physik*, (6) 5, 197, 1949.

W. Heisenberg, (a) *Z. Naturforsch.*, 2a, 185 (1947); (b) *Z. Naturforsch.*, 8a, 65 (1948); (c) *Göttingen Nachr. Math.-Physik. Klasse*, 1947, p. 23; (d) *Ann. Physik*, 8, 289 (1948).

H. Koppe, (a) *Z. Naturforsch.*, 4a, 79 (1949); (b) *Ergeb. exakt. Naturw.*, 28, 283, (1950).

*See Heisenberg reference in footnote 1.

* Compare A. B. Pippard, *Proc. Roy. Soc. A* 208, 195, 210, (1950).

(b) We shall not change any of the fundamental equations enumerated in Chap. 3 except the relation between supercurrent density \mathbf{i} and the supercurrent momentum \mathbf{G} , i. e., we abandon eqs. VIII and VIII a, but retain all the other equations indicated by roman numerals. The new relation will be left open to a considerable extent, it being required only that it shall be uniquely reversible and go over to the linear relation VIII (or VIII a) for sufficiently weak currents; that a change of sign of \mathbf{i} shall cause a change of sign of \mathbf{G} , and the angle between \mathbf{i} and \mathbf{G} shall always be acute so that

$$(\mathbf{i} \cdot \mathbf{G}) > 0 \quad (20-1)$$

For a given direction of \mathbf{i} the absolute value of \mathbf{G} and the absolute value of \mathbf{i} increase simultaneously.

The most important restriction, however, arises from the energy principle. Equation 5-4 can be taken over immediately, and by eq. IX we can put in that equation

$$(\mathbf{E} \cdot \mathbf{i}) = \left(\mathbf{i} \cdot \frac{\partial \mathbf{G}}{\partial t} \right) \quad (20-2)$$

We require that the integral

$$F' \equiv \int \left(\mathbf{i} \cdot \frac{\partial \mathbf{G}}{\partial t} \right) dt \quad (20-3)$$

shall depend only on the final supercurrent density when the latter is zero at the beginning, being independent of the intermediate states through which it has passed. Owing to the assumption of unique reversibility of the relation between \mathbf{i} and \mathbf{G} we can also state that F' depends only on the momentarily existing supercurrent momentum \mathbf{G} , or alternatively, that the integral

$$F' = \int_0^G (\mathbf{i} \cdot d\mathbf{G}) \quad (20-4)$$

shall be independent of the path of integration in \mathbf{G} -space. Otherwise the theory would lead to energy transformations within the superconductor contradictory to observation. Under these conditions eq. 20-4 becomes the definition of the density of free energy F' associated with the supercurrent. The mathematical expression for these conditions is:

$$\frac{\partial G_\alpha}{\partial G_\beta} - \frac{\partial F'}{\partial G_\beta} = 0 \quad (\alpha, \beta = 1, 2, 3) \quad (20-5)$$

This ensures that the integral appearing in the equation

²In the integrand it is to be understood that \mathbf{i} and \mathbf{g} are variables of integration that assume the values \mathbf{i} and \mathbf{g} at the upper limit. The relation between \mathbf{i} and \mathbf{g} is naturally the same as between \mathbf{i} and \mathbf{G} .

$$F_i = (i \cdot G) - \int_0^i (g \cdot i) \quad (20-6)$$

shall be independent of the path of integration in l_a space and leads to conditions equivalent with eq. 20-5, namely,

$$\frac{\partial G_a}{\partial l_i} - \frac{\partial G_i}{\partial l_a} = 0 \quad (\alpha, \beta = 1, 2, 3) \quad (20-7)$$

From eq. 20-1 it then follows that

$$F_i > 0 \quad (20-8)$$

Equation 20-4 may now be integrated in G_a space along the straight line that connects the origin (zero G) with the end of the vector G . On this line increments dG_a are proportional to G_a and have the same sign, so that $(i \cdot dG) > 0$ along the whole path. The same argument applied to the l_a space proves that the integral in eq. 20-6 is positive. It therefore follows that

$$F_i < (i \cdot G) \quad (20-9)$$

The surfaces $F_i = \text{constant}$ will be closed shells in both G_a space and in l_a space. They will have the same symmetry as that of the crystal class about the origin as center. As long as the linear approximation VIII holds, eq. 20-7 goes over into the symmetry condition $\lambda_{\alpha\beta} = \lambda_{\beta\alpha}$, and the surfaces are ellipsoids or spheres for the cubic system. In the general case they have less simple forms, and in general i and G are different in direction even for the cubic system. If i happens to coincide in direction with an axis of rotation, G must do the same because of the uniqueness of their relationship. Of course this is true for any crystal class.

The possibility cannot be excluded that there exists a surface in l_a space, at a finite distance from the origin, corresponding to infinite free energy $F_i = \infty$. The vector i could then never grow beyond that surface, and there would exist a maximum current density dependent on direction. At such a surface G would also become infinite, for otherwise F_i must remain finite by eq. 20-9. Under these circumstances the energy principle (compare eq. 5-5) takes the form

$$\frac{\partial}{\partial t} \left\{ \frac{1}{2} E^2 + \frac{1}{2} H^2 + F_i \right\} + (i^0 \cdot E) + c \operatorname{div} [E \times H] = 0 \quad (20-10)$$

Just as in Chap. 5, we can conclude from this that space charges in a superconductor compensate each other in a short time, or move to the surface until the total density $\rho = \rho^0 + \rho'$ vanishes. We do not learn anything from this theory about ρ' itself.

By integrating the integral in eq. 20-6 along the same straight line in l_a space one can put

$$(g \cdot i) = \left[\frac{(g \cdot i)}{|i|} \right] d|i|$$

For the linear theory the component $(g \cdot i)/|i|$ of the vector g in the direction i becomes proportional to $|i|$, as shown by the straight line in Fig. 20-1. We then find (in agreement with eq. 5-6)

$$\int_0^i (g \cdot di) = \frac{1}{2} (G \cdot i), \quad F_i = \frac{1}{2} (G \cdot i)$$

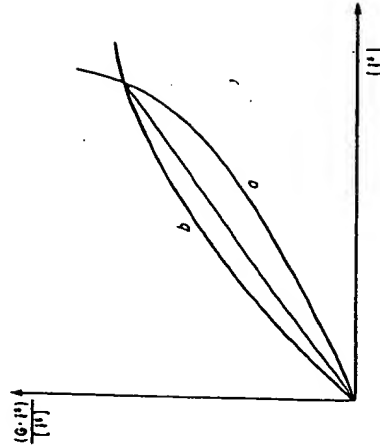


Fig. 20-1. Schematic representation of the types of nonlinear relations between supercurrent momentum G and supercurrent density i . Abscissa: magnitude of the supercurrent i . Ordinate: component of supercurrent momentum in direction of the supercurrent.

In the nonlinear theory the relation between $(g \cdot i)/|i|$ and $|i|$ can be represented for example by a curve of the type a in Fig. 20-1. Then clearly

$$\int_0^i (g \cdot di) < \frac{1}{2} (G \cdot i), \quad F_i > \frac{1}{2} (G \cdot i) \quad (20-11)$$

while for a curve of the type b in Fig. 20-1 we would have

$$\int_0^i (g \cdot di) > \frac{1}{2} (G \cdot i), \quad F_i < \frac{1}{2} (G \cdot i) \quad (20-12)$$

The existence of a maximum current density corresponds to the case a because here G increases more rapidly than proportional to i .

(c) We now have to find out to what extent the results of the linear theory still apply, and we start with the Meissner effect.⁴

⁴The equation 7-4 is still valid because in proving it the relation between G and i is never used. However we cannot take over the proof of the uniqueness theorem following eq. 7-4 because the difference field between two possible fields is no longer itself a possible field, i. e., one that satisfies the fundamental equations.

Let us first consider, as in Chap. 7, the stationary state with all field quantities depending only on x_3 . Because of $\text{div } \mathbf{r} = 0$ and $\text{div } \mathbf{H} = 0$, we get as before $i_3' = 0$, $H_3 = 0$, but G_3 is generally different from zero. Equation X, under this assumption, yields

$$-c \frac{dG_1}{dx_3} = H_3, \quad c \frac{dG_2}{dx_3} = H_1 \quad (20-13)$$

whereas from II,

$$-i_1' = c \frac{dH_2}{dx_3}, \quad i_3' = c \frac{dH_1}{dx_3} \quad (20-14)$$

Elimination of H leads to the partial differential equations

$$c^2 \frac{d^2 G_1}{dx_3^2} = i_1', \quad c^2 \frac{d^2 G_2}{dx_3^2} = i_3' \quad (20-15)$$

in which G_1 and G_2 have to be regarded as functions of i_1' and i_3' respectively. These equations replace the former differential equation $\Delta u - \beta^2 u = 0$. Taking the product of the first of these with G_1 and the second with G_2 and adding the results we obtain

$$G_1 \frac{d^2 G_1}{dx_3^2} + G_2 \frac{d^2 G_2}{dx_3^2} = \frac{1}{c^2} (i_1' \cdot G)$$

and by eq. 20-13:

$$\frac{d^2}{dx_3^2} (G_1^2 + G_2^2) = \frac{2 (i_1' \cdot G)}{c^2} + \left(\frac{dG_1}{dx_3} \right)^2 + \left(\frac{dG_2}{dx_3} \right)^2 \quad (20-16)$$

On the other hand, if we multiply the left-hand equations of 20-13 and 20-14 together, and also the right-hand equations, and add the results, we find, by using eq. 20-4 that

$$\frac{dF_1}{dx_3} = \frac{1}{2} \frac{d(H^2)}{dx_3} \quad (20-17)$$

or, by introducing an arbitrary integration constant C ,

$$F_1 = \frac{1}{2} H^2 - C \quad (20-18)$$

Using eqs. 20-18 and 20-15 gives

$$\frac{d^2}{dx_3^2} (G_1^2 + G_2^2) = \frac{2}{c^2} [(i_1' \cdot G) + F_1 + C] \quad (20-19)$$

Here $(i_1' \cdot G)$ and F_1 are to be regarded as known functions of i_1' and i_3' just as are G_1 and G_2 .

In order to discuss eq. 20-19, we now write z for x_3 and put $G_1^2 + G_2^2 \equiv u(z)$. According to eq. 20-16 $u'' > 0$, so the curve of $u(z)$ is everywhere concave upwards. To within the linear approximation $(i_1' \cdot G)$ as well as F_1 are proportional to $(G_1^2 + G_2^2)$, the proportionality factor depending on the ratio G_1/G_2 . In any case, on this approximation eq. 20-19 assumes the form

$$u'' = A^2 (u + C')$$

where A is a constant and C' another constant proportional to C . The solution in terms of another integration constant B is

$$u + C' = B \exp [\pm A (z - z_0)]$$

We use the lower sign and choose $C = 0$, therefore also $C' = 0$. Then u and therefore also G_1 and G_2 approach zero with increasing z . By eqs. 20-13 and 20-14 i_1' and H decrease exponentially with increasing z , in agreement with Chap. 7. However, $(G_1^2 + G_2^2)$ increases in the negative z direction because of the positive u'' , finally without limit. It depends upon the relation between i_1' and G whether u increases without limit at a finite z or only at infinite z . In any case we can, by choosing a suitable value for z_0 , arrange for $H^2 = c^2 [(dG_1/dx_3)^2 + (dG_2/dx_3)^2]$ to have any prescribed value H_0^2 at $z = x_3 = 0$. To obtain also a prescribed direction for H at the origin we must also be free to choose the ratio G_1/G_2 at any point appropriately.

Let the superconductor occupy the half space $x_3 > 0$ as in Chap. 7, while a homogeneous magnetic field H^0 exists where $x_3 < 0$. Then the solutions just discussed will yield the Meissner effect, i. e., the restriction of the magnetic field in the superconductor to a protecting layer close under the surface.

For a plane parallel plate of finite thickness, C differs from zero. Indeed $C < 0$ if a current is passed through the plate without producing an additional magnetic field. Then $H = 0$ exactly at the center of the plate, by symmetry, but i_1' and with it F_1 are different from zero. If instead we prescribe that the magnetic field H^0 shall be the same at the two surfaces without passing a current through it, then $i_1' = 0$ but H differs from zero and therefore $C > 0$ at the middle.⁵

⁵H. Koppe (see footnote 1) integrated the differential equation under the arbitrary assumption that

$$G = \frac{\lambda \mu}{\sqrt{1 - \mu^2/i_m^2}}$$

His result is represented in Fig. 20-2, which shows the field distribution in the superconducting half of space, $z > 0$. In this figure

$$i = \frac{|i_1'|}{i_m}, \quad h = \frac{H}{\sqrt{\lambda} i_m}, \quad \varepsilon = \frac{C}{c \sqrt{\lambda} i_m}, \quad w = \frac{F_1}{\lambda i_m^2}$$

the unit for x_3 is $\exp \sqrt{\lambda}$. The boundary surface of the superconductor has to be so chosen that it coincides with the prescribed value of H^0 . If this value is comparatively small, the boundary lies fairly far to the left in the diagram and the field quantities decrease exponentially with increasing x_3 . If H^0 is relatively large, the boundary lies far to the right and the current density in the protecting layer is not much less than i_m over a wide region.

(d) In a cylinder carrying a current (Chap. 8) the situation becomes rather complicated unless the direction of the current coincides with a crystallographic axis of rotation, so that, by section (b), the vectors \mathbf{G} and \mathbf{i} are parallel. In this case we can use simply the magnitudes G and i .

Introducing cylindrical coordinates as in Chap. 8, G and i become functions of the radius vector only. The same is true of the component of the magnetic field H_θ in the θ direction. Equation X then yields,

$$\frac{dG}{dr} = H_\theta \quad (20-20)$$

and from eq. II, (compare eq. 8-1)

$$i = \frac{c}{r} \frac{d(r H_\theta)}{dr} \quad (20-21)$$

We proceed as in section (c). Eliminate H and multiply the last two equations, and we then obtain

$$\frac{d}{dr} \left(r \frac{dG}{dr} \right) = \frac{2r}{c^2} (G i + H_\theta^2) \quad (20-22)$$

i. e.,

$$r \frac{dG}{dr} = \frac{2}{c} \int_0^r r (G i + H_\theta^2) dr$$

and after integration

$$F_i = \frac{1}{2} H_\theta^2 + \int_0^r \frac{H_\theta^2}{r} dr + F_\theta^i \quad (20-23)$$

The integration constant F_θ^i represents the energy density at the axis $r = 0$. According to eq. 20-22, $dG/dr > 0$, and this represents the Meissner effect.

Apply eq. 20-23 at the surface of the wire ($r = R$) where the field is H^0 . If R is large compared with a suitably defined penetration depth d , then the integral is at most of the order of magnitude $(H^0)^2 d/R$, and therefore small compared with $\frac{1}{2} (H^0)^2$. The same is true of F_i . Consequently just as in eq. 20-18 where $C = 0$ for the "thick" superconductor,

$$F_i = \frac{1}{2} (H^0)^2 \quad (20-24)$$

However, it is possible for $F_i \gg \frac{1}{2} (H^0)^2$, if $F_\theta^i \gg \frac{1}{2} H_\theta^2$, i. e., if the current is more or less uniformly distributed over the cross section of the cylinder.

(e) London's theorems concerning persistent currents (eqs. 12-11 and 12-13) remain unchanged. The proof of these equations does not use any relation between G and i . Likewise eq. 12-21 is still valid; the left-hand side is still positive for any really existing field even though it no longer represents the total free energy of the field. Thus on the nonlinear theory there still exist no magnetic fields that are not produced by one of the three following causes: annular currents in a superconductor, ohmic currents in

a normal conductor, and permanent magnetism. The proof that these causes determine the field uniquely cannot be given in the same way as in Chap. 12, because now the difference field is no longer a possible field as it was in the linear theory.

(f) Sections (c) to (e) show how little the nonlinear theory differs from the linear one for stationary fields. It is difficult to decide between them on the basis of experimental evidence at present available. The decisive question is whether on the nonlinear theory there also exists a stress tensor Θ , depending on the supercurrent density as in Chap. 13 and exerting a volume force on a homogeneous superconductor that exactly cancels the force due to the Maxwell stress tensor. The fact that the resistance vanishes demands this unequivocally.

We now proceed to prove the impulse theorem 13-10 for the nonlinear theory. The force equation

$$\Theta_{\alpha\beta} = i_\beta^i G_\alpha - \delta_{\alpha\beta} F_i \quad (20-25)$$

provides the required proof, because actually it does not differ from eq. 13-1 if we write $P = i$, $Q = G$, because then $F_i = \frac{1}{2} \sum i_\alpha^i G_\alpha$. The proof follows the earlier calculation of $\text{div } \Theta$. The x_1 component of this vector is defined in eq. 13-3, and we have to put

$$\Theta_{11} = i_1^i G_1 - F_i, \quad \Theta_{12} = i_2^i G_1, \quad \Theta_{13} = i_3^i G_1 \quad (20-26)$$

The differential coefficient $\partial F_i / \partial x_1$ appears in the result.

F_i depends both on i and on certain parameters p_n which are present also in the relation between G and i . The p_n 's are functions of the temperature and differ from substance to substance. Whenever the superconductor is inhomogeneous, whether due to temperature differences or to differences in chemical composition (as in alloys at soldered boundaries), the p_n 's are functions of the coordinates x . From eq. 20-4 it therefore follows that

$$\frac{\partial F_i}{\partial x_1} = \sum_\alpha i_\alpha^i \frac{\partial G_\alpha}{\partial x_1} + \sum_{n,\gamma} \frac{\partial p_n}{\partial x_1} \int_0^G \left(\frac{\partial i_\gamma}{\partial p_n} \right) d\epsilon_\gamma$$

The suffix g indicates differentiation at constant g . Using eq. 20-26 the calculation yields

$$\text{div}_1 \Theta = \sum_{n=1}^{10} B_n$$

where

$$B_1 = i_1^i \frac{\partial G_1}{\partial x_1}, \quad B_2 = G_1 \frac{\partial i_1^i}{\partial x_1}, \quad B_3 = -i_1^i \frac{\partial G_1}{\partial x_1}$$

$$B_4 = -i_2^i \frac{\partial G_2}{\partial x_1}, \quad B_5 = -i_3^i \frac{\partial G_3}{\partial x_1}$$

$$B_6 = - \sum_{n,\gamma} \frac{\partial p_n}{\partial x_1} \int_0^G \left(\frac{\partial i_\gamma}{\partial p_n} \right) d\epsilon_\gamma$$

$$B_7 = i_2' \frac{\partial G_1}{\partial x_3}, \quad B_8 = G_1 \frac{\partial i_2'}{\partial x_3}$$

$$B_9 = i_3' \frac{\partial G_1}{\partial x_3}, \quad B_{10} = G_1 \frac{\partial i_3'}{\partial x_3}$$

One sees at once that

$$B_1 + B_9 = 0, \quad B_2 + B_8 + B_{10} = G_1 \operatorname{div} i'$$

$$B_4 + B_7 = -i_2' \operatorname{curl}_3 G, \quad B_5 + B_6 = i_3' \operatorname{curl}_2 G$$

Therefore

$$\operatorname{div} \Theta = G \operatorname{div} i' - [i' \times \operatorname{curl} G] - \sum_{n,\gamma} \operatorname{grad} p_n \int_0^{\Theta} \left(\frac{\partial i_\gamma}{\partial p_n} \right) d\epsilon_\gamma \quad (20-27)$$

This agrees with eq. 13-5 apart from the form of the term representing inhomogeneity. The argument following eq. 13-5 in Chap. 13 does not make use of the relation between G and i' , and therefore applies in the present case and leads to the impulse theorem (compare eq. 13-10)

$$-\operatorname{div} [T(E) + T(H) + \Theta] = \rho^0 E + \frac{1}{c} [i^0 \times H] +$$

$$+ \sum_{n,\gamma} \operatorname{grad} p_n \int_0^{\Theta} \left(\frac{\partial i_\gamma}{\partial p_n} \right) d\epsilon_\gamma + \frac{\partial}{\partial t} \left[\frac{1}{c} [E \times H] + \rho^0 G \right] \quad (20-28)^a$$

The whole discussion that follows the impulse theorem concerning the volume forces and the torque due to asymmetry of the tensor

$$\Theta_{33} - \Theta_{33} = [G \times i']_1, \text{ etc.}$$

remains valid here. The new fact that arises is that this asymmetry appears now even in cubic crystal superconductors, at least when we go beyond the region where the linear approximation is sufficient.

(g) Differences from the linear theory appear when we discuss the individual stress components. If we choose the x_1 direction parallel to i'

^aFrom eq. 20-8 it follows by differentiation with respect to p_n at constant i' and G that

$$\sum_{\gamma} \int_0^{\Theta} \left(\frac{\partial i_\gamma}{\partial p_n} \right) d\epsilon_\gamma = - \sum_{\gamma} \int_0^{\Theta} \left(\frac{\partial \epsilon_\gamma}{\partial p_n} \right) di_\gamma$$

The third term on the right-hand side of eq. 20-28 can therefore also be written in the alternative form given by M. von Laue (footnote 1)

$$- \sum_{n,\gamma} \operatorname{grad} p_n \int_0^{\Theta} \left(\frac{\partial \epsilon_\gamma}{\partial p_n} \right) di_\gamma$$

at some point in space, four of the nine components of Θ vanish there and the others have the values:

$$\Theta_{11} = (i' \cdot G) - F', \quad \Theta_{22} = \Theta_{33} = -F', \quad \Theta_{21} = i_1' G_2, \quad \Theta_{31} = i_1' G_3 \quad (20-29)$$

The components Θ_{21} and Θ_{31} also vanish if i' and G are parallel, and then the current line is, just as before, one of the principal axes of rotational symmetry of the tensor Θ . A tension F' acts perpendicular to the current line, and a pressure acts along it because $\Theta_{22} = \Theta_{33} < 0$ while $\Theta_{11} > 0$ according to eqs. 20-8 and 20-9. However, the pressure is no longer equal to the tension, but, by eq. 20-11 is smaller than the tension when G and i' are related as in curve a of Fig. 20-1, and greater for the curve b .

In any case, according to eq. 20-29 a supercurrent flowing parallel to the surface of a superconductor must exert a force that has both a tangential and a normal component across the surface into the interior amounting to F' per unit area. The work done by this field upon a surface element $d\sigma$ displaced a distance ∂u toward the interior of the superconductor amounts therefore to $F' d\sigma \partial u$. Therefore the thermodynamic equilibrium condition at the boundary between normally and superconducting phases of the same substance is (compare Chap. 17)

$$F' = \frac{(i' \cdot G)}{V} \quad (20-30)$$

while at the free (outside) surface of the superconductor

$$F' \leq \frac{(i' \cdot G)}{V} \quad (20-31)$$

In so far as $F' = \frac{1}{2} (i' \cdot G)$ this agrees with eqs. 17-3 and 17-4.

For very thick specimens we can write $\frac{1}{2} (H^0)^2$ for F' , by eq. 20-24 and so get exactly the form 17-6 and 17-7 for the equilibrium conditions. As the whole of the thermodynamics of this transition can be derived from this condition, according to Chap. 17, it remains unaffected by altering the electrostatics in the above manner. For a plate of finite thickness however $C > 0$ in eq. 20-18 by section (c). If the magnetic field on both sides of the plate has the critical value H_c , then by eq. 20-31, F' at the boundary has a lower value than the critical one. We then have to increase the external field to bring F' to its critical value, i. e., for thin superconductors the critical field strength is greater than for thick ones. This agrees qualitatively with the results of Chap. 18, which however no longer hold quantitatively in the nonlinear theory. The results depend on the relation between G and i' so that it should in principle be possible to derive conclusions about this relation from experimental data on the dependency of the critical magnetic field on the thickness of the plate.

(h) We now turn to the case where there does exist a maximum current density i_m , i. e., the family of surfaces in i' space converge upon a finite surface on which F' becomes infinite.

We consider first the superconductor of section (c), occupying half of space. If i_1' at the surface is only a little below i_m , while $i_2' = 0$ (this can

always be done by choosing the appropriate direction for the coordinates x_1 and x_2 , then by eq. 20-15 G_1 decreases with increasing x_3 , but not as in Chap. 7 (exponentially in one way or another) but much more slowly, approximately in the form of a parabola. By eq. 20-13 H_s thus becomes a linear function of x_3 (compare Fig. 20-2), and this causes the protecting layer to become thicker than on the linear theory. As a matter of fact, to completely shield the field H^0 the Maxwell theory would require a total surface current cH^0 , and this, when the current density is limited, would have to be distributed over a thicker protecting layer. The penetration depth therefore becomes greater than in the linear theory and dependent on H^0 .

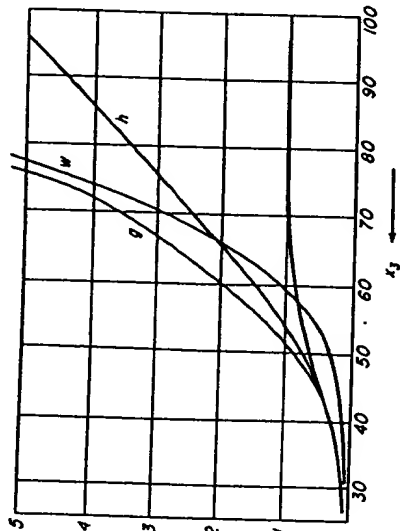


Fig. 20-2. Field distribution in the superconductor filling half space $x_3 > 0$ according to Koppe (see footnote 1, Chapter 20). Abscissa: x_3 in units of $\exp \sqrt{\lambda}$. Ordinate:

$$i = |E|/i_m, \quad h = H/\sqrt{\lambda} i_m, \\ g = C/c \sqrt{\lambda} i_m, \quad w = F^2/\lambda i_m^2$$

When a cylinder of radius R (section d) carries a current, the field H^0 at the surface is definitely less than the value $R i_m/2c$ that would exist if the current density were equal to i_m over the whole cross section. In spite of this limitation on H^0 , F^2 can by eq. 20-23 attain any value at the surface, including the critical value given by eq. 20-31, so long as F^0 already has approximately this value, i. e., so long as the current is somewhat uniformly distributed over the cross section.⁷ But F^2 is nowhere so great as it is at the surface, and it is there that the greatest danger to the superconductivity lies, and it is also there that the breakdown starts as soon as F^2 reaches the critical value. This is true no matter how great the critical value may

⁷ The same conclusion can be drawn from eq. 20-18 with $C < 0$.

be or how small the maximum current density. The upper limit of the current density is therefore not a new condition for the stability of the supercurrent; the thermodynamic relations 20-30 or 20-31 are still necessary and sufficient.⁸

(⁸) Although the nonlinear theory agrees at least qualitatively, and in many important problems even quantitatively, with the linear theory for all stationary fields, in discussing oscillatory fields the linear theory can only be regarded as an approximation for oscillations of sufficiently small amplitude.

APPENDIX

Proof of Equation 14-8

If matter undergoes an arbitrary but continuous displacement ∂u then the change δP of an arbitrary vector P at a moving (material) point is related with the change δP at a given point in space through the equation

$$\delta P_a = \partial P_a + \sum_y \partial u_y \frac{\partial P_a}{\partial x_y} + \frac{1}{2} [P \times \text{curl } \partial u]_a$$

Therefore

$$\begin{aligned} d(P_a P_b) &= \partial(P_a P_b) + P_a \left\{ \sum_y \partial u_y \frac{\partial P_b}{\partial x_y} + \frac{1}{2} [P \times \text{curl } \partial u]_b \right\} \\ &\quad + P_b \left\{ \sum_y \partial u_y \frac{\partial P_a}{\partial x_y} + \frac{1}{2} [P \times \text{curl } \partial u]_a \right\} \end{aligned} \quad (a)$$

$P_a P_b$ are the components of a symmetrical tensor, say t_{ab} . For the most general formulation of the symmetrical tensor we have to combine three noncoplanar vectors P, Q, R as follows:

$$P_a P_b + Q_a Q_b + R_a R_b$$

The two additional terms do not alter the form of the transformation of $d t_{ab}$ into ∂t_{ab} , so we confine ourselves to the definition

$$t_{ab} = P_a P_b$$

Transcribing (a) we then have

$$d t_{11} = \partial t_{11} + \sum_y \partial u_y \frac{\partial t_{11}}{\partial x_y} + \frac{1}{2} (t_{12} \text{curl}_3 \partial u - t_{13} \text{curl}_2 \partial u)$$

⁸ According to the above considerations (see M. von Laue, footnote 1), Silsbee's hypothesis [compare Chap. 1 (e)] is now valid only for sufficiently "thick" superconductors.

$$d\ell_{23} = \partial\ell_{23} + \sum_{\gamma} \partial u_{\gamma} \frac{\partial \ell_{23}}{\partial x_{\gamma}} + \frac{1}{2} \{ (\ell_{33} - \ell_{22}) \text{curl}_1 \partial u + \ell_{13} \text{curl}_2 \partial u - \ell_{12} \text{curl}_3 \partial u \}$$

etc.

Just as in Chap. 14 we now assume that all the $d\ell_{\alpha\beta}$'s are zero so that

$$\begin{aligned} \partial\ell_{11} &= - \sum_{\gamma} \partial u_{\gamma} \frac{\partial \ell_{11}}{\partial x_{\gamma}} - \frac{1}{2} (\ell_{13} \text{curl}_2 \partial u - \ell_{12} \text{curl}_3 \partial u) \\ \partial\ell_{23} &= - \sum_{\gamma} \partial u_{\gamma} \frac{\partial \ell_{23}}{\partial x_{\gamma}} + \frac{1}{2} \{ (\ell_{22} - \ell_{33}) \text{curl}_1 \partial u - \ell_{12} \text{curl}_2 \partial u + \ell_{13} \text{curl}_3 \partial u \} \end{aligned} \quad (b)$$

Let Q be another arbitrary vector. In (b) collect all the terms with $\text{curl}_1 \partial u$, all those with $\text{curl}_2 \partial u$ and all those with $\text{curl}_3 \partial u$, and obtain

$$\begin{aligned} \frac{1}{2} \sum_{\alpha\beta} Q_{\alpha} Q_{\beta} \partial\ell_{\alpha\beta} &= \frac{1}{2} Q_1^2 \partial\ell_{11} + \dots + Q_2 Q_3 \partial\ell_{23} + \dots = \\ &- \frac{1}{2} \sum_{\alpha\beta\gamma} Q_{\alpha} Q_{\beta} \frac{\partial \ell_{\alpha\beta}}{\partial x_{\gamma}} \partial u_{\gamma} \\ &+ \frac{1}{2} \{ \text{curl}_1 \partial u [(Q_3^2 - Q_2^2) \partial\ell_{33} + Q_1 Q_3 \ell_{12} - Q_1 Q_2 \ell_{13} + Q_2 Q_3 (\ell_{22} - \ell_{33})] \\ &+ \text{curl}_2 \partial u [\text{a similar factor to the above}] \\ &+ \text{curl}_3 \partial u [\text{a similar factor to the above}] \} \end{aligned}$$

This equation can be simplified by introducing the following vector:

$$R_{\alpha} \equiv \sum_{\beta} \ell_{\alpha\beta} Q_{\beta}$$

We then obtain

$$\frac{1}{2} \sum_{\alpha\beta} Q_{\alpha} Q_{\beta} \partial\ell_{\alpha\beta} = - \frac{1}{2} \sum_{\alpha\beta} Q_{\alpha} Q_{\beta} (\partial u \cdot \nabla \ell_{\alpha\beta}) + \frac{1}{2} (\text{curl} \partial u \cdot [R \times Q]) \quad (c)$$

Finally writing ℓ in place of Q , G for R and $\ell_{\alpha\beta}$ for $\ell_{\alpha\beta}$ we confirm eq. 14-8.

INDEX

- | | |
|--------------------------------------|--------------------------------------------------|
| Acceleration theory, 18 | Magnetic field |
| Bessel equation, 35 | — critical value, 4, 6, 105, 112, 120, 126 |
| — functions, 36 | — at transition temperature, 108 |
| Cathode rays, 19, 20 | — temperature dependence, 5, 108 |
| Crystals, and superconduction, 15—17 | — thin superconductors, 27, 112—120, 135 |
| Debye's law, 110 | — distortion, 7, 112 |
| Eddy currents, 102 | — circular cylinder, 55 |
| Electrons mean free path, 102, 103 | — sphere, 58 |
| Energy, 20—22 | — external, penetration of, 121 |
| — electric, 9 | — in superconductors, 6—8, 30 |
| — free, 22, 104; 106 | — intensification factor, 112 |
| — density, 127—137 | — moment, 70 |
| — temperature dependence, 106 | Maxwell equations, 13 |
| — magnetic, 9 | — from least action principle, 9, 10 |
| — total density, 21 | Maxwell-London theory, 12 |
| Entropy, 106, 107 | Maxwell stresses, 75—84 |
| Equilibrium conditions, 105, 109 | — and torque, 82, 84 |
| — stable, 71 | — tensors of, 77 |
| Extinction coefficient, 92 | Maxwell theory, 6 |
| Hankel function, 44 | Meissner effect, 7, 27, 30, 66, 80, 106, 129—132 |
| Induction, coefficient, 12, 14 | — and skin effect, 94 |
| — equations, 9, 11 | — superconducting states, 107 |
| Kirchhoff's rule 8, 9 | — disappearance of, 121 |
| Lattice structure 4 | Momentum law, equation of, 78 |
| — and conducting phase, 103 | Multiply connected region, 62 |
| Lines of force, for sphere, 60 | Nernst theorem, 106, 108 |
| — thin cylinder, 52 | Ohmic current, 106 |
| London's fundamental equations, 14 | — distribution in superconductor, 72 |
| — relativistic form, 14 | — existence of, 94 |
| London stresses, 75—84, 118 | Penetration depth, 3, 126 |
| — and torque, 82 | — and alternating currents, 94—103 |
| — surface divergence, 18 | — mean free path of electrons, 102, 103 |
| — tension, 104 | — non-linear theory, 136 |
| | — of magnetic field, 27 |
| | — increase, 67 |

- Penetration near transition temperature, 32
 - relation to flux of induction, 75
- Persistent current, 3, 10, 61, 75, 132
 - energy, 73, 74, 91
 - in doubly connected body, 41, 49
 - ring, 68
 - production, 70
- Potential, scalar and vector, 61
 - superconduction 63
 - period of, 65, 67, 85
- Poynting sector, 21, 78, 96
- Refractive index, 92, 93
- Silsbee hypothesis, 6, 118
- Skin effect, 94, 103
- Specific heat, 107, 108
 - of conduction electrons, 110
 - at transition temperature, 110
- Stress tensor, 76
 - and non-linear theory, 135
- Superconductivity
 - atomic theory, 126
 - breakdown, 105, 126
 - quenching, 7, 8, 112
 - for thin specimen, 113
 - sphere, 121
 - permanent magnetism, 89, 106
 - Superconductor, crystal systems, 2
 - current distribution, 11
 - displacement of current lines 72
- Superconductor field free state, 7, 103
 - homogeneous cubic, 26
 - inhomogeneous, 88
 - magnetic field, 4, 12
 - space charges, 19, 20, 128
 - thin, 27, 34
- Super current 3, 4
 - critical value of 6, 114, 115
 - in circular cylinder, 35
 - in elliptic cylinder, 53
 - hollow cylinder, 44
 - stationary field, 68
 - maximum density, 126, 137
 - stability of 75, 76
 - velocity of 83, 84
- Supermomentum, 78
- Thermal expansion coefficient 3
- Thermodynamics, 7, 103, 112
 - equilibrium, 105, 119
- Transition from normal to superconductivity, 4
 - magnetic effect, 13
- Transition temperature
 - and magnetic field, 108
 - penetration depth, 32
 - resistance, 1, 2
 - specific heat, 110
 - of metals, 2
- Uniqueness theorem, 25, 68

BRIEF ATTACHMENT AU

NEW SUPERCONDUCTIVE COMPOUNDS HAVING HIGH TRANSITION
TEMPERATURE, AND METHODS FOR THEIR USE AND PREPARATION

CROSS REFERENCE TO RELATED APPLICATION

see serial 8/87
③

DESCRIPTION

Technical Field

5 This invention relates to a new class of superconducting
compositions having high superconducting transition
temperatures and methods for using and preparing these
compositions, and more particularly to superconducting
compositions including copper and/or other transition
10 metals, the compositions being characterized by a
superconducting phase and a layer-like structure.

Background Art

15 Superconductivity is usually defined as the complete
loss of electrical resistance of a material at a well-
defined temperature. It is known to occur in many ma-
terials, including about a quarter of the elements of
the periodic table and over 1000 alloys and other
multi-component systems. Generally, superconductivity

is considered to be a property of the metallic state of a material since all known superconductors are metallic under the conditions that cause them to be superconducting. A few normally non-metallic materials, for example, become superconducting under very high pressure wherein the pressure converts them to metals before they exhibit superconducting behavior.

Superconductors are known to be very attractive for the generation and energy-saving transport of electrical power over long distances, and as materials used to form the coils of very strong magnets. These magnets are used in, for example, plasma and nuclear physics, nuclear magnetic resonance medical diagnosis systems, and in connection with the magnetic levitation of fast trains. Other potential uses of superconducting materials occur in power generation systems using thermonuclear fusion where very large magnetic fields must be provided, superconducting magnets being the only possible means for providing such high fields. In addition to these applications, superconductors are known in high speed switching devices, such as Josephson type switches, and in high density packaging and circuit layouts. Superconductors also are used in different types of elec-

tronic instrumentation, such as magnetic susceptometers and magnetometers.

While the advantages of superconductors are quite obvious to scientists and engineers, the common disadvantage of all presently known superconductive materials lies in their very low transition temperature. This temperature is often called the critical temperature T_c and is the temperature above which superconductivity will not exist. Usually T_c is on the order of a few degrees Kelvin. The element with the highest T_c is niobium whose T_c is 9.2°K . The composition having the highest previously known T_c is Nb_3Ge which exhibits a T_c of about 23°K at ambient pressure. Transition metal alloy compounds of the $\text{A15}(\text{Nb}_3\text{Sn})$ and $\text{B1}(\text{NbN})$ structure have been shown to have high superconducting transition temperatures. Among the A15 compounds is the aforementioned composition Nb_3Ge . Some of these compositions are described in J. Muller, Rep. Prog. Phys. 43, 663 (1980), and M. R. Beasley et al, Phys. Today, 37 (10), 60 (1984).

It is known in the art that a small number of oxides will exhibit superconductivity. Reference is made to D.C. Johnston et al, Mat. Res. Bull. 8, 777 (1973), which describes high temperature superconductivity in the Li-

5 *added (A)
8/1/87* Ti-O system with superconducting onsets as high as 13.7°K. These materials have multiple crystallographic phases including a spinel structure exhibiting the high T_c . Other metallic oxides, such as the perovskite Ba-Pb-Bi-O system, can exhibit superconductivity due to high electron-phonon coupling in a mixed valent compound, as described by G. Binnig et al, Phys. Rev. Lett., 45, 1352 (1980), and A.W. Sleight et al, Solid State Communications, 17, 27 (1975).

10 As is evident from the foregoing, superconductors presently known require liquid helium for cooling and this, in turn, requires an elaborate technology and a considerable investment in cost and energy. Accordingly, it is a primary object of the present invention to provide
15 new compositions which exhibit high T_c and methods for using and producing the same.

20 It is another object of the present invention to provide new superconducting compositions and methods for using and making them where cooling with liquid helium is not required in order to have superconductive properties in the compositions.

It is another object of the present invention to provide novel superconductive materials that are multi-valent oxides including transition metals, the compositions having a perovskite-like structure.

5 It is a further object of the present invention to provide novel superconductive compositions that are oxides including rare earth and/or rare earth-like atoms, together with copper or other transition metals that can exhibit mixed valent behavior.

10 It is a still further object of the present invention to provide novel superconductive compositions exhibiting high T_c , where the compositions are oxides including a phase having a layer-like structure and including copper.

15 It is a still further object of the present invention to provide new superconductive compositions exhibiting high T_c , where the superconductive compositions include layered structures including a rare earth and/or rare earth-like element and a transition metal.

20 It is another object of this invention to provide a new class of superconducting compositions characterized by

a T_c greater than 26 °K, and methods for making and using these compositions.

It is another object of this invention to provide new compositions and methods for using them, where the compositions include a multi-valent oxide of copper and exhibit a T_c greater than 26°K.

The basis for our invention has been described by us in the following previously published article: J.G.

Bednorz and K.A. Muller, Zeitschrift fur Physik B - Condensed Matter, 64, pp. 189-193, ^{Sept} (1986)

Another article of interest by us is J.G. Bednorz, K.A. Muller, M. Takashige, Europhysics Letters, 3(3), pp. 379-385 (1987).

Summary of the Invention

This invention relates to novel compositions exhibiting superconductivity at temperatures higher than those obtained in prior known superconductive materials, and to methods for using and forming these compositions. These compositions can carry supercurrents (i.e., electrical

Amend
8/5/79

currents in a substantially zero resistance state of the composition) at temperatures ~~at~~ greater than 26°K. In general, the compositions are characterized as mixed transition metal oxide systems where the transition metal oxide can exhibit multivalent behavior. These compositions have a layer-type crystalline structure, often perovskite-like, and can contain a rare earth or rare earth-like element. A rare earth-like element (sometimes termed a near rare earth element, ~~is~~ ^{is} one whose properties make it essentially a rare earth element. An example is a group IIIB element of the periodic table, such as La. Substitutions can be found in the rare earth (or rare earth-like) site or in the transition metal sites of the compositions. For example, the rare earth site can also include alkaline earth elements selected from group IIA of the periodic table, or a combination of rare earth or rare earth-like elements and alkaline earth elements. Examples of suitable alkaline earths include Ca, Sr, and Ba. The transition metal site can include a transition metal exhibiting mixed valent behavior, and can include more than one transition metal. A particularly good example of a suitable transition metal is copper. As will be apparent later, Cu-oxide based systems provide unique and excellent properties as high T_c superconductors.

Amend
B
8/187

Amend
8/79

An example of a superconductive composition having high T_c is the composition represented by the formula RE-TM-O, where RE is a rare earth or rare earth-like element, TM is a nonmagnetic transition metal, and O is oxygen. Examples of transition metal elements include Cu, Ni, Cr etc. In particular, transition metals that can exhibit multi-valent states are very suitable. The rare earth elements are typically elements 58-71 of the periodic table, including Ce, Nd, etc. If an alkaline earth element (AE) were also present, the composition would be represented by the general formula RE-AE-TM-O.

The ratio (AE,RE) : TM is generally approximately 1:1, but can vary from this as will be shown by examples where the ratio (AE,RE) : TM is 2:1. Of course, the amount of oxygen present in the final composition will adjust depending upon the processing conditions and will be such that the valence requirements of the system are satisfied.

The methods by which these superconductive compositions can be made can use known principles of ceramic fabrication, including the mixing of powders containing the rare earth or rare earth-like, alkaline earth, and

transition metal elements, coprecipitation of these materials, and heating steps in oxygen or air.

A particularly suitable superconducting material in accordance with this invention is one containing copper as the transition metal. Copper can exist in a Cu^{2+} or Cu^{3+} mixed valence state. The state(s) assumed by copper in the overall composition will depend on the amount of oxygen present and on any substitutions in the crystalline structure. Very high T_c has been found in Cu-oxide systems exhibiting mixed valence states, as indicated by conductivity and other measurements. Copper oxide systems including a rare earth or rare earth-like element, and an alkaline earth element, are unique examples of this general class of superconducting layered copper oxides which exhibit T_c greater than 26°K.

These and other objects, features, and advantages will be apparent from the following more particular description of the preferred embodiments.

Brief Description of the Drawings

FIG. 1 is a schematic illustration of a representative circuit used to measure dc conductivity in the high T_c superconductors of this invention.

FIG. 2 is a plot of the temperature dependence and resistivity in the composition $Ba_x La_{5-x} Cu_5 O_{5(3-y)}$ for samples with $x(Ba)=1$ (upper two curves, left scale) and $x(Ba)=0.75$ (lower curve, right scale). The influence of current density through the composition is also shown.

FIG. 3 is a plot of the low temperature dependence of resistivity in the composition $Ba_x La_{5-x} Cu_5 O_{5(3-y)}$ with $x(Ba)=1$, for different annealing conditions (i.e., temperature and oxygen partial pressure).

FIG. 4 is a plot of the low-temperature resistivity of the composition $Ba_x La_{5-x} Cu_5 O_{5(3-y)}$ with $x(Ba)=0.75$, recorded for different densities of electrical current through the composition.

Description of the Preferred Embodiments

The superconductive compositions of this invention are transition metal oxides generally having a mixed valence and a layer-like crystalline structure, and exhibit T_c 's higher than those of previously known superconducting materials. These compositions can also include a rare earth site in the layer-like structure where this site can be occupied by rare earth and rare earth-like atoms, and also by alkaline earth substitutions such as Ca, Sr, and Ba. The amount of oxygen present will be such that the valence requirements of the system are satisfied, the amount of oxygen being somewhat a function of the processing steps used to make the the superconductive compositions. Non-stoichiometric amounts of oxygen can be present in these compositions. The valence state of the elements in the oxide will be determined by the final composition in a manner well known to chemists. For example, the transition metal Cu may be present in some compositions in both a Cu^{2+} and a Cu^{3+} state.

An example of a superconductive compound having a layer-type structure in accordance with the present invention is an oxide of the general composition RE_2TMO_4 , where RE stands for the rare earths (lanthanides) or rare earth-like elements and TM stands for a transition metal. In these compounds the RE portion can be par-

tially substituted by one or more members of the alkaline earth group of elements. In these particular compounds, the oxygen content is at a deficit.

For example, one such compound that meets this general description is lanthanum copper oxide La_2CuO_4 in which the lanthanum - which belongs to the IIIB group of elements - is in part substituted by one member of the neighboring IIA group of elements, viz. by one of the alkaline earth metals (or by a combination of the members of the IIA group), e.g., by barium. Also, the oxygen content of the compound can be incomplete such that the compound will have the general composition

$\text{La}_{2-x}\text{Ba}_x\text{CuO}_{4-y}$, wherein $x \leq 0.3$ and $y < 0.5$.

Another example of a compound meeting this general formula is lanthanum nickel oxide wherein the lanthanum is partially substituted by strontium, yielding the general formula $\text{La}_{2-x}\text{Sr}_x\text{NiO}_{4-y}$. Still another example is cerium nickel oxide wherein the cerium is partially substituted by calcium, resulting in $\text{Ce}_{2-x}\text{Ca}_x\text{NiO}_{4-y}$.

The following description will mainly refer to barium as a partial replacement for lanthanum in a La_2CuO_4 compound because it is in the Ba-La-Cu-O system that

many laboratory tests have been conducted. Some compounds of the general Ba-La-Cu-O system have been described by C. Michel and B. Raveau in Rev. Chim. Min. 21 (1984) 407, and by C. Michel, L. Er-Rakho and B. Raveau in Mat. Res. Bull., Vol. 20, (1985) 667-671. They did not, however, find or try to find superconductivity. These references and their teachings regarding perovskite-like layered oxides of mixed valent transition metals, and their preparation, are herein incorporated by reference.

Experiments conducted in connection with the present invention have revealed that high- T_c superconductivity is present in compounds where the rare earth or rare earth-like element is partially replaced by any one or more of the members of the IIA group of elements, i.e., the alkaline earth metals. Actually, the T_c of $\text{La}_2\text{CuO}_{4-y}$ with the substitution Sr^{2+} is higher and its superconductivity-induced diamagnetism larger than that found with the substitutions Ba^{2+} and Ca^{2+} .

The Ba-La-Cu-O system can exhibit a number of crystallographic phases, namely with mixed-valent copper constituents which have itinerant electronic states between non-Jahn-Teller Cu^{3+} and Jahn-Teller Cu^{2+} ions.

This applies likewise to systems where nickel is used in place of copper, with Ni^{3+} being the Jahn-Teller constituent, and Ni^{2+} being the non-Jahn-Teller constituent. The existence of Jahn-Teller polarons in conducting crystals was postulated theoretically by K.H. Hoeck, H. Nickisch and H. Thomas in Helv. Phys. Acta 56 (1983) 237. Polarons have large electron-phonon interactions and, therefore, are favorable to the occurrence of superconductivity at higher critical temperatures.

Amend
8/5/87

Samples in the Ba-La-Cu-O system, when subjected to X-ray analysis, revealed three individual crystallographic phases, viz.

- a first layer-type perovskite-like phase, related to the

K_2NiF_4 structure, with the general composition

$\text{La}_{2-x}\text{Ba}_x\text{CuO}_{4-y}$, with

$x \ll 1$ and $y \geq 0$;

- a second, non-conducting CuO phase; and

- a third, nearly cubic perovskite phase of the general composition $\text{La}_{1-x}\text{Ba}_x\text{CuO}_{3-y}$ which appears to be independent of the exact starting composition.

Of these three phases the first one appeared to be responsible for the observed high- T_c superconductivity, the critical temperature showing a dependence on the barium concentration in that phase. Obviously, the Ba^{2+} substitution caused a mixed-valent state of Cu^{2+} and Cu^{3+} to preserve charge neutrality. It is assumed that the oxygen deficiency, y , is the same in the doped and undoped crystallites.

In this application, the terms transition metal oxide, copper oxide, Cu-oxide, etc. are meant to broadly include the oxides which exhibit superconductivity at temperatures greater than 26°K. Thus, the term copper oxide can mean, among other things, an oxide such as CuO_{4-y} in the mixed oxide composition $La_{2-x}Ba_xCuO_{4-y}$.

Both La_2CuO_4 and $LaCuO_3$ are metallic conductors at high temperatures in the absence of barium. Actually, both are metals like $LaNiO_3$. Despite their metallic character, the Ba-La-Cu-O type materials are essentially ceramics, as are the other compounds of the RE_2MO_4 type, and their manufacture generally follows the known principles of ceramic fabrication. The preparation of a superconductive Ba-La-Cu-O compound, for example, in

accordance with the present invention typically involves the following manufacturing steps:

5 • Preparing aqueous solutions of the respective nitrates of barium, lanthanum and copper and coprecipitation thereof in their appropriate ratios,

 • adding the coprecipitate to oxalic acid and forming an intimate mixture of the respective oxalates.

10 • decomposing the precipitate and causing a solid-state reaction by heating the precipitate to a temperature between 500 and 1200°C for one to eight hours.

15 • pressing the resulting product at a pressure of about 4 kbar to form pellets.

 • re-heating the pellets to a temperature between 500 and 900°C for one half hour to three hours for sintering.

It will be evident to those skilled in the art that if the partial substitution of lanthanum by another alkaline earth element, such as strontium or calcium, is desired, the particular nitrate thereof will have to be used in place of the barium nitrate of the example process described above. Also, if the copper of this example is to be replaced by another transition metal, the nitrate thereof will obviously have to be employed. Other precursors of metal oxides, such as carbonates or hydroxides, can be chosen in accordance with known principles.

Experiments have shown that the partial contents of the individual compounds in the starting composition play an important role in the formation of the phases present in the final product. While, as mentioned above, the final Ba-La-Cu-O system obtained generally contains the said three phases, with the second phase being present only in a very small amount, the partial substitution of lanthanum by strontium or calcium (and perhaps beryllium) will result in only one phase existing in the final $\text{La}_{2-x}\text{Sr}_x\text{CuO}_{4-y}$ or $\text{La}_{2-x}\text{Ca}_x\text{CuO}_{4-y}$, respectively, provided $x < 0.3$.

With a ratio of 1:1 for the respective (Ba, La) and Cu contents, it is expected that the three phases will occur in the final product. Setting aside the second phase, i.e. the CuO phase whose amount is negligible, the relative volume amounts of the other two phases are dependent on the barium content in the $\text{La}_{2-x}\text{Ba}_x\text{CuO}_{4-y}$ complex. At the 1:1 ratio and with an $x = 0.02$, the onset of a localization transition is observed, i.e., the resistivity increases with decreasing temperature, and there is no superconductivity.

With $x = 0.1$ at the same 1:1 starting ratio, there is a resistivity drop at the very high critical temperature of 35°K .

With a (Ba, La) versus Cu ratio of 2:1 in the starting composition, the composition of the La_2CuO_4 :Ba phase, which appears to be responsible for the superconductivity, is imitated, with the result that now only two phases are present, the CuO phase not existing. With a barium content of $x = 0.15$, the resistivity drop occurs at $T_c = 26^\circ\text{K}$.

The method for preparing these Ba-La-Cu-O sample complexes used two heat treatments for the precipitate at

an elevated temperature for several hours. In the experiments carried out in connection with the present invention it was found that best results were obtained at 900°C for a decomposition and reaction period of 5 hours, and again at 900°C for a sintering period of one hour. These values apply to a 1:1 ratio composition as well as to a 2:1 ratio composition.

For the 2:1 ratio composition, a somewhat higher temperature is permissible owing to the higher melting point of the composition in the absence of excess copper oxide. However, a one-phase compound was not achieved by a high temperature treatment.

Conductivity Measurements (FIGS. 1-4)

5 The dc conductivity of representative Ba-La-Cu-O compositions was measured to determine their low temperature behavior and to observe their high T_c . These measurements were performed using the well known four-point probe technique, which is schematically illustrated in FIG. 1. Rectangular shaped samples 10 of

10 $Ba_xLa_{5-x}CuO_{5(3-y)}$ were cut from sintered pellets, and provided with gold sputtered electrodes 12A and 12B, about 0.5 microns thick. Indium wires 14A and 14B contact electrodes 12A and 12B, respectively. The sample was contained in a continuous flow cryostat 16

(Leybold-Heraeus) and measurements were made over a temperature range 300-^{4.2}412°K.

15 Electrodes 12A and 12B are connected in a circuit including a current source 18 and a variable resistor 20. Indium leads 22A and 22B are pressed into contact with sample 10 and fixed with silver paint 24. Leads 22A, 22B are connected to a voltage reading instrument 26.

20 Since the current and voltage are accurately determined, the resistivity of the sample 10 is then known. In the configuration used for these measurements, a computer was used to provide a computer-controlled fully-

automatic system for temperature variation, data acquisition and processing.

In FIG. 2, the low temperature dependence of resistivity ρ (measured in ohm-cms) in the composition

8/5/87
 $\text{Ba}_x\text{La}_{5-x}\text{Cu}_5\text{O}_{5(3-y)}$ is plotted for two different values of x . For the upper two curves, the value of $x(\text{Ba})$ is 1 and the left side vertical scale is used. For the lower curve, the value of x is 0.75, and the resistivity scale on the right hand side of the figure is used. The data is taken for different values of current density: 0.25 A/cm^2 for the top curve and 0.50 A/cm^2 for the middle and bottom curves.

For barium-doped samples with $x(\text{Ba}) < 1.0$, for example with $x < 0.3$, at current densities of 0.5 A/cm^2 , a high-temperature metallic behavior with an increase in resistivity at low temperatures was found as depicted in FIG. 2. At still lower temperatures, a sharp drop in resistivity ($> 90\%$) occurred which for higher current densities became partially suppressed (FIG. 1 upper curves, left scale). This characteristic drop was studied as a function of the annealing conditions, i.e. temperature and oxygen partial pressure as shown in FIG. 2. For samples annealed in air, the transition from

itinerant to localized behavior , as indicated by the minimum in resistivity in the 80°K range, was not found to be very pronounced. Annealing in a slightly reducing atmosphere, however, led to an increase in resistivity and a more pronounced localization effect. At the same time, the onset of the resistivity drop was shifted towards the 30°K region. Curves 4 and 5 (FIG. 3), recorded for samples treated at 900°C, show the occurrence of a shoulder at still lower temperatures, more pronounced in curve 6. At annealing temperatures of 1040°C, the highly conducting phase has almost vanished. Long annealing times and/or high temperatures will generally destroy the superconductivity.

The mixed-valent state of copper is of importance for electron-phonon coupling. Therefore, the concentration of electrons was varied by the Ba/La ratio. A typical curve for a sample with a lower Ba concentration of 0.75 is shown in FIG. 2(right scale). Its resistivity decreases by at least three orders of magnitude, giving evidence for the bulk being superconducting below 13°K with an onset around 35°K, as shown in FIG. 4 on an expanded temperature scale. FIG. 4 also shows the influence of the current density, typical for granular

compounds. Current densities of 7.5, 2.5, and 0.5 A/cm² were passed through the superconducting composition.

When cooling the samples from room temperature, the resistivity data first show a metal-like decrease. At low temperatures, a change to an increase occurs in the case of Ca substituted compounds and for the Ba-substituted samples. This increase is followed by a resistivity drop, showing the onset of superconductivity at $22 \pm 2^\circ\text{K}$ and $33 \pm 2^\circ\text{K}$ for the Ca and Ba compounds, respectively. In the Sr compound, the resistivity remains metallic down to the resistivity drop at $40 \pm 1^\circ\text{K}$. The presence of localization effects, however, depends strongly on alkaline-earth ion concentration and sample preparation, that is to say, on annealing conditions and also on the density, which have to be optimized. All samples with low concentrations of Ca, Sr, and Ba show a strong tendency to localization before the resistivity drops occur.

Apparently, the onset of the superconductivity, i.e. the value of the critical temperature T_c , is dependent on, among other parameters, the oxygen content of the final compound. It seems that for certain materials, an oxygen deficiency is necessary for the material to have a

high- T_c behavior. In accordance with the present invention, the method described above for making the $\text{La}_2\text{CuO}_4\text{:Ba}$ complex is complemented by an annealing step during which the oxygen content of the final product can be adjusted. Of course, what was said in connection with the formation of the $\text{La}_2\text{CuO}_4\text{:Ba}$ compound likewise applies to other compounds of the general formula $\text{RE}_2\text{TMO}_4\text{:AE}$ (where AE is an alkaline earth element), such as, e.g. $\text{Nd}_2\text{NiO}_4\text{:Sr}$.

In the cases where a heat treatment for decomposition and reaction and/or for sintering was performed at a relatively low temperature, i.e., at no more than 950°C , the final product is subjected to an annealing step at about 900°C for about one hour in a reducing atmosphere.

It is assumed that the net effect of this annealing step is a removal of oxygen atoms from certain locations in the matrix of the RE_2TMO_4 complex, thus creating a distortion in its crystalline structure. The O_2 partial pressure for annealing in this case may be between 10^{-1} and 10^{-5} bar.

In those cases where a relatively high temperature (i.e., above 950°C) is employed for the heat treatment, it might be advantageous to perform the annealing step

in a slightly oxidizing atmosphere. This would make up for an assumed exaggerated removal of oxygen atoms from the system owing to the high temperature and resulting in a too severe distortion of the system's crystalline structure.

Resistivity and susceptibility measurements as a function of temperature of Sr^{2+} and Ca^{2+} -doped $\text{La}_2\text{CuO}_{4-y}$ ceramics show the same general tendency as the Ba^{2+} -doped samples: a drop in resistivity ρ (T), and a crossover to diamagnetism at a slightly lower temperature. The samples containing Sr^{2+} actually yielded a higher onset than those containing Ba^{2+} and Ca^{2+} . Furthermore, the diamagnetic susceptibility is about three times as large as for the Ba samples. As the ionic radius of Sr^{2+} nearly matches that of La^{3+} , it seems that the size effect does not cause the occurrence of superconductivity. On the contrary, it is rather adverse, as the data on Ba^{2+} and Ca^{2+} indicate.

The highest T_c for each of the dopant ions investigated occurred for those concentrations where, at room temperature, the $\text{RE}_{2-x}\text{TM}_x\text{O}_{4-y}$ structure is close to the orthorhombic-tetragonal structural phase transition, which may be related to the substantial electron-phonon

interaction enhanced by the substitution. The alkaline-earth substitution of the rare earth metal is clearly important, and quite likely creates TM ions with no e_g Jahn-Teller orbitals. Therefore, the absence of these Jahn-Teller orbitals, that is, Jahn-Teller holes near the Fermi energy, probably plays an important role in the T_c enhancement.

While examples have been given using different transition metal elements in the superconducting compositions, copper oxide compositions having mixed valence appear to be unique and of particular importance, having superconducting properties at temperatures in excess of 26°K. These mixed valent copper compositions can include a rare earth element and/or a rare earth-like element which can be substituted for by an alkaline earth element. The amount of oxygen in these compositions will vary depending upon the mode of preparation and will be such as to meet the valence requirements of the composition. These copper-based compositions have a layer-like structure, often of a perovskite type. For a more detailed description of some of the types of crystallographic structures that may result, reference is made to the aforementioned publication by Michel and

Raveau in Rev. Chim. Min. 21, 407 (1984), and to C. Michel et al, Mat. Res. Bull., Vol. 20, 667-671 (1985).

5 While the invention has been described with respect to particular embodiments thereof, it will be apparent to those of skill in the art that variations can be made therein without departing from the spirit and scope of the present invention. For example, while the range of compositions includes rare earth elements and transition metal elements, the ratios of these elements can be
10 varied because the crystalline structure can accommodate vacancies of these elements and still retain a layer-like structural phase exhibiting superconductivity.

15 Further, the stoichiometry or degree of non-stoichiometry of oxygen content (i.e., oxygen deficit or surplus) of these compositions can be varied by using reducing or oxidizing atmospheres during formation of the compounds and by using different doping amounts in the rare earth and transition metal sites of the crystal structure. This type of distortion of the crystal
20 structure and the many forms that it can encompass are readily apparent from reference to the aforementioned Michel and Raveau publications. Thus, the invention broadly relates to mixed (doped) transition metal oxides

having a layer-like structure that exhibit superconducting behavior at temperatures in excess of 26°K. Of these materials, a mixed copper oxide having multivalent states provides high T_c and favorable superconducting properties.

5

CLAIMS

Having thus described our invention what we claim as new
and desire to secure as Letters Patent, is:

- 1 1. A superconductive composition having a transition
2 temperature greater than 26°K, the composition in-
3 cluding a rare earth or ~~near~~^{rare} rare earth-like ele-
4 ment, a transition metal element capable of
5 exhibiting multivalent states and oxygen, and in-
6 cluding at least one phase that exhibits
7 superconductivity at temperature in excess of 26°K.

- 1 2. The composition of claim 1, further including an
2 alkaline earth element substituted for at least one
3 atom of said rare earth or rare earth-like element
4 in said composition.

- 1 3. The composition of claim 2, where said transition
2 metal is Cu.

to be
amended
2/6/91

1 4. The composition of claim 3, where said alkaline earth
2 element is selected from the group consisting of
3 ^{Be}
~~B~~, Ca, Ba, and Sr.

1 5. The composition of claim 1, where said transition
2 metal element is selected from the group consisting
3 of Cu, Ni, and Cr.

1 6. The composition of claim 2, where said rare earth
2 or rare earth-like element is selected from the
3 group consisting of La, Nd, and Ce.

1 7. The composition of claim 1, where said phase is
2 crystalline with a perovskite-like structure.

1 8. The composition of claim 2, where said phase is
2 crystalline with a perovskite-like structure.

1 9. The composition of claim 1, where said phase exhibits
2 a layer-like crystalline structure.

1 10. The composition of claim 1, where said phase is a
2 mixed copper oxide phase.

1 11. The composition of claim 1, where said composition
2 is comprised of mixed oxides with alkaline earth
3 doping.

1 12. A superconducting combination, including a
2 superconductive composition having a transition
3 temperature $> 26^{\circ}\text{K}$,

4 means for passing a superconducting electrical
5 current through said composition while said compo-
6 sition is at a temperature $> 26^{\circ}\text{K}$., and

7 cooling means for cooling said composition to a
8 superconducting state at a temperature in excess
9 of 26°K .

1 13. The combination of claim 12, where said
2 superconductive composition includes a transition
3 metal oxide.

1 14. The combination of claim 12, where said
2 superconductive composition includes Cu-oxide.

1 15. The combination of claim 12, where said
2 superconductive composition includes a multivalent
3 transition metal, oxygen, and at least one addi-
4 tional element.

1 16. The combination of claim 15, where said transition
2 metal is Cu.

1 17. The combination of claim 15, where said additional
2 element is a rare earth or rare earth-like element.

1 18. The combination of claim 15, where said additional
2 element is an alkaline earth element.

1 19. The combination of claim 12, where said composition
2 includes a perovskite-like superconducting phase.

1 20. The combination of claim 12, where said composition
2 includes a substituted transition metal oxide.

1 21. The combination of claim 20, where said substituted
2 transition metal oxide includes a multivalent
3 transition metal element.

1 22. The combination of claim 20, where said substituted
2 transition metal oxide is an oxide of copper.

1 23. The combination of claim 20, where said substituted
2 transition metal oxide has a layer-like structure.

1 24. A method including the steps of forming a transition
2 metal oxide having a phase therein which exhibits
3 a superconducting state at a critical temperature
4 in excess of 26° K,

5 ^{maintaining} [lowering] the temperature of said material at ^{a temperature less than} [least
6 to] said critical temperature to produce said
7 superconducting state in said phase, and

8 passing an electrical supercurrent through said
9 transition metal oxide while it is in said super-
10 conducting state.

1 25. The method of claim 24, where said transition metal
2 oxide is comprised of a transition metal capable
3 of exhibiting multivalent states.

1 26. The method of claim 24, where said transition metal
2 oxide is comprised of a Cu oxide.

1 27. A superconducting composition having a transition
2 temperature in excess of 26°K, said composition
3 being a substituted Cu-oxide including a supercon-
4 ducting phase having a structure substantially
5 close to the orthorhombic-tetragonal phase transi-
6 tion of said composition.

1 28. The composition of claim 27, where said substituted
2 Cu-oxide includes a rare earth or rare earth-like
3 element.

1 29. The composition of claim 27, where said substituted
2 Cu-oxide includes an alkaline earth element.

1 30. The composition of claim 29, where said alkaline
2 earth element is atomically large with respect to
3 Cu.

1 31. The composition of claim 27, where said composition
2 has a crystalline structure which enhances
3 electron-phonon interactions to produce
4 superconductivity at a temperature in excess of
5 26°K.

1 32. The composition of claim 31, where said crystalline
2 structure is layer-like, enhancing the number of
3 Jahn-Teller polarons in said ~~composite~~ -- composition --

1 33. A superconducting composition having a supercon-
2 ducting onset temperature in excess of 26°K., the
3 composition being comprised of a copper oxide doped
4 with an alkaline earth element where the concen-

A.Y.
Amendment
" "
2/8/91

5 tration of said alkaline earth element is near to
6 the concentration of said alkaline earth element
7 where the superconducting copper oxide phase in
8 said composition undergoes an orthorhombic to
9 tetragonal structural phase transition.

1 34. A superconducting composition having a supercon-
2 ducting onset temperature in excess of 26°K, the
3 composition being comprised of a mixed copper oxide
4 doped with an element chosen to create Cu³⁺ ions
5 in said composition.

1 35. The composition of claim 34, where said doping el-
2 ement includes an alkaline earth element.

1 36. A combination comprising:
2 a composition having a superconducting onset tem-
3 perature in excess of 26°K, said composition being
4 comprised of a substituted copper oxide exhibiting
5 mixed valence states and at least one other element
6 in its crystalline structure,

7 means for passing a superconducting electrical
8 current through said composition while said compo-
9 sition is at a temperature in excess of 26°K ~~and~~.

10 cooling means for cooling said composition to a
11 superconducting state at a temperature in excess
12 of 26°K ~~and~~.

1 37. The combination of claim 36, where said at least
2 one other element is an alkaline earth element.

1 38. The combination of claim 36, where said at least
2 one other element is an element which creates Cu^{3+}
3 ions in said composition.

1 39. The composition of claim 36, where said at least
2 one other element is an element chosen to create
3 the presence of both Cu^{2+} and Cu^{3+} ions in said
4 composition.

1 40. A superconductor exhibiting a superconducting onset
2 at a temperature in excess of 26°K, said supercon-
3 ductor being comprised of at least four elements,
4 none of which is itself superconducting.

1 41. The superconductor of claim 40, where said elements
2 include a transition metal and oxygen.

1 42. A superconductor having a superconducting onset
2 temperature greater 26°K, said superconductor being
3 a doped transition metal oxide, where said transi-
4 tion metal is itself non-superconducting.

1 43. The superconductor of claim 42, where said doped
2 transition metal oxide is multivalent in said
3 superconductor.

1 44. The superconductor of claim 42, further including
2 an element which creates a mixed valent state of
3 said transition metal.

1 45. The superconductor of claim 43, where said transi-
2 tion metal is Cu.

1 46. A superconductor having a superconducting onset
2 temperature greater than 26°K, said superconductor
3 being an oxide having multivalent oxidation states
4 and including a ^{transition} metal, said oxide having a crys-
5 talline structure which is oxygen deficient.

Amended
8/87

1 47. The superconductor of claim 46, where said transi-
2 tion metal is Cu.

1 48. A superconductive composition comprised of a tran-
2 sition metal oxide having substitutions therein,
3 the amount of said substitutions being sufficient
4 to produce sufficient electron-phonon interactions.
5 in said composition that said composition exhibits
6 a superconducting onset at temperatures greater
7 than 26°K.

1 49. The composition of claim 48, where said transition
2 metal oxide is multivalent in said composition.

1 50. The composition of claim 48, where said transition
2 metal is Cu.

1 51. The composition of claim 48, where said substi-
2 tutions include an alkaline earth element.

1 52. The composition of claim 48, where said substi-
2 tutions include a rare earth or rare earth-like
3 element.

1 53. A superconductor comprised of a copper oxide having
2 a layer-like crystalline structure and at least one
3 additional element substituted in said crystalline
4 structure, said structure being oxygen deficient
5 and exhibiting a superconducting onset temperature
6 in excess of 26°K.

1 54. The superconductor of claim 53, where said addi-
2 tional element creates a mixed valent state of said
3 copper oxide in said superconductor.

1 55. A combination, comprising:

2 a transition metal oxide having an oxygen defi-
3 ciency, said transition metal being non-
4 superconducting and said oxide having multivalent
5 states,

6 means for passing an electrical superconducting
7 current through said oxide while said oxide is at
8 a temperature greater than 26°K and

9 ~~cooling means for cooling said oxide in a super-~~
10 ~~conducting state at a temperature greater than~~
11 ~~26°K~~]

1 56. The combination of claim 55, where said transition
2 metal is Cu.

1 57. A combination including;
2
3 a superconducting oxide having a superconducting onset
4 temperature in excess of 26°K and containing at least 3
5 non-superconducting elements,
6
7 means for passing a supercurrent through said oxide
8 while said oxide is maintained at a temperature greater
9 than 26°K, and
10
11 means for maintaining said oxide in a superconducting
12 state at a temperature greater than 26°K.

1 58. A combination, comprised of:
2
3 a copper oxide superconductor including an element which
4 creates a mixed valent state in said oxide, said oxide
5 being crystalline and having a layer-like structure,
6
7 means for passing a supercurrent through said copper
8 oxide while it is maintained at a temperature greater
9 than 26°K, and
10
11

8
8/87

8 means for ^{maintaining} [cooling] said copper oxide ⁱⁿ (to) a superconductive
9 state at a temperature greater than 26°K.

1 59. A combination, comprised of:

2 a superconducting ceramic-like material having an
3 onset of superconductivity at a temperature in ex-
4 cess of 26°K.,

5 means for passing a supercurrent through said
6 superconducting ceramic-like material while said
7 ceramic-like material is maintained at a temper-
8 ature in excess of 26°K., and

8
8/87

9 means for ^{maintaining} [cooling] said superconducting ceramic-like
10 material ⁱⁿ to a superconductive state at a temper-
11 ature greater than 26°K.

1 60. A superconductor comprised of a transition metal
2 oxide, and at least one additional element, said
3 superconductor having a distorted crystalline
4 structure characterized by an oxygen deficiency and

5 exhibiting a superconducting onset temperature in
6 excess of 26°K.

1 61. The superconductor of claim 60, where said transi-
2 tion metal is Cu.

1 62. A superconductor comprised of a transition metal
2 oxide and at least one additional element, said
3 superconductor having a distorted crystalline
4 structure characterized by an oxygen excess and
5 exhibiting a superconducting onset temperature in
6 excess of 26°K.

1 63. The superconductor of claim 62, where said transi-
2 tion metal is Cu.

1 64. A combination, comprising:
2 a mixed copper oxide composition having enhanced
3 polaron formation, said composition including an
4 element causing said copper to have a mixed valent

5 state in said composition, said composition further
6 having a distorted octahedral oxygen environment
7 leading to a T_c greater than 26°K.,

8 means for providing a supercurrent through said
9 composition at temperatures greater than 26°K. [~~and~~

10 ~~cooling means for cooling said composition~~ to a
11 ~~temperature greater than 26°K.~~]

ancel
B
8/87

1 65. A superconducting composition exhibiting
2 superconductivity at temperatures greater than
3 26°K, said composition being a ceramic-like mate-
4 rial in the RE-AE-TM-O system, where RE is a rare
5 earth or near rare earth element, AE is an alkaline
6 earth element, TM is a multivalent transition metal
7 element having at least two valence states in said
8 composition, and O is oxygen, the ratio of the
9 amounts of said transition metal in said two va-
10 lence states being determined by the ratio RE : AE.

1 66. A superconductive composition having a transition
2 temperature greater than 26°K, the composition in-

3 cluding a multivalent transition metal oxide and
4 at least one additional element, said composition
5 having a distorted orthorhombic crystalline struc-
6 ture.

1 67. The composition of claim 66, where said transition
2 metal oxide is a mixed copper oxide.

1 68. The composition of claim 67, where said one addi-
2 tional element is an alkaline earth element.

1 69. A superconductive combination, comprising:

2 a superconducting composition exhibiting a super-
3 conducting transition temperature greater than
4 26°K, said composition being a transition metal
5 oxide having a distorted orthorhombic crystalline
6 structure, and

7 means for passing a superconducting electrical
8 current through said composition while said compo-
9 sition is at a temperature greater than 26°K.

1 70. The combination of claim 69, where said transition
2 metal oxide is a mixed copper oxide.

1 71. The combination of claim 70, where said mixed copper
2 oxide includes an alkaline earth element.

1 72. The combination of claim 71, where said mixed copper
2 oxide further includes a rare earth or rare earth-
3 like element.

1 73. A method for making a superconductor having a
2 superconducting onset temperature $> 26^{\circ}\text{K}$, said
3 method including the steps of:

4 preparing powders of oxygen-containing compounds
5 of a rare earth or rare earth-like element, an
6 alkaline earth element, and copper,

7 mixing said compounds and firing said mixture to
8 create a mixed copper oxide composition including
9 said alkaline earth element and said rare earth or
10 rare earth-like element, and

11 annealing said mixed copper oxide composition at
12 an elevated temperature less than about 950°C in
13 an atmosphere including oxygen to produce a super-
14 conducting composition having a mixed copper oxide
15 phase exhibiting a superconducting onset temper-
16 ature greater than 26°K, said superconducting com-
17 position having a layer-like crystalline structure
18 after said annealing step.

1 74. The method of claim 73, where the amount of oxygen
2 incorporated into said composition is adjusted by
3 said annealing step, the amount of oxygen therein
4 affecting the critical temperature T_c of the
5 superconducting composition.

1 75. A method for making a superconductor having a
2 superconducting onset temperature greater than
3 26°K, said superconductor being comprised of a rare
4 earth or rare earth-like element (RE), an alkaline
5 earth element (AE), copper (CU), and oxygen (O) and
6 having the general formula RE-AE-CU-O, said method
7 including the steps of combining said rare earth
8 or rare earth-like element, said alkaline earth

9 element and said copper in the presence of oxygen
10 to produce a mixed copper oxide including said rare
11 earth or rare earth-like element and said alkaline
12 earth element therein, and

13 heating said mixed copper oxide to produce a
14 superconductor having a crystalline layer-like
15 structure and exhibiting a superconducting onset
16 temperature greater than 26°K, the critical tran-
17 sition temperature of said superconductor being
18 dependent on the amount of said alkaline earth el-
19 ement therein.

1 76. The method of claim 75, where said heating step is
2 done in an atmosphere including oxygen.

1 77. A combination, comprising:

2 a mixed copper oxide composition including an
3 alkaline earth element (AE) and a rare earth or
4 rare earth-like element (RE), said composition
5 having a layer-like crystalline structure and
6 multi-valent oxidation states, said composition

amend
to
9/87

7 exhibiting a substantially zero resistance to the
8 flow of electrical current therethrough when ⁱⁿ [cooled
9 to] a superconducting state at a temperature in ex-
10 cess of 26°K, and

11 electrical means for passing an electrical super-
12 current through said composition when said compo-
13 sition exhibits substantially zero resistance at a
14 temperature greater than 26°K.

1 78. The combination of claim 77, where the ratio
2 (AE,RE) : Cu is substantially 1:1.

amend
to
9/87

1 79. The combination of claim 77, where the ratio
2 (AE,RE) : Cu is substantially ² 1:1.

1 80. The combination of claim 77, where said crystalline
2 structure is perovskite-like.

1 81. The combination of claim 77, where said mixed copper
2 oxide composition has a non-stoichiometric amount
3 of oxygen therein.

1 82. A method for making a superconductor having a
2 superconducting onset temperature greater than 26° ,
3 said superconductor being comprised of a rare earth
4 or rare earth-like element (RE), an alkaline earth
5 element (AE), a transition metal element (TM), and
6 oxygen (O) and having the general formula
7 RE-AE-TM-O, said method including the steps of
8 combining said rare earth or rare earth-like ele-
9 ment, said alkaline earth element and said transi-
10 tion metal element in the presence of oxygen to
11 produce a mixed transition metal oxide including
12 said rare earth or rare earth-like element and said
13 alkaline earth element therein, and

14 heating said mixed transition metal oxide to
15 produce a superconductor having a crystalline
16 layer-like structure and exhibiting a supercon-
17 ducting onset temperature greater than 26°K , said
18 superconductor having a non-stoichiometric amount
19 of oxygen therein.

and
of
8/87

1 83. The method of claim 82, where said transition metal
2 is copper.

1 84. A superconducting combination, comprising:

2 a mixed transition metal oxide composition con-
3 taining a non-stoichiometric amount of oxygen
4 therein, a transition metal and at least one addi-
5 tional element, said composition having substan-
6 tially zero resistance to the flow of electricity
7 therethrough when ⁱⁿ [cooled to] a superconducting state
8 at a temperature greater than 26°K, and

ended
6
8/17

9 electrical means for passing an electrical super-
10 current through said composition when said compo-
11 sition is in said superconducting state at a
12 temperature greater than 26°K.

1 85. The combination of claim 84, where said transition
2 metal is copper.

1 86. A method, comprising the steps of:

2 forming a composition including a transition metal,
3 a rare earth or rare earth-like element, an
4 alkaline earth element, and oxygen, where said
5 composition is a mixed transition metal oxide hav-
6 ing a non-stoichiometric amount of oxygen therein
7 and exhibiting a superconducting state at a tem-
8 perature greater than 26°K,

amend
8
8/17 9 ^{maintaining} [cooling] said composition ⁱⁿ [to] said superconducting
10 state at a temperature greater than 26°K, and

11 passing an electrical current through said compo-
12 sition while said composition is in said supercon-
13 ducting state.

1 87. The method of claim 86, where said transition metal
2 is copper.

1 88. A method, including the steps of:

2 forming a composition exhibiting a superconductive
3 state at a temperature in excess of 26°K,

B
1/17

4 ^{maintaining}
[cooling] said composition ^{at} [to] a temperature in excess
5 of 26°K at which temperature said composition ex-
6 hibits said superconductive state, and

7 passing an electrical current through said compo-
8 sition while said composition is in said
9 superconductive state.

1 89. The method of claim 88, where said composition is
2 comprised of a metal oxide.

1 90. The metal of claim 88, where said composition is
2 comprised of a transition metal oxide.

BRIEF ATTACHMENT AV

IN THE UNITED STATES PATENT AND TRADEMARK OFFICE

In re Patent Application of

Applicants: Bednorz et al.

Serial No.: 08/479,810

Filed: June 7, 1995

For: NEW SUPERCONDUCTIVE COMPOUNDS HAVING HIGH TRANSITION
TEMPERATURE, METHODS FOR THEIR USE AND PREPARATION

Date: March 1, 2004

Docket: YO987-074BZ

Group Art Unit: 1751

Examiner: M. Kopec

Commissioner for Patents
P.O. Box 1450
Alexandria, VA 22313-1450

FIFTH SUPPLEMENTAL AMENDMENT

Sir:

In response to the Office Action dated February 4, 2000:

ATTACHMENT 6

AV

電氣抵抗せよ

明の臣民がゼロになる前に
 現象を、明治三〇年（明治
 二十九年）の「博士」に
 心起す新す「博士」に
 された。今「博士」の研究が
 高田田原作の可能性を示した
 物質で、この時と東京工芸学
 理工学部の田中「博士」教授らのク

スナール型を保持することを願ひました。

和伝母材料で作つたパイルに一度融した重晶石水が凝れれば、その重晶石で強い母材が得られるなど、利用価値は極めて大きい。しかし、和伝母現象を起こす融解程度が低すぎるものが多かった。

すでに実用化されている二ナフ命も、融解程度は絶対温度二〇〇度以下。実験室での融解程度でさえ、三二二度前後で、この計算は一七五三年以来変わらなかつた。

現在、実用化されている和伝母装置は、最少物質の液体ヘリウム（純粋絶対零度四度）で冷やされている。日本で使われる液体ヘリウムは、金帝アメリカ

などからの輸入に頼っている。歐州銀度が三〇度になれば、純度が純銀銀度二〇度の液体水素や四二七度の液体ネオンの使用が可能となる。

石伝導石、医学用の石伝導板、電氣共聴断脈診所装設など石伝導材料を便する設備は増えているので、高度で動く石伝導材料の開発は世界中の研究がしのぎを削つていた。

DISCOVERY OF NEW SUPERCONDUCTING MATERIAL

" CERAMIC WITH SUFFICIENT SUPERCONDUCTIVE POWER IN HIGH TEMPERATURE REGION "

A new ceramic with a very high T_c of 30K of the superconducting transition has been found. The possibility of high T_c - superconductivity has been reported by scientists in Switzerland in this spring. The group of Prof. Shoji TANAKA, Dept. Appl. Phys. Faculty of Engineering at the University of Tokyo confirmed in November, that this is true. T_c 's of all superconducting materials which we have in practical application till now are lower than 20K. Therefore we need large amount of liquid He for cooling. Note that the price of liquid He is very expensive. But with this new material we can use cheaper liquid H_2 for cooling. We can expect great from this material to the applications such as linear motorcars, electricity transport systems, etc.

The ceramic newly discovered, is an oxide compound of La and Cu with Ba, which has a structure of the so-called perovskite and shows metal-like properties. Prof. Tanaka's laboratory confirmed that this material shows diamagnetism (Meissner effect) up to 30K, which is the most important indication of the existence of superconductivity.

There are a lot of possibilities for practical applications of superconductors. For example very strong magnets, made of superconducting coils, etc. But one handicap is that T_c is too low in each material we know till now.

The T_c of Nb-alloys which are already in practical use are lower than 20K. The record of T_c in a laboratory is around 23.2K. This record has not been broken since 1973.

Nowadays each instrument using superconductors is operated by liquid He cooling, and He is a very rare material with a boiling point of 4K. Liquid He used in present Japan is exclusively imported from the USA. If we could get a material with a high T_c of 30K, we can not only use liquid H_2 but also liquid Ne with a boiling point of 27K.

Since the application of superconductors to many fields, such as very strong magnets, medical use of NMR machines, etc. show rapid increasing, research field of high T_c superconductivity is highly competitive all over the world.

BRIEF ATTACHMENT AW

IN THE UNITED STATES PATENT AND TRADEMARK OFFICE

In re Patent Application of

Applicants: Bednorz et al.

Serial No.: 08/479,810

Filed: June 7, 1995

For: NEW SUPERCONDUCTIVE COMPOUNDS HAVING HIGH TRANSITION
TEMPERATURE, METHODS FOR THEIR USE AND PREPARATION

Date: March 1, 2004

Docket: YO987-074BZ

Group Art Unit: 1751

Examiner: M. Kopec

Commissioner for Patents
P.O. Box 1450
Alexandria, VA 22313-1450

FIFTH SUPPLEMENTAL AMENDMENT

Sir:

In response to the Office Action dated February 4, 2000:

ATTACHMENT 23

AW

COPPER OXIDE SUPERCONDUCTORS

Charles P. Poole, Jr.
Timir Datta
Horacio A. Farach

with help from

M. M. Rigney
C. R. Sanders

*Department of Physics and Astronomy
University of South Carolina
Columbia, South Carolina*



WILEY

A Wiley-Interscience Publication

JOHN WILEY & SONS

New York • Chichester • Brisbane • Toronto • Singapore

Copyright © 1988 by John Wiley & Sons, Inc.

All rights reserved. Published simultaneously in Canada.

Reproduction or translation of any part of this work beyond that permitted by Section 107 or 108 of the 1976 United States Copyright Act without the permission of the copyright owner is unlawful. Requests for permission or further information should be addressed to the Permissions Department, John Wiley & Sons, Inc.

Library of Congress Cataloging in Publication Data:

Poole, Charles P.

Copper oxide superconductors · Charles P. Poole, Jr., Timir Datta,
and Horacio A. Farach: with help from M. M. Rigney and C. R. Sanders.
p. cm.

"A Wiley-Interscience publication."

Bibliography: p.

Includes index.

I. Copper oxide superconductors. I. Datta, Timir. II. Farach,
Horacio A. III. Title.

QC611.98.C64P66 1988

S39.6'23-dc 19 88-18569 CIP

ISBN 0-471-62342-3

Printed in the United States of America

10 9 8 7 6 5 4 3 2 1

A2

PREFACE

The unprecedented worldwide effort in superconductivity research that has taken place over the past two years has produced an enormous amount of experimental data on the properties of the copper oxide type materials that exhibit superconductivity above the temperature of liquid nitrogen. The time is now ripe to bring together in one place the results of this research effort so that scientists working in this field can better acquire an overall perspective, and at the same time have available in one place a collection of detailed experimental data. This volume reviews the experimental aspects of the field of oxide superconductivity with transition temperatures from 30 K to above 120 K, from the time of its discovery by Bednorz and Müller in April 1986 until a few months after the award of the Nobel Prize to them in October 1987. During this period a consistent experimental description of many of the properties of the principal superconducting compounds such as BiSrCaCuO , LaSrCuO , TlBaCaCuO , and YBaCuO has emerged. At the same time there has been a continual debate on the extent to which the BCS theory and the electron-phonon interaction mechanism apply to the new materials, and new theoretical models are periodically proposed. We discuss these matters and, when appropriate, make comparisons with transition metal and other previously known superconductors. Many of the experimental results are summarized in figures and tables.

The field of high-temperature superconductivity is still evolving, and some ideas and explanations may be changed by the time these notes appear in print. Nevertheless, it is helpful to discuss them here to give insights into work now in progress, to give coherence to the present work, and to provide guidance for future work. It is hoped that in the not too distant future the field will settle down enough to permit a more definitive monograph to be written.

vi PREFACE

The literature has been covered almost to the end of 1987, and some 1988 work has been discussed. This has been an enormous task, and we apologize for any omissions in the citing and discussion of articles.

We wish to thank the following for giving us some advanced notice about their work: R. Barrio, B. Battlogg, L. A. Boatener, G. Burns, J. Drumheller, H. Enomoto, P. K. Gallagher, R. Goldfarb, J. E. Graebner, R. L. Greene, J. Heremans, T. C. Johnson, J. K. Karamas, M. Levy, J. W. Lynn, A. Malozemoff, K. A. Müller, T. Nishino, N. Nucker, J. C. Phillips, R. M. Silver, G. Shirane, J. Stankowski, B. Stridzker, S. Tanigawa, G. A. Thomas, and W. H. Weber. We appreciate comments on the manuscript from S. Alterowitz, C. L. Chien, D. K. Finnamore, J. Goodenough, J. R. Morton, and C. Uher, and helpful discussions with J. Budnick, M. H. Cohen, M. L. Cohen, R. Creswick, S. Deb, M. Fluss, A. Freeman, D. U. Gubser, A. M. Hermann, V. Z. Kresin, H. Ledbetter, W. E. Pickett, M. Tinkham, C. E. Violet, and S. A. Wolf. Support from the University of South Carolina, the Naval Research Laboratory, and the National Science Foundation Grant ISP 80 11451 is gratefully acknowledged.

Michael A. Poole helped to develop the computer data storage techniques that were used. Jesse S. Cook is thanked for editorial comments on the manuscript. C. Almasan, S. Atkas, J. Estrada, N. Hong, O. Lopez, M. Mesa, T. Mouzghi, and T. Usher are thanked for their interest in this project.

CHARLES P. POOLE, JR.
TIMIR DATTA
HORACIO A. FARACH

*Columbia, South Carolina
July 1988*

ects of the BCS theory, however,

id detailed treatment of the prop-
see the extent to which they con-
ey agree with some of the other
n these two chapters.

V

PREPARATION AND CHARACTERIZATION OF SAMPLES

A. INTRODUCTION

Copper oxide superconductors with a purity sufficient to exhibit zero resistivity or to demonstrate levitation (Early) are not difficult to synthesize. We believe that this is at least partially responsible for the explosive worldwide growth in these materials. Nevertheless, it should be emphasized that the preparation of these samples does involve some risks since the procedures are carried out at quite high temperatures, often in oxygen atmospheres. In addition, some of the chemicals are toxic, and in the case of thallium compounds the degree of toxicity is extremely high so ingestion, inhalation, and contact with the skin must be prevented.

The superconducting properties of the copper oxide compounds are quite sensitive to the method of preparation and annealing. Multiphase samples containing fractions with T_c above liquid nitrogen temperature (Monec) can be synthesized using rather crude techniques, but really high-grade single-phase specimens require careful attention to such factors as temperature control, oxygen content of the surrounding gas, annealing cycles, grain sizes, and pelletizing procedures. The ratio of cations in the final sample is important, but even more critical and more difficult to control is the oxygen content. However, in the case of the Bi- and Tl-based compounds, the superconducting properties are less sensitive to the oxygen content.

Figure V-1 illustrates how preparation conditions can influence superconducting properties. It shows how the calcination temperature, the annealing time, and the quenching conditions affect the resistivity drop at T_c of a BiSrCa-CuO pellet, a related copper-enriched specimen, and an aluminum-doped coun-

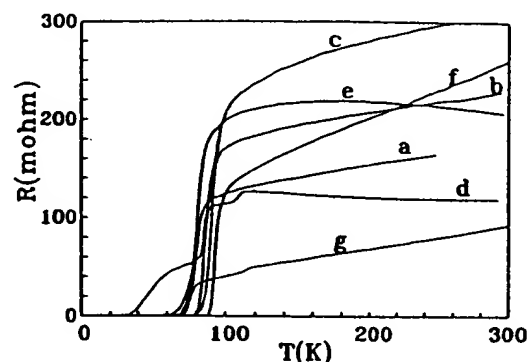


Fig. V-1. Effects of heat treatments on the resistivity transition of BiSrCaCuO_{7-x} (a) calcined at 860°C , (b) calcined at 885°C , (c) calcined at 901°C , (d) aluminum-doped sample calcined at 875°C , prolonged annealing, (e) copper-rich sample calcined at 860°C , (f) aluminum-doped sample calcined at 885°C , slow quenching and (g) calcined at 885°C , prolonged annealing, and slow quenching (Chuz5).

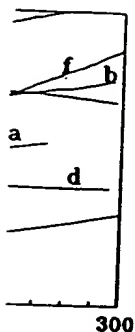
terpart (Chuz5). These samples were all calcined and annealed in the same temperature range and air-quenched to room temperature.

Polycrystalline samples are the easiest to prepare, and much of the early work was carried out with them. Of greater significance is work carried out with thin films and single crystals, and these require more specialized preparation techniques. More and more of the recent work has been done with such samples.

Many authors have provided sample preparation information, and others have detailed heat treatments and oxygen control. Some representative techniques will be discussed.

The beginning of this chapter will treat methods of preparing bulk superconducting samples in general, and then samples of special types such as thin films and single crystals. The remainder of the chapter will discuss ways of checking the composition and quality of the samples. The thermodynamic or subsolidus phase diagram of the ternary Y-Ba-Cu oxide system illustrated in Fig. V-2 contains several stable stoichiometric compounds such as the end-point oxide Y_2O_3 , BaO , and CuO at the apices, the binary oxides stable at 950° , $(\text{Ba}_2\text{CuO}_4)$ Ba_2CuO_3 , BaCuO_2 , $\text{Y}_2\text{Cu}_2\text{O}_5$, $\text{Y}_4\text{Ba}_3\text{O}_9$, Y_2BaO_4 , and $(\text{Y}_2\text{Ba}_4\text{O}_7)$, along the edges, and ternary oxides such as $(\text{YBa}_3\text{Cu}_2\text{O}_7)$, the semiconducting green phase Y_2BaCuO_5 , and the superconducting black solid $\text{YBa}_2\text{Cu}_3\text{O}_{7-x}$ in the interior (Bey2, Bour3, Cap01, Eag11, Frase, Hosoy, Jonel, Kaise, Kurth, Kuz2, Leez3, Lian1, Mali1, Schn1, Schn1, Schu1, Takay, Torra, Wagne). Compounds in parentheses are not on the figure, but are reported by other workers. The existence of a narrow range of solid solution was reported (Panso), and the argued against (Wagne) by the same group.

AMPLES



transition of $\text{BiSrCaCuO}_{7.4}$ (a) at 901°C , (d) aluminum-doped copper-rich sample calcined at low quenching and (g) calcined (25).

annealed in the same temperature.

and much of the early work was carried out with thin film specialized preparation technique with such samples.

information, and others some representative techniques.

preparing bulk superconducting types such as thin films discuss ways of checking thermodynamic or subsolidus illustrated in Fig. V-2 contains the end-point oxides table at 950° , (Ba_3CuO_4), and ($\text{Y}_2\text{Ba}_4\text{O}_7$), along the superconducting green phase $\text{YBa}_2\text{Cu}_3\text{O}_{7.6}$ in the interior, Kaise, Kurth, Kuzzz, Wagne). Compounds listed by other workers. The reported (Panso), and then

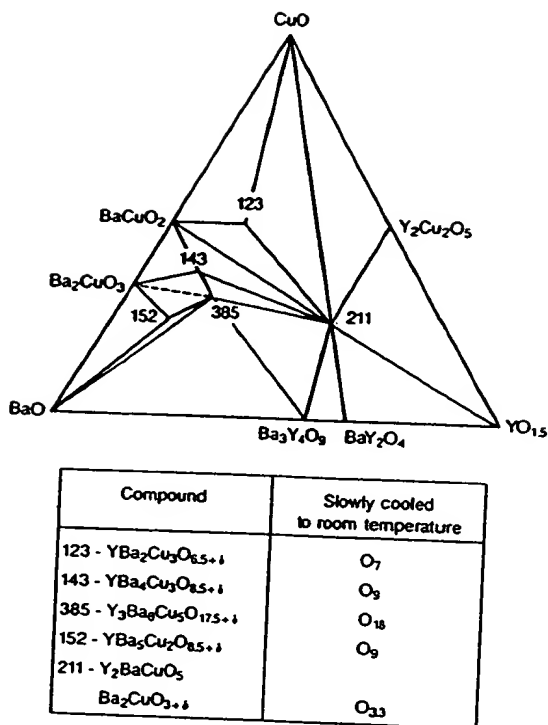


Fig. V-2. Ternary phase diagram of the Y_2O_3 - BaO - CuO system at 950°C . The green phase [Y_2BaCuO_5 , (211)] the superconducting phase [$\text{YBa}_2\text{Cu}_3\text{O}_{7.6}$, (123)], and three other compounds are shown in the interior of the diagram (DeLee).

B. METHODS OF PREPARATION

In this section three methods of preparation will be described, namely, the solid state, the coprecipitation, and the sol-gel techniques (Hatfi). The widely used solid-state technique permits off-the-shelf chemicals to be directly calcined into superconductors, and it requires little familiarity with the subtle physicochemical processes involved in the transformation of a mixture of compounds into a superconductor. The coprecipitation technique mixes the constituents on an atomic scale and forms fine powders, but it requires careful control of the pH and some familiarity with analytical chemistry. The sol-gel procedure requires more competence in analytical procedures.

In the solid-state reaction technique one starts with oxygen-rich compounds of the desired components such as oxides, nitrates, or carbonates of Ba, Bi, La, Sr, Tl, Y, or other elements. Sometimes nitrates are formed first by dissolving oxides in nitric acid and decomposing the solution at 500°C before calcination

(e.g., Davis, Holla, Kelle). These compounds are mixed in the desired atomic ratios and ground to a fine powder to facilitate the calcination process. Then these room-temperature-stable salts are reacted by calcining for an extended period (≈ 20 hr) at elevated temperatures ($\approx 900^\circ\text{C}$). This process may be repeated several times, with pulverizing and mixing of the partially calcined material at each step. As the reaction proceeds, the color of the charge changes. The process usually ends with a final oxygen anneal followed by a slow cool down to room temperature of the powder, or pellets made from the powder, by sintering in a cold or hot press. Sintering is not essential for the chemical process, but for transport and other measurements it is convenient to have the material pelletized. A number of researchers have provided information on this solid-state reaction approach (e.g., Allge, Finez, Galla, Garla, Gopal, Gubse, Hajk1, Hatan, Herrm, Hika1, Hirab, Jayar, Maen1, Mood1, Mood2, Neume, Poepp, Polle, Qadri, Rhyne, Ruzic, Saito, Sait1, Sawal, Shamo, Takit, Tothz, Wuzz3).

Some of the earlier works on foils, thick films, wires, or coatings employed a suspension of the calcined powder in a suitable organic binder, and the desired product was obtained by conventional industrial processes such as extruding, spraying, or coating.

In the second or coprecipitation process the starting materials for calcination are produced by precipitating them together from solution (e.g., Asela, Bedno, Leez7, Wang2). This has the advantage of mixing the constituents on an atomic scale. In addition the precipitates may form fine powders whose uniformity can be controlled, which can eliminate some of the labor. Once the precipitate has been dried, calcining can begin as in the solid-state reaction procedure. A disadvantage of this method, at least as far as the average physicist or materials scientist is concerned, is that it requires considerable skill in chemical procedures.

Another procedure for obtaining the start-up powder is the sol-gel technique in which an aqueous solution containing the proper ratios of Ba, Cu, and Y nitrates is emulsified in an organic phase and the resulting droplets are gelled by the addition of a high-molecular-weight primary amine which extracts the nitric acid. This process was initially applied to the La materials, but has been perfected for YBaCuO as well (Cimaz, Hatfi).

When using commercial chemical supplies to facilitate the calcination process a dry or wet (acetone) pregrinding with an agate mortar and pestle or a ball mill is recommended. Gravimetric amounts of the powdered precursor materials are thoroughly mixed and placed in a platinum or ceramic crucible. Care must be taken to ensure the compatibility of the ceramic crucible with the chemicals to obviate reaction and corrosion problems.

Complete recipes for the YBa \star material have been described (e.g., Gran2). Typically, the mixture of unreacted oxides is calcined in air or oxygen around 900°C for 15 hr. During this time the YBaCuO mixture changes color from the green Y_2BaCuO_5 phase to the dark gray $\text{YBa}_2\text{Cu}_3\text{O}_{7-\delta}$ compound. Then the charge is taken out, crushed, and scanned with X rays to determine its purity. If warranted by the powder pattern X-ray scan, the calcination process is repeated. Often, at this stage the material is very oxygen poor, and electrically it is semi-

BRIEF ATTACHMENT AX

IN THE UNITED STATES PATENT AND TRADEMARK OFFICE

In re Patent Application of

Applicants: Bednorz et al.

Serial No.: 08/479,810

Filed: June 7, 1995

Date: March 1, 2004

Docket: YO987-074BZ

Group Art Unit: 1751

Examiner: M. Kopec

For: NEW SUPERCONDUCTIVE COMPOUNDS HAVING HIGH TRANSITION
TEMPERATURE, METHODS FOR THEIR USE AND PREPARATION

Commissioner for Patents
P.O. Box 1450
Alexandria, VA 22313-1450

FIFTH SUPPLEMENTAL AMENDMENT

Sir:

In response to the Office Action dated February 4, 2000:

ATTACHMENT 3

AX

Possible High T_c Superconductivity in the Ba-La-Cu-O System

J.G. Bednorz and K.A. Müller

IBM Zürich Research Laboratory, Rüschlikon, Switzerland

Received April 17, 1986

Metallic, oxygen-deficient compounds in the Ba-La-Cu-O system, with the composition $\text{Ba}_x\text{La}_{5-x}\text{Cu}_3\text{O}_{5(3-y)}$ have been prepared in polycrystalline form. Samples with $x=1$ and 0.75 , $y>0$, annealed below 900°C under reducing conditions, consist of three phases, one of them a perovskite-like mixed-valent copper compound. Upon cooling, the samples show a linear decrease in resistivity, then an approximately logarithmic increase, interpreted as a beginning of localization. Finally an abrupt decrease by up to three orders of magnitude occurs, reminiscent of the onset of percolative superconductivity. The highest onset temperature is observed in the 30 K range. It is markedly reduced by high current densities. Thus, it results partially from the percolative nature, but possibly also from 2D superconducting fluctuations of double perovskite layers of one of the phases present.

I. Introduction

"At the extreme forefront of research in superconductivity is the empirical search for new materials" [1]. Transition-metal alloy compounds of $A15$ (Nb_3Sn) and $B1$ (NbN) structure have so far shown the highest superconducting transition temperatures. Among many $A15$ compounds, careful optimization of Nb-Ge thin films near the stoichiometric composition of Nb_3Ge by Gavalev et al. and Testardi et al. a decade ago allowed them to reach the highest $T_c=23.3$ K reported until now [2, 3]. The heavy Fermion systems with low Fermi energy, newly discovered, are not expected to reach very high T_c 's [4].

Only a small number of oxides is known to exhibit superconductivity. High-temperature superconductivity in the Li-Ti-O system with onsets as high as 13.7 K was reported by Johnston et al. [5]. Their x-ray analysis revealed the presence of three different crystallographic phases, one of them, with a spinel structure, showing the high T_c [5]. Other oxides like perovskites exhibit superconductivity despite their small carrier concentrations, n . In Nb-doped SrTiO_3 , with $n=2 \times 10^{20} \text{ cm}^{-3}$, the plasma edge is below the highest optical phonon, which is therefore unshielded

[6]. This large electron-phonon coupling allows a T_c of 0.7 K [7] with Cooper pairing. The occurrence of high electron-phonon coupling in another metallic oxide, also a perovskite, became evident with the discovery of superconductivity in the mixed-valent compound $\text{BaPb}_{1-x}\text{Bi}_x\text{O}_3$ by Sleight et al., also a decade ago [8]. The highest T_c in homogeneous oxygen-deficient mixed crystals is 13 K with a comparatively low concentration of carries $n=2-4 \times 10^{21} \text{ cm}^{-3}$ [9]. Flat electronic bands and a strong breathing mode with a phonon feature near 100 cm^{-1} , whose intensity is proportional to T_c , exist [10]. This last example indicates that within the BCS mechanism, one may find still higher T_c 's in perovskite-type or related metallic oxides, if the electron-phonon interactions and the carrier densities at the Fermi level can be enhanced further.

Strong electron-phonon interactions in oxides can occur owing to polaron formation as well as in mixed-valent systems. A superconductivity (metallic) to bipolaronic (insulator) transition phase diagram was proposed theoretically by Chakraverty [11]. A mechanism for polaron formation is the Jahn-Teller effect, as studied by Höck et al. [12]. Isolated Fe^{4+} , Ni^{3+} and Cu^{2+} in octahedral oxygen environment

show strong Jahn-Teller (J.T.) effects [13]. While SrFe(VI)O_3 is a distorted perovskite insulator, LaNi(III)O_3 is a J.T. undistorted metal in which the transfer energy b_π of the J.T. e_g electrons is sufficiently large [14] to quench the J.T. distortion. In analogy to Chakraverty's phase diagram, a J.T.-type polaron formation may therefore be expected at the borderline of the metal-insulator transition in mixed perovskites, a subject on which we have recently carried out a series of investigations [15]. Here, we report on the synthesis and electrical measurements of compounds within the Ba-La-Cu-O system. This system exhibits a number of oxygen-deficient phases with mixed-valent copper constituents [16], i.e., with itinerant electronic states between the non-J.T. Cu^{3+} and the J.T. Cu^{2+} ions, and thus was expected to have considerable electron-phonon coupling and metallic conductivity.

II. Experimental

1. Sample Preparation and Characterization

Samples were prepared by a coprecipitation method from aqueous solutions [17] of Ba-, La- and Cu-nitrate (SPECPURE JMC) in their appropriate ratios. When added to an aqueous solution of oxalic acid as the precipitant, an intimate mixture of the corresponding oxalates was formed. The decomposition of the precipitate and the solid-state reaction were performed by heating at 900 °C for 5 h. The product was pressed into pellets at 4 kbar, and reheated to 900 °C for sintering.

2. X-Ray Analysis

X-ray powder diffractograms (System D 500 SIEMENS) revealed three individual crystallographic phases. Within a range of 10° to 80° (2 θ), 17 lines could be identified to correspond to a layer-type perovskite-like phase, related to the K_2NiF_4 structure ($a=3.79$ Å and $c=13.21$ Å) [16]. The second phase is most probably a cubic one, whose presence depends on the Ba concentration, as the line intensity decreases for smaller $x(\text{Ba})$. The amount of the third phase (volume fraction > 30% from the x-ray intensities) seems to be independent of the starting composition, and shows thermal stability up to 1,000 °C. For higher temperatures, this phase disappears progressively, giving rise to the formation of an oxygen-deficient perovskite ($\text{La}_3\text{Ba}_3\text{Cu}_6\text{O}_{14}$) as described by Michel and Raveau [16].

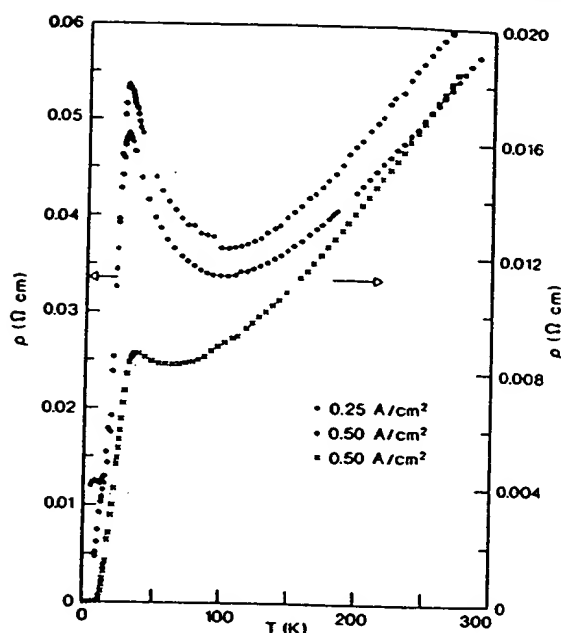


Fig. 1. Temperature dependence of resistivity in $\text{Ba}_x\text{La}_{3-x}\text{Cu}_2\text{O}_{5(3-x)}$ for samples with $x(\text{Ba})=1$ (upper curves, left scale) and $x(\text{Ba})=0.75$ (lower curve, right scale). The first two cases also show the influence of current density

3. Conductivity Measurements

The dc conductivity was measured by the four-point method. Rectangular-shaped samples, cut from the sintered pellets, were provided with gold electrodes and contacted by In wires. Our measurements between 300 and 4.2 K were performed in a continuous-flow cryostat (Leybold-Heraeus) incorporated in a computer-controlled (IBM-PC) fully-automatic system for temperature variation, data acquisition and processing.

For samples with $x(\text{Ba}) \leq 1.0$, the conductivity measurements, involving typical current densities of 0.5 A/cm², generally exhibit a high-temperature metallic behaviour with an increase in resistivity at low temperatures (Fig. 1). At still lower temperatures, a sharp drop in resistivity (> 90%) occurs, which for higher currents becomes partially suppressed (Fig. 1: upper curves, left scale). This characteristic drop has been studied as a function of annealing conditions, i.e., temperature and O_2 partial pressure (Fig. 2). For samples annealed in air, the transition from itinerant to localized behaviour, as indicated by the minimum in resistivity in the 80 K range, is not very pronounced. Annealing in a slightly reducing atmosphere, however, leads to an increase in resistivity and a more pronounced localization effect. At the same time, the onset of the resistivity drop is shifted

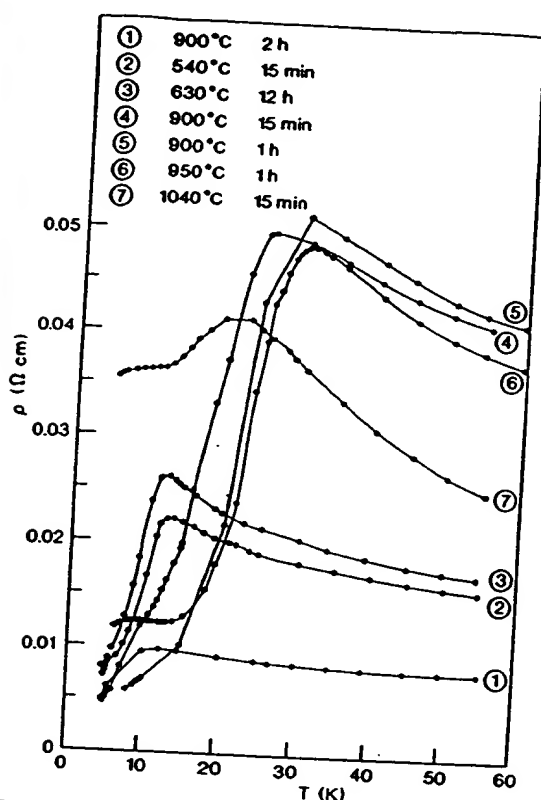


Fig. 2. Low-temperature resistivity of samples with $x(\text{Ba})=1.0$, annealed at O_2 partial pressure of 0.2 bar (curve ①) and 0.2×10^{-4} bar (curves ② to ⑦)

towards the 30 K region. Curves ④ and ⑤, recorded for samples treated at 900 °C, show the occurrence of a shoulder at still lower temperature, more pronounced in curve ④. At annealing temperatures of 1,040 °C, the highly conducting phase has almost vanished. As mentioned in the Introduction, the mixed-valent state of copper is of importance for electron-phonon coupling. Therefore, the concentration of electrons was varied by the Ba/La ratio. A typical curve for a sample with a lower Ba concentration of 0.75 is shown in Fig. 1 (right scale). Its resistivity decreases by at least three orders of magnitude, giving evidence for the bulk being superconducting below 13 K with an onset around 35 K, as shown in Fig. 3, on an expanded temperature scale. The latter figure also shows the influence of the current density, typical for granular compounds.

III. Discussion

The resistivity behaviour of our samples, Fig. 1, is qualitatively very similar to the one reported in the Li-Ti-O system, and in superconducting

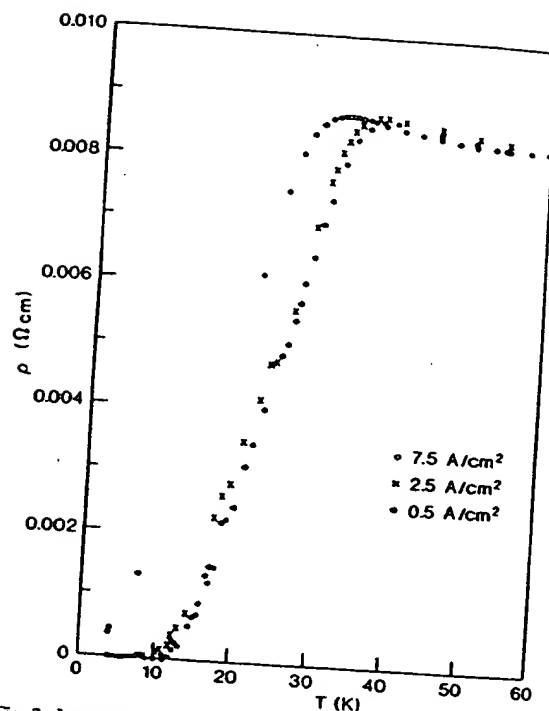


Fig. 3. Low-temperature resistivity of a sample with $x(\text{Ba})=0.75$, recorded for different current densities

$\text{BaPb}_{1-x}\text{Bi}_x\text{O}_3$ polycrystalline thin films [5, 18]. Upon cooling from room temperature, the latter exhibit a nearly linear metallic decrease of $\rho(T)$, then a logarithmic type of increase, before undergoing the transition to superconductivity. One could, of course, speculate that in our samples a metal-to-metal structural phase transition occurs in one of the phases. The shift in the drop in $\rho(T)$ with increasing current density (Fig. 3), however, would be hard to explain with such an assumption, while it supports our interpretation that we observe the onset of superconductivity of percolative nature, as discussed below. In $\text{BaPb}_{1-x}\text{Bi}_x\text{O}_3$, the onset of superconductivity has been taken at the resistivity peak [18]. This assumption appears to be valid in percolative systems, i.e., in the thin films [18] consisting of polycrystals with grain boundaries, or when different crystalline phases with interpenetrating grains are present, as found in the Li-Ti-O [5] or in our Ba-La-Cu-O system. The onset can also be due to fluctuations in the superconducting wave functions. We assume one of the Ba-La-Cu-O phases exhibits this behaviour. Therefore, under the above premises, the peak in $\rho(T)$ at 35 K, observed for an $x(\text{Ba})=0.75$ (Fig. 1), has

to be identified as the start to superconductive cooperative phenomena in the isolated grains. It should be noted that in granular Al, Cooper pairs in coupled grains have been shown to exist already at a point where $\rho(T)$ upon cooling has decreased by only 20% of its highest value. This has been proven qualitatively [19] and more recently also quantitatively [20] by the negative frequency shift occurring in a microwave cavity. In 100 Å films, a shoulder in the frequency shift owing to 2D fluctuations was observed above the T_c of the grains. In our Ba—La—Cu—O system, a series of layer-like phases with considerable variety in compositions are known to exist [16, 21], and therefore 2D correlations can be present.

The granularity of our system can be justified from the structural information, and more quantitatively from the normal conductivity behaviour. From the former, we know that more than one phase is present and the question arises how large are the grains. This can be inferred from the logarithmic fingerprint in resistivity. Such logarithmic increases are usually associated with beginning of localization. A most recent example is the Anderson transition in granular Sn films [22]. Common for the granular Sn and our samples is also the resistivity at 300 K, lying in the range of 0.06 to 0.02 Ωcm , which is near the microscopic critical resistivity of $\rho_c = 10 L_0 \hbar / e^2$ for localization. From the latter formula, an interatomic distance L_0 in the range of 100 Å is computed, thus a size of superconducting grains of this order of magnitude must be present. Upon cooling below T_c , Josephson junctions between the grains phase-lock progressively [23] and the bulk resistivity gradually drops to zero by three orders of magnitude, for sample 2 (Fig. 1). At larger current densities, the weaker Josephson junctions switch to normal resistivity, resulting in a temperature shift of the drop, as shown in Fig. 3. The plateau in resistivity occurring below the 80% drop (Fig. 1) for the higher current density of 0.5 A/cm², and Fig. 2 curve ⑥) may be ascribed to switching of junctions to the normal state.

The way the samples have been prepared seems to be of crucial importance: Michel et al. [21] obtained a single-phase perovskite by mixing the oxides of La and Cu and BaCO₃ in an appropriate ratio and subsequent annealing at 1,000 °C in air. We also applied this annealing condition to one of our samples, obtained by the decomposition of the corresponding oxalates, and found no superconductivity. Thus, the preparation from the oxalates and annealing below 950 °C are necessary to obtain a non-perovskite-type phase with a limited temperature range of stability exhibiting this new behaviour. The formation of this phase at comparatively low temperatures is favoured by the intimate mixture of the compo-

nents and the high reactivity of the oxalates owing to the evolution of large amounts of H₂O and CO₂ during decomposition.

IV. Conclusion

In the concentration range investigated, compounds of the Ba—La—Cu—O system are metallic at high temperatures, and exhibit a tendency towards localization upon cooling. Samples annealed near 900 °C under reducing conditions show features associated with an onset of granular superconductivity near 30 K. The system consists of three phases, one of them having a metallic perovskite-type layer-like structure. The characterization of the new, apparently superconducting, phase is in progress. An identification of that phase may allow growing of single crystals for studying the Meissner effect, and collecting specific-heat data to prove the presence of high T_c bulk superconductivity.

The authors would like to thank H.E. Weibel for his help in getting familiar with the conductivity measurement system, E. Courtens and H. Thomas for discussions and a critical reading of the manuscript.

References

1. Tinkham, M., Beasley, M.R., Larbalestier, D.C., Clark, A.F., Finnemore, D.K.: Workshop on Problems in Superconductivity, Copper Mountain, Colorado, August 1983, p. 12
2. Beasley, M.R., Geballe, T.H.: Phys. Today 36 (10), 60 (1984)
3. Müller, J.: Rep. Prog. Phys. 43, 663 (1980)
4. Ott, H.R.: Unconventional Superconductivity. Zürich Phys. Soc. Seminar, Zürich, February 13, 1986
5. Johnston, D.C., Prakash, H., Zachariasen, W.H., Viswanathan, R.: Mat. Res. Bull. 8, 777 (1973)
6. Baratoff, A., Binnig, G.: Physics 108 B, 1335 (1981)
7. Baratoff, A., Binnig, G., Bednorz, J.G., Gervais, F., Servoin, J.L.: In: Superconductivity in *d*- and *f*-Band Metals, Proceedings IV Conference in 'Superconductivity in *d*- and *f*-Band Metals'. Buckel, W. and Weber, W. (eds), p. 419, Kernforschungszentrum Karlsruhe 1982
8. Binnig, G., Baratoff, A., Hönig, H.E., Bednorz, J.G.: Phys. Rev. Lett. 45, 1352 (1980)
9. Sleight, A.W., Gillson, J.L., Bierstedt, F.E.: Solid State Commun. 17, 27 (1975)
10. Batlogg, B.: Physica 126 B, 275 (1984)
11. Thanh, T.D., Koma, A., Tanaka, S.: Appl. Phys. 22, 205 (1980)
12. Mattheis, F., Hamann, D.R.: Phys. Rev. B 26, 2682 (1982); *ibid.* 28, 4227 (1983)
13. Chakraverty, B.K.: J. Phys. Lett. 40, L99 (1979); J. Phys. 42, 1351 (1981)
14. Höck, K.-H., Nickisch, H., Thomas, H.: Helv. Phys. Acta 56, 237 (1983)
15. Englmann, R.: In: The Jahn-Teller Effect in Molecules and Crystals. London, New York: Wiley Interscience 1972
16. Goodenough, J.B., Longo, M.: Magnetic and other properties of oxide and related compounds. In: Landolt-Boernstein New

- Series. Vol III/4a: Crystal and solid state physics. Hellwege, K.H., Hellwege, A.M. (eds.), p. 262, Fig. 73. Berlin, Heidelberg, New York: Springer-Verlag 1970
15. Bednorz, J.G., Müller, K.A.: (in preparation)
 16. Michel, C., Raveau, B.: *Chim. Min.* 21, 407 (1984)
 17. Bednorz, J.G., Müller, K.A., Arend, H., Gränicher, H.: *Mat. Res. Bull.* 18 (2), 181 (1983)
 18. Suzuki, M., Murakami, T., Inamura, T.: *Shinku* 24, 67 (1981) (in Japanese)
Enomoto, Y., Suzuki, M., Murakami, T., Inukai, T., Inamura, T.: *Jpn. J. Appl. Phys.* 20, L661 (1981)
 19. Müller, K.A., Pomerantz, M., Knoedler, C.M., Abraham, D.: *Phys. Rev. Lett.* 45, 832 (1980)
 20. Stocker, E., Buttat, J.: *Solid State Commun.* 53, 915 (1985)
 21. Michel, C., Er-Rakho, L., Raveau, B.: *Mat. Res. Bull.* 20, 667 (1985)
 22. Van Haesendonck, C., Bruynsraede, Y.: *Phys. Rev. B* 33, 1684 (1986)
 23. Deutscher, G., Entin-Wohlman, O., Fishman, S., Shapira, Y.: *Phys. Rev. B* 21, 5041 (1980)

J.G. Bednorz
K.A. Müller
IBM Zürich Research Laboratory
Säumerstrasse 4
CH-8803 Rüschlikon
Switzerland

Note Added in Proof

Chemical analysis of the bulk composition of our samples revealed a deviation from the ideal La/Ba ratios of 4 and 5.66. The actual ratios are 16 and 18, respectively. This is in agreement with an identification of the third phase as CuO.

BRIEF ATTACHMENT AY

INTRODUCTION

Exploring Superconductivity

Georg Bednorz

In 1987, Georg Bednorz shared the Nobel Prize in Physics with his partner and mentor, K. Alex Müller "For their important breakthrough in the discovery of superconductivity in ceramic materials." Their breakthrough, accomplished in an IBM research lab in Switzerland, centered around the fabrication of a new copper-oxide compound that was superconducting at temperatures high enough to dramatically extend the applications of superconductors. To comprehend the significance of Bednorz's work, one must first understand the history of research in superconductivity.

Early investigations of superconductors that operate at temperatures higher than 23.2° K focused on metallic compounds that are good conductors of current at room temperature. In 1957 John Bardeen, Leon N. Cooper, and J. Robert Schrieffer (Nobel Prize in Physics, 1972) of the University of Illinois presented a new theory of superconductivity that changed the focus of research. In ordinary conductors some energy is lost to resistance because the conducting electrons scatter off impurities and vibrating atoms, known as phonons. According to the BCS theory (named for the initials of its originators), superconducting current is carried by pairs of electrons. This pairing keeps individual electrons from scattering off impurities, thus preventing resistance and establishing the superconducting state. Furthermore, it is the interaction between the electrons and the atomic structure of the superconductor that is responsible for the electron pairing.

With this new theory, the search for high-temperature superconductors shifted from metals and metal alloys to materials that display a strong interaction between the electron pairs and the underlying atomic structure. Scientists turned to oxides, which are normally insulators.


The initial research led to modest advances. In 1973 David Johnston at the University of California at San Diego discovered superconductivity in lithium-titanium oxide at 13.7° K. In 1975 Arthur Sleight at Du Pont Research observed barium-lead-bismuth oxide superconducting at 13° K. X-ray analysis indicated the presence of significant interaction between electrons and the vibrations of the structural atoms (phonons). This fit the BCS theory and suggested that further research on metal oxides might prove rewarding.

In 1983 Alex Müller, who had been conducting research on insulators, proposed that Bednorz collaborate with him in a search for high-temperature superconductors in metal oxides. Bednorz agreed because he felt the combination of Müller's vision and his expertise in solid-state physics would lead to success.

They first experimented with nickel oxides, but had disappointing results. Progress was slow and the amount of time and energy they could devote to this work was limited because it was not a major focus at the IBM research facility. The two men persevered, however, because they knew that oxide materials satisfied the requirements of the current BCS theory and that under the proper conditions such a material should prove to be superconducting at high temperatures.

[Click here](#)  To hear Georg Bednorz describe their early work.

Then in the fall of 1985 Bednorz read a paper by Claude Michel, L. Er-Rakho, and Bernard Raveau (from the University of Caen) that described their work with copper-oxide compounds. Bednorz immediately realized that a mixture of copper and barium would have the properties he was seeking, and on that very day he fabricated the new compound, a ceramic insulator composed of lanthanum, barium, and copper oxide. Since he could not duplicate the exact conditions under which the French scientists prepared their compound, he used a different preparation scheme. As it turned out, that "chance" modification led to the Nobel Prize.

[Click here](#)  To hear Georg Bednorz describing the results of their modification.

In January 1986 the new material was tested and the resistance analysis indicated that it was superconducting. Bednorz recalls that "when it happened, I didn't trust my eyes." The fabrication scheme he used had a different amount of oxygen and a more moderate heating process than the original French one; this turned out to be a key to its superconducting character. Bednorz's compound--and all subsequent metal-oxide superconductors--contained very thin sheets of copper oxide separated by layers of other metal oxides. There appears to be a direct correlation between the number of copper-oxide layers in a superconductor and its critical temperature. In general, the greater the number of copper-oxide layers, the higher the critical temperature. By varying the barium content and heating conditions, Bednorz was able to produce a material that was superconducting at temperatures as high as 30° K, seven degrees higher than the existing record.

When Bednorz's laboratory detected the initial data supporting the high-temperature superconductivity of the copper-oxide ceramic material, Bednorz and Müller had to make a difficult decision. There had been many unsubstantiated and overrated claims of high-temperature superconductors, and they wondered if they should publish their results immediately in a prominent journal or wait until they substantiated their results with the more rigorous magnetic tests (to detect the Meissner effect). Delays at this stage would mean that others working on similar projects could publish their findings first and receive the credit. They decided to submit their results at once to a journal that would not have many specialists as readers. They also wanted a journal with a fair amount of time between submission and publication, which would allow them to complete the magnetic testing before the article appeared. Their initial results were submitted to the Swiss Journal Zeitschrift fur Physik on April 17, 1986, and were published in the September issue. The paper received little attention, and by mid-October they had final confirmation of superconductivity.

[Click here](#)  To hear Georg Bednorz describing their thoughts on publishing their results.

Bednorz and Müller announced their discovery to the physics community, which was initially skeptical. Their colleagues questioned the validity of the data, and many laboratories throughout the world set out to verify their claims. After confirmation by the University of Tokyo, the University of Houston, and Bell Laboratories, the scientific community began to realize that their claim of high-temperature superconductivity was valid.

Attention in the scientific community then focused on raising the temperature, and by the end of 1986 Bednorz raised the critical temperature of the barium-lanthanum-copper oxide system to 40° K by replacing barium with strontium. Researchers from the University of Houston and the University of Alabama, led by Paul Chu, then found that they could raise the compound's critical temperature to 52° K by applying pressure to the present metal oxide superconductor. This connection between compression of a crystal and an elevated critical temperature led Paul Chu to replace lanthanum with a smaller atom, yttrium. On February 16, 1987, his research group established the critical temperature of yttrium-

barium-copper oxide at 92° K. This advance was particularly significant because this compound could be cooled with cheap and readily available liquid nitrogen. These new materials were dubbed high-temperature superconductors.

The newest members of the superconductor family contain bismuth or thallium. On January 22, 1988, Hiroshi Maeda of Tsukuba Laboratories of the National Research Institute of Metals discovered a critical temperature of 105° K for a bismuth-calcium-strontium-copper oxide compound. On January 26, 1988, Paul Chu reported a critical temperature of 120° K for the same system. On February 22, 1988, Zhengzhi Sheng and Allen Hermann of the University of Arkansas announced that a compound of thallium-calcium-barium-copper oxide exhibited an onset critical temperature of 120° K. Many research groups are now working diligently to find new materials that display even higher critical temperature.

It is worth noting that there is no accepted theory to explain the high-temperature behavior of this type of compound. The BCS theory, which has proven to be a useful tool in understanding lower-temperature materials, does not adequately explain how the Cooper pairs in the new compounds hold together at such high temperatures. When Bednorz was asked how high-temperature superconductivity works, he replied, "If I could tell you, many of the theorists working on the problem would be very surprised."

[Back to Interactive Learning Studio](#)

BRIEF ATTACHMENT AZ

April 2002

“A Snapshot View of High Temperature Superconductivity 2002”

Ivan K. Schuller¹, Arun Bansil², Dimitri N. Basov¹, Malcolm R. Beasley³, Juan C. Campuzano⁴, Jules P. Carbotte⁵, Robert J. Cava⁶, George Crabtree⁴, Robert C. Dynes¹, Douglas Finnemore⁷, Theodore H. Geballe³, Kenneth Gray⁴, Laura H. Greene⁸, Bruce N. Harmon⁷, David C. Larbalestier⁹, Donald Liebenberg¹⁰, M. Brian Maple¹, William T. Oosterhuis¹⁰, Douglas J. Scalapino¹¹, Sunil K. Sinha¹, Zhixun Shen³, James L. Smith¹², Jerry Smith¹⁰, John Tranquada¹³, Dale J. van Harlingen⁸, David Welch¹³

¹University of California, San Diego, ²Northeastern University, ³Stanford University, ⁴Argonne National Laboratory, ⁵McMaster University, ⁶Princeton University, ⁷Ames Laboratory, ⁸University of Illinois, ⁹University of Wisconsin, ¹⁰U.S. Department of Energy, ¹¹University of California, Santa Barbara, ¹²Los Alamos National Laboratory, ¹³Brookhaven National Laboratory

Table of Contents

- I. **Summary**
- II. **Structure, Bonding and New Systems**
 - 1. Synthesis and Fabrication
 - a) *Bulk*
 - b) *Thin films*
 - c) *Doping in the Cuprate Superconductors*
 - 2. Other Topics of Interest:
 - a) *Applied pressure*
 - b) *Spin, lattice, and charge correlations*
 - 3. Conclusion
- III. **Electronic structure and quasiparticle dynamics**
 - 1. Techniques
 - a) *Electron Tunneling*
 - b) *Angular Resolved Photoemission Spectroscopy (ARPES)*
 - c) *Infrared Spectroscopy*
 - 2. Magnetism, Competing Order, and Phonons
 - a) *Magnetism and Spin Fluctuations*
 - b) *Competing Orders*
 - c) *Phonons and Electron-Phonon Interactions*
- IV. **Vortices**
 - 1. Single Vortex Physics
 - a) *Confinement*
 - b) *Pseudovortices and Vortex Core States*
 - c) *Hybrid Materials*
 - 2. Multivortex Physics
 - a) *Disordered Glassy and Liquid States*
 - b) *Dynamic Phases*
 - c) *Josephson Vortices and Crossing Lattices*
 - 3. Instrumentation
- V. **Proximity and Interface Effects**
- VI. **Nonequilibrium Effects**
- VII. **Theory**
 - 1. Preamble
 - 2. Phenomenological Approach
 - a) *Status*
 - b) *Key issues and opportunities*
 - 3. Numerical Studies of Hubbard and t-J Models
 - a) *Status*
 - b) *Key issues and opportunities*
 - 4. Electronic Structure
 - a) *Status*
 - b) *Key issues and opportunities*
- VIII. **Defects and Microstructure with an Eye to Applications**

I. Summary

This report outlines the conclusions of a workshop on High Temperature Superconductivity held April 5-8, 2002 in San Diego. The purpose of this report is to outline and highlight some outstanding and interesting issues in the field of High Temperature Superconductivity. The range of activities and new ideas that arose within the context of High Temperature Superconductors is so vast and extensive that it is impossible to summarize it in a brief document. Thus this report does not pretend to be all-inclusive and cover all areas of activity. It is a restricted snapshot and it only presents a few viewpoints. The complexity and difficulties with high temperature superconductivity is well illustrated by the Buddhist parable of the blind men trying to describe "experimentally" an elephant. These very same facts clearly illustrate that this is an extremely active field, with many unanswered questions, and with a great future potential for discoveries and progress in many (sometimes unpredictable) directions.

It is very important to stress that independently of any current or future applications, this is a very important area of basic research.

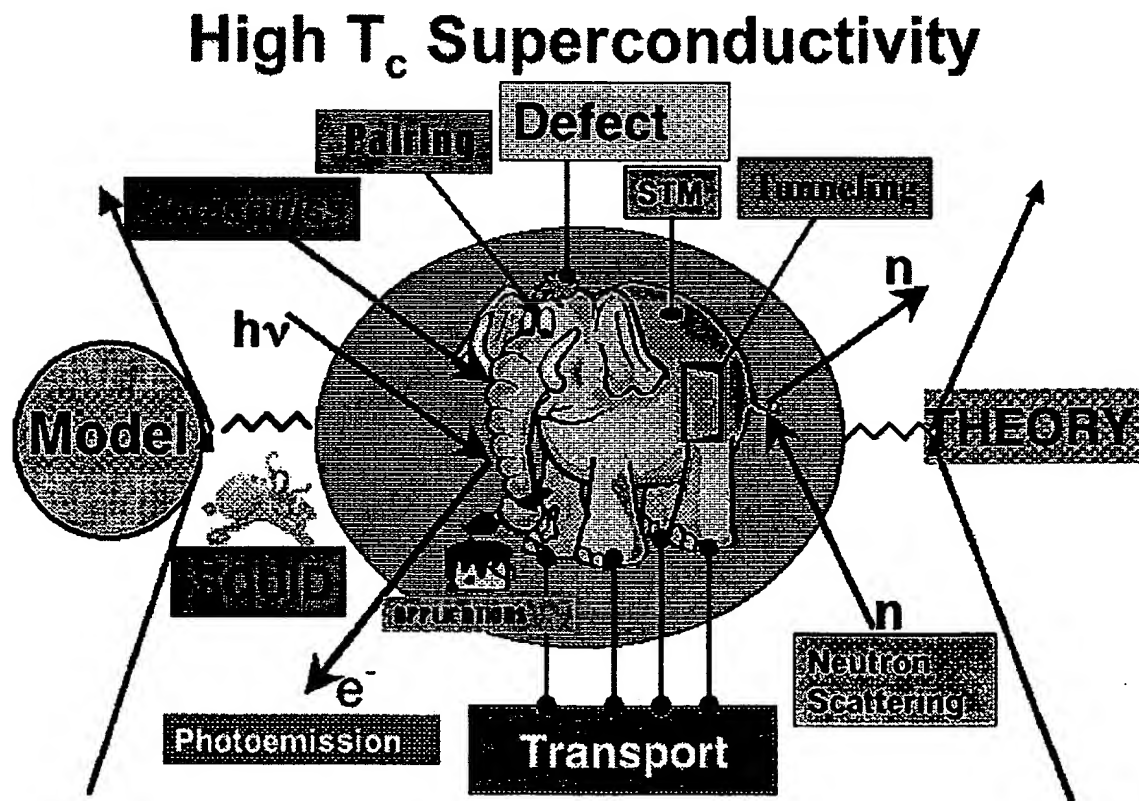


Fig. 1 Status of High Temperature Superconductivity.[1]

Basic research in high temperature superconductivity, because the complexity of the materials, brings together expertise from materials scientists, physicists and chemists, experimentalists and theorists. Much of the research in High T_c superconductivity has spilled over to other areas of research where complex materials play an important role such as magnetism in the manganites, complex oxides, two and one dimensional magnets, etc. Applications could greatly benefit from the discovery of new superconductors which are more robust and allow easier manufacturing. Perhaps this is not possible since a naive inspection of superconductors seems to indicate that the higher the T_c the more complex the material. An excellent review where many target needs for applications have been outlined is an NSF report of ~5 years ago. Many of the comments made there regarding applied needs, are still valid[2].

It is important to realize that this field is based on complex materials and because of this materials science issues are crucial. Microstructures, crystallinity, phase variations, nonequilibrium phases, and overall structural issues play a crucial role and can strongly affect the physical properties of the materials. Moreover, it seems that to date there are no clear-cut directions for searches for new superconducting phases, as shown by the serendipitous discovery of superconductivity in MgB_2 . Thus studies in which the nature of chemical bonding and how this arises in existing superconductors may prove to be fruitful. Of course, "enlightened" empirical searches either guided by chemical and materials intuition or systematic searches using well-defined strategies may prove to be fruitful. It is interesting to note that while empirical searches in the oxides, gave rise to many superconducting systems, similar (probable?) searches after the discovery of superconductivity in MgB_2 have not uncovered any new superconductors. Anyhow, this illustrates that superconductivity is pervasive in many systems and thus future work should not be restricted to a particular type of materials systems. See Chapter II.

Research in the electronic properties of High T_c superconductors has proven to be particularly fruitful. This has lead to improvements in electronic structure techniques which unquestionably have an effect on other fields. The improvement on real and reciprocal space resolution uncovered many interesting properties. However, it is not clear at the present time whether many of these properties are related in some essential way to superconductivity or they are just accidentally present. It seems that the presence of competing phenomena is present in most high temperature superconductors. Thus it is natural to investigate systems which are close to some form of instability such as the metal-insulator transition, magnetic phases, electronic instabilities such as stripe phases, etc. Comparisons of classical infrared spectroscopy, and photoemission measurements with tunneling may prove to be fruitful. In particular, mapping with high resolution (in real and reciprocal space) the electronic structure may prove to hold some of the keys to the mechanism of superconductivity. To make these useful, issues such as surface contamination, surface segregation, and in general heterogeneity of the materials close to surfaces or interfaces must be addressed, and are particularly important in these very short coherence length superconductors. This is particularly important for surface sensitive probes such as photoemission. Several techniques such as Raman scattering, NMR and muon spin depolarization are not addressed in this snapshot, although they give

valuable information and are heavily researched. Complementary measurements are particularly useful if a whole battery of tests, **in the same sample**, which are structurally characterized in detail, are performed. The "quality" of samples on the other hand, must be well established by structural criteria which are well defined "a-priori" and not based on circular or theoretical arguments. See Chapter III.

The properties of High Temperature Superconductors in a magnetic field have proven to be particularly interesting. A myriad of new phases have been uncovered in the vortex system and have lead to the establishment of a very complex phase diagram the details of which are still being established. The presence of many phases and the interaction/competition/closeness to magnetic phases allows for much new research using artificially structured pinning. New lithography and preparation techniques allow modifications and confinement of these materials in length scales approaching the superconducting coherence length and certainly the penetration depth. Moreover, novel imaging techniques are arising which can give detailed microscopic images of the vortex system. This of course can provide the microscopic picture of the magnetic state of high temperature superconductors and will probably also help improvements on their use. See Chapter IV.

Many basic research studies and a large number of applications require the High Temperature Superconductors to be in proximity with other materials. Thus issues of proximity effects, spatial variations close to an interface or surface, structural and materials variations are particularly important in thin film and/or nanoscopic structures. For this purpose it is important to investigate the mutual interaction between superconductors and other materials. This requires careful preparation and detailed characterization of inhomogeneous materials, together with superconducting measurements as a function of well-defined structural parameters. This may also allow addressing issues such as the importance of the proximity to other ordered phases such as magnetic and electronic inhomogeneities which are naturally existent or are artificially engineered. It is not even clear in the various models of high temperature superconductivity or even experimentally how the proximity effect occurs. What is the dependence of the order parameter in an ordinary or magnetic metal, or a low temperature superconductor when in proximity with a d-wave superconductor? See Chapter V

Contrary to low temperature superconductors, high T_c ones have received very little attention under nonequilibrium (time dependent, strongly driven, exposed to varying radiations, etc.) conditions. This may prove to be a very interesting and novel direction for ceramic oxides. These types of studies may hold important clues to the mechanism of superconductivity, may unravel new physics and are important in many applications. For instance, simple issues such as the microscopic nature or even existence of critical slowing down close to the superconducting phase transition has not been firmly established. See Chapter VI.

The theory of high temperature superconductivity has proven to be elusive to date. This is probably as much caused by the fact that in these complex materials it is

very hard to establish uniquely even the experimental phenomenology, as well as by the evolution of many competing models, which seem to address only particular aspects of the problem. The Indian story[1] of the blind men trying to characterize the main properties of an elephant by touching various parts of its body seems to be particularly relevant. It is not even clear whether there is a single theory of superconductivity or whether various mechanisms are possible. Thus it is impossible to summarize, or even give a complete general overview of all theories of superconductivity and because of this, this report will be very limited in its theoretical scope. The general view point (determined by "majority vote") seems to be that low temperature superconductors are phonon mediated whereas high T_c ones are somehow "unconventional" and anisotropic, although the origin of the anisotropy remains controversial. Because of this, numerical studies in well-defined theoretical models may prove to be particularly illuminating and may help uncover the essence of superconductivity. Particularly, understanding and further developing the t-J model looks like a promising numerical direction. Electronic structure calculations combined with well developed methodologies seem to explain quantitatively many aspects of superconductors with moderate T_c s. How far can these type of approaches be pushed? Could they in fact explain ab-initio superconductivity in some of the cuprates? Moreover, first principle electronic calculations may be very useful in providing parameters for model hamiltonians. Another approach which at least allows parametrizing in some useful way the properties of superconductors has also been used. How far can these type of models go and how universally can they explain the (superconducting or normal) properties is not clear at this stage. There are several important issues which must be kept in mind. It may be that there is a theoretical model which has the essence of the problem in it and it either has not yet been developed or has not yet percolated to the conscience of the community. Moreover, it seems that to date no theory has been developed which has predictive power as far as materials system are concerned. Since purely theoretical approaches have difficulties so far in identifying a clear avenue for search, empirical studies in which materials parameters and properties are correlated with superconducting properties may prove useful[3]. This may serve at a later stage as a test ground for theories. Comparisons of theoretical ideas which rely only on the layered material of high T_c ceramics, with artificially engineered layered superlattices should not be neglected and may prove to be useful. See Chapter VII.

Finally, there seems to be still much work needed to understand in detail the connections, control and effect of defects on high temperature superconductivity. This of course is very important for applications, particularly those which require high critical currents such as power applications. Moreover, the intrinsic brittleness highlights that understanding and controlling the mechanical properties while not directly related to superconductivity, is a very important and promising new area of research, especially in connections with large scale applications. See Chapter VIII.

In the rest of this paper we will expand on these issues and attempt to outline some well defined promising directions of research. The focus is mostly on basic research challenges and opportunities, which hold back progress.

II. Structure, Bonding and New Systems

The discovery of new superconducting materials has played an important role in the advancement of the field of superconductivity research since its inception[4-7]. This was perhaps most dramatically displayed by the discovery of the high T_c cuprates in 1986. The influence of new superconducting systems continues to this day, for example through the discovery in 2001[8] of MgB_2 . Thus far, the existence of a totally new superconductor has proven impossible to predict from first principles. Therefore their discovery has been based largely on empirical approaches, intuition, and even serendipity. This unpredictability is at the root of the excitement that the condensed matter community displays at the discovery of a new material that is superconducting at high temperature. New systems can be found by either bulk methods or thin film methods, each of which has its own advantages, disadvantages, challenges and opportunities. The search for new materials has always been[9], and remains an important area of research in the field of superconductivity.

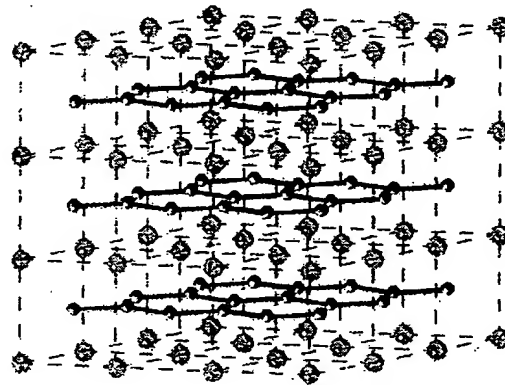


Fig. 2 The crystal structure of MgB_2 . The graphite-like array of boron (shown in black) is critical to the occurrence of high temperature superconductivity in this compound.

Also important for the development of potentially practical materials and the understanding of the complex physical phenomena which occur in superconducting materials has been the use of chemical doping or manipulation to influence the electronic and magnetic properties of the superconducting systems. An example of the former chemical doping is the introduction of small flux pinning chemical precipitates in conventional intermetallic superconductors and 123-type superconductors. Examples of the latter are found in the "lightly doped" cuprates and other perovskite structure transition metal oxides where the concepts of charge and orbital ordering have recently emerged as important considerations in attempts to understand magnetic and electronic properties. These cooperative states join other such states such as charge density waves and spin density waves as critically influential in determining the ultimate electronic

ground state of complex materials. Chemical doping has played an essential role in these areas. Importantly, it allows for the systematic variation of electronic properties as a function of variables such as lattice size, carrier concentration, and magnetic or non-magnetic disorder, providing a basis for the development of theoretical models. This area of research is highly active in the field of superconductivity, and will continue to be of great importance in the future.

1. Synthesis and Fabrication

a) Bulk

In the high density of states conventional intermetallic superconductors, the BCS coupling through the lattice may be viewed as a general lattice phenomenon. In more recently discovered superconductors, such as MgB_2 , it has been found that one particular phonon mode – an in-plane boron mode that modulates bond lengths and angles within the flat B honeycomb lattice in the case of MgB_2 – is responsible for coupling to the conduction electrons and is the driving force for superconductivity[10, 11]. Conclusions about the nature of the phonons and electrons that are responsible for the superconductivity in a particular material can be arrived at nowadays by sophisticated experimental study and theoretical analysis. In particular the band-structure experts can calculate the effect that a particular phonon has on the electrons at the Fermi energy in a particular superconductor by doing “frozen phonon calculations”. Such calculations are highly instructive for superconducting materials like MgB_2 .

This analysis is after the fact, unfortunately, for people whose interest is in finding the new superconductors in the first place. So given the fact that undirected combinatorial chemistry will never get through all the possible element/treatment combinations in a search for superconducting materials, one important issue to be resolved in future research is to translate the physics of superconductivity into a set of chemical hypotheses to guide the search for new ones. The era of finding new high temperature superconductors in intermetallic compounds like Nb_3Ge appears to be long gone. The new breed of high T_c superconductors is quite different – even beyond the cuprates, which are their own special case. The difference lies in the type of chemical bonding these superconductors display, even in what look like classic intermetallic compounds such as MgB_2 and $\text{LuNi}_2\text{B}_2\text{C}$ [12]. Thus one important issue for future research is to explore how the nature of the chemical bonding present influences the superconductivity in “conventional” intermetallic compounds.

Initially promising reports of electronic doping through charge injection into a variety of organic and inorganic compounds in FET device structures have recently been called into question[13]. Nonetheless, conceptually they point out that another area of future research in new superconducting systems should be that non-thermodynamic synthetic methods should be actively pursued. Modulation doping, the chemical analogue of charge injection, for transferring charge between layers in fine scaled multilayered films, has potential which is yet to be exploited. Other methods for non-thermodynamic synthesis with high potential for success include quenching from high pressure or from

the vapor, epitaxial thin film layer by layer or block-by-block growth, photodoping, electrochemical synthesis at low temperatures, ion exchange, framework stabilization of structures, and electrochemical intercalation.

b) Thin Films.

There are many examples of stabilization of non thermodynamic compounds in thin films in both the cuprate superconductors and in dielectric or ferroelectric materials by using epitaxy with substrate or buffer layers. In the most extreme examples of this type of metastable material it may be a single atomic layer or even an interface that has the desired properties. On such short length scales, chemical bonding is the predominant influencing factor. Different physical and chemical methods of growth influence the behavior of surfaces and very thin layers. Great progress has been made in characterization after growth – such as Transmission Electron Microscopy (TEM) and X-ray probes, but a great deal more may be gained in the future by incorporating techniques that can be used *in situ* to characterize surfaces during growth.

Of particular interest in the search for new materials is the “phase spread method” used with success by some materials physicists. In this method, thin films are made by intentionally introducing composition gradients, for example by having three atomic sources in a triangular geometry, such that their deposition areas only partially overlap. The film thus fabricated contains mixtures of the source atoms in systematically varying ratios depending on proximity of substrate to one or another of the source. Annealing of such composition spreads under different conditions can be employed to search significant areas of phase space.

Photoexcitation provides another non-thermodynamic method to perform doping studies on thin films in a reproducible way without changing material, thus avoiding the inherent difficulties with controlling stoichiometry, uniformity, and homogeneity of the samples[14, 15]. Persistent photoexcitation has been performed in many cuprate superconductors and on the magnetic manganites at low temperatures below 100K. Large changes in conductivity, Hall effect, mobility, and superconducting transition temperatures have been observed. In the best model for this process, light generates an electron hole pair and the electron is trapped in a defect thus changing the hole doping in the electronically active layer providing a potentially useful way to trim device properties and “write” artificial nanostructures without need for lithography.

c) Doping in the Cuprate Superconductors.

The properties of the cation-substituted and oxygen-doped high-temperature superconductors have been studied in detail since 1987. In general, the physical properties (temperature-dependent resistivity, superconducting transition temperature, Hall effect, etc.) and the structural properties of the HTS cuprates behave quite differently as a function of substitutions in comparison to conventional superconductors. Doping and ion-induced disorder have shown that a small change in physical structure can induce a dramatic change in the electronic structure in these materials. This was one

of the first indications that they were unconventional superconductors. The details of the effects of atomic substitutions or doping are not yet fully understood in the cuprate superconductors, and this represents an active area of current research. Concentrating on $\text{YBa}_2\text{Cu}_3\text{O}_{7-\delta}$ (YBCO) for example, some of these issues are:

i) *Doping on the Y-site.*

Doping with the heavy Rare Earth (RE) ions on the Y-site, even with Gd, does not affect T_c , except for substitutions of the Y with Pr. The effects of Pr-doping remain controversial.

ii) *Doping on the CuO chains.*

Substitutions of 3+ ions (e.g., Al, Co, Fe) primarily replace Cu in the CuO chains. Extra oxygen is simultaneously incorporated into the chain layer, the c-axis lattice constant increases, and an orthorhombic to tetragonal transition occurs. Since the extra oxygen compensates for the valence of the substituted cation, it remains an open question as to whether the resulting doped materials are underdoped or overdoped. Also, it has long been known that not only is the T_c of YBCO dependent on the oxygen concentration, but also on how the oxygen is ordered. Open issues remain, such as why do the chain oxygens need to be ordered to maximize the T_c ?

iii) *Doping in the CuO_2 planes.*

Both Ni and Zn predominately replace copper in the CuO_2 planes without significant structural change. However, T_c falls faster in these cases than it does with increased 3+-cation doping on the chains or oxygen doping on the chains. That is an indication that the loss of structural continuity of the CuO_2 plane is more detrimental to the superconducting transition temperature than the lattice changes that occur due to doping on the CuO chains. There are interesting data comparing the Ni and Zn-doping: T_c falls faster with increasing the Zn doping than with increasing the Ni doping. Conversely, the room temperature resistivity increases faster and the Relative Resistance Ratio (RRR) [$R(300) / R(0)$ -extrapolated] reduces faster with increasing Ni doping than increasing Zn doping. Therefore, Zn destroys the superconducting phase faster and the Ni destroys the normal metal phase faster. Remaining issues are: Why do Ni and Zn substitution reduce T_c so dramatically? and Why does Zn suppress the superconducting state faster than Ni, while Ni suppresses the normal state faster than Zn?

iv) *The Role of the Charge Reservoir Layers.*

The cuprates containing Hg, Tl and Bi ions in their charge reservoir layers have unusually high T_c s. These ions are known to charge disproportionate, which makes them negative U-centers. Under some circumstances it is known that negative U-centers can be superconducting pairing centers. It is of great interest to determine whether superconducting pairing on the charge reservoir layers is responsible for the enhanced T_c s.

of the Hg, Bi and Tl cuprates, and if so whether the negative U approach can be turned into a general method for finding and enhancing superconductivity.

2. Other Topics of Interest

a) *Applied Pressure.*

The investigation of high temperature superconductors under high pressure has the advantage that the basic interactions responsible for superconductivity can be changed without introducing disorder into the system as encountered in alloying experiments. The drawback is that one has to deal with massive high pressure cells, small sample sizes, and technical difficulties that increase with the higher the pressure range of interest. Measurements of the pressure dependence of T_c are the most straightforward since this can be accomplished through measurements of the electrical resistivity and the ac magnetic susceptibility under pressure. The electrical resistivity in the normal state, which can be accessed even below T_c by suppressing superconductivity with a magnetic field, yields complimentary information about phonons and magnetic excitations that are responsible for the superconductivity. Other types of measurements such as NMR and specific heat have been made under pressure. It would be useful to develop techniques for making other types of measurements under pressure and extending the range of pressures currently accessible.

b) *Spin, Lattice, and Charge Correlations.*

"Doping" generally refers to the introduction of charge carriers into the conduction or valence bands of a material. However, because of the large coupling between charge, spin and lattice in the cuprate superconductors and other transition metal oxides, doping of these materials with charge carriers can also be accompanied by the formation of static and dynamic spin and/or charge ordered phases on a microscopic scale. These "stripe phases," have recently been observed in many perovskite based transition metal oxides, including several cuprates, and may be a general feature of transition metal oxides[16, 17]. The role these microscopic inhomogeneous spin or charge phases play in high temperature superconductivity, magnetism, and other effects that have been attributed to them, is, however, unclear at this time.

The comprehensive understanding of spin/charge self-organization in oxides is a challenging task. This is a new viewpoint in the survey of strongly correlated phenomena in solids – a field that until recently has been primarily focused on the properties of nominally homogeneous systems. Intrinsically inhomogeneous spin and charge systems in transition metal oxides call for both original theoretical approaches and for the development of novel experimental tools suitable to deliver important information. Existing experimental information on the electronic and lattice properties of stripes systems is incomplete and therefore many fundamental problems related to spin/charge ordered regime in solids remain unresolved.

3. Conclusion

We believe that the opportunities for new materials to greatly influence the future of superconductivity research remain large, both from the point of view of fundamental science and the development of practical superconducting materials. We believe that chemical doping, non-thermodynamic synthesis, the discovery of totally new materials, the investigation of strongly correlated charge and electronic systems, and the use of chemical principles to help answer questions about the nature of superconductivity are exciting areas for future research.

III. Electronic Structure and Quasiparticle Dynamics

High- T_c superconductivity is achieved when a moderate density of electrons or holes is introduced in antiferromagnetic (AF) Mott-Hubbard insulator hosts by chemical or field-effect doping. Gross features of the evolution of the electronic structure as doping progresses from Mott insulator to d-wave superconductor are known from the systematic transport, photoemission and optical studies[18-21]. The doping-driven phase diagram of high- T_c systems is exceptionally rich owing at least in part to the fact that at the verge of the metal-insulator transition boundary magnetic, electronic, lattice and orbital degrees of freedom are all characterized by similar energy scales. Optimally doped cuprates (having highest T_c for a given series) reveal a well-defined Fermi surface in close agreement with the results of the band structure calculations[22]. Nevertheless, the dynamics of charge carriers appears to be highly anomalous defying the grounding principles of the Fermi liquid theory. Numerous attempts to describe the electronic properties using strong coupling Eliashberg theory have been only partially successful[23-25]. Using this approach it became possible to find a consistent description of many of the features established through a combination of tunneling, photoemission, optical and neutron scattering measurements for YBCO and the Bi2212 families of materials. However, many other systems of cuprates fail to follow the same patterns[26, 27]. Moreover, because of the extremely strong inelastic scattering established for most high T_c superconductors the concept of strongly interacting quasiparticles underlying the Eliashberg formalism is in question.

Early on it became established that superconducting currents in cuprates are carried by *pairs* of holes or electrons similar to that of conventional BCS superconductors. However, a viable description of the pairing interaction is yet to be found. Numerous experimental results indicate that the process of the condensate formation in cuprates is much more complex than the BCS picture of a pairing instability of the Fermi gas. One example of a radical departure from the BCS scenario is that the opening of the superconducting gap in cuprates is preceded by the formation of a partial gap (pseudogap)[28]. There is still a debate as to whether this pseudogap is related to the superconductivity. The pseudogap appears to be strongly anisotropic around the Fermi surface mirroring the anisotropy of the superconducting gap. These observations prompted the "precursor to superconductivity" scenarios for the pseudogap. Within this

view, the formation of pairs precedes the development of global phase coherence between paired states[29]. Observations of vortex-like excitations[30] as well as of finite superfluid stiffness[31] at $T > T_c$ are in accord with the preformed pairs hypothesis. The process of the superconducting condensate formation in high- T_c cuprates also appears to be notably different from the BCS scenario. In particular, the energy scales involved in the formation of the superconducting condensate are anomalously broad and exceeds the magnitude of the superconducting energy gap by more than one order of magnitude[32, 33]. These latter results inferred from optical spectroscopy are consistent with the view that the kinetic energy is lowered in the superconducting state. Similar conclusions also emerged from the detailed analysis of the photoemission spectra[34]. The electronic properties of the high- T_c superconductors have been probed by several complementary techniques. These techniques have shown substantial technological improvements in part driven by the need for higher energy and k resolution. In addition there is a growing belief that these materials may have real space inhomogeneities and so that a high resolution real space probe is desirable. Among the techniques that have revealed substantial insight because of technical improvements, we discuss electron tunneling, angular resolved photoemission spectroscopy, and infrared spectroscopy.

1. Techniques

a) *Electron Tunneling.*

Electron tunneling (both quasiparticle and Josephson tunneling) has been a powerful technique to probe the excitation spectrum, the superfluid density and the pair wave function phase of conventional superconductors. With high T_c cuprates, the technique has been no less informative. Currently, much of our understanding of the order parameter symmetry has come from Josephson effect studies[35] and the non-BCS nature of the excitation spectrum that comes about from the symmetry has been clearly observed[36]. C-axis and a-b plane quasiparticle tunneling have illustrated the extreme anisotropy of these superconductors and shown that surfaces are very different with possible bound states due to the broken symmetry at the a-b interface[37]. Intrinsic c-axis tunneling[38] has attempted to address the relationship between the superconducting gap and the pseudo gap. The debate over whether the pseudogap and the gap are intrinsically coupled continues.

STM studies offer an important additional feature that has already yielded some surprises. STM quasiparticle tunneling has allowed both microscopy and spectroscopy with good energy resolution and the spatial resolution to study the gap parameter on a length scale smaller than the superconducting coherence length[39]. Some of the current thinking on the high T_c superconductors concludes that there are intrinsic inhomogeneities (especially in the underdoped limits) in the superconducting properties. Coupling the high energy resolution with the high spatial resolution, along with the recently developed superconducting STM[40] will allow direct spatial studies of the energy gap, bound states and the superfluid density. Recent investigations have illustrated the local effects of non-magnetic and magnetic impurities[41] in the high T_c materials and a background periodicity in the electronic density[42] (charge density wave

or spin density wave?) which requires further investigation. It is not clear whether this periodicity in the electronic density is associated with the superconductivity in these materials. Finally, the combination of high resolution quasiparticle spectroscopy and Josephson probe will allow quantitative investigation of spatial variations of the order parameter and superfluid density around impurities, at interfaces and proximity junctions. In conventional superconductors these two quantities are related but with spatial inhomogeneities, it is no longer required. For the high T_c materials, some theoretical models require inhomogeneities that would result in the superfluid density having different behavior than the energy gap. This will allow us to address both fundamental issues and applications. For example, current studies show that a magnetic impurity does not suppress the energy gap[31]. It has been concluded that superconductivity is not affected but the superfluid density has not yet been investigated. In addition, much is still to be learned about the proximity effect at the interface between the high T_c materials and other metals. Tunneling will allow us to probe this interface.

b) Angular Resolved Photoemission Spectroscopy (ARPES).

ARPES experiments have contributed to our understanding of the electronic structure and superconducting properties by revealing the Fermi surface information,[43] and a large superconducting gap anisotropy that is consistent with d-wave pairing state.[44]

Recent improved resolution, both in energy and in \mathbf{k} have resulted in unprecedented data which allow us to map the electronic dispersion curves (E vs. \mathbf{k}) for bands below the Fermi level E_F [45, 46]. Angle resolved photoemission studies are now mapping the dispersion curves for several cuprates (and other perovskite oxides). As a result of the enhanced energy and \mathbf{k} resolution, it has been demonstrated that in addition to E and \mathbf{k} , the linewidths ΔE (related to scattering rate $1/\tau$) and Δk (related to the inverse mean free path $1/\ell$) can also be determined. While mapping these quantities over an extensive phase space of E and \mathbf{k} is still to be done, these measurements have revealed some very important insight already. Close to E_F an electron mass enhancement[47-49] (E vs. \mathbf{k} measures the velocity and hence the effective mass m^*) is observed in the dispersion curves which is both energy and temperature dependent. These measurements can be thought of as directly probing the self-energy of the carriers with all their dressings as a result of the interactions the carriers experience. In conventional superconductors, these interactions and mass enhancements are a result of the electron-phonon interaction; the mechanism responsible for superconductivity in the simple materials. Indeed, for many in the field it was the measurement of the strength of the electron-phonon interaction (via tunneling for example) which confirmed the phonon mechanism of superconductivity. The measurements of ARPES are being carried out in several laboratories in the U.S. and elsewhere and the mass renormalization effects are observed at several facilities and in several materials.

There is still disagreement as to some of the details of these measurements and to their interpretation[48, 50, 51]. Electron-phonon interactions, electron-spin interactions and electron-electron interactions have all been suggested and all result in enhanced mass

due to the interactions. Temperature dependent studies also illustrate that these interactions are at low energy and result from strong interactions.

It is clear that mapping of these dispersion curves over a wider volume of the E-k phase space is important. It is especially critical with the high T_c cuprates because of the large electronic anisotropy of the materials. Furthermore, because of the symmetry of the order parameter, mapping of the self energy effects as a function of \mathbf{k} around the Fermi surface is especially critical. If these observed renormalizations are the signature of the mechanism responsible for superconductivity in the high T_c materials, an extensive map of the electronic renormalized map will be valuable if the analogy with low T_c superconductors is relevant. In the case of low T_c materials the renormalized mass $m^* = m(1 + \lambda)$ where λ = electron-phonon interaction averaged over the Fermi surface.

Current ARPES measurements could be determining quantitatively the strength of the interaction and the mechanism of superconductivity. As a final caveat, it must be remembered that both APRES and tunneling are surface probes.

In this connection, inelastic X-ray scattering (IXS), which is not sensitive to surfaces or defects, is a valuable probe of bulk states. For high momentum and energy transfers IXS directly measures the ground state momentum density of electrons, while spin density is measured in magnetic IXS scattering. With improved resolution that has been achieved with synchrotron light sources, IXS has revealed surprising electron correlation effects with simple metals and has been extended to study the electronic excitations of the present compound of high T_c superconductors. Its application to ceramic superconductors would be most worthwhile.[52, 53]

c) *Infrared Spectroscopy.*

Infrared (IR) and optical spectroscopy is ideally suited for the studies of superconductivity because of the ability of these techniques to probe such fundamental parameters as the energy gap and the super fluid density[54]. Notably, IR spectroscopy allows one to investigate the *anisotropy* in these parameters through measurements performed with the polarized light[55]. Because IR/optical information is representative of the bulk and measurements can be performed on the micro-crystals, these studies allow one to examine common patterns of a large variety of materials which may not be suitable for examination with other techniques. Optical techniques offer means to probe strong coupling effects in the response of quasiparticles. In this context IR, tunneling and ARPES results are complimentary to each other. It is therefore desirable to "map" renormalization effects using a combination of several spectroscopic methods. Charge- and spin-ordered states in solids can be conveniently examined through the analysis of the IR-active phonon modes. The latter circumstance is important for the investigation of self-organization effects which dominate the dynamics of charge carriers at least in under-doped cuprates.

IR measurements can be performed in high magnetic field. Present work in the use of IR in high field experiments is restricted to a few experiments but several groups

are actively involved into adapting IR instrumentation for these challenging measurements. These studies promise to yield detailed information on dynamics of both pancake and Josephson vortices. More importantly, DC fields currently available in optical cryostats (up to 33 T) are sufficient to destroy superconductivity thus giving spectroscopic access to the *normal* state properties at $T \ll T_c$. Transport measurements in strong magnetic field highlighted anomalies of the normal state in LaSrCuO (LSCO) series of cuprates[56]. Spectroscopic measurements will be instrumental in distinguishing between (conflicting) interpretations of these results and will also help to unravel generic trends of the normal state behavior at $T \ll T_c$ between several classes of superconductors.

2. Magnetism, Competing Order, and Phonons

a) *Magnetism and Spin Fluctuations.*

As discussed earlier, superconductivity in the cuprates is achieved by doping holes or electrons into an antiferromagnetic-insulator state. The magnetism is essentially an electronic effect, as it results from strong Coulomb repulsion between pairs of conduction electrons on the same Cu atom, together with the Pauli exclusion principle. Considerable knowledge of antiferromagnetism (AF) and spin fluctuations in the cuprates[57, 58]. has been obtained experimentally using neutron scattering, nuclear magnetic resonance (NMR), and muon spin rotation (μ SR) spectroscopy. The general significance of antiferromagnetic correlations and spin fluctuations in theoretical mechanisms of high-temperature superconductivity is motivated by this experimental work.

In hole-doped cuprates, 2% holes doped into the CuO_2 planes are generally sufficient to destroy AF long-range order, but a minimum of 5-6% are necessary to induce superconductivity. Considerable attention has been devoted to characterizing the evolution of the AF spin fluctuations with doping. The bandwidth of the magnetic excitations, ~ 300 meV in the ordered AF, appears to change relatively little with doping. In LSCO, the low-energy spin fluctuations become incommensurate as doping increases, with a characteristic wave vector displaced from that of the AF by an amount δ . Similar incommensurability has been observed in YBCO, but additional features are the presence of a gap in the low-energy fluctuation spectrum followed by a commensurate "resonance" peak. The gap and peak energies both increase with hole concentration up to optimum doping, at which the resonance-peak energy is ~ 40 meV. Recent results on other families of superconducting cuprates indicate that the resonance peak is a common, although not universal, feature[59].

Electron doping has a weaker effect on the AF state, with a transition directly from AF order to superconductivity occurring at an electron concentration near 12%. Initial neutron measurements indicate that the AF spin fluctuations remain commensurate in the superconducting phase. Studies over a broad energy range are made challenging by the presence of crystal-field excitations from the rare-earth ions.

Progress in the characterization of spin fluctuations has been enabled by the development and improvement of techniques for growing large single crystals and by forming large-volume mosaics of small crystals. Neutron scattering studies of hole-doped cuprate systems other than LSCO and YBCO are in early stages, and considerable progress is likely in the next few years. Improvement in the homogeneity of large underdoped YBCO crystals would be helpful for some of the issues discussed below. The availability of sufficient access to appropriate neutron scattering facilities may also be a limiting factor.

b) Competing Orders.

A phenomenon known as "stripe" order has been observed by neutron and X-ray diffraction in several variants of the LSCO family[60, 61]. Spin-stripe order is indicated by the appearance of elastic magnetic superlattice peaks at the same incommensurate wave vectors at which the low-energy spin fluctuations occur. These are usually accompanied by the observation of another set of superlattice peaks split about fundamental Bragg points, indicative of charge-stripe order. The presence of stripe order is generally (although not always, as in the case of $\text{La}_2\text{CuO}_{4+y}$) associated with a reduction in the superconducting transition temperature. However, there is also a linear correlation between T_c and the incommensurability of the spin fluctuations in the absence of stripe order.

There is also some evidence of stripe correlations in $\text{YBa}_2\text{Cu}_3\text{O}_{6+x}$ O chains. The temperature dependence of the associated superlattice intensities suggests a coupling to electronic correlations, and possibly to charge stripes[62]. Certain spin fluctuations have been found to have an incommensurability similar to that found in LSCO; however, the cause of the incommensurability is controversial.

The recent scanning tunneling microscope (STM) observations of spatial modulations of the electronic density of states (DOS) in the CuO_2 planes of BSCCO has stimulated considerable speculation. The observed period of $4a$ (a , the in-plane lattice constant) suggests a connection with the charge and spin stripes found in LSCO. Clearly, a combination of tunneling and scattering studies is needed to clarify the nature of the modulations.

There are many unresolved issues associated with the problem of stripes. Is stripe order a type of electronic instability, like conventional charge-density-wave order, that only competes with and limits superconductivity? Is it possible for a stripe-liquid phase to exist? Are stripe correlations common to all superconducting cuprate families, or do they only occur in special cases? Are spin stripes always associated with charge stripes, or are these distinct types of order? Do stripes (or possibly another type of inhomogeneity) exist in electron-doped cuprates? Studies with a wide range of techniques will be needed to answer these questions. Stripes are but one kind of order that has been proposed to have a connection with the various "pseudogap" phenomena that are observed in underdoped cuprates[63]. A number of theories have put forward the hypothesis that a new order parameter appears in the pseudogap regime. Two particular

examples are quadrupolar orbital currents, and the staggered flux phase or d-density-wave (DDW) state. In both cases, orbital currents result in local magnetic moments that should be, in principle, detectable by neutron scattering. So far, neutron scattering experiments have been unable to find evidence for such phases, which predict no breaking of translational symmetry; however, the presence of quadrupolar currents provides a possible explanation for the recent observation of time-reversal-symmetry breaking by photoemission[64]. The possible existence of orbital moments remains an open issue.

c) *Phonons and Electron-Phonon Interactions.*

The role of electron-phonon interactions in the cuprates has been the subject of renewed interest, motivated in part by a recent interpretation of ARPES data.[28] An important technique for characterizing phonon dispersions and densities of states is inelastic neutron scattering. (Note that neutron measurements of the phonon DOS in MgB_2 provided an important validation of the theoretical evaluations of electron-phonon coupling in that system.) Dispersion anomalies in the Cu-O bond-stretching modes, clearly associated with some kind of electron-phonon coupling, have been the subject of controversy for several years. The experiments are constrained by weak scattering cross sections and limited crystal size. Further experimental studies, together with serious theoretical analysis, are necessary in order to make real progress in this area. Inelastic X-ray scattering has also been used recently to study optical phonons in a cuprate.

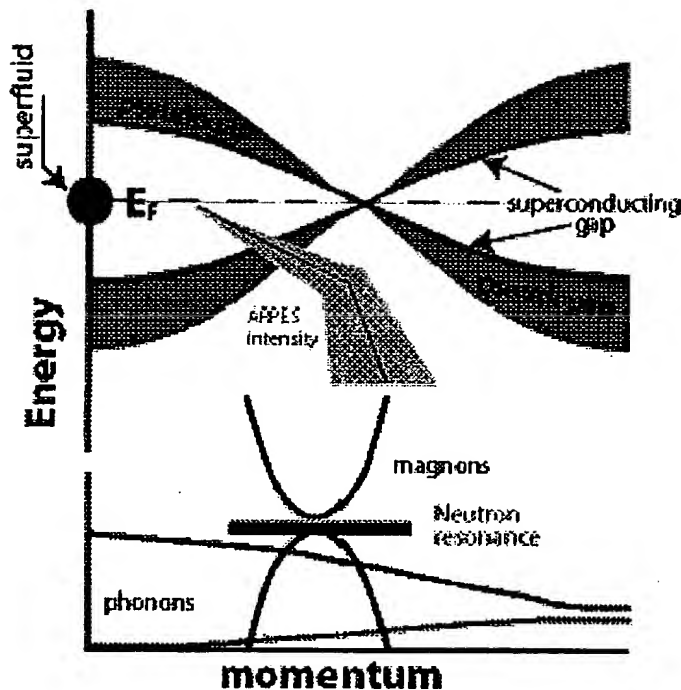


Figure 3. Schematic representation of excitations and collective modes in high- T_c superconductors. A remarkable variety of effects in these materials have typical energy scales of about 50-70 meV, including: phonons, magnetic resonance, superconducting gap and pseudogap as well as "kinks" in the ARPES spectra. Competition, interplay and interdependence between these effects are responsible for complexity of the strongly correlated state in these materials.

IV. Vortices

Most of the electromagnetic properties of Type II superconductors are determined by vortices in static and dynamic configurations. Rapid progress in manipulating and measuring vortices in recent years has greatly expanded the limits of known and imaginable vortex phenomena. This chapter outlines several research directions that are now within reach and that will develop new concepts and strategies for fundamental science and applications.

1. Single Vortex Physics.

a) Confinement.

Advances in micro- and nano-scale patterning and in high sensitivity measurements now enable studies of *single* vortices, allowing a wide range of new physics to be explored. Vortices enter mesoscopic samples[65-68] one-at-a-time at field intervals determined by flux quantization, $\Delta H \sim \Phi_0/L^2$ where Φ_0 is the flux quantum and L the sample dimension. The entry of each vortex produces a step change in the magnetization, corresponding to a *first order* phase transition. In circular disks, vortices are predicted to configure in shell patterns[69] reminiscent of electrons in atoms and leading to magic numbers of high stability. At certain fields a collection of discrete Abrikosov vortices transforms to a single *giant vortex* containing the same number of flux quanta and a circulating current at the outer edge of the sample. This phase transition is reminiscent of Wigner localization in electronic systems. In lower symmetry disks such as squares, vortices and antivortices coexist to simultaneously satisfy flux quantization and rotational symmetry[67].

Studies of confined vortices can be extended to layered superconductors such as NbSe_2 and the cuprates, where the superconducting coherence length ξ and the magnetic penetration depth λ are quite different, and to other experimental probes like STM that directly image the superconducting order parameter. Confinement need not be limited to a single disk. Arrays of disks, each containing confined vortices, can interact through a superconducting substrate. Confinement in a line geometry[65] allows *motion* of confined vortices to be studied[70]. Confined disks connected by lines offer many analogies to single electron behavior including the Coulomb blockade and single electron tunneling.

Individual vortices in an array can be manipulated by imposing an artificial mesoscopic template. One approach is to lithographically pattern a superconducting film with an array of holes, or antidots, each of which traps one or more vortices[71-74]. Trapping vortices one-by-one has practical implications: it can dramatically enhance the pinning effectiveness and critical current, and it can lead to extremely sharp switching effects at matching fields. These switching features offer the potential for three terminal devices, where the supercurrent across the antidot array is modulated by a control magnetic field operating near the matching field. Antidots are predicted to trap vortices

with multiple flux quanta if the hole size is large compared to the coherence length. The properties of these multiquanta vortices are largely unexplored. Such antidots, for example, could enable the construction of information storage devices operating with integer rather than conventional binary bits.

Mesoscopic templating can be extended in several exciting directions. The technique can be applied to cuprate high temperature superconductors[75], where the nanoscale coherence length enables many tens of flux quanta to be trapped in a single mesoscopic hole. Unlike low T_c superconductors, the cuprates have clearly defined lattice, liquid, and glassy phases that will react quite differently to the imposed order of the templates. First order vortex lattice melting, for example, is expected to be fundamentally modified by commensurate or incommensurate templates. Aperiodic templates provide another new direction. The vortices trapped in the holes create aperiodic scattering centers for free interstitial vortices whose dynamics will be quite different from those in ordered or random pinning arrays. Templates created to date have been limited by lithography to lattice spacings slightly less than one micron, putting the first matching field at about 20 Gauss. Electron beam and self-assembly techniques, for example based on diblock copolymers[76] anodic aluminum oxide[77] or inverse micelles[78], can be used to make templates with nanometer lattice constants. This much smaller spacing puts the commensurate vortex lattice in the strong interaction limit where collective effects dramatically alter its behavior. The one study on dense templates reported so far[79] shows that strong pinning persists well below T_c . High density templates bring the first matching field up to the kG range, much more interesting for applications than the tens of Gauss range accessible to lithographic templates. High density templates offer an intriguing new strategy for pinning the vortex liquid, where eliminating shear motion requires one pin site per vortex. In BSCCO and YBCO this opens large areas of the H-T phase diagram to practical use.

b) Pseudovortices and Vortex Core States.

The observation of unusual thermomagnetic effects in the underdoped region of LSCO above the superconducting transition temperature and below the pseudogap temperature[80] suggests that vortex-like excitations may be associated with the pseudogap state. The properties of these pseudovortices are still under examination and may hold important insights into the underdoped state. Pseudovortices may be observable as fluctuations using experiments with short time scales and local resolution, such as magnetic resonance or muon spin rotation.

The suppression of the superconducting energy gap in the vortex core creates a natural potential well that captures observable bound states in cuprate superconductors[81, 82]. These bound states provide a window on the nature of pairing, because they are sensitive to the presence of nodes in the gap that distort the core potential. STM sees not only the bound state, but also the anisotropy of the energy gap around the core, providing direct information on the nodal structure. These experiments would be particularly valuable if performed systematically for under and over doped regimes, where the nature of the normal and superconducting states changes

continuously. In other organic and heavy fermion superconductors where the order parameter is a complex vector, the core states will display subtle details reflecting the exotic pairing. These core states are within reach experimentally but remain unexplored.

In the vortex core the superconducting order parameter is suppressed, providing a fascinating opportunity to search for competing types of order without physically altering the material. Indications of spin density waves[42] and pseudogaps[83] in the cores of BSCCO suggest a strong interplay of these types of order with superconductivity. The same approach could be employed to search for competition with antiferromagnetism[84] charge stripes, and other proposed ordered states.

The existence of two superconducting gaps[85] in MgB_2 raises fundamental questions about their effect on the core states. Strong variations in the core potential and the bound states are expected as the relative strength of the two gaps varies with temperature and field. This fascinating area is now within reach and is virtually unexplored.

c) *Hybrid Materials.*

We are now entering a new era of materials sophistication allowing studies of superconductors exposed to *internal* magnetic fields. Such internal fields arise in magnetic/superconducting hybrid structures[86], including naturally occurring $\text{RuSr}_2\text{GdCu}_2\text{O}_8$ [87] and the magnetic borocarbides[88, 89], and artificial hybrid structures containing patterned magnetic and superconducting layers[90]. There are fundamental questions regarding how superconductors respond to internal magnetic fields: the conventional mechanisms of Meissner shielding and vortex penetration for external fields are not necessarily adequate.

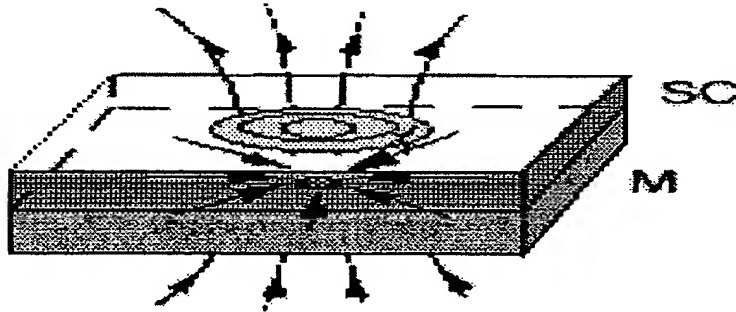


Fig 4. Superconductor/magnet bilayer. The vortex field polarizes the magnet locally, producing a radial magnetic texture.

In bilayer hybrids, the field of an individual vortex in the superconducting layer locally polarizes the adjacent magnetic layer creating a tiny *magnetic texture*. [91] Fig 4 shows a radial magnetic texture, where the vertical arrows represent the vortex magnetic

field and the horizontal arrows the induced polarization of the magnetic layer. The coupled vortex-magnetic texture pair is a new compound object whose static and dynamic properties are virtually unexplored. One important element is the interaction between pairs, which is mediated by dipole and exchange interactions in the magnetic layer, Lorentz forces in the superconducting layer, and magnetostatic interactions between the layers. The resultant interaction potential is distinctively more complex than the simple repulsive potential of bare vortices. Dynamics brings in yet another element, the de-polarization and re-polarization of the magnetic layer that is required if a vortex in the superconducting layer is to move. Beyond the new physics of vortex-texture pairs, there is an additional attractive feature. The properties of the hybrid can be tuned by selecting the materials (e.g., the easy direction and the anisotropy in the magnetic layer), the relative thickness of the two layers, and the magnetic field direction. In multilayer hybrids with parallel applied field, an array of π -Josephson vortices can be formed, while tipping the field away from the layers induces Abrikosov-texture pairs.

There are equally fascinating possibilities in hybrids composed of magnetic dots deposited on a superconducting layer. Here the magnetic dot is a pin site that is isolated from the superconductor, avoiding deleterious effects of the pinning defect on current flow. Recent work on superconducting/magnetic dot hybrids[92-94] has defined several important issues, such as (i) the spontaneous creation of vortices and antivortices in zero applied field, (ii) the annihilation of antivortices by external field-generated vortices, (iii) the nature of matching field effects, (iv) the effect of magnetic dot repolarization at high field, and (v) the dynamics of dot-generated vortices under a driving Lorentz force. These basic unexplored issues become even more fascinating when the scale of the magnetic dot array is reduced from present day lithographic dimensions to much smaller self-assembled dimensions. The interaction of flexible and compressible vortex lattices with rigid pinning geometries has many analogies in epitaxial growth, absorption of noble gases on surfaces and even plasma physics in confined geometries. Thus progress in this area has broad relevance well beyond the field of superconductivity.

2. Multivortex Physics

a) *Disordered Glassy and Liquid States.*

The *collective behavior* of vortices is much like that of atoms: their mutual interaction energy creates lattices, quenched disorder by random pinning produces glasses, and thermal disorder melts the lattice or glass to a novel liquid state. The liquid and glassy states of vortex matter offer major challenges for understanding the magnetic properties of superconductors. Two kinds of glassy state have been proposed, the vortex glass[95] for disorder by point defects, and the Bose glass[96] for disorder by line defects. While experiments confirm the second order Bose glass melting transition, the tilt modulus and the resistive behavior of these disordered systems are at odds with each other and with theory[97]. For point disorder, even the voltage-current scaling behavior expected at melting is not observed[98]. Experimentally, lattice and glassy melting coexist in the same phase diagram[99-101], sometimes accompanied by novel "inverse melting" regions. Quasi crystals are another disordered phase of vortex matter, triggered

by pentagonal or decagonal boundaries. The thermodynamics of melting in this phase intermediate between lattice and glass will be fascinating.

The vortex liquid shows equally fascinating behavior arising from *thermal* disorder rather than quenched disorder. Recent specific heat measurements[102] reveal two liquid phases separated by a second order phase transition. Understanding the nature of these two phases and the transition between them is a challenge not only for vortex matter but also other line liquids like polymers and liquid crystals. The vortex liquid offers another promising opportunity, to study the *interplay* of thermal and quenched disorder. The addition of quenched disorder to the liquid shifts the freezing transition up for columnar defects, down for point defects. The effect of the two kinds of quenched disorder on liquid state thermodynamics and on its driven dynamics is ripe for incisive experiments. Disordered vortices offer a rich complexity that is easily accessible experimentally yet so far defies theoretical description. Their behavior is fundamental to applications of superconductivity, and to the basic science of condensed matter systems generally.

b) *Dynamic Phases.*

The rich equilibrium phase diagram of vortices is matched by its driven dynamic behavior. The onset of motion at the critical current is a complex dynamic process governed by the distribution of pinning strengths, the vortex-vortex interactions, the temperature, and the driving Lorentz force. The plastic motion that normally accompanies depinning can now be directly observed through Lorentz microscopy[103] and magneto-optical imaging[104]. This emerging spatio-temporal resolution opens possibilities for systematic experimental studies to characterize the depinning process as a function of the basic variables. Such previously hidden onset phenomena as vortex channeling, vortex hopping from pin site to pin site, and the distinction between avalanche and continuous onset are becoming observable. This wealth of experimental information drives new theoretical descriptions of the depinning process. The plastic motion inherent in depinning makes its description in terms of partial differential equations of hydrodynamics challenging. However, statistical descriptions in terms of time dependent position and velocity correlation functions can be created that break new ground for describing the onset of plastic motion. Beyond depinning, there are a host of dynamic phenomena that are now amenable to observation, including vortex creep, thermally assisted flux flow, hysteresis in I-V curves, and memory effects. The concept of vortex *focusing* and *rectification* through the ratchet effect is especially interesting[105]. A fundamental microscopic understanding of these phenomena would lead to better engineered superconducting devices where stability and high depinning forces are crucial [106].

c) *Josephson Vortices and Crossing Lattices.*

Highly layered cuprates such as BSCCO support naturally occurring Josephson vortices, where the absence of a core and the large lateral penetration depth fundamentally alter the behavior typical of Abrikosov vortices. The two kinds of vortices co-exist and interact in the presence of a tilted applied field, where the perpendicular field

induces a pancake vortex lattice and the parallel field induces a Josephson vortex lattice. The two *crossing lattices* interact to produce a complex phase diagram[107], containing spontaneous vortex stripes and intricate melting behavior for fields very close to the *ab* plane[108]. Advances in scanning Hall probe technology[109] and magneto-optical imaging[110] now allow these crossing lattice states to be imaged, directly illuminating these phase transitions in real space. The dynamic properties of Josephson lattices are also fascinating. Because they have no core and no conventional pinning, Josephson vortices can be driven at very high speeds. They are predicted to undergo a dynamic phase transition, from a highly distorted hexagonal structure at low speed to a stacked configuration at high speed[111]. The most remarkable prediction is that the high speed Josephson lattice emits Terahertz radiation with a frequency inversely proportional to the transit time for one lattice constant[112]. This offers the appealing possibility to create a new class of Terahertz radiation sources from dc components, with an adjustable frequency determined by the driving current and applied magnetic field.

3. Instrumentation.

Advances in STM, scanning Hall probes, magneto-optical imaging, Lorentz microscopy, high sensitivity specific heat and magnetization have driven recent and rapid progress in vortex physics. Further advances in instrumentation are on the horizon. Lorentz microscopy of vortex systems has recently been achieved at 1 MeV, showing unexpected changes in vortex orientation in BSCCO films[113] and dynamic structure in apparently static crossing lattices[114]. Magneto-optical imaging can now see single vortices[104], opening a new window on real space dynamics. Higher resolution can be achieved with development of *near field* magneto-optical imaging, an advance that is within reach using available techniques. Specific heat experiments are ripe for much higher sensitivity using MEMS (micromachines) to eliminate addenda corrections and innovative temperature sensing. This new instrumentation will drive not only vortex physics but also will advance many other areas of condensed matter physics.

V. Proximity and Interface Effects

The superconducting proximity effect involves the mutual influence of neighboring superconducting and non-superconducting materials across an interface[115]. Such mutual influences can be profound. They can affect greatly the physical properties of both materials and are important in any application or scientific measurement that involves interfaces. Related effects occur at vacuum interfaces at the surface of a superconductor. The proximity effect is central to the physics of the coupling of superconductivity across non-superconducting barriers that make possible the Josephson junctions used in high- T_c superconducting electronics[116] and the grain boundary interfaces that are presently the primary factor limiting current flow in high-current superconducting tapes[117]. The proximity effect is also central to the broader application of the extremely powerful but surface sensitive techniques of photoemission spectroscopy and the growing arsenal of scanning local probes to these materials. The importance of grain boundaries as current limiting factors in HTS tapes is also discussed in

Chapter VII of this report. And the importance of surface effects in the application of ARPES and scanning probes is discussed in Chapter III.

To all of this must be added the possibility of surface doping through the use of charge transfer from deposited over-layers or the electrostatic field effect. The recent determination of scientific misconduct in some reported results using field-effect doping to induce high-temperatures superconductivity does not undermine the basic scientific rationale for such work. Indeed, field effect doping (both capacitive[118] and ferroelectric[119]) has a long history that continues up to today. The situation has been reviewed recently[120]. Clearly, charge transfer and field-effect doping remain potentially elegant approaches to creating new superconductors and developing model systems for studying two-dimensional superconductivity.

For all these reasons mastery of the proximity and interface effects in the high temperature superconductors is essential to progress in the field.

In conventional, low- T_c superconductors the understanding of the proximity effect is relatively well developed for interfaces with normal metals[121]. The reasons are the power of BCS theory along with the simplification provided by the generally long superconducting coherence lengths typical of low- T_c materials (and conventional normal metals). These long coherence lengths tend to average out and temper interface effects and thereby permit the use of simple, phenomenological boundary conditions for most purposes. The proximity effect with a ferromagnet is qualitatively different, however, and its understanding remains under developed. The new twist here is that the pair wave function has an oscillatory decay in the ferromagnetic (FM) material[122], in contrast to the simple exponential decay found in the normal-metal case.

High- T_c superconductors are very different. The very short coherence lengths characteristic of these materials make them much more susceptible to the influence of neighboring materials and internal defects virtually at the atomic level. Hence, the use of phenomenological boundary conditions is problematic, and microscopic theory will have to play a larger role. Of course, there is no well developed microscopic theory of the high- T_c superconductors. In addition, the strong doping dependence of the cuprate superconductors makes them sensitive to charge transfer at interfaces, where there is a tendency to form npn-like junctions[123], introducing further new complexity. The d-wave nature of the pairing also leads to new features in the proximity effect (and the related Andreev scattering process at interfaces) that have not been fully explored. One now well-accepted example is the reduction of the pair wave function to zero at surfaces whose normal points along the direction of the nodes in the energy gap[124].

There are also intriguing experimental results that suggest new physics is operating in the proximity effect with the high- T_c superconductors. The anomalous normal state properties of the cuprates, particularly in the pseudo-gap regime at low doping, seems incompatible with the use of the conventional theory (based on low- T_c

superconductors and normal metallic behavior) to describe the proximity effect with these phases. In addition, various systematic studies of the proximity Josephson coupling of the ab-planes of the cuprate superconductors across these normal phases imply characteristic lengths of the proximity coupling that are larger than can be readily explained with conventional ideas[125]. The alternative possibility that longer coherence lengths are possible in the normal planes and/or that the range of the proximity effect with conventional normal metals on the c-axis of BSCCO is shorter than can be readily explained with conventional ideas[126] is intriguing.

From the theoretical perspective, understanding of the proximity effect with a material near a quantum phase transition (such as the superconductor/insulator or metal/insulator transitions) with their associated quantum fluctuations is lacking even in the case of conventional superconductivity. It is presumably even more challenging in the case of the cuprates, which exhibit several such transitions as a function of doping, due to their highly correlated nature. In addition, there are speculations that negative U centers in the blocking layers are playing a role in the high- T_c of some cuprates in a kind of internal proximity effect[127].

Finally, the ability to exploit widely the powerful but inherently surface sensitive electronic probes of the high- T_c superconductors such as ARPES and the various emerging scanning probes will depend on dealing somehow with their complicated surface chemistry and altered doping of the CuO_2 planes near the surface due to the lack in general of a charge neutral cleavage plane in the unit cell of the cuprates, with the notable exception of $\text{Bi}_2\text{Sr}_2\text{CaCu}_2\text{O}_x$ (2212 BSCCO).

Key to understanding proximity and interface effects is the controlled preparation and characterization at the atomic level of the various interfaces of interest. Only by creating and understanding such model interfaces can the necessary phenomenology be developed that can guide applications (with their real, more complicated interfaces) and permit unambiguous scientific study of these materials with surface sensitive techniques.

Fortunately, recent advances in the controlled thin film deposition of highly refined interfaces of various kinds have been developed for the high- T_c superconductors and complex oxides more generally[128]. Atomic layer (or block by block) epitaxial growth has been achieved in some cases. Grading of individual layers as a film is built up may be necessary and likely is possible. The same techniques may also be useful in preparing the surfaces of bulk single crystals for study by ARPES and/or scanning probes.

The techniques capable of such refined interface preparation involve the combination of very well controlled deposition techniques with various *in-situ* means of monitoring the growth. These include Molecular Beam Epitaxy (MBE), Pulsed Laser Deposition (PLD) and sputtering. The need for an oxidizing atmosphere presents technical problems, but these are increasingly under control. *In-situ* Reflection High Energy Electron Diffraction (RHEED) is now commonly available for structural characterization and techniques to measure *in-situ* and in real time the temperature and

composition of a growing film are likely to become available. Such instrumentation will greatly facilitate progress. *Ex-situ*, post-deposition characterization is necessary, however, in order to confirm the structure away from the growth conditions.

At the same time, techniques for preparing well-defined grain boundaries of various types for physical study in both crystals and thin films have been developed. Advances in electron microscopy have also been developed that permit not only the structural characterization of the grain boundaries but also determination of the spatial dependence of the electric potential (and therefore the distribution of charge) across the boundary, at least on average. Such information will greatly facilitate progress in understanding the electrical properties of these grain boundaries. Still needing development are probes capable of characterizing the lateral dependence of the structure and properties of these interfaces (particularly electrical transport). Presumably local scanning probes can be brought to bear usefully on these questions. Similarly, techniques need to be developed that can reveal the point defects present near the boundaries that are not visible in TEM and may be playing a significant role in achieving charge neutrality near the boundary.

In concert with better sample preparation and more thorough physical study will need to be the systematic development of phenomenological theories that incorporate appropriately the known physics of the high- T_c superconductors and the realities of the materials themselves. First principle predictive value is probably not possible nor is it necessary from the point of view of furthering the science. Phenomenological models may provide useful models of interfaces for applications and guide the empirical process of materials optimization.

In summary, study of the proximity effect is a critical element in the evolving study of the high temperature superconductors. The key issues are: developing the model materials systems that will enable understanding at the required atomic level; developing tools to make and measure such interfaces, in particular scanning probes; surface doping and charge transfer studies, developing a unified theory of the proximity effect that deals with the material realities and the novel physics of the high- T_c superconductors; and applying all this knowledge in surface sensitive studies of these materials.

VI. Nonequilibrium Effects

A very general case of nonequilibrium dynamics in an electronic system starts by creating a high-energy electron (e.g., by optical absorption) followed by a cascade of excited states with smaller and smaller energies until the excess energy can escape the system, generally by phonons. In superconductors, nonequilibrium effects also occur with a transport current, for example, at interfaces exhibiting proximity effects, including grain boundaries (see Chapters V and VIII). The nonequilibrium effects of currents are especially important when magnetic vortices appear either from applied fields or the self-field of the current. The excitation energies are not too large ($< k_B T_c$) in these cases, which are discussed in the dynamic phases of vortices part of Chapter IV and under pinning in Chapter VIII.

Returning to the cascade processes mentioned at the start, these are indicated schematically in Fig. 5. They include electron-phonon and electron-electron scattering and are relatively fast, being $\sim 10^{-12}$ sec to achieve thermal energies[129]. The eventual loss of excess energy results from the escape of phonons from a finite sized sample and it is much slower, being generally $\sim 10^{-6}$ sec, due to the small velocity of sound and significant phonon-electron scattering. In the case of a superconductor, this strongly affects the final relaxation step, the recombination into Cooper pairs and escape of the excess energy by phonons. In superconductors, scattering between electron-like and hole-like branches (see Fig. 5) only occurs after 'thermalization' to energy scales of order of the energy gap. In high-temperature superconductors (HTS), the d-wave energy gap depends on the momentum direction, exhibiting nodes along the (π, π) wave vectors. Thus a new element of nonequilibrium processes in HTS is the relaxation of momentum around the Fermi surface.

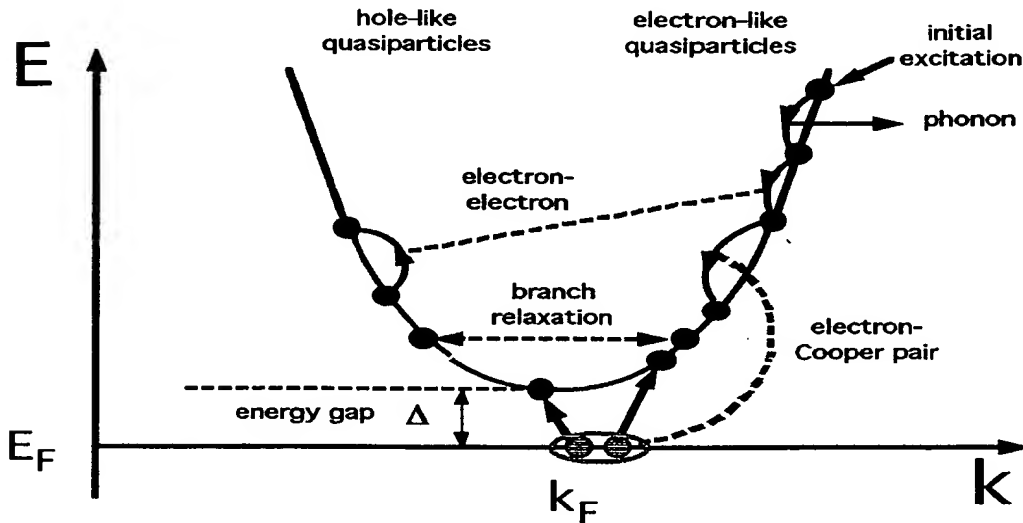


Fig. 5. Energy, E , versus momentum, k , for quasiparticle excitations in a superconductor with energy gap, Δ , showing electron-like ($k > k_F$) and hole-like ($k < k_F$) excitation branches. Also shown schematically are possible relaxation cascade processes for an initial electron-like excitation of energy, $E \gg \Delta$. Energy relaxation occurs by emission of a phonon, scattering off another quasiparticle or breaking a Cooper pair. Relaxation between the electron-like and hole-like branches occurs preferentially when $E \sim \Delta$. The final step (not shown) is the relaxation of the excess quasiparticle density back to Cooper pairs and the concomitant escape of a phonon with energy $\sim 2\Delta$.

Progress has been made to understand the fast scattering rates in HTS using thermal Hall conductivity[130], microwave absorption[131] and optical pump-probe experiments[132-136], but crucial pieces are missing. These include systematic studies

that cover a wide spectrum of pump and probe frequencies, other complementary experiments and connections to theoretical predictions. Less attention has been paid to the traditional nonequilibrium studies[137, 138] in LTS that have addressed a wide range of effects of excess quasiparticle densities and/or branch imbalances between electron-like and hole-like quasiparticles. The opportunities in the latter case are exotic, numerous and largely untapped.

It is quite interesting that the scattering times derived from thermal conductivity[130], microwave absorption[131] and optical pump-probe experiments[132] exhibit a very similar magnitude and temperature dependence. While the first two probe nodal quasiparticles at the (π, π) points of the k -dependent d -wave density of states at an energy scale of $\sim k_B T$, most pump-probe experiments excite the HTS with 1.5 eV photons whose energy is $\sim 200 k_B T_c$ and the cascade can include all k states. In addition, the probe response, which measures the reflectivity changes after optical pumping, varies dramatically with probe frequency (even changing sign) so the specific property of the nonequilibrium distribution being addressed is less clear. One expects that these probe-frequency dependencies will reflect features of the electronic system such as the plasma frequency as well as the changes due to these nonequilibrium states. For example, the temperature dependence of the amplitude of the 90 meV probe energy response to a 1.5 eV pump energy[133], shows a strong correlation with the amplitude of the neutron resonant spin excitation[139]. The resolutions of these fascinating mysteries promise a rich new field of research that can bring considerable insight into non-thermal processes in electronic oxides and possibly into the mechanism of HTS. For these experiments, it seems that much could be answered if another probe, like tunneling, could be done on such fast time scales (~ 10 psec) to complement the optical data.

The eventual recombination and energy transfer to phonons has been addressed in mm-wave absorption measurements that probe the reflectivity at a frequency of ~ 0.3 meV. The authors find relaxation times in the 10^{-6} sec range and intuit a more significant bottleneck than LTS due to the unique properties of the nodal quasiparticles. They also suggest an analogy to the T relaxation process[140] found for He. The long relaxation time means that the traditional nonequilibrium effects found in LTS, which have addressed the effects of excess quasiparticle densities and/or branch imbalances between electron-like and hole-like quasiparticles, should be observable in HTS. Such nonequilibrium effects in high-temperature superconductors (HTS) comprise a research area that is ready for exploitation.

Numerous effects of perturbations by tunnel-junction injection of quasiparticles (unpaired electrons), microwave or optical illumination, etc. are readily observed in low T_c superconductors (LTS) and these have been understood in terms of electron-phonon scattering[137, 138]. This is consistent with the electron-phonon coupling mechanism for these superconductors. Occasionally the effects of direct electron-electron (Coulomb) scattering must also be considered. In HTS the situation is potentially much more interesting for at least two reasons. The d -wave symmetry of the order parameter admits a momentum-dependence to the quasiparticle energy spectrum and there are additional spin and charge excitations that have been suggested as potential candidate bosons for the

attractive interaction. The latter excitations are seen by neutron scattering and would be expected to interact with quasiparticles. By studying the relaxation processes in nonequilibrium it may be possible to address the importance of these excitations if their effects on the relaxation of nonequilibrium quasiparticle distributions can be identified.

Nonequilibrium states are here classified as those states for which the quasiparticle (or, e.g., phonon) distribution exhibits an energy profile different from thermal equilibrium. No matter how high the energy of the fundamental excitation process, in a fairly short time the excess energy of the perturbation relaxes, predominantly, into a state for s-wave superconductors in which it resonates between phonons of energy 2Δ and quasiparticles of energy $\sim\Delta$. This is due to the high density of quasiparticle states near Δ in the BCS density of states and it results in a bottleneck for the escape of the 2Δ recombination phonons into the thermal bath since they are resonantly reabsorbed by the high density of Cooper pairs. This increases the effective recombination time above the bare value (typically by one to two orders-of-magnitude).

The observations of many diverse nonequilibrium effects observed in low T_c superconductors (LTS) benefit from the long time constants for the ultimate recombination into Cooper pairs. This is due to the 2Δ -phonon bottleneck and the small energy scale of Δ in LTS also contributes to a long bare recombination time due to the small phase space available in the decay channel via phonons (density of phonon states $\sim\omega^2$). Nonequilibrium studies in LTS have discovered new effects, like energy gap enhancement by microwave or tunnel-junction injection, branch or charge imbalance and new applications, like weak-link Josephson devices, superconducting three-terminal devices and particle detectors. See Ref. 9 for more complete reviews of these topics. The greater richness of the interactions in HTS, together with the nonconventional order parameter, large energy gap and the naturally layered structure can be anticipated to provide additional phenomena and applications. Examples include the coupling of ac Josephson oscillations to phonons or the possibility of terahertz oscillators enabled by the coupling of coherent Josephson vortex flow in BSCCO to Josephson plasmons to produce electromagnetic radiation. For instance, in the latter case, one can test predictions of the occurrence of dynamically stabilized vortex configurations and the interaction with Josephson vortices with Josephson plasmons. In addition, the large energy gap in HTS cuprates make them attractive candidates to extend the frequency range of tunnel-junction mixers beyond that of LTS junctions. Although energy gap enhancement, by microwave illumination[141, 142] or tunnel junction injection[143], is well established in LTS, the discovery of photoinduced superconductivity in underdoped cuprates is unique and unexpected—it produces substantial increases in T_c that are persistent[14].

The large Δ_0 in HTS, compared to LTS, may be expected to lead to shorter bare recombination times, but under many circumstances nonequilibrium effects can still occur. For example, the longer effective relaxation time due to resonant 2Δ -phonon adsorption mentioned above is largely a geometrical escape factor that may be quite similar[134] to that found in LTS. This resonant adsorption is usually referred to as phonon trapping since the nonequilibrium perturbation energy must be converted into,

and carried away by, phonons. Phonons can be expected to play that same role in HTS, since, e.g., spin and charge excitations cannot leave the electronic system. But also, an additional trapping mechanism may occur due to the nodes of the d-wave order parameter. This proposed effect is the momentum-space analogy of the real-space quasiparticle traps devised for LTS superconductive detectors[144]. In such detectors, Cooper pairs in a large volume of superconductor (with a relatively large gap, Δ_1) interact strongly with incident irradiation to produce excess quasiparticles. The detector is arranged so that the quasiparticles have a high probability of diffusing into an attached superconductor with a smaller gap, Δ_s , before the energy escapes the system via phonons. The smaller Δ_s results in a *longer bare recombination time* due to the smaller phase space of phonons of energy $\omega=2\Delta_s$. In addition, the excess energy of quasiparticles, $\sim\Delta_1$, converts into a greater number of quasiparticles with $E\sim\Delta_s$.

In a proposed relaxation mechanism, quasiparticles produced in the high- Δ regions away from the nodes at the (π, π) points would diffuse to traps in momentum space at the lower energy states near the nodes. Several mechanisms can be envisioned, e.g., direct scattering of quasiparticles by phonons or spin excitations and pair breaking into near-nodal quasiparticle states by nonequilibrium phonons or spin excitations. The interpretation of nonequilibrium data in these regimes could be connected to models for the mechanism of HTS (see Chapter VII). It will be interesting to explore the relation of the specific momenta of spin excitations with relaxation processes across the d-wave Fermi surface. The multiplying factor upon energy degradation implies that a single 1.5 eV photon could create up to 4000 quasiparticles trapped at the nodal points with an energy scale of ~ 4 K. As pointed out above, measurable recombination times in excess of 10^{-6} sec have been reported in HTS.

The ease of fabrication of thin-film superconductor-insulator-superconductor tunnel junctions was also a vital component of previous studies of LTS materials. Making junctions with two HTS electrodes has proved much more difficult and most tunneling studies have relied on point-contact or STM tunnel junctions. However significant progress has been made using MBE growth of multilayers of HTS with lattice-matched insulators as well as the internal junctions of BSCCO crystals offer another opportunity that is unique to the HTS cuprates. In the latter case, it seems necessary to intercalate molecules (e.g., iodine or mercury bromide) between the Bi-O bilayers to reduce the current for injection near the energy gap, 2Δ , and avoid a significant weakening of the superconducting state[145].

VII. Theory

1. Preamble

Since the discovery of high T_c superconducting materials, there have been many ideas put forth to explain their unusual and often perplexing physical properties. Here, rather than attempting to survey the field, we offer three individual perspectives.

2. Phenomenological Approach

a) *Status.*

The cuprates are highly correlated systems close to the Hubbard-Mott antiferromagnetic insulating state. In the underdoped regime, pseudogap signatures[28] go well beyond ordinary metallic behavior. Here we will limit the discussion to the optimally doped case where Hubbard-Mott modifications may not be so severe. In this case generalizations of techniques developed for ordinary superconductors may be applicable with appropriate modifications and give valuable insight. For conventional superconductors phonon structures in current-voltage characteristics of planar tunneling were exploited to derive a complete picture of the electron-phonon spectral density $\alpha^2F(\omega)$ [146]. This function defines the kernels that enter the Eliashberg equations. The theory accurately predicts (at the 10% level) the many deviations from universal BCS laws which have been seen in a broad range of experiments[146]. Similar equations suitably generalized to include d-wave symmetry[23, 147, 148] can lead to an equally good understanding of the observed superconducting properties of optimally doped YBCO. In this approach the general framework of a boson exchange mechanism is retained with a boson exchange spectral density (denoted by $I^2\chi(\omega)$), to be determined from experimental data. In the high temperature oxides, rather than tunneling, including STM, the technique of choice has so far been the infrared conductivity, from which one can construct a model of $I^2\chi(\omega)$. [23, 147, 148] When applied to the conventional s-wave case the method reproduces the tunneling derived model for $\alpha^2F(\omega)$ [149, 150]. In the oxides the optical scattering is dominated by a fluctuation spectrum which is largely featureless and which extends over a large energy scale of order several hundred meV (the order of J in the t-J model). Such a spectrum is expected in spin fluctuation theories such as the nearly antiferromagnetic Fermi liquid (NAFL)[151, 152] or in the marginal Fermi liquid (MFL)[153].

In the superconducting state a new phenomenon has been identified. One finds increased scattering at some definite finite value of ω associated with the growth of a new optical resonance in the charge carrier boson spectral density, the energy of which (ω_n) corresponds exactly to the energy of the spin resonance measured by inelastic neutron scattering (when available). This correspondence does not prove, but provides support for a spin fluctuation mechanism (rather than the MFL). Moreover the spectral density derived from the infrared data, (at T_c in optimally doped YBCO) shows a form characterized by a spin fluctuation energy ω_{sf} [152]. This form is progressively modified by the growth of the resonance at ω_n and attendant reduction of spectral weight at smaller energies as the temperature is lowered below T_c . The spectrum obtained depends on temperature (through feedback effects due to the onset of superconductivity)[154, 155], and leads to good agreement with observed properties of the superconducting state. While the generalized (for d-wave) Eliashberg equations are not as firmly grounded in

the basic microscopic theory as in the phonon case, they do offer a phenomenology within which superconducting properties can be understood. These include the condensation energy per copper atom, the fraction of total spectral weight which condenses into Cooper pairs at $T=0$, the temperature dependence of the superfluid density, the peak observed in microwave data as a function of temperature and its shift in position with microwave frequency, the similar peak in the thermal conductivity, and the frequency dependence of the infrared conductivity

b) Key Issues and Opportunities.

An important issue for the future is to extend the calculations to the underdoped regime. There is as yet no systematic quantification of pseudogap effects and contradictory views exist as to their origin. In the preformed pair model[29] the pseudogap and superconducting gap have a common origin with the superconducting transition related to the onset of phase coherence. In the d-density wave model[156] (DDW) a new order parameter competes with superconductivity. Another problem that needs resolution is understanding the new ARPES data which have been interpreted as giving strong signatures of phonon effects[157-159]. The dressed quasiparticle energies must also contain important renormalization due to the spin fluctuations. Certainly a pure phonon model is incompatible with the infrared optical data. However, it is well known that transport and quasiparticle scattering rates are different. In transport, backward collisions assume additional importance in the depletion of current, as compared with quasiparticle scattering. The quasiparticle electron-boson spectral density may have important contributions from both phonons and spin fluctuations, while the transport spectral density may be dominated by spin fluctuations. An important aim for the future should be to achieve a common understanding of ARPES, optical and tunneling data simultaneously.

3. Numerical Studies of Hubbard and t-J Models

a) Status.

Numerical studies of the high T_c cuprate problem have been used to determine what types of correlations are significant in specific models. They have shown that the 2D Hubbard and t-J models exhibit antiferromagnetic[160, 161], striped domain wall[162], and $d_{x^2-y^2}$ pairing correlations[162-165]. The similarity of this behavior to the phenomena observed in the cuprate materials support the notion that the Hubbard and t-J models contain much of the essential physics of the cuprate problem.

This is really quite remarkable when one considers that these are basically two parameter models involving U/t or J/t and the doping $x = 1-n$. Furthermore, boundary conditions or added next-nearest-neighbor hopping terms can shift the nature of the dominant correlations showing that the antiferromagnetic, stripe, and pairing correlations are delicately balanced in these models, reminding us of the behavior of the materials themselves.

b) Key Issues and Opportunities.

While we have seen that many of the basic cuprate phenomena appear as properties of these models, the interplay of the various correlations and the nature of the underlying pairing mechanism remain open. Thus a key issue is to determine whether the underlying physics is to be understood in terms of spin-charge separation[166, 167], SO(5) symmetry[130], stripes[168], spin-fluctuation exchange[169], or whether additional phonon mediated interactions may play a supporting role[46, 170]. With the understanding which has been gained and with further development of computational techniques, we have the opportunity of addressing these issues. Here it is important to realize that the search for the appropriate theoretical framework for understanding the cuprates also includes seeking to determine what type of models (and ultimately materials) are described by various scenarios. For example, we would like to understand what types of strongly correlated models exhibit spin-charge separation or more generally some type of fractionalization. Is there a sufficient temperature range for strongly correlated 2-leg ladders to renormalize so that an SO(5) description is appropriate? Do stripes suppress or enhance pairing? What role do phonons play and how is the electron-phonon interaction affected by strong Coulomb interactions? What is the structure of the phase diagram for these models? What new materials or material modifications will the answers to these questions suggest?

It should also be noted that theoretical progress in first-principles band theory simulations of ARPES intensities in the high- T_c 's has been made and the inclusion of the electron-phonon and strong correlation effects in these simulations can advance the interpretation of the data[171].

We are in a position to address these issues and we also have the opportunity to take advantage of more than a decade and a half of advances driven by the cuprate discovery. As part of this effort we need to continue the development of numerical techniques. We should also work to establish closer connections to the electronic structure and quantum chemistry communities for key information on the basic orbitals and effective parameters that enter model descriptions of real materials.

4. Electronic Structure

a) Status.

The discovery of superconductivity in MgB_2 and the subsequent response by the computational community demonstrated the remarkable progress that has been achieved in first principles calculations for the electronic properties of conventional (phonon mediated) superconductors. Indeed, $\alpha^2F(\omega)$ can now be calculated accurately for fairly complex materials using density functional methods. For example, first principles evaluation of the electron-phonon interaction was used to calculate the superconducting transition temperature of the simple hexagonal phase of Si under high pressure[172]. Not only can the electron-phonon coupling be obtained, but also complete phonon dispersion curves for the whole Brillouin Zone (BZ) are being calculated using perturbation theory

(harmonic approximation). If anharmonic terms are important, frozen phonon calculations yield total energies as a function of the relevant lattice distortions. Indeed, structural phase transitions involving soft phonon modes are frequently analyzed via such total energy calculations. While phonon frequencies and eigenvectors are needed to

evaluate $\alpha^2F(\omega)$, it is difficult to draw conclusions about superconductivity from phonon dispersion curves. It is interesting however, that first principles calculations of phonons in the cuprates have in general yielded good agreement with neutron scattering experiments (see for example [173] and references therein).

When Local Density Approximation (LDA) calculations were unable to produce the insulating antiferromagnetic state in the cuprate phase diagram [174], it became clear that new approaches for dealing with correlation and moving beyond standard band structure techniques were needed. The first of these new "band structure" approaches, the LDA+U method, introduces a Hubbard U term into the LDA equations, affecting the orbitals for which the correlations are strong [175]. The more recent LDA++, and Dynamical Mean Field Theory (DMFT) methods make a more direct attack at calculating the electron self-energy, $\Sigma(\mathbf{k}, \omega)$ [176-179]. The computational resources for evaluating the dynamics are demanding, and while good progress is being made, results have only been obtained for prototype systems. Although there is not yet a satisfactory band structure based technique for treating spin fluctuations when going from the Mott-Hubbard insulating state to optimally doped high T_c materials, straight forward band structure calculations of the doped cuprates yield Fermi surface geometries in remarkably good agreement with precise angle resolved photoemission experiments. Band structure calculations have also been valuable in identifying the relevant orbitals and in estimating values of the parameters that enter more phenomenological models.

b) Key Issues and Opportunities.

A key ingredient in solving the Eliashberg equation for phonon mediated superconductivity is the simplification made possible by Migdal's theorem. In exploring other boson mechanisms with higher frequency spectra the role of the retarded Coulomb interaction, μ^* , needs to be revisited [180]. It has been suggested that for vanadium the effective μ^* is larger than expected because of the pair-breaking influence of spin fluctuations [181]. In the one band Hubbard model it has also been argued that strong correlations suppress the electron phonon coupling in α^2F and transport quantities [182]. The recent angle resolved photoemission measurements which show mass renormalization for bands passing through the Fermi energy may provide a quantitative measure of the electron-phonon interaction for specific states [159]. A comparison with first principles calculated values would be most interesting.

There are many other questions, many identified in this document, which are now being approached with model Hamiltonians. While electronic structure practitioners are eager to participate in and learn from such studies, and to provide parameters and insights where possible, there is a strong desire to develop the apparatus required for a real first principles treatment of the phenomena. There are many insights and ideas that need to be

developed first. Perhaps the situation today is not so different than in the early 1960s when the Fermi surface was considered exotic. The dividends from the investment in physics of that period are the basis for what is now considered "routine" materials science, with applications ranging from Stockpile Stewardship to material processing to drug design. Solving the "high T_c problem" will likewise result in valuable tools and insights leading to future applications.

VIII. Defects and Microstructure with an Eye to Applications

Crystal lattice defects and their organization on the scale of nanometers to micrometers ("microstructure" for short) play a very significant role in the science and technology of superconducting materials: [183-188] For one thing, defects are unavoidable in the world of "real materials," and it is vital to characterize their nature and distribution so as to understand their effects on superconductivity. It is also vital to control the defect distribution in the polycrystalline, large-scale microstructure of conductors since appropriate nanoscale defects are responsible for developing high critical current densities, J_c , within grains. But planar defects, especially grain boundaries, block grain-to-grain transmission of the current, dictating the geometry of conductors because of the sensitivity of J_c to strain defects, etc. Defects can also provide insights into fundamental questions, e.g., the use of grain-boundary junctions in the investigation of order-parameter symmetry in cuprate superconductors. HTS conductors are available from several companies worldwide and have been used to demonstrate large components of the electric power grid such as power cables, motors, transformers and fault current limiters. Josephson-junction devices and other electronic devices based on HTS technology are in an advancing state of commercial development. However, we are still far from understanding or being able to optimize HTS material properties in the way that we have learned to do for the workhorse conductor of LTS (Nb-Ti). The main point is that our ability to adequately control defects and microstructures is still rudimentary. Some of the remaining key issues derive from the anisotropic nature of the cuprates and their low carrier density. These characteristics result in inadequate magnetic flux pinning, percolative current flow past many interfacial barriers, inability to control the phase state, and a general lack of materials control.

Extensive investigation of the cuprates has developed a firm understanding of some of their microstructure-sensitive properties. First of all, it is painfully clear that crystallographic texture and phase purity must be tightly controlled for high J_c in cuprates. It also seems unavoidable that magnetic flux pinning at temperatures, above about 30K, is inadequate in the present conductor material, Bi-2223. It is just too anisotropic for magnetic field applications, though adequate for self-field use in power cables at 77K. YBCO has much greater potential for applications in fields at 77K than Bi-2223, because its mass anisotropy is about 7, rather than the ~100 of Bi-2223, even though its T_c is 92 K rather than the 110 K of Bi-2223. By contrast it has been quickly established that MgB_2 has only a small anisotropy (values vary from about 2 to 7, though with a greater weight on lower numbers) and that grain boundaries are not serious obstacles to current flow. Flux pinning also appears to be strong, leading to high critical current densities in prototype wires. In many respects MgB_2 appears to be exactly what

its 39 K T_c suggests, intermediate in properties between LTS and HTS, benefiting in particular from lower anisotropy and relatively insensitive to planar defects.

It is not surprising at all that understanding of defects in cuprate superconductors is such a hard-won commodity, because these are very complex materials (the most practically important material, Bi-2223 $(\text{Bi,Pb})_2\text{Sr}_2\text{Ca}_2\text{Cu}_3\text{O}_{10-x}$) forms a 7-component system when embedded in Ag). The continued attention to grain boundaries and to the search to understand flux-pinning defects has enhanced and will continue to increase our knowledge of defects in complex oxides in a much wider context, e.g., the understanding of defects in manganites, ferroelectric perovskites, etc. Continued investment in the materials physics of defects in HTS materials is attractive, not just because of the implications for superconductivity technology

What, then, are some of the outstanding issues in this field and how can we solve them? We need a new phenomenology, which combines the new physics of HTS with a realistic description of defects and microstructure in these complex materials. At present, almost all of the phenomenological discussion of the effects of defects and microstructure on the superconducting properties of HTS materials is based on theoretical concepts appropriate to s wave LTS. How do defects in HTS materials really interact with correlated-electron phenomena, stripe-phases, and electronic phase separation? We will not understand the answers to such questions without a basic theory of defects in complex oxides that takes account of their complex electronic state and proximity to the metal insulator transition.

Knowledge of lattice defects and microstructure in HTS materials is mostly confined to YBCO (and other 123-structure cuprates) and to the 2212 and 2223 phases of BSCCO. Why stick to these "old favorites?" To a very large degree, this reflects a "tyranny of practicality and materials complexity," which inhibits the development of a wider knowledge needed to understand broader aspects of the materials physics of HTS materials. Many HTS materials are much more complex to make and appropriate recipes for "good sample" manufacture are lacking. It is believed that much might be learned from infinite layer materials. For example, their structures are not neatly divisible into charge reservoir and superconducting blocks. Since grain boundaries in HTS are believed to be disruptive to current precisely because charge transfer to the conducting cuprate planes is perturbed, their study in infinite layers might be particularly valuable.

Many issues involving magnetic flux pinning in HTS materials remain to be clarified. Although much is known about the thermodynamics and phase-diagrams of vortex matter in HTS materials, (see Chapter IV), much remains to be learned about the elementary interactions between vortices and defects, e.g., the physics of the elementary pinning forces, f_p , for various types of defects and their systematic variation among various cuprates. Furthermore, the knowledge of the behavior of defects, such as dislocations and plastic flow in vortex lattices themselves, is mostly extrapolated from the LTS case and almost certainly needs revision in such strongly anisotropic cases as Bi-2223, where line vortices in LTS materials break up into largely, but not completely disconnected pancake vortices. Experiments need to be designed specifically to

illuminate the fundamental nature of defect-vortex interactions in HTS materials. These would be particularly valuable when combined with parallel conductor development activities. The intermediate nature of MgB_2 makes the nature of elementary pinning forces, vortex-lattice elasticity and plasticity very interesting. Are these properties fundamentally different or similar to those of Nb_3Sn and other LTS intermetallic compounds? Does the complex electronic band structure and anisotropy of MgB_2 make it's flux-pinning fundamentally different from that in the A15 compounds?

What is learned about the interactions between defects and correlated-electron phenomena in HTS materials will pay dividends in a wider range of materials, e.g., manganites, and phenomena, e.g., magnetism and metal-insulator transitions. In fact, the interactions between defects and transport properties in the normal state of cuprates are very poorly understood, too. A better understanding here would greatly improve the ability to characterize the nature and concentration of defects in cuprates in a quantitative manner.

There are many needs and opportunities in the science of defects and microstructure of cuprates, in addition to the direct connection to superconductivity (e.g., flux-pinning and weak links). The latter provides the motivation for microstructural control, but understanding of the basic materials science of defects and microstructure is needed to exercise such control efficiently. Here, too, experiments and theory designed to gain basic understanding that can couple to the activity driven by practical considerations would be very valuable. For example, there is a considerable lack of serious theory and modeling, as well as of basic experimental studies, of the thermodynamics, kinetics, and mechanisms of nucleation and growth of epitaxial oxides of relevance to coated conductors (including buffer layers, etc.), despite there being a large amount of process development in this area. Understanding of the fundamentals of phase formation in cuprate systems is sparse. There is also a serious need for quantitative understanding of the elementary defects, such as point defects, dislocations, twin boundaries, stacking faults, etc., which are the "elementary particles" of microstructure in HTS phases. This, together with quantitative descriptions of microstructure and defect chemistry, is needed to develop an adequate phenomenology of current transport and flux pinning in HTS systems.

Another area of fundamental materials physics that is relatively unexplored for HTS materials is that of mechanical properties, especially elasticity, anelasticity, and fracture. There is a paucity of basic experimental data, and these complex materials require theoretical methods more advanced than those needed for simpler materials, including ferroelasticity, non-linear and microcontinuum elasticity, and models of non-linear lattice statics and dynamics. Furthermore, an understanding of the coupling of elastic strain fields to the superconductivity of HTS materials is needed to understand interactions between defects and superconductivity, as well as to predict the behavior of conductors in devices such as high field magnets where large stresses arise during device operation.

The quantitative description of HTS-based conductors also requires improved methods of modeling the physical properties of composites, including mechanical, thermal and electromagnetic properties. The latter is particularly challenging, involving current and magnetic induction distributions in polycrystalline, defect-containing, multiphase composites.

The discussion above indicates the great complexity of the defect physics and microstructural science of HTS superconductors, which are both of fundamental interest and of enormous relevance to practical applications. However, powerful instrumental tools are available to help meet this challenge, especially modern transmission electron microscopy and local scanning probe microscopies and spectroscopies. These tools now permit the characterization of atomic and electronic structure, as well as elastic strain fields, over length scales ranging from atomic resolution to micrometers. This affords an unprecedented ability to obtain images and spectroscopy of atomic, charge, and strain distributions, which will revolutionize our quantitative understanding of defects and microstructure. The use of such instrumental tools, together with microscale electromagnetic characterization, coupled with the development of HTS-appropriate theoretical phenomenology, has the potential to yield important new insights into this complex problem, with wider implications for many complex new materials of the future.

References

1. Buddhist Udana, Circa 100 B.C..
2. B.J. Battlogg. 1997, National Science Foundation.
3. J.E. Hirsch, Phys. Rev. B **55**, 9007 (1997).
4. R. Flukiger, in *Concise Encyclopedia of Magnetic and Superconducting Material*, Jan Evetts, Editor. 1992, Pergamon Press, Inc. p. 1.
5. O. Fisher and M.B. Maple, in *Superconductivity in Ternary Compound*, I. O. Fischer and M.B. Maple, Editors. 1982, Springer-Verlag: Berlin. p. 1.
6. J. Etourneau, in *Solid State Chemistry: Compounds*, A.K. Cheetham and Peter Day, Editors. 1992, Clarendon Press: Oxford. p. 60.
7. S.V. Vonsovsky, Yu A. Izyunov, and E.Z. Kurmaev, in *Springer Series in Solid State Sciences*. 1982, Springer-Verlag: Berlin. p. 259.
8. J. Nagamatsu, N. Nakagawa, Y.Z. Murakana, and J. Akimitsu, Nature **410**, 63 (2001).
9. C.M. Varma, W. Buckel and W. Weber, Editors. 1982, Kernforschungszentrum Karlsruhe, GmbH: Karlsruhe. p. 603.

10. S. L. Bud'ko, G. Lapertot, C. Petrovic, C.E. Cunningham, N. Anderson, and P.C. Canfield, Phys. Rev. Lett. **86**, 1877 (2001).
11. T. Yildirim, O. Gulseren, J.W. Lynn, and C.M. Brown, Phys. Rev. Lett. **87**, 037001 (2001).
12. T. Siegrist, H. W. Zandbergen, R. J. Cava, J. J. Krajewski, and W.F. Peck, Jr., Nature **367**, 254 (1994).
13. http://www.lucnt.com/news_events/researchreview.html
14. A. Gilabert, A. Hoffmann, M.-G. Medici and I.K. Schuller, J. Supercond. **13**, 1 (2000).
15. R. Cauro, A. Gilabert, J. P. Contour, R. Lyonnet, M.-G. Medici, J. C. Grenet, C. Leighton, and I. K. Schuller, Phys. Rev. B **63**, 174423 (2001).
16. J.M. Tranquada, B.J. Sternlieb, J.D. Axe, Y. Nakamura, and S. Uchida, Nature **375**, 561 (1995).
17. M. Abu-Shiekh, O. Bakharev, H. B. Brom, and J. Zaanen, Phys. Rev. Lett. **87**, 237201 (2001).
18. J. Orenstein, G.A. Thomas, A.J. Millis, S.L. Cooper, D.H. Rapkine, T. Timusk, L.F. Schneemeyer, and J.V. Waszczak, Phys. Rev. B **42**, 6342 (1990).
19. S. Uchida, T. Ido, H. Takagi, T. Arima, Y. Tokura, and S. Tajima, Phys. Rev. B **43**, 7942 (1991).
20. M. Imada, A. Fujimori, and Y. Tokura, Rev. Mod. Phys. **70**, 1039 (1998).
21. A. Damascelli, Z.-X. Shen, and Z. Hussain, Cond-Matt/0208504, (2002).
22. W.E. Pickett, H. Krakauer, R.E. Cohen, and D.J. Singh, Science **225**, 46 (1992).
23. J.P. Carbotte, E. Schachinger, and D.N. Basov, Nature **401**, 354 (1999).
24. A. Abanov, A.V. Chubukov, and J. Schmalian, J. Jour. El. Spect. Rel. Phen. **117-118**, 129 (2001).
25. M.R. Norman and H. Ding, Phys. Rev. B **57**, 11088 (1998).
26. A. Lanzara, P.V. Bogdanov, X.J. Zhou, S.A. Kellar, D.L. Feng, E.D. Lu, Yoshida T, H. Elsaki, A. Fujimori, K. Kishio, J.-I. Shimoyama, T. Noda, S. Uchida, Z. Hussain, and Z.-X. Shen, Nature **412**, 510 (2001).

27. E.J. Singley, D.N. Basov, K. Kurahashi, T. Uefuji, and K. Yamada, *Phys. Rev. B* **64**, 224503 (2001).
28. T. Timusk and B. Statt, *Rep. Prog. Phys.* **62**, 61 (1999).
29. V. J. Emery and S. A. Kivelson, *Nature* **374**, 434 (1995).
30. Z.A. Xu, N.P. Ong, Y. Wang, T. Kakeshita, and S. Uchida, *Nature* **406**, 486 (2000).
31. J. Corson, R. Mallozzi, J. Orenstein, J.N. Eckstein, and I. Bozovic, *Nature* **398**, 221 (1999).
32. D.N. Basov, S.I. Woods, A.S. Katz, E.J. Singley, R.C. Dynes, M. Xu, D.C. Hinks, C.C. Homes, and M. Strongin, *Science* **283**, 49 (1999).
33. H.J.A. Molengraaf, C. Pressura, D. Van Der Marel, P.H. Kes, and M. Li, *Science* **295**, 2239 (2002).
34. M.R. Norman, M. Randeria, B. Janko, and J.C. Campuzano, *Phys. Rev. B* **61**, 14742 (2000).
35. D. van Harlingen, *DOE Workshop, High Temperature Superconductivity*. April 2002.
36. Ch. Renner, B. Revaz, J.-Y. Genoud, K. Kadowaki, and O. Fischer, *Phys. Rev. Lett.* **80**, 149 (1998).
37. M. Covington and L.H. Greene, *Phys. Rev. B* **62**, 12440 (2002).
38. V.M. Krasnov, *Arxiv: Condensed Matter/0201287*.
39. S.H. Pan, J.P. O'Neal, R.L. Badzey, C. Chamon, H. Ding, J.R. Engelbrecht, Z. Wang, H. Eisaki, S. Uchida, A.K. Gupta, K.-W. Ng, E.W. Hudson, K.M. Lang, and J.C. Davis, *Nature* **413**, 282 (2001).
40. O. Naaman, W. Teizer, and R.C. Dynes, *Phys. Rev. Lett.* **87**, 097004 (2001).
41. E.W. Hudson, K.M. Lang, V. Madhavan, S.H. Pan, H. Eisaki, S. Uchida, and J.C. Davis, *Nature* **411**, 920 (2001).
42. J. E. Hoffman, E. W. Hudson, K. M. Lang, V. Madhavan, H. Eisaki, S. Uchida, and J.C. Davis, *Science* **295**, 466 (2002).

43. C.G. Olson, R. Liu, A.B. Yang, D.W. Lunch, A.J. Arko, R.S. List, B.W. Veal, Y.C. Chang, P.Z. Jiang, and A.P. Paulikas, *Science* **245**, 731 (1989).
44. Z.X. Shen, D.S. Dessau, B.O. Wells, D.M. King, W.E. Spicer, A.J. Arko, D.S. Marshall, L.W. Lambardo, A. Kapitulnik, P. Dickinson, S. Doniach, and J. Dicarolo, *Phys. Rev. Lett.* **70**, 1553 (1993).
45. A. Kaminski, M. Randeria, J.C. Campuzano, M.R. Norman, H. Fretwell, J. Mesot, T. Sato, Takahashi, and K. Kadowaki, *Phys. Rev. Lett.* **86**, 1070 (2002).
46. P.V. Bogdanov, A. Lanzara, S.A. Kellar, Z.J. Zhou, E.D. Lu, W.J. Zheng, G. Gu, J.-I. Shinoyama, K. Kishio, H. Ikeda, R. Yoshizaki, Z. Hussain, and Z.X. Shen, *Phys. Rev. Lett.* **85**, 2581 (2000).
47. A. D. Gromko, A. V. Fedorov, Y. -D. Chuang, J. D. Koralek, Y. Aiura, Y. Yamaguchi, K. Oka, Yoichi Ando, and D. S. Dessau, *Arxiv.: Condensed Matter/0202329*.
48. Z.-X. Shen, A. Langara, S. Ishihara, and N. Nagaosa, *Phil Mag.* **B82**, 1349 (2002).
49. T. Valla, *Arxiv.: Condensed Matter/0204003*.
50. P.D. Johnson, T. Valla, A.V. Fedorov, Z. Yusof, B.O. Wells, Q. Li, A.R. Moodenbaugh, G.D. Gu, N. Koshizuka, C. Kendziora, C. Sha Jian, and D.G. Hinks, *Phys. Rev. Lett.* **87**, 177077 (2002).
51. M.R. Norman, M. Eschrig, A. Kaminski, and J.C. Campuzano, *Phys. Rev. B* **64**, 184508 (2001).
52. Y. Sakurai, Y. Tanaka, A. Bansil, S. Kaprzyk, A.T. Stewart, Y. Nagashima, T. Hyodo, S. Nanao, H. Kawata, and N. Shiotani, *Phys. Rev. Lett.* **74**, 2252 (1995).
53. J. Laukkanen, K. Hamalainen, S. Manninen, A. Shukla, T. Takahashi, K. Yamada, B. Barbiellini, S. Kapryzk, and A. Bansil, *J. Phys. Chem. Sol.* **62**, 2249 (2001).
54. D.N. Basov and T. Timusk, in *Handbook on the Physics and Chemistry of Rare Earths*. 2001, Elsevier Science B.V. p. 437.
55. D.N. Basov, R. Liang, D.A. Bonn, W.N. Hardy, B. Dabrowski, M. Quijada, D.B. Tanner, J.P. Rice, D.M. Ginsberg, and T. Timusk, *Phys. Rev. Lett.* **74**, 598 (1995).

56. G.S. Boebinger, Y. Ando, A. Passner, T. Kimura, M. Okuya, J. Shimoyama, K. Kishio, K. Tamasaku, N. Ichikawa, and S. Uchida, *Phys. Rev. Lett.* **77**, 5417 (1996).
57. T. E. Mason, in *Handbook on the Physics and Chemistry of Rare Earths*, K. A. Gschneidner, Jr., L. Eyring, and M. B. Maple, Editors. 2001, Elsevier: Amsterdam.
58. M.A. Kastner, R.J. Birgeneau, G. Shirane, and Y. Endoh, *Rev. Mod. Phys.* **70**, 897 (1998).
59. H. He, P. Bourges, Y. Sidis, C. Ulrich, L.P. Regnault, S. Pailhes, N.S. Berzigiarova, N.N. Kolesnikov, and B. Keimer, *Science* **295**, 1045 (2002).
60. J. Orenstein and A. J. Millis, *Science* **288**, 468 (2000).
61. V.J. Emery, S.A. Kivelson, and J.M. Tranquada, *Proc. Natl. Acad. Sci.* **96**, 8814 (1999).
62. Z. Islam, Arxiv: Condensed Matter/0110390.
63. M. Buchanan, *Nature* **409**, 8 (2001).
64. A. Kaminski, S. Rosenkranz, H. M. Fretwell, J. C. Campuzano, Z. Li, H. Raffy, W. G. Cullen, H. You, C. G. Olson, C. M. Varma, and H. Höchst, *Nature* **416**, 610 (2002).
65. J. Guimpel, L. Civale, F. de la Cruz, J.M. Murduck, and I.K. Schuller, *Phys. Rev. B* **38**, 2342 (1988).
66. A. K. Geim, S.V. Dubonos, J.J. Palacios, I.V. Grigorieva, M. Henini, and J.J. Schermer, *Phys. Rev. Lett.* **85**, 1528 (2000).
67. L. F. Chibotaru, A. Ceulemans, V. Bruyndoncx, and V.V. Moshchalkov, *Nature* **408**, 833 (2000).
68. B. J. Baelus and F. M. Peeters, *Phys. Rev. B* **65**, 104515 (2002).
69. Yu. E. Lozovik, E.A. Rakoch, and S. Yu. Volkov, *Phys. Solid State* **44**, 22 (2002).
70. R. Besseling, R. Niggebrugge, and P. H. Kes, *Phys. Rev. Lett.* **82**, 3144 (1999).
71. J. I. Martin, M. Velez, E.M. Gonzalez, A. Hoffmann, D. Jaque, M.I. Montero, E. Navarro, J.E. Villegas, I.K. Schuller, and J.L. Vicent, *Physica C* **369**, 135 (2002).

72. A. Grigorenko, G.D. Howells, S.J. Bending, J. Bekaert, M.J. Van Bael, L. Van Look, V.V. Moshchalkov, Y. Bruynseraede, G. Borghs, I.I. Kaya, and R.A. Stradling, *Phys. Rev. B* **63**, 052504 (2001).
73. M. Baert, V.V. Metlushko, R. Jonckheere, V.V. Moshchalkov, and Y. Bruynseraede, *Phys. Rev. Lett.* **74**, 3269 (1995).
74. V. Metlushko, U. Welp, G.W. Crabtree, R. Osgood, S.D. Bader, L.E. DeLong, Zhao Zhang, S.R.J. Brueck, B. Illic, K. Chung, and P.J. Hesketh, *Phys. Rev. B* **60**, R12585 (1999).
75. A. Castellanos, R. Wordenweber, G. Ockenfuss, A. V.D. Hart, and K. Keck, *Appl. Phys. Lett.* **71**, 962 (1997).
76. M. Park, C. Harrison, P. Chaikin, R.A. Register, and D.H. Adamson, *Science* **276**, 1401 (1997).
77. H. Masuda and H. Fukuda, *Science* **268**, 1466 (1995).
78. B. Koslowski, S. Strobel, Th. Herzog, B. Heinz, H.G. Boyen, R. Notz, P. Ziemann, J.P. Spatz, and M. Moller, *J. Appl. Phys.* **87**, 7533 (2000).
79. U. Welp, Z. L. Xiao, J. S. Jiang, V. K. Vlasko-Vlasov, S. D. Bader, G. W. Crabtree, J. Liang, H. Chik, and J. M. Xu, *Arxiv Condensed Matter/0204535*.
80. Yayu Wang, Z.A. Xu, T. Kakeshita, S. Uchida, S. Ono, Y. Ando, and N.P. Ong, *Phys. Rev. B* **64**, 224519 (2001).
81. S.H. Pan, E.W. Hudson, A.K. Gupta, K.-W. Ng, H. Elsaki, S. Uchida, and J.C. Davis, *Phys. Rev. Lett.* **85**, 1536 (2000).
82. I. Maggio-Aprile, Ch. Renner, A. Erb, E. Walker, and O. Fischer, *Phys. Rev. Lett.* **75**, 2754 (1995).
83. B.W. Hoogenboom, K. Kadowaki, B. Revaz, M. Li, Ch. Renner, and O. Fischer, *Phys. Rev. Lett.* **87**, 267001 (2001).
84. S.-C. Zhang, *Science* **275**, 1089 (1997).
85. A.Y. Liu, I.I. Mazin, and J. Kortus, *Phys. Rev. Lett.* **87**, (2001).
86. C. Uher, R. Clarke, G.-G. Zheng, and I.K. Schuller, *Phys. Rev. B* **30**, 453 (1984).
87. J. Jorgensen, *Phys. Rev. B* **63**, 054440 (2001).
88. T.K. Ng and C.M. Varma, *Phys. Rev. Lett.* **78**, 330 (1997).

89. S.-M. Choi, J.W. Lynn, D. Lopez, P.L. Gammel, P.C. Canfield, and S.L. Bud'ko, *Phys. Rev. Lett.* **87**, 107001 (2001).
90. M.I. Montero, Kai Liu, O.M. Stoll, A. Hoffmann, Ivan K. Schuller, Johan J. Åkerman, J.I. Martin, J.L. Vicent, S.M. Baker, T.P. Russell, C. Leighton and J. Nogues, *J. Phys. D*, **35**, 2398 (2002).
91. S. Erdin, I.F. Lyuksyutov, V.L. Pokrovsky, and V.M. Vinokur, *Phys. Rev. Lett.* **88**, 017001 (2002).
92. O.M. Stoll, M.I. Montero, J. Guimpel, J.J. Åkerman, and I.K. Schuller, *Phys. Rev. B* **65**, 104518 (2002).
93. M. Velez, D. Jaque, J.I. Martin, M.I. Montero, I.K. Schuller, and J.L. Vicent, *Phys. Rev. B* **65**, 104511 (2002).
94. M.J. Van Bael, J. Bekaert, K. Temst, L. Van Look, V.V. Moschchalkov, Y. Bruynseraede, G.D. Howells, A.N. Grigorenko, S.J. Bending, and G. Borghs, *Phys. Rev. Lett.* **86**, 155 (2001).
95. D. S. Fisher, M.P. A. Fisher, and D. A. Huse, *Phys. Rev. B* **43**, 130 (1991).
96. David R. Nelson and V. M. Vinokur, *Phys. Rev. B* **48**, 13060 (1993).
97. A. W. Smith, H.M. Jaeger, T.F. Rosenbaum, W.K. Kwok, and G.W. Crabtree, *Phys. Rev. B* **63**, 064514 (2001).
98. A. M. Petrean, L.M. Paulius, W.-K. Kwok, J.A. Fendrich, and G.W. Crabtree, *Phys. Rev. Lett.* **84**, 5852 (2000).
99. Y. Paltiel, E. Zeldov, Y. Myasoedov, M.L. Rappaport, G. Jung, S. Bhattacharya, M.J. Higgins, Z.L. Xiao, E.Y. Andrei, P.L. Gammel, and D.J. Bishop, *Phys. Rev. Lett.* **85**, 3712 (2000).
100. W. K. Kwok, R.J. Olsson, G. Karapetrov, L.M. Paulius, W.G. Moulton, D.J. Hofman, and G.W. Crabtree, *Phys. Rev. Lett.* **84**, 3706 (2000).
101. N. Avraham, B. Khaykevich, Y. Myasoedov, M. Rappaport, H. Shtrikman, D.E. Feldman, T. Tamegai, P.H. Kes, Ming Li, M. Konczykowski, K. Van der Beek, K. Yamada, and E. Zeldov, *Nature* **411**, 451 (2001).
102. F. Bouquet, C. Marcenat, E. Steep, R. Calemczuk, W.K. Kwok, U. Welp, G.W. Crabtree, R.A. Fisher, N.E. Phillips, and A. Schilling, *Nature* **411**, 448 (2001).

103. T. Matsuda, K. Harada, H. Kasai, O. Kamimura, and A. Tonomura, *Science* **271**, 1393 (1996).
104. P.E. Goa, H. Hauglin, M. Baziljevich, E. Il'yashenko, P.L. Gammel, and T.H. Johansen, *Supercond. Sci. Tech.* **14**, 729 (2001).
105. C.J. Olson, C. Reichhardt, B. Janko, and F. Nori, *Phys. Rev. Lett.* **87**, 177002 (2001).
106. M.N. Kunchur, B.I. Ivlev, and J.M. Knight, *Phys. Rev. Lett.* **87**, 177001 (2001).
107. A. E. Koshelev, *Phys. Rev. Lett.* **83**, 187 (1999).
108. J. Mirkovic, S.E. Savelev, E. Sugahara, and K. Kadowaki, *Phys. Rev. Lett.* **86**, 886 (2001).
109. A. Grigorenko, S. Bending, T. Tamegal, S. Ooi, and M. Henini, *Nature* **414**, 728 (2001).
110. V.K. Vlasko-Vlasov, *Arxiv Condensed Matter/0203145*.
111. A.E. Koshelev and I. Aranson, *Phys. Rev. B* **64**, 174508 (2001).
112. M. Machida, T. Koyama, and M. Tachiki, *Phys. Rev. Lett.* **83**, 4618 (1999).
113. A. Tonomura, H. Kasai, O. Kamimura, T. Matsuda, K. Harada, Y. Nakayama, J. Shimoyama, K. Kishio, T. Hanaguri, K. Kitazawa, M. Sasase, and S. Okayasu, *Nature* **412**, 620 (2001).
114. T. Matsuda, O. Kamimura, H. Kasai, K. Harada, T. Yoshida, T. Akashi, A. Tonomura, Y. Nakayama, J. Shimoyama, K. Kishio, T. Hanaguri, and K. Kitazawa, *Science* **294**, 2136 (2001).
115. For a good classic discussion of proximity effects, see the chapter by G. Deutscher and P.G. de Gennes, in *Superconductivity*, R. D. Parks, Editor. 1969, Marcel Dekker.
116. For a useful entrée into the literature, see: L. Antognazza, B.H. Moeckly, T.H. Geballe and K. Char, *Phys. Rev.*, *Phys. Rev. B* **52**, 4559 (1995).
117. For an authoritative review, see: H. Hilgenkamp and J. Mannhart, *Rev. Mod. Phys.* **74**, 485 (2002).
118. R.E Glover and M.D. Sherill, *Phys. Rev. Lett.* **5**, 248 (1960).
119. H.L. Stradler, *Phys. Rev. Lett.* **14**, 979 (1965).

120. C.H. Ahn, J.-M Triscone, and J. Mannhart, (To be published in Nature).
121. For a contemporary entrée into the literature, see: Y.V. Fominov, N.M. Chtchelkatchev and A.A. Golubov, Arxiv-cond. matt. *Nonmonotonic critical temperature in superconductor/ferromagnet bilayers*.
122. See for example: A. Rusanov, R. Boogaard, M. Hesselberth, H. Sellier and J Aarts, Arxiv.: Condensed Matter/0111178.
123. See section VII-D, Rev. Mod. Phys. **74**, 485 (2002).
124. Y. Tanaka, and S. Kashiwaya, Phys. Rev. Lett. **74**, 3451 (1995).
125. For one example and useful references, see Y. Suzuki, J.M. Triscone, E.B. Eom, M.R. Beasley, and T.H. Geballe, Phys. Rev. Lett. **73**, 328 (1994).
126. R.C. Dynes, this DOE Workshop.
127. T.H. Geballe and B.Y. Mozyzhes, Physica C **341**, 1821 (2000).
128. See, for instance, I. Bozovic IEEE Trans. Appl. Superconductivity **11**, 2686 (2001).
129. Philip B. Allen, Phys. Rev. Lett. **59**, 1460 (1987).
130. Y. Zhang, N. P. Ong, P. W. Anderson, D. A. Bonn, R. Liang, and W. N. Hardy, Phys. Rev. Lett. **86**, 890 (2001).
131. A. Hosseini, R. Harris, S. Kamal, P. Dosanjh, J. Preston, Ruixing Liang, W.N. Hardy, and D.A. Bonn, Phys. Rev. B **60**, 1349 (1999).
132. G.P. Segre, N. Gedik, J. Orenstein, D.A. Bonn, Ruixing Liang, and W.N. Hardy, Phys. Rev. Lett. **88**, 137001 (2002).
133. R.A. Kaindl, M. Woerner, T. Elsaesser, D.C. Smith, J.F. Ryan, G.A. Farnan, M.P. McCurry, and D.G. Walmsley, Science **287**, 470 (2000).
134. B.J. Feenstra, J. Schutzmann, D. van der Marel, R. Perez Pinaya, and M. Decroux, Phys. Rev. Lett. **79**, 4890 (1997).
135. R.D. Averitt, G. Rodriguez, A. I. Lobad, J. L. W. Siders, S. A. Trugman, and A. J. Taylor, Phys. Rev. B **63**, 140502 (2001).
136. J. Demsar, R. Hudej, J. Karpinski, V.V. Kabanov, and D. Mihailovic, Phys. Rev. B **63**, 054519 (2001).

137. *Nonequilibrium Superconductivity, Phonons, and Kapitza Boundaries*, ed. K.E. Gray. 1981, New York: Plenum Press.
138. D.N. Langenberg and A.I. Larkin. 1986, New York: North-Holland.
139. P. Dai, H.A. Mook, S.M. Hayden, G. Aeppli, T.G. Perring, R.D. Hunt, and F. Dogan, *Science* **284**, 1344 (1999).
140. D. Vollhardt and P. Wölfle. 1990, London: Taylor & Francis.
141. A.F.G. Wyatt, V. M. Dmitriev, W. S. Moore, and F. W. Sheard, *Phys. Rev. Lett.* **16**, 1166 (1966).
142. A.H. Dayem and J.J. Wiegand, *Phys. Rev.* **155**, 419 (1967).
143. K.E. Gray, *Solid State Commun.* **26**, 633 (1978).
144. N.E. Booth, *Appl. Phys. Lett.* **50**, 293 (1987).
145. A. Yurgens, D. Winkler, T. Claeson, Seong-Ju Hwang, and Jin-Ho Choy, *Int. J. Mod. Phys.* **13**, 3758 (1999).
146. J. P. Carbotte, *Rev. Mod. Phys.* **62**, 1027 (1990).
147. E. Schachinger, J.P. Carbotte, and D.N. Basov, *Europhys. Lett.* **54**, 380 (2001).
148. E. Schachinger and J. P. Carbotte, *Phys. Rev. B* **65**, 064514 (2002).
149. A. Puchkov, D.N. Basov, and T. Timusk, *J. Phys: Condens. Matter* **8**, 10049 (1996).
150. F. Marsiglio, T. Startseva, and J.P. Carbotte, *Phys. Lett. A* **245**, 172 (1998).
151. N. E. Bickers, D. J. Scalapino, and S. R. White, *Phys. Rev. Lett.* **62**, 96 (1989).
152. A. J. Millis, H. Monien, and D. Pines, *Phys. Rev. B* **42**, 167 (1990).
153. C.M. Varma, P.B. Littlewood, S. Schmitt-Rink, E. Abrahams, and A.E. Ruckenstein, *Phys. Rev. Lett.* **63**, 1996 (1989).
154. C.H. Pao and N.E. Bickers, *Phys. Rev. Lett.* **72**, 1870 (1994).
155. P. Monthoux and D.J. Scalapino, *Phys. Rev. Lett.* **72**, 1874 (1994).

156. S. Chakravarty, R.B. Laughlin, D.K. Morr, and C. Nayak, Phys. Rev. B **63**, 094503 (2001).
157. P.D. Johnson, T. Valla, A.V. Fedorov, Z. Yusof, B.O. Wells, Q. Q. Li, A.R. Moodenbaugh, G.D. Gu, N. Koshizuka, C. Kendziora, Sha Jian, and D.G. Hinks, Phys. Rev. Lett. **87**, 177007 (2001).
158. A. Lanzara, Arxiv. Condensed Matter/10102227.
159. Z. X. Shen, Arxiv: Condensed Matter/10102244.
160. J. E. Hirsch, Phys. Rev. B **31**, 4403 (1985).
161. J. D. Reger and A. P. Young, Phys. Rev. B **37**, 5978 (1988).
162. D. J. Scalapino and S. R. White, Phys. Rev. **31**, 5978 (2001).
163. S. Sorella, G.B. Martins, F. Becca, C. Gazza, L. Capriotti, A. Parola, and E. Dagotto, Arxiv: Condensed Matter/0110460.
164. D. Poilblanc, J. Riera, and E. Dagotto, Phys. Rev. B **49**, 12318 (1994).
165. P. W. Leung, Arxiv: Condensed Matter/0201031.
166. G. Baskaran, Z. Zou, and P. W. Anderson, Sol. State. Comm. **63**, 973 (1987).
167. T. Senthil and M. P. A. Fisher, Arxiv: Condensed Matter/9910224.
168. V. J. Emery, S. A. Kivelson, and O. Zachar, Phys. Rev. **56**, 6120 (1997).
169. V. Chubukov, D. Pines, and J. Schmalian, Arxiv: Condensed Matter/9910224.
170. D.J. Scalapino, Phys. Reports **250**, 329 (1995).
171. A. Bansil and M. Lindroos, Phys. Rev. Lett. **83**, 5154 (1999).
172. K.J. Chang, M.M. Dacorogna, M.L. Cohen, J.M. Mignot, G. Chouteau, and G. Martinez, Phys. Rev. Lett. **54**, 2375 (1985).
173. Cheng-Zhang Wang, Rici Yu, and H. Krakauer, Phys. Rev. B **59**, 9278 (1999).
174. T. C. Leung, X. W. Wang, and B. N. Harmon, Phys. Rev. B **37**, 384 (1988).
175. V. I. Anisimov, F. Aryasetiawan, and A.I. Lichtenstein, J. Phys.: Condens. Matter **9**, 767 (1997).

176. M.I. Katsnelson and A.I. Lichtenstein, *J. Phys.: Condens. Mat.* **11**, 1037 (1999).
177. A. Georges, G. Kotliar, W. Krauth, and M.J. Rozenberg, *Rev. Mod. Phys.* **68**, 13 (1996).
178. For a recent cluster DMFT application to the Hubbard model and d-wave superconductivity, see A. I. Lichtenstein and M. I. Katsnelson, *Phys. Rev. B* **62**, R9283 (2000).
179. An application of DMFT to ARPES spectra see Th. A. Meier, Th. Pruschke, and M. J  rrell, cond-mat/0201037.
180. H. Rietschel and L. J. Sham, *Phys. Rev. B* **28**, 5100 (1983).
181. H. Rietschel, H. Winter, and W. Reichardt, *Phys. Rev. B* **22**, 4284 (1980).
182. Miodrag L. Kuli   and Roland Zeyher, *Phys. Rev. B* **49**, 4395 (1994).
183. Z.-X. Cai and Yimei Zhu. 1998: World Scientific.
184. M.E. McHenry and R.A. Sutton, *Prog. Mater. Sci.* **38**, 159 (1994).
185. G. Blatter, M.V. Feigel'man, V.B. Geshkenbein, A.I. Larkin, and V.M. Vinokur, *Revs. Mod. Phys.* **66**, 1125 (1994).
186. Superconductors Science and Technology, July 1997. Special issue to mark 10 years of high-Tc superconductivity, .
187. C. Buzea and T. Yamashita, *Superconductor Science and Technology* **14**, R115 (2001).
188. D. Larbalestier, A. Gurevich, D.M. Feldman, and A. Polyanskii, *Nature* **414**, 368 (2001).

BRIEF ATTACHMENT BA

IN THE UNITED STATES PATENT AND TRADEMARK OFFICE

In re Patent Application of

Applicants: Bednorz et al.

Serial No.: 08/479,810

Filed: June 7, 1995

Date: March 1, 2004

Docket: YO987-074BZ

Group Art Unit: 1751

Examiner: M. Kopec

For: NEW SUPERCONDUCTIVE COMPOUNDS HAVING HIGH TRANSITION
TEMPERATURE, METHODS FOR THEIR USE AND PREPARATION

Commissioner for Patents
P.O. Box 1450
Alexandria, VA 22313-1450

FIFTH SUPPLEMENTAL AMENDMENT

Sir:

In response to the Office Action dated February 4, 2000:

ATTACHMENT 43

BA



http://catnyp.nypl.org/search/q

CATNYP: The Online Catalog of The New York Public Library
The Research Libraries

ANOTHER
SEARCH

START
OVER

EXPORT

You searched **AUTHOR**

rao

in **Entire**

Limited to: Words in the TITLE "new directions in s"

Call #

JSD 88-446

Author

Rao, C. N. R. (Chintamani Nagesa Ramachandra), 1934-

Title

New directions in solid state chemistry : structure, synthesis, properties, reactions
Rao, J. Gopalakrishnan.

Imprint

Cambridge [Cambridgeshire] ; New York : Cambridge University Press, 1986

LOCATION	CALL #
Science & Business Lib	JSD 88-446

Location

Science & Business Lib

Descript

x, 516 p. : ill. ; 23 cm.

Series

Cambridge solid state science series

Note

Includes index.

Subject

Bibliography: p. [475]-503.

Add'l name

Solid state chemistry.

Gopalakrishnan, J. (Jagannatha), 1939-

ANOTHER
SEARCH

START
OVER

EXPORT

CATNYP: The Online Catalog of The New York Public Library

Daniel P. Morris, Ph.D.
Staff Counsel
IBM Research
IP Law Department Yorktown
Tie line: 8-862-3217
Phone: 914-945-3217
Fax: 914-945-3281



RECEIPT

IN THE UNITED STATES PATENT AND TRADEMARK OFFICE

In re Patent Application of
Applicants: Bednorz et al.

Serial No.: 08/479,810

Filed: June 7, 1995

For: NEW SUPERCONDUCTIVE COMPOUNDS HAVING HIGH TRANSITION
TEMPERATURE, METHODS FOR THEIR USE AND PREPARATION



Date: March 1, 2004

Docket: YO987-074BZ

Group Art Unit: 1751

Examiner: M. Kopec

Commissioner for Patents
P.O. Box 1450
Alexandria, VA 22313-1450

FIFTH SUPPLEMENTAL AMENDMENT

Sir:

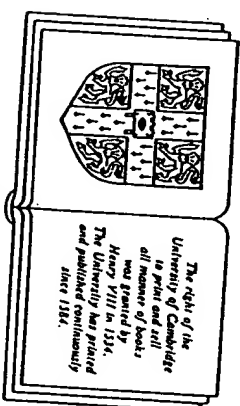
In response to the Office Action dated February 4, 2000:

C. N. R. RAO, FRS
J. GOPALAKRISHNAN

*Solid State and Structural Chemistry Unit, Indian Institute of Science,
Bangalore, India*

New directions in solid state chemistry

Structure, synthesis, properties, reactivity
and materials design



*The right of the
University of Cambridge
to print and sell
all manner of books
was granted by
Henry VIII in 1534.
The University has printed
and published continuously
since 1584.*

CAMBRIDGE UNIVERSITY PRESS
Cambridge

*London New York New Rochelle
Melbourne Sydney*



bulk metals. Metal particulates (similar to those on the surfaces of supported metal catalysts (Chapter 8)) constitute a type of metal aggregate somewhere between high nuclearity metal clusters and bulk metals.

There are families of metal cluster compounds (Fig. 6.37) containing metal clusters surrounded by ligands (Lewis & Green, 1982). In small cluster compounds, the electrons are paired, but in large clusters there will be closely spaced electronic levels, as in metal particles. In such clusters, quantum size effects would be expected. Benfield *et al.* (1982) have found intrinsic paramagnetism in $\text{H}_2\text{Os}_6(\text{CO})_{24}$ below 70 K as expected of an osmium particle of approximate diameter of 10 Å; the excess paramagnetism increases with cluster size in osmium compounds (Johnson *et al.*, 1985).

Metal cluster compounds simulate surface species produced by the interaction of molecules with metal surfaces (Muettteries *et al.*, 1979) and this is of value in understanding heterogeneous catalysis. The development of selective catalysts for the C_1 chemical industry employing CO (and possibly CO_2) as the raw material has resulted in major efforts in metal cluster research. Criteria have been developed to distinguish between cluster catalysis and mononuclear catalysis. Typical of the catalysts investigated hitherto are $[\text{Ir}_4(\text{CO})_{12-x}(\text{PPh}_3)_x]$ where $\text{Ph} = \text{phenyl}$ and $x = 1, 2$ or 3.

6.7 Mixed-valence compounds

Chemical compounds consisting of an element (usually a metal) in two different formal oxidation states are said to exhibit mixed valency. Mixed-valence chemistry is as old as chemistry itself, some of the well known mixed-valence compounds being Prussian blue ($\text{Fe}_4[\text{Fe}(\text{CN})_6]_3 \cdot 14\text{H}_2\text{O}$), magnetite (Fe_3O_4), and heteropoly tungsten and molybdenum blues. Mixed-valence chemistry, however, encompasses a large variety of solids with fascinating properties (Table 6.6) formed by nearly a third of the elements in the periodic table, and there has been a recent upsurge of interest in the subject (Day, 1981). Since variable valency is a prerequisite for mixed valency, it is quite common among the compounds of transition metals, Ce, Eu and Tb, as well as some of the post-transition elements with stable ns^2 and ns^0 electronic configurations such as Ga, Sn, Sb, Tl, Pb and Bi. Most mixed-valency compounds contain electronegative counterpart anions such as halides, oxide, sulphide or molecular ligands containing electronegative atoms. In order for a solid to be called a mixed-valence compound, we should be able to assign definite oxidation states that differ by integral numbers (one or at the most two units) to the element showing mixed valency.

Fe_3O_4 consisting of iron in the 2^+ and 3^+ oxidation states, is a mixed-valence compound, whereas the alloy Nb_3Ge , where we cannot specify the oxidation states of the constituents, is not. We should also make a distinction between the mixed-valence compounds of the Fe_3O_4 type and valence-fluctuating systems such as Ce and SmS, where a fluctuation in the electron configuration between $4f^n$ and $4f^{n-1}d^1$ occurs (Falicov *et al.*, 1981). (see Section 2.2.7). Electronic properties associated with f -electrons receiving much attention recently are those arising from heavy fermion behaviour (e.g. CeCu_2Si_2 , UPt_3) wherein the carriers exhibit large effective masses (Stewart, 1984).

In certain mixed-valence compounds, the presence of more than one oxidation state can be recognized from the formula, as for example Pb_3O_4 and $\text{V}_n\text{O}_{2n-1}$, while in some others the formula indicates an apparently integral oxidation state although the oxidation state is rather unusual for the element in question. Typical examples of the latter category are Sb_2O_4 , BaBiO_3 and $\text{Pt}(\text{NH}_3)_2\text{Cl}_3$; experimental evidence shows that we are not dealing with $\text{Sb}(\text{IV})$, $\text{Bi}(\text{IV})$ and $\text{Pt}(\text{III})$ states in these compounds but with $\text{Sb}(\text{III})$, V , $\text{Bi}(\text{III})$, V and $\text{Pt}(\text{II})$, IV , and these solids should indeed be formulated as $\text{Sb}^{3+}\text{Sb}^{5+}\text{O}_4$, $\text{BaBi}_6^{3+}\text{Bi}_6^{5+}\text{O}_3$ and $[\text{Pt}(\text{NH}_3)_4]^{2+}[\text{PtCl}_6]^{2-}$. In all such systems, X-ray photoelectron

Table 6.6 Typical mixed-valence solids

Compound	Classification in the Robin-Day scheme	Importance
Pb_3O_4	Class I	Red lead
Sb_2O_4	Class I	Mineral cervantite
$\text{Fe}_4[\text{Fe}(\text{CN})_6]_3 \cdot 14\text{H}_2\text{O}$	Class II	Dye and pigment (Prussian blue)
$\text{V}_n\text{O}_{2n-1}$	Class II	Semiconductor-metal transitions
$\text{Li}_x\text{Ni}_{1-x}\text{O}$	Class II	Hopping semiconductor
$\text{La}_{1-x}\text{Sr}_x\text{MnO}_3$	Class II	Ferromagnetism
$\text{BaBi}_{1-x}\text{Pb}_x\text{O}_3$	Class III	Superconductivity
LiTi_2O_4	Class III	Superconductivity
$\text{K}_2\text{Pt}(\text{CN})_4\text{Br}_{0.30} \cdot 3\text{H}_2\text{O}$	Class III	Molecular metal; Peter's instability
Na_xWO_3	Class III	Bronze lustre and metallic at high x
$\text{M}_x\text{Mo}_6\text{S}_8$	Class III	Superconductivity
Fe_4S_4 Ferredoxins	Class III	Electron transfer (enzymes)

spectroscopy can readily identify the presence of mixed valency (Rao *et al.*, 1979).

Robin & Day (1967) have proposed a classification of mixed-valence compounds based on the valence delocalization coefficient, α , the magnitude of which depends on the energy difference between the two states $M_A^n M_B^{n+1}$ and $M_A^{n+1} M_B^n$, where A and B are two different sites. When ΔE is large as in Pb_3O_4 , α is small; such compounds belong to class I. If the two sites are similar but crystallographically distinguishable, the compounds are considered to belong to class II. In class III, α becomes large and the two sites occupied by the mixed-valent cations are identical. Properties associated with the different classes would be different (Table 6.6). For example, in class I compounds, electron hopping between the sites is not favoured since ΔE is large. In class III compounds, on the other hand, the electrons would be delocalized. The ligands which bridge the cations play a role in determining the intervalence transfer; the greater the metal-ligand overlap, the higher the probability of electron transfer (Mayoh & Day, 1972). In order to describe the electron transfer in mixed-valence compounds properly, one would have to consider the coupling between the electronic and vibrational motions. Experimentally, the frequency of optical intervalence transition gives an estimate of the energy required for thermally activated electron transfer. The intensity of the optical intervalence transition gives information on α . One of the most characteristic features of mixed-valent class II compounds is the structureless broad intervalence absorption band in the visible and infrared. A vibrational coupling model has been developed to calculate the absorption profiles (Piepho *et al.*, 1978); a good example of analysis of such absorption profiles is the recent study of $(CH_3NH_3)_2SbSn_{1-x}Cl_x$ by Prassides & Day (1984). When the electrons are not completely delocalized and they hop from site to site in marginal semiconductors, the strength of interaction between the electrons and the lattice (polarons) becomes an important factor.

Mixed valency occurs in minerals (e.g. Fe_2O_3), metal-chain compounds, dimers and oligomers and metal complexes, and even in organic and biological systems (Brown, 1980; Day, 1981). Among the dimeric and oligomeric metal complexes exhibiting mixed valency, the pyrazine-bridged Ru (II, III) ammine complex,



synthesized by Creutz & Taube (1973), has received much attention. The important question with regard to this family of complexes is whether they belong to class II or III. With identical ligands around each metal ion, the first impression is to consider the *Creutz-Taube complex* as belonging to class III. Optical absorption shows an intense band in the visible (550 nm), which is characteristic of Ru(II). It certainly supports the idea that a distinct Ru(II) can be identified on the time scale of optical transition (10^{-14} s). However, the intervalence band centred at ~ 1550 nm is insensitive to solvent effects and a bit too narrow to be called a class II behaviour. XPS shows doublets in the core-level Ru(3d) and (3p) spectra, indicating that the individual oxidation states can be distinguished on this time scale (10^{-16} s) as well. Hush (1975) has argued that the creation of core-hole by photoionization would relax the system into a localized state even if it were originally delocalized; core-shell photoelectron spectroscopy therefore does not appear to provide the means to determine the extent of localization or delocalization in the valence shell. Infrared spectroscopy has shown that the NH_3 rocking mode (800 cm^{-1}), $Ru-NH_3$ stretching mode (449 cm^{-1}) and Ru -pyrazine stretching mode (316 cm^{-1}) of the Creutz-Taube complex all occur at values intermediate between those of the corresponding Ru(II) and Ru(III) complexes. This has been taken as evidence that the valence electron is delocalized in the time scale of infrared spectroscopy (10^{-12} – 10^{-13} s). Results of the various measurements on this complex are somewhat conflicting because of the different time scales; it appears that the electron-transfer rate is somewhere between 10^5 – 10^{12} s^{-1} . Mixed valency in compounds like $La_{1-x}Sr_xCoO_3$ (Rao *et al.*, 1975, 1977) is determined by rate of electron transfer and so by composition; that in $MoFe_2O_4$ and other solids resulting from fast electron transfer is discussed (Ramdani *et al.*, 1985).

In the metal-chain compounds, we can distinguish two types of mixed valent systems, one where the chain is entirely composed of metal atoms (class III) and the other in which the metal and the bridging ligand alternate (class II). Wolfram's red salt, $[Pt(C_2H_5NH_2)_4][Pt(C_2H_5NH_2)_4Cl_4] \cdot 4H_2O$ is an example of the former, consisting of Pt(II) and Pt(IV) ions bridged by chloride ions. In KCP type of mixed-valent compounds, mixed valency is achieved by partly oxidizing the Pt ions to an average oxidation state $(2+x)$ with $x \approx 0.3$. Partial oxidation is accomplished by removing some of the cations as in $K_{1.75}Pt(CN)_4 \cdot 1.5H_2O$ or by introducing extra anions $K_2Pt(CN)_4Br_{0.3} \cdot 3H_2O$. Even the Hg chain compound $Hg_{3-x}AsF_6$ (see Section 4.9) is mixed-valent.

Fe_3O_4 has the inverse spinel structure, with all the Fe^{2+} ions and half of the Fe^{3+} ions located in octahedral sites (B sites) in the oxygen network and the remaining half of the Fe^{3+} ions located on tetrahedral sites (A sites). It undergoes a ferimagnetic-paramagnetic transition around 850 K and another transition around $T_V = 123$ K (Verwey transition). The material is a semiconductor both above and below the Verwey transition. Some changes in properties have also been observed near 200 K and 12 K, but these are not very significant. The properties of Fe_3O_4 in the region of the Verwey transition and above have been a subject of great interest, and an entire issue of the *Philosophical Magazine* (B42, No. 10, 1980) was devoted to the transition.

Detailed structural investigations employing neutron diffraction and other techniques suggest that charge ordering of Fe^{2+} and Fe^{3+} ions (and therefore the long-range order) is established below T_V . Cation strings, *a* and *b*, run along the $[110]$ and $[\bar{1}10]$ directions respectively (on alternate (001) planes). While three Fe^{2+} ions in succession are followed by a Fe^{3+} ion along one chain, on an adjacent *a* chain three Fe^{3+} ions are followed by one Fe^{2+} . In the *b* chain, cation ordering occurs with a pair of Fe^{3+} ions followed by a pair of Fe^{2+} ions in alternation. Successive *b*-*a*-*b*- planes are stacked, perpendicular to the *c* axis, in such a way that proximate cations in three successive planes are in groups, forming hexagonal rings of alternate Fe^{2+} and Fe^{3+} ions. All the cations along *b* strings are members of rings and only a quarter of the *a*-string cations are involved in ring formation. The synchronous displacement of three electrons to their nearest-neighbour position inside any ring produces an interchange of Fe^{2+} with Fe^{3+} . A significant fraction of hexagonal rings always exists in the 'inverted' charge configuration, thereby randomizing charge along the *b* strings, but leaving three-quarters of the *a*-chain constituents in an ordered arrangement below T_V . This rationalizes earlier experimental findings that it is the *a*-plane cations which order at low temperatures.

The existence of superstructure lines just above T_V in critical neutron scattering and the detailed investigation of elastic and inelastic neutron scattering show the existence of a soft mode with wave vector $k = (00\frac{1}{2})$ that 'condenses' at $k = (00\frac{1}{2})$. Proceeding from one Fe^{2+} (or from one Fe^{3+}) ion in the *a* plane at $z = \frac{1}{8}$ to the corresponding position in the *a* plane at $z = \frac{5}{8}$, one arrives at the complementary charge (namely, Fe^{3+} or Fe^{2+}) respectively. One has to advance by twice the unit lattice distance along *c* to duplicate the same ionic configuration at $z = \frac{1}{8}$ that prevails at $z = \frac{5}{8}$. Formally, this corresponds to the existence of a charge-density wave (with wave length $\lambda = 2c$) which couples strongly to the corresponding phonon mode with the same wave vector. At the transition, the ordering of the charges (leading to the establishment of the CDW)

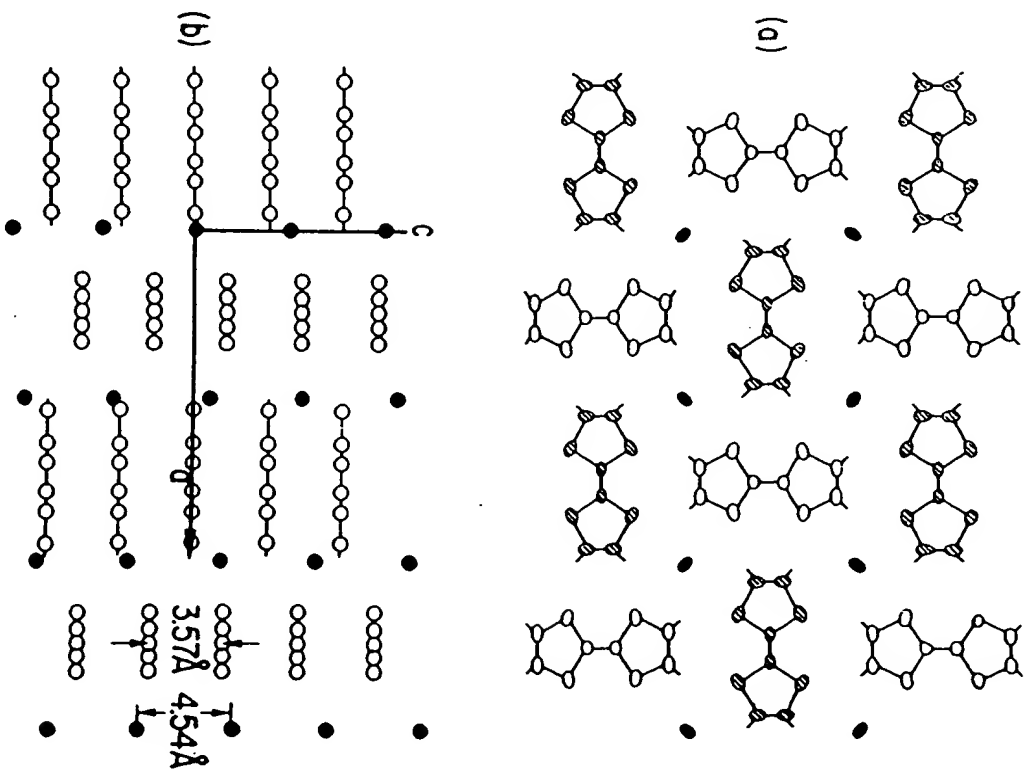
occurs simultaneously with a net atomic displacement that lowers the symmetry.

Although the structural characterization of Fe_3O_4 near the Verwey transition is fairly satisfactory, many finer details are not yet understood, (Honig, 1982, 1986), including the actual structure of the low-temperature phase (rhombohedral, orthorhombic, monoclinic or triclinic). Electrical properties around T_V are also not fully characterized. There is uncertainty regarding the nature of variation of conductivity with temperature. It is not clear whether the itinerant character of charge carriers assumed by some workers is valid. Most of the data on transport properties seem to suggest a small polaron model. What is rather puzzling is that the resistivity decreases by two orders of magnitude at T_V , accompanied by the loss of long-range order. Recent studies have shown that the Verwey transition and the associated changes in conductivity and heat capacity are very sensitive to oxygen stoichiometry (Honig, 1986).

There are several interesting families of inorganic mixed-valence compounds that we have not discussed here (see Yvon, 1979; McCauley, 1982). For example, there are metal-cluster compounds such as the Chevrel phases, $\text{M}_x\text{Mo}_6\text{X}_8$ ($\text{X} = \text{S}$ or Se) and condensed metal-cluster chain compounds such as TiMo_3Se_3 , Ti_3Te_4 , NaMo_4O_6 and $\text{M}_x\text{Pt}_3\text{O}_4$. TTF halides and TTF-TCNQ complexes (Section 1.9) constitute molecular mixed-valent systems in which the mixed valency is associated with an entire molecule; the charge on TTF in such compounds is non-integral. The structure of TTF- $\text{Br}_{0.79}$ and such solids consists of stacks of TTF molecules parallel to the *c*-axis. The Br^- ions are also arranged in columns parallel to the *c*-axis. However, the repeat distances of the cation (3.57 Å) and anion (4.54 Å) columns are different (Fig. 6.38). The structure is incommensurate along the *c*-axis because the lattice periodicities of the two subunits are not simple multiples (or fractions) of one another. It is important to note that the periodicity of the TTF sublattice is independent of stoichiometry, whereas that of the bromide sublattice is stoichiometry dependent. Hence the charge transfer in the salt can be expressed as $f = 3.57/c(\text{Br})$. Nonstoichiometric compositions in the TTF-halide systems seem to be stabilized because of electrostatic (Madelung) factors. Calculations show that the Madelung energy is maximum around a halogen content of 0.7 to 0.8. Beyond this composition, repulsion between like charges along the stacking axis begins to dominate, decreasing the net binding energy. Optical absorption shows a new peak around 0.7 eV in TTF- $\text{Br}_{0.79}$. The peak, which is not present in the spectra of stoichiometric salts, has been assigned to a mixed-valence intrastack charge-transfer transition between a neutral TTF and adjacent TTF $^+$.

The structure of HMTTF-TCNQ, a typical TTF-TCNQ-type complex, is shown in Fig. 6.39. The segregated stacking in this structure is a characteristic feature of the highly conducting organic charge-transfer system of the TTF-TCNQ family. In HMTTF-TCNQ (HMTTF-hexamethylenetetrafulvalene), the separation between donor molecules is 3.57 Å while that between TCNQ molecules is 3.23 Å along the stacks. To make the anion and cation sublattices com-

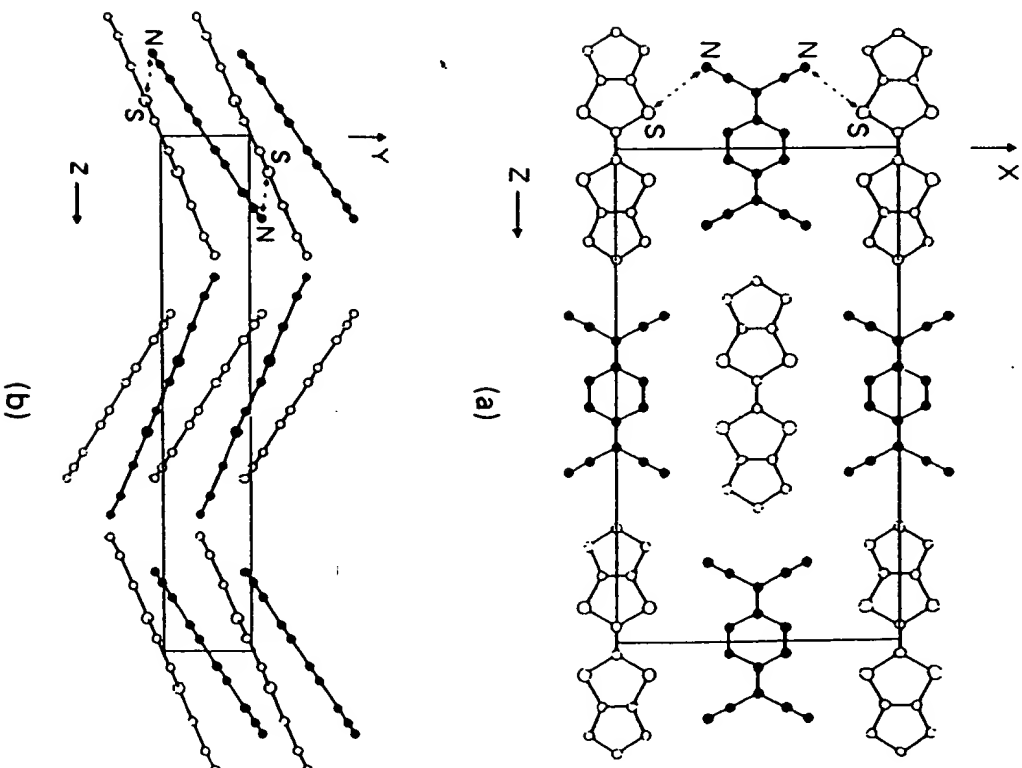
Figure 6.38. Crystal structure of TTF-Br_{0.79}. Projections (a) down the *a*-axis and (b) down the *b*-axis. (After Torrance & Silverman, 1977.)



mensurate with each other, the molecules are stacked in a staggered configuration such that the normals to the molecular planes are not parallel to the stacking axis but make an angle with it. The angles are different for the donor and acceptor stacks; in the HMTTF-TCNQ structure, the values are respectively 23.8° and 34.2°.

What makes the TTF-TCNQ family distinct from the other salts of TCNQ with cations, such as alkali metals and tetramethylammonium, is

Figure 6.39. Crystal structure of HMTTF-TCNQ. (a) Projection on the plane perpendicular to the stacking axis and (b) projection on a plane containing the stacking axis. (After Greene *et al.*, 1976.)



that the charge transfer, f , in the TTF-TCNQ family is incomplete ($f < 1$). TTF-TCNQ members are also different from the TTF-halides; in the TTF-halides, where the charge on each halide atom is unity, partial charge transfer (mixed valency) is realized by the formation of non-stoichiometric materials, while in the TTF-TCNQ family, the composition is stoichiometric (1:1), but mixed valence arises because of partial electron-transfer.

Evidence for incomplete electron transfer (mixed valency) has come from a number of physical studies. Optical absorption studies show a low energy peak at 0.3 eV, which is not present in insulating salts such as $K^+(TCNQ)^-$. Moreover, the absorption is polarized parallel to the stack axis. The absorption is therefore clearly due to mixed-valence intrastack electronic transition. TTF-TCNQ undergoes a transition from conducting to insulating state at 59 K. This transition is characterized by a subtle periodic modulation of the lattice due to a coupling of the conduction electrons with the lattice (CDW). This shows up in the form of satellite reflections surrounding the Bragg peaks in the diffraction experiment. Because the structure is sinusoidally modulated, the Bragg peaks caused by the average structure remain essentially unchanged. Since the satellite peaks are the result of interaction between conduction electrons and the lattice, their positions are determined by the extent of charge transfer f ; a value of $f = 0.59$ has been obtained for TTF-TCNQ from the diffraction satellites. A comparison of charge transfer in a variety of TCNQ salts with the reduction potential of cations shows that only those cations with a reduction potential $E_r = 0.0$ to 0.5 V vs. SCE lead to mixed-valence or incomplete transfer (Torrance, 1979). When the potential is too high (perylene, pyrene, anthracene etc.), there is no charge transfer and when it is too low, the transfer is complete.

The effect of f on the conductivity of TCNQ salts can be visualized as follows: for electrical conduction to occur, electrons must move from one TCNQ to another. When the charge transfer is complete, the process can be represented as



which involves creation of a dianion. Understandably the energy involved would be prohibitive and hence TCNQ salts with $f = 1$ are insulators. In the mixed-valence salts, the electrons can move easily along the stack by the process, $TCNQ^- + TCNQ^0 \longrightarrow TCNQ^0 + TCNQ^-$, which does not require creation of dianions. This localized picture is, however, only qualitative. A more accurate description would involve the band model. The relation between mixed-valence and

electrical properties is seen in HMTTF-TCNQ and HMTTF-TCNQF₄. Both are isostructural but HMTTF-TCNQ is metallic, while the tetrafluoro-substituted TCNQ salt is semiconducting; the conductivity of the latter is about seven orders of magnitude less than the former. This difference arises because TCNQF₄ is a much stronger acceptor than TCNQ and hence the charge transfer is complete in HMTTF-TCNQF₄.

6.8 Low-dimensional solids

Chemists are by and large preoccupied with three-dimensional structures and most of solid state chemistry deals with three-dimensional solids. However, there has been increasing interest in lower-dimensional solids which show spectacular anisotropy in their properties. One is familiar with graphite that is metallic in two dimensions and a semiconductor in the third dimension; the striking directional differences in the properties of mica(sheet) and asbestos (fibre) are common experience. The platinum chain compound KCP referred to earlier reflects visible light and conducts electricity like a metal only in the chain direction. If one looks at a crystal of KCP with a polaroid oriented so that the electric vector of the light is parallel to the chain axis, it is highly reflecting and copper-coloured; if the polaroid is turned through a right angle, it is pale yellow and transparent like any other ionic crystal. The situation is similar with Wolfram's red salt. Most of the synthetic metals or molecular metals are low-dimensional solids; many of the exotic materials being tried for superconductivity are also low-dimensional (Keller 1975, 1977; Miller & Epstein, 1978; Hatfield, 1978; Alacer, 1980; Miller, 1982).

It is convenient to classify low-dimensional solids into two categories, chain (essentially one-dimensional) and layer (essentially two-dimensional). Examples of the chain compounds are KCP and other Pt-chain compounds, polymeric (SN)_{*x*}, polyacetylene, Hg_{3-*x*}AsF₆ with Hg chains, [(CH₃)₄N]MnCl₃, KCuF₃ and RbFeCl₃. Examples of layer compounds are graphite-related systems, Ta and Nb chalcogenides, K₂NiF₄, (RNH₂)₂MCl₄ and CoCl₂ (R = CH₃ etc., M = Cr, Mn etc.). We shall briefly examine the magnetic, electrical and optical properties as well as phase transitions of typical members of this extraordinary class of materials. (Day, 1983; Subramanyam & Naik, 1985) also see Phil. Trans. Roy. Soc. London 1985, A314.

In understanding the magnetic behaviour of solids it is necessary to take into account not only the dimensionality of the lattice (1 to 3), but also the dimensionality of the spin or of the order parameter (1 to 3), which give rise to nine possible types of magnetic systems. In addition,

BRIEF ATTACHMENT BB

IN THE UNITED STATES PATENT AND TRADEMARK OFFICE

In re Patent Application of

Applicants: Bednorz et al.

Serial No.: 08/479,810

Filed: June 7, 1995

For: NEW SUPERCONDUCTIVE COMPOUNDS HAVING HIGH TRANSITION
TEMPERATURE, METHODS FOR THEIR USE AND PREPARATION

Date: March 1, 2004

Docket: YO987-074BZ

Group Art Unit: 1751

Examiner: M. Kopec

Commissioner for Patents
P.O. Box 1450
Alexandria, VA 22313-1450

FIFTH SUPPLEMENTAL AMENDMENT

Sir:

In response to the Office Action dated February 4, 2000:

ATTACHMENT 49

The following tables give properties of a number of high temperature superconductors. Table 1 lists the crystal structure (space group and lattice constants) and the critical transition temperature T_c for the more important high temperature superconductors so far studied. Table 2 gives energy gap, critical current density, and penetration depth in the superconducting state. Table 3 gives electrical and thermal properties of some of these materials in the normal state. The tables were prepared in November 1992 and updated in November 1994.

REFERENCES

1. Ginsburg, D.M., Ed., *Physical Properties of High-Temperature Superconductors*, Vols. I—III, World Scientific, Singapore, 1989—1992.
2. Rao, C.N.R., Ed., *Chemistry of High-Temperature Superconductors*, World Scientific, Singapore, 1991.
3. Shackelford, J.F., *The CRC Materials Science and Engineering Handbook*, CRC Press, Boca Raton, 1992, 98—99 and 122—123.
4. Kaldis, E., Ed., *Materials and Crystallographic Aspects of HT_c Superconductivity*, Kluwer Academic Publ., Dordrecht, The Netherlands, 1992.
5. Malik, S.K. and Shah, S.S., Ed., *Physical and Material Properties of High Temperature Superconductors*, Nova Science Publ., Commack, N.Y., 1994.
6. Chmaissem, O. et al., *Physica*, C230, 231—238, 1994.
7. Antipov, E.V. et al., *Physica*, C215, 1—10, 1993.

Table 1
Structural Parameters and Approximate T_c Values of High-Temperature Superconductors

Material	Structure	T_c /K (maximum value)
* 1 $\text{La}_2\text{CuO}_{4.8}$	Bmab; $a = 5.355$, $b = 5.401$, $c = 13.15$ Å	39
2 $\text{La}_{2-x}\text{Sr}_x(\text{Ba}_{1-x}\text{CuO}_4)$	I4/mmm; $a = 3.779$, $c = 13.23$ Å	35
3 $\text{La}_2\text{Ca}_{1-x}\text{Sr}_x\text{Cu}_2\text{O}_6$	I4/mmm; $a = 3.825$, $c = 19.42$ Å	60
4 $\text{YBa}_2\text{Cu}_3\text{O}_7$	Pmmm; $a = 3.821$, $b = 3.885$, $c = 11.676$ Å	93
5 $\text{YBa}_2\text{Cu}_4\text{O}_8$	Ammm; $a = 3.84$, $b = 3.87$, $c = 27.24$ Å	80
6 $\text{Y}_2\text{Ba}_4\text{Cu}_7\text{O}_{15}$	Ammm; $a = 3.851$, $b = 3.869$, $c = 50.29$ Å	93
* 7 $\text{Bi}_2\text{Sr}_2\text{CuO}_6$	Amaa; $a = 5.362$, $b = 5.374$, $c = 24.622$ Å	10
* 8 $\text{Bi}_2\text{CaSr}_2\text{Cu}_2\text{O}_8$	A ₂ aa; $a = 5.409$, $b = 5.420$, $c = 30.93$ Å	92
* 9 $\text{Bi}_2\text{Ca}_2\text{Sr}_2\text{Cu}_3\text{O}_{10}$	A ₂ aa; $a = 5.39$, $b = 5.40$, $c = 37$ Å	110
* 10 $\text{Bi}_2\text{Sr}_2(\text{La}_{1-x}\text{Ce}_x)_2\text{Cu}_2\text{O}_{10}$	P4/mmm; $a = 3.888$, $c = 17.28$ Å	25
* 11 $\text{Ti}_2\text{Ba}_2\text{CuO}_6$	A ₂ aa; $a = 5.468$, $b = 5.472$, $c = 23.238$ Å; I4/mmm; $a = 3.866$, $c = 23.239$ Å	92
* 12 $\text{Ti}_2\text{CaBa}_2\text{Cu}_2\text{O}_8$	I4/mmm; $a = 3.855$, $c = 29.318$ Å	119
* 13 $\text{Ti}_2\text{Ca}_2\text{Ba}_2\text{Cu}_3\text{O}_{10}$	I4/mmm; $a = 3.85$, $c = 35.9$ Å	128
14 $\text{Ti}(\text{BaLa})\text{CuO}_5$	P4/mmm; $a = 3.83$, $c = 9.55$ Å	40
15 $\text{Ti}(\text{SrLa})\text{CuO}_5$	P4/mmm; $a = 3.7$, $c = 9$ Å	40
* 16 $(\text{Ti}_{0.5}\text{Pb}_{0.5})\text{Sr}_2\text{CuO}_5$	P4/mmm; $a = 3.738$, $c = 9.01$ Å	40
* 17 $\text{TiCaBa}_2\text{Cu}_2\text{O}_7$	P4/mmm; $a = 3.856$, $c = 12.754$ Å	103
* 18 $(\text{Ti}_{0.5}\text{Pb}_{0.5})\text{CaSr}_2\text{Cu}_2\text{O}_7$	P4/mmm; $a = 3.80$, $c = 12.05$ Å	90
19 $\text{TiSr}_2\text{Y}_{0.5}\text{Ca}_{0.5}\text{Cu}_2\text{O}_7$	P4/mmm; $a = 3.80$, $c = 12.10$ Å	90
* 20 $\text{TiCa}_2\text{Ba}_2\text{Cu}_3\text{O}_8$	P4/mmm; $a = 3.853$, $c = 15.913$ Å	110
* 21 $(\text{Ti}_{0.5}\text{Pb}_{0.5})\text{Sr}_2\text{Ca}_2\text{Cu}_3\text{O}_9$	P4/mmm; $a = 3.81$, $c = 15.23$ Å	120
22 $\text{TiBa}_2(\text{La}_{1-x}\text{Ce}_x)_2\text{Cu}_2\text{O}_9$	I4/mmm; $a = 3.8$, $c = 29.5$ Å	40
23 $\text{Pb}_2\text{Sr}_2\text{La}_{0.5}\text{Ca}_{0.5}\text{Cu}_3\text{O}_8$	Cmmm; $a = 5.435$, $b = 5.463$, $c = 15.817$ Å	70
24 $\text{Pb}_2(\text{SrLa})_2\text{Cu}_2\text{O}_6$	P2 ₂ 2 ₁ ; $a = 5.333$, $b = 5.421$, $c = 12.609$ Å	32
25* $(\text{Pb,Cu})\text{Sr}_2(\text{La,Ca})\text{Cu}_2\text{O}_7$	P4/mmm; $a = 3.820$, $c = 11.826$ Å	50
26 $(\text{Pb,Cu})(\text{Sr,Eu})(\text{Eu,Ce})\text{Cu}_2\text{O}_x$	I4/mmm; $a = 3.837$, $c = 29.01$ Å	25
* 27 $\text{Nd}_{2-x}\text{Ce}_x\text{CuO}_4$	I4/mmm; $a = 3.95$, $c = 12.07$ Å	30
* 28 $\text{Ca}_{1-x}\text{Sr}_x\text{CuO}_2$	P4/mmm; $a = 3.902$, $c = 3.35$ Å	110
29 $\text{Sr}_{1-x}\text{Nd}_x\text{CuO}_2$	P4/mmm; $a = 3.942$, $c = 3.393$ Å	40
* 30 $\text{Ba}_{0.6}\text{K}_{0.4}\text{BiO}_3$	Pm3m; $a = 4.287$ Å	31
* 31 Rb_2CsCuO	$a = 14.493$ Å	31
32 $\text{NdBa}_2\text{Cu}_3\text{O}_7$	Pmmm; $a = 3.878$, $b = 3.913$, $c = 11.753$	58

HIGH TEMPERATURE SUPERCONDUCTORS (continued)

Table 1
Structural Parameters and Approximate T_c Values of High-Temperature Superconductors
(continued)

Material	Structure	T_c /K (maximum value)
33 SmBaSrCu ₃ O ₇	14/mmm; $a = 3.854$, $c = 11.62$	84
34 EuBaSrCu ₃ O ₇	14/mmm; $a = 3.845$, $c = 11.59$	88
35 GdBaSrCu ₃ O ₇	14/mmm; $a = 3.849$, $c = 11.53$	86
36 DyBaSrCu ₃ O ₇	Pmmm; $a = 3.802$, $b = 3.850$, $c = 11.56$	90
37 HoBaSrCu ₃ O ₇	Pmmm; $a = 3.794$, $b = 3.849$, $c = 11.55$	87
38 ErBaSrCu ₃ O ₇ (multiphase)	Pmmm; $a = 3.787$, $b = 3.846$, $c = 11.54$	82
39 TmBaSrCu ₃ O ₇ (multiphase)	Pmmm; $a = 3.784$, $b = 3.849$, $c = 11.55$	88
40 YBaSrCu ₃ O ₇	Pmmm; $a = 3.803$, $b = 3.842$, $c = 11.54$	84
* 41 HgBa ₂ CuO ₄	14/mmm; $a = 3.878$, $c = 9.507$	94
* 42 HgBa ₂ CaCu ₂ O ₆ (annealed in O ₂)	14/mmm; $a = 3.862$, $c = 12.705$	127
* 43 HgBa ₂ Ca ₂ Cu ₃ O ₈	Pmmm; $a = 3.85$, $c = 15.85$	133
* 44 HgBa ₂ Ca ₃ Cu ₄ O ₁₀	Pmmm; $a = 3.854$, $c = 19.008$	126

Table 2
Superconducting Properties

$J_c(0)$: Critical current density extrapolated to 0 K
 λ_{ab} : Penetration depth in a - b plane
 k_B : Boltzmann constant

Material	Form	Energy gap (Δ)		$10^{-4} \times J_c(0)/A \text{ cm}^{-2}$	λ_{ab}/λ
		$2\Delta_{pp}/k_B T_c^*$	$2\Delta_{fn}/k_B T_c^\dagger$		
YBa ₂ Cu ₃ O ₇	Single Crystal	5-6	4-5	30 (film)	1400
Bi ₂ Sr ₂ CaCu ₂ O ₈	Single Crystal	8-9	5.5-6.5	2	2700
Tl ₂ Ba ₂ CaCu ₂ O ₈	Ceramic	6-7	4-6	10 (film, 80 K)	2000
La _{2-x} Sr _x CuO ₄ , $x = 0.15$	Ceramic	7-9	4-6		
Nd _{2-x} Ce _x CuO ₄	Ceramic	8	4-5	0.2 (film)	

* Obtained from peak to peak value.

† Obtained from fit to BCS-type relation.

BRIEF ATTACHMENT BC

IN THE UNITED STATES PATENT AND TRADEMARK OFFICE

In re Patent Application of

Applicants: Bednorz et al.

Serial No.: 08/479,810

Filed: June 7, 1995

Date: March 1, 2004

Docket: YO987-074BZ

Group Art Unit: 1751

Examiner: M. Kopec

For: NEW SUPERCONDUCTIVE COMPOUNDS HAVING HIGH TRANSITION
TEMPERATURE, METHODS FOR THEIR USE AND PREPARATION

Commissioner for Patents
P.O. Box 1450
Alexandria, VA 22313-1450

FIFTH SUPPLEMENTAL AMENDMENT

Sir:

In response to the Office Action dated February 4, 2000:

ATTACHMENT 50

ERCONDUCTIVITY

Temperature

Temperature

Temperature

Superconductivity

Physics

conductors

Superconductivity

ima)

kshop on Towards the
factors

ity

opics — 1st Asia-Pacific

1 Superconductivity

Temperature

Superconductivity

PHYSICAL PROPERTIES OF HIGH TEMPERATURE SUPERCONDUCTORS I

Editor

Donald M. Ginsberg

Professor of Physics

University of Illinois at Urbana-Champaign



World Scientific

Singapore • New Jersey • London • Hong Kong

Published by

World Scientific Publishing Co. Pte. Ltd.
P O Box 128, Farrer Road, Singapore 9128

USA office: World Scientific Publishing Co., Inc.
687 Hartwell Street, Teaneck, NJ 07666, USA

UK office: World Scientific Publishing Co. Pte. Ltd.
73 Lynton Mead, Totteridge, London N20 8DH, England

537.623

Physic

1989

*This book is de
rised to the big*

PHYSICAL PROPERTIES OF HIGH TEMPERATURE SUPERCONDUCTORS I

Copyright © 1989 by World Scientific Publishing Co. Pte. Ltd.

All rights reserved. This book, or parts thereof, may not be reproduced in any form or by any means, electronic or mechanical, including photocopying, recording or any information storage and retrieval system now known or to be invented, without written permission from the Publisher.

ISBN 9971-50-683-1
9971-50-894-X (pbk)

Printed in Singapore by Utopia Press.

315

CONTENTS

Preface	vii
Chapter 1: Introduction, History, and Overview of High Temperature Superconductivity <i>D.M. Ginsberg</i>	1
Chapter 2: Thermodynamic Properties, Fluctuations, and Anisotropy of High Temperature Superconductors <i>M.B. Salamon</i>	39
Chapter 3: Macroscopic Magnetic Properties of High Temperature Superconductors <i>A.P. Malozemoff</i>	71
Chapter 4: Neutron Scattering Studies of Structural and Magnetic Excitations in Lamellar Copper Oxides — A Review <i>R.J. Birgeneau and G. Shirane</i>	151
Chapter 5: Normal State Transport and Elastic Properties of High T_c Materials and Related Compounds <i>P.B. Allen, Z. Fisk, and A. Migliori</i>	213
Chapter 6: Rare Earth and Other Substitutions in High Temperature Oxide Superconductors <i>J.T. Markert, Y. Dalichaouch, and M.B. Maple</i>	265
Chapter 7: Infrared Properties of High T_c Superconductors <i>T. Timusk and D.B. Tanner</i>	339
Chapter 8: Raman Scattering in High- T_c Superconductors <i>C. Thomsen and M. Cardona</i>	409
Subject Index	509

PHYSICAL PROPERTIES OF HIGH TEMPERATURE SUPERCONDUCTORS II

Editor

Donald M. Ginsberg

Department of Physics

University of Illinois at Urbana — Champaign



World Scientific

Singapore • New Jersey • London • Hong Kong

Published by

World Scientific Publishing Co. Pte. Ltd.

P O Box 128, Farrer Road, Singapore 9128

USA office: 687 Hartwell Street, Teaneck, NJ 07666

UK office: 73 Lynton Mead, Totteridge, London N20 8DH

*Thi.
John*

**PHYSICAL PROPERTIES OF HIGH TEMPERATURE
SUPERCONDUCTORS II**

Copyright © 1990 by World Scientific Publishing Co. Pte. Ltd.

All rights reserved. This book, or parts thereof, may not be reproduced in any form or by any means, electronic or mechanical, including photocopying, recording or any information storage and retrieval system now known or to be invented, without written permission from the Publisher.

ISBN 981-02-0124-9

981-02-0190-7 (pbk)

Printed in Singapore by JBW Printers & Binders Pte. Ltd.

CONTENTS

Preface	vii
Chapter 1. Introduction: A Description of Some New Materials and An Overview of This Book <i>D.M. Ginsberg</i>	1
Chapter 2. Specific Heat of High Temperature Superconductors: A Review <i>A. Junod</i>	13
Chapter 3. Crystal Structures of High-Temperature Superconductors <i>R.M. Hazen</i>	121
Chapter 4. The Microstructure of High-Temperature Oxide Superconductors <i>C.H. Chen</i>	199
Chapter 5. Nuclear Resonance Studies of $\text{YBa}_2\text{Cu}_3\text{O}_{7-\delta}$ <i>C.H. Pennington and C.P. Slichter</i>	269
Chapter 6. Electronic Structure, Surface Properties, and Interface Chemistry of High Temperature Superconductors <i>H.M. Meyer III and J. H. Weaver</i>	369
Chapter 7. The Hall Effect and its Relation to other Transport Phenomena in the Normal State of the High-Temperature Superconductors <i>N.P. Ong</i>	459
Chapter 8. Oxygen Stoichiometric Effects and Related Atomic Substitutions in the High- T_c Cuprates <i>L.H. Greene and B.G. Bagley</i>	509
Chapter 9. The Pairing State of $\text{YBa}_2\text{Cu}_3\text{O}_{7-\delta}$ <i>J.F. Annett, N. Goldenfeld and S.R. Renn</i>	571
Subject Index	687
Appendix A	697
Appendix B	699

BRIEF ATTACHMENT BD

IN THE UNITED STATES PATENT AND TRADEMARK OFFICE

In re Patent Application of

Applicants: Bednorz et al.

Serial No.: 08/479,810

Filed: June 7, 1995

Date: March 1, 2004

Docket: YO987-074BZ

Group Art Unit: 1751

Examiner: M. Kopec

For: NEW SUPERCONDUCTIVE COMPOUNDS HAVING HIGH TRANSITION
TEMPERATURE, METHODS FOR THEIR USE AND PREPARATION

Commissioner for Patents
P.O. Box 1450
Alexandria, VA 22313-1450

FIFTH SUPPLEMENTAL AMENDMENT

Sir:

In response to the Office Action dated February 4, 2000:

ATTACHMENT 51

BD

CHEMISTRY OF HIGH TEMPERATURE SUPERCONDUCTORS

Edited by

C. N. R. RAO, F. R. S.

*CSIR Centre of Excellence in Chemistry and
Solid State and Structural Chemistry Unit
Indian Institute of Science, Bangalore, India*



World Scientific

Singapore • New Jersey • London • Hong Kong

Published by

World Scientific Publishing Co. Pte. Ltd.

P O Box 128, Farrer Road, Singapore 9128

USA office: Suite 1B, 1060 Main Street, River Edge, NJ 07661

UK office: 73 Lynton Mead, Totteridge, London N20 8DH

Library of Congress Cataloging-In-Publication Data

Chemistry of high-temperature: superconductors/edited by C.N.R. Rao.

p. cm.

Includes bibliographical references.

ISBN 9810208057

1. High temperature superconductors. 2. Superconductivity-Chemistry. 3. Solid state chemistry. I. Rao, C. N. R.

(Chintamani Nagesa Ramachandra), 1934-

QC611.98.H54C47 1991

527.623--dc20

91-32649

CIP

Copyright © 1991 by World Scientific Publishing Co. Pte. Ltd.

All rights reserved. This book, or parts thereof, may not be reproduced in any form or by any means, electronic or mechanical, including photocopying, recording or any information storage and retrieval system now known or to be invented, without written permission from the Publisher.

Printed in Singapore by Utopia Press.

Library

University of Miami

PREFACE

Superconductivity has become one of the most active areas of research in physical sciences in the last few years, because of the advent of high temperature superconductivity in oxide materials, especially the cuprates. Since the initial discovery of 30 K superconductivity in the La-Ba-Cu system by Bednorz and Müller, a variety of materials with novel structural features have been synthesized and characterized. Several interesting relations between the structure and the properties of superconducting materials have been unravelled. While most cuprate superconductors contain holes as charge carriers, electron superconducting cuprates have also been discovered. There are also a few oxide superconductors which contain copper in them. In all these developments, chemists have made important contributions. In this volume an effort has been made to present the status of the chemistry of high-temperature oxide superconductors. It is possible that certain aspects such as crystal growth and measurement of single crystals have not been adequately covered in this volume. However, the various articles presented here should cover most of the salient features of high-temperature oxide superconductors with respect to their structure, and properties. Wherever possible preparative aspects are highlighted and two review articles deal with thin films besides one article on tapes. I believe that by going through the articles in this volume, one will be able to get a nearly complete picture of the present status of the physical aspects of high-temperature oxide superconductors, with a useful references to most of the recent literature. It is hoped that some of the topics mentioned in these articles would also stimulate further research.

High-temperature superconductivity itself is going through a rapid phase today. Newer materials are likely to be discovered in the near future. We already have the alkali metal doped buckminsterfullerene, C_{60} , with superconductivity around 40 K.

I do hope that the present volume will be found useful by students, teachers and practitioners.

C.N.R.
Bangalore
July

CONTENTS

Preface	v
Crystal Chemistry and Superconductivity in the Copper Oxides <i>J. B. Goodenough and A. Manthiram</i>	1
Defects and Microstructures in Layered Copper Oxides <i>M. Hervieu, B. Domengès, C. Michel, and B. Raveau</i>	57
Important Common Features of the Cuprate Superconductors: Relation Between the Electronic Structure and Superconductivity <i>C. N. R. Rao</i>	87
Design of New Cuprate Superconductors and Prediction of Their Structures <i>Takahisa Arima and Yoshinori Tokura</i>	104
Structure and Superconductivity in Y-123 and Related Compounds <i>G. V. Subba Rao and U. V. Varadaraju</i>	126
Chemistry of Superconducting Bismuth, Thallium and Lead Cuprates <i>J. Gopalakrishnan</i>	156
The Modulation in Bismuth Cuprates and Related Materials <i>J. W. Tarascon, W. R. McKinnon, and Y. LePage</i>	186
Electron-Doped High T_c Cuprate Superconductors <i>Carmen C. Almasan and M. Brian Maple</i>	205
Application of High-Pressure and High Oxygen Pressure to Cu-Oxides <i>M. Takano, Z. Hiroi, M. Azuma, and Y. Takeda</i>	243
Copper-Less Oxide Superconductors <i>A. M. Umarji</i>	267
Synthesis, Structure and Properties of $\text{La}_2\text{NiO}_{4+\delta}$ <i>Douglas J. Buttrey and Jurgen M. Honig</i>	283

Thermodynamics of Y-Ba-Cu-O System and Related Aspects	306
<i>S. F. Pashin and Yu. D. Tretyakov</i>	
Investigation of the Electronic Structure of the Cuprate Superconductors Using High-Energy Spectroscopies	348
<i>D. D. Sarma</i>	
Field Modulated Microwave Absorption in High-Temperature Superconducting Oxides	379
<i>Micky Puri and Larry Kevan</i>	
Grain Alignment and its Effect on Critical Current Properties of $\text{Bi}_2\text{Sr}_2\text{Ca}_1\text{Cu}_2\text{O}_x/\text{Ag}$ Superconducting Tape	399
<i>K. Togano, H. Kumakura, H. Maeda, and J. Kase</i>	
High T_c Superconducting Thin Films - Processing Methods and Properties	411
<i>S. Mohan</i>	
High Temperature Superconductor Thin Films by Pulsed Laser Ablation	454
<i>S. B. Ogale</i>	
Magnetic Properties and Field Modulated Microwave Absorption of $\text{YBa}_2\text{Cu}_3\text{O}_7$ Thin Films	484
<i>C. Schlenker, J. Dumas, C. L. Liu, and S. Revenaz</i>	

Published by

World Scientific Publishing Co. Pte. Ltd.

P O Box 128, Farrer Road, Singapore 9128

USA office: Suite 1B, 1060 Main Street, River Edge, NJ 07661

UK office: 73 Lynton Mead, Totteridge, London N20 8DH

Library of Congress Cataloging-in-Publication Data

Chemistry of high-temperature: superconductors/edited by C.N.R.
Rao.

p. cm.

Includes bibliographical references.

ISBN 9810208057

1. High temperature superconductors. 2. Superconductivity-
Chemistry. 3. Solid state chemistry. I. Rao, C. N. R.
(Chintamani Nagesa Ramachandra), 1934-

QC611.98.H54C47 1991

527.623-dc20

91-32649

CIP

Copyright © 1991 by World Scientific Publishing Co. Pte. Ltd.

All rights reserved. This book, or parts thereof, may not be reproduced in any form or by any means, electronic or mechanical, including photocopying, recording or any information storage and retrieval system now known or to be invented, without written permission from the Publisher.

Printed in Singapore by Utopia Press.

Library
University of Miami

Su
in pl
temp
Since
system
featu
tions
mater
holes
discov
copp
impor
the st
is pos
single
the v
high-t
struct
lighte
tapes
be ab
mical
refere
menti
Hig
phase
We al
super
I de
and p

BRIEF ATTACHMENT BE

IN THE UNITED STATES PATENT AND TRADEMARK OFFICE

In re Patent Application of

Applicants: Bednorz et al.

Serial No.: 08/479,810

Filed: June 7, 1995

For: NEW SUPERCONDUCTIVE COMPOUNDS HAVING HIGH TRANSITION
TEMPERATURE, METHODS FOR THEIR USE AND PREPARATION

Date: March 1, 2004

Docket: YO987-074BZ

Group Art Unit: 1751

Examiner: M. Kopec

Commissioner for Patents
P.O. Box 1450
Alexandria, VA 22313-1450

FIFTH SUPPLEMENTAL AMENDMENT

Sir:

In response to the Office Action dated February 4, 2000:

ATTACHMENT 52

BE

The CRC Materials Science and Engineering Handbook

Editor

James F. Shackelford

Professor of Materials Science and Engineering

Division of Materials Science and Engineering

and

Associate Dean of the College of Engineering

University of California, Davis

Associate Editor

William Alexander

Research Engineer

Division of Materials Science and Engineering

University of California, Davis



CRC Press

Boca Raton Ann Arbor London

Library of Congress Cataloging-in-Publication Data

Catalog record is available from the Library of Congress

ISBN 0-8493-4276-7

This book represents information obtained from authentic and highly regarded sources. Reprinted material is quoted with permission, and sources are indicated. A wide variety of references are listed. Every reasonable effort has been made to give reliable data and information, but the author and the publisher cannot assume responsibility for the validity of all materials or for the consequences of their use.

All rights reserved. This book, or any parts thereof, may not be reproduced in any form without written consent from the publisher.

Direct all inquiries to CRC Press, Inc., 2000 Corporate Blvd., N. W., Boca Raton, Florida, 33431.

© 1992 by CRC Press, Inc.

International Standard Book Number 0-8493-4276-7

Printed in the United States 0 1 2 3 4 5 6 7 8 9

TABLE OF CONTENTS

The Elements	1
Elements for Engineering Materials	2
Elements in the Earth's Crust	4
The Periodic Table of The Elements	6
The Metallic Elements	7
The Elements in Ceramic Materials	8
The Elements in Polymeric Materials	9
The Elements in Semiconducting Materials	10
Available Stable Isotopes of the Elements	12
Properties of Selected Elements	20
Melting Points of Selected Elements	26
Densities of Selected Elements	28
Crystal Structure of the Elements	30
Atomic and Ionic Radii of the Elements	34
Atomic Radii of the Elements	39
Ionic Radii of the Elements	41
Selected Properties of Superconductive Elements	43
T_c for Thin Films of Superconductive Elements	44
Engineering Compounds	47
Engineering Ceramics	48
Refractories, Ceramics, and Salts	53
Type II Superconducting Compounds:	
Critical Temperature and Crystal Structure Data	65
High Temperature Superconducting Compounds:	
Critical Temperature and Crystal Structure Data	98
Crystal Structure Types	101
Critical Temperature Data for	
Type II Superconducting Compounds	104
Selected Superconductive Compounds And Alloys:	
Critical Field Data	121
T_c Data for High Temperature Superconducting Compounds	122
Bonding, Thermodynamic, and Kinetic Data	125
Bond Strengths in Diatomic Molecules	
(Listed by Molecule)	126
(Listed by Bond Strength)	135
Bond Strengths of Polyatomic Molecules	
(Listed by Molecule)	144
(Listed by Bond Strength)	147

terial is quoted
has been made
e validity of all

n consent from

Table of Contents (Continued)

Carbon Bond Lengths (Periodic Table Presentation)	150
Carbon Bond Lengths	151
Bond Length Values Between Elements	
(Listed by Bond)	154
(Listed by Bond Length)	156
Bond Angle Values Between Elements	
(Listed by Bond)	158
(Listed by Bond Angle)	159
Heat of Formation of Selected Inorganic Oxides	160
Heats of Sublimation (at 25°C) of Selected Metals and their Oxides	173
Melting Points of Selected Elements and Inorganic Compounds	
(Listed by Element or Compound)	174
(Listed by Melting Point)	186
Melting Points of Ceramics	
(Listed by Compound)	198
(Listed by Melting Point)	202
Heat of Fusion For Selected Elements and Inorganic Compounds	206
Surface Tension of Liquid Elements	218
Vapor Pressure of the Elements	
(Very Low Pressures)	235
(Moderate Pressures)	237
(High Pressures)	240
Specific Heat of Selected Elements at 25 °C	
(Listed by Element)	243
(Listed by Specific Heat)	248
Heat Capacity of Selected Ceramics	253
Specific Heat of Selected Polymers	255
Phase Change Thermodynamic Properties	
for Selected Elements	260
for Selected Oxides	269
Thermodynamic Coefficients	
Description	281
for Selected Elements	283
for Selected Oxides	292
Thermal Conductivity of Metals	
at Cryogenic Temperatures	305
at 100 to 3000 K	321

Table of Contents (Continued)

Thermal Conductivity of Selected Ceramics	334
Thermal Conductivity of Special Concretes	345
Thermal Conductivity of Cryogenic Insulation and Supports	346
Thermal Conductivity of Selected Polymers	348
Thermal Expansion of Selected Tool Steels	355
Thermal Expansion and Thermal Conductivity of Selected Alloy Cast Irons	356
Thermal Expansion of Selected Ceramics	357
Thermal Expansion Coefficients for Materials used in Integrated Circuits	374
Thermal Expansion of Selected Polymers	376
Values of The Error Function	384
Diffusion in Selected Metallic Systems	385
Diffusivity Values of Metals into Metals	406
Diffusion in some Non-Metallic Systems	416
Diffusion in Semiconductors	417
Temper Designation System for Aluminum Alloys	424
Structure, Compositions, and Phase Diagram Sources	425
The Seven Crystal Systems	426
The Fourteen Bravais Lattices	427
Structure of Selected Ceramics	428
Density of Selected Tool Steels	434
Density of Selected Alloy Cast Irons	435
Density of Selected Ceramics	436
Specific Gravity of Selected Polymers	439
Composition Limits of Selected Tool Steels	450
Composition Limits of Selected Gray Cast Irons	459
Composition Limits of Selected Ductile Irons	464
Composition Ranges for Selected Malleable Irons	468
Composition Ranges for Selected Carbon Steels	470
Composition Ranges for Selected Resulfurized Carbon Steels	475
Composition Ranges for Selected Alloy Steels	478
Composition Ranges for Selected Cast Aluminum Alloys	498
Composition Ranges for Selected Wrought Aluminum Alloys	502
Typical Composition of Selected Glass-Ceramics	506
Phase Diagram Sources	510

Table of Contents (Continued)

Mechanical Properties	511
Mechanical Properties of Selected Tool Steels	512
Tool Steel Softening After 100 Hours for Various Temperatures	518
Mechanical Properties of Selected Gray Cast Irons	519
Mechanical Properties of Selected Ductile Irons	521
Average Mechanical Properties of Treated Ductile Irons	523
Mechanical Properties of Selected Malleable Iron Castings	525
Young's Modulus of Selected Ceramics	528
Modulus of Elasticity in Tension for Selected Polymers	534
Poisson's Ratio for Selected Ceramics	538
Yield Strength of Selected Cast Aluminum Alloys (Listed by Alloy)	541
(Listed by Yield Strength)	544
Yield Strength of Selected Wrought Aluminum Alloys (Listed by Alloy)	547
(Listed by Yield Strength)	555
Yield Strength of Selected Polymers	563
Tensile Strength of Selected Aluminum Casting Alloys (Listed by Alloy)	567
(Listed by Tensile Strength)	570
Tensile Strength of Selected Wrought Aluminum Alloys (Listed by Alloy)	573
(Listed by Tensile Strength)	581
Tensile Strength of Selected Ceramics	589
Tensile Strength of Selected Polymers	593
Total Elongation of Selected Cast Aluminum Alloys (Listed by Alloy)	601
(Listed by Total Elongation)	604
Total Elongation of Selected Polymers	607
Elongation at Yield of Selected Polymers	615
Shear Strength of Selected Wrought Aluminum Alloys (Listed by Alloy)	617
(Listed by Shear Strength)	624
Hardness of Selected Wrought Aluminum Alloys (Listed by Alloy)	631
(Listed by Hardness)	636
Hardness of Selected Ceramics	641
Hardness of Selected Polymers	647

El

Cl

Table of Contents (Continued)

Impact Strength of Selected Polymers	657
Compressive Yield Strength of Selected Polymers.....	666
Compressive Strength of Selected Polymers	669
Modulus of Elasticity in Flexure of Selected Polymers	674
Flexural Strength of Selected Polymers	683
Fatigue Strength of Selected Wrought Aluminum Alloys (Listed by Alloy)	691
(Listed by Fatigue Strength).....	695
Coefficient of Static Friction for Selected Polymers	699
Abrasion Resistance of Selected Polymers	701
Electrical, Magnetic, and Optical Properties	705
Electrical Resistivity of Selected Alloy Cast Irons	706
Resistivity of Selected Ceramics	707
Volume Resistivity of Selected Polymers	713
Dielectric Strength of Selected Polymers.....	722
Dielectric Constant of Selected Polymers	731
Dissipation Factor for Selected Polymers	740
Arc Resistance of Selected Polymers	751
Dispersion of Optical Materials at 298 K	757
Transmission Range of Glass Ceramics	766
Transparency of Selected Polymers	770
Refractive Index of Selected Polymers	776
Chemical Properties	781
Composition of Sea Water	782
Anions in Sea Water	783
Water Absorption of Selected Polymers	784
Flammability of Selected Polymers	793

BRIEF ATTACHMENT BF

IN THE UNITED STATES PATENT AND TRADEMARK OFFICE

In re Patent Application of

Applicants: Bednorz et al.

Serial No.: 08/479,810

Filed: June 7, 1995

For: NEW SUPERCONDUCTIVE COMPOUNDS HAVING HIGH TRANSITION
TEMPERATURE, METHODS FOR THEIR USE AND PREPARATION

Date: March 1, 2004

Docket: YO987-074BZ

Group Art Unit: 1751

Examiner: M. Kopec

Commissioner for Patents
P.O. Box 1450
Alexandria, VA 22313-1450

FIFTH SUPPLEMENTAL AMENDMENT

Sir:

In response to the Office Action dated February 4, 2000:

ATTACHMENT 53

BF

Materials and Crystallographic Aspects of HT_C-Superconductivity

edited by

E. Kaldis

Laboratorium für Festkörperphysik,
Eidgenössische Technische Hochschule Hönggerberg,
Zürich, Switzerland

*NATO Science Committee,
technological knowledge,
ties.*

s in conjunction with the

ng Corporation
v York

ic Publishers
on and London

rg, New York, London,

liographical references
tions from international

rs:

ESRIN,

retrieval software in
E Technologies Inc.

urd of Publishers or



Kluwer Academic Publishers

Dordrecht / Boston / London

Published in cooperation with NATO Scientific Affairs Division

Proceedings of the NATO Advanced Study Institute on
Materials and Crystallographic Aspects of HT_c-Superconductivity
Erice, Sicily, Italy
May 17-30, 1993

A C.I.P. Catalogue record for this book is available from the Library of Congress.

ISBN 0-7923-2773-X

Published by Kluwer Academic Publishers,
P.O. Box 17, 3300 AA Dordrecht, The Netherlands.

Kluwer Academic Publishers incorporates the publishing programmes of
D. Reidel, Martinus Nijhoff, Dr W. Junk and MTP Press.

Sold and distributed in the U.S.A. and Canada
by Kluwer Academic Publishers,
101 Philip Drive, Norwell, MA 02061, U.S.A.

In all other countries, sold and distributed
by Kluwer Academic Publishers Group,
P.O. Box 322, 3300 AH Dordrecht, The Netherlands.

Printed on acid-free paper

All Rights Reserved

© 1994 Kluwer Academic Publishers and copyright holders as specified on appropriate pages within

No part of the material protected by this copyright notice may be reproduced or utilized in any form or by any means, electronic or mechanical, including photocopying, recording or by any information storage and retrieval system, without written permission from the copyright owner.

Printed in the Netherlands

TABLE OF

Preface

Part I: Stru

M. Marezio
A classificat
between the

A.W. Hewat
Neutron pow
superconduct

T. Egami
Local structu
temperature s

D. Hohlwein
Superstructun

V.I. Simonov
Accurate X-ra
materials

C. Chaillout a
Structural and

John B. Good
Electron energ

John B. Good
The system La

John B. Good
The n-type cor

TABLE OF CONTENTS

Preface	ix
Part I: Structure and Structure-Properties Relationship	
<i>M. Marezio and C. Chaillout</i>	
A classification of the copper oxide superconductors and the relationship between the CU valence and the superconducting properties	3
<i>A.W. Hewat</i>	
Neutron powder diffraction on the ILL high flux reactor and high T_c superconductors	17
<i>T. Egami</i>	
Local structural distortion: implication to the mechanism of high temperature superconductivity	45
<i>D. Hohlwein</i>	
Superstructures in 123 compounds X-ray and neutron diffraction	65
<i>V.I. Simonov</i>	
Accurate X-ray structural investigations of single crystals of high- T_c materials	83
<i>C. Chaillout and M. Marezio</i>	
Structural and physical properties of superconducting $\text{La}_2\text{CuO}_{4.8}$	129
<i>John B. Goodenough</i>	
Electron energies in oxides	145
<i>John B. Goodenough</i>	
The system $\text{La}_{2-x}\text{Sr}_x\text{CuO}_4$	161
<i>John B. Goodenough</i>	
The n-type copper oxide superconductors	175

1 appro-

uced or
photo-
t written

<i>Shin-ichi Uchida</i> Charge dynamics in high T_c copper oxides	187	<i>J. Mannhart, J.</i> High- T_c thin fil
<i>Y. Maeno</i> Lattice instabilities and superconductivity in La-214 compounds	203	<i>J. Alarco, Yu. B.</i> <i>Z. Ivanov, V.K.</i> <i>J. Ramos, E. St</i> Engineered grain applications
Part II: Physics of HTSC		
<i>D. Brinkmann</i> Probing crystallographic and materials properties of Y-Ba-Cu-O superconductors by NMR and NQR	225	Part IV: Organ
<i>Z. Schlesinger, R.T. Collins, L.D. Rotter, F. Holtzberg, C. Feild,</i> <i>U. Welp, G.W. Crabtree, J.Z. Liu and Y. Fang</i> Infrared properties of selected high T_c superconductors	249	<i>J. Fink, P. Adeln</i> <i>M. Knupfer, M. A</i> <i>and E. Sohmen</i> High-energy spec superconductors
<i>H. Keller</i> Probing high-temperature superconductivity with positive muons	265	<i>G. van Tendeloo</i> Electron microscop materials and full
<i>T. Schneider</i> Extreme type II superconductors: Universal properties and trends	289	<i>Jack M. Williams,</i> <i>Urs Geiser, John</i> <i>Eugene L. Venturi</i> Structure-property and anion-based (c use in the design o
<i>G. Ruani</i> IR-excited Raman spectroscopy on HT $_c$ superconductors	311	Part V: Phase Dia
<i>I. Morgenstern, J.M. Singer, Th. Hußlein and H.-G. Matuttis</i> Numerical simulation of high temperature superconductors	331	<i>J. Karpinski, K. Co</i> <i>and E. Kaldis</i> Phase diagram, syn oxygen pressure Pc
<i>J. Röhrler</i> Evidence from EXAFS for an axial oxygen centered lattice instability in YBa $_2$ Cu $_3$ O $_{7.8}$?	353	<i>G.F. Voronin</i> Thermodynamic sta
<i>A.M. Hermann, M. Paranthaman and H.M. Duan</i> Single crystal growth and characterization of thallium cuprate superconductors - A review	373	
Part III: Flux Pinning, Pinning Centers, Applications		
<i>P.H. Kes</i> Flux pinning in high-temperature superconductors	401	
<i>M. Murakami</i> Flux pinning of high temperature superconductors and their applications	433	

187	<i>J. Mannhart, J.G. Bednorz, A. Catana, Ch. Gerber and D.G. Schlom</i> High-T _c thin films. Growth modes - structure - applications	453
203	<i>J. Alarco, Yu. Boikov, G. Brorsson, T. Claeson, G. Daalmans, J. Edstam, Z. Ivanov, V.K. Kaplunenko, P.-Å. Nilsson, E. Olsson, H.K. Olsson, J. Ramos, E. Stepantsov, A. Tzalenchuk, D. Winkler and Y.-M. Zhang</i> Engineered grain boundary junctions - characteristics, structure, applications	471
225	Part IV: Organic Superconductors	
249	<i>J. Fink, P. Adelman, M. Alexander, K.-P. Bohnen, M.S. Golden, M. Knupfer, M. Merkel, N. Nücker, E. Pellegrin, H. Romberg, M. Roth and E. Sohmen</i> High-energy spectroscopic studies of fullerene and cuprate superconductors	493
265	<i>G. van Tendeloo and S. Amelinckx</i> Electron microscopy and the structural studies of superconducting materials and fullerites	521
311	<i>Jack M. Williams, K. Douglas Carlson, Aravinda M. Kini, H. Hau Wang, Urs Geiser, John A. Schlueter, Arthur J. Schultz, James E. Schirber, Eugene L. Venturini, Donald L. Overmyer and Myung-Hwan Whangbo</i> Structure-property relationships in radical-cation (electron-donor molecule) and anion-based (including fullerides) organic superconductors and their use in the design of new materials	539
353	Part V: Phase Diagrams of HTSC	
373	<i>J. Karpinski, K. Conder, Ch. Krüger, H. Schwer I. Mangelschots, E. Jilek and E. Kaldis</i> Phase diagram, synthesis and crystal growth of YBaCuO phases at high oxygen pressure $P_{O_2} < 3000$ bar.	555
401	<i>G.F. Voronin</i> Thermodynamic stability of superconductors in the Y-Ba-Cu-O system	585
433		



BRIEF ATTACHMENT BG

IN THE UNITED STATES PATENT AND TRADEMARK OFFICE

In re Patent Application of

Applicants: Bednorz et al.

Serial No.: 08/479,810

Filed: June 7, 1995

Date: March 1, 2004

Docket: YO987-074BZ

Group Art Unit: 1751

Examiner: M. Kopec

For: NEW SUPERCONDUCTIVE COMPOUNDS HAVING HIGH TRANSITION
TEMPERATURE, METHODS FOR THEIR USE AND PREPARATION

Commissioner for Patents
P.O. Box 1450
Alexandria, VA 22313-1450

FIFTH SUPPLEMENTAL AMENDMENT

Sir:

In response to the Office Action dated February 4, 2000:

ATTACHMENT 54

**PHYSICAL AND MATERIAL
PROPERTIES OF
HIGH TEMPERATURE
SUPERCONDUCTORS**

**Edited by
S.K. Malik and S.S. Shah**

NOVA SCIENCE PUBLISHERS, INC.

Yonkers, NY

QC
611
-98
-H54 P48

Art Director: Christopher Concannon
Graphics: Elenor Kallberg and Maria Ester Hawrys
Book Production: Michael Lyons, Roseann Pena,
Casey Pfalzer, June Martino,
Tammy Sauter, and Michelle Lalo
Circulation: Irene Kwartiroff, Annette Hellinger,
and Benjamin Fung

Library of Congress Cataloging-in-Publication Data

Physical and material properties of high temperature
superconductors / edited by S.K. Malik and S.S. Shah.
p. cm.

Includes bibliographical references and index.
ISBN 1-56072-114-6 : \$145.00

1. High temperature superconductors. 2. High
temperature superconductivity. I. Malik, S.K. II. Shah, S.S.
QC611.98.H54P48 1993 93-8788
537.623-dc20 CIP

© 1994 Nova Science Publishers, Inc.
6080 Jericho Turnpike, Suite 207
Commack, New York 11725
Tele. 516-499-3103 Fax 516-499-3146
E Mail Novasci1@aol.com

All rights reserved. No part of this book may be reproduced,
stored in a retrieval system or transmitted in any form or by any
means: electronic, electrostatic, magnetic, tape, mechanical,
photocopying, recording or otherwise without permission from
the publishers.

Printed in the United States of America

LIBRARY
University Of Miami

Contents

Preface	xi
Chemistry and Superconductivity of $(\text{TLA})(\text{Ba}, \text{Sr}, \text{Ln})_2(\text{Cu}, \text{MO})_{5\pm\delta}$ 1201 Thallium Cuprates <i>M. Greenblatt and M.-H. Pan</i>	1
Phase Formation and Superconducting Properties of $\text{LnBaSrCu}_3\text{O}_7$ Compounds <i>V. Badri, U.V. Varadaraju, and G.V. Subba Rao</i>	35
Structure and Properties of Electron Superconductors <i>G. Balakrishnan</i>	49
The Influence of Pr and Cm on the Superconducting Properties of High- T_c Oxides <i>L. Soderholm and C.W. Williams</i>	59
Synthesis, Crystal Structure and Physical Properties of the $\text{Pb}_2\text{Sr}_2\text{RCu}_3\text{O}_{8+\delta}$ System <i>J.S. Xue, M. Reedyk and J.E. Greedan</i>	77
Current Directions in the Architecture of High- T_c Superconducting Oxides — A Review <i>Y.V. Yakimi and R.M. Iyer</i>	121
Characterization of Superconducting Fullerenes <i>J.D. Thompson, G. Sparr, K. Holczer, O. Klein, G. Gruner, R.B. Kaner, F. Diederich, and R.L. Whetten</i>	139
Transport Properties in Y-Doped Bi- and Tl-Based Superconductors <i>B. Ghosh, A. Poddar, P. Mandal, A.N. Das, and P. Choudhury</i>	149
On the Magnitude of Resistivity in High-Temperature Cuprate Superconductors <i>P. Ganguly</i>	163
Chemical Doping and Charge Balance in High Temperature Superconductors <i>E.E. Alp and S.M. Mini</i>	181

Hidden Aspects of the Valence and Superconductivity
X.Oudet

Valence Fluctuation in Metallic and Superconducting Oxides
M.S. Hegde

Magnetic Ordering in Oxide Superconductors
J.W. Lynn

Rare Earth Magnetism and Superconductivity in $\text{Pr}_{2-x}\text{Ce}_x\text{CuO}_4$ and $\text{Y}_{1-x}\text{Pr}_x\text{Ba}_2\text{Cu}_3\text{O}_7$: A Neutron Scattering Study
C.-K. Loong and L. Soderholm

Magnetism, Superconductivity and Upper Critical Fields in $\text{R}_{1-x}\text{Pr}_x\text{Ba}_2\text{Cu}_3\text{O}_{7-\delta}$ (R = Rare Earth) Compounds
S.K. Malik and C.V. Tomy

Low Temperature Specific Heat and AC-Susceptibility of $\text{REBa}_2\text{Cu}_3\text{O}_{7-\delta}$ (RE = Y, Nd, Eu, Gd, Dy, Ho, Er, Tm and Yb)
H. Kierspel, F. Oster, H. Drössler, U. Callies, H. General, H. Geus, G. Jackel, H.D. Jostarndt, J. Langen, A. Waldorf, R. Müller, W. Schlabit, and D. Wohlleben

Fluctuation Diamagnetic Susceptibility in High Temperature Superconductors
R. Srinivasan

Flux-Lattice Melting in High-Temperature Superconductors
K.N. Shrivastava

Reversible Magnetization of Copper Oxide Superconductors in the Mixed State
U. Welp, S. Fleshler, W.K. Kwok, R.A. Klemm, V.M. Vinokur, J. Downey, and G.W. Crabtree

Vibrating Reed Studies of Flux Line Dynamics in Superconductors
Lance E. De Long, Zhigang Xu, Ji-Chang Hou and Joseph Brill

Diffraction from the Flux-Line Lattice in High Temperature Superconductors
D. McKenzie Paul and T. Forgan

Measurements on
Line in Type I

R. Kumar, S.

Quantized Lorentz

Resonance in H

K.N. Shrivastava

Crystal Growth and

S.C. Gadkari, M.

the Department

Magnetic Properties

Ming Xu

Recent Theories of F

K.P. Sinha

Critical Current in H

P. Bhattachary

Critical State Model

Demagnetization

P.N. Chaddah and

High- T_c Josephson Ju

A.K. Gupta

Structural, Morpholo

Films of High- T_c

Laser Ablation

S.B. Ogale, S.M.

K.R. Viswanathan,

at Institute of

In-Situ Growth of Su

R. Pinto

Preparation and Cha

A.M. D.K. Aswal, M.F.

S.K. Gupta, and

ides	2	Measurements on Inhomogeneous Magnetic States and Irreversibility Line in Type-I and Type-II Superconductors <i>R. Kumar, S. Ramakrishnan, and A.K. Grover</i>	421
	2	Quantized Lorentz Force, Microwave Absorption and Magnetic Resonance in High Temperature Superconductors <i>K.N. Shrivastava</i>	445
$x\text{CuO}_4$ and	2	Crystal Growth and Characterization of Oxide Superconductors <i>S.C. Gadkari, M.K. Gupta, and S.C. Sabharwal</i>	477
in	2	Magnetic Properties in $\text{Bi}_2\text{Sr}_2\text{CaCu}_2\text{O}_x$ Single Crystals <i>Ming Xu</i>	497
	2	Recent Theories of High T_c Superconductivity <i>K.P. Sinha</i>	529
nd Yb)	30	Critical Current in High Temperature Superconductors <i>P. Bhattacharyya</i>	541
teral,		Critical State Model for Samples with Non-Zero Demagnetization Factor <i>P. Chaddah and K.V. Bhagwat</i>	557
orf,	32	High- T_c Josephson Junctions—A Review <i>A.K. Gupta</i>	571
s	34	Structural, Morphological and Superconducting Properties of the Thin Films of High- T_c Oxide Superconductors Deposited by Pulsed Laser Ablation <i>S.B. Ogale, S.M. Kanetkar, R.D. Vispute, R. Viswanathan, and S.T. Bendre</i>	591
s in the		In-Situ Growth of Superconducting $\text{YBa}_2\text{Cu}_3\text{O}_{7-\delta}$ Thin Films <i>R. Pinto</i>	629
Vinokur,	38	Preparation and Characterization of $\text{YBa}_2\text{Cu}_3\text{O}_{7-\delta}$ Thick Films <i>D.K. Aswal, M.K. Gupta, A.K. Debnath, S.K. Gupta, and S.C. Sabharwal</i>	649
uctors			
i Brill			

Containerless Melt Processing of $\text{REBa}_2\text{Cu}_3\text{O}_{7-x}$ (RE = Y, Gd, Nd)
High Temperature Superconductors

R.W. McCallum, M.J. Kramer, T.J. Folkerts, S.R. Arrasmith,
B.D. Merkle, S.I. Yoo, Youwen Xu and K.W. Dennis

Fabrication of High T_c Oxide Superconductors

R. Prasad, N.C. Soni, K. Adhikary, and S.K. Malik

Influence of Zn, Ni and Co Substitution on Flux-Pinning and Critical
Current in $\text{YBa}_2\text{Cu}_3\text{O}_{7-\delta}$

R.G. Kulkarni

Magnetic Resonance Imaging (MRI)—A Programme in Superconductivity

R.S. Chaughule

Subject Index

The idea of a
Temperature Sup
during February
ment of Physics,
by the Departme
Institute of Fund
Aurangabad, and Inc

It was decide
in the form of a
Workshop many t
was, therefore, felt
should invite articl
are very happy to

We are indebt
and made it self-su
Science and Techno
al Research, Mara
Colleges and Indus

S.K. Malik
Tata Institute of F
Bombay 400 005, I

S.S. Shah
Marathwada Unive
Aurangabad 431 0

BRIEF ATTACHMENT BH

IN THE UNITED STATES PATENT AND TRADEMARK OFFICE

In re Patent Application of

Applicants: Bednorz et al.

Serial No.: 08/479,810

Filed: June 7, 1995

Date: March 1, 2004

Docket: YO987-074BZ

Group Art Unit: 1751

Examiner: M. Kopec

For: **NEW SUPERCONDUCTIVE COMPOUNDS HAVING HIGH TRANSITION
TEMPERATURE, METHODS FOR THEIR USE AND PREPARATION**

Commissioner for Patents
P.O. Box 1450
Alexandria, VA 22313-1450

FIFTH SUPPLEMENTAL AMENDMENT

Sir:

In response to the Office Action dated February 4, 2000:

ATTACHMENT 55



ELSEVIER

Physica C 230 (1994) 231-238

PHYSICA C

Synthesis and characterization of $\text{HgBa}_2\text{Ca}_{n-1}\text{Cu}_n\text{O}_{2n+2+\delta}$ ($n=1, 2$, and 3)

O. Chmaissem, L. Wessels, Z.Z. Sheng *

Department of Physics, and High Density Electronics Center, University of Arkansas, Fayetteville, AR 72701, USA

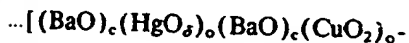
Received 17 May 1994; revised manuscript received 20 June 1994

Abstract

We have successfully prepared the first three members of the mercury-based superconducting compounds $\text{HgBa}_2\text{Ca}_{n-1}\text{Cu}_n\text{O}_{2n+2+\delta}$, namely Hg-1201, Hg-1212 and Hg-1223 with high purity and very good quality. The influence of the synthesis parameters is studied in detail. Using the sealed quartz tube method, very simple procedures are found to ensure a 100% reproducibility of nearly 100% pure Hg-1201 and 85-90% Hg-1212 and Hg-1223. Oxygen annealing of the sample Hg-1201 at 300°C for 18 h results in an enhancement of its critical temperature up to 97 K. The symmetry of the first and second members is tetragonal with lattice parameters $a=3.8831(1)$ Å, $c=9.5357(2)$ Å, and $a=3.8624(1)$ Å, $c=12.7045(2)$ Å, respectively. X-ray diffraction lines of Hg-1223 can be indexed in a tetragonal cell with $a=3.8564(1)$ Å and $c=15.8564(9)$ Å as well as in an orthorhombic cell with lattice parameters $a=5.4537(1)$ Å, $b=5.4247(1)$ Å, and $c=15.8505(7)$ Å.

1. Introduction

Following the discovery of superconductivity with $T_c=94$ K in the one-layer $\text{HgBa}_2\text{CuO}_{4+\delta}$ compound [1], a variety of new mercury cuprates have been synthesized [2-10]. $\text{HgBa}_2\text{CuO}_{4+\delta}$ (Hg-1201) is the first member of the homologous series $\text{HgBa}_2\text{Ca}_{n-1}\text{Cu}_n\text{O}_{2n+2+\delta}$. The $T_{c\text{onset}}$ of the first, second and third members are 94 K, 127 K and 134 K, respectively. $\text{HgBa}_2\text{Ca}_{n-1}\text{Cu}_n\text{O}_{2n+2+\delta}$ are isostructural to the Tl based superconductors $\text{TlBa}_2\text{Ca}_{n-1}\text{Cu}_n\text{O}_{2n+3}$ [11,12] but unlike the thallium compounds the mercury layers are heavily oxygen deficient. The structure of the Hg based superconductors $\text{HgBa}_2\text{Ca}_{n-1}\text{Cu}_n\text{O}_{2n+2+\delta}$ can be described as a sequence of layers:



in which blocks $(\text{BaO})_c(\text{HgO}_\delta)_o(\text{BaO})_c$ having the rock-salt structure and a thickness of about 5.5 Å alternate with blocks $(\text{CuO}_2)_o\{((n-1)(\text{Ca})_c(\text{CuO}_2)_o)\}$ having a perovskite-like structure and an approximate thickness $[4.00 + (n-1) \times 3.16]$ Å. The subscripts o and c indicate if the cation is at the origin or at the center of the mesh in each layer. All Hg-1201 [13,14], Hg-1212 [3] and Hg-1223 [15] are found to crystallize with symmetry of space group $P4/mmm$. An orthorhombic symmetry was also proposed by Meng et al. [16] for Hg-1223.

The research conducted on the thallium-based compounds showed that these materials offer a wide variety of possible substitutions on the different sites of their structures. Many compounds were prepared having their T_c above 100 K. As we mentioned above many new mercury-related compounds were already successfully synthesized with T_c around 100 K. Fur-

* Corresponding author.

thermore, Chu et al. [17] found that under very high pressures of about 150 kbar, the third member Hg-1223 becomes superconducting at 153 K. This result was confirmed by Nunez Regueiro et al. [18] who showed that their Hg-1223 samples if pressed to 235 kbar have a T_c as high as 157 K. As these results have no practical value because of the enormous pressure required, one may speculate that substituting some elements by smaller ions could imitate the effect of the high pressures and increase T_c to much higher values. The search for such new elements of substitution requires a well-controlled synthesis technique.

The synthesis of the Hg-Ba-Ca-Cu-O superconducting compounds of high purity remained a serious challenge until this date. One of the reasons for the fact that the preparation of these materials is so delicate is the decomposition of the mercury oxide HgO at low temperature (between 500 and 600°C), and by consequence, the formation of the superconducting phases is due to the reaction between vapor and solid. Two major methods were used:

- (1) the high-pressure methods in which the decomposition of HgO is slow, and
- (2) the sealed quartz tube methods.

Several groups reported their success in preparing samples of good quality using the sealed quartz tube method. Using this method, many classical synthesis routes were employed. Meng et al. [16] reported the synthesis of the mercury compounds ($n=2$ and 3) using an original method in which the Hg vapor is controlled by the insertion of precursor pellets in the sealed quartz tube together with pellets of nominal composition $\text{HgBa}_2\text{Ca}_{n-1}\text{Cu}_n\text{O}_x$. However, the synthesis of the mercury compounds has proved to be very delicate and requires good control of all the different preparation procedures such as starting materials, heating temperature, heating time, etc. The aim of our work was to study the influence of all these parameters and to find a more convenient method which guarantees to us the high reproducibility of the desired superconducting phases with high purity. We report herein the optimization of the synthesis of samples of good quality and 100% reproducibility using the sealed quartz tube method.

2. Experimental

Several methods were tried before we finally succeeded in synthesizing samples of high purity and 100% reproducibility. Attempts were first made to prepare superconducting samples using the single-step method (mixing the high-purity oxides all together and heating between 750°C and 850°C. The other preparations were all based on the two-step method in which we first prepared precursors of $\text{Ba}_2\text{Ca}_{n-1}\text{Cu}_n\text{O}_x$. The best precursors were those obtained by mixing $\text{Ba}(\text{NO}_3)_2$, CaO and CuO in appropriate amounts corresponding to the stoichiometric formula [19]. The mixture is placed in an alumina crucible and introduced into a preheated furnace at 650°C for 1–2 h, the temperature is then increased to 750°C and maintained for 1–2 h before the temperature is increased to 800–930°C. The sample is heated at this temperature for 16–18 h before being cooled down to room temperature by turning the furnace off. All of the heating cycle is done under a flowing gas of oxygen. The resulting materials are immediately transferred to a dry box. Some of the precursors are pelletized and the remaining powder is mixed with HgO in a molar ratio of 1:1 and then pelletized. Pellets of $\text{Ba}_2\text{Ca}_{n-1}\text{Cu}_n\text{O}_x$ (P) and of $\text{HgBa}_2\text{Ca}_{n-1}\text{Cu}_n\text{O}_{2n+2+\delta}$ (non-reacted HBCCO) (total weight about 1.8 g) were sealed together in a vacuum quartz tube (0.6 cm inner diameter, 1.0 cm outer diameter, and 8–9 cm long) which was in turn placed in a steel container as a safety precaution against possible explosion and then slowly heated (1–3.5°C/min) to 800–950°C. The temperature was maintained for 3 to 10 h before cooling slowly (1–3.5°C/min.) to 20–600°C. The furnace was then turned off.

The as-prepared samples were subjected to a heating treatment in a flowing gas of oxygen: the samples were introduced into a preheated furnace at 300°C and heated for a period of 18 h. The samples were then pulled out and quenched to room temperature in a dry box.

The samples were characterized using the X-ray diffraction technique, the AC magnetic susceptibility and the resistivity measurements. X-ray experiments were performed on a "Philips 1830" diffractometer with Cu K α radiation and showed that the superconducting phases were the majority phases in all the

samples prepared under the conditions described above together with some impurity phases which may be estimated to be in the order of 5–20%. These impurity phases are mainly CaHgO_2 and CaO . The AC magnetic susceptibility measurements showed that the samples prepared at temperatures above 900°C and the samples heated for more than 10 h were not superconducting. These experiments also showed sharp transitions from the normal state to the superconducting state with ΔT_c in the order of 5 K.

3. Results

3.1. Hg-1201

As the first member of the homologous series $\text{HgBa}_2\text{Ca}_{n-1}\text{Cu}_n\text{O}_{2n+2+\delta}$, Hg-1201 does not contain calcium; its synthesis can be done very easily using our procedures with very good quality and a sharp superconducting transition. The precursor was first heated at 750°C (1–2 h) and after the total decomposition of the barium nitrate the temperature was raised to 900°C for 20 h before being pulled out and quenched to room temperature in the dry box. Slow cooling in the furnace gave the same good quality of precursors. The resulting precursor was partially melted and very well crystallized. An appropriate amount of HgO was added to the precursor and pelletized. Pellets of both precursor (P) and non-reacted mixture of HgO +precursor (HBCCO) were sealed together at a weight ratio (P/HBCCO) of 0.48 and slowly heated ($3^\circ\text{C}/\text{min}$) to 810°C maintained for 6 h, and then slowly cooled ($3.5^\circ\text{C}/\text{min}$) to 575°C . The power was then shut off and the furnace was naturally cooled to room temperature.

X-ray diffraction pattern of a Hg-1201 sample prepared under these conditions is presented in Fig. 1 and shows that Hg-1201 is the majority phase ($>95\%$) and that the compound is nearly single phased. The structure is tetragonal with the space group $P4/\text{mmm}$, and there is no evidence of any kind of special extinction. The refined cell parameters of the as-synthesized sample are: $a=3.8831(1) \text{ \AA}$ and $c=9.5357(2) \text{ \AA}$.

AC magnetic susceptibility and resistivity measurements (Fig. 2) performed on Hg-1201 samples show a sharp superconducting transition and a zero

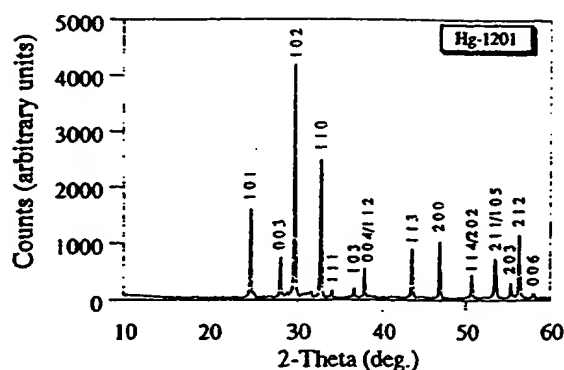


Fig. 1. X-ray diffraction pattern of an as-prepared Hg-1201 sample. The lines are indexed in a tetragonal cell with lattice constants $a=3.8831(1) \text{ \AA}$ and $c=9.5357(2) \text{ \AA}$.

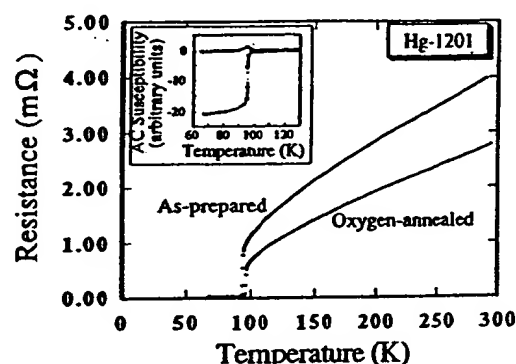


Fig. 2. Resistivity measurements carried out on a Hg-1201 sample. A sharp drop of the resistivity is observed at 94 K in the as-synthesized sample, it increases up to 97 K in the oxygen-annealed sample (300°C , 18 h). AC magnetic measurements (real and imaginary parts) are shown in the inset.

resistance at 94 K. Annealing the sample in O_2 at 300°C for 18 h results in an increase of its critical temperature up to 97 K. The curves presented in Fig. 2 show the resistivity measurements of the as-prepared and the oxygen-annealed sample. The oxygen-annealed samples were checked by X-ray diffraction and found to be remaining intact with no sign of any apparent change in the structure.

3.2. Hg-1212

With the introduction of the calcium into the structure, the synthesis procedures become more del-

icate and special care should be taken in the different stages of the preparation.

Some groups have reported the successful synthesis of Hg-1212 and Hg-1223 using the single-step method [20-24]. However, their procedures included the preparation of fresh oxides of BaO and CaO and the isolation of the sample from the quartz walls by wrapping the materials with a gold or silver foil [21-23] or even by using alumina tubes to be inserted in the quartz tubes [24]. Our experiments using this method were not successful probably because the samples were introduced in the quartz tubes without wrapping. Unlike the preparations based on the two-step method, the samples are rudely reacted with the quartz even at temperature as low as 750°C and the resulting materials were multi-colored powders with no sign of any homogeneity and particularly no superconductivity.

Our Hg-1212 samples were prepared by repeating the same procedures employed for the synthesis of Hg-1201. The purity of the samples was estimated by both the X-ray diffraction patterns and the AC magnetic-susceptibility measurements. We found that samples prepared at temperatures between 825°C and 860°C contain not more than 65% of the superconducting phase Hg-1212. Table 1 shows the dependence of the Hg-1212 volume percentage on the preparation conditions. The best samples were obtained by heating at relatively low temperature 790°C for 10 h. X-ray diffraction pattern and the superconducting properties are shown in Figs. 3 and 4, respectively. Hg-1212 is also tetragonal with lattice param-

eters $a=3.8624(1)$ Å and $c=12.7045(2)$ Å. The $T_{\text{c onset}}$ of the as-prepared samples is between 110 K and 120 K. Samples annealed in O₂ at 300°C for 18 h have their $T_{\text{c zero R}}$ increased up to 127 K.

3.3. Hg-1223

Ba₂Ca₂Cu₃O₇ precursors were prepared by heating the starting materials at 935°C for 7 h. Details are in the experimental section. The first preparations based on these precursors were partially successful as we were able to obtain a superconducting volume in the order of 60%. However, the superconducting phase was Hg-1212 rather than Hg-1223 (according to the X-ray diffraction patterns). Table 2 shows two sets of experiments with detailed synthesis conditions of Hg-1212 from nominal 1223 composition. The upper part of the table concerns the preparations in which the weight ratio P/HBCCO=0. The introduced pellets were only those with the nominal composition Hg_xBa₂Ca₂Cu₃O₇, assuming that the prepared precursors had their initial composition. The mercury oxide was added in excess to the stoichiometric formula in order to compensate the loss resulting from its reaction with the quartz tube. In the lower part of the table are presented the experiments of the Hg controlled vapor by using the method described in the experimental section with the weight ratio P/HBCCO>0. In these preparations the estimated superconducting volume (Hg-1212) is ranging between 0 and 60%. These estimations are based on the X-ray diffraction patterns which also showed

Table 1
Selected experiments carried out for the preparation of Hg-1212. The nominal composition of the precursors used in these experiments is Ba₂CaCu₂O₃. Column 2 gives the weight ratio Precursor/HgBa₂CaCu₂O₇

Name	Weight ratio	Heating rate (°C/min)	Cooling rate (°C/min)	Temp. (°C)	Time (h)	Hg-1212 vol. (%)
ch26	0.386	3	2→565°C	825	6	65
ch27	0.412	3	2→565°C	845	8	65
ch28	0.388	2.5	1→515°C	860	5	25
ch30	0.257	3	2→515°C	835	6	65
ch31	0.184	3	2→515°C	835	6	65
ch32	0.314	3	2→515°C	835	6	65
ch33	0.398	2	1→565°C	835	6	55
ch34	0.325	2	1→565°C	835	6	50
ch35	0.410	3	2→565°C	790	10	85
ch36	0.210	3	2→565°C	790	10	25

2) Å. The
veen 110 K
0°C for 18

1 by heating
etails are in
itions based
ssful as we
lume in the
cting phase
rding to the
ws two sets
onditions of
on. The up-
arations in
The intro-
minal com-
at the pre-
osition. The
he stoichio-
the loss re-
tube. In the
xperiments
method de-
the weight
ons the esti-
12) is rang-
ns are based
also showed

se experiments

1212
(%)

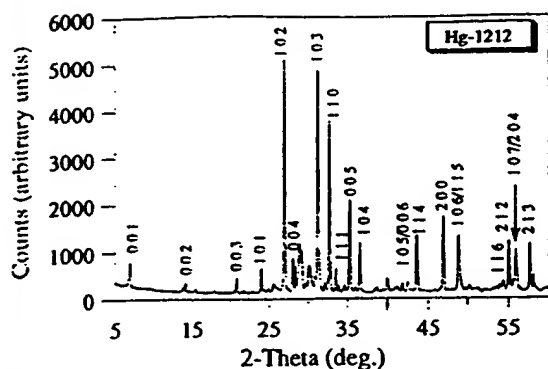


Fig. 3. X-ray diffraction pattern of an as-prepared Hg-1212 sample. The diffraction lines are indexed in a tetragonal cell with the lattice parameters $a=3.8624(1)$ Å and $c=12.7045(2)$ Å.

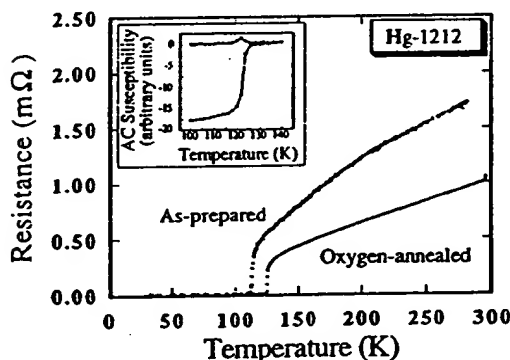


Fig. 4. Resistivity measurements of a sample Hg-1212. The figure shows clearly the increase of the $T_{c\text{onset}}$ from 117 K (as-synthesized sample) to 127 K (oxygen-annealed sample). The inset shows the AC magnetic measurements (real and imaginary parts) performed on an oxygen-annealed sample.

that the impurity phases are CaHgO_2 and CaO , with traces of a weak unknown phase. It is clear from the table that the formation of the superconducting phase is favored by the presence of the precursor pellets. The highest superconducting volume is obtained when heating to temperatures close to 850°C . At 870°C the sample (ch11) is still superconducting but with a decreased volume down to 40% and the sample is partially melted, indicating that preparations above this temperature could not be carried out successfully.

This work was carried out simultaneously with attempts to synthesize the fourth member of the mercury-based series, namely Hg-1234. The first results showed that the superconducting phase obtained with precursors assumed to be $\text{Ba}_2\text{Ca}_3\text{Cu}_4\text{O}_9$ (234) was

Hg-1223. By consequence, we started a new series of experiments based on the 234 precursors for the synthesis of Hg-1223.

Nominal $\text{Hg}_x\text{Ba}_2\text{Ca}_3\text{Cu}_4\text{O}_9$ pellets and $\text{Ba}_2\text{Ca}_3\text{Cu}_4\text{O}_9$ pellets were sealed together and treated as described in Table 3. Very good Hg-1223 samples with a volume $\approx 90\%$ were obtained with temperatures between 870°C and 885°C . The samples prepared at 900°C were partially melted and presented only 30 to 40% superconducting volume (samples ch2 and ch5), a longer reaction time at this temperature results in the destruction of the superconducting phase (sample ch19). The reproducibility of the Hg-1223 phase using these procedures is 100%. Using precursors obtained from different batches and following the same conditions given in Table 3 gave 90% Hg-1223 at each time. Together with the superconducting pellets were found drops of mercury inside the closed quartz tube.

X-ray diffraction pattern is given in Fig. 5 which shows the good quality of our Hg-1223 sample. Based on the tetragonal symmetry [4,15] of space group $P4/mmm$, the refined lattice parameters were found to be $a=3.8564(1)$ Å and $c=15.8564(9)$ Å. During indexing the diffraction pattern we found that many peaks were doubled and cannot all be indexed in the tetragonal symmetry, indicating that the symmetry might be orthorhombic. Refinements in an orthorhombic cell were equally successful and the doubled strong lines were all indexed in a unit cell of lattice parameters $a=5.4537(1)$ Å, $b=5.4247(1)$ Å and $c=15.8505(7)$ Å.

The AC magnetic susceptibility and the resistivity measurements for a Hg-1223 phasic sample are given in Fig. 6. The $T_{c\text{onset}}$ is around 105 K for the as-prepared samples. A $T_{c\text{onset}}$ of 135 K can be easily obtained by following the same annealing treatment performed on Hg-1201 and Hg-1212 (O_2 , 300°C , 18 h). The resistivity measurement shows a sharp transition at 135 K and a zero resistance is achieved around 134 K.

4. Discussion

As we stated above, the preparation of Hg-1201, Hg-1212, and Hg-1223 was carried out using the sealed quartz tube method. The insertion of

Table 2

Selected preparation conditions of samples in the phase-formation experiments. The resultant superconducting phase is Hg-1212, and the nominal composition of the precursors is $\text{Ba}_2\text{Ca}_x\text{Cu}_3\text{O}_7$. Column 2 gives the weight ratio Precursor/ $\text{Hg}_x\text{Ba}_2\text{Ca}_x\text{Cu}_3\text{O}_7$, where $x=1$ for the preparation marked with an asterisk and $x=1.5$ for all the other preparations

Name	Weight ratio	Heating rate ($^{\circ}\text{C}/\text{min}$)	Cooling rate ($^{\circ}\text{C}/\text{min}$)	Temp. ($^{\circ}\text{C}$)	Time (h)	Hg-1212 vol. (%)
Hg1*	0	4	1.5 \rightarrow room temp.	800	8	0
Hg2	0	30	power shut off	850	7	7
Hg3	0	preheated furnace	power shut off	750	7	2
hg12	0	1.5	power shut off	860	8	6
hg16	0	3.5	power shut off	850	5	10
hg11	0.33	4.5	power shut off	850	5	55
hg13	0.35	4.5	power shut off	850	5	55
hg14	0.50	3.5	power shut off	830	5	50
hg15	0.40	2.5	power shut off	850	5	55
hg17	0.26	2.5	power shut off	850	8	65
ch11	0.40	3.5	power shut off	870	5	40

Table 3

Selected experiments carried out for the preparation of Hg-1223. The nominal composition of the precursors used in these experiments is $\text{Ba}_2\text{Ca}_x\text{Cu}_4\text{O}_8$. Column 2 gives the weight ratio Precursor/ $\text{Hg}_x\text{Ba}_2\text{Ca}_x\text{Cu}_4\text{O}_8$, where $x=1.5$ for the preparations marked with an asterisk and $x=1.0$ for all the other preparations

Name	Weight ratio	Heating rate ($^{\circ}\text{C}/\text{min}$)	Cooling rate ($^{\circ}\text{C}/\text{min}$)	Temp. ($^{\circ}\text{C}$)	Time (h)	Hg-1223 vol. (%)
ch14	0	1.5	1.0 \rightarrow room temp.	870	5	50
ch10	0.40	3.5	2.5 \rightarrow 600 $^{\circ}\text{C}$	870	5	90
ch15	0.40	3.5	2.5 \rightarrow 600 $^{\circ}\text{C}$	870	5	90
ch16	0.40	3.5	2.5 \rightarrow 600 $^{\circ}\text{C}$	870	5	90
ch13	0.40	3.5	1.5 \rightarrow 550 $^{\circ}\text{C}$	870	5	90
ch17	0.40	3.5	2.5 \rightarrow 600 $^{\circ}\text{C}$	880	8	90
ch18	0.38	3.5	2.5 \rightarrow room temp.	885	5	90
ch19	0.49	1.0	1.0 \rightarrow room temp.	900	10	0
ch4*	0.41	2.5	power shut off	880	10	0
hg1*	0.39	2.5	power shut off	870	8	65
hg3*	0.35	2.5	power shut off	900	5	40
ch2*	0.40	2.5	2.5 \rightarrow 140 $^{\circ}\text{C}$	900	10	40
ch3*	0.42	2.5	power shut off	950	3	0
ch5*	0.40	1.0	power shut off	900	3	30

$\text{Ba}_2\text{Ca}_{n-1}\text{Cu}_n\text{O}_y$ pellets (P) together with Hg- $\text{Ba}_2\text{Ca}_{n-1}\text{Cu}_n\text{O}_y$ pellets (HBCCO) in the sealed quartz tubes suggests that the total amount of the material inside the tube is mercury deficient. Surprisingly, drops of mercury were observed in almost all the experiments. The formation of Hg-1212 instead of Hg-1223 from nominal 1223 composition and the formation of Hg-1223 instead of Hg-1234 from nominal 1234 composition mean that there are some calcium and copper left. CaHgO_2 was observed as the major impurity phase and there are negligible traces

of CuO and its related compounds. One may speculate that the copper and the mercury cations are mixed. The substitution of Cu for 8% Hg was observed by Wagner et al. [13] in their Hg-1201 sample. As a consequence, they found additional extra oxygen atoms on the edges of the mercury layer ($\frac{1}{2}$, 0, z) together with the already existing extra oxygen atoms at ($\frac{1}{2}$, $\frac{1}{2}$, 0). In the first, second, third and fifth member of the mercury-based series the mercury atoms are found to have an unusually high temperature factor [14,15,25-27]. This can be reduced to a more

base is Hg-1212, and
Cu₂O₃, where $x=1$ for

Hg-1212 vol. (%)
0
7
2
6
10
55
55
50
55
65
40

in these experiments
marked with an asterisk

Hg-1223 vol. (%)
50
90
90
90
90
90
90
0
0
65
40
40
0
30

One may specu-
cations are
8% Hg was ob-
ir Hg-1201 sam-
additional extra
mercury layer ($\frac{1}{2}$,
ing extra oxygen
d, third and fifth
s the mercury at-
high temperature
duced to a more

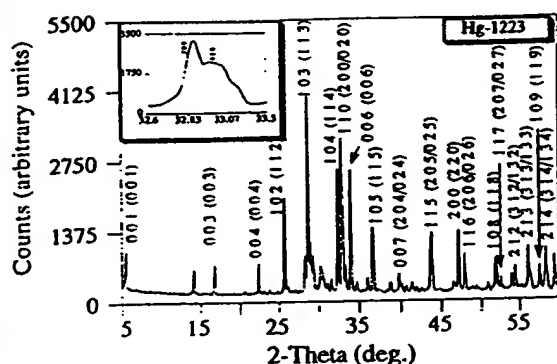


Fig. 5. X-ray diffraction pattern of an as-prepared Hg-1223 sample. The diffraction lines are indexed in both tetragonal cell with lattice constants $a=3.8564(1)$ Å and $c=15.8565(9)$ Å and orthorhombic cell (in parentheses) with lattice constants $a=5.4537(1)$ Å, $b=5.4247(1)$ Å and $c=15.8505(7)$ Å. The inset shows the splitting of the line (110) (tetragonal symmetry) into two lines, 200 and 020 (orthorhombic symmetry).

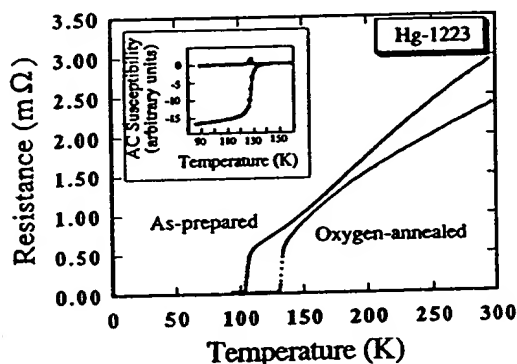


Fig. 6. Resistivity measurements carried out on both as-synthesized and oxygen-annealed Hg-1223 samples. The T_{onset} (originally 105 K) is increased up to 135 K. The curve shows a sharp transition around 135 K with a zero resistance at about 134 K. The real and imaginary parts of the AC magnetic-susceptibility measurements carried out on an oxygen-annealed sample are shown in the inset.

reasonable value by mixing the mercury cations with atoms like copper for example. This possibility was investigated but not proved. The successful preparation of nearly "100%" pure Hg-1201 samples using our method where the mercury cations enclosed in the quartz tube present only 0.57 mole to 1 mole of the precursor $\text{Ba}_2\text{CuO}_{3+x}$ confirms that the mixing of Cu and Hg is very possible. The increase of T_{onset} (97 K) might be due to this mixing. However, this conclusion must be interpreted with some caution. A

molar ratio Hg/Cu of 0.57 seems to be rather small compared to 0.85 found by Wagner et al.. Even though our sample looks pure using the X-ray diffraction technique, it might not really be the case. An undetectable (by X-rays) amorphous Ba-Cu-O substance could exist in the powder as well. Such observation was reported by Dolhert et al. [28] who studied the low detectability of excess yttrium and barium in $\text{YBa}_2\text{Cu}_3\text{O}_7$ by X-ray diffraction. Thus the X-ray "pure" sample may not be actually very pure. However, the formation of $(\text{Hg}, \text{Cu})\text{Ba}_2\text{Ca}_{n-1}\text{Cu}_n\text{O}_{2n+2+\delta}$ is possible and seems to be dependent on the preparation conditions. More details need to be studied. As the X-rays are not too sensitive to the oxygen anions, neutron experiments are needed to determine the value of the extra oxygen atoms and their location and to confirm the occupancy of the mercury sites and also to investigate the possibility of any change in the structure.

Our Hg-1223 phase is very likely to be orthorhombic. The orthorhombicity of our samples is observed by the splitting of some of the X-ray diffraction lines. The possibility of the coexistence of two phases with very high rate of overlapped lines would suggest that these two phases are both members of the mercury-based series and by consequence we must be able to observe at least two well-defined superconducting transitions in our measurements. As this was not the case and as the lines (00l) are singles and not split we may conclude that our Hg-1223 phase is orthorhombic. The refined cell parameters are in good agreement with those reported by Meng et al. [16] and Huang et al. [29] for their orthorhombic samples.

Acknowledgements

We thank John Shultz for his assistance in powder X-ray diffraction. This work was supported by the Advanced Research Projects Agency and the Arkansas Energy Office, USA.

References

- [1] S.N. Putilin, E.V. Antipov, O. Chmaissem and M. Marezio, Nature (London) 362 (1993) 226.

- [2] A. Shilling, M. Cantoni, J.D. Guo and M.R. Ott, *Nature* (London) 363 (1993) 56.
- [3] S.N. Putilin, E.V. Antipov and M. Marezio, *Physica C* 212 (1993) 266.
- [4] E.V. Antipov, S.M. Loureiro, C. Chaillout, J.J. Capponi, P. Bordet, J.L. Tholence, S.N. Putilin and M. Marezio, *Physica C* 215 (1993) 1.
- [5] C. Martin, M. Huve, G. Van Tendeloo, A. Maignan, C. Michel, M. Hervieu and B. Raveau, *Physica C* 212 (1993) 274.
- [6] A. Maignan, C. Michel, G. Van Tendeloo, M. Hervieu and B. Raveau, *Physica C* 216 (1993) 1.
- [7] R.S. Liu, D.S. Shy, S.F. Hu and D.A. Jefferson, *Physica C* 216 (1993) 237.
- [8] F. Goutenoire, P. Daniel, M. Hervieu, G. Van Tendeloo, C. Michel, A. Maignan and B. Raveau, *Physica C* 216 (1993) 243.
- [9] D. Pelloquin, M. Hervieu, C. Michel, G. Van Tendeloo, A. Maignan and B. Raveau, *Physica C* 216 (1993) 257.
- [10] M. Hervieu, G. Van Tendeloo, A. Maignan, C. Michel, F. Goutenoire and B. Raveau, *Physica C* 216 (1993) 264.
- [11] Z.Z. Sheng and A.M. Hermann, *Nature* (London) 332 (1988) 55.
- [12] Z.Z. Sheng and A.M. Hermann, *Nature* (London) 332 (1988) 138.
- [13] J.L. Wagner, P.G. Radaelli, D.G. Hinks, J.D. Jorgensen, J.F. Mitchell, B. Dabrowski, G.S. Knapp and M.A. Beno, *Physica C* 210 (1993) 447.
- [14] O. Chmaissem, Q. Huang, S.N. Putilin, M. Marezio and A. Santoro, *Physica C* 212 (1993) 259.
- [15] O. Chmaissem, Q. Huang, E.V. Antipov, S.N. Putilin, M. Marezio, S.M. Loureiro, J.J. Capponi, J.L. Tholence and A. Santoro, *Physica C* 217 (1993) 265.
- [16] R.L. Meng, L. Beauvais, X.N. Zhang, Z.J. Huang, Y.Y. Sun, Y.Y. Xue and C.W. Chu, *Physica C* 216 (1993) 21.
- [17] C.W. Chu, L. Gao, F. Chen, Z.J. Huang, R.L. Meng and Y.Y. Xue, *Nature* (London) 365 (1993) 323.
- [18] M. Nunez-Regueiro, J.L. Tholence, E.V. Antipov, J.J. Capponi and M. Marezio, *Science* 262 (1993) 97.
- [19] Z.Z. Sheng, Y.F. Li and K.C. Goretta, *Mod. Phys. Lett. B*, to be published.
- [20] P.G. Radaelli, J.L. Wagner, B.A. Hunter, B.A. Beno, G.S. Knapp, J.D. Jorgensen and D.G. Hinks, *Physica C* 216 (1993) 29.
- [21] M. Itoch, A. Tokiwa-Yamamoto, S. Adachi and H. Yamauchi, *Physica C* 212 (1993) 271.
- [22] A. Tokiwa-Yamamoto, K. Isawa, M. Itoch, S. Adachi and H. Yamauchi, *Physica C* 216 (1993) 250.
- [23] W.J. Zhu, Y.Z. Huang, L.Q. Chen, C. Dong, B. Yin and Z.X. Zhao, *Physica C* 218 (1993) 5.
- [24] M. Paranthaman, *Physica C* 222 (1994) 7.
- [25] S.M. Loureiro, E.V. Antipov, J.L. Tholence, J.J. Capponi, O. Chmaissem, Q. Huang and M. Marezio, *Physica C* 17 (1993) 253.
- [26] E.V. Antipov, J.J. Capponi, C. Chaillout, O. Chmaissem, S.M. Loureiro, M. Marezio, S.N. Putilin, A. Santoro and J.L. Tholence, *Physica C* 218 (1993) 348.
- [27] Q. Huang, O. Chmaissem, J.J. Capponi, C. Chaillout, M. Marezio, J.L. Tholence and A. Santoro, *Physica C* 227 (1994) 1.
- [28] L.E. Dolhert and N.D. Spencer, *Mater. Lett.* 9 (1990) 537.
- [29] Z.J. Huang, R.L. Meng, X.D. Qiu, Y.Y. Sun, J. Kulik, Y.Y. Xue and C.W. Chu, *Physica C* 217 (1993) 1.

The synthesis and characterization of the $\text{HgBa}_2\text{Ca}_2\text{Cu}_3\text{O}_{8+\delta}$ and $\text{HgBa}_2\text{Ca}_3\text{Cu}_4\text{O}_{10+\delta}$ phases

E.V. Antipov ^{a,b}, S.M. Loureiro ^b, C. Chaillout ^b, J.J. Capponi ^b, P. Bordet ^b, J.L. Tholence ^c,
S.N. Putilin ^a and M. Marezio ^{b,d}

^a Department of Chemistry, Moscow State University, 119899 Moscow, Russian Federation

^b Laboratoire de Cristallographie CNRS-UJF, BP 166, 38042 Grenoble Cedex 09, France

^c CRTBT, CNRS-UJF, BP 166, 38042 Grenoble Cedex 09, France

^d AT&T Bell Laboratories, Murray Hill, NJ 07974, USA

Received 28 June 1993

Revised manuscript received 9 July 1993

The third (Hg-1223) and the fourth (Hg-1234) members of the recently-discovered homologous series $\text{HgBa}_2\text{Ca}_{n-1}\text{Cu}_n\text{O}_{2n+2+\delta}$ have been synthesized by solid state reaction, carried out at 950°C under 50 kbar at different annealing times. These phases have a tetragonal cell with lattice parameters: $a=3.8532(6)$ Å, $c=15.818(2)$ Å and $a=3.8540(3)$ Å, $c=19.006(3)$ Å, respectively. The c parameters are in agreement with the formula $c \approx 9.5 + 3.2(n-1)$. Electron microscopy study showed similar lattice parameters as well as the occurrence of different intergrowths and stacking faults. A periodicity of 22 Å has also been detected, which may be attributed to the existence of the Hg-1245 phase. EDS analysis data of several grains of Hg-1223 and Hg-1234 are in agreement with the proposed chemical formulae. AC susceptibility measurements show that an increase of the superconducting transition temperature with n in the $\text{HgBa}_2\text{Ca}_{n-1}\text{Cu}_n\text{O}_{2n+2+\delta}$ series occurs till the third member, after which a saturation seems to be achieved.

1. Introduction

Superconductivity at about 94 K and well above 120 K has been recently reported for $\text{HgBa}_2\text{CuO}_{4+\delta}$ (Hg-1201) [1] and $\text{HgBa}_2\text{CaCu}_2\text{O}_{6+\delta}$ (Hg-1212) [2], respectively. These phases are the first and the second members of the Hg-based homologous series of layered Cu mixed oxides. Their structures contain rock-salt-like slabs, such as $(\text{BaO})(\text{HgO}_2)(\text{BaO})$ alternating with either one (CuO_2) layer in the former or an anion-deficient perovskite-like slab, such as $(\text{CuO}_2)(\text{CaO})(\text{CuO}_2)$, in the latter. A superconducting transition temperature as high as 133 K has been reported for a multiphasic sample in the Hg-Ba-Ca-Cu-O system by Schilling et al. [4]. These authors could not identify by X-ray diffraction the phases responsible for the superconductivity at this temperature, but proved by high resolution electron microscopy that the sample contained the Hg-1212 and Hg-1223 phases as well as different intergrowths. Putilin et al. [2] showed that in the sample

containing Hg-1212 as the majority phase, a small drop on the AC susceptibility curve versus T occurred at about 132 K which could be attributed to the third member of the Hg-bearing series.

Putilin et al. also showed [2] that it was possible to synthesize the Hg-1212 phase, practically in pure form, under high pressure (40–60 kbar) and at 800°C for about 1 h. The high pressure synthesis allows one to lower the mercury oxide decomposition. This decomposition occurs at ambient pressure at a temperature at which the reactivity of the other components is very low. It was suggested that the same technique could be used for obtaining the higher members of the series. We found that the reactions have to be carried out at higher temperatures (950°C) and for longer annealing times. The same occurs for the higher members of the Bi- or Tl-based Cu oxide series, which are formed by the formation, at the initial stages of the reaction, of the lower members of the corresponding families. We report herein the synthesis and characterization of the Hg-

$\text{Ba}_2\text{Ca}_2\text{Cu}_3\text{O}_{8+\delta}$ (Hg-1223) and $\text{HgBa}_2\text{Ca}_3\text{Cu}_4\text{O}_{10+\delta}$ (Hg-1234) phases. The reactions were carried out in a belt-type apparatus under high pressure (50 kbar) at 950°C for 3 and 3.5 h, respectively.

2. Synthesis and characterization by X-ray and EDS analysis

Powder samples containing the $\text{HgBa}_2\text{Ca}_2\text{Cu}_3\text{O}_{8+\delta}$ and $\text{HgBa}_2\text{Ca}_3\text{Cu}_4\text{O}_{10+\delta}$ phases were obtained by high-pressure and high-temperature reactions using the belt-type apparatus of the Laboratoire de Cristallographie. A precursor with the nominal composition $\text{Ba}_2\text{Ca}_2\text{Cu}_3\text{O}_x$ was prepared by mixing high-purity nitrates: $\text{Ba}(\text{NO}_3)_2$ (Aldrich, > 99%), $\text{Ca}(\text{NO}_3)_2 \cdot 4\text{H}_2\text{O}$ (Normapur Prolabo, analytical reagent) and $\text{Cu}(\text{NO}_3)_2 \cdot 3\text{H}_2\text{O}$ (Strem Chemical Inc., 99.5%). The mixture thus obtained was initially heated at 600°C in air for 12 h, then reground and annealed at 925°C for 72 h in an oxygen flow with three intermediate regrindings. Then, the stoichiometric amount of yellow HgO (Aldrich, > 99%) was added and the mixture was thoroughly grounded in an agate mortar and sealed in a Pt capsule specific for high pressure synthesis. Various temperatures and annealing times at a pressure of 50 kbar were tried in order to obtain the Hg-1223 and Hg-1234 phases. In these experiments the pressure was first increased to 50 kbar, subsequently the temperature was raised to the desired value during 1 h, then the temperature and the pressure were kept constant for 1–4 h. After this, the furnace power was shut off and the pressure decreased to normal conditions in 30 min.

The samples were studied by X-ray powder diffraction, performed with a Guinier focusing camera and Fe K α radiation (1.93730 Å). Finely powdered silicon ($a = 5.43088$ Å at 25°C) was used as an internal standard. The intensities of the reflections were evaluated by an automatic film scanner. The SCAN3 and SCANPI programs were used for processing the data [5].

The phase $\text{HgBa}_2\text{Ca}_2\text{Cu}_3\text{O}_{8+\delta}$ was present in the sample synthesized at 950°C for 3 h (sample I) together with a smaller amount of Hg-1212, CaO and CuO, and traces of CaHgO_2 [6] and of an unknown phase whose intensities were less than 4%. The X-ray

diffraction pattern of sample I after background subtraction is shown in fig. 1. The 20 reflections corresponding to Hg-1223 were indexed on a tetragonal cell with lattice parameters $a = 3.8532(6)$ Å, $c = 15.818(2)$ Å. The characteristic 001 reflection is shown in the insert. No systematic absences were observed, leading to space group P4/mmm and one formula per unit cell. The measured value of the c parameter of Hg-1223 corresponded to the expected value calculated by the formula $c \cong 9.5 + 3.2(n-1)$ with $n = 3$ [1].

A scanning electron microscope JEOL 840A equipped with an energy-dispersive spectroscopy (EDS) attachment was used for the analysis of the cation composition of the two prepared samples. K α lines were used for the analysis of the Ca and Cu cations, and L α lines for the Ba and Hg ones. EDS analysis of several well crystallized and flat grains showed that besides Hg, Ba, Ca, Cu and O no other element was present in the samples. The average metal ratio found for four grains was $\text{Hg}:\text{Ba}:\text{Ca}:\text{Cu} = 13(2):24(1):26(1):38(1)$, with standard deviations between parentheses. The cation stoichiometry is in good agreement with the expected formula of the Hg-1223 phase.

The lattice parameters of Hg-1212 refined from ten reflections ($a = 3.859(4)$ Å, $c = 12.68(2)$ Å) are in agreement with the data of Putlin et al. [2]. It should be noted that there is severe overlapping between the $hk0$ reflections of the Hg-1212 and those of the Hg-1223 phases. Moreover, the $hk4$ reflections of Hg-1212 overlap with the $hk5$ reflections of Hg-1223. These overlappings did not allow us to determine all the intensities of the two phases. However, the ratio of the intensities of the strongest lines for Hg-1212 (102 and 103) and Hg-1223 (103 and 104) shows clearly that the Hg-1223 is the predominant phase in sample I (fig. 1).

The presence in sample I of the lower member together with the initial oxides, CuO and CaO, obviously indicates that the formation of Hg-1223 was not complete after a 3 h annealing period. The synthesis carried out at 900°C for 2 h led to the formation of Hg-1212 which was found to be the main phase in the sample together with the starting compounds. These data show that the formation of Hg-1223 occurs through the synthesis of the lower members of the series. The increase of the annealing

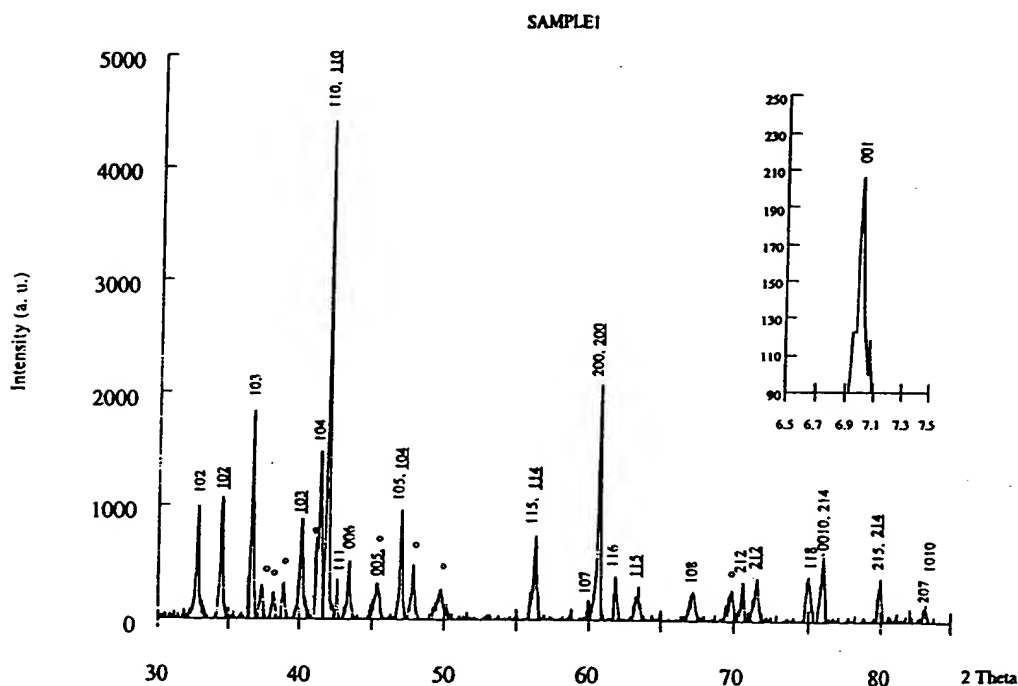


Fig. 1. X-ray powder pattern for sample I. Indexed XRD intensities correspond to Hg-1223 and Hg-1212 (underline). Impurities of CaO, CuO, CaHgO_2 and an unknown phase are marked by (*). The inset displays the characteristic intensity of 001 for Hg-1223.

time up to 3.5 and 4 h at 950°C and the same pressure led to the expected disappearance of Hg-1212 as well as of CaO. In these samples the formation of a new phase was detected. Its amount was relatively high (more than 50%) in samples annealed for 3.5 h (sample II). A total of 17 reflections of this phase were indexed on a tetragonal cell with lattice parameters $a = 3.8540(3) \text{ \AA}$, $c = 19.006(3) \text{ \AA}$. As for Hg-1223 no systematic absences were observed, leading to space group $P4/\text{mmm}$. Similar parameters were found by electron diffraction (see below). The c parameters of this phase corresponded to the value calculated from the formula $c \cong 9.5 + 3.2(n-1)$ for $n=4$. This strongly suggested that the new phase was the fourth member of the Hg-based series: $\text{HgBa}_2\text{Ca}_3\text{Cu}_4\text{O}_{10+s}$. The approximate cations ratio determined by EDS analysis of five well-crystallized and flat grains was $\text{Hg}:\text{Ba}:\text{Ca}:\text{Cu} = 9(1):18(1):29(2):44(2)$. These data are in good agreement with the proposed formula for the new compound.

Besides Hg-1234 as the main phase, a smaller amount of Hg-1223 was present in sample II together with small amounts of CuO and of an unknown phase. This unknown phase was predominant in a sample treated for 5 h in the same conditions which did not contain any member of the Hg-based series and did not exhibit any superconductivity. The presence of the latter oxides can be explained as a result of the decomposition of Hg-1223 and the formation of Hg-1234. Hg-1212 was absent in this sample as well as in that annealed for 4 h. The X-ray diffraction pattern of sample II after background subtraction is shown in fig. 2. The ratio of the main intensities for both Hg-based layered cuprates, 104 for Hg-1223 and 105 for Hg-1234, shows that the latter was the main phase in this sample. As for sample I the overlapping of $hk0$ reflections for both phases occurs because of the similarity of the two a parameters. Moreover, the $hk6$ reflections of Hg-1234 are overlapped with the $hk5$ ones of Hg-1223.

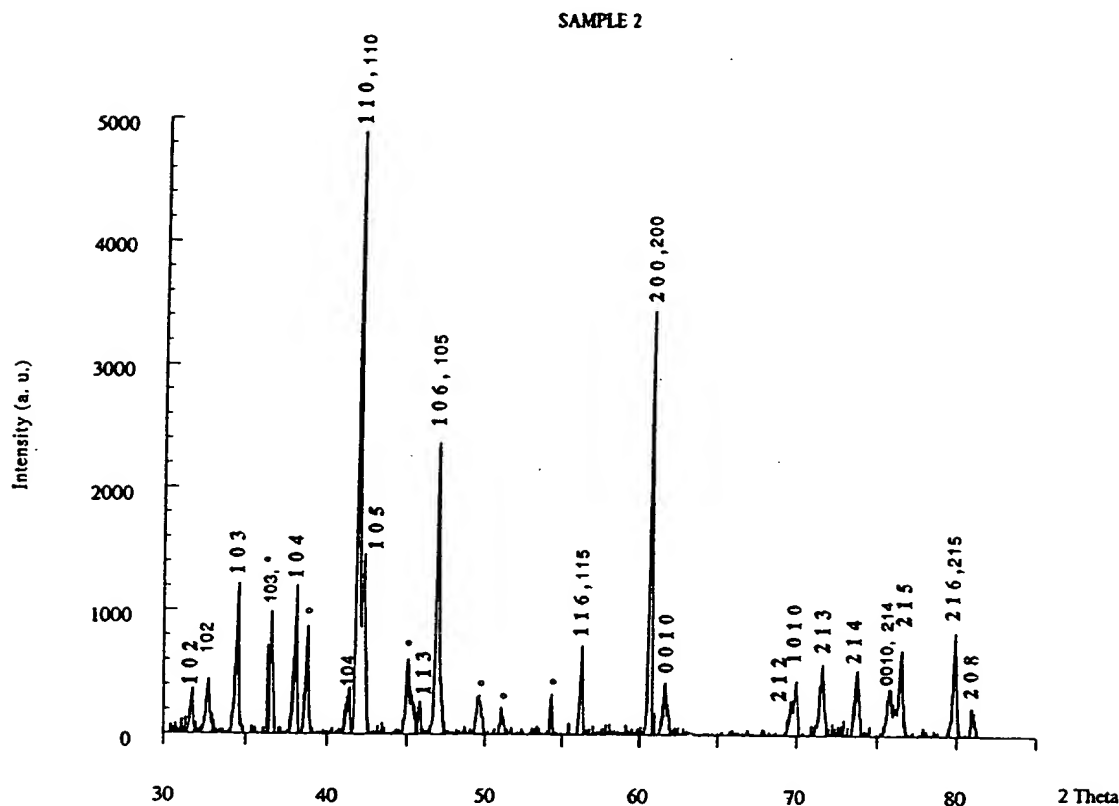


Fig. 2. X-ray powder pattern for sample II. Indexed XRD intensities correspond to Hg-1234 (bold) and Hg-1223. Impurities of CuO and an unknown phase are marked by (*).

3. Electron microscopy

The I and II samples were studied by electron microscopy. A suspension of crystals in acetone was grounded in an agate mortar. The crystallites were recovered from the suspension on a porous carbon film. A Philips EM 400T operating at 120 kV was used.

Figure 3 (a) and (b) shows two diffraction patterns obtained for sample I corresponding to the [001] and the $\langle 110 \rangle$ zone axes of the $\text{HgBa}_2\text{Ca}_2\text{Cu}_3\text{O}_{8+\delta}$ (Hg-1223) phase, respectively. In both cases, the diffraction spots are sharp, which indicates that the crystal is well ordered. In fig. 3(b), one can notice a modulation of the intensity of the diffraction spots along the c^* -axis, with maxima for hkl reflections with $l = 5n$ ($n = 0, 1, 2, \dots$). On the micrograph (fig. 3(c)) corresponding to the diffraction pattern shown in fig. 3(b), one can see the very

regular periodicity of the fringes separated by 15.8 Å. During the observation under the electron beam, dark spots appeared near the edge of the crystal, probably due to the decomposition of the crystal.

Some diffraction patterns obtained for other crystals present diffuse lines parallel to the c^* -axis and passing through the Bragg spots (fig. 4 (a)). They are due to the presence of intergrowths as given evidence for by fig. 4(b). On this micrograph, two different spacings of 15.8 Å and 12.7 Å can be measured, attributed to Hg-1223 and Hg-1212, respectively.

In the case of sample II, almost all the observed crystallites have diffraction patterns corresponding to the Hg-1234 phase ($\text{HgBa}_2\text{Ca}_3\text{Cu}_4\text{O}_{10+\delta}$) with cell parameters $a = b = 3.85$ Å and $c = 19$ Å. Figure 5(a) and (b) give examples of the [001] and $\langle 100 \rangle$ zone axes, respectively. As for Hg-1223, also for Hg-1234 the intensity of the Bragg spots varies according to

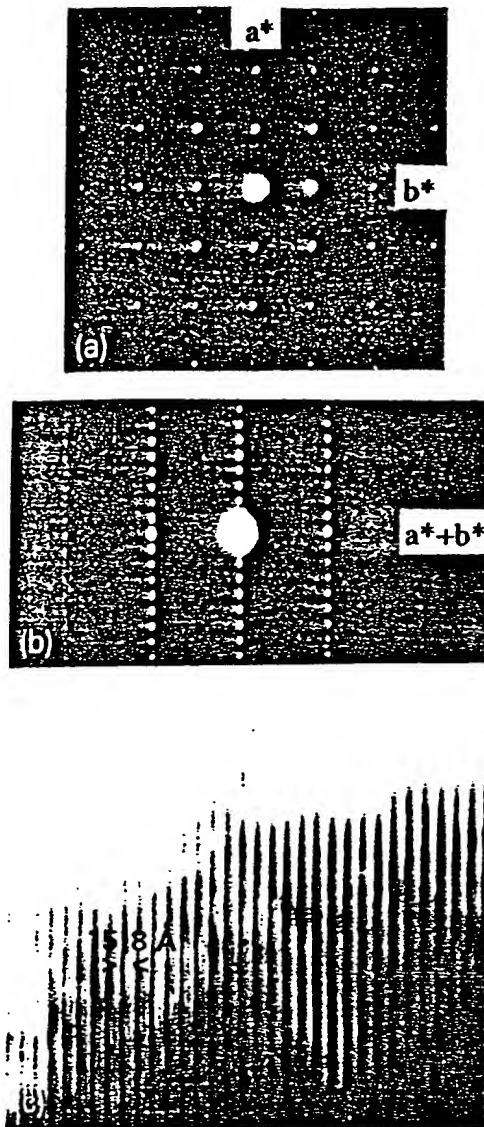


Fig. 3. Electron diffraction patterns of Hg-1223 taken along $[001]$ (a) and $\langle 110 \rangle$ (b) zone axes. (c) Micrograph corresponding to the diffraction pattern (b). The interfringe spacing is 15.8 \AA .

the value of the l index, the maxima of intensity being obtained for $l=6n$ ($n=0, 1, 2, \dots$). This intensity pattern might be explained by the fact that $c/6$ is equal to 3.17 \AA , which corresponds to the distance between two neighboring (CuO_2) layers. The increase of the layer number n in the structure leads to the increase of the intensity of the hkl reflections with

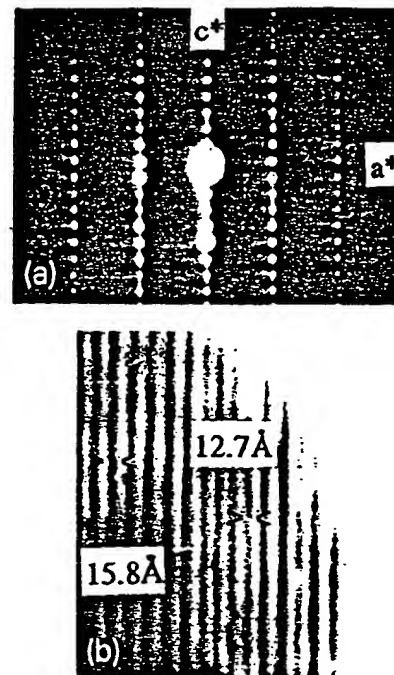


Fig. 4. Electron diffraction pattern of sample 1 along $\langle 100 \rangle$ and corresponding micrograph showing the intergrowths of Hg-1223 and Hg-1212.

$l=n+2$. These periodicities of the (CuO_2) layers explain the overlapping of such reflections on the X-ray powder pattern (see above). Most of the images taken along the $\langle 100 \rangle$ zone axis show very regular fringes separated by 19 \AA (fig. 5(c)). However, some crystals present intergrowths between the Hg-1223 and Hg-1234, as revealed in fig. 6. In this case, the following sequence is observed over about 500 \AA : $-19 \text{ \AA}-19 \text{ \AA}-19 \text{ \AA}-19 \text{ \AA}-19 \text{ \AA}-22 \text{ \AA}-$. On the corresponding diffraction pattern, besides the diffraction spots of the Hg-1234 phase, additional spots related to the 22 \AA periodicity are present. Such a periodicity may be attributed to a 1245 phase ($\text{HgBa}_2\text{Ca}_4\text{Cu}_5\text{O}_{12+\delta}$). The fact that the extra diffraction spots are sharp indicates that this phase is well ordered at least over a certain number of cells in these crystals.

4. AC susceptibility measurements

The critical temperature T_c , and the apparent su-

Theta
es of CuO

by 15.8
on beam,
crystal,
crystal.
her crys-
axis and
)). They
even evi-
two dif-
be mea-
Hg-1212,

observed
sponding
with cell
ure 5(a)
 $\langle 100 \rangle$ zone
Hg-1234
ording to

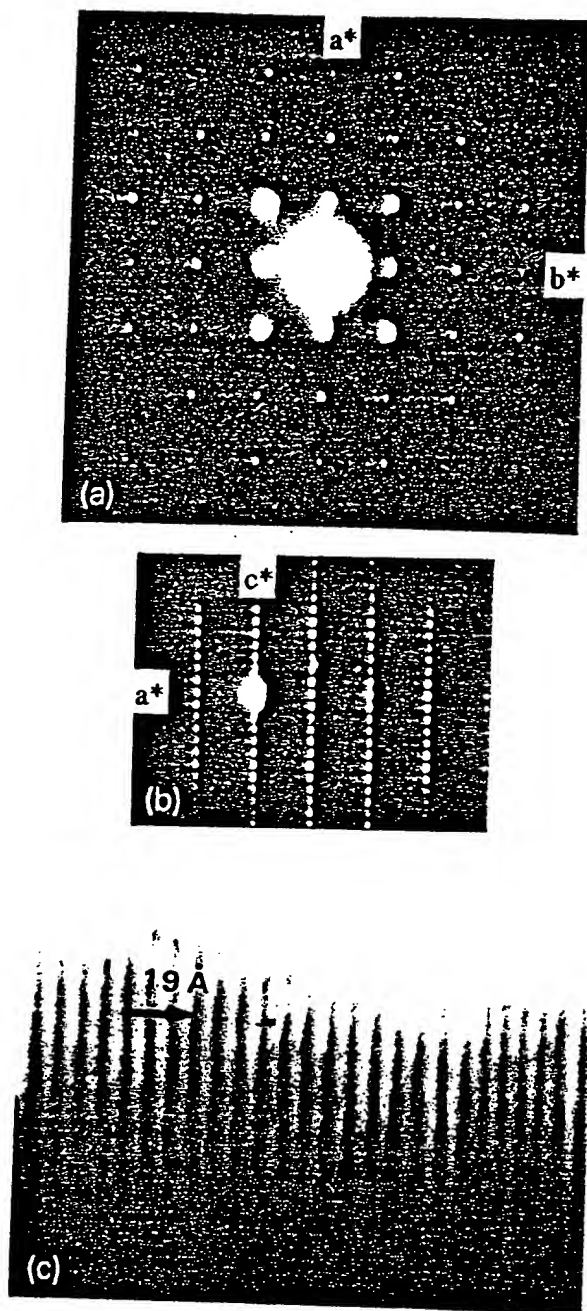


Fig. 5. Electron diffraction patterns of Hg-1234 taken along $[001]$ (a) and $\langle 100 \rangle$ (b) zone axes. (c) Micrograph corresponding to the diffraction pattern of (b). The interfringe spacing is 19 Å.

perconducting volume of samples I and II have been determined from AC susceptibility measurements on fine powder samples. This avoids overestimates of the superconducting volume due to the larger screenings in sintered samples. The AC susceptibility was measured with an alternating maximum field of 0.01 Oe and a frequency of 119 Hz. The temperature was measured by a calibrated 100 Ω platinum thermometer.

The as-synthesized sample I undergoes a transition from the paramagnetic to the diamagnetic state with an onset above 133 K (fig. 7). Several measurements were made with the same sample and the reproducibility of T_c is ± 1 K (mainly due to the thermal contact between the sample and the thermometer). The estimated magnetic susceptibility at 4 K corresponds to a large volume of ideal diamagnetism indicating the bulk nature of superconductivity. We can suggest that the sharp and large drop on the AC susceptibility curve above 133 K should correspond to the Hg-1223 phase because Hg-1212, which is present in this sample as the minority phase, has a T_c not higher than 126 K [3].

The as-synthesized sample II undergoes a transition from the paramagnetic to the diamagnetic state with an onset as high as 132 K. Actually, two onsets at two different temperatures are visible, the smaller one at 132 K and the larger one at about 126 K. There are two Hg-based layered cuprates in this sample: Hg-1234 as the main phase and Hg-1223 as the minority one. Taking into consideration the results of sample I, we might suggest that the first onset (132 K) corresponds to Hg-1223 and the larger one at the lower temperature (126 K) to Hg-1234. In any case, it is obvious that T_c for Hg-1234 is not higher than that for Hg-1223.

5. Discussion

The synthesized $\text{HgBa}_2\text{Ca}_2\text{Cu}_3\text{O}_{8+\delta}$ (Hg-1223) and $\text{HgBa}_2\text{Ca}_3\text{Cu}_4\text{O}_{10+\delta}$ (Hg-1234) phases are the third and the fourth members of the $\text{Hg-Ba}_2\text{Ca}_{n-1}\text{Cu}_n\text{O}_{2n+2+\delta}$ series. In analogy with those of Hg-1201 [1,7,8] and Hg-1212 [2] their structures can be schematized as containing rock-salt-like slabs, $(\text{BaO})(\text{HgO}_\delta)(\text{BaO})$, alternating with perovskite-like slabs, consisting in three (Hg-1223) or

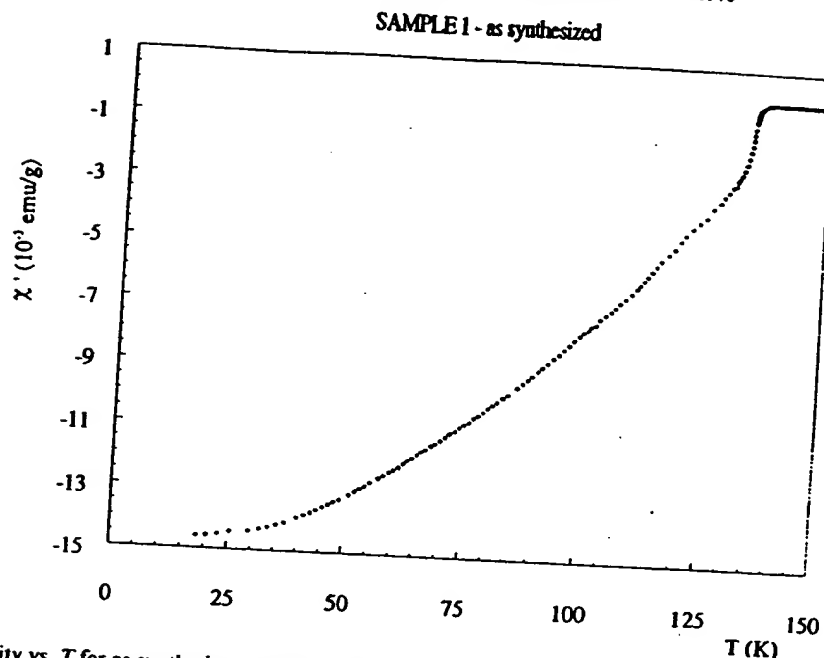


Fig. 7. AC susceptibility vs. T for as-synthesized sample I, where Hg-1223 is present as the main phase and Hg-1212 as the minority phase.

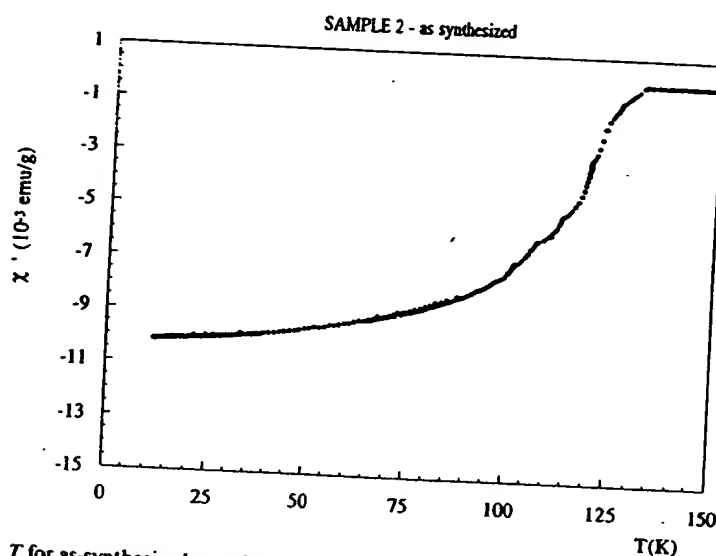


Fig. 8. AC susceptibility vs. T for as-synthesized sample II showing the presence of Hg-1234 as the main phase and of Hg-1223 as the minority phase.

1212. The appropriate treatment for Hg-1234 can possibly change T_c for this phase. Therefore, we can only conclude that for the as-prepared samples a saturation of T_c seems to occur in the Hg-Ba-Ca-Cu-O system at the third member. A similar behavior

occurs for the $\text{TlBa}_2\text{Ca}_{n-1}\text{Cu}_n\text{O}_{2n+3+\delta}$ homologous series, for which T_c increases up to the third member (120 K) also [9].

One can see in table 1 that for the Hg series, the increase of T_c is accompanied by a decrease of the a

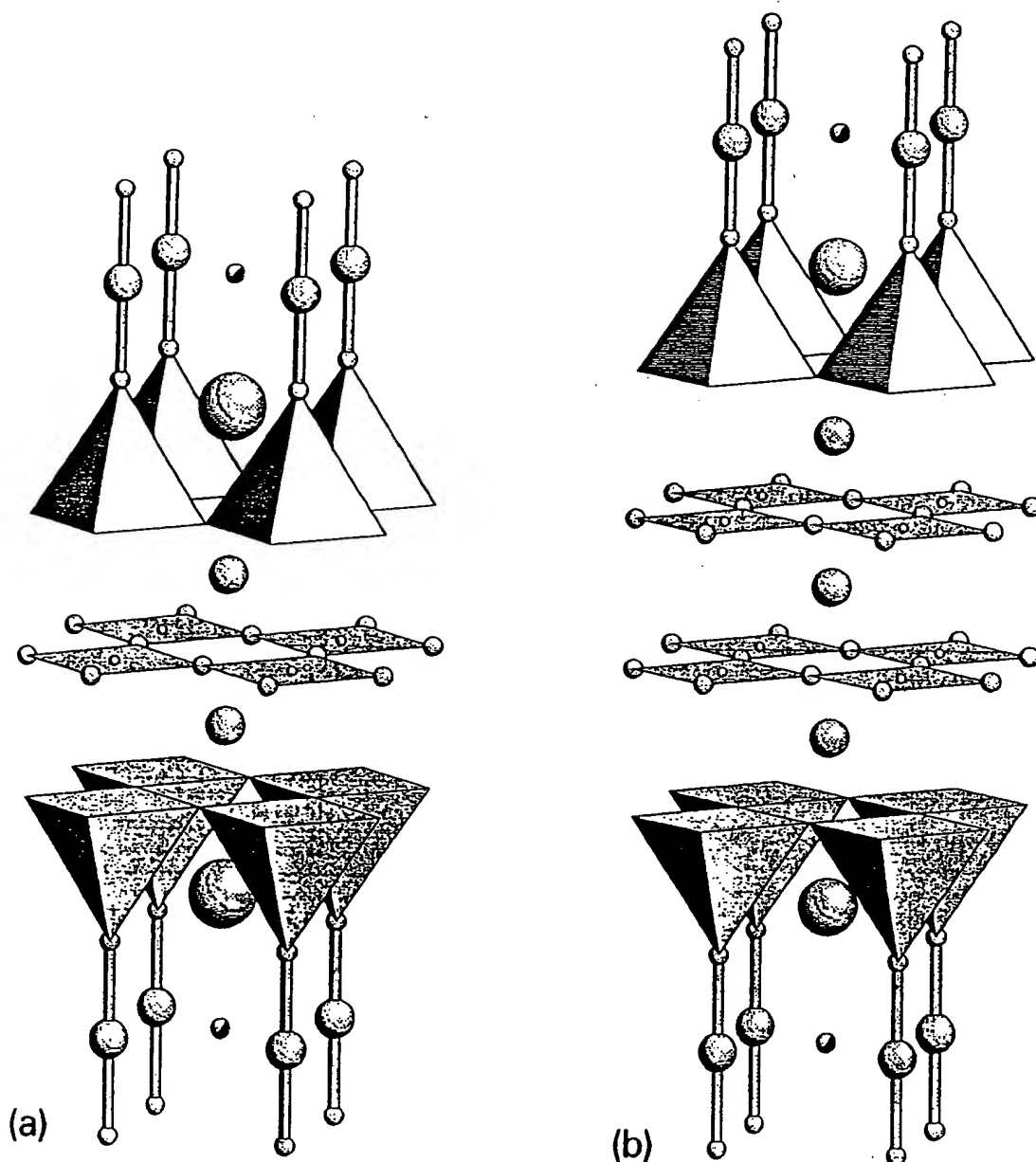


Fig. 9. The crystal structures of Hg-1223 (a) and Hg-1234 (b). The largest and medium large circles refer to Ba and Ca atoms, respectively. The Cu atoms are the smallest circles. Those at the base of the shaded pyramids are not shown. The circles forming the squares around the Cu are oxygen atoms. The dumbbells around the Hg atoms are formed by apical oxygen atoms. Partially filled circles refer to the partially occupied oxygen sites on the Hg layer.

parameter and just at T_c it remains practically constant between Hg-1223 and Hg-1234.

The electron microscopy study of Hg-1201 [10]

revealed the absence of intergrowths and this was attributed to the absence of the Ca^{2+} cations in the system. On the contrary, the addition of Ca layers in

Table I
Lattice parameters and transition temperatures for Hg-based Cu oxides

Formula	Short form	a (Å)	c (Å)	T_{c}^{on} (K)	Ref.
$\text{HgBa}_2\text{CuO}_{4+\delta}$	Hg-1201	3.8797(5)	9.509(2)	94	[1]
$\text{HgBa}_2\text{CaCu}_2\text{O}_{6+\delta}$	Hg-1212	3.8556(8)	12.652(4)	121	[2]
$\text{HgBa}_2\text{Ca}_2\text{Cu}_3\text{O}_{8+\delta}$	Hg-1223	3.8532(6)	15.818(2)	126	[3]
$\text{HgBa}_2\text{Ca}_3\text{Cu}_4\text{O}_{10+\delta}$	Hg-1234	3.8540(3)	19.006(3)	133	[4], this work
				< 132	this work

the system leads to intergrowths due to different numbers of (CuO_2) and Ca layers in the perovskite-like slabs. Such intergrowths were already reported in ref. [4]. Possibly, the occurrence of different intergrowths may explain why the variation versus temperature of the AC susceptibility does not present distinct and abrupt transitions which could be attributed to pure Hg-1212, 1223 and 1234 phases.

The synthesis of the higher members of the Hg-based homologous series as bulk samples has been performed at higher temperatures than that used for Hg-1212 and with longer treatment times. We suggest that the synthesis of such phases occurs through the formation at an initial state and subsequent decomposition of the lower members of the series. This feature is similar to that existing for the $\text{Ti-Ba}_2\text{Ca}_{n-1}\text{Cu}_n\text{O}_{2n+3-\delta}$ homologous series [9]. The use of high pressure, possibly, lowers the mercury oxide decomposition. It also leads to a decrease of stability of CaHgO_2 , whose synthesis at the first stage of the reaction inhibits the formation of Hg-based compounds.

Acknowledgements

The authors would like to thank M.F. Gorius, M.

Perroux and R. Argoud for their technical assistance. The visit of EVA has been supported by the fund from the French Ministry of Foreign Affairs. EVA and SNP would like to thank the support of the Russian Scientific Council on Superconductivity (Project "Poisk"). SML was supported by the Erasmus Students Exchange Program.

References

- [1] S.N. Putilin, E.V. Antipov, O. Chmaissem and M. Marezio, *Nature* (London) 362 (1993) 226.
- [2] S.N. Putilin, E.V. Antipov and M. Marezio, *Physica C* 212 (1993) 266.
- [3] S.M. Loureiro and J.J. Capponi, private communication.
- [4] A. Schilling, M. Cantoni, J.D. Guo and H.R. Ott, *Nature* (London) 363 (1993) 56.
- [5] K.E. Johansson, T. Palm and P.-E. Werner, *J. Phys. E: Sci. Instrum.* 13 (1980) 1289.
- [6] S.N. Putilin, M.G. Rozova, D. Kashporov, E.V. Antipov and L.M. Kovba, *Zh. Neorganicheskoi Khimii* 36 (1991) 1645 (in Russian).
- [7] O. Chmaissem, Q. Huang, S.N. Putilin, M. Marezio and A. Santoro, *Physica C* 212 (1993) 259.
- [8] J.L. Wagner, P.G. Radaelli, D.G. Hinks, J.D. Jorgensen, J.F. Mitchell, B. Dabrowski, G.S. Knapp and M.A. Beno, *Physica C* 210 (1993) 447.
- [9] S. Nakajima, M. Kikuchi, Y. Syono, T. Oku, D. Shindo, K. Hiraga, N. Kobayashi, H. Iwasaki and Y. Muto, *Physica C* 158 (1989) 471.
- [10] I. Bryntse and S.N. Putilin, *Physica C* 212 (1993) 223.

BRIEF ATTACHMENT BI

IN THE UNITED STATES PATENT AND TRADEMARK OFFICE

In re Patent Application of

Applicants: Bednorz et al.

Serial No.: 08/479,810

Filed: June 7, 1995

For: NEW SUPERCONDUCTIVE COMPOUNDS HAVING HIGH TRANSITION
TEMPERATURE, METHODS FOR THEIR USE AND PREPARATION

Date: March 1, 2004

Docket: YO987-074BZ

Group Art Unit: 1751

Examiner: M. Kopec

Commissioner for Patents
P.O. Box 1450
Alexandria, VA 22313-1450

FIFTH SUPPLEMENTAL AMENDMENT

Sir:

In response to the Office Action dated February 4, 2000:

ATTACHMENT 56

BI

The synthesis and characterization of the $\text{HgBa}_2\text{Ca}_2\text{Cu}_3\text{O}_{8+\delta}$ and $\text{HgBa}_2\text{Ca}_3\text{Cu}_4\text{O}_{10+\delta}$ phases

E.V. Antipov^{a,b}, S.M. Loureiro^b, C. Chaillout^b, J.J. Capponi^b, P. Bordet^b, J.L. Tholence^c, S.N. Putilin^a and M. Marezio^{b,d}

^a Department of Chemistry, Moscow State University, 119899 Moscow, Russian Federation

^b Laboratoire de Cristallographie CNRS-UJF, BP 166, 38042 Grenoble Cedex 09, France

^c CRTBT, CNRS-UJF, BP 166, 38042 Grenoble Cedex 09, France

^d AT&T Bell Laboratories, Murray Hill, NJ 07974, USA

Received 28 June 1993

Revised manuscript received 9 July 1993

The third (Hg-1223) and the fourth (Hg-1234) members of the recently-discovered homologous series $\text{HgBa}_2\text{Ca}_{n-1}\text{Cu}_n\text{O}_{2n+2+\delta}$ have been synthesized by solid state reaction, carried out at 950°C under 50 kbar at different annealing times. These phases have a tetragonal cell with lattice parameters: $a=3.8532(6)$ Å, $c=15.818(2)$ Å and $a=3.8540(3)$ Å, $c=19.006(3)$ Å, respectively. The c parameters are in agreement with the formula $c \approx 9.5 + 3.2(n-1)$. Electron microscopy study showed similar lattice parameters as well as the occurrence of different intergrowths and stacking faults. A periodicity of 22 Å has also been detected, which may be attributed to the existence of the Hg-1245 phase. EDS analysis data of several grains of Hg-1223 and Hg-1234 are in agreement with the proposed chemical formulae. AC susceptibility measurements show that an increase of the superconducting transition temperature with n in the $\text{HgBa}_2\text{Ca}_{n-1}\text{Cu}_n\text{O}_{2n+2+\delta}$ series occurs till the third member, after which a saturation seems to be achieved.

1. Introduction

Superconductivity at about 94 K and well above 120 K has been recently reported for $\text{HgBa}_2\text{CuO}_{4+\delta}$ (Hg-1201) [1] and $\text{HgBa}_2\text{CaCu}_2\text{O}_{6+\delta}$ (Hg-1212) [2], respectively. These phases are the first and the second members of the Hg-based homologous series of layered Cu mixed oxides. Their structures contain rock-salt-like slabs, such as $(\text{BaO})(\text{HgO}_2)(\text{BaO})$ alternating with either one (CuO_2) layer in the former or an anion-deficient perovskite-like slab, such as $(\text{CuO}_2)(\text{CaO})(\text{CuO}_2)$, in the latter. A superconducting transition temperature as high as 133 K has been reported for a multiphasic sample in the Hg-Ba-Ca-Cu-O system by Schilling et al. [4]. These authors could not identify by X-ray diffraction the phases responsible for the superconductivity at this temperature, but proved by high resolution electron microscopy that the sample contained the Hg-1212 and Hg-1223 phases as well as different intergrowths. Putilin et al. [2] showed that in the sample

containing Hg-1212 as the majority phase, a small drop on the AC susceptibility curve versus T occurred at about 132 K which could be attributed to the third member of the Hg-bearing series.

Putilin et al. also showed [2] that it was possible to synthesize the Hg-1212 phase, practically in pure form, under high pressure (40–60 kbar) and at 800°C for about 1 h. The high pressure synthesis allows one to lower the mercury oxide decomposition. This decomposition occurs at ambient pressure at a temperature at which the reactivity of the other components is very low. It was suggested that the same technique could be used for obtaining the higher members of the series. We found that the reactions have to be carried out at higher temperatures (950°C) and for longer annealing times. The same occurs for the higher members of the Bi- or Tl-based Cu oxide series, which are formed by the formation, at the initial stages of the reaction, of the lower members of the corresponding families. We report herein the synthesis and characterization of the Hg-

$\text{Ba}_2\text{Ca}_2\text{Cu}_3\text{O}_{8+x}$ (Hg-1223) and $\text{HgBa}_2\text{Ca}_3\text{Cu}_4\text{O}_{10+x}$ (Hg-1234) phases. The reactions were carried out in a belt-type apparatus under high pressure (50 kbar) at 950°C for 3 and 3.5 h, respectively.

2. Synthesis and characterization by X-ray and EDS analysis

Powder samples containing the $\text{HgBa}_2\text{Ca}_2\text{Cu}_3\text{O}_{8+x}$ and $\text{HgBa}_2\text{Ca}_3\text{Cu}_4\text{O}_{10+x}$ phases were obtained by high-pressure and high-temperature reactions using the belt-type apparatus of the Laboratoire de Cristallographie. A precursor with the nominal composition $\text{Ba}_2\text{Ca}_2\text{Cu}_3\text{O}_x$ was prepared by mixing high-purity nitrates: $\text{Ba}(\text{NO}_3)_2$ (Aldrich, > 99%), $\text{Ca}(\text{NO}_3)_2 \cdot 4\text{H}_2\text{O}$ (Normapur Prolabo, analytical reagent) and $\text{Cu}(\text{NO}_3)_2 \cdot 3\text{H}_2\text{O}$ (Strem Chemical Inc., 99.5%). The mixture thus obtained was initially heated at 600°C in air for 12 h, then reground and annealed at 925°C for 72 h in an oxygen flow with three intermediate regrindings. Then, the stoichiometric amount of yellow HgO (Aldrich, > 99%) was added and the mixture was thoroughly grounded in an agate mortar and sealed in a Pt capsule specific for high pressure synthesis. Various temperatures and annealing times at a pressure of 50 kbar were tried in order to obtain the Hg-1223 and Hg-1234 phases. In these experiments the pressure was first increased to 50 kbar, subsequently the temperature was raised to the desired value during 1 h, then the temperature and the pressure were kept constant for 1–4 h. After this, the furnace power was shut off and the pressure decreased to normal conditions in 30 min.

The samples were studied by X-ray powder diffraction, performed with a Guinier focusing camera and $\text{Fe K}\alpha$ radiation (1.93730 Å). Finely powdered silicon ($a = 5.43088$ Å at 25°C) was used as an internal standard. The intensities of the reflections were evaluated by an automatic film scanner. The SCAN3 and SCANPI programs were used for processing the data [5].

The phase $\text{HgBa}_2\text{Ca}_2\text{Cu}_3\text{O}_{8+x}$ was present in the sample synthesized at 950°C for 3 h (sample I) together with a smaller amount of Hg-1212, CaO and CuO, and traces of CaHgO_2 [6] and of an unknown phase whose intensities were less than 4%. The X-ray

diffraction pattern of sample I after background subtraction is shown in fig. 1. The 20 reflections corresponding to Hg-1223 were indexed on a tetragonal cell with lattice parameters $a = 3.8532(6)$ Å, $c = 15.818(2)$ Å. The characteristic 001 reflection is shown in the insert. No systematic absences were observed, leading to space group $P4/mmm$ and one formula per unit cell. The measured value of the c parameter of Hg-1223 corresponded to the expected value calculated by the formula $c \cong 9.5 + 3.2(n-1)$ with $n=3$ [1].

A scanning electron microscope JEOL 840A equipped with an energy-dispersive spectroscopy (EDS) attachment was used for the analysis of the cation composition of the two prepared samples. $K\alpha$ lines were used for the analysis of the Ca and Cu cations, and $L\alpha$ lines for the Ba and Hg ones. EDS analysis of several well crystallized and flat grains showed that besides Hg, Ba, Ca, Cu and O no other element was present in the samples. The average metal ratio found for four grains was $\text{Hg}:\text{Ba}:\text{Ca}:\text{Cu} = 13(2):24(1):26(1):38(1)$, with standard deviations between parentheses. The cation stoichiometry is in good agreement with the expected formula of the Hg-1223 phase.

The lattice parameters of Hg-1212 refined from ten reflections ($a = 3.859(4)$ Å, $c = 12.68(2)$ Å) are in agreement with the data of Putlin et al. [2]. It should be noted that there is severe overlapping between the $hk0$ reflections of the Hg-1212 and those of the Hg-1223 phases. Moreover, the $hk4$ reflections of Hg-1212 overlap with the $hk5$ reflections of Hg-1223. These overlappings did not allow us to determine all the intensities of the two phases. However, the ratio of the intensities of the strongest lines for Hg-1212 (102 and 103) and Hg-1223 (103 and 104) shows clearly that the Hg-1223 is the predominant phase in sample I (fig. 1).

The presence in sample I of the lower member together with the initial oxides, CuO and CaO, obviously indicates that the formation of Hg-1223 was not complete after a 3 h annealing period. The synthesis carried out at 900°C for 2 h led to the formation of Hg-1212 which was found to be the main phase in the sample together with the starting compounds. These data show that the formation of Hg-1223 occurs through the synthesis of the lower members of the series. The increase of the annealing

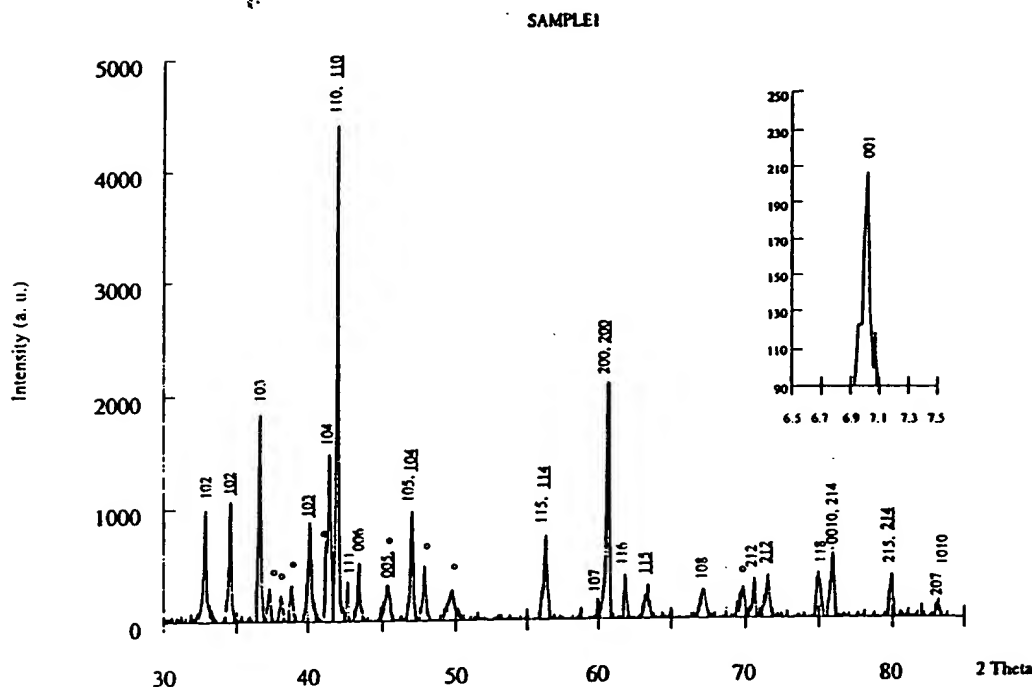


Fig. 1. X-ray powder pattern for sample I. Indexed XRD intensities correspond to Hg-1223 and Hg-1212 (underline). Impurities of CaO, CuO, CaHgO_2 and an unknown phase are marked by (*). The inset displays the characteristic intensity of 001 for Hg-1223.

time up to 3.5 and 4 h at 950°C and the same pressure led to the expected disappearance of Hg-1212 as well as of CaO. In these samples the formation of a new phase was detected. Its amount was relatively high (more than 50%) in samples annealed for 3.5 h (sample II). A total of 17 reflections of this phase were indexed on a tetragonal cell with lattice parameters $a=3.8540(3)$ Å, $c=19.006(3)$ Å. As for Hg-1223 no systematic absences were observed, leading to space group $P4/mmm$. Similar parameters were found by electron diffraction (see below). The c parameters of this phase corresponded to the value calculated from the formula $c \cong 9.5 + 3.2(n-1)$ for $n=4$. This strongly suggested that the new phase was the fourth member of the Hg-based series: $\text{HgBa}_2\text{Ca}_3\text{Cu}_4\text{O}_{10+\delta}$. The approximate cations ratio determined by EDS analysis of five well-crystallized and flat grains was Hg:Ba:Ca:Cu = 9(1):18(1):29(2):44(2). These data are in good agreement with the proposed formula for the new compound.

Besides Hg-1234 as the main phase, a smaller amount of Hg-1223 was present in sample II together with small amounts of CuO and of an unknown phase. This unknown phase was predominant in a sample treated for 5 h in the same conditions which did not contain any member of the Hg-based series and did not exhibit any superconductivity. The presence of the latter oxides can be explained as a result of the decomposition of Hg-1223 and the formation of Hg-1234. Hg-1212 was absent in this sample as well as in that annealed for 4 h. The X-ray diffraction pattern of sample II after background subtraction is shown in fig. 2. The ratio of the main intensities for both Hg-based layered cuprates, 104 for Hg-1223 and 105 for Hg-1234, shows that the latter was the main phase in this sample. As for sample I the overlapping of $hk0$ reflections for both phases occurs because of the similarity of the two a parameters. Moreover, the $hk6$ reflections of Hg-1234 are overlapped with the $hk5$ ones of Hg-1223.

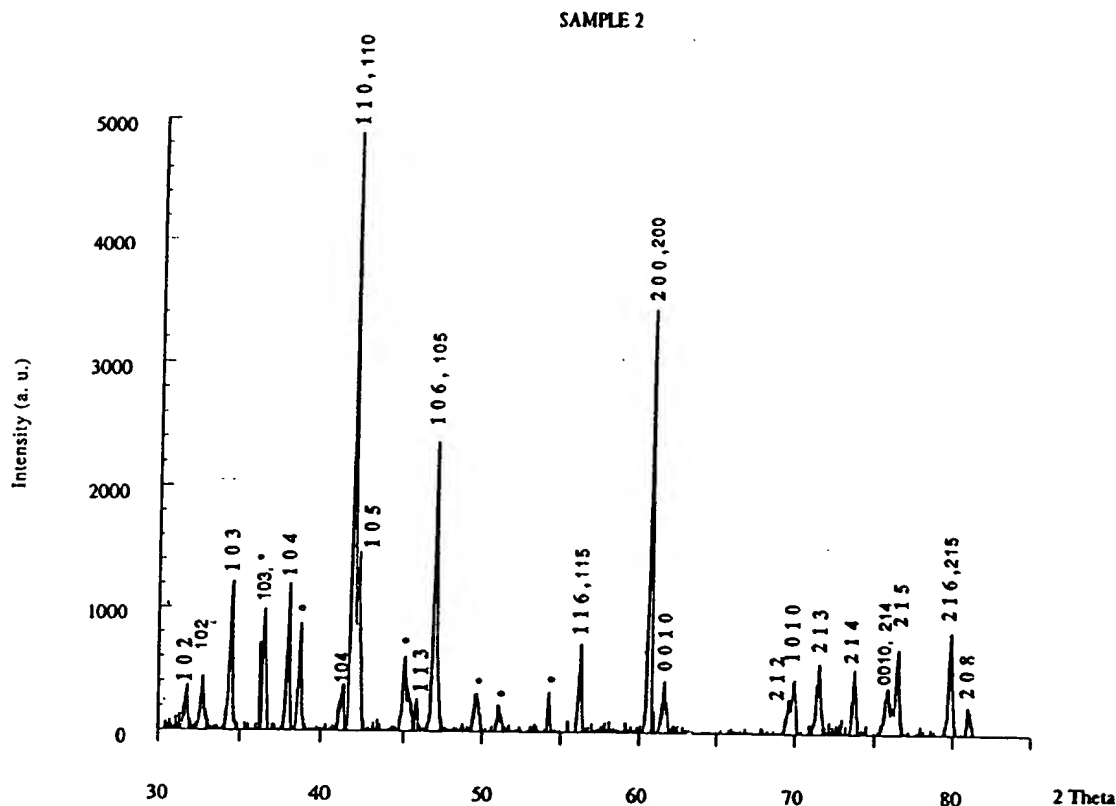


Fig. 2. X-ray powder pattern for sample II. Indexed XRD intensities correspond to Hg-1234 (bold) and Hg-1223. Impurities of CuO and an unknown phase are marked by (*).

3. Electron microscopy

The I and II samples were studied by electron microscopy. A suspension of crystals in acetone was grounded in an agate mortar. The crystallites were recovered from the suspension on a porous carbon film. A Philips EM 400T operating at 120 kV was used.

Figure 3 (a) and (b) shows two diffraction patterns obtained for sample I corresponding to the $[001]$ and the $\langle 110 \rangle$ zone axes of the $\text{HgBa}_2\text{Ca}_2\text{Cu}_3\text{O}_{8+\delta}$ (Hg-1223) phase, respectively. In both cases, the diffraction spots are sharp, which indicates that the crystal is well ordered. In fig. 3(b), one can notice a modulation of the intensity of the diffraction spots along the c^* -axis, with maxima for hkl reflections with $l=5n$ ($n=0, 1, 2, \dots$). On the micrograph (fig. 3(c)) corresponding to the diffraction pattern shown in fig. 3(b), one can see the very

regular periodicity of the fringes separated by 15.8 Å. During the observation under the electron beam, dark spots appeared near the edge of the crystal, probably due to the decomposition of the crystal.

Some diffraction patterns obtained for other crystals present diffuse lines parallel to the c^* -axis and passing through the Bragg spots (fig. 4 (a)). They are due to the presence of intergrowths as given evidence for by fig. 4(b). On this micrograph, two different spacings of 15.8 Å and 12.7 Å can be measured, attributed to Hg-1223 and Hg-1212, respectively.

In the case of sample II, almost all the observed crystallites have diffraction patterns corresponding to the Hg-1234 phase ($\text{HgBa}_2\text{Ca}_3\text{Cu}_4\text{O}_{10+\delta}$) with cell parameters $a=b=3.85$ Å and $c=19$ Å. Figure 5(a) and (b) give examples of the $[001]$ and $\langle 100 \rangle$ zone axes, respectively. As for Hg-1223, also for Hg-1234 the intensity of the Bragg spots varies according to

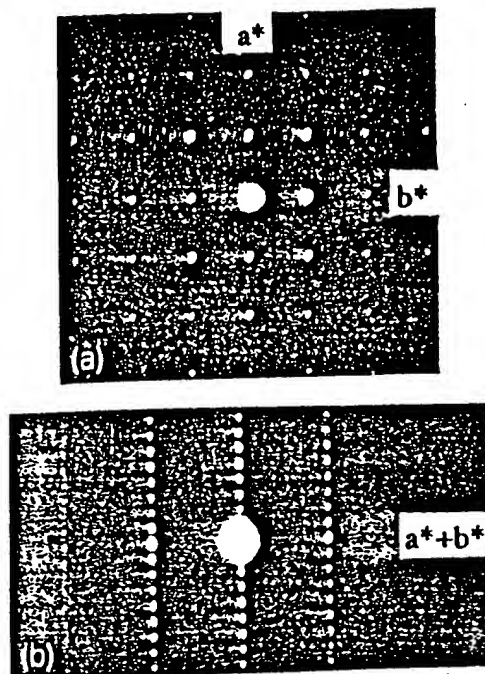


Fig. 3. Electron diffraction patterns of Hg-1223 taken along $[001]$ (a) and $[110]$ (b) zone axes. (c) Micrograph corresponding to the diffraction pattern (b). The interfringe spacing is 15.8 \AA .

the value of the l index, the maxima of intensity being obtained for $l=6n$ ($n=0, 1, 2, \dots$). This intensity pattern might be explained by the fact that $c/6$ is equal to 3.17 \AA , which corresponds to the distance between two neighboring (CuO_2) layers. The increase of the layer number n in the structure leads to the increase of the intensity of the hkl reflections with

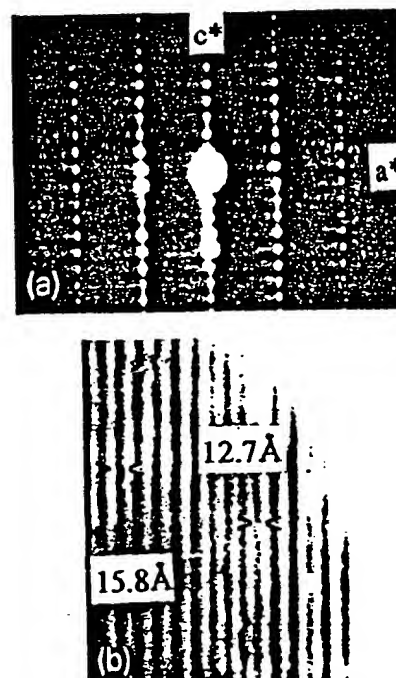


Fig. 4. Electron diffraction pattern of sample I along $\langle 100 \rangle$ and corresponding micrograph showing the intergrowths of Hg-1223 and Hg-1212.

$l=n+2$. These periodicities of the (CuO_2) layers explain the overlapping of such reflections on the X-ray powder pattern (see above). Most of the images taken along the $\langle 100 \rangle$ zone axis show very regular fringes separated by 19 \AA (fig. 5(c)). However, some crystals present intergrowths between the Hg-1223 and Hg-1234, as revealed in fig. 6. In this case, the following sequence is observed over about 500 \AA : $-19 \text{ \AA}-19 \text{ \AA}-19 \text{ \AA}-19 \text{ \AA}-19 \text{ \AA}-22 \text{ \AA}-$. On the corresponding diffraction pattern, besides the diffraction spots of the Hg-1234 phase, additional spots related to the 22 \AA periodicity are present. Such a periodicity may be attributed to a 1245 phase ($\text{Hg-Ba}_2\text{Ca}_4\text{Cu}_5\text{O}_{12+\delta}$). The fact that the extra diffraction spots are sharp indicates that this phase is well ordered at least over a certain number of cells in these crystals.

4. AC susceptibility measurements

The critical temperature T_c , and the apparent su-

beta

s of CuO

by 15.8 \AA
beam,
crystal,
ystal.
er crys-
xis and
). They
ven evi-
two dif-
mea-
g-1212.

bserved
onding
with cell
re 5(a)
)> zone
lg-1234
ding to

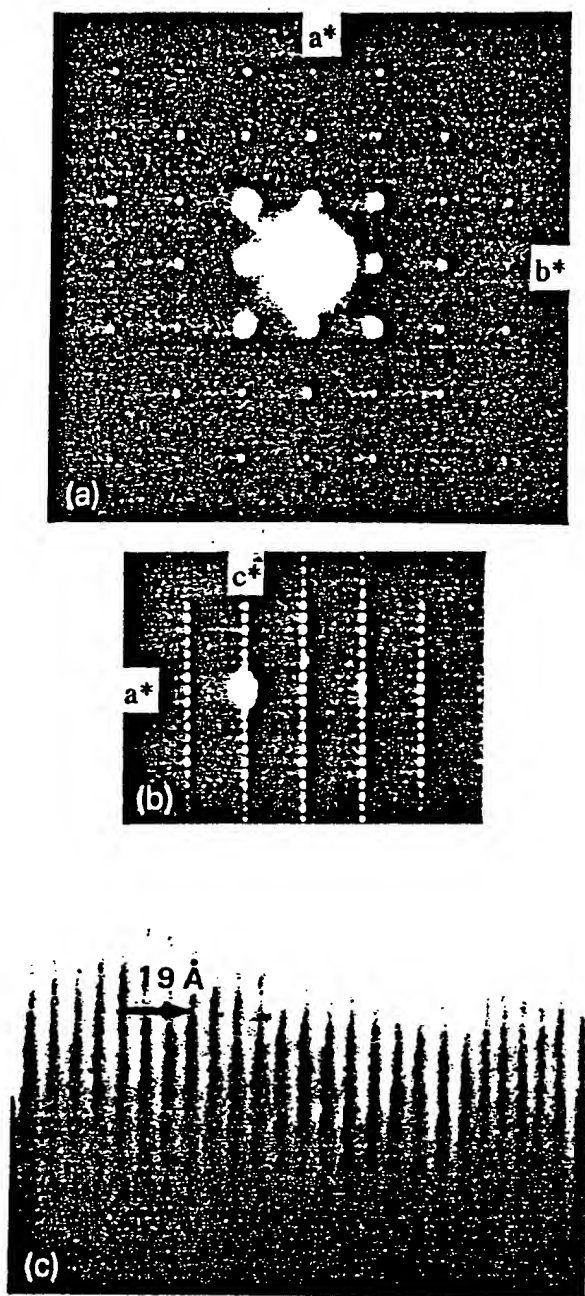


Fig. 5. Electron diffraction patterns of Hg-1234 taken along $[001]$ (a) and $\langle 100 \rangle$ (b) zone axes. (c) Micrograph corresponding to the diffraction pattern of (b). The interfringe spacing is 19 \AA .

perconducting volume of samples I and II have been determined from AC susceptibility measurements on fine powder samples. This avoids overestimates of the superconducting volume due to the larger screenings in sintered samples. The AC susceptibility was measured with an alternating maximum field of 0.01 Oe and a frequency of 119 Hz . The temperature was measured by a calibrated $100 \text{ } \Omega$ platinum thermometer.

The as-synthesized sample I undergoes a transition from the paramagnetic to the diamagnetic state with an onset above 133 K (fig. 7). Several measurements were made with the same sample and the reproducibility of T_c is $\pm 1 \text{ K}$ (mainly due to the thermal contact between the sample and the thermometer). The estimated magnetic susceptibility at 4 K corresponds to a large volume of ideal diamagnetism indicating the bulk nature of superconductivity. We can suggest that the sharp and large drop on the AC susceptibility curve above 133 K should correspond to the Hg-1223 phase because Hg-1212, which is present in this sample as the minority phase, has a T_c not higher than 126 K [3].

The as-synthesized sample II undergoes a transition from the paramagnetic to the diamagnetic state with an onset as high as 132 K . Actually, two onsets at two different temperatures are visible, the smaller one at 132 K and the larger one at about 126 K . There are two Hg-based layered cuprates in this sample: Hg-1234 as the main phase and Hg-1223 as the minority one. Taking into consideration the results of sample I, we might suggest that the first onset (132 K) corresponds to Hg-1223 and the larger one at the lower temperature (126 K) to Hg-1234. In any case, it is obvious that T_c for Hg-1234 is not higher than that for Hg-1223.

5. Discussion

The synthesized $\text{HgBa}_2\text{Ca}_2\text{Cu}_3\text{O}_{8+\delta}$ (Hg-1223) and $\text{HgBa}_2\text{Ca}_3\text{Cu}_4\text{O}_{10+\delta}$ (Hg-1234) phases are the third and the fourth members of the $\text{Hg-Ba}_2\text{Ca}_{n-1}\text{Cu}_n\text{O}_{2n+2+\delta}$ series, in analogy with those of Hg-1201 [1,7,8] and Hg-1212 [2] their structures can be schematized as containing rock-salt-like slabs, $(\text{BaO})(\text{HgO}_2)(\text{BaO})$, alternating with perovskite-like slabs, consisting in three (Hg-1223) or

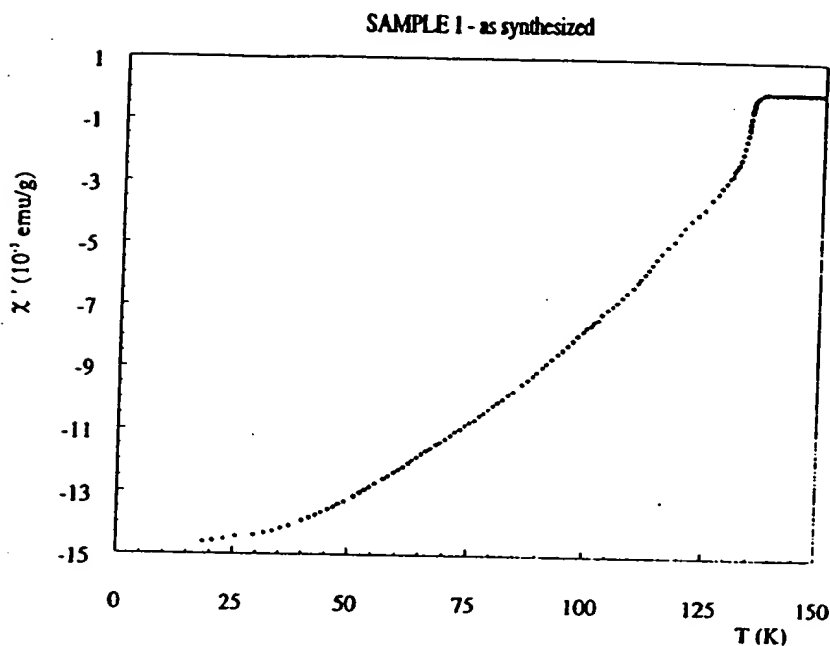


Fig. 7. AC susceptibility vs. T for as-synthesized sample I, where Hg-1223 is present as the main phase and Hg-1212 as the minority phase.

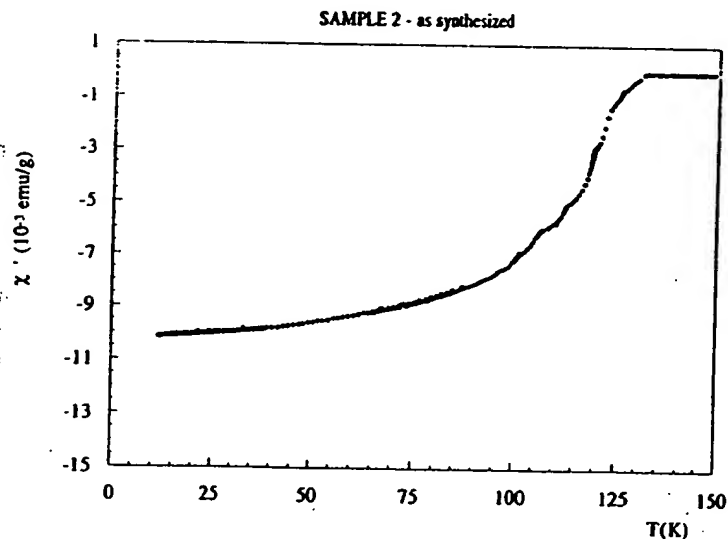


Fig. 8. AC susceptibility vs. T for as-synthesized sample II showing the presence of Hg-1234 as the main phase and of Hg-1223 as the minority phase.

1212. The appropriate treatment for Hg-1234 can possibly change T_c for this phase. Therefore, we can only conclude that for the as-prepared samples a saturation of T_c seems to occur in the Hg-Ba-Ca-Cu-O system at the third member. A similar behavior

occurs for the $\text{TlBa}_2\text{Ca}_{n-1}\text{Cu}_n\text{O}_{2n+3+\delta}$ homologous series, for which T_c increases up to the third member (120 K) also [9].

One can see in table 1 that for the Hg series, the increase of T_c is accompanied by a decrease of the a

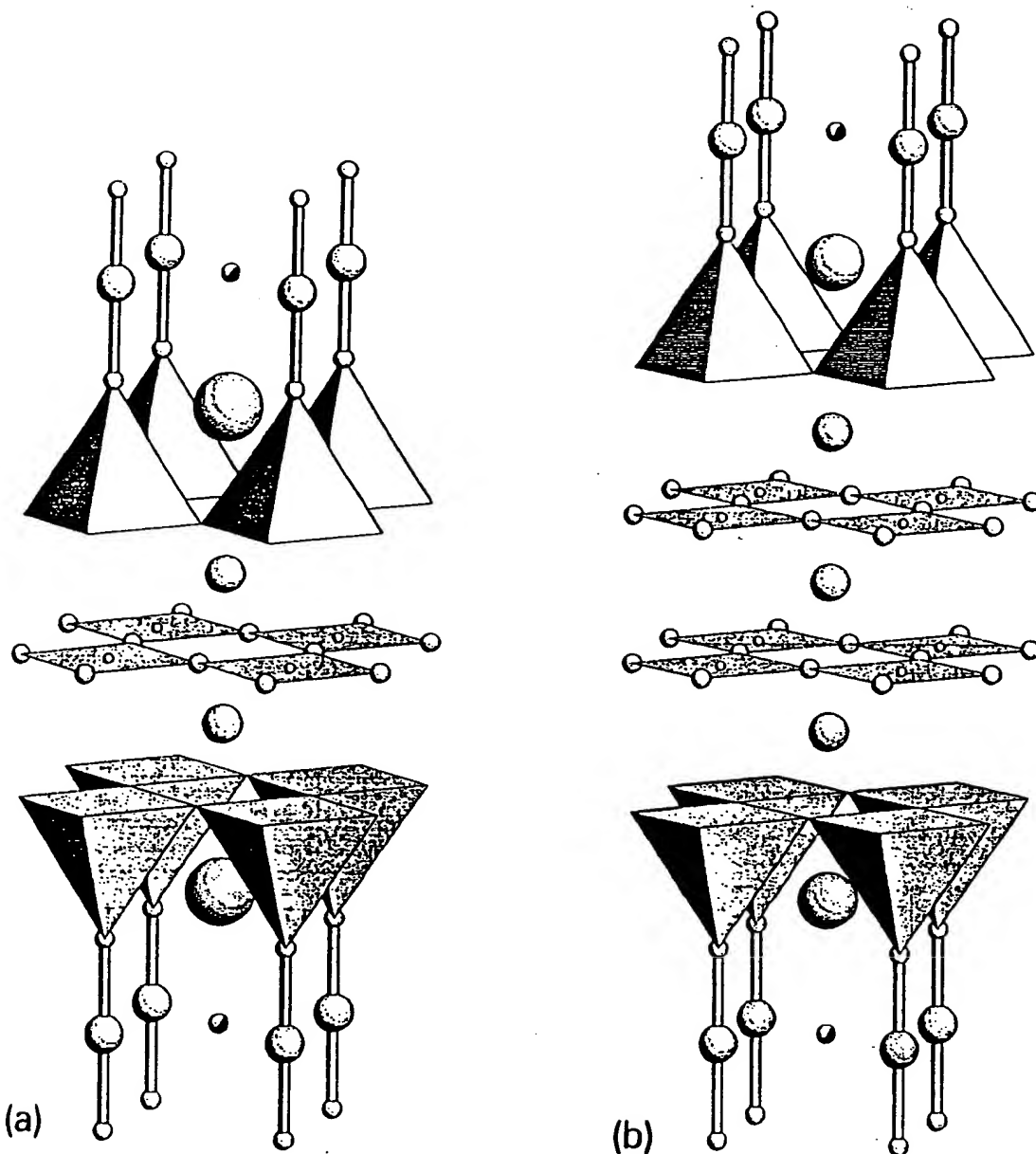


Fig. 9. The crystal structures of Hg-1223 (a) and Hg-1234 (b). The largest and medium large circles refer to Ba and Ca atoms, respectively. The Cu atoms are the smallest circles. Those at the base of the shaded pyramids are not shown. The circles forming the squares around the Cu are oxygen atoms. The dumbbells around the Hg atoms are formed by apical oxygen atoms. Partially filled circles refer to the partially occupied oxygen sites on the Hg layer.

parameter and just at T_c it remains practically constant between Hg-1223 and Hg-1234.

The electron microscopy study of Hg-1201 [10]

revealed the absence of intergrowths and this was attributed to the absence of the Ca^{2+} cations in the system. On the contrary, the addition of Ca layers in

Table I
Lattice parameters and transition temperatures for Hg-based Cu oxides

Formula	Short form	<i>a</i> (Å)	<i>c</i> (Å)	<i>T_c</i> (K)	Ref.
HgBa ₂ CuO _{4+δ}	Hg-1201	3.8797(5)	9.509(2)	94	[1]
HgBa ₂ CaCu ₂ O _{8+δ}	Hg-1212	3.8556(8)	12.652(4)	121	[2]
				126	[3]
HgBa ₂ Ca ₂ Cu ₂ O _{8+δ}	Hg-1223	3.8532(6)	15.818(2)	133	[4], this work
HgBa ₂ Ca ₃ Cu ₄ O _{10+δ}	Hg-1234	3.8540(3)	19.006(3)	< 132	this work

the system leads to intergrowths due to different numbers of (CuO₂) and Ca layers in the perovskite-like slabs. Such intergrowths were already reported in ref. [4]. Possibly, the occurrence of different intergrowths may explain why the variation versus temperature of the AC susceptibility does not present distinct and abrupt transitions which could be attributed to pure Hg-1212, 1223 and 1234 phases.

The synthesis of the higher members of the Hg-based homologous series as bulk samples has been performed at higher temperatures than that used for Hg-1212 and with longer treatment times. We suggest that the synthesis of such phases occurs through the formation at an initial state and subsequent decomposition of the lower members of the series. This feature is similar to that existing for the Tl-Ba₂Ca_{*n*-1}Cu_{*n*}O_{2*n*+3-δ} homologous series [9]. The use of high pressure, possibly, lowers the mercury oxide decomposition. It also leads to a decrease of stability of CaHgO₂, whose synthesis at the first stage of the reaction inhibits the formation of Hg-based compounds.

Acknowledgements

The authors would like to thank M.F. Gorius, M.

Perroux and R. Argoud for their technical assistance. The visit of EVA has been supported by the fund from the French Ministry of Foreign Affairs. EVA and SNP would like to thank the support of the Russian Scientific Council on Superconductivity (Project "Poisk"). SML was supported by the Erasmus Students Exchange Program.

References

- [1] S.N. Putilin, E.V. Antipov, O. Chmaissem and M. Marezio, *Nature* (London) 362 (1993) 226.
- [2] S.N. Putilin, E.V. Antipov and M. Marezio, *Physica C* 212 (1993) 266.
- [3] S.M. Loureiro and J.J. Capponi, private communication.
- [4] A. Schilling, M. Cantoni, J.D. Guo and H.R. Ott, *Nature* (London) 363 (1993) 56.
- [5] K.E. Johansson, T. Palm and P.-E. Werner, *J. Phys. E: Sci. Instrum.* 13 (1980) 1289.
- [6] S.N. Putilin, M.G. Rozova, D. Kashporov, E.V. Antipov and L.M. Kovba, *Zh. Neorganicheskoi Khimii* 36 (1991) 1645 (in Russian).
- [7] O. Chmaissem, Q. Huang, S.N. Putilin, M. Marezio and A. Santoro, *Physica C* 212 (1993) 259.
- [8] J.L. Wagner, P.G. Radaelli, D.G. Hinks, J.D. Jorgensen, J.F. Mitchell, B. Dabrowski, G.S. Knapp and M.A. Beno, *Physica C* 210 (1993) 447.
- [9] S. Nakajima, M. Kikuchi, Y. Syono, T. Oku, D. Shindo, K. Hiraga, N. Kobayashi, H. Iwasaki and Y. Muto, *Physica C* 158 (1989) 471.
- [10] I. Bryntse and S.N. Putilin, *Physica C* 212 (1993) 223.

BRIEF ATTACHMENT BJ

IN THE UNITED STATES PATENT AND TRADEMARK OFFICE

In re application of:

Date: November 6, 2006

Applicants: Bednorz, et al.

Docket: YO987-074BZ

Serial No.: 08/479,810

Group Art Unit: 1751

Filed: June 7, 1995

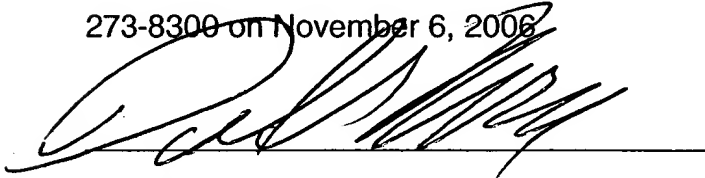
Examiner: M. Kopec

For: NEW SUPERCONDUCTIVE COMPOUNDS HAVING HIGH TRANSITION
TEMPERATURE, METHODS FOR THEIR USE AND PREPARATION

Commissioner for Patents
P.O. Box 1450
Alexandria, VA 22313-1450
(571) 273-8300

CERTIFICATE OF FACSIMILE TRANSMISSION

I hereby certify that this Ninth Response After Final Rejection (_4_ pages)
is being facsimile transmitted to the U.S. Patent and Trademark Office to (571)
273-8300 on November 6, 2006



Dr. Daniel P. Morris, Esq.
Reg. No. 32,053

NINTH SUPPLEMENTAL RESPONSE

Sir:

In response to Office Action dated October 20, 2005, please consider the
following:

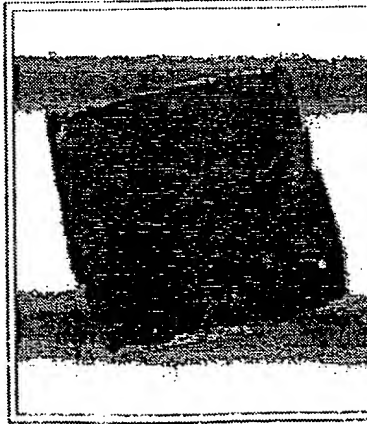
Bismuth strontium calcium copper oxide

From Wikipedia, the free encyclopedia

Bismuth strontium calcium copper oxide, or **BSCCO** (pronounced "bisko"), is a family of high-temperature superconductors having the generalized chemical formula $\text{Bi}_2\text{Sr}_2\text{Ca}_n\text{Cu}_{n+1}\text{O}_{2n+6}$.

Specific types of BSCCO are usually referred to using the sequence of the numbers of the metallic ions. Thus **BSCCO-2212** ($\text{Bi}_2\text{Sr}_2\text{Ca}_1\text{Cu}_2\text{O}_8$) has a critical temperature of 95 K and **BSCCO-2223** ($\text{Bi}_2\text{Sr}_2\text{Ca}_2\text{Cu}_3\text{O}_{10}$) has $T_c = 107$ K. Both these critical temperatures are above the temperature of liquid nitrogen. BSCCO was also the first high-temperature superconductor to be discovered which did not contain a rare earth element.

BSCCO-2212 is the first high-temperature superconductor to be used for making conducting wires. Although it has the same problems with weak links at crystal grain boundaries as YBCO, for BSCCO this can be overcome by a texture evolution during the rolling process due to Van-der-Waals coupled BiO layers, which are not present in YBCO. However, its critical current density in magnetic fields at elevated temperatures is about a factor 10 less than that of YBCO.

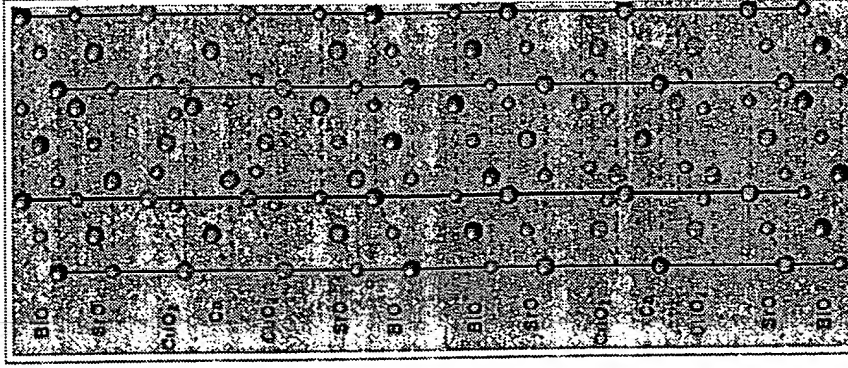


A small sample of the high-temperature superconductor BSCCO-2223. (The two lines in the background are 1 mm apart.)

Retrieved from

"http://en.wikipedia.org/wiki/Bismuth_strontium_calcium_copper_oxide"

Categories: Bismuth compounds | Strontium compounds | Calcium compounds
| High-temperature superconductors



The unit cell of BSCCO-2212. The other BSCCO family members have very similar structures: 2201 has one less CuO_2 in its top and bottom half and no Ca layer, while 2223 has an extra CuO_2 and Ca layer in each half.

- This page was last modified 14:15, 14 July 2006.
 - All text is available under the terms of the GNU Free Documentation License. (See Copyrights for details.)
- Wikipedia® is a registered trademark of the Wikimedia Foundation, Inc.

ATTACHMENT BK

IN THE UNITED STATES PATENT AND TRADEMARK OFFICE

In re Patent Application of

Applicants: Bednorz et al.

Serial No.: 08/479,810

Filed: June 7, 1995

For: NEW SUPERCONDUCTIVE COMPOUNDS HAVING HIGH TRANSITION
TEMPERATURE, METHODS FOR THEIR USE AND PREPARATION

Date: November 25, 2006

Docket: YO987-074BZ

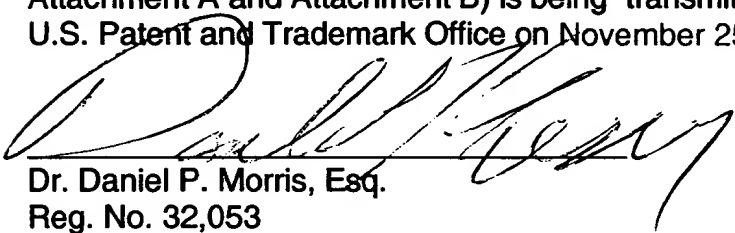
Group Art Unit: 1751

Examiner: M. Kopec

Commissioner for Patents
Box AF
P.O. Box 1450
Alexandria, VA 22313-1450

CERTIFICATE OF FIRST CLASS TRANSMISSION

I hereby certify that this Supplementary Response, (3 Pages Plus
Attachment A and Attachment B) is being transmitted by first class mail to the
U.S. Patent and Trademark Office on November 25, 2006.



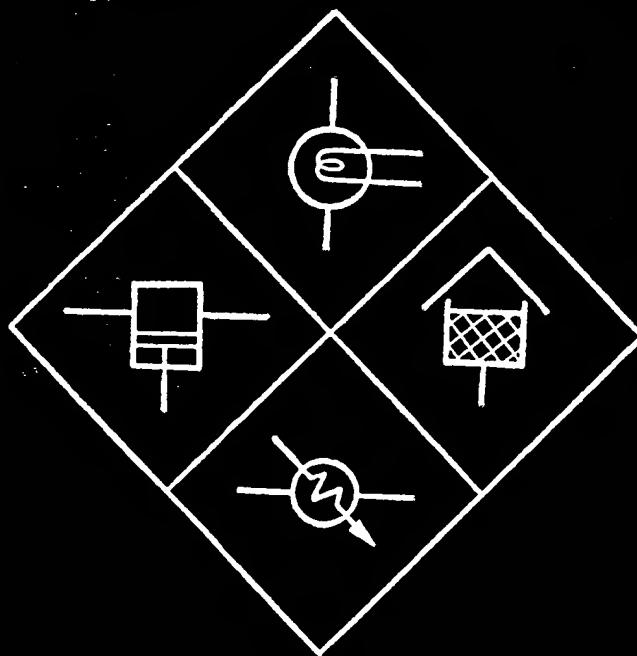
Dr. Daniel P. Morris, Esq.
Reg. No. 32,053

FOURTEENTH SUPPLEMENTARY RESPONSE

In response to the Office Action dated October 20, 2005 please consider the
following:

ATTACHMENT A

Cryogenic Engineering



Edited by
B.A.HANDS

YORE

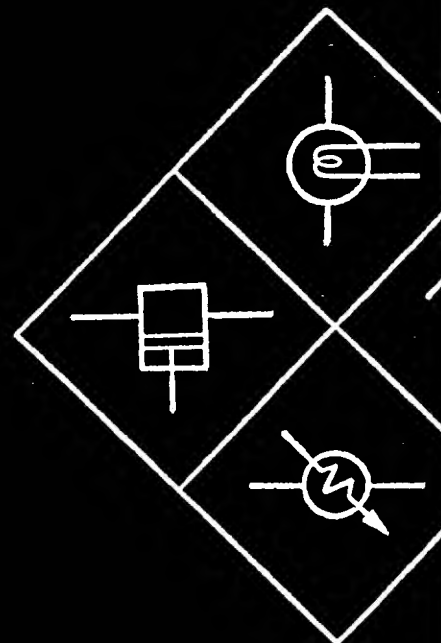
438929

TP 482.C74
1986
COPY 1

HANDS

Cryogenic Engineering

Cryogenic Engineering



Edited by
B.A.HAN

0.12.322990.1

TP
482.
C74

1986

YORE 1

Cryogenic Engineering

Edited by

B. A. Hands

*Department of Engineering Science, University of Oxford,
and St. Hilda's College, Oxford, England*

1986



Academic Press

Harcourt Brace Jovanovich, Publishers

London Orlando New York San Diego Austin
Boston Tokyo Sydney Toronto

ACADEMIC PRESS INC. (LONDON) LTD.
24/28 Oval Road, London NW1 7DX

United States Edition published by
ACADEMIC PRESS, INC.
Orlando, Florida 32887

Copyright © 1986 by
Academic Press Inc. (London) Ltd.

All rights reserved. No part of this book may be reproduced
or transmitted in any form or by any means, electronic or
mechanical, including photocopy, recording, or any
information storage and retrieval system without permission
in writing from the publishers

British Library Cataloguing in Publication Data

Cryogenic engineering.
1. Low temperature engineering
I. Hands, B.A.
621.5'9 TP482

ISBN 0-12-322990-1
ISBN 0-12-322991-X (Pbk)

Computer typeset and printed by
Page Bros (Norwich) Ltd

C. A. Bail
eering S
and Fell
R. A. Byrn
Formerly
Californ
D. Dew-H
versity o
versity C
D. Evans
00X, Er
E. J. Grego
Fordhou
B. A. Hand
eering Sc
and G.E
G. Krafft
Karlsruh
J. T. Morg
OX11 0C
N. Nambud
Bombay
Engineer
B. W. Rick
inghamsh
J. M. Robe
Establish
H. Sixsmitt
Hampshir
W. L. Swin
Hampshir
W. J. Tallis
Science, I
R. M. Thor
Chemical
T. J. Webst
England.

Contributors

- C. A. Bailey** University Lecturer, Cryogenics Laboratory, Department of Engineering Science, University of Oxford, Parks Road, Oxford OX1 3PJ, England and Fellow of Keble College, Oxford
- R. A. Byrns** Consultant, 2457 Marin Avenue, Berkeley, California 94708, U.S.A. *Formerly* Staff Senior Scientist, Lawrence Berkeley Laboratory, University of California, Berkeley, California 94720, U.S.A.
- D. Dew-Hughes** University Lecturer, Department of Engineering Science, University of Oxford, Parks Road, Oxford OX1 3PJ, England and Fellow of University College, Oxford
- D. Evans** Rutherford Appleton Laboratory, Chilton, Didcot, Oxfordshire OX11 0QX, England
- E. J. Gregory** Chief Process Engineer, Marston-Palmer Limited, Wobaston Road, Fordhouses, Wolverhampton WV10 6QJ, England
- B. A. Hands** Research Associate, Cryogenics Laboratory, Department of Engineering Science, University of Oxford, Parks Road, Oxford OX1 3PJ, England and G.E.C. Lecturer in Engineering, St. Hilda's College, Oxford
- G. Krafft** Koordinationstelle Technologietransfer, Kernforschungszentrum Karlsruhe GmbH, Postfach 3640, D-7500 Karlsruhe 1, West Germany
- J. T. Morgan** Rutherford Appleton Laboratory, Chilton, Didcot, Oxfordshire OX11 0QX, England
- N. Nambudripad** Tata Institute of Fundamental Research, Homi Bhabha Road, Bombay 400 005, India. *Formerly* of the Cryogenics Laboratory, Department of Engineering Science, University of Oxford
- B. W. Ricketson** Cryogenic Calibrations Limited, Pitchcott, Aylesbury, Buckinghamshire HP22 4HT, England
- J. M. Robertson** Heat Transfer and Fluid Flow Service, Atomic Energy Research Establishment, Harwell, Oxfordshire OX11 0RA, England
- H. Sixsmith** Creare Inc., PO Box 71, Great Hollow Road, Hanover, New Hampshire 03755, U.S.A.
- W. L. Swift** Creare Inc., PO Box 71, Great Hollow Road, Hanover, New Hampshire 03755, U.S.A.
- W. J. Tallis** Design Engineer, Cryogenics Laboratory, Department of Engineering Science, University of Oxford, Parks Road, Oxford OX1 3PJ, England
- R. M. Thorogood** Director, Cryogenic Research Programs, Air Products and Chemicals Inc., PO Box 538, Allentown, Pennsylvania 18105, U.S.A.
- T. J. Webster** Consultant, 38 Parkland Grove, Ashford, Middlesex TW15 2JR, England. *Formerly* Safety Manager, British Oxygen Company Ltd., England

Preface

The 1960s saw great activity in the field of cryogenic engineering, stimulated particularly by the American space effort and by developments in superconductivity. As a result, a number of books on cryogenic engineering in general were published. Since then, most volumes have concentrated on a particular aspect of the subject, rather than attempting a comprehensive review. In view of the steady, if unspectacular, advances made since that time, it seems opportune to attempt a new account of the basic science and of the engineering methods employed.

Cryogenic engineering covers a wide spectrum of disciplines, in traditional terms embracing much of electrical, mechanical and chemical engineering, its distinguishing feature being the use of temperatures well below ambient. In order to produce a volume of reasonable length, it was decided to assume that the reader should have knowledge appropriate to that of a final-year or graduate engineer or physicist. Further, since much of the body of knowledge of engineering at room-temperature can be applied directly to cryogenic problems, reference in such cases is made to standard textbooks, although since this book is biased towards engineering, the physicist may need to consult rather more of them than the engineer.

It was also decided, again on the grounds of overall length, to restrict the account of superconductivity. The design of superconducting magnets is very largely an electrical engineering problem, the cryogenic design, apart from training problems and stabilisation, being relatively straightforward. Further, the monograph "Superconducting Magnets" by M. N. Wilson (Oxford University Press, 1985) treats the subject comprehensively, and is required reading for anyone with other than a superficial interest in magnet design. Thus, the coverage of this topic is deliberately brief.

There are some other deliberate omissions, also. In particular, an account of refrigeration using hydrogen and neon is omitted, on the grounds that the techniques involved are broadly the same as those used for helium. Similarly, the particular problems involved with cryogenics in space are given only passing mention, since most of the design principles involved are also applicable to earth-based equipment. There is no attempt to provide complete property data; general trends are indicated, and, it is hoped, enough references for the reader to locate detailed data as necessary. However, since the book is intended for potential (and practising) cryogenic engineers, details of practical methods and current practices have been included.

The production of this book has been a co-operative effort, and I thank the authors for their tolerance of the editor's quirks. I should like to acknowledge those who have read parts of my own contributions and assisted with the provision of information, photographs and diagrams, particularly Dr A. Acton, Dr V. D. Arp, Mr R. J. Allam, Dr C. A. Bailey, Dr M. L. Christie, Dr. G. Davey, Prof G. B. Donaldson, Mr R. Harper, Dr D. B. R. Kenning, Dr R. D. McCarty, Dr W. Obert, Dr. C. Ruiz, Dr L. Solymar and Dr. R. M. Thorogood. Acknowledgements and sources for diagrams and photographs are given as appropriate in the text; I am most grateful to the organisations which supplied these and gave permission for their use. I am indebted to Johanne Beaulieu for preparing much of the text, to Mrs Judith Takacs for drawing the diagrams with her usual patience and skill, and to Mrs Stella Seddon for preparing the index. Finally, gratitude is due to my family for their tolerance, and for foregoing the use of the dining table for many months.

Oxford, 1985

B. A. Hands

In the tables of data, a dash indicates that information was not available.

Contributo
Preface

1.1 Introd
1.2 The C
1.3 Featur
1.4 Liquef
1.5 Air Se
1.6 Liquic
1.7 Liquic
1.8 Super
1.9 Cryog
1.10 Cryog
1.11 Medic
1.12 Cryop
1.13 Instru
Refere
Journ
Gener
Bibliog
Non-sq

2.1 Introdu
2.2 Propert
2.3 Hydrog
2.4 Helium
2.5 Equatic

PREFACE

and I thank the
knowledge those
the provision of
Dr V. D. Arp,
ay, Prof G. B.
Carty, Dr W.
nowledgements
in the text; I
permission for
of the text, to
and skill, and
e to my family
many months.

A. Hands

able.

Contents

Contributors
Preface

v
vii

1. A Survey of Cryogenic Engineering

B. A. Hands

1.1 Introduction	1
1.2 The Cryogenic Temperature Range	2
1.3 Features of Cryogenic Engineering	3
1.4 Liquefied Natural Gas (LNG)	6
1.5 Air Separation	10
1.6 Liquid Hydrogen	15
1.7 Liquid Helium	18
1.8 Superconducting Magnets and Machinery	19
1.9 Cryogenic Electronics	26
1.10 Cryogenics in Space	29
1.11 Medical and Biological Applications	29
1.12 Cryopumping	30
1.13 Instrumentation	33
References	34
Journals	36
General Bibliography	36
Bibliography of Specific Topics	36
Non-specialist Reading	37

2. Properties of the Cryogenic Fluids

B. A. Hands

2.1 Introduction	39
2.2 Property Data	40
2.3 Hydrogen	43
2.4 Helium	46
2.5 Equations of State	50

2.6 The Two-phase Region	54	5.9
2.7 Computer Packages	56	5.10
2.8 Approximate Equations	58	5.11
2.9 Properties of Mixtures	59	5.12
References	63	5.13
Sources of Data	63	5.14

3. Cryogenic Safety

T. J. Webster

3.1 Introduction	67	
3.2 Organisation for Safety	68	6.1 I
3.3 Relationship between Fluid Properties and Safety	68	6.2 I
3.4 First Aid	76	6.3 I
3.5 Combustion	77	6.4 I
3.6 Oxygen Hazards	79	6.5 I
3.7 Unexpected Hazards	83	6.6 I
3.8 Fluorine Safety	87	I
Bibliography	87	

4. Thermal Design

C. A. Bailey and B. A. Hands

4.1 Conservation of Energy Considerations	89	7.1 I
4.2 General Energy Requirements	90	7.2 I
4.3 Specific Heat	93	7.3 F
4.4 Thermal Contraction	97	7.4 F
4.5 Thermal Conductivity of Solids	100	F
4.6 Conduction through Gases	106	
4.7 Radiative Heat Transfer	107	
4.8 Thermal Insulations	112	
4.9 Applications to Design	116	
References	121	
Bibliography	121	

8.1 I
8.2 R
8.3 C
8.4 P
R

5. Fluid Dynamics

B. A. Hands

5.1 Introduction	123	
5.2 Pressure Drop Calculations	124	
5.3 Single-phase Pressure Drop	125	
5.4 Characteristics of Two-phase Flow	128	
5.5 Two-phase Pressure Drop	130	
5.6 Critical (Choked) Flow	131	9.1 I
5.7 Cooldown Behaviour	131	9.2 S
5.8 Introduction to Instabilities	132	9.3 F

CONTENTS

54
56
58
59
63
63

CONTENTS

- 5.9 Density Wave Oscillations
5.10 The Ledinegg Instability and Pressure-drop Oscillations
5.11 Geysering
5.12 Thermoacoustic Oscillations
5.13 Stratification, Thermal Overfill and Rollover
5.14 Sloshing
References

xi

134
136
138
141
143
146
148

6. Heat Transfer to Fluids

J. M. Robertson

67
68
68
76
77
79
83
87
87

- 6.1 Introduction
6.2 Heat Transfer to Single-phase Fluids
6.3 Heat Transfer Rates
6.4 Pool Boiling
6.5 Boiling in Channels
6.6 In-tube Condensing
References

151
153
156
157
160
166
168

7. Heat Transfer Below 10 K

G. Krafft

89
90
93
97
100
106
107
112
116
121
121

- 7.1 Introduction
7.2 Basic Considerations
7.3 Heat Transfer to Supercritical Helium
7.4 Heat Transfer to Two-phase Helium
References

171
172
174
181
191

8. Heat Exchangers

E. J. Gregory

- 8.1 Introduction
8.2 Regenerators
8.3 Coiled Tube Heat Exchangers
8.4 Plate and Fin Heat Exchangers
References

193
195
197
199
216

9. Electrical Conductors at Low Temperatures

D. Dew-Hughes

123
124
125
128
130
131
131
132

- 9.1 Introduction
9.2 Simple Theory of Electrical Resistivity
9.3 Real Conductors at Low Temperatures

217
219
221

9.4 Magnetoresistance	223	1
9.5 Superconductivity	225	
9.6 Theories of Superconductivity	229	
9.7 Flux-pinning and Critical Current Density	232	
9.8 Conductor Stability	235	13.1
9.9 Stress Effects	236	13.2
9.10 Commercial Superconductors	238	13.3
Bibliography	240	13.4
		13.5
		13.6
		13.7
		13.8
		13.9
		13.10
		13.11

10. Mechanical Design with Metals

B. A. Hands

10.1 Introduction	241	
10.2 Elastic Moduli	242	
10.3 Plastic Behaviour	243	
10.4 Fracture Behaviour	246	
10.5 Fatigue Behaviour	252	
10.6 Aluminium Alloys	254	
10.7 Stainless Steels	257	
10.8 Nickel-Iron Alloys	262	
10.9 Titanium Alloys	265	14.1 Ir
10.10 Copper Alloys	266	14.2 T
10.11 General Discussion	267	14.3 G
References	269	14.4 P
Bibliography	270	14.5 T
		14.6 P
		14.7 C
		R

11. Design with Non-metallic Materials

D. Evans and J. T. Morgan

11.1 Introduction	271	
11.2 Mechanical Properties of Polymers and their Relation to Structure	276	
11.3 Thermal Contraction	285	15.1 S
11.4 Thermal Conductivity	289	15.2 I
Bibliography	292	15.3 T
		15.4 I
		15.5 C
		15.6 I
		15.7 I
		15.8 C
		15.9 I
		15.10 I
		15.11 I
		15.12 T
		15.13 I
		15.14 I

12. Construction and Assembly Methods

W. J. Tallis

12.1 General Design Considerations	293	
12.2 Permanent Joints	295	
12.3 Demountable Joints	302	
12.4 General Comments	309	

CONTENTS

223
225
229
232
235
236
238
240

241
242
243
246
252
254
257
262
265
266
267
269
270

271
276
285
289
292

293
295
302
309

CONTENTS

xiii

13. Principles of Refrigeration, Liquefaction and Gas Separation

C. A. Bailey and B. A. Hands

13.1 Refrigeration	313
13.2 Liquefaction	314
13.3 Cooling Methods	316
13.4 Simple Cycles	320
13.5 Irreversibility	324
13.6 Second Law Violations	324
13.7 Compound Cycles	325
13.8 The Separation of Gases	328
13.9 Principles of Distillation	329
13.10 The Single Column Linde System	336
13.11 The Double Column	339
References	340

14. Cryogenic Turbines and Pumps

H. Sixsmith and W. L. Swift

14.1 Introduction	341
14.2 Turboexpander Design	342
14.3 Gas Bearings	344
14.4 Protective Devices	348
14.5 Turbine Performance	349
14.6 Pumps	352
14.7 Conclusions	355
References	355

15. Large Helium Refrigeration and Liquefaction Systems

R. A. Byrns

15.1 Specification of Heat Load and Capacity	357
15.2 Design of J-T Stage	360
15.3 The Claude Cycle	362
15.4 Design and Optimisation	364
15.5 Compressors	366
15.6 Heat Exchangers	368
15.7 Expanders	369
15.8 Control, Instrumentation, Purity and Gas Management	371
15.9 Distribution and Cooling Methods	372
15.10 Large Helium Plants	375
15.11 Large Purification Liquefiers	375
15.12 The 1500 W Refrigerator	376
15.13 Lawrence Livermore National Laboratory (3000 W) System	379
15.14 Fermi National Accelerator Laboratory (23 kW) System	381

15.15 Brookhaven 24.8 kW Refrigerator	388
15.16 Refrigeration Equipment Cost	389
References	389

16. Large Gas Separation and Liquefaction Plants

R. M. Thorogood

16.1 Introduction	391
16.2 Cryogenic Air Separation Processes	392
16.3 Natural Gas Processes	409
16.4 Natural Gas Liquefaction Processes	411
16.5 Equipment for Large Air Separation Plants	418
16.6 Equipment for Natural Gas Plants	424
16.7 Operation and Safety	427
Acknowledgements	428
References	428

17. Small Refrigerators

N. Nambudripad

17.1 Introduction	431
17.2 The Stirling Refrigerator	433
17.3 The Gifford-McMahon Refrigerator	438
17.4 The Pulse-tube Refrigerator	441
17.5 The Vuilleumier Refrigerator	443
17.6 Losses in Regenerative Mechanical Coolers	445
17.7 Regenerators	447
17.8 Magnetic Refrigeration	452
References	453

18. Thermometry

B. W. Ricketson

18.1 Introduction	457
18.2 Temperature and Accuracy	458
18.3 Criteria for Choosing a Sensor	459
18.4 Sensors	460
18.5 Thermal Anchorage for Electrical Leads	467
18.6 Measurement	468
18.7 Temperature from the Measurement	473
18.8 Conclusion	476
References	476

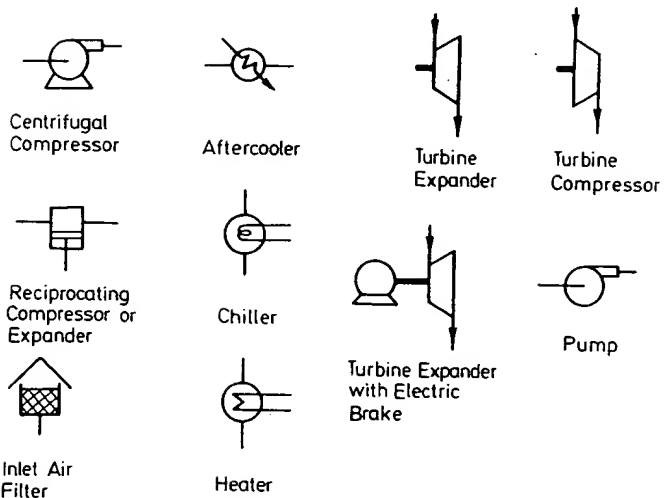
Appendix	477
Index	485

CONTENTS

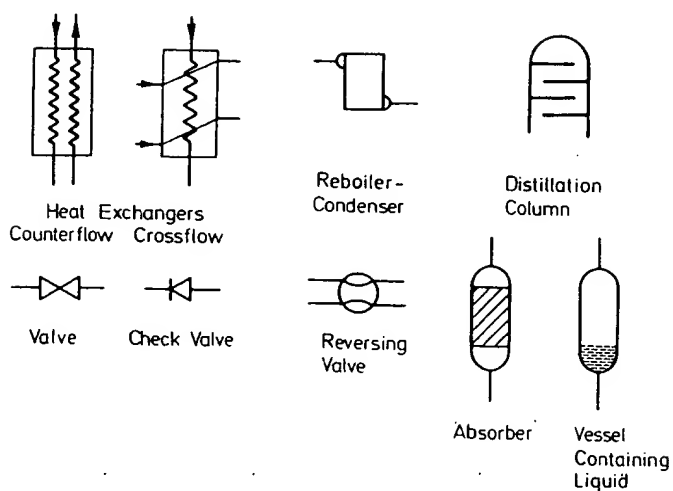
388
389
389

Symbols Used

391
392
409
411
418
424
427
428
428



431
433
438
441
443
445
447
452
453



457
458
459
460
467
468
473
476
476

477
485

A Survey of Cryogenic Engineering

B. A. HANDS

1.1 Introduction	1
1.2 The Cryogenic Temperature Range	2
1.3 Features of Cryogenic Engineering	3
1.4 Liquefied Natural Gas (LNG)	6
1.5 Air Separation	10
1.6 Liquid Hydrogen	15
1.7 Liquid Helium	18
1.8 Superconducting Magnets and Machinery	19
1.9 Cryogenic Electronics	26
1.10 Cryogenics in Space	29
1.11 Medical and Biological Applications	29
1.12 Cryopumping	30
1.13 Instrumentation	33
References	34
Journals	36
General Bibliography	36
Bibliography of Specific Topics	36
Non-specialist Reading	37

1.1 Introduction

Most of this book is concerned with an outline of the theory and practice of cryogenic engineering. It has not been possible within a volume of reasonable size to explore every aspect in detail, nor has it been possible to give a detailed account of all the applications of cryogenics. This chapter is intended to give an impression of the wide range of cryogenic engineering. After a discussion of the meaning of cryogenics, the chapter covers the uses of the commoner cryogenic liquids (natural gas, oxygen, nitrogen, hydrogen and helium), and then deals with superconductivity and cryo-

pumping. The chapter concludes with a brief outline of cryogenic instrumentation.

1.2 The Cryogenic Temperature Range

The 1960s were a decade which saw a rapid expansion both in low-temperature physics and in the commercial exploitation of low-temperature techniques. Towards the end of this period, a need was felt for the standardisation of low-temperature terminology, and, on the initiative of Professor Nicholas Kurti, the Comité d'étude des termes techniques français organised a meeting in 1969, at which was formed a small international committee to consider the terminology of low temperatures, remembering the necessity of unambiguous translation between English and French, and paying due regard to current practice in the United States. As an example of the confusion which then existed, temperature levels in Britain were, by some people, referred to as 'low' (below 0°C), 'very low' (around 100 K), 'deep low' (around 4 K) and 'ultra low' (less than 0.3 K), although the French had only two terms 'basse' and 'très basse'. It was never clear how the British users of this terminology would refer to temperatures in the microkelvin region!

The working group, with members from six countries, made its recommendations in 1971 [1.1], and these have largely been accepted by the scientific community. 'Cryogenics' and the corresponding prefix 'cryo' were to refer to 'all phenomena, processes, techniques or apparatus occurring or used at temperatures below 120 K' approximately, that is, around or below the normal boiling point of liquefied natural gas. It was recognised, however, that some inconsistencies were unavoidable, in particular the use, on historical grounds, of the terms cryohydrate, cryoscopy, cryochemistry and the French cryodessication, all of which refer to temperatures well above 120 K; and, because they use cryogenic fluids and techniques, cryosurgery, cryomedicine and cryobiology. Otherwise, the temperature range between 120 K and 0°C is covered by 'refrigeration' technology.

The scientific community has, on the whole, adhered to these proposals, but they have not been rigidly adopted by industry, where the technology of handling liquid ethylene (at around 150 K) is, with some justification on the grounds of the equipment used, included in the cryogenic domain, and 'cryogenic' is also used, with less justification, to describe equipment designed for use at still higher temperatures. However, since all fluids and materials used in cryogenics must at some time be brought to room temperature, properties and processes in the temperature range up to room temperature cannot be ignored.

1. A SURVEY OF CRYOGENICS

In this book, we shall refer to 'cryogenic engineering' to refer to the most widely used liquefied natural gas and liquid hydrogen (LH2). The importance of hydrogen in the temperature range, the product of which is regarded as 'physics' at present to experimental demagnetisation and will be covered in this volume.

1.3 Features of Cryogenics

It is worth considering 'ordinary' (or room temperature) properties of materials that the properties of a particular material accepted that, in fact, they behave similarly to cryogenic materials. The ability to recognise and use the use of low temperature different from that of room temperature. The design criteria with identification of methods to achieve cryogenic should, therefore, be in its own right.

There are, however, engineering temperature ranges—fluidity—the ability of a material to be a superfluid state has been achieved. The superfluid state has been achieved. The other phenomena of electrical resistance different for each material.

* According to [1.1], the wide acceptance.

cryogenic

In this book, we follow the 1971 recommendation and take 'cryogenic engineering' to refer to the temperature range below about 120 K. The most widely used liquids, in order of descending normal boiling point, are liquefied natural gas (LNG), liquid oxygen (LOX), liquid nitrogen (LIN), liquid hydrogen (LH₂) and liquid helium (LHe), although at present the importance of hydrogen has declined. At the lower end of the temperature range, the production of temperatures less than about 1.5 K may be regarded as 'physics' rather than 'engineering', since their use is restricted at present to experimental work. Therefore, techniques such as adiabatic demagnetisation and the use of the light isotope of helium (He³) will not be covered in this volume.

1.3 Features of Cryogenic Engineering

It is worth considering at this stage the differences between cryogenic and 'ordinary' (or room temperature) engineering. For a long time, it was felt that the properties of cryogenic fluids were in some way peculiar, so that a particular mystique arose around this area of engineering. It is now accepted that, in fact, cryogenics (with the exception of superfluid helium) behave similarly to other fluids, and that the art of cryogenics lies in the ability to recognise and cater for the particular problems which arise through the use of low temperatures *per se*. This requirement is, of course, no different from that required in any other branch of engineering: an assessment of design criteria and possible causes of equipment failure, together with identification of the best techniques, materials and construction methods to achieve safe, efficient and reliable operation. Cryogenics should, therefore, be regarded more as a special art rather than as a subject in its own right.

There are, however, two phenomena peculiar to the cryogenic engineering temperature range which merit special consideration. One is superfluidity—the ability of liquid helium to behave as if it has zero viscosity. The superfluid state has been investigated by both experimental and theoretical physicists for many years, and a deep understanding of its behaviour has been achieved. From the engineer's point of view, it is of interest because of the very high rates of heat transfer which can be attained.

The other phenomenon is that of superconductivity,* the complete loss of electrical resistance below some well-defined temperature which is different for each metal. Superconductivity is of increasing technical import-

* According to [1.1], the proper term is superconduction, but this word has never achieved wide acceptance.

ance in the provision of high and very stable magnetic fields, and its application to heavy electrical engineering is being extensively studied. In 1962, the discovery of the Josephson effect opened the door to a new range of superconducting electronic devices.

The penalty of operating in the cryogenic temperature range is that work must be done to reach and maintain the low temperature required; from the second law of thermodynamics, it is clear that the work will increase roughly in inverse proportion to the magnitude of the absolute temperature. For instance, to extract 1 J of heat reversibly at 77 K requires about 3.7 J of work, while to extract 1 J at 4.2 K requires about 68 J of work. In practice, of course, reversibility cannot be achieved, and the work actually required is somewhat larger, by a few tens of percent at the higher cryogenic temperatures, to a factor of ten in the liquid helium range. Thus, on economic grounds there is every incentive to avoid the use of cryogenics wherever possible.

Cryogenics can be considered to have been born towards the end of 1877, when the first liquefaction of oxygen was achieved, by Raoul Pictet in Geneva, Switzerland, and by Louis Cailletet in Chatillon-sur-Seine in France.* Each used a different technique. Pictet's was to cool oxygen at 470 bars to about 140 K using successively liquid sulphur dioxide and solid carbon dioxide, at which temperature he allowed the oxygen to escape through a valve, and saw a mixture of liquid and vapour in the resulting jet. Cailletet, on the other hand, cooled his oxygen to only -29°C using liquid sulphur dioxide, and then performed an adiabatic expansion to form a mist of droplets in his glass vessel. It is perhaps of interest to observe that Pictet's method of 'cascade' cooling followed by Joule-Thomson expansion is still used in many designs of refrigerator and liquefier, although usually in association with external-work machines.

The next significant step was the invention of the vacuum flask by James Dewar, which enabled liquefied gases to be stored for long periods and paved the way for the liquefaction of hydrogen and helium. Until Dewar's invention, the liquids were stored in the innermost of a number of concentric vessels, each containing in turn a boiling liquid of higher temperature. The vacuum insulated, glass flask is now well known to the general public as a 'Thermos'; in the scientific community the name 'dewar' is preferred and is also used for small storage vessels of metallic or polymeric construction.

Developments during the next two decades proceeded apace, with Claude in France and Linde in Germany developing techniques for the liquefaction and fractional distillation of air to produce oxygen and nitrogen, and

* Which scientist was first is of no concern to us here, nor is the ensuing controversy, which has been discussed recently by Kurti [1.2].

1. A SURVEY

forming cor today to m the 'permar afterwards j above the li plentiful su Leiden from especially fo

Between t production (process of 'a: 100 m³ (100 t was still a co duction being basis, and the the world.

Immediate Massachusset liquefier usin making liquid the same tim during the 192 comparatively

As a result, produced in q conducting ma was readily ava those research since the savir water-cooled s As confidence constructed, so tens of supercc refrigerators in engines were d several kilowatt

As to the fut argon by the frac process for man present forms a v in importance as are developed. F

olds, and its
y studied. In
a new range

is that work
quired; from
will increase
emperature.
; about 3.7 J
of work. In
ork actually
er cryogenic
e. Thus, on
f cryogenics

the end of
Raoul Pictet
sur-Seine in
ol oxygen at
de and solid
n to escape
he resulting
-29°C using
sion to form
observe that
n expansion
ugh usually

sk by James
periods and
til Dewar's
f concentric
ature. The
l public as a
eferred and
onstruction.
with Claude
liquefaction
rogen, and

roversy, which

forming companies which are still in the forefront of cryogenic engineering today to market their inventions. Finally, in 1908, helium, the last of the 'permanent' gases, was liquefied by Kamerlingh Onnes, who shortly afterwards produced superfluid helium by reducing the vapour pressure above the liquid using a vacuum pump. It is worth noting, in these days of plentiful supplies, that Onnes's helium was painstakingly extracted at Leiden from large quantities of monazite sand imported from India especially for the purpose.

Between the two World Wars, there was a steady development in the production of oxygen and nitrogen by the distillation of liquid air (the process of 'air separation'), and during the 1930s plants producing around 100 m³ (100 t) of liquid oxygen per day were in operation. Liquid helium was still a comparatively rare and expensive commodity, the rate of production being limited to a litre or two per hour, often only on an intermittent basis, and the liquid being available in only very few laboratories throughout the world.

Immediately after the Second World War, Professor Sam Collins, at the Massachusetts Institute of Technology, developed a new design of helium liquefier using reciprocating expansion engines, which was capable of making liquid on a continuous basis at a rate of several litres per hour. At the same time, the extraction of helium from natural gas wells, begun during the 1920s, had greatly increased, so that helium gas, although still comparatively expensive, was no longer a rare commodity.

As a result, when, during the 1960s, Type II superconducting wire was produced in quantity on a commercial basis, enabling high-field superconducting magnets to be constructed for the first time, liquid helium was readily available for cooling. This development was quickly exploited by those research establishments concerned with high-energy nuclear physics, since the saving in energy costs compared with those of an equivalent water-cooled system quickly outweighed the much higher capital cost. As confidence was gained, magnets of increasingly complex design were constructed, so that each of the major laboratories now contain several tens of superconducting magnets. In parallel with these developments, refrigerators incorporating expansion turbines rather than reciprocating engines were developed; a number of refrigerators capable of extracting several kilowatts at 4 K have now been built.

As to the future, it is clear that the production of oxygen, nitrogen and argon by the fractional distillation of liquid air will remain a major industrial process for many years. The transport of liquefied natural gas by sea at present forms a vital link in the world's fuel supply system, but will decrease in importance as supplies of natural gas diminish and other energy sources are developed. Hydrogen may well be one of these fuels, but at present in

energy terms it is expensive to produce, requiring large amounts of primary energy, and the liquefaction process also consumes much energy. Liquid hydrogen, therefore, may never be economically viable as a fuel other than for a few specialised applications.

Superconducting magnet technology has assumed great importance, and since it is economically attractive compared with the use of conventional magnets and can also produce more uniform and time-invariant fields, applications are expanding. For a number of years, superconducting magnets have been routinely manufactured for experimental work in physics and chemistry, notably for nuclear magnetic resonance (NMR) and electron spin resonance (ESR). These methods have recently been extended to biological applications and now to medical diagnosis. This latter provides the first truly large-scale, commercial application of superconductivity.

Although superconducting motors, generators, transmission lines, and so on have been under active development in a number of countries, the scenario so far has been that each advance in superconducting electrical engineering has been matched by an advance in the corresponding room-temperature technology. Since the latter is usually less complex, it has been more attractive on the grounds of both cost and reliability.

In electronic engineering, the Josephson effect opened new prospects in the precise determination of voltage, in the measurement of very small magnetic fields and in rf applications. Devices based on the Josephson effect are now used on a routine basis.

Thus, although cryogenics is a field of relative antiquity, there has been an unusually long time between the discovery of some phenomena and their commercial exploitation. This was particularly so in the case of superconductivity, which was discovered in 1911 but only ceased to be a laboratory curiosity some 50 years later. On the other hand, devices using the Josephson effect were marketed within a few years of its prediction and discovery.

1.4 Liquefied Natural Gas (LNG)

Natural gas is typically composed of 85–95% methane, the remainder being mainly nitrogen, ethane, propane and butane, although quantities of heavier hydrocarbons, carbon dioxide, water, sulphur compounds and, occasionally, mercury, may also be present, the precise composition depending upon the reservoir from which it is extracted. Certain sources, notably in Kansas, are comparatively rich (about 0.4%) in helium and are the major sources of this element. Natural gas is extracted by drilling in a way similar to that used for oil production and is somewhat refined before

1. A SUR

use: the
or as liq
reduced.

Natur:
century
pipeline
of Amer
relied en
of Japan
Europe :

Y

19

19

19

19

1980

1990

* F

Sources
with the r
of large de
southward
is liquefie
decrease i
pressurisa

The fir
from Lake
and as a re
to Canvey
Twenty ye
Europe, fi

amounts of primary
uch energy. Liquid
as a fuel other than

at importance, and
use of conventional
ne-invariant fields;
perconducting mag-
tal work in physics
NMR) and electron

been extended to
This latter provides
perconductivity.
mission lines, and
er of countries, the
conducting electrical
rresponding room-
omplex, it has been
ility.

ed new prospects in
ment of very small
l on the Josephson

ity, there has been
ne phenomena and
so in the case of
only ceased to be a
hand, devices using
of its prediction and

ane, the remainder
though quantities of
ir compounds and,
recise composition
ed. Certain sources,
s) in helium and are
cted by drilling in a
what refined before

use: the heavier hydrocarbons are separated as natural gas liquid (NGL) or as liquefied petroleum gas (LPG), and the nitrogen content may be reduced.

Natural gas was used on a local basis in the United States during the 19th century for both fuel and heating; by the 1940s it was being distributed by pipeline throughout much of the country and now provides about a quarter of America's energy requirements. Since about 1975, Great Britain has relied entirely on natural gas for its gas supplies; it forms a significant part of Japan's energy consumption; and its use is widespread throughout Europe and the USSR (Table 1.1).

Table 1.1
Past and Projected Consumption of LNG (10^6 t/year)^a

Year	Japan	United States	Western Europe	Total
1975	5.0	0.25	8	13.3
1980	19	11	11	41
1985	44	39	22-36	105-119
1990	47-55	50-105	33-39	130-199

Sources of natural gas (10^6 t/year)^a

	Americas	USSR	Middle East	Far East	Africa	Total
1980	1	—	3	15	22	41
1990	6-30	9-35	13-17	35-39	67-78	130-199

^a From Thorogood [1.3].

Sources of natural gas are scattered relatively evenly around the globe, with the result that a trade has developed in transferring the gas to areas of large demand. Thus there are, for instance, major pipelines from Alaska southwards, and from the USSR to Western Europe. However, much gas is liquefied for both transport and storage to take advantage of the large decrease in specific volume which is achieved without the necessity for pressurisation.

The first shipments of LNG by sea were made on an experimental basis from Lake Charles, United States, to Canvey Island, England, during 1959, and as a result of the success of these voyages a regular service from Algeria to Canvey Island was instituted in 1961, carrying about 700,000 t/year. Twenty years later, routes had been established from Algeria and Libya to Europe, from Algeria to the United States, and from Alaska, Abu Dhabi,

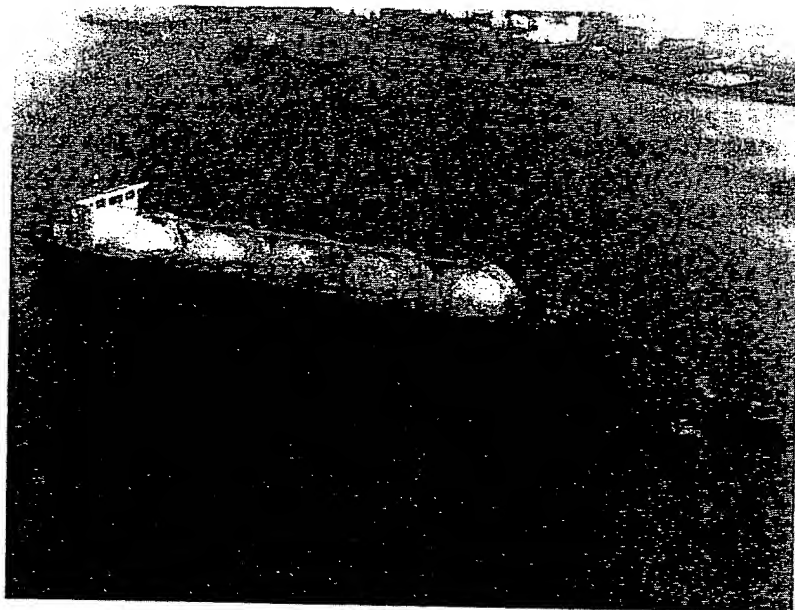
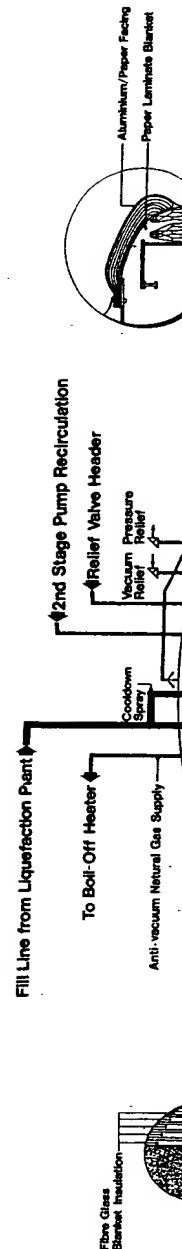


Fig. 1.1 The LNG tanker 'LNG Aquarius', launched in 1977, L.O.A. 285 m. The LNG is carried in 5 spherical aluminium tanks, each of 25,260 m³ capacity. (Courtesy of British Gas Corporation.)

Indonesia and Brunei to Japan, and another ten or so routes were under active development [1.4]. The shipping terminals are supplied by large liquefiers with up to 5000 t/day capacity in a single train (Fig. 16.22).

Apart from storage at liquefaction plants and trading terminals, natural gas is stored as liquid for 'peak shaving' operations, that is, to provide an additional source of gas during periods of peak demand when the normal supply system is inadequate (usually in winter). Liquefaction, using small (200 t/day) plants takes place during periods of low demand in the summer. Storage tanks may be as big as 100 m in diameter and 30 m in height, containing tens of thousands of tonnes of liquid (Fig. 1.2). In the past, they were usually constructed of either aluminium or 9% nickel steel; now, prestressed concrete (with a suitable thin metal liner to eliminate porosity problems) is being increasingly used. During the 1960s, a number of tanks were formed by excavating a hole in the ground and installing a thin steel liner, but this design has proved to be unsatisfactory due to large evaporation rates and to an ever-increasing area of frozen ground around the tank, although new designs are now being developed in Japan.



The LNG
y of British

are under
by large
(22).
s, natural
rovide an
e normal
ing small
summer.
n height,
ast, they
el; now,
porosity
of tanks
g a thin
to large
d around
n.

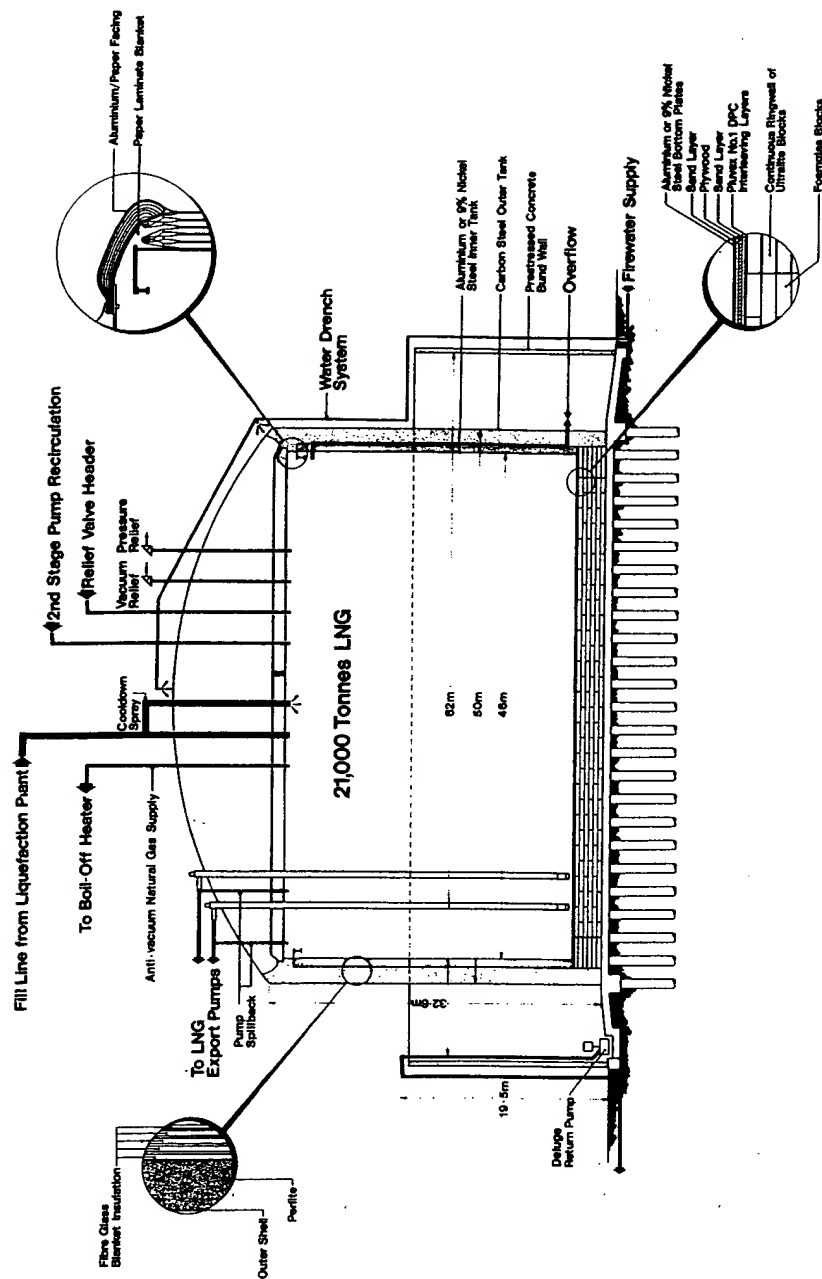


Fig. 1.2 A 50,000 m³ tank for the storage of liquefied natural gas for peak shaving. A bund is provided to retain the liquid in case of leakage. The insulated interspace, which contains natural gas vapour, is open to the vapour above the liquid, so that there will be no pressure differential. The horizontal ceiling above the liquid is insulated with glass fibre. The outer tank is designed as a pressure vessel, and in some designs might be reinforced concrete rather than carbon steel. (Courtesy of British Gas Corporation.)

Besides these large-scale facilities, in some areas it has proved economic to distribute LNG by truck and to keep it in small storage vessels close to the point of use. The technology adopted is similar to the well-established methods used for oxygen and nitrogen.

Purification ('upgrading') of natural gas is achieved by cryogenic methods. Many natural gas sources contain significant quantities of nitrogen and carbon dioxide, which reduce the calorific value and render the gas incompatible with other supplies to the pipeline distribution network. Upgrading plants are based on successive liquefaction and separation of the various components of natural gas and are frequently installed at the well-head. In these plants, solid impurities (sand, etc.) are filtered, and then water, sulphur compounds and carbon dioxide are removed using either molecular sieves or chemical absorption, for example, using glycol to absorb water or monoethanol amine to absorb carbon dioxide. Liquefaction can then take place without blocking the low-temperature heat exchangers with frozen components of the gas. Currently, natural gas companies are projecting a significant increase in the number and size of such plants. This increase is associated with the use of nitrogen injection into the gas wells to enhance gas recovery, thus creating a double use of cryogenics for both injection and rejection, since the nitrogen will be produced on-site by the fractional distillation of liquid air.

1.5 Air Separation

The production of oxygen, nitrogen and argon by the fractional distillation of air, or 'air separation' as it is known, forms a vital part of the infrastructure of the industrialised world. The major developments have occurred since the Second World War: in 1948, a system to produce 140 t/day of liquid oxygen was built in the United States; in the 1970s, plants with ten times that capacity were under construction in various parts of the world. The daily world production of oxygen is now about 5×10^5 t (Fig. 1.3), a purity of around 99.5% being easily achievable even on this scale.

By far the greatest amount of oxygen is consumed by the chemical and steel industries (Table 1.2). Since the daily consumption of a chemical or steel works may amount to several hundred tonnes per day, it has become common practice to build an air separation plant on an adjacent site and deliver the oxygen by pipeline. Because a continuous supply is essential, stringent conditions may be imposed by the user, and emergency electrical generators and back-up storage vessels may have to be provided to guarantee a supply until faults can be rectified or oxygen brought in by road.

A consic
compressed
hospitals. C
oxidation o
methanol p
and in the t

I
—
—
Stu

Nc
Fa
Ch
I
/
7
F
V
C

Pol
Mis

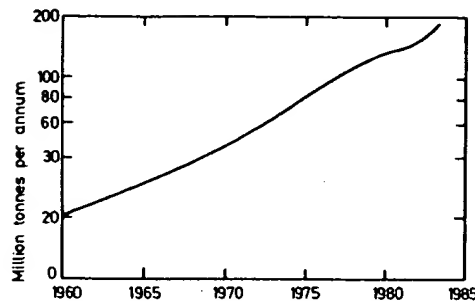


Fig. 1.3 Worldwide annual production rate of oxygen. (Courtesy of R. M. Thorogood.)

A considerable quantity of oxygen is produced in gaseous form and compressed into cylinders to be used, for instance, for welding, in diving and hospitals. Other important and growing uses for oxygen are in the partial oxidation of coal and heavy hydrocarbons to synthesise gas mixtures for methanol production and to produce hydrogen for ammonia production, and in the treatment of waste water by activated sludge processes. The use

Table 1.2
Industrial Consumption of Oxygen in the United States in 1979*

Percent of total consumption		
Steel making		
Basic oxygen process	39.6	
Open hearth process	9.3	
Electric furnace	1.7	
Cutting, welding, blast furnace air enrichment	14.8	
Total		65.4
Non-ferrous metals		3.0
Fabricated metal products		7.0
Chemicals		
Ethylene oxide	8.2	
Acetylene	3.8	
Titanium dioxide	2.8	
Propylene oxide	2.3	
Vinyl acetate	2.3	
Other	0.6	
Total		20.0
Pollution control		3.0
Miscellaneous		1.6

* From Thorogood [1.3].

of oxygen in the production of fuels from coal is expected to increase as oil reserves diminish, an important aspect of this being the very large consumption which will be required at an individual site, perhaps 20,000–30,000 t/day: the SASOL II complex which is operational in South Africa uses 15,000 t of oxygen per day.

Liquid oxygen is also produced in quantity for use in aerospace activities, both as a fuel oxidiser and for life support systems. The amounts required can be large: for instance, each Apollo flight to the moon consumed about 2000 t (Fig. 1.4), and the annual consumption of the American space programme at its peak was about 400,000 t [1.5].

At the same time as oxygen is separated from air, nitrogen is also, of

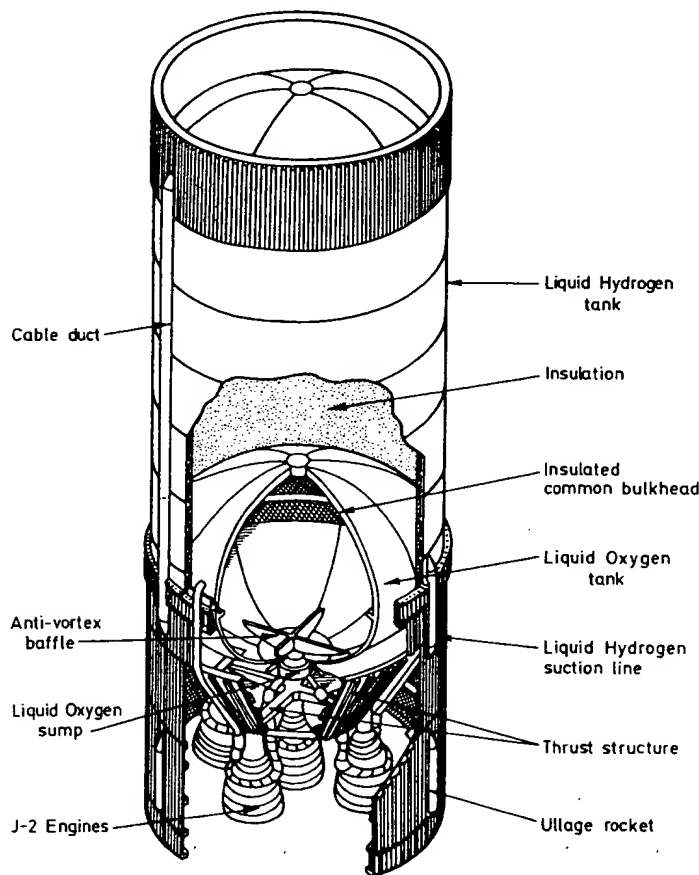


Fig. 1.4 Second stage of the Saturn V rocket launcher used for the Apollo flights to the moon. This stage was about 25 m high and 10 m diameter.

1. A SURVEY C

course, produc
oxygen. In th
by-product an
developed an
production.

Liquid nitro
cations, such a

(1) for coc
tamination mu

(2) for free
uses up to 700

(3) in the r
either side of t
whole system;

(4) in recla
of many metal
cold motor ve

constituents se
can be shattere

which does no
treated. In Bel;

being fragment
consumption o

(5) in defla
deflashing can

each item indiv

(6) in the h
resistance of ce

(7) for the
the cattle indus

(8) in astro

(9) in grow
to be performe

(10) in bon
porarily harmle

However, th
for various che
dependent upor
for such applica
and chemical t

course, produced, the current world-wide consumption being about that of oxygen. In the early years of the industry, nitrogen was considered a by-product and sold relatively cheaply. However, new uses have been developed and some plants are now biased more towards nitrogen production.

Liquid nitrogen is a useful source of cold and finds a diversity of applications, such as:

- (1) for cooling cold traps in vacuum systems, especially where contamination must be avoided, as in semi-conductor device manufacture;
- (2) for freezing food: one major fast-food franchise in the United States uses up to 700 t/day for freezing hamburgers;
- (3) in the repair of pipelines: by freezing the liquid in the pipeline on either side of the fracture, a repair can be effected without emptying the whole system;
- (4) in reclamation processes, where use is made of the embrittlement of many metals and polymers at low temperatures, when, for instance, cold motor vehicle tyres can be pulverised, and the steel and polymer constituents separated and re-used; the polymer coating of electric cables can be shattered into small pieces while the copper or aluminium conductor, which does not become brittle, remains intact. Large items can also be treated. In Belgium, for example, complete automobiles are cooled before being fragmented; it is claimed that the process reduces the overall energy consumption of the process and makes it easier to separate the ferrous from the non-ferrous (non-embrittled) scrap;
- (5) in deflashing of moulded polymer products: in the embrittled state, deflashing can be achieved by a tumbling process rather than by treating each item individually;
- (6) in the heat treatment of metals: for instance, to improve the wear resistance of certain tool steels;
- (7) for the storage of biological specimens, especially bull semen for the cattle industry;
- (8) in astronautics, for pre-cooling fuel tanks prior to filling with oxygen;
- (9) in ground freezing, to enable tunnelling and excavation operations to be performed in wet and unstable soils;
- (10) in bomb disposal, for freezing explosives to render them temporarily harmless.

However, the widest use for nitrogen is as an inert blanketing gas for various chemical and metallurgical processes. The purity required is dependent upon use, with medium purities (1-3% oxygen) being acceptable for such applications as blast furnace feed systems, coal handling systems and chemical tank purging. High purity (less than 10 ppm oxygen) is

essential for many purposes, of which steel annealing, float glass manufacture and fabrication of semi-conducting devices are important examples. Gaseous nitrogen is also used as a feedstock for the production of some chemicals, particularly ammonia. For large-scale uses, the nitrogen is supplied by an on-site plant or by pipeline. In other cases, it is often convenient to store the nitrogen as liquid rather than as gas in cylinders and vaporise it as required.

As already mentioned, a relatively recent and growing use of nitrogen is as a displacing medium in the recovery of oil and gas. By forcing oil or natural gas out of the well under pressure, a significant increase in the percentage extracted can be achieved. Such applications are of large volume and require delivery pressures between 130 and 700 bars.

The other major constituent of air is argon, which is in great demand for inert blanketing when nitrogen is too reactive, and for inert gas-shielded welding (TIG, MIG, etc.), although helium tends to be preferred in the United States. Because a very high purity (>99.9%) is required for most purposes, the impure product from several air-separation plants may be sent to a central point for purification. The air-separation industry is, in fact, so competitive that the recovery of argon may be necessary to prevent a plant running at a loss. The demand for argon is increasing rapidly, and it is possible that in the future some air-separation plants will be operated for the production of argon only, the nitrogen and oxygen being discarded. Although much argon is supplied as compressed gas, it is more economical for even moderate users to receive and store argon as liquid.

Of the minor constituents of air (Table 1.3), neon, krypton and xenon are extracted mainly for use in the lamp industry and laboratory instruments. It is not at present economic to recover helium due to its availability from LNG wells.

Table 1.3
Potential Yield of Atmospheric Rare Gases from a 1000 t/day Oxygen Plant*

	Total in air passing through plant (m ³ /hr at NTP)	Typical yield (%)	Cylinders per day
Argon	1395	55	2800
Neon	2.7	60	6
Helium	0.75	60	2
Krypton	0.17	30	0.2
Xenon	0.014	30	0.015

* From Thorogood [1.3].

1. A SURV

1.6 Liquid

Hydrogen explosive (0.02 mJ at no unusual 1970s, when its importance for example

Hydrogen hydrocarbon gas or fuel scale, electric due mainly hydrocarbon burning by Electrolytic hydrogen. Since it clears the resulting tigation of thermochemical

Hydrogen (Chapters 1 higher. A carbon and para (C conversion) being usual. Care must be taken oxygen which believed, carbon temperature par

Liquid hydrogen nuclear physics a target for from the engine to measure interactions; volume of liquid of a charged a piston in oil

1.6 Liquid Hydrogen

Hydrogen gas is a somewhat hazardous substance to handle due to its wide explosive concentration range with air (4–72%) and its low ignition energy (0.02 mJ at 30% concentration), although the liquid itself appears to present no unusual problems and was in wide use for cooling purposes until the 1970s, when liquid helium became more easily available in large quantities. Its importance as a cryogen has declined considerably since then, so that, for example, in Great Britain it is no longer commercially available.

Hydrogen gas is produced on a large scale by the reaction of steam with hydrocarbons, particularly natural gas, or by the partial oxidation of natural gas or fuel oil. The gasification of coal may also be used. On a smaller scale, electrolysis of water is used, in spite of its higher cost, which is due mainly to the higher binding energy of hydrogen in water than in hydrocarbons, to the high cost of electricity (itself often produced by burning hydrocarbons), and to the low efficiency of electrolytic cells. Electrolytic hydrogen may cost twice as much as the cheapest 'chemical' hydrogen. There is currently interest in developing hydrogen as a fuel, but since it clearly does not make sense to produce it from other fuels (with the resulting overall loss in available energy), there is widespread investigation of methods for producing hydrogen from water using various thermochemical methods.

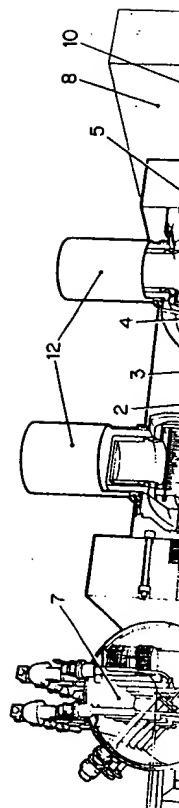
Hydrogen may be liquefied using cycles similar to those in use for helium (Chapters 13 and 15), except that the cycle pressures are about five times higher. A complication is that, because hydrogen exists in two forms, ortho and para (Chapter 2), the inclusion of catalysts to promote ortho-to-para conversion must be considered. Great care must be taken with safety, it being usual to provide a blast wall between the liquefier and its operators. Care must also be taken to free the hydrogen from impurities, especially oxygen which can promote unwanted ortho-para conversion, and, it is believed, cause an explosion if accumulated as solid in the lower temperature parts of the plant.

Liquid hydrogen still finds two particular applications. In high-energy nuclear physics experiments, liquid hydrogen or deuterium may be used as a target for the particles produced from the accelerator. More interesting from the engineering point of view is the bubble chamber, which is used to measure the properties of charged particles and to elucidate their interactions and decays. A bubble chamber consists essentially of a closed volume of liquid held at a pressure well above saturation. On the passage of a charged particle, the pressure is rapidly reduced, usually by means of a piston in one wall of the chamber, so that the liquid is in the superheated

state, and bubbles form along the track of the particle. A stereo photograph is taken, and the liquid is recompressed before bulk boiling occurs, the whole cycle taking a few tens of milliseconds. A large magnet surrounds the chamber so that the momentum of the particle can be deduced from the curvature of the track. Bubble chambers containing hydrocarbons and helium have been built, but hydrogen and deuterium are particularly favoured because their simpler nuclear structure allows a more straightforward interpretation of any interactions which occur. Hydrogen bubble chambers have been built as large as 3 m in length and containing several cubic metres of liquid, but they have now been superseded by other methods of detection, and the present tendency is to use smaller chambers surrounded by electronic detectors (Fig. 1.5).

The other application for which liquid hydrogen is still produced in quantity is as a fuel for space vehicles. When used with oxygen, it has a high propulsive energy per unit mass, and on this basis was, for instance, chosen for the fuel of the second and third stages of the rocket for the Apollo manned space flights to the moon, each of which consumed about 90 tonnes (1300 m^3) of liquid hydrogen (Fig. 1.4): in the late 1960s, the American space programme was using about 40,000 t/year [1.5]. In the 1980s, each launch of the space shuttle consumes about 120 tonnes (1700 m^3). Although on a mass basis hydrogen has a calorific value about three times higher than kerosene (which was used for the first stage of Apollo), its calorific value per unit volume is about three times lower. Thus rockets fuelled with hydrogen have to be much larger than those fuelled with kerosene, and this can entail problems of structural stability, particularly bending oscillations during flight.

There has been widespread discussion of the possibility of using hydrogen as a fuel for aircraft and automobiles as oil supplies diminish, although as already mentioned, a novel and energy-efficient means of producing hydrogen must be developed before this becomes a reality. On the question of safety, it can be argued that although hydrogen is more easily ignited than hydrocarbon fuels, its flame radiates little heat. Also, since hydrogen is lighter than air, it spreads upwards rather than outwards, so that overall there is probably little to choose between the two fuels. The storage of hydrogen is, however, a major problem. Storage as metal hydrides imposes a large weight and cost penalty because of the metals used and their low absorption capacity. Storage as liquid is clearly convenient, but requires large fuel tanks as mentioned earlier, although some saving in volume (about 15%) can be made by using a mixture of solid and liquid—'slush hydrogen'. Considerable care would have to be taken in the disposal of boil-off in a safe way. Perhaps a more serious drawback is the energy required for liquefaction, which may amount to as much as a third of the



B. A. HANDS

o photograph
g occurs, the
net surrounds
duced from
ocarbons and
particularly
ore straight-
rogen bubble
ining several
led by other
ler chambers

produced in
gen, it has a
for instance,
cket for the
sumed about
e 1960s, the
[1.5]. In the
120 tonnes
value about
irst stage of
lower. Thus
fuelled with
particularly

ng hydrogen
h, although
f producing
he question
asily ignited
e hydrogen
that overall
storage of
des imposes
d their low
ut requires
in volume
uid—'slush
disposal of
the energy
hird of the

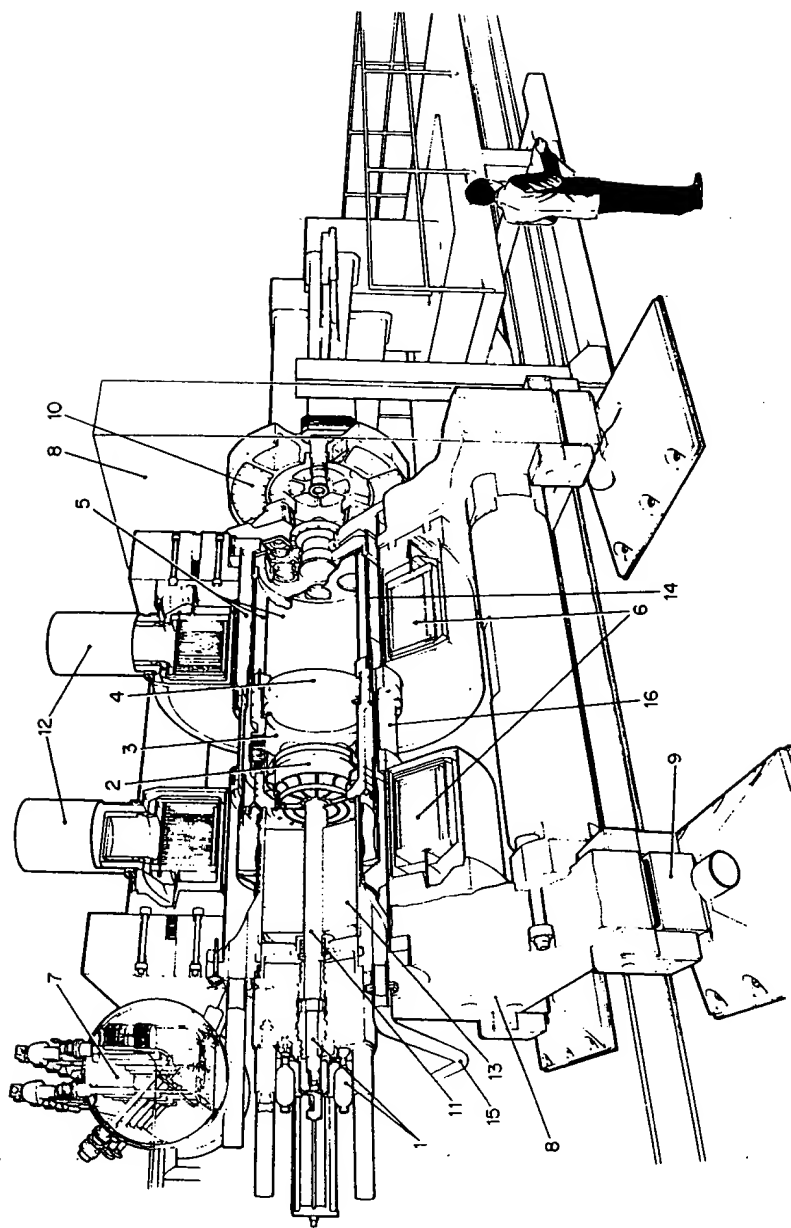


Fig. 1.5 Rapid-cycling hydrogen bubble chamber built for high-energy nuclear physics experiments. (1) Hydraulic actuator, (2) glass-reinforced plastic piston and bellows, (3) active volume (250 l), (4) main optical window, (5) vacuum enclosure, (6) superconducting magnet coils, (7) chamber refrigeration control vessel, (8) iron support structure, (9) damped mountings, (10) cameras and light-source assembly, (11) piston shaft, (12) magnet lead and transfer line enclosures, (13) thermal insulation, (14) radiation shield cooled by helium gas at 20 K, (15) safety vent and (16) outer vacuum vessel. (Courtesy of the SERC, Rutherford Appleton Laboratory.)

calorific value of the fuel liquefied. This, together with the present high cost of production from non-hydrocarbon sources, makes hydrogen economically unattractive, although several experimental automobiles have been successfully run with liquid hydrogen as fuel for a number of years.

1.7 Liquid Helium

The importance of helium to the physicist and cryogenic engineer is that it is the only route to temperatures below about 10 K, apart from magnetic cooling methods which are unlikely to become practical on anything but a very small scale. The provision of helium refrigeration is, therefore, a necessary adjunct to the use of superconducting magnets.

The largest sources of helium in the western world are currently the natural gas wells of the states of Texas and Kansas in the United States. Wells in Poland, Northern Germany and the USSR (at Orenburg) also produce large quantities. Helium is present in these wells at a concentration of about 0.2–0.7% and is extracted by liquefying the other constituents. Although at present there is plenty of helium available, there are worries that if the growth in both size and number of superconducting magnets continues at the present pace, there could be a severe shortage in a few decades as natural gas wells become exhausted, even though the United States has considerable quantities of helium stored in underground porous rock—a result of the so-called ‘conservation’ programme which has now been discontinued [1.6]. Outside America, ‘conservation’ has a rather different connotation—that of recycling the gas after use, rather than exhausting it to the atmosphere. Such recovery is usually justifiable on economic grounds alone, since gaseous helium is not cheap, but it is worth noting that large quantities are used in welding and in oxygen–helium atmospheres for diving, from which helium recovery is not feasible.

A major landmark in the development of helium technology came in 1946 with the design by Professor Sam Collins of a liquefier which did not require the feed helium to be pre-cooled and which could be operated continuously for long periods. Previous to this, small-scale experiments were done by liquefying helium *in situ*, for example, by precooling with liquid hydrogen (sometimes itself produced *in situ*) and then adiabatically expanding. Continuous liquefaction was achieved using cascade cooling with liquid air (or nitrogen) and hydrogen followed by Joule–Thomson expansion. The latter method could produce a few litres of helium per hour, but required the simultaneous operation of both a hydrogen and a helium liquefier, the liquid air or nitrogen usually being available from a commercial source.

1. A SURVEY OF

The Collins proved to be a meant that fairl still marketed to bearings were d liquefiers, and s refrigerators. Tl engine, have no high efficiency. liquefiers.

Another probl to compress the since all will free is especially imp to be run conti contaminations I believed that w blockages in one received general based, piston rin compressors, bei reciprocating cor require a sophisti for a malfunction refrigerator itself more frequent m for more massiv tamination is sim

1.8 Superconduct

Perhaps the one has been the ex conductivity or tl phenomenon was major part in elec was destroyed by presence of a mag remained unfulfil ‘high-field’ superc remain supercond

present high
hydrogen econ-
omobiles have
number of years.

reer is that it
om magnetic
anything but a
therefore, a

currently the
nited States.
enburg) also
oncentration
constituents.
are worries
ing magnets
age in a few
the United
ound porous
ich has now
as a rather
rather than
ustifiable on
at it is worth
ygen-helium
asible.

ogy came in
hich did not
be operated
experiments
cooling with
adiabatically
ade cooling
le-Thomson
helium per
rogen and a
lable from a

The Collins liquefier, which used a reciprocating expansion engine, proved to be a reliable machine, although the presence of rubbing seals meant that fairly frequent maintenance was required; its derivatives are still marketed today. During the 1950s, high-speed turbines running on gas bearings were developed as the external work components for hydrogen liquefiers, and soon afterwards this technique was incorporated in helium refrigerators. These turbines, although less robust than a reciprocating engine, have no rubbing surfaces and can achieve a large throughput at high efficiency. They are now usually specified for large refrigerators and liquefiers.

Another problem in the design of refrigerators arises from the necessity to compress the gas. The helium feed must be free of oil, water and air, since all will freeze at some point in the system and cause blockages: this is especially important today, when superconducting systems may have to be run continuously for many months. To achieve such service, oil contaminations less than 1 part in 10^7 may have to be specified, and it is believed that water contamination of about 3 parts in 10^8 has caused blockages in one system [1.7]. Two types of compressor appear to have received general acceptance, reciprocating compressors with dry, polymer-based, piston rings, and oil-flooded screw compressors. Oil-flooded screw compressors, being rotating machines, suffer from fewer problems than reciprocating compressors and are more compact and vibration-free, but require a sophisticated oil-removal system. Furthermore, it is not unknown for a malfunction to occur such that much of the oil is delivered into the refrigerator itself. Reciprocating compressors have the disadvantage of more frequent maintenance intervals, more vibration and a requirement for more massive foundations, but the equipment for removal of contamination is simpler.

1.8 Superconducting Magnets and Machinery

Perhaps the one major disappointment in the development of cryogenics has been the exploitation of the "electrical engineers' dream"—superconductivity or the complete absence of electrical resistivity. After this phenomenon was discovered in 1911, hopes persisted that it would play a major part in electrical engineering, even though the superconducting state was destroyed by the passage of a current of only a few amperes or the presence of a magnetic field of only a few tenths of a tesla, but the dream remained unfulfilled for some 50 years. In the late 1950s, a range of 'high-field' superconductors were discovered, so called because they would remain superconducting in fields of tens of tesla. Also, their critical tem-

peratures, instead of being at the most 9.25 K (niobium) were 5–10 K higher. It was discovered, however, that the construction of a superconducting magnet involved more than just winding the wire into a coil, and that copper had to be incorporated to 'stabilise' the magnet and allow it to operate at the fields which a short sample of the wire could sustain. In order to optimise the performance, many subtle techniques had to be learnt, and even today new designs are not always completely successful. Nevertheless, magnets are now made commercially on a production-line basis, and, for large magnets at least, at a cost less than their water-cooled copper equivalents, to which they are superior on running costs and in stability of field.

Superconducting magnets have found widespread applications in research

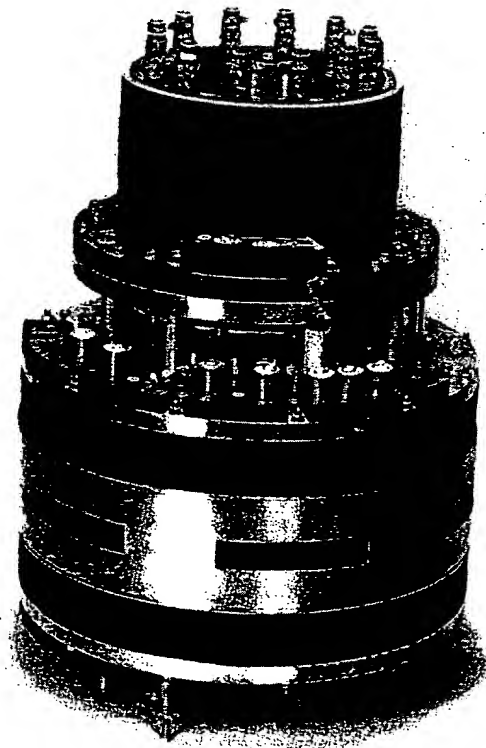


Fig. 1.6 Small superconducting magnet for research use. This is a split-pair magnet, wound partly from niobium-tin wire and partly from niobium-titanium, producing 10 T in a 70 mm bore. The maximum diameter is about 25 cm. The 12 resistors on top of the assembly are used to absorb energy should the magnet unexpectedly change from the superconducting to the normal state ('quench'). (Courtesy of Oxford Instruments Ltd.)

1. A SURVEY

laboratory cubic centimetre of NMR assembly use into channels in which the incoming nucleus (proton) radiation, the magnetic field between 0.1 and 10 T, the x, y and z coordinates correlating information may intensity of the wave. Since the wave body, a 3-dimensional lattice and structure acquired. The (Fig. 1.7), wave and a stability

Still at a Spectroscopy nuclei due to resonant frequency *in vivo*. Process tissue during ^{23}Na nucleus, Because the mass of protons; magnetic

No adverse MRI or MRS. field, which can be necessary), and ferrous objects

For MRS and used, the latter cryogenics for environments. conductivity, the per year worldwide Large magnets

(niobium) were 5–10 K construction of a superconducting wire into a coil, use the magnet and allow the wire could sustain. Little techniques had to be very completely successful. Only on a production-line basis than their water-cooled on running costs and in

d applications in research

1. A SURVEY OF CRYOGENIC ENGINEERING

21

laboratories. Small magnets, providing a uniform field over a few tens of cubic centimetres, are mainly used by physicists (Fig. 1.6); the development of NMR and ESR techniques for analytical purposes has extended their use into chemistry and biology [1.8], and more recently, into medicine, in which the technique known as MRI (Magnetic Resonance Imaging) is coming into routine clinical use. In MRI, the resonance of the hydrogen nucleus (proton) is stimulated by applying radiofrequency electromagnetic radiation, the resonant frequency being directly proportional to the applied magnetic field. The patient is subjected to a uniform magnetic field of between 0.5 and 1.5 T, upon which are superimposed small gradients in the x , y and z directions. By changing the applied rf frequency and correlating the resonant frequency with the local field, 3-dimensional information may be obtained. The primary information is obtained from the intensity of the resonance, which depends upon the local proton density. Since the water and lipid content is different in the various tissues of the body, a 3-dimensional image of the body structure may be produced and abnormalities such as tumours may be located. Measurement of the spin-lattice and spin-spin relaxation times enable further information to be acquired. The magnets for whole-body MRI require a bore of about 1.0 m (Fig. 1.7), with a field homogeneity as good as 0.1 ppm of the main field and a stability of 0.1 ppm per hour [1.8].

Still at a more experimental stage is MRS (Magnetic Resonance Spectroscopy). Slight variations in the local magnetic environment of the nuclei due to different chemical surroundings produce small shifts in the resonant frequency, and this enables chemical reactions to be followed *in vivo*. Processes which have been investigated include changes in muscle tissue during exercise using the ^{31}P nucleus, cellular biochemistry using the ^{23}Na nucleus, and the kinetics of enzyme reactions using the ^{13}C nucleus. Because the magnetic moments of these nuclei are much weaker than those of protons, magnetic fields of about 6 T are generally required.

No adverse physiological effects are believed to occur with the use of MRI or MRS. The main safety problems are control of the stray magnetic field, which can be limited by the use of iron shielding (some 20 t may be necessary), and the prevention of personnel from inadvertently carrying ferrous objects into the region of the stray field.

For MRS and MRI, both conventional and superconducting magnets are used, the latter giving superior resolution but requiring some expertise in cryogenics for its operation which may not be available in some hospital environments. This is the first large-scale, non-research use of superconductivity, the current production rate being several hundred magnets per year worldwide.

Large magnets have been used since the mid-1960s by high-energy

is a split-pair magnet, wound
., producing 10 T in a 70 mm
on top of the assembly are
from the superconducting to
Ltd.)

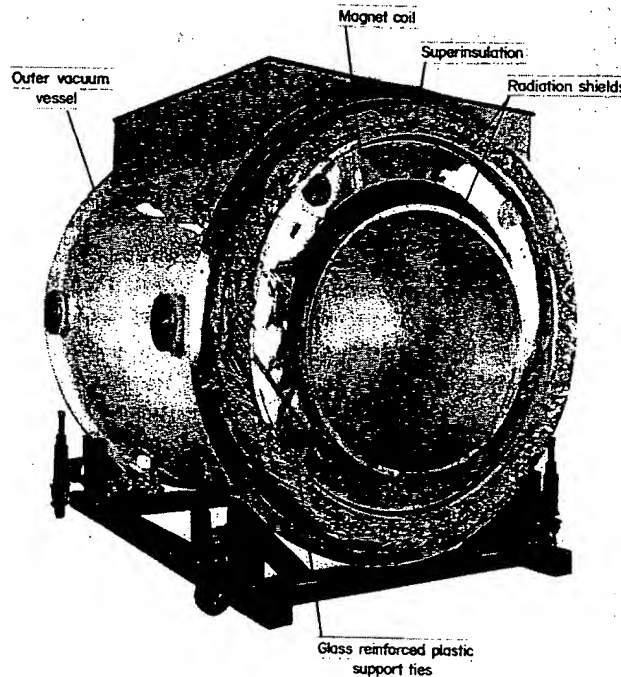


Fig. 1.7 A superconducting magnet, designed for whole-body scanning, during assembly. A field in the range 0.5–1.5 T is produced in a bore of 1 m. (Courtesy of Oxford Magnet Technology Ltd.)

nuclear physics establishments, at first for the focusing of ionised particle beams between the accelerator and the experiment, and lately in the accelerator itself. Such magnets are often one or two metres long with a bore of around 10 cm; besides simple solenoids, quadrupole and other configurations have been constructed. A great variety of superconducting magnets for other uses has now been made, for example, simple solenoids of several metres bore for use with bubble chambers; toroidal magnets for plasma physics experiments; and a 'yin-yang' configuration, weighing 341 t, for a nuclear fusion experiment (Fig. 1.8). Fields in the region of 10 T are commonplace, and some magnets are pulsed on a routine basis. High-energy nuclear physics and nuclear fusion have both given great stimulus to the development of magnet technology.

Applications in the generation and transmission of electric power have not been as successful, the enthusiasm of the manufacturers being counter-

1. A SURVEY

balanced by the story has ahead of the mission line system would [1.10]. Ten temperature studies had transmission continuously overload.

Similarly, construction power generated 1000–3000 M over conversion smaller by a at the most, reliable than therefore, p the western programmes reported in 1 switched into construction

At present an electricity magnet capital substation of Energy is transferred controlled with supply [1.13] time of 10 m shaving' energy way as pump

There has most promising given power, generator is generally of rapid speed thus removing

balanced by the caution (realism?) of the utility companies [1.9]. In general, the story has been that advances in 'conventional' technology have remained ahead of the possibilities of using superconductors. Superconducting transmission lines are a good example. In 1973, it seemed that a superconducting system would be economically viable for powers greater than about 1 GVA [1.10]. Ten years later, due to advances in insulation technology of room temperature systems, the figure had risen to 5 or 10 GVA, and experimental studies had been largely abandoned, even though in 1984 the prototype ac transmission line at the Brookhaven National Laboratory [1.11] was run continuously for 4 weeks at 1 GW, and its stability demonstrated at 100% overload.

Similarly, in the 1970s there was considerable activity in the design and construction of models and prototypes of superconducting alternators for power generation aimed at eventual machines in the capacity range of 1000-3000 MW. Superconducting alternators have two major advantages over conventional designs: a greater efficiency, and a size and weight smaller by a factor of about two. However, the increase in efficiency is 1% at the most, and this is easily negated if the alternators prove to be less reliable than the machines currently in use. The generating authorities are, therefore, proceeding with extreme caution, and again by 1985, activity in the western world in this field had considerably diminished, with only small programmes remaining in the USA, Japan and Germany. However, it was reported in 1985 [1.12] that in the USSR, an experimental alternator was switched into the Leningrad supply in the summer of 1984, and that construction of 300 MVA alternators is proceeding.

At present, only one superconducting device is believed to be in use by an electricity supply authority in the western world. A superconducting magnet capable of storing 38 MJ of energy has been installed at the Tacoma substation of the Bonneville Power Administration in the United States. Energy is transferred between the magnet and the transmission line in a controlled way to damp out subsynchronous oscillations in the ac electricity supply [1.13]. An advantage of the system is the relatively fast response time of 10 ms. Much larger magnets have also been proposed as 'peak shaving' energy storage devices, which would be used in much the same way as pumped water storage is now.

There has been considerable interest in superconducting motors. The most promising application appears to be for ship propulsion, where, for a given power, a superconducting motor combined with a superconducting generator is much smaller than a conventional system. The motors are generally of the dc homopolar type. The small rotating mass facilitates rapid speed changes, and the motor will operate efficiently at low speed, thus removing the need for a gear box. However, on economic grounds a

conventional system is still superior, and the main use for a superconducting unit may be in naval vessels, for which flexibility and small size are important advantages, and in icebreakers, because of the frequent reversals of direction at low speed.

A different form of power unit is the linear motor, which, when combined with magnetic levitation, forms a suitable system for driving high-speed trains. Japanese National Railways has pursued such a development [1.14], intended for the commuter line between Kobe and Tokyo, which was predicted to reach full capacity soon after 1980. Work started in the 1960s, and the first prototype was successfully tested in 1975. Since then, the design has been considerably refined, and in 1979 the version known as ML-500 ran at 517 km/hr, a world record. Propulsion is by linear synchronous motor, the high-frequency ac power being provided by coils mounted on the track. Guidance and support are both achieved using a repulsive electromagnetic inductive method, which requires the train itself to be equipped with powerful magnets. In the Japanese system, each vehicle (28.8 m long and weighing about 10 t) is provided with eight superconducting magnets of 700 kA-turns each and on-board refrigeration (Fig. 1.9). Although the project is well advanced, there are no plans yet to introduce the train into commercial service, since passenger density on the line has increased slower than originally predicted.

Finally, one other use of superconducting magnets is showing commercial promise. In the 1960s, it was established that kaolin, which is used in paper-

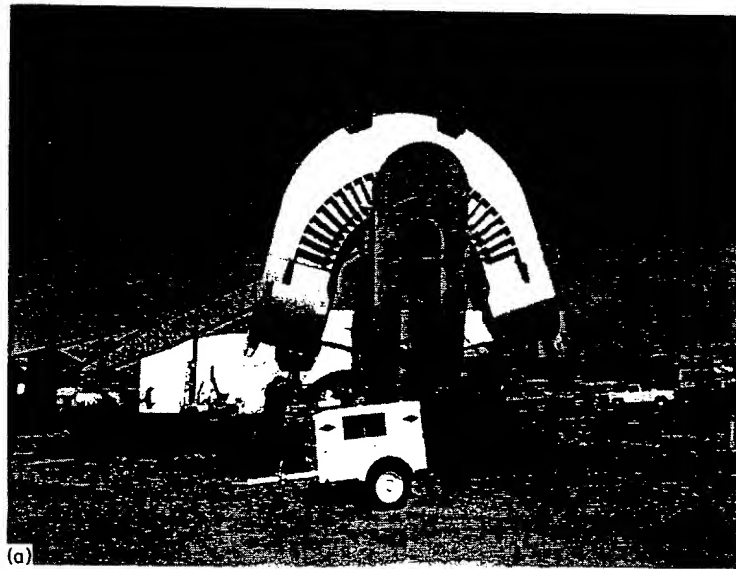


Fig. 1.8 'Yin
(a) Opposite: Cc
Laboratory). (b)
diameter. The (re
can also be seen
photograph indic
University of Cal
Energy.)

HANDS

ducting
portant
of direc-

mbined
h-speed
t [1.14],
ich was
e 1960s,
en, the
own as
achron-
ounted
pulsive
f to be
vehicle
super-
n (Fig.
yet to
on the

mercial
paper-



(b)

Fig. 1.8 'Yin-yang' magnet for the Mirror Fusion Test Facility in Berkeley, California. (a) *Opposite*: Coil-box assembly (courtesy of University of California Lawrence Berkeley Laboratory). (b) Magnet during installation in the vacuum vessel, which is about 20 m in diameter. The (rectangular) end views of six cryopump modules for maintaining a high vacuum can also be seen, arranged radially around the top two-thirds of the vacuum vessel. This photograph indicates the complexity of a modern large cryogenic installation. (Courtesy of University of California Lawrence Livermore National Laboratory and U.S. Department of Energy.)

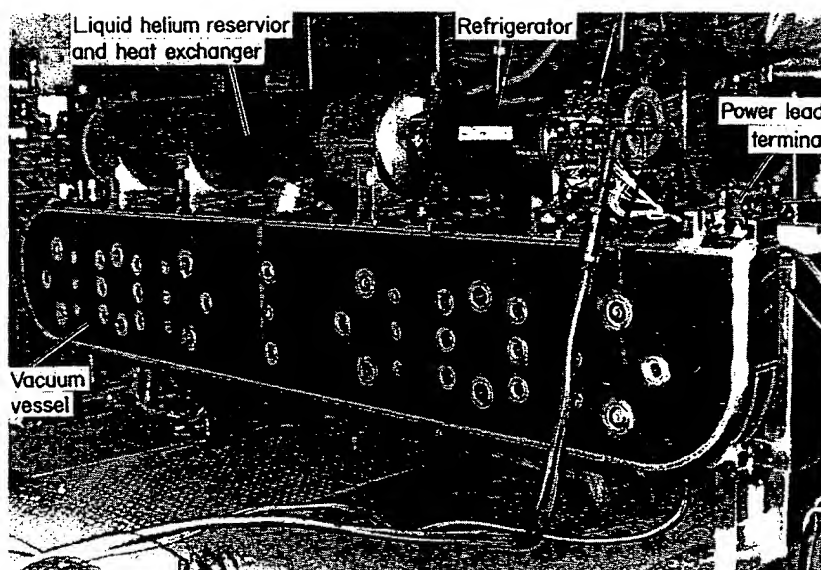


Fig. 1.9 A magnet-refrigerator assembly for the Japanese magnetically levitated train. The magnet coil is within the vacuum vessel. (Courtesy of Japanese National Railways.)

making, could be whitened by removing the discolourants, which are principally due to traces of iron, by passing the clay through a magnetic field gradient. Since then, applications have been found in the separation of ores, in the purification of chemicals, in the desulphurisation of coal and in the cleaning of flue gases and liquid effluents. The separation of red blood cells from plasma is also possible. Although many of these processes require only comparatively low magnetic fields, the use of superconducting magnets may be advantageous for certain applications [1.15].

1.9 Cryogenic Electronics

Many active electronic devices can be operated in a cryogenic environment [1.16]. They are generally of the field-effect transistor (FET) type and are based on silicon or gallium arsenide. For instrumentation purposes, there are clear advantages in placing at least some of the electronic circuitry close to the sensing head. However, there may also be inherent advantages in operating transistors at low temperatures, such as increased switching speed or lower noise. A serious problem is the effect on device reliability of the stresses induced by thermal cycling.

1. A SURVEY

Superconductivity is a phenomenon involving two phenomena: zero resistance and perfect flux, which is more complex than extremely small amount of the Josephson effect. Lead or niobium oxide film at such a layer. Superconducting superconducting function of the Josephson junction uncertainty in

The superconducting from a superconductor. If the loop is because it is a wave function there is a phase difference of the

The rf SQUID loop, which can drive a current measure of the Josephson junction through the current is the Superconducting technologies similar methods may be dc SQUID is be approached a known distance be measured

Among a local anomaly and archaeological routinely used satellite trans investigation



ated train.
lways.)

uch are
agnetic
variation
oal and
of red
ocesses
ducting

nment
nd are
there
close
ges in
speed
of the

Superconducting electronic devices are in a different class. They rely on two phenomena—the Josephson effect and the quantisation of magnetic flux, which are described in a simple way in [1.17], for example, while a more complete account is given in [1.18]. The quantum of magnetic flux is extremely small: 2.07×10^{-15} Wb, which is approximately equal to the amount of the earth's field enclosed by a ring $10 \mu\text{m}$ in diameter. The Josephson effect is observed when two pieces of superconductor (commonly lead or niobium) are separated by a very thin insulating layer, perhaps an oxide film about 20 nm thick. Not only can single electrons tunnel through such a layer, but so can the pairs of electrons (Cooper pairs) to which superconductivity is attributed, so that the insulating layer behaves as a superconductor, although there is a discontinuity in the phase of the wave function of the Cooper pairs across the junction. The characteristics of the Josephson junction are now used to define the volt, and have enabled the uncertainty in the maintained standard to be reduced to about $0.1 \mu\text{V}$.

The superconducting quantum interference device (SQUID) is formed from a superconducting loop containing at least one Josephson junction. If the loop encloses some magnetic flux, there must be a circulating current because it is superconducting. This current consists of Cooper pairs whose wave functions form standing waves round the ring. Across the junction, there is a phase discontinuity which is a function of the current flowing and hence of the magnetic flux.

The rf SQUID is formed from a single junction in a superconducting loop, which is inductively coupled to a resonant circuit. This is arranged to drive a current round the loop, so that the voltage across the circuit is a measure of the magnetic flux being measured. In the dc SQUID, two Josephson junctions are made in the loop, and a dc current is passed through the parallel circuit so formed. The voltage required to produce the current is then a function of the magnetic field trapped inside the loop. Superconducting quantum interference devices may be fabricated by technologies similar to those used for integrated circuits, although other methods may also be used. The rf device is the easier to make and use; the dc SQUID is the more sensitive, and the quantum limit of sensitivity can be approached. By forming the superconducting loop from two rings with a known distance between their planes, small magnetic field gradients may be measured in the presence of a large uniform field.

Among a variety of applications, SQUIDs have been used to map local anomalies in the earth's magnetic field (of interest to geologists and archaeologists, for example) and for navigational purposes. They are routinely used as mixers and amplifiers for receiving weak signals from satellite transmissions, and are also used in infra-red detectors. In medical investigations, SQUIDs are used to record the varying magnetic fields

associated with bodily activity, the fluctuations ranging from 10^{-11} T (from the heart) down to 10^{-15} T (from the brain) [1.19]. Gradiometer arrangements are often used in an attempt to reduce to an acceptably low level the effects of local field fluctuations due to electrical equipment and ionospheric phenomena. Advantages over the use of ECG and EEG are that electrodes do not have to be attached to the patient, and that the measurements are localised rather than averaged over some distance. By spatial scanning, a 3-dimensional image of, for example, brain activity can be constructed and the position of a malfunction pin-pointed. With a single detector, such an image may take several days to produce, but attempts are being made to develop multiple arrays using several tens of SQUIDS to reduce the scanning time. It may be observed that whereas MRI (Section 1.8) gives information about the structure of tissue, these magnetic field measurements give information about the functional behaviour of the tissue. SQUIDS have also been used to detect accumulations of ferromagnetic material in various parts of the body.

Josephson junctions may be arranged in a variety of ways for other purposes. For instance, a sampling oscilloscope has been made with a time resolution of 2 psec. But perhaps the best-known application is to computers. Combinations of Josephson junctions can be designed to act as a very fast switch with low power dissipation or as a memory element. The theoretical switching time is about 10 psec and the power dissipation about $1 \mu\text{W}$, giving a product of switching time and power consumption—the figure of merit used for switching devices—several orders of magnitude better than that of transistors. The fabrication of logic elements using such devices allows in principle the construction of a large capacity, compact, high-speed computer [1.20]. Much development work was carried out on this concept during the 1970s, especially by IBM. However, after '15 years and an estimated 100 million dollars' [1.21], IBM announced in 1983 that the project was abandoned, although development work in fact continues at a lower level. During that time, complete logic boards had been developed and tested. Major problems with the technology are that large fan-out ratios are difficult to achieve and that superconducting circuits have a very low inherent impedance and so are difficult to couple with conventional elements at room temperature. There were also manufacturing problems, since the boards could only be tested when in the superconducting state at a low temperature, and some logic gates were always destroyed due to thermal cycling. Another factor was that, as in other branches of superconductivity, room-temperature devices were being developed which approached the advantages offered by the superconducting system; for instance, at the end of 1985, it was reported that miniature ceramic circuit boards and hot electron devices were being developed by Fujitsu of Japan for use in an ambient-temperature computer which would be very much

1. A SURV

faster than
construct
there hav
architect

1.10 Cryo

The large
engineering ha
and hydr
precooling
carried f
tanks. Th
is at a pre
insulation
problems
currents
these pro
small acc
fuel tank

The sn
urements
wavelength
of the ex
supercon
17) is al
utterly re
alternati
then has

1.11 Met

Cryogen
fields. Th
been dis
more di
particula
difficult,
processe
by the th
chemical

ations ranging from 10^{-11} T (the brain) [1.19]. Gradiometer to reduce to an acceptably low level to electrical equipment and the use of ECG and EEG are close to the patient, and that the signal is spread over some distance. By using, for example, brain activity can be localised pin-pointed. With a single channel, it is difficult to produce, but attempts are being made using several tens of SQUIDS. It is noted that whereas MRI (Section 1.10) is of tissue, these magnetic field measurements are a functional behaviour of the system to detect accumulations of ferro-magnetic material.

There is a variety of ways for other applications. One type has been made with a time delay line. One application is to compute. It can be designed to act as a very fast memory element. The problem is the power dissipation about the system and power consumption—the power is several orders of magnitude more than of logic elements using such as a large capacity, compact, system. Recent work was carried out on the IBM. However, after 15 years of work, IBM announced in 1983 that the development work in fact continues. The logic boards had been developed. The technology are that large fan-cooled superconducting circuits have a great advantage to couple with conventional circuits. Also manufacturing problems, in the superconducting state at low temperatures were always destroyed due to the fact that as in other branches of superconductivity were being developed which are a superconducting system; for example, that miniature ceramic circuit developed by Fujitsu of Japan or which would be very much

faster than a Josephson machine. However, work continues towards the construction of a complete superconducting computer in Japan, where there have recently been striking advances in fabrication technology and architecture.

1.10 Cryogenics in Space

The large-scale applications of cryogenic technology to aerospace engineering have already been mentioned, in particular the use of liquid oxygen and hydrogen to power launch vehicles, and the use of liquid nitrogen for precooling purposes. In addition, liquid or cold supercritical oxygen is carried for life support, and helium may be carried for pressurising fuel tanks. The technology is similar to that used on earth, except that weight is at a premium, and, once in the space environment, only minimal thermal insulation may be needed. However, the absence of gravity poses serious problems, since liquid no longer separates from vapour and convection currents are non-existent. Special devices have to be used to overcome these problems. In the case of rocket motors, the vehicle may be given a small acceleration by an auxiliary rocket to drive the liquid towards the fuel tank outlet so that the engines may be started reliably.

The small-scale applications are mainly concerned with scientific measurements, including astronomy covering the whole range of electromagnetic wavelengths, recording of magnetic fields and observations of the surface of the earth. The instruments used often include a cooled detector or a superconducting device. The provision of a small refrigerator (see Chapter 17) is attractive, but the device must be of long life (several years), utterly reliable and low in power consumption, weight and vibration. The alternative is to provide a store of cryogenic liquid, but the experiment then has a comparatively short lifetime. Both methods are, in fact, used.

1.11 Medical and Biological Applications

Cryogenics has found a number of applications in the medical and biological fields. The use of superconducting magnets in MRS and MRI has already been discussed, as has the use of SQUIDS. Low temperatures are used more directly to enable biological materials to be frozen and stored, particularly thin tissues and blood. The preservation of large items is more difficult, since the cells suffer damage during the cooling and warming processes, the rapidity of which is inevitably controlled to a great extent by the thermal conductivity of the material, although the injection of certain chemicals can minimise the damage in some cases. On the other hand, this

damage is put to good use in the elimination of tumours by freezing. A major difficulty here lies in the monitoring and control of the frozen region. There is also insufficient understanding of the mechanisms by which cells are killed. Nevertheless, successful results have been obtained in the treatment of some conditions, and it is probable that cryosurgery will be more widely used in the future [1.22].

In agriculture, for many years cattle semen has been routinely preserved in liquid nitrogen for subsequent artificial insemination, and this has made a major contribution to the development of the industry, especially in the underdeveloped countries.

1.12 Cryopumping

Cryopumping—the removal of gas from a system by solidification onto a cold surface—has a number of advantages over other methods of producing vacua. A cryopump consists essentially of a metal plate cooled to a low temperature, and, therefore, can be made easily and economically in a large size, with considerable freedom in design configuration [1.23]. It is a 'clean' pump, since the only working substance is the refrigerant used for cooling, which does not come into contact with the vacuum space. Lastly, all gases except helium can be pumped to extremely low partial pressures (Fig. 1.10).

Although the concept of the cryopump is straightforward, the construction requires some sophisticated design, since the low-temperature parts must be carefully shielded from room-temperature radiation while

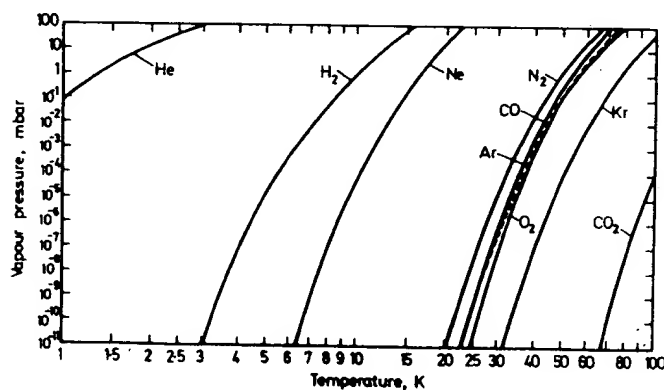


Fig. 1.10 Vapour pressure-temperature curves for atmospheric gases.

Down Lines for
Thermocouple

LN₂ Cooling

Top Manifold
and Radiation
Shield

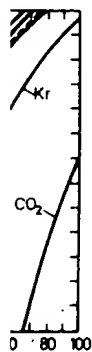
Module
Manifolds

by freezing. A
e frozen region.
s by which cells
obtained in the
osurgery will be

tinely preserved
d this has made
especially in the

ification onto a
ds of producing
cooled to a low
onomically in a
on [1.23]. It is a
gerant used for
n space. Lastly,
artial pressures

ward, the con-
ow-temperature
radiation while



ic gases.

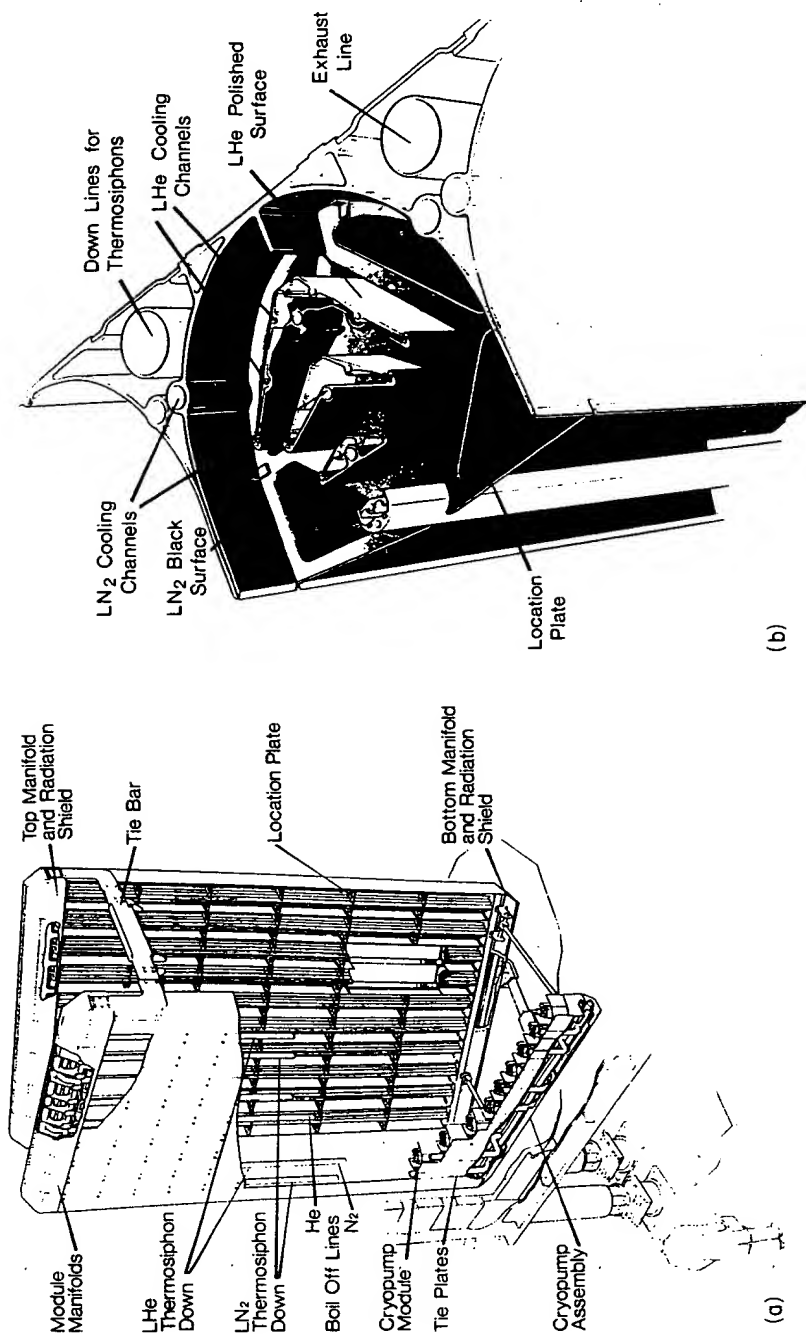


Fig. 1.11 Cryopump designed for the neutral injector assembly of the JET nuclear fusion experiment at Culham, England. The complete assembly is shown in (a). Each module (b) is 0.30×0.35 m in section and 6 m in height. (Courtesy of JET Joint Undertaking.)

allowing free access to gas molecules. This is especially so for cryopumps with stages at 20 K or 4 K, which must be shielded with panels at around 80 K. Since some molecules are scattered away from the cryopumping surface itself by the shields, the overall capture coefficient (which is usually between 0.35 and 0.5 depending on the design) is much less than that of the bare panel and, in fact, is not much different from that of a large diffusion pump.

Very large cryopumps were developed during the 1950s for use in space simulation chambers. Frequently, these used panels cooled to 20 K using a refrigerator with helium gas as the working fluid, and radiation shields cooled either with liquid nitrogen or with helium gas at around 100 K. The residual hydrogen and helium was extracted using conventional high-vacuum pumps. The cryopumps usually covered almost the whole of the interior surface of the vacuum vessel, which typically might be several hundred square metres in area.

Recently, attention has turned to the provision of cryopumps for nuclear fusion experiments. These are required to pump hydrogen at speeds of 10^6 – 10^7 l/sec and to pressures of the order of 10^{-5} mbar or better, so that the coolant must be liquid helium at around 3.5 K. A number of large pumps of this type have now been constructed; advantage has been taken of the geometrical freedom mentioned earlier to produce some interesting configurations [1.24] such as that shown in Fig. 1.11.

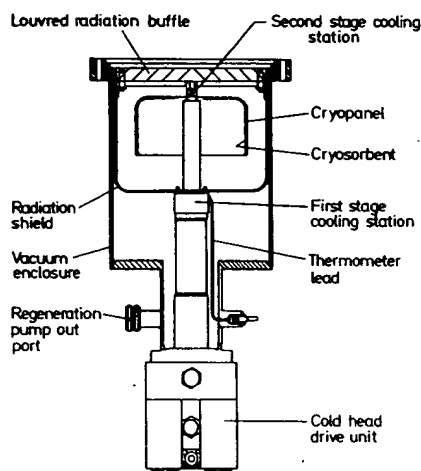


Fig. 1.12 Typical design of a small cryopump attached to a displacer refrigerator and intended to replace a diffusion pump.

At the other cryopumps for i be scrupulously apertures of a direct replacem contained retri provides retri of course, pum temperature p residual hydrog and zeolites ha low pressures restricted by a

1.13 Instrumen

The instrumen meter, prot lation. The lat if accurate an procedures, as examined in C

The measure liquids, float g allow the gas temperature of resistors or dic measuring curr in the liquid, a change in heat unreliable beca heat transfer c and a static liq of the liquid al

In the autho hydrostatic heat to room tempe temperature er rising up the n that the liquid

ryopumps
ls at around
ryopumping
ich is usually
than that of
t of a large

use in space
o 20 K using
ation shields
ound 100 K.
tional high-
whole of the
t be several

s for nuclear
it speeds of
tter, so that
er of large
been taken
interesting

rigerator and

At the other end of the size scale, there is an increasing interest in small cryopumps for industrial purposes, especially where oil contamination must be scrupulously avoided as in the semi-conductor industry. These have apertures of a few tens of centimetres and are frequently designed to be a direct replacement for a diffusion pump. They are cooled with a small self-contained refrigerator based on a displacer cycle (see Chapter 17) which provides refrigeration at around 100 K for the radiation shield (which also, of course, pumps water vapour), and cooling at around 20 K for the lower temperature panel, which is equipped with a sorbent material to pump residual hydrogen (Fig. 1.12). Sorbent materials such as activated charcoal and zeolites have attracted attention on account of their ability to achieve low pressures at comparatively high temperatures. However, their use is restricted by a low pumping speed and a limited absorption capacity.

1.13 Instrumentation

The instrument most commonly used in cryogenic engineering is the thermometer, probably on account of its cheapness and simplicity of installation. The latter is deceptive, however, and great care must be taken if accurate and reliable measurements are to be obtained. Installation procedures, as well as the many different types of sensor available, are examined in Chapter 18.

The measurement of liquid level can present problems. For the denser liquids, float gauges can be used, provided that the float is designed to allow the gas inside to contract or even condense, depending on the temperature of the liquid. A popular electronic device is a chain of carbon resistors or diodes which essentially act as resistance thermometers. The measuring current is adjusted so that when the sensor ceases to be immersed in the liquid, a large temperature change of the sensor occurs due to the change in heat transfer coefficient. However, the method tends to be unreliable because the current must be carefully adjusted and because the heat transfer coefficient can be similar in a fast-flowing stream of vapour and a static liquid. Difficulties can also arise if the saturation temperature of the liquid alters due to a change in pressure.

In the author's view, the most reliable method is simply to measure the hydrostatic head of liquid, using pressure tappings which are brought up to room temperature to a suitable differential pressure gauge. At the low-temperature end, to eliminate hydrostatic head errors due to the liquid rising up the measuring tube, the tube must be arranged horizontally so that the liquid boils in the horizontal portion. Boiling can be ensured by

using a small heater if the natural heat leak from room temperature is not sufficient. Errors may occur because of unknown temperature gradients in the liquid and also in the vapour, whose density is often not negligible compared with that of the liquid, especially in helium systems.

For liquid helium in the absence of strong magnetic fields, the superconducting gauge is undoubtedly the most convenient and accurate, measuring level to within a few millimetres. The sensor consists of a length of Type II superconducting wire, which is heated so that it is superconducting below the liquid level, but normal above, so that the resistance is just proportional to the length of wire above the free surface. The state of the wire when in the vapour will again depend on the local heat transfer coefficient, but nevertheless a well-designed sensor appears to be unaffected by high velocity flows of cold gas. The heater is sometimes separate from the wire, sometimes the measuring current itself is sufficient.

Many types of flowmeter have been used at cryogenic temperatures, with varied success, although it is usual to measure the flow at room temperature if possible. The low viscosity of the liquids, and their low density, means that turbine meters are not responsive to changes in flow rate, and also may be damaged by overspeeding due to the large gas flows during cooldown of the system; a bypass may therefore be necessary. If the liquid is near saturation, vapour may be formed in the throats of orifice plates and venturi meters unless the pressure differential is so low that it is difficult to measure. Again, the measuring equipment may be damaged during cooldown because of the large pressure differentials which may be developed. Ultrasonics and thermal anemometry have been used with some success, but the equipment is expensive and difficult to install in a cryogenic environment. Except for very small pipelines, the vortex-shedding meter may be the best type to use.

A wide range of other instruments has been used in a cryogenic environment. Generally, instruments used for room-temperature applications can be adapted, with a careful choice of materials, unless the measuring phenomenon itself is very sensitive to temperature or does not exist in the cryogenic temperature range. Many types of transistors will operate satisfactorily right down to liquid helium temperatures [1.16, 1.25], and this fact has been exploited in the design of many instruments.

References

- 1.1 N. Kurti, 'Low Temperature Terminology', *Proc. XIII Int. Congr. Refrig.*, Vol. I, pp. 593-597 (Int. Inst. Refrig., 1973).

1. A SURVEY OF
- 1.2 N. Kurti, 'F
- 1.3 Data kindly
- 1.4 E. K. Farida
Gastech 81 1
1982).
- 1.5 A. O. Tisch
1-10 (1966).
- 1.6 E. F. Hamn
(1980); A. F.
there a crisis
- 1.7 C. H. Rode
Cryog. Engi
- 1.8 L. J. Neurin
pp. 32-43, F.
'Supercondu
53.
- 1.9 B. J. Maddo
Cryog. Eng.
conducting a
598, Genova
- 1.10 B. C. Belan
in the U.S.
(1975).
- 1.11 E. B. Forsyt
Cryogenics 1
- 1.12 *Cryogenics* 1
- 1.13 R. I. Scherl
storage syste
123-132 (19
- 1.14 T. Ohtsuka
in 'Japan',
(1984).
- 1.15 J. H. P. Wa
presented at
- 1.16 R. K. Kirsch
- 1.17 H. M. Rose
- 1.18 T. van Duz
Edward Arr
- 1.19 S. J. Williar
22, 129-201
- 1.20 J. Matisoo,
1980).
- 1.21 *The Times*.
- 1.22 P. Le Piver
Engng Conf
- 1.23 B. A. Hand
- 1.24 B. A. Hand
- 1.25 B. Lengeler
genics 14, 4.

temperature is not
erature gradients in
often not negligible
systems.

ic fields, the super-
and accurate, meas-
nsists of a length of
is superconducting
e resistance is just
ce. The state of the
local heat transfer
ars to be unaffected
imes separate from
ficient.

temperatures, with
t room temperature
low density, means
rate, and also may
during cooldown of
the liquid is near
e plates and venturi
difficult to measure.
g cooldown because
ed. Ultrasonics and
, but the equipment
onment. Except for
be the best type to

cryogenic environ-
re applications can
ess the measuring
does not exist in
istors will operate
..16, 1.25], and this
nts.

1. A SURVEY OF CRYOGENIC ENGINEERING

35

- 1.2 N. Kurti, 'From Cailletet and Pictet to microkelvin', *Cryogenics* 18, 451-458 (1978).
- 1.3 Data kindly supplied by R. M. Thorogood.
- 1.4 E. K. Faridany, 'International trade in LNG: present projects and future outlook', *Proc. Gastech 81 LNG/LPG Conference*, pp. 21-35 (Gastech Ltd., Rickmansworth, England, 1982).
- 1.5 A. O. Tischler, 'The impact of the space age on cryogenics', *Adv. Cryog. Engng* 11, 1-10 (1966).
- 1.6 E. F. Hammel, 'Helium: its past, present and future', *Adv. Cryog. Engng* 25, 810-821 (1980); A. Francis, D. Keierleber and D. Swartz, 'Helium prospects for the future: is there a crisis?', *Adv. Cryog. Engng* 29, 9-17 (1984).
- 1.7 C. H. Rode, 'Cryogenic system for a 100 km superconducting collider', *Proc. 10th Int. Cryog. Engng Conf.*, pp. 760-770, Helsinki, Finland (1984).
- 1.8 L. J. Neuringer, 'NMR in biology and medicine', *Proc. 10th Int. Cryog. Engng Conf.*, pp. 32-43, Helsinki, Finland (1984); M. F. Wood, I. L. MacDougall and P. H. Winson, 'Superconducting magnets for NMR imaging and in-vivo spectroscopy', *ibid.*, pp. 44-53.
- 1.9 B. J. Maddock and W. T. Norris, 'Superconductivity in electricity supply', *Proc. 7th Int. Cryog. Engng Conf.*, pp. 245-259, London, England (1978); J. G. Steel, 'Superconducting a.c. generators - a utility view', *Proc. 8th Int. Cryog. Engng Conf.*, pp. 590-598, Genova, Italy (1980).
- 1.10 B. C. Belanger, 'Superconducting and resistive cryogenic power transmission research in the U.S. - an opportunity for cryogenic innovation', *Adv. Cryog. Engng* 20, 1-22 (1975).
- 1.11 E. B. Forsyth, 'Cryogenic engineering for the Brookhaven power transmission project', *Cryogenics* 17, 3-7 (1977).
- 1.12 *Cryogenics* 25, 50 (1985).
- 1.13 R. I. Schermer *et al.*, 'Design and operation of the 30 MJ superconducting magnetic storage system on the Bonneville Power Administration bus', *Adv. Cryog. Engng* 29, 123-132 (1984).
- 1.14 T. Ohtsuka and Y. Kyotani, 'Recent progress on superconducting magnetic levitation in Japan', *Proc. 10th Int. Cryog. Engng Conf.*, pp. 750-759, Helsinki, Finland (1984).
- 1.15 J. H. P. Watson, 'Status report on magnetic separation using superconducting magnets', presented at *10th Int. Cryog. Engng Conf.*, Helsinki, Finland (1984).
- 1.16 R. K. Kirschman, 'Cold electronics: an overview', *Cryogenics* 25, 115-122 (1985).
- 1.17 H. M. Rosenberg, *The Solid State*, 2nd edn, Clarendon Press (1978).
- 1.18 T. van Duzer and C. W. Turner, *Principles of Superconductive Devices and Circuits*, Edward Arnold (1981).
- 1.19 S. J. Williamson and L. Kaufman, 'Biomagnetism', *J. Magnetism and Magn. Materials* 22, 129-201 (1981).
- 1.20 J. Matisoo, 'The superconducting computer', *Scientific American* 282 (5), 38-53 (May 1980).
- 1.21 *The Times*, London, 1 December 1983, p. 19.
- 1.22 P. Le Pivert, 'Cryosurgery: current issues and future trends', *Proc. 10th Int. Cryog. Engng Conf.*, pp. 551-557, Helsinki, Finland (1984).
- 1.23 B. A. Hands, 'Introduction to cryopump design', *Vacuum* 26, 11-16 (1976).
- 1.24 B. A. Hands, 'Recent developments in cryopumping', *Vacuum* 32, 603-612 (1982).
- 1.25 B. Lengeler, 'Semiconductor devices suitable for use in cryogenic environments', *Cryogenics* 14, 439-447 (1974).

Journals

The most useful regular cryogenic publications are:

- Cryogenics*, a journal published by Butterworth Scientific Ltd., Guildford, England.
- Advances in Cryogenic Engineering*, which is published by Plenum Press and is the proceedings of the biennial Cryogenic Engineering Conference and the concurrent International Cryogenic Materials Conference held in the USA. It is referred to in this volume as *Adv. Cryog. Engng.*
- Proceedings of the International Cryogenic Engineering Conference series (ICEC), published by Butterworth Scientific Ltd., Guildford, England, and predecessors.
- Proceedings of the LNG and GasTech Conferences, which contain information on developments in LNG technology.
- IC SQUID, proceedings of the International Conferences on SQUIDS.
- International Institute of Refrigeration (IIR) conference proceedings.
- Proceedings of the Applied Superconductivity Conference series.

General Bibliography

In reverse order of publication:

- R. F. Barron, *Cryogenic Systems*, 2nd edn, Oxford University Press (1985).
- K. D. Williamson, Jr. and F. J. Edeskuty (eds), *Liquid Cryogens Vol. 1: Theory and Equipment; Vol. 2: Properties and Applications*, CRC Press (1983).
- A. Arkharov, I. Marfenina and Ye. Mikulin, *Theory and Design of Cryogenic Systems*, MIR Publishers (1981).
- G. K. White, *Experimental Techniques in Low-Temperature Physics*, 3rd edn, Clarendon Press (1979).
- A. C. Rose-Innes, *Low Temperature Laboratory Techniques. The Use of Liquid Helium in the Laboratory*, 2nd edn, English Universities Press (1973).
- C. A. Bailey (ed.), *Advanced Cryogenics*, Plenum Press (1971).
- G. G. Haselden (ed.), *Cryogenic Fundamentals*, Academic Press (1971).
- H. Weinstock (ed.), *Cryogenic Technology*, Boston Tech. Publ. (1969).
- R. H. Kropschot, B. W. Birmingham and D. B. Mann (eds), *Technology of Liquid Helium*, NBS Monograph 111 (1968).
- R. B. Scott, W. H. Denton and C. M. Nicholls (eds), *Technology and Uses of Liquid Hydrogen*, Pergamon Press (1964).
- J. H. Bell, *Cryogenic Engineering*, Prentice Hall (1963).
- R. W. Vance (ed.), *Cryogenic Technology*, John Wiley (1963).
- R. W. Vance and W. M. Duke (eds), *Applied Cryogenic Engineering*, John Wiley (1962).
- R. B. Scott, *Cryogenic Engineering*, Van Nostrand (1959).

Bibliography of Specific Topics

In alphabetical order of author:

- A. Barone and G. Paternò, *Physics and Applications of the Josephson Effect*, Wiley-Interscience (1982).
- N. R. Braton, *Cryogenic Recycling and Processing*, CRC Press (1980).

1. A SU

British C
Mech
J. R. Bu
A. J. Cr
B. Deav
T. van E
Arnol
R. C. F.
Press,
D. Fishl
S. Fonei
Appli
R. A. H
(Engli
H. von
W. L. L
W. R. P
Topic
M. Recl
A. C. R
Press
R. P. Sh
B. B. S
Plenu
F. H. T
M. N. V

Non-sp

K. Men
Weide
D. Wils
(1979)

1. A SURVEY OF CRYOGENIC ENGINEERING

- British Cryogenics Council, *Cryogenics Safety Manual - A Guide to Good Practice*, 2nd edn, Mechanical Engineering Publications, Bury St. Edmunds (1982).
- J. R. Bumby, *Superconducting Rotating Electrical Machines*, Clarendon Press (1983).
- A. J. Croft, *Cryogenic Laboratory Equipment*, Plenum Press (1970).
- B. Deaver and J. Ruvalds (eds), *Advances in Superconductivity*, Plenum Press (1983).
- T. van Duzer and C. W. Turner, *Principles of Superconductive Devices and Circuits*, Edward Arnold (1981).
- R. C. Ffooks, *Natural Gas by Sea*, Gentry Books, London (1979); *Gas Carriers*, Fairplay Press, London (1984).
- D. Fishlock (ed.), *A Guide to Superconductivity*, Macdonald-Elsevier (1969).
- S. Foner and B. B. Schwartz (eds), *Superconducting Machines and Devices - Large Systems Applications*, Plenum Press (1974).
- R. A. Haefler, *Kryo-Vakuumtechnik: Grundlagen und Anwendungen*, Springer-Verlag (1981) (English translation to be published by Oxford University Press).
- H. von Leden and W. G. Cahan, *Cryogenics in Surgery*, H. K. Lewis (1971).
- W. L. Lom, *Liquefied Natural Gas*, Applied Science Publishers (1974).
- W. R. Parrish, R. O. Voth, J. G. Hust, T. M. Flynn, C. F. Sindt and N. A. Olien, *Selected Topics on Hydrogen Fuel*, NBS Special Publication 419 (1975).
- M. Rechowicz, *Electric Power at Low Temperatures*, Clarendon Press (1975).
- A. C. Rose-Innes and E. H. Rhoderick, *Introduction to Superconductivity*, 2nd ed., Pergamon Press (1978).
- R. P. Shutt (ed.), *Bubble and Spark Chambers, Vol. 1*, Academic Press (1967).
- B. B. Schwartz and S. Foner (eds), *Superconductor Applications: SQUIDS and Machines*, Plenum Press (1977).
- F. H. Turner, *Concrete and Cryogenics*, Cement and Concrete Ass., England (1979).
- M. N. Wilson, *Superconducting Magnets*, Clarendon Press (1983).

Non-specialist Reading

- K. Mendelssohn, *The Quest for Absolute Zero; the Meaning of Low Temperature Physics*, Weidenfeld & Nicholson (1966).
- D. Wilson, *Supercold, an Introduction to Low Temperature Technology*, Faber & Faber (1979).

logy of Liquid Helium,

g, John Wiley (1962).

sephson Effect, Wiley-

0).

ATTACHMENT BL

IN THE UNITED STATES PATENT AND TRADEMARK OFFICE

In re Patent Application of

Applicants: Bednorz et al.

Serial No.: 08/479,810

Filed: June 7, 1995

For: NEW SUPERCONDUCTIVE COMPOUNDS HAVING HIGH TRANSITION
TEMPERATURE, METHODS FOR THEIR USE AND PREPARATION

Date: November 25, 2006

Docket: YO987-074BZ

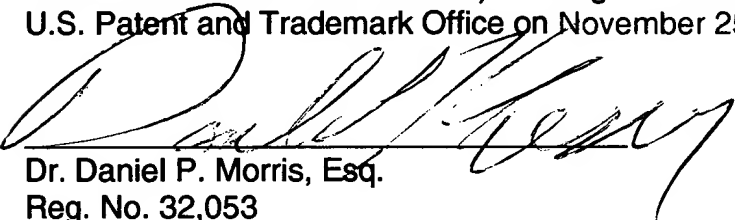
Group Art Unit: 1751

Examiner: M. Kopec

Commissioner for Patents
Box AF
P.O. Box 1450
Alexandria, VA 22313-1450

CERTIFICATE OF FIRST CLASS TRANSMISSION

I hereby certify that this Supplementary Response, (3 Pages Plus
Attachment A and Attachment B) is being transmitted by first class mail to the
U.S. Patent and Trademark Office on November 25, 2006.



Dr. Daniel P. Morris, Esq.
Reg. No. 32,053

FOURTEENTH SUPPLEMENTARY RESPONSE

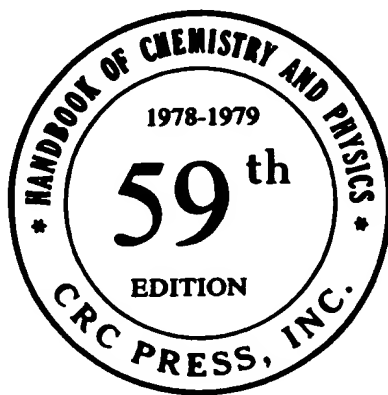
In response to the Office Action dated October 20, 2005 please consider the
following:

ATTACHMENT B

VCE
tion
ogy,
VCE

CRC Handbook OF Chemistry and Physics

A Ready-Reference Book of Chemical and Physical Data



EDITOR

ROBERT C. WEAST, Ph.D.

*Vice President, Research, Consolidated Natural Gas Service Company, Inc.
Formerly Professor of Chemistry at Case Institute of Technology*

ASSOCIATE EDITOR

MELVIN J. ASTLE, Ph.D.

*Formerly Professor of Organic Chemistry at Case Institute of Technology
and
Manager of Research at Glidden-Durkee Division of SCM Corporation*

SES

In collaboration with a large number of professional chemists and physicists whose assistance is acknowledged in the list of general collaborators and in connection with the particular tables or sections involved.



CRC PRESS, Inc.

2255 Palm Beach Lakes Blvd., West Palm Beach, Florida 33409

Superconductivity*

B.W. ROBERTS

General Electric Research Laboratory, Schenectady, New York

The following tables on superconductivity include superconductive properties of chemical elements, thin films, a selected list of compounds and alloys, and high-magnetic-field superconductors.

The historically first observed and most distinctive property of a superconductive body is the near total loss of resistance at a critical temperature (T_c) that is characteristic of each material. Figure 1(a) below illustrates schematically two types of possible transitions. The sharp vertical discontinuity in resistance is indicative of that found for a single crystal of a very pure element or one of a few well annealed alloy compositions. The broad transition, illustrated by broken lines, suggests the transition shape seen for materials that are not homogeneous and contain unusual strain distributions. Careful testing of the resistivity limits for superconductors shows that it is less than 4×10^{-23} ohm-cm, while the lowest resistivity observed in metals is of the order of 10^{-13} ohm-cm. If one compares the resistivity of a superconductive body to that of copper at room temperature, the superconductive body is at least 10^{17} times less resistive.

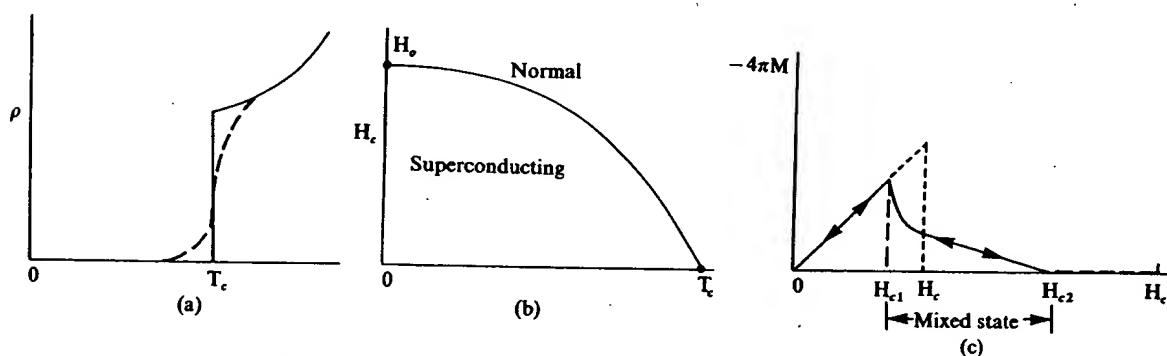


Figure 1. PHYSICAL PROPERTIES OF SUPERCONDUCTORS

- (a) Resistivity versus temperature for a pure and perfect lattice (solid line). Impure and/or imperfect lattice (broken line).
- (b) Magnetic-field temperature dependence for Type-I or "soft" superconductors.
- (c) Schematic magnetization curve for "hard" or Type-II superconductors.

The temperature interval ΔT_c , over which the transition between the normal and superconductive states takes place, may be of the order of as little as 2×10^{-5} °K or several °K in width, depending on the material state. The narrow transition width was attained in 99.9999 percent pure gallium single crystals.

A Type-I superconductor below T_c , as exemplified by a pure metal, exhibits perfect diamagnetism and excludes a magnetic field up to some critical field H_c , whereupon it reverts to the normal state as shown in the H-T diagram of Figure 1(b).

The difference in entropy near absolute zero between the superconductive and normal states relates directly to the electronic specific heat, γ : $(S_s - S_n)_{T \rightarrow 0} = -\gamma T$.

The magnetization of a typical high-field superconductor is shown in Figure 1(c). The discovery of the large current-carrying capability of Nb_3Sn and other similar alloys has led to an extensive study of the physical properties of these alloys. In brief, a high-field superconductor, or Type-II superconductor, passes from the perfect diamagnetic state at low magnetic fields to a mixed state and finally to a sheathed state before attaining the normal resistive state of the metal. The magnetic field values separating the four stages are given as H_{c1} , H_{c2} , and H_{c3} . The superconductive state below H_{c1} is perfectly diamagnetic, identical to the state of most pure metals of the "soft" or Type-I

*Prepared for Office of Standard Reference Data, National Bureau of Standards, by Standard Reference Data Center on Superconductive Materials, Schenectady, N.Y.

superconductor. Between H_{c1} and H_{c2} a "mixed superconductive state" is found in which fluxons (a minimal unit of magnetic flux) create lines of normal superconductor in a superconductive matrix. The volume of the normal state is proportional to $-4\pi M$ in the "mixed state" region. Thus at H_{c2} the fluxon density has become so great as to drive the interior volume of the superconductive body completely normal. Between H_{c2} and H_{c3} the superconductor has a sheath of current-carrying superconductive material at the body surface, and above H_{c3} the normal state exists. With several types of careful measurement, it is possible to determine H_{c1} , H_{c2} , and H_{c3} . Table 2-35 contains some of the available data on high-field superconductive materials.

High-field superconductive phenomena are also related to specimen dimension and configuration. For example, the Type-I superconductor, Hg, has entirely different magnetization behavior in high magnetic fields when contained in the very fine sets of filamentary tunnels found in an unprocessed Vycor glass. The great majority of superconductive materials are Type II. The elements in very pure form and a very few precisely stoichiometric and well annealed compounds are Type-I with the possible exceptions of vanadium and niobium.

Metallurgical Aspects. The sensitivity of superconductive properties to the material state is most pronounced and has been used in a reverse sense to study and specify the detailed state of alloys. The mechanical state, the homogeneity, and the presence of impurity atoms and other electron-scattering centers are all capable of controlling the critical temperature and the current-carrying capabilities in high-magnetic fields. Well annealed specimens tend to show sharper transitions than those that are strained or inhomogeneous. This sensitivity to mechanical state underlines a general problem in the tabulation of properties for superconductive materials. The occasional divergent values of the critical temperature and of the critical fields quoted for a Type-II superconductor may lie in the variation in sample preparation. Critical temperatures of materials studied early in the history of superconductivity must be evaluated in light of the probable metallurgical state of the material, as well as the availability of less pure starting elements. It has been noted that recent work has given extended consideration to the metallurgical aspects of sample preparation.

REFERENCES

References to the data presented in this section, to additional entries of superconductive materials, and to those materials specifically tested and found non-superconductive to some low temperature may be found in the following publications:

"Superconductive Materials and Some of Their Properties", *Progress in Cryogenics*, B.W. Roberts, Vol. IV, Heywood and Co., 1964, pp. 160-231.

"Superconductive Materials and Some of Their Properties", B.W. Roberts, National Bureau of Standards Technical Notes 408 and 482, U.S. Government Printing Office, 1966 and 1969.

SELECTED PROPERTIES OF THE SUPERCONDUCTIVE ELEMENTS

Conversion Factors

$$\text{Oe} \times 79.57 = \text{A/m}; \text{katm} \times 1.013 \times 10^5 = \text{N/m}^2; \text{kb} \times 1.0 \times 10^3 = \text{N/m}^2$$

Element	$T_c(\text{K})$	$H_0(\text{oersteds})$	$\theta_D(\text{K})$	$\gamma(\text{mJmole}^{-1} \text{deg} \cdot \text{K}^2)$
Al	1.175	104.93	420	1.35
Be	0.026			0.21
Cd	0.518, 0.52	29.6	209	0.688
Ga	1.0833	59.3	325	0.60
Ga (β)	5.90, 6.2	560		
Ga (γ)	7.62	950		
Ga (δ)	7.85	815		
Hg (α)	4.154	411	87, 71.9	1.81
Hg (β)	3.949	339	93	1.37
In	3.405	281.53	109	1.672
Ir	0.14, 0.11	19	425	3.27
La (α)	4.88	808, 798	142	10.0, 11.3
La (β)	6.00	1,096	139	11.3
Mo	0.916	90, 98	460	1.83
Nb	9.25	1,970	277, 238	7.80
Os	0.655	65	500	2.35
Pa	1.4			
Pb	7.23	803	96.3	3.0
Re	1.697	188, 211	415	2.35
Ru	0.493	66	580	3.0
Sb	2.6-2.7			
Sn	3.721	305	195	1.78
Ta	4.47	831	258	6.15
Tc	7.73, 7.78	1,410	411	4.84, 6.28
Th	1.39	159.1	165	4.31
Ti	0.39	56, 100	429, 412	3.32
Tl	2.332, 2.39	181	78.5	1.47
V	5.43, 5.31	1,100, 1,400	382	9.82
W	0.0154	1.15	550	0.90
Zn	0.875	55	319.7	0.633
Zr	0.53	47	290	2.78
Zr (ω)	0.65			

Thin Films Condensed at Various Temperatures

Element	$T_c(\text{K})$
Al	1.18-~5.7
Be	~0.3, ~9.6; 6.5-10.6 ^a ; 10.2 ^b
Bi	~2-~5, 6.11, 6.154, 6.173
Cd	0.53-0.91
Ga	6.4-6.8, 7.4-8.4, 8.56
In	3.43-4.5; 3.68-4.17 ^c
La	5.0-6.74
Mo	3.3-3.8, 4-6.7
Nb	6.2-10.1
Pb	~2-7.7
Re	~7
Sn	3.6, 3.84-6.0
Ta	<1.7-4.25, 3.16-4.8
Ti	1.3
Tl	2.64
V	5.14-6.02
W	<1.0-4.1
Zn	0.77-1.48

^aWith KCl.

^bWith Zn etioporphyrin.

^cIn glass pores.

SELECTED PROPERTIES OF THE SUPERCONDUCTIVE ELEMENTS (Continued)

Data for Elements Studied Under Pressure

Element	$T_c(K)$	Pressure
As	0.31-0.5 0.2-0.25	220-140 kb ~140-100 kb
Ba II	~1.3	55 kb
Ba III	3.05 ~5.2	85-88 kb >140 kb
Bi II	3.916 3.90 3.86	25 katm 25.2 katm 26.8 katm
Bi III	6.55 7.25	~37 kb 27-28.4 katm
Bi IV	7.0	43, 43-62 kb
Bi V	8.3, 8.55	81 kb
Bi VI	8.55	90, 92-101 kb
Ce	1.7	50 kb
Cs	~1.5	>~125 kb
Ga II	6.24, 6.38	≥35 katm
Ga II'	7.5	≥35 katm ($P \rightarrow 0$)
Ge	4.85-5.4 5.35	~120 kb 115 kb
La	~5.5-11.93	0-~140 kb
P	4.7 5.8	>100 kb 170 kb
Pb II	3.55, 3.6	160 kb
Sb	3.55 3.52 3.53 3.40	85 kb 93 kb 100 kb ~150 kb
Se II	6.75, 6.95	~130 kb
Si	6.7, 7.1	120 kb
Sn II	5.2 4.85	125 kb 160 kb
Sn III	5.30	113 kb
Te II	2.05 3.4	43 kb 50 kb
Te III	4.28	70 kb
Te IV	4.25	84 kb
Tl, cub.	1.45	35 kb
Tl, hex.	1.95	35 kb
U	2.3	10 kb
Y	~1.2, ~2.7	120-170 kb

From Roberts, B. W., Properties of Selected Superconductive Materials, 1974 Supplement, NBS Technical Note 825, U.S. Government Printing Office, Washington, D.C., 1974, 10.

All compositions are denoted on an atomic basis, i.e., AB, A_xB_y or AB_3 for compounds, unless noted. Solid solutions or odd compositions may be denoted as A_xB_{1-x} or A_xB . A series of three or more alloys is indicated as A_xB_{1-x} or by actual indication of the atomic fraction range, such as $A_{0-0.6}B_{1-0.4}$. The critical temperature of such a series of alloys is denoted by a range of values or possibly the maximum value.

The selection of the critical temperature from a transition in the effective permeability, or the change in resistance, or possibly the incremental changes in frequency observed by certain techniques is not often obvious from the literature. Most authors choose the mid-point of such curves as the probable critical temperature of the idealized material, while others will choose the highest temperature at which a deviation from the normal state property is observed. In view of the previous discussion concerning the variability of the superconductive properties as a function of purity and other metallurgical aspects, it is recommended that appropriate literature be checked to determine the most probable critical temperature or critical field of a given alloy.

A very limited amount of data on critical fields, H_c , is available for these compounds and alloys; these values are given at the end of the table.

SYMBOLS: n = number of normal carriers per cubic centimeter for semiconductor superconductors.

Substance	$T_c, ^\circ K$	Crystal structure type††	Substance	$T_c, ^\circ K$	Crystal structure type††
$Ag_xAl_{1-x}Zn_{1-x-y}$	0.5-0.845	Cubic	$Al_{0.8}Ge_{0.2}Nb_3$	20.7	Al5
$Ag_7BF_4O_8$	0.15		$AlLa_3$	5.57	DO ₁₉
$AgBi_2$	3.0-2.78		Al_2La	3.23	Cl5
$Ag_7F_{0.25}N_{0.75}O_{10.25}$	0.85-0.90		$AlMg_2$	0.84	Cubic, f.c.
Ag_7FO_8	0.3		$AlMo_3$	0.58	Al5
Ag_2F	0.066	Cubic	$AlMo_6Pd$	2.1	
$Ag_{0.8-0.3}Ga_{0.2-0.7}$	6.5-8		AlN	1.55	B4
Ag_4Ge	0.85		Al_2NNb_3	1.3	Al3
$Ag_{0.438}Hg_{0.562}$	0.64		$AlNb_3$	18.0	Al5
$AgIn_2$	~2.4		Al_xNb_{1-x}	<4.2-13.5	D8 ₈
$Ag_{0.1}In_{0.9}Te$ ($n = 1.40 \times 10^{22}$)	1.20-1.89	Bl	Al_xNb_{1-x}	12-17.5	Al5
$Ag_{0.2}In_{0.8}Te$ ($n = 1.07 \times 10^{22}$)	0.77-1.00	Bl	$Al_{0.27}Nb_{0.73-0.48}V_{0-0.25}$	14.5-17.5	Al5
$AgLa$ (9.5 kbar)	1.2	B2	$AlNb_xV_{1-x}$	<4.2-13.5	
$AgNO_{11}$	1.04	Cubic	$AlOs$	0.39	B2
Ag_xPb_{1-x}	7.2 max.	Cubic	Al_3Os	5.90	
Ag_xSn_{1-x} (film)	2.0-3.8		$AlPb$ (films)	1.2-7	
Ag_xSn_{1-x}	1.5-3.7		Al_2Pt	0.48-0.55	Cl
$AgTe_3$	2.6		Al_5Re_{24}	3.35	Al2
$AgTh_2$	2.26		Al_3Th	0.75	DO ₁₉
$Ag_{0.03}Tl_{0.97}$	2.67	Cl6	$Al_xTi_yV_{1-x-y}$	2.05-3.62	Cubic
$Ag_{0.94}Tl_{0.06}$	2.32		$Al_{0.108}V_{0.892}$	1.82	Cubic
Ag_xZn_{1-x}	0.5-0.845		Al_xZn_{1-x}	0.5-0.845	
Al (film)	1.3-2.31		$AlZr_3$	0.73	Li ₂
Al (1 to 21 katm)	1.170-0.687	Al	$AsBiPb$	9.0	
$AlAu_4$	0.4-0.7	Like Al3	$AsBiPbSb$	9.0	
Al_2CMo_3	10.0	Al3	$As_{0.33}InTe_{0.67}$ ($n = 1.24 \times 10^{22}$)	0.85-1.15	Bl
Al_2CMo_3	9.8-10.2	Al3 + trace 2nd phase	$As_{0.5}InTe_{0.5}$ ($n = 0.97 \times 10^{22}$)	0.44-0.62	Bl
Al_2CaSi	5.8	Cubic	$As_{0.50}Ni_{0.06}Pd_{0.44}$	1.39	C2
$Al_{0.131}Cr_{0.088}V_{0.781}$	1.46		$AsPb$	8.4	
$AlGe_2$	1.75		$AsPd_2$ (low- temperature phase)	0.60	Hexagonal
$Al_{0.5}Ge_{0.5}Nb$	12.6	Al5	$AsPd_2$ (high-temp. phase)	1.70	C22

††See key at end of table.

Substance	T_c , °K	Crystal structure type††	Substance	T_c , °K	Crystal structure type††
AsPd ₅	0.46	Complex	BW ₂	3.1	Cl6
AsRh	0.58	B31	B ₆ Y	6.5-7.1	
AsRh _{1.4-1.6}	<0.03-0.56	Hexagonal	B ₁₂ Y	4.7	
AsSn	4.10		BZr	3.4	Cubic
AsSn			B ₁₂ Zr	5.82	
($n = 2.14 \times 10^{22}$)	3.41-3.65	BI	BaBi ₃	5.69	Tetragonal
As ₂ Sn ₃	3.5-3.6, 1.21-1.17		Ba _x O ₃ Sr _{1-x} Ti ($n = 4.2-11 \times 10^{19}$)	<0.1-0.55	
As ₃ Sn ₄			Ba _{0.13} O ₃ W	1.9	Tetragonal
($n = 0.56 \times 10^{22}$)	1.16-1.19	Rhombohedral	Ba _{0.14} O ₃ W	<1.25-2.2	Hexagonal
Au ₃ Ba	0.4-0.7	D2 _d	BaRh ₂	6.0	Cl5
AuBe	2.64	B20	Be ₂₂ Mo	2.51	Cubic, like Be ₂₂ Re
Au ₂ Bi	1.80	Cl5			
Au ₅ Ca	0.34-0.38	Cl5 _b	Be ₈ Nb ₅ Zr ₂	5.2	
AuGa	1.2	B31	Be _{0.98-0.92} Re _{0.02-0.08} (quenched)	9.5-9.75	Cubic
Au _{0.40-0.92} Ge _{0.60-0.08}	<0.32-1.63	Complex	Be _{0.957} Re _{0.043}	9.62	Cubic, like Be ₂₂ Re
AuIn	0.4-0.6	Complex			
AuLu	<0.35	B2	BeTc	5.21	Cubic
AuNb ₃	11.5	Al5	Be ₂₂ W	4.12	Cubic, like Be ₂₂ Re
AuNb ₃	1.2	A2			
Au _{0-0.3} Nb _{1-0.7}	1.1-11.0		Be ₁₃ W	4.1	Tetragonal
Au _{0.02-0.98} Nb ₃ Rh _{0.98-0.02}	2.53-10.9	Al5	Bi ₃ Ca	2.0	
AuNb _{3(1-x)}} V _{3x}	1.5-11.0	Al5	Bi _{0.5} Cd _{0.13} Pb _{0.25} Sn _{0.12} (weight fractions)	8.2	
AuPb ₂	3.15		BiCo	0.42-0.49	
AuPb ₂ (film)	4.3		Bi ₂ Cs	4.75	Cl5
AuPb ₃	4.40		Bi _x Cu _{1-x} (electrodeposited)	2.2	
AuPb ₃ (film)	4.25		BiCu	1.33-1.40	
Au ₂ Pb	1.18, 6-7	Cl5	Bi _{0.019} In _{0.981}	3.86	
AuSb ₂	0.58	C2	Bi _{0.05} In _{0.95}	4.65	α -phase
AuSn	1.25	B8 ₁	Bi _{0.10} In _{0.90}	5.05	α -phase
Au _x Sn _{1-x} (film)	2.0-3.8		Bi _{0.15-0.30} In _{0.85-0.70}	5.3-5.4	α - and β -phases
Au ₃ Sn	0.7-1.1	A3	Bi _{0.34-0.48} In _{0.66-0.52}	4.0-4.1	
Au ₃ Te ₅	1.62	Cubic	Bi ₂ In ₅	4.1	
AuTh ₂	3.08	Cl6	BiIn ₂	5.65	β -phase
AuTi	1.92		Bi ₂ Ir	1.7-2.3	
AuV ₃	0.74	Al5	Bi ₂ Ir (quenched)	3.0-3.96	
Au _x Zn _{1-x}	0.50-0.845		BiK	3.6	
AuZn ₃	1.21	Cubic	Bi ₂ K	3.58	Cl5
Au _x Zr ₇	1.7-2.8	A3	BiLi	2.47	Ll ₀ , α -phase
AuZr ₃	0.92	Al5	Bi ₄₋₉ Mg	0.7-~1.0	
BCMo ₂	5.4	Orthorhombic	Bi ₃ Mo	3-3.7	
B _{0.03} C _{0.51} Mo _{0.47}	12.5		BiNa	2.25	Ll ₀
BCMo ₂	5.3-7.0	Orthorhombic	BiNb ₃ (high pressure and temperature)	3.05	Al5
BHf	3.1	Cubic	BiNi	4.25	B8 ₁
B ₆ La	5.7		Bi ₃ Ni	4.06	Orthorhombic
B ₁₂ Lu	0.48		Bi ₁₋₀ Pb ₀₋₁	7.26-9.14	
BMo	0.5 (extrap- olated)		Bi ₁₋₀ Pb ₀₋₁ (film)	7.25-8.67	
			Bi _{0.05-0.40} Pb _{0.95-0.60}	7.35-8.4	Hexagonal, c.p., to ϵ -phase
BMo ₂	4.74	Cl6			
BNb	8.25	B _f			
BRe ₂	2.80, 4.6				
B _{0.3} Ru _{0.7}	2.58	D10 ₂			
B ₁₂ Sc	0.39				
BTa	4.0	B _f			
B ₆ Th	0.74		BiPbSb	8.9	

††See key at end of table.

SELECTED SUPERCONDUCTIVE COMPOUNDS AND ALLOYS (Continued)

	Substance	$T_c, ^\circ K$	Crystal structure type††	Substance	$T_c, ^\circ K$	Crystal structure type††
	$\text{Bi}_{0.5}\text{Pb}_{0.31}\text{Sn}_{0.19}$ (weight fractions)	8.5		$\text{C}_{0.44}\text{Mo}_{0.56}$	1.3	BI
	$\text{Bi}_{0.5}\text{Pb}_{0.25}\text{Sn}_{0.25}$	8.5		$\text{C}_{0.5}\text{Mo}_x\text{Nb}_{1-x}$	10.8–12.5	BI
	BiPd_2	4.0		$\text{C}_{0.6}\text{Mo}_{4.8}\text{Si}_3$	7.6	D8 ₈
al	$\text{Bi}_{0.4}\text{Pd}_{0.6}$	3.7–4	Hexagonal, ordered	$\text{CMo}_{0.2}\text{Ta}_{0.8}$	7.5	BI
	BiPd	3.7	Orthorhombic	$\text{CMo}_{0.5}\text{Ta}_{0.5}$	7.7	BI
al	Bi_2Pd	1.70	Monoclinic, α -phase	$\text{CMo}_{0.75}\text{Ta}_{0.25}$	8.5	BI
al	Bi_2Pd	4.25	Tetragonal, β -phase	$\text{CMo}_{0.8}\text{Ta}_{0.2}$	8.7	BI
	BiPdSe	1.0	C2	$\text{CMo}_{0.85}\text{Ta}_{0.15}$	8.9	BI
22Re	BiPdTe	1.2	C2	$\text{CMo}_x\text{Ti}_{1-x}$	10.2 max.	BI
	BiPt	1.21	B8 ₁	$\text{CMo}_{0.83}\text{Ti}_{0.17}$	10.2	BI
	BiPtSe	1.45	C2	$\text{CMo}_x\text{V}_{1-x}$	2.9–9.3	BI
	BiPtTe	1.15	C2	$\text{CMo}_x\text{Zr}_{1-x}$	3.8–9.5	BI
22Re	Bi_2Pt	0.155	Hexagonal	$\text{C}_{0.1-0.9}\text{Nb}_{0.9-0.1}\text{Nb}$	8.5–17.9	
	Bi_2Rb	4.25	CI5	$\text{C}_{0-0.38}\text{Nb}_{1-0.62}\text{Ta}$	10.0–11.3	
	BiRe_2	1.9–2.2		CNb (whiskers)	7.5–10.5	
22Re	BiRh	2.06	B8 ₁	$\text{C}_{0.984}\text{Nb}$	9.8	BI
al	Bi_3Rh	3.2	Orthorhombic, like NiB_3	CNb (extrapolated)	~14	
	Bi_4Rh	2.7	Hexagonal	$\text{C}_{0.7-1.0}\text{Nb}_{0.3-0}$	6–11	BI
	Bi_3Sn	3.6–3.8		CNb ₂	9.1	
	BiSn	3.8		$\text{CNb}_x\text{Ta}_{1-x}$	8.2–13.9	
	Bi_2Sn_y	3.85–4.18		$\text{CNb}_x\text{Ti}_{1-x}$	<4.2–8.8	BI
	Bi_3Sr	5.62		$\text{CNb}_{0.6-0.9}\text{W}_{0.4-0.1}$	12.5–11.6	BI
	Bi_3Te	0.75–1.0		$\text{CNb}_{0.1-0.9}\text{Zr}_{0.9-0.1}$	4.2–8.4	BI
	Bi_3Ti_3	6.4		CRb _x (gold)	0.023–0.151	Hexagonal
	$\text{Bi}_{0.26}\text{Ti}_{0.74}$	4.4		$\text{CRc}_{0.01-0.08}\text{W}$	1.3–5.0	
	$\text{Bi}_{0.26}\text{Ti}_{0.74}$	4.15		$\text{CRc}_{0.06}\text{W}$	5.0	
phases	Bi_2Y_3	2.25		CTa	~11 (extrapolated)	
	Bi_3Zn	0.8–0.9		$\text{C}_{0.987}\text{Ta}$	9.7	
	$\text{Bi}_{0.3}\text{Zr}_{0.7}$	1.51		$\text{C}_{0.848-0.987}\text{Ta}$	2.04–9.7	
	BiZr_3	2.4–2.8		CTa (film)	5.09	BI
	CCs_x	0.020–0.135	Hexagonal	CTa_2	3.26	L ₃
	C_8K (gold)	0.55		$\text{CTa}_{0.4}\text{Ti}_{0.6}$	4.8	BI
	CGaMo_2	3.7–4.1	Hexagonal, H-phase	$\text{CTa}_{1-0.4}\text{W}_{0-0.6}$	8.5–10.5	BI
ase	$\text{CHf}_{0.5}\text{Mo}_{0.5}$	3.4	BI	$\text{CTa}_{0.2-0.9}\text{Zr}_{0.8-0.1}$	4.6–8.3	BI
	$\text{CHf}_{0.3}\text{Mo}_{0.7}$	5.5	BI	CTc (excess C)	3.85	Cubic
	$\text{CHf}_{0.23}\text{Mo}_{0.75}$	6.6	BI	$\text{CTi}_{0.5-0.7}\text{W}_{0.5-0.3}$	6.7–2.1	BI
	$\text{CHf}_{0.7}\text{Nb}_{0.3}$	6.1	BI	CW	1.0	
	$\text{CHf}_{0.6}\text{Nb}_{0.4}$	4.5	BI	CW_2	2.74	L ₃
	$\text{CHf}_{0.5}\text{Nb}_{0.5}$	4.8	BI	CW_2	5.2	Cubic, f.c.
	$\text{CHf}_{0.4}\text{Nb}_{0.6}$	5.6	BI	CaIr ₂	6.15	CI5
mbic	$\text{CHf}_{0.25}\text{Nb}_{0.75}$	7.0	BI	$\text{Ca}_x\text{O}_3\text{Sr}_{1-x}\text{Ti}$ ($n = 3.7-11.0 \times 10^{19}$)	<0.1–0.55	
	$\text{CHf}_{0.2}\text{Nb}_{0.8}$	7.8	BI	$\text{Ca}_{0.1}\text{O}_3\text{W}$	1.4–3.4	Hexagonal
	$\text{CHf}_{0.9-0.1}\text{Ta}_{0.1-0.9}$	5.0–9.0	BI	CaPb	7.0	
al,	Ck (excess K)	0.55	Hexagonal	CaRh ₂	6.40	CI5
	C_8K	0.39	Hexagonal	$\text{Cd}_{0.3-0.5}\text{Hg}_{0.7-0.5}$	1.70–1.92	
	$\text{C}_{0.40-0.44}\text{Mo}_{0.60-0.56}$	9–13		CdHg	1.77, 2.15	Tetragonal
	CMo	6.5, 9.26		$\text{Cd}_{0.0075-0.05}\text{In}_{1-x}$	3.24–3.36	Tetragonal
	CMo ₂	12.2	Orthorhombic	$\text{Cd}_{0.97}\text{Pb}_{0.03}$	4.2	
				CdSn	3.65	
				$\text{Cd}_{0.17}\text{Ti}_{0.83}$	2.3	
				$\text{Cd}_{0.18}\text{Ti}_{0.82}$	2.54	
				CeCo ₂	0.84	CI5
				$\text{CeCo}_{1.67}\text{Ni}_{0.33}$	0.46	CI5

††See key at end of table.

Substance	T_c , °K	Crystal structure type††	Substance	T_c , °K	Crystal structure type††
CeCo _{1.67} Rh _{0.33}	0.47	Cl5	CuSSe	1.5-2.0	Cl8
Ce _x Gd _{1-x} Ru ₂	3.2-5.2	Cl5	CuSe ₂	2.3-2.43	Cl8
CeIr ₃	3.34		CuSeTe	1.6-2.0	Cl8
CeIr ₅	1.82		Cu _x Sn _{1-x}	3.2-3.7	
Ce _{0.005} La _{0.995}	4.6		Cu _x Sn _{1-x} (film)		
Ce _x La _{1-x}	1.3-6.3		(made at 10°K)	3.6-7	
Ce _x Pr _{1-x} Ru ₂	1.4-5.3	Cl5	Cu _x Sn _{1-x} (film)		
Ce ₂ Pt _{1-x}	0.7-1.55		(made at 300°K)	2.8-3.7	
CeRu ₂	6.0	Cl5	CuTe ₂	<1.25-1.3	Cl8
Co _x Fe _{1-x} Si ₂	1.4 max.	Cl	CuTh ₂	3.49	Cl6
CoHf ₂	0.56	E9 ₃	Cu _{0-0.027} V	3.9-5.3	A2
CoLa ₃	4.28		Cu ₂ Zn _{1-x}	0.5-0.845	
CoLu ₃	~0.35		Er _x La _{1-x}	1.4-6.3	
Co _{0-0.01} Mo _{0.8} Re _{0.2}	2-10		Fe _{0-0.04} Mo _{0.8} Re _{0.2}	1-10	
Co _{0.02-0.10} Nb ₃ Rh _{0.98-0.90}	2.28-1.90	Al5	Fe _{0.05} Ni _{0.05} Zr _{0.90}	~3.9	
Co _x Ni _{1-x} Si ₂	1.4 max.	Cl	Fe ₃ Th ₇	1.86	D10
Co _{0.5} Rh _{0.5} Si ₂	2.5		Fe _x Ti _{1-x}	3.2 max.	Fe in α-Ti
Co _x Rh _{1-x} Si ₂	3.65 max.		Fe _x Ti _{1-x}	3.7 max.	Fe in β-Ti
Co _{-0.3} Sc _{-0.7}	~0.35		Fe _x Ti _{0.6} V _{1-x}	6.8 max.	
CoSi ₂	1.40, 1.22	Cl	FeU ₆	3.86	D2 _c
Co ₃ Th ₇	1.83	D10 ₂	Fe _{0.1} Zr _{0.9}	1.0	A3
Co _x Ti _{1-x}	2.8 max.	Co in α-Ti	Ga _{0.5} Ge _{0.5} Nb ₃	7.3	Al5
Co _x Ti _{1-x}	3.8 max.	Co in β-Ti	GaLa ₃	5.84	
CoTi ₂	3.44	E9 ₃	Ga ₂ Mo	9.5	
CoTi	0.71	A2	GaMo ₃	0.76	Al5
CoU	1.7	B2, distorted	Ga ₄ Mo	9.8	
CoU ₆	2.29	D2 _c	GaN (black)	5.85	B4
Co _{0.28} Y _{0.72}	0.34		GaNb ₃	14.5	Al5
CoY ₃	<0.34		Ga ₂ Nb ₃ Sn _{1-x}	14-18.37	Al5
CoZr ₂	6.3	Cl6	Ga _{0.7} Pt _{0.3}	2.9	Cl
Co _{0.1} Zr _{0.9}	3.9	A3	GaPt	1.74	B20
Cr _{0.6} Ir _{0.4}	0.4	Hexagonal, c.p.	GaSb (120 kbar, 77°K, annealed)	4.24	A5
Cr _{0.65} Ir _{0.35}	0.59	Hexagonal, c.p.	GaSb (unannealed)	~5.9	
Cr _{0.7} Ir _{0.3}	0.76	Hexagonal, c.p.	Ga _{0.1} Sn ₁₋₀ (quenched)	3.47-4.18	
Cr _{0.72} Ir _{0.28}	0.83		Ga ₀₋₁ Sn ₁₋₀ (annealed)	2.6-3.85	
Cr ₃ Ir	0.45	Al5	Ga ₃ V ₂	3.55	Tetragonal, Mn ₂ Hg ₅ type
Cr _{0-0.1} Nb _{1-0.9}	4.6-9.2	A2			
Cr _{0.80} Os _{0.20}	2.5	Cubic	GaV ₃	16.8	Al5
Cr _x Re _{1-x}	1.2-5.2		GaV _{2.1-3.5}	6.3-14.45	Al5
Cr _{0.40} Re _{0.60}	2.15	D8 ₆	GaV _{4.5}	9.15	
Cr _{0.8-0.6} Rh _{0.2-0.4}	0.5-1.10	A3	Ga ₃ Zr	1.38	
Cr ₃ Ru (annealed)	3.3	Al5	Gd _x La _{1-x}	<1.0-5.5	
Cr ₂ Ru	2.02	D8 ₆	Gd _x Os ₂ Y _{1-x}	1.4-4.7	
Cr _{0.1-0.5} Ru _{0.9-0.5}	0.34-1.65	A3	Gd _x Ru ₂ Th _{1-x}	3.6 max.	Cl5
Cr _x Ti _{1-x}	3.6 max.	Cr in α-Ti	GeIr	4.7	B31
Cr _x Ti _{1-x}	4.2 max.	Cr in β-Ti	Ge ₂ La	1.49, 2.2	Orthorhombic, distorted ThSi ₂ -type
Cr _{0.1} Ti _{0.3} V _{0.6}	5.6				
Cr _{0.0175} U _{0.9825}	0.75	β-phase			
Cs _{0.32} O ₃ W	1.12	Hexagonal	GeMo ₃	1.43	Al5
Cu _{0.15} In _{0.85} (film)	3.75		GeNb ₂	1.9	
Cu _{0.04-0.08} In _{1-x}	4.4		GeNb ₃ (quenched)	6-17	Al5
CuLa	5.85		Ge _{0.25} Nb _{0.75}	6	Al5
Cu _x Pb _{1-x}	5.7-7.7		Ge _x Nb ₃ Sn _{1-x}	17.6-18.0	Al5
CuS	1.62	B18	Ge _{0.5} Nb ₃ Sn _{0.5}	11.3	
CuS ₂	1.48-1.53	Cl8			

††See key at end of table.

SELECTED SUPERCONDUCTIVE COMPOUNDS AND ALLOYS (Continued)

Substance	T_c , °K	Crystal structure type††	Substance	T_c , °K	Crystal structure type††
GePt	0.40	B3I	InSb	2.1	
Ge ₃ Rh ₅	2.12	Orthorhombic, related to InNi ₂	(InSb) _{0.95-0.10} Sn _{0.05-0.90} (various heat treatments)	3.8-5.1	
			(InSb) _{0-0.07} Sn _{1-0.93}	3.67-3.74	
Ge ₂ Sc	1.3		In ₃ Sn	~5.5	
Ge ₃ Te ₄ (n = 1.06 × 10 ²²)	1.55-1.80	Rhombohedral	In _x Sn _{1-x}	3.4-7.3	
Ge _x Te _{1-x} (n = 8.5-64 × 10 ²⁰)	0.07-0.41		In _{0.82-1} Te	1.02-3.45	BI
GeV ₃	6.01	BI	In _{1.000} Te _{1.002}	3.5-3.7	BI
Ge ₂ Y	3.80	Al5	In ₃ Te ₄ (n = 0.47 × 10 ²²)	1.15-1.25	Rhombohedral
Ge _{1.62} Y	2.4	C _c	In _x Tl _{1-x}	2.7-3.374	
H _{0.33} Nb _{0.67}	7.28	Cubic, b.c.	In _{0.8} Tl _{0.2}	3.223	
H _{0.1} Nb _{0.9}	7.38	Cubic, b.c.	In _{0.62} Tl _{0.38}	2.760	
H _{0.05} Nb _{0.95}	7.83	Cubic, b.c.	In _{0.78-0.69} Tl _{0.22-0.31}	3.18-3.32	Tetragonal
H _{0.12} Ta _{0.88}	2.81	Cubic, b.c.	In _{0.69-0.62} Tl _{0.31-0.38}	2.98-3.3	Cubic, f.c.
H _{0.08} Ta _{0.92}	3.26	Cubic, b.c.	Ir ₂ La	0.48	CI5
H _{0.04} Ta _{0.96}	3.62	Cubic, b.c.	Ir ₃ La	2.32	DI0 ₂
HfN _{0.989}	6.6	BI	Ir ₃ La ₇	2.24	DI0 ₂
Hf _{0-0.5} Nb _{1-0.5}	8.3-9.5	A2	Ir ₅ La	2.13	
Hf _{0.75} Nb _{0.25}	>4.2		Ir ₂ Lu	2.47	CI5
HfOs ₂	2.69	CI4	Ir ₃ Lu	2.89	CI5
HfRe ₂	4.80	CI4	IrMo	<1.0	A3
Hf _{0.14} Re _{0.86}	5.86	Al2	IrMo ₃	8.8	Al5
Hf _{0.99-0.96} Rh _{0.01-0.04}	0.85-1.51		IrMo ₃	6.8	D8 ₈
Hf _{0-0.55} Ta _{1-0.45}	4.4-6.5 ~	A2	IrNb ₃	1.9	Al5
HfV ₂	8.9-9.6	CI5	Ir _{0.4} Nb _{0.6}	9.8	D8 ₈
Hg _x In _{1-x}	3.14-4.55		Ir _{0.37} Nb _{0.63}	2.32	D8 ₈
HgIn	3.81		IrNb	7.9	D8 ₈
Hg ₂ K	1.20	Orthorhombic	Ir _{0.02} Nb ₃ Rh _{0.98}	2.43	Al5
Hg ₃ K	3.18		Ir _{0.05} Nb ₃ Rh _{0.95}	2.38	Al5
Hg ₄ K	3.27		Ir _{0.287} O _{0.14} Ti _{0.573}	5.5	E9 ₃
Hg ₈ K	3.42		Ir _{0.265} O _{0.035} Ti _{0.65}	2.30	E9 ₃
Hg ₃ Li	1.7	Hexagonal	Ir _x Os _{1-x}	0.3-0.98	
Hg ₂ Na	1.62	Hexagonal		(max.)-0.6	
Hg ₄ Na	3.05		IrOsY	2.6	CI5
Hg _x Pb _{1-x}	4.14-7.26		Ir _{1.5} Os _{0.5}	2.4	CI4
HgSn	4.2		Ir ₂ Sc	2.07	CI5
Hg _x Tl _{1-x}	2.30-4.109		Ir _{2.5} Sc	2.46	CI5
Hg ₅ Tl ₂	3.86		IrSn ₂	0.65-0.78	CI
Ho _x La _{1-x}	1.3-6.3		Ir ₂ Sr	5.70	CI5
InLa ₃	9.83, 10.4	LI ₂	Ir _{0.5} Te _{0.5}	~3	
InLa ₃ (0-35, kbar)	9.75-10.55		IrTe ₃	1.18	C2
In _{1-0.86} Mg _{0-0.14}	3.395-3.363		IrTh	<0.37	B _f
InNb ₃ (high pressure and temp.)	4-8, 9.2	A15	Ir ₂ Th	6.50	CI5
In _{0-0.3} Nb ₃ Sn _{1-0.7}	18.0-18.19	Al5	Ir ₃ Th	4.71	
In _{0.5} Nb ₃ Zr _{0.5}	6.4		Ir ₃ Th ₇	1.52	DI0 ₂
In _{0.11} O ₃ W	<1.25-2.8	Hexagonal	Ir ₅ Th	3.93	D2 ₄
In _{0.95-0.83} Pb _{0.05-0.15}	3.6-5.05		IrTi ₃	5.40	Al5
In _{0.98-0.91} Pb _{0.02-0.09}	3.45-4.2		IrV ₂	1.39	Al5
InPb	6.65		IrW ₃	3.82	
InPd	0.7	B2	Ir _{0.28} W _{0.72}	4.49	
InSb (quenched from 170 kbar into liquid N ₂)	4.8	Like A5	Ir ₂ Y	2.18, 1.38	CI5
			Ir _{0.69} Y _{0.31}	1.98, 1.44	CI5
			Ir _{0.70} Y _{0.30}	2.16	CI5

††See key at end of table.

SELECTED SUPERCONDUCTIVE COMPOUNDS AND ALLOYS (Continued)

<i>Substance</i>	<i>T_c, °K</i>	<i>Crystal structure type††</i>	<i>Substance</i>	<i>T_c, °K</i>	<i>Crystal structure type††</i>
Ir ₂ Y	1.09	CI5	Mo ₃ Si	1.30	A15
Ir ₂ Y ₃	1.61		MoSi _{0.7}	1.34	
Ir _x Y _{1-x}	0.3-3.7		Mo _x SiV _{3-x}	4.54-16.0	A15
Ir ₂ Zr	4.10	CI5	Mo _x Tc _{1-x}	10.8-15.8	
Ir _{0.1} Zr _{0.9}	5.5	A3	Mo _{0.16} Ti _{0.84}	4.18, 4.25	
K _{0.27-0.31} O ₃ W	0.50	Hexagonal	Mo _{0.913} Ti _{0.087}	2.95	Cubic
K _{0.40-0.57} O ₃ W	1.5	Tetragonal	Mo _{0.04} Ti _{0.96}	2.0	
La _{0.55} Lu _{0.45}	2.2	Hexagonal, La type	Mo _{0.025} Ti _{0.975}	1.8	
La _{0.8} Lu _{0.2}	3.4	Hexagonal, La Type	Mo _x U _{1-x}	0.7-2.1	
LaMg ₂	1.05	CI5	Mo _x V _{1-x}	0-~5.3	CI5
LaN	1.35		Mo ₂ Zr	4.27-4.75	
LaOs ₂	6.5	CI5	NNb (whiskers)	10-14.5	
LaPt ₂	0.46	CI5	NNb (diffusion wires)	16.10	
La _{0.28} Pt _{0.72}	0.54	CI5	NNb (film)	6-9	BI
LaRh ₃	2.60		N _{0.988} Nb	14.9	BI
LaRh ₅	1.62		N _{0.824-0.988} Nb	14.4-15.3	BI
La ₇ Rh ₃	2.58	DI0 ₂	N _{0.70-0.795} Nb	11.3-12.9	Cubic and tetragonal
La ₇ Ru ₃	1.63	CI5	NNb ₂ O ₇	13.5-17.0	BI
LaRu ₂	6.5	D7 ₃	NNb ₂ O ₇	6.0-11	
La ₃ S ₄	8.6	D7 ₃	N _{100-42 w/o} Nb _{0-58 w/o} Ti†	15-16.8	
La ₃ Se ₄	2.3	C _c	N _{100-75 w/o} Nb _{0-25 w/o} Zr†	12.5-16.35	
La _x Y _{1-x}	1.7-5.4		NNb ₂ Zr _{1-x}	9.8-13.8	BI
LaZn	1.04	B2	N _{0.93} Nb _{0.85} Zr _{0.15}	13.8	BI
LiPb	7.2		N _x O _y Ti _z	2.9-5.6	Cubic
LuOs ₂	3.49	CI4	N _x O _y V _z	5.8-8.2	Cubic
Lu _{0.275} Rh _{0.725}	1.27	CI5	N _{0.34} Re	4-5	Cubic, f.c.
LuRh ₅	0.49		NTa	12-14	BI
LuRu ₂	0.86	CI4		(extrapolated)	
Mg-0.47Ti-0.53	2.75	B2	NTa (film)	4.84	BI
Mg ₂ Nb	5.6		N _{0.6-0.987} Ti	<1.17-5.8	BI
Mn _x Ti _{1-x}	2.3 max.	Mn in α-Ti	N _{0.82-0.99} V	2.9-7.9	BI
Mn _x Ti _{1-x}	1.1-3.0	Mn in β-Ti	NZr	9.8	BI
MnU ₆	2.32	D2 _c	N _{0.906-0.984} Zr	3.0-9.5	BI
MoN	12	Hexagonal	Na _{0.28-0.35} O ₃ W	0.56	Tetragonal
Mo ₂ N	5.0	Cubic, f.c.	Na _{0.28} Pb _{0.72}	7.2	
Mo _x Nb _{1-x}	0.016-9.2		NbO	1.25	
Mo ₃ Os	7.2	A15	NbOs ₂	2.52	A12
Mo _{0.62} Os _{0.38}	5.65	D8 _h	Nb ₃ Os	1.05	A15
Mo ₃ P	5.31	DO _c	Nb _{0.6} Os _{0.4}	1.89, 1.78	D8 _h
Mo _{0.5} Pd _{0.5}	3.52	A3	Nb ₃ Os _{0.02-0.10} Rh _{0.98-0.90}	2.42-2.30	A15
Mo ₃ Re	10.0		Nb _{0.6} Pd _{0.4}	1.60	D8 _f plus cubic
Mo _x Re _{1-x}	1.2-12.2		Nb ₃ Pd _{0.02-0.10} Rh _{0.98-0.90}	2.49-2.55	A15
MoRe ₃	9.25, 9.89	A12	Nb _{0.62} Pt _{0.38}	4.21	D8 _h
Mo _{0.42} Re _{0.58}	6.35	D8 _h	Nb ₃ Pt	10.9	A15
Mo _{0.52} Re _{0.48}	11.1		Nb ₂ Pt ₃	3.73	D8 _h
Mo _{0.57} Re _{0.43}	14.0		Nb ₃ Pt _{0.02-0.98} Rh _{0.98-0.02}	2.52-9.6	A15
Mo-0.60Re-0.395	10.6		Nb _{0.38-0.18} Re _{0.62-0.82}	2.43-9.70	A12
MoRh	1.97	A3	Nb ₃ Rh	2.64	A15
Mo _x Rh _{1-x}	1.5-8.2	Cubic, b.c.	Nb _{0.60} Rh _{0.40}	4.21	D8 _h plus other
MoRu	9.5-10.5	A3	Nb ₃ Rh _{0.98-0.90} Ru _{0.02-0.10}	2.42-2.44	A15
Mo _{0.61} Ru _{0.39}	7.18	D8 _h	Nb _x Ru _{1-x}	1.2-4.8	
Mo _{0.2} Ru _{0.8}	1.66	A3	NbS ₂	6.1-6.3	Hexagonal, NbSe ₂ type
Mo ₃ Sb ₄	2.1				

†w/o denotes weight percent.

††See key at end of table.

SELECTED SUPERCONDUCTIVE COMPOUNDS AND ALLOYS (Continued)

<i>Substance</i>	<i>T_c, °K</i>	<i>Crystal structure type††</i>	<i>Substance</i>	<i>T_c, °K</i>	<i>Crystal structure type††</i>
NbS ₂	5.0-5.5	Hexagonal, three-layer type	Os ₂ Zr	3.0	Cl4
Nb ₃ Sb _{0-0.7} Sn _{1-0.3}	6.8-18	A15	Os _x Zr _{1-x}	1.50-5.6	
NbSe ₂	5.15-5.62	Hexagonal, NbS ₂ type	PPb	7.8	
Nb _{1-1.05} Se ₂	2.2-7.0	Hexagonal, NbS ₂ type	PPd _{3.0-3.2}	<0.35-0.7	DO ₁₁
Nb ₃ Si	1.5	Li ₂	P ₃ Pd ₇ (high temperature)	1.0	Rhombohedral Complex
Nb ₃ SiSnV ₃	4.0	A15	P ₃ Pd ₇ (low temp.)	0.70	
Nb ₃ Sn	18.05	A15	PRh	1.22	
Nb _{0.8} Sn _{0.2}	18.18, 18.5	A15	PRh ₂	1.3	Cl
Nb ₂ Sn _{1-x} (film)	2.6-18.5		PW ₃	2.26	DO ₄
NbSn ₂	2.60	Orthorhombic	Pb ₂ Pd	2.95	Cl6
Nb ₃ Sn ₂	16.6	Tetragonal	Pb ₄ Pt	2.80	Related to Cl6
NbSnTa ₂	10.8	A15	Pb ₂ Rh	2.66	Cl6
Nb ₂ SnTa	16.4	A15	PbSb	6.6	
Nb _{2.5} SnTa _{0.5}	17.6	A15	PbTe (plus 0.1 w/o Pb)†	5.19	
Nb _{2.75} SnTa _{0.25}	17.8	A15	PbTe (plus 0.1 w/o Tl)†	5.24-5.27	
Nb _{3x} SnTa _{3(1-x)}	6.0-18.0		PbTl _{0.27}	6.43	
NbSnTaV	6.2	A15	PbTl _{0.17}	6.73	
Nb ₂ SnTa _{0.5} V _{0.5}	12.2	A15	PbTl _{0.12}	6.88	
NbSnV ₂	5.5	A15	PbTl _{0.075}	6.98	
Nb ₂ SnV	9.8	A15	PbTl _{0.04}	7.06	
Nb _{2.5} SnV _{0.5}	14.2	A15	Pb _{1-0.26} Tl _{0-0.74}	7.20-3.68	
Nb _x Ta _{1-x}	4.4-9.2	A2	PbTl ₂	3.75-4.1	
NbTc ₃	10.5	A12	Pb ₃ Zr ₃	4.60	D8 ₈
Nb _x Ti _{1-x}	0.6-9.8		PbZr ₃	0.76	A15
Nb _{0.6} Ti _{0.4}	9.8		Pd _{0.9} Pt _{0.1} Te ₂	1.65	C6
Nb _x U _{1-x}	1.95 max.		Pd _{0.05} Ru _{0.05} Zr _{0.9}	~9	
Nb _{0.88} V _{0.12}	5.7	A2	Pd _{2.3} S (quenched)	1.63	Cubic
Nb _{0.75} Zr _{0.25}	10.8		PdSb ₂	1.25	C2
Nb _{0.66} Zr _{0.33}	10.8		PdSb	1.50	B8 ₁
Ni _{0.3} Th _{0.7}	1.98	D10 ₂	PdSbSe	1.0	C2
NiZr ₂	1.52		PdSbTe	1.2	C2
Ni _{0.1} Zr _{0.9}	1.5	A3	Pd ₄ Se	0.42	Tetragonal
O ₃ Rb _{0.27-0.29} W	1.98	Hexagonal	Pd ₆₋₇ Se	0.66	Like Pd ₄ Te
O ₃ SrTi			Pd _{2.8} Se	2.3	
(n = 1.7-12.0 × 10 ¹⁹)	0.12-0.37		Pd _x Se _{1-x}	2.5 max.	
O ₃ SrTi			PdSi	0.93	B3I
(n = 10 ¹⁸ -10 ²¹)	0.05-0.47		PdSn	0.41	B3I
O ₃ SrTi			PdSn ₂	3.34	
(n = ~10 ²⁰)	0.47		Pd ₃ Sn	0.41	C37
OTi	0.58		Pd ₃ Sn ₂	0.47-0.64	B8 ₂
O ₃ Sr _{0.08} W	2-4	Hexagonal	PdTe	2.3, 3.85	B8 ₁
O ₃ Tl _{0.30} W	2.0-2.14	Hexagonal	PdTe _{1.02-1.08}	2.56-1.88	B8 ₁
OV ₃ Zr ₃	7.5	E9 ₃	PdTe ₂	1.69	C6
OW ₃ (film)	3.35, 1.1	A15	PdTe _{2.1}	1.89	C6
OsReY	2.0	Cl4	PdTe _{2.3}	1.85	C6
Os ₂ Sc	4.6	Cl4	Pd _{1.1} Te	4.07	B8 ₁
OsTa	1.95	A12	PdTh ₂	0.85	Cl6
Os ₃ Th ₇	1.51	D10 ₂	Pd _{0.1} Zr _{0.9}	7.5	A3
Os ₂ W _{1-x}	0.9-4.1		PtSb	2.1	B8 ₁
OsW ₃	~3		PtSi	0.88	B3I
Os ₂ Y	4.7	Cl4	PtSn	0.37	B8 ₁
			PtTe	0.59	Orthorhombic
			PtTh	0.44	B _f
			Pt ₃ Th ₇	0.98	D10 ₂
			Pt ₅ Th	3.13	

†w/o denotes weight percent.

††See key at end of table.

SELECTED SUPERCONDUCTIVE COMPOUNDS AND ALLOYS (Continued)††See key at end of table.

A
A
A
A
A
A
A
A
A
A
A
B1
B2
B3
B4
B8
B8
B1
B1
B1
B2
B2
B3
B3
B3
B3
B_j
B₉
B_k
B_i
C1
C1
C2
C6
C1
C1
C1
C1

*Sec "H2

SELECTED SUPERCONDUCTIVE COMPOUNDS AND ALLOYS (Continued)

CRITICAL FIELD DATA

<i>Substance</i>	<i>H_c oersteds</i>	<i>Substance</i>	<i>H_c oersteds</i>
Ag ₂ F	2.5	InSb	1,100
Ag ₇ NO ₁₁	57	In _x Tl _{1-x}	252-284
Al ₂ CMo ₃	1,700	In _{0.8} Tl _{0.2}	252
BaBi ₃	740	Mg _{~0.47} Tl _{~0.53}	220
Bi ₂ Pt	10	Mo _{0.16} Ti _{0.84}	<985
Bi ₃ Sr	530	NbSn ₂	620
Bi ₅ Tl ₃	>400	PbTl _{0.27}	756
CdSn	>266	PbTl _{0.17}	796
CoSi ₂	105	PbTl _{0.12}	849
Cr _{0.1} Ti _{0.3} V _{0.6}	1,360	PbTl _{0.075}	880
In _{1-0.86} Mg _{0-0.14}	272.4-259.2	PbTl _{0.04}	864

KEY TO CRYSTAL STRUCTURE TYPES

<i>"Strukturbericht" type*</i>	<i>Example</i>	<i>Class</i>	<i>"Strukturbericht" type*</i>	<i>Example</i>	<i>Class</i>
A1	Cu	Cubic, f.c.	C15 ₈	AuBe ₅	Cubic
A2	W	Cubic, b.c.	C16	CuAl ₂	Tetragonal, b.c.
A3	Mg	Hexagonal, close packed	C18	FeS ₂	Orthorhombic
A4	Diamond	Cubic, f.c.	C22	Fe ₂ P	Trigonal
A5	White Sn	Tetragonal, b.c.	C23	PbCl ₂	Orthorhombic
A6	In	Tetragonal, b.c. (f.c. cell usually used)	C32	AlB ₂	Hexagonal
A7	As	Rhombohedral	C36	MgNi ₂	Hexagonal
A8	Se	Trigonal	C37	Co ₂ Si	Orthorhombic
A10	Hg	Rhombohedral	C49	ZrSi ₂	Orthorhombic
A12	α-Mn	Cubic, b.c.	C54	TiSi ₂	Orthorhombic
A13	β-Mn	Cubic	C _c	Si ₂ Th	Tetragonal, b.c.
A15	"β-W" (WO ₃)	Cubic	DO ₃	BiF ₃	Cubic, f.c.
B1	NaCl	Cubic, f.c.	DO ₁₁	Fe ₃ C	Orthorhombic
B2	CsCl	Cubic	DO ₁₈	Na ₃ As	Hexagonal
B3	ZnS	Cubic	DO ₁₉	Ni ₃ Sn	Hexagonal
B4	ZnS	Hexagonal	DO ₂₀	NiAl ₃	Orthorhombic
B8 ₁	NiAs	Hexagonal	DO ₂₂	TiAl ₃	Tetragonal
B8 ₂	Ni ₂ In	Hexagonal	DO _e	Ni ₃ P	Tetragonal, b.c.
B10	PbO	Tetragonal	D1 ₃	Al ₄ Ba	Tetragonal, b.c.
B11	γ-CuTi	Tetragonal	D1 _c	PtSn ₄	Orthorhombic
B17	PtS	Tetragonal	D2 ₁	CaB ₆	Cubic
B18	CuS	Hexagonal	D2 _c	MnU ₆	Tetragonal, b.c.
B20	FeSi	Cubic	D2 ₄	CaZn ₅	Hexagonal
B27	FeB	Orthorhombic	D5 ₂	La ₂ O ₃	Trigonal
B31	MnP	Orthorhombic	D5 ₈	Sb ₂ S ₃	Orthorhombic
B32	NaTl	Cubic, f.c.	D7 ₃	Th ₃ P ₄	Cubic, b.c.
B34	PdS	Tetragonal	D7 _b	Ta ₃ B ₄	Orthorhombic
B _f	δ-CrB	Orthorhombic	D8 ₁	Fe ₃ Zn ₁₀	Cubic, b.c.
B _g	MoB	Tetragonal, b.c.	D8 ₂	Cu ₅ Zn ₈	Cubic, b.c.
B _h	WC	Hexagonal	D8 ₃	Cu ₉ Al ₄	Cubic
B _i	γ-MoC	Hexagonal	D8 ₈	Mn ₅ Si ₃	Hexagonal
C1	CaF ₂	Cubic, f.c.	D8 _b	CrFe	Tetragonal
C1 _b	MgAgAs	Cubic, f.c.	D8 _i	Mo ₂ B ₅	Rhombohedral
C2	FeS ₂	Cubic	D10 ₂	Fe ₃ Th ₇	Hexagonal
C6	CdI ₂	Trigonal	E2 ₁	CaTiO ₃	Cubic
C11b	MoSi ₂	Tetragonal, b.c.	E9 ₃	Fe ₃ W ₃ C	Cubic, f.c.
C12	CaSi ₂	Rhombohedral	L1 ₀	CuAu	Tetragonal
C14	MgZn ₂	Hexagonal	L1 ₂	Cu ₃ Au	Cubic
C15	Cu ₂ Mg	Cubic, f.c.	L2 _b	ThH ₂	Tetragonal, b.c.
			L'3	Fe ₂ N	Hexagonal

*See "Handbook of Lattice Spacing and Structures of Metals", W.B. Pearson, Vol. I, Pergamon Press, 1958, p. 79. and Vol. II, Pergamon Press, 1967, p. 3.

HIGH CRITICAL MAGNETIC-FIELD SUPERCONDUCTIVE COMPOUNDS AND ALLOYS

With Critical Temperatures, H_{c1} , H_{c2} , H_{c3} , and the Temperature of Field Observations, T_{obs}

Substance	T_c , °K	H_{c1} , kg	H_{c2} , kg	H_{c3} , kg	T_{obs} , °K†
Al_2CMo_3	9.8–10.2	0.091	156		1.2
$AlNb_3$		0.375			
$Ba_xO_3Sr_{1-x}Ti$	<0.1–0.55	0.0039 max.			
$Bi_{0.5}Cd_{0.1}Pb_{0.27}Sn_{0.13}$			>24		3.06
Bi_2Pb_{1-x}	7.35–8.4	0.122 max.	~30 max.		4.2
$Bi_{0.56}Pb_{0.44}$	8.8		15		4.2
$Bi_{7.5}w/oPb_{92.5}w/o†$			2.32		
$Bi_{0.099}Pb_{0.901}$		0.29	2.8		
$Bi_{0.02}Pb_{0.98}$		0.46	0.73		
$Bi_{0.53}Pb_{0.32}Sn_{0.16}$			>25		3.06
$Bi_{1-0.93}Sn_{0-0.07}$			0–0.032		3.7
Bi_5Ti_3	6.4		>5.56		3.35
C_6K (excess K)	0.55		0.160 (H⊥c)		0.32
			0.730 (H c)		0.32
			0.025 (H⊥c)		0.32
C_8K	0.39		0.250 (H c)		0.32
$Co_{0.44}Mo_{0.56}$	12.5–13.5	0.087	98.5		1.2
CNb	8–10	0.12	16.9		4.2
$CNb_{0.4}Ta_{0.6}$	10–13.6	0.19	14.1		1.2
CTa	9–11.4	0.22	4.6		1.2
$Ca_xO_3Sr_{1-x}Ti$	<0.1–0.55	0.002–0.004			
$Cd_{0.1}Hg_{0.9}$ (by weight)		0.23	0.34		2.04
$Cd_{0.05}Hg_{0.95}$		0.28	0.31		2.16
$Cr_{0.10}Ti_{0.30}V_{0.60}$	5.6	0.071	84.4		0
GaN	5.85	0.725			4.2
Ga_xNb_{1-x}			>28		4.2
GaSb (annealed)	4.24		2.64		3.5
$GaV_{1.95}$	5.3		73***		
$GaV_{2.1-3.5}$	6.3–14.45		230–300**		0
GaV_3		0.4	350***		0
			500**		
$GaV_{4.5}$	9.15		121*		0
$HfNb_3$			>52–>102		1.2
$HfTa_3$			>28–>86		1.2
$Hg_{0.05}Pb_{0.95}$		0.235	2.3		
$Hg_{0.101}Pb_{0.899}$		0.23	4.3		4.2
$Hg_{0.15}Pb_{0.85}$	~6.75		>13		2.93
$In_{0.98}Pb_{0.02}$	3.45	0.1		0.12	2.76
$In_{0.96}Pb_{0.04}$	3.68	0.1	0.12	0.25	2.94
$In_{0.94}Pb_{0.06}$	3.90	0.095	0.18	0.35	3.12
$In_{0.913}Pb_{0.087}$	4.2	~0.17	0.55	2.65	
$In_{0.916}Pb_{0.084}$		0.155	3.7		4.2
$In_{0.17}Pb_{0.83}$			2.8	5.5	4.2
$In_{1.000}Te_{1.002}$	3.5–3.7		1.2*		0
$In_{0.95}Tl_{0.05}$		0.263	0.263		3.3
$In_{0.90}Tl_{0.10}$		0.257	0.257		3.25
$In_{0.83}Tl_{0.17}$		0.242	0.39		3.21
$In_{0.75}Tl_{0.25}$		0.216	0.50		3.16
LaN	1.35	0.45			0.76
La_3S_4	6.5	~0.15	>25		1.3
La_3Se_4	8.6	~0.2	>25		1.25
$Mo_{0.52}Re_{0.48}$	11.1		14–21	22–33	4.2
			18–28	37–43	1.3
			14–20	20–37	4.2
$Mo_{0.6 \pm 0.05}Re_{0.395}$	10.6		19–26	26–37	1.3
			~75*		0
$Mo_{-0.5}Tc_{-0.5}$			98.7*		0
$Mo_{0.16}Ti_{0.84}$	4.18	0.028	36–38		3.0
			~15		4.2
$Mo_{0.913}Ti_{0.087}$	2.95	0.060	>25		
$Mo_{0.1-0.3}U_{0.9-0.7}$	1.85–2.06		~30		
$Mo_{0.17}Zr_{0.83}$	15.2		>9.5		13.2
$N_{(12.8 w/o)}Nb$	16.1		153*		0
NNb (wires)			132		4.2
			95		8
			53		12
NNb_xO_{1-x}	13.5–17.0		~38		
NNb_xZr_{1-x}	9.8–13.8		4–>130		4.2
$N_{0.93}Nb_{0.85}Zr_{0.15}$	13.8		>130		4.2
$Na_{0.086}Pb_{0.914}$		0.19	6.0		
$Na_{0.016}Pb_{0.984}$		0.28	2.05		

†w/o denotes weight percent.

HIGH CRITICAL MAGNETIC-FIELD SUPERCONDUCTIVE COMPOUNDS AND ALLOYS (Continued)

Substance	T_c , °K	H_{c1} , kg	H_{c2} , kg	H_{c3} , kg	T_{c2} , °K†
Nb	9.15		2.020		1.4
Nb			1.710		4.2
Nb (unstrained)		0.4-1.1	3-5.5		4.2
Nb (strained)		1.1-1.8	3.40	6-9.1	4.2
Nb (cold-drawn wire)		1.25-1.92	3.44	6.0-8.7	4.2
Nb (film)		2.48	4.10	≈ 10	4.2
NbSc			> 25		4.2
Nb ₃ Sn		0.170	> 30		
			221		4.2
			70		14.15
			54		15
			34		16
			17		17
Nb _{0.1} Ta _{0.9}		0.084	0.154		4.195
Nb _{0.2} Ta _{0.8}			10		4.2
Nb _{0.65-0.73} Ta _{0.02-0.10} Zr _{0.25}			> 70-90		4.2
Nb _x Ti _{1-x}			148 max.		1.2
			120 max.		4.2
Nb _{0.222} U _{0.778}		1.98	23		1.2
Nb _x Zr _{1-x}			127 max.		1.2
			94 max.		4.2
O ₃ SrTi	0.43	.0049*	.504*		0
O ₃ SrTi	0.33	.00195*	.420*		0
PbSb ₁ w/o (quenched)			> 1.5		4.2
PbSb ₁ w/o (annealed)			> 0.7		4.2
PbSb _{2.8} w/o (quenched)			> 2.3		4.2
PbSb _{2.8} w/o (annealed)			> 0.7		4.2
Pb _{0.871} Sn _{0.129}		0.45	1.1		
Pb _{0.965} Sn _{0.035}		0.53	0.56		
Pb _{1-0.26} Tl _{0-0.74}	7.20-3.68		2-6.9*		0
PbTl _{0.17}	6.73		4.5*		0
Rc _{0.26} W _{0.74}			> 30		
Sb _{0.93} Sn _{0.07}			0.12		3.7
SiV ₃	17.0	0.55	156***		
Sn _x Te _{1-x}		0.00043-0.00236	0.005-0.0775		0.012-0.079
Ta (99.95%)		0.425	1.850		1.3
		0.325	1.425		2.27
		0.275	1.175		2.66
		0.090	0.375		3.72
Ta _{0.5} Nb _{0.5}			3.55		4.2
Ta _{0.65-0.73} Ti _{0.35-1}	4.4-7.8		> 14-138		1.2
Ta _{0.5} Ti _{0.5}			138		1.2
Te	~3.3	0.25*			0
Tc _x W _{1-x}	5.75-7.88		8-44		4.2
Ti				2.7	4.2
Ti _{0.75} V _{0.25}	5.3	0.029*	199*		0
Ti _{0.775} V _{0.225}	4.7	0.024*	172*		0
Ti _{0.615} V _{0.385}	7.07	0.050	~34		4.2
Ti _{0.516} V _{0.484}	7.20	0.062	~28		4.2
Ti _{0.415} V _{0.585}	7.49	0.078	~25		4.2
Ti _{0.12} V _{0.88}			17.3	28.1	4.2
Ti _{0.09} V _{0.91}			14.3	16.4	4.2
Ti _{0.06} V _{0.94}			8.2	12.7	4.2
Ti _{0.03} V _{0.97}			3.8	6.8	4.2
Ti _x V _{1-x}			108 max.		1.2
V	5.31	~0.8	~3.4		1.79
		~0.75	~3.15		2
		~0.45	~2.2		3
		~0.30	~1.2		4
V _{0.26} Zr _{0.74}	≈ 5.9	0.238			1.05
		0.227			1.78
		0.185			3.04
		0.165			3.5
W (film)	1.7-4.1		> 34		1

† Temperature of critical field measurement.

* Extrapolated.

** Linear extrapolation.

*** Parabolic extrapolation.

TABLES OF PROPERTIES OF SEMICONDUCTORS

Compiled by Dr. Brian Randall Pamplin

The term "semiconductor" is applied to a material in which electric current is carried by electrons or holes and whose electrical conductivity when extremely pure rises exponentially with temperature and may be increased from this low "intrinsic" value by many orders of magnitude by "doping" with electrically active impurities.

Semiconductors are characterised by an energy gap in the allowed energies of electrons in the material which separates the normally filled energy levels of the *valence band* (where "missing" electrons behave like positively charged current carriers "holes") and the *conduction band* (where electrons behave rather like a gas of free negatively charged carriers with an effective mass dependent on the material and the direction of the electrons' motion). This energy gap depends on the nature of the material and varies with direction in anisotropic crystals. It is slightly dependent on temperature and pressure, and this dependence is usually almost linear at normal temperatures and pressures.

The data is presented in three tables. Table I "General Properties of Semiconductors" lists the main crystallographic and semiconducting properties of a large number of semiconducting materials in three main categories; "Tetrahedral Semiconductors" in which every atom is tetrahedrally co-ordinated to four nearest neighbour atoms (or atomic sites) as for example in the diamond structure; "Octahedral Semiconductors" in which every atom is octahedrally co-ordinated to six nearest neighbour atoms—as for example in the halite structure; and "Other Semiconductors".

Table II gives more detailed information about some better known semiconductors, while Table III gives some information about the electronic energy band structure parameters of the best known materials.

**This Page is Inserted by IFW Indexing and Scanning
Operations and is not part of the Official Record**

BEST AVAILABLE IMAGES

Defective images within this document are accurate representations of the original documents submitted by the applicant.

Defects in the images include but are not limited to the items checked:

- ☒ **BLACK BORDERS**
- ☐ **IMAGE CUT OFF AT TOP, BOTTOM OR SIDES**
- ☒ **FADED TEXT OR DRAWING**
- ☐ **BLURRED OR ILLEGIBLE TEXT OR DRAWING**
- ☐ **SKEWED/SLANTED IMAGES**
- ☒ **COLOR OR BLACK AND WHITE PHOTOGRAPHS**
- ☐ **GRAY SCALE DOCUMENTS**
- ☒ **LINES OR MARKS ON ORIGINAL DOCUMENT**
- ☐ **REFERENCE(S) OR EXHIBIT(S) SUBMITTED ARE POOR QUALITY**
- ☐ **OTHER:** _____

IMAGES ARE BEST AVAILABLE COPY.

As rescanning these documents will not correct the image problems checked, please do not report these problems to the IFW Image Problem Mailbox.